UNIVERSITY OF CALIFORNIA
SANTA CRUZ

NON-MIGRATORY INTERNAL PLASTICIZATION OF POLY(VINYL CHLORIDE) VIA PENDANT TRIAZOLES BEARING ALKYL OR POLYETHER ESTERS

A dissertation submitted in partial satisfaction
of the requirements for the degree of

DOCTOR OF PHILOSOPHY

in

CHEMISTRY

by

Chad Masaharu Higa

September 2018

The Dissertation of Chad Masaharu Higa is approved:

_____
Professor Rebecca Braslau, Advisor

_____
Professor Pradip Mascharak, Chair

_____
Assistant Professor Jevgenij Raskatov

_____
Lori Kletzer
Vice Provost and Dean of Graduate Studies

Table of Contents

List of Figures, Schemes, and Tables ..... **vii**

Abstract ..... **xx**

Dedication ..... **xxii**

Acknowledgements ..... **xxiii**

1 Introduction: Internal Plasticization of Poly(vinyl chloride) **1**

1.1 Poly(vinyl chloride): History and Discovery 1

1.2 Global Demand and General Applications of PVC 2

1.3 Synthesis and Physical Properties of PVC 4

1.4 Plasticization Theory 11

1.5 Compatibility Factors Essential for Efficient Plasticization 26

1.6 Phthalate Plasticizers 31

1.7 Adverse Biological Effects: Phthalates 34

1.8 Phthalate Plasticizer Alternatives for PVC 49

1.9 Thioether Internally Plasticized Poly(vinyl chloride) (PVC) 51

1.10 Natural Product-Derived Internally Plasticized Poly(vinyl chloride) (PVC) 66

1.11 Synthetic 1,2,3-Triazole Internally Plasticized Poly(vinyl chloride) (PVC) 75

1.12 Conclusion 89

1.13 References 90

2 Direct and Single Hexyl Tethered Alkyl Triazole Phthalate Mimics **103**

2.1 The 1,3-Dipolar Cycloaddition 103

2.2 1,3-Dipolar Cycloaddition: Electron-Deficient Alkynes 106

2.3 PVC Plasticization: Direct PVC Modification with Triazole-Phthalate Mimics 109

2.4 DSC Analysis: 1st Generation Triazole-Phthalate Mimics on PVC 119

2.5 2nd Generation Plasticizer: Single Hexyl Tether Alkyl Phthalate Mimics on PVC . 123

2.6 DSC Analysis: 2nd Generation Single Hexyl Tether Triazole Phthalate Mimics on PVC…… 141

2.7 DSC Analysis: 1st Generation Versus 2nd Generation Triazole Phthalate Mimics on PVC…..... 143

2.8 Plasticizer Efficiencies: 1st and 2nd Generation Systems Versus DEHP-PVC 155

2.9 Thermogravimetric Analysis: 1st and 2nd Generation Systems 160

2.10 References 167

3 Double Hexyl Tethered Alkyl Triazole Phthalate Mimics 170

3.1 Increasing Plasticizing Efficiency Utilizing Alkyl Plasticizer Chains with the Triazole Anchoring Strategy 170

3.2 Synthetic Challenges: Esterification of Acetylenedicarboxylic Acid with Hexyl Tethered Alcohols Containing Pendant Alkyl Triazole Phthalate Mimics..... 172

3.3 Synthesis of Acetylenedicarboxylate Esters with Hexyl Tethered Alcohols Containing Pendant Alkyl Triazole Phthalate Mimics 180

3.4 Synthetic Optimization and Analysis of Acetylenedicarboxylate Esters with Hexyl Tethered Alcohols Containing Pendant Alkyl Triazole Phthalate Mimics..... 184

3.5 3rd Generation Plasticizer: Synthesis and Characterization of Double Hexyl Tethered Alkyl Triazole Phthalate Mimics on PVC..... 191

3.6 DSC Analysis: Double Hexyl Tethered Alkyl Triazole Phthalate Mimics on PVC. 196

3.7 Plasticizer Efficiencies: Generations 1 - 3 Triazole Plasticizers Versus DEHP-PVC 200

3.8 Thermogravimetric Analysis: Double Hexyl Tethered Alkyl Triazole Phthalate Mimics on PVC 206

3.9 References 209

4 Poly(ethylene oxide) Triazole Phthalate Mimics 211

4.1 Miscibility of Polyethers with PVC 211

4.2 Synthesis of Type 0D Poly(ethylene oxide) Triazole-Plasticized PVC 216

4.3 Synthesis of Type 1 Poly(ethylene oxide) Triazole Plasticizers 223

4.4 Synthesis of Type 2 Poly(ethylene oxide) Triazole Plasticizer 229

4.5 Synthesis of Type 0M Poly(ethylene oxide) Triazole Plasticizer 235

4.6 DSC Analysis: 4th Generation PEO Triazole-Plasticizers 240

4.7 Plasticizer Efficiencies: 4th Generation PEO Triazole-Plasticizers Versus DEHP-PVC 244

4.8 Cumulative Thermal Analysis and Plasticizer Efficiencies: Triazole-Based Internally Plasticized PVC Versus DEHP-PVC 248

4.9 Thermogravimetric Analysis: PEO-Triazole Internal Plasticizers 256

4.10 Plasticizer Migration: *n*-Hexane Extraction of Triazole-Based Internally Plasticized PVC Versus DEHP-PVC 259

4.11 Conclusion 262

4.12 References 263

5 Plasticizing Triazole Monomers For Copolymerization With Vinyl Chloride 265

5.1 Synthesis of Vinyl Acetate Triazole Phthalate Mimics 265

5.2 Polymerization Experiments of Vinyl Acetate Triazole-Phthalate Mimics 269

5.3 Synthesis of Acrylate Hexyl Tethered Triazole Phthalate Mimics 275

5.4 Conclusion 278

5.5 References 280

6 Experimental Section 281

6.1 General Materials and Methods 281

6.2 Instrumentation 282

6.3 Plasticizer Migration Studies 283

6.4 Warning on Organic Azides 284

6.5 Chapter 2 Experimental Section 284

6.6 Chapter 3 Experimental Section 305

6.7 Chapter 4 Experimental Section 322

6.8 Chapter 5 Experimental Section 353

6.9 References 359

Appendix 360

Bibliography 725

List of Figures, Schemes, and Tables

Scheme 1.1 Vinyl Chloride Monomer Polymerized To Poly(vinyl chloride) 1

Figure 1.1 Di-(2-Ethylhexyl) Phthalate (DEHP) 3

Scheme 1.2 Direct and Oxychlorination Methods of Ethylene to Obtain VCM 4

Scheme 1.3 Head-to-Tail and Head-to-Head Addition of VCM to the Propagating Chain..... 5

Figure 1.2 Tacticity Present in PVC 9

Figure 1.3 Defects Present in PVC 11

Figure 1.4 Graphical representation of the phase transition between liquid to glass 17

Figure 1.5 Specific Temperature-Volume Curves for Polystyrene 19

Figure 1.6 Top: T_g values of PS vs molecular weight (M_n), Bottom: T_g values of PS vs M^{-1} 19

Figure 1.7 Log(η_T/η_{217}) vs M at 110, 140 and 160 °C for PS 20

Table 1.1 Viscosities and Viscosity-Temperature Coefficients (E_T) of Polystyrene 21

Table 1.2 Flory-Huggins Interaction Parameter Values for Crosslinked PVC and Plasticizer 28

Table 1.3 Flory-Huggins Interaction Parameter Values *via* Anagnostopoulos' Micromethod 28

Table 1.4 Bigg's X Values of PVC-Plasticizer (Improved Hot-Stage Microscope) 29

Table 1.5 Tomaselli's PVC-Plasticizer Flory-Huggins Interaction Values 29

Table 1.6 Flory-Huggins Interaction Values of PVC-Plasticizer Utilizing Automatic Photodiode Microtechnique 30

Table 1.7 Compiled Flory-Huggins Interaction Parameter Values of PVC-Plasticizers 30

Figure 1.8 DEHP versus DNBP Structure 31

Figure 1.9 Generalized Phthalic Acid Ester and Di-*iso*nonyl Phthalate (DINP) 32

Table 1.8 Risk Assessment of Selected Phthalates 35

Scheme 1.4 DEHP Metabolic Products 38

Figure 1.10 PVC Bearing Thiophenol 51

Figure 1.11 Structures of Michel's PVC Thiolate Derivatives of 2-Ethylhexyl Esters 51

Table 1.9 Michel's PVC Thiosalicylate and Thioglycolate Thermal Data 52

Scheme 1.5 Reinecke's Modification Reaction of PVC with Halogenated Thiolates 53

Scheme 1.6 Synthesis of Mercapto-Phthalate Derivatives 54

Figure 1.12 Reinecke's Mercapto-Phthalate Derivatives 54

Scheme 1.7 PVC S_N2 by Mercapto-Phthalate Derivatives 55

Scheme 1.8 Acid Chloride Mediated Synthesis of Thiophenol Based Plasticizer 56

Scheme 1.9 Isocyanate Mediated Synthesis of Thiophenol Based Plasticizer 56

Scheme 1.10 Chlorosulfonyl Mediated Synthesis of Thiophenol Based Plasticizer 56

Scheme 1.11 S_N2 by Aliphatic Thiolate Derivatives on PVC 57

Table 1.10 Reinecke's Aliphatic Thiolphenol PVC Results 58

Scheme 1.12 Preparation of TCTA-Based PVC Plasticizers 59

Scheme 1.13 Reinecke's Attachment of Thiolate Triazine to PVC 59

Figure 1.13 Functional Groups Utilized in TCTA-PVC Investigation 60

Table 1.11 Reinecke's TCTA-PVC Plasticizer Results 60

Figure 1.14 PVC-TCTA JEFFAMINE™ Structures 62

Table 1.12 Reinecke's JEFFAMINE™ PVC-TCTA Plasticizer Results 63

Table 1.13 Non-Covalent DEHP-PVC Standard Mixture Data 64

Figure 1.15 PVC-TCTA Jeff600 Comparison 65

Figure 1.16 PVC-TCTA Jeff1000 Comparison 65

Figure 1.17 PVC-TCTA Jeff2070 Comparison 65

Scheme 1.15 Preparation of Tung Oil-Derived Internally Plasticized PVC 67

Table 1.14 Tung Oil-Derived Internally Plasticized PVC Data 68

Scheme 1.16 Zhou's Cardanol PVC Synthesis 70

Table 1.15 Zhou's T_g Data for PVC and PVC-Cardanol 70

Scheme 1.17 Yang's Cardanol Alkyne Synthesis 71

Scheme 1.18 Yang's PVC-Azide and Cardanol Alkyne Cu-Mediated Cycloaddition 71

Table 1.16 Yang's T_g Data for Standards and PVC-Triazole-Cardanol 72

Scheme 1.19 Zhou's Triethyl Citrate Internally Plasticized PVC Synthesis 73

Table 1.17 Zhou's Thermal Data for PVC-Triazole-Citrate Study 74

Scheme 1.20 Kwak's Hyperbranched Polyglycerol (HPG-C6) Alkyne Synthesis 76

Scheme 1.21 Kwak's PVC-*g*-HPG-C6 Synthesis 76

Table 1.18 PVC-*g*-HPG-C6 GPC and DSC Results 76

Figure 1.18 PVC-*g*-HPG-C6 T_g versus Mol% 77

Scheme 1.22 Poly(ε-caprolactone) Triazole Functionalized PVC Synthesis 79

Table 1.19 Poly(ε-caprolactone) Triazole Functionalized PVC Data 79

Scheme 1.23: Esterification and Copper-Free Azide-Alkyne Cycloaddition to Yield Phthalate Mimics 80

Figure 1.19: Structural Comparison of DEHP and 2-Ethylhexyl Triazole Phthalate Mimic 81

Table 1.20: Thermal Azide-Alkyne Cycloaddition Optimization Reaction Conditions 81

Scheme 1.24: Small Molecule Model Azides and PVC-N_3 Synthesis 82

Scheme 1.25: Fischer Esterification Synthesis of Dialkyl Acetylenedicarboxylates 82

Scheme 1.26: Thermal Azide-Alkyne Cycloaddition Optimization 82

Scheme 1.27: Thermal Huisgen 1,3-Dipolar Cycloaddition Reactions 83

Scheme 1.28: Cu-Mediated and Thermal AAC PVC-Triazole-Phthalate Syntheses 85

Scheme 1.29: Braslau's Three Propargyl Alkyne Tethered Phthalate Synthetic Pathways 86

Scheme 1.30: Braslau's Propiolic Alkyne Phthalate Synthesis 87

Scheme 1.31: Cu-Mediated and Thermal AAC Model Reactions 88

Table 1.21: Braslau's Thermal Data for PVC-Triazole-DEHP Derivatives 88

Scheme 2.1 Azide-Alkyne Thermal Dipolar Cycloaddition Furnishing a PVC-Triazole Phthalate Mimic 103

Scheme 2.2 1,3-Dipolar Cycloaddition Mechanism of a Dipole and Alkyne 104

Table 2.1 Examples of 1,3-Dipoles 104

Scheme 2.3 Wittig and Krebs' Phenyl Azide and Cyclooctyne Cycloaddition 105

Figure 2.1 Second-Order Rate Constants of Reactions Between Alkyl Azide and Bertozzi's Cyclooctynes 106

Scheme 2.4 Michael's Azide-Alkyne Cycloaddition 107

Scheme 2.5 Huisgen's Diazoalkane Reaction with Electron-Deficient Alkynes 108

Scheme 2.6 Onset Temperatures for Brook's Azide-Alkyne Cycloadditions with Electron-Deficient Alkynes 108

Scheme 2.7 Synthesis of PVC-Azide **2.1** 109

Figure 2.2 FTIR Spectrum of 15% PVC-Azide **2.1** 110

Figure 2.3 ^{1}H-NMR Spectrum of 15% PVC-Azide **2.1** in $CDCl_3$ 111

Figure 2.4 ^{13}C-NMR Spectrum of 15% PVC-Azide **2.1** in $CDCl_3$ 111

Scheme 2.8 Fischer Esterification of Acetylenedicarboxylic Acid to Form Electron-Deficient Alkynes **2.2 - 2.3** 112

Scheme 2.9 Azide-Alkyne Cycloadditions of PVC-Azide **2.1** and Electron-Deficient Alkynes DMAD, **2.2 - 2.3** 114

Figure 2.5 FTIR Monitoring of Cycloaddition Between 15% PVC-Azide **2.1** and DEHAD **2.3** at 90 °C 115

Figure 2.6 ^{1}H-NMR Spectra of DEHAD (**2.3**) and 15% PVC-TRZ-DiEH (**2.6**) 116

Figure 2.7 ^{13}C-NMR Spectra of DEHAD (**2.3**) and 15% PVC-TRZ-DiEH (**2.6**) 118

Figure 2.8 DSC Second Heat Scan of 15% PVC-TRZ-DiEH 120

Figure 2.9 T_g Values of PVC and PVC-Azide 121

Table 2.2 DSC Data of PVC Standards and 1st Generation PVC Triazole Phthalate Mimics 121

Figure 2.10 DSC Data for 1st Generation Triazole Phthalate Mimics 121

Table 2.3 Changes in Glass Transition Temperatures (ΔT_g PVC) of 1st Generation Triazole Phthalate Mimics With Respect To Unmodified PVC 122

Figure 2.11 Difference in Glass Transition Temperatures of 1st Generation Triazole Phthalate Mimics with Respect to Unmodified PVC 122

Figure 2.12 Illustration of a Single Hexyl Tether Between PVC and Triazole Phthalate Mimic 124

Scheme 2.10 Synthesis of 6-Azidohexan-1-ol **2.7** Hexyl Tether Precursor 125

Scheme 2.11 Syntheses of Hexyl Tether Alkyl Triazolo-Alcohol Precursors 126

Figure 2.13 ^{1}H-NMR Comparing 6-Azidohexan-1-ol (**2.7**) and TRZ-DiMe Hexanol (**2.8**) 127

Figure 2.14 ^{13}C-NMR Comparing 6-Azidohexan-1-ol (**2.7**) and TRZ-DiMe Hexanol (**2.8**)... 128

Scheme 2.12 Fischer Esterification of Propiolic Acid and Triazolo-Alcohols **2.8 - 2.10** to Form Propiolates **2.11 - 2.13** Containing Hexyl Tethered Alkyl Triazole Phthalate Mimics 130

Figure 2.15 ^{1}H-NMR and ^{13}C-NMR of TRZ-DiMe Hexyl Propiolate **2.11** 132

Scheme 2.13 Thermal Azide-Alkyne Cycloaddition of PVC-Azide **2.1** and Propiolate Hexyl Tethered Triazole Phthalate Mimics **2.11 - 2.13** 133

Figure 2.16 FTIR Comparison of TRZ-DiMe Hexyl Propiolate **2.11** and 15% PVC-Azide **2.1** 134

Figure 2.17 FTIR Reaction Monitoring Between 15% PVC-Azide **2.1** and **2.11** 135

Figure 2.18 ^{1}H-NMR Spectra Comparing TRZ-DiMe Hexyl Propiolate (**2.11**) and 15% PVC-TRZ-Hexyl-TRZ-DiMe (**2.14**) 137

Figure 2.19 Primary Triazole Regioisomers Formed By 2nd Generation Hexyl Tethered Triazole-Based Phthalate Mimics 138

Figure 2.20 ^{13}C-NMR Spectra Comparing TRZ-DiMe Hexyl Propiolate (**2.11**) and 15% PVC-TRZ-Hexyl-TRZ-DiMe (**2.14**) 140

Table 2.4 DSC Data of PVC Standards and 2nd Generation Single Hexyl Tethered Triazole Phthalate Mimics 141

Figure 2.21 DSC Data of 2nd Generation Single Hexyl Tethered Triazole Phthalate Mimics 142

Table 2.5 Changes in Glass Transition Temperature (ΔT_g PVC) of 2nd Generation Single Hexyl Tethered Triazole Phthalate Mimics with Respect to Unmodified PVC 142

Figure 2.22 Difference in Glass Transition Temperature (ΔT_g PVC) of 2nd Generation Single Hexyl Tethered Triazole Phthalate Mimics with Respect to Unmodified PVC 143

Figure 2.23 DSC Data Comparing 1st and 2nd Generation Triazole Phthalate Mimics 144

Table 2.6 DSC Data of PVC Standards with 1st and 2nd Generation Triazole Phthalate Mimics 145

Table 2.7 ΔT_g PVC of 1st and 2nd Generation Triazole Phthalate Mimics 146

Table 2.8 ΔT_g PVC and ΔT_g Between 1st and 2nd Generation Systems Grouped By Ester Alkyl Chain 146

Figure 2.24 Difference in Glass Transition Temperature (ΔT_g PVC) of 1st and 2nd Generation Systems with Respect to Unmodified PVC 147

Figure 2.25 Structural Comparison of 1st and 2nd Generation Triazole Phthalate Mimics ... 147

Figure 2.26 Structural Breakdown to Calculate Weight Percent Plasticizer 148

Table 2.9 Elemental Analysis of PVC-Azide Samples..... 149

Table 2.10 Glass Transition Temperatures of DEHP-PVC Standard Mixtures with Respect to Weight Percent DEHP Plasticizer 152

Table 2.11 Glass Transition Temperatures and Weight Percentages of 1st and 2nd Generation Triazole-Based Phthalate Mimics in Modified PVC..... 153

Figure 2.27 Overlay of T_g Values Versus Weight Percent of Plasticizer with DEHP-PVC Standard Mixtures and Generations 1-2 Triazole Phthalate Mimics..... 153

Table 2.12 Plasticization Efficiencies of 5 Mol % 1st and 2nd Generation Triazole Internally Plasticized PVC Ranked by Descending EΔT_g Values..... 158

Table 2.13 Plasticization Efficiencies of 15 Mol % 1st and 2nd Generation Triazole Internally Plasticized PVC Ranked by Descending EΔT_g Values..... 158

Figure 2.28 Efficiency Values ($E\Delta T_g$) of 1st and 2nd Generation Internally Plasticized PVC 159

Figure 2.29 TGA (Green) and DTG (Blue) of Unmodified PVC (Air) 162

Table 2.14 Degradation Temperatures of PVC and PVC-Azide (5 and 15 Mol % Azide)..... 162

Table 2.15 TGA/DTG Degradation Temperatures of Unmodified PVC, PVC-Azide and 1st Generation Internally Plasticized PVC 163

Table 2.16 TGA/DTG Degradation Temperatures of Unmodified PVC, PVC-Azide and 2nd Generation Internally Plasticized PVC 165

Figure 3.1 Structures of 1st, 2nd, and 3rd Generation Triazole Phthalate Mimics..... 171

Scheme 3.1 Attempted Syntheses to Obtain Double Hexyl Tethered Alkynes..... 172

Scheme 3.2 Garcia and Miranda's DCC Coupling of ADA and 4-Methoyphenol 173

Scheme 3.3 Volonterio's Carbodiimide Reaction with ADA Monoesters 174

Scheme 3.4 Volonterio's DFT Mechanism Pathways 175

Scheme 3.5 Kunishima's DMTMM Coupling Reaction Cycle..... 176

Scheme 3.6 Heyl and Fessner's DMTMM Coupling of ADA and Amines..... 177

Scheme 3.7 Kunishima's DMTMM Coupling of Carboxylic Acids and Amines in Alcohol Solvents..... 179

Table 3.1 Kunishima's DMTMM Coupling Data of Amines in Alcohol Solvents..... 179

Scheme 3.8 Ruggli's Attempt to Synthesize ADACl..... 180

Scheme 3.9 Diels and Thiele's Putative Synthesis of ADACl 181

Scheme 3.10 Krueger and McDonald's Attempt to Synthesize ADACl..... 181

Scheme 3.11 Maier and Jung's Synthesis of ADACl 182

Scheme 3.12 Synthesis of Double Hexyl Tethered Acetylenedicarboxylate Esters 183

Figure 3.2 ^{13}C-NMR Comparison of Acetylenedicarboxylic Acid and Dibromofumaric Acid (**3.1**) 185

Figure 3.3 ^{1}H-NMR Comparison of TRZ-DiMe Hexanol (**2.8**) and Bis(TRZ-DiMe Hexyl) Dibromofumarate (**3.3**) 187

Figure 3.4 ^{13}C-NMR Comparison of TRZ-DiMe Hexanol (**2.8**) and Bis(TRZ-DiMe Hexyl) Dibromofumarate (**3.3**) 189

Figure 3.5 ^{1}H-NMR and ^{13}C-NMR of Bis(TRZ-DiMe Hexyl) Acetylenedicarboxylate **3.6**..... 190

Figure 3.6 Magnetic Anisotropic Shielding Cones 191

Scheme 3.13 Thermal Azide-Alkyne Cycloaddition of PVC-Azide **2.1** and Double Hexyl Tethered Alkyl Triazole Phthalate Mimics **3.6 - 3.8**..... 192

Figure 3.7 FTIR Monitoring of Cycloaddition Between 15% PVC-Azide **2.1** and Bis(TRZ-DiMe Hexyl) Acetylenedicarboxylate **3.6**..... 193

Figure 3.8 ^{1}H-NMR Spectra of Bis(TRZ-DiMe Hexyl) Acetylenedicarboxylate (**3.6**) and 15% PVC-TRZ-DiHexyl-TRZ-DiMe (**3.9**)..... 194

Figure 3.9 ^{13}C-NMR Spectra of Bis(TRZ-DiMe Hexyl) Acetylenedicarboxylate (**3.6**) and 15% PVC-TRZ-DiHexyl-TRZ-DiMe (**3.9**)..... 195

Table 3.2 DSC Data of PVC Standards, 5 and 15 Mol % Double Hexyl Tethered Alkyl Triazole Phthalate Mimics..... 196

Figure 3.10 DSC Data of 3rd Generation Double Hexyl Tethered Triazole Phthalate Mimics 197

Table 3.3 DSC Data of PVC Standards and Generations 1-3 Triazole-Plasticizers 197

Figure 3.11 DSC Data Comparing Generations 1-3 Triazole Phthalate Mimics..... 198

Figure 3.12 Overlay of T_g Values Versus Weight Percent Plasticizer of DEHP-PVC and Generations 1-3 Alkyl Triazole Phthalate Mimics 199

Table 3.4 Glass Transition Temperatures and Weight Percentages of Generations 1-3 Alkyl Triazole Phthalate Mimics 199

Table 3.5 $E\Delta T_g$ Values of 5 Mol % 3rd Generation Internally Plasticized PVC 201

Table 3.6 $E\Delta T_g$ Values of 15 Mol % 3rd Generation Internally Plasticized PVC 201

Figure 3.13 Efficiency Values ($E\Delta T_g$) of 3rd Generation Internally Plasticized PVC 201

Table 3.7 Plasticization Efficiencies of 5 Mol % Generations 1-3Internally Plasticized PVC Ranked By Descending $E\Delta T_g$ Values 202

Figure 3.14 Efficiency Values ($E\Delta T_g$) of Generations 1-3 Internally Plasticized PVC..... 203

Table 3.8 Plasticization Efficiencies of 15 Mol % Generations 1-3 Internally Plasticized PVC Ranked By Descending $E\Delta T_g$ Values 203

Table 3.9 TGA/DTG Degradation Temperatures of Unmodified PVC, PVC-Azide and 3rd Generation Internally Plasticized PVC 206

Scheme 4.1 Kwak's Alkyl-HPG External PVC Plasticizer 213

Figure 4.1 Kwak's Polyglycerol-Based Internal Plasticizer: PVC-*g*-HPG-C6..... 214

Table 4.1 DSC and GPC Data: Kwak's PVC-*g*-HPG-C6..... 214

Figure 4.2 Reinecke's PVC Internal Plasticizer: TCTA Incorporating JEFFAMINEs™ 215

Figure 4.3 "Type" Designations of PVC Triazole-Plasticizers..... 216

Scheme 4.2 Fischer Esterification of PEO and Acetylenedicarboxylic Acid to Form Type 0D Internally Plasticized PVC 217

Figure 4.4 FTIR Monitoring of Reaction Between 5% PVC-Azide **2.1** and Di(PEO_{164}Me) Acetylenedicarboxylate **4.1** at 90 °C 218

Figure 4.5 Blue Fluorescence of Di(PEO_{164}Me) Acetylenedicarboxylate **4.1** Under Irradiation with a Short Wave UV Lamp 219

Figure 4.6 ^{1}H-NMR of Di($PEO_{164}Me$) Acetylenedicarboxylate (**4.1**) and Type 0D 15% PVC-TRZ-Di$PEO_{164}Me$ (**4.4**) 220

Figure 4.7 ^{13}C-NMR of Di($PEO_{164}Me$) Acetylenedicarboxylate (**4.1**) and Type 0D 15% PVC-TRZ-Di$PEO_{164}Me$ (**4.4**) 222

Scheme 4.3 Synthesis of PEO Triazolo-Alcohols 224

Scheme 4.4 Synthesis of Type 1 PEO Triazole-Plasticizers Attached to PVC 224

Figure 4.8 ^{1}H-NMR of TRZ-Di$PEO_{164}Me$ Hexyl Propiolate (**4.9**) and Type 1 5% PVC-TRZ-Hexyl-Di$PEO_{164}Me$ (**4.11**) 226

Figure 4.9 ^{13}C-NMR of TRZ-Di$PEO_{164}Me$ Hexyl Propiolate (**4.9** @ 125 MHz) and Type 1 15% PVC-TRZ-Hexyl-TRZ-Di$PEO_{164}Me$ (**4.11** @ 200 MHz) 228

Scheme 4.5 Synthesis of Type 2 PEO Triazole-Plasticizer Attached to PVC 230

Figure 4.10 ^{1}H-NMR of Bis(Hexyl-TRZ-Di$PEO_{164}Me$) Acetylenedicarboxylate (**4.14**) and Type 2 15% PVC-TRZ-DiHexyl-TRZ-Di$PEO_{164}Me$ (**4.15**) 232

Figure 4.11 ^{13}C-NMR of Bis(Hexyl-TRZ-Di$PEO_{164}Me$) Acetylenedicarboxylate (**4.14** @ 125 MHz) and Type 2 15% PVC-TRZ-DiHexyl-TRZ-Di$PEO_{164}Me$ (**4.15** @ 200 MHz) 234

Scheme 4.6 Synthesis of Type 0M PEO Triazole-Plasticizer Attached to PVC 236

Figure 4.12 ^{1}H-NMR Spectra of $PEO_{1000}Me$ Propiolate (**4.16**) and Type 0M 15% PVC-TRZ-$PEO_{1000}Me$ (**4.18**) 237

Figure 4.13 ^{13}C-NMR Spectra of $PEO_{1000}Me$ Propiolate (**4.16** @ 125 MHz) and Type 0M 15% PVC-TRZ-$PEO_{1000}Me$ (**4.18** @ 200 MHz) 239

Table 4.1 Glass Transition Temperatures and Weight Percentages of 4th Generation PEO Triazole Plasticizers 241

Figure 4.14 DSC Data for 4th Generation PEO Triazole Plasticizers 241

Figure 4.15 Overlay of T_g Values *vs.* Weight Percent of Plasticizer with DEHP-PVC Standard Mixtures and 4th Generation Triazole Plasticizers 242

Figure 4.16 Glass Transition Temperatures Versus Weight Percent Plasticizer of Type 0M PEO PVC and DEHP-PVC Standards 243

Table 4.3 Plasticization Efficiencies of 5 Mol % 4th Generation PEO Internally Plasticized PVC Ranked By Descending EΔT_g Values 244

Table 4.4 Plasticization Efficiencies of 15 Mol % 4th Generation PEO Internally Plasticized PVC Ranked By Descending EΔT_g Values 244

Figure 4.17 Efficiency Values (EΔT_g) of 4th Generation Internally Plasticized PVC 245

Figure 4.18 DSC Data for All Triazole Internally Plasticized PVC 248

Figure 4.19 T_g Values Versus Weight Percent Plasticizer with DEHP-PVC Standard Mixtures and All Triazole Internally Plasticized PVC 249

Table 4.5 Glass Transition Temperatures of All Triazole Internally Plasticized PVC Ordered By Ascending T_g Values 250

Table 4.6 Plasticization Efficiencies of All 5 Mol% Triazole Internally Plasticized PVC Ranked By Descending EΔT_g Values 251

Table 4.7 Plasticization Efficiencies of All 15 Mol% Triazole Internally Plasticized PVC Ranked By Descending EΔT_g Values 251

Figure 4.20 Efficiency Values of All Triazole Internally Plasticized PVC 252

Table 4.8 TGA/DTG Degradation Temperatures of 4th Generation PEO-Functionalized Internally Plasticized PVC 257

Table 4.9 Plasticizer Migration Data (*n*-Hexane) of DEHP-PVC (60 Wt % DEHP) Versus 15% PVC-TRZ-PEO_{2000}Me, 15% PVC-TRZ-PEO_{1000}Me and 15% PVC-TRZ-DiPEO_{550}Me 261

Figure 4.21 Degree of Plasticizer Migration (*n*-Hexane). 261

Scheme 5.1 Synthesis of Vinyl Acetate Containing Pendant Triazole-Phthalate Mimics 266

Figure 5.1 ^{1}H-NMR and ^{13}C-NMR Spectra of VAc-TRZ-DiEH **5.4** 267

Figure 5.2 Structures of Azobisisobutyronitrile (AIBN) and Trigonox 23..... 269

Scheme 5.2 Copolymerization of Vinyl Chloride Monomer (VCM) and Vinyl Acetate 269

Table 5.1 (Co)Polymerization Results of Vinyl Chloride and Vinyl Acetate at 50 °C 270

Scheme 5.3 Copolymerization of Vinyl Chloride and Vinyl Acetates Containing Pendant Triazole-Phthalate Mimics..... 270

Table 5.2 (Co)Polymerization Results of Vinyl Chloride and Vinyl Acetates Containing Pendant Triazole-Phthalate Mimics 271

Figure 5.3 ^{1}H-NMR Spectra of Exp 2: VAc-TRZ-DiEH **5.4** Homopolymerizations as a Function of Temperature After 24 Hours..... 271

Figure 5.4 ^{1}H-NMR Spectra of VCM and VAc-TRZ-DiEH **5.4** Copolymerizations as a Function of Solvent (Top DMSO, Middle: DMF, Bottom: THF)..... 272

Figure 5.5 ^{1}H-NMR of Exp 6: VCM and VAc-TRZ-DiBu **5.3** Copolymerization (THF-d_8)..... 274

Figure 5.6 ^{1}H-NMR of Exp 7: VCM and VAc-TRZ-DiBu **5.3** Copolymerization at 70 °C Using DMSO ([VAc-TRZ-DiBu]/[VCM] = 90/10) 274

Scheme 5.5 Synthesis of Acrylate Containing Hexyl Tethered 2-Ethylhexyl Triazole Phthalate Mimic **5.6** 275

Figure 5.7 ^{1}H-NMR and ^{13}C-NMR Spectra of Acrylate-Hexyl-TRZ-DiEH **5.6** 277

Scheme 5.6 Copolymerization of Vinyl Chloride and Acrylate **5.6** Containing Hexyl Tethered 2-Ethylhexyl Triazole Phthalate Mimic 278

Scheme 5.7 Copolymerization of VCM with PEO Acrylate and PEO Methacrylate..... 278

Abstract

NON-MIGRATORY INTERNAL PLASTICIZATION OF POLY(VINYL CHLORIDE) VIA PENDANT TRIAZOLES BEARING ALKYL OR POLYETHER ESTERS

Chad Masaharu Higa

Poly(vinyl chloride) (PVC) is one of the most utilized thermoplastics on Earth. However, PVC by itself is brittle and not readily processable. This material reached the success of its worldwide demand because of phthalates, a cost-effective additive (emollient) that imparts flexibility and resistivity towards weathering, temperature extremes and electrical conductivity. The use of phthalates as plastic emollients is widespread, representing approximately three quarters of all plasticizers globally, with applications ranging from industrial to consumer products. The pervasive utilization of low molecular weight blended phthalates as emollients inevitably leads to leaching, contamination and exposure. Phthalates and their metabolites have displayed negative effects on various organs and act as potent endocrine disrupting chemicals that cause deleterious pre- and postnatal developmental effects, notably in males. Bans of phthalates by the European Union and the United States in children's articles have spurred the development of less toxic PVC plasticizer alternatives.

Branched and linear non-migratory internal plasticizers attached to PVC by a pendant triazole linkage were synthesized. Copper-free azide-alkyne thermal cycloaddition was employed to covalently bind triazole-based phthalate mimics to poly(vinyl chloride) (PVC). To systematically investigate the effect of plasticizer structure on glass transition temperature, several architectural motifs were explored. Free volume theory was considered when designing many of these internal plasticizers: hexyl-tethers were utilized to generate additional space between the triazole-phthalate mimic and the polymer backbone. Miscibility of these triazole-plasticizers in PVC is important: variation of the ester moieties on the triazole

possessing alkyl and/or poly(ethylene oxide) (PEO) chains produced a wide range of glass transition temperatures (T_g): from anti-plasticizing 96 °C, to highly efficient plasticized materials exhibiting T_g values as low as -42 °C.

Triazole methyl esters directly appended to PVC displays an inherent anti-plasticization effect originating from the aromatic ring, which diminishes with increasing molecular weight and branching of the alkyl ester chains. Introduction of a flexible hexyl tether to the secondary triazole group acts as additional molecular weight and branching, further lowering T_g values. Attachment of two hexyl tethered secondary triazoles follows this trend by enforcing another branch point and increasing molecular weight. Utilization of PEO esters in all architectural types significantly enhances T_g depressions, with longer PEO chains exhibiting remarkable results. Single PEO triazole esters readily prepared from propiolic esters using low-cost, commercially available materials combine excellent plasticization with straightforward synthesis, making these non-migratory internal plasticizers extremely attractive for industrial applications.

An alternative strategy to post-polymerization direct modification of PVC to obtain internally plasticized materials involves the copolymerization of vinyl chloride monomer (VCM) with a monomer functionalized with a triazole-phthalate mimic. Electron-rich vinyl acetate monomers with an appended triazole-plasticizer were synthesized for this purpose. Copolymerizations with the vinyl acetate triazole monomers and VCM were largely unsuccessful. It was envisaged that an acrylate derivative should remedy the low reactivity of these vinyl acetate monomers. An acrylate incorporating a hexyl-tethered triazole-phthalate mimic served two purposes: 1) generate space between the triazole and polymerizing vinyl group to prevent monomer deactivation and, 2) enhance the plasticization efficiency of the triazole.

Dedication

This Dissertation is dedicated to my parents, Zachary and Elayne Higa.

I owe everything to you: For the endless amount of support, understanding, and love, you are the constant in my life. Through the prosperous times and through the arduous times, you have been there. As my shadow surely follows me on the sunniest of days, you are always with me in my heart and soul. You are the source of inspiration that gives life meaning. Without you, this would have not been possible.

Acknowledgements

First and foremost, I would like to thank my parents, Zachary and Elayne Higa for supporting me throughout this arduous endeavor. The journey was long, but the rewards are great. Despite having a doctorate in chemistry, I still have a lot to learn from you. I strive to attain your level of compassion, understanding, and patience. I would like to thank my dissertation reading committee for the invaluable advice and wisdom during the past few years in graduate school. Thank you, Pradip Mascharak for serving as my committee chair for all these years. You have taught me to creatively problem solve and unintentionally gave me insight to seek solutions beyond my field of expertise. We all share somewhat myopic views in many ways: sometimes the answers are just ahead, but we cannot see the big picture. Thank you, Jevgenij Raskatov for serving as my third committee member, and Stephen Branz for serving as the outside member on my qualifying exam. I must extend my gratitude to Rudy Wojtecki and Andy Tek at the IBM Almaden Research Center for thermally characterizing all of my samples. Without your assistance, this dissertation would not be possible. I look forward to many years of fascinating discovery and science with you. Thank you Jorge Coelho and Armenio Serra at the University of Coimbra, Portugal for polymerizing my monomers. A special thanks to Jack (Hsiau-Wei) Lee for always helping me with NMR. I have learned a great deal from you: you have taught me to fill the NMRs with liquid nitrogen, maintenance and troubleshooting of these awesome instruments. We have developed a friendship that I will treasure for the rest of my life.

Thank you to the members of the Braslau Lab during my graduate school experience. To Aruna Earla, it was always nice to interact with you. I gained the basic laboratory skills required to pursue my research from you. A planted seed starts off small, but with adequate nurturing, can become a tree. Thank you for teaching me all those years ago: your help will never be forgotten. A very special thank you to Longbo Li: you have come a long way since

you joined the lab. You became one of the best friends I have made in graduate school. I will miss the dinners after all those strenuous days after lab. I will miss those good old days in lab, those moments of happiness, those moments of struggle, trial, and tribulation, those moments of excessive difficulty, all spent with you. When times got difficult, you were always there to help. A person such as you is rare in today's society: never lose your charm and happy disposition. Although graduate school seems like an eternal struggle, there is an end. That end is you earning a doctorate, I can sense it. Do not let the pervasive negativity that surrounds you take away your happiness. Your positivity is refreshing and is one of your best attributes. With that said, I eagerly await your visit to Hilo. To Wiley Schultz-Simonton, thanks for being an excellent lab mate. Your culinary insights are enlightening and the discussions we had throughout the years on random topics have always been fun. I will forever remember struggling together in lab. I wish you the best of luck in completing your degree. Thank you Jennifer Petraitis for the memories: we entered the lab together simultaneously, and shared many of the early tribulations of graduate school together. Our conversations on food, pop culture, and fashion were always enjoyable. To Wendell Scott, my former student and undergraduate researcher, you have overcome so much and persevered as a graduate student at UCLA. I commend your inner-fortitude, your work ethic, and your ability to see the big picture. Thank you for being a part of my journey. I often reminisce of those evenings at Mission Street BBQ with you, devouring brisket, pulled pork, and occasionally, the Mission Sandwich. It warms my heart to see that you have truly moved on to bigger and better things: all the best to you.

A very special thanks to my dear friend Mauricio Rojas-Andrade: we are finally here. After all those difficult years, we made it. From day one, you have been kind to me, regardless of not being a student in my lab. When I moved to Santa Cruz in 2012, I truly felt alone, as my family and friends back in Hawaii were 2300 miles across the ocean. You helped me transition to California, when I knew no one. You made a foreign place feel like

home. It is so easy for a person to ignore the strife of others, as often is the case, but you were there. Maybe it's being a country kid from South Lake Tahoe that makes you so personable. More likely than that, it is just because you are a good person, with a good soul. You are one of the best friends I have made here in California. You may or may not know, but I have learned an important life lesson from you. You showed me how to live in the moment, as I am often agonizing about the future. While it is true that the future is determined by the actions we take in the present, it is the moments we live in the present that should be reveled and enjoyed. After all, we cannot change the past, nor can we predict the future, so why not enjoy the present? Thank you for opening my eyes to this point of view and philosophy. Thank you to the students in Bakthan Singaram's Lab: Christopher Bailey, Christopher Murphy, Rachel Snelling, Angel Resendez, and Gabriella Amberchan. Your advice at the beginning of graduate school was invaluable. Your assistance in obtaining chemicals that I required for my research is immensely appreciated. To the students in Pradip Mascharak's Lab: Jorge Jimenez and Miguel Pinto, thank you for the help in making KBr pellets for FTIR. More importantly, thank you for being good friends. Much appreciation to past and present administrators Janet Jones, Karen Meece, Yat Li, and Ilan Benjamin for assuring that the correct paperwork and requirements were clear and seen to in a timely fashion. Thank you, Caitlin Binder for being a motivational and positive educator. The time I have spent with you teaching has been insightful. I appreciate you giving me the opportunity to present organic chemistry lectures. I have learned much from you, and strive to as energetic as you.

To my friends from Hawaii, thank you for always being a connection to the place I still call home. We can be thousands of miles apart, but you made time to check in to see how I was doing. As they say, "you can take the boy from the island, but not the island from the boy." Although it has been years, things never change. That is the definition of true friends: we just pick up where we left off. You have kept me planted, kept me humble, during these tumultuous years in the mainland. I look forward to the years ahead, and all that it brings.

1 Introduction: Internal Plasticization of Poly(vinyl chloride)

1.1 Poly(vinyl chloride): History and Discovery

Poly(vinyl chloride) (PVC) is a synthetic polymer made from the polymerization of vinyl chloride monomer (VCM). Among the thermoplastics, PVC is ranked second in terms of production only to polyolefins such as poly(ethylene) and poly(propylene).[1] PVC is a thermoplastic, which is defined as a synthetic resin that becomes malleable, ductile, or moldable above a specific temperature, and subsequently solidifies after cooling.[2] Thermoplastics may be reheated and reformed, while a thermoset cannot be recycled. The origins of PVC date back to 1835, with the discovery of vinyl chloride monomer by Liebig and Regnault.[3] Historically, the newly discovered vinyl chloride gas was left in a sealed container exposed to sunlight, thereafter leaving a brittle white solid deposit within the confines of the flask; however this anecdote is considered to be apocryphal. In 1878, Eugen Baumann rediscovered PVC, when studying the effect of sunlight on vinyl chloride, which, once again, gave a white solid when exposed to the sun. In both instances, there were no recorded follow up studies on the brittle, white substance, as it was presumably difficult to manipulate. While investigating the addition of several chemicals to acetylene in 1913, Klatte rediscovered the light induced polymerization of VCM. Klatte also described the polymerization of VCM by oxygen-containing compounds such as peroxides and ozone, and is now credited as the inventor of the free-radical polymerization of VCM with peroxides.[3] Klatte discovered that it was also possible to process PVC under heat and pressure; this was the first description of PVC as a thermoplastic material. Nevertheless, PVC remained a challenging substance to manipulate due to its relatively low thermal stability in comparison with other polymeric substances of the time. Industrial applications of PVC remained esoteric until 1926, when

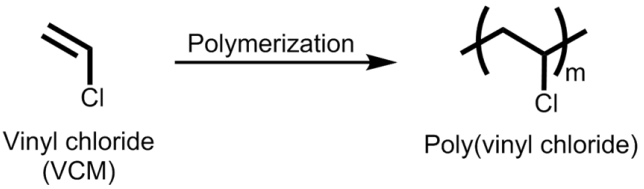

Scheme 1.1 Vinyl Chloride Monomer Polymerized To Poly(vinyl chloride)

Waldo Semon, a B.F. Goodrich employee in Akron, Ohio, discovered plasticized PVC when attempting to dehydrohalogenate high molecular weight PVC to obtain a polymer which could potentially bond rubber to metal.[4] This serendipitous discovery by Semon was an unexpected byproduct of his primary work, but nevertheless, led to the commercialization and globalization of PVC as a popular plastic material.[3]

1.2 Global Demand and General Applications of PVC

Global demand for PVC is substantial: in 2015, 18.3 percent of thermoplastics consumed was PVC, behind poly(ethylene) at 20.3 percent, and poly(propylene) at 26.8 percent.[5] Overall demand for PVC in relation to all plastic types accounted for 16 percent of total global plastics.[5] PVC in this statistical analysis was the overall second largest resin type consumed behind all combined types of polyolefins. In North America, PVC accounted for 15.3 percent of total combined sales, considering all plastic types in 2015.[6]

Applications of PVC are widespread and vast, ranging from consumer items to industrial materials. In 2014, the European Union utilized PVC for profiles (28%, profiles are specialty millwork that are applied in buildings to create a finished appearance for windows and doors), pipes and fittings (22%), rigid films (9%), miscellaneous rigids and bottles (7%), cables (7%), flex film and sheet (6%), flooring (6%), coated fabrics (4%), flex tubes and profiles (2%), rigid plates (2%), and other (8%).[7] In 2007, North America used PVC for siding, accessories and skirting (35%), windows, doors, fencing and decking (22%), film and sheets (16%), wire and cable (11%) and other extruded/molded products (16%).[8] Much of the consumption of PVC is by the construction industry, which utilizes the polymer for profiles, pipes, fittings, siding, skirting, flooring, doors, wiring, fencing, and decking. Other consumer goods include toys, automotive parts, and medical supplies.

PVC possesses the largest market share of any dedicated polymeric material in the medical field, comprising 40 percent of all polymeric medical items.[9] In medicine, PVC is the

first choice of polymeric material due to its transparency, strength, biocompatibility, and facility of sterilization *via* autoclave and gamma irradiation.[9] As it is cost effective, PVC products are ideal for single use medical devices, which greatly reduce the occurrence of contamination. Medical products that are composed of PVC include intravenous tubing, urine continence containers, catheters, inflatable stints, inhalation masks, pill packs, respiratory tubing, and blood bags.

There has been a rising concern in recent years about the utilization of PVC in medical equipment due to concerns over the major plasticizer in these products:[10] di-(2-ethylhexyl) phthalate (DEHP), also known as di-octyl phthalate (DOP) (**Figure 1.1**). While an excellent monomeric plasticizer for this application, the constant contact with biological fluids in medical devices results in the extraction of DEHP from the PVC material. The consequences of leaching DEHP from a blood bag to the patient, for example, can have long term medical ramifications.[11]

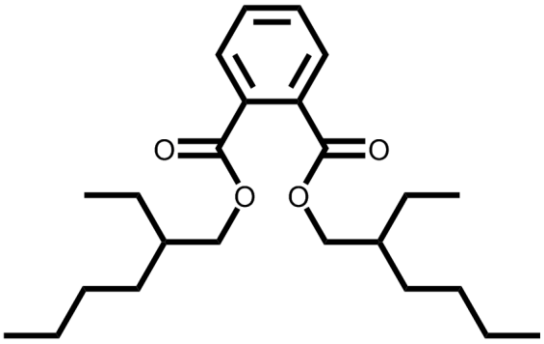

Figure 1.1 Di-(2-Ethylhexyl) Phthalate (DEHP)

With broad applications and high global demand, PVC has a large impact on humanity. The awareness of phthalate leaching presents a challenging, yet intriguing problem: how to replace phthalates in PVC with safe, non-leaching alternatives. Herein, the physical properties, synthesis, plasticization of PVC, along with the inherent health concerns of phthalates, and an overview of current research investigating internally plasticizing PVC will be discussed.

1.3 Synthesis and Physical Properties of PVC

Poly(vinyl chloride) in its pure, unmodified state is an odorless, brittle white solid. The precursor to PVC, vinyl chloride monomer (VCM) is a gas at room temperature and pressure, with a boiling point of -13.4 °C.[12] In industry, VCM is handled as a compressed toxic volatile liquid in all types of polymerization operations. VCM is produced predominantly by two industrial reactions: (1) the hydrochlorination of acetylene and (2) thermal cracking of ethylene dichloride (EDC) produced by direct chlorination or oxychlorination of ethylene. To clarify, under the direct chlorination method, ethylene, chlorine, and iron (III) chloride catalyst are charged into a reactor to form EDC. The oxychlorination method involves charging a reactor with ethylene, recycled hydrogen chloride (HCl) from the direct chlorination process, copper (II) chloride catalyst, and oxygen (or air) to obtain EDC. Subsequently, ethylene dichloride is thermally cracked to VCM (**Scheme 1.2**). Most of the VCM produced globally

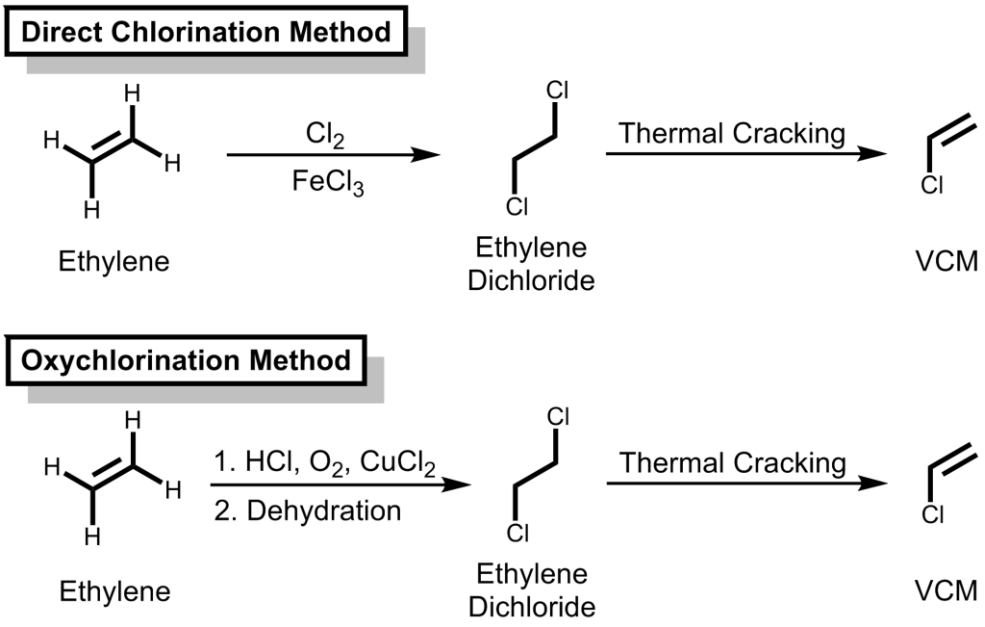

Scheme 1.2 Direct and Oxychlorination Methods of Ethylene to Obtain VCM

involves the direct chlorination and oxychlorination process. According to Alfrey-Price *Q-e* schemes,[13] VCM is classified as a non-conjugated weakly electron-withdrawing vinyl

monomer. Briefly, the *Q*-*e* scheme postulates that two reactivity ratios in a binary copolymerization can be expressed mathematically. Parameters *Q* and *e* are associated with resonance stability and polarity, respectively.[14] VCM possess *Q* and *e*-values of 0.44 and 0.22.[15] These values indicate that VCM has relatively low reactivity, while the resulting radical is highly reactive. Due to the high reactivity of the propagating radical, there is a tendency for chain transfer reactions to occur with other species during polymerization. Species suffering chain transfer can include VCM, initiator, and polymer,[15] resulting in defects in the final polymeric structure. Thus, control over morphology and polydispersity during VCM polymerization utilizing conventional peroxide initiators is difficult, resulting in PVC with high polydispersity index (PDI) values and imperfect chain morphology. Although solution polymerization of VCM with an α-hydrogen nitroxide shows excellent PDI values, this method of polymerization has not been adopted industrially, due to its extra cost.[16] Conventionally, the propagation phase of VCM to PVC determines the overall molecular weight and structural defects of the final polymer.[15] VCM can add to the propagating chain by head-to-head or head-to-tail radical addition (**Scheme 1.3**). Evidence points to predominantly head-to-tail addition of the propagating chain to VCM.[17] Commercial PVC is produced in one of three

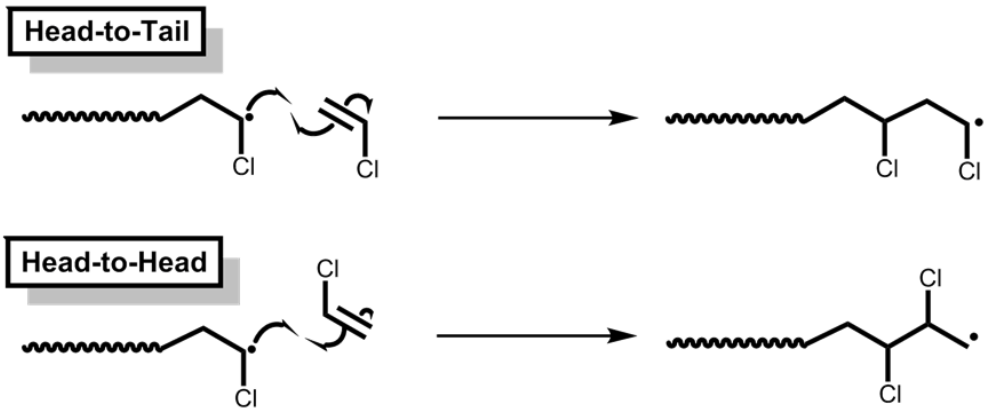

Scheme 1.3 Head-to-Tail and Head-to-Head Addition of VCM to the Propagating Chain[15]

radical polymerization methods: suspension polymerization (80% of world production), bulk polymerization (8%), and emulsion polymerization (12%).[12]

Suspension polymerization is a heterogeneous radical polymerization process in which an agitator mixes the monomer in a liquid phase, causing the polymerization to be carried out in globular droplets. Generally, under high pressure, liquid VCM is dispersed in water by vigorous stirring in an autoclave with baffles, which promotes agitation.[12] A protective colloid, also known as a granulating agent, and a monomer-soluble free radical initiator are part of the reaction mixture. The primary function of the protective colloid is to control grain size, porosity, and morphological properties of the final PVC: an important aspect of quality control in industry. Customarily, these protective colloids are cellulose ether derivatives, partially hydrolyzed poly(vinyl acetates), or poly(vinyl alcohols).[12] A range of peroxide initiators are utilized in the suspension polymerization of VCM, such as benzoyl peroxide, diacetyl peroxide, peroxydicarbonates, and alkyl peroxyesters. In industry, “recipes” of these reagents are charged into reactors with specific proportions of each component. The components are heated to 45 °C to 75 °C, which initiates homolysis of the radical initiator and subsequent polymerization of VCM inside the droplets. At the beginning of the process, VCM is distributed into 30 to 40 μm droplets under the influence of stirring, mixing and agitation in the reactor with the water-soluble protective colloid, which is absorbed at the water-VCM interface. As the reaction proceeds with thermal initiation *via* a peroxide initiator, graft-like polymerization of PVC occurs at the interfacial layer formed by the protective colloid, causing droplet coalescence at 4-5% conversion. Droplet coalescence negatively alters the ability of the protective colloid to control grain size and morphology.[12] As polymerization proceeds, the PVC chains become larger. The coalescence process stops after approximately 20% conversion; hereon, the grain size remains fairly constant.

The highly exothermic suspension polymerization process is controlled *via* heat removal. This is accomplished by cooling jackets and/or evaporation of the monomer into

condensers, which is recovered and returned to the reactor for further polymerization. Industrial plants producing PVC generally assess polymerization progress by the heat emanated to the cooling jackets: the coolant temperature is carefully monitored. A consistent reactor temperature is accomplished by altering the temperature of the coolant throughout the duration of the polymerization. The increase of heat emanated during the reaction requires a concomitant decrease in coolant temperature. Likewise, once the polymerziation nears completion, the emanated heat from the reaction decreases, requiring increased coolant temperatures to maintain the constant reactor temperature. Pressure is also monitored throughout the suspension polymerization process of VCM to PVC to assess reaction progress. Once the polymerization nears 70%, a noticeable decrease in pressure occurs in the reactor, due to the depletion of liquefied VCM.[12] Termination is generally determined by a preset reactor pressure, upon which the remaining VCM is vented off to a recovery plant and/or a terminating agent is added to the reactor. The crude PVC is then passed through a stripping column to remove residual VCM.

Bulk polymerization of VCM to PVC is nearly analogous to the process found in suspension polymerization. The chemical mechanism is similar, with the crucial distinction residing in the mechanical operation.[12] First, VCM and initiator are charged in a reactor at a temperature of 62 °C to 75 °C, which causes an initial, brisk polymerization of VCM. Large 100 μm aggregates are formed, made up of many 0.1 μm PVC particles. These particles form seeds for the final PVC grain. This initial batch of PVC is transferred to another reactor with fresh VCM and initiator, and undergoes a secondary polymerization with the PVC seed grains, fusing to form final PVC grains of 130-160 μm. Cooling of the reactor during the polymerization process is done strictly by evaporation of VCM *via* condensation. In theory, this process is more economical,[12] as it does not require a drying phase as with suspension polymerization, which uses water. In contrast to suspension polymerization, bulk polymerization utilizes a primary and secondary reactor, along with PVC seed particles.

Industrially, removing traces of VCM and PVC from the reactors becomes challenging in a two reactor setup. Residual VCM and PVC contamination causes dispersion faults, yielding oversized polymer chains.[18]

Emulsion polymerization involves polymerizing VCM in an aqueous environment with a surfactant and a water-soluble radical initiator. The “emulsion” formed by the reaction conditions inherently form PVC lattices: colloidal dispersions of PVC particles ranging between 0.1 and 3.0 μm, made up of agglomerates of PVC latex particles.[12] The term “emulsion” is a historic misnomer, as the polymerization of VCM is performed in latex particles, not emulsion droplets. The surfactant prevents coalescence of the latex particles by electrostatic repulsion. Industrial emulsion polymerization of VCM occurs in high pressure reactors between 40 °C to 60 °C, with exothermic heat evolution controlled in a similar manner to other polymerization methods. Surfactants are a critical component of the polymerization process, determining the final PVC latex characteristics and physical properties. Commonly utilized surfactants include sodium salts of alkyl sulfates, alkyl sulfonates, dialkyl sulfosuccinates, alkyl ethoxysulfates, and fatty acid soaps.[12] Initiators are customarily water-soluble, which include ammonium or potassium peroxosulfate. In the beginning of a typical emulsion polymerization process, an emulsifier is chosen based on the critical concentration at which the molecules aggregate to form micelles. The choice of emulsifier ultimately imparts the final properties to the PVC latex. At the specific critical micelle concentration (CMC), PVC latex formation is controlled within micelles which solubilize VCM and become the loci of polymerization. If a low critical micellar concentration is used, high concentrations of latex particles are obtained, resulting in greater polymerization rates over the suspension method.[19] Once the initial nucleation phase ends, the surfactant absorbs onto PVC latex particles, causing micellar breakdown. Polymerization is typically terminated at 90% conversion, with subsequent removal of VCM to a recovery tank.[12] PVC lattices are subsequently milled to produce fine particles, which readily mix with plasticizers to

form suspensions. The surfactant layer surrounding latex particles does not allow the plasticizer to be absorbed within the particles: this forms a plastisol, which is a liquid that can be sprayed on items such as fabrics, or poured into molds to create consumer products such flooring and toys.

PVC is structurally heterogeneous and possesses relative pseudochirality, also known as tacticity.[20] Tacticity is defined as the relative conformation of pseudoasymmetric centers formed as a consequence of sequential stereogenic centers.[21] The same configuration of adjacent pseudoasymmetric carbon atoms in a head-to-tail vinyl polymer is designated isotactic,[22] while an alternating arrangement is designated syndiotactic.[23] PVC is considered atactic if both isotactic and syndiotactic configurations exist in short segments of the same chain (**Figure 1.2**).[24]

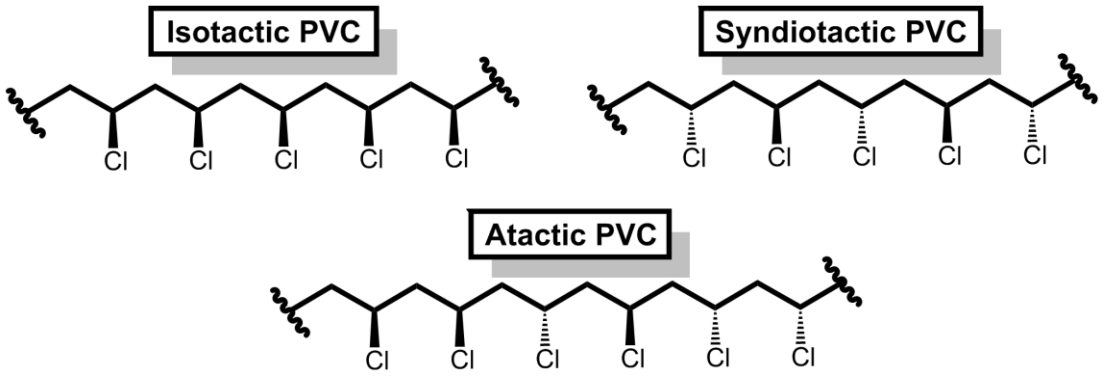

Figure 1.2 Tacticity Present in PVC[20-24]

One of the consequences of uncontrolled VCM polymerization is a randomization of the chlorine atom orientation throughout PVC. By definition, the entire polymer must contain either an isotactic or syndiotactic sequence of pseudochiral carbon-chlorine centers to be considered truly such. An investigation into the thermodynamics of VCM polymerization revealed that the activation energy of isotactic addition is higher than syndiotactic addition.[24] A noticeable decrease in syndiotactic segments was observed with an increase of reaction temperature. Intuitively, this is logical; the relatively large atomic radius of chlorine may cause

steric interactions between the radical chain end and VCM. Electrostatically, the dipole-dipole interaction energy between two successive chlorine substituents in PVC was calculated to be 0.7 kcal/mol greater in an isotactic sequence versus a syndiotactic arrangement.[24] At higher temperatures, steric and electrostatic effects play less of a role in monomer addition: thus, an increase in isotactic segments is observed.

The physical properties and thermal stability of PVC is greatly influenced by tacticity. Crystallinity present in PVC is usually attributed to syndiotactic sequences.[15] Syndiotactic carbon-chlorine dipole moments can associate strongly with adjacent chain segments containing similar dipoles, which ultimately provide the means to induce crystallinity. The melting point of conventionally synthesized PVC is between 115-205 °C due to anomalous defects present throughout the polymer.[25] In theory, perfectly syndiotactic PVC would have a melting point of 400 °C, due to the maximized presence of dipole-dipole interactions between analogous chain segments.[25] Heating neat, atactic PVC above 100 °C initiates degradation *via* emission of hydrochloric acid (HCl) from the chlorinated backbone, creating alkenes.[15] The presence of HCl further catalyzes elimination reactions from adjacent monomeric units. This process occurs iteratively, until short polyene segments are present throughout the polymer. Continued heating result in the initiation of secondary reactions, such as crosslinking, scission, and cyclization.[26] Cyclization leads to the formation of aromatic compounds, which induce dramatic changes to the physical properties of the polymer. The suspected origin of HCl elimination is related to structure: chlorine atoms adjacent to alkene defects present in the main chain from polymerization, and tertiary chlorine atoms at branch point defects are considered culprits for initial elimination.[15] Tertiary chlorine defects are more abundant than allylic chlorine defects; therefore, the current consensus is that tertiary sites are the major proponent of HCl-mediated thermal degradation of PVC.[27]

Due to the highly reactive nature of the propagating radical, side reactions occur during the uncontrolled radical polymerization of VCM. Defects in the main chain are intrinsically introduced, resulting in a myriad of abnormal morphologies involving the repeating units or chain ends in PVC (**Figure 1.3**).[27-28] An example of the formation of a defect occurs with the head-to-head addition of VCM and the propagating radical (**Scheme 1.3**). The presence of a 1,2-dichlorine arrangement can lead to chlorine migration and subsequent chlorine radical elimination at the chain end.[28a] The result of repeating unit and chain end defects induce an overall decrease in thermal stability to PVC.[29]

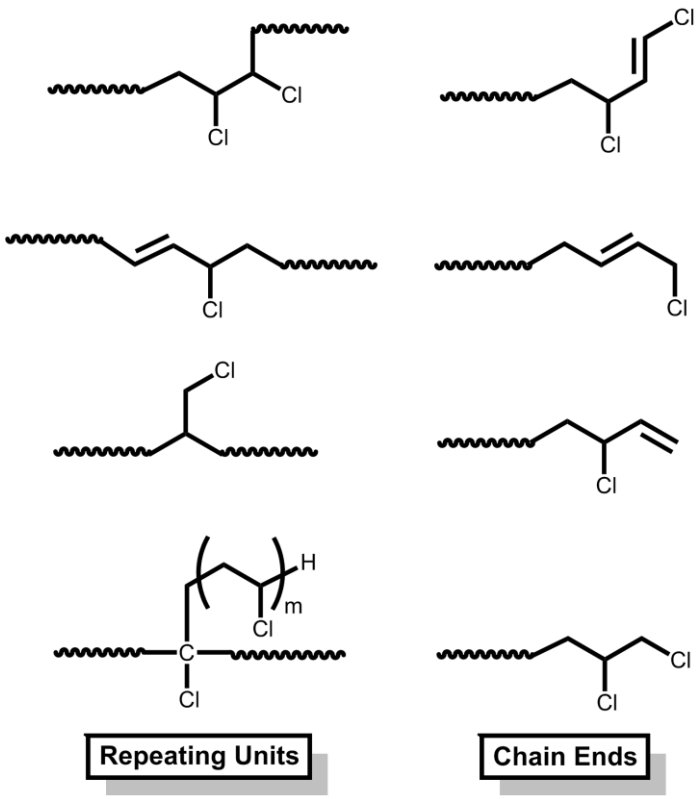

Figure 1.3 Defects Present in PVC[27-28]

1.4 Plasticization Theory

PVC in its unadulterated form is a brittle white solid with limited applications. When a plasticizer is introduced into PVC, vastly different physical properties such as flexibility, increased thermal stability, and transparency are achieved. Gaining an understanding of how a plasticizer imparts ductility and malleability is essential in designing an efficient, novel internally plasticized system for PVC. Multiple qualitative theories on plasticization arose in the mid-20th century.[30] Due to the absence of complex computing during this era, initial

theories were generally qualitative observations describing plasticization. In the formative years of classical plasticization theory, two separate but interconnected ideologies were developed to rationalize how a plasticizer functions in a polymeric matrix: lubricity theory and gel theory.[30] Subsequently, free volume theory was developed to quantitatively characterize plasticization properties.

The lubricity theory of plasticization states that the function of a plasticizer is to reduce intermolecular friction between the main chains of a polymer.[31] Lubricity theory is credited to Kirkpatrick,[32] Clark,[33] and Houwink.[34] Each author conceptualized polymer chains slipping over each other in space. Rigidity of the resin is thought to arise from intermolecular friction. The plasticizer lubricates polymer chains by reducing the internal friction and resistance between chains, thereby imparting flexibility to the plastic.

Kirkpatrick[32] stated that plasticization may result from: (1) solvent action, (2) simple lubrication of plastic micellae, and (3) a combination of the two preceding actions. As a whole, Kirkpatrick emphasized a few imperative factors that were important for plasticization to occur: (1) a plasticizer must contain mutual points of attraction between the polymer *via* specific functional group interactions, (2) within the plasticizer and polymer, these mutual functional group attraction points must be positioned in such a way that permits the facile attraction between both entities at a molecular level, and (3) the plasticizer must possess the proper shape to impart the necessary physical characteristics required. Clark[33] theorized that plasticizing properties were consequent of filling large voids in a three-dimensional polymeric matrix, leading to the formation of glide planes. The plasticizer acts as a lubricant, which results in the fluidic movement between planes upon the application of physical force on the polymer. In this way, Clark envisioned plasticized polymers as alternating layers of plasticizer and base resin, in which the polarity of each entity must be similar to obtain plasticization, stemming from the adage “like dissolves like.” Houwink[34] also envisioned polymeric glide planes and the importance of polymer-plasticizer polarity, in a cognate manner to Clark.

Houwink however, considered swelling and dissolving factors, whereas Clark did not. The purpose of the plasticizer is to interact with the polymer by swelling, which is directly dependent on the polarities of each species. In the case of an infinitely swelling polymer, all inter-chain bonds are completely detached; likewise, a partially swollen polymer would contain partially detached inter-chain bonding. Plasticization *via* swelling of a polymer can be justified by two gliding mechanisms: (1) the glide planes are in the bulk of the plasticizer, which would preferentially adhere to the main chain of the polymer, allowing the plasticizer to slip over each other, and (2) the glide planes are at the surface of the polymer backbone. This would create three possible physical interactions between polymer and plasticizer: (1) a polymer-polymer interaction, (2) a plasticizer-plasticizer interaction, and (3) a polymer-plasticizer interaction. Houwink states that the energy involved in separating the polymer-polymer and plasticizer-plasticizer interactions are greater than that of the polymer-plasticizer interaction. This causes the glide plane to exist near the polymer backbone.

The gel theory of plasticization states that polymers are formed by a honeycomb structure maintained by *non-covalent* centers of attachment between main chains.[30] The three-dimensional nature of a polymer is the main cause of rigidity in its plasticized state; the predominant factor contributing to rigidity exists within the interlocked centers between backbones. According to gel theory, the function of the plasticizer is to break these intermittent non-covalent attachments, which allows the polymer to deform. Therefore, a dynamic solvation-desolvation equilibrium exists between the polymer and plasticizer, simultaneously causing the aggregation-disaggregation of the main chain.

Aiken[35] described gel theory when studying the tensile creep behavior of PVC with different plasticizers. Aiken rationalized that polar groups in the plasticizer arranged *via* solvating dipoles along the main chain of PVC were efficient at imparting softness. Non-polar alkyl tails of a plasticizer would aggregate in the matrix, resulting in a portion of unshielded polar polymer chain. It was theorized that these unshielded polar regions on PVC would

interact and create a gel-like structure, which is responsible for the viscous flow observed in plasticized PVC. Thus, a proposed mechanism of plasticization for PVC was devised: a plasticizer will induce micro-Brownian motion between the main chain segments, thereby imparting flexibility to the polymer-plasticizer mixture. Aiken realized that pure segmental motion would not satisfactorily explain elasticity unaccompanied by flow in plasticized PVC systems: if a polymer exists as a three-dimensional network, plasticizers can convey flexibility in space by two possibilities: (1) a dynamic equilibrium involving a solvation-desolvation process of plasticizer to polymer main chain, and (2) a static mechanism that defines the mean lifetime of the polymer-plasticizer interaction to be longer than the mean lifetime of segmental motion of the polymer backbone. In the dynamic solvation-desolvation process, the plasticizer is envisioned to move through the three-dimensional polymer matrix *via* diffusion, which would temporarily disconnect polymer-polymer interactions, creating a gel-interface between main chains. Although Aiken's perception of plasticization was largely in accordance with current gel theory, there were some factors not explained.

Busse[36] described gel plasticization by the presence of four factors in a polymer-plasticizer mixture: (1) groups of atoms which form strong flexible fibrous units, (2) weak or uniform cohesive forces around the fibers, (3) an interlocking of fibers at a few locations along the main chain of the polymer to form a three-dimensional network, which can occur by various forms of non-covalent bonding, secondary valence forces, or mechanical entanglement, and (4) a means of storing free energy in the fibers during deformation. The main difference between Aiken's description of gel plasticization lays in Busse's third factor: the *interlocking* of fibers along the backbone of the polymer at a few locations to form a three-dimensional network. Aiken largely neglected to explain how a three-dimensional network was held together by interactions between adjacent polymers chains during plasticization. The focus of Aiken's work[35] was on the solvation-desolvation of a plasticizer. Although Busse

accounted for inter-chain interactions and the role of a plasticizer to disrupt these centers of attachment, little in terms of quantitative data was gathered to substantiate this theory.

In 1947, Doolittle,[37] while studying solvent action kinetics on macromolecular systems, was the first author to substantiate gel theory with experimental results. Doolittle described cohesive forces originating at definite points along the polymer as “active centers,” which can be broken apart by thermal agitation.[37a] Like Aiken, Doolittle stated that solvation occurs when solvent and solute macromolecules are joined together, while the interaction of solute macromolecules is called aggregation. The reverse processes are desolvation and disaggregation. To gain a quantitative understanding of gel plasticization, a resin solution was titrated into a nonsolvent, in accordance to a modified procedure by the American Society for Testing and Materials (ASTM) D-268-T. By varying the concentration of solvent-diluent mixture *via* titration, a point is reached where the rate of solvation barely exceeds the initial rate of desolvation. At this point, the solvent molecules that penetrate the matrix will become bound to a certain fraction of active centers in the polymer. These active centers are statistically eliminated as inter-chain attraction points and a quantifiable amount of disaggregation occurs. As the titration continues, the rate of solvation increases, which causes the aggregation-disaggregation equilibrium to shift toward complete disaggregation of the polymer. A plasticizer in this description may be considered a non-volatile solvent, which disrupts the active centers within a polymer. Ultimately, the data showed that plasticization depends on the strength of attraction between polymer and plasticizer and the overall mobility of the plasticizer with the polymer matrix. Doolittle asserted that, “the nonvolatile plasticizer still remains in the film and by its presence prevents, to an extent determined by its amount and solvent strength, further desolvation of the resin. Wherever the active centers of the resin macromolecules are masked by solvation, resin-resin contact at that point is prevented. Thus, the extent of plasticization becomes equivalent to the degree to which three-dimensional aggregation of the resin macromolecules is prevented by the solvent action of the

plasticizer."[37a] In this perspective, the performance of a plasticizer should be dependent on its relative solvent strength in a polymer. With a plasticizer containing strong solvency character, less must be added to the resin to obtain a desired amount of flexibility, relative to a plasticizer with weaker solvency properties. Interestingly, Doolittle mentions that the term "flexible" is ambiguous, "since each of the principal fields of application has appropriated the term to represent its own particular viewpoint." At the time of publication (1947), there was no quantifiable method to determine the "flexibility" of a polymer; the elongation modulus and torsion test were the only two methods reported by the author as a measure of flexibility.

Gel theory rationalizes why covalently bound internally plasticized systems are comparatively inefficient to non-covalently bound externally plasticized systems:[30] an external plasticizer is free to solvate and desolvate at the "active centers" within the polymer. The non-covalently bound plasticizer is able to more efficiently displace three-dimensional inter-chain interactions than a covalently bound internal plasticizer, which does not experience the same freedom of diffusion and solvation-desolvation. By design, an internal plasticizer is less effective at disassociating active centers due to its inability to move throughout the matrix: in a sense, these plasticizers are constantly solvating the main chain due to its covalent attachment. This ultimately diminishes the emollient's ability to induce desolvation and disaggregation between polymer chains.

Free volume theory of plasticization involves the quantitative measurements of polymer physical properties. Qualitatively, free volume theory describes the empty space between polymer chains, which depend on the amount of polymer end groups, side chain flexibility, and polymer molecular weight. Some of these metrics are measured in terms of temperature, viscosity, specific volume, and glass transition temperature (T_g). This theory lends itself to quantifying plasticization *via* the glass transition temperature of a polymer. Empirically, as temperature decreases, the volume between molecules during the transition of a liquid to a glass *diminishes*. This sudden reduction in free volume occurs at a specific

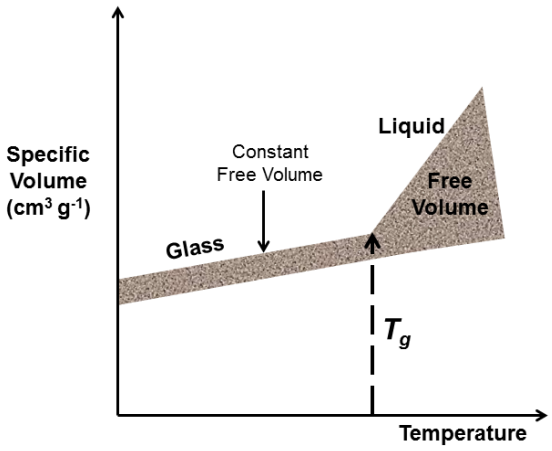

Figure 1.4 Graphical representation of the phase transition between liquid to glass

temperature, hence the term "glass transition temperature." **Figure 1.4** describes the phase transition from a liquid to a glass in terms of free volume and temperature. From a macromolecular perspective, a polymer will experience increased rotational and translational motion at higher temperatures due to a greater abundance of volume, while the same polymer will have less volume to rotate and translate at lower temperatures. Hence, when a polymer is flexible at room temperature, it will possess a low glass transition temperature: a lower temperature is required to achieve a glass-like physical state with the flexible polymer, than a polymer that exhibits greater rigidity.

In 1950, Flory and Fox[38] were the first to postulate the free volume theory in terms of specific volumes in polystyrene (PS) as a function of the second-order transition temperature (T_g) and molecular weight. The glass transition temperature was proposed as an iso-free volume state, as opposed to an iso-viscosity state, which was the contemporary consensus of that era. In the publication, the authors state that, "the second-order transition is not an equilibrium transition in a thermodynamic sense, but originates from kinetic limitations on the rates of the internal adjustments occasioned by changes in temperature."[38] The authors rationalize that at temperatures below the T_g, the internal mobility of the polymer is "insufficient for maintenance of the equilibrium internal configuration and hence, of the equilibrium volume."[38] Macroscopic viscosity is also mentioned as an inverse measure of internal mobility of a monomeric species, in which a second order transition occurs at a viscosity of approximately 10^{12} poises. However, the authors state that with a polymer, the macroscopic viscosity depends on the mobility of each chain segment *and* an "intersegment

cooperation factor," that increases with molecular weight.[39] These factors do not exist with a monomeric species: measurements of macroscopic viscosity at the time of publication neglected chain mobility and intersegmental motion as factors, with the viscosity of a polymer always decreasing with an increase of temperature or molecular weight.

In the study,[38] specific volumes of fractionated polystyrene *via* pycnometer measurements was investigated using a previously published method.[40] Polystyrene samples were heated to 217 °C due to the known densities of the polymer from absolute specific volume measurements at this temperature.[38] Dilatometry, a thermo-analytical method to measure the specific volume of a material over a controlled temperature protocol, was performed on polystyrene by placing a bubble-free sample into a bulb of a glass dilatometer, with special attention to avoid heating the polymer. Polystyrene ranged in size from 2970 to 85000 g/mol. Mercury was introduced at 0.005 mm Hg; the amount of mercury in the dilatometer was determined by weighing. The volume of polystyrene and mercury was determined at the calibration temperature (217 °C).[38] From here, measurements of the mercury in the dilatometer were taken at intervals of 10 °C below the calibration temperature of 217 °C. At all temperatures except those in the vicinity of the T_g, volume equilibrium was established, with no further changes in volume observed after 24 hours. To account for volume equilibrium within polystyrene above the T_g, each sample was allowed to stand for 10 to 60 minutes before taking a dilatometric reading. Any measurement taken at temperatures lower than the T_g required 6 to 12 hours of equilibration time.

In polystyrene samples below 25000 g/mol, specific volume measurements determined at 217 °C decrease with increasing molecular weight. In contrast, any sample above 25000 g/mol possesses similar specific volumes regardless of molecular weight. When the dilatometric data is graphed, with temperature (°C) as the abscissa, and specific volume as the ordinate axis (mL/g), the glass transition temperatures of the polystyrene samples are observed (**Figure 1.5**). There are two distinct lines that make up the specific temperature-

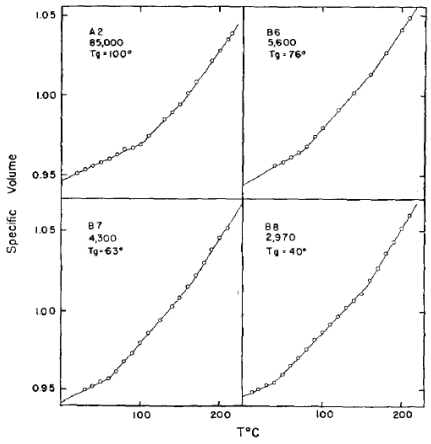

Figure 1.5 Specific Temperature-Volume Curves for Polystyrene[38]

volume curves, with different volume-temperature coefficients, represented by the slope of each line. The intersection point of the two lines is the glass transition temperature (T_g). In the proximity of 160 °C however, the volume-temperature coefficient (the slope of the line) exhibits a further increase with increasing temperature.[38] The T_g of polystyrene above 25000 g/mol is nearly independent of molecular weight, while T_g values of samples less than 25000 g/mol rapidly declined with decreasing molecular weight (**Figure 1.6**). According to the authors, the derivative specific volume-temperature coefficient $(dv/dT)_3$ (below the T_g), appears to be *independent* of molecular weight with an average value of 2.5×10^{-4} (mL/g)/°C, albeit with experimental error over limited temperature ranges.[38] The slope of the line at the bottom of **Figure 1.6** is defined as **Equation 1.1**:

$$T_g = 100 - 1.7x10^5/M \qquad \textbf{Equation 1.1}$$

The line at the bottom of **Figure 1.5** was calculated from the curve at the top. The authors conclude that the specific volume of polystyrene below the T_g does not depend on molecular weight in its glass state. In contrast, the specific volume of the polymer is dependent on molecular weight at temperatures over the T_g.

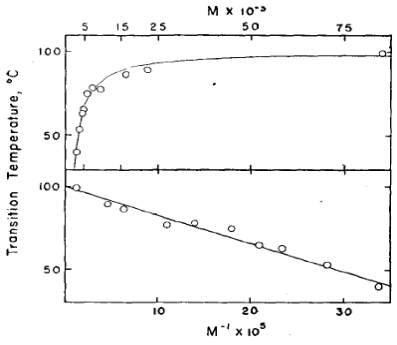

Figure 1.6 Top: T_g values of PS vs molecular weight (M_n), Bottom: T_g values of PS vs M^{-1}[38]

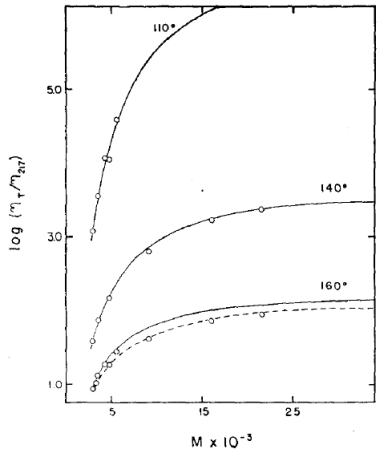

Figure 1.7 Log(η_T/η_{217}) vs M at 110, 140 and 160 °C for PS[38]

The viscosities of the polystyrene samples were also investigated. At the calibration temperature (217 °C), the viscosity (η_{217}) was in agreement with previous data at high molecular weights. However, at lower molecular weights, η_{217} showed values 10 percent higher than larger molecular weight polystyrene, due to degradation of the smaller polymers.[38] To show the relationship of the viscosity at 217 °C (η_{217}) to the viscosity at a set temperature (η_T), data at a specific temperature for each polymer was obtained. Taking the logarithm of the ratio between η_T and η_{217} versus molecular weight revealed the viscosity changes present in different molecular weight samples at different set temperatures (**Figure 1.7**). The relationships between $\log(\eta_T/\eta_{217})$ and 1/T (in °K) were shown to be non-linear, and dependent on molecular weight. At 25000 g/mol or lower, polystyrene exhibits increased $\log(\eta_T/\eta_{217})$ values with increasing molecular weight; above 25000 g/mol, polystyrene $\log(\eta_T/\eta_{217})$ values remain constant. With this data, the authors derive an equation that relates viscosity to specific volume and molecular weight (**Equation 1.2**):

$$\log\left(\frac{\eta_T}{\eta_{217}}\right) = F(T)e^{-2530/M} \qquad \textbf{Equation 1.2}$$

where F(T) is a function of absolute temperature. The viscosity-temperature function at infinite molecular weight, M=∞, along with the values of F(T) obtained from the calculations from **Figure 1.7**, were found to be linear relationships of $1/T^6$. Inserting this data into **Equation 1.1**, the authors obtain **Equation 1.3**, which expresses the dependence of the viscosity-temperature relationship on temperature and molecular weight:

$$\log\left(\frac{\eta_T}{\eta_{217}}\right) = 2.92x10^{16}\left(\left(\frac{1}{T^6}\right) - \left(\frac{1}{490^6}\right)\right)e^{-2530/M} \qquad \textbf{Equation 1.3}$$

Differentiating **Equation 1.3** yields an expression for the "apparent energy of activation for viscous flow,"[39a] also known as the viscosity-temperature coefficient, given by E_T (cal/mol) in **Equation 1.4**:

$$E_T = \left(\frac{8.1x10^{17}}{T^5}\right) e^{-2530/M} \qquad \textbf{Equation 1.4}$$

The values of log η_T and E_T were calculated for the polystyrene samples at their respective glass transition temperatures. Using the equations above, the authors obtained the data displayed in **Table 1.1**.

M_n (g/mol)	T_g (°C)	logη at T_g	E_T at T_g (kcal/mol)
300000	99	14.19	112
100000	98	12.40	112
50000	97	11.40	111
25000	93	10.93	111
15000	89	10.57	110
10000	83	10.58	110
5000	66	10.66	109
4000	58	10.69	108
3000	43	11.31	111

Table 1.1 Viscosities and Viscosity-Temperature Coefficients (E_T) of Polystyrene[38]

The viscosities (logη) of the polystyrene samples are not consistent, exhibiting considerable changes with molecular weight. At molecular weights above 25000 g/mol, the viscosity decreases while at molecular weights below 25000 g/mol, viscosities remain constant. Throughout the entire spectrum of molecular weights, the energy of activation of viscous flow (also known as the viscosity-temperature coefficient, E_T) is constant, with values of 110 ± 2 kcal/mol. From **Equation 1.4**, the authors obtain a relationship of temperature (T) at which a sample with molecular weight M has a value of E_T analogous to polystyrene of an infinite molecular weight (M = ∞), possessing a glass transition temperature ($T_{g,\infty}$) (**Equation 1.5**):

$$\frac{8.1x10^{17}}{T^5{}_{g,\infty}} = \frac{8.1x10^{17}}{T^5} e^{-2530/M} \qquad \textbf{Equation 1.5}$$

Solving for T and using the two terms of the series expansion of the exponential term, the authors obtain **Equation 1.6**:

$$T = T_{g,\infty}(1 - 506/M) \qquad \textbf{Equation 1.6}$$

Finally, inserting the value for $T_{g,\infty}$ of 373 °K, then converting to °C, **Equation 1.7** is obtained, which incidentally, is the same as **Equation 1.1** (within limits of experimental accuracy):

$$T_g = 100 - 1.9x10^5/M \qquad \textbf{Equation 1.7}$$

From the data obtained during the study, Flory and Fox derived an equation, known contemporarily as the Flory-Fox equation (**Equation 1.8**):

$$T_g = T_{g,\infty} - \frac{K}{M_n} \qquad \textbf{Equation 1.8}$$

Where T_g is the glass transition temperature, $T_{g,\infty}$ is the maximum glass transition temperature that can be achieved at a theoretical infinite molecular weight, K is an intrinsic constant associated with a polymer type, and M_n, which is the molecular weight of the polymer. From **Equation 1.8**, it is clear that M_n influences the T_g of a polymer sample, where a larger molecular weight (M_n) increases the T_g of the sample.

The second-order transition temperatures (T_g) for the polystyrene series are not iso-viscous, as was believed at the time of publication. At the glass transition temperature, the viscosity-temperature coefficient (E_T) is independent of molecular weight; in this way, the authors prove that T_g is a function of iso-free volume, rather than an iso-viscous state. Essentially, local segmental motion of a polymer is an imperative factor which directly influences the T_g by creating free volume between adjacent chains. This phenomenon can be rationalized *via* the length of a polymer chain which is directly related to M_n: as the polymer chain increases in length, so does the inter-chain interactions between adjacent polymers while in shorter polymer chains, there are less interactions. Prior to this study, macroscopic viscosity was thought to be an ideal measurement to justify the decrease in T_g for short

versus long polymers, by initial interpretation of viscosity data with respect to polymer size. However, according to the data gathered by the authors, the viscosity-temperature coefficient (E_T) is independent of chain length, which leaves free volume between polymers as the major contributing factor affecting T_g.

Flory and Fox[38] rationalized that the change in T_g of the polystyrene samples were dependent on chain length and the abundance of chain ends. The increase of specific volume in the samples as molecular weight decreased can be attributed to the end groups of a polymer acting "like a foreign substance, in disrupting the local configurational order of the styrene units, and this is manifested by an increase in the specific volume…"[38] The free volume between segments which Flory and Fox deemed as "holes," are a result of local segmental motion *and* mobile chain ends, which open voids between polymer main chains. Conceptually, a short polymer would inherently contain a higher abundance of chain ends over a longer polymer per unit volume. The nearest intermolecular neighbor distance is greater between a chain end and an adjacent main chain, relative to the length of the short covalent bonds that make up the polymer. An increased presence of chain ends generates more free volume. This is a source of internal plasticization in a polymeric species. As a result, a longer polymer with less chain ends will experience a higher T_g compared to a short polymer. A polymer with a lower T_g possesses more free volume than a polymer with a higher T_g; this implies that a plasticizer which creates more free space between polymers will decrease the T_g and increase the pliability of the system.

In terms of a binary polymer-plasticizer system, Fox[41] subsequently developed a means to determine how glass transition temperatures change when a low molecular weight diluent (a plasticizer) is added to a polymer. A plasticizer introduced to a polymer matrix should increase the free volume between polymer chains, thereby lowering the T_g of the mixture. The Fox equation, (**Equation 1.9**), describes a binary polymer-plasticizer system and its respective effect on the overall glass transition temperature on a mixture:

$$\frac{1}{T_g} = \frac{w_1}{T_{g,1}} + \frac{w_2}{T_{g,2}}$$ **Equation 1.9**

In **Equation 1.9**, w_1 and w_2 are the respective weight fractions of each component. The Fox equation relies on many assumptions about the binary system of interest. These assumptions are: (1) the pure polymer glass transition temperatures are constant with blend composition with the plasticizer, (2) the contributions of the polymer components are equally additive, (3) the two polymers are miscible and amorphous; and (4) that the heat capacity changes at the phase transition are the same for the two materials. The component masses are simply added together in this model, which will inherently result in a minor depression of T_g due to the small increase in entropy and free volume, with the absence of interactions between plasticizer and polymer chain. In this sense, **Equation 1.9** does not account for the specific volume and expansion coefficients of both components. The Gordon-Taylor equation[42] (**Equation 1.10**) accounts for the specific volume and expansion coefficients of each component by the addition of factor *k* into the Fox equation:

$$T_g = \frac{w_1 T_{g,1} + k w_2 T_{g,2}}{w_1 + k w_2}$$ **Equation 1.10**

Gordon and Taylor[42] based their model on a linear change in volume with temperature.[43] Factor *k* depends on the change in the thermal expansion coefficient (α) as the components change from a glassy to a flexible state, as described in **Equation 1.11**:

$$k = \left(\frac{V_2}{V_1}\right)\left(\frac{\Delta\alpha_2}{\Delta\alpha_1}\right)$$ **Equation 1.11**

In **Equation 1.11**, the specific volumes (V) at corresponding T_g values are accounted for along with the thermal expansion coefficient (α). If applying the Boyer-Simha rule[44] to the Gordon-Taylor equation, in which $\Delta\alpha \cdot T_g$ = constant, α is removed from factor *k* to simplify calculations, resulting in **Equation 1.12**:[43]

$$k \approx \left(\frac{V_2 T_{g,1}}{V_1 T_{g,2}}\right)$$ **Equation 1.12**

In this manner, it is possible to predict the T_g of a binary polymer-plasticizer mixture, based on the concept of free volume. A lower T_g should result in a polymer that is more flexible. According free volume theory, when a plasticizer is added to PVC, PVC should become more flexible, due to the increase in free volume generated by a compatible external plasticizer. The plasticizer would enter interstitial "holes" generated in the polymer by structural defects or chain ends and eventually surround the backbone, thereby increasing free volume between the polymer chains. This in turn would increase segmental motion between polymer chains, reduce inter-chain interactions, and decrease the T_g due to an increase in free volume.

To recapitulate, the free volume of a polymer comes from three sources:[30] (1) motion of chain ends, (2) motion of side chains, and (3) segmental motion of the main chain. Therefore, free volume can be increased by:[30] (1) increasing the number of end groups, (2) increasing the number of side chains, as a form of internal plasticization, (3) increasing the probability for main chain movement by inclusion of segments of low steric hindrance and low intermolecular interaction, as another form of internal plasticization, and (4) the inclusion of a compatible compound of lower molecular weight that facilitates factors 1 through 3 as a form of external plasticization. According to Marcilla and Beltran,[30] increasing the molecular weight of an external plasticizer should introduce more free volume, and as a result, an increase in plasticizing efficiency. Likewise, a branched plasticizer should be more efficient than a linear one, as the branching would supposedly induce more free volume between main chains of the PVC.

1.5 Compatibility Factors Essential for Efficient Plasticization

The compatibility of a plasticizer is a measure of its solubility within the polymer of interest: the adage “like dissolves like” comes to mind. While researchers have alluded to solubility as a factor in plasticizing efficiency,[32-35, 37] quantitative solubility parameters in the formative years of plasticization theory were scarce. Empirical methods yield results which generally agree with each other throughout the literature. However, these methods are challenging to apply to increasingly complex systems, due to the lack of an adequate qualitative measure of compatibility between polymer and plasticizer. Consequently, qualitative methods have been developed to describe the solubility, and therefore compatibility of a plasticizer with a polymer. While many approaches were developed to predict the solubility of a plasticizer, such as the Hansen solubility parameters,[45] and the Hildebrand solubility parameter,[46] the most developed theory of PVC compatibility with plasticizers is the Flory-Huggins theory.[47] Therefore, the Flory-Huggins theory will be the primary focus for the current discussion on compatibility.

The Flory-Huggins theory was developed to quantify the ability of a polymer and plasticizer to mix as a process determined by a combination of thermodynamic factors.[48] This process is described in part by the Gibbs free energy of mixing equation (**Equation 1.13**):

$$\frac{\Delta G}{RT} = x_1 ln\varphi_1 + x_2 ln\varphi_2 + \chi_1\varphi_1\varphi_2\left(x_1 + x_2\frac{V_2}{V_1}\right) \qquad \textbf{Equation 1.13}$$

Where ΔG is the Gibbs free energy of mixing and x_1 and x_2 are mole fractions of plasticizer and polymer, respectively. The factors φ_1 and φ_2 are volume fractions of plasticizer and polymer. Finally, X_1 is the Flory-Huggins interaction parameter. The first two terms in **Equation 1.13** are a result of the entropy of mixing experienced by the plasticizer and polymer: these terms are always negative. The Flory-Huggins interaction parameter (X_1) is dimensionless and represents the difference in interaction energy between a molecule of

plasticizer in the pure polymer and the interaction energy of a molecule of plasticizer immersed in a pure solution of itself. The Huggins interaction parameter is then used to derive an equation to characterize plasticizer activity, as shown in **Equation 1.14**:

$$\ln a_1 = \frac{\Delta\mu_1}{RT} = \ln(1-\varphi_2) + \varphi_2 + \chi_1\varphi_2^2 \qquad \textbf{Equation 1.14}$$

where a_1 is the plasticizer activity and μ_1 is the chemical potential of the plasticizer. Generally, a value of 0.55 or less for X_1 deems a plasticizer sufficiently compatible with a polymer.[49] A mixture with a Flory-Huggins interaction parameter value between 0.55 and 0.3 is considered to possess moderate solubility, while any value below 0.3 predicts excellent compatibility between plasticizer and polymer.[49] Historically, the interaction between PVC and plasticizer has been studied to determine overall compatibility with respect to the Flory-Huggins interaction parameter (X_1).

In an early study by Zable and Doty,[50] a variety of aliphatic plasticizers were investigated to determine the Flory-Huggins interaction parameters in PVC *via* swelling measurements. PVC was chosen as the model polymer due to its tendency to crosslink when heated. This crosslinking factor was essential to this study, as the equation derived to determine X introduced a parameter M_c which, according to the authors, "can be interpreted as the average molecular weight between crosslinks." **Equation 1.15** accounts for M_c, which was utilized to determine X *via* equilibrium swelling due to the crosslinks introduced into PVC, which formed a gel structure:

$$\chi v_2^2 = -\ln(1-v_2) - v_2 - \rho_2 V_1 v_2^{1/3} / M_c \qquad \textbf{Equation 1.15}$$

where v_2 is the volume fraction of PVC at swelling equilibrium, ρ_2 is the density of pure PVC and V_1 is the molal volume in solvent. The authors determined the degree of swelling with freshly crosslinked PVC in three standard solvents, thereby obtaining standardized values for M_c. A mixture of an appropriate amount of plasticizer into crosslinked PVC was measured in

terms of the degree of swelling, which led to the calculation of X. Selected X values of PVC-plasticizer mixtures are shown in **Table 1.2**.

Plasticizer	X (at 76°C)
Di-*n*-Hexyl Phthalate	-0.09
Di-*n*-Butyl Phthalate	-0.01
Di-*Iso*octyl Phthalate	0.03
Di-Ethyl Phthalate	0.40
Di-Methyl Phthalate	0.53

Table 1.2 Flory-Huggins Interaction Parameter Values for Crosslinked PVC and Plasticizer[50]

A subsequent study done by Anagnostopoulos et al.,[51] describes X values utilizing a microdetermination method in which a single PVC particle in the presence of excess diluent (plasticizer) is measured going from a gel-state to a sol-state on a hot-stage microscope. A drop of plasticizer was placed on a microslide with a few granules of PVC and mixed with a microspatula. Anagnostopoulos accounts for the "apparent melting temperature" of PVC, while Zable and Darby[50] solely utilized the degree of swelling to determine X. The study also accounts for ΔH_u, which is the heat of fusion per mole of repeating monomer unit, the melting point of the pure polymer ($T°_m$), and the depressed melting temperature (T_m) (**Equation 1.16**):

$$1/T_m - 1/T_m^\circ = (R/\Delta H_u)(V_u/V_1)(v_1 - \chi v_1^2) \qquad \textbf{Equation 1.16}$$

where V_u and V_1 are the molar volumes of the polymer repeating unit and plasticizer, respectively, and v_1 is the volume fraction of the plasticizer. Select Flory-Huggins interaction parameter data obtained from the experiment are shown in **Table 1.3**.

Plasticizer	Flory-Huggins Interaction Parameter (X)
Di-*n*-Butyl Phthalate	-0.05
Di-*n*-Hexyl Phthalate	-0.04
Di-*Iso*octyl Phthalate	-0.03
Di-Ethyl Phthalate	0.34
Di-Methyl Phthalate	0.52

Table 1.3 Flory-Huggins Interaction Parameter Values *via* Anagnostopoulos' Micromethod[51]

In a similar study, Bigg[49] investigated Flory-Huggins interaction parameters for PVC and plasticizers. Bigg utilizes the same method as Anagnostopoulos,[51] with the only major difference being the use of a more sophisticated transmitted-light hot-stage microscope apparatus. The modern equipment achieved better contrast, leading to increased accuracy.[51] **Table 1.4** gives Flory-Huggins interaction parameter data obtained from the experiment:

Plasticizer	Flory-Huggins Interaction Parameter (X)
Di-*n*-Butyl Phthalate	0.04
Di-*Iso*octyl Phthalate	0.05
n-Butyl Benzyl Phthalate	0.17

Table 1.4 Bigg's X Values of PVC-Plasticizer (Improved Hot-Stage Microscope)[49]

Tomaselli et al.[52] described Flory-Huggins interaction parameters for PVC and aliphatic ester plasticizers in a similar manner to Anagnostopoulos[51] and Bigg.[49] However, in the study, mixtures of plasticizers were investigated, along with the single plasticizer systems previously investigated. Of particular interest to the current topic of discussion are the single component plasticizer systems; the X values are listed in **Table 1.5**.

Plasticizer	Flory-Huggins Interaction Parameter (X)
Di-*Iso*octyl Phthalate	-0.24
Di-*n*-Butyl Phthalate	-0.22
Di-Octyl Decyl Phthalate	-0.16
n-Butyl Benzyl Phthalate	-0.09
Di-*Iso*decyl Phthalate	-0.07

Table 1.5 Tomaselli's PVC-Plasticizer Flory-Huggins Interaction Values[52]

In a relatively recent study, Brown and coworkers[53] developed an automated microtechnique as a modification of Anagnostopoulos' method[51] to determine the apparent melting temperature of PVC in excess plasticizer. A microscope equipped with a photodiode sensor was utilized to measure the amount of light transmitted through a plasticizer sample containing a PVC particle as the temperature is increased at a fixed rate.[53] The apparent melting temperature of the mixture is characterized by a sigmoidal change in the light

transmitted through a fixed area. Different heating rates were executed, ultimately yielding the X values displayed in **Table 1.6**:

Plasticizer	Heating Rate (°C/min)	Flory-Huggins Parameter (X)
Di-Methyl Phthalate	0.2	0.34
	1.0	0.35
Di-*n*-Butyl Phthalate	0.2	-0.30
	1.0	-0.23
Di-*Iso*octyl Phthalate	0.2	-0.31
	1.0	-0.23

Table 1.6 Flory-Huggins Interaction Values of PVC-Plasticizer Utilizing Automatic Photodiode Microtechnique[53]

The studies measuring the Flory-Huggins interaction parameter with PVC and plasticizer agree with one another, as seen in **Table 1.7**:

Plasticizer	X Zable[50]	X Anagnostopoulos[51]	X Bigg[49]	X Tomaselli[52]	X Brown[53]
Di-*n*-Butyl Phthalate	-0.01	-0.05	0.04	-0.22	-0.30 (0.2 °C/min)
					-0.23 (1.0 °C/min)
Di-*n*-Hexyl Phthalate	-0.09	-0.04	-	-	-
Di-*Iso*octyl Phthalate	0.03	-0.03	0.05	-0.24	-0.31 (0.2 °C/min)
					-0.23 (1.0 °C/min)
Di-Ethyl Phthalate	0.40	0.34	-	-	-
Di-Methyl Phthalate	0.53	0.52	-	-	0.34 (0.2 °C/min)
					0.35 (1.0 °C/min)
n-Butyl Benzyl Phthalate	-	-	0.17	-0.09	-
n-Octyl *n*-Decyl Phthalate	-	-	-	-0.16	-
Di-*Iso*decyl Phthalate	-	-	-	-0.07	-

Table 1.7 Compiled Flory-Huggins Interaction Parameter Values of PVC-Plasticizers[49-53]

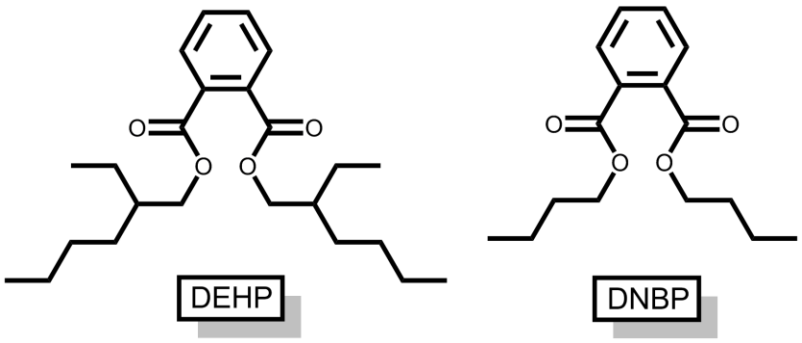

Figure 1.8 DEHP versus DNBP Structure

In terms of plasticizer structure, a plasticizer will most efficiently solvate a polymer chain when the polarity of both entities are similar.[48] The interactions between the polymer backbone and plasticizer will have the lowest energy of interaction and readily dissolves when mixed. In a thermodynamic sense, the energy of interaction between a polymer and a plasticizer must be greater than the energy of interaction between plasticizer-plasticizer and polymer-polymer interactions. There must be the existence of functional groups within each entity which establish solubility and therefore compatibility. When taking into consideration the quantitative Flory-Huggins interaction parameter, di-*n*-butyl phthalate (DNBP) and DEHP possess similar values across all studies, which implies that DEHP is a superior plasticizer from the perspective of free volume theory. Per unit plasticizer, DEHP should impart more free volume to PVC due to its structure. The aliphatic chains in DEHP are large and contain a chiral center, which creates a branch point in the chain, as a mixture of diastereomers, increasing the disorder. DNBP, on the other hand, contains less carbon atoms and does not possess a branch point (**Figure 1.8**). Therefore, DEHP should possess superior plasticization efficiency over DNBP as an external plasticizer for PVC due its similar compatibility with PVC and larger, bulkier structure.

1.6 Phthalate Plasticizers

Historically, phthalates were introduced in the 1920s as a PVC plasticizer to replace camphor, which has an odor and high volatility.[54] The commercial availability of PVC in 1931, and the synthesis of DEHP (**Figure 1.1, 1.8**) in 1933, spurred the growth and development of

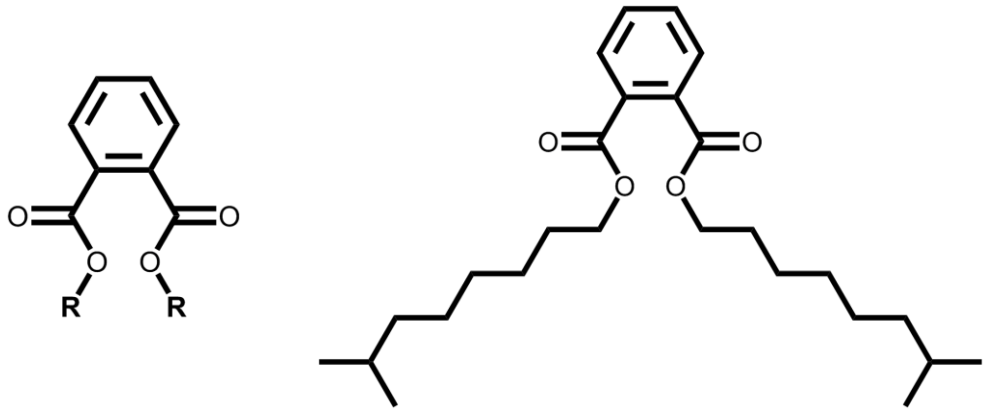

Figure 1.9 *Left:* Generalized Phthalic Acid Ester, *Right:* Di-*iso*nonyl Phthalate (DINP)

the flexible PVC industry.[54] Phthalic acid esters also known as phthalates, are the most prevalent plasticizer type utilized globally. Structurally, all phthalates contain a benzene-1,2-dicarboxylate moiety with a myriad of chemical groups that may be utilized as the "R" groups. Di-*iso*nonyl phthalate (DINP) (**Figure 1.9**) is currently the second most common phthalate plasticizer, second only to DEHP worldwide.[55]

Today, flexible PVC accounts for 80-90% of the total world plasticizer consumption.[56] According to IHS Chemical, in 2014, phthalates made up 70% of the global plasticizer market, while DEHP made up 37% of the plasticizer market: DEHP is the largest-volume plasticizer globally.[56] Another source, Micromarket Monitor, found that DEHP made up 45.7% of the global plasticizer market in 2014.[55] Overall phthalate consumption has decreased since 2005, when phthalates made up 88% of the global plasticizer market.

As mentioned previously, DEHP has an array of applications in combination with PVC, ranging from the construction industry to the medical service field. Nearly 40 percent of all plastic items in a medical setting are PVC-DEHP mixtures.[9] While the medical applications of PVC-DEHP mixtures are immense, DEHP is the major component utilized in blood bags.[9] The blood bag was invented by Dr. Carl Walter in 1947,[57] leading to its widespread use in 1955.[58] PVC-DEHP was chosen as the material of choice by Walter due to its elastic

properties, while being robust enough to permit sterilization *via* steam.[57] Early on, PVC-DEHP was observed to reduce the onset of bacterial infections during blood storage.[57] Interestingly, DEHP also has the ability to impart desirable optical and pliant properties to the PVC-based blood bag, while osmotically stabilizing red blood cells[59] up to 9% better than systems without it.[60] The retention of normal morphology and reduction in hemolysis of the red blood cells is directly attributed to DEHP.[60] DEHP enhances the rate of *in vivo* patient recovery by preserving red blood cells up to 24% better after reinfusion as compared to the equivalent trimellitate-plasticized blood bag.[60] The presence of PVC-DEHP blood bags in medicine has been a cornerstone of medical practice for more than half a century; thus the industry has a large amount of experience with the material. As a result, manufacturers are careful to not introduce additional risks through changes in product specifications which may result in weaker bags.[58]

Despite the benefits of DEHP in blood-bearing medical supplies, DEHP is known to leach out of these materials directly into the blood at high concentrations:[61] this is due to DEHP not being covalently bound to PVC.[62] Adverse health effects stemming from DEHP and its phthalate relatives have called legislators around the world to put restrictions on its use as a plasticizer in many consumer products.[63] The European Union (EU) has banned the use of certain phthalates in toys, food containing materials, and cosmetics.[64] The United States has banned DEHP, along with di-*n*-butyl phthalate (DNBP) and *n*-butyl benzyl phthalate (BBzP) in any amount greater than 0.1 weight percent in child care products, while placing restrictions on DINP, di-*iso*decyl phthalate (DIDP), and di-*n*-octyl phthalate (DNOP) on any product that may enter the mouth of a child.[65] Phthalates leach[66] from consumer and medical products, enter the body, and act as endocrine disrupting chemicals (EDC).[62] The adverse biological effects of phthalates on human physiology are of major concern, and are discussed herein.

1.7 Adverse Biological Effects: Phthalates

Human exposure to these plasticizers is imminent and unavoidable, due to the ubiquitous presence in consumer products. Routes of exposure to phthalates comes in many forms: ingestion, inhalation, dermal absorption, and intravenous injection.[67] Ingestion has been shown to be the primary source of phthalate exposure in the general population through dietary intake of contaminated food.[67] Medical devices also introduce phthalates (predominately DEHP) to hospital patients *via* containers holding blood, nutritional formulas, and respiratory gases.[67] Toys designed for children made of PVC softened with phthalates is another oral source of exposure. Inhalation by baking polymer modelling clay at home has been shown to be a route of exposure, with many clay samples containing 3.5% to 14% phthalate by weight.[68] House dust and indoor air is another route for inhalation exposure, stemming from outgassing plastics present in household products such as furniture, flooring, toys, and automobile parts.[69] Dermal absorption of phthalates occur when coming into direct contact with cosmetics, sunscreens, polymer modelling clay, toys, shower curtains, and yoga pads. Fortunately, studies have shown that the rate of phthalate dermal absorption is generally slow in both rodents and humans.[70] Often, the highest levels of exposure occurs intravenously, through leaching of DEHP from PVC blood bags and tubing. DEHP frequently comprises more than 40-50 percent of the weight in the material used in flexible medical PVC.[9]

The leaching action of DEHP from PVC blood bags was first noted in an early study by Jaeger and Rubin in 1970.[61] In 1972, Jaeger and Rubin[71] further investigated the migration of DEHP from PVC blood bags, measuring the rate of extraction of the plasticizer in human and dog blood at 4 °C. DEHP was found to migrate at 0.25±0.03 mg per 100 mL of blood per day.[71] The plasticizer was found in lipid and lipid-free fractions of blood plasma, while red blood cells contained only minute amounts of DEHP. In 1973, the same authors[72] found DEHP localized in the liver, lung, spleen, and adipose tissue of patients in a hospital

setting. In addition, the authors were the first to describe phthalate metabolites in the urine as a method of detection.[72] Leaching of DEHP from flexible PVC varies with lipid content, temperature, storage time, and agitation.[67] Due to the hydrophobic nature of DEHP, a higher lipid content of the intravenous liquid increases leaching and exposure of the phthalate to the patient.[73] Knowledge in the years following Jaeger and Rubin's discovery of DEHP leaching into the blood of patients spurred the establishment of a tolerable daily intake (TDI), a reference dose level (RfD), and minimum risk levels (MRL) by a variety of expert panels worldwide. **Table 1.8** describes the TDI, RfD, and MRL of select phthalates for humans.[62]

The United States Environmental Protection Agency (US-EPA), Agency for Toxic Substances and Disease Registry (ATSDR), Scientific Committee on Toxicity, Ecotoxicity and the Environment (CSTEE), and the European Chemicals Bureau (ECB) all rate DEHP as a fairly toxic chemical, with tolerable exposures ranging from 0.02 to 0.100 milligrams per

Phthalate	Region	Committee	Year	mg/kg bw/day	MRL/TDI/RfD
DEHP	USA	US-EPA	1991	0.020	RfD (Chronic)
		ATSDR	2002	0.100	MRL (Intermediate)
	EU	CSTEE	1998	0.050	TDI
		ECB/EU	2004	0.020	TDI (Newborns,Women)
	CAN	Health Canada	1994	0.044	TDI
DNBP	USA	US-EPA	1990	0.1	RfD (Chronic)
		ATSDR	2001	0.5	MRL (Acute Oral)
	EU	CSTEE	1998	0.1	TDI
	CAN	Health Canada	1994	0.06	TDI
DINP	EU	CSTEE	1998	0.15	TDI
DIDP	EU	CSTEE	1998	0.25	TDI

Table 1.8 Risk Assessment of Selected Phthalates[62]

kilogram per body weight per day (mg/kg bw/day). DNBP, DINP, and DIDP are rated as less toxic than DEHP, with higher RfD, MRL and TDI values ranging from 0.06 to 0.5 mg/kg bw/day. Phthalates are not acutely toxic, with median lethal dose (LD_{50}) values ranging 1 to 30 gram(s) per kilogram of body weight.[62] The inherent danger of DEHP lies in its subacute

toxic effects on organs, not its acute toxicity. DEHP has been studied in the lungs,[74] heart,[75] kidneys,[76] liver,[77] ovaries,[78] and the testis.[79]

Recently, phthalate exposure assessment has increasingly focused on human biomonitoring.[80] Urinary analysis is a common method to measure internal exposure of phthalates in humans.[62] In an early study, Albro and Moore[81] studied rat urinary metabolites of phthalates, which were administered orally. High-pressure liquid chromatography (HPLC) was used to determine the primary and secondary metabolites in urine samples. Low molecular weight phthalates such as dimethyl and di-*n*-butyl phthalate are metabolized into their monoesters and excreted.[81] Dimethyl phthalate is excreted as a significant component in urine, while di-*n*-butyl phthalate was found to be a trace component during urinary analysis. Higher molecular weight phthalates such as di-*n*-octyl phthalate are hydrolyzed to the monoester, then subsequently metabolized into smaller alkyl chain derivatives by ω and ω-1 oxidation, followed by α or β oxidation. Albro[82] postulated that there are a myriad of metabolic pathways that play a role in converting DEHP to water-soluble excretion products. DEHP is initially metabolized into its primary metabolite, mono-(2-ethylhexyl) phthalate (MEHP), which result from gut lipase hydrolysis. The liver, kidney, lungs, pancreas and plasma also contain enzymes capable of converting DEHP to MEHP, however to a lesser degree than the intestinal tract.[11] At least 98% of ^{14}C present in the urine of rats given carbonyl ^{14}C-labeled DEHP either orally or intravenously was accounted for by 20 metabolites, none of which is the parent diester phthalate.[82] Moreover, 2-ethylhexanol, another primary metabolite of DEHP, is further metabolized into at least 7 secondary metabolites.[83] Both MEHP and 2-ethylhexanol are subsequently metabolized in the liver into various secondary metabolites, which specifically depend on the mammal of interest. For example, primates generally glucuronidate MEHP prior to excretion,[84] while rodents metabolize MEHP *via* oxidation pathways.[11] In this capacity, MEHP is subsequently modified by various side-chain hydroxylation and oxidation biochemical reactions.[85] Major DEHP metabolites currently

known are mono-(2-ethylhexyl) phthalate (MEHP), mono-(2-ethyl-5-hydroxylhexyl) phthalate (5OH-MEHP), mono-(2-ethyl-5-oxohexyl) phthalate (5oxo-MEHP), mono-(2-ethyl-5-carboxypentyl) phthalate (5cx-MEPP), and mono-[2(carboxymethyl)hexyl] phthalate (2cx-MMHP) (**Scheme 1.4**).[85] In rat[84] and hamster[86] models, Lhuguenot and co-workers determined that the predominant oxidation pathway for DEHP was *via* ω-1, due to the prevalence of these metabolites in both mammalian model systems. DEHP metabolism is both time and dose dependent. An increase in peroxisome proliferation was noted in the rat model, but not the hamster model. For context, the peroxisome is an organelle that is responsible for the oxidation of fatty acid chains and the production of hydroxyl and superoxide radicals.[87] Hamsters are known to be resistant to peroxisome proliferation,[86] and as a result the ω-1 oxidized products were found as water soluble glucuronide conjugates, as sometimes found in primate models. In rats however, the ω-1 oxidized products were found in their respective non-water soluble, non-conjugated forms. DEHP belongs to a class of molecules known as peroxisome proliferators (PPs), which cause increased oxidative stress due to the overexpression of H_2O_2-generating peroxisomal fatty acyl-COA oxidase and the overproduction of other reactive oxygen species.[87b] Therefore, the peroxisome proliferation effect of DEHP may explain the origin of the oxidized secondary metabolites of MEHP found to be prevalent in bioanalysis of rodent and human exposure to DEHP.

For decades, MEHP was the sole biomarker utilized in identifying internal exposure to DEHP.[88] This was due to initial evidence showing that MEHP, not DEHP, was one of the major causative agents of toxicity.[89] However, using MEHP as the sole biomarker to determine phthalate exposure may prove to be an inefficient means of analysis. MEHP is externally formed from DEHP by abiotic processes and can exist as a standalone environmental contaminant.[62] When investigating individuals for exposure to phthalates in a 2541 person study,[88] MEHP levels were much lower than expected, despite the ubiquity of

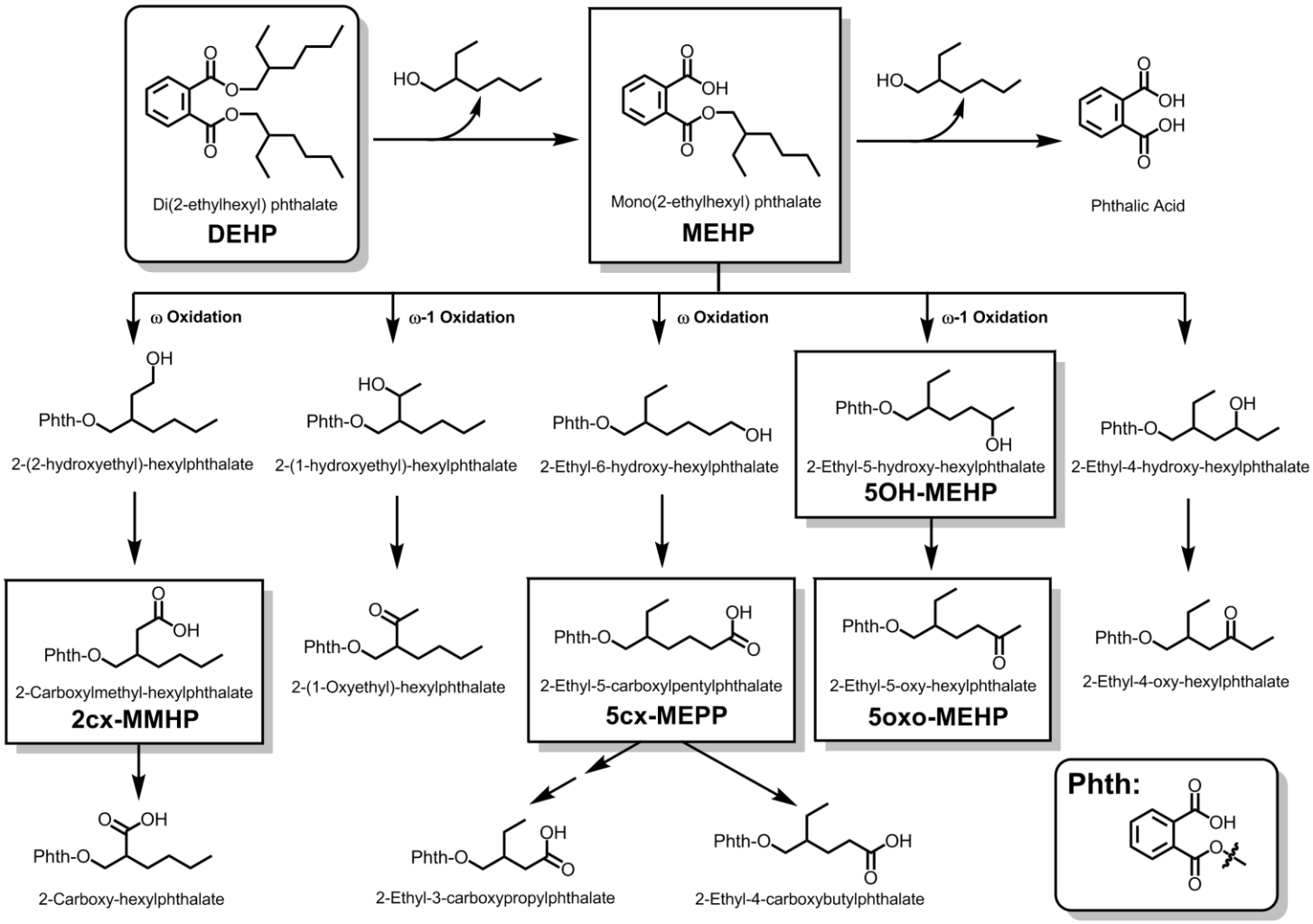

Scheme 1.4 DEHP Metabolic Products[85]

DEHP in consumer products: this brought in to question the accuracy of using MEHP as a biomarker for assessing DEHP exposure.

In a study done by Koch,[85] MEHP represented only 7.3% of the original DEHP dose administered, as analyzed in urine, while possessing the shortest half-life of elimination compared to other metabolites investigated. Oxidized secondary metabolites have been shown to be up to 100 times more embryotoxic than MEHP, with considerably longer half-lives.[62, 85] In humans, secondary metabolites such as 5OH-MEHP and 5oxo-MEHP make up 38.5% of the oral DEHP dose given after 24 hours.[85] In total, approximately 70% of DEHP metabolites found in urine are oxidized secondary metabolites, which include 5OH-MEHP, 5oxo-MEHP, 5cx-MEPP, and 2cx-MMHP.[90] Half-lives of DEHP metabolites were found to be: 5 hours (MEHP), 10 hours (5OH-MEHP and 5oxo-MEHP), 12 to 15 hours (5cx-MEPP) and 24 hours (2cx-MMHP).[85] Unlike MEHP, accurate analysis of these oxidized secondary metabolites is not subject to external environmental contamination. In combination with longer half-lives, higher toxicity and lower contamination risks than MEHP, urinary analysis of DEHP exposure has been shifting toward these oxidized species as biomarkers.

Androgens are steroids essential to the development of the male internal and external male reproductive tract.[91] During fetal development, androgens are produced by the testes and mediate the formation of the mesonephric (Woffian) duct. In proto-male development, the mesonephric duct differentiates into the vas deferens, epididymis, ejaculatory ducts, and seminal vesicles. This masculinization process is regulated *via* testosterone. External male genitalia and prostate development are mediated by a potent metabolite of testosterone, dihydrotestosterone (DHT). The role of the endocrine system in male reproductive development is easily affected by endocrine disrupting chemicals (EDCs) such as DEHP, which interfere with the production, distribution, and action of androgens. DEHP and other phthalates have been shown to profoundly disrupt the physical development of the male reproductive tract in rodent models, in an array of *in vivo* studies.[92] In general,

physical abnormalities caused by DEHP during and post-natal development of rodent models include: malformed external genitalia, hypospadias, cryptorchidism, Leydig cell hyperplasia, seminiferous cord and prostate abnormalities, malformation of the epididymis and vas deferens, retention of thoracic nipples/areolae, and reductions in anogenital distance (AGD).[93] For context, AGD is the distance between the anus and genitals, and is considered an important endpoint for hormonally regulated sex differentiation in rodents, as it is controlled by dihydrotestosterone, a potent steroid agonist of the androgen receptor (AR).[94] AGDs are normally twice as long in males (compared to females) in both rodents and humans.[95]

A study by Vinggaard and co-workers[96] observed the biochemical effects of DEHP on gonocytes and Leydig cells. Quantitative reverse transcription polymerase chain reactions revealed reduced testicular mRNA expression of many steroidogenesis related factors.[96] Nuclear receptor SF-1 (a Leydig cell product responsible for the first phase of testicular descent during fetal development) is crucial in regulating key steps of steroid biosynthesis, germ cell survival, bone metabolism, and INSL-3.[97] Decreased expression of SF-1 led to reduced INSL-3 levels, which is commonly associated with cryptorchidism. Immunochemistry studies showed a decrease in SR-B1 (an integral membrane protein involved in the uptake of cholesteryl esters from high-density lipoproteins in the liver), StAR (a transport protein that regulates cholesterol transfer in the mitochondria, which is the rate-limiting step in steroidogenesis), PBR (a translocator protein of the steroidogenic machinery mediating cholesterol delivery from the outer to the inner mitochondrial membrane), and P450scc (cholesterol side-chain cleavage enzyme, a mitochondrial enzyme that normally catalyzes the conversion of cholesterol to pregnenolone) levels in Leydig cells. From the immunology assays, a particular protein of interest is PPARγ: a peroxisome proliferator-activated receptor, which regulates fatty acid storage and glucose metabolism, also experienced decreased expression. The decrease in expression of these key receptors and enzymes are involved in

the downregulation of steroidogenesis, which may explain the observed physical effects in the mis-development of the male reproductive tract.[96]

Oxidized secondary metabolites of MEHP are the chemical agents responsible for reprotoxic effects in rodent models. Parks[98] investigated the mechanism by which DEHP affects transgenerational reproductive toxicity in a rat model. DEHP causes a decrease of testosterone (T) levels in male fetal and neonatal specimens upon maternal treatment with DEHP from gestation to postnatal day. Anogenital distance (AGD) was reduced by 36% in exposed male, but not in female specimens. After 20 days post-gestation, DEHP maternal exposure significantly reduced testicular mass. The authors note large, less dispersed clusters of Leydig cells (LC) in 3β-hydroxysteroid dehydrogenase (3β-HSD) staining in the testes of the treatment group than for the control. 3β-HSD is an enzyme responsible for converting androstenediol to testosterone. Using a human androgen receptor (hAR) transfected COS cell line, neither DEHP nor MEHP exhibited affinity for hAR receptor at concentrations up to 10 μM *in vitro*. An anti-androgenic effect is observed *in vivo*, but not *in vitro*, with DEHP or MEHP. This implies that the metabolites subsequently produced from MEHP, not MEHP itself, are the cause for developmental dysfunction of male sexual organs in the rat model, which can be transmitted in a transgenerational manner between mother and male fetus.

Foster et al.[93a] investigated phthalate esters and their effect on HepG2 cells transfected with AR and a reporter gene. Examination from testes of fetal rats indicated markedly lower T levels and increased Leydig cell abundance after phthalate exposure to pregnant female rats. Malformations of the epididymis, vas deferens, and hypospadias were observed in DEHP treated specimens. Anogenital distance was reduced in males, as in the study done by Parks et al.,[98] while a retention of thoracic nipples/areolae was also noted. Adenomas of Leydig cells were also observed to form approximately 100 days after birth. All male offspring with maternal treatment of DEHP experienced similar phenotypes, while the

mother exhibited no symptoms, despite treatment with DEHP. Neither DNBP, DEHP, nor their major primary metabolites (MEHP) interacted with human or rodent androgen receptors in transcriptional activation assays *in vitro*. Once again, evidence of the anti-androgenic effect of DEHP in male mammalian development points to the secondary metabolites of DEHP/MEHP as the toxic causative agent, in agreement with the study by Parks.[98]

Stroheker et al.[99] reported that neither DEHP nor MEHP appeared to be androgen receptor (AR) agonists in the breast cancer cell line MDA-MB453. Neither phthalate species antagonized dihydrotestosterone (DHT) activity on the MDA-MB453 cell line. However, when 5OH-MEHP and 5oxo-MEHP were tested, both oxidized metabolites of DEHP *were* anti-androgenic *in vitro*. Furthermore, the Hershberger assay was used on an immature castrated rat model, which examined the antagonism of DEHP on the testosterone propionate androgenic effect with respect to accessory sex organ development. The bulbocavernosus and levator ani muscles, prostate, and seminal vesicle masses were shown to decrease with increasing exposure of DEHP, while liver mass increased with exposure. Increase in liver mass may be correlated to the peroxisome proliferation effect DEHP has *in vivo*, which has been shown to cause hepatocellular tumors in rodent models.[87a] Therefore, concomitant with the observations made by Parks[98] and Foster,[93a] DEHP or MEHP acts as an anti-androgenic agent *in vivo*, while no androgenic effect is observed *in vitro*. The oxidized secondary metabolites of DEHP, 5OH-MEHP and 5oxo-MEHP, have an anti-androgenic effect *in vivo* due to the eventual metabolic breakdown of DEHP/MEHP into these anti-androgenic agents, while *in vitro*, there are no metabolic processes to produce the oxidized secondary metabolites from DEHP or MEHP: no anti-androgenic effect is observed. Ultimately, the studies done by Parks,[98] Foster,[93a] and Stroheker[99] demonstrate that DEHP and its monoester metabolite MEHP are not necessarily the major causative agent of illness: rather, the oxidized secondary metabolites post-hydrolysis may be the toxic agents, possessing anti-androgenic effects on developing male rodent models.

In terms of human exposure, urinary metabolites from DEP, DNBP, BBzP and DEHP were known to be highly prevalent in the population of the United States since 1999-2000, when the Nation Health and Nutrition Examination Survey (NHANES) first systematically quantified phthalate metabolites.[63] Higher concentrations of phthalate metabolites are commonly found in different sociodemographic populations, including children,[80] females,[100] non-white populations,[100b] and individuals of lower socioeconomic status.[101] From data gathered throughout the years, DEHP's action is known to be dose, time, gender, and age dependent.[87b] From the studies done on rats,[93a, 98-99] it is evident that two particularly vulnerable demographics for DEHP exposure are male children and pregnant women carrying a male fetus.

Infants and young children between 0.5 and 4 years of age consume more phthalate per kilogram of body weight than any other age demographic;[94] this is presumably due to oral exposure *via* toys and other childcare articles softened with DEHP. DEHP calculated exposure of children sucking or chewing toys and miscellaneous items reaches up to 0.085 mg/kg bw/day.[62] DINP exposures ranged from 0.005 to 0.040 mg/kg bw/day, with 99th percentiles reaching up to 0.183 mg/kg bw/day.[89] Adolescents younger than 19 years of age are the next second largest consumers of phthalates. In Canada, estimations of DEHP consumption for infants are 0.009 mg/kg bw/day, 0.019 mg/kg bw/day for toddlers, 0.014 mg/kg bw/day for children, and 0.006 mg/kg bw/day for adults.[102] In 2006, a European study found concomitant results with these statistics: exposure of DEHP and other phthalates through oral, dermal and inhalation pathways are statically higher in infants and toddlers than other age demographics.[103] In infants and toddlers, mean exposure of DINP and DIDP are calculated to be higher than the maximum exposure to any other phthalate, including DEHP. This is probably due to legislation by the European Union[64d] to ban the use of DEHP in toys and articles used by children, which was subsequently replaced with DINP and DIDP. The maximum exposure of infants and toddlers to DEHP and DINP is higher than 0.100 mg/kg

bw/day, mainly by mouthing of toys, and the ingestion of food and dust contaminated with these phthalates.[103] This level of exposure exceeds the recommended levels prescribed by panels in the European Union (CSTEE, ECB/EU) and Canada (Health Canada) for DEHP and DINP as shown in **Table 1.8**.

The high level of phthalate exposure to developing fetuses, infants, toddlers, and children has been shown to have an array of pre and postnatal developmental effects, notably in males. Low sperm counts, hypospadias, cryptorchidism, and testicular germ cell cancer are interrelated disorders comprising testicular dysgenesis syndrome (TDS), also known as phthalate syndrome.[91] TDS likely stems from environmental exposure of phthalates to pregnant women carrying a male fetus.[104] In 2005, Swan and co-workers[105] investigated the effect of prenatal environmental exposure to phthalates on human genital development. A relationship between anogenital distance (AGD) and maternal urinary concentrations of phthalate was noted. A standardized measure of AGD in 134 boys between 2 to 36 months of age was obtained, correlating penile volume with AGD. The authors created an anogenital index (AGI), which is defined as the AGD divided by the child's weight at examination. From here, an age-adjusted AGI by regression analysis was performed. Maternal prenatal urinary samples of 85 pregnant women were examined for four phthalate metabolites: monoethyl phthalate (MEP), mono-*n*-butyl phthalate (MNBP), monobenzyl phthalate (MBzP) and mono-*iso*butyl phthalate (MIBP), which were measured as predictors of AGD due to their inverse relation to age-adjusted AGI. After age adjustment, p-values were calculated for regression coefficients. For context, p-values test a null hypothesis of which the coefficient is equal to zero. If a p-value is less than 0.05, one can reject the null hypothesis, meaning that there is a meaningful addition to a statistical model. The authors obtained p-values for this metric ranging from 0.007 to 0.097. A summary phthalate score was defined to quantify the joint exposure to the four phthalates in the study. Ultimately, the data shows that the age-adjusted AGI decreased with increasing phthalate score. The authors report that the median

concentration of phthalate metabolites that are associated with a small AGI and incomplete testicular descent are below those found in 25% of the female population in the United States, and that the data support the hypothesis that prenatal exposure to environment phthalates can affect male reproductive tract develop in humans.[105]

Subsequently in 2008, Swan et al.[106] investigated AGD and other genital parameters in human infants with respect to phthalate exposure, as an extension to the 2005 study. Physical examination data of 140 boys and 153 girls was taken between the ages of 2 to 36 months of age. In this population subset, 75% of the subjects also had corresponding phthalate data from maternal urine. In this case, 106 mother-son pairs with urine data and AGD were investigated. In boys, mean AGD was 70.4 mm while in girls AGD averaged 47.3 mm: males possessed on average an AGD 49% longer than females. Mothers with DEHP urinary metabolite concentrations several times higher than average gave birth to boys with shorter AGDs compared to the mean. Residual AGD correlated with penile width and length was also calculated: penile width, not length, was significantly associated with concentration of the sum of DEHP metabolites and MEHP.[106] Of the boys in the study who possessed information on testicular location and phthalate concentrations (n = 119), 12 had incomplete testicular descent, representing 10% of the subset. Higher DEHP metabolite concentrations were correlated with a greater probability of incomplete testicular descent. Summary phthalate scores ranged from 0 to 15, with a median value of 9. Of the 29 boys with shorter AGDs, none were born to a mother with a low summary phthalate score.[106] In juxtaposition, 28 of the boys with longer than average AGD values, only 1 was born to a mother with a high phthalate summary score. Once again, the authors report that urinary phthalate metabolite concentrations in prenatal development of males have an effect on AGD, and transitively, on male genital development.

Studies on the effect of phthalates on human male development are scarce, as one cannot treat expecting human mothers with phthalates and observe if the newborn male

possesses malformations of the reproductive system. It is of utmost importance to understand the effects of phthalates on developing human males, therefore a method of investigating the effects of these endocrine disruptors was developed in a rodent model using xenographed human fetal testis tissue.[107] Heger and co-workers[108] investigated the effect of di-*n*-butyl phthalate (DNBP) on human fetal testis xenographed rats. *In utero* rat models exposed to phthalate are susceptible to multinucleated germ cell (MNG) induction and suppressed steroidogenic gene expression and testosterone production in the fetal testis.[108] Multinucleated germ cells in males are spermatozoa with more than one nucleus, where normally only a single nucleus exists.[109] In contrast, mice models exhibited only MNG induction, without any steroidogenic inhibition, supporting a species-specific sensitivity to phthalate mediated suppression of steroidogenesis in Leydig cells. The rationale behind the study was to investigate human fetal testis response to phthalates, on the premise of species specific responses. Fetal rat, mouse and human testes were xenographed into immunodeficient rodent hosts. These rodent hosts were not castrate-type specimens, and as a result, the presence of host testosterone may skew the results obtained during the study.[107] The xenographed specimens were dosed with DNBP in corn oil for up to 3 consecutive days. AGD was assessed by treating rodent hosts at 3 days *postnatal* with DNBP. The authors deem this method "*in utero*," however, this implies that the unborn rodent would be in the maternal host. AGD data shows reduction in rat, but not mouse postnatal models. Rats with xenographed fetal testicular tissue exhibited similar trends: fetal rat testes displayed MNG induction and suppressed gene expression of steroidogenic genes, while xenographed fetal mice testes experienced MNG induction without suppressed expression of steroidogenic genes. Xenographed fetal human testes exhibited similar results to the mice xenograph: induction of MNG without suppression of steroidogenic genes. Malformation of the seminiferous cords was observed, which is a result of MNG induction. The authors conclude "phthalate exposure of grafted human fetal testis altered germ cells but did not reduce expression of genes that regulate fetal testosterone biosynthesis."[108] The phthalate under

study was DNBP, which may not produce the same toxic secondary metabolites as DEHP, which have unequivocally been shown to be reprotoxic.[93a, 98-99] As a result, one cannot generalize to any phthalate, and a direct comparison of DNBP and DEHP in a species-specific study may not yield comparable results *in utero* or otherwise.

In a similar study by Mitchell and co-workers,[110] the effect of DNBP exposure on testosterone production by normally human fetal testis xenographs was investigated. The human fetal testes were xenographed into castrate nude mice, which were treated for 4 to 21 days with DNBP or MDBP. All mice were treated with human chorionic gonadotropin to mimic normal human pregnancy. As a control, rat fetal testis xenografts were exposed for 4 days to DNBP. The results show that human fetal testis xenographs have a high survival rate of approximately 80%. Total graft weight, serum testosterone levels, and seminal vesicle (SV) weight did not change in DNBP or MNBP treated specimens compared to xenographed mice without treatment with DNBP. Rat xenographed specimens experienced reduced SV weight and testis Cyp11a1/StAR expression, along with reduced testosterone levels.[110] The conclusion is that DNBP does not suppress testosterone production in human fetal testis xenographed specimens, while rat fetal xenographs are highly susceptible to the reprotoxic effects of DNBP. This conclusion is sound, as it does not generalize all phthalates as the same reprotoxic molecule. DNBP does indeed appear not to affect testosterone biosynthetic production in xenographed human fetal testes. However, the effect of DEHP on human xenographed specimens has not been investigated, and a direct comparison of DNBP to DEHP should not be made. The studies done by Heger[108] and Mitchell[110] indicate that DNBP may mechanistically affect germ and Sertoli cells differently: the anti-androgenic effects of DNBP on Leydig cell steroidogenic processes are not required to cause malformations in the seminiferous cord.[107] In a review, Spade[107] comments that the human fetal testis tissues utilized in the xenographed rodents were not from the range of gestational ages identified as in the “masculinization programing window,” where phthalates would have the greatest

impact on male reproductive tract development.[111] Therefore, studies utilizing the xenograft method with human male fetal testis cells from the proper masculinization programming window of development with DNBP, DEHP, and their respective oxidized secondary metabolites would more effectively exhibit the effects of these phthalates on human male development.

Desdoits-Lethimonier et al.[112] examined human male testis explants and NCI-H295R adrenocortical human cells cultured *in vitro* with DEHP or MEHP to investigate the effect that the phthalates would have on an organotypic adult human testis culture. Orangotypic culturing, also known as *ex-vivo* 3D culturing, involves explanting human testis tissue from prostate cancer patients in a cube, into a polyethylene terephthalate insert at the interface of air and culturing media. This maintains the three-dimensional organization of cells and extracellular matrix within the organ or tissue, giving a more accurate depiction of the subcellular biological system being investigated.[113] In this study, the culturing media, Dulbecco's modified Eagle's medium, contained DMSO as a control, or DEHP at different concentrations. In both human male testis explant and NCI-H295R cells, lower testosterone levels were observed. INSL3 production by Leydig cells were not affected after incubation. Reduction in fetal expression of INSL-3 is commonly associated with testicular dysgenesis syndrome.[97] The unaffected INSL-3 production implies that DEHP and MEHP effect solely steroidogenic pathways. Inhibin B production by Sertoli cells was also unaffected by DEHP or MEHP. Sertoli cells are somatic cells of the testis that are key in testis formation and spermatogenesis.[114] Inhibin B is a protein complex that downregulates follicle stimulating hormone (FSH) secretion *via* a negative feedback loop. There is a strong positive correlation of serum inhibin B levels with testicular volume and sperm counts.[115] Low DEHP and MEHP concentrations were reported in the human testis explant. Again, it is probable that the oxidized secondary metabolites of MEHP are responsible for the reprotoxic effects observed in mammals. The paper concluded: "the DEHP-induced inhibition of testosterone production

by our models most probably results from the activities of MEHP and 5OH-MEHP. The decline in the anti-androgenic effects observed after 48 hours of culture most likely results from this biotransformation."[112] Overall, the study provides direct evidence that DEHP is able to suppress human testicular steroidogenesis.

1.8 Phthalate Plasticizer Alternatives for PVC

There is unequivocal evidence that phthalates, most notably DEHP, have adverse health effects on young developing human males. Phthalate exposure from multiple modalities during gestation results in testicular dysgenesis syndrome, which can lead to infertility, hypospadias, cryptorchidism, and testicular germ cell cancer later in life. The reprotoxic effects of DEHP outweigh its benefits as an efficient plasticizer for PVC. Global bans of DEHP by the European Union (EU)[64] and the United States[65] in children's articles, along with restrictions in other items has spurred the development and implementation of less toxic PVC plasticizer alternatives.[9] Examples of these alternative plasticizers include terephthalates,[116] citrates,[117] trimellitates,[118] succinates,[119] sebacates,[120] and isosorbates.[121] While these purportedly less toxic plasticizers are used to soften PVC, they all share a common detriment with phthalates: they migrate and leach out of PVC.

Plasticizer migration and leaching is most effectively prevented through covalent attachment of a plasticizer to PVC,[62-63] also known as internal plasticization. In the case of phthalates, DEHP leaching has led to ubiquitous contamination of materials and solvents used in the laboratory setting.[122] Grob and Fankhauser-Noti[123] noted the pervasive contamination and concurrent interference of laboratory equipment measurements with DEHP and DNBP from plastic articles, solvents, and air. Marega et al.[124] examined the absorption of phthalates from the laboratory air on the outer wall of the syringe needle, which contributes to blank problems during gas chromatography-mass spectroscopy (GC-MS) injections. Oca and co-workers[125] expressed the challenge in determining the presence of

plasticizers and other additives from plastic materials, when the substances were already present in the laboratory environment, leading to contamination of their equipment and results.

Another factor to consider with an internally plasticized PVC system is longevity of the PVC item. When a plasticizer migrates out of the PVC matrix, the original physical properties imparted by the plasticizer are decreased, and leads to degradation of the plastic over time. Ito and Nagai[126] artificially weathered plasticized PVC sheets by irradiation *via* a xenon discharge lamp with a cyclic spray of distilled water and thermal degradation at 100 °C. A decrease in tensile strength was noted, along with a decrease in DEHP concentration after 600 hours of xenon irradiation. Prodigious DEHP migration between 1000 and 2000 hours of irradiation was observed.[126] Thermally mediated migration of DEHP occurred, but not to the extent of xenon irradiation. Degradation of DEHP was not noted by GC-MS analysis. Chen and co-workers[127] noted the migration of DEHP from PVC following shortwave ultraviolet radiation (UV, 254 nm), resulting in increased hydrophilicity with longer exposure times. DEHP migration out of PVC were determined by extracting DEHP-PVC films after different irradiation times, then subsequently analyzing the solutions *via* high-pressure liquid chromatography (HPLC). DEHP migrated out of PVC while forming MEHP and phthalic acid after shortwave UV exposure.

The requirement of a non-migratory plasticizer for PVC is crucial: deleterious health effects for humans and wildlife, environmental contamination, and loss of desirable properties over time with conventional externally plasticized PVC systems are all prevalent reasons to develop covalently bound PVC systems. Recent efforts have been explored to create internal plasticizers that prevent the migration of emollients out of flexible PVC. Three tethering strategies are presented in the literature: 1) thioether, 2) amine (using natural product derived plasticizers), and 3) azide-alkyne cycloaddition.

1.9 Thioether Internally Plasticized Poly(vinyl chloride) (PVC)

The requirement for non-leaching poly(vinyl chloride) (PVC) plasticizers globally has spurred the recent development of novel, internally plasticized poly(vinyl chloride) systems. In 1982, Martinez and co-workers[128] developed a methodology to perform S_N2 nucleophilic substitution on PVC using sodium thiophenolate (**Figure 1.10**). This method involved preparing sodium thiophenolate using purified sodium and thiolphenol in refluxing *p*-xylene. The S_N2 reaction was performed by dissolving the sodium thiophenolate in cyclohexanone. Next, PVC was dissolved in another portion of cyclohexanone and combined with the thiolphenolate solution at -15 °C under an inert atmosphere ranging from 1 to 240 hours. Substitution was confirmed by UV-Vis spectroscopy. This initial study demonstrated that S_N2 substitution occurs on the PVC chain in three different regimes with decreasing rate constants. Subsequently, in 1986, Michel et al.[129] utilized 2-ethylhexyl esters of thiosalicylate **1.2** and thioglycolate **1.3** as plasticizing agents *via* nucleophilic substitution of the chlorine atoms in PVC. Final products contained thioether grafted (*g*) thiosalicylate and thioglycolate esters (**Figure 1.11**). In this investigation, the authors performed nucleophilic substitution reactions on poly(vinyl chloride) with thiolates **1.2**

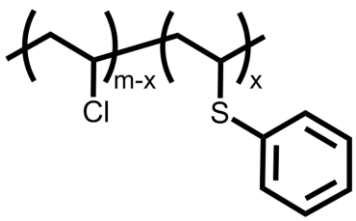

Figure 1.10 PVC Bearing Thiophenol[128]

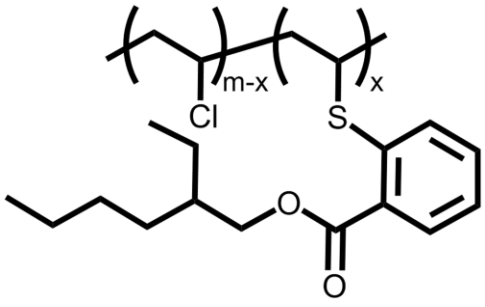

1.2 PVC-*g*-2-Ethylhexyl Thiosalicylate

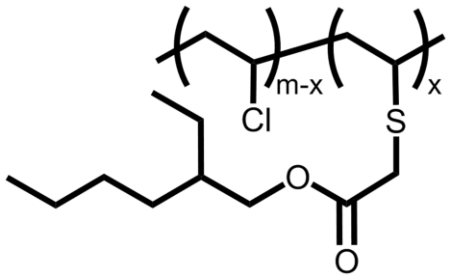

1.3 PVC-*g*-2-Ethylhexyl Thioglycolate

Figure 1.11 Structures of Michel's PVC Thiolate Derivatives of 2-Ethylhexyl Esters[129]

and **1.3** using thermomechanical treatments simulating industry operations with the aid of a HAAKE™ Rheomix 600 internal mixer. Solution substitution reactions were carried out for these two reagents at 160 °C in cyclohexanone with a modified version of their previously described method.[128] The authors describe decreasing glass transition temperatures (T_g) with increasing nucleophilic substitution of the chlorine atoms on PVC, as shown in **Table 1.9** below:

Sample	Nucleophile	Mol% of Nucleophile	T_g (°C)
10	Sodium 2-Ethylhexyl Thiosalicylate	0.018	66.0
11	Sodium 2-Ethylhexyl Thiosalicylate	0.082	66.0
12	Sodium 2-Ethylhexyl Thiosalicylate	0.150	59.0
13	Sodium 2-Ethylhexyl Thioglycolate	0.154	55.5
14	Sodium 2-Ethylhexyl Thioglycolate	0.126	63.3
15	HSR (Non-Grafted Thioglycolate)	0.066	13.4
16	HSR (Non-Grafted Thioglycolate)	0.102	10.0
17	HSR (Non-Grafted Thioglycolate)	0.153	17.4

Table 1.9 Michel's PVC Thiosalicylate and Thioglycolate Thermal Data[129]

As a reference, the T_g of unmodified PVC is 83 °C.[130] Sample 12, containing approximately 15 mole percent of the 2-ethylhexyl thiosalicylate ester gave a T_g of 59.0 °C, while sample 13, containing a similar mole percent of the 2-ethylhexyl thioglycolate ester gave a T_g of 55.5 °C. The depression in T_g can be justified by the presence of a rigid aromatic ring in the thiosalicylate; the aromatic ring may impart rigidity to PVC, which will inherently increase the T_g over a covalently bound plasticizer without an aromatic group. In juxtaposition, non-grafted 2-ethylhexyl thioglycolate ester mixed with PVC exhibited the lowest glass transition temperatures, as demonstrated by samples 15, 16, and 17, yielding T_g values of 10.0 °C to 17.4 °C. The non-covalently bound thioglycolate esters gave the lowest T_g values, presumably due to more degrees of freedom for the plasticizer to move and create free volume within the PVC matrix, relative to the covalently bound species.

In 2008, Reinecke et al.[131] described an aromatic thiol substitution system, based on work previously done by Martinez[128] and Michel.[129] In a similar vein, Reinecke performed S_N2 substitution of the chlorine atoms on PVC with different derivatives of sodium thiophenolate

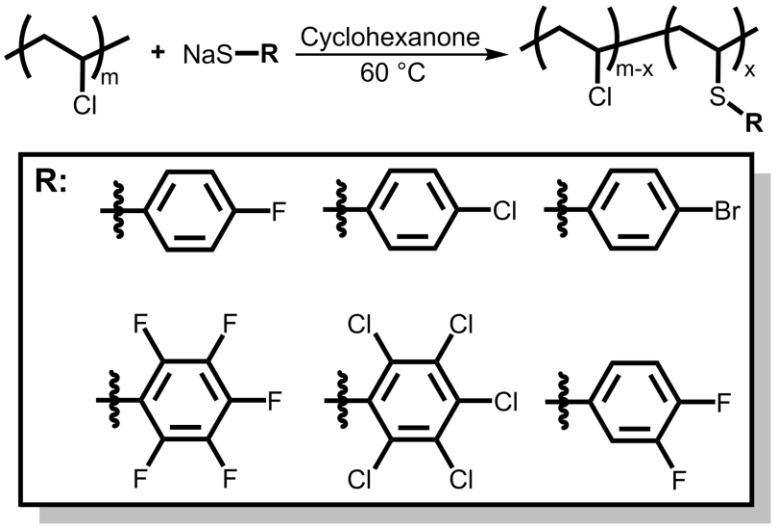

Scheme 1.5 Reinecke's Modification Reaction of PVC with Halogenated Thiolates[131]

(**Scheme 1.5**). In this formative demonstration, Reinecke reported that a myriad of halogenated thiolates were a ble to modify PVC without side reactions, such as elimination. Changing the halogen atoms present on the aromatic ring altered the final degree of substitution; the 4-bromo-thiophenol derivative exhibited the fastest reaction times while obtaining the highest degree of modification to PVC relative to other halogenated derivatives. However, when using potassium carbonate as a base, the reactivity of the thiolates invert: the highest degree of modification is achieved using the 4-fluoro-thiophenolate derivative.[131] This tendency relates to the acidity of the thiol, which in turn correlates to nucleophilicity of the thiolate; the thiolate anion is further stabilized by induction *via* fluorine versus bromine. Conceptually, this justifies why the brominated derivative is more nucleophilically reactive under neutral conditions, and the fluorinated derivative is more active under basic conditions. Interestingly, the authors noted that at short reaction times under neutral conditions, the fastest reacting species was the 4-fluoro derivative. This may be attributed to the physically larger size of the other halogenated derivatives over the 4-fluoro substituted ring, and may support the observed kinetic effect. In this study, the authors were clearly not attempting to plasticize PVC: rather, this study prototypically demonstrated the substitution properties of the thiophenol system before moving to plasticizing derivatives. Glass transition temperatures

were measured, displaying relatively minute changes ranging from 85.4 °C (in the case of 12 mol% PVC-F5-Thiophenolate) to 54.3 °C (in the case of 55 mol% PVC-F-Thiophenolate).

Subsequently, Reinecke et al.[132] investigated the possibility of internally plasticizing PVC utilizing mercapto-phthalate derivatives. In a three step synthesis, the desired 2-ethylhexyl-mercapto-phthalate derivatives were obtained (**Scheme 1.6**).

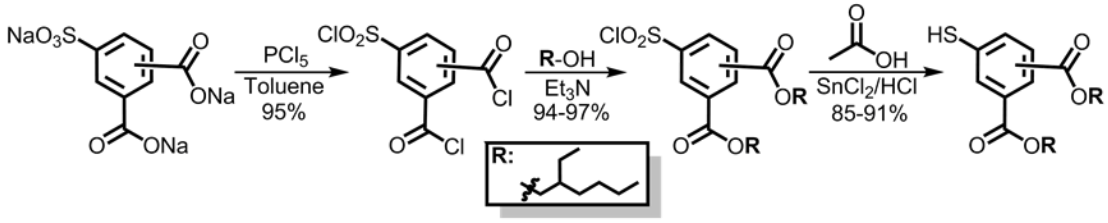

Scheme 1.6 Synthesis of Mercapto-Phthalate Derivatives[132]

First, acid chloride activation of the carboxylate salt was performed, allowing the concurrent formation of the 2-ethylhexyl ester and chlorosulfone. The chlorosulfone was reduced to the mercapto-phthalate by tin(II) chloride, hydrochloric and acetic acid. Two 2-ethylhexyl-mercapto-phthalate derivatives were obtained, DEHP-SH **1.4** and ^{iso}DEHP-SH **1.5** (**Figure 1.12**).

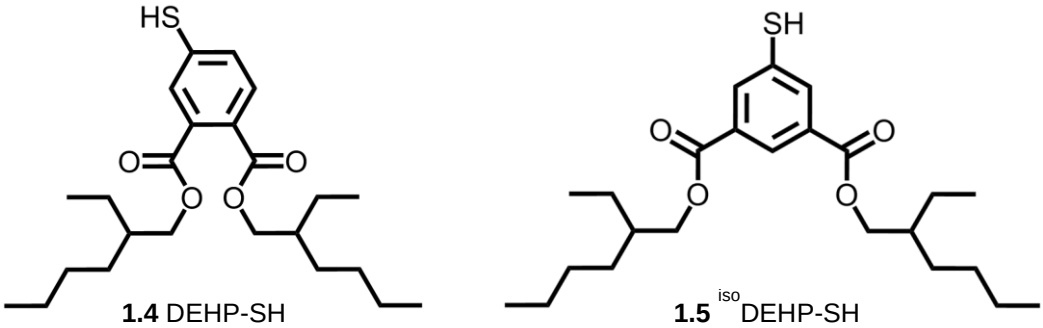

1.4 DEHP-SH **1.5** ^{iso}DEHP-SH

Figure 1.12 Reinecke's Mercapto-Phthalate Derivatives[132]

Once the 2-ethylhexyl-mercapto-phthalates were obtained, PVC, cyclohexanone and potassium carbonate were collectively stirred at 60 °C with either **1.4** or **1.5** to yield thioether-tethered 2-ethylhexyl-phthalate functionalized PVC (**Scheme 1.7**).

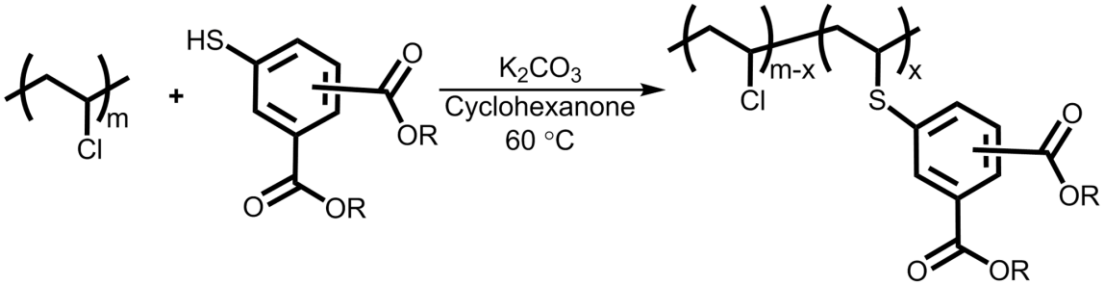

Scheme 1.7 PVC S_N2 by Mercapto-Phthalate Derivatives[132]

The nucleophilic substitution of DEHP-SH with PVC was characterized by ^{1}H-NMR, noting an increase in proton shifts at 7.0-8.0 ppm, indicating the presence of the aromatic group present in DEHP-SH. A simultaneous increase in aliphatic proton shifts between 0.5-1.8 ppm was also observed, due to the presence of 2-ethylhexyl chains in the plasticizing moiety. No olefinic proton shifts were observed, which indicates the absence of deleterious elimination reactions on the backbone of PVC. Under the optimized reaction conditions, the amount of mercapto-phthalate substituted onto PVC was 23 mole percent (DEHP-SH-PVC) and 31 mole percent (^{iso}DEHP-SH-PVC), giving T_g values of 0 °C and 20 °C, respectively. These low T_g values require a large mole percent of mercapto-phthalate to plasticize effectively. In contrast to the industry standard DEHP-PVC blend, 14.8 mol% DEHP gives a T_g of -35 °C.[130] Migration studies of the covalently bound thioether-linked plasticizer with *n*-heptane exhibits no detectable amount of DEHP-SH in solution, while the standard DEHP-PVC mixture experiences near complete extraction of DEHP within 3 hours from PVC.

The Reinecke group[133] further developed the use of thiophenolates in 2016, utilizing aliphatic non-phthalate analogs toward plasticizing PVC. The authors employed acid chloride

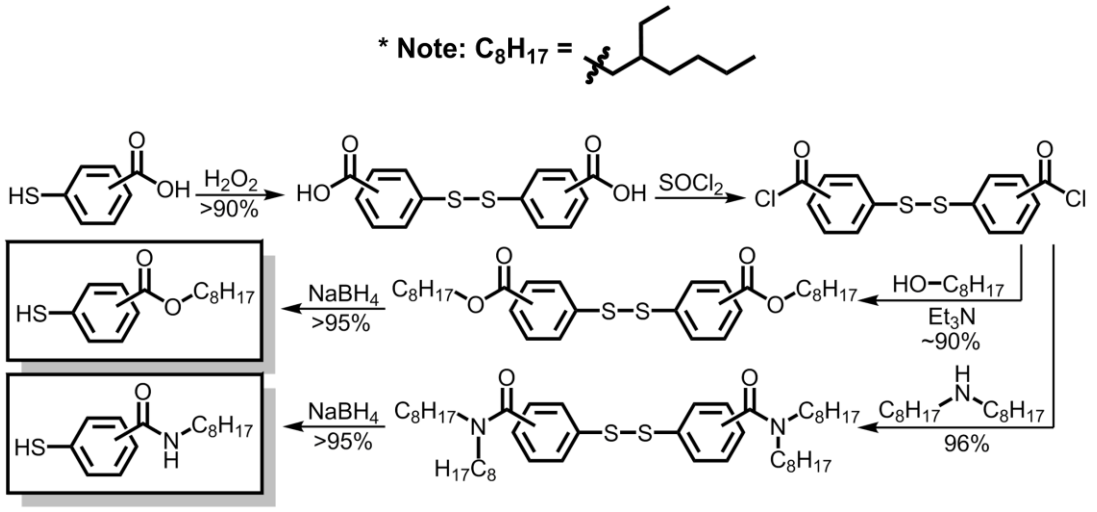

Scheme 1.8 Acid Chloride Mediated Synthesis of Thiophenol Based Plasticizer[133]

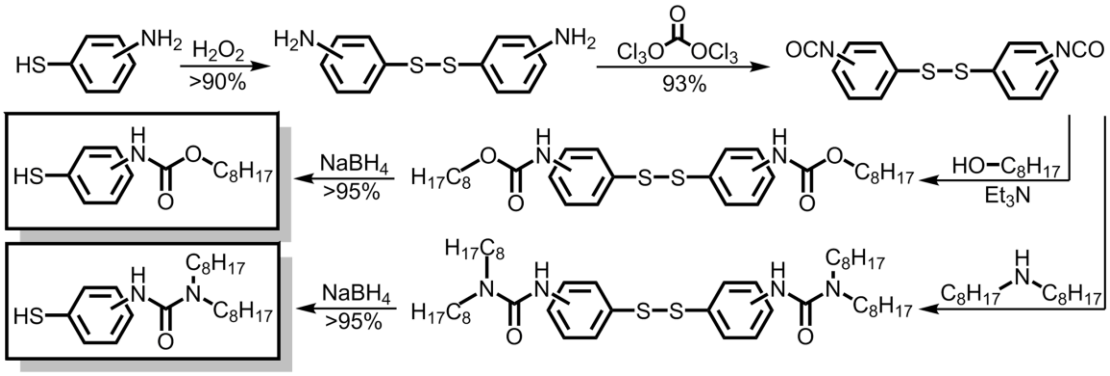

Scheme 1.9 Isocyanate Mediated Synthesis of Thiophenol Based Plasticizer[133]

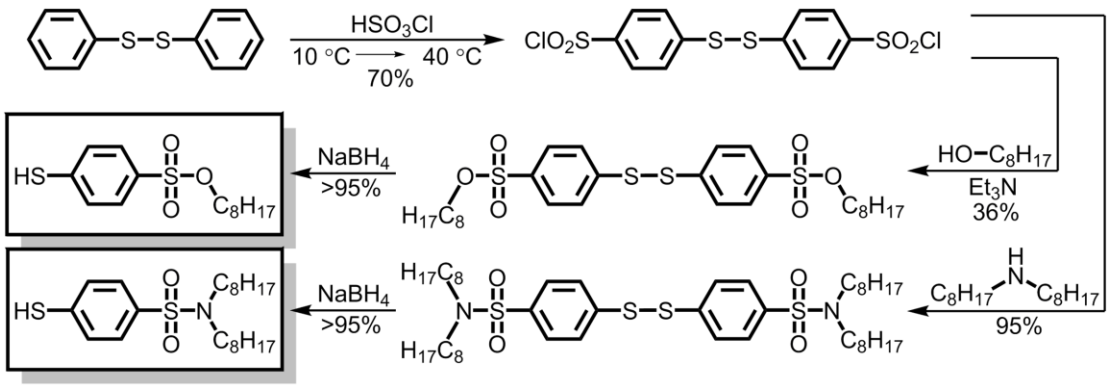

Scheme 1.10 Chlorosulfonyl Mediated Synthesis of Thiophenol Based Plasticizer[133]

(**Scheme 1.8**), isocyanate (**Scheme 1.9**), and chlorosulfonyl (**Scheme 1.10**) functional groups as intermediates in the synthesis of the thiolphenol plasticizer.[133] Subsequently, these aliphatic thiophenol plasticizers were treated with an equimolar amount of sodium hydroxide in dry ethanol, transforming the thiolphenols to the thiolate salts. The salt solution was added to another reaction flask containing PVC dissolved in a 4:1 mixture of acetone/tetrahydrofuran, and heated for 2 hours at 85 °C, as shown in **Scheme 1.11**.

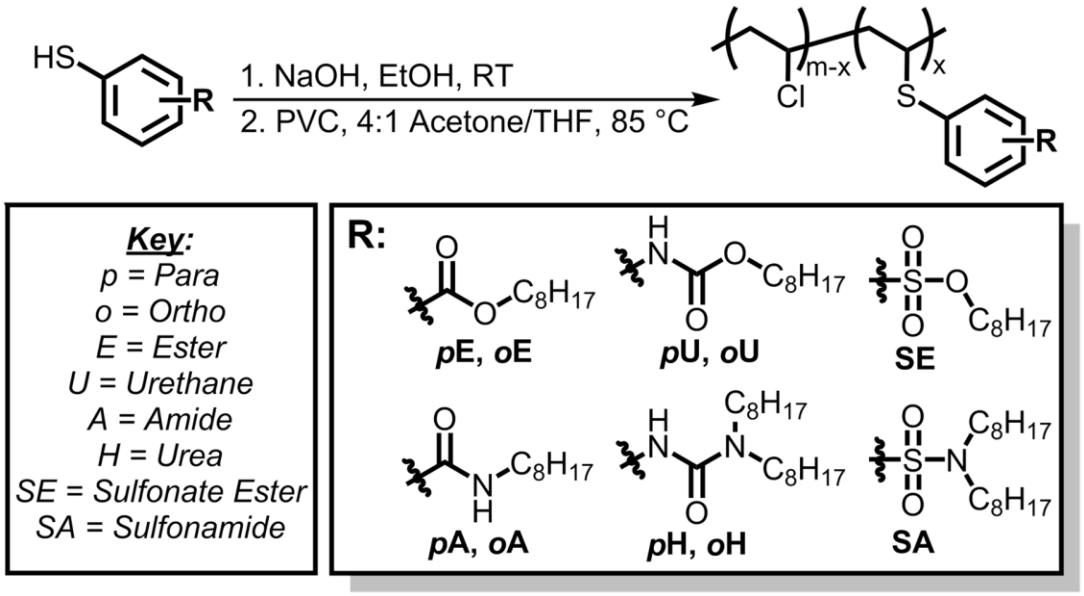

Scheme 1.11 S_N2 by Aliphatic Thiolate Derivatives on PVC[133]

PVC was treated with 20 and 40 weight percent aliphatic thiolate, yielding ten polymer types, with a grand total of twenty polymers. Nucleophilic substitution of the chlorides on PVC was not quantitative, as shown in **Table 1.10**. The degree of modification was determined *via* ^{1}H-NMR, by comparing the aliphatic region in the plasticizer (~0.9 ppm) to the methane protons (C**H**Cl) on PVC at 4.5 ppm. Anchorage efficiency was defined as the degree of modification divided by the total weight percentage expected. Efficiency of the substitution reaction by thiophenolates ranged from 69.5% to 97%. The sulfonic ester derivative (**SE**) did not undergo significant substitution due to the strong electron withdrawing character of the sulfonic ester,

Polymer	Modifier in Mixture (Wt %)	Covalently Bound Modifier (Wt %)	Degree of Anchorage (%)	T_g (°C)
*o*E	20	14.4	72.0	55
	40	34.1	85.2	35
*o*A	20	18.5	92.5	56
	40	37.8	94.5	37
*p*E	20	18.7	93.5	51
	40	38.8	97.0	29
*p*A	20	18.6	93.0	53
	40	38.8	97.0	32
*o*U	20	13.9	69.5	54
	40	32.2	77.0	38
*o*H	20	14.8	74.0	62
	40	30.8	77.0	41
*p*U	20	13.9	69.5	53
	40	31.2	78.0	39
*p*H	20	17.2	86.1	60
	40	35.1	87.8	33
SE	20	Unreported	Unreported	-
	40	Unreported	Unreported	-
SA	20	15.1	75.5	49
	40	36.3	90.8	28

Table 1.10 Reinecke's Aliphatic Thiolphenol PVC Results[133]

which inherently decreases the nucleophilic character of the thiolate. Ester and amide derivatives were efficient nucleophiles, generally achieving anchorage efficiencies greater than 90%, with the exception of the *ortho*-ester (***o*E**) due to steric hindrance of the *ortho*-positioned aliphatic chain relative to the thiolate. Urethane and urea derivatives experienced lower anchorage efficiencies, stemming from the electron withdrawing character of these functional groups. As expected, glass transition temperatures decrease as the weight percent of plasticizer increases. The *para*-ester (***p*E**) derivative at 40 weight percent gave a T_g of 29 °C, while the sulfonamide derivative (**SA**) at approximately the same weight percent gave a T_g of 28 °C. Despite lower glass transition temperatures compared to unmodified PVC, deficiencies in plasticization efficiency compared to traditional DEHP-PVC blends were observed, due to the inherent nature of having a plasticizer covalently bound to PVC. According to the authors, this may induce rigidity to those chain segments in which the bulky additive is attached.[133]

In subsequent studies by the Reinecke group,[133-134] a one-pot approach using trichlorotriazine chemistry to internally plasticize PVC was published in 2016. Trichlorotriazine (TCTA, **Scheme 1.12**) according to the authors, is an interesting and versatile substance, as it contains three chlorine atoms of different reactivities.[135] This, in theory, would allow one to selectively substitute different nucleophiles in a stepwise manner on the heterocyclic molecule. Synthetically, two equivalents of aliphatic amine were linked to TCTA, while the third chlorine was transformed to the thiouronium salt, which is subsequently hydrolyzed into the thiolate functionality used for PVC functionalization (**Scheme 1.12**).

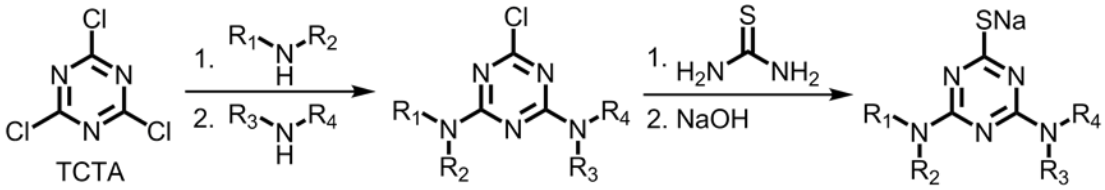

Scheme 1.12 Preparation of TCTA-Based PVC Plasticizers[133-134]

After the thiolate triazine derivative was prepared, the crude reaction mixture was poured into a sealable flask with the desired amount of PVC under nitrogen, and heated at 85 °C for 2 hours (**Scheme 1.13**). The authors claim that the sealed flask contained only modified PVC with NaCl dissolved in acetone after reaction completion. The final polymer was obtained by casting the acetone solution or by precipitation in methanol/water.

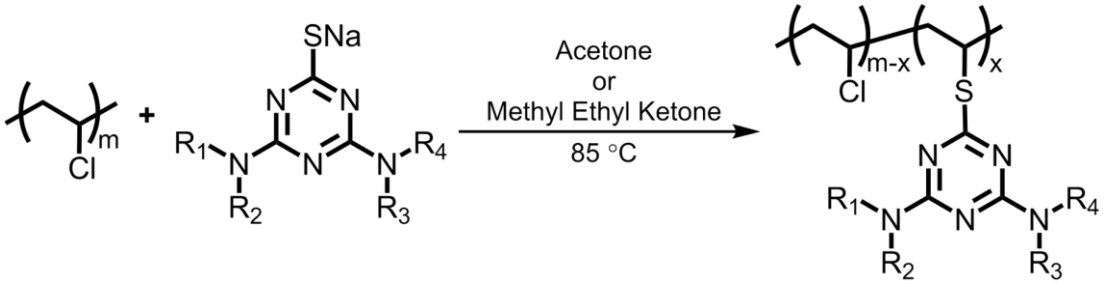

Scheme 1.13 Reinecke's Attachment of Thiolate Triazine to PVC[133-134]

In the first study,[133] five aliphatic thiolate triazine derivatives were synthesized with 20 and 40 weight percent plasticizer, relative to PVC. In the second study,[134] six unique polymeric derivatives were synthesized in the same manner as the first study.[133] The ^{1}H-NMR spectra of the polymers showed increased signal in the aliphatic region and at 3.4 ppm (which is presumably the methylene signal adjacent to the methane bearing the aromatic heteroatom linkage). **Figure 1.13** is a graphical representation of the functional group abbreviations. **Table 1.11** summarizes the polymers obtained in the studies.[133-134]

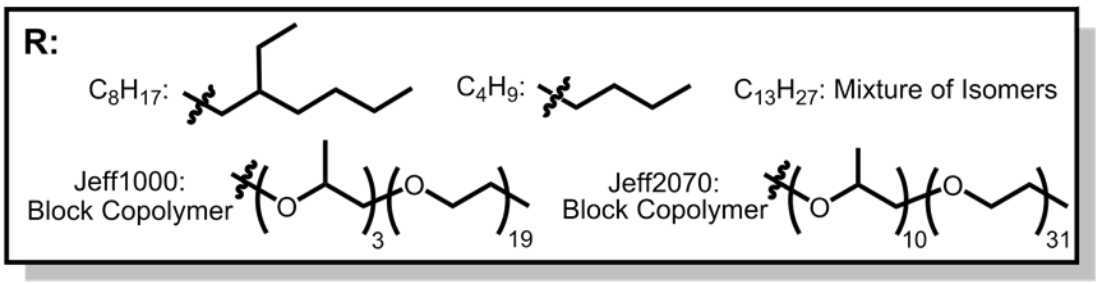

Figure 1.13 Functional Groups Utilized in TCTA-PVC Investigation[133]

Polymer	R1	R2	R3	R4	Modifier in Mixture (Wt %)	T_g (°C)
1	C_8H_{17}	C_8H_{17}	C_8H_{17}	C_8H_{17}	20	43
					40	35
					55	27
					75	22
2	C_4H_9	C_4H_9	C_4H_9	C_4H_9	20	72
					40	55
3	$C_{13}H_{27}$	$C_{13}H_{27}$	C_4H_9	C_4H_9	20	54
					40	35
4	H	C_8H_{17}	C_8H_{17}	C_8H_{17}	20	47
					40	31
5	H	Jeff1000	C_4H_9	C_4H_9	20	14
					40	-17
6	H	Jeff2070	H	Jeff2070	20	10
					40	-22
7	O (Ether)	C_2H_5	C_8H_{17}	C_8H_{17}	20	43
					40	37
8	O (Ether)	C_8H_{17}	O (Ether)	C_8H_{17}	20	-
					40	-
9	S (Thioether)	C_8H_{17}	S (Thioether)	C_8H_{17}	20	-
					40	-

Table 1.11 Reinecke's TCTA-PVC Plasticizer Results[133-134]

To clarify, polymer samples **8** and **9** did not completely covalently attach to PVC, according to ^{1}H-NMR. As a result, thermal data was not obtained on these polymers. The authors observed that only amine substituted thiolate triazine examples were quantitatively attached to PVC. For polymer **1** (also shown in **Table 1.10**), T_g values at 20 weight percent and 40 weight percent were 43 °C and 35 °C, respectively. Maximum plasticization occurs at 75 weight percent plasticizer to PVC (22 °C). Results for polymer **2** are not improved from polymer **1**, with modest T_g depressions of 72 °C and 55 °C for 20 and 40 weight percent, respectively. Polymers **3**, **4**, and **7** did not see improved T_g values over polymer **1**. However, polymer **5**, which contains the polyether Jeff1000, displayed marked improvements in T_g values at both 20 (14 °C) and 40 (-17 °C) weight percent. Polymer **6** (Jeff2070) exhibited the lowest T_g values, with 20 weight percent yielding 10 °C, while 40 weight percent displayed an impressive -22 °C. It is clear that the Jeffamine-TCTA derivatives were the most effective in this series at internally plasticizing PVC. The polyether chains effectively depress T_g values over any alkyl derivative at an equivalent weight percent of plasticizer. As an interesting comparison, polymers **5** and **6** show the expected T_g depressions, with an increase in molecular weight of the plasticizer, at an equivalent weight percent relative to PVC. In a mole percent perspective, the TCTA derivative utilized in polymer **6** is the most effective plasticizer, as its higher molecular weight (approximately four times) over the TCTA derivative in polymer **5** makes it a more efficient plasticizer per molar unit, requiring less thiol substitution sites on PVC to achieve similar glass transition temperatures. One can take away from this study that a large polyether plasticizer should increase plasticization efficiency over alkyl counterparts while imparting desirable plasticization properties to PVC, with fewer substitution sites.

In light of the promising plasticizing efficiency of polyether plasticizer systems demonstrated in the initial TCTA studies,[133-134] Reinecke and co-workers[130] published a subsequent paper focusing on the ubiquitous issue present in all covalently bound plasticizer systems: decreased plasticizer efficiency due to induced rigidity of segments where the

plasticizer is linked. The authors claim that compatibility of the plasticizer with PVC should play a key role in increasing plasticizing efficiency.[130] The greater the compatibility of the plasticizer with the polymer, the higher the tendency for the plasticizer to interrupt chain-chain interactions, which in theory, should yield a material with superior malleability and flexibility. The use of TCTA, in combination with poly(propylene oxide) (PPO) and poly(ethylene oxide) (PEO) oligomers as a plasticizing entity for PVC were investigated.[130] These TCTA based plasticizers employ JEFFAMINEs™, which are amine terminated block copolymers of poly(propylene oxide) and poly(ethylene oxide) with specified molecular weight ranges.[136] The synthetic route taken by the authors was essentially identical to their previous work[133-134] (**Scheme 1.12, Scheme 1.13**), with the quintessential difference being the utilization of JEFFAMINEs™ varying from 600 to 3085 molecular weight.[130] It is worth mentioning that Jeff600 and Jeff2005 are considered hydrophobic, while Jeff1000, Jeff2070, and Jeff3085 are considered hydrophilic, according to the manufacturer, Huntsman Corporation.[136] Poly(ethylene oxide) is completely miscible with PVC, while poly(propylene oxide) is somewhat immiscible with PVC.[137] The intention of Reinecke's study[130] was to determine the influence of molecular weight and composition on the efficiency of the covalently linked plasticizer system with polyethers. The PPO/PEO monoamines, along with a representative structure of the modified PVC are presented in **Figure 1.14**. A full set of data for the JEFFAMINE™ TCTA thiophenol plasticizers is provided with all T_g values (**Table 1.12**).

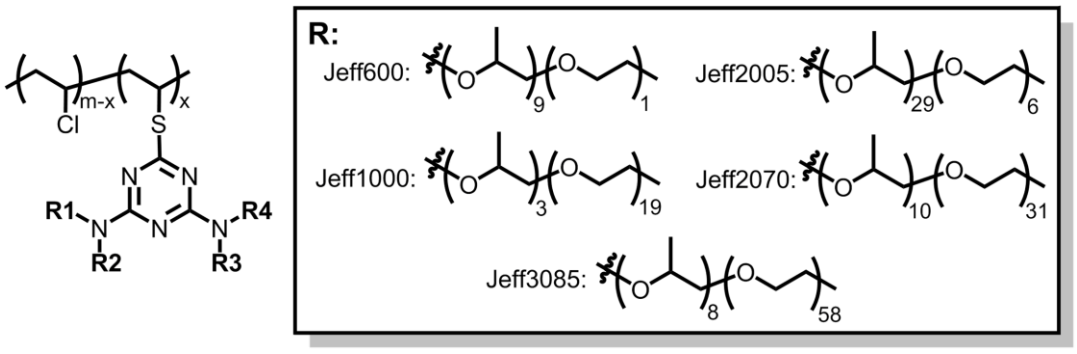

Figure 1.14 PVC-TCTA JEFFAMINE™ Structures[130]

Modifier	R1	R2	R3	R4	MW (g/mol)	Modifier in Mixture (Wt %)	Mol%	T_g (°C)
Bis-600	Jeff600	H	Jeff600	H	1310	16	0.90	47
						22	1.33	38
						29	1.91	27
						39	2.96	7
						48	4.22	9
						64	7.82	-9
Mono-600	Jeff600	H	*n*-C_4H_9	*n*-C_4H_9	840	21	1.94	55
						30	3.09	40
						40	3.82	24
						47	6.19	22
Bis-1000	Jeff1000	H	Jeff1000	H	2100	18	0.65	35
						28	1.14	24
						32	1.39	12
						38	1.79	0
						45	2.34	-18
						73	7.44	-41
Mono-1000	Jeff1000	H	*n*-C_4H_9	*n*-C_4H_9	1240	21	1.32	36
						27	1.83	25
						42	3.52	4
						49	4.62	-5
Bis-2005	Jeff2005	H	Jeff2005	H	4100	13	0.27	56
						19	0.36	67
						28	0.59	61
						35	0.81	57
						45	1.23	43
Mono-2005	Jeff2005	H	*n*-C_4H_9	*n*-C_4H_9	2240	13	0.41	68
						19	0.65	46
						33	1.35	38
Bis-2070	Jeff2070	H	Jeff2070	H	4250	13	0.22	48
						19	0.34	36
						22	0.41	26
						29	0.60	10
						40	0.97	-16
						62	2.35	-50
Mono-2070	Jeff2070	H	*n*-C_4H_9	*n*-C_4H_9	2310	26	0.94	27
						33	1.32	23
						42	1.92	-5
						56	3.33	-20
Bis-3085	Jeff3085	H	Jeff3085	H	6280	8	0.09	59
						14	0.16	43
						18	0.22	33
						26	0.35	16
						34	0.53	-2
						62	1.60	-46

Table 1.12 Reinecke's JEFFAMINE™ PVC-TCTA Plasticizer Results[130]

Relative to previous studies, the JEFFAMINE™ TCTA derivatives exhibit excellent low glass transition temperatures, which imply that these covalently modified PVC samples are malleable and flexible. Comparing traditional DEHP-PVC T_g values (**Table 1.13**) to the JEFFAMINE™ system (by wt%) reveals an equivalent plasticizing efficiency to free DEHP.

Modifier	MW (g/mol)	Modifier in PVC (Wt %)	Mol%	T_g (°C)
DEHP	390	0	0	83
		21	4.1	28
		32	7.0	12
		43	10.8	-24
		52	14.8	-35
		57	17.5	-43
		78	36.2	-70

Table 1.13 Non-Covalent DEHP-PVC Standard Mixture Data[130]

As a standard, at 21 weight percent, DEHP-PVC gives a T_g of 28 °C. At similar weight percentages, T_g values for the novel JEFFAMINE™ system are near DEHP-PVC values: Bis-2070 (22 wt%, 26°C), Mono-2070 (26 wt%, 27 °C), and Bis-3085 (18 wt%, 33 °C). At a higher weight percent of 32, DEHP-PVC shows a T_g of 12 °C. With the JEFFAMINE™ system, Bis-1000 (32 wt%, 12 °C), Bis-2070 (29 wt%, 10°C) and Bis-3085 (34 wt%, -2 °C) show equivalent or lower T_g values when compared to DEHP-PVC at approximately the same weight percentage of plasticizer. Analogous trends continue at higher weight percentages of JEFFAMINE™ TCTA plasticizer. Also noteworthy is the overall composition of these novel polyether plasticizers. In all instances, the major constituent of the most efficacious plasticizer derivatives is poly(ethylene glycol), not poly(propylene glycol). Hydrophobic JEFFAMINE™ analogs (Jeff600, Jeff2005) containing predominantly poly(propylene glycol) do not display comparable glass transition temperatures to DEHP-PVC. These derivatives are inefficient plasticizers, likely due to the incompatibility of PVC with poly(propylene oxide).[137] Clearly, miscibility of the plasticizer is essential for effective plasticization with PVC, especially when covalently bound to the backbone of the polymer. Another interesting trend shows that the greater the molecular weight of the plasticizing species, the more efficient the plasticizing

efficiency relative to smaller, yet higher mole percentage plasticizer, despite an equivalent weight percent in PVC. The “Bis” derivatives displayed an overall better plasticizing efficiency over the “Mono” functionalized plasticizers. These trends are shown for PVC-TCTA Jeff600 (**Figure 1.15**), PVC-TCTA Jeff1000 (**Figure 1.16**), and PVC-TCTA Jeff2070 (**Figure 1.17**).

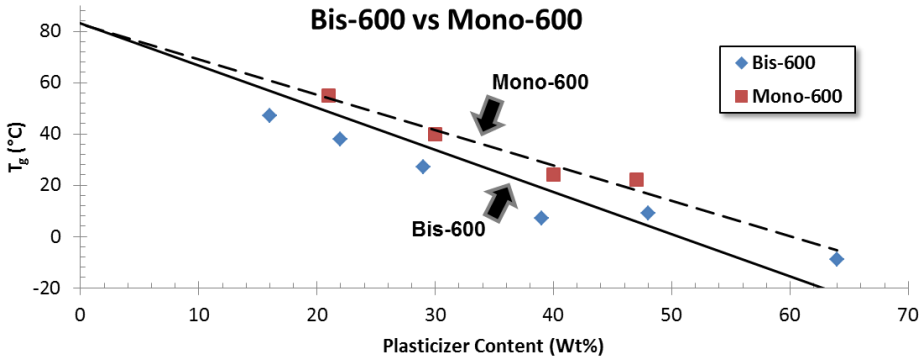

Figure 1.15 PVC-TCTA Jeff600 Comparison[130]

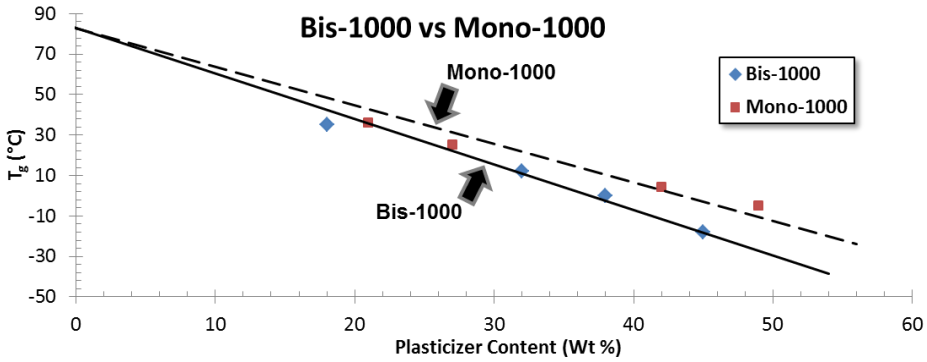

Figure 1.16 PVC-TCTA Jeff1000 Comparison[130]

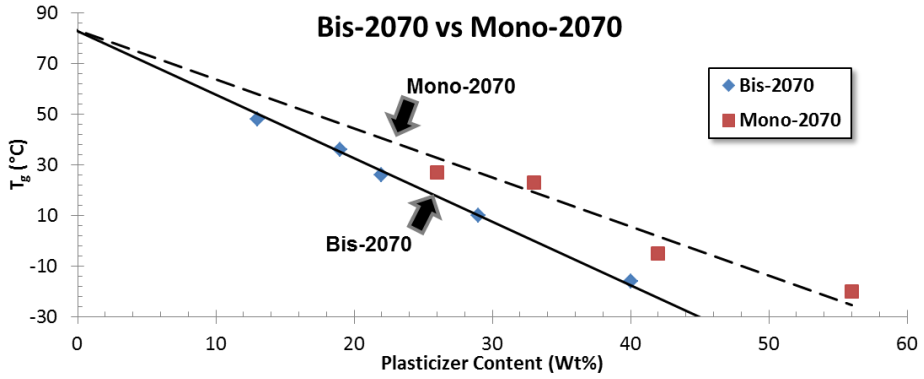

Figure 1.17 PVC-TCTA Jeff2070 Comparison[130]

Reinecke formulated three conclusions that can be drawn from each graph (**Figures 1.15-1.17**) regardless of the JEFFAMINE™ utilized. First, the glass transition temperature decreases linearly with increasing amount of plasticizer. Second, trend lines corresponding to the higher molecular weight plasticizers are situated below those of their lower molecular weight counterparts, and lastly, trend lines of higher molecular weight plasticizers show a larger negative slope than lower molecular weight analogs. Reinecke postulated that these effects stem from the amount of anchoring sites present on PVC. Recall that this system utilizes TCTA, an aromatic heterocycle which contains three conjugated sp^2 bonds. The planar, rigid nature of this aromatic heterocycle imparts rigidity to localized regions of the polymer where the plasticizer is covalently linked. In extreme cases, π-stacking may occur between the aromatic anchors, which will inherently induce crystallinity and additional rigidity in the polymer. As a result, larger molecular weight plasticizers requiring less anchoring points to achieve the same weight percent of plasticizer content compared to a lower molecular weight counterpart should provide improved plasticization properties. The glass transition temperature data above corroborates this theory, and alludes to the fact that one may be able to achieve superior plasticization character by eliminating rigid anchoring points to the main chain of PVC, such as aromatic functional groups. This implies that the ultimate covalently-bound internally plasticized PVC system should contain predominantly poly(ethylene oxide), devoid of any rigid anchoring groups. The combination of compatibility between PVC and poly(ethylene oxide), and the absence of rigid functional groups should unquestionably enhance the plasticization efficiency of a covalently bound system, regardless of the mobility penalty accrued with attachment to the backbone of PVC.

1.10 Natural Product-Derived Internally Plasticized Poly(vinyl chloride) (PVC)

The demand for an affordable phthalate replacement has grown in recent years, with many countries around the world banning DEHP as a plasticizer for PVC. An avenue toward an economical and ecologically renewable plasticizer may be found in nature. Zhou and

coworkers[138] investigated aminated tung oil as an internal plasticizer for PVC. Tung oil, a drying oil extracted from tung tree seeds, is a poly-unsaturated triacylglycerol. It has found use in wood finishing,[139] water-proofing,[140] biodiesel,[141] and as a light lubricant for porous materials.[142] In Zhou's publication, a tung oil derived aliphatic amide was synthesized, *via* a diamine, which ultimately yields a nucleophilic (and basic) terminal amine (**Scheme 1.14**).

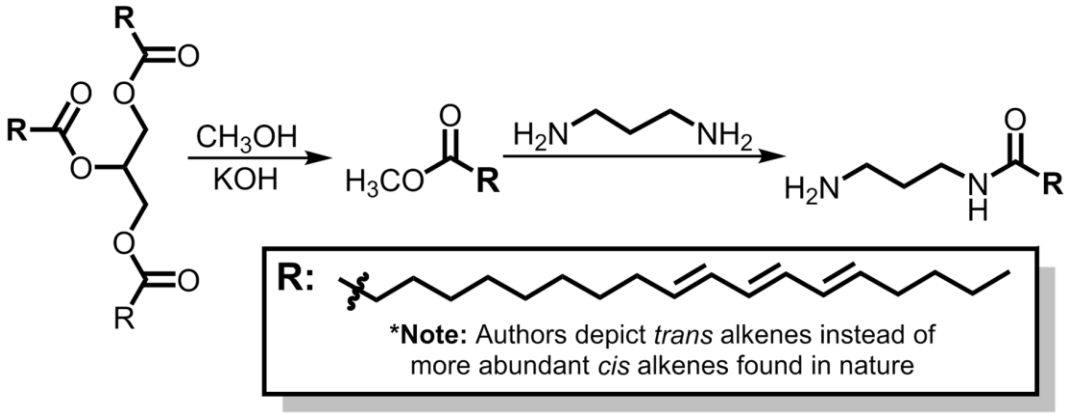

Scheme 1.14 Zhou's Tung Oil Plasticizer Synthesis[138]

In a two-step reaction sequence, transesterification was performed on tung oil with methanol and potassium hydroxide, furnishing the methyl ester. Next, the aliphatic methyl ester was treated with propylenediamine to yield the final plasticizer. To obtain the internally plasticized polymer, both PVC and tung oil amine plasticizer were dissolved in DMF and heated to 80 °C, as shown in **Scheme 1.15**.

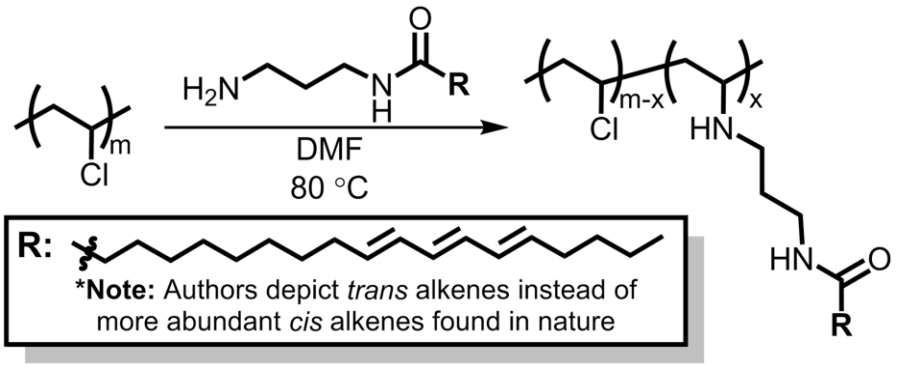

Scheme 1.15 Preparation of Tung Oil-Derived Internally Plasticized PVC[138]

While the authors performed S_N2 substitution on PVC with the tung oil amine, there is a possibility of competing elimination reactions with the neural amine and PVC, despite it not being mentioned in the publication. Alkenes present in the tung oil plasticizer may overlap with olefinic ^{1}H-NMR signals formed as a result of elimination of HCl via amine on PVC.

Analysis of the PVC-tung oil system by FTIR, ^{1}H-NMR, and ^{13}C-NMR was performed. Gel permeation chromatography (GPC) was carried out on PVC and the four modified polymers to determine the molecular weights of each species. DSC and TGA analyses were also done for each polymer. **Table 1.14** summarizes the GPC and DSC data.

Polymer	M_n (g/mol)	T_g (°C)
PVC	15100	85
PVC-Tung	18100	71
	21400	57
	22600	51
	23800	44

Table 1.14 Tung Oil-Derived Internally Plasticized PVC Data[138]

Curiously, unmodified PVC in this study exhibited a higher than normal T_g value (85 °C): this may be due to the absence of purification of PVC prior to measurement, the molecular weight, and/or inconsistent heat-cool-heat cycling of the polymer during DSC measurements. Upon careful inspection, the protocol for the DSC measurements in the experimental section states, "the temperature was over a range of -40 to -120 °C at a heating of 20 °C min^{-1}. ... The DSC data were collected from first cycle of heating."[138] The standard heat-cool-heat cycling to erase the polymer's thermal history was not performed. This major deficiency in the thermal protocol will inevitably yield inconsistent and inaccurate glass transition temperatures. Therefore, these T_g values must be taken provisionally, with the knowledge that the thermal measurements are conceivably erroneous. As predicted, an inversely proportional trend is observed: as substitution of the chlorine atoms with the tung oil derivative increases, the T_g values decrease. This is due to the greater presence of the tung oil-based plasticizer within the PVC matrix, which disrupt chain-chain interactions of PVC. At

the maximum level of substitution, the tung oil system gave a T_g of 44 °C. Using the M_n value of 23800 and comparing to the standard PVC value of 15100, one can approximate the weight percentage of plasticizer to be 36.5 percent. In this study, the authors did not report T_g values of standard DEHP-PVC mixtures to compare to their internally plasticized system. Comparing data gathered from others in the literature,[130] DEHP-PVC exhibits a characteristic T_g value of 12 °C at 32 weight percent DEHP and -24 °C at 42 weight percent DEHP. Generating a second order quadratic trend line from the general literature data on DEHP-PVC mixtures (**Table 1.13**)[130] reveals a predicted T_g value of -5.3 °C at 36.5 weight percent DEHP. With this approximate standard T_g value in mind, the covalently bound tung oil derived plasticizer system is not commensurate with the traditional DEHP-PVC system, despite exhibiting lower than standard glass transition temperatures over unmodified PVC.

Zhou and co-workers[143] also developed an approach to covalently attach a Mannich base cardanol-derived plasticizer to PVC. Cardanol is a renewable organic resource, originating from the thermal decomposition of anacardic acids. The molecule is the predominant component in the oil of cashew nutshells, commonly referred to as “cashew nutshell liquid” (CNSL) in industry.[144] CNSL is commonly employed as a surface coating, adhesive, varnish, and paint. The authors utilized a Mannich reaction to create an amine-terminated long chain tether. The cardanol-amine possesses the nucleophilic properties to displace chlorine on PVC (**Scheme 1.16**); however, elimination of HCl by the amine is also expected to be a significant side reaction.

FTIR and ^{1}H-NMR were performed to confirm the final structure of the internally plasticized polymer. Four separate polymer samples with varying levels of substitution were synthesized, with number average molecular weights (M_n) of 17900, 18900, 21000, and 24500 grams per mole. Standard PVC possessed a M_n value of 15100 grams per mole. DSC measurements were performed on each of the four PVC-Cardanol polymers, along with standard PVC as shown in **Table 1.15**.

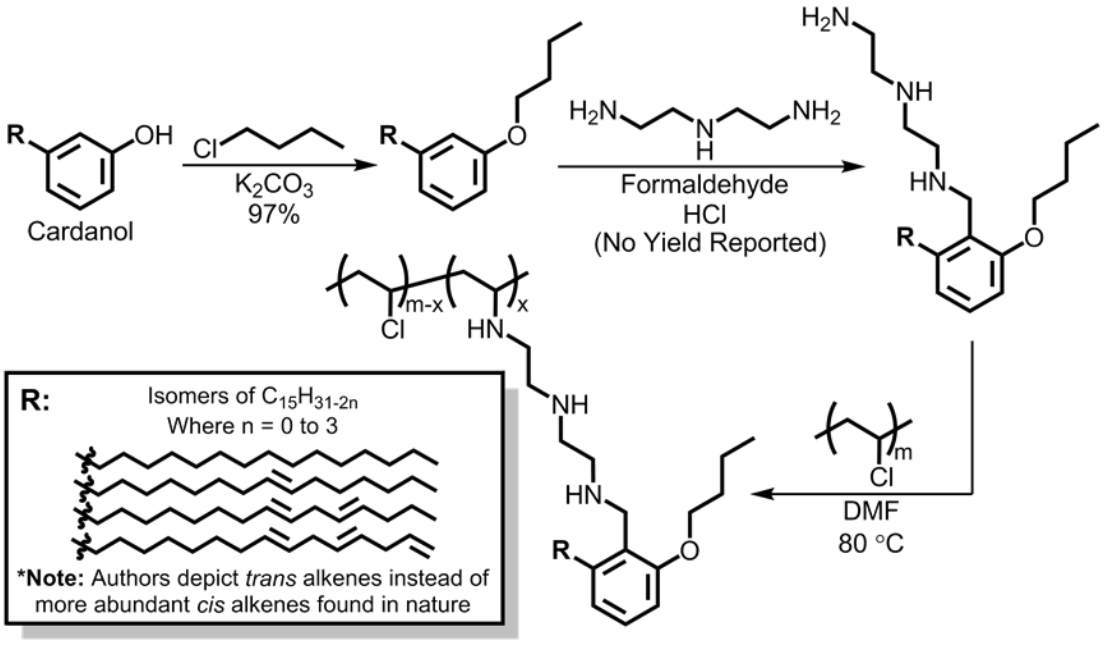

Scheme 1.16 Zhou's Cardanol PVC Synthesis[143]

Polymer	M_n (g/mol)	T_g (°C)
PVC	15100	85.6
PVC-Cardanol	17900	69.1
	18900	58.8
	21000	56.5
	24500	49.3

Table 1.15 Zhou's T_g Data for PVC and PVC-Cardanol[143]

Once again, as in Zhou's previous study,[138] a higher than standard T_g for PVC is presented at 85.6 °C. To recapitulate, the protocol for the DSC measurements did not incorporate the standard heat-cool-heat cycling to erase the thermal history of the polymeric samples.[143] Thus, these thermal values may be inaccurate. As the molecular weight of the polymer increases, due to the concurrent increase in substitution of chlorine on PVC with the cardanol plasticizer, the T_g values unsurprisingly decrease. Using the M_n values given by the authors, at maximum substitution, 38.4 weight percent of the polymer is comprised of cardanol plasticizer, yielding a T_g of 49.3 °C. With the glass transition data gathered from the literature on DEHP-PVC mixtures (**Table 1.13**),[130] a T_g value of -9.1 °C is extrapolated at 38.4

weight percent of DEHP. The T_g values remain inferior to non-covalent DEHP-PVC systems, and thus does not possess the same plasticizing efficiency as DEHP.

Yang and co-workers developed an alternative strategy to covalently attach cardanol to PVC.[145] Cardanol was affixed to PVC using the copper-mediated azide-alkyne cycloaddition reaction (CuAAC). In contrast to Zhou,[143] Yang utilizes the phenolic alcohol on cardanol as the attachment point for the propargyl group under basic conditions, yielding a terminal alkyne derivative of cardanol. The synthesis of the cardanol alkyne is shown in **Scheme 1.17**. The copper-mediated cycloaddition of the alkyne to PVC-N_3 is shown in **Scheme 1.18**.

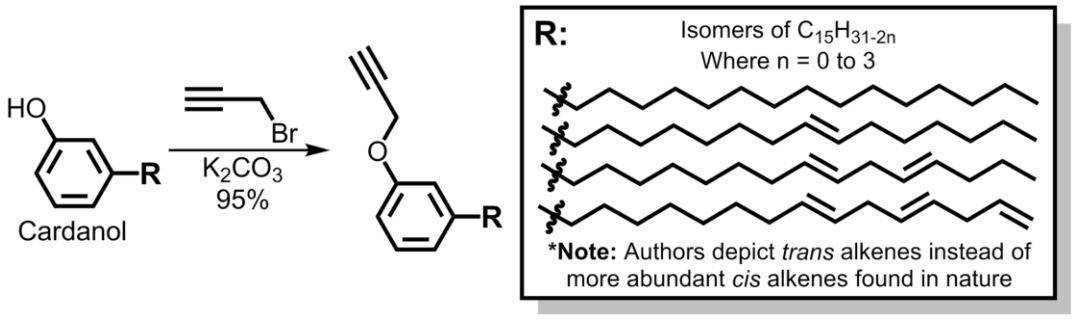

Scheme 1.17 Yang's Cardanol Alkyne Synthesis[145]

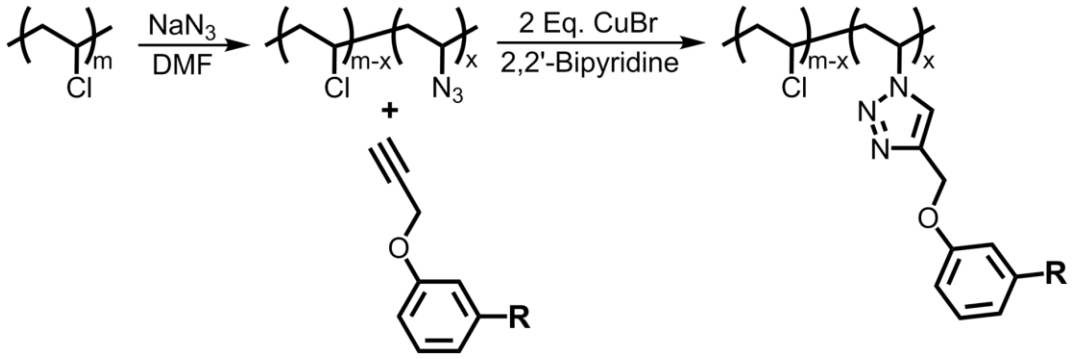

Scheme 1.18 Yang's PVC-Azide and Cardanol Alkyne Copper-Mediated Cycloaddition[145]

For the S_N2 substitution by azide on PVC, the authors reported that 10 percent of the chlorine atoms were displaced based on elemental analysis. Subsequently, the authors

monitored the progress of the copper-mediated cycloaddition *via* FTIR, paying close attention to the azide (N_3) absorption at 2114 cm^{-1}, the internal alkyne carbon absorption at 2123 cm^{-1}, and the terminal alkyne carbon absorption at 3308 cm^{-1}. Reaction completion was determined by the disappearance of the azide and both alkyne absorptions after filtration of the copper salts and precipitation in methanol. ^{1}H-NMR spectra exhibited the typical proton shifts of PVC-triazole, aromatics, and lipids present in the polymeric matrix. Glass transition temperatures are reported in **Table 1.16**.

Polymer	T_g (°C)
PVC	87.1
PVC-N_3 (10% Azide)	81.0
PVC-Triazole-Cardanol	51.0
PVC-DEHP (8.7 Wt% DEHP)	48.8

Table 1.16 Yang's T_g Data for Standards and PVC-Triazole-Cardanol[145]

At approximately 10 mole percent triazole-cardanol on PVC, a T_g of 51.0 °C was observed. In comparison to standard PVC (87.1 °C): the cardanol derivative appears to act as a plasticizer, lowering the T_g of PVC by 36.1 °C. Although the T_g value for unmodified PVC is higher than the standard literature accepted value of 83 °C, the authors performed the necessary heat-cool-heat cycling of the polymer samples. A systematic calibration error of the DSC instrument may potentially be the cause of the elevated T_g value of PVC. Thermal gravimetric analysis of PVC-DEHP and PVC-triazole-cardanol was also performed. The non-covalent PVC-DEHP showed poor thermal stability caused by the volatilization of DEHP at high temperatures; in contrast, the cardanol sample displayed improved thermal stability throughout the temperature range, possibly due to the covalent linkage of the plasticizer to the main chain of PVC. The 1%, 5%, and 50% weight loss temperatures for PVC-DEHP were 107 °C, 160 °C, and 296 °C, respectively. PVC-triazole-cardanol gave weight loss temperatures of 143 °C, 225 °C, and 387 °C. Plasticizer migration was also investigated by treating PVC-DEHP and PVC-triazole-cardanol with *n*-heptane at 40 °C. The PVC-triazole-cardanol derivative did not show any significant migration of the cardanol plasticizer, while

the PVC-DEHP standard displayed considerable leaching of DEHP into the *n*-heptane solution.

Citric acid, a molecule ubiquitously found in citrus plants, was explored as a basis for a novel, covalently bound, plasticizing system for PVC.[146] Zhou et al. also employed the copper-mediated azide-alkyne cycloaddition as an attachment strategy. Citric acid is a tricarboxylic acid, manufactured globally in large quantities.[147] The free-acid has a multitude of applications ranging from preservatives, cosmetics, pharmaceuticals, beverage additives, and dyes.[147] Cost-effective, renewable, and easy to manufacture, citric acid is a commodity chemical that has the potential to be an excellent internal plasticizer to PVC due to its branched structure, which allows the facile functionalization of multiple chemical moieties bearing plasticizing entities. In this study however, the authors purchased commercially available triethyl citrate for use as the main plasticizing moiety. The synthesis of the citrate alkyne and its subsequent attachment to PVC using the copper-mediated azide-alkyne cycloaddition is shown in **Scheme 1.19**.

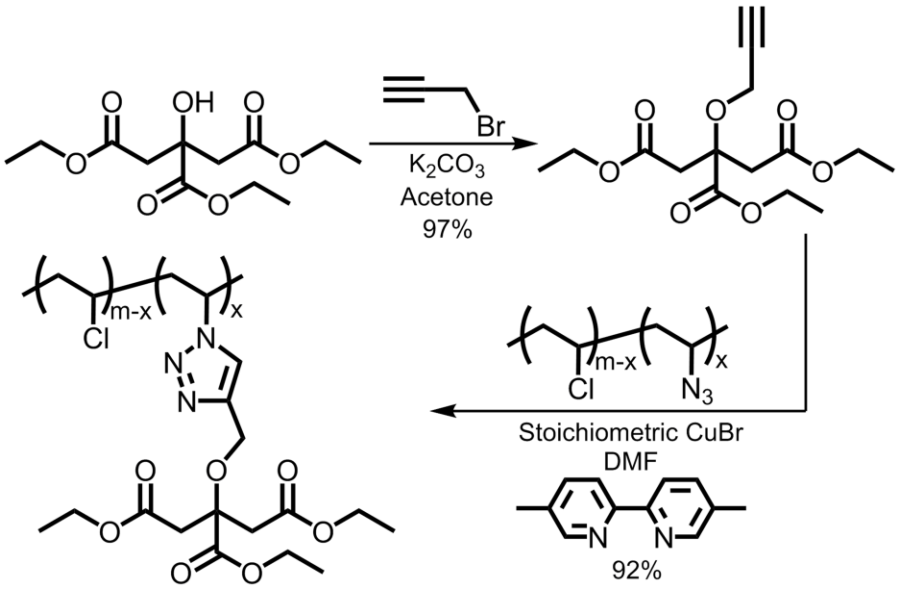

Scheme 1.19 Zhou's Triethyl Citrate Internally Plasticized PVC Synthesis[146]

Triethyl citrate was treated with propargyl bromide and potassium carbonate in acetone, at 65 °C for 12 hours in 97% yield. PVC-N_3 was synthesized by dissolving PVC and sodium azide in DMF at 30 °C for 24 hours, and was subsequently precipitated in a 1:1 water/methanol solution. The key azide-alkyne cycloaddition was performed with stoichiometric copper (I) bromide and 5,5'-dimethyl-2,2'-bipyridine in DMF at 30 °C for 24 hours. Polymer samples were characterized by FTIR, ^{1}H-NMR, ^{13}C-NMR, GPC, DSC, and TGA. Mechanical properties were also investigated. **Table 1.17** shows the DSC results of the polymer samples, with corresponding molecular weights.

Sample	M_n (g/mol)	T_g (°C)
PVC	19529	87.6
PVC-Triazole-Citrate	29602	35.7
PVC-DEHP (40 Wt% DEHP)	19529	11.7

Table 1.17 Zhou's Thermal Data for PVC-Triazole-Citrate Study[146]

To reprise what was previously stated, Zhou et al. does not perform a heat-cool-heat cycle on each polymer sample, leaving the potential thermal history of the polymer unperturbed when measuring the glass transition temperatures. Thus, the T_g data presented in this study may not be accurate compared to experiments following the standard cycling conditions. That aside, the PVC-citrate derivative exhibited a T_g of 35.7 °C, approximately 52 °C lower than the T_g of unmodified PVC. In comparison to their PVC-DEHP mixture, the citrate derivative falls short in terms of glass transition temperature by 24 °C. Elemental analysis was performed on the PVC-N_3, giving values of 35.13% C, 8.21% H, 18.47% N, and 38.19% Cl; however, the authors failed to determine the actual degree of azidation on PVC. Using the molecular weights given by GPC, the PVC-citrate sample gained 10073 grams per mole over standard PVC, which equates to 34 weight percent triazole-citrate plasticizer. TGA revealed that the triazole-citrate plasticizer imparts improved thermal stability to the sample, by possessing higher degradation temperatures at 5, 15, and 50 percent weight loss over PVC or PVC-DEHP. Migration studies on PVC-citrate and PVC-DEHP were carried out to

ASTMD1239-98 standards with four different solvents. In distilled water, 10% (v/v) aqueous ethanol, petroleum ether, and 30% (w/v) acetic acid, DEHP migrated to a greater extent than the triazole-citrate system, which experienced no migration in any solvent, due to its covalent bond to PVC.

1.11 Synthetic 1,2,3-Triazole Internally Plasticized Poly(vinyl chloride) (PVC)

The copper-mediated azide-alkyne cycloaddition (CuAAC)[148] is currently *en vogue* as a facile means to couple organic molecules together, and is quickly becoming popular in all fields of chemistry. Consequently, CuAAC is gaining prevalence in the polymer realm as an approach to covalently attach plasticizers to PVC. In the preceding section discussing naturally-derived plasticizers, two studies[145-146] harnessed the straightforward nature of the copper-mediate cycloaddition to attach plasticizers to PVC. While these two studies dealt with naturally-derived plasticizers, there are a multitude of publications that utilize wholly synthetic plasticizers covalently bonded to PVC *via* a copper-mediated azide-alkyne cycloaddition.

Kwak and coworkers developed a hyperbranched polyglycerol (HPG) plasticizer, which was grafted onto PVC utilizing copper-mediated azide-alkyne cycloaddition.[149] A hexyl ester-terminated HPG (HPG-C6) was synthesized with each HPG-C6 unit containing one alkyne. HPG was synthesized by an anionic ring-opening polymerization (AROP) of glycidol with propargyl alcohol under basic conditions as shown in **Scheme 1.20**. The hyperbranched polyglycerol alkyne was then mixed neat with hexanoic anhydride at 120 °C for 3 hours, yielding the final HPG-C6 alkyne. To obtain PVC with the grafted hyperbranched HPG derivative (PVC-*g*-HPG-C6), HPG-C6-alkyne and PVC-N_3 at varying degrees of azidation were combined with copper (I) bromide and *N,N,N',N'',N''*-pentamethyldiethylenetriamine (PMDETA) in DMF, at 50 °C, for 24 hours (**Scheme 1.21**).

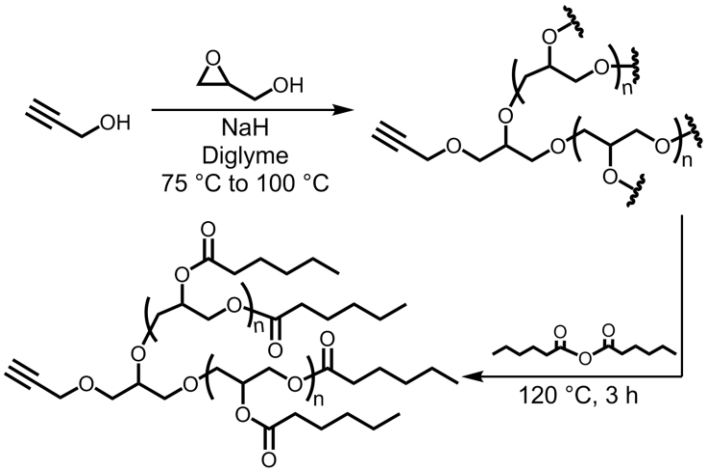

Scheme 1.20 Kwak's Hyperbranched Polyglycerol (HPG-C6) Alkyne Synthesis[149]

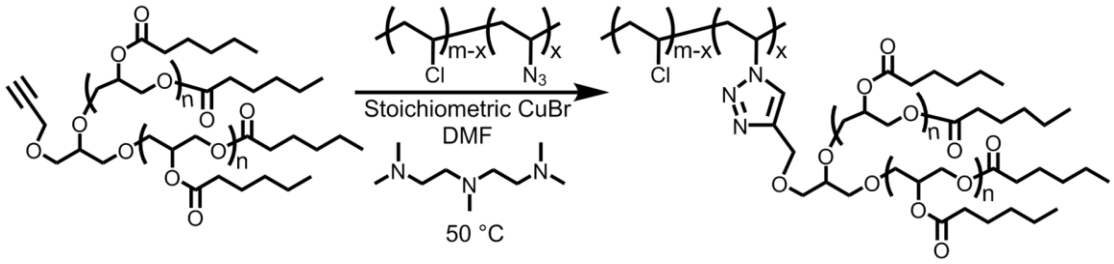

Scheme 1.21 Kwak's PVC-*g*-HPG-C6 Synthesis[149]

The PVC-N_3 used by the authors possessed different degrees of azidation ranging from 1.8% to 9.0%, depending on reaction time. A multitude of analyses were performed on the PVC-*g*-HPG-C6 derivatives. Beginning with the thermal data, the authors observe a progressive, significant enhancement in glass transition temperatures in the PVC-*g*-HPG-C6 samples (**Table 1.18**). Unmodified PVC exhibits a glass transition temperature of 81.3 °C. At 1.8 mole percent HPG-C6, a decrease in T_g is observed at 38.6 °C, representing a 42.7 °C depression

Sample	Triazole Content (mol%)	M_n (g/mol)	T_g (°C)	ΔT_g (°C)
PVC	0	42271	81.3	-
$PVC_{1.8}$-*g*-HPG-C6	1.8	50251	38.6	42.7
$PVC_{3.6}$-*g*-HPG-C6	3.6	57763	16.4	64.9
$PVC_{5.8}$-*g*-HPG-C6	5.8	83883	-4.5	85.8
$PVC_{9.0}$-*g*-HPG-C6	9.0	88404	-28.9	110.2

Table 1.18 PVC-*g*-HPG-C6 GPC and DSC Results[149]

compared to standard PVC. At twice the mole percent substitution (3.6%), the grafted material displays a T_g of 16.4 °C. At 5.8 mole percent, $PVC_{5.8}$-*g*-HPG-C6 gave a T_g of -4.5 °C. At 9.0 mole percent, $PVC_{9.0}$-*g*-HPG-C6 showed an impressive T_g value of -28.9 °C, a 110.2 °C depression compared to standard PVC. The glass transition temperature depressions show an exponential decrease from 81.3 °C to -28.9 °C (**Figure 1.18**). The authors report that the decline in T_g is comparable to conventional PVC-DEHP at 60 parts per hundred resin (phr).

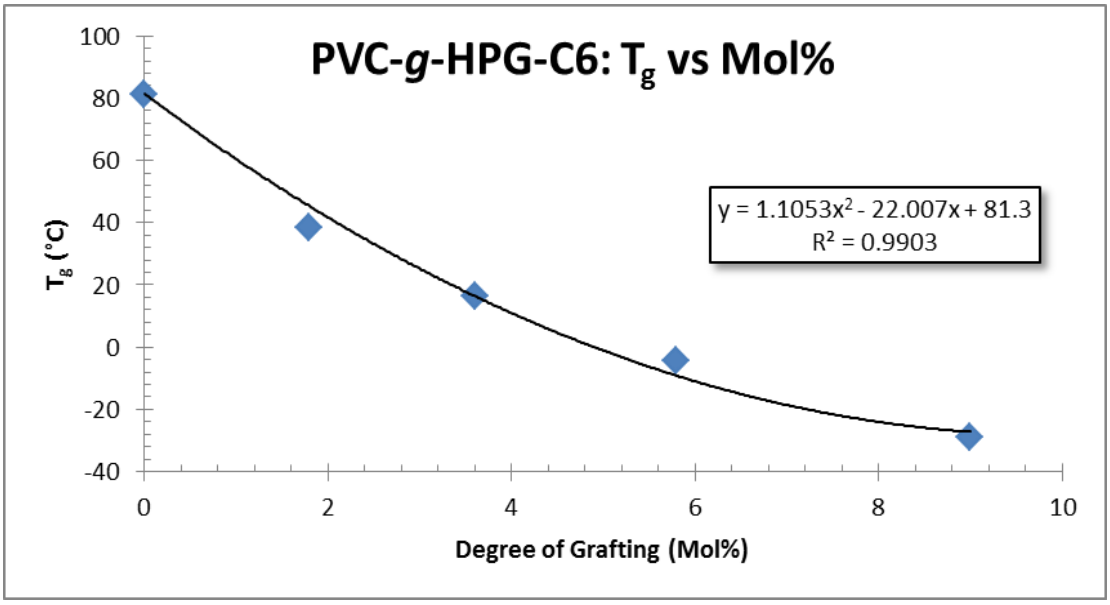

Figure 1.18 PVC-*g*-HPG-C6 T_g versus Mol%[149]

At 60 parts per hundred resin DEHP to PVC, a T_g of -23.8 °C was obtained. The authors rationalized the decrease in T_g, writing, "the amorphous, unentangled, and bulky dendritic structure, as well as the numerous mobile polyether segments of HPG-C6 efficiently increase the free volume of the PVC-*g*-HPG-C6." What may also contribute to the efficacy of the HPG-C6 system is the presence of the polyether segments. While the authors mention mobility of the polyglycerol segments, a statement on the *miscibility* of the polyether with PVC is absent. The storage modulus (*E'*) and loss tangent (tanδ) were obtained as a function of temperature. The storage modulus of PVC-*g*-HPG-C6 decreased as the temperature

increased, indicating energy dissipation. Other observations included the onset of *E'* drop and *E'* value at 25 °C, which decreased from 46.1 °C to -15 °C, and from 235 to 0.12 MPa, respectively. The α-relaxation temperature was lowered in PVC-*g*-HPG-C6 and increased the height of the tanδ peak. The authors concluded that these values indicate that grafted HPG-C6 increases segmental motion to PVC, and consequently, improves the malleability of the polymer at room temperature. To contrast, a mixture of PVC-DEHP (60 phr) exhibited onset of *E'* drop and α-relaxation temperatures between 5.8 mole percent and 9.0 mole percent PVC-*g*-HPG-C6, which corresponds with the T_g values taken of these samples. The *E'* value at 25 °C of PVC-DEHP is between the 3.6 mole percent and 5.8 mole percent PVC-*g*-HPG-C6; this phenomenon indicates that PVC-DEHP is less flexible and ductile at 25 °C than 5.8 and 9.0 mole percent PVC-*g*-HPG-C6, despite having similar T_g values.[149]

The mechanical properties of the PVC-*g*-HPG-C6 derivatives were also investigated. To investigate the effect of covalent bonding of HPG-C6 to PVC, PVC-*g*-HPG-C6 and mixtures of PVC with unbound HPG-C6 were subjected to stress-strain tests. With both grafted and unbound HPG-C6, tensile strength decreased with higher molar percentages of HPG-C6. All tensile strength values for PVC-*g*-HPG-C6 were higher than the unbound analogs, due to the covalent attachment of HPG-C6 to PVC, which imparts strength to the polymer. Elongation at break significantly increased in all covalently grafted samples versus the unbound mixtures. The maximum elongation at break value was observed for the 9.0 mole percent PVC-$_g$-HPG-C6 samples, to be 912% (380 times greater than pure PVC). For comparison, a maximum value of 153% was obtained for the unbound samples, which corresponded to 1.7 mole percent of unbound HPG-C6. Tensile strength and elongation of break of PVC-DEHP (60 phr) values were similar to that of the 3.6 mole percent PVC-*g*-HPG-C6 derivative.

In another study which utilized CuAAC for the covalent attachment of a polymeric species to PVC, Tasdelen and Demirici[150] grafted poly(ε-caprolactone) to PVC. The authors synthesize poly(ε-caprolactone) alkyne *via* a ring opening polymerization of ε-caprolactone using $Sn(Oct)_2$ and propargyl alcohol as shown in **Scheme 1.22**.

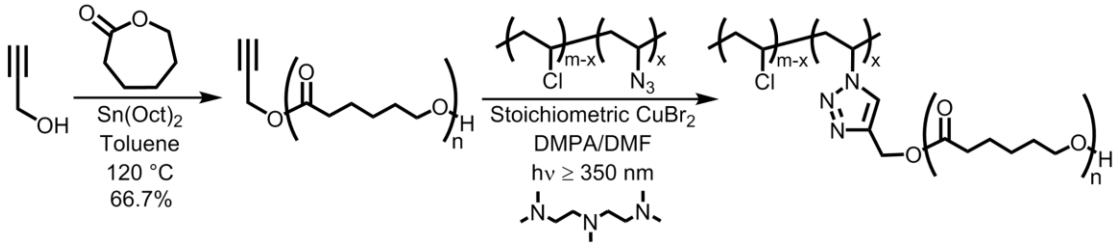

Scheme 1.22 Poly(ε-caprolactone) Triazole Functionalized PVC Synthesis[150]

The subsequent azide-alkyne-cycloaddition is carried out with stoichiometric copper (II) dibromide, PMDETA, and 2,2-dimethoxy-2-phenylacetophenone (DMPA) as a photoinitiator in DMF at 60 °C. With respect to PVC-N_3, there was no indication of the degree of azidation nor elemental analysis to describe the amount of azide substitution on the PVC, although the authors reference another study that utilized similar reaction conditions to obtain PVC-N_3.[151] However, that reference ran the S_N2 with sodium azide for 92 hours versus 42 hours, as in Tasdelen and Demirci's current study. According to the secondary reference, after 92 hours, the azidation percentage was reported to be 8.0 mole percent.[151] Regardless of the absence of this important data, the photoinduced copper-mediated cycloaddition was monitored by FTIR, noting the disappearance of the azide stretch at 2110 cm^{-1} after reaction completion. Other methods of characterization were carried out such as GPC and DSC, as seen in **Table 1.19**.

Sample	M_n (g/mol)	T_g (°C)
PVC	57800	-
PVC-N_3	58400	87
PCL-Alkyne	8000	-
PVC-*g*-PCL	88000	76

Table 1.19 Poly(ε-caprolactone) Triazole Functionalized PVC Data[150]

The authors observe a glass transition temperature of 87 °C for PVC-N_3 and 76 °C for PVC-*g*-PCL. Pure PVC was not measured for T_g as a standard. The modest T_g decrease of PVC-*g*-PCL is accompanied by a large increase in M_n compared to PVC (Δ 30200g/mol) or PVC-N_3 (Δ 29600 g/mol). If using PVC-N_3 as the standard, the difference in M_n would equate to a 33.6 weight percent increase, which can be accounted for by the cycloaddition of the poly(ε-caprolactone) alkyne. Overall, efficient plasticization was not achieved; poly(ε-caprolactone) does not appear to be an effective means of plasticizing PVC.

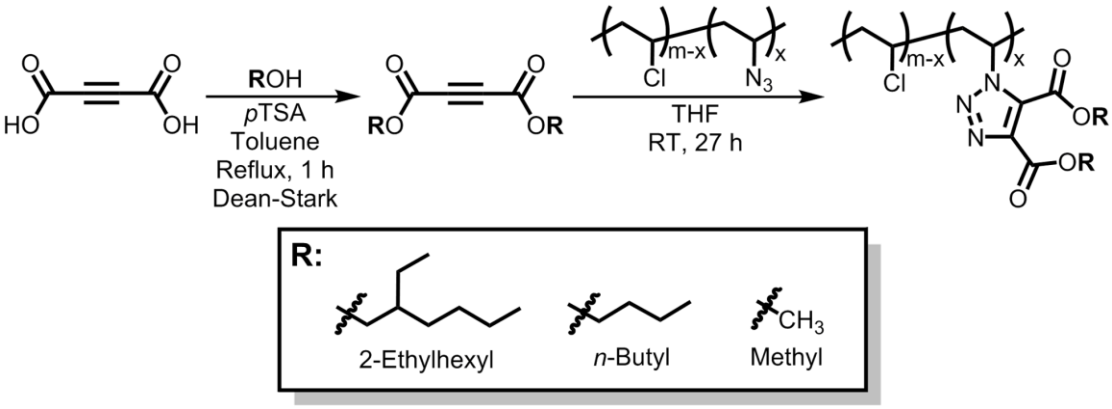

Scheme 1.23: Esterification and Copper-Free Azide-Alkyne Cycloaddition to Yield Phthalate Mimics[152]

Braslau and Earla[152] employed the use of a mild, copper-free azide-alkyne cycloaddition, to attach acetylenedicarboxylate esters bearing alkyl groups, with the intended purpose of creating phthalate analogs directly attached to PVC. The general synthesis of the acetylenedicarboxylate ester and the final PVC product are shown in **Scheme 1.23**. In this reaction scheme, acetylenedicarboxylate was esterified using one of three alcohols, *p*-toluenesulfonic acid (*p*-TSA) and toluene. The reaction was heated to reflux for one hour with a Dean-Stark apparatus to enable facile reaction completion. PVC-N_3 was then treated with the dialkyl acetylenedicarboxylate in THF at room temperature for 27 hours. After subsequent precipitation once in methanol, the final polymers were obtained with varying degrees of functionalization, bearing triazole-based phthalate mimics. As an example, the 2-ethylhexyl

triazole derivative **1.7** is compared to standard DEHP **1.6** (**Figure 1.19**). As seen in **Figure 1.19**, the structure of the novel triazole-based phthalate mimic is nearly analogous to the phthalate, except for two differences. The first difference is the presence of the triazole heterocycle. The five membered ring is aromatic, as is the phenyl group in di-(2-ethylhexyl) phthalate. The second difference is the facile nature of covalently attaching an alkyl group *via* the triazole, designated $\mathbf{R_1}$ in **1.7**. In the present study, the covalently attached alkyl group is PVC, which is formed from a simple thermal 1,3-dipolar cycloaddition of the azide and an electron poor alkyne.

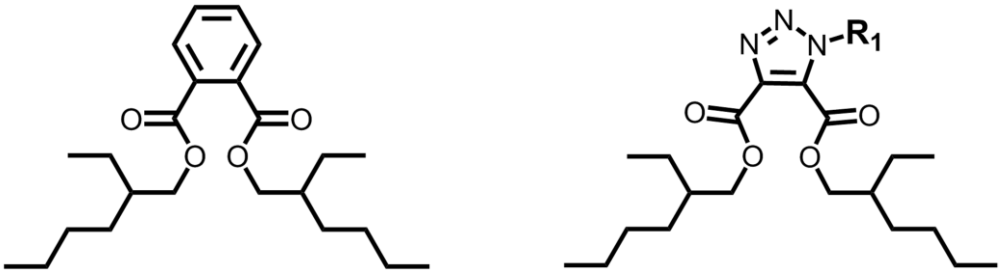

1.6 Di(2-Ethylhexyl) Phthalate (DEHP) **1.7** 2-Ethylhexyl Triazole Phthalate Mimic

Figure 1.19: Structural Comparison of DEHP and 2-Ethylhexyl Triazole Phthalate Mimic

Small molecule azides and PVC-N_3 were synthesized as depicted in **Scheme 1.24**. Once the small molecule azides were prepared, three derivatives of dialkyl acetylenedicarboxylate were synthesized *via* Fischer esterification (**Scheme 1.25**). Next, the thermal azide-alkyne cycloaddition was optimized using commercially available dimethyl acetylenedicarboxylate and 4-ethylbenzyl azide at varying temperatures and molar equivalents of the electron-poor alkyne (**Scheme 1.26**, **Table 1.20**).

Equivalents Alkyne	Solvent	Temperature (°C)	Time	Yield
50	Neat	100	40 min	91%
5	Neat	50	40 min	ND
5	Neat	RT	40 min	ND
1.5	Neat	RT	22 h	ND
1.5	$CDCl_3$	RT	22 h	89%

Table 1.20: Thermal Azide-Alkyne Cycloaddition Optimization Reaction Conditions[152]

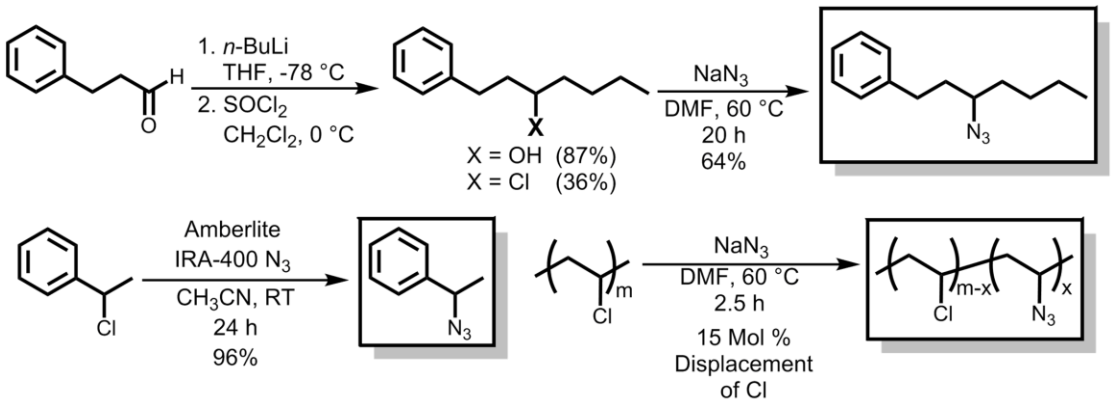

Scheme 1.24: Small Molecule Model Azides and PVC-N_3 Synthesis[152]

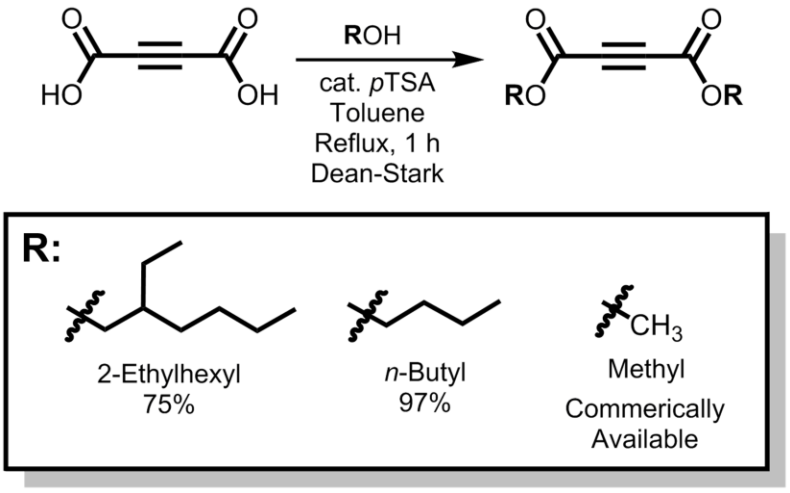

Scheme 1.25: Fischer Esterification Synthesis of Dialkyl Acetylenedicarboxylates[152]

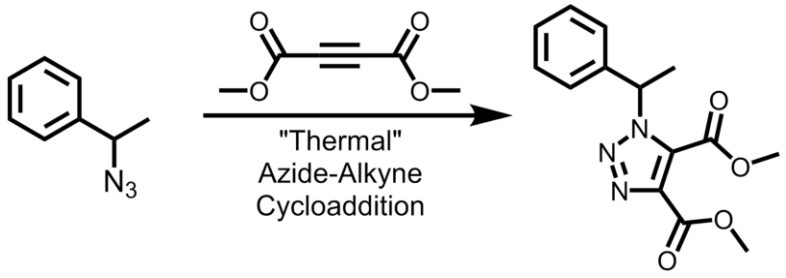

Scheme 1.26: Thermal Azide-Alkyne Cycloaddition Optimization[152]

In the literature prior to this optimization study, it was reported that 50 equivalents of alkyne were required for a thermal cycloaddition to occur at 100 °C.[153] Aruna Earla discovered that the reaction proceeds at lower temperatures and vastly less equivalents of alkyne. Although reaction times increased from 40 minutes to 22 hours, the thermal azide-alkyne cycloaddition was optimized to perform under mild conditions. This is possibly due to the nature of the alkyne, which bears two electron-withdrawing esters adjacent to the sp^1 carbons of the alkyne. This lowers the lowest unoccupied molecular orbital (LUMO), thus activating the alkyne and allowing the cycloaddition to occur at lower equivalents, concentrations, and temperatures. After reaction optimization, the small molecule model azides and PVC-N_3 were treated with dialkyl acetylenedicarboxylates at room temperature for approximately a day, resulting in the key thermal Huisgen 1,3-dipolar cycloaddition occurs on the azide models and PVC-N_3 (**Scheme 1.27**).

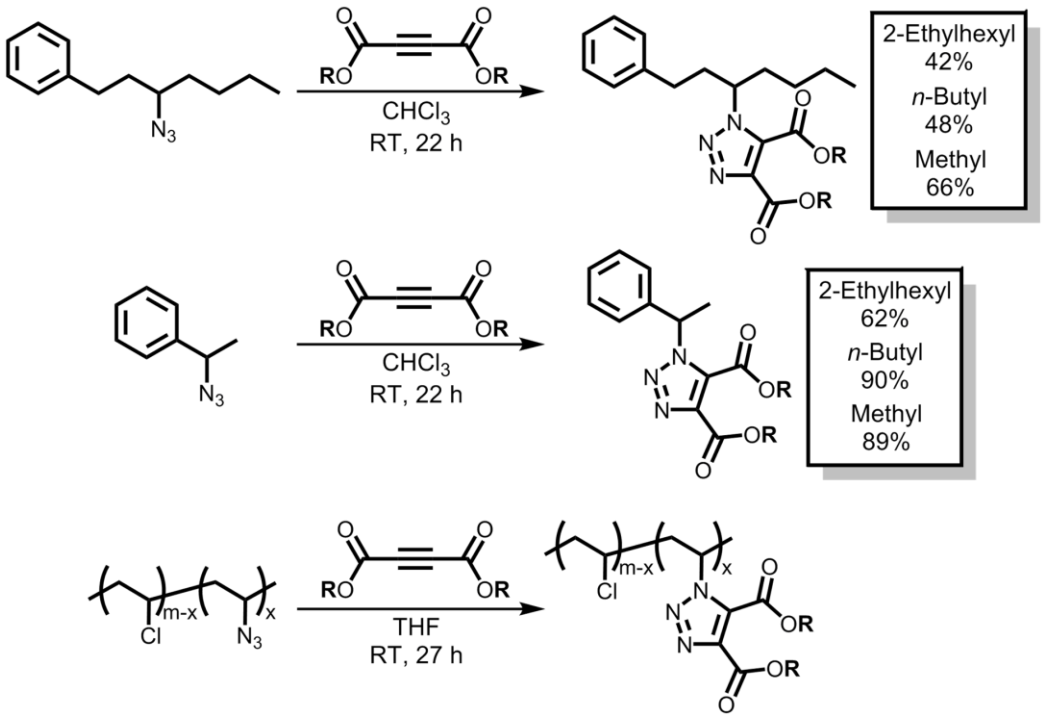

Scheme 1.27: Thermal Huisgen 1,3-Dipolar Cycloaddition Reactions[152]

The thermal cycloadditions were monitored by FTIR. The disappearance of the characteristic azide stretch at 2100-2000 cm^{-1} is a clear indicator that the cycloaddition of azide and alkyne had transpired. In all instances, the cycloaddition occurred at room temperature. Despite PVC-N_3 containing somewhat sterically hindered 2° azide sites, the cycloaddition reached completion, yielding PVC-triazole. To determine the degree of azidation, elemental analysis was carried out on PVC-N_3, which revealed the composition of the polymer to be 38.17% C, 4.70% H, and 9.81% N. This corresponds to 14.7% substitution of chloride with azide. Other forms of analysis were performed such as ^{1}H-NMR, ^{13}C-NMR, and DEPT. Differential scanning calorimetry (DSC) results were absent in the publication: likewise, no T_g values were obtained. This formative investigation led to future research on the plasticizing capabilities of these triazole-based phthalate mimics covalently attached to PVC.

In 2017, Braslau, Earla, Li, and Costanzo[154] further explored the prospect of internally plasticizing PVC with triazole tethered phthalate mimics, utilizing either copper-mediated or thermal Huisgen 1,3-dipolar cycloaddition as a strategy to covalently attach the plasticizing entities (**Scheme 1.28**). It was envisaged that a phthalate covalently attached to PVC *via* the azide-alkyne cycloaddition may plasticize PVC in an efficient manner. This, in combination with a flexible linker to the final plasticizing moiety,[154] was theorized to increase plasticization efficiency over a triazole phthalate mimic directly attached to PVC.[152] The short, flexible linker imparts mobility to the phthalate moiety, allowing the plasticizer to disrupt chain-chain interactions, thereby generating additional free volume more efficiently than an analogous triazole plasticizer tethered directly to the backbone of PVC.

Three synthetic paths were developed (**Scheme 1.29**) to prepare the propargyl-phthalate derivative. Briefly, **Path 1** involves a Diels-Alder cycloaddition with dimethyl acetylenedicarboxylate to give a diene, which was subsequently oxidized, forming the aromatic methyl ester phthalate. Benzylic bromination with *N*-bromosuccinimide yielded the

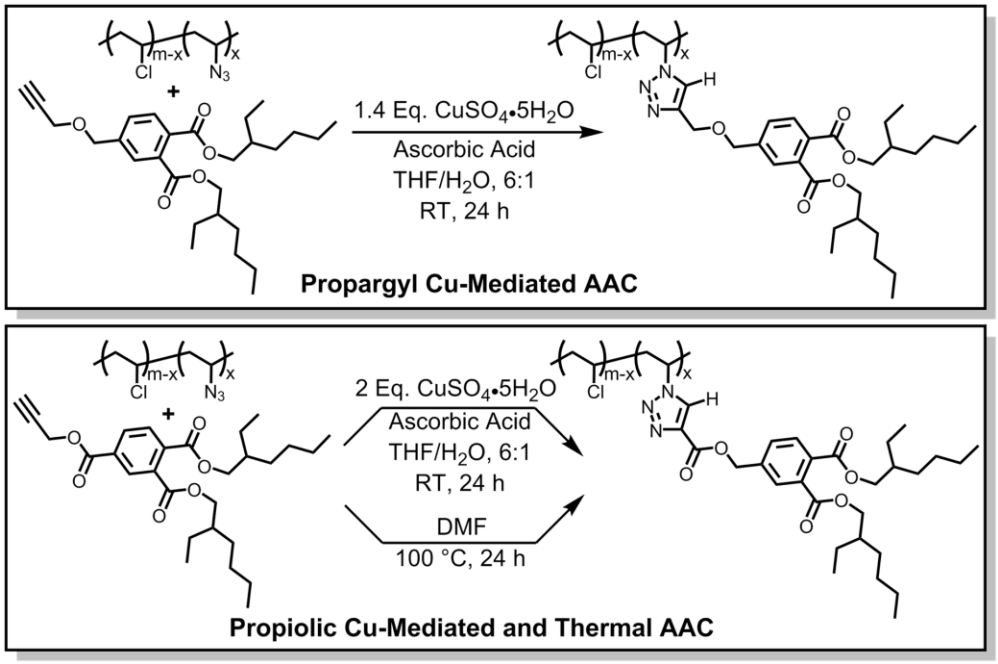

Scheme 1.28: Cu-Mediated and Thermal AAC PVC-Triazole-Phthalate Syntheses[154]

benzyl bromide, which was subsequently treated with propargyl alcohol and sodium hydride to install the alkyne as a benzylic ether. Finally, 2-ethylhexyl alcohol was treated with sodium hydride and the propargyl phthalate methyl ester underwent a transesterification to yield the final propargyl 2-ethylhexyl phthalate derivative. **Path 2** is more convergent; first a Diels-Alder cycloaddition was performed on di(2-ethylhexyl) acetylenedicarboxylate and isoprene, using activated silica as a catalyst. The reaction was exposed to air, oxidizing the 1,4-diene to the tolyl-2-ethylhexyl phthalate intermediate. Subsequently, the benzylic methyl was brominated using *N*-bromosuccinimide, yielding the benzylic bromide, which was treated with propargyl alcohol and sodium hydride to give the desired propargyl-phthalate derivative. **Path 3** utilizes 4-methylphthalic anhydride to obtain the final product. First, 4-methylphthalic anhydride was treated with *N*-bromosuccinimide to give the benzyl brominated anhydride. Next, anhydride opening and Fischer esterification with 2-ethylhexyl alcohol gave the benzylic brominated 2-ethylhexyl phthalate. Analogous to **Path 2**, the brominated phthalate intermediate was treated with propargyl alcohol and sodium hydride to obtain the propargyl

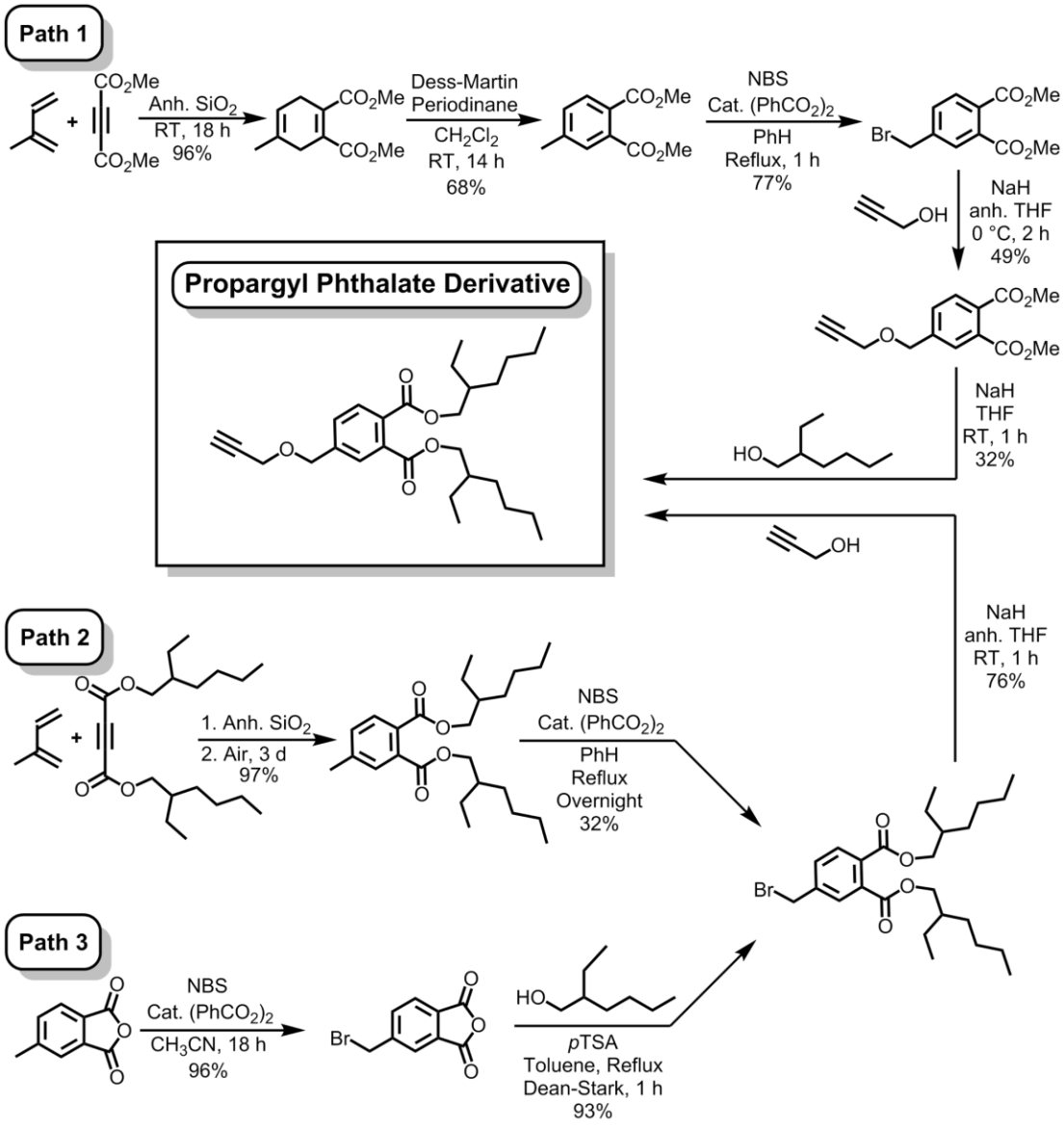

Scheme 1.29: Braslau's Three Propargyl Alkyne Tethered Phthalate Synthetic Pathways[154]

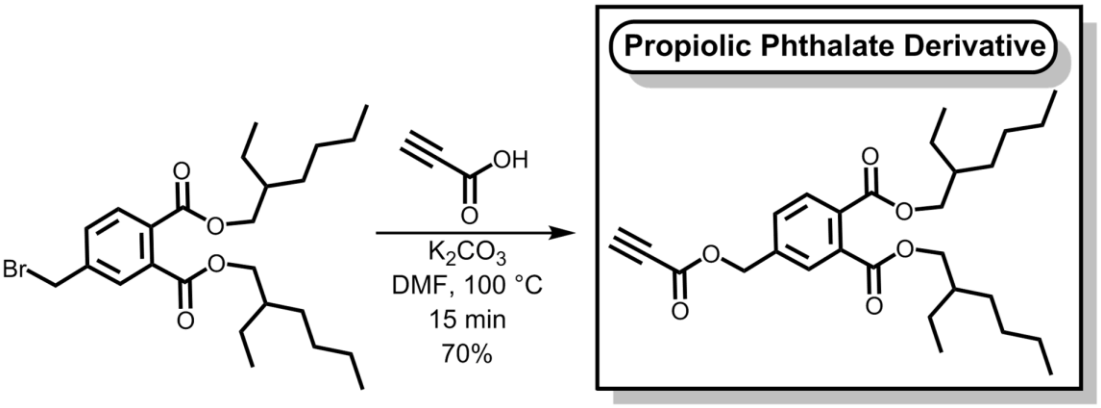

Scheme 1.30: Braslau's Propiolic Alkyne Phthalate Synthesis[154]

phthalate derivative. Fortunately, either **Path 2** or **Path 3** may be used to synthesize the advanced brominated intermediate shared in the syntheses of the propargyl and propiolic derivatives. In a single step, propiolic acid and potassium carbonate in DMF were heated to 100 °C for 15 minutes, to give the propiolic-phthalate derivative (**Scheme 1.30**). Once the ether and ester alkyne derivatives were prepared, model reactions were performed to investigate the feasibility of both the copper-mediated and thermal AAC with a small molecule azide model: 1-phenethyl azide (**Scheme 1.31**). This permitted the straightforward characterization of the product by FTIR, NMR and HRMS: the final polymeric species is not as amenable to these analytical methods. FTIR, NMR, and HRMS all confirmed the formation of the triazole under both copper-catalyzed and thermal conditions with 1-phenethyl azide. The conditions shown in **Scheme 1.31** were then applied to PVC-N_3. The propargyl and propiolic phthalate derivatives were each combined with PVC-N_3 (**Scheme 1.32**) to furnish PVC with covalently attached phthalate derivatives bound by a triazole with a short, flexible ether or ester linker.

Differential scanning calorimetry was performed on a multitude of polymeric samples in this study (**Table 1.21**). Unmodified PVC exhibits the common literature value for the glass transition temperature of 82 °C, while PVC-N_3 at 5 mole percent gives a slightly higher T_g of 84 °C. PVC-N_3 at 15 mole percent gives a marginally lower T_g of 75 °C.

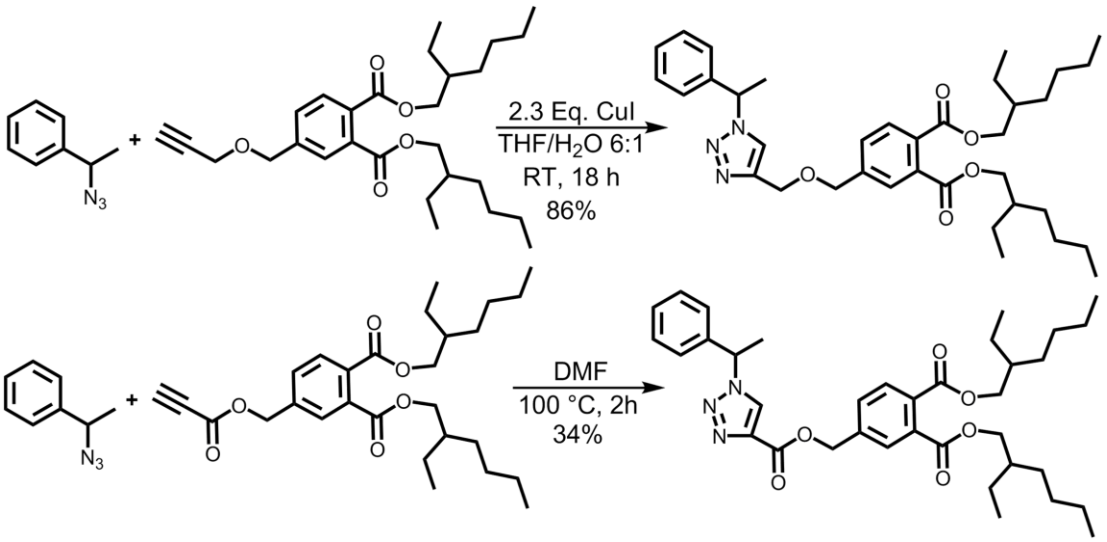

Scheme 1.31: Cu-Mediated and Thermal AAC Model Reactions[154]

Sample	Mol% Substitution	T_g (°C)
PVC	0	82
PVC-N_3	5	84
	15	75
PVC-DEHT*	5	61
	15	65
PVC-DEHP-Ether	5	69
	15	55
PVC-DEHP-Ester (Cu Cat.)	5	69
	15	60
PVC-DEHP-Ester (Thermal)	5	77
	15	60
PVC-DEHP (Conventional Mixture)	5 (Wt %)	74
	15 (Wt %)	75

Table 1.21: Braslau's Thermal Data for PVC-Triazole-DEHP Derivatives[154]
**Note: DEHT = Di(2-Ethylhexyl) Triazole*

Interestingly, PVC bearing a triazole with 2-ethylhexyl esters (PVC-DEHT) exhibited a higher T_g at 15 mole percent substitution (65 °C) over the 5 mole percent analog (61 °C). This phenomenon may be rationalized by the presence of the aromatic triazole on PVC. As seen with Reinecke's mercapo-phthalate derivatives,[132] direct aromatic substitution on the backbone of PVC possibly impedes plasticization efficiency, due to an increase of rigidity of the PVC chain due to crystallinity or π-stacking of the aromatic rings. PVC-DEHP-ester,

which is mimicked by PVC-DEHT, displayed decreased T_g values, whether prepared by copper-catalysis or dipolar cycloaddition, ranging from 77 °C for the 5 mole percent thermally coupled sample to 60 °C for both copper and thermal 15 mole percent samples. PVC-DEHP-ether gave the lowest T_g in this study: 55 °C for the 15 mole percent sample. This can be justified as previously discussed, where rigidity is induced by aromatic planarity. The sp^2 carbonyl bond of the ester appears to convey additional rigidity to PVC in juxtaposition to the ether counterpart. T_g values of the 15 mole percent ester linker were 60 °C, compared to 55 °C in the ether linked DEHP. From this data, the key concept exemplified is that any molecule bestowing rigidity to the main chain of PVC will presumably decrease plasticization efficiency at higher chlorine substitution levels.

1.12 Conclusion

While the studies discussed achieve varying levels of plasticization, design rules for covalently bound emollients on PVC have not yet been firmly established: this dissertation aims to systematically investigate the effect of plasticizer structure on glass transition temperature. Factors such as branching, plasticizing group composition, and miscibility were explored. Non-migratory plasticizers attached to pendant triazole linkages were investigated. Copper-free thermal azide-alkyne cycloadditions are employed to functionalize PVC with an array of triazole-based phthalate mimics.

1.13 References

1. Starnes, W. H. Structural and Mechanistic Aspects of the Thermal Degradation of Poly(vinyl chloride). *Progress in Polymer Science* **2002,** *27* (10), 2133-2170.

2. Shubhra, Q. T. H.; Alam, A. K. M. M.; Quaiyyum, M. A. Mechanical Properties of Polypropylene Composites: A Review. *Journal of Thermoplastic Composite Materials* **2013,** *26* (3), 362-391.

3. Braun, D. PVC - Origin, Growth, and Future. *Journal of Vinyl and Additive Technology* **2001,** *7* (4), 168-176.

4. Semon, W. L.; Stahl, G. A. History of Vinyl-Chloride Polymers. *Journal of Macromolecular Science-Chemistry* **1981,** *A 15* (6), 1263-1278.

5. *World Plastics Statistics 2015*. https://committee.iso.org/files/live/sites/tc61/files/The%20Plastic%20Industry%20Berlin%20Aug%202016%20-%20Copy.pdf. (accessed Sept 13, 2017).

6. U.S. Resin Production & Sales 2016 vs. 2015. https://plastics.americanchemistry.com/Sales-Data-by-Resin.pdf (accessed Sept 8, 2017).

7. The European Council of Vinyl Manufacturers, How is PVC Used? http://www.pvc.org/en/p/how-is-pvc-used (accessed Sept 13, 2017).

8. Whitfield & Associates. The Economic Benefits of Polyvinyl Chloride in the United States and Canada. http://www.pvc.org/upload/documents/The_Economics_of_PVC.pdf. (accessed Sept 13, 2017).

9. Chiellini, F.; Ferri, M.; Morelli, A.; Dipaola, L.; Latini, G. Perspectives on Alternatives to Phthalate Plasticized Poly(vinyl chloride) in Medical Devices Applications. *Progress in Polymer Science* **2013,** *38* (7), 1067-1088.

10. Hakkarainen, M. New PVC Materials for Medical Applications - The Release Profile of PVC/Polycaprolactone-Polycarbonate Aged in Aqueous Environments. *Polymer Degradation and Stability* **2003,** *80* (3), 451-458.

11. Tickner, J. A.; Schettler, T.; Guidotti, T.; McCally, M.; Rossi, M. Health Risks Posed by Use of Di-2-Ethylhexyl Phthalate (DEHP) in PVC Medical Devices: A Critical Review. *American Journal of Industrial Medicine* **2001,** *39* (1), 100-111.

12. Fischer, I.; Schmitt, W. F.; Porth, H.-C.; Allsopp, M. W.; Vianello, G. Poly(Vinyl Chloride). In *Ullmann's Encyclopedia of Industrial Chemistry*, Wiley-VCH Verlag GmbH & Co. KGaA: 2000; pp 1-29.

13. Alfrey, T.; Price, C. C. Relative Reactivities in Vinyl Copolymerization *Journal of Polymer Science* **1947,** *2* (1), 101-106.

14. Laurier, G. C.; Odriscoll, K. F.; Reilly, P. M. Estimating Reactivity in Free-Radical Copolymerizations. *Journal of Polymer Science-Polymer Symposia* **1985,** (72), 17-26.

15. Endo, K. Synthesis and Structure of Poly(vinyl chloride). *Progress in Polymer Science* **2002,** *27* (10), 2021-2054.

16. Abreu, C. M. R.; Mendonça, P. V.; Serra, A. C.; Noble, B. B.; Guliashvili, T.; Nicolas, J.; Coote, M. L.; Coelho, J. F. J. Nitroxide-Mediated Polymerization of Vinyl Chloride at Low Temperature: Kinetic and Computational Studies. *Macromolecules* **2016,** *49* (2), 490-498.

17. Enomoto, S. Polymerization of Vinyl Chloride. *Journal of Polymer Science Part A: Polymer Chemistry* **1969,** *7*, 1255-1267.

18. Fischer, N. Morphology of Mass PVC. *Journal of Vinyl Technology* **1984,** *6* (1), 35-49.

19. Ugelstad, J.; Mork, P. C.; Dahl, P.; Rangnes, P. A Kinetic Investigation of the Emulsion Polymerization of Vinyl Chloride. *Journal of Polymer Science Part C: Polymer Symposia* **1969,** *27* (1), 49-68.

20. Pham, Q.-T.; Millan, J.-L.; Madruga, E. L. Thermodynamics of the Stereosequence Propagations in the Radical Polymerization of Vinyl Chloride Studied by ^{13}C-NMR and IR. *Die Makromolekulare Chemie* **1974,** *175* (3), 945-952.

21. Crowther, M. W.; Szeverenyi, N. M.; Levy, G. C. Absolute Tacticity Assignments of Poly(vinyl chloride) via the Two-Dimensional NMR Spin-Lock RELAY Experiment. *Macromolecules* **1986,** *19* (5), 1333-1336.

22. Natta, G. Une Nouvelle Classe de Polymeres d'α-Olefines Ayant une Régularité de Structure Exceptionnelle. *Journal of Polymer Science* **1955,** *16* (82), 143-154.

23. Natta, G.; Corradini, P. The Structure of Crystalline 1,2-Polybutadiene and of Other “Syndyotactic Polymers”. *Journal of Polymer Science* **1956,** *20* (95), 251-266.

24. Fordham, J. W. L. Stereoregulated Polymerization in the Free Propagating Species. I. Theory. *Journal of Polymer Science* **1959,** *39* (135), 321-334.

25. Gouinlock, E. V. The Fusion of Highly Crystalline Poly(vinyl chloride). *Journal of Polymer Science: Polymer Physics Edition* **1975,** *13* (8), 1533-1542.

26. Minsker, K. S.; Lisitsky, V. V.; Kolesov, S. V.; Zaikov, G. E. New Developments in Degradation and Stabilization of Polymers Based on Vinyl Chloride. *Journal of Macromolecular Science, Part C* **1981,** *20* (2), 243-308.

27. Hjertberg, T.; Sörvik, E. M. Formation of Anomalous Structures in PVC and Their Influence on the Thermal Stability: 2. Branch Structures and Tertiary Chlorine. *Polymer* **1983,** *24* (6), 673-684.

28. (a) Hjertberg, T.; Sörvik, E. M. Formation of Anomalous Structures in PVC and Their Influence on Thermal Stability. I. Endgroup Structures and Labile Chlorine Substituted by Phenol. *Journal of Macromolecular Science: Part A - Chemistry* **1982,** *17* (6), 983-1004; (b) Hjertberg, T.; Sörvik, E. M. Formation of Anomalous Structures in PVC and Their Influence on the Thermal Stability: 3. Internal Chloroallylic Groups. *Polymer* **1983,** *24* (6), 685-692.

29. Braun, D.; Böhringer, B.; Iván, B.; Kelen, T.; Tüdös, F. Structural Defects in Poly(vinyl chloride)—IV. Thermal Degradation of Vinyl Chloride/Acetylene Copolymers. *European Polymer Journal* **1986,** *22* (1), 1-4.

30. Marcilla, A.; Beltran, M. 5 - Mechanisms of Plasticization A2 - Wypych, George. In *Handbook of Plasticizers (Third Edition)*, ChemTec Publishing: 2017; pp 119-134.

31. Daniels, P. H. A Brief Overview of Theories of PVC Plasticization and Methods Used to Evaluate PVC-Plasticizer Interaction. *Journal of Vinyl & Additive Technology* **2009,** *15* (4), 219-223.

32. Kirkpatrick, A. Some Relations Between Molecular Structure and Plasticizing Effect. *Journal of Applied Physics* **1940,** *11* (4), 255-261.

33. Clark, F. W. Plasticizers. *Chemistry & Industry (London, U. K.)* **1941**, 228-230.

34. Houwink, R. *Proceedings of the XIth International Congress of Pure and Applied Chemistry: London, 17th-24th July, 1947*. Hepworth: London, 1947.

35. Aiken, W.; Alfrey, T., Jr.; Janssen, A.; Mark, H. Creep Behavior of Plasticized Vinylite VYNW. *Journal of Polymer Science* **1947,** *2*, 178-198.

36. Busse, W. F. The Physical Structure of Elastic Colloids. *The Journal of Physical Chemistry* **1932,** *36*, 2862-2879.

37. (a) Doolittle, A. K. Application of a Mechanistic Theory of Solvent Action to Plasticizers and Plasticization. *Journal of Polymer Science* **1947,** *2*, 121-141; (b) Doolittle, A. K. Mechanism of Solvent Action. Influence of Molecular Size and Shape on Temperature Dependence of Solvent Ability. *Industrial & Engineering Chemistry* **1946,** *38*, 535-540; (c) Doolittle, A. K. Mechanism of Solvent Action. *Industrial & Engineering Chemistry* **1944,** *36*, 239-244.

38. Fox, T. G., Jr.; Flory, P. J. Second-Order Transition Temperatures and Related Properties of Polystyrene. I. Influence of Molecular Weight. *Journal of Applied Physics* **1950,** *21*, 581-591.

39. (a) Fox, T. G.; Flory, P. J. Viscosity-Molecular Weight and Viscosity-Temperature Relationships for Polystyrene and Polyisobutylene. *Journal of the American Chemical Society* **1948,** *70* (7), 2384-2395; (b) Flory, P. J. Kinetics of the Degradation of Polyesters by alcohols. *Journal of the American Chemical Society* **1940,** *62*, 2255-2261.

40. Flory, P. J. Viscosities of Linear Polyesters. An Exact Relationship between Viscosity and Chain Length. *Journal of the American Chemical Society* **1940,** *62* (5), 1057-1070.

41. Fox, T. G. Influence of Diluent and of Copolymer Composition on the Glass Temperature of a Polymer System. *Bull. Am. Phys. Soc. [2]* **1956,** *1*, 123.

42. Gordon, M.; Taylor, J. S. Ideal Copolymers and the Second-Order Transitions of Synthetic Rubbers. i. Non-Crystalline Copolymers. *Journal of Applied Chemistry* **1952,** *2* (9), 493-500.

43. Pinal, R. Entropy of Mixing and the Glass Transition of Amorphous Mixtures. *Entropy* **2008,** *10* (3), 207-223.

44. Simha, R. On A General Relation Involving Glass Temperature and Coefficients of Expansion of Polymers. *Journal of Chemical Physics* **1962,** *37* (5), 1003-1007.

45. Hansen, C. M. The Three Dimensional Solubility Parameter and Solvent Diffusion Coefficient : Their Importance in Surface Coating Formulation. Copenhagen Danish Technical Press, Denmark, 1967.

46. (a) Hildebrand, J. H.; Scott, R. L. *The Solubility of Nonelectrolytes*. Dover Publications: New York, 1964; (b) Hildebrand, J. H. A Critique of the Theory of Solubility of Non-Electrolytes. *Chemical Reviews* **1949,** *44* (1), 37-45.

47. (a) Flory, P. J. Thermodynamics of High Polymer Solutions. *The Journal of Chemical Physics* **1942,** *10* (1), 51-61; (b) Flory, P. J. Thermodynamics of High Polymer Solutions. *The Journal of Chemical Physics* **1941,** *9* (8), 660-661; (c) Huggins, M. L. Solutions of Long Chain Compounds. *The Journal of Chemical Physics* **1941,** *9* (5), 440.

48. Senichev, V. Y.; Tereshatov, V. V.; Wypych, G. Chapter 6 - Theories of Compatibility. In *Handbook of Plasticizers (Third Edition)*, ChemTec Publishing: 2017; pp 135-164.

49. Bigg, D. C. H. Comparison of Methods for Assessing the Degree of Interaction Between Plasticizers and Poly(vinyl chloride). *Journal of Applied Polymer Science* **1975,** *19* (11), 3119-3127.

50. Doty, P.; Zable, H. S. Determination of Polymer–Liquid Interaction by Swelling Measurements. *Journal of Polymer Science* **1946,** *1* (2), 90-101.

51. Anagnostopoulos, C. E.; Coran, A. Y.; Gamrath, H. R. Polymer–Diluent Interactions. I. A New Micromethod for Determining Polyvinyl Chloride-Diluent Interactions. *Journal of Applied Polymer Science* **1960,** *4* (11), 181-192.

52. Tomaselli, F.; Gupta, V. P.; Calderon, H. S.; Brown, G. R. Poly(vinyl chloride)/Plasticizer-Mixture Interactions. Mixtures of Various Plasticizers of Industrial Importance. *Journal of Vinyl and Additive Technology* **1989,** *11* (1), 9-14.

53. Caldas, V.; Radiotis, T.; Brown, G. R. Automated Microscopic Technique for Evaluating Poly(vinyl chloride)-Plasticizer Compatibility. *Journal of Applied Polymer Science* **1994,** *52* (13), 1939-1947.

54. Graham, P. R. Phthalate Ester Plasticizers--Why and How They Are Used. *Environmental Health Perspectives* **1973,** *3*, 3-12.

55. Steady Growth Predicted in Global Markets for DINP and DOP Phthalate Plasticizers. *Additives for Polymers* **2015,** *2015* (9), 11.

56. IHS Chemical. Chemical Economics Handbook: Plasticizers. https://www.ihs.com/products/plasticizers-chemical-economics-handbook.html (accessed September 25, 2017).

57. Walter, C. W. Invention and Development of the Blood Bag. *Vox Sanguinis* **1984,** *47* (4), 318-324.

58. Sampson, J.; de Korte, D. DEHP-Plasticised PVC: Relevance to Blood Services*. *Transfusion Medicine* **2011,** *21* (2), 73-83.

59. Horowitz, B.; Stryker, M. H.; Waldman, A. A.; Woods, K. R.; Gass, J. D.; Drago, J. Stablization of Red Blood-Cells By the Plasticizer, Diethylhexylphthalate. *Vox Sanguinis* **1985,** *48* (3), 150-155.

60. AuBuchon, J.; Estep, T.; Davey, R. The Effect of the Plasticizer Di-2-ethylhexyl Phthalate on the Survival of Stored RBCs. *Blood* **1988,** *71* (2), 448-452.

61. Jaeger, R. J.; Rubin, R. J. Plasticizers From Plastic Devices: Extraction, Metabolism, and Accumulation By Biological Systems. *Science* **1970,** *170* (3956), 460-462.

62. Heudorf, U.; Mersch-Sundermann, V.; Angerer, J. Phthalates: Toxicology and Exposure. *International Journal of Hygiene and Environmental Health* **2007,** *210* (5), 623-634.

63. Zota, A. R.; Calafat, A. M.; Woodruff, T. J. Temporal Trends in Phthalate Exposures: Findings from the National Health and Nutrition Examination Survey, 2001-2010. *Environmental Health Perspectives* **2014,** *122* (3), 235-241.

64. (a) Commission Directive 2007/19/EC of 30 March 2007 Amending Directive 2002/72/EC Relating to Plastic Materials and Articles Intended to Come into Contact with Food and Council Directive 85/572/EEC Laying Down the List of Simulants to Be Used for Testing Migration of Constituents of Plastic Materials and Articles Intended to Come into Contact with Foodstuffs. In *European Union*, 2007; Vol. L 91, pp 17-36; (b) Directive 2005/84/EC of the European Parliament and of the Council 14 December 2005 Amending for the 22nd time Council Directive 76/769/EEC on the Approximation of the Laws, Regulations and Administrative Provisions of the Member States Relating to Restrictions on the Marketing and Use of Certain Dangerous Substances and Preparations (Phthalates in Toys and Childcare Articles). In *European Union*, 2005; Vol. L 344, pp 40-43; (c) Commission Directive 2004/93/EC of 21 September 2004 Amending Council Directive 76/768/EEC for the Purpose of Adapting Its Annexes II and III to Technical Progress. In *European Union*, 2004; Vol. L 300, pp 13-41; (d) 1999/815/EC: Commission Decision of 7 December 1999 Adopting Measures Prohibiting the Placing on the Market of Toys and Childcare Articles Intended to be Placed in the Mouth by Children Under Three Years of Age Made of Soft PVC Containing One or More of the Substances Di-iso-nonyl Phthalate (DINP), Di(2-ethylhexyl) Phthalate (DEHP), Dibutyl Phthalate (DBP), Di-iso-decyl Phthalate (DIDP), Di-n-octyl Phthalate (DNOP), and Butylbenzyl Phthalate (BBP). In *European Union*, 1999; Vol. L 315, pp 46-49.

65. *U.S. Environmental Protection Agency: Child-Specific Exposure Factors Handbook (Final Report)*; United States of America, 2008.

66. Hill, S. S.; Shaw, B. R.; Wu, A. H. B. The Clinical Effects of Plasticizers, Antioxidants, and Other Contaminants in Medical Polyvinylchloride Tubing During Respiratory and Non-Respiratory Exposure. *Clinica Chimica Acta* **2001,** *304* (1-2), 1-8.

67. Schettler, T. Human Exposure to Phthalates via Consumer Products. *International Journal of Andrology* **2006,** *29* (1), 134-139.

68. Maas, R. P.; Patch, S. C.; Pandolfo, T. J. Inhalation and Ingestion of Phthalate Compounds from Use of Synthetic Modeling Clays. *Bulletin of Environmental Contamination and Toxicology* **2004,** *73* (2), 227-234.

69. (a) Rudel, R. A.; Brody, J. G.; Spengler, J. C.; Vallarino, J.; Geno, P. W.; Sun, G.; Yau, A. Identification of Selected Hormonally Active Agents and Animal Mammary Carcinogens in Commercial and Residential Air and Dust Samples. *Journal of the Air &*

Waste Management Association **2001,** *51* (4), 499-513; (b) Becker, K.; Seiwert, M.; Angerer, J.; Heger, W.; Koch, H. M.; Nagorka, R.; Roßkamp, E.; Schlüter, C.; Seifert, B.; Ullrich, D. DEHP Metabolites in Urine of Children and DEHP in House Dust. *International Journal of Hygiene and Environmental Health* **2004,** *207* (5), 409-417.

70. (a) Scott, R. C.; Dugard, P. H.; Ramsey, J. D.; Rhodes, C. In Vitro Absorption of Some o-Phthalate Diesters Through Human and Rat Skin. *Environmental Health Perspectives* **1987,** *74*, 223-227; (b) Elsisi, A. E.; Carter, D. E.; Sipes, I. G. Dermal Absorbtion of Phthalate Diesters in Rats. *Fundamental and Applied Toxicology* **1989,** *12* (1), 70-77.

71. Jaeger , R. J.; Rubin , R. J. Migration of a Phthalate Ester Plasticizer from Polyvinyl Chloride Blood Bags into Stored Human Blood and Its Localization in Human Tissues. *New England Journal of Medicine* **1972,** *287* (22), 1114-1118.

72. Rubin, R. J.; Jaeger, R. J. Some Pharmacologic and Toxicologic Effects of Di-2-ethylhexyl Phthalate (DEHP) and Other Plasticizers. *Environmental Health Perspectives* **1973,** *3*, 53-59.

73. Safety Assessment of Di(2-Ethylhexyl) Phthalate (DEHP) Released From Medical Devices. United States Food and Drug Administration, United States of America, 2001.

74. Roth, B.; Herkenrath, P.; Lehmann, H. J.; Ohles, H. D.; Homig, H. J.; Benzbohm, G.; Kreuder, J.; Younossihartenstein, A. Di-(2-Ethylhexyl)-Phthalate as Plasticizer in PVC Respiratory Tubing Systems-Indications of Hazardous Effects on Pulmonary-Function in Mechanically Ventilated, Preterm Infants. *European Journal of Pediatrics* **1988,** *147* (1), 41-46.

75. Rock, G.; Labow, R. S.; Franklin, C.; Burnett, R.; Tocchi, M. Hypotension and Cardiac-Arrest in Rats After Infusion of Mono(2-Ethylhexyl)phthalate (MEHP), a Contaminant of Stored-Blood. *New England Journal of Medicine* **1987,** *316* (19), 1218-1219.

76. Crocker, J. F. S.; Safe, S. H.; Acott, P. Effects of Chronic Phthalate Exposure on the Kidney. *Journal of Toxicology and Environmental Health* **1988,** *23* (4), 433-444.

77. Kevy, S. V.; Jacobson, M. S. Hepatic Effects of a Phthalate Ester Plasticizer Leached from Poly(vinyl chloride) Blood Bags Following Transfusion. *Environmental Health Perspectives* **1982,** *45*, 57-64.

78. Davis, B. J.; Maronpot, R. R.; Heindel, J. J. Di-(2-Ethylhexyl) Phthalate Suppresses Estradiol and Ovulation in Cycling Rats. *Toxicology and Applied Pharmacology* **1994,** *128* (2), 216-223.

79. (a) Arcadi, F. A.; Costa, C.; Imperatore, C.; Marchese, A.; Rapisarda, A.; Salemi, M.; Trimarchi, G. R.; Costa, G. Oral Toxicity of Bis(2-ethylhexyl) Phthalate During Pregnancy and Suckling in the Long-Evans Rat. *Food and Chemical Toxicology* **1998,** *36* (11), 963-970; (b) Wolf, C.; Lambright, C.; Mann, P.; Price, M.; Cooper, R. L.; Ostby, J.; L. Earl Gray, J. Administration of Potentially Antiandrogenic Pesticides (Procymidone, Linuron, Iprodione, Chlozolinate, p,p'-DDE, and Ketoconazole) and Toxic Substances (Dibutyl- and Diethylhexyl Phthalate, PCB 169, and Ethane Dimethane Sulphonate) During Sexual Differentiation Produces Diverse Profiles of Reproductive Malformations in the Male Rat. *Toxicology and Industrial Health* **1999,** *15* (1-2), 94-118.

80. Wittassek, M.; Koch, H. M.; Angerer, J.; Bruening, T. Assessing Exposure to Phthalates - The Human Biomonitoring Approach. *Molecular Nutrition and Food Research* **2011,** *55* (1), 7-31.

81. Albro, P. W.; Moore, B. Identification of the Metabolites of Simple Phthalate Diesters in Rat Urine. *Journal of Chromatography A* **1974,** *94* (1), 209-218.

82. Albro, P. W. Absorption, Metabolism, and Excretion of Di(2-ethylhexyl) Phthalate by Rats and Mice. *Environmental Health Perspectives* **1986,** *65*, 293-298.

83. Albro, P. W. The Metabolism of 2-Ethylhexanol in Rats. *Xenobiotica* **1975,** *5* (10), 625-636.

84. Lhuguenot, J.-C.; Mitchell, A. M.; Milner, G.; Lock, E. A.; Elcombe, C. R. The Metabolism of Di(2-ethylhexyl) Phthalate (DEHP) and Mono-(2-ethylhexyl) Phthalate (MEHP) in Rats: In Vivo and In Vitro Dose and Time Dependency of Metabolism. *Toxicology and Applied Pharmacology* **1985,** *80* (1), 11-22.

85. Koch, H. M.; Bolt, H. M.; Preuss, R.; Angerer, J. New Metabolites of Di(2-ethylhexyl)phthalate (DEHP) in Human Urine and Serum After Single Oral Doses of Deuterium-Labelled DEHP. *Archives of Toxicology* **2005,** *79* (7), 367-376.

86. Lhuguenot, J. C.; Mitchell, A. M.; Elcombe, C. R. The Metabolism of Mono-(2-Ethylhexyl) Phthalate (Mehp) and Liver Peroxisome Proliferation in the Hamster. *Toxicology and Industrial Health* **1988,** *4* (4), 431-441.

87. (a) Bentley, P.; Calder, I.; Elcombe, C.; Grasso, P.; Stringer, D.; Wiegand, H. J. Hepatic Peroxisome Proliferation in Rodents and its Significance for Humans. *Food and Chemical Toxicology* **1993,** *31* (11), 857-907; (b) Latini, G. Potential Hazards of Exposure to Di-(2-ethylhexyl)-Phthalate in Babies. *Biology of the Neonate* **2000,** *78* (4), 269-276.

88. Barr, D. B.; Silva, M. J.; Kato, K.; Reidy, J. A.; Malek, N. A.; Hurtz, D.; Sadowski, M.; Needham, L. L.; Calafat, A. M. Assessing Human Exposure to Phthalates Using Monoesters and Their Oxidized Metabolites as Biomarkers. *Environmental Health Perspectives* **2003,** *111* (9), 1148-1151.

89. Kavlock, R.; Boekelheide, K.; Chapin, R.; Cunningham, M.; Faustman, E.; Foster, P.; Golub, M.; Henderson, R.; Hinberg, I.; Little, R.; Seed, J.; Shea, K.; Tabacova, S.; Tyl, R.; Williams, P.; Zacharewski, T. NTP Center for the Evaluation of Risks to Human Reproduction: Phthalates Expert Panel Report on the Reproductive and Developmental Toxicity of Di(2-ethylhexyl) Phthalate. *Reproductive Toxicology* **2002,** *16* (5), 529-653.

90. (a) Koch, H. M.; Preuss, R.; Angerer, J. Di(2-ethylhexyl)phthalate (DEHP): Human Metabolism and Internal Exposure – An Update and Latest Results. *International Journal of Andrology* **2006,** *29* (1), 155-165; (b) Preuss, R.; Koch, H. M.; Angerer, J. Biological Monitoring of the Five Major Metabolites of Di-(2-ethylhexyl)phthalate (DEHP) in Human Urine Using Column-Switching Liquid Chromatography–Tandem Mass Spectrometry. *Journal of Chromatography B* **2005,** *816* (1), 269-280.

91. Fisher, J. S. Environmental Anti-Androgens and Male Reproductive Health: Focus on Phthalates and Testicular Dysgenesis Syndrome. *Reproduction* **2004,** *127* (3), 305-315.

92. (a) Foster, P. M. D. Disruption of Reproductive Development in Male Rat Offspring Following In Utero Exposure to Phthalate Esters. *International Journal of Andrology* **2006,** *29* (1), 140-147; (b) Howdeshell, K. L.; Furr, J.; Lambright, C. R.; Rider, C. V.; Wilson, V. S.; Gray, L. E. Cumulative Effects of Dibutyl Phthalate and Diethylhexyl Phthalate on Male Rat Reproductive Tract Development: Altered Fetal Steroid Hormones and Genes. *Toxicological Sciences* **2007,** *99* (1), 190-202; (c) MacLeod, D. J.; Sharpe, R. M.; Welsh, M.; Fisken, M.; Scott, H. M.; Hutchison, G. R.; Drake, A. J.; van den Driesche, S. Androgen Action in the Masculinization Programming Window and Development of Male Reproductive Organs. *International Journal of Andrology* **2010,** *33* (2), 279-286; (d) Hannas, B. R.; Lambright, C. S.; Furr, J.; Howdeshell, K. L.; Wilson, V. S.; Gray, L. E. Dose-Response Assessment of Fetal Testosterone Production and Gene Expression Levels in Rat Testes Following In Utero Exposure to Diethylhexyl Phthalate, Diisobutyl Phthalate, Diisoheptyl Phthalate, and Diisononyl Phthalate. *Toxicological Sciences* **2011,** *123* (1), 206-216.

93. (a) Foster, P. M. D.; Mylchreest, E.; Gaido, K. W.; Sar, M. Effects of Phthalate Esters on the Developing Reproductive Tract of Male Rats. *Human Reproduction Update* **2001,** *7* (3), 231-235; (b) Mylchreest, E.; Sar, M.; Cattley, R. C.; Foster, P. M. D. Disruption of Androgen-Regulated Male Reproductive Development by Di(*n*-Butyl) Phthalate During Late Gestation in Rats is Different from Flutamide. *Toxicology and Applied Pharmacology* **1999,** *156* (2), 81-95.

94. Lyche, J. L.; Gutleb, A. C.; Bergman, A.; Eriksen, G. S.; Murk, A. J.; Ropstad, E.; Saunders, M.; Skaare, J. U. Reproductive and Developmental Toxicity of Phthalates. *Journal of Toxicology and Environmental Health-Part B-Critical Reviews* **2009,** *12* (4), 225-249.

95. Salazar-Martinez, E.; Romano-Riquer, P.; Yanez-Marquez, E.; Longnecker, M. P.; Hernandez-Avila, M. Anogenital Distance in Human Male and Female Newborns: A Descriptive, Cross-Sectional Study. *Environmental Health* **2004,** *3* (1), 8.

96. Borch, J.; Metzdorff, S. B.; Vinggaard, A. M.; Brokken, L.; Dalgaard, M. Mechanisms Underlying the Anti-Androgenic Effects of Diethylhexyl Phthalate in Fetal Rat Testis. *Toxicology* **2006,** *223* (1), 144-155.

97. Ivell, R.; Anand-Ivell, R. Biology of Insulin-Like Factor 3 in Human Reproduction. *Human Reproduction Update* **2009,** *15* (4), 463-476.

98. Parks, L. G.; Ostby, J. S.; Lambright, C. R.; Abbott, B. D.; Klinefelter, G. R.; Barlow, N. J.; Gray, L. E. The Plasticizer Diethylhexyl Phthalate Induces Malformations by Decreasing Fetal Testosterone Synthesis During Sexual Differentiation in the Male Rat. *Toxicological Sciences* **2000,** *58* (2), 339-349.

99. Stroheker, T.; Cabaton, N.; Nourdin, G.; Regnier, J.-F.; Lhuguenot, J.-C.; Chagnon, M.-C. Evaluation of Anti-Androgenic Activity of Di-(2-ethylhexyl) Phthalate. *Toxicology* **2005,** *208* (1), 115-121.

100. (a) Silva, M. J.; Barr, D. B.; Reidy, J. A.; Malek, N. A.; Hodge, C. C.; Caudill, S. P.; Brock, J. W.; Needham, L. L.; Calafat, A. M. Urinary levels of Seven Phthalate Metabolites in the U.S. Population from the National Health and Nutrition Examination Survey (NHANES) 1999-2000. *Environ. Health Perspect.* **2004,** *112* (3), 331-338; (b) Trasande, L.; Attina, T. M.; Sathyanarayana, S.; Spanier, A. J.; Blustein, J. Race/Ethnicity-Specific Associations of Urinary Phthalates with Childhood Body Mass in a Nationally Representative Sample. *Environmental Health Perspectives* **2013,** *121* (4), 501-506.

101. Kobrosly, R. W.; Parlett, L. E.; Stahlhut, R. W.; Barrett, E. S.; Swan, S. H. Socioeconomic Factors and Phthalate Metabolite Concentrations Among United States Women of Reproductive Age. *Environmental Research* **2012,** *115*, 11-17.

102. Meek, M. E.; Chan, P. K. L. Bis(2-ethylhexyl)phthalate: Evaluation of Risks to Health From Environmental Exposure in Canada. *Journal of Environmental Science and Health, Part C* **1994,** *12* (2), 179-194.

103. Wormuth, M.; Scheringer, M.; Vollenweider, M.; Hungerbühler, K. What Are the Sources of Exposure to Eight Frequently Used Phthalic Acid Esters in Europeans? *Risk Analysis* **2006,** *26* (3), 803-824.

104. (a) Skakkebaek, N. E.; Rajpert-De Meyts, E.; Main, K. M. Testicular Dysgenesis Syndrome: An Increasingly Common Developmental Disorder with Environmental Aspects. *Human Reproduction* **2001,** *16* (5), 972-978; (b) Sharpe, R. M.; Franks, S. Environment, Lifestyle and Infertility - an Inter-Generational Issue. *Nature Medicine* **2002,** *8*, 33-40.

105. Swan, S. H.; Main, K. M.; Liu, F.; Stewart, S. L.; Kruse, R. L.; Calafat, A. M.; Mao, C. S.; Redmon, J. B.; Ternand, C. L.; Sullivan, S.; Teague, J. L.; Study Future Families Res, T. Decrease in Anogenital Distance Among Male Infants with Prenatal Phthalate Exposure. *Environmental Health Perspectives* **2005,** *113* (8), 1056-1061.

106. Swan, S. H. Environmental Phthalate Exposure in Relation to Reproductive Outcomes and Other Health Endpoints in Humans. *Environmental Research* **2008,** *108* (2), 177-184.

107. Spade, D. J.; McDonnell, E. V.; Heger, N. E.; Sanders, J. A.; Saffarini, C. M.; Gruppuso, P. A.; De Paepe, M. E.; Boekelheide, K. Xenotransplantation Models to Study the Effects of Toxicants on Human Fetal Tissues. *Birth Defects Research Part B-Developmental and Reproductive Toxicology* **2014,** *101* (6), 410-422.

108. Heger, N. E.; Hall, S. J.; Sandrof, M. A.; McDonnell, E. V.; Hensley, J. B.; McDowel, E. N.; Martin, K. A.; Gaido, K. W.; Johnson, K. J.; Boekelheide, K. Human Fetal Testis Xenografts Are Resistant to Phthalate-Induced Endocrine Disruption. *Environmental Health Perspectives* **2012,** *120* (8), 1137-1143.

109. Fisher, J. S.; Macpherson, S.; Marchetti, N.; Sharpe, R. M. Human 'Testicular Dysgenesis Syndrome': A Possible Model Using In-Utero Exposure of the Rat to Dibutyl Phthalate. *Human Reproduction* **2003,** *18* (7), 1383-1394.

110. Mitchell, R. T.; Childs, A. J.; Anderson, R. A.; van den Driesche, S.; Saunders, P. T. K.; McKinnell, C.; Wallace, W. H. B.; Kelnar, C. J. H.; Sharpe, R. M. Do Phthalates Affect Steroidogenesis by the Human Fetal Testis? Exposure of Human Fetal Testis Xenografts to Di-*n*-Butyl Phthalate. *The Journal of Clinical Endocrinology and Metabolism* **2012,** *97* (3), E341-E348.

111. Scott, H. M.; Mason, J. I.; Sharpe, R. M. Steroidogenesis in the Fetal Testis and Its Susceptibility to Disruption by Exogenous Compounds. *Endocrine Reviews* **2009,** *30* (7), 883-925.

112. Desdoits-Lethimonier, C.; Albert, O.; Le Bizec, B.; Perdu, E.; Zalko, D.; Courant, F.; Lesne, L.; Guille, F.; Dejucq-Rainsford, N.; Jegou, B. Human Testis Steroidogenesis Is Inhibited by Phthalates. *Human Reproduction* **2012,** *27* (5), 1451-1459.

113. Shamir, E. R.; Ewald, A. J. Three-Dimensional Organotypic Culture: Experimental Models of Mammalian Biology and Disease. *Nature Reviews Molecular Cell Biology* **2014,** *15* (10), 647-664.

114. Griswold, M. D. The Central Role of Sertoli Cells in Spermatogenesis. *Seminars in Cell & Developmental Biology* **1998,** *9* (4), 411-416.

115. Meachem, S. J.; Nieschlag, E.; Simoni, M. Inhibin B in Male Reproduction: Pathophysiology and Clinical Relevance. *European Journal of Endocrinology* **2001,** *145* (5), 561-571.

116. (a) Deyo, J. A. Carcinogenicity and Chronic Toxicity of Di-2-Ethylhexyl Terephthalate (DEHT) Following a 2-Year Dietary Exposure in Fischer 344 Rats. *Food and Chemical Toxicology* **2008,** *46* (3), 990-1005; (b) Eckert, E.; Munch, F.; Goen, T.; Purbojo, A.; Muller, J.; Cesnjevar, R. Comparative Study On the Migration of Di-2-Ethylhexyl Phthalate (DEHP) and Tri-2-Ethylhexyl Trimellitate (TOTM) Into Blood From PVC Tubing Material of a Heart-Lung Machine. *Chemosphere* **2016,** *145*, 10-16.

117. Johnson, W. Final Report on the Safety Assessment of Acetyl Triethyl Citrate, Acetyl Tributyl Citrate, Acetyl Trihexyl Citrate, and Acetyl Trioctyl Citrate. *International Journal of Toxicology* **2002,** *21* (5), 1-17.

118. ter Veld, M. G. R.; Schouten, B.; Louisse, J.; Es, D. S. van; Saag, P. T. van der; Rietjens, I. M. C. M.; Murk, A. J. Estrogenic Potency of Food-Packaging-Associated Plasticizers and Antioxidants As Detected in ERα and ERβ Reporter Gene Cell Lines. *Journal of Agricultural and Food Chemistry* **2006**, *54* (12), 4407-4416

119. Stuart, A.; McCallum, M. M.; Fan, D. M.; LeCaptain, D. J.; Lee, C. Y.; Mohanty, D. K. Poly(vinyl chloride) Plasticized With Succinate Esters: Synthesis and Characterization. *Polymer Bulletin* **2010,** *65* (6), 589-598.

120. Bonora, S.; Ercoli, L.; Torreggiani, A.; Fini, G. Influence of Sebacate Plasticizers on the Thermal Behaviour of Dipalmitoylphosphatidylcholine Liposomes. *Thermochimica Acta* **2002,** *385* (1-2), 51-61.

121. Yin, B.; Hakkarainen, M. Oligomeric Isosorbide Esters as Alternative Renewable Resource Plasticizers for PVC. *Journal of Applied Polymer Science* **2011,** *119* (4), 2400-2407.

122. Erythropel, H. C.; Maric, M.; Nicell, J. A.; Leask, R. L.; Yargeau, V. Leaching of the Plasticizer Di(2-ethylhexyl)phthalate (DEHP) From Plastic Containers and the Question of Human Exposure. *Applied Microbiology and Biotechnology* **2014,** *98* (24), 9967-9981.

123. Fankhauser-Noti, A.; Grob, K. Blank Problems In Trace Analysis of Diethylhexyl and Dibutyl Phthalate: Investigation of the Sources, Tips and Tricks. *Analytica Chimica Acta* **2007,** *582* (2), 353-360.

124. Marega, M.; Grob, K.; Moret, S.; Conte, L. Phthalate Analysis By Gas Chromatography-Mass Spectrometry: Blank Problems Related to the Syringe Needle. *Journal of Chromatography A* **2013,** *1273*, 105-110.

125. Oca, M. L.; Rubio, L.; Sarabia, L. A.; Ortiz, M. C. Dealing With the Ubiquity of Phthalates In the Laboratory When Determining Plasticizers By Gas Chromatography/Mass Spectrometry and PARAFAC. *Journal of Chromatography A* **2016,** *1464*, 124-140.

126. Ito, M.; Nagai, K. Analysis of Degradation Mechanism of Plasticized PVC Under Artificial Aging Conditions. *Polymer Degradation and Stability* **2007,** *92* (2), 260-270.

127. Hankett, J. M.; Collin, W. R.; Chen, Z. Molecular Structural Changes of Plasticized PVC After UV Light Exposure. *Journal of Physical Chemistry B* **2013,** *117* (50), 16336-16344.

128. Martinez, G.; Mijangos, C.; Millan, J. Selective Substitution Reactions on PVC. Lability of Some Normal Structures. *Journal of Macromolecular Science Chemistry* **1982,** *A17* (7), 1129-1148.

129. Mijangos, C.; Martinez, A.; Michel, A. Fonctionnalisation du Polychlorure de Vinyle: Greffage de Fonctions Plastifiantes (Type Ester d'Ethyle-Hexyle). *European Polymer Journal* **1986,** *22* (5), 417-421.

130. Navarro, R.; Gacal, T.; Ocakoglu, M.; Garcia, C.; Elvira, C.; Gallardo, A.; Reinecke, H. Nonmigrating Equivalent Substitutes for PVC/DOP Formulations as Shown by a TG Study of PVC with Covalently Bound PEO-PPO Oligomers. *Macromolecular Rapid Communications* **2017,** *38* (6).

131. Navarro, R.; Bierbrauer, K.; Mijangos, C.; Goiti, E.; Reinecke, H. Modification of Poly(Vinyl Chloride) with New Aromatic Thiol Compounds. Synthesis and Characterization. *Polymer Degradation and Stability* **2008,** *93* (3), 585-591.

132. Navarro, R.; Perrino, M. P.; Tardajos, M. G.; Reinecke, H. Phthalate Plasticizers Covalently Bound to PVC: Plasticization with Suppressed Migration. *Macromolecules* **2010,** *43* (5), 2377-2381.

133. Navarro, R.; Perrino, M. P.; Garcia, C.; Elvira, C.; Gallardo, A.; Reinecke, H. Opening New Gates for the Modification of PVC or Other PVC Derivatives: Synthetic Strategies for the Covalent Binding of Molecules to PVC. *Polymers* **2016,** *8* (4), 152-165.

134. Navarro, R.; Perrino, M. P.; Garcia, C.; Elvira, C.; Gallardo, A.; Reinecke, H. Highly Flexible PVC Materials Without Plasticizer Migration as Obtained by Efficient One-Pot Procedure Using Trichlorotriazine Chemistry. *Macromolecules* **2016,** *49* (6), 2224-2227.

135. Blotny, G. Recent Applications of 2,4,6-Trichloro-1,3,5-Triazine and its Derivatives in Organic Synthesis. *Tetrahedron* **2006,** *62* (41), 9507-9522.

136. Technical Bulletin: JEFFAMINE™ Polyetheramines. http://www.huntsman.com/performance_products/a/Products/Amines/Polyetheramines%20%20%20JEFFAMINE_R (accessed Sept 7, 2017).

137. Castro, R. E. N.; Toledo, E. A.; Rubira, A. F.; Muniz, E. C. Crystallisation and Miscibility of Poly(Ethylene Oxide)/Poly(Vinyl Chloride) Blends. *Journal of Materials Science* **2003,** *38* (4), 699-703.

138. Jia, P. Y.; Hu, L. H.; Yang, X. H.; Zhang, M.; Shang, Q. Q.; Zhou, Y. H. Internally Plasticized PVC Materials via Covalent Attachment of Aminated Tung Oil Methyl Ester. *RSC Advances* **2017,** *7* (48), 30101-30108.

139. Yoo, Y.; Youngblood, J. P. Tung Oil Wood Finishes with Improved Weathering, Durability, and Scratch Performance by Addition of Cellulose Nanocrystals. *ACS Applied Materials & Interfaces* **2017,** *9* (29), 24936-24946.

140. Ahmed, S. A.; Moren, T.; Sehlstedt-Persson, M.; Blom, A. Effect of Oil Impregnation On Water Repellency, Dimensional Stability and Mold Susceptibility of Thermally Modified European Aspen and Downy Birch Wood. *Journal of Wood Science* **2017,** *63* (1), 74-82.

141. (a) Yang, J. B.; Feng, Y. Y.; Zeng, T.; Guo, X. T.; Li, L.; Hong, R. Y.; Qiu, T. Synthesis of Biodiesel via Transesterification of Tung Oil Catalyzed By New Bronsted Acidic Ionic Liquid. *Chemical Engineering Research & Design* **2017,** *117*, 584-592; (b) Qi, D. H.; Yang, K.; Zhang, D.; Chen, B.; Wei, Q.; Zhang, C. H. Experimental Investigation of a Turbocharged CRDI Diesel Engine Fueled with Tung Oil-Diesel-Ethanol Microemulsion Fuel. *Renewable Energy* **2017,** *113*, 1201-1207.

142. Žlahtič, M.; Mikac, U.; Serša, I.; Merela, M.; Humar, M. Distribution and Penetration of Tung Oil in Wood Studied by Magnetic Resonance Microscopy. *Industrial Crops and Products* **2017,** *96*, 149-157.

143. Jia, P.; Hu, L.; Shang, Q.; Wang, R.; Zhang, M.; Zhou, Y. Self-Plasticization of PVC Materials via Chemical Modification of Mannich Base of Cardanol Butyl Ether. *ACS Sustainable Chemistry & Engineering* **2017,** *5* (8), 6665-6673.

144. Tyman, J. H. P.; Wilczynski, D.; Kashani, M. A. Phenolic Lipids. Part XI. Compositional Studies on Technical Cashew Nutshell Liquid (CNSL) by Chromatography and Mass Spectroscopy. *Journal of the American Oil Chemists' Society* **1978,** *55* (9), 663-668.

145. Yang, P.; Yan, J.; Sun, H. Z.; Fan, H. J.; Chen, Y.; Wang, F.; Shi, B. Novel Environmentally Sustainable Cardanol-Based Plasticizer Covalently Bound to PVC via Click Chemistry: Synthesis and Properties. *RSC Advances* **2015,** *5* (22), 16980-16985.

146. Jia, P. Y.; Hu, L. H.; Feng, G. D.; Bo, C. Y.; Zhang, M.; Zhou, Y. H. PVC Materials Without Migration Obtained by Chemical Modification of Azide-Functionalized PVC and Triethyl Citrate Plasticizer. *Materials Chemistry and Physics* **2017,** *190*, 25-30.

147. Apelblat, A.; Korin, E.; Manzurola, E. Thermodynamic Properties of Aqueous Solutions with Citrate Ions. Compressibility Studies in Aqueous Solutions of Citric Acid. *Journal of Chemical Thermodynamics* **2013,** *64*, 14-21.

148. (a) Himo, F.; Lovell, T.; Hilgraf, R.; Rostovtsev, V. V.; Noodleman, L.; Sharpless, K. B.; Fokin, V. V. Copper(I)-Catalyzed Synthesis of Azoles. DFT Study Predicts Unprecedented Reactivity and Intermediates. *Journal of the American Chemical Society* **2005,** *127* (1), 210-216; (b) Rostovtsev, V. V.; Green, L. G.; Fokin, V. V.; Sharpless, K. B. A Stepwise Huisgen Cycloaddition Process: Copper(I)-Catalyzed Regioselective "Ligation" of Azides and Terminal Alkynes. *Angewandte Chemie International Edition* **2002,** *41* (14), 2596-2599.

149. Lee, K. W.; Chung, J. W.; Kwak, S. Y. Structurally Enhanced Self-Plasticization of Poly(vinyl chloride) via Click Grafting of Hyperbranched Polyglycerol. *Macromolecular Rapid Communications* **2016,** *37* (24), 2045-2051.

150. Demirci, G.; Tasdelen, M. A. Synthesis and Characterization of Graft Copolymers by Photoinduced CuAAC Click Chemistry. *European Polymer Journal* **2015,** *66*, 282-289.

151. Pawlak, M.; Mistlberger, G.; Bakker, E. In Situ Surface Functionalization of Plasticized Poly(Vinyl Chloride) Membranes by Click Chemistry. *Journal of Materials Chemistry* **2012,** *22* (25), 12796-12801.

152. Earla, A.; Braslau, R. Covalently Linked Plasticizers: Triazole Analogues of Phthalate Plasticizers Prepared by Mild Copper-Free "Click" Reactions with Azide-Functionalized PVC. *Macromolecular Rapid Communications* **2014,** *35* (6), 666-671.

153. Rathwell, K.; Sperry, J.; Brimble, M. A. Synthesis of Triazole Analogues of the Nanaomycin Antibiotics Using 'Click Chemistry'. *Tetrahedron* **2010,** *66* (23), 4002-4009.

154. Earla, A.; Li, L. B.; Costanzo, P.; Braslau, R. Phthalate Plasticizers Covalently Linked to PVC via Copper-Free or Copper Catalyzed Azide-Alkyne Cycloadditions. *Polymer* **2017,** *109*, 1-12.

2 Direct and Single Hexyl Tethered Alkyl Triazole Phthalate Mimics

2.1 The 1,3-Dipolar Cycloaddition

A facile method to create a phthalate mimic covalently bound to poly(vinyl chloride) (PVC) was investigated: factors considered included cost, simplicity, and ease of implementation in an industrial setting. The azide-alkyne cycloaddition was quickly recognized as an efficient method to incorporate triazole-based phthalate mimics directly bound to PVC. The PVC 1,2-diester triazole moiety closely resembles a phthalate plasticizer such as DEHP (**Scheme 2.1**). In this way, two simple synthetic steps are required to create the desired plasticizer without a metal catalyst, as compared to the copper-mediated azide alkyne cycloaddition (CuAAC) popularized by Sharpless and coworkers.[1] A metal-free reaction is preferred in most industrial modalities, as contamination can lead to deleterious post-production effects.

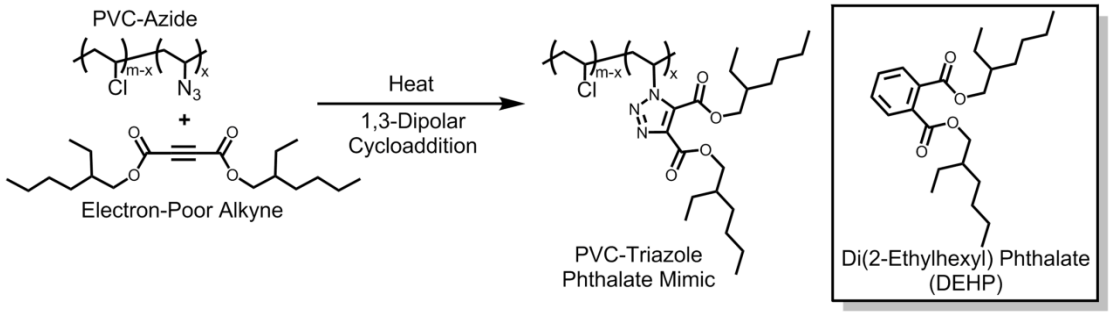

Scheme 2.1 Azide-Alkyne Thermal Dipolar Cycloaddition Furnishing a PVC-Triazole Phthalate Mimic

The azide-alkyne cycloaddition (AAC) belongs to a class of reactions called 1,3-dipolar cycloadditions, which generally involve an electron-rich 1,3-dipole and an electron-poor dipolarophile, forming a neutral five-membered ring (**Scheme 2.2**).[2] Mechanistically, this reaction is pericyclic and concerted. The cycloaddition obeys the Woodward-Hoffman[3] and Dewar-Zimmermann[4] rules. According to the Woodward-Hoffmann definition, frontier molecular orbitals of the 1,3-dipole and dipolarophile overlap in a suprafacial π4s + π2s symmetry allowed manner. In the Dewar-Zimmerman Möbius-Hückel approach, the 1,3-

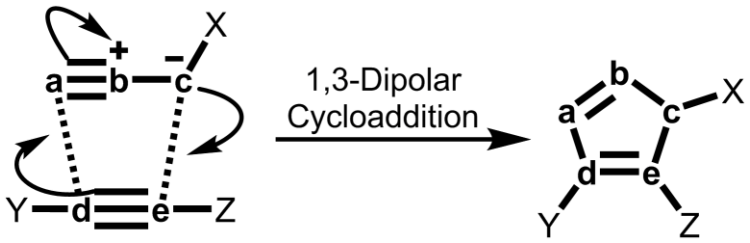

Scheme 2.2 1,3-Dipolar Cycloaddition Mechanism of a Dipole and Alkyne

dipolar cycloaddition is considered a Hückel 4n+2, six-electron system with two phase inversions: therefore this reaction is thermally allowed and photochemically forbidden.

1,3-Dipole	1 ↘ a≡b–c ↙ 3
Azide	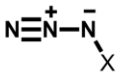
Diazoalkane	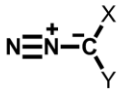
Nitrous Oxide	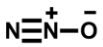
Nitrile Ylide	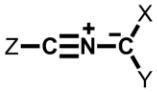
Nitrilimine	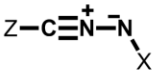
Nitrile Oxide	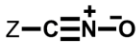

Table 2.1 Examples of 1,3-Dipoles

The 1,3-dipole is a zwitterionic species, systematically designated "*a*-*b*-*c*" (**Table 2.1**). In the case of an azide-alkyne cycloaddition, the 1,3-dipole is an azide, while the dipolarophile is an alkyne (designated "*d*-*e*", **Scheme 2.2**). Taking into account the number of atoms in the 1,3-dipole (3) and dipolarophile (2), this reaction can also be designated as a (3+2) cycloaddition. Molecular orbitals of the dipole and dipolarophile must sufficiently overlap to allow the concerted movement of electrons to form the five-membered ring. Therefore, reaction efficiency is determined by the energy gap between the highest occupied molecular orbital (HOMO) of the azide and the lowest unoccupied molecular orbital (LUMO) of the alkyne.[5] Increased cycloaddition reactivity can be achieved by utilizing a strained or electron-deficient alkyne. In a strained alkyne, the angle of two p-orbitals of the sp-hybridized carbon-carbon bond are bent further apart than that in the analogous π-bond of ethylene.[6] The overlap of the p-orbitals is less than in a

standard sp^2 or sp carbon-carbon bond: this raises the HOMO and lowers the LUMO in strained systems.

In 1961, Wittig and Krebs[7] observed the explosive reaction of cyclooctyne and phenyl azide, forming the triazole product (**Scheme 2.3**). The strained alkyne present in cyclooctyne has a lower LUMO than a non-strained analogue. The bond angles of the sp carbons in cyclooctyne are ~160°, with approximately 18 kcal/mol of ring strain, which distorts the orbitals toward the transition state and final product of the cycloaddition.[8] In contrast to linear alkynes, the reaction takes place vigorously under mild heating.

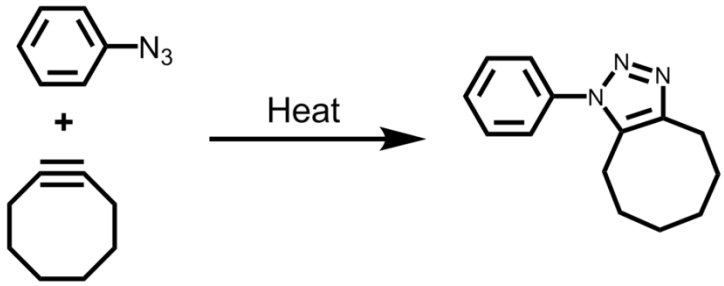

Scheme 2.3 Wittig and Krebs' Phenyl Azide and Cyclooctyne Cycloaddition[7]

Inspired by this early work, the Bertozzi group[8-9] pioneered a copper-free strain-promoted azide-alkyne cycloaddition (SPAAC) as a useful strategy to carry out chemical reactions that are biorthogonal: they do not interfere with biological processes.[9a] Copper-catalyzed azide-alkyne cycloadditions (CuAAC)[10] are fast, easy to work up, have no side products, and have a broad scope of applications. The system developed by Bertozzi does not require excessive heat nor a cytotoxic transition metal catalyst: the triazole is formed under biocompatible conditions. Cyclooctynes with functional groups that allow future coupling to fluorophores were synthesized (**Figure 2.1**). However, the second-order rate constants of the prototypical molecules were not sufficient to mediate the dipolar cycloaddition under ambient conditions. In order to increase the rate, fluorine atoms were placed on one of the α-carbons adjacent to the alkyne. Subsequently, aromatic groups were

fused on the cyclooctyne ring to enhance the reaction rate by further increasing the strain on the triple bond.[9a]

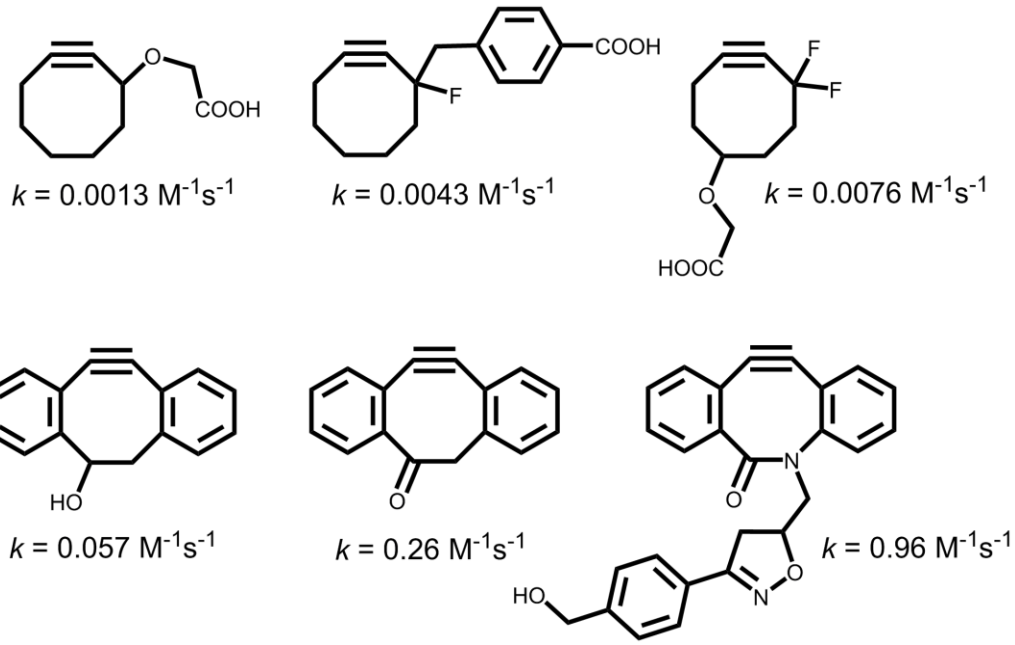

Figure 2.1 Second-Order Rate Constants of Reactions Between Alkyl Azide and Bertozzi's Cyclooctynes[8-9]

While SPAAC works well for small-scale biological applications, the cyclooctynes are challenging to synthesize and expensive to purchase. Another strategy to lower the alkyne's LUMO involves placing strong electron-withdrawing groups directly on the sp-carbons, thereby creating an electron-deficient alkyne. Electron-withdrawing groups (EWG) include halides, sulfonates, cyano, nitro groups and carbonyls such as esters, amides, ketones, aldehydes, and carboxylic acids. Synthetically, the carbonyl alkynes are often easily accessed. Enhanced cyclization rates and low temperatures are desirable reaction attributes when forming the triazole phthalate mimics on PVC.

2.2 1,3-Dipolar Cycloaddition: Electron-Deficient Alkynes

In 1893, Arthur Michael first described the thermal dipolar azide-alkyne cycloaddition.[11] In this seminal publication, Michael combined phenyl azide and dimethyl

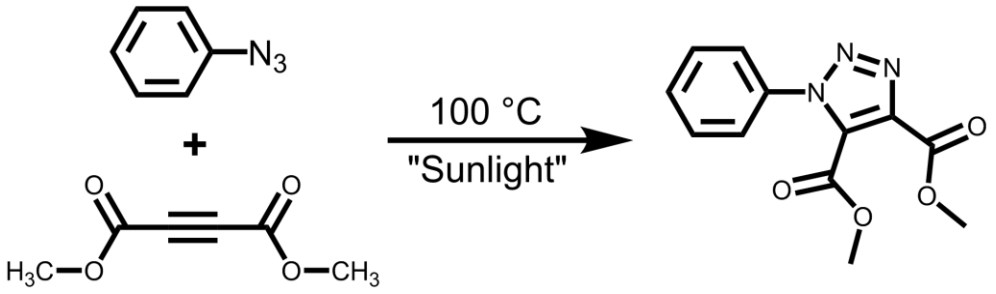

Scheme 2.4 Michael's Azide-Alkyne Cycloaddition[11]

acetylenedicarboxylate in a sealed tube at 100 °C for 8 hours under sunlight (**Scheme 2.4**). White needles were obtained, which possessed a molecular formula of $C_{12}H_{11}N_3O_4$. Michael commented on the similarity of the reaction done by Buchner and Witter[12] the same year, in which methyl diazoacetate and dimethyl acetylenedicarboxylate were combined to produce what was then called "pyrazoltricarbonsaureester," or pyrazole tri-carbon acid ester. In this era of chemistry, cycloadditions were novel, uncommon reactions. For perspective, the thermal azide-alkyne cycloaddition done by Michael predates the Nobel Prize winning work of Diels and Alder[13] by 35 years. The 1,3-dipolar cycloaddition was rediscovered nearly seven decades later by Huisgen,[14] who recognized that reactions of this nature had been previously investigated. However, the mechanistic details, scope and applications were not thoroughly understood by Michael[11] 70 years prior. Huisgen[15] observed a trend corresponding to the rate of a 1,3-dipolar cycloaddition between diazoalkanes (a similar 1,3 dipole to azide), and electron-poor alkynes (**Scheme 2.5**). As more electron-withdrawing groups are added to the alkyne, a rate enhancement occurs. A single electron-withdrawing ester attached to a terminal alkyne increases the relative rate of the reaction 903-fold, compared to the phenyl acetylene standard. When two esters are attached to the alkyne, the rate increases 8203-fold over the standard. From these data it is clear that as an alkyne becomes more electron-poor, the rate of cyclization increases.

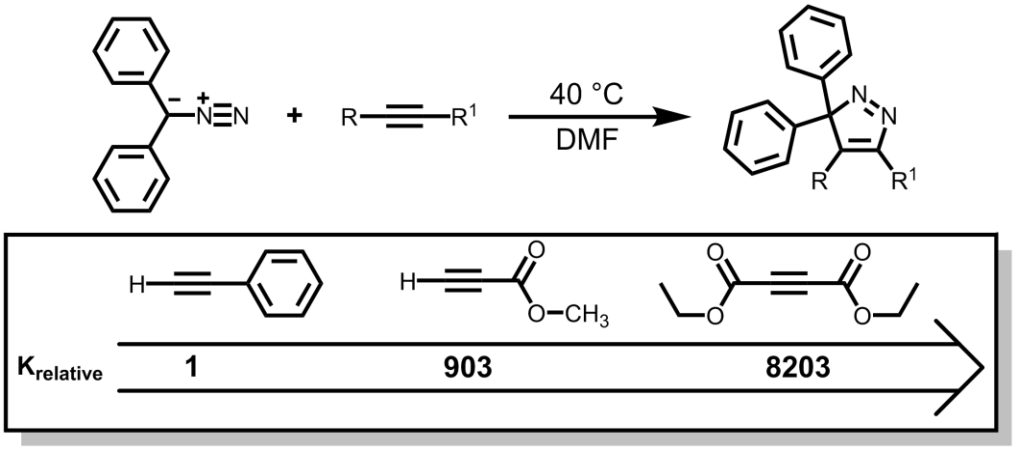

Scheme 2.5 Huisgen's Diazoalkane Reaction with Electron-Deficient Alkynes[15]

Brook and coworkers[5] studied the onset cycloaddition temperatures for a variety of alkynes and an alkyl azide *via* differential scanning calorimetry (**Scheme 2.6**). Similar to Huisgen's observations of reaction rates involving diazoalkanes, the relative onset temperature decreases with increasing electron-withdrawing substitution on the alkyne. Diethyl acetylenedicarboxylate, with two electron-withdrawing esters, has a low onset temperature of 37 °C. Benzyl propiolate, with a single ester, displays an intermediate onset temperature of 51 °C, while its amide derivative begins cyclization at 72 °C. The electron-donating trimethylsilane in 4-(trimethylsilyl)-3-butyn-2-one displays a high onset temperature of 90 °C. The data implies that as an alkyne becomes more electron-deficient, the amount of thermal energy to overcome E_A decreases.

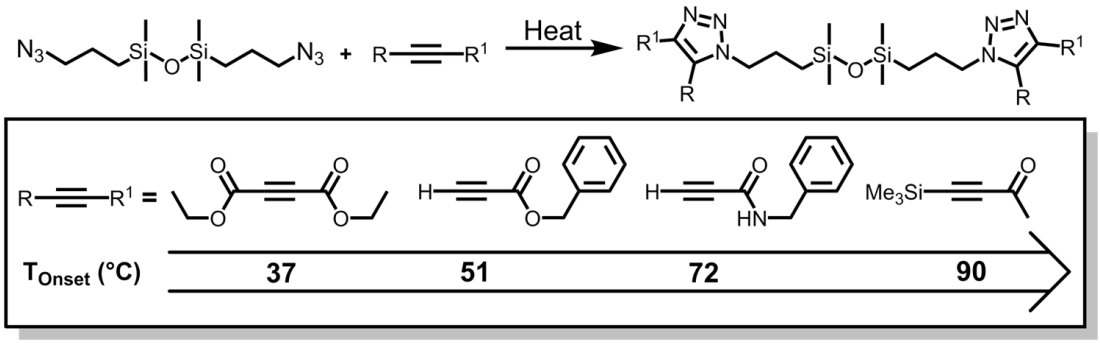

Scheme 2.6 Onset Temperatures for Brook's Azide-Alkyne Cycloadditions with Electron-Deficient Alkynes[5]

2.3 PVC Plasticization: Direct PVC Modification with Triazole-Phthalate Mimics

The azide-alkyne cycloaddition (AAC) was chosen as the simplest synthetic method to directly attach a phthalate mimic to the backbone of PVC. Development of electron-poor alkynes bearing two electron withdrawing groups facilitated decreased reaction times and improved yields. This thermal azide-alkyne cycloaddition system is modular, is synthetically simpler than current methods involving strained cyclooctynes, and creates a straightforward approach to covalently functionalize PVC with phthalate mimics. Thoughtful selection of EWGs with functionalizable tethering capabilities enables a multitude of applications under mild, copper-free conditions.

First, PVC-Azide **2.1** was synthesized in accordance to the procedure of Rusen and coworkers[16] (**Scheme 2.7**). Azide is an excellent nucleophile and a poor base: previous studies by the Braslau group[17] showed no indications of undesirable side reactions such as elimination.

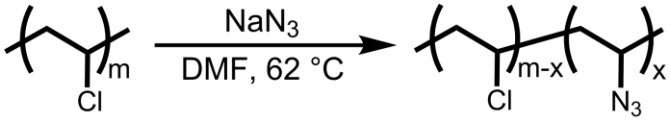

Reaction Time	Mol % Azide
30 min	5 %
2 h	15 %

Scheme 2.7 Synthesis of PVC-Azide **2.1**

PVC (Sigma-Aldrich, M_w: 43000 g/mol, PDI: 1.95) was purified by dissolving in tetrahydrofuran (THF) and precipitating in methanol three times. Next, PVC was treated with sodium azide in dimethylformamide (DMF) at 62 °C for either 30 minutes to give 5 mole percent azide or 2 hours to give 15 mole percent azide. The amount of chloride displaced by azide was determined by elemental analysis.[17b] After purification of PVC-azide *via* precipitation, FTIR verified that the reaction occurred, as indicated by the presence of the highly distinguishable azide stretch at 2114 cm^{-1} (**Figure 2.2**).

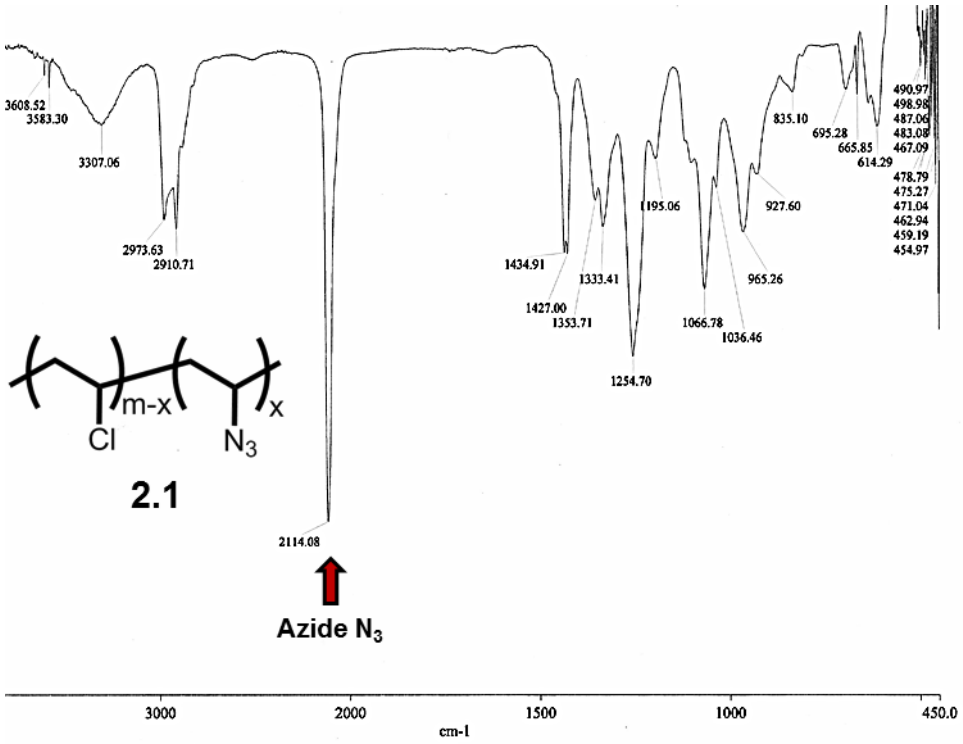

Figure 2.2 FTIR Spectrum of 15% PVC-Azide **2.1**

^{1}H-NMR and ^{13}C-NMR verified reaction completion. The ^{1}H-NMR of PVC-azide in $CDCl_3$ shows characteristic shifts (**a** and **c**) between δ1.77 – 2.46 ppm for the methylene protons of N_3-CH-C**H$_2$**, and Cl-CH-C**H$_2$** (**Figure 2.3**). Further downfield at δ 4.09 and δ 4.20 ppm, broad singlets are observed which correspond to the methine protons **d** of N_3-C**H**-CH_2. The remaining shifts are methine protons **a** adjacent to chlorine, Cl-C**H**-CH_2. ^{13}C-NMR in $CDCl_3$ exhibits small signals between δ 42.8 – 44.0 ppm, belonging to methylene carbons **C** adjacent to the azide (N_3-C-**C**H_2) (**Figure 2.4**). A family of peaks between δ 44.8 – 47.3 ppm are indicative of methylene carbons **A** adjacent to carbon bearing chloride (Cl-C-**C**H_2). Finally, methine shifts are observed for isotactic (δ 54.9 – 55.1 ppm), heterotactic (δ 55.7 – 56.1 ppm), and syndiotactic (δ 56.9 – 58.0 ppm) carbons **B** and **D** belonging to N_3-**C**H-CH_2 and Cl-**C**H-CH_2. In both ^{1}H-NMR and ^{13}C-NMR, no appreciable amount of elimination (alkene signals) were observed. Competing elimination reactions with certain nucleophiles (e.g., amine) give

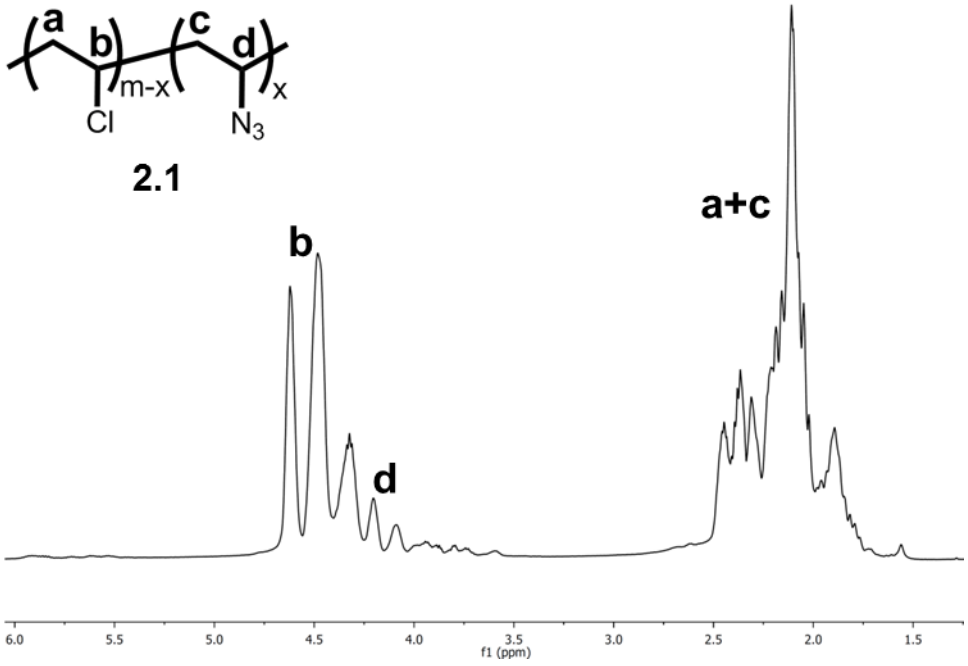

Figure 2.3 ^{1}H-NMR Spectrum of 15% PVC-Azide **2.1** in $CDCl_3$

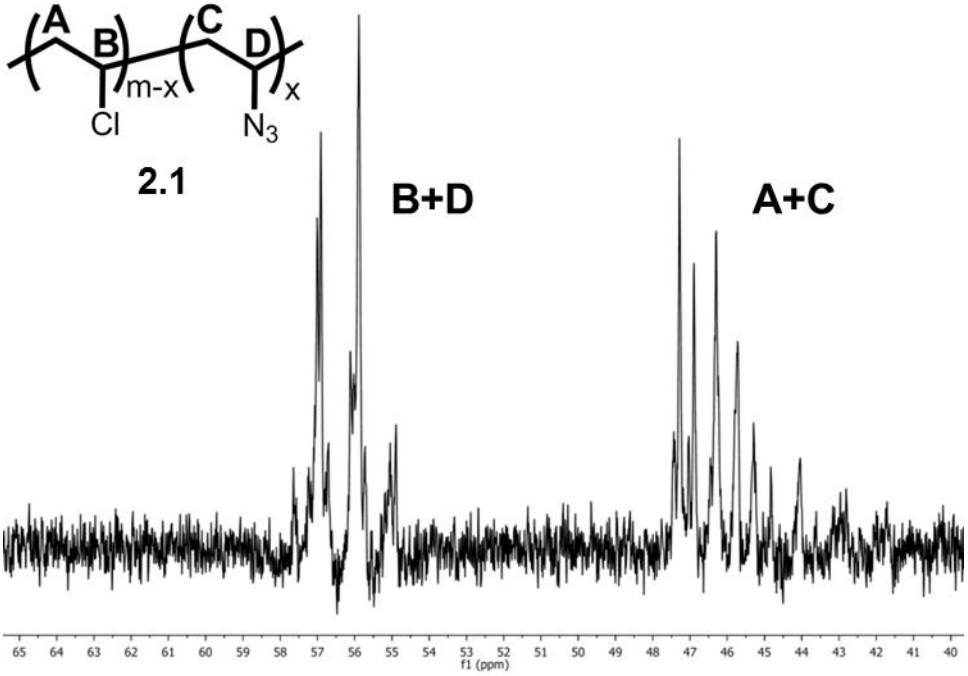

Figure 2.4 ^{13}C-NMR Spectrum of 15% PVC-Azide **2.1** in $CDCl_3$

rise to olefins during the S_N2 substitution on PVC. The presence of HCl byproduct catalyzes additional elimination reactions at the adjacent monomeric units. This process iteratively occurs until short polyene segments are formed throughout the main chain.[18]

Electron-deficient alkynes were synthesized with the intent of directly functionalizing PVC with triazole-based phthalate mimics. Following the synthesis described by Braslau and Earla,[17b] Fischer esterifications were performed. Acetylenedicarboxylic acid was treated with either *n*-butanol or 2-ethylhexyl alcohol and catalytic *p*-toluenesulfonic acid (*p*TSA) in toluene (**Scheme 2.8**). To drive the chemical equilibrium toward the di-ester in accordance with Le Chatelier's principle, a Dean-Stark apparatus was utilized to trap water formed as a by-product of the condensation. After 1 hour under reflux, di(*n*-butyl) acetylenedicarboxylate (DBuAD, **2.2**) and di(2-ethylhexyl) acetylenedicarboxylate (DEHAD, **2.3**) were obtained in 95 and 74 percent yield, respectively.

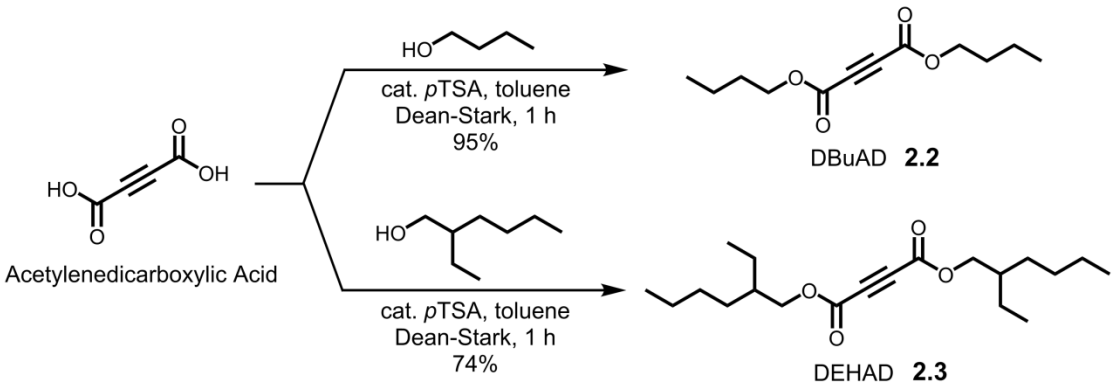

Scheme 2.8 Fischer Esterification of Acetylenedicarboxylic Acid to Form Electron-Deficient Alkynes **2.2 - 2.3**

In both DBuAD and DEHAD, two electron-withdrawing esters are directly attached to the sp-carbons of the alkyne, lowering the LUMO and enabling enhanced reaction rates with increased thermal efficiency. These factors are imperative for the cyclization with PVC-azide: the azide is somewhat sterically hindered as it is attached to a secondary carbon. In the original publication by Braslau and Earla,[17b] PVC-azide and alkyne di-esters were combined

in tetrahydrofuran (THF) and stirred at room temperature for 27 hours. According to the dissertation of Earla,[19] the cycloaddition of DEHAD with PVC-azide took 7 days to complete at room temperature, as monitored by FTIR.

A myriad of reaction conditions for the expeditious formation of the triazole-based phthalate mimic was explored. An aspect that affects reaction efficiency is the solvent: the thermal nature of azide-alkyne cycloadditions (AAC) may be exploited to increase the reaction rate. THF has a boiling point of 66 °C under ambient conditions. Therefore, the maximum amount of heat that the system can experience is relatively low: by utilizing a higher boiling solvent, the reaction will proceed at an accelerated rate. Investigation of a suitable solvent began with 1,2-dichloroethane, which dissolved PVC, but caused the reaction to darken at its boiling point (83 °C) presumably due to degradation. Likewise, DMF at elevated temperatures (80 – 100 °C) resulted in discoloration. Inspiration came from the construction industry, which commonly uses a technique called “solvent welding” to fuse materials (e.g., PVC pipe connectors): a specialty solvent is applied to two plastic components, which temporarily dissolves the polymer chains at room temperature, allowing one to join the pieces together. A search of common solvents for this purpose revealed that ketones are able to solubilize PVC. Cyclohexanone was effective at dissolving both PVC and the alkynes at temperatures of 90 to 100 °C. However, this solvent proved difficult to work with when precipitating the polymer following cycloaddition. If the system is too dilute, the functionalized PVC will not effectively precipitate in the anti-solvent, methanol. This issue can be mitigated by concentrating the reaction *in vacuo*. Unfortunately, cyclohexanone creates an operationally challenging workup: it has an excessively high boiling point (155 °C) that makes it difficult to concentrate. After this setback, butanone (also known as methyl ethyl ketone, MEK) was considered. Although MEK dissolves PVC, its somewhat low boiling point (79 °C) limits the range of temperature tunability. After much deliberation, 3-pentanone was chosen as the final optimized solvent for the cyclization. 3-Pentanone (boiling point: 102 °C) offers a

large array of reaction temperatures, while maintaining the ability to be readily evaporated *in vacuo*. The boiling point also acts as a safety parameter with respect to PVC degradation, as the reaction cannot exceed 102 °C. HCl elimination is reported to commence above 100 °C.[20] In addition, 3-pentanone does not impart discoloration during the cyclization.

Copper-free azide-alkyne cycloadditions (AAC) were performed with PVC-azide (5 and 15 mole percent azide) and dimethyl acetylenedicarboxylate (DMAD, commercially available), DBuAD, or DEHAD in 3-pentanone. The reactions were carried out at 90 °C, for 24 hours with 2.5 – 3.0 equivalents of alkyne to each equivalent of azide (**Scheme 2.9**). A concentration ranging between 0.026 to 0.120 M (relative to azide) was chosen depending on the solubility of the alkyne and PVC-azide. Reaction progress was monitored *via* FTIR, noting the disappearance of the azide stretch (N_3) at ~2110 cm^{-1} and the appearance of the triazole

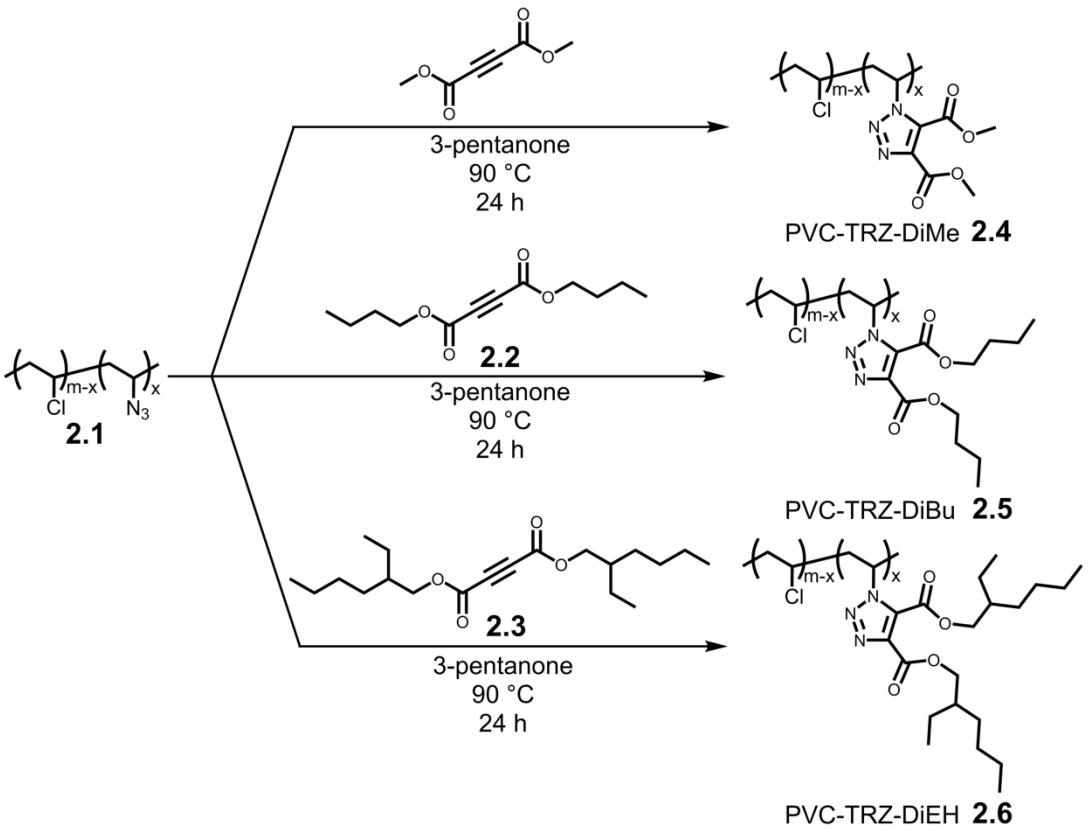

Scheme 2.9 Azide-Alkyne Cycloadditions of PVC-Azide **2.1** and Electron-Deficient Alkynes DMAD, **2.2 - 2.3**

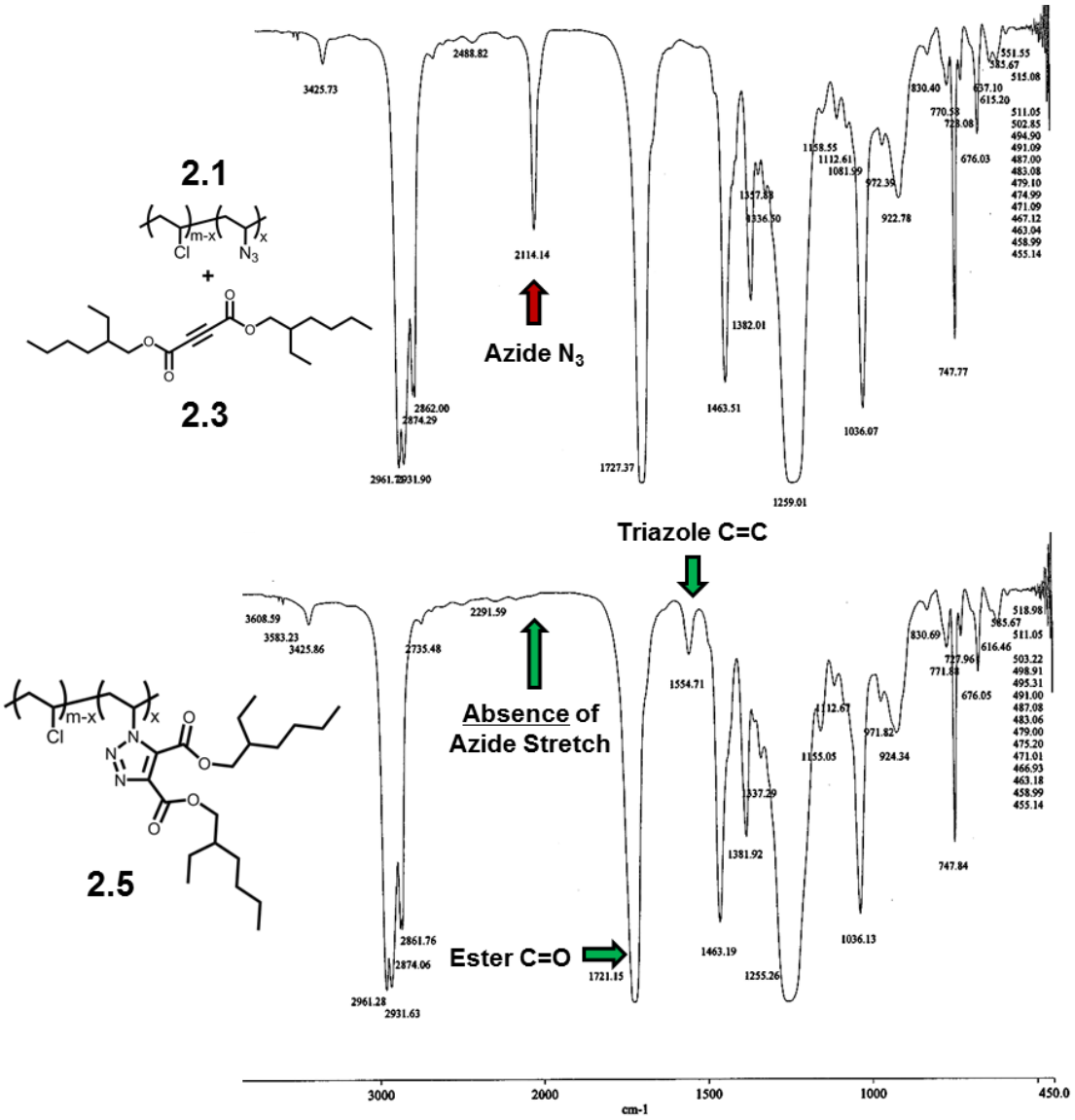

Figure 2.5 FTIR Monitoring of Cycloaddition Between 15% PVC-Azide **2.1** and DEHAD **2.3** at 90 °C
Top: After 15 Minutes
Bottom: After 24 Hours

(TRZ) sp^2 carbon-carbon stretch (C=C) at ~1550 cm^{-1} (**Figure 2.5**). After purification, the presence of an ester carbonyl stretch (C=O) at ~1730 cm^{-1} was also indicative of the successful formation of the triazole phthalate mimic on PVC.

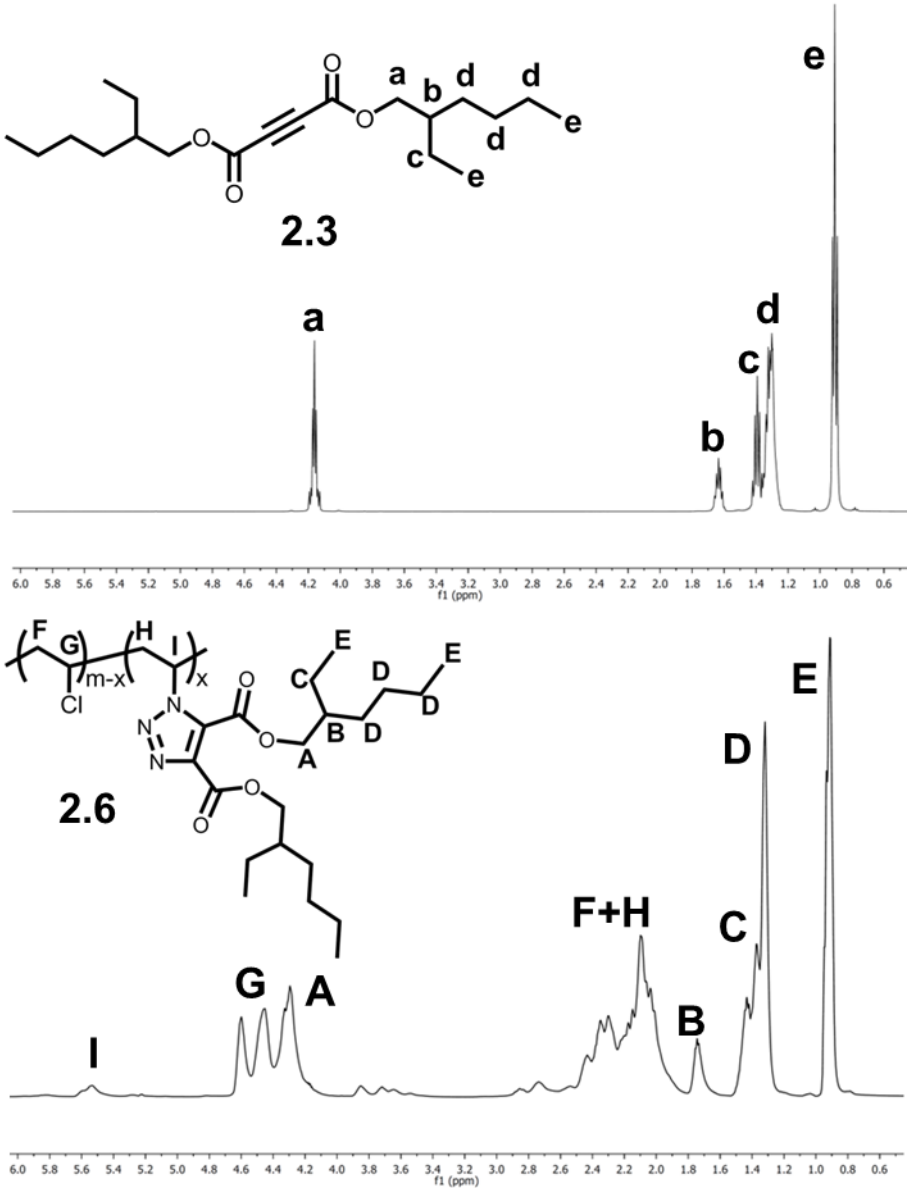

Figure 2.6 ^{1}H-NMR Spectra of DEHAD (**2.3**, Top)
and 15% PVC-TRZ-DiEH (**2.6**, Bottom)

^{1}H-NMR and ^{13}C-NMR were acquired for PVC-TRZ-DiMe, PVC-TRZ-DiBu, and PVC-TRZ-DiEH bearing both 5 and 15 mole percent triazole phthalate mimics in $CDCl_3$. Broadening of proton signals is ubiquitous in polymers due to heterogeneity, large size, and lack of isotropic molecular tumbling. Common to all directly modified PVC-triazole phthalate

mimics are characteristic ^{1}H-NMR signals **F** between δ 1.80 – 2.50 ppm, representing the methylene protons of Cl-CH-C**H$_2$** (**Figure 2.6**). Further downfield at δ 2.50 – 2.90 ppm are the β-position methylene protons **H** of PVC with respect to the triazole (TRZ-CH-C**H$_2$**). Between δ 4.10 – 4.70 ppm are a series of broad singlets which correspond to the methine protons **G** of Cl-C**H**-CH$_2$. Finally, methine protons **I** of PVC adjacent to a triazole appear in the range of δ 5.35 – 5.65 ppm (triazole-C**H**-CH$_2$); these are shifted downfield due to the newly formed aromatic ring's deshielding magnetic anisotropic effect.

In PVC-TRZ-DiMe, the ^{1}H signals of the methyl esters (TRZ Ester-O-C**H$_3$**) generally appear in the range of δ 4.00 – 4.10 as a series of singlets. In PVC-TRZ-DiBu and PVC-TRZ-DiEH, peaks ranging from δ 4.20 – 4.40 belong to the plasticizing alkyl chain methylene signals of TRZ Ester-O-C**H$_2$**-C. These overlap with the methine protons of PVC. The alkoxy-ester protons (Ester-O-C**H$_2$**-C) move further downfield once the triazole is formed due to the same deshielding anisotropic effect as the main chain methine protons (Cl-C**H**-CH$_2$). This is presented in **Figure 2.6** using 15% PVC-TRZ-DiEH **2.6** as an example: the alkoxy-protons (Ester-O-C**H$_2$**-C) of DEHAD **2.3** at δ 4.13 – 4.19 ppm show a well-defined multiplet **a** due to the ability of this small molecule to undergo sufficient isotropic tumbling in solution NMR. In contrast, analogous alkoxy-ester protons **A** of the triazole (TRZ Ester-O-C**H$_2$**-C) shift downfield and broaden due to attachment to PVC. PVC-triazole exhibits a significant amount of signal broadening due to a lack of isotropic tumbling, stemming from non-averaged anisotropic interactions. The multitude of proton signals present in the PVC-triazole spectra originate from various macromolecular regions that experience unique chemical environments. This leads to an array of peaks which become broadened and difficult to interpret.

For each PVC-triazole phthalate mimic, ^{13}C-NMR was measured in $CDCl_3$ (**Figure 2.7**). Carbon shifts common to all samples relate to the main chain of PVC. Methylene

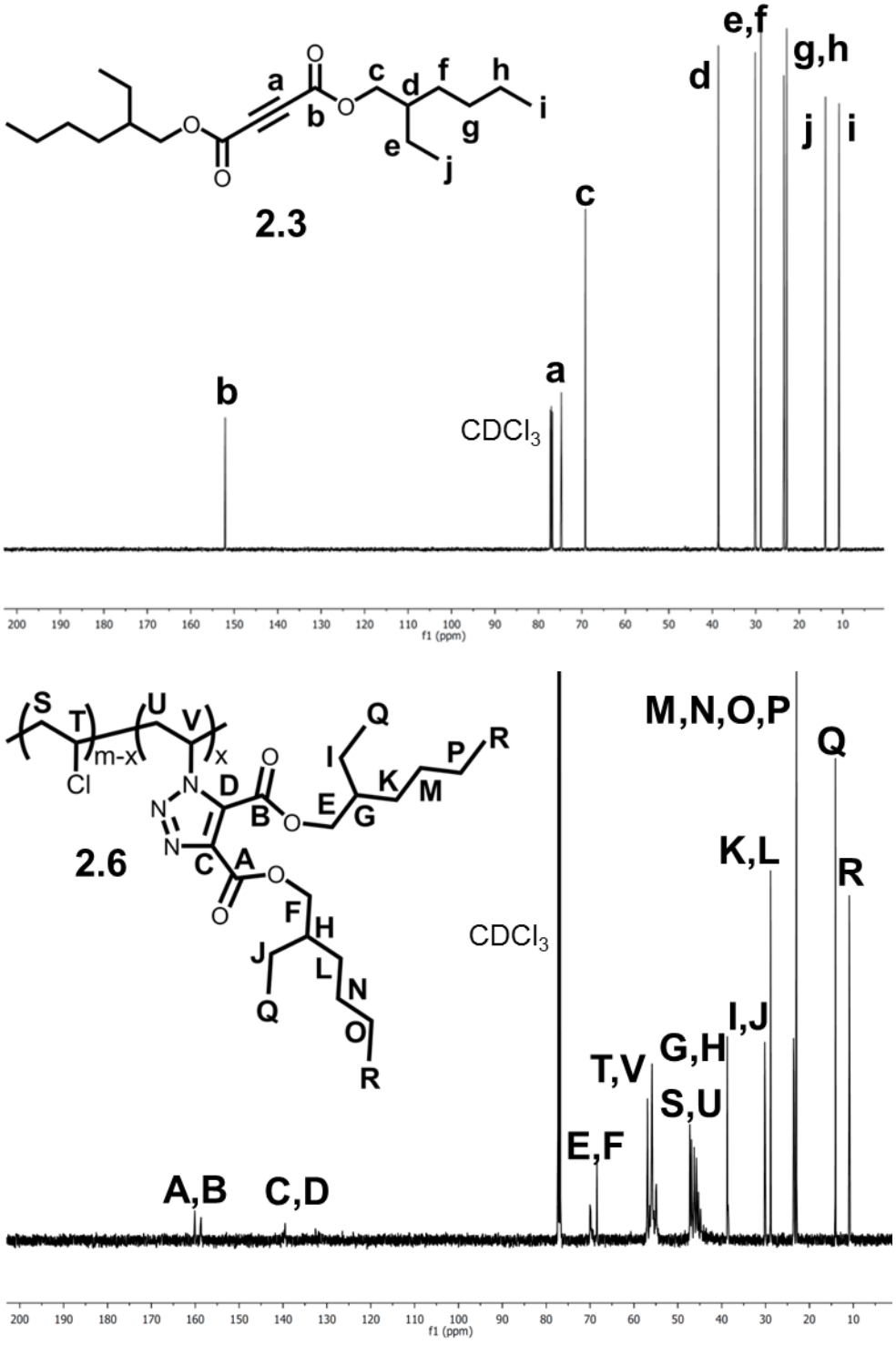

Figure 2.7 ^{13}C-NMR Spectra of DEHAD (**2.3**, Top) and 15% PVC-TRZ-DiEH (**2.6**, Bottom)

carbons **S** between δ 44.8 – 47.3 ppm are representative of Cl-CH-**C**H_2. Methine shifts **T** of isotactic (δ 54.9 – 55.1 ppm), atactic (δ 55.7 – 56.1 ppm), and syndiotactic (δ 56.9 – 57.0 ppm) carbons belong to Cl-**C**H-CH_2. If the polymer concentration is high enough, methine carbons **V** of TRZ-**C**H-CH_2 are visible at δ 56.4 ppm and δ 53.8 ppm. Formation of a triazole on PVC imparts new carbon peaks relative to the parent alkyne. Most of the ester alkyl carbons are present in the ^{13}C-NMR of the triazole-functionalized polymer, albeit shifted and increased in number due to a loss of symmetry following cyclization. The disappearance of the alkyne quaternary sp-carbon signal **a** at δ 74.7 ppm is indicative of cycloaddition and thorough purification of the plastic. If the functionalized PVC is not properly precipitated, peak **a** at δ 74.7 ppm remains, due to leftover alkyne precursor in the polymeric matrix. In the same vein, two weak quaternary carbon signals **C** and **D** belonging to the triazole appear at approximately δ 133.0 and δ 139.5 ppm. In addition, two carbonyl ester signals **A** and **B** appear at approximately δ 158.0 and δ 160.0 ppm. For reference, the parent alkyne carbonyl ester signal **b** appears at δ 152.0 ppm.

2.4 DSC Analysis: 1st Generation Triazole-Phthalate Mimics on PVC

After the PVC internally plasticized by triazole phthalate mimics were characterized via ^{1}H-NMR, ^{13}C-NMR and FTIR, thermal analyses were performed by collaborators Dr. Rudy Wojtecki and Andy Tek at the IBM Almaden Research Center. Differential scanning calorimetry (DSC) was measured in order to quantitatively determine the level of plasticization of each sample. Modulated Differential Scanning Calorimetry (MDSC) was performed on each polymer using a TA Instruments DSC Q2000 with a heat-cool-heat protocol. The general scanning ranges of MDSC analyses ranged from -90 °C to 200 °C, with an increase of 10 °C per minute. Typically, a heat-cool-reheat protocol is utilized in differential scanning calorimetry to erase the thermal history of each polymer sample. The first heat cycle assesses the “as-present” thermal properties of the sample. Workup, processing, and storage can alter the properties of a polymer, resulting in varied glass transition temperatures

for an analogous sample. Once the polymer is heated above its melt temperature, it is cooled at a controlled rate. All samples in the data set were subjected to the same cooling rate: this imparts a consistent thermal history for each polymer. The second heat cycle is subsequently performed to obtain the true glass transition temperature (T_g) of the sample. This is a quantitative indicator of the level of plasticization imparted by the novel internal plasticizer. Low T_g values indicate a high degree of plasticization. A detailed discussion on the free volume theory of plasticization with respect to T_g is discussed in *Chapter 1*.

In a DSC scan, there are two regions that represent the physical state of the polymer, as seen by the top bold green line in **Figure 2.8**. The abscissa is the temperature (°C) and the ordinate is a reversing signal of heat flow, also known as the "heat capacity component" (J/g·°C). Starting from the highest temperature, a plateau is observed, which corresponds to a polymer in its flexible state. A sharp decrease occurs as the system cools down: this drop eventually stabilizes as a secondary plateau, which represents the glass state. The inflection point of this descent is the glass transition temperature (T_g).

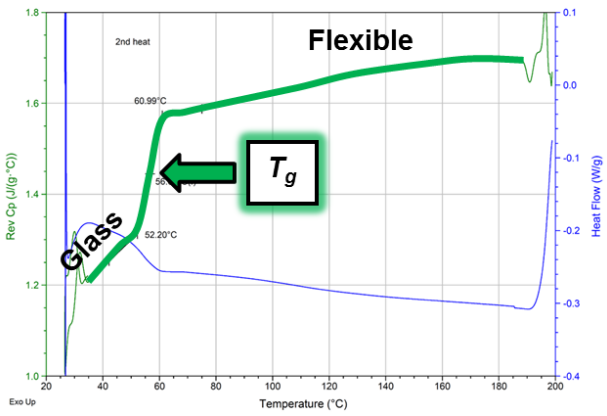

Figure 2.8 DSC Second Heat Scan of 15% PVC-TRZ-DiEH

DSC scans of PVC, 5% PVC-azide and 15% PVC-azide were measured as reference standards. Unmodified, purified PVC exhibits a T_g of 81 °C. PVC-azide displays a T_g of 83 °C at 5 mole percent azide, and 78 °C at 15 mole percent azide (**Figure 2.9**). This information provides standard T_g values to assess the efficacy of the triazole phthalate mimics as internal plasticizers (**Figure 2.10**). **Table 2.2** summarizes the T_g values of all samples synthesized.

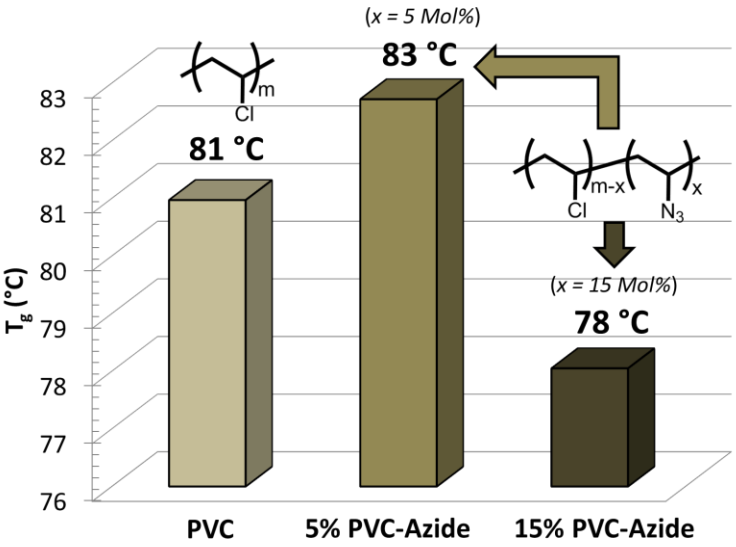

Figure 2.9 T_g Values of PVC and PVC-Azide

Polymer	5 Mol% T_g (°C)	15 Mol% T_g (°C)
PVC	*81 °C*	
PVC-Azide	83	78
PVC-TRZ-DiMe	88	96
PVC-TRZ-DiBu	76	74
PVC-TRZ-DiEH	65	57

Table 2.2 DSC Data of PVC Standards and 1st Generation PVC Triazole Phthalate Mimics

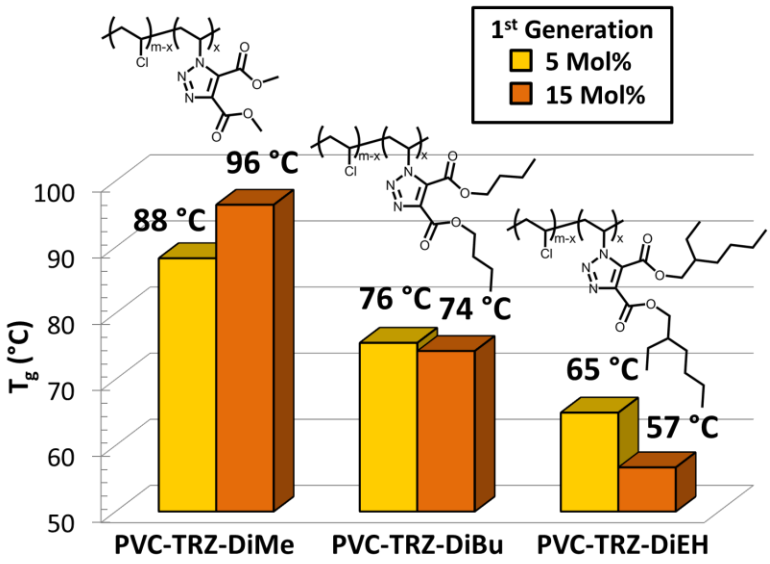

Figure 2.10 DSC Data for 1st Generation Triazole Phthalate Mimics

Differences in the glass transition temperature between a given polymer sample and unmodified PVC is defined as (**Equation 2.1**):

$$\Delta T_g\ PVC = T_{g\ Triazole\ Plasticized\ PVC} - T_{g\ Unmodified\ PVC} \qquad \textbf{Equation 2.1}$$

These ΔT_g PVC values are shown in **Table 2.3** and are graphically illustrated in **Figure 2.11**.

Polymer	5 Mol% ΔT_g TRZ (°C)	15 Mol% ΔT_g TRZ (°C)
PVC	*81 °C*	
PVC-TRZ-DiMe	+7	+15
PVC-TRZ-DiBu	-5	-7
PVC-TRZ-DiEH	-16	-24

Table 2.3 Changes in Glass Transition Temperatures (ΔT_g PVC) of 1st Generation Triazole Phthalate Mimics With Respect To Unmodified PVC

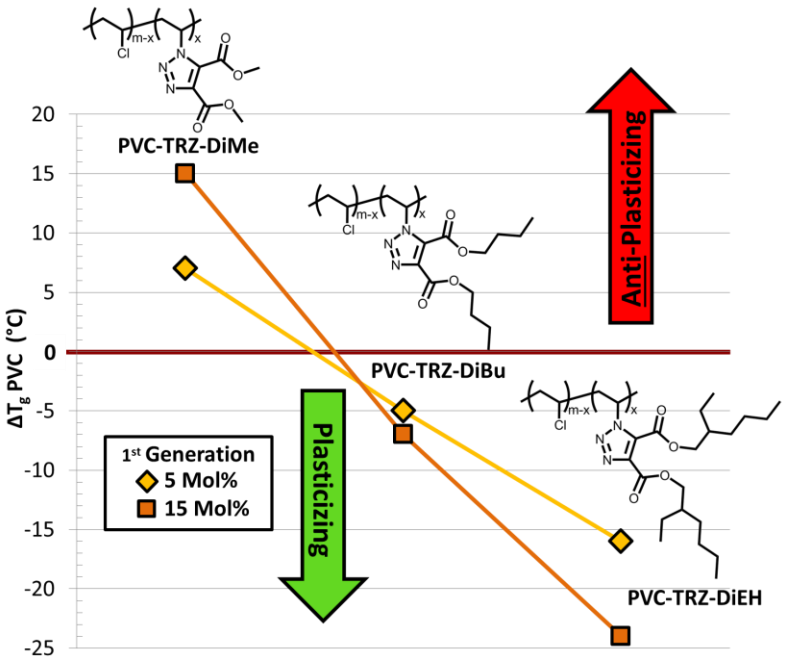

Figure 2.11 Difference in Glass Transition Temperatures of 1st Generation Triazole Phthalate Mimics with Respect to Unmodified PVC

Beginning with the 5 mole percent triazole samples, modest glass transition temperature depressions from unmodified PVC are observed. Interestingly, 5% PVC-TRZ-DiMe gives an *elevated* T_g of 88 °C compared to pure PVC (81 °C): this effect is called *anti-plasticization*. It appears that the absence of sufficiently large alkyl plasticizing chains in PVC-

TRZ-DiMe increases its rigidity, presumably due to π-π or edge-to-face stacking and enhanced crystallinity engendered by the directly appended aromatic triazole rings. Hypothetically, an intensified anti-plasticization effect should occur in the analogous sample containing a three-fold molar increase of this methyl ester triazole (15% PVC-TRZ-DiMe).

Glass transition temperatures at the 15 mole percent modification level are intensified compared to the 5 mole percent polymers (**Figure 2.11, Table 2.3**). PVC-TRZ-DiEH, at 15 mole percent displays a notable T_g depression (57 °C) from pure PVC (ΔT_g *PVC* = -24 °C) and the 5 mole percent analogue (ΔT_g = -8 °C). The T_g of 15% PVC-TRZ-DiBu (T_g = 74 °C) remains nearly identical to its 5 mole percent relative (ΔT_g = -2 °C). A remarkable T_g *increase* of 15% PVC-TRZ-DiMe (T_g = 96 °C) is observed compared to unmodified PVC (ΔT_g *PVC* = +15 °C) and its 5 percent congener (ΔT_g = +8 °C). The stronger anti-plasticizing effect in 15% PVC-TRZ-DiMe compared to its 5 mole percent counterpart clearly indicates the detrimental effect of direct attachment of an aromatic triazole on plasticization efficiency. This phenomenon has been previously implicated in the work of both Reinecke[21] and Braslau.[17a] The data imply that an increased amount of triazole directly attached to PVC leads to decreased plasticization efficiency; this explains the increase in glass transition temperatures of 5 and 15 mole percent PVC-TRZ-DiMe, and the diminutive depressions observed in PVC modified with triazoles containing *n*-butyl and 2-ethylhexyl moieties, despite the 3-fold mole percent increase of triazole-based plasticizer.

2.5 2nd Generation Plasticizer: Single Hexyl Tether Alkyl Phthalate Mimics on PVC

In order to overcome the aromatic anti-plasticization penalty furnished by the triazole, free volume theory[22] was considered when designing a new family of 2nd generation triazole-based internal plasticizers. Accordingly, the more space that exists between polymer chains, the more flexible the plastic will become. DSC data gathered from the 1st generation polymers imply that plasticization occurs, albeit inefficiently, due to the presence of rigid aromatic rings

on the polymeric backbone. It was envisaged that a tether between a triazole attachment to PVC (primary triazole; 1°TRZ) and a triazole phthalate mimic (secondary triazole; 2°TRZ) would boost plasticizing efficiency by distancing the plasticizer from the main chain (**Figure 2.12**). In effect, this extension would generate additional free space, while maintaining covalent attachment to PVC. This novel tethering approach also preserves the non-leaching attributes of the 1st generation system. The tether should overcome the anti-plasticization effects of the primary triazole to improve plasticizer efficacy. Although the thermal azide-alkyne cycloaddition remains the method of attachment to PVC (retaining the deleterious *1°TRZ*), the facile nature and reliability of this dipolar cycloaddition continues to be an appealing method to functionalize PVC.

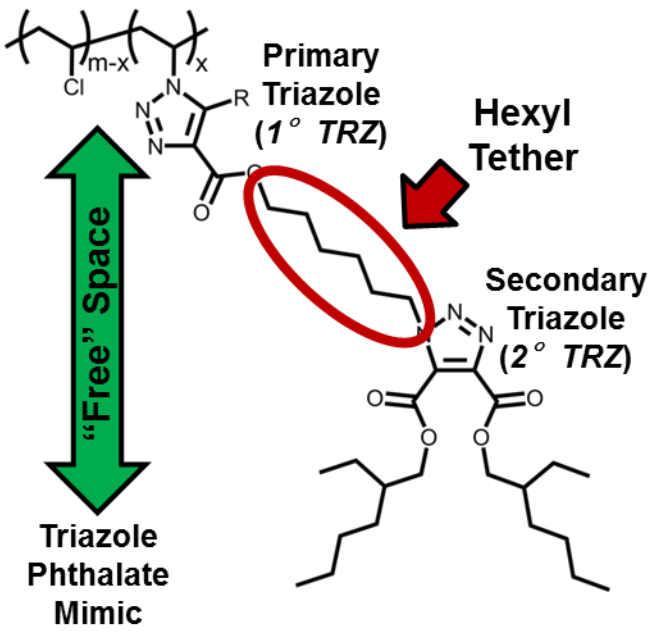

Figure 2.12 Illustration of a Single Hexyl Tether Between PVC and Triazole Phthalate Mimic

Numerous long chain tethers were investigated. Economic feasibility was of utmost significance during the selection process of a suitable tether. Synthetic accessibility and structural simplicity are desirable attributes for the tether: 6-chlorohexan-1-ol was the best candidate for this purpose. The process to obtain the desired azide is trivial and has literature precedence. Following the procedure of Park,[23] synthesis of the hexyl tether began with azidation of 6-chlorohexan-1-ol *via* an S_N2 reaction using sodium azide in DMSO at 50 °C. Reaction progress was preliminarily monitored by ^{1}H-NMR in d_6-DMSO to determine the amount of time the reaction takes to complete. Once it was established that the reaction took

24 hours, non-deuterated DMSO was utilized in subsequent large scale syntheses. Reliable quantitative conversion to 6-azidohexan-1-ol **2.7** required no chromatographic purification (**Scheme 2.10**). Organic azides can be dangerous in nature: low molecular weight organic azides have a propensity to violently decompose. A formula to determine if an organic azide is safe to handle has been created:[24] $(N_{Carbon} + N_{Oxygen}) / N_{Azide\ Nitrogen} \geq 3$, where N = number of azide nitrogen atoms. While 6-azidohexan-1-ol **2.7** and PVC-Azide **2.1** did not violently decompose, it should be noted that extreme caution should be taken at all times when synthesizing or handling organic azides.

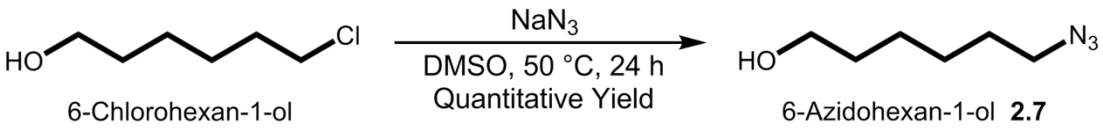

Scheme 2.10 Synthesis of 6-Azidohexan-1-ol **2.7** Hexyl Tether Precursor[23]

Without further purification, 6-azidohexan-1-ol **2.7** and DMAD, DBuAD **2.2**, or DEHAD **2.3** were stirred in chloroform for 24 hours at 50 °C to give the hexyl tethered triazolo-alcohol phthalate mimics **2.8 - 2.10** (**Scheme 2.11**). High yields (98% to 99%) were achieved after column chromatography. The reaction concentration was set at 0.3 M, with the acetylenedicarboxylate esters used in a 1.3 equivalent excess to 6-azidohexan-1-ol **2.7**. These cycloadditions were monitored *via* TLC. The product R_f values were significantly reduced compared to the alkyne starting materials due to the polar nature of the alcohol and pendant triazole. Furthermore, the triazole is extremely UV-active, whereas 6-azidohexan-1-ol and the alkynes are not. This provided a clear qualitative indicator of product formation.

^{1}H-NMR was performed to confirm the structures and assess purity (**Figure 2.13**). A downfield shift of the methylene protons **A** adjacent to the secondary triazole at δ 4.6 ppm (Tether-C**H$_2$**-2°TRZ) from the protons **a**, next to the azide (δ 3.25 ppm, C**H$_2$**-N_3) is observed, stemming from an aromatic anisotropic effect. The methylene **D** adjacent to the alcohol (HO-C**H$_2$**-Tether) is present at δ 3.6 ppm, while peaks between δ 1.3 – 1.6 ppm are central

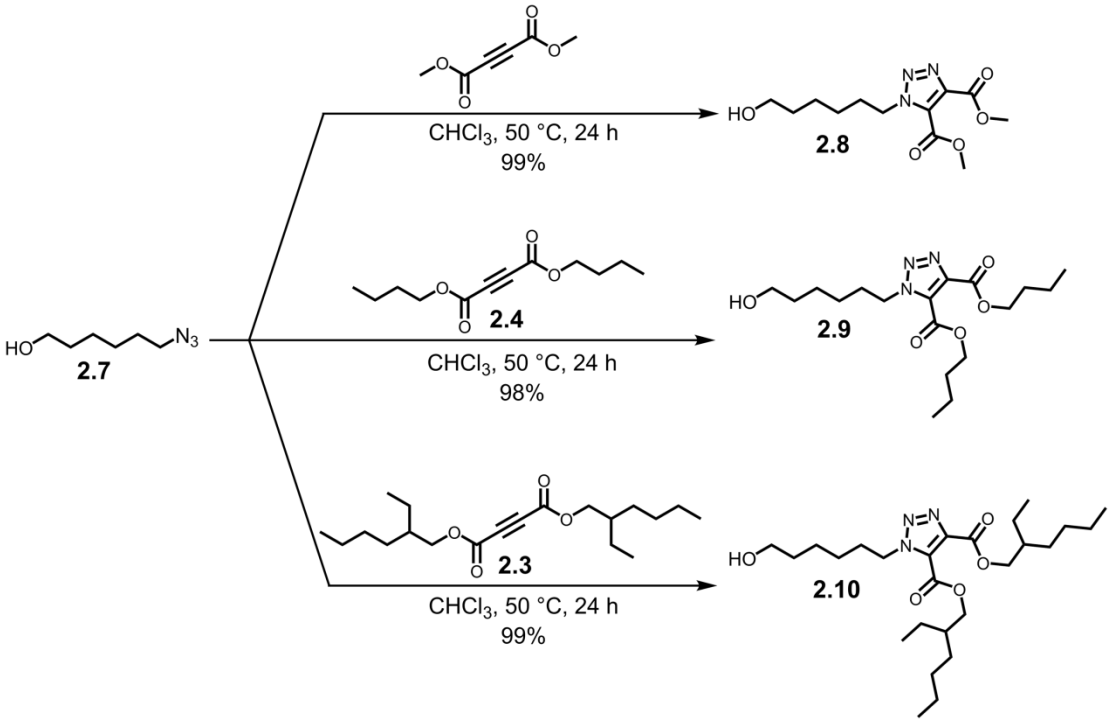

Scheme 2.11 Syntheses of Hexyl Tether Alkyl Triazolo-Alcohol Precursors

methylene protons **C** of the hexyl tether (Tether-C**H**$_2$-C**H**$_2$-Tether). Proton signal **B** two carbons away from the secondary triazole (Tether-C**H**$_2$-CH$_2$-2°TRZ) moves downfield to δ 1.9 ppm (from δ 1.5 ppm in the azide). This is possibly due to an inductive electron-withdrawing effect of the triazole esters, in conjunction with anisotropy. Regioisomeric TRZ-DiMe hexanol **2.8** methyl ester protons **F** (2°TRZ Ester-O-C**H**$_3$) appear at δ 3.96 and δ 3.99 ppm as a pair of singlets (**Figure 2.13**). In TRZ-DiBu **2.9** and TRZ-DiEH hexanol **2.10**, alkoxy-protons (2°TRZ Ester-O-C**H**$_2$-C) belonging to the secondary triazole ester appear between δ 4.22 – 4.36 ppm.

^{13}C-NMR of the hexyl tethered triazolo-alcohols were performed and analyzed (**Figure 2.14**). Triazole ester carbonyl peaks **I** and **J** at δ 159.0 and δ 160.5 ppm are present in all of the derivatives. ^{13}C signals **H** and **G** appearing at approximately δ 130 and δ 140 ppm

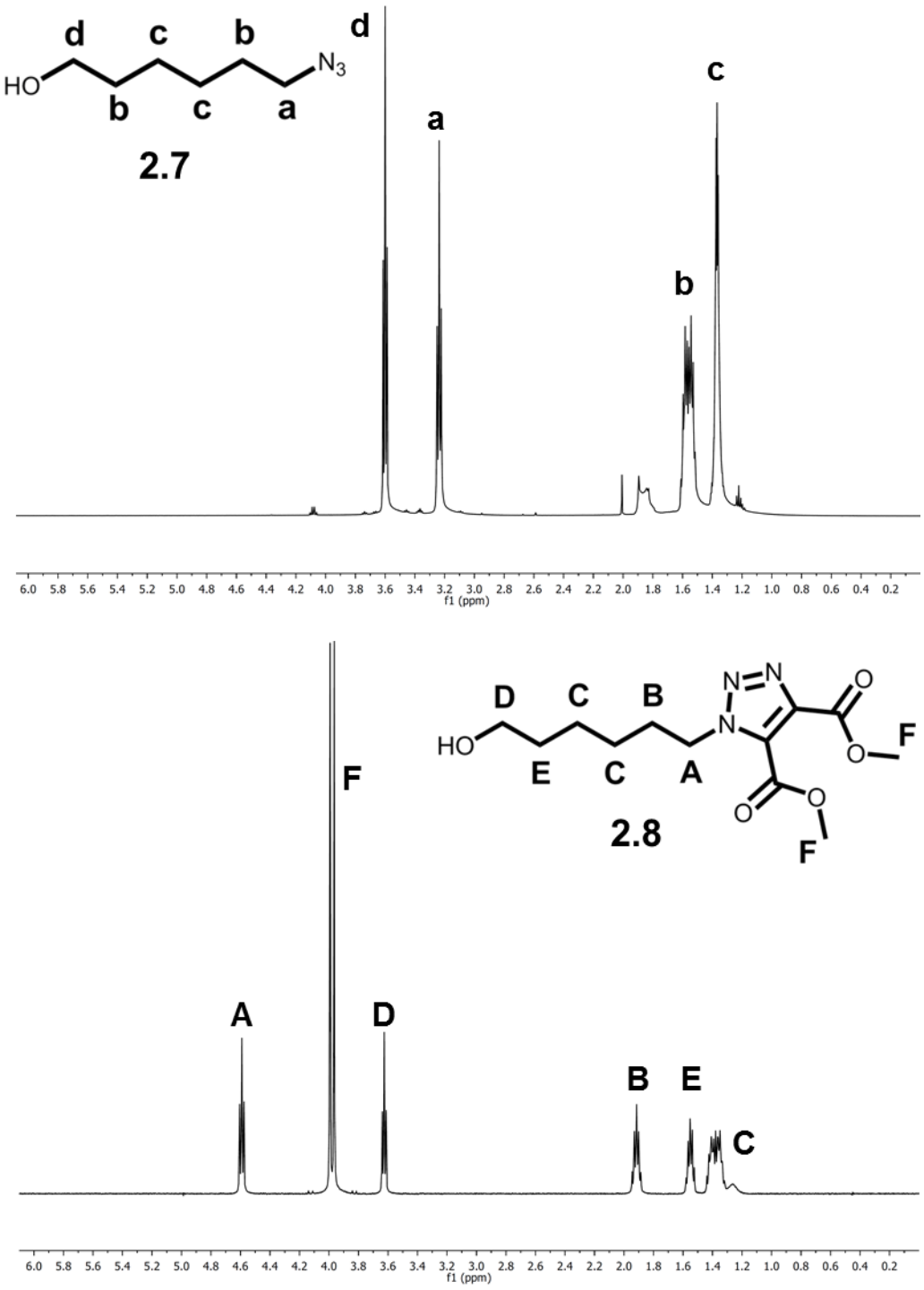

Figure 2.13 ^{1}H-NMR Comparing 6-Azidohexan-1-ol (**2.7**, Top) and TRZ-DiMe Hexanol (**2.8**, Bottom)

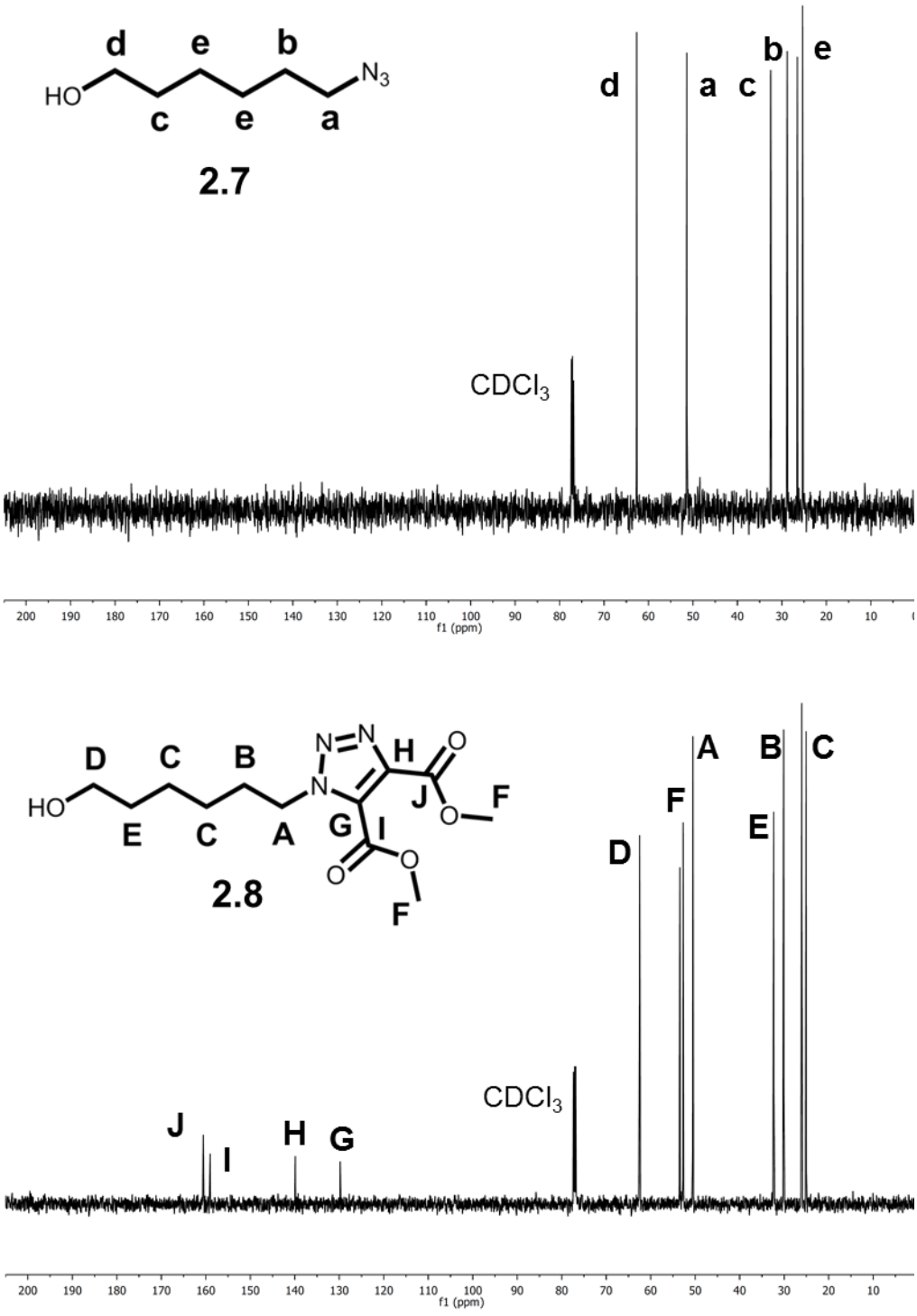

Figure 2.14 ^{13}C-NMR Comparing 6-Azidohexan-1-ol (**2.7**, Top) and TRZ-DiMe Hexanol (**2.8**, Bottom)

belong to the quaternary carbons in the triazole ring (**C**=**C**). A ubiquitous peak present in all samples is the methylene carbon **D** adjacent to the alcohol at δ 62.5 ppm (HO-**C**H_2-Tether). The methylene carbon **A** adjacent to the triazole (Tether-**C**H_2-2°TRZ) was observed at δ 50.4 ppm. Generally, signals in the range of δ 25 – 32 ppm belong to the hexyl tether: in the instance of TRZ-DiBu hexanol **2.9** and TRZ-DiEH hexanol **2.10**, some of the carbon signals originating from the aliphatic ester chains overlap with the tether.

Propiolic acid was chosen as the electron-deficient alkyne precursor: its relatively low-cost and straight-forward esterification procedures were attractive attributes. All of the 1st generation alkynes had been symmetrical acetylenedicarboxylate diesters. While these alkynes possess two electron-withdrawing groups, making the triple-bond more amenable to cycloaddition, acetylenedicarboxylic acid is substantially more expensive than propiolic acid and proves obdurate when performing esterifications with complex alcohols. The works of Huisgen[15] and Brook[5] show that the presence of a single electron-withdrawing ester in a propiolate leads to enhanced cycloaddition rates compared to non-activated alkynes. Therefore, a propiolate should be adequately activated to facilitate thermal triazole formation with PVC-azide without a transition metal catalyst.

Fischer esterifications were performed to obtain mono-ester electron-deficient alkynes (**Scheme 2.12**). Propiolic acid was treated with triazolo-alcohols **2.8 - 2.10**, *p*-toluenesulfonic acid (*p*TSA) as an acid catalyst, and toluene. A Dean-Stark apparatus was employed to trap water formed as the condensation by-product. The esterifications were complete after 2 hours, with yields ranging from 66% to 72% after purification via column chromatography.

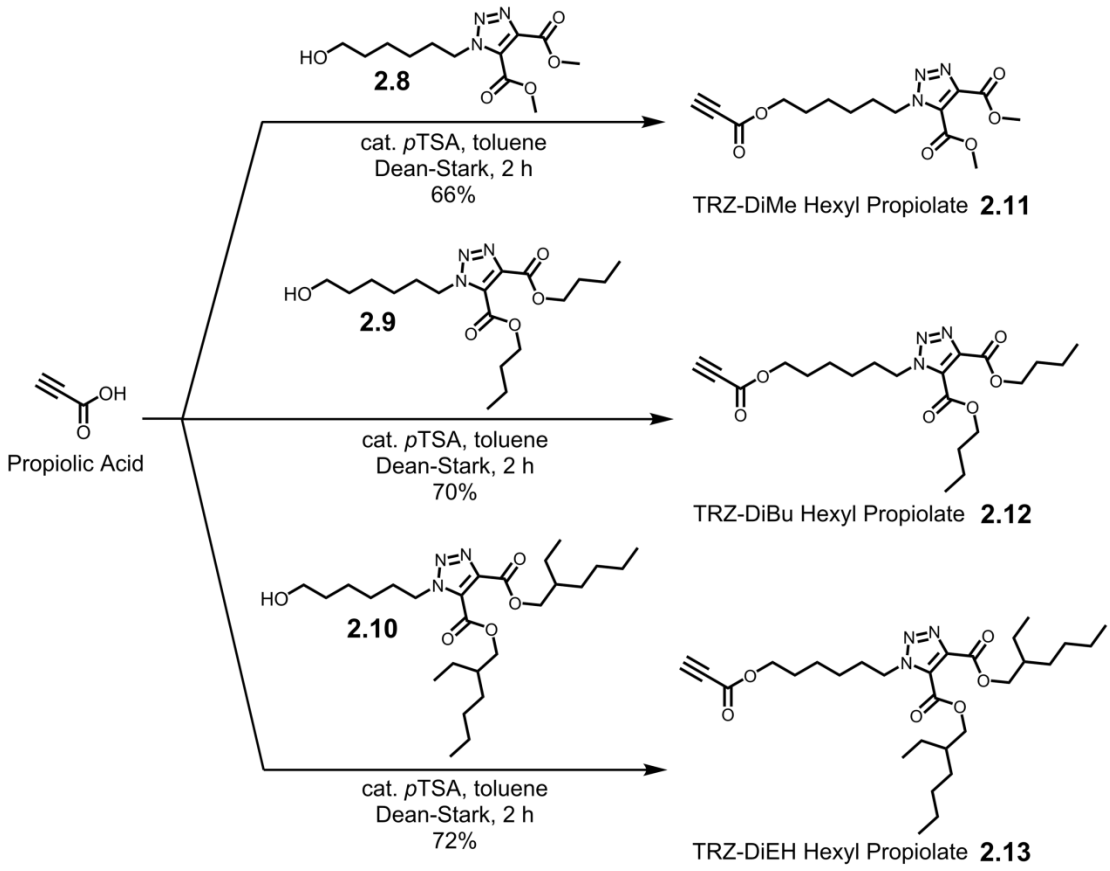

Scheme 2.12 Fischer Esterification of Propiolic Acid and Triazolo-Alcohols **2.8 - 2.10** to Form Propiolates **2.11 - 2.13** Containing Hexyl Tethered Alkyl Triazole Phthalate Mimics

Syntheses of the final propiolates with hexyl tethers **2.11 - 2.13** proceeded without incident. Triazolo-alcohols **2.8 - 2.10** were used in a 1.2 to 1.3 equivalent excess to propiolic acid, in 1.0 M toluene. Purification involved concentrating the crude reaction *in vacuo*, then immediately performing flash chromatography to obtain the pure product. Reaction progress was monitored via TLC: all propiolate derivatives have larger R_f values than their respective parent alcohols. Propitiously, the triazolo-alcohols are not exceptionally visible on TLC with potassium permanganate ($KMnO_4$), while the final propiolates are instantly visible. The oxidizing TLC stain reacts rapidly with the terminal alkyne to form a yellow spot on a magenta background. In contrast, the triazolo-alcohols do not possess functional groups that are easily oxidized by $KMnO_4$, requiring heat to visualize these molecules on TLC.

For the future, an alternative synthetic strategy could use propiolic acid in stoichiometric excess to the triazolo-alcohol. The acid would be washed away during aqueous workup with a weak base, leading to increased reaction yields and simplified purification. In the reactions performed, excess alcohol was utilized to thoroughly consume the propiolic acid: this was a historic reaction practice coming from the original acetylenedicarboxylate syntheses to fully convert the expensive di-acid to the desired di-ester. However, in the case of propiolic acid, one can use more of the carboxylic acid due to its relative affordability over acetylenedicarboxylic acid. This optimization would allow for the complete conversion of the hexyl tether alcohol: an aspect that would be industrially desirable, as the triazolo-alcohol involves a multistep synthesis, whereas propiolic acid is obtained through the oxidation of propargyl alcohol via an electrochemical process.[25]

^{1}H-NMR and ^{13}C-NMR spectra of the hexyl tethered propiolates are similar to those of the parent alcohols (**Figure 2.15**). In the ^{1}H-NMR, methylene protons **d** neighboring the ester (Propiolate Ester-O-C**H$_2$**-Tether) exhibit a significant downfield shift to δ 4.2 ppm, (from approximately δ 3.6 ppm as the alcohol) due to the presence of the carbonyl which deshields the ester alkoxy-methylene protons more than the alcohol due to anisotropic deshielding and the electronegative carbonyl. Furthermore, methylenes **e** two carbons away from the propiolate ester (Propiolate Ester-O-CH$_2$-C**H$_2$**) move slightly downfield (from δ 1.55 to δ 1.70 ppm). A lone proton **g** at δ 2.90 ppm belongs to the terminal alkyne.

^{13}C-NMR spectra of the hexyl tethered propiolates gives three additional signals compared to their parent alcohols (**Figure 2.15**). First, a propiolate ester carbonyl **K** (**C**=O) appears at δ 152.7 ppm in all derivatives. In addition, sp-hybridized carbons of the terminal alkyne show two signals at δ 74.6 ppm (**M**, alkyne CH) and δ 74.7 ppm (**L**, alkyne 4°).

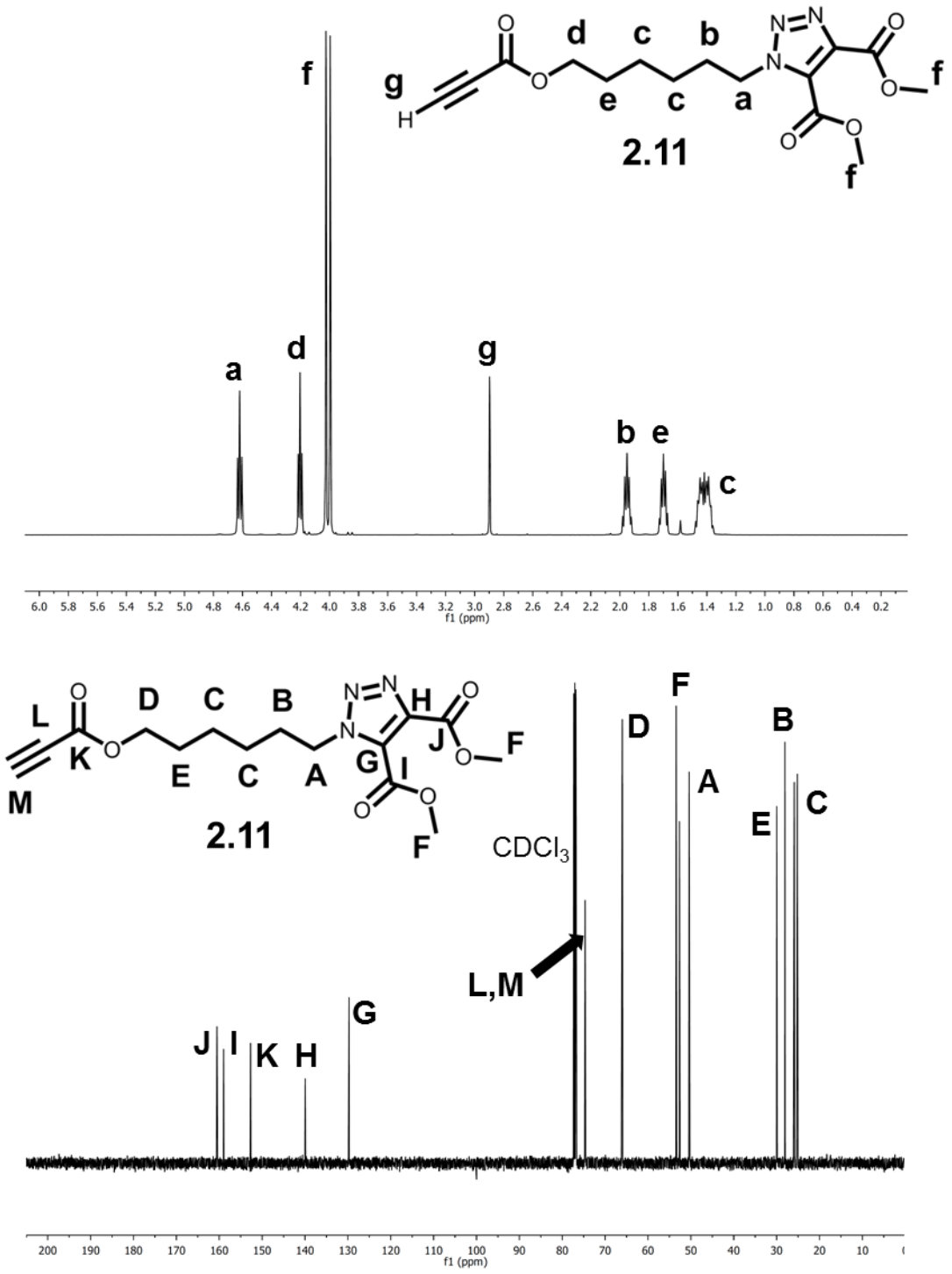

Figure 2.15 ^{1}H-NMR and ^{13}C-NMR of TRZ-DiMe Hexyl Propiolate **2.11**

Furthermore, a minor downfield shift of the propiolate ester alkoxy-methylene carbon **D** (Propiolate Ester-O-**C**H_2-C) at δ 66.0 ppm (from δ 62.5 ppm as the alcohol) is indicative of the electronegative influence of the carbonyl on the neighboring carbon atoms. All other ^{13}C signals are nearly analogous to those of the alcohol precursors.

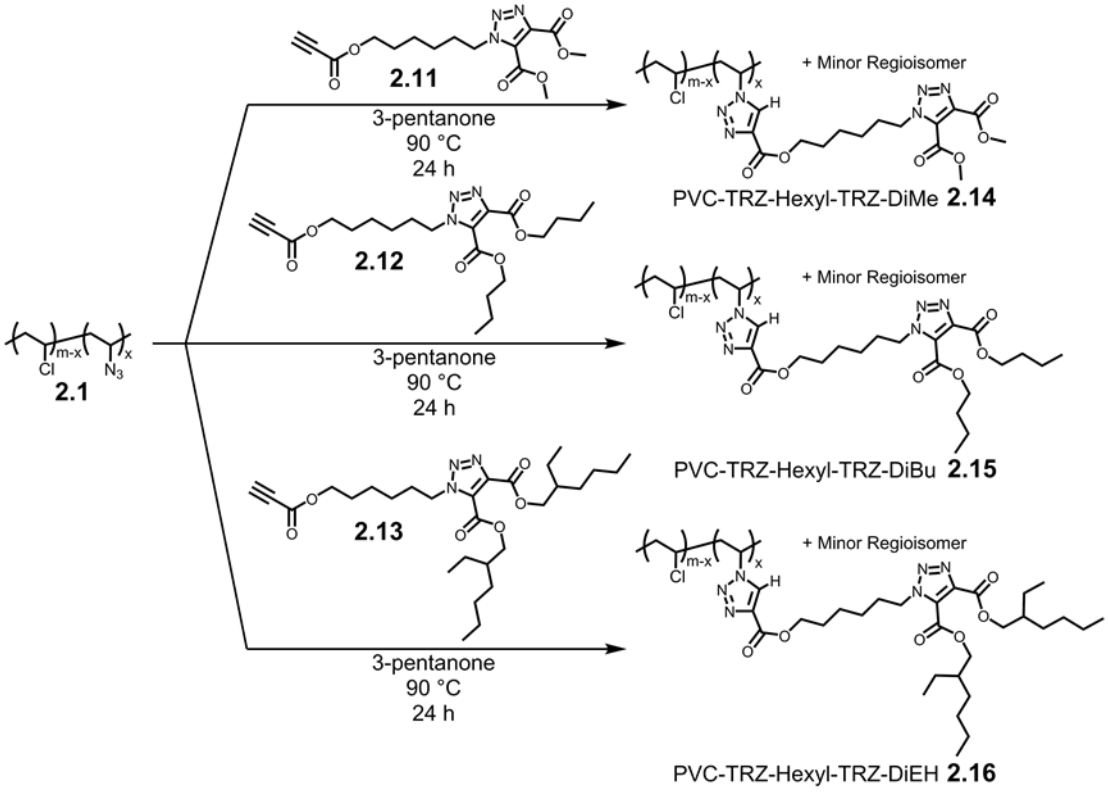

Scheme 2.13 Thermal Azide-Alkyne Cycloaddition of PVC-Azide **2.1** and Propiolate Hexyl Tethered Triazole Phthalate Mimics **2.11 - 2.13**

As with the 1st generation phthalate mimics, copper-free thermal azide-alkyne cycloadditions (AAC) were performed with PVC-azide (5 and 15 mole percent azide) in 3-pentanone. Reactions were carried out at 90 °C for 24 hours, with 2.5 – 3.0 equivalents of alkyne for each equivalent of azide (**Scheme 2.13**). The reaction concentrations ranged from 0.04 M to 0.12 M (relative to azide). Thermal azide-alkyne cycloaddition of propiolate hexyl tethered phthalate mimics **2.11 - 2.13** and PVC-azide **2.1** was tracked *via* FTIR. Distinctive

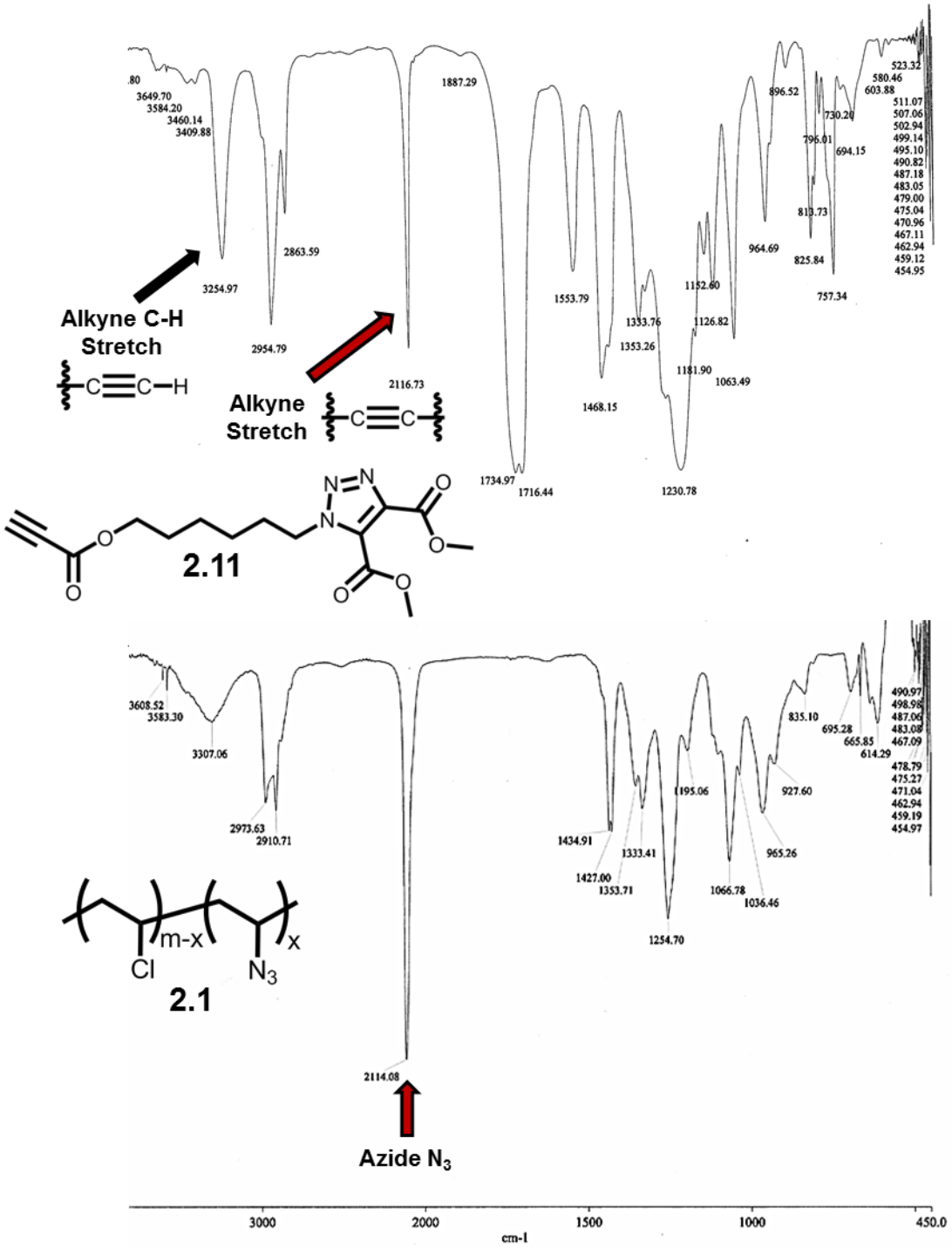

Figure 2.16 FTIR Comparison of TRZ-DiMe Hexyl Propiolate **2.11** and 15% PVC-Azide **2.1**
(*NOTE: Overlapping Alkyne and Azide Stretches at ~ 2114 cm^{-1}*)

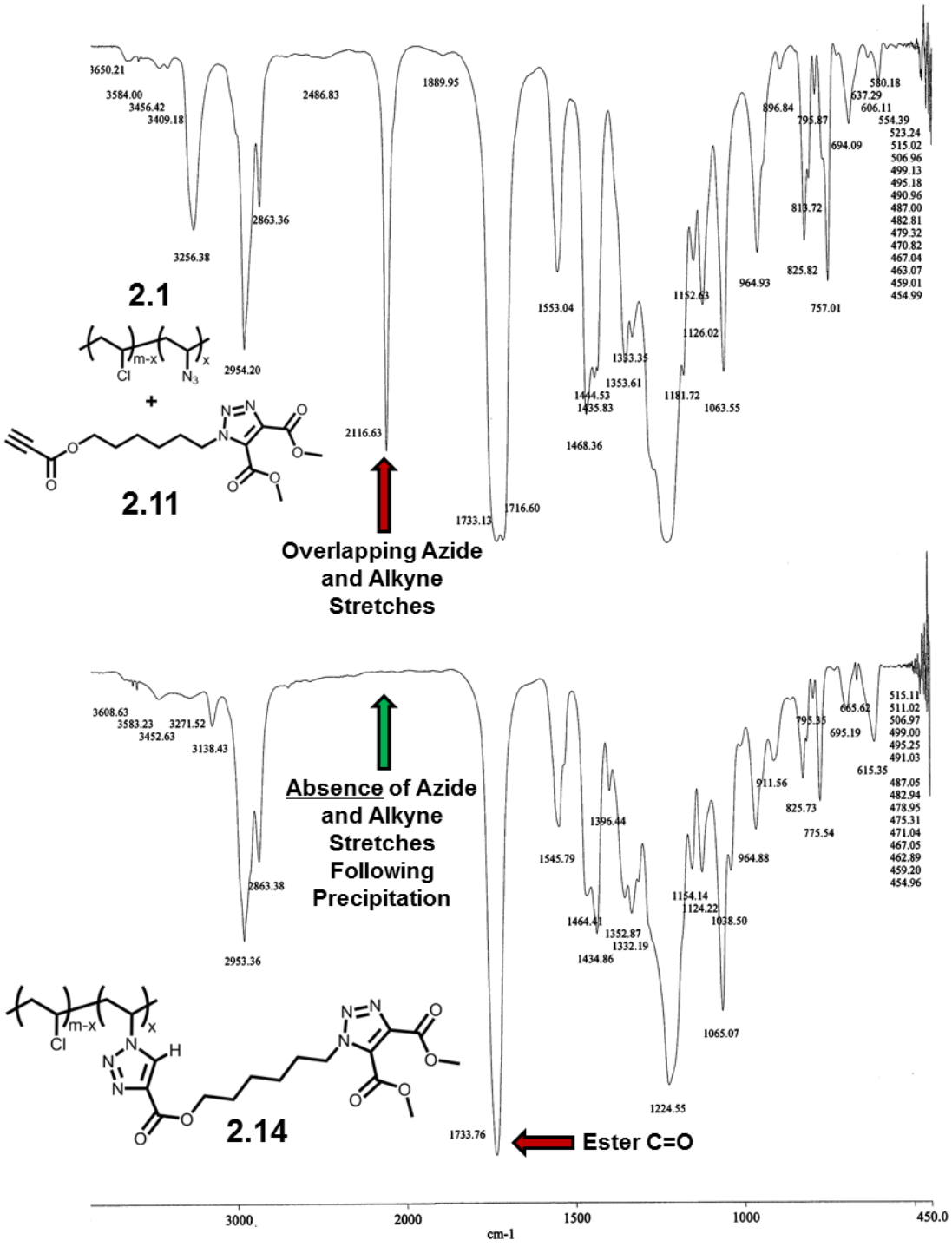

Figure 2.17 FTIR Reaction Monitoring Between 15% PVC-Azide **2.1** and **2.11**
Top: After 15 Minutes
Bottom: After 24 Hours Following Precipitation to Remove Excess Alkyne

terminal alkyne stretches appear at approximately 3255 cm^{-1} (alkyne C-H) and 2116 cm^{-1} (alkyne CC). As shown in **Figure 2.16**, this presents a technical challenge with respect to PVC-azide: a strong azide stretch resides at approximately 2114 to 2116 cm^{-1}, which overlaps with the propiolate's alkyne carbon-carbon stretch. Therefore, reaction monitoring using FTIR proved difficult compared to the cycloaddition of PVC-azide with the first generation acetylenedicarboxylate esters. The 1st generation's symmetrical internal alkyne diester does not absorb at the same wavenumber as azide (2114 cm^{-1}), allowing one to clearly monitor the disappearance of the azide stretch and easily determine reaction progress. Because the cyclization with PVC-azide requires an excess of electron-deficient alkyne, the propiolate stretch at 2116 cm^{-1} will never disappear regardless of reaction completion. This deceptive coincidence may lead to the false pretense that functionalization through AAC was not complete. To circumvent this complication, aliquots of the reaction mixture were taken at 12 hour intervals, and precipitated three times in methanol to assure that the disappearance of the azide stretch at 2114 cm^{-1} had occurred. In this manner, the propiolate was removed from the polymeric matrix. Cycloadditions with PVC-azide were complete after 24 hours according to FTIR of the precipitated reaction aliquots (**Figure 2.17**). The relatively high reaction temperature of 90 °C, along with a single electron-withdrawing ester on the alkyne smoothly furnished PVC modified with a variety of 2nd generation, single hexyl tethered triazole phthalate mimics **2.14 - 2.16**.

Once the polymers were synthesized, ^{1}H-NMR and ^{13}C-NMR was acquired to confirm structure and purity of both 5 and 15 mole percent PVC functionalized with single hexyl tethered triazole phthalate mimics. Common to all PVC containing these 2nd generation triazole plasticizers are characteristic ^{1}H signals **G** and **G'** between δ 8.10 – 8.29 ppm, which

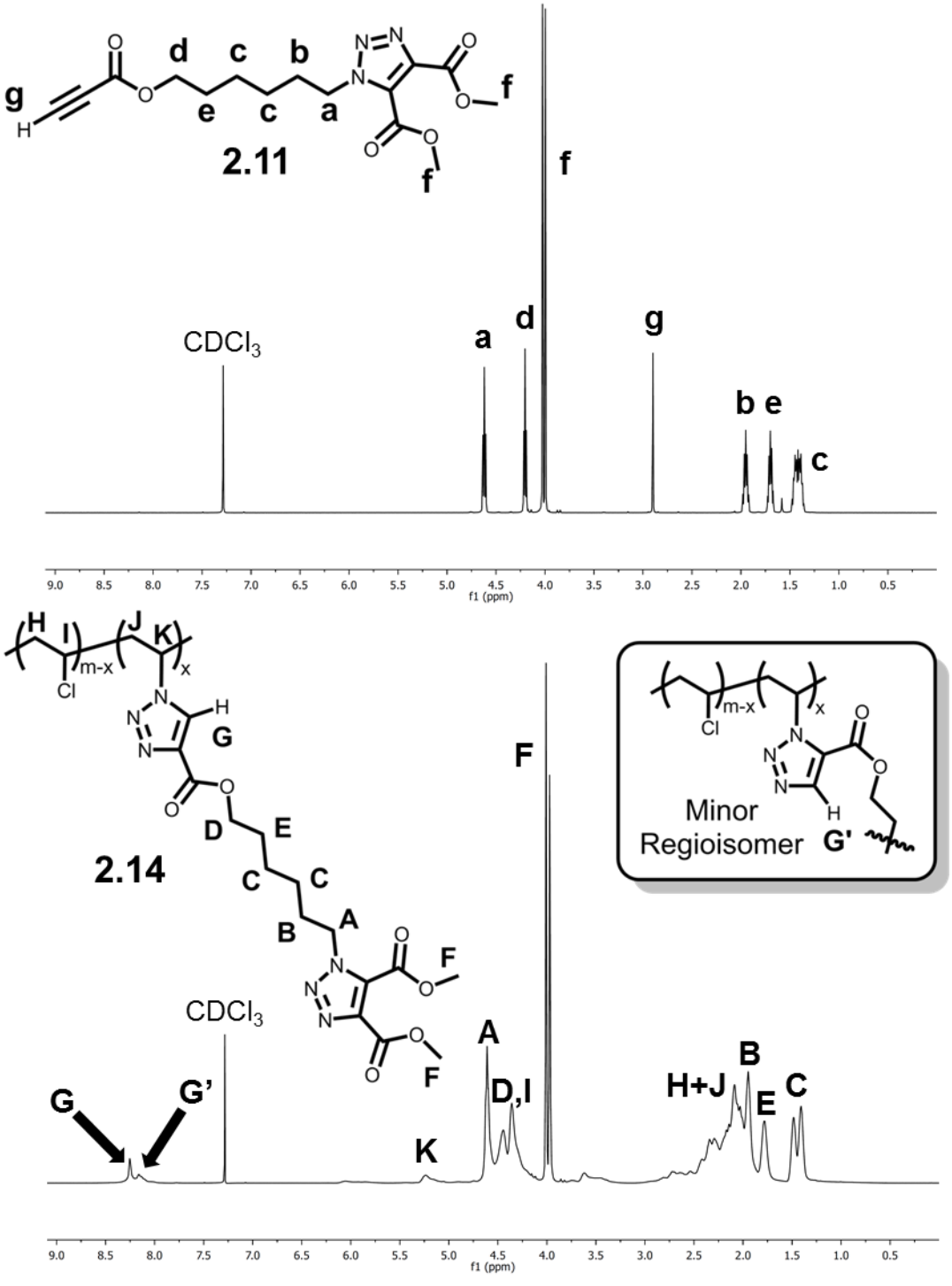

Figure 2.18 ^{1}H-NMR Spectra Comparing TRZ-DiMe Hexyl Propiolate (**2.11**, Top) and 15% PVC-TRZ-Hexyl-TRZ-DiMe (**2.14**, Bottom)

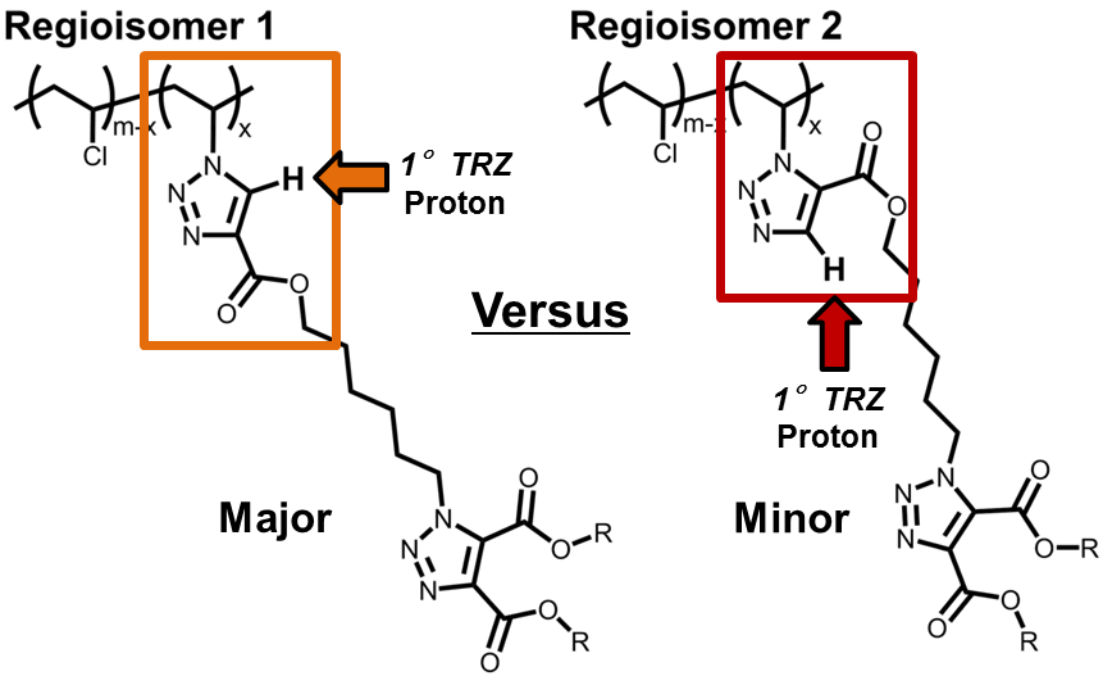

Figure 2.19 Primary Triazole Regioisomers Formed By 2nd Generation Hexyl Tethered Triazole-Based Phthalate Mimics

represent the regioisomeric protons directly attached to the triazole ring (PVC-1°TRZ-**H**) (**Figure 2.18**). Major *Regioisomer 1* places the hexyl tether away from PVC: the less bulky 1°TRZ proton is closer to the main chain (**Figure 2.19**). Conversely, in the minor *Regioisomer 2*, the hexyl tether is adjacent to the polymeric backbone, with its concomitant proton further away. *Regioisomer 1* is favored over *2* due to steric constraints: the less sterically hindered orientation in *Regioisomer 1* forms preferentially. As a result, the two peaks in the range of δ 8.10 – 8.30 ppm are not equal in size. The downfield signal (~ δ 8.30 ppm) is larger and is assigned to *Regioisomer 1*.

Other ^{1}H-NMR features of PVC functionalized with 2nd generation triazole phthalate mimics include a myriad of hexyl tether methylene proton signals **C** and **E** between δ 1.25 – 1.90 ppm (**Figure 2.18**). Methylene protons **D** at δ 4.20 ppm are adjacent to the primary triazole ester oxygen (PVC-1°TRZ Ester-O-C**H**$_2$-Tether). The methylene directly attached to the secondary triazole **A** (PVC-1°TRZ-Tether-C**H**$_2$-2°TRZ) shows a peak at δ 4.60 ppm.

Plasticizing alkyl chains common to the 1st generation phthalate mimics (2-ethylhexyl and *n*-butyl derivatives) appear between δ 0.86 – 1.98 ppm, overlapping with the hexyl tether and PVC signals. Methine protons **K** of PVC adjacent to the primary triazole appear in the range of δ 5.10 – 5.30 ppm (PVC-C**H**-1°TRZ). All other proton shifts belonging to the polymer chain are in the same general location as in unmodified PVC.

^{13}C-NMR spectra of PVC functionalized with the 2nd generation triazole phthalate mimics appear similar to those of the parent propiolates with a few key differences (**Figure 2.20**). Signals of the hexyl tether methylene carbons (**B**, **C** and **E**), quaternary carbons of the secondary triazole (**G** and **H**, at δ 133 ppm and δ 140 ppm), and secondary triazole carbonyl peaks (**I** and **J**, at δ 158 ppm and δ 160 ppm), along with its respective alkyl chain carbons are present in the ^{13}C-NMR. Main chain PVC carbons remain predominately unaltered. The disappearance of the quaternary sp-carbon signals **l** and **m**, at δ 74.6 and δ 74.7 ppm is indicative of cycloaddition and thorough purification of the plastic.

The primary triazole ester carbonyl signal **K** is not appreciably present: this is presumably due to the small signal of the quaternary carbonyl carbons and the presence of regioisomers. Unlike the 1st generation acetylenedicarboxylate derivatives, which possess two esters and no regioisomers, the single hexyl tethered primary triazole has a lone carbonyl, which is averaged between two regioisomers. The carbonyl ^{13}C shift is not readily visualized with a 500 MHz NMR with a room-temperature probe. ^{13}C spectra of select triazole-based internal plasticizers on PVC were acquired for subsequent generations of polymers with an 800 MHz NMR equipped with a cryoprobe, which successfully detected carbonyl signals corresponding to the primary triazoles.

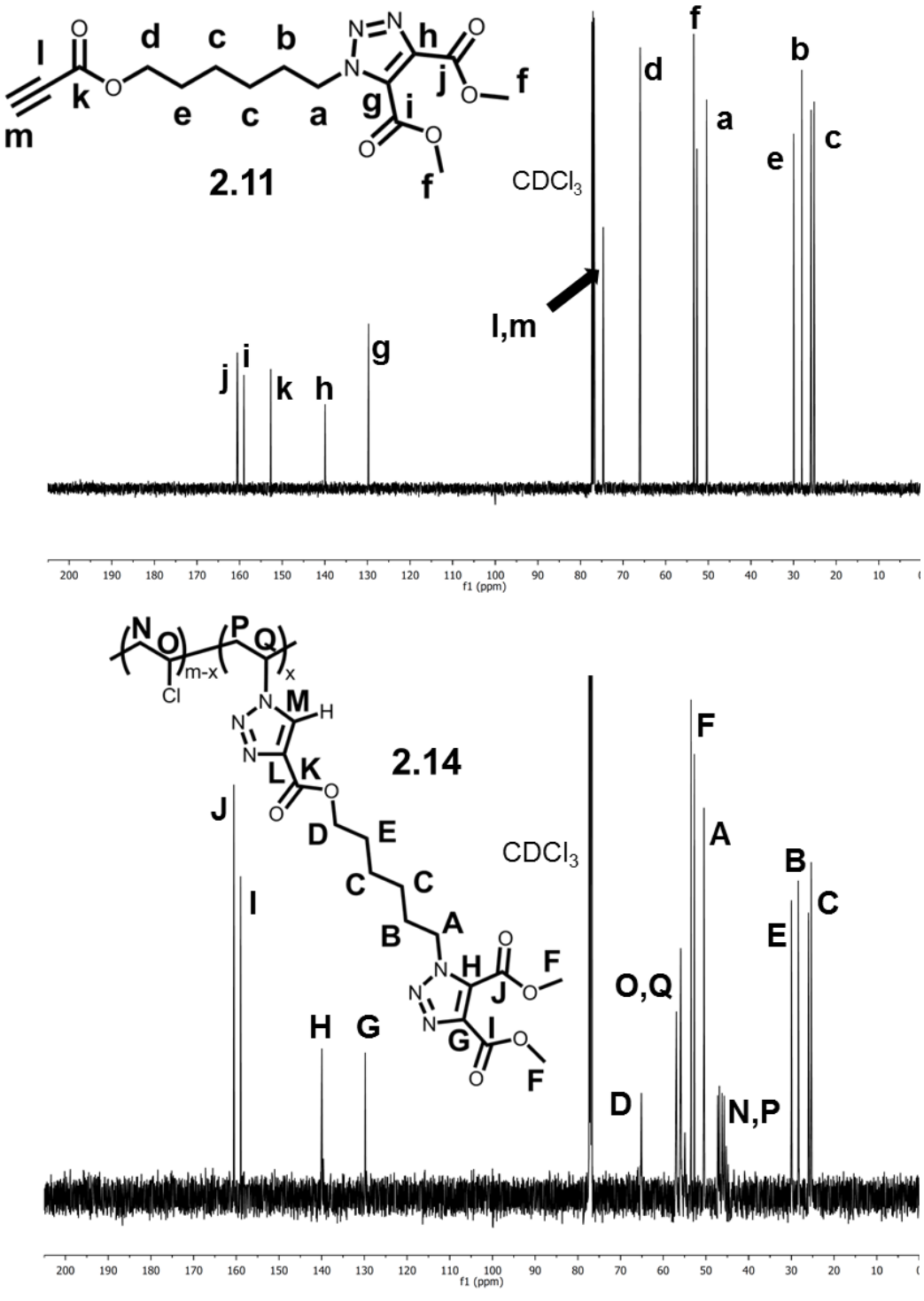

Figure 2.20 ^{13}C-NMR Spectra Comparing TRZ-DiMe Hexyl Propiolate (**2.11**, Top) and 15% PVC-TRZ-Hexyl-TRZ-DiMe (**2.14**, Bottom)

2.6 DSC Analysis: 2nd Generation Single Hexyl Tether Triazole Phthalate Mimics on PVC

Thermal analyses of PVC functionalized with 2nd generation single hexyl tethered triazole phthalate mimics were performed by our collaborators at IBM Almaden in an analogous fashion to 1st generation triazole-phthalate mimics in *Section 2.4*, to quantitatively determine the degree of plasticization. **Table 2.4** summarizes the T_g values of these PVC derivatives with standards; these data are presented in **Figure 2.21**. The focus of this section will compare these 2nd generation to the 1st generation system.

Glass transition temperatures of all 2nd generation derivatives exhibit decreased values compared to unmodified PVC. No significant anti-plasticization was observed. Beginning with the 5 mole percent samples, PVC-TRZ-Hexyl-TRZ-DiMe maintains a T_g similar to unmodified PVC (T_g = 82 °C). PVC-TRZ-Hexyl-TRZ-DiBu (T_g = 65 °C) displays a much lower glass transition temperature, while PVC-TRZ-Hexyl-TRZ-DiEH (T_g = 56 °C) shows a significant depression relative to unmodified PVC. At 15 mole percent, 2nd generation triazole-based plasticizers revealed lower glass transition temperatures compared to the 5 mole percent analogues and to standard PVC: PVC-TRZ-Hexyl-TRZ-DiMe (T_g = 75 °C), PVC-TRZ-Hexyl-TRZ-DiBu (T_g = 54 °C), and PVC-TRZ-Hexyl-TRZ-DiEH (T_g = 41 °C).

Polymer	5 Mol% T_g (°C)	15 Mol% T_g (°C)
PVC	*81 °C*	
PVC-Azide	83	78
PVC-TRZ-Hexyl-TRZ-DiMe	82	75
PVC-TRZ-Hexyl-TRZ-DiBu	65	54
PVC-TRZ-Hexyl-TRZ-DiEH	56	41

Table 2.4 DSC Data of PVC Standards and 2nd Generation Single Hexyl Tethered Triazole Phthalate Mimics

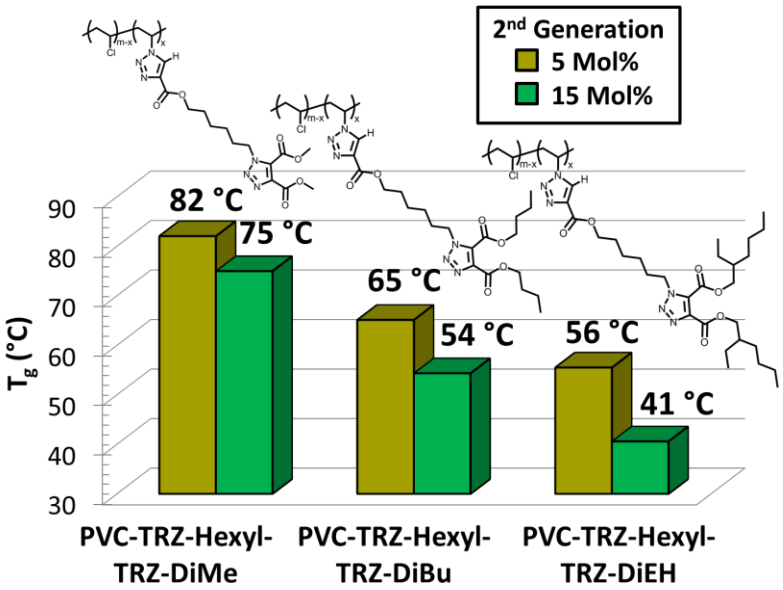

Figure 2.21 DSC Data of 2nd Generation Single Hexyl Tethered Triazole Phthalate Mimics

Polymer	5 Mol% ΔT_g PVC (°C)	15 Mol% ΔT_g PVC (°C)
PVC	*81 °C*	
PVC-TRZ-Hexyl-TRZ-DiMe	+1	-6
PVC-TRZ-Hexyl-TRZ-DiBu	-16	-27
PVC-TRZ-Hexyl-TRZ-DiEH	-25	-40

Table 2.5 Changes in Glass Transition Temperature (ΔT_g PVC) of 2nd Generation Single Hexyl Tethered Triazole Phthalate Mimics with Respect to Unmodified PVC

The glass transition temperatures of PVC functionalized with 2nd generation triazole phthalate mimics display multiple observable phenomena. **Table 2.5** shows the glass transition difference (ΔT_g PVC) between unmodified PVC and each 2nd generation plasticized sample (**Equation 2.1**). As seen in the 1st generation triazole-based plasticizers, T_g values decrease as longer alkyl ester chains are introduced, with considerable depressions observed in the 15 mole percent PVC derivatives compared to the 5 mole percent analogues. As the plasticizer becomes structurally larger, there is a non-linear plasticization effect that occurs between the 5 and 15 mole percent samples. In **Figure 2.22**, ΔT_g PVC values taken from **Table 2.5** show that PVC-TRZ-Hexyl-TRZ-DiEH, the largest alkyl ester discussed thus far, displays the most substantial intensification of plasticization from 5 to 15 mole percent. As

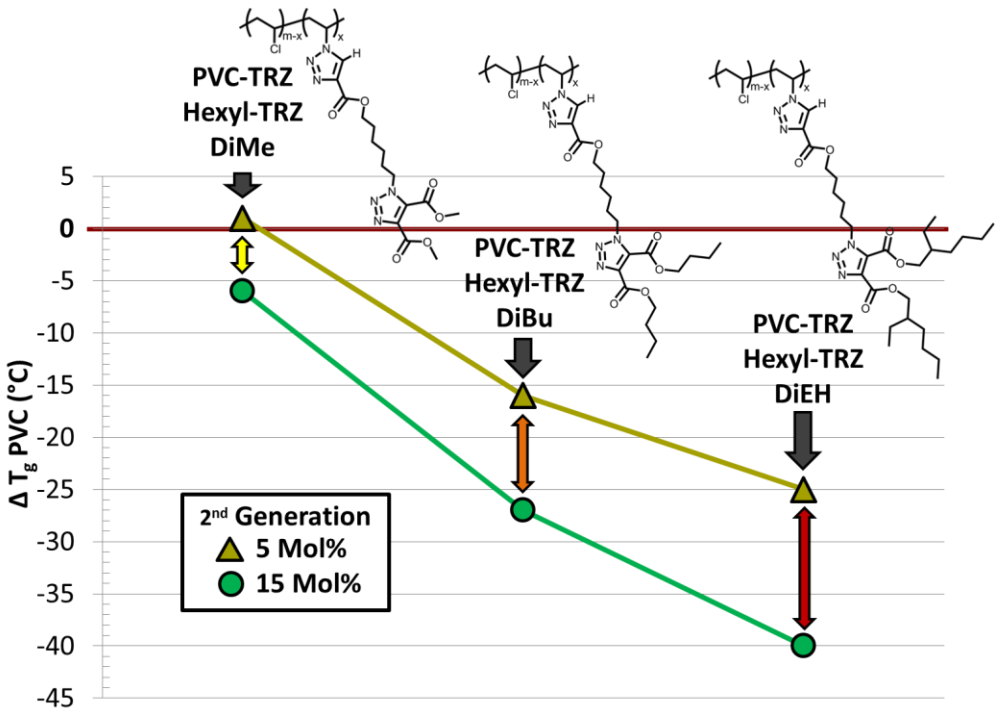

Figure 2.22 Difference in Glass Transition Temperature (ΔT_g PVC) of 2nd Generation Single Hexyl Tethered Triazole Phthalate Mimics with Respect to Unmodified PVC

the molecular weight of internal plasticizer decreases, so does this phenomenon: PVC-TRZ-Hexyl-TRZ-DiBu demonstrates a moderate boost in plasticization, while PVC-TRZ-Hexyl-TRZ-DiMe exhibits a minute T_g depression. Therefore, long and sterically bulky triazole emollients are superior internal PVC plasticizers. Conceptually, this is logical: as plasticizer molecular weight increases, so will its weight percent in the final material.

2.7 DSC Analysis: 1st Generation Versus 2nd Generation Triazole Phthalate Mimics on PVC

The 1st generation primary triazole directly attached to PVC conveys a slight anti-plasticization effect. This issue was alleviated in the 2nd generation system by adding a hexyl-tether to provide an efficient means of plasticization by allowing the secondary triazole-phthalate mimic to create more free volume between the PVC main chains compared to the 1st generation system.

The efficacy of the 2nd generation triazole-phthalate mimics was determined by comparing DSC data to the 1st generation system (**Figure 2.23**). PVC samples containing hexyl-tethers exhibit lower overall T_g values than their 1st generation analogues. **Table 2.6** collectively illustrates the glass transition temperatures of internally plasticized PVC encompassing 1st and 2nd generation derivatives. The aromatic anti-plasticization penalty seen with the 1st generation samples has largely been mitigated by the hexyl tether.

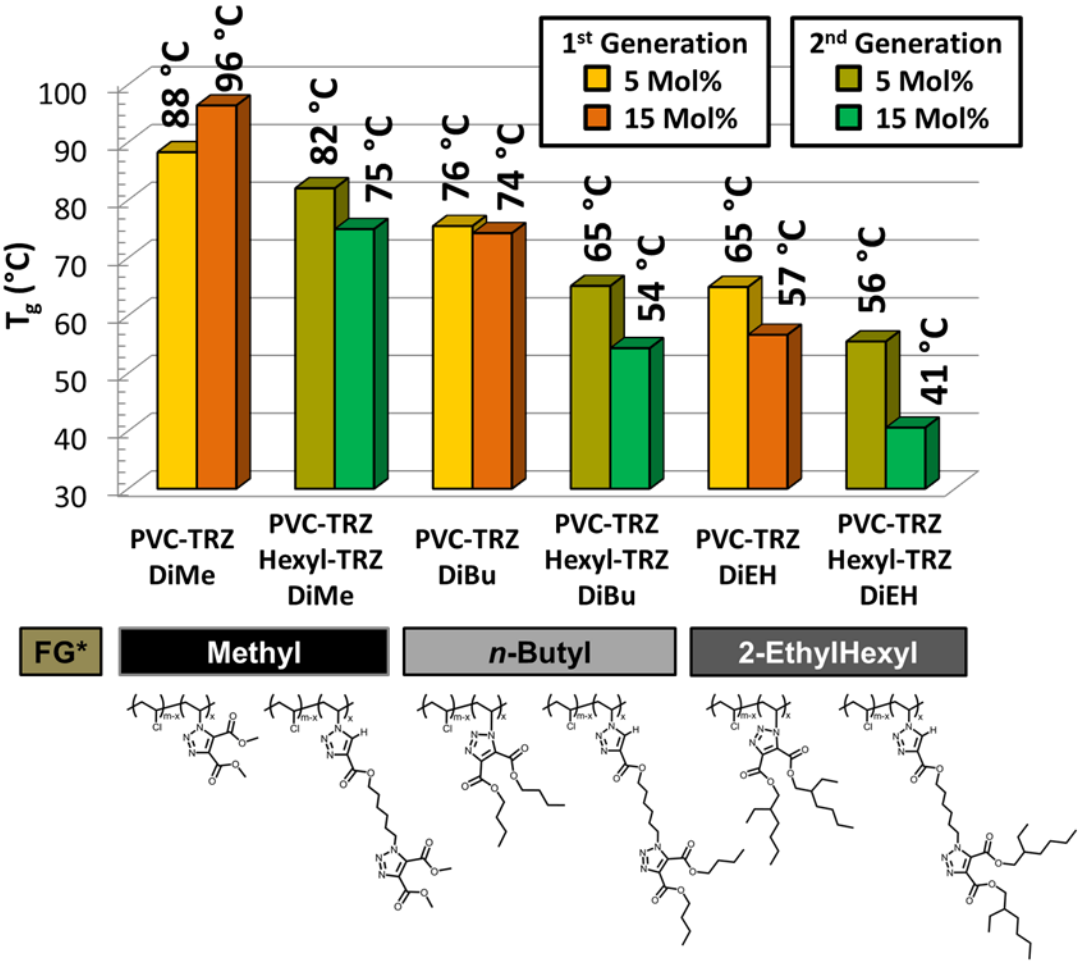

Figure 2.23 DSC Data Comparing 1st and 2nd Generation Triazole Phthalate Mimics (**FG = Functional Group*)

Generation	Polymer	5 Mol% T_g (°C)	15 Mol% T_g (°C)
Standards	*PVC*	*81 °C*	
	PVC-Azide	83	78
1st Gen.	PVC-TRZ-DiMe	88	96
	PVC-TRZ-DiBu	76	74
	PVC-TRZ-DiEH	65	57
2nd Gen.	PVC-TRZ-Hexyl-TRZ-DiMe	82	75
	PVC-TRZ-Hexyl-TRZ-DiBu	65	54
	PVC-TRZ-Hexyl-TRZ-DiEH	56	41

Table 2.6 DSC Data of PVC Standards with 1st and 2nd Generation Triazole Phthalate Mimics

ΔT_g *PVC* values of 1st and 2nd generation systems are presented in **Table 2.7**. The crystallinity engendered by the aromatic triazole is counterbalanced by the incorporation of the hexyl tether. Both 5 and 15 mole percent methyl triazole congeners belonging to the 1st generation (PVC-TRZ-DiMe) convey anti-plasticization properties to PVC. On the other hand, 2nd generation internally plasticized PVC containing the analogous secondary methyl triazole (PVC-TRZ-Hexyl-TRZ-DiMe) displays lower T_g values. This represents a 6 °C depression between 5 mole percent methyl ester generations, and a staggering 21 °C decrease between the 15 mole percent relatives (**Table 2.8**). The hexyl tether unequivocally alleviates the deleterious rigidification conveyed by the primary triazole, despite largely absent plasticizing alkyl chains in the secondary dimethyl ester triazole. Comparing *n*-butyl ester relatives reveals a similar trend (**Table 2.8**): noteworthy T_g depressions between generations of 5 and 15 mole percent analogues are observed (ΔT_g 5 Mol% = -11 °C and ΔT_g 15 Mol% = -20 °C). In the same vein, 2-ethylhexyl congeners exhibited similar glass transition temperature depressions (ΔT_g 5 Mol% = -9 °C and ΔT_g 15 Mol% = -16 °C).

On average, the 5 mole percent derivatives exhibited a T_g reduction of 9 °C, while the 15 mole percent polymers saw an average decline of 19 °C. Intensified glass transition temperature depressions occur in the 15 mole percent samples compared to the 5 mole percent analogues (**Figure 2.24**). As the primary anchoring triazole becomes more ubiquitous on the backbone in the 2nd generation system, a concomitant inclusion of two new moieties

appears: 1) a hexyl tether and 2) a secondary plasticizing triazole. In contrast, the 1st generation system relies exclusively on a single plasticizing triazole directly bound to PVC (**Figure 2.25**). The hexyl tether of the 2nd generation system may synergistically enhance plasticization by acting as a pseudo-plasticizing entity, in addition to distancing the secondary triazole from the main chain of PVC. As a result, the structural configuration of the 2nd generation system may function as more than one triazole phthalate mimic per attachment point versus the 1st generation, which contains only one phthalate mimic equivalent.

Generation	**Polymer**	**5 Mol% ΔT_g PVC (°C)**	**15 Mol% ΔT_g PVC (°C)**
	PVC	*81 °C*	
1st Gen.	PVC-TRZ-DiMe	+7	+15
	PVC-TRZ-DiBu	-5	-7
	PVC-TRZ-DiEH	-16	-24
2nd Gen.	PVC-TRZ-Hexyl-TRZ-DiMe	+1	-6
	PVC-TRZ-Hexyl-TRZ-DiBu	-16	-27
	PVC-TRZ-Hexyl-TRZ-DiEH	-25	-40

Table 2.7 ΔT_g PVC of 1st and 2nd Generation Triazole Phthalate Mimics

FG	**Polymer**	**5% ΔT_gPVC**	**ΔT_g Gen 5%**	**15% ΔT_gPVC**	**ΔT_g Gen 15%**
	PVC	*81 °C*			
Me	PVC-TRZ-DiMe	+7	-6	+15	-21
	PVC-TRZ-Hexyl-TRZ-DiMe	+1		-6	
n-Bu	PVC-TRZ-DiBu	-5	-11	-7	-20
	PVC-TRZ-Hexyl-TRZ-DiBu	-16		-27	
2-EH	PVC-TRZ-DiEH	-16	-9	-24	-16
	PVC-TRZ-Hexyl-TRZ-DiEH	-25		-40	

Table 2.8 ΔT_g PVC and ΔT_g Between 1st and 2nd Generation Systems Grouped By Ester Alkyl Chain

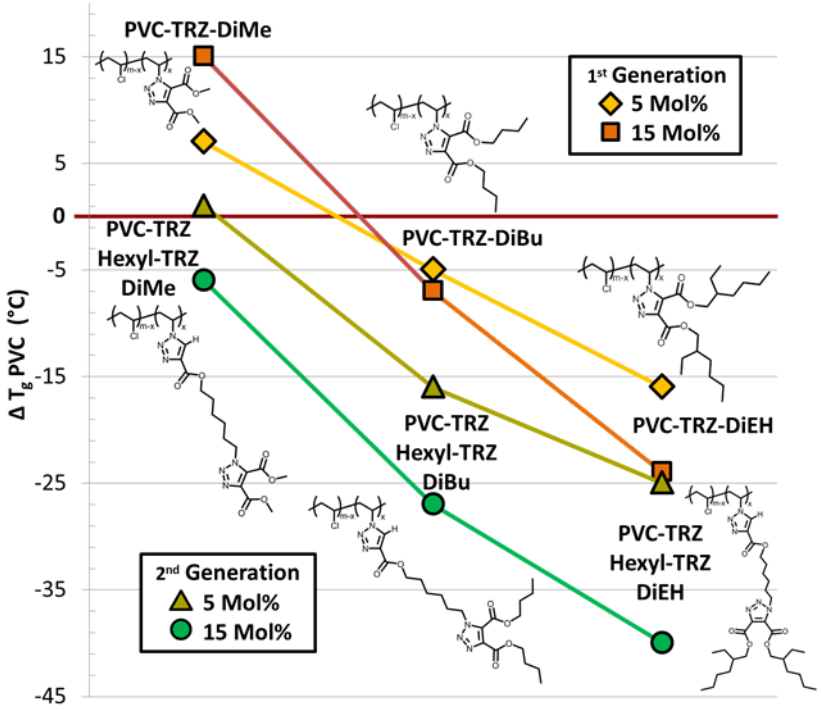

Figure 2.24 Difference in Glass Transition Temperature (ΔT_g PVC) of 1st and 2nd Generation Systems with Respect to Unmodified PVC

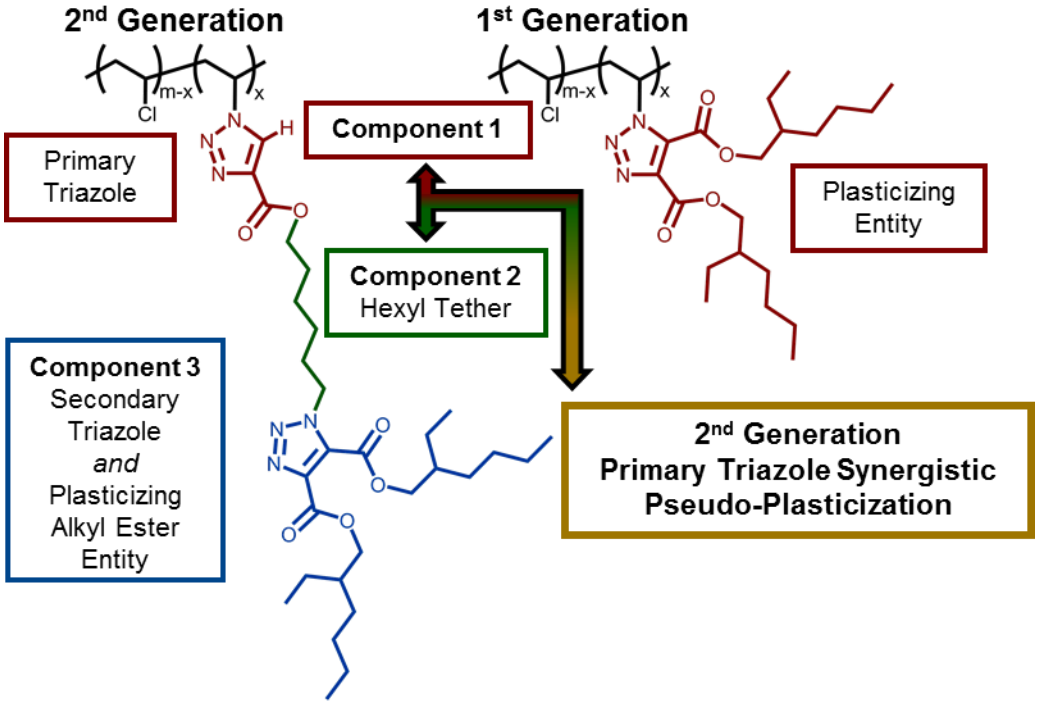

Figure 2.25 Structural Comparison of 1st and 2nd Generation Triazole Phthalate Mimics

Thus far, all internally plasticized polymers were examined in terms of mole percent triazole present on PVC. A valuable alternate analytical perspective evaluates glass transition temperatures as a function of weight percentage of plasticizer. In this manner, one can simplify alterations to the plasticizer solely by considering molecular weight. Most publications utilize *weight percent* of plasticizer as a standard metric to determine plasticization efficiency. **Figure 2.26** graphically illustrates the method to obtain the weight percent of triazole-based internal plasticizer in functionalized PVC.

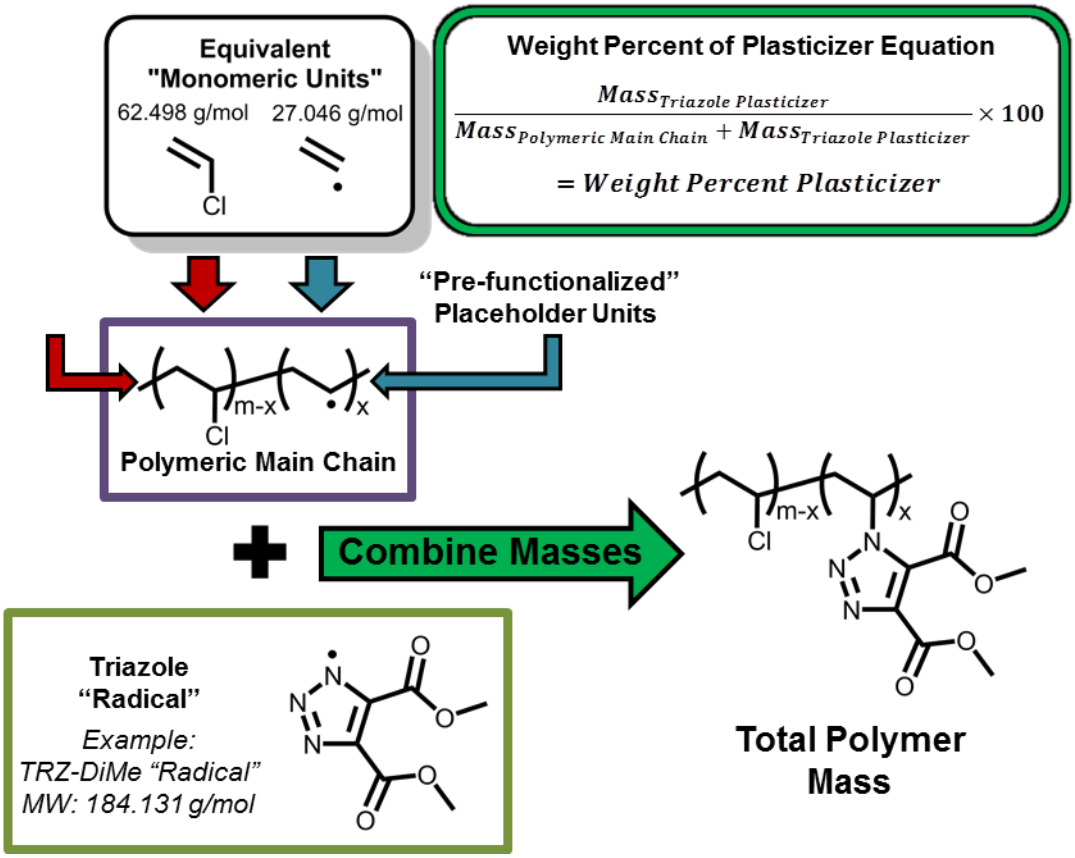

Figure 2.26 Structural Breakdown to Calculate Weight Percent Plasticizer

A mathematical expression was devised to calculate the weight percent of triazole-phthalate mimic in PVC (**Equation 2.3**):

$$X_{Mass\ PVC} + Y_{Mass\ Plasticizer} = Z_{Mass\ Total} \qquad \textbf{Equation 2.2}$$

$$\frac{Y_{Mass\ Plasticizer}}{Z_{Mass\ Total}} \times 100 = Wt\%\ Plasticizer\ in\ PVC \qquad \textbf{Equation 2.3}$$

On first inspection, this calculation seems fairly rudimentary; however, one must bear in mind that there was a loss of chloride on PVC, as a consequence of substitution with azide. To determine the weight percent of plasticizer, one must elucidate how many moles of azide are on PVC after S_N2 substitution. Elemental analysis data of the 5 and 15 mole percent substituted PVC-azide gives the moles of nitrogen present, thus the moles of azide can be solved mathematically.

Polymer	Alleged Mol%	Carbon (Wt%)	Hydrogen (Wt%)	Nitrogen (Wt%)
PVC-Azide	5	38.97	4.98	**3.10**
	15	38.17	4.70	**9.81**

Table 2.9 Elemental Analysis of PVC-Azide Samples

For 100 grams of sample, the weight percentage of each atom directly translates to a mass. For the approximately 15 mole percent azide polymer, 9.81 grams out of the total 100 grams of plastic is nitrogen. Utilizing the atomic weight of nitrogen (14.01 g/mol), the moles of nitrogen atoms in the 100 gram polymer is calculated (**Equation 2.4**):

$$9.81\ grams\ Nitrogen\ \left(\frac{1\ Mole}{14.01\ grams\ Nitrogen}\right) = 0.700\ moles\ Nitrogen \qquad \textbf{Equation 2.4}$$

Likewise, the moles of carbon in the sample are determined from the data in **Table 2.9** (**Equation 2.5**):

$$38.7\ grams\ Carbon\ \left(\frac{1\ Mole}{12.01\ grams\ Carbon}\right) = 3.178\ moles\ Carbon \qquad \textbf{Equation 2.5}$$

The molar value of nitrogen is divided by 3 to account for each atom present in the azide moiety (**Equation 2.6**). Carbon is divided by 2 to account for each atom present in a monomeric unit of the entire polymer (**Equation 2.7**):

$$\frac{0.700\ Moles\ Nitrogen}{3} = 0.233\ Moles\ of\ Azide \qquad \textbf{Equation 2.6}$$

$$\frac{3.178\ Moles\ Carbon}{2} = 1.589\ Moles\ in\ Each\ Carbon\ Monomeric\ Unit \qquad \textbf{Equation 2.7}$$

The value for nitrogen and carbon are taken as a molar ratio and multiplied by 100 to give the degree of azidation in the polymer (**Equation 2.8**):

$$\frac{0.233\ Moles\ of\ Azide}{1.589\ Moles\ in\ Each\ Carbon\ Monomeric\ Unit} \times 100 \qquad \textbf{Equation 2.8}$$

$$= 14.69\ Azide\ Moieties\ Per\ 100\ Monomeric\ Units$$

The calculation for the "5%" PVC-azide sample yields 4.547 azide moieties per 100 monomeric units. To account for the mole percent of plasticizer, an arbitrary 100 millimoles (mmol) of PVC is multiplied by the value elucidated for degree of azidation, which is directly related to the millimoles of plasticizer on modified PVC (**Equation 2.9**):

$$100\ mmol\ Polymer - 14.69\ mmol\ Plasticizer = 85.31\ mmol\ Unmodified\ PVC \qquad \textbf{Equation 2.9}$$

The mass of unmodified PVC is calculated from the molecular weight for vinyl chloride monomer (62.498 g/mol) and the mmol value obtained from **Equation 2.9** (**Equation 2.10**):

$$85.31\ mmol\ PVC\left(\frac{62.498\ grams}{1000\ mmol}\right) = 5.332\ grams\ of\ Unmodified\ PVC \qquad \textbf{Equation 2.10}$$

The amount of plasticizer in mmol is identical to the amount of chlorine atoms lost, due to S_N2 displacement with azide in the first substitution reaction. This equates to the millimolar equivalents of polymerized "monomeric units" with a triazole. The total mass of the unfunctionalized backbone (the main chain mass of PVC without chlorine or triazole) must be

determined at the specific mole percent substitution of plasticizer chosen (5 or 15 Mol%). A theoretical ethylene radical (MW: 27.05 g/mol, **Figure 2.26**) is utilized as a "pre-functionalized unit placeholder" for the incorporation of a future triazole, thereby factoring the loss of chlorine into the mass calculation of the main chain (**Equation 2.11**):

$$14.69\ mmol\ Ethylene\ Radical\left(\frac{27.05\ grams}{1000\ mmol}\right) \qquad \textbf{Equation 2.11}$$

$$= 0.397\ grams\ \text{of}\ Pre-Functionalized\ Units$$

The masses of unmodified PVC and the pre-functionalized placeholder are combined to yield 5.729 grams of polymeric main chain, which includes unmodified and pre-functionalized units (**Equation 2.12**). In "5" mole percent samples, there is 6.089 grams of polymeric main chain.

$$5.332\ grams\ Unmodified\ PVC + 0.397\ grams\ Pre\ Functionalized\ Units \qquad \textbf{Equation 2.12}$$

$$= 5.729\ grams\ of\ Polymeric\ Main\ Chain$$

To account for the triazole phthalate mimic, a theoretical triazole "radical" acts as a means to determine the molecular weight of "pure" triazole plasticizer (**Figure 2.26**). As an *example*, methyl ester triazole (found in PVC-TRZ-DiMe) is calculated based on its "radical" form, which selectively gives the molecular weight of the plasticizer (in this instance, 184.13 g/mol, **Figure 2.26**). The triazole's molecular weight, in combination with the known mmol value of plasticizer attached to PVC (**4.547 mmol for 5 Mol% or 14.69 mmol for 15 Mol%**), allows one to calculate the mass of "pure" triazole-phthalate mimic present in the final material (**Equation 2.13**):

$$14.69\ mmol\ Triazole\ Plasticizer\left(\frac{184.13\ grams}{1000\ mmol}\right) \qquad \textbf{Equation 2.13}$$

$$= 2.705\ grams\ Triazole\ Plasticizer$$

Finally, the weight percent of triazole-based plasticizer present in PVC is calculated using the general equation below (**Equation 2.14**):

$$\frac{Mass_{Triazole\ Plasticizer}}{Mass_{Polymeric\ Main\ Chain} + Mass_{Triazole\ Plasticizer}} \times 100 = Weight\ Percent\ Plasticizer$$ **Equation 2.14**

The mass of the triazole plasticizer is divided by the total mass of the polymer, which consists of the plasticizer and polymeric main chain. This accurately yields the weight percent of plasticizer present for the modified PVC. For the example with approximately 5 mole percent dimethyl ester triazole (PVC-TRZ-DiMe), a sample calculation is illustrated by **Equation 2.15**:

$$\frac{2.705\ grams\ Triazole\ Plasticizer}{5.729\ grams\ Polymeric\ Main\ Chain + 2.705\ grams\ Triazole\ Plasticizer} \times 100 = 32.07\%\ Triazole\ Phthalate\ Plasticizer$$ **Equation 2.15**

These calculations were applied to the first two generations of internally plasticized PVC.

DEHP-PVC mixtures were prepared to establish a standard T_g curve following the current industry benchmark. By comparing the T_g values of the DEHP-PVC standards, it is possible to determine the efficacy of the triazole-based system with respect to DEHP. Glass transition temperatures of DEHP-PVC standard mixtures are listed in **Table 2.10**.

Polymer	Wt % DEHP Plasticizer	T_g Standards (°C)
DEHP-PVC	0	80.97
	20	19.39
	30	-3.52
	40	-26.57
	50	-43.40
	60	-56.85
	70	-67.02

Table 2.10 Glass Transition Temperatures of DEHP-PVC Standard Mixtures with Respect to Weight Percent DEHP Plasticizer

Weight percentages and glass transition temperatures of the 1st and 2nd generation polymers are presented in **Table 2.11**. An overlay of these T_g values versus weight percent plasticizer with DEHP-PVC standards is illustrated in **Figure 2.27**.

Generation	Polymer	Mol %	Wt % Plasticizer	T_g (°C)
1st Gen.	PVC-TRZ-DiMe	5	12.1	88
		15	32.1	96
	PVC-TRZ-DiBu	5	16.7	76
		15	40.8	74
	PVC-TRZ-DiEH	5	22.1	65
		15	49.4	57
2nd Gen.	PVC-TRZ-Hexyl-TRZ-DiMe	5	22.1	82
		15	49.3	75
	PVC-TRZ-Hexyl-TRZ-DiBu	5	25.7	65
		15	54.3	54
	PVC-TRZ-Hexyl-TRZ-DiEH	5	30.1	56
		15	59.6	41

Table 2.11 Glass Transition Temperatures and Weight Percentages of 1st and 2nd Generation Triazole-Based Phthalate Mimics in Modified PVC

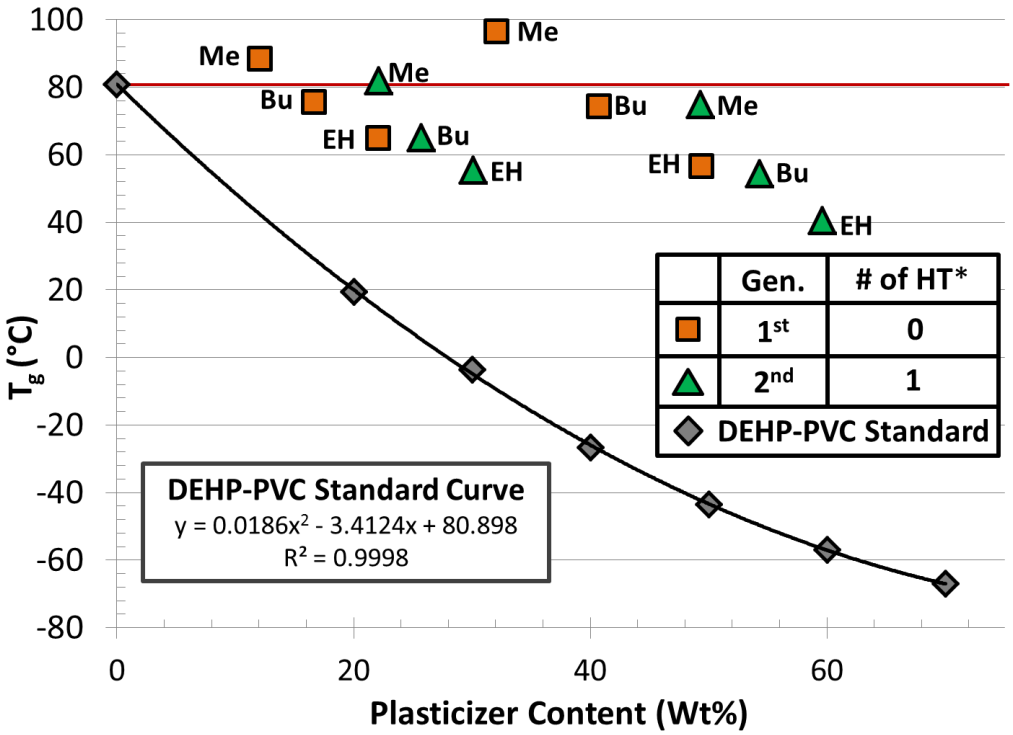

Figure 2.27 Overlay of T_g Values Versus Weight Percent of Plasticizer with DEHP-PVC Standard Mixtures and Generations 1-2 Triazole Phthalate Mimics
(**HT = Hexyl Tethers*)

There are two major clusters of data in **Figure 2.27**. The first cluster, located approximately between 10 and 30 weight percent plasticizer, correlates to the 5 mole percent derivatives, while samples between 32 and 60 weight percent belong to the 15 mole percent polymers. The red line in **Figure 2.27** represents the standard glass transition temperature of unmodified PVC (T_g = 81 °C). Three samples are above the red line, demonstrating anti-plasticizing properties: both 5 and 15% PVC-TRZ-DiMe, along with 5% PVC-TRZ-Hexyl-TRZ-DiMe exhibit T_g values higher than PVC. A decrease in T_g for all species is concomitant with the enlargement of the alkyl plasticizing chain, regardless of mole percent or generation. A striking juxtaposition of glass transition temperatures can be seen between 15% PVC-TRZ-DiMe (T_g = 96 °C, 32.1 Wt% Plasticizer) and 5% PVC-TRZ-Hexyl-TRZ-DiEH (T_g = 56 °C, 30.1 Wt% Plasticizer): despite the similarity in weight percentage of plasticizer, 5% PVC-TRZ-Hexyl-TRZ-DiEH has a ΔT_g of -40 °C when compared to 5% PVC-TRZ-DiMe, illustrating the advantage of a long, bulky ester chain and tether. Likewise, 5% PVC-TRZ-DiEH (T_g = 65 °C, 22.2 Wt% Plasticizer) and 5% PVC-TRZ-Hexyl-TRZ-DiMe (T_g = 82 °C, 22.1 Wt% Plasticizer) show significantly different glass transition temperatures (ΔT_g = -17 °C). In a similar vein, 15% PVC-TRZ-DiEH (T_g = 57 °C, 49.4 Wt% Plasticizer) and 15% PVC-TRZ-Hexyl-TRZ-DiMe (T_g = 75 °C, 49.3 Wt% Plasticizer) also demonstrate decreased T_g values (ΔT_g = -18 °C) with similar weight percentages of plasticizer. While PVC-TRZ-Hexyl-TRZ-DiMe has a hexyl-tether, it lacks long, bulky alkyl moieties to effectively create free space between chains of PVC, whereas PVC-TRZ-DiEH has no tether, but contains the longest, most sterically hindered and branched plasticizing chains.

Analyzing **Figure 2.27** horizontally, inspection of the 5 mole percent cluster shows that PVC-TRZ-DiEH (T_g = 65 °C, 22.1 Wt% Plasticizer) and PVC-TRZ-Hexyl-TRZ-DiBu (T_g = 65 °C, 25.7 Wt% Plasticizer) have the same glass transition temperature, despite a slight difference in weight percentage of plasticizer. While PVC-TRZ-Hexyl-TRZ-DiBu has a tether, PVC-TRZ-DiEH contains the large, branched 2-ethylhexyl chains, furnishing nearly

analogous glass transition temperatures at a lower weight percent. A corresponding observation in the 15 mole percent samples of PVC-TRZ-DiEH (T_g = 57 °C, 49.4 Wt% Plasticizer) and PVC-TRZ-Hexyl-TRZ-DiBu (T_g = 54 °C, 54.3 Wt% Plasticizer) was found: regardless of the greater percentage of plasticizer by weight present in PVC-TRZ-Hexyl-TRZ-DiBu, the difference in glass transition temperatures relative to PVC-TRZ-DiEH is marginal (ΔT_g = -3 °C). It is evident that a long and branched alkyl plasticizing moiety is essential for plasticization efficacy. The hexyl tether merely enhances the ability of a secondary triazole with smaller ester alkyl chains to work in a similar fashion to its larger-chain congeners. Therefore, a combination of a tether with 2-ethylhexyl groups on the secondary triazole should provide the most pronounced plasticization effect with the lowest weight percentage of plasticizer. This phenomenon was observed between 5% PVC-TRZ-Hexyl-TRZ-DiEH (T_g = 56 °C, 30.1 Wt% Plasticizer) and 15% PVC-TRZ-Hexyl-TRZ-DiBu (T_g = 54 °C, 54.3 Wt% Plasticizer); comparable glass transition temperatures were found for both polymers despite a large difference in weight percent of plasticizer (ΔWt% Plasticizer = 24.2%). Another example occurs comparing plasticizers containing 2-ethylhexyl groups: 5% PVC-TRZ-Hexyl-TRZ-DiEH (T_g = 56 °C, 30.1 Wt% Plasticizer) and 15% PVC-TRZ-DiEH (T_g = 57 °C, 49.4 Wt% Plasticizer) gave nearly identical T_g values, but contain a vastly disparate weight percentage of plasticizer (ΔWt% Plasticizer = 19.3%). The major difference in the architecture of these two 2-ethylhexyl functionalized plasticizers lies in the presence of the hexyl-tether. Evidently, the tether maximizes the ability of the secondary triazole to soften PVC and requires significantly less plasticizer to attain comparable T_g values.

2.8 Plasticizer Efficiencies: 1st and 2nd Generation Systems Versus DEHP-PVC

Thus far, the analysis of DSC data from the 1st and 2nd generation systems has been framed in comparative terms to unmodified PVC. However, industry rarely uses PVC in its pure brittle form and most frequently mixes in DEHP to provide a cost-effective method to access flexibility and resistivity towards weathering, temperature extremes, and electrical

conductivity. Therefore, a more accurate measure of triazole-based plasticizer efficacy is a comparison with the ubiquitous DEHP-PVC system. Plasticizer efficiency related to the reduction in T_g of polyglycerol externally plasticized PVC, with respect to pure PVC and a PVC standard with a matched weight percentage of DEHP to polyglycerol has been previously reported.[26] A modification of this calculation was adopted for the current study. The plasticizer efficiency percentage ($E\Delta T_g$) is determined as follows (**Equation 2.16**):

$$E\Delta T_g = \frac{\Delta T_g\ TRZ}{\Delta T_g\ DEHP} \times 100 \qquad \textbf{Equation 2.16}$$

In order to obtain ΔT_g TRZ, one must calculate the difference of T_g between unmodified PVC ($T_{g\ PVC}$) and the triazole modified PVC (T_g TRZ) (**Equation 2.17**):

$$\Delta T_g\ TRZ = T_{g\ PVC} - T_g\ TRZ \qquad \textbf{Equation 2.17}$$

where T_g TRZ is the observed glass transition temperature of the novel triazole-based system, and $T_{g\ PVC}$ is 80.97 °C, obtained by experimental DSC.

A similar process is employed to determine ΔT_g DEHP (**Equation 2.18**):

$$\Delta T_g\ DEHP = T_{g\ PVC} - T_g DEHP \qquad \textbf{Equation 2.18}$$

To determine ΔT_g DEHP, a standard curve was generated using various weight percentages of DEHP in PVC. Utilizing the identical DSC heat-cool-heat protocol as all other measured polymer samples, glass transition temperature data (**Table 2.10**) was obtained and an equation for a DEHP-PVC standard curve was generated in terms of weight percent DEHP versus T_g, following **Figure 2.27** (**Equation 2.19**):

$$y = 0.0186x^2 - 3.4124x + 80.898 \qquad \textbf{Equation 2.19}$$

where *x* represents the weight percentage of DEHP in a PVC mixture, and *y* is the T_g of the DEHP-PVC mixture. Employing the weight percentage calculation method outlined in *Section*

2.7, the weight percent of triazole-based plasticizer was obtained: this value is substituted for *x* in **Equation 2.19**. This yields the predicted T_g of the DEHP-PVC blend with the identical weight percentage of DEHP emollient as the triazole-based system, in terms of *y*. The output value for *y* is applied in the calculation of ΔT_g *DEHP*, the difference in T_g between the DEHP-PVC mixture and pure PVC (**Equation 2.20**):

$$\Delta T_g\ DEHP = 80.97 - y \qquad \textbf{Equation 2.20}$$

By placing the ΔT_g values from **Equation 2.19 and 2.20** into **Equation 2.16**, the plasticizer efficiency percentage ($E\Delta T_g$) is obtained for any triazole-based plasticized PVC sample (**Equation 2.21**):

$$E\Delta T_g = \frac{80.97 - T_{g\ Triazole\ Plasticized\ PVC}}{80.97 - y} \times 100 \qquad \textbf{Equation 2.21}$$

$E\Delta T_g$ is a value representing how similar the triazole-plasticizers compare to the standard DEHP-PVC mixture. Conveniently, the large variability of plasticizer weight percentages between triazole functionalized PVC samples is compensated in this calculation. The effectiveness of covalently-bound plasticizers can be directly compared and analyzed without regard to weight percent plasticizer, as each internally plasticized sample is now standardized to DEHP-PVC. A range from 0 to 100 is typical for $E\Delta T_g$. However, a value below zero indicates anti-plasticization, while a value above 100 describes an emollient more efficient than DEHP at a specific weight percent of plasticizer. $E\Delta T_g$ values for all 1st and 2nd generation samples were calculated and are presented in **Table 2.12** (5 mole percent) and **Table 2.13** (15 mole percent), organized in descending order of efficiency percentages. $E\Delta T_g$ values for 3rd generation polymers are depicted as a bar graph in **Figure 2.28**.

Utilizing the quantitative $E\Delta T_g$ values from **Table 2.12** and **Table 2.13**, it is apparent that 5 and 15 mole percent polymers require slightly different structural configurations to achieve high efficiency percentages. For the 5 mole percent triazole samples, the presence

Polymer	Wt% TRZ (*x*)	T_g TRZ	ΔT_g TRZ	DEHP T_g (*y*)	ΔT_g DEHP	$E\Delta T_g$
5% PVC TRZ-Hexyl-TRZ-DiEH	30.1	55.5	25.5	-4.9	85.9	**29.7**
5% PVC TRZ-DiEH	22.1	65	16.0	14.5	66.5	**24.1**
5% PVC TRZ-Hexyl-TRZ-DiBu	25.7	65	15.8	5.5	75.5	**21.0**
5% PVC TRZ-DiBu	16.7	75.5	5.5	29.1	51.9	**10.5**
5% PVC TRZ-Hexyl-TRZ-DiMe	22.1	82.1	-1.1	14.6	66.3	**-1.6**
5% PVC TRZ-DiMe	12.1	88.3	-7.3	42.4	38.6	**-19.0**

Table 2.12 Plasticization Efficiencies of 5 Mol % 1st and 2nd Generation Triazole Internally Plasticized PVC Ranked by Descending $E\Delta T_g$ Values

Polymer	Wt% TRZ (*x*)	T_g TRZ	ΔT_g TRZ	DEHP T_g (*y*)	ΔT_g DEHP	$E\Delta T_g$
15% PVC TRZ-Hexyl-TRZ-DiEH	59.6	40.6	40.4	-56.4	137.4	**29.4**
15% PVC TRZ-Hexyl-TRZ-DiBu	54.3	54.4	26.6	-49.6	130.5	**20.4**
15% PVC TRZ-DiEH	49.4	56.7	24.3	-42.3	123.2	**19.7**
15% PVC TRZ-DiBu	40.8	74.3	6.7	-27.3	108.3	**6.2**
15% PVC TRZ-Hexyl-TRZ-DiMe	49.3	75.0	6.0	-42.1	123.1	**4.9**
15% PVC TRZ-DiMe	32.1	96.4	-15.4	-9.4	90.4	**-17.1**

Table 2.13 Plasticization Efficiencies of 15 Mol % 1st and 2nd Generation Triazole Internally Plasticized PVC Ranked by Descending $E\Delta T_g$ Values

of 2-ethylhexyl moieties appears to be more important than the hexyl tether in engendering better plasticization efficiencies (**Table 2.12**). A sequential decrease in $E\Delta T_g$ is observed with the 2nd generation PVC-TRZ-Hexyl-TRZ-DiEH, exhibiting the highest value of 29.7, while the 1st generation PVC-TRZ-DiEH ($E\Delta T_g$ = 24.1), 2nd generation PVC-TRZ-Hexyl-TRZ-DiBu ($E\Delta T_g$ = 21.0) and 1st generation PVC-TRZ-DiBu ($E\Delta T_g$ = 10.5) show lower efficiencies. Both generations of derivatives containing methyl-triazole (PVC-TRZ-DiMe and PVC-TRZ-Hexyl-TRZ-DiMe) give negative $E\Delta T_g$ values, indicating anti-plasticization. The 1st generation sample, PVC-TRZ-DiMe ($E\Delta T_g$ = -19.0) is much less efficient than its 2nd generation analogue, PVC-TRZ-Hexyl-TRZ-DiMe ($E\Delta T_g$ = -1.6) at conveying flexibility to PVC. The addition of the hexyl tether enhances the efficiency between generations of methyl-triazoles by 17.4%.

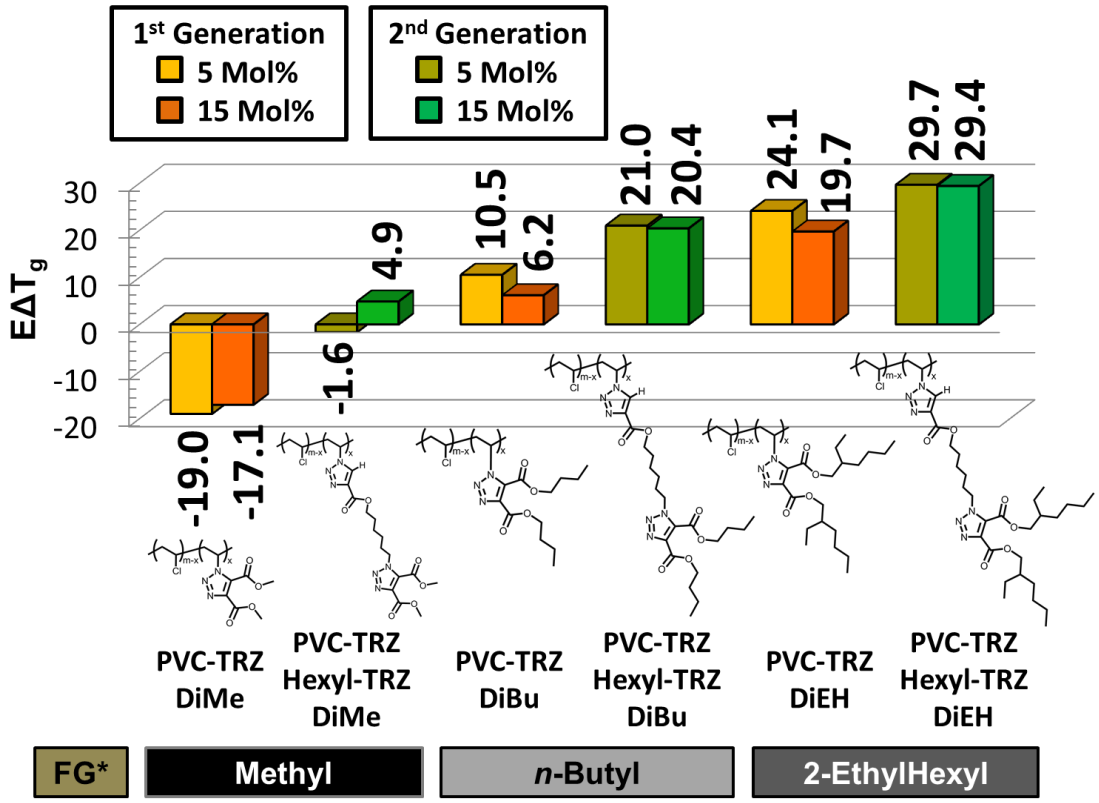

Figure 2.28 Efficiency Values ($E\Delta T_g$) of 1st and 2nd Generation Internally Plasticized PVC (**FG = Functional Group*)

In the 15 mole percent samples, the hexyl tether in 2nd generation triazole plasticizers plays a critical role in enhancing plasticizing efficiency (**Table 2.13**). The highest efficiencies are observed in 2nd generation samples PVC-TRZ-Hexyl-TRZ-DiEH ($E\Delta T_g$ = 29.4) and PVC-TRZ-Hexyl-TRZ-DiBu ($E\Delta T_g$ = 20.4), with the 1st generation PVC-TRZ-DiEH ($E\Delta T_g$ = 19.7) coming in a close third. The 1st generation PVC TRZ-DiBu ($E\Delta T_g$ = 6.2) experiences a severe reduction in $E\Delta T_g$ relative to its 2nd generation hexyl tethered analogue, PVC-TRZ-Hexyl-TRZ-DiBu, corresponding to a 14.2% deficit. Methyl-triazole analogues at 15 mole percent are also not effective in plasticizing PVC: the 1st generation sample, PVC-TRZ-DiMe, displays anti-plasticization characteristics ($E\Delta T_g$ = -17.1), while the 2nd generation relative, PVC-TRZ-Hexyl-TRZ-DiMe ($E\Delta T_g$ = 4.9), effectively counteracts anti-plasticization. Interestingly, PVC-TRZ-DiMe shows decreased efficiencies at 5 mole percent compared to 15 mole percent

($E\Delta T_g$ 5 Mol% = -19.0, $E\Delta T_g$ 15 Mol% = -17.1) despite a significant increase in T_g at the higher mole percentage of triazole.

In this capacity, the plasticizers in both 1st and 2nd generations remain less effective from a weight percentage perspective than traditional non-covalently bound DEHP. While effective plasticization is achieved with these triazole phthalate mimics, as the weight percentage of plasticizer increases, the chasm of glass transition temperatures between the novel triazole-plasticized polymers progressively widens compared to the traditional DEHP-PVC blends. At 5 mole percent of covalently-bound plasticizer, the triazole system appears to approach closer to the DEHP standard T_g curve than the 15 mole percent samples. This effect likely stems from the reduced presence of aromatic anchoring points in the internal plasticizers: a spacing strategy containing a primary triazole will accumulate a commensurate amount of rigid moieties on the backbone of PVC as the mole percent increases. As the molar presence of the stiff triazole rings escalates, a paradoxical magnification of anti-plasticization occurs, thereby diminishing the efficacy of the phthalate mimic. This may be due in part to the π-π stacking of the triazole rings in the three-dimensional matrix of PVC, which imparts crystallization and firmness to the composite. Ideally, the next generation of internal plasticizers would possess a higher molecular weight per triazole attachment point and will be designed to reduce stacking of primary triazoles on the PVC backbone, while conveying flexibility to the secondary triazole. This should contribute to lower glass transition temperatures per weight percent of plasticizer and improve plasticization efficacy compared to the 1st and 2nd generation systems.

2.9 Thermogravimetric Analysis: 1st and 2nd Generation Systems

The thermal stability of PVC and its internally plasticized analogues was measured by our collaborators at IBM Almaden Research Center through derivative thermogravimetry (DTG) and thermogravimetric analyses (TGA) with a TA Instruments TGA Q500. The TGA

standard protocol specifies a scanning range of 30 °C to 500 °C with a heating rate of 10 °C per minute, in both air and nitrogen atmospheres.

TGA provides a general indication of weight (in units of Wt%) lost during the decomposition process of a polymer. The atmosphere around the polymer often affects this process; the relative amounts of different decomposition products vary with the gas utilized. DTG affords information on specific decomposition constituents of a polymer at specific temperatures as peaks, corresponding to the first derivative of a TGA curve in units of derivative weight (Wt% / °C).

DTG of unmodified PVC reveals two peaks, indicative of a multistage decomposition process with an initial decrease in mass at the first derivative peak ($T_{d,PVC1}$) of 289 °C, and a second loss ($T_{d,PVC2}$) at 442 °C when measured using air as the surrounding atmosphere (**Figure 2.29**). The first peak ($T_{d,PVC1}$) signifies a complete dehydrochlorination of PVC with concomitant loss of hydrochloric acid, formation of various cyclic aromatic compounds and vinyl chloride. Between 227 °C and 277 °C, hydrogen chloride gas is evolved in a near quantitative manner by a chain stripping mechanism.[27] The second peak ($T_{d,PVC2}$) represents the loss of higher molecular weight hydrocarbon fragments due to chain scission of the carbonaceous backbone. Between 440 °C and 477 °C, hydrogen is evolved during carbonization with a subsequent cyclization of these products. An explicit discussion on PVC degradation was outlined in *Chapter 1*.

DTG of PVC-azide at 5 and 15 mole percent azide exhibit lower degradation temperatures compared to unmodified PVC (**Table 2.14**). The first degradation peak ($T_{d,PVC1}$) of 5% PVC-azide occurs at 227 °C in a nitrogen (N_2) atmosphere and 229 °C when surrounded by air. The second degradation peak ($T_{d,PVC2}$) was observed at 447 °C (N_2) and 453 °C (air). A progressive decrease in degradation temperature occurs with an increasing amount of azide substituted on PVC. In 15% PVC-azide, $T_{d,PVC1}$ occurs at 214 °C (N_2) and

219 °C (air), while $T_{d,PVC2}$ was observed at 444 °C (N_2) and 451 °C (air). Degradation temperatures of PVC internally plasticized by the 1st generation system is given in **Table 2.15**, while the 2nd generation polymers are shown in **Table 2.16**.

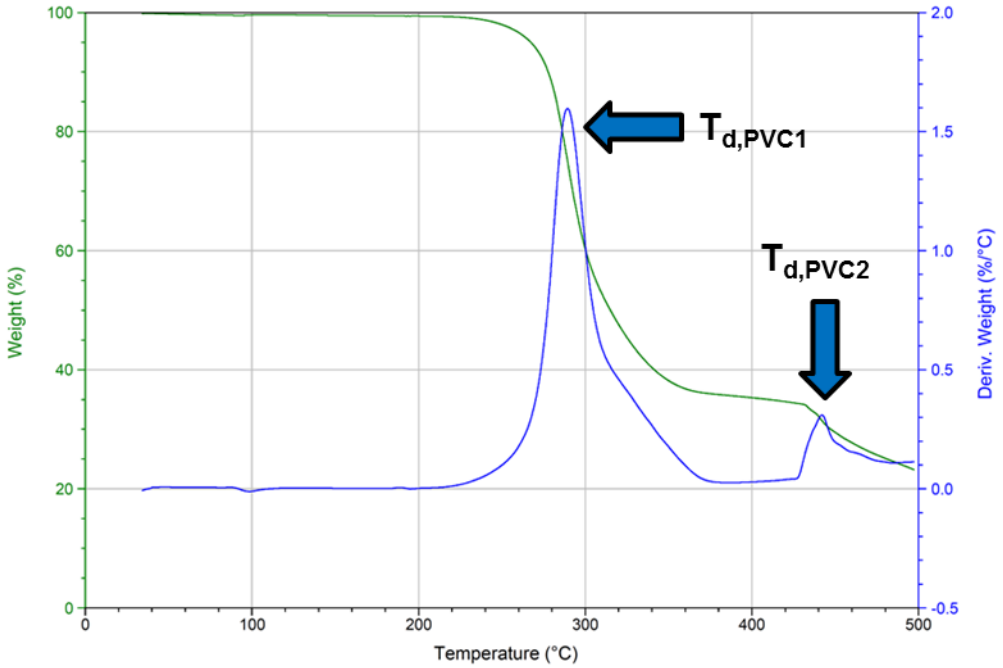

Figure 2.29 TGA (Green) and DTG (Blue) of Unmodified PVC (Air)

Polymer	Atm	$T_{d,PVC1}$ (°C)	$T_{d,PVC2}$ (°C)
Unmodified PVC	N_2	283	319 and 327
	Air	289	442
5% PVC-Azide	N_2	227	447
	Air	229	453
15% PVC-Azide	N_2	214	444
	Air	219	451

Table 2.14 Degradation Temperatures of PVC and PVC-Azide (5 and 15 Mol % Azide)

Polymer	Atm	$T_{d,PVC1}$ (°C)	$T_{d,PVC2}$ (°C)	$T_{d,EH}$ (°C)	$T_{d,TRZ1}$ (°C)	$T_{d,TRZ2}$ (°C)	$T_{d,TRZ3}$ (°C)
Unmodified PVC	N_2	283	-	-	-	-	-
	Air	289	442	-	-	-	-
5% PVC-Azide	N_2	227	447	-	-	-	-
	Air	229	453	-	-	-	-
15% PVC-Azide	N_2	214	444	-	-	-	-
	Air	219	451	-	-	-	-
5% PVC-TRZ-DiMe	N_2	269	442	-	432	-	-
	Air	274	440	-	-	-	465
15% PVC-TRZ-DiMe	N_2	248	440	-	429 (w)	-	-
	Air	254	441	-	-	455 (w)	-
5% PVC-TRZ-DiBu	N_2	268	446	-	434 (w)	-	-
	Air	275	443	-	-	-	464 (w)
15% PVC-TRZ-DiBu	N_2	279	448	-	435	-	-
	Air	290	444	-	-	457 (w)	-
5% PVC-TRZ-DiEH	N_2	270	446	-	433	-	-
	Air	280	451	-	429	457 (w)	466 (w)
15% PVC-TRZ-DiEH	N_2	285	-	367	436	455	-
	Air	306	-	416 (w)	-	456 (w)	-

Table 2.15 TGA/DTG Degradation Temperatures of Unmodified PVC, PVC-Azide and 1st Generation Internally Plasticized PVC

PVC-TRZ-DiMe displays lower $T_{d,PVC1}$ temperatures than unmodified PVC at 5 mole percent (269 °C N_2, 274 °C air) and 15 mole percent (248 °C N_2, 254 °C air). PVC second degradation temperatures ($T_{d,PVC2}$) in these methyl triazole functionalized samples remain similar to unmodified PVC at 5 mole percent (442 °C N_2, 440 °C air) and 15 mole percent (440 °C N_2, 441 °C air). DTG events occurring at 432 °C (5% PVC-TRZ-DiMe, N_2) and 429 °C (15% PVC-TRZ-DiMe, N_2) represent the triazole ester hydrolyzing into its respective alcohol and carboxylic acid. $T_{d,TRZ2}$ (465 °C, 5% PVC-TRZ-DiMe) and $T_{d,TRZ3}$ (455 °C, 15% PVC-TRZ-DiMe) appear as weak DTG peaks when the measurements are performed in air. This is presumably due to the degradation of an oxidized triazole species.

Dehydrochlorination peaks ($T_{d,PVC1}$) of PVC-TRZ-DiBu appear as slightly lower values at 5 mole percent (268 °C N_2, 275 °C air), while similar values to unmodified PVC was

recorded at 15 mole percent (279 °C N_2, 290 °C air). Weak DTG peaks at 434 °C (5 Mol %, N_2) and 435 °C (15 Mol %, N_2) originate from triazole hydrolyzation. Equivalent DTG peaks seen in PVC-TRZ-DiMe occur with PVC-TRZ-DiBu at 464 °C (5 Mol %, air) and 457 °C (15 Mol %, air), stemming from an oxidized triazole degradation process.

The 1st generation polymers display common degradation events relating to the triazole (**Table 2.15**). At 5 mole percent, PVC-TRZ-DiEH exhibits depressed $T_{d,PVC1}$ values (270 °C N_2, 280 °C air) and elevated $T_{d,PVC2}$ values (446 °C N_2, 451 °C air) compared to unmodified PVC. Minor $T_{d,TRZ1}$ (433 °C N_2, 429 °C air) and $T_{d,TRZ2}$ (457 °C air, 466 °C air) peaks represent analogous triazole degradation processes seen in PVC-TRZ-DiMe and PVC-TRZ-DiBu. At 15 mole percent, PVC-TRZ-DiEH displays increased $T_{d,PVC1}$ temperatures (285 °C N_2, 306 °C air) with respect to unmodified PVC, while $T_{d,PVC2}$ was not readily visible. In nitrogen, a strong $T_{d,TRZ1}$ peak (436 °C, N_2) may overlap with $T_{d,PVC2}$. An additional DTG peak at 455 °C (N_2) was noted, which might originate from the delayed degradation of PVC main chain regimes functionalized with the 2-ethylhexyl triazole, or the hydrolyzation of the triazole itself. A broad shoulder at 367 °C (N_2) represents the degradation of the 2-ethylhexyl groups on the triazole. When the thermogravimetric scan was performed in air for 15% PVC-TRZ-DiEH, less prominent DTG peaks are observed from approximately 400 °C, compared to measurements in nitrogen. Two weak yet discernable degradation events at 416 °C and 456 °C are indicative of the oxidized 2-ethylhexyl triazole. No $T_{d,PVC2}$ peak is observed when scanned in air.

The 2nd generation polymers exhibit similar degradation trends to the 1st generation samples (**Table 2.16**). At 5 mole percent, PVC-TRZ-Hexyl-TRZ-DiMe displays decreased $T_{d,PVC1}$ temperatures (243 °C N_2, 248 °C air) with concomitant elevated $T_{d,PVC2}$ values (450 °C N_2, 445 °C air). A minor DTG peak at 437 °C (N_2) is indicative of triazole ester hydrolyzation or an alternate regime of the PVC main chain degradation. A broad shoulder originating from an oxidized triazole degradation ($T_{d,TRZ3}$) is observed when measured in air (459 °C). At 15

mole percent, PVC-TRZ-Hexyl-TRZ-DiMe gives significantly lower $T_{d,PVC1}$ values (221 °C N_2, 227 °C air) compared to unmodified PVC. $T_{d,TRZ1}$ peaks at 428 °C (air) and 432 °C (weak, N_2) are indicative of triazole ester hydrolysis.

Polymer	Atm	T_d PVC1 (°C)	T_d PVC2 (°C)	T_d EH (°C)	T_d Hexyl (°C)	T_d TRZEH (°C)	T_d TRZ1 (°C)	T_d TRZ2 (°C)	T_d TRZ3 (°C)
Unmodified PVC	N_2	283	-	-	-	-	-	-	-
	Air	289	442	-	-	-	-	-	-
5% PVC-Azide	N_2	227	447	-	-	-	-	-	-
	Air	229	453	-	-	-	-	-	-
15% PVC-Azide	N_2	214	444	-	-	-	-	-	-
	Air	219	451	-	-	-	-	-	-
5% PVC-TRZ-Hexyl-TRZ-DiMe	N_2	243	450	-	-	-	437	-	-
	Air	248	445	-	-	-	-	-	459
15% PVC-TRZ-Hexyl-TRZ-DiMe	N_2	221	442	-	-	-	432	-	-
	Air	227	442	-	-	-	428	449	460
5% PVC-TRZ-Hexyl-TRZ-DiBu	N_2	271	441	-	-	-	-	-	-
	Air	274	438	-	-	-	-	-	-
15% PVC-TRZ-Hexyl-TRZ-DiBu	N_2	271	442	-	350	-	-	452	-
	Air	273	442	-	325	-	419	-	-
5% PVC-TRZ-Hexyl-TRZ-DiEH	N_2	271	445	-	358	-	434	-	-
	Air	275	441	-	-	-	-	-	462
15% PVC-TRZ-Hexyl-TRZ-DiEH	N_2	267	448	303	360	-	-	-	-
	Air	279	442	307	340	403	413	-	461

Table 2.16 TGA/DTG Degradation Temperatures of Unmodified PVC, PVC-Azide and 2nd Generation Internally Plasticized PVC

It appears that regardless of generation, methyl triazoles cause a notable decrease in $T_{d,PVC1}$, particularly in 15 mole percent samples. This may stem from the amount of energy that is required to hydrolyze the methyl ester on the triazole, compared to congeners with larger alkyl esters. If the methyl ester requires less energy to hydrolyze than the alkyl analogues containing *n*-butyl or 2-ethylhexyl groups, the resulting triazole carboxylic acid and alcohol are formed at lower temperatures, thereby initiating the acid-catalyzed dehydrochlorination of PVC ($T_{d,PVC1}$). This is observed in 1st and 2nd generation polymers:

triazoles with large alkyl groups exhibit progressively elevated $T_{d,PVC1}$ temperatures as the size of the carbon chain increases (**Table 2.15** and **Table 2.16**). For example, PVC-TRZ-Hexyl-TRZ-DiBu and PVC-TRZ-Hexyl-TRZ-DiEH give $T_{d,PVC1}$ temperatures lower than unmodified PVC, but greater than all methyl triazole derivatives.

Broad DTG peaks exclusively observed in 2nd generation samples occur in 15 mole percent PVC-TRZ-Hexyl-TRZ-DiBu at 325 °C (air) and 350 °C (N_2). This may originate from the hexyl tether (**Table 2.16**). In the 2nd generation polymers, the tether is attached to the primary triazole by a single ester: this may hydrolyze and cause the loss in mass observed in the TGA and DTG. Likewise, 15 mole percent PVC-TRZ-Hexyl-TRZ-DiEH exhibits analogous degradation events at 340 °C (air) and 360 °C (N_2). As with the 1st generation samples, the primary or secondary triazole esters in the 2nd generation polymers should take more energy to hydrolyze as the alkyl chains increase in size. The DTG data of the 2nd generation samples corroborates this hypothesis, showing elevated degradation temperatures originating from the hexyl tether ($T_{d,Hexyl}$) between *n*-butyl and 2-ethylhexyl derivatives. Comparable degradation events occurring only in air are observed with PVC-TRZ-Hexyl-TRZ-DiBu (15%, 413 °C) and PVC-TRZ-Hexyl-TRZ-DiEH (15%, 419 °C). This may stem from the hydrolysis of the primary or secondary triazole esters. PVC-TRZ-Hexyl-TRZ-DiEH displays additional DTG peaks ($T_{d,EH}$) not seen in any other 1st or 2nd generation derivative at 303 °C (N_2) and 307 °C (air). This is possibly due to regimes of PVC heavily functionalized with 2nd generation plasticizers containing 2-ethylhexyl triazole esters. The acid strength of the catalyst determines the rate of thermal degradation in PVC.[28] The presence of internal plasticizer may deter the initial dehydrochlorination of PVC in these localized regions due to the larger pK_a value of the triazole carboxylate (pK_a = 2.95)[29] relative to HCl ($pK_a \approx -7$). The pK_a value associated with the carboxylate implicate a slower onset of dehydrochlorination by sequestering some of the thermal energy required to hydrolyze the triazole esters, that would have otherwise gone towards the elimination of HCl from the main chain.

2.10 References

1. Rostovtsev, V. V.; Green, L. G.; Fokin, V. V.; Sharpless, K. B. A Stepwise Huisgen Cycloaddition Process: Copper(I)-Catalyzed Regioselective "Ligation" of Azides and Terminal Alkynes. *Angewandte Chemie International Edition* **2002,** *41* (14), 2596-2599.

2. Huisgen, R. Kinetics and Mechanism of 1,3-Dipolar Cycloadditions. *Angewandte Chemie International Edition in English* **1963,** *2* (11), 633-645.

3. Woodward, R. B.; Hoffmann, R. Stereochemistry of Electrocyclic Reactions. *Journal of the American Chemical Society* **1965,** *87* (2), 395-397.

4. Zimmerman, H. E. On Molecular Orbital Correlation Diagrams, the Occurrence of Möbius Systems in Cyclization Reactions, and Factors Controlling Ground- and Excited-State Reactions. I. *Journal of the American Chemical Society* **1966,** *88* (7), 1564-1565.

5. Pascoal, M.; Brook, M. A.; Gonzaga, F.; Zepeda-Velazquez, L. Thermally Controlled Silicone Functionalization Using Selective Huisgen Reactions. *European Polymer Journal* **2015,** *69* (Supplement C), 429-437.

6. Fleming, I. Ionic Reactions—Reactivity. In *Molecular Orbitals and Organic Chemical Reactions*, John Wiley & Sons, Ltd: 2010; pp 145-203.

7. Wittig, G.; Krebs, A. Zur Existenz Niedergliedriger Cycloalkine, I. *Chemische Berichte* **1961,** *94* (12), 3260-3275.

8. Jewett, J. C.; Bertozzi, C. R. Cu-free click cycloaddition reactions in chemical biology. *Chemical Society Reviews* **2010,** *39* (4), 1272-1279.

9. (a) Sletten, E. M.; Bertozzi, C. R. From Mechanism to Mouse: A Tale of Two Bioorthogonal Reactions. *Accounts of Chemical Research* **2011,** *44* (9), 666-676; (b) Jewett, J. C.; Sletten, E. M.; Bertozzi, C. R. Rapid Cu-Free Click Chemistry with Readily Synthesized Biarylazacyclooctynones. *Journal of the American Chemical Society* **2010,** *132* (11), 3688-3690.

10. Kolb, H. C.; Finn, M. G.; Sharpless, K. B. Click Chemistry: Diverse Chemical Function From A Few Good Reactions. *Angewandte Chemie-International Edition* **2001,** *40* (11), 2004-2021.

11. Michael, A. Ueber die Einwirkung von Diazobenzolimid auf Acetylendicarbonsauremethylester. *Journal für Praktische Chemie* **1893,** *48*, 94-95.

12. Buchner, E.; Witter, H. III. Synthese der Pyrazolin-3,4,5-tricarbonsäure. *Justus Liebigs Annalen der Chemie* **1893,** *273* (2-3), 239-245.

13. Diels, O.; Alder, K. Synthesen in der Hydroaromatischen Reihe. *Justus Liebigs Annalen der Chemie* **1928,** *460* (1), 98-122.

14. Huisgen, R. 1,3-Dipolar Cycloadditions. Past and Future. *Angewandte Chemie International Edition in English* **1963,** *2* (10), 565-598.

15. Huisgen, R.; Stangl, H.; Sturm, H. J.; Wagenhofer, H. Kinetik und Mechanismus der 1.3-dipolaren Additionen der Diazoalkane. *Angewandte Chemie* **1961,** *73* (5), 170.

16. Rusen, E.; Marculescu, B.; Butac, L.; Preda, N.; Mihut, L. The Synthesis and Characterization of Poly Vinyl Chloride Chemically Modified with C60. *Fullerenes, Nanotubes and Carbon Nanostructures* **2008,** *16* (3), 178-185.

17. (a) Earla, A.; Li, L. B.; Costanzo, P.; Braslau, R. Phthalate Plasticizers Covalently Linked to PVC via Copper-Free or Copper Catalyzed Azide-Alkyne Cycloadditions. *Polymer* **2017,** *109*, 1-12; (b) Earla, A.; Braslau, R. Covalently Linked Plasticizers: Triazole Analogues of Phthalate Plasticizers Prepared by Mild Copper-Free "Click" Reactions with Azide-Functionalized PVC. *Macromolecular Rapid Communications* **2014,** *35* (6), 666-671.

18. (a) Hjertberg, T.; Sörvik, E. M. Formation of Anomalous Structures in PVC and Their Influence on the Thermal Stability: 3. Internal Chloroallylic Groups. *Polymer* **1983,** *24* (6), 685-692; (b) Minsker, K. S.; Lisitsky, V. V.; Kolesov, S. V.; Zaikov, G. E. New Developments in Degradation and Stabilization of Polymers Based on Vinyl Chloride. *Journal of Macromolecular Science, Part C* **1981,** *20* (2), 243-308.

19. Earla, Aruna. Plasticization of PVC: Covalently Linked Plasticizers Using Thermal or Copper-Catalyzed Azide-Alkyne Cycloadditions. Ph.D. Dissertation. University of California Santa Cruz, United States of America, California, Santa Cruz, 2016.

20. Endo, K. Synthesis and Structure of Poly(vinyl chloride). *Progress in Polymer Science* **2002,** *27* (10), 2021-2054.

21. Navarro, R.; Perrino, M. P.; Tardajos, M. G.; Reinecke, H. Phthalate Plasticizers Covalently Bound to PVC: Plasticization with Suppressed Migration. *Macromolecules* **2010,** *43* (5), 2377-2381.

22. Fox, T. G., Jr.; Flory, P. J. Second-Order Transition Temperatures and Related Properties of Polystyrene. I. Influence of Molecular Weight. *Journal of Applied Physics* **1950,** *21*, 581-591.

23. Pak, H. K.; Han, J.; Jeon, M.; Kim, Y.; Kwon, Y.; Park, J. Y.; Rhee, Y. H.; Park, J. Synthesis of Enamides by Ruthenium-Catalyzed Reaction of Alkyl Azides with Acid Anhydrides in Ionic Liquid. *ChemCatChem* **2015,** *7* (24), 4030-4034.

24. Brase, S.; Gil, C.; Knepper, K.; Zimmermann, V. Organic Azides: An Exploding Diversity of a Unique Class of Compounds. *Angewandte Chemie-International Edition* **2005,** *44* (33), 5188-5240.

25. Riemenschneider, W. Carboxylic Acids, Aliphatic. In *Ullmann's Encyclopedia of Industrial Chemistry*, Wiley-VCH Verlag GmbH & Co. KGaA: 2000; p 108.

26. Lee, K. W.; Chung, J. W.; Kwak, S.-Y. Synthesis and Characterization of Bio-Based Alkyl Terminal Hyperbranched Polyglycerols: A Detailed Study of Their Plasticization Effect and Migration resistance. *Green Chemistry* **2016,** *18* (4), 999-1009.

27. Elakesh, E. O.; Richard Hull, T.; Price, D.; Carty, P. Thermal Decomposition of Chlorinated Poly(vinyl chloride) (CPVC). *Journal of Vinyl and Additive Technology* **2003,** *9* (3), 116-126.

28. Tiemblo, P.; Martinez, G.; Millan, J. L. A Verification by FTIR Spectroscopy of the Effect of Some Local Chain Conformations on the Specific Molecular Interactions of Solvents, Esters, and Polyesters with PVC. *Journal of Polymer Science Part A: Polymer Chemistry* **1995,** *33* (8), 1243-1255.

29. Franz, R. G. Comparisons of pKa and log P Values of Some Carboxylic and Phosphonic Acids: Synthesis and Measurement. *AAPS PharmSci* **2001,** *3* (2), 1-13.

3 Double Hexyl Tethered Alkyl Triazole Phthalate Mimics

3.1 Increasing Plasticizing Efficiency Utilizing Alkyl Plasticizer Chains with the Triazole Anchoring Strategy

In a quest to increase plasticizing efficiency of the direct triazole attachment system, data from the first two generations of plasticizers were analyzed, revealing intriguing trends. As discussed in *Chapter 2*, there are quintessential structural attributes that must exist in the covalently-bound triazole-based phthalate mimics to achieve maximal emollient capabilities. When utilizing alkyl esters, long, sterically hindered plasticizer chains are required, as any species with the 2-ethylhexyl moiety demonstrates improved plasticizing efficacy over its congeners with smaller, non-branched aliphatic groups. Despite containing a lower weight percentage of plasticizer when compared to *n*-butyl and methyl triazole derivatives, polymers possessing the 2-ethylhexyl triazole proved more effective at imparting decreased glass transition temperatures and therefore increased pliability to the final plastic. Additionally, samples at 5 mole percent triazole plasticizer exhibited T_g values closer to the standard curve comprised of DEHP-PVC mixtures than the 15 mole percent analogues. The data imply that at higher substitution levels, the aromatic triazole ring engenders rigidity to the backbone of PVC, which may stem from π-π or edge-to-face stacking. Hexyl tethers of the 2nd generation system enhanced the plasticization abilities of the triazole-based phthalate mimics over its directly tethered first generation counterparts. This is due to the additional space generated between the secondary plasticizing triazole and PVC. The single hexyl tethered triazole phthalate mimics is engineered to maximize the mobility of secondary triazole within the polymer matrix relative to the original 1st generation triazole diester emollients. This 2nd generation system was created due to ease of synthetic access and low cost of the final plasticized material. Although plasticization was achieved in the first two generations of triazole-based plasticizers, efficiency of these internally plasticized systems still falls short of the industry standard DEHP-PVC system.

Thus, an improved triazole-based plasticizer must contain higher molecular weight substituents per anchoring point on PVC compared to its predecessors. A decreased amount of attachment points to the backbone should suppress aromatic stacking, which is expected to enable augmented plasticization per unit weight of plasticizer. Structurally, a plasticizer with the 2-ethylhexyl plasticizing entity should convey the lowest glass transition temperatures, in juxtaposition to smaller alkyl groups. With this in mind, the endeavor to create a superior plasticizer was pursued. In the 1st generation plasticizers, a double-sided alkyne was synthesized as a precursor to generate the directly bound triazole phthalate mimic. It was envisaged that a double hexyl tethered plasticizer would satisfy the goals of the 3rd generation system: the larger size will expand on the steric properties of the emollient, while increasing the molecular weight of the plasticizer per anchoring point (**Figure 3.1**). Likewise, the inclusion of the hexyl tether will supplement the ability of the secondary triazole to better generate free volume in the polymeric matrix.

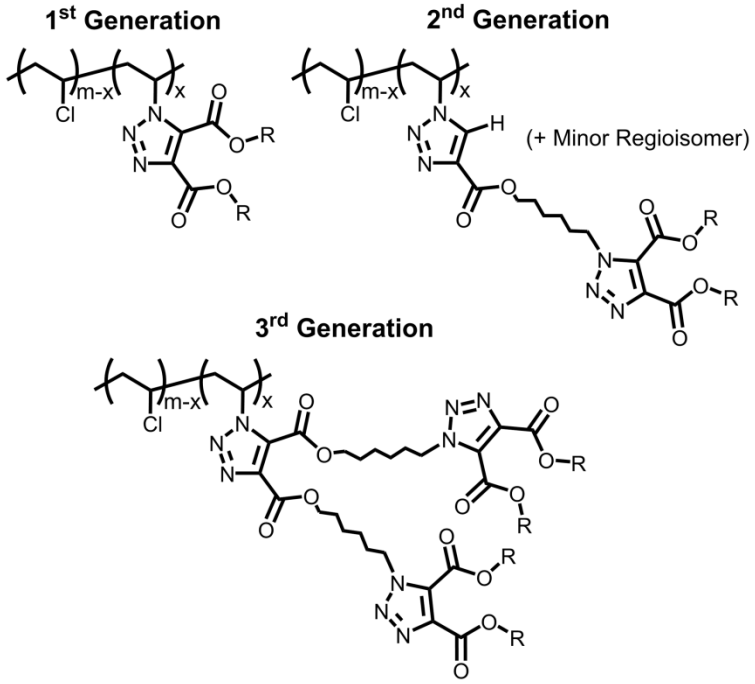

Figure 3.1 Structures of 1st, 2nd, and 3rd Generation Triazole Phthalate Mimics

3.2 Synthetic Challenges: Esterification of Acetylenedicarboxylic Acid with Hexyl Tethered Alcohols Containing Pendant Alkyl Triazole Phthalate Mimics

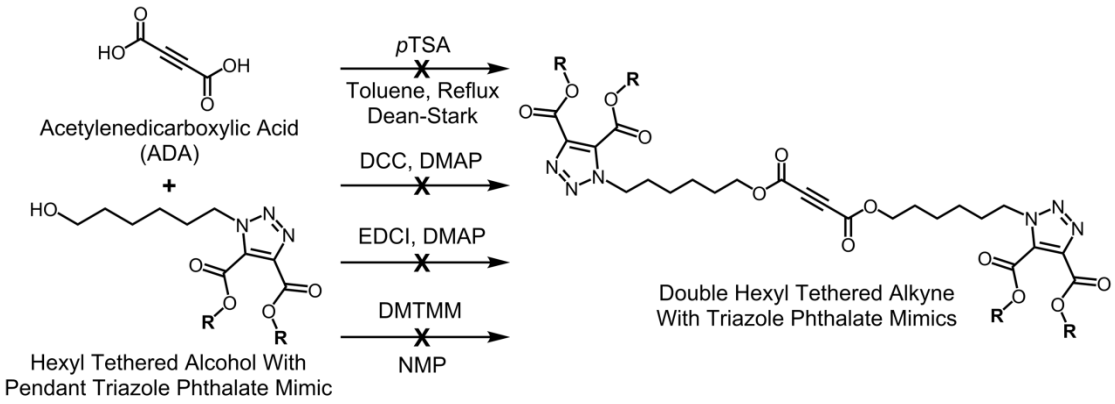

Scheme 3.1 Attempted Syntheses to Obtain Double Hexyl Tethered Alkynes

As a starting point, acetylenedicarboxylic acid (ADA) was employed as the precursor to create the double hexyl tethered plasticizers. Synthesis of the hexyl tether triazolo-alcohols were outlined in *Chapter 2*. Overall, esterification of acetylenedicarboxylic acid is a challenging prospect when utilizing complex alcohols (**Scheme 3.1**). Initially, esterification of ADA was attempted with triazolo-alcohols **2.8 - 2.10** *via* the Fischer method, to no avail. This was in contrast with earlier attempts in the 1st and 2nd generation system, which proved straightforward and high yielding. The key difference in the two syntheses is the alcohols: in the 1st generation esterifications, simple alkyl alcohols were used, while in this 3rd generation system, complex hexyl tether alcohols must be utilized. In the 2nd generation syntheses, Fischer esterification of alcohols **2.8 - 2.10** with propiolic acid occurred without incident. To alleviate this synthetic issue with ADA, other esterification methods were pursued using carbodiimide coupling chemistry. First, Steglich esterifications with *N,N'*-dicyclohexylcarbodiimide (DCC) and 4-dimethylaminopyridine (DMAP) were performed in a range of solvents at different temperatures with no success.[1] Next, a water soluble coupling agent, 1-ethyl-3-(3-dimethylaminopropyl)carbodiimide (EDCI) with DMAP as a catalyst was employed: no appreciable diester was formed.[2] Upon further literature research on these

carbodiimide-based methods, Garcia and Miranda[3] attempted to couple ADA with 4-methoxyphenol using DCC and DMAP as a catalyst. The symmetric diester was not detected: instead an assortment of products including an asymmetric ester amide, an alleged substituted uracil, and cyclohexylisocyanate were formed (**Scheme 3.2**).

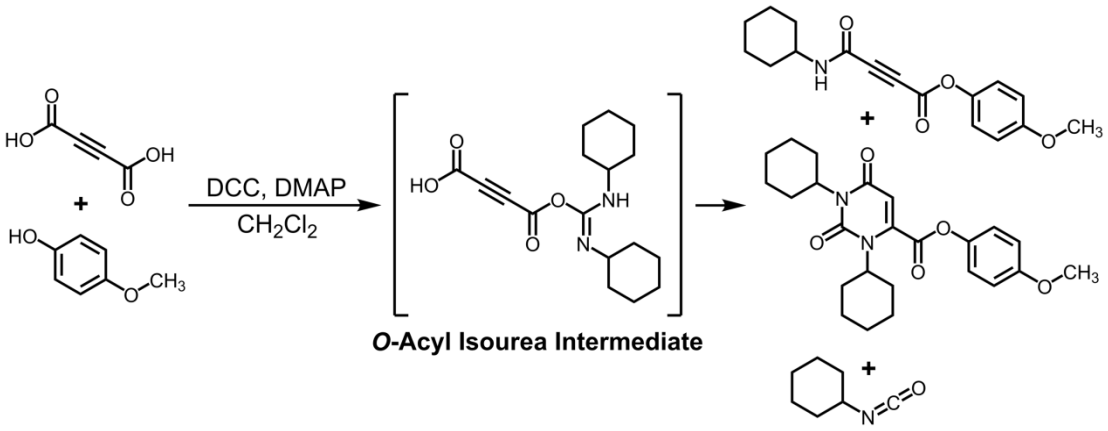

Scheme 3.2 Garcia and Miranda's DCC Coupling of ADA and 4-Methoxyphenol[3]

The available concentrations of the reactive species are of great importance to the rate of carbodiimide couplings: the carboxylate anion and protonated carbodiimide must both be present in appreciable amounts in order for amidation or esterification to occur. The rate determining step is the reaction between a carboxylic acid and the carbodiimide.[4] Acetylenedicarboxylic acid (ADA) has pK_a values of 1.73 and 4.40 in water.[5] The first pK_a of ADA (1.73) is much lower than most carbodiimide reagents (EDCI in water, pK_a = 4.7),[4] which allows smooth coupling of the first carboxylic acid with the alcohol. Once the first coupling occurs, acetylenedicarboxylate monoester's remaining carboxylic acid *should* possess a pK_a of approximately 4. The newly formed ester is strongly electron-withdrawing and should decrease the pK_a of the second carboxylic acid by better stabilizing the conjugate base. The presence of DMAP as a base enables anion formation on the remaining carboxylic acid, which *increases* electron density of the alkyne. Thus far, one would expect that the second carboxylic acid should readily couple with the triazolo-alcohols using carbodiimide chemistry.

However, once the second carboxylate anion forms the *O*-acyl isourea intermediate, the alkyne becomes significantly more electron-deficient, further increasing its susceptibility to nucleophilic addition. Presumably, the amine of the isourea acts as a nucleophile, in an intramolecular Michael addition to the triple bond; as been demonstrated with activated α,β-unsaturated carboxylic acids.[6] Volonterio and coworkers[7] describe the synthesis of hydantoins under mild conditions through a regiospecific domino process involving carbodiimides and acetylenedicarboxylate monoesters (**Scheme 3.3**). The *O*-acyl isourea is formed by the condensation of the carbodiimide and carboxylic acid. Next, a nucleophilic aza-Michael addition to the activated alkyne occurs, leading to an imino-oxazolidinone, which subsequently undergoes an acid-mediated O→N acyl migration.[7] This furnishes the reported 1,3,5-trisubstituted hydantoins.

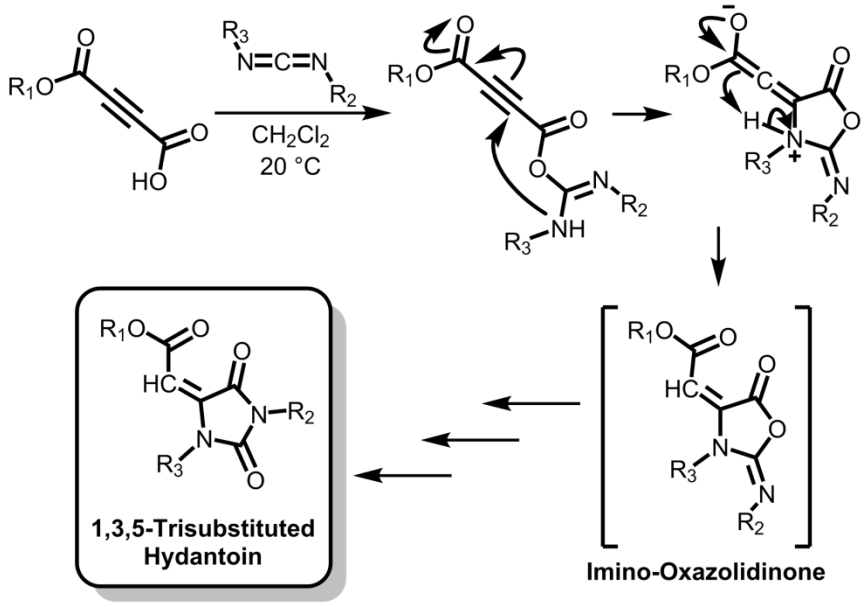

Scheme 3.3 Volonterio's Carbodiimide Reaction with ADA Monoesters[7]

Subsequently, Volonterio et al.[6c] utilized density functional theory (DFT) calculations to determine the mechanism of hydantoin formation. B3LYP and MPW1K functionals were used with the 6-311+G(2d,2p) basis set. The B3LYP functional results best matched the experimental data than the MPW1K results. In this study, two mechanistic pathways were

considered: 1) through an imino-oxazolidinone intermediate and 2) through an *N*-acyl urea intermediate (**Scheme 3.4**). The calculations indicate that both reaction pathways have similar overall barriers, with B3LYP showing a preference for Pathway 1. This occurs when the *O*-acyl isourea is formed, followed by *E*/*Z* isomerization and an 1,3 O→N acyl shift. Interestingly, a Bucherer-Bergs-like isomerization[8] with an isocyanate intermediate was not considered as an alternative mechanistic pathway.

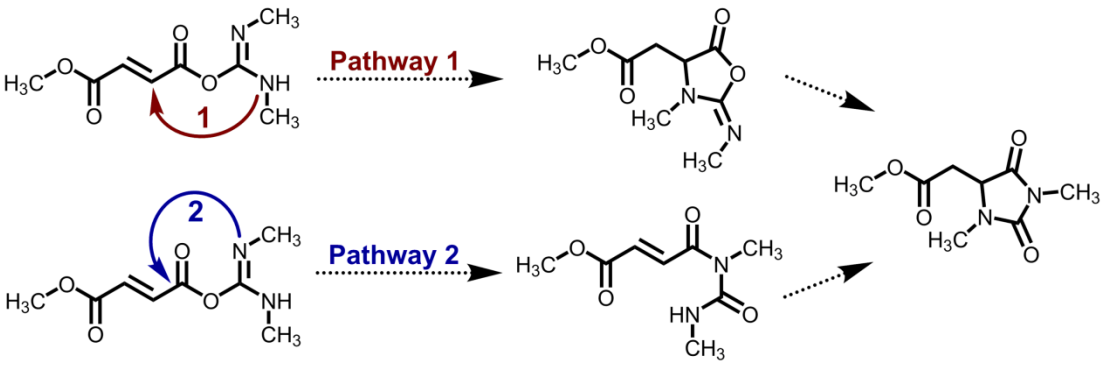

Scheme 3.4 Volonterio's DFT Mechanism Pathways[6c]

Upon careful observation, Volonterio's hydantoins synthesized from acetylenedicarboxylate monoesters[7] and the substituted uracil described by Garcia and Miranda[3] are constitutional isomers, if the same monoester and carbodiimide were used. It is possible that the alleged uracil was actually the hydantoin, following the plausible mechanism outlined by Volonterio and co-workers.[6c] Historically, nucleic acid thymine bases are known to give hydantoins *via* free-radical oxidation.[9] This may justify the observance of the uracil derivative, which may have not yet oxidized to its hydantoin congener. However, this is unlikely given the DFT data.[6c]

The triazene coupling reagent 4-(4,6-dimethoxy-1,3,5-triazin-2-yl)-4-methyl-morpholinium chloride (DMTMM) with *N*-methyl-2-pyrrolidone (NMP) as a solvent, was utilized, which is expected to function through a directly-activated ester mechanism similar to that of carbodiimide reagents (**Scheme 3.5**).[10] However, DMTMM does not form a

nucleophilic species in the activated acyloxytriazine intermediate. This is in contrast to DCC and EDCI, which contain a nucleophilic amine in the *O*-acyl isourea species. Therefore, using an acyloxytriazine should prevent intramolecular Michael addition, thus mitigating the formation of hydantoins.

In the original publication describing DMTMM by Kunishima and coworkers,[10a] there is a detailed discussion on the possible mechanism of condensation (**Scheme 3.5**). The authors state that carboxylic acids reacts slower with DMTMM than carboxylate anions: therefore, premixing the carboxylic acid and amine to form the ammonium carboxylate salt is essential.[10a] This assists in forming the active species, acyloxytriazine, and the hydrochloride salt of *N*-methylmorpholine (NMM·HCl). Furthermore, generation of the ammonium carboxylate salt prevents the free amine from attacking DMTMM. The amine is regenerated from NMM·HCl, thereby restoring its nucleophilicity and ability to react with the

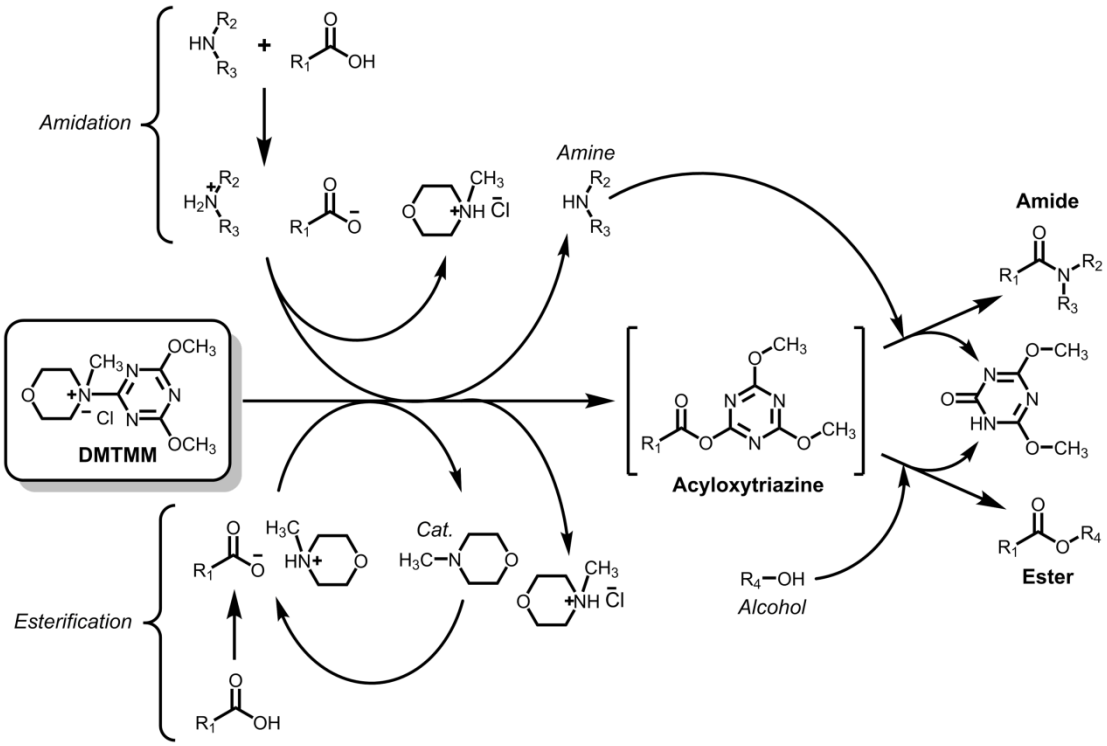

Scheme 3.5 Kunishima's DMTMM Coupling Reaction Cycle[10a]

acyloxytriazine to give the amide. The presence of an amine base is imperative for this reaction to proceed efficiently. By contrast, an alcohol is not basic and does not have the ability to deprotonate carboxylic acids. In order to mitigate this problem, esterifications were carried out with the addition of catalytic *N*-methylmorpholine (NMM). NMM acts as a tertiary amine base, enabling the reaction to proceed with a neutral nucleophile such as an alcohol: this promotes the formation of carboxylate anions, thereby generating the acyloxytriazine intermediate. Addition of an alcohol yields the ester.

Fessner and Heyl[11] successfully employed DMTMM in the synthesis of acetylenedicarboxamides directly from ADA with an assortment of primary and secondary amines with yields ranging from 52 to 80% (**Scheme 3.6**). With respect to acetylenedicarboxylic acid, the ammonium carboxylate intermediate generated in the first step of the reaction increases the electron density of the triple bond *via* the carboxylate anion, thereby deactivating the alkyne from nucleophilic attack.[12] This ionic intermediate present during DMTMM's coupling cycle led the authors to utilize the reagent in synthesizing the acetylenedicarboxyamides. The choice of solvent played a key role in obtaining the symmetrical diamide: tetrahydrofuran (THF) and ethyl acetate gave gels with erratic yields during the initial formation of the ammonium carboxylate salt. Dimethylformamide (DMF) and *N*-methyl-2-pyrrolidone (NMP) gave the best results, probably due to these solvent's ability to

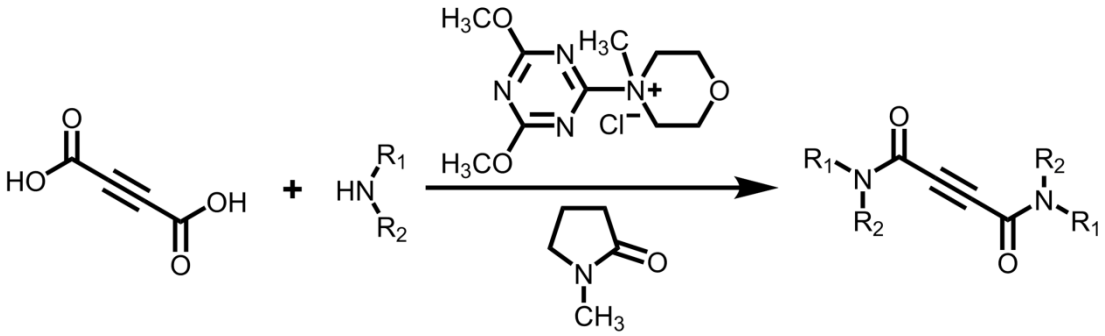

Scheme 3.6 Heyl and Fessner's DMTMM Coupling of ADA and Amines[11]

solubilize polar, ionic compounds. Methanol gave low yields, while aqueous mixtures of DMF and NMP (10% H_2O v/v) exhibited remarkably lower yields. Pure water did not afford the diamide. Generally, nucleophilic acyl substitutions are performed in aprotic solvents, as hydrogen bonding to the nucleophile will hinder its attack on the electrophile. Primary and secondary amines can hydrogen bond to water and other protic solvents, possibly explaining why protic solvents were unproductive. The reactions were performed at 0 °C to prevent degradation of the acetylenedicarboxylate and DMTMM, and were effective for coupling a multitude of amines with ADA.

With this in mind, DMTMM coupling seemed like a promising prospect to obtain the diesters of ADA and the long chain tethers containing pendant triazole-phthalate mimics. However, esterifications using DMTMM and triazolo-alcohols **2.8 - 2.10** proved fruitless; as the desired diesters were not obtained after many reaction trials in either DMF and NMP. NMM was utilized as a base to deprotonate ADA with the aim of generating the essential ammonium carboxylate salt: no appreciable esterification was observed. A factor that may have contributed to unsuccessful diesterification is the nucleophilicity of the alcohol. While the alcohol is primary in the hexyl tethered triazole precursor, it may not be sufficiently nucleophilic to react with the activated intermediate. The greater nucleophilicity of an amine compared to an alcohol increases the rate of acyl substitution when utilizing DMTMM.

This concept is illustrated by Kunishima; amines were preferentially coupled with carboxylic acids, despite the use of alcohol solvents (**Scheme 3.7**, **Table 3.1**).[10b] DMTMM exhibited excellent selectivity for amines, forming 98-99% of the desired amide. On the other hand, carbodiimides demonstrated low yields and poor selectivity, with DCC giving 27% amide (with 21% *N*-acylurea isolated) and 7% ester, while EDCI furnished 53% amide and 16% ester. The authors commented on the key reaction attributes that will lead to a successful acyl substitution with an active-ester coupling agent: first, a coupling agent should

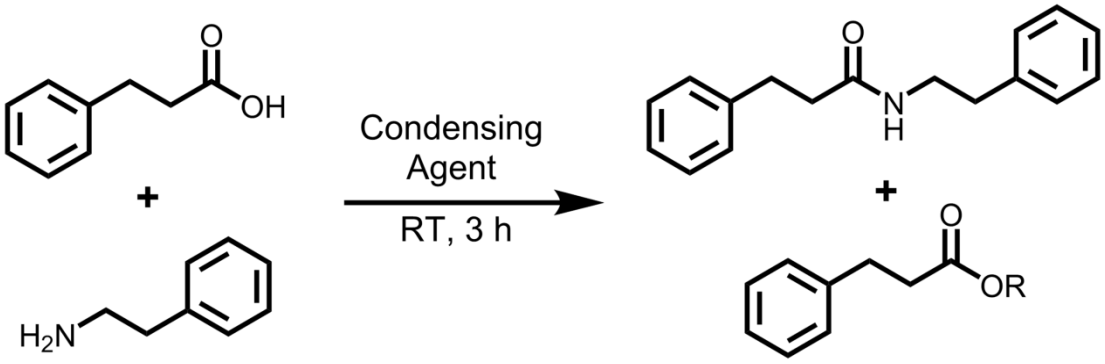

Scheme 3.7 Kunishima's DMTMM Coupling of Carboxylic Acids and Amines in Alcohol Solvents[10b]

Condensing Agent	Solvent	Amide (%)	Ester (%)	Amide/Ester
DMTMM	MeOH	98	1.0	98
DMTMM	EtOH	99	0.7	141
DMTMM	*i*-PrOH	96	0.7	137
DCC	MeOH	27	7.0	4
EDCI	MeOH	53	16	3.3

Table 3.1 Kunishima's DMTMM Coupling Data of Amines in Alcohol Solvents[10b]

be stable and soluble in a chosen solvent and react selectively with the carboxyl group to produce the activated acid-derivatives faster than the solvent or nucleophile can react with the reagent itself. Furthermore, the reaction between the activated acid derivative and the selected nucleophile must be faster than solvolysis. According to the original publication by the same group,[10a] DMTMM does not experience solvolysis in water or methanol. Therefore, the triazolo-alcohol is not reactive enough to form esters. Paradoxically, the monoester's electron-withdrawing nature should increase the propensity for esterification with the second carboxylate: this was observed by Kunishima when investigating substituted aromatic carboxylic acids and alcohols.[10a] Despite this, esterifications using DMTMM typically require an extreme excess of alcohol, and is often used as the solvent.[10a] This makes acyl substitution with the triazolo-alcohols impractical, as the advanced intermediate is not commercially available and must be synthesized through a convergent three-step process.

3.3 Synthesis of Acetylenedicarboxylate Esters with Hexyl Tethered Alcohols Containing Pendant Alkyl Triazole Phthalate Mimics

An alternative to Fischer esterification, carbodiimide, and triazine couplings is through a reaction of an alcohol with an acid halide intermediate. The acid chloride of acetylenedicarboxylic acid remains elusive in the literature: this is due to the internal alkyne's high reactivity, caused by two adjacent electron-withdrawing carbonyls. A number of studies have demonstrated the facile nature of nucleophiles adding to ADA's triple bond.[13] Therefore, obtaining the acid chloride through the direct chlorination of ADA has proven challenging throughout the last century.

In 1920, Ruggli[14] attempted to synthesize acetylenedicarboxylate acid chloride (ADACl) from phosgene and a Grignard derivative of acetylene. Unfortunately, the reaction gave a viscous tar, likely resulting from the extremely reactive acetylene acyl chloride intermediate (**Scheme 3.8**).

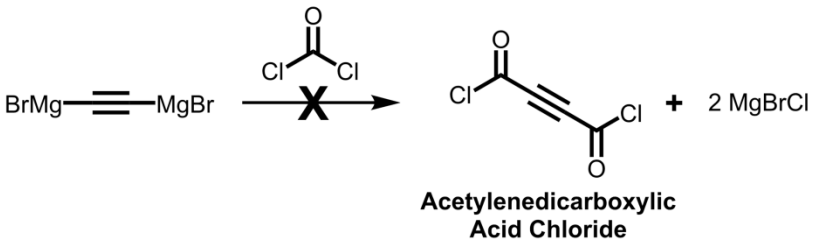

Scheme 3.8 Ruggli's Attempt to Synthesize ADACl[14]

In 1938, Diels and Thiele[15] described a method to obtain ADACl through thermal decomposition. The authors cite that ADACl cannot be obtained through conventional synthetic methods due to the formation of HCl during the direct chlorination of ADA with PCl_5, which adds to the triple bond; this gave chlorofumaryl dichloride. In the publication, the Diels-Alder adduct of maleic anhydride and anthracene was obtained, then subsequently subjected to chlorination *via* PCl_5, yielding 9,10-dihydro-9,10-ethenoanthracene-11,12-dicarbonyl dichloride. Next, the chlorinated anthracene derivative was heated for 4 hours in a sealed

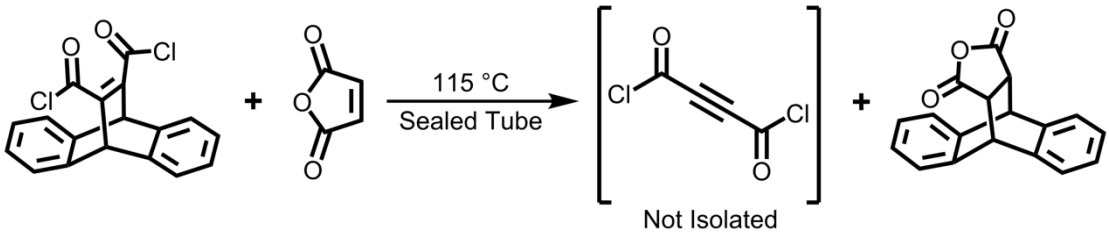

Scheme 3.9 Diels and Thiele's Putative Synthesis of ADACl[15]

tube at 115 °C (**Scheme 3.9**). Although it was claimed that ADACl was obtained, it is unclear whether the compound was isolated, due to the lack of instrumentation available at the time of publication that could definitively characterize the putative diacid chloride product.

In 1963, Krueger and McDonald[16] attempted to synthesize acetylenedicarboxylic chloride using thionyl chloride ($SOCl_2$) in DMF: after work up, dichloromaleic anhydride was isolated in 63% yield with sulfur as a byproduct (**Scheme 3.10**). The authors state that this process appears to be a, "*cis*-chlorination of the triple bond and dehydration of the diacid to the anhydride."[16] Interestingly, the reaction forms tars without DMF and commercial samples of $SOCl_2$ give variable yields of the anhydride. In addition to DMF, pyridine and triethylamine also act as catalysts, albeit resulting in lower yields of the anhydride product. It is hypothesized that the catalysts complex with $SOCl_2$, thereby enabling the *cis*-addition of the chlorides, and accounts for the elemental sulfur byproduct found in the reaction.

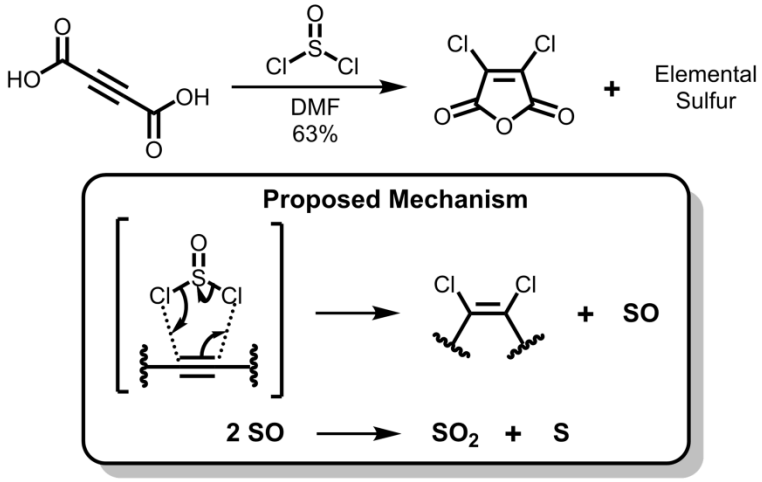

Scheme 3.10 Krueger and McDonald's Attempt to Synthesize ADACl[16]

In 1982, Maier and Jung[17] claimed that they successfully synthesized acetylenedicarboxylic acid chloride with PCl_5 in CCl_4 under a stream of argon (**Scheme 3.11**). However, the authors did not succeed in isolating ADACl due to its high reactivity: an FTIR, ^{13}C-NMR and HRMS was obtained of the alleged molecule. According to the publication, ADACl can readily undergo Diels-Alder reactions with dienes to cleanly form adducts.

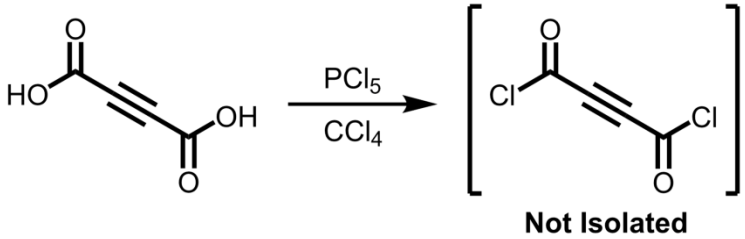

Scheme 3.11 Maier and Jung's Synthesis of ADACl[17]

The collective problem with the syntheses of acetylenedicarboxylic acid chloride stems from the highly reactive triple bond. In order to mitigate this issue, the alkyne can be inactivated by increasing the electron density in the triple bond, or *via* a protecting group to inhibit unwanted nucleophilic addition. The method of protection must be reversible and produce the desired acetylenic diesters in high yields. In 1912, Ott[18] synthesized a protected form of ADA, dibromofumaric acid (DBFA), by direct bromination. The process to obtain dibromofumaric acid is challenging, involving bubbling bromine gas through a solution of ADA for several days, in the absence of light. Ott also reported the synthesis of dibromofumaric acid chloride by treating dibromofumaric acid with PCl_5 in petroleum ether at room temperature. This advanced intermediate should allow one to perform esterifications that would eventually lead to the diester of ADA.

In order to mitigate nucleophilic addition to the triple bond, a strategy involving protection of the alkyne was carried out. Charlton and Chee[19] described the synthesis of ADA chiral esters using bromine as a protecting group to obtain dibromofumaric acid.[12, 18] A slightly modified version of Charlton and Chee's approach was performed to obtain the double hexyl

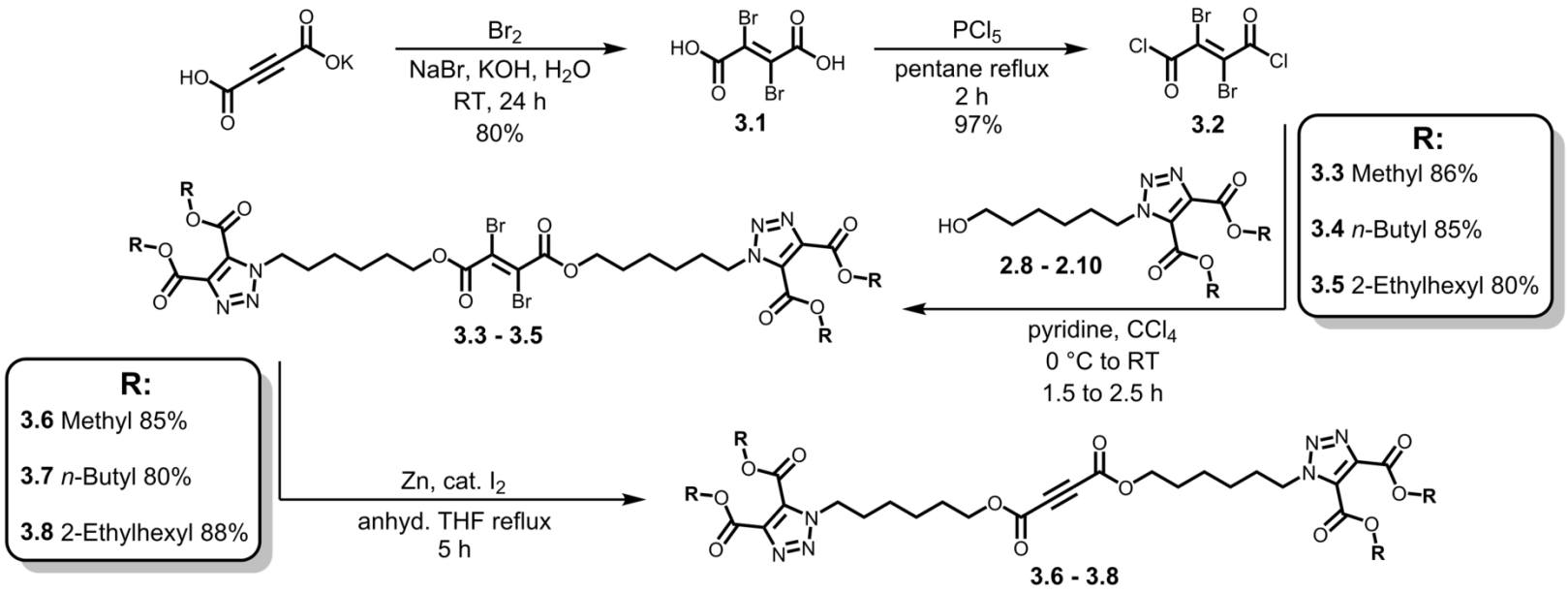

Scheme 3.12 Synthesis of Double Hexyl Tethered Acetylenedicarboxylate Esters

tethered acetylenedicarboxylate esters (**Scheme 3.12**). To protect ADA, acetylenedicarboxylic acid monopotassium salt was neutralized with an aqueous KOH solution. Sodium bromide aqueous solution was combined with the neutralized ADA. Bromine was added and allowed to stand overnight, giving dibromofumaric acid **3.1** in 80% yield. The acid chloride was made *via* Ott's procedure with slight modifications.[18] Dibromofumaric acid **3.1** was treated with PCl_5 in pentanes under reflux for 2 hours, affording dibromofumaryl chloride **3.2** in 97% yield. Next, triazolo-alcohols **2.8 - 2.10** were diluted in carbon tetrachloride with pyridine, then cooled to 0 °C under nitrogen. Dibromofumaryl chloride **3.2** was added dropwise and stirred for 1.5 to 2.5 hours to give the brominated diesters **3.3 - 3.5** in 80% to 86% yield. Deprotection involved refluxing the protected ester with granular zinc and catalytic iodine in anhydrous THF, to give the final double-sided hexyl tethered alkynes **3.6 - 3.8** in 80% to 88% yield.

3.4 Synthetic Optimization and Analysis of Acetylenedicarboxylate Esters with Hexyl Tethered Alcohols Containing Pendant Alkyl Triazole Phthalate Mimics

During the synthesis of dibromofumaric acid **3.1**, it was found that concentrated HCl solution was required to reprotonate the anion of DBFA. Also, the use of saturated aqueous sodium bisulfite was necessary to thoroughly quench any remaining bromine. Purification *via* reprecipitation was carried out using diethyl ether and chloroform. Subsequently, ^{13}C-NMR was performed to assess the presence and purity of dibromofumaric acid **3.1** (**Figure 3.2**). Acetone-d_6 was selected as the NMR solvent over D_2O,[19b] due to the enhanced solubility and increased signal strength of acetylenedicarboxylic acid (ADA) and dibromofumaric acid in acetone. A substantial downfield movement of the alkyne quaternary carbons in ADA is observed after bromination: ADA displays a signal **a** at δ 74.6 ppm, while the brominated sp^2 carbon **A** in DBFA exhibit a signal at δ 111.7 ppm. The carbonyl signal also moves downfield from δ 151.8 ppm in ADA (**b**) to δ 162.8 ppm in dibromofumaric acid (**B**). ^{1}H-NMR was not performed, as both ADA and dibromofumaric acid **3.1** possess only carboxylic acid protons.

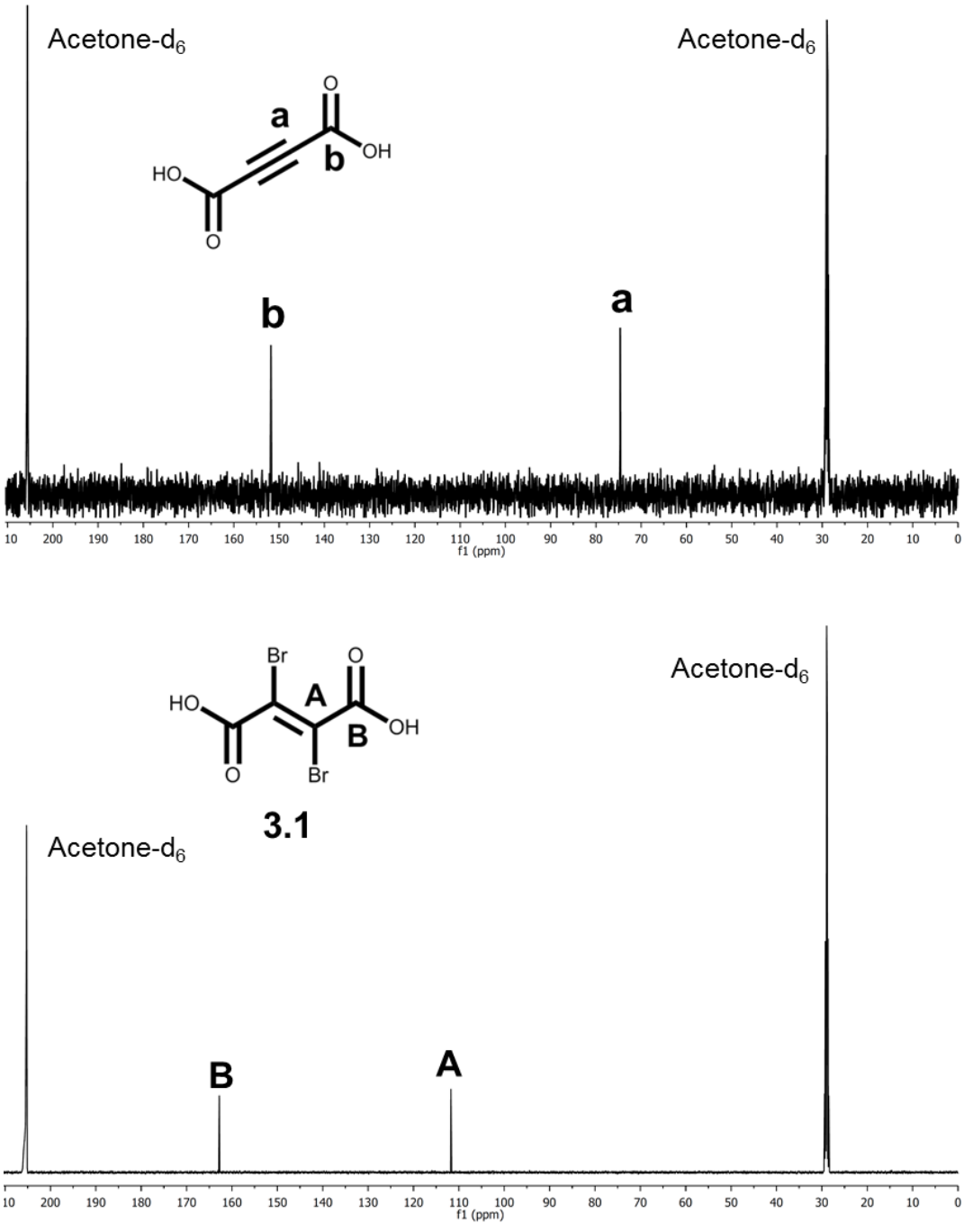

Figure 3.2 ^{13}C-NMR Comparison of Acetylenedicarboxylic Acid (Top) and Dibromofumaric Acid (**3.1**, Bottom)

During the synthesis of dibromofumaryl chloride **3.2**, it was discovered that raising the reaction temperature to pentanes reflux furnished the acid chloride rapidly, in comparison to previous methods.[18-19] Reaction times were reduced by 50%, as prior publications required five hours at room temperature. Oddly, no acid chloride was observed following the literature procedure[18] using petroleum ether as the solvent, whereas using pentanes gave the desired acid chloride. Reaction monitoring was done visually: the solids present in the reaction mixture are insoluble in pentanes. Once the chlorination is complete, the reaction becomes *transparent* yellow, due to the greater solubility of **3.2** in pentanes. Workup involved pouring the crude reaction mixture on ice to quench PCl_5 and solubilize any acids formed during the chlorination. This seems counterintuitive, as water hydrolyzes acid chlorides. However, the use of extremely non-polar pentanes in combination with ice proved effective in eliminating residual acids while retaining the acid chloride.

When the acyl substitution reactions were conducted with triazolo-alcohols **2.8 - 2.10**, 2.2 equivalents of alcohol was typically added to assure complete esterification. In contrast to other methods, which require an extreme excess of alcohol,[10] exact equivalents may be utilized with dibromofumaryl chloride **3.2**: this allows one to employ precious alcohol intermediates in this esterification. The couplings were monitored *via* TLC; protected diester R_f values increased significantly relative to both precursors, due to the conversion of the polar alcohol and acid chloride to the diester. As with the propiolate esters discussed in *Chapter 2*, the triazole present in the starting material and product is extremely UV-active, providing a clear indicator of product formation. Both ^{1}H-NMR and ^{13}C-NMR of the brominated diesters **3.3 - 3.5** were similar to the parent alcohols (**Figure 3.3**). Methylene protons **d** (HO-C**H$_2$**-Tether) of the triazolo-alcohol displays a downfield shift from ~δ 3.6 ppm to δ 4.2 ppm as the diester **D**. This stems from the greater deshielding effect of the newly formed ester compared to the alcohol. Likewise, tether methylenes **E** two carbons away from the oxygen of the dibromofumatate esters (Ester-O-CH_2-C**H$_2$**-Tether) move downfield from δ 1.55 ppm as the

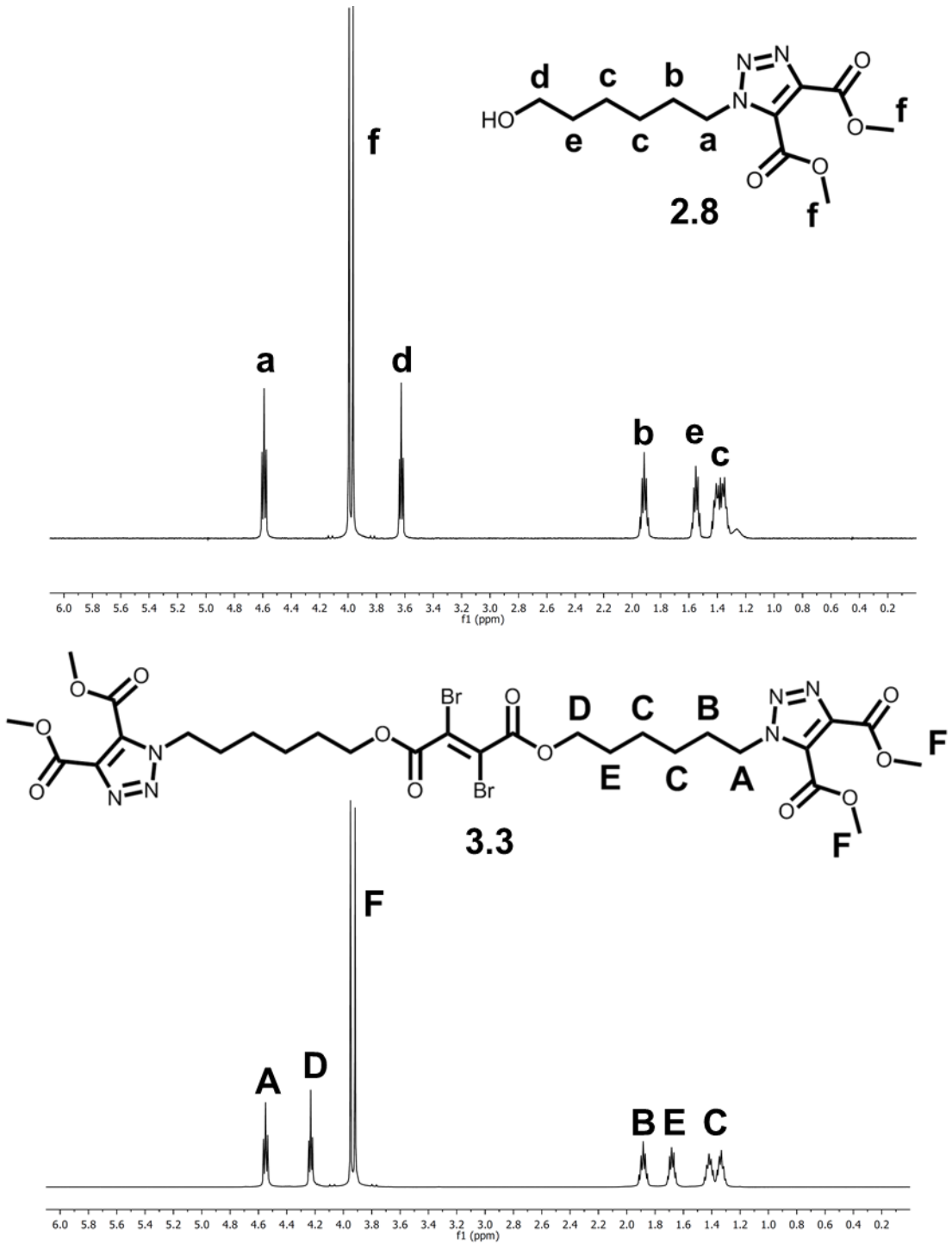

Figure 3.3 ^{1}H-NMR Comparison of TRZ-DiMe Hexanol (**2.8**, Top) and Bis(TRZ-DiMe Hexyl) Dibromofumarate (**3.3**, Bottom)

alcohol to δ 1.68 ppm as the ester. ^{13}C-NMR reveals two additional signals relative to the parent alcohol (**Figure 3.4**). A new carbonyl peak **K** appears at δ 162.2 ppm in all dibrominated ester derivatives. Also, a downfield shift of carbon carbon **D** directly attached to the ester (Ester-O-**C**H_2-C) occurs at δ 66.8 ppm. The brominated central sp^2 carbon **L** is noted by a signal at δ 112.7 ppm. All other ^{13}C signals are nearly analogous to the alcohol precursor.

During the final deprotection reaction with zinc, addition of catalytic elemental iodine assured complete formation of the alkyne **3.6 - 3.8**. Similar to the initial bromination, sodium bisulfite was used to quench any residual iodine, although it was not part of the literature procedure.[19] Successful deprotection of the dibromofumarate esters **3.3 - 3.5** was not readily apparent *via* TLC monitoring. The loss of two bromines does not drastically alter the alkyne's polarity, making reaction evaluation difficult. Eventually, the difference in the oxidative susceptibility between the starting material and product was utilized to determine reaction completion. Potassium permanganate stain ($KMnO_4$) reacts with readily oxidizable functional groups such as alkenes and alkynes. Dibromofumarates are not especially reactive with $KMnO_4$ stain, whereas the alkynes are extremely reactive, instantly showing a yellow spot when stained. Although not quantitative, this method permits one to quickly identify alkyne formation. The zinc deprotection was allowed to react for five hours, which was the maximum length specified in the literature.[19] Once the reaction was complete, ^{1}H-NMR and ^{13}C-NMR confirmed the presence of alkynes **3.6 - 3.8** (**Figure 3.5**). ^{1}H-NMR of the deprotected molecules was generally uninformative, with trivial changes of proton signals relative to the dibromofumarates. In contrast, ^{13}C-NMR produced pertinent information on the double hexyl tethered alkynes. Carbonyl signal **K** belonging to the ester adjacent to the alkyne (Alkyne-**C**=O-O-C) experiences a considerable upfield shift with respect to the dibromofumarate precursor at δ 151.8 ppm. Similarly, the quaternary carbon **L** of the alkyne displays an upfield

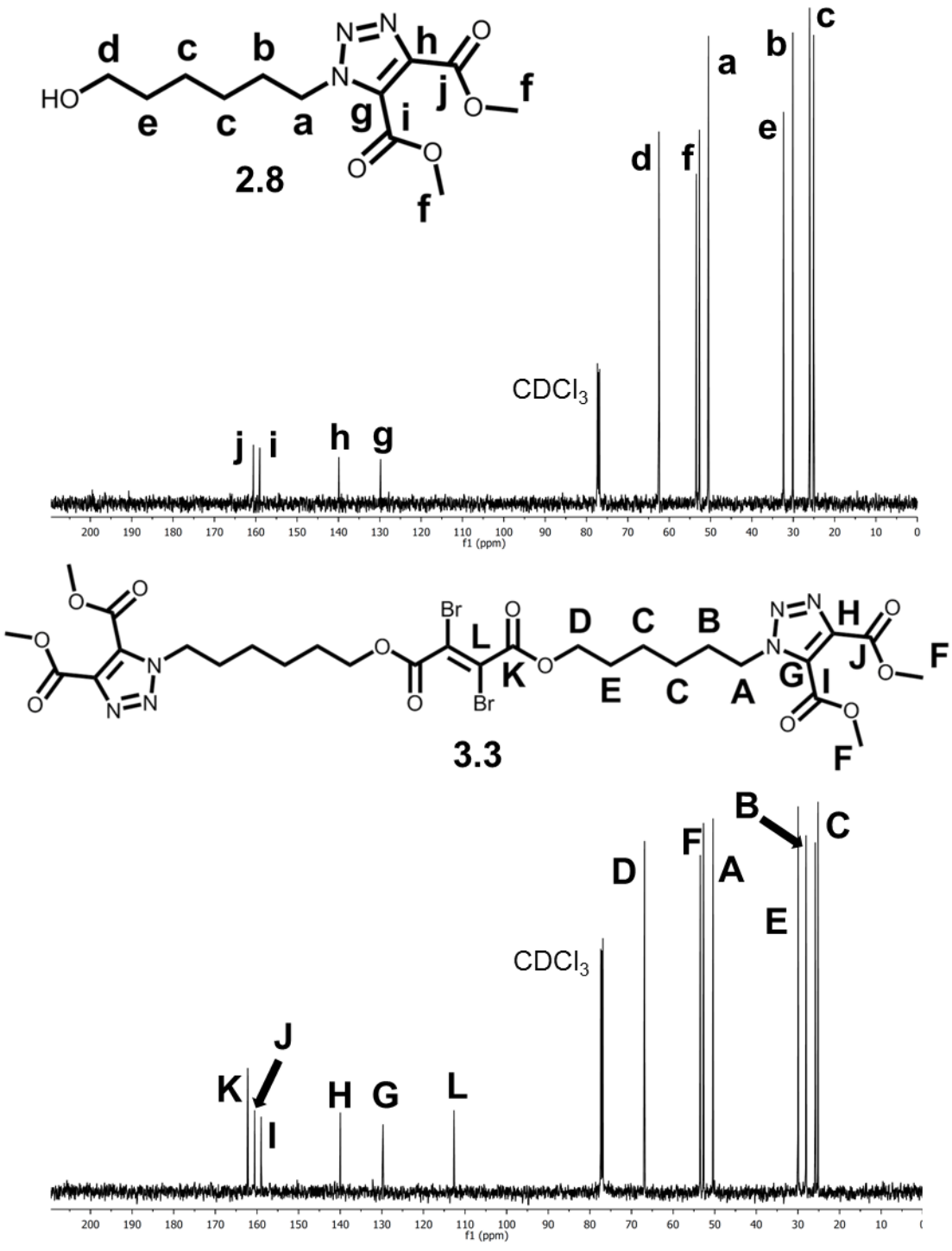

Figure 3.4 ^{13}C-NMR Comparison of TRZ-DiMe Hexanol (**2.8**, Top) and Bis(TRZ-DiMe Hexyl) Dibromofumarate (**3.3**, Bottom)

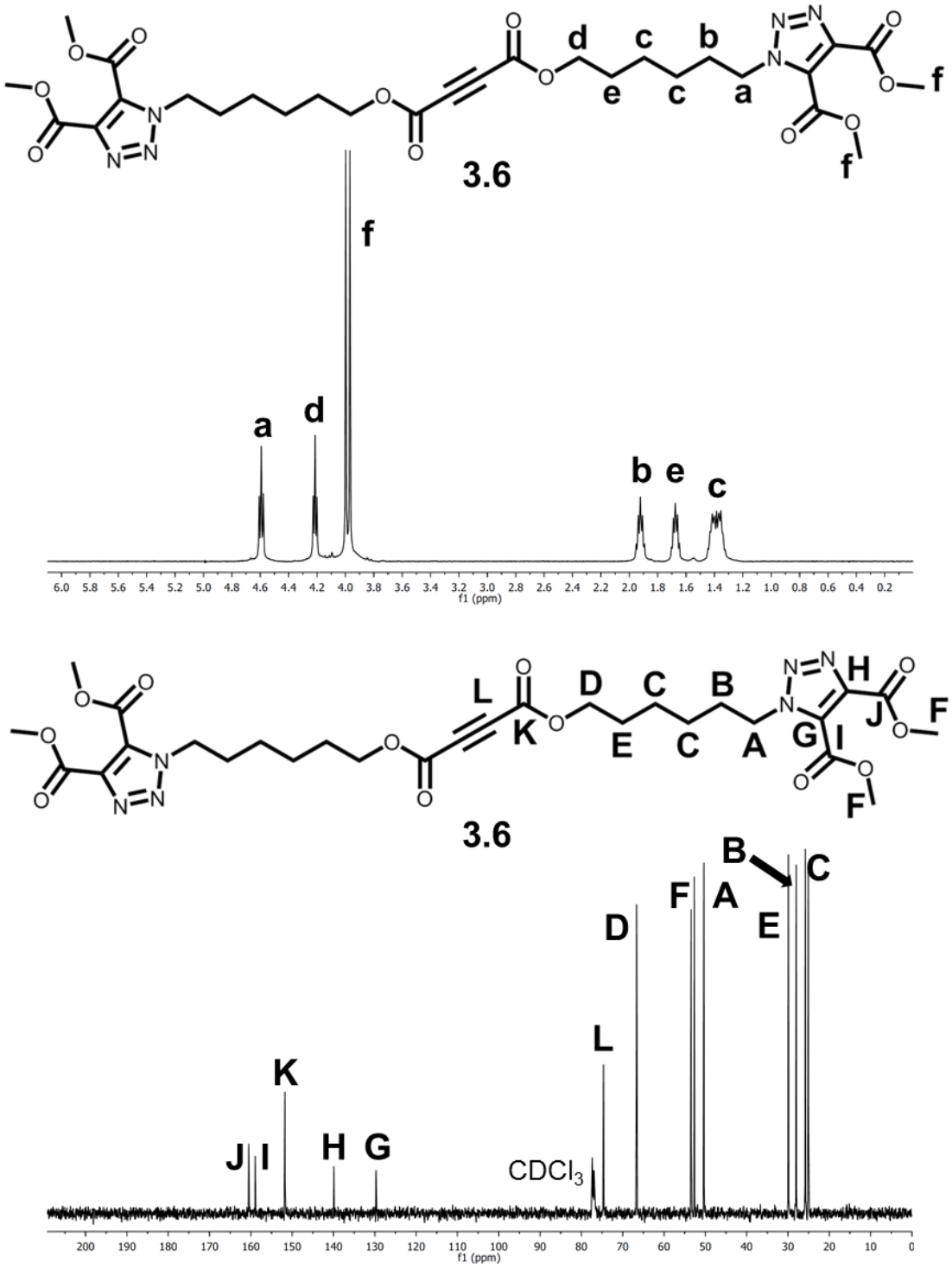

Figure 3.5 ^{1}H-NMR and ^{13}C-NMR of Bis(TRZ-DiMe Hexyl) Acetylenedicarboxylate **3.6**

shift to δ 74.7 ppm, from δ 112.7 ppm in the dibromofumarate. These perturbations in the ^{13}C-NMR of all doubly hexyl tethered alkynes stem from the loss of two bromine atoms. This is due to a major change in the magnetic anisotropic shielding cone going from the dibromofumarate to the acetylenedicarboxylate (**Figure 3.6**). The observed downfield chemical signals of the dibrominated alkene occur due to an increased amount of electron circulation when the sp^2 carbons are perpendicular to the magnetic field.[20] In contrast, the shielding cone of an acetylene[21] is oriented 90 degrees relative to an alkene. This is partially due to the cylindrical symmetry of the alkyne. As a result of these shielding cones possessing perpendicular orientations relative to each other, the carbon signals from the dibrominated alkene to the internal alkyne shift upfield: the sp-carbons in the final product is directly in the shielding cone of the alkyne.

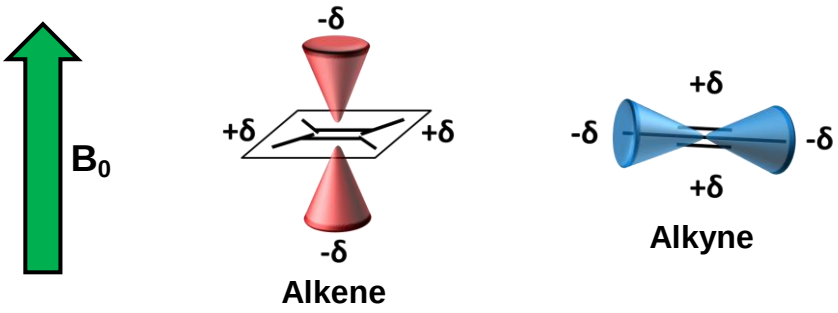

Figure 3.6 Magnetic Anisotropic Shielding Cones

3.5 3rd Generation Plasticizer: Synthesis and Characterization of Double Hexyl Tethered Alkyl Triazole Phthalate Mimics on PVC

As with the first two generations of triazole-based phthalate mimics, copper-free azide-alkyne cycloadditions (AAC) were performed with PVC-azide in 3-pentanone (**Scheme 3.13**). Reactions were typically carried out at 90 °C for 24 hours with 2.5 to 3.0 equivalents of alkyne to each equivalent of azide. Some cyclizations took up to 36 hours to complete. AAC of the ADA hexyl tethered phthalate mimics **3.6 - 3.8** and PVC-azide **2.1** were tracked *via*

FTIR, noting the disappearance of the azide stretch (N_3) at ~2110 cm^{-1} and the appearance of the triazole sp^2 carbon-carbon stretch (C=C) at ~1550 cm^{-1} (**Figure 3.7**). No issues in reaction monitoring occurred with these 3rd generation plasticizers, as the internal alkyne does not possess the terminal CC stretch at 2116 cm^{-1}, present in the 2nd generation hexyl

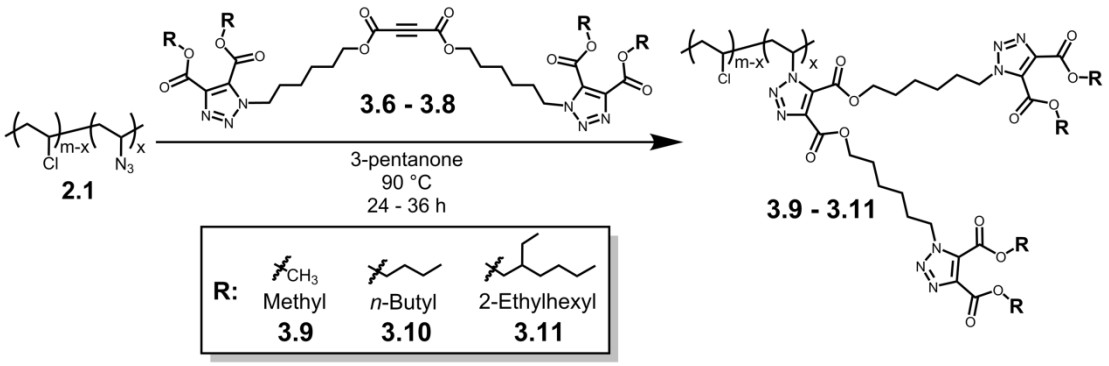

Scheme 3.13 Thermal Azide-Alkyne Cycloaddition of PVC-Azide **2.1** and Double Hexyl Tethered Alkyl Triazole Phthalate Mimics **3.6 - 3.8**

tethered propiolates.

Once the doubly hexyl tethered internally plasticized PVC samples **3.9 - 3.11** were synthesized, ^{1}H-NMR and ^{13}C-NMR was performed to confirm structure and purity. Spectra of both 5 and 15 mole percent 3rd generation plasticized polymers were measured in $CDCl_3$. Similar to the 2nd generation single tether analogues, PVC containing two hexyl tethers with pendant triazole-phthalate mimics include a number of methylene tether signals (**Figure 3.8**): δ 1.30 – 1.90 ppm are central tether protons **C** (Tether-C**H**$_2$-C**H**$_2$-Tether), while methylene protons **D** adjacent to the primary triazole esters (PVC-1°TRZ Ester-O-C**H**$_2$-Tether) appear at δ 4.30 – 4.40 ppm. The signal at δ 4.60 ppm originates from methylene **A** directly attached to the secondary triazole (Tether-C**H**$_2$-2°TRZ). Plasticizing alkyl chains on the secondary triazole (2-ethylhexyl and *n*-butyl) appear between δ 0.86 – 1.98 ppm, which overlap with the hexyl-tether and PVC signals. Methine protons **J** of PVC adjacent to the primary triazole (PVC-C**H**-1°TRZ) appear in the range of δ 5.10 – 5.65 ppm. All other proton signals

belonging to these 3rd generation internally plasticized PVC samples are in the same general location as those in unmodified PVC.

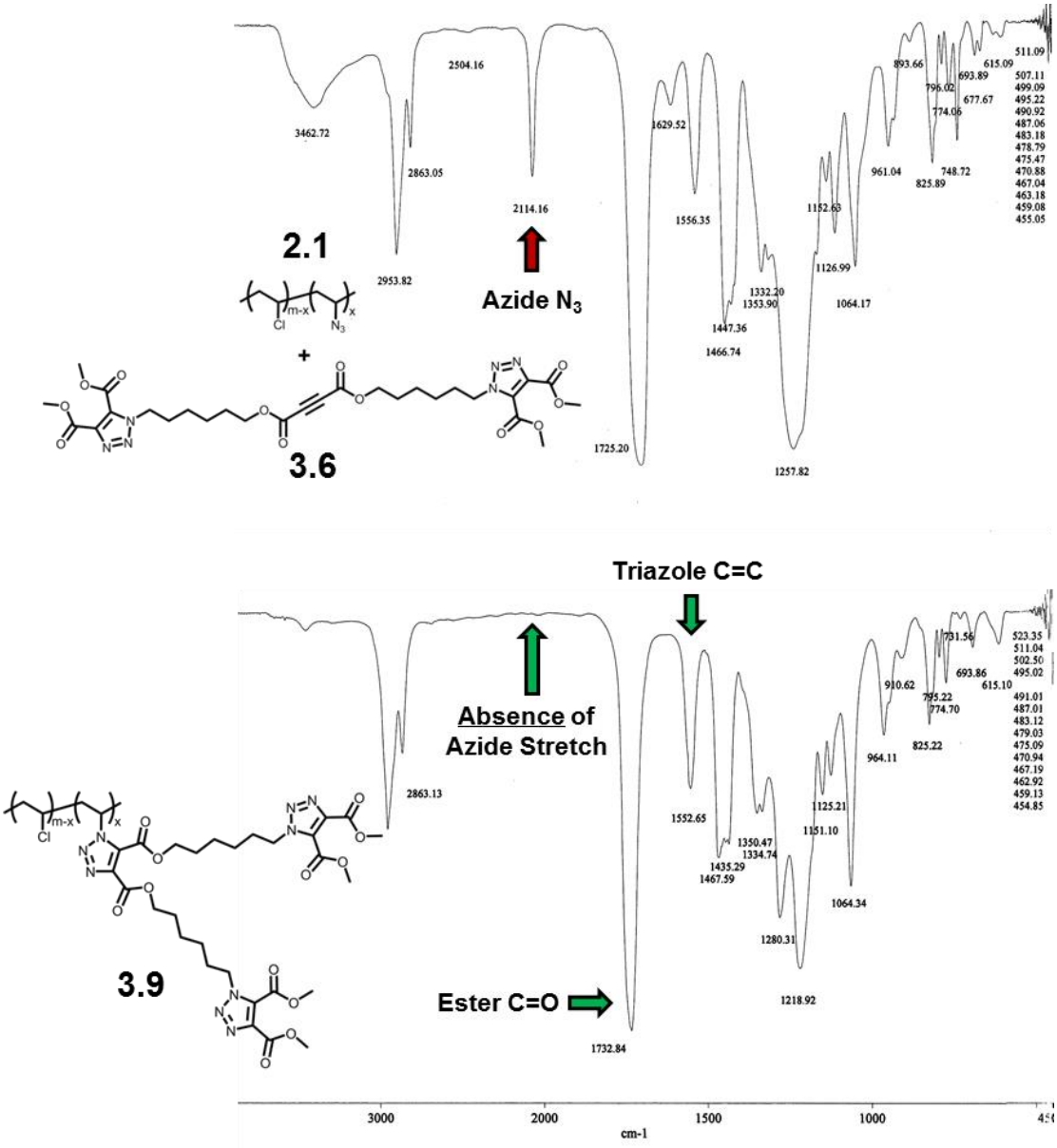

Figure 3.7 FTIR Monitoring of Cycloaddition Between 15% PVC-Azide **2.1** and Bis(TRZ-DiMe Hexyl) Acetylenedicarboxylate **3.6**
Top: Reaction After 15 Minutes
Bottom: Reaction After 24 Hours

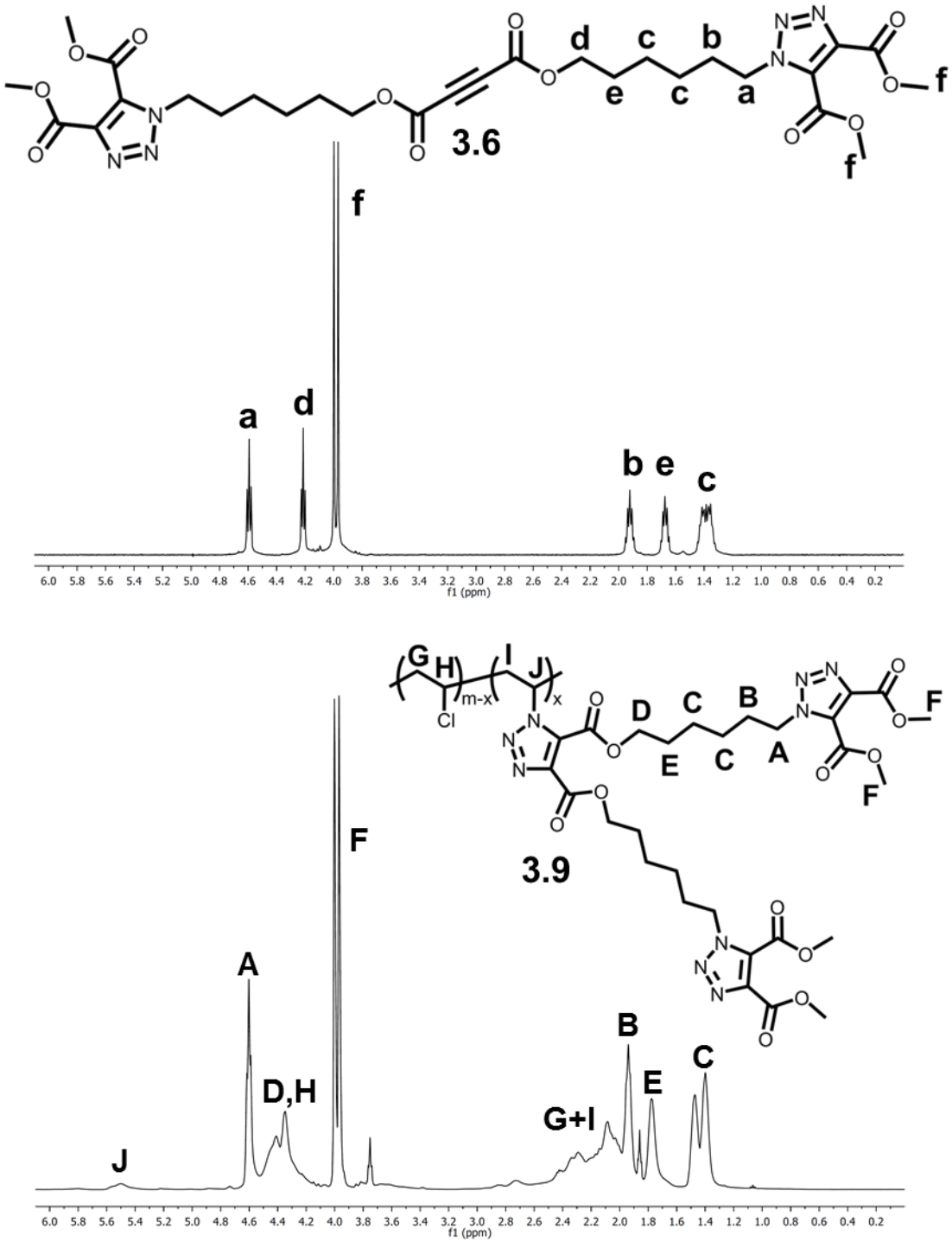

Figure 3.8 ^{1}H-NMR Spectra of Bis(TRZ-DiMe Hexyl) Acetylenedicarboxylate (**3.6**, Top) and 15% PVC-TRZ-DiHexyl-TRZ-DiMe (**3.9**, Bottom)

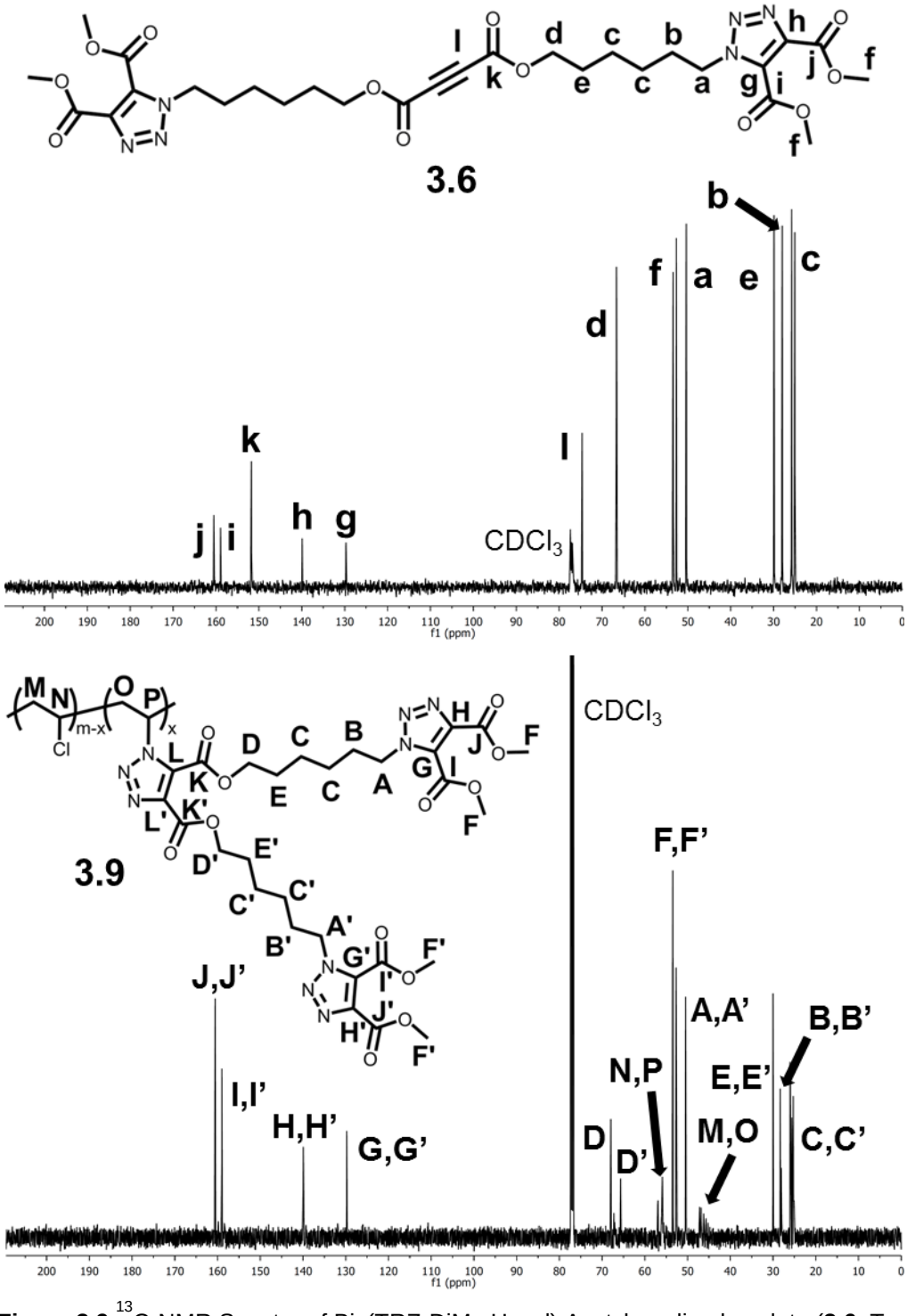

Figure 3.9 ^{13}C-NMR Spectra of Bis(TRZ-DiMe Hexyl) Acetylenedicarboxylate (**3.6**, Top) and 15% PVC-TRZ-DiHexyl-TRZ-DiMe (**3.9**, Bottom)

^{13}C-NMR of polymers **3.9 - 3.11** functionalized with 3rd generation plasticizers appear similar to the parent acetylenedicarboxylates **3.6 - 3.8** with a few key differences (**Figure 3.9**). The regioisomeric primary triazole ester carbonyl signals **K** and **K'** were not observed due to a lack of isotropic molecular tumbling. The bulky, sterically congested doubly hexyl tethered plasticizer bound to PVC leads to non-averaged anisotropic interactions, thereby weakening the carbonyl signal. Furthermore, the primary triazole quaternary carbons **L** and **L'** are not readily visible in the ^{13}C-NMR. Distinct ^{13}C-signals of the hexyl tether include the quaternary carbons of the secondary triazole (**G,G'** at δ 129.6 ppm and **H,H'** at δ 140 ppm) and the secondary triazole carbonyls (**I,I'** at δ 159 ppm and **J,J'** at δ 161 ppm). Each 3rd generation polymer contains aliphatic carbon signals similar to the parent alkyne, which originate from the alkyl chains on the secondary triazole. Main chain PVC carbons remain largely unaltered. The absence of signals at δ 74.6 and δ 74.7 ppm indicates polymers free of excess alkyne.

3.6 DSC Analysis: Double Hexyl Tethered Alkyl Triazole Phthalate Mimics on PVC

Thermal analyses of PVC functionalized with 3rd generation double hexyl tethered triazole phthalate mimics were performed by collaborators at IBM Almaden in an analogous fashion to the previous generations of polymers. Differential scanning calorimetry (DSC) was performed on all 3rd generation polymers to determine the extent of plasticization and degradation properties. **Table 3.2** summarizes the T_g values of these derivatives and PVC standards. DSC results of the 3rd generation polymers are displayed in **Figure 3.10**.

Polymer	**5 Mol % T_g (°C)**	**15 Mol % T_g (°C)**
PVC	*81 °C*	
PVC-Azide	83	78
PVC-TRZ-DiHexyl-TRZ-DiMe	66	48
PVC-TRZ-DiHexyl-TRZ-DiBu	42.8	12
PVC-TRZ-DiHexyl-TRZ-DiEH	43.5	-6

Table 3.2 DSC Data of PVC Standards, 5 and 15 Mol %
Double Hexyl Tethered Alkyl Triazole Phthalate Mimics

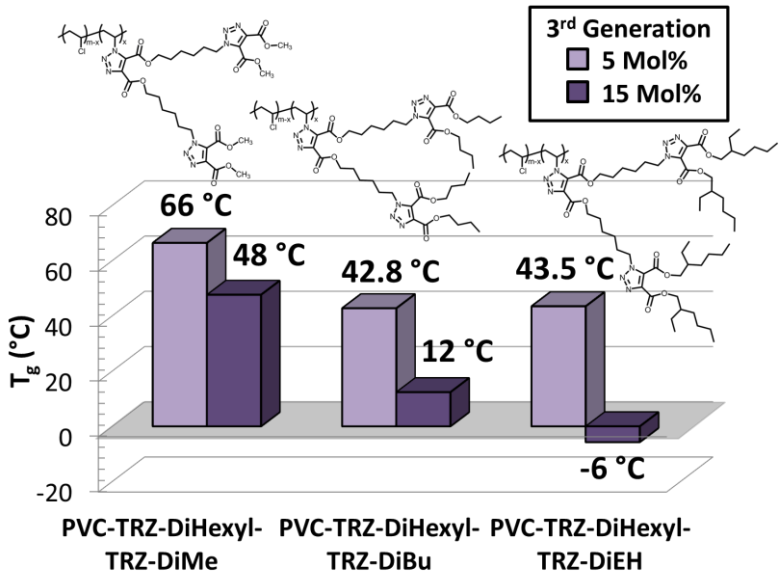

Figure 3.10 DSC Data of 3rd Generation Double Hexyl Tethered Triazole Phthalate Mimics

The first sub-zero glass transition temperature employing the copper-free triazole anchoring strategy was observed with the 3rd generation polymer, PVC-TRZ-DiHexyl-TRZ-DiEH, at 15 mole percent (T_g = -6 °C). The glass transition temperatures of the 1st, 2nd and 3rd generations of triazole-plasticizers are presented in **Figure 3.11** and **Table 3.3**. Progressive T_g depressions in the 3rd generation samples relative to the prior generations of internal plasticizers stem from the addition of two hexyl tethers containing pendant triazole-phthalate mimics. The lowest T_g values were observed with the 3rd generation triazole-plasticizers functionalized with *n*-butyl or 2-ethylhexyl groups.

Generation	Polymer	5 Mol% T_g (°C)	15 Mol% T_g (°C)
Standards	*PVC*	*81 °C*	
	PVC-Azide	83	78
1st Gen.	PVC-TRZ-DiMe	88	96
	PVC-TRZ-DiBu	76	74
	PVC-TRZ-DiEH	65	57
2nd Gen.	PVC-TRZ-Hexyl-TRZ-DiMe	82	75
	PVC-TRZ-Hexyl-TRZ-DiBu	65	54
	PVC-TRZ-Hexyl-TRZ-DiEH	56	41
3rd Gen.	PVC-TRZ-DiHexyl-TRZ-DiMe	66	48
	PVC-TRZ-DiHexyl-TRZ-DiBu	42.8	12
	PVC-TRZ-DiHexyl-TRZ-DiEH	43.5	-6

Table 3.3 DSC Data of PVC Standards and Generations 1-3 Triazole-Plasticizers

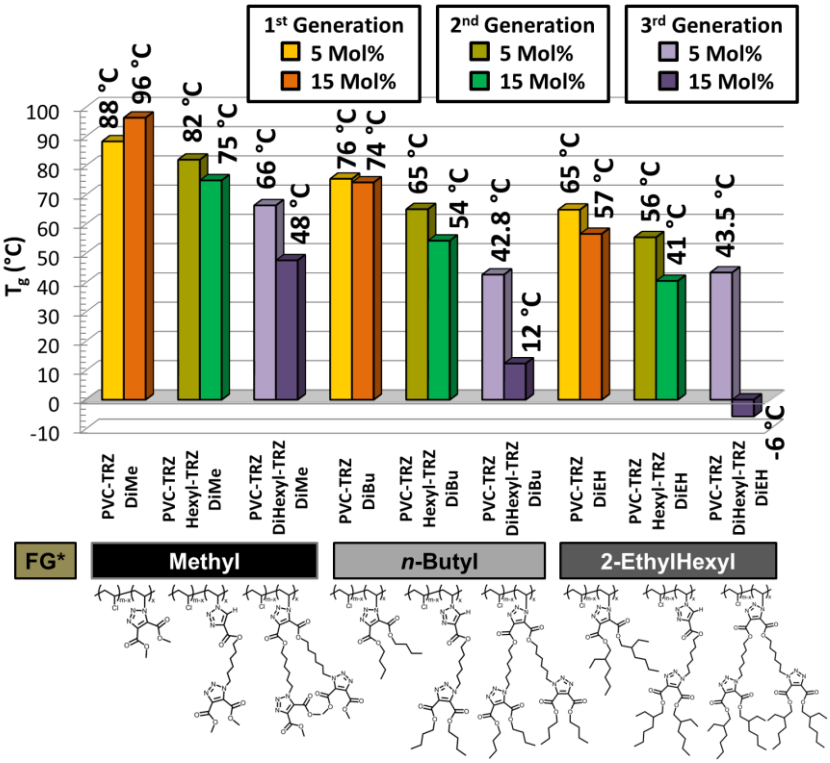

Figure 3.11 DSC Data Comparing Generations 1-3 Triazole Phthalate Mimics (**FG = Functional Group*)

Weight percentages of all plasticizers hitherto utilizing the method outlined in *Chapter 2* are displayed in **Figure 3.12** and **Table 3.4**. At 15 mole percent, T_g values exhibit a roughly exponential decrease in the 3rd generation system with increasing size of the alkyl chain on the triazole ester. However, at 5 mole percent, there appears to be an anomalous glass transition temperature belonging to PVC-TRZ-DiHexyl-TRZ-DiEH (T_g = 43.5 °C). A slightly higher T_g compared to PVC-TRZ-DiHexyl-TRZ-DiBu (T_g = 42.8 °C) is observed despite a larger amount of plasticizer by weight present in the 2-ethylhexyl analogue. Free volume theory[22] may offer a possible explanation for the elevated glass transition temperature of 5 mole percent PVC-TRZ-DiHexyl-TRZ-DiEH: larger polymer chains containing more surface area and a low relative abundance of chain ends will inherently give higher glass transition temperatures in comparison to smaller polymers with less surface area and a greater relative abundance of chain ends. Purification of all samples involved iterative precipitation of the

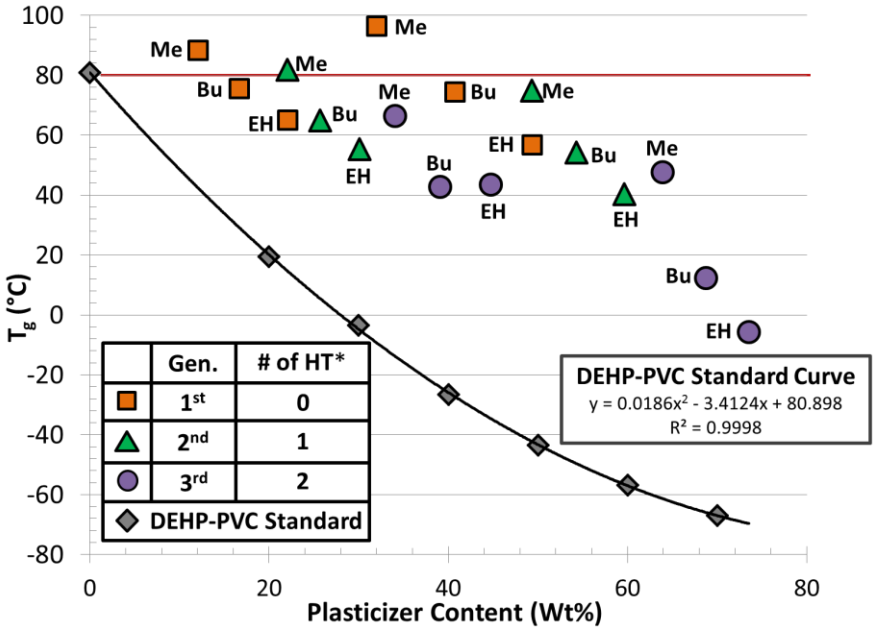

Figure 3.12 Overlay of T_g Values Versus Weight Percent Plasticizer of DEHP-PVC and Generations 1-3 Alkyl Triazole Phthalate Mimics (**HT = Hexyl Tethers*)

Generation	Polymer	Mol%	Wt % Plasticizer	T_g (°C)
1st Gen.	PVC-TRZ-DiMe	5	12.1	88
		15	32.1	96
	PVC-TRZ-DiBu	5	16.7	76
		15	40.8	74
	PVC-TRZ-DiEH	5	22.1	65
		15	49.4	57
2nd Gen.	PVC-TRZ-Hexyl-TRZ-DiMe	5	22.1	82
		15	49.3	75
	PVC-TRZ-Hexyl-TRZ-DiBu	5	25.7	65
		15	54.3	54
	PVC-TRZ-Hexyl-TRZ-DiEH	5	30.1	56
		15	59.6	41
3rd Gen.	PVC-TRZ-DiHexyl-TRZ-DiMe	5	34.0	66
		15	63.9	48
	PVC-TRZ-DiHexyl-TRZ-DiBu	5	39.1	42.8
		15	68.8	12
	PVC-TRZ-DiHexyl-TRZ-DiEH	5	44.7	43.5
		15	73.5	-6

Table 3.4 Glass Transition Temperatures and Weight Percentages of Generations 1-3 Alkyl Triazole Phthalate Mimics

dissolved polymer in methanol. This method may inadvertently fractionate the internally plasticized sample, thereby leading to preferential isolation of lengthier main chains. Longer polymers tend to precipitate more readily than those of shorter lengths: oligomeric polymers often become suspensions if the polarity of the anti-solvent is not conducive toward precipitation. Likewise, for the PVC samples covalently modified with 3rd generation triazole-plasticizers containing *n*-butyl or 2-ethylhexyl moieties, the difference in size of the alkyl chain may play a role in the ability of the polymer to precipitate out of methanol and may result in different chain lengths between samples. It is possible that PVC covalently functionalized with triazoles containing different length plasticizing alkyl chains produce varied free volume effects as a function of the interaction within the 3-dimensional matrix of PVC. Plasticizer compatibility was discussed in *Chapter 1*: phthalates are known to exhibit a range of different Flory-Huggins interaction parameters in PVC. Perhaps the 3rd generation *n*-butyl derivative at 5 mole percent is more soluble in PVC than the 2-ethylhexyl analogue due to less carbons on the secondary triazoles. In addition, the enhanced miscibility of the *n*-butyl triazole phthalate mimic may impart increased polar properties to the functionalized main chain, thereby increasing the solubility of PVC-TRZ-DiHexyl-TRZ-DiBu in methanol.

3.7 Plasticizer Efficiencies: Generations 1 – 3 Triazole Plasticizers Versus DEHP-PVC

To gain an understanding of how efficient the doubly hexyl tethered PVC samples are with respect to DEHP-PVC, plasticizer efficiencies ($E\Delta T_g$) were determined for all 3rd generation samples at both 5 mole percent (**Table 3.5**) and 15 mole percent (**Table 3.6**). $E\Delta T_g$ values for 3rd generation polymers are presented as a bar graph in **Figure 3.13**. The 3rd generation system exhibits superior $E\Delta T_g$ values compared to the 1st and 2nd generation triazole-plasticizers, as illustrated in **Table 3.7** and **Table 3.8**. $E\Delta T_g$ values for PVC samples internally plasticized by generation 1-3 emollients are depicted as a bar graph in **Figure 3.14**.

Polymer	Wt% TRZ	T_g TRZ (°C)	ΔT_g TRZ	DEHP T_g (°C)	ΔT_g DEHP	$E\Delta T_g$
PVC-TRZ-DiHexyl-TRZ-DiBu	39.1	**42.8**	38.2	-24.1	105.0	**36.4**
PVC-TRZ-DiHexyl-TRZ-DiEH	44.7	**43.5**	37.5	-34.5	115.5	**32.5**
PVC-TRZ-DiHexyl-TRZ-DiMe	34.0	**66**	14.5	-13.7	94.7	**15.4**

Table 3.5 Descending $E\Delta T_g$ Values of 5 Mol % 3rd Generation Internally Plasticized PVC

Polymer	Wt% TRZ	T_g TRZ (°C)	ΔT_g TRZ	DEHP T_g (°C)	ΔT_g DEHP	$E\Delta T_g$
PVC-TRZ-DiHexyl-TRZ-DiEH	73.5	**-6**	86.7	-69.5	150.4	**57.6**
PVC-TRZ-DiHexyl-TRZ-DiBu	68.8	**12**	68.6	-65.8	146.8	**46.7**
PVC-TRZ-DiHexyl-TRZ-DiMe	63.9	**48**	33.3	-61.2	142.2	**23.4**

Table 3.6 Descending $E\Delta T_g$ Values of 15 Mol % 3rd Generation Internally Plasticized PVC

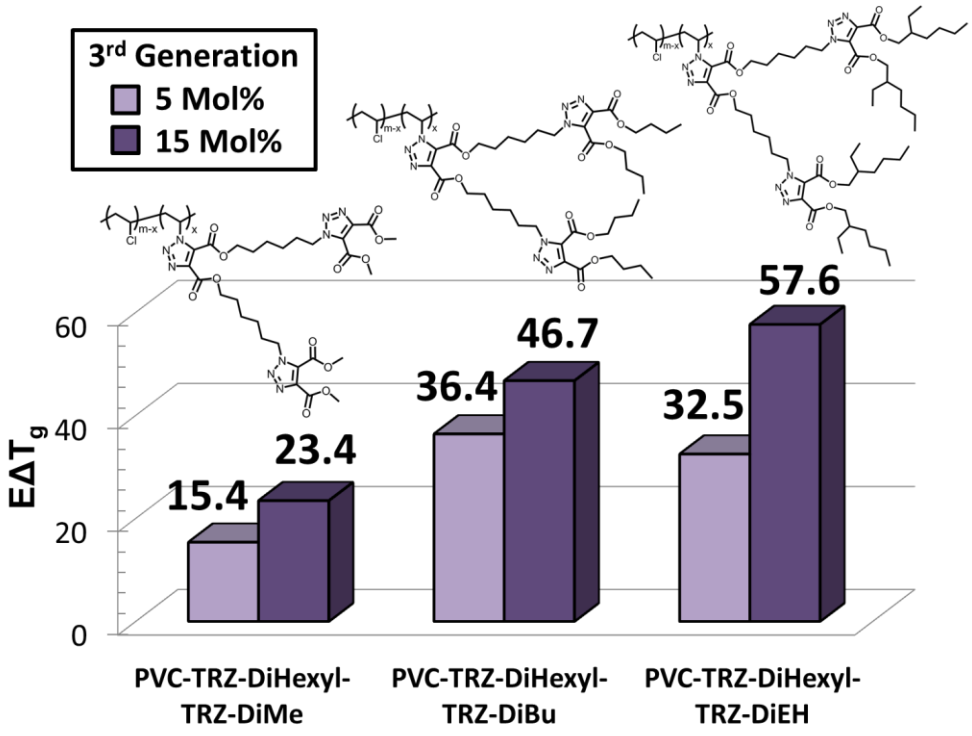

Figure 3.13 Efficiency Values ($E\Delta T_g$) of 3rd Generation Internally Plasticized PVC

At 5 mole percent, the $E\Delta T_g$ for PVC-TRZ-DiHexyl-TRZ-DiBu ($E\Delta T_g$ = 36.4) is greater than PVC-TRZ-DiHexyl-TRZ-DiEH ($E\Delta T_g$ = 32.5) by 3.9%. At 15 mole percent however, PVC-TRZ-DiHexyl-TRZ-DiEH ($E\Delta T_g$ = 57.6) displays a 10.9% increase in efficiency compared to PVC-TRZ-DiHexyl-TRZ-DiBu ($E\Delta T_g$ = 46.7). Within the 3rd generation polymers, it is clear that the alkyl plasticizing chains on the secondary triazole significantly contribute toward plasticizing efficiency. The 2-ethylhexyl group enhances plasticizing efficiency at high mole percentages, while the *n*-butyl moiety appears to be more efficient at lower mole percentages. The methyl triazoles demonstrate decent plasticization efficiencies, but are approximately 50% less efficient than other 3rd generation congeners incorporating longer alkyl chains.

At 5 mole percent, the top two efficiencies belong to 3rd generation polymers PVC-TRZ-DiHexyl-TRZ-DiBu ($E\Delta T_g$ = 36.4) and PVC TRZ-DiHexyl-TRZ-DiEH ($E\Delta T_g$ = 32.5). The 2nd generation sample PVC-TRZ-Hexyl-TRZ-DiEH ($E\Delta T_g$ = 29.7) is 2.8% less efficient than its 3rd generation counterpart, PVC-TRZ-DiHexyl-TRZ-DiEH. Furthermore, the 1st generation

Polymer	Wt% TRZ	T_g TRZ (°C)	ΔT_g TRZ	DEHP T_g (°C)	ΔT_g DEHP	$E\Delta T_g$
5% PVC-TRZ-DiHexyl-TRZ-DiBu	39.1	**42.8**	38.2	-24.1	105.0	**36.4**
5% PVC-TRZ-DiHexyl-TRZ-DiEH	44.7	**43.5**	37.5	-34.5	115.5	**32.5**
5% PVC-TRZ-Hexyl-TRZ-DiEH	30.1	**56**	25.5	-4.9	85.9	**29.7**
5% PVC-TRZ-DiEH	22.1	**65**	16.0	14.5	66.5	**24.1**
5% PVC-TRZ-Hexyl-TRZ-DiBu	25.7	**65**	15.8	5.5	75.5	**21.0**
5% PVC-TRZ-DiHexyl-TRZ-DiMe	34.0	**66**	14.5	-13.7	94.7	**15.4**
5% PVC-TRZ-DiBu	16.7	**76**	5.5	29.1	51.9	**10.5**
5% PVC-TRZ-Hexyl-TRZ-DiMe	22.1	**82**	-1.1	14.6	66.3	**-1.6**
5% PVC-TRZ-DiMe	12.1	**88**	-7.3	42.4	38.6	**-19.0**

Table 3.7 Plasticization Efficiencies of 5 Mol % Generations 1-3 Internally Plasticized PVC Ranked By Descending $E\Delta T_g$ Values

Polymer	Wt% TRZ	T_g TRZ (°C)	ΔT_g TRZ	DEHP T_g (°C)	ΔT_g DEHP	$E\Delta T_g$
15% PVC-TRZ-DiHexyl-TRZ-DiEH	73.5	**-6**	86.7	-69.5	150.4	**57.6**
15% PVC-TRZ-DiHexyl-TRZ-DiBu	68.8	**12**	68.6	-65.8	146.8	**46.7**
15% PVC-TRZ-Hexyl-TRZ-DiEH	59.6	**41**	40.4	-56.4	137.4	**29.4**
15% PVC-TRZ-DiHexyl-TRZ-DiMe	63.9	**48**	33.3	-61.2	142.2	**23.4**
15% PVC-TRZ-Hexyl-TRZ-DiBu	54.3	**54**	26.6	-49.6	130.5	**20.4**
15% PVC-TRZ-DiEH	49.4	**57**	24.3	-42.3	123.2	**19.7**
15% PVC-TRZ-DiBu	40.8	**74**	6.7	-27.3	108.3	**6.2**
15% PVC-TRZ-Hexyl-TRZ-DiMe	49.3	**75**	6.0	-42.1	123.1	**4.9**
15% PVC-TRZ-DiMe	32.1	**96**	-15.4	-9.4	90.4	**-17.0**

Table 3.8 Plasticization Efficiencies of 15 Mol % Generations 1-3 Internally Plasticized PVC Ranked By Descending $E\Delta T_g$ Values

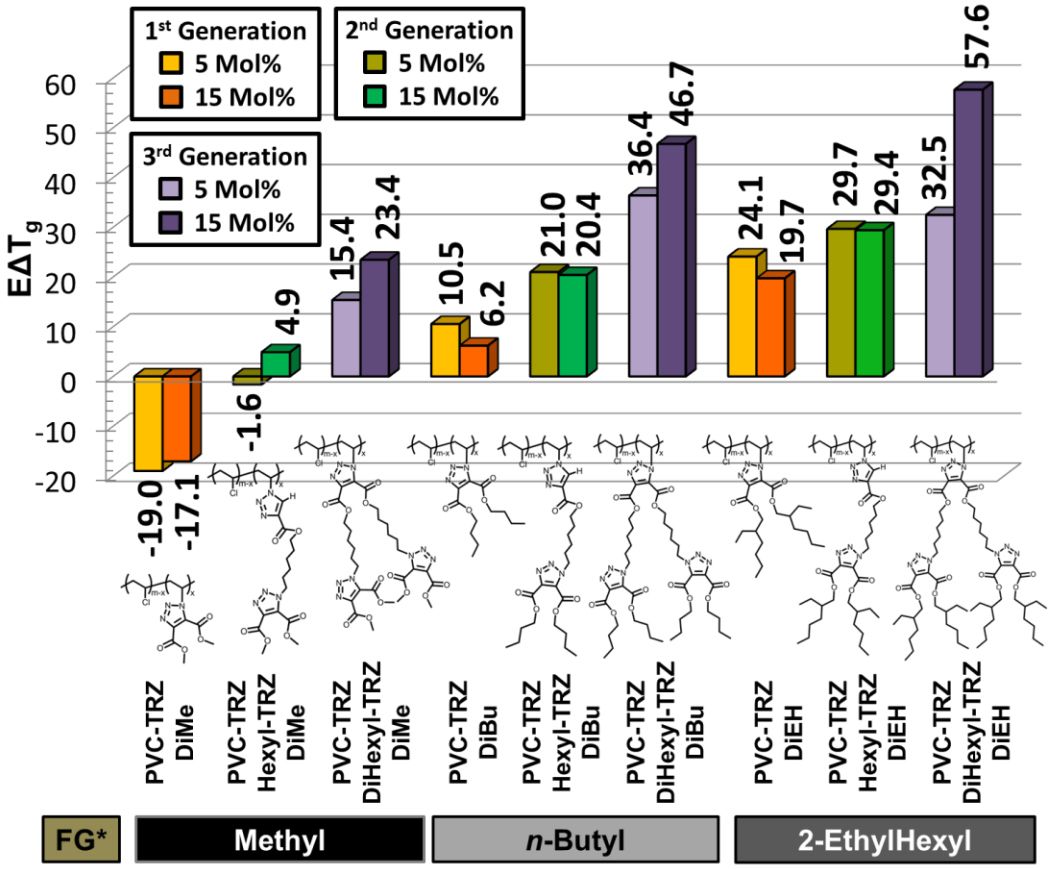

Figure 3.14 Efficiency Values ($E\Delta T_g$) of Generations 1-3 Internally Plasticized PVC (**FG = Functional Group*)

polymer PVC-TRZ-DiEH ($E\Delta T_g$ = 24.1) is 5.6% less efficient than its 2nd generation analogue, PVC-TRZ-Hexyl-TRZ-DiEH. It is evident that regardless of generation, the 2-ethylhexyl moiety is essential in engendering efficient plasticization properties to PVC at 5 mole percent. While PVC-TRZ-DiHexyl-TRZ-DiBu was calculated to have the highest plasticization efficiency at 5 mole percent, all three generations of 2-ethylhexyl internal plasticizers exhibit relatively high efficiencies giving the second, third and fourth best $E\Delta T_g$ values (**Table 3.7**, **Figure 3.14**). These 2-ethylhexyl relatives display descending $E\Delta T_g$ values according to generation: 3rd generation PVC TRZ-DiHexyl-TRZ-DiEH possesses the highest plasticization efficiency ($E\Delta T_g$ = 32.5), 2nd generation PVC-TRZ-Hexyl-TRZ-DiEH exhibits medium efficiency ($E\Delta T_g$ = 29.7), and 1st generation PVC-TRZ-DiEH ($E\Delta T_g$ = 24.1) gives the lowest $E\Delta T_g$ value. Unsurprisingly, 2nd generation PVC-TRZ-Hexyl-TRZ-DiBu ($E\Delta T_g$ = 21.0) with a single hexyl tether displays the fifth highest $E\Delta T_g$, representing a 3.1% efficiency decrease relative to 1st generation PVC-TRZ-DiEH. The 3rd generation methyl ester triazole, PVC-TRZ-DiHexyl-TRZ-DiMe ($E\Delta T_g$ = 15.4) is 4.8% more efficient than 1st generation PVC-TRZ-DiBu ($E\Delta T_g$ = 10.5): this implies that the hexyl tethers in the double hexyl tethered internal plasticizers may synergistically act as pseudo-1st generation plasticizers while conveying increased flexibility and mobility to the secondary triazoles. Incorporation of hexyl tethers appears to be a successful solution to counteract the anti-plasticization engendered by the primary triazole, most noticeable in the 1st generation PVC-TRZ-DiMe samples.

A similar trend in plasticizing efficiencies is observed in polymers functionalized with 15 mole percent triazole plasticizer, as the 5 mole percent analogues (**Table 3.8**, **Figure 3.14**). Ranked by $E\Delta T_g$, the top five samples correspond to 2nd or 3rd generation systems: the two highest efficiency values belong to 3rd generation double hexyl tethered plasticizers containing 2-ethylhexyl ($E\Delta T_g$ = 57.6) and *n*-butyl ($E\Delta T_g$ = 46.7) triazole esters. The 2nd generation sample, PVC-TRZ-Hexyl-TRZ-DiEH ($E\Delta T_g$ = 29.4), is 17.4% less efficient than the 3rd generation PVC-TRZ-DiHexyl-TRZ-DiBu ($E\Delta T_g$ = 46.7). In terms of $E\Delta T_g$, the next best

polymer is 3rd generation PVC-TRZ-DiHexyl-TRZ-DiMe ($E\Delta T_g$ = 23.4). A 3.1% decrease in plasticization efficiency was calculated for PVC-TRZ-Hexyl-TRZ-DiBu ($E\Delta T_g$ = 20.4) relative to PVC-TRZ-DiHexyl-TRZ-DiMe. This is likely due to the greater weight percentage of plasticizer in PVC-TRZ-DiHexyl-TRZ-DiMe (63.9 Wt% Plasticizer) compared to PVC-TRZ-Hexyl-TRZ-DiBu (54.3 Wt% Plasticizer). As discussed in *Chapter 2*, the calculation of $E\Delta T_g$ compensates for weight percentage of plasticizer between samples, suggesting that branching at the primary triazole and solubility is critical in enhancing plasticizing efficiencies. The next best $E\Delta T_g$ value in **Table 3.8** belongs to 1st generation PVC-TRZ-DiEH ($E\Delta T_g$ = 19.7), which is a mere 0.7% less efficient than 2nd generation PVC-TRZ-Hexyl-TRZ-DiBu ($E\Delta T_g$ = 20.4). A considerable 13.5% decrease in $E\Delta T_g$ is observed between PVC-TRZ-DiBu ($E\Delta T_g$ = 6.2) and PVC-TRZ-DiEH ($E\Delta T_g$ = 19.7).

It appears that extended branching, at both the primary and secondary triazoles, are necessary to convey the maximum efficiencies when utilizing alkyl plasticizing groups. Significant increases in $E\Delta T_g$ is achieved by incorporating two hexyl tethers into the primary triazole, evidenced by all generations of methyl functionalized triazoles at 15 mole percent (**Table 3.8**): PVC-TRZ-DiHexyl-TRZ-DiMe ($E\Delta T_g$ = 23.4), PVC-TRZ-Hexyl-TRZ-DiMe ($E\Delta T_g$ = 4.9), and PVC-TRZ-DiMe ($E\Delta T_g$ = -17.0). A similar trend in $E\Delta T_g$ also occurs at 5 mole percent (**Table 3.7**): PVC-TRZ-DiHexyl-TRZ-DiMe ($E\Delta T_g$ = 15.4), PVC-TRZ-Hexyl-TRZ-DiMe ($E\Delta T_g$ = -1.6), and PVC-TRZ-DiMe ($E\Delta T_g$ = -19.0). Regardless of the rigidification engendered by the methyl triazole, the inclusion of hexyl tethers counteracts this anti-plasticization effect. Steric bulk generated by alkyl moieties on the secondary triazole enhances the efficacy of the covalently-bound plasticizers. Branching at the primary triazole (not necessarily limited to hexyl tethers), in combination with large alkyl chains on either triazole should furnish improved $E\Delta T_g$ values that better match the plasticization efficiency of traditional DEHP-PVC blends.

3.8 Thermogravimetric Analysis: Double Hexyl Tethered Alkyl Triazole Phthalate Mimics on PVC

The thermal stability of PVC and the 3rd generation internally plasticized analogues were measured by our collaborators by derivative thermogravimetry (DTG) and thermogravimetric analyses (TGA) with a TA Instruments TGA Q500 in both air and nitrogen atmospheres, with a heating rate of 10 °C per minute. Degradation temperatures of PVC internally plasticized by the 3rd generation system are given in **Table 3.9**.

Polymer	Atm	T_d PVC1 (°C)	T_d PVC2 (°C)	T_d Hexyl (°C)	T_d TRZ (°C)	T_d TRZ1 (°C)	T_d TRZ2 (°C)	T_d TRZ3 (°C)
Unmodified PVC	N_2	283	-	-	-	-	-	-
	Air	289	442	-	-	-	-	-
5% PVC-Azide	N_2	227	447	-	-	-	-	-
	Air	229	453	-	-	-	-	-
15% PVC-Azide	N_2	214	444	-	-	-	-	-
	Air	219	451	-	-	-	-	-
5% PVC-TRZ-DiHexyl-TRZ-DiMe	N_2	231	446	-	-	-	-	-
	Air	236	447	-	-	-	-	-
15% PVC-TRZ-DiHexyl-TRZ-DiMe	N_2	223	442	-	-	431	-	-
	Air	231	-	-	-		452	461
5% PVC-TRZ-DiHexyl-TRZ-DiBu	N_2	264	447	-	-	436	-	-
	Air	286	439	-	-	-	-	469
15% PVC-TRZ-DiHexyl-TRZ-DiBu	N_2	279	439	337	-	-	448	-
	Air	284	443	337	413	427	-	-
5% PVC-TRZ-DiHexyl-TRZ-DiEH	N_2	261	446	-	-	433	-	-
	Air	270	441	-	-	427	-	459
15% PVC-TRZ-DiHexyl-TRZ-DiEH	N_2	311	442	353	-	-	-	-
	Air	317	441	351	-	422	453	-

Table 3.9 TGA/DTG Degradation Temperatures of Unmodified PVC, PVC-Azide and 3rd Generation Internally Plasticized PVC

PVC-TRZ-DiHexyl-TRZ-DiMe at 5 mole percent plasticizer exhibits decreased $T_{d,PVC1}$ temperatures (231 °C N_2, 236 °C air) with slightly elevated $T_{d,PVC2}$ temperatures (446 °C N_2, 447 °C air) relative to unmodified PVC. At 15 mole percent, PVC-TRZ-DiHexyl-TRZ-DiMe

gives drastically lower $T_{d,PVC1}$ values (223 °C N_2, 231 °C air) compared to PVC. A DTG peak at 431 °C (weak, N_2) is indicative of triazole hydrolyzation. As noted with the 1st and 2nd generation methyl triazole analogues, a decrease in $T_{d,PVC1}$ is observed in the 3rd generation samples containing methyl triazoles relative to unmodified PVC. Presumably, the methyl ester requires less energy to hydrolyze than the larger alkyl analogues, liberating the alcohol and the carboxylic acid from the triazole ester. This results in a lower degradation temperature ($T_{d,PVC1}$) when the dehydrochlorination of PVC occurs. With 15 mole percent PVC-TRZ-DiHexyl-TRZ-DiMe measured in air, the second PVC degradation event ($T_{d,PVC2}$) is not observed at 442 °C: this peak appears to be buried in the large oxidized triazole degradation peak at 452 °C.

$T_{d,PVC1}$ values increased in PVC-TRZ-DiHexyl-TRZ-DiBu relative to PVC-TRZ-DiHexyl-TRZ-DiMe. At 5 mole percent, weak DTG peaks corresponding to triazole degradation occur at 436 °C (N_2) and 469 °C (air). At 15 mole percent, PVC-TRZ-DiHexyl-TRZ-DiBu exhibits hexyl tether hydrolyzation at 337 °C. Likewise, at the same mole percentage of plasticizer, PVC-TRZ-DiHexyl-TRZ-DiEH demonstrates hexyl tether degradation events at 353 °C (N_2) and 351 °C (air). At both substitution levels, PVC-TRZ-DiHexyl-TRZ-DiEH displays triazole ester hydrolyzation events at 427 °C (5 mol %, air) and 422 °C (15 mol %, air). Significantly elevated $T_{d,PVC1}$ values with 15 mole percent PVC-TRZ-DiHexyl-TRZ-DiEH (311 °C N_2, 317 °C air) are observed, compared to all triazole plasticized PVC samples and unmodified PVC. Apparently, the enhanced thermal stability of this 3rd generation sample containing 2-ethylhexyl triazole esters originates from the large alkyl moieties and high weight percentage of plasticizer (73.5 Wt%). Alkyl degradation processes ensue at much higher temperatures than PVC dehydrochlorination ($T_{d,PVC1}$). Because 15 mole percent PVC-TRZ-DiHexyl-TRZ-DiEH is comprised of predominately alkyl-based triazole plasticizer, in combination with difficult to hydrolyze 2-ethylhexyl esters, $T_{d,PVC1}$ occurs at elevated temperatures relative to unmodified PVC. Enhanced thermal stability may also

stem from the overall polarity of the polymeric matrix. This sample contains primarily non-polar alkyl groups.[23] The pK_a values (in water) of hydrochloric acid ($pK_a \approx -7$) and triazole carboxylic acid ($pK_a = 2.95$)[24] are dependent on the nature of the surrounding environment. The low polarity of the modified polymeric matrix raises these pK_a values, thereby delaying the initial thermal degradation of 15 mole percent PVC-TRZ-DiHexyl-TRZ-DiEH.

3.9 References

1. Sinirlioglu, D.; Muftuoglu, A. E. Synthesis of an Inorganic-Organic Hybrid Material Based on Polyhedral Oligomeric Silsesquioxane and Polystyrene via Nitroxide-Mediated Polymerization and Click Reactions. *Designed Monomers and Polymers* **2011,** *14* (3), 273-286.

2. Su, Y. C.; Lo, Y. L.; Hwang, C. C.; Wang, L. F.; Wu, M. H.; Wang, E. C.; Wang, Y. M.; Wang, T. P. Azide-Alkyne Cycloaddition For Universal Post-Synthetic Modifications of Nucleic Acids and Effective Synthesis of Bioactive Nucleic Acid Conjugates. *Organic & Biomolecular Chemistry* **2014,** *12* (34), 6624-6633.

3. Alvaro, M.; García, H.; Miranda, M. A.; Primo, J. Preparation and Photolysis of Diaryl Esters of Acetylenedicarboxylic Acid. *Tetrahedron* **1992,** *48* (16), 3437-3444.

4. Chan, L. C.; Cox, B. G. Kinetics of Amide Formation through Carbodiimide/N-Hydroxybenzotriazole (HOBt) Couplings. *The Journal of Organic Chemistry* **2007,** *72* (23), 8863-8869.

5. Brown, H. C.; McDaniel, D. H.; Hafliger, O. Chapter 14 - Dissociation Constants - Braude, E.A. In *Determination of Organic Structures by Physical Methods*, Nachod, F. C., Ed. Academic Press: 1955; pp 567-662.

6. (a) Volonterio, A.; Zanda, M. Domino Condensation/Aza-Michael/O→N Acyl Migration of Carbodiimides with Activated α,β-Unsaturated Carboxylic Acids to Form Hydantoins. *Tetrahedron Letters* **2003,** *44* (47), 8549-8551; (b) Volonterio, A.; Ramirez de Arellano, C.; Zanda, M. Synthesis of 1,3,5-Trisubstituted Hydantoins by Regiospecific Domino Condensation/Aza-Michael/O→N Acyl Migration of Carbodiimides with Activated α,β-Unsaturated Carboxylic Acids. *The Journal of Organic Chemistry* **2005,** *70* (6), 2161-2170; (c) Marcelli, T.; Olimpieri, F.; Volonterio, A. Domino Synthesis of 1,3,5-Trisubstituted Hydantoins: A DFT Study. *Organic & Biomolecular Chemistry* **2011,** *9* (14), 5156-5161.

7. Bellucci, M. C.; Marcelli, T.; Scaglioni, L.; Volonterio, A. Synthesis Of Diverse Spiroisoxazolidinohydantoins By Totally Regio- and Diasteroselective 1,3-Dipolar Cycloadditions. *RSC Advances* **2011,** *1* (7), 1250-1264.

8. Chubb, F. L.; Edward, J. T.; Wong, S. C. Simplex Optimization of Yields in the Bucherer-Bergs reaction. *Journal of Organic Chemistry* **1980,** *45* (12), 2315-2320.

9. (a) Hoss, M.; Jaruga, P.; Zastawny, T. H.; Dizdaroglu, M.; Paabo, S. DNA Damage and DNA Sequence Retrieval From Ancient Tissues. *Nucleic Acids Research* **1996,** *24* (7), 1304-1307; (b) Hofreiter, M.; Serre, D.; Poinar, H. N.; Kuch, M.; Paabo, S. Ancient DNA. *Nature Reviews Genetics* **2001,** *2* (5), 353-359; (c) Cadet, J.; Davies, K. J. A.; Medeiros, M. H. G.; Di Mascio, P.; Wagner, J. R. Formation and Repair of Oxidatively Generated Damage in Cellular DNA. *Free Radical Biology and Medicine* **2017,** *107*, 13-34.

10. (a) Kunishima, M.; Kawachi, C.; Morita, J.; Terao, K.; Iwasaki, F.; Tani, S. 4-(4,6-Dimethoxy-1,3,5-triazin-2-yl)-4-methyl-morpholinium Chloride: An Efficient Condensing Agent Leading to the Formation of Amides and Esters. *Tetrahedron* **1999,** *55* (46), 13159-13170; (b) Kunishima, M.; Kawachi, C.; Hioki, K.; Terao, R.; Tani, S. Formation of Carboxamides by Direct Condensation of Carboxylic Acids and Amines in Alcohols Using a New Alcohol- and Water-Soluble Condensing Agent: DMT-MM. *Tetrahedron* **2001,** *57* (8), 1551-1558.

11. Heyl, D.; Fessner, W. D. Facile Direct Synthesis of Acetylenedicarboxamides. *Synthesis-Stuttgart* **2014,** *46* (11), 1463-1468.

12. Eichelberger, L. Iodination of Acetylene Derivatives. I. The Preparation of Diiodofumaric Acid. *Journal of the American Chemical Society* **1926,** *48*, 1320-1322.

13. Winterfeldt, E. Additions to the Activated CC Triple Bond. *Angewandte Chemie-International Edition* **1967,** *6* (5), 423-434.

14. Ruggli, P. Uber Versuche zur Darstellung von Derivaten des Diamido-acetylens. 4. Mitteilung über Acetylenderivate. *Helvetica Chimica Acta* **1920,** *3*, 559-572.

15. Diels, O.; Thiele, W. E. Zur Kenntnis der Dien-Synthesen, XXX. Mitteil.: Über das Chlorid der Acetylendicarbonsäure. *Berichte der Deutschen Chemischen Gesellschaft (A and B Series)* **1938,** *71* (6), 1173-1178.

16. McDonald, R. N.; Krueger, R. A. The Catalyzed Reaction of Acetylenedicarboxylic Acid and Thionyl Chloride. *The Journal of Organic Chemistry* **1963,** *28* (10), 2542-2544.

17. Maier, G.; Jung, W. A. Acetylenedicarbonyl Dichloride. *Chemische Berichte-Recueil* **1982,** *115* (2), 804-807.

18. Ott, E. Über Symmetrische und Asymmetrische Dicarbonsäurechloride. *Justus Liebigs Annalen der Chemie* **1912,** *392* (3), 245-285.

19. (a) Charlton, J. L.; Chee, G. Synthesis of Chiral Esters of Acetylenedicarboxylic Acid. *Tetrahedron Letters* **1994,** *35* (34), 6243-6246; (b) Charlson, J. L.; Chee, G.; McColeman, H. Synthesis of Acetylenedicarboxylic Acid Esters and Asymmetric Diels-Alder Reactions of the Bis(methyl (S)-lactyl) Ester. *Canadian Journal of Chemistry* **1995,** *73* (9), 1454-1462.

20. Abraham, R. J.; Canton, M.; Griffiths, L. Proton Chemical Shifts In NMR: Part 17. Chemical Shifts In Alkenes And Anisotropic And Steric Effects Of The Double Bond. *Magnetic Resonance in Chemistry* **2001,** *39* (8), 421-431.

21. Abraham, R. J.; Reid, M. Proton Chemical Shifts In NMR. Part 16. Proton Chemical Shifts In Acetylenes And The Anisotropic And Steric Effects Of The Acetylene Group. *Journal of the Chemical Society-Perkin Transactions 2* **2001,** (7), 1195-1204.

22. Fox, T. G., Jr.; Flory, P. J. Second-Order Transition Temperatures and Related Properties of Polystyrene. I. Influence of Molecular Weight. *Journal of Applied Physics* **1950,** *21*, 581-591.

23. Tiemblo, P.; Martinez, G.; Millan, J. L. A Verification by FTIR Spectroscopy of the Effect of Some Local Chain Conformations on the Specific Molecular Interactions of Solvents, Esters, and Polyesters with PVC. *Journal of Polymer Science Part A: Polymer Chemistry* **1995,** *33* (8), 1243-1255.

24. Franz, R. G. Comparisons of pK_a and log P Values of Some Carboxylic and Phosphonic Acids: Synthesis and Measurement. *AAPS PharmSci* **2001,** *3* (2), 1-13.

4 Poly(ethylene oxide) Triazole Phthalate Mimics

4.1 Miscibility of Polyethers with PVC

Polyethers are miscible with PVC and thus may increase the efficiency of an internal plasticizer compared to a system that is predominantly comprised of alkyl groups. Muniz and coworkers[1] investigated the miscibility of blends containing PVC and poly(ethylene oxide) (PEO) with viscosimetric, microscopic and thermal analyses. In accordance with Sun theory[2], attractive forces between PEO and PVC were evaluated by the determination of α parameters. Thermal and viscosimetric data indicate that the PEO/PVC blends are miscible at all weight percentages of PEO tested. Polymer-polymer interaction parameters (X_{12}) determined by depression of the melting temperature (T_m) were found to be negative (-0.028 to -0.102) and dependent on the molecular weight of PVC: this implies that PEO and PVC are miscible. X_{12} values calculated utilized T_m values that were not at equilibrium when measured. Scanning electron microscopy (SEM) revealed PVC rich phases in the PEO/PVC blends, indicating non-homogenous mixing. The authors suggested that the polar interactions between chlorine atoms in PVC and oxygen atoms in PEO are responsible for the miscibility between the two components.

Subsequently, Muniz[3] described the crystallization properties of PEO and its influence on miscibility with PVC. Isothermal crystallization of PEO was influenced by PVC as determined by the various temperatures and crystallization times noted during the experiments of different ratios of these two components. PEO/PVC blends were analyzed by differential scanning calorimetry (DSC), using PEO as a reference. The Hoffmann-Weeks[4] plot procedure was utilized to determine the equilibrium melt temperatures ($T_m°$), while the Nishi-Wang equation was employed to quantify the polymer-polymer interaction parameter (X_{12}) of pure PEO and PEO/PVC blends. From the melting depression data, mixtures of PEO/PVC containing 20 to 60 percent by weight PVC, has an X_{12} (X_{PEO}/X_{PVC}) value of -0.02, indicating miscibility. According to the authors, a minute $T_m°$ depression was noted by

increasing the PVC content, suggesting that PEO miscibility can be affected with different weight percentages of PVC. Blends richer in PEO have higher crystallization rates. As the content of PVC increases, the mobility of the PEO chains as melted segments toward the interface of the growing PEO crystals decreases, implying that PVC may interfere with the PEO nucleation process and can alter its miscibility.

The influence of PVC on PEO was also described by Fatou[5] through dynamic and isothermal crystallization methods: a progressive reduction in the overall rate of PEO crystallization occurs with increasing PVC content. The publication states that "when a polymer chain crystallizes in the presence of a non-crystallizable component, the accumulation of the non-crystallizable component outside the crystalline regions will cause a depression in the melting point… [of the crystalizable component]."[5] In this study, the X_{12} interaction parameter between PEO and PVC is -0.094, suggesting that the blends are thermodynamically stable in the melt for compositions greater than 40 percent by weight of PVC. The authors report a lower interaction value (X_{12}) than in previous studies due to the lower molecular weight of the PEO; this caused a higher entropic contribution to the free energy of the blend and a decreased X_{12} value.

Kwak[6] investigated alkyl terminated hyperbranched polyglycerols (alkyl-HPG) as external PVC plasticizers (**Scheme 4.1**). The polyglycerol emollient was synthesized by reacting glycidol with trimethylolpropane via anionic ring opening polymerization followed by esterification using an anhydride or acid chloride. A number of HPGs with various amounts of glycerol repeat units, along with different chain lengths of terminating alkyl groups were investigated. Solubility parameters were measured using density, group molar attraction constants, and molecular weight. Substances with similar solubility parameters values of ±1.8 $cal^{1/2}$ $cm^{3/2}$ are considered miscible.[7] PVC has a solubility parameter of 9.66 $cal^{1/2}$ $cm^{3/2}$. Solubility parameter values of alkyl-HPGs in PVC are reported to be between 8.32 and 8.82 $cal^{1/2}$ $cm^{3/2}$, while non-alkylated HPG derivatives are between 12.46 and 12.85 $cal^{1/2}$ $cm^{3/2}$.

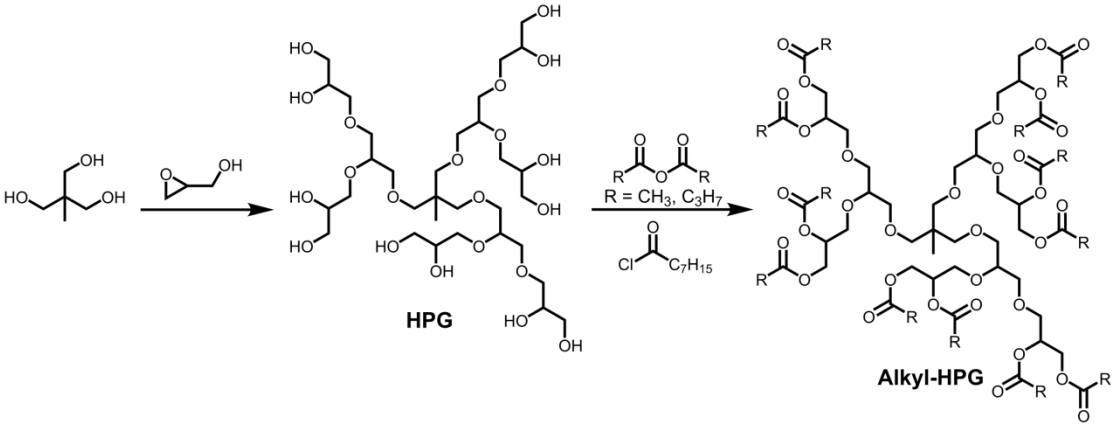

Scheme 4.1 Kwak's Alkyl-HPG External PVC Plasticizer[6]

The authors demonstrated that polyglycerol is miscible with PVC when alkylated. In contrast, non-alkylated HPG derivatives were shown to be immiscible. External alkyl-HPG plasticizers are effective at decreasing the glass transition temperature (T_g) of PVC. Increasing the amount of polyether repeat units did not entail a concurrent decrease in T_g: higher values were observed due to the diminishing presence of chain ends relative to the larger polyether core.[8] Furthermore, reduced T_g values were reported as the amount of carbons in the terminating group grew. Using HPG with nine repeat units terminated by either two, four and eight carbon moieties exhibited progressive T_g depressions (-32.6 °C, -65.4 °C, and -71.4 °C).

Currently, there are only two publications that describe PVC internal plasticizers incorporating polyether groups.[9] Kwak[9a] functionalized PVC by grafting alkyl terminated hyperbranched polyglycerol onto PVC via copper-mediated azide-alkyne cycloaddition (CuAAC): **Figure 4.1**. Hyperbranched polyglycerol (HPG) was synthesized by anionic ring-opening polymerization of glycidol initiated by propargyl alcohol. The propargyl-HPG intermediate was treated with hexanoic anhydride to furnish the hexyl-terminated HPG-C6 alkyne. This was grafted onto PVC-azide containing 1.8 to 9.0 mole percent azide, resulting in PVC-*g*-HPG-C6 analogues with various quantities of internal plasticizer.

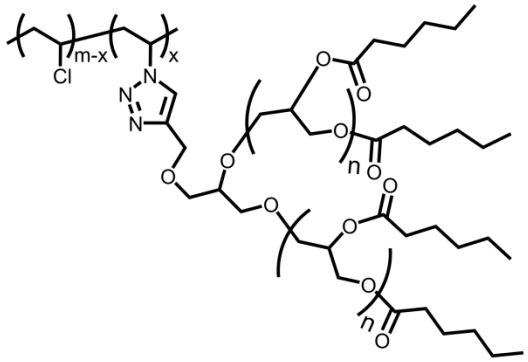

Figure 4.1 Kwak's Polyglycerol-Based Internal Plasticizer: PVC-*g*-HPG-C6[9a]

Sample	Triazole Content (mol%)	M_n (g/mol)	T_g (°C)	ΔT_g (°C)
PVC	0	42271	81.3	-
$PVC_{1.8}$-*g*-HPG-C6	1.8	50251	38.6	42.7
$PVC_{3.6}$-*g*-HPG-C6	3.6	57763	16.4	64.9
$PVC_{5.8}$-*g*-HPG-C6	5.8	83883	-4.5	85.8
$PVC_{9.0}$-*g*-HPG-C6	9.0	88404	-28.9	110.2

Table 4.1 DSC and GPC Data: Kwak's PVC-*g*-HPG-C6[9a]

As shown in **Table 4.1**, a decline in glass transition temperatures with increasing triazole content was observed. The authors report comparable T_g depressions of the HPG-*g*-C6 system to a traditional DEHP-PVC blend at 60 parts per hundred resin (T_g DEHP 60 phr = -23.8 °C). Polyglycerol segment mobility was mentioned as a possible mechanism leading to efficient PVC plasticization. However, a statement on the miscibility of the polyether with PVC was absent from this paper. It should be noted that these same authors published a study eight months earlier on the solubility of external alkyl-HPG emollients in PVC.[6]

Reinecke[9b] covalently modified PVC with trichlorotriazines (TCTA) containing nucleophilic thiolates (**Figure 4.2**). These TCTA derivatives were functionalized with JEFFAMINEs™, which are amine terminated block copolymers of poly(propylene oxide) and poly(ethylene oxide) with specified molecular weight ranges.[10] A range of glass transition temperatures were reported from 68 °C to -50 °C. All T_g values from this study were given in *Chapter 1* (**Table 1.12**). A previous publication by the same group showed that incorporation

of JEFFAMINEs into the internal plasticizer greatly decreased T_g values of the modified PVC samples compared to TCTA functionalized exclusively with alkyl chains.[11]

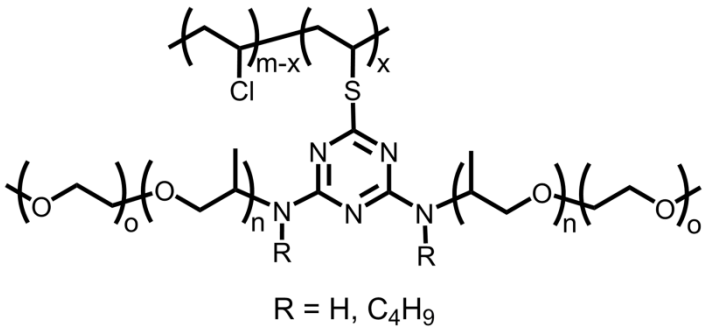

Figure 4.2 Reinecke's PVC Internal Plasticizer: TCTA Incorporating JEFFAMINEs™[9b]

The advantageous use of polyethers in the literature prompted an investigation into PEO-based internal plasticizers using the thermal copper-free azide-alkyne cycloaddition anchoring strategy. Due to the synthetic modularity of the first three generations of triazole-plasticizers, the alkyl chains were interchanged with various lengths of poly(ethylene oxide) monomethyl ethers (PEO). Each PEO contains a single alcohol functional group per molecule, allowing for selective esterification with acetylenedicarboxylic acid or propiolic acid.

A new nomenclature based on the triazole plasticizer architecture was devised to streamline the identification of the internally plasticized PVC samples spanning all three generations. Three types of triazole-plasticizers were developed: "Type 0" has no tether, "Type 1" contains a single hexyl tether, and "Type 2" possesses two hexyl tethers. The "D" or "M" designation represents *di*-substituted or *mono*-substituted triazoles (Type 0D and Type 0M). In this way, the "Type" designation consolidates all generations of internal plasticizer into a unified naming system and allows one to quickly identify the overall structure of the triazole-based emollient.

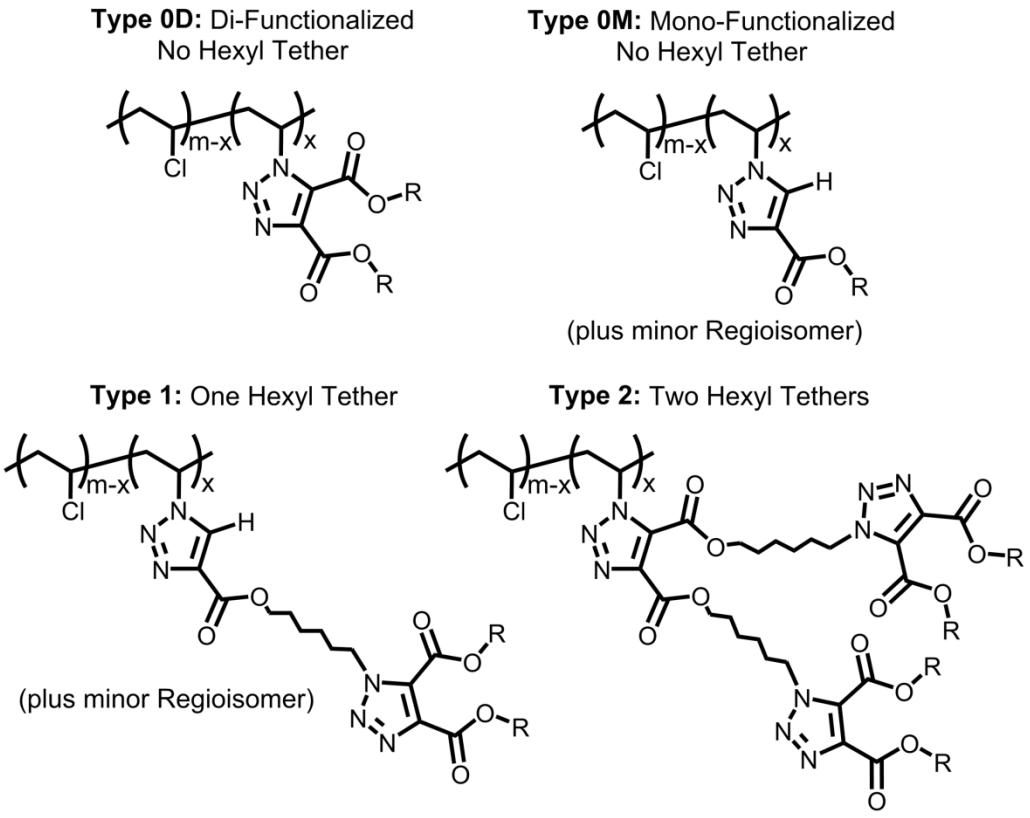

Figure 4.3 "Type" Designations of PVC Triazole-Plasticizers

4.2 Synthesis of Type 0D Poly(ethylene oxide) Triazole-Plasticized PVC

Commercially available poly(ethylene oxide) monomethyl ethers (PEO) were utilized in the synthesis of electron-deficient alkynes to directly functionalize PVC, with improved miscibility between the internal plasticizer and PVC. Acetylenedicarboxylic acid was treated with poly(ethylene oxide) monomethyl ethers with a molecular weight of exactly 164 g/mol ($PEO_{164}Me$), an average of 350 g/mol ($PEO_{350}Me$), or an average of 550 g/mol ($PEO_{550}Me$) and catalytic sulfuric acid (H_2SO_4) in toluene (**Scheme 4.2**). To drive the chemical equilibrium toward the diester in accordance with Le Chatelier's principle, a Dean-Stark apparatus was utilized to trap the water formed as a by-product of the condensation. After 1 hour under reflux, di($PEO_{164}Me$) acetylenedicarboxylate **4.1**, di($PEO_{350}Me$) acetylenedicarboxylate **4.2**,

and di($PEO_{550}Me$) acetylenedicarboxylate **4.3** were obtained in 75%, 61%, and 78% yields, respectively.

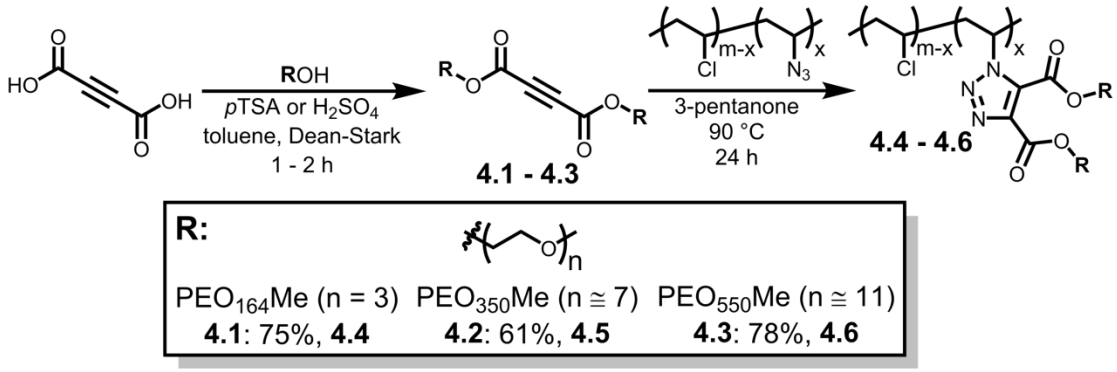

Scheme 4.2 Fischer Esterification of PEO and Acetylenedicarboxylic Acid to Form Type 0D Internally Plasticized PVC

Copper-free thermal azide-alkyne cycloadditions (AAC) were performed with PVC-azide (5 and 15 mole percent azide) and **4.1** - **4.3** in 3-pentanone. The reactions were carried out at 90 °C for 24 hours with 2.5 – 3.0 equivalents of alkyne to each equivalent of azide (**Scheme 4.2**). Reaction progress was monitored *via* FTIR, noting the disappearance of the azide stretch at ~2110 cm^{-1} and the appearance of the triazole sp^2 carbon-carbon stretch at ~1550 cm^{-1} (**Figure 4.4**). After purification by precipitation in methanol three times, the presence of an ester carbonyl stretch (C=O) at ~1730 cm^{-1} was indicative of the successful formation of the triazole-plasticizer attached to PVC (**4.4 - 4.6**). Polyether stretches at ~1250 cm^{-1} and ~1100 cm^{-1} are present in all polymers containing PEO.

^{1}H-NMR in $CDCl_3$ was acquired for all Type 0D PEO acetylenedicarboxylates as well as PVC-TRZ-Di($PEO_{164}Me$), PVC-TRZ-Di($PEO_{350}Me$), and PVC-TRZ-Di($PEO_{550}Me$). For NMR analysis, di($PEO_{164}Me$) acetylenedicarboxylate and PVC-TRZ-Di($PEO_{164}Me$) are chosen, as they are representative of the other Type 0D PEO-functionalized polymers (**Figure 4.5**). Di($PEO_{164}Me$) acetylenedicarboxylate **4.1** displays a 4H multiplet between δ 4.39 – 4.31 ppm, corresponding to the ester methylene protons **a** (Ester-O-C**H$_2$**-C-O). Although one would expect a triplet, it appears that alkynes containing PEO esters may self-

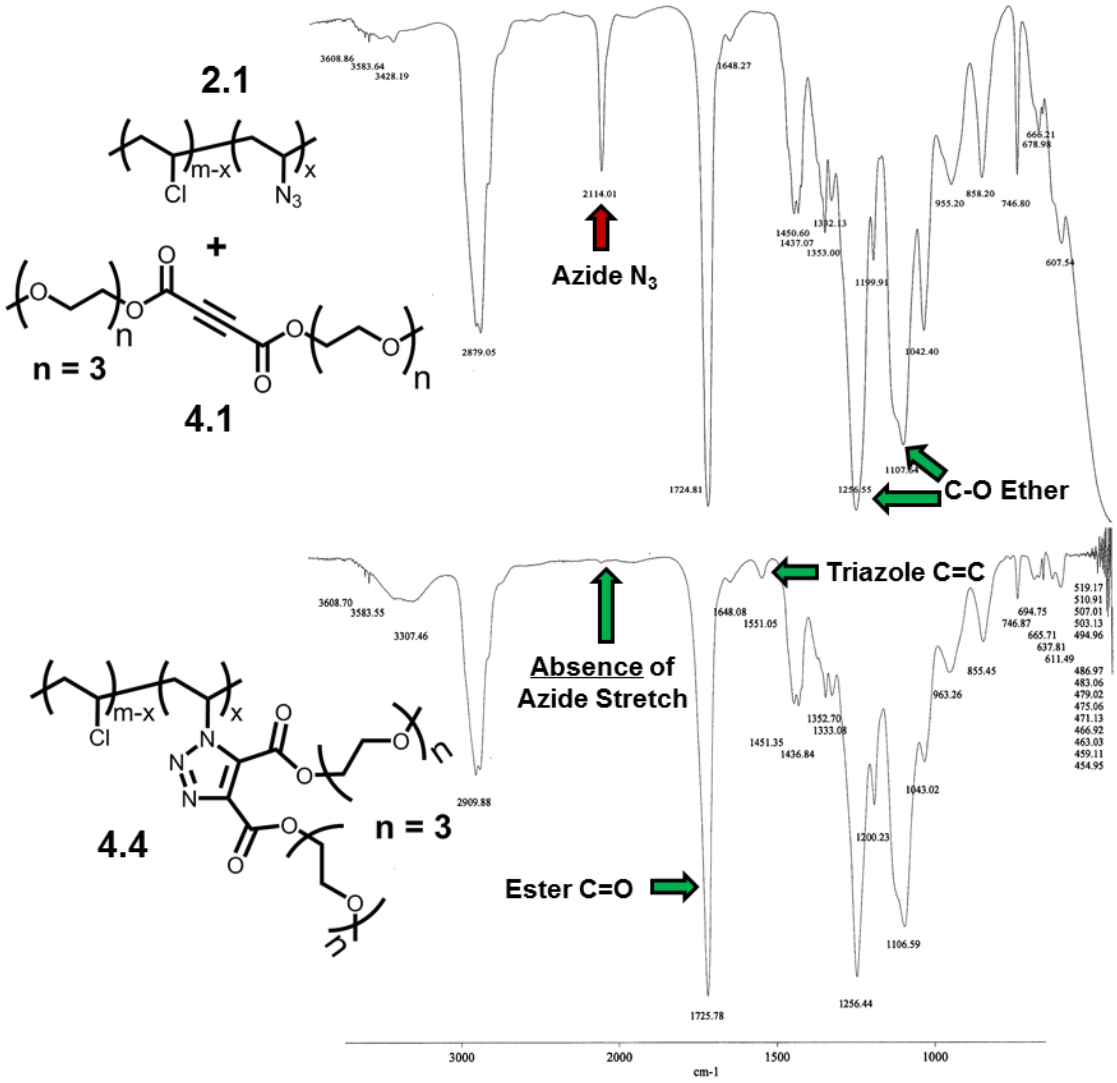

Figure 4.4 FTIR Monitoring of Reaction Between 5% PVC-Azide **2.1** and Di(PEO_{164}Me) Acetylenedicarboxylate **4.1** at 90 °C
Top: After 15 Minutes
Bottom: After 24 Hours

assemble in $CDCl_3$, which widens the proton shifts. Irradiation of the alkyne with a short wave UV lamp gives blue fluorescence (**Figure 4.5**). Aggregation of the PEO-functionalized alkynes may lead to the observed fluorescence and ^{1}H-NMR signal broadening. Another 4H multiplet **b** at δ 3.74 – 3.70 ppm is assigned to the second methylene away from the ester carbonyl (Ester-O-C-C**H$_2$**-O). Central methylene ether signals **c** overlap with each other as a

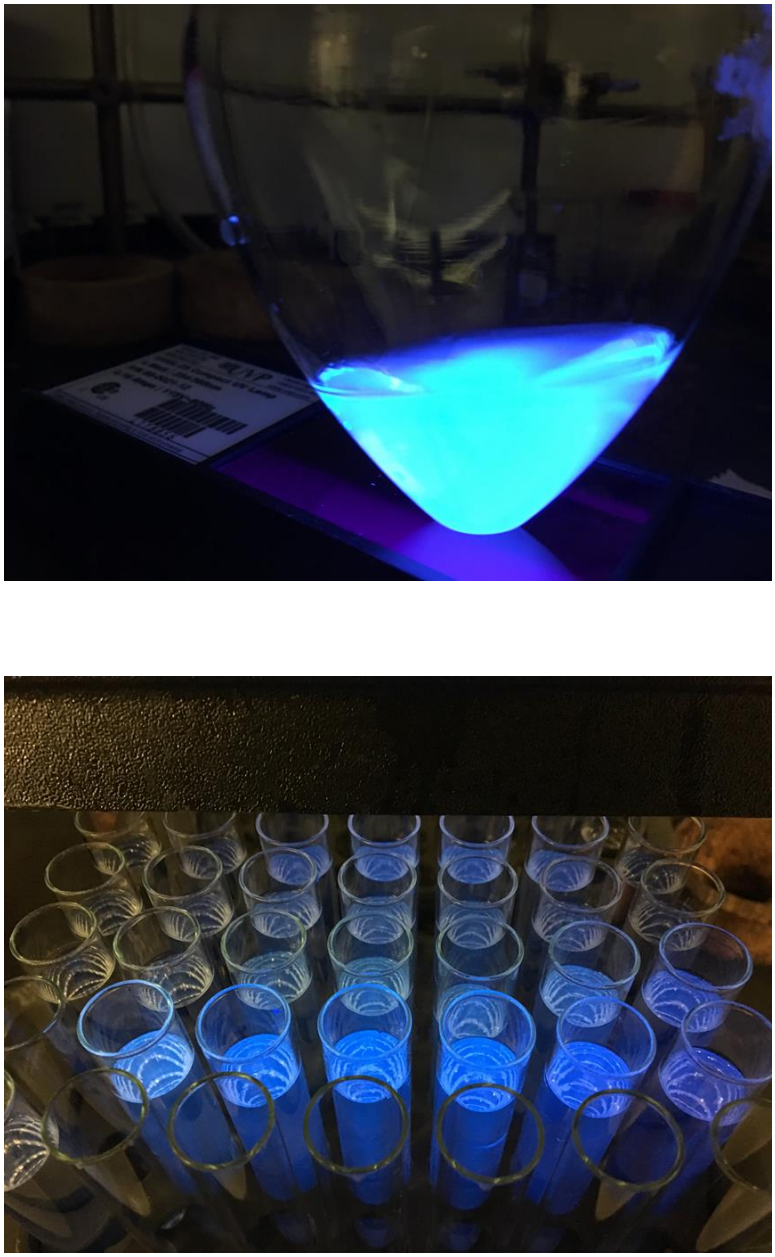

Figure 4.5 Blue Fluorescence of Di(PEO_{164}Me) Acetylenedicarboxylate **4.1** Under Irradiation with a Short Wave UV Lamp

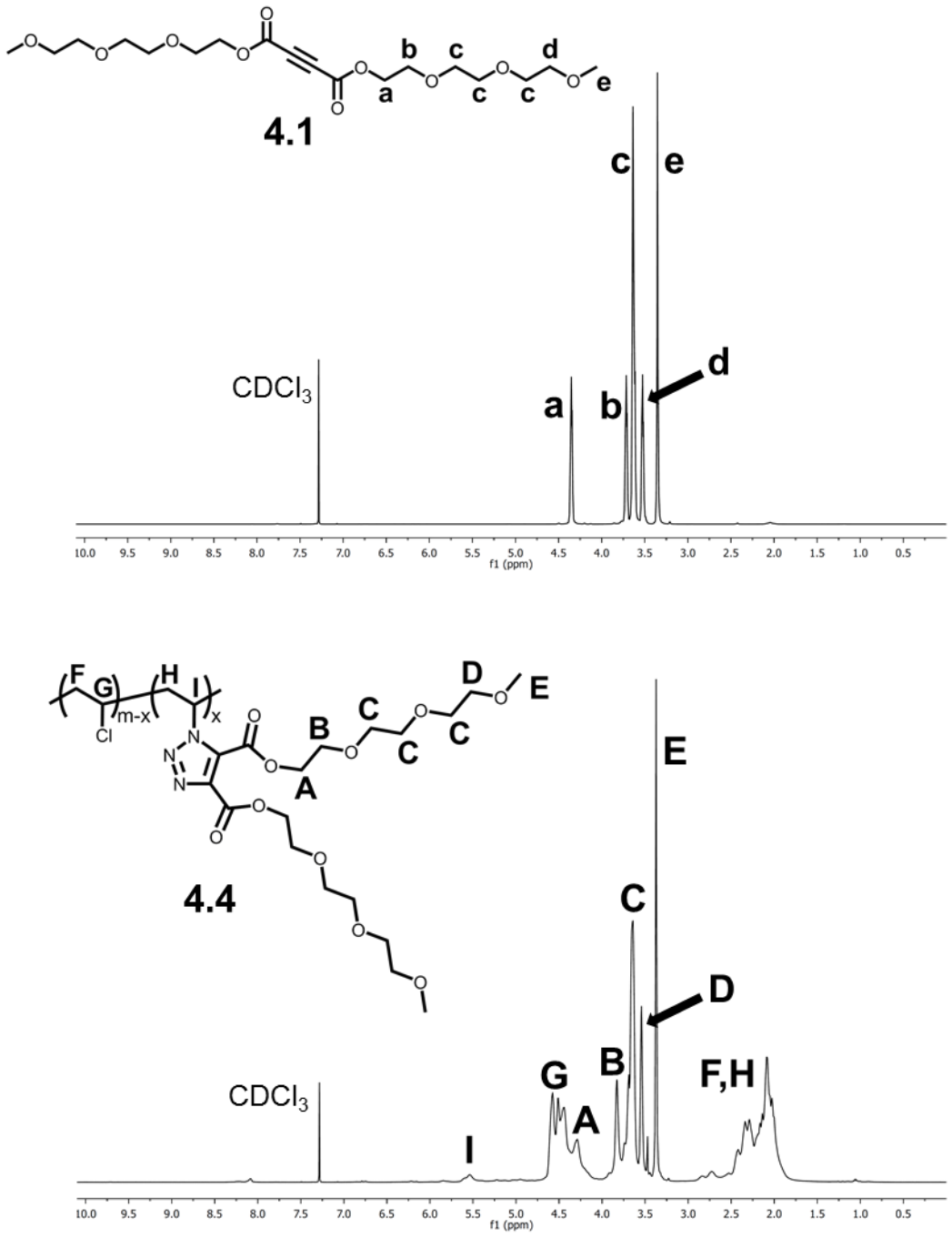

Figure 4.6 ^{1}H-NMR of Di($PEO_{164}Me$) Acetylenedicarboxylate (**4.1**, Top) and Type 0D 15% PVC-TRZ-Di$PEO_{164}Me$ (**4.4**, Bottom)

12H broad multiplet at δ 3.65 – 3.60 ppm. The methylene adjacent to the terminal ether oxygen **d** (PEO-C**H**$_2$-O-CH$_3$) is represented as a 4H multiplet at δ 3.56 – 3.49 ppm. The terminal methyl groups overlap as a 6H singlet **e** at δ 3.37 – 3.33 ppm (PEO-C**H**$_3$).

Common to all PEO triazole-plasticized PVC are characteristic ^{1}H-NMR shifts between δ 5.65 – 5.35 ppm (PVC-C-C**H**-1°TRZ) **I**: the methines bearing triazoles are shifted downfield relative to unperturbed methines due to the newly formed aromatic ring's deshielding magnetic anisotropic effect (**Figure 4.6**). At δ 4.70 – 4.10 ppm are a series of broad singlets **G** which correspond to the methine protons of Cl-C**H**-CH$_2$. Further upfield at δ 2.50 – 2.90 ppm are the methylene protons **H** of PVC in the β-position with respect to the triazole (PVC-C**H**$_2$-CH-1°TRZ). Finally, the methylene protons **F** of Cl-CH-C**H**$_2$ are observed between δ 1.80 – 2.50 ppm. In internally plasticized Type 0D PEO PVC, the shifts of the ester methylene protons **A** (PVC-1°TRZ-Ester-O-C**H**$_2$) appear in the range of δ 4.54 – 4.39 as a broad singlet, which slightly overlaps with PVC methine protons **G**. Polyether methylene protons **B**, **C**, **D** and **E** appear in approximately the same ranges as the alkyne precursor, albeit broadened due the lack of isotropic molecular tumbling of the primary triazole ester directly attached to PVC.

^{13}C-NMR spectra taken in CDCl$_3$ of Type 0D PEO alkynes exhibit a characteristic ester carbonyl signal **f** at δ 151.6 ppm (**Figure 4.7**). The alkyne quaternary carbons **g** appear at δ 74.7 ppm. Ester methylene carbons **a** (Ester-O-**C**H$_2$-C-O) are present at δ 71.9 ppm. Adjacent methylenes two carbons away from the ester **b** (Ester-O-C-**C**H$_2$-O) are observed at δ 68.4 ppm. Large overlapping peaks at δ 70.7 and δ 70.6 ppm represent centrally located poly(ethylene oxide) methylene carbons **c**. The PEO methylene carbon **d** adjacent to the terminal ether oxygen (PEO-**C**H$_2$-O-CH$_3$) appears at δ 65.8 ppm. The terminal PEO methyl carbon **e** is represented by a peak at δ 58.9 ppm (PEO-C-O-**C**H$_3$).

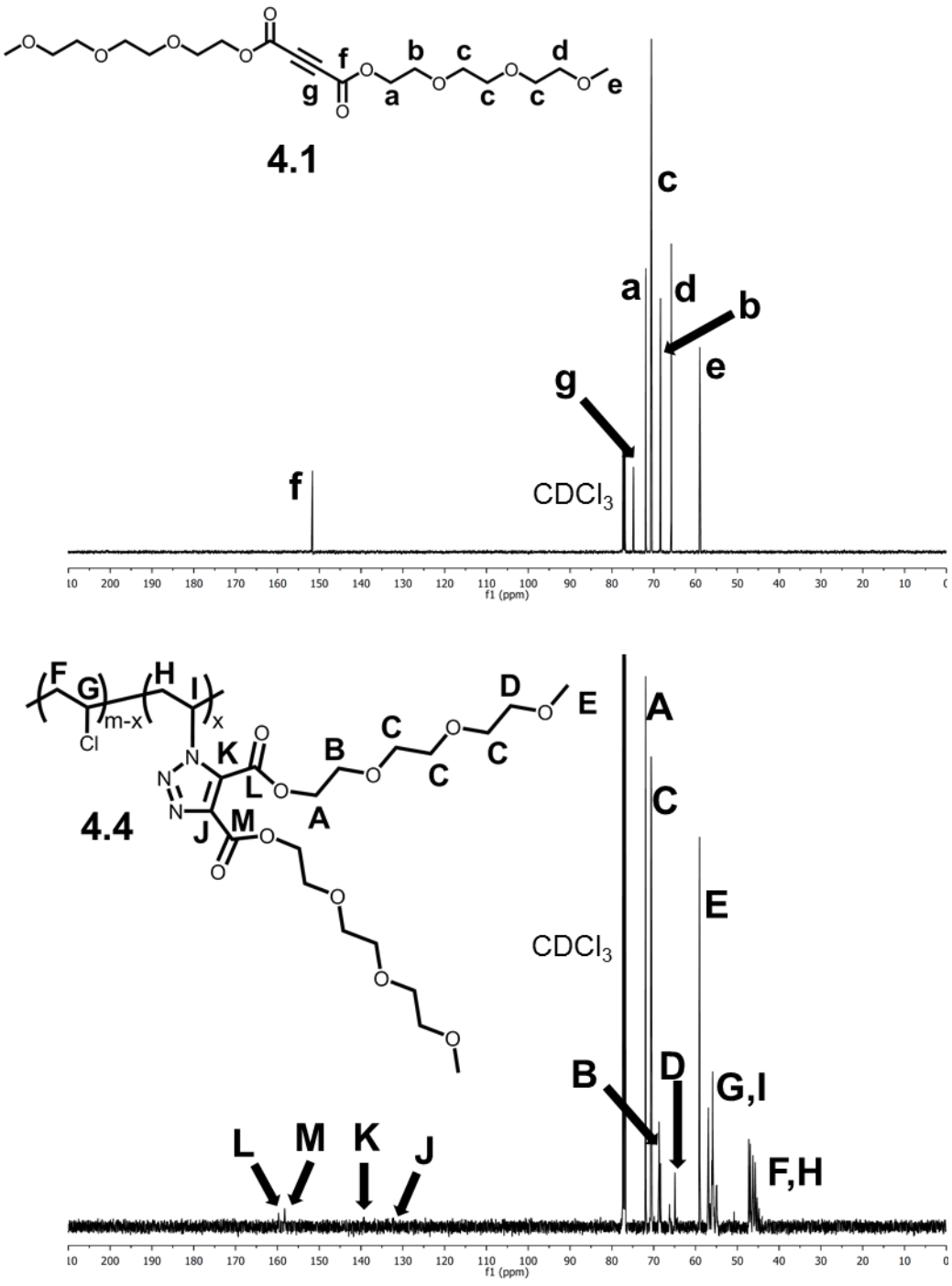

Figure 4.7 ^{13}C-NMR of Di($PEO_{164}Me$) Acetylenedicarboxylate (**4.1**, Top) and Type 0D 15% PVC-TRZ-Di$PEO_{164}Me$ (**4.4**, Bottom)

All PEO triazole-plasticized PVC possess characteristic ^{13}C-NMR signals originating from the main chain of PVC (**Figure 4.7**). Methylene carbons **F** and **H** between δ 44.8 – 47.3 ppm are representative of Cl-CH-**C**H_2. Methine shifts of isotactic (δ 54.9 – 55.1 ppm), atactic (δ 55.7 – 56.1 ppm), and syndiotactic (δ 56.9 – 57.0 ppm) carbons **G** and **I** belong to Cl-**C**H-CH_2. The PEO esters on the triazole in Type 0D PEO plasticized PVC undergo desymmetrization relative to the alkyne precursor. Two new regioisomeric triazole ester peaks, δ 159.7 and δ 158.3 ppm, appear as the carbonyl signals **L** and **M**. Weak quaternary triazole carbon peaks appear at δ 138.6 and δ 131.7 ppm as signals **K** and **J**. The ester methylene carbons **A** (1°TRZ Ester-O-**C**H_2) appear at δ 71.9 and δ 72.5 ppm. Polyether methylene carbons **B** appear at δ 68.7 and 68.4 ppm. Central polyether methylene carbons **C** are observed as overlapping signals at δ 70.6 and δ 70.5 ppm. The methylene carbons **D** adjacent to the terminal ether oxygen (PEO-**C**H_2-O-CH_3) is noted at δ 64.9 ppm. The terminal methyl carbons **E** are present at δ 59.0 ppm (PEO-C-O-**C**H_3). The disappearance of the alkyne quaternary sp-carbon signal at δ 74.7 ppm is indicative of cycloaddition and thorough purification of the plastic from the excess alkyne.

4.3 Synthesis of Type 1 Poly(ethylene oxide) Triazole Plasticizers

Synthesis of Type 1 PEO plasticizers began with 6-chlorohexan-1-ol, which was converted to 6-azidohexan-1-ol **2.7**. Di(PEO_{164}Me) acetylenedicarboxylate **4.1** or di(PEO_{350}Me) acetylenedicarboxylate **4.2** was stirred in chloroform with azide **2.7** for 24 hours at 50 °C to give the hexyl tether triazolo-alcohols **4.7** and **4.8** (**Scheme 4.3**). Satisfactory yields of 74% and 86% were achieved after column chromatography. The acetylenedicarboxylate esters were used in a 1.3 equivalent excess to 6-azidohexan-1-ol **2.7**, with cycloadditions monitored *via* TLC.

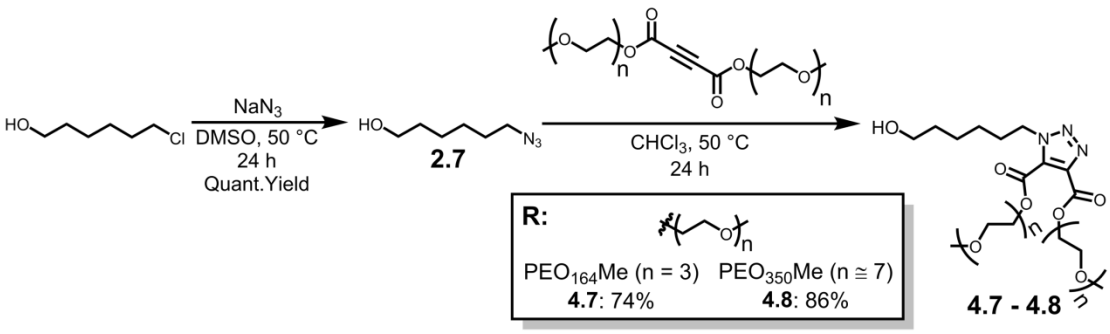

Scheme 4.3 Synthesis of PEO Triazolo-Alcohols

Fischer esterifications were performed to obtain Type 1 monoester electron-deficient alkynes (**Scheme 4.3**). Propiolic acid was treated with TRZ-Di(PEO_{164}Me) hexanol **4.7** or TRZ-Di(PEO_{350}Me) hexanol **4.8**, H_2SO_4 as an acid catalyst, and toluene using a Dean-Stark apparatus. The PEO triazolo-alcohols **4.7** and **4.8** were used in a 1.2 – 1.3 equivalent excess compared to propiolic acid, under concentrated conditions (1.0 M). The reactions were complete within 2 hours, furnishing TRZ-Di(PEO_{164}Me) hexyl propiolate **4.9** in 60% yield and TRZ-Di(PEO_{350}Me) hexyl propiolate **4.10** in 77% yield. Purification involved concentrating the crude reaction *in vacuo*, then performing flash chromatography. Reaction progress was monitored *via* TLC. All propiolate derivatives have slightly larger R_f values than their respective parent alcohols.

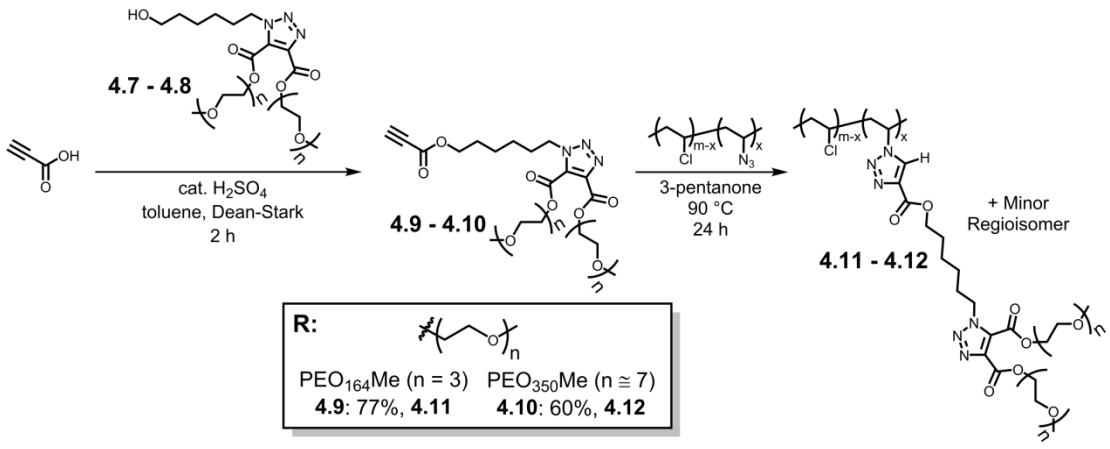

Scheme 4.4 Synthesis of Type 1 PEO Triazole-Plasticizers Attached to PVC

Copper-free azide-alkyne cycloadditions (AAC) were performed with PVC-azide (5 and 15 mole percent) in 3-pentanone. Reactions were carried out at 90 °C for 24 hours, with 2.5 – 3.0 equivalents of alkyne for each equivalent of azide (**Scheme 4.4**). Cyclizations of Type 1 PEO propiolates **4.9** and **4.10** with PVC-azide were tracked *via* FTIR. Aliquots of the reaction mixture were taken at 12 hour intervals, then precipitated three times in methanol to determine if the disappearance of the azide stretch at 2114 cm^{-1} had occurred. AAC between Type 1 alkynes and PVC-azide were complete after 24 hours.

^{1}H-NMR of Type 1 PEO hexyl tethered propiolates and their corresponding internally plasticized PVC analogues were performed (**Figure 4.8**). For this discussion, TRZ-Di($PEO_{164}Me$) hexyl propiolate and PVC-TRZ-Hexyl-TRZ-Di($PEO_{164}Me$) were chosen as representative Type 1 PEO-functionalized examples. In TRZ-Di($PEO_{164}Me$) hexyl propiolate, protons **f** belong to the hexyl tether methylene connected to the secondary triazole (Tether-C**H**$_2$-2°TRZ), giving a 2H triplet at δ 4.59 ppm. Another set of 2H triplets, upfield at δ 4.50 and 4.54 ppm correspond to methylene protons **a** of both regioisomeric PEO triazole esters (2°TRZ Ester-O-C**H**$_2$-C-O). Methylene protons producing signal **j** at δ 4.2 ppm belong to the hexyl tether next to the propiolate ester (Propiolate Ester-O-C**H**$_2$-Tether). The PEO methylenes producing signal **b** is a 4H overlapping triplet at δ 3.82 ppm (2°TRZ Ester-O-C-C**H**$_2$-O-). A broad 12H multiplet **c** between δ 3.72 – 3.60 ppm are central PEO methylenes. Methylenes **d** at the ends of the PEO chains (PEO-C**H**$_2$-O-CH_3) are seen as a 4H multiplet between δ 3.57 – 3.49 ppm. Terminal PEO methyl groups appear as two 3H singlets **e** at δ 3.36 and 3.37 ppm (PEO-C-O-C**H**$_3$). A lone proton **k** at δ 2.93 ppm belongs to the terminal alkyne. Hexyl-tether methylene protons **g**, two carbons from the secondary triazole (Tether-C**H**$_2$-CH_2-2°TRZ) are observed as a 2H pentet at δ 1.93 ppm. In the same vein, methylene protons **i**, two carbons away from the propiolate ester (Propiolate Ester-O-CH_2-C**H**$_2$-Tether), are present as a 2H multiplet at δ 1.68 ppm. Two adjacent hexyl tether methylene protons **h**

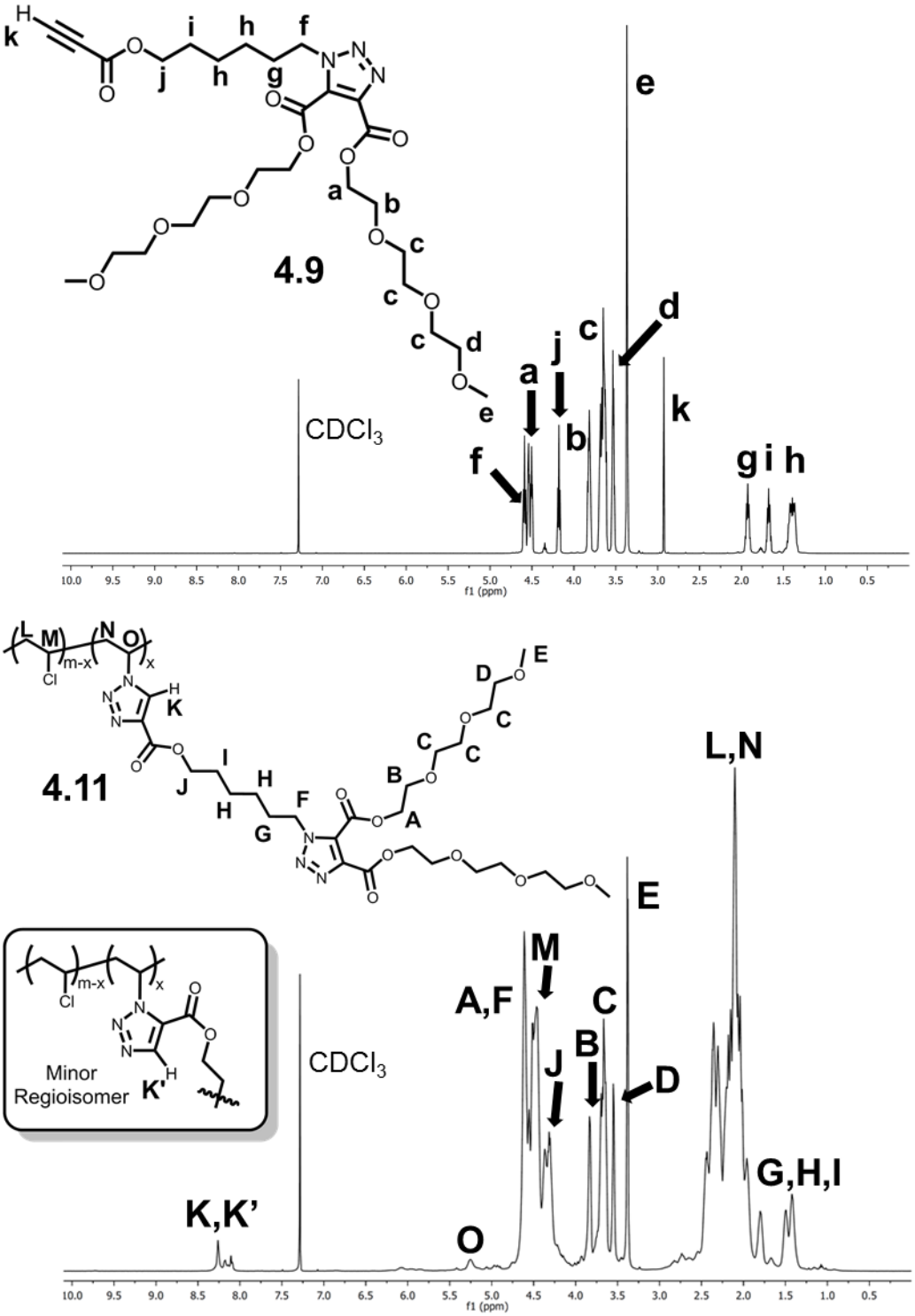

Figure 4.8 ^{1}H-NMR of TRZ-DiPEO$_{164}$Me Hexyl Propiolate (**4.9**, Top) and Type 1 5% PVC-TRZ-Hexyl-DiPEO$_{164}$Me (**4.11**, Bottom)

are represented by an overlapping 4H multiplet between δ 1.45 – 1.34 ppm (Propiolate Ester-O-C-C-C**H$_2$**-C**H$_2$**-).

^{1}H-NMR spectra of Type 1 PEO functionalized polymers at both 5 and 15 mole percent triazole plasticizer give characteristic signals between δ 8.05 and 8.35 ppm, representing the proton directly attached to the primary triazole ring, as **K** (and **K'**) in **Figure 4.8** (PVC-1°TRZ-**H**). There are two broadened peaks in this region due to triazole regioisomers. The less sterically hindered regioisomer in **4.11** predominates. A broad multiplet **J** belonging to the alkoxy-protons adjacent to the primary triazole (PVC-1°TRZ-Ester-O-C**H$_2$**-Tether) displays a downfield shift at δ 4.26 – 4.41 ppm from the parent alkyne signal **j** at δ 4.2 ppm. Methylene protons **I**, two carbons away from the primary triazole (PVC-1°TRZ-O-CH$_2$-C**H$_2$**-Tether) move downfield between δ 1.72 – 1.86 ppm, from δ 1.68 ppm in the parent alkyne. The methylene directly attached to the secondary triazole **F** (PVC-1°TRZ-Tether-C-C**H$_2$**-2°TRZ) gives a broad multiplet between δ 4.59 – 4.70 ppm, exhibiting a downfield shift from δ 4.59 ppm in the parent alkyne: This signal overlaps with PEO signal **A** and PVC main chain chlorinated methine **M**. Signal **O**, corresponding to the methine of PVC covalently bonded to the primary triazole (PVC-C**H**-1°TRZ), appears as a broadened multiplet between δ 5.12 – 5.32 ppm. All other proton shifts of the PVC main chain (**L** and **N**) are in the same general location as in unmodified PVC.

^{13}C-NMR spectra of Type 1 PEO alkynes show the newly formed propiolate ester carbonyl signal **m** at δ 152.7 ppm (**Figure 4.9**). Also, the sp-hybridized carbons of the terminal alkyne are present as two peaks at δ 74.6 ppm (Alkyne CH) **k** and δ 74.7 ppm (Alkyne 4°) **l**. A minor downfield shift of the propiolate ester hexyl tether methylene **j** (Propiolate Ester-O-**C**H$_2$-C) at δ 65.6 ppm, from δ 62.5 ppm (HO-**C**H$_2$-C) in the alcohol, is indicative of the electronegative influence of the carbonyl on the proximal carbon atom. Secondary triazole esters **p** and **q** are observed at δ 158.4 and 160.1 ppm. Quaternary carbons **n** and **o** of the secondary triazole appear at δ 129.6 and 140.0 ppm. The hexyl tether

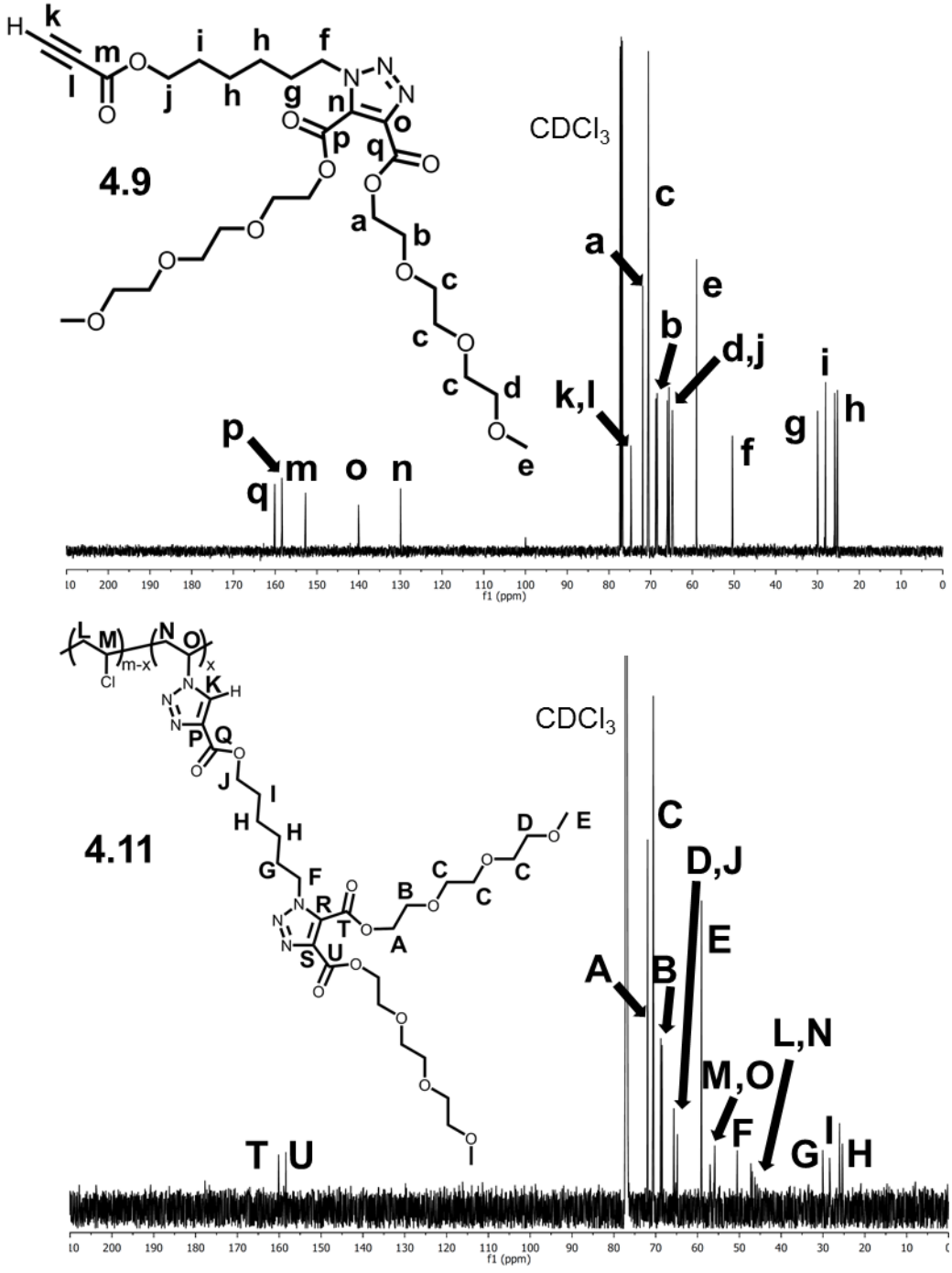

Figure 4.9 ^{13}C-NMR of TRZ-DiPEO$_{164}$Me Hexyl Propiolate (**4.9**, Top @ 125 MHz) and Type 1 15% PVC-TRZ-Hexyl-TRZ-DiPEO$_{164}$Me (**4.11**, Bottom @ 200 MHz)

methylene **f**, attached to the secondary triazole ester, displays a peak at δ 50.4 ppm (Tether-**C**H_2-2°TRZ). The tether methylene two carbons away from the secondary triazole ester **g**, displays a peak at δ 30.0 ppm (Tether-**C**H_2-CH_2-2°TRZ). The methylene **i** two carbons away from the propiolate ester, produces a peak at δ 28.1 ppm (Propiolate Ester-O-C-**C**H_2-Tether). Central hexyl tether carbons **h** are observed at δ 25.2 ppm and δ 25.9 ppm. Secondary triazole ester methylenes **a** (2°TRZ-Ester-O-**C**H_2-C-O) are observed at δ 71.9 ppm and δ 72.5 ppm. Three overlapping peaks at δ 70.5 ppm, δ 70.6 ppm, and δ 70.7 ppm represent centrally located PEO carbons **c**. Regioisomeric methylenes two carbons away from the secondary triazole ester **b** (2°TRZ-Ester-O-C-**C**H_2-O) are noted at δ 68.4 ppm and δ 68.7 ppm. PEO carbons **d** adjacent to the terminal ether oxygen (PEO-**C**H_2-O-CH_3) appear at δ 64.8 and δ 66.0 ppm. The PEO methyl carbon **e** appears at δ 59.0 ppm (PEO-O-**C**H_3).

Type 1 PEO internally plasticized PVC samples did not produce ^{13}C signals corresponding to the primary triazole carbons **K** and **P** (**Figure 4.9**). Likewise, the primary triazole carbonyl **Q** is not observed. However, the peaks corresponding to the secondary triazole carbonyls (**T** and **U**) are observed at δ 158.4 ppm and δ 160.2 ppm. The disappearance of the alkyne quaternary sp-carbon signals **k** and **l** at δ 74.6 ppm and δ 74.7 ppm is indicative of cycloaddition and thorough purification. The hexyl tether carbon **J** directly attached to the primary triazole (PVC-1°TRZ Ester-O-**C**H_2-Tether) produces a significantly weaker signal than the parent alkyne at δ 65.2 ppm, while the methylene two carbons from the primary triazole **I** (PVC-1°TRZ Ester-O-C-**C**H_2-Tether) displays a signal at δ 28.4 ppm, representing a slight downfield shift from the parent alkyne. All other ^{13}C signals in Type 1 PEO internally plasticized PVC are similar to the parent Type 1 PEO alkyne.

4.4 Synthesis of Type 2 Poly(ethylene oxide) Triazole Plasticizer

Protective bromination of the electron-deficient alkyne in acetylenedicarboxylic acid,[12] followed by acid chloride activation[13] was used to generate the Type 2 PEO double hexyl

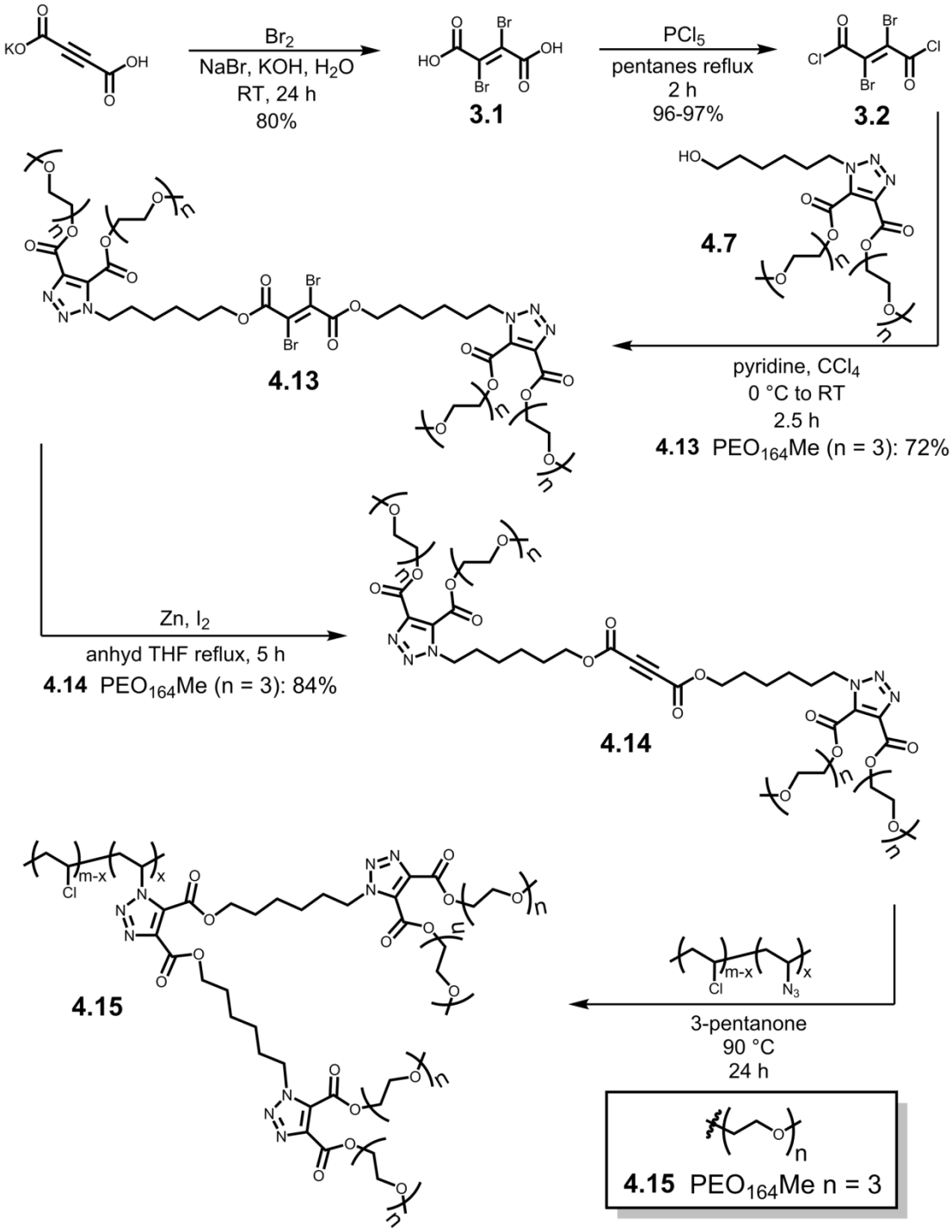

Scheme 4.5 Synthesis of Type 2 PEO Triazole-Plasticizer Attached to PVC

tethered alkyne (**Scheme 4.5**). TRZ-Di($PEO_{164}Me$) hexanol **4.7** was diluted in carbon tetrachloride (CCl_4) and pyridine, then allowed to react with dibromofumaryl chloride **3.2** for 2.5 hours: This furnished the brominated diester **4.13** in 72% yield. Deprotection involved refluxing the protected di-ester with granular zinc and catalytic iodine in anhydrous THF, affording Type 2 PEO alkyne **4.14** in 84% yield after purification via column chromatography. Copper-free azide-alkyne cycloaddition was performed with PVC-azide in 3-pentanone (**Scheme 4.5**). Reactions were carried out at 90 °C for 24 hours, with 3.0 equivalents of alkyne to each equivalent of azide. Cyclizations were monitored *via* FTIR, noting the disappearance of the azide stretch at ~2110 cm^{-1} and the appearance of the triazole sp^2 carbon-carbon stretch at ~1550 cm^{-1}.

^{1}H-NMR spectra of bis(hexyl TRZ-Di$PEO_{164}Me$) acetylenedicarboxylate **4.14** and the Type 2 PEO PVC analogues (PVC-TRZ-DiHexyl-TRZ-Di$PEO_{164}Me$, **4.15**) were acquired (**Figure 4.10**). In $CDCl_3$, bis(hexyl TRZ-Di$PEO_{164}Me$) acetylenedicarboxylate **4.14** gave broadened signals, akin to that observed in Type 0D PEO alkynes. d_6-Benzene produced better splitting patterns: however, PVC-TRZ-DiHexyl-TRZ-Di$PEO_{164}Me$ **4.15** was not soluble in d_6-benzene, making comparative analysis of the precursor and final polymer difficult. As a result, NMR results measured in $CDCl_3$ will be discussed, as alkyne **4.14** and its polymers **4.15** were sufficiently soluble in $CDCl_3$ to give analytically useful spectra. Bis(hexyl TRZ-Di$PEO_{164}Me$) acetylenedicarboxylate methylene protons **j** proximal to the alkyne ester (Alkyne Ester-O-C**H_2**-Tether), give a 4H broad multiplet at δ 4.22 ppm. Type 2 PEO plasticizers containing two hexyl tethers display numerous methylene signals: δ 1.30 – 1.50 ppm are tether protons **h**, δ 1.63 – 1.73 ppm are protons **i**, and δ 1.85 – 1.97 ppm belong to protons **g**. Terminal PEO methyl protons **e** are observed as overlapping signals between δ 3.32 – 3.40 ppm. PEO methylene protons **d** are present between δ 3.49 – 3.57 ppm. Protons originating from central PEO methylenes **c** exhibit signals between δ 3.57 – 3.73 ppm.

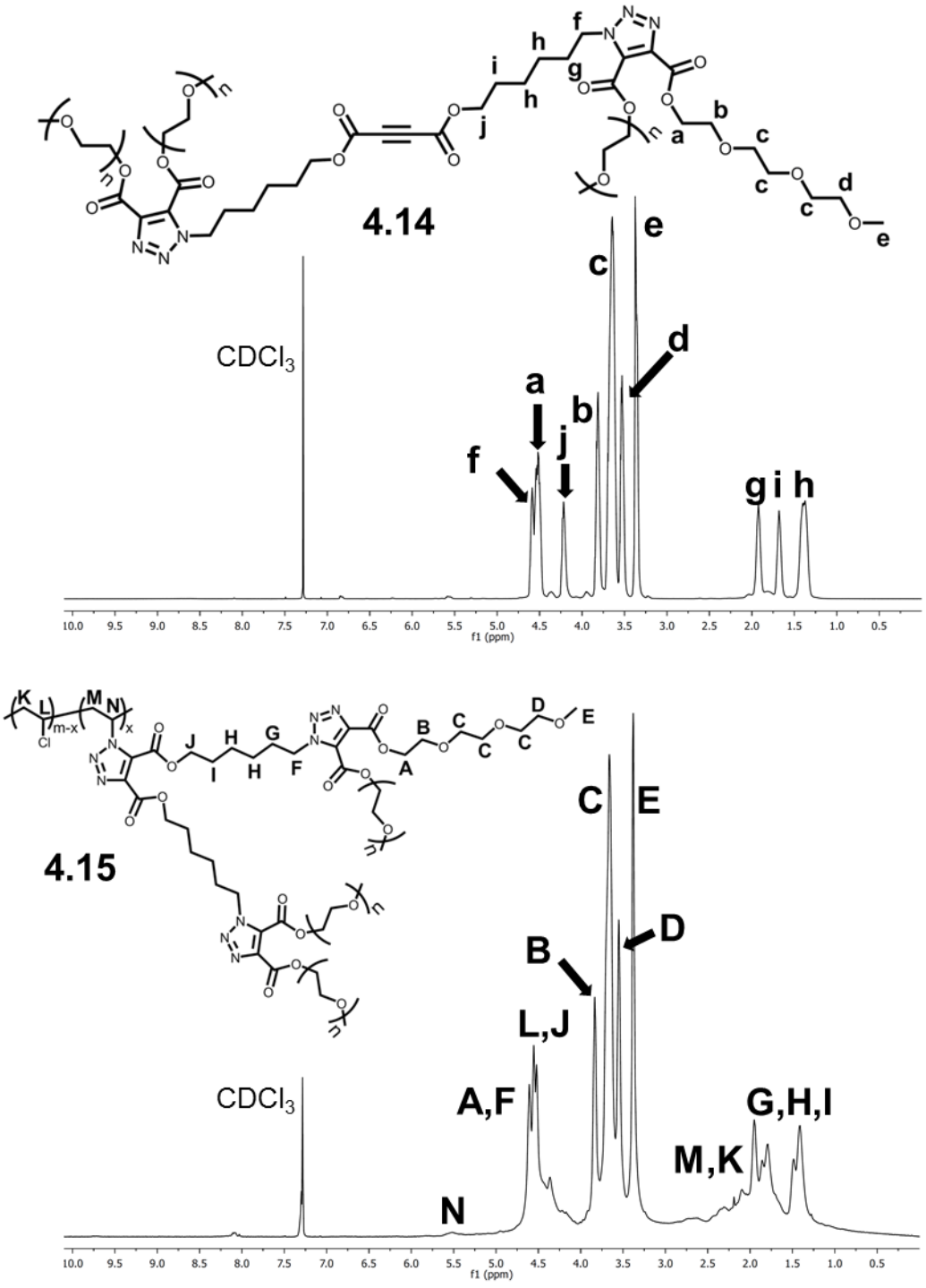

Figure 4.10 ^{1}H-NMR of Bis(Hexyl-TRZ-DiPEO$_{164}$Me) Acetylenedicarboxylate (**4.14**, Top) and Type 2 15% PVC-TRZ-DiHexyl-TRZ-DiPEO$_{164}$Me (**4.15**, Bottom)

Methylene protons **b** two carbons away from the secondary triazole (2°TRZ Ester-O-C-C**H**$_2$-O)appear as a broad multiplet between δ 3.77 and 3.86 ppm. PEO methylene protons **a** directly attached to the secondary triazole ester (2°TRZ Ester-O-C**H**$_2$-C-O) give peaks at δ 4.46 – 4.55 ppm. Methylene protons **f** of the hexyl tether (Tether-C**H**$_2$-2°TRZ) display signals between δ 4.55 – 4.63 ppm.

^{1}H-NMR of Type 2 PEO functionalized PVC **4.15** is presented in **Figure 4.10**. The broad multiplet **J** of the hexyl tether proximal to the primary triazole (PVC-1°TRZ-Ester-O-C**H**$_2$-Tether) demonstrates a significant downfield shift and signal weakening at δ 4.24 – 4.39 ppm, compared to the parent alkyne peak **j** at δ 4.22 ppm. Hexyl tether methylene **I** (PVC-1°TRZ-Ester-O-C-C**H**$_2$-Tether) also moves downfield to δ 1.60 – 1.89 ppm, compared to the parent alkyne. Methylene **F** directly attached to the secondary triazole (PVC-1°TRZ-Tether-C-C**H**$_2$-2°TRZ) gives a broad multiplet between δ 4.58 – 4.67 ppm: this signal overlaps with PEO signal **A** and PVC main chain chlorinated methine **L**. Signal **N** corresponding to the PVC methine covalently bound to the primary triazole (PVC-C**H**-1°TRZ) appears as a broad multiplet between δ 5.35 – 5.65 ppm. All other proton shifts belonging to the PVC main chain (**K** and **M**) are in the same location as unmodified PVC.

^{13}C-NMR of Type 2 PEO alkyne **4.14** displays an upfield shift of the carbonyls adjacent to the alkyne at δ 151.8 ppm, from δ 162.2 ppm as the dibromofumarate (**Figure 4.11**). Likewise, quaternary carbons of the internal alkyne move upfield from δ 112.7 ppm as the brominated sp^2 alkene, to δ 74.7 ppm as the alkyne. Methylene **j** of the hexyl tether (Alkyne Ester-O-**C**H$_2$-C) is present at δ 66.7 ppm. Secondary triazole esters **o** and **p** are observed at δ 158.4 and 160.1 ppm. Secondary triazole quaternary carbons **m** and **n** appear at δ 129.9 and 140.0 ppm. Methylene **f** attached to the secondary triazole ester displays a peak at δ 50.4 ppm (Tether-**C**H$_2$-2°TRZ). Methylene **g** of the hexyl tether, two carbons away from the secondary triazole ester, produce a peak at δ 30.0 ppm (Tether-**C**H$_2$-CH$_2$-2°TRZ), while methylene **i** give a signal at δ 28.0 ppm (Alkyne Ester-O-C-**C**H$_2$-Tether). Central hexyl

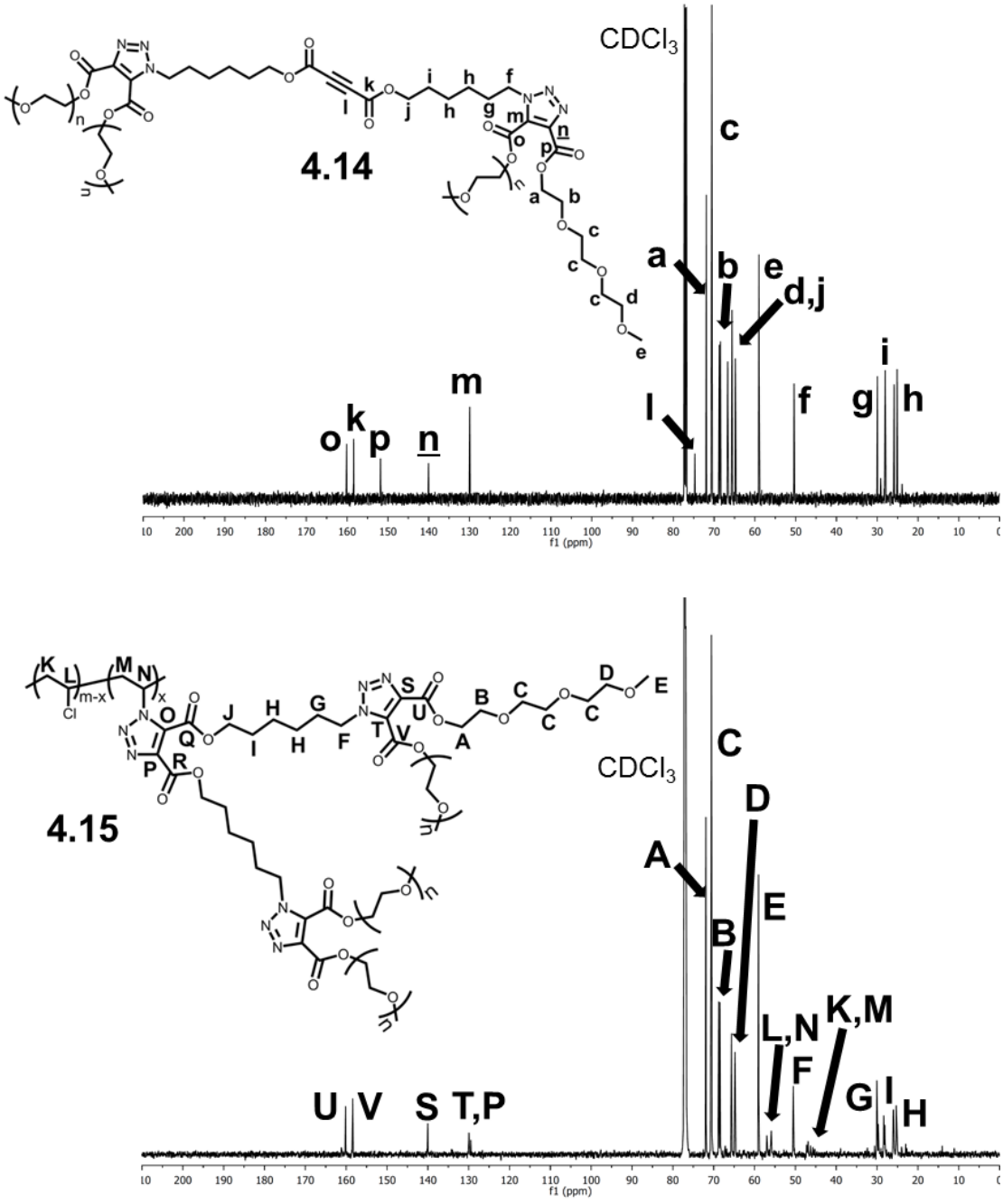

Figure 4.11 ^{13}C-NMR of Bis(Hexyl-TRZ-DiPEO$_{164}$Me) Acetylenedicarboxylate (**4.14**, Top @ 125 MHz) and Type 2 15% PVC-TRZ-DiHexyl-TRZ-DiPEO$_{164}$Me (**4.15**, Bottom @ 200 MHz)

tether carbons **h** are observed at δ 25.1 and 25.9 ppm. Three peaks at δ 70.55, 70.59 and 70.67 ppm represent centrally located PEO carbons **c**. Secondary triazole ester methylene **a** (2°TRZ-Ester-O-**C**H_2-C-O) gives a signal at δ 71.9 ppm. Methylenes **b** two carbons away from the secondary triazole ester (2°TRZ-Ester-O-C-**C**H_2-O) are observed at δ 68.5 and 68.7 ppm. PEO carbons **d** proximal to the terminal ether oxygen (PEO-**C**H_2-O-CH_3) appears at δ 64.8 and 65.6 ppm. PEO methyl carbon **e** displays a peak at δ 59.0 ppm (PEO-**C**H_3).

^{13}C-NMR spectra of PVC functionalized with the Type 2 PEO triazole-plasticizer **4.15** appear similar to the parent acetylenedicarboxylate with a few key differences (**Figure 4.11**). The sterically congested acetylenedicarboxylate containing two hexyl tethers does not display ^{13}C signals originating from the primary triazole carbonyls **Q** and **R**, quaternary carbon **O**, nor hexyl tether methylene **J** (1°TRZ Ester-O-**C**H_2-Tether). However, utilization of a ^{13}C-NMR at 200 MHz equipped with a cryoprobe, produce a primary triazole quaternary carbon signal **P** at δ 129.5 ppm. The remaining hexyl tether carbons **H** (δ 25.2, 25.3, 25.96, 26.0 ppm), **I** (δ 28.1, 28.4 ppm), and **G** (δ 29.7, 30.0 ppm) are observed. The secondary triazole quaternary carbons **S** and **T** (δ 129.9 ppm, 140 ppm) and its associated carbonyl peaks **U** and **V** (δ 158.4 ppm, 160.1 ppm) are also present. The remaining PEO chain signals are similar to the alkyne precursor. Absence of the quaternary sp-carbon signal at δ 74.7 ppm indicates pure internally plasticized PVC samples, free of excess precursor. Main chain PVC carbons remain predominately unaltered relative to the Type 1 PEO system.

4.5 Synthesis of Type 0M Poly(ethylene oxide) Triazole Plasticizer

In a quest to decrease the number of synthetic steps while increasing plasticization efficiency, propiolates of large PEO chains were synthesized (**Scheme 4.6**). PEO with average molecular weights of 1000 g/mol or 2000 g/mol were utilized to incorporate substantial amounts of poly(ethylene oxide) to the primary triazole, while avoiding the use of acetylenedicarboxylic acid required in Type 1 and 2 triazole-plasticizers. A single Fischer

esterification, involving propiolic acid and PEO using catalytic H_2SO_4 and toluene under Dean-Stark conditions gave $PEO_{1000}Me$ propiolate **4.16** and $PEO_{2000}Me$ propiolate **4.17** in yields of 56% and 77%. Cycloadditions to PVC-azide were carried out in the same manner as Type 1 derivatives, furnishing Type 0M PEO plasticized PVC **4.18** and **4.19**. The entire reaction sequence to obtain Type 0M PEO PVC from unmodified PVC requires only three synthetic steps.

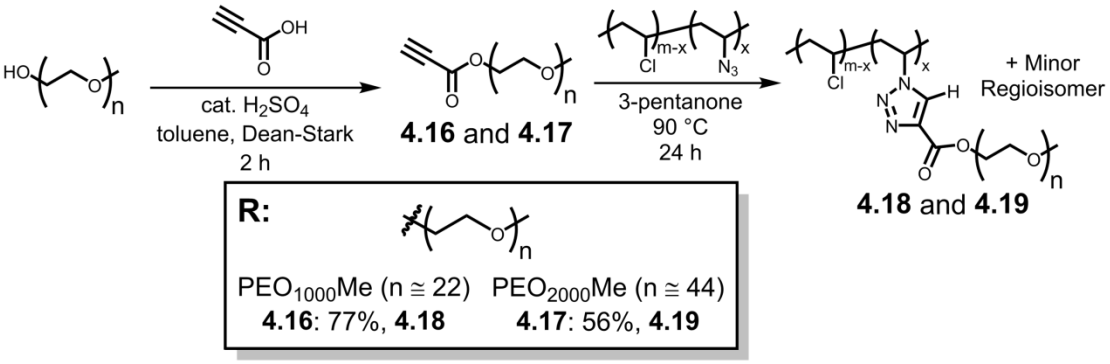

Scheme 4.6 Synthesis of Type 0M PEO Triazole-Plasticizer Attached to PVC

^{1}H-NMR was acquired for Type 0M PEO propiolates and PVC functionalized with both 5 and 15 mole percent Type 0M triazole-plasticizer in $CDCl_3$. For this analysis, $PEO_{1000}Me$ propiolate **4.16** and PVC-TRZ-$PEO_{1000}Me$ **4.18** were chosen as representative Type 0M PEO triazole-plasticizers (**Figure 4.12**). $PEO_{1000}Me$ propiolate gives a broad 2H multiplet between δ 4.32 – 4.37 ppm, corresponding to the ester methylene protons **a** (Propiolate Ester-O-C**H$_2$**-C-O). Another broad 2H multiplet **b** at δ 3.72 – 3.76 ppm is the second methylene from the ester (Propiolate Ester-O-C-C**H$_2$**-O). Central PEO methylene proton signals **c** overlap with each other as an extremely large broad multiplet at δ 3.58 – 3.72 ppm. The PEO methylene protons adjacent to the terminal ether oxygen **d** (PEO-C**H$_2$**-O-CH_3) are represented as another broad 2H multiplet at δ 3.53 – 3.58 ppm. The terminal methyl groups overlap as a singlet **e** at δ 3.35 – 3.42 ppm (PEO-C-O-C**H$_3$**). A 1H singlet **f** at δ 2.99 ppm belongs to the terminal alkyne.

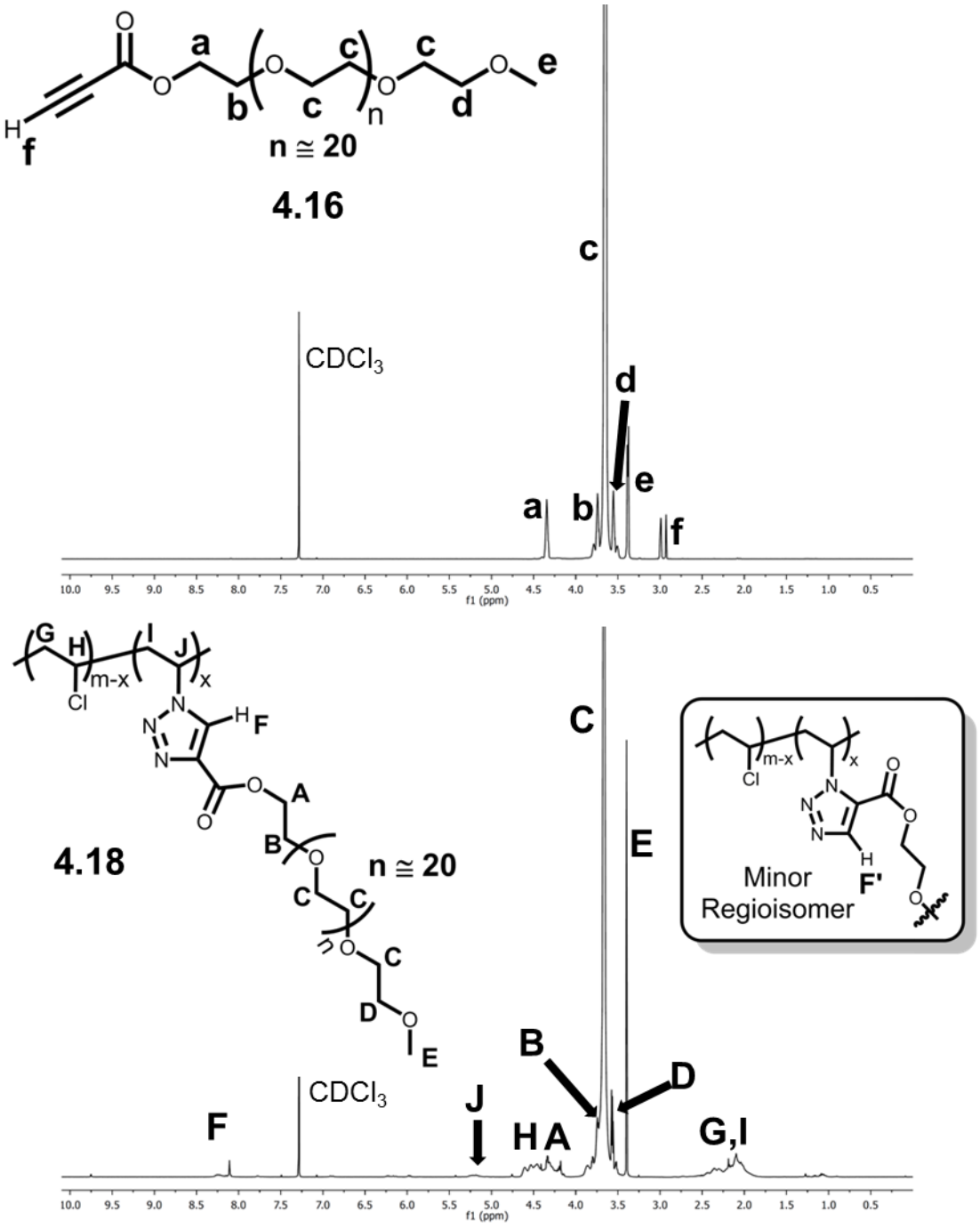

Figure 4.12 ^{1}H-NMR Spectra of PEO_{1000}Me Propiolate (**4.16**, Top) and Type 0M 15% PVC-TRZ-PEO_{1000}Me (**4.18**, Bottom)

The ^{1}H-NMR spectrum of Type 0M PEO internally plasticized PVC gives signals between δ 8.07 – 8.29 ppm, representing the proton directly attached to the primary triazole ring, as **F** in **Figure 4.12** (PVC-1°TRZ-**H**). The two broadened peaks originating from triazole regioisomers observed in Type 1 derivatives are not as pronounced in the Type 0M PEO polymers. The primary triazole ester methylene protons **A** (PVC-1°TRZ-Ester-O-C**H$_2$**) appear in the range of δ 4.50 – 4.56 as a broad multiplet, which overlaps with PVC protons **H**. PEO methylene protons **B** are downfield shifted from the propiolate precursor at δ 3.82 – 3.95 ppm. Central PEO methylene signals **C** (δ 3.59 – 3.82 ppm), methylene protons adjacent to the terminal ether oxygen **D** (δ 3.54 – 3.58 ppm) and PEO methyl groups **E** (δ 3.38 – 3.41 ppm) appear in approximately the same ranges as the alkyne precursor, albeit broadened. The absence of the terminal alkyne proton signal **f** indicates pure Type 0M PEO PVC free of propiolate.

The ^{13}C-NMR spectrum of Type 0M PEO propiolate measured in $CDCl_3$ exhibits an ester carbonyl signal **h** at δ 152.6 ppm (**Figure 4.13**). Alkyne sp-carbons **f** and **g** produce signals at δ 74.5 and 75.3 ppm. Propiolate ester methylene carbons **a** (Propiolate Ester-O-**C**H$_2$-C-O) are present at δ 71.9 ppm. Adjacent methylenes two carbons away from the ester **b** (Propiolate Ester-O-C-**C**H$_2$-O) are observed at δ 68.5 ppm. Large overlapping peaks at δ 70.55, 70.64 and 70.7 ppm represent centrally located PEO methylene carbons **c**. PEO methylene carbons **d** adjacent to the terminal ether oxygen (PEO-**C**H$_2$-O-CH$_3$) appears at δ 65.2 ppm, while the PEO methyl carbon **e** gives a signal at δ 59.0 ppm (PEO-C-O-**C**H$_3$).

The ^{13}C-NMR spectrum of Type 0M PEO internally plasticized PVC displays a primary triazole ester carbonyl signal **L** at δ 161.0 ppm (**L'** minor regioisomer at δ 160.4 ppm), with concomitant quaternary carbon **K** (δ 138.1 ppm) and aromatic triazole carbon **F** (δ 129.7 ppm) as shown in **Figure 4.13**. Regioisomeric methylenes **A** adjacent to the primary triazole ester (1°TRZ Ester-O-**C**H$_2$) are observed at δ 71.9 and δ 72.5 ppm. PEO methylene carbon **B**

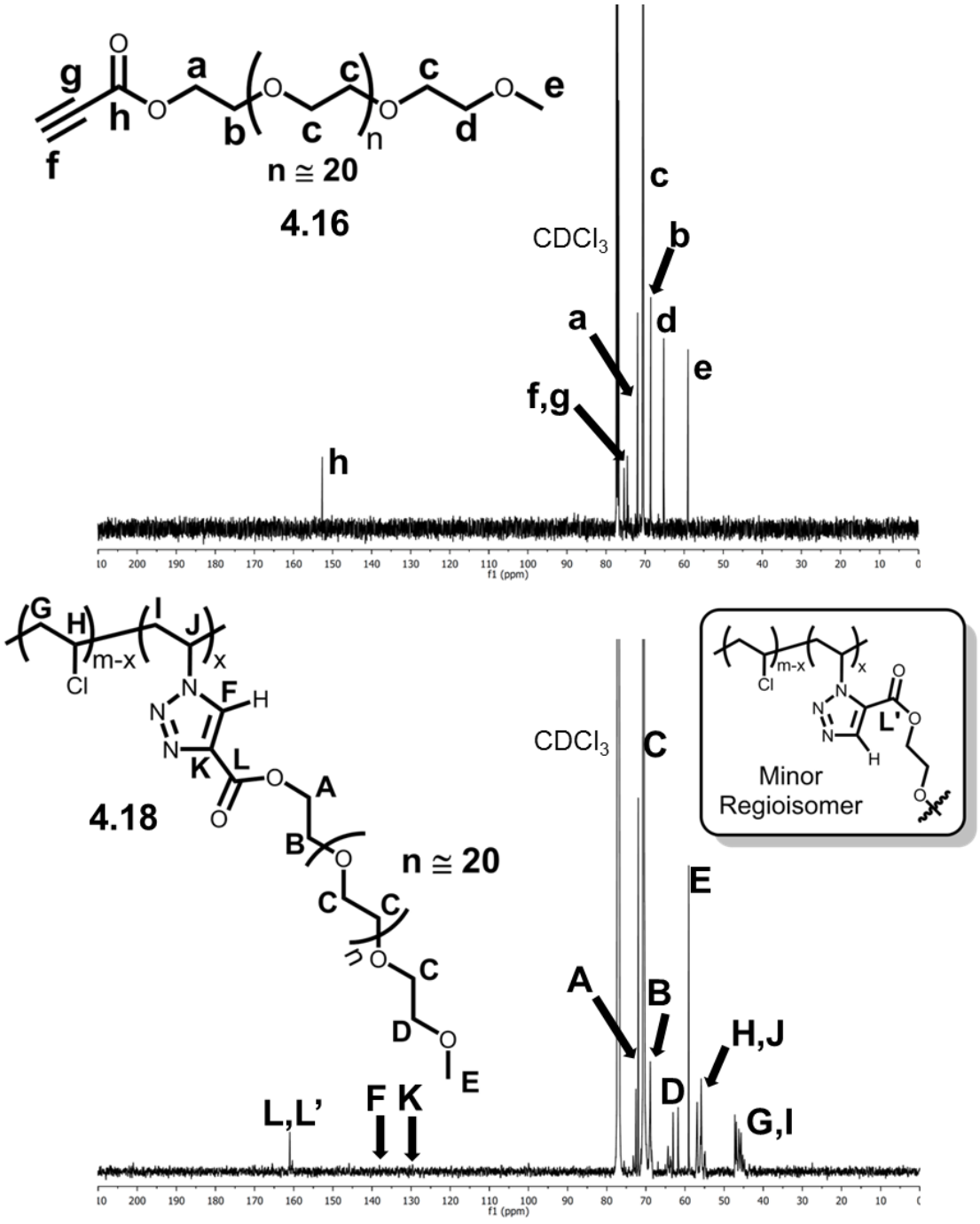

Figure 4.13 ^{13}C-NMR Spectra of PEO_{1000}Me Propiolate (**4.16**, Top @ 125 MHz) and Type 0M 15% PVC-TRZ-PEO_{1000}Me (**4.18**, Bottom @ 200 MHz)

(1°TRZ Ester-O-C-**C**H_2-O) appears at δ 68.9 ppm. PEO methylene carbons **C** produce overlapping signals at δ 70.6 ppm. Carbons **D** next to the terminal ether oxygen (PEO-**C**H_2-O-CH_3) are noted at δ 63.0 and 64.9 ppm. PEO methyl carbons **E** are visible at δ 59.0 and 61.8 ppm (PEO-C-O-**C**H_3). The disappearance of the precursor PEO propiolate sp-carbon signals **f** and **g** (δ 74.5 and 75.3 ppm) is indicative of thorough polymer purification. Main chain PVC carbons remain predominately unaltered relative to the Type 0D PEO system.

4.6 DSC Analysis: 4th Generation PEO Triazole-Plasticizers

All 4th generation polymers contain PEO. Thermal analyses of PVC functionalized with 4th generation triazole-phthalate mimics were performed by our collaborators at IBM Almaden in an analogous fashion to samples internally plasticized by all prior generations of plasticizers. Differential scanning calorimetry (DSC) was performed for each 4th generation polymer to quantitatively determine the degree of plasticization. **Table 4.2** summarizes the T_g values and weight percentages of the 4th generation internally plasticized polymers with unmodified PVC. DSC results of PVC with PEO triazole-plasticizers are illustrated as a bar graph in **Figure 4.14**. Glass transition temperatures versus weight percent plasticizer of 4th generation analogues with DEHP-PVC standards are presented in **Figure 4.15**. DSC data reveals numerous samples with sub-zero glass transition temperatures. Common to all samples displaying sub-zero T_g values are high weight percentages of plasticizer at 15 mole percent functionalization: PVC-TRZ-DiPEO_{350}Me contains the lowest weight percent plasticizer (67.8 Wt% Plasticizer), while PVC-TRZ-PEO_{2000}Me has the highest weight percent plasticizer (84.3 Wt% Plasticizer). Interestingly, Type 1 PVC-TRZ-Hexyl-TRZ-DiPEO_{350}Me at 72.3 weight percent plasticizer displayed a higher than expected glass transition temperature T_g = -1 °C) when compared to its other 4th generation congeners. The closest relative to Type 1 PVC-TRZ-Hexyl-TRZ-DiPEO_{350}Me is another Type 1 analogue, PVC-TRZ-Hexyl-TRZ-DiPEO_{164}Me functionalized with three ethylene oxide repeat units in the PEO chain (T_g = 18 °C, 62.3 Wt% Plasticizer). Other 4th generation plasticizers gave lower glass transition

Polymer	Type	Mol %	Wt % Plasticizer	T_g (°C)
PVC-TRZ-DiPEO$_{164}$Me	0D PEO	5	25.1	61
		15	53.5	42
PVC-TRZ-Hexyl-TRZ-DiPEO$_{164}$Me	1 PEO	5	32.5	57
		15	62.3	18
PVC-TRZ-DiHexyl-TRZ-DiPEO$_{164}$Me	2 PEO	5	47.7	24
		15	75.8	-17
PVC-TRZ-DiPEO$_{350}$Me	0D PEO	5	38.0	49
		15	67.8	-3
PVC-TRZ-Hexyl-TRZ-DiPEO$_{350}$Me	1 PEO	5	43.2	71
		15	72.3	-1
PVC-TRZ-DiPEO$_{550}$Me	0D PEO	5	47.7	27
		15	75.8	-29
PVC-TRZ-PEO$_{1000}$Me	0M PEO	5	45.0	65
		15	73.7	-35
PVC-TRZ-PEO$_{2000}$Me	0M PEO	5	61.0	22
		15	84.3	-42

Table 4.1 Glass Transition Temperatures and Weight Percentages of 4th Generation PEO Triazole Plasticizers

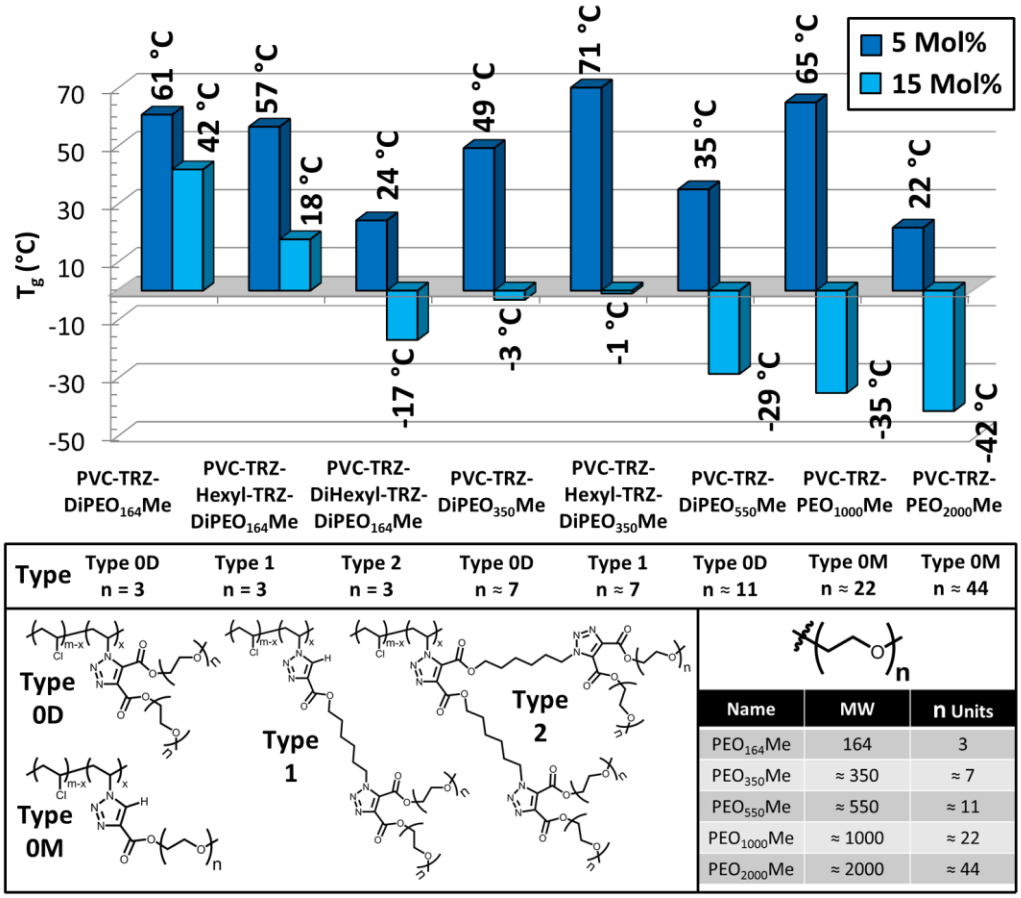

Figure 4.14 DSC Data for 4th Generation PEO Triazole Plasticizers

temperatures than Type 1 PVC-TRZ-Hexyl-TRZ-DiPEO$_{350}$Me with about the same amount of plasticizer. For example, Type 0D PVC-TRZ-DiPEO$_{350}$Me containing less plasticizer by weight (67.8 Wt% Plasticizer) has a glass transition temperature of -3 °C, while PVC-TRZ-DiPEO$_{550}$Me at a marginally higher weight percent plasticizer (75.8 Wt% Plasticizer) exhibits a T_g of -29 °C. Likewise, Type 2 PVC-TRZ-DiHexyl-TRZ-DiPEO$_{164}$Me (T_g= -17 °C, 75.8 Wt% Plasticizer) displays a lower T_g than Type 1 PVC-TRZ-Hexyl-TRZ-DiPEO$_{350}$Me. At 5 mole percent, Type 1 PEO plasticizers displayed anomalous glass transition temperatures: PVC-TRZ-Hexyl-TRZ-DiPEO$_{164}$Me (T_g = 57 °C, 32.5 Wt% Plasticizer) and PVC-TRZ-Hexyl-TRZ-DiPEO$_{350}$Me (T_g = 71 °C, 43.2 Wt% Plasticizer) gave higher T_g values than many of the 4th generation relatives.

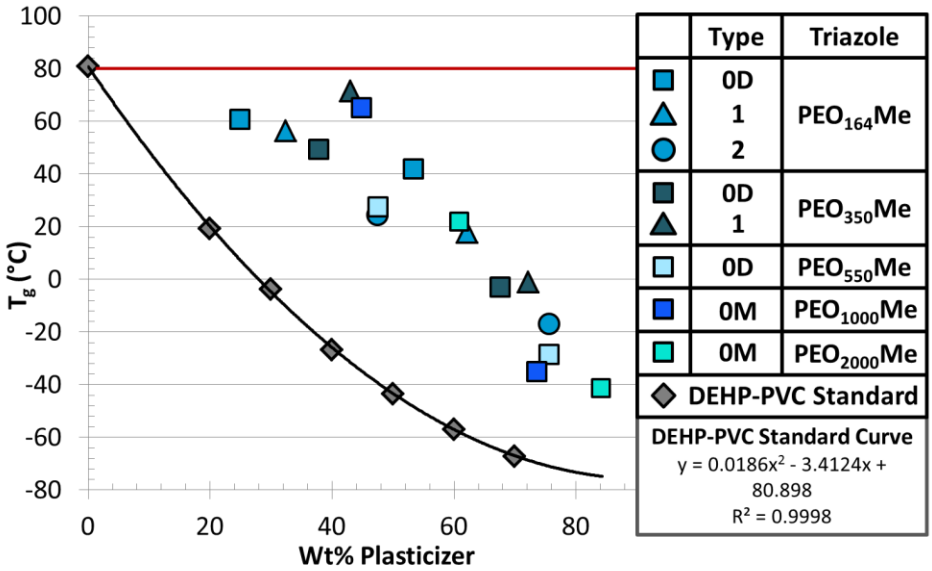

Figure 4.15 Overlay of T_g Values *vs.* Weight Percent of Plasticizer with DEHP-PVC Standard Mixtures and 4th Generation Triazole Plasticizers

Out of all the 4th generation plasticizers synthesized and tested, Type 0M samples PVC-TRZ-PEO$_{1000}$Me (T_g = -35 °C, 73.7 Wt% Plasticizer) and PVC-TRZ-PEO$_{2000}$Me (T_g = -42 °C, 84.3 Wt% Plasticizer) at 15 mole percent gave the lowest glass transition temperatures. Type 0M PVC-TRZ-PEO$_{1000}$Me containing less plasticizer by weight than Type 0D PVC-TRZ-DiPEO$_{550}$Me (T_g = -29 °C, 75.8 Wt% Plasticizer) has a lower T_g (T_g = -35 °C).

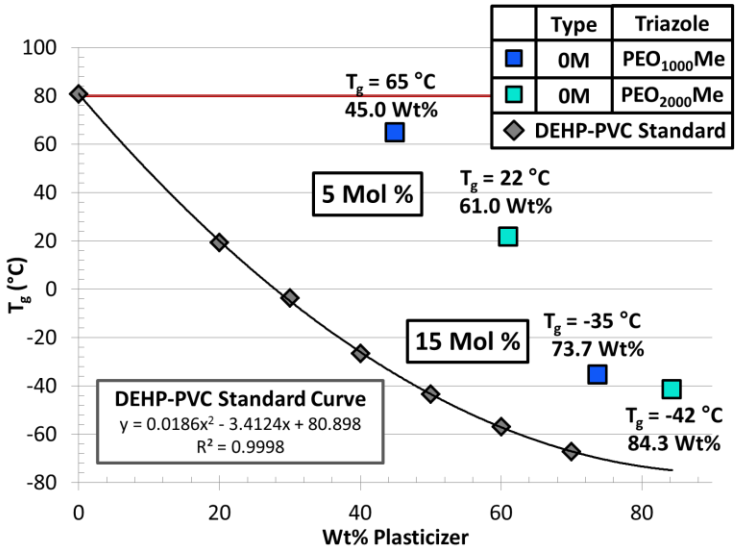

Figure 4.16 Glass Transition Temperatures Versus Weight Percent Plasticizer of Type 0M PEO PVC and DEHP-PVC Standards

A large disparity in glass transition temperatures is noted between Type 0M PVC-TRZ-$PEO_{1000}Me$ and PVC-TRZ-$PEO_{2000}Me$ (**Figure 4.16**). At 5 mole percent, PVC-TRZ-$PEO_{1000}Me$ (T_g = 65 °C, 45.0 Wt% Plasticizer) exhibits a much higher T_g relative to PVC-TRZ-$PEO_{2000}Me$ (T_g = 22 °C, 61.0 Wt% Plasticizer). In contrast, 15 mole percent PVC-TRZ-$PEO_{1000}Me$ (T_g = -35 °C, 73.7 Wt% Plasticizer) displays a similar T_g to PVC-TRZ-$PEO_{2000}Me$ (T_g = -42 °C, 84.3 Wt% Plasticizer). This phenomenon can be explained by the plasticizer weight percentages when utilizing $PEO_{2000}Me$ versus $PEO_{1000}Me$. PVC-TRZ-$PEO_{2000}Me$ has 16.0% more plasticizer by weight than PVC-TRZ-$PEO_{1000}Me$. Increasing the plasticizer molecular weight by the addition of PEO repeat units per triazole anchoring point leads to vastly decreased glass transition temperatures: this highlights the necessity of large molecular weight internal plasticizers with small amounts of covalent attachment points to PVC. As demonstrated by the 15 mole percent Type 0M samples, an increase of anchoring points diminishes the plasticization effect stemming from increased plasticizer molecular weight: the presence of low molecular weight plasticizers is compensated by more covalent attachment points, which incorporates more plasticizer into the PVC matrix.

4.7 Plasticizer Efficiencies: 4th Generation PEO Triazole-Plasticizers Versus DEHP-PVC

Plasticization efficiency ($E\Delta T_g$) values were calculated for 5 mole percent (**Table 4.3**) and 15 mole percent (**Table 4.4**) polymers incorporating 4th generation PEO triazole internal plasticizers. $E\Delta T_g$ values for 4th generation polymers are depicted in **Figure 4.17**.

Polymer	Wt% TRZ	T_g TRZ (°C)	ΔT_g TRZ	DEHP T_g (°C)	ΔT_g DEHP	$E\Delta T_g$	Type
PVC-TRZ-DiHexyl-TRZ-DiPEO$_{164}$Me	47.7	24	56.8	-39.5	120.5	**47.1**	**2 PEO**
PVC-TRZ-DiPEO$_{550}$Me	47.7	27	53.6	-39.5	120.5	**44.5**	**0D PEO**
PVC-TRZ-PEO$_{2000}$Me	61.0	22	59.2	-58.0	139.0	**42.6**	**0M PEO**
PVC-TRZ-DiPEO$_{350}$Me	38.0	49	31.8	-21.9	102.9	**30.9**	**0D PEO**
PVC-TRZ-DiPEO$_{164}$Me	25.1	61	20.3	7.0	74.0	**27.5**	**0D PEO**
PVC-TRZ-Hexyl-TRZ-DiPEO$_{164}$Me	32.5	57	24.5	-10.3	91.2	**26.8**	**1 PEO**
PVC-TRZ-PEO$_{1000}$Me	45.0	65	16.1	-34.9	115.9	**13.9**	**0M PEO**
PVC-TRZ-Hexyl-TRZ-DiPEO$_{350}$Me	43.1	71	9.5	-31.7	112.7	**8.5**	**1 PEO**

Table 4.3 Plasticization Efficiencies of 5 Mol % 4th Generation PEO Internally Plasticized PVC Ranked By Descending $E\Delta T_g$ Values

Polymer	Wt% TRZ	T_g TRZ (°C)	ΔT_g TRZ	DEHP T_g (°C)	ΔT_g DEHP	$E\Delta T_g$	Type
PVC-TRZ-PEO$_{2000}$Me	84.3	-42	122.5	-74.6	155.6	**78.7**	**0M PEO**
PVC-TRZ-PEO$_{1000}$Me	73.7	-35	116.3	-69.6	150.6	**77.2**	**0M PEO**
PVC-TRZ-DiPEO$_{550}$Me	75.8	-29	109.7	-70.9	151.8	**72.2**	**0D PEO**
PVC-TRZ-DiHexyl-TRZ-DiPEO$_{164}$Me	75.8	-17	98.0	-70.9	151.8	**64.5**	**2 PEO**
PVC-TRZ-DiPEO$_{350}$Me	67.8	-3	84.1	-65.0	145.9	**57.7**	**0D PEO**
PVC-TRZ-Hexyl-TRZ-DiPEO$_{350}$Me	72.3	-1	82.0	-68.6	149.5	**54.8**	**1 PEO**
PVC-TRZ-Hexyl-TRZ-DiPEO$_{164}$Me	62.3	18	63.3	-59.5	140.4	**45.1**	**1 PEO**
PVC-TRZ-DiPEO$_{164}$Me	53.5	42	39.2	-48.4	129.4	**30.3**	**0D PEO**

Table 4.4 Plasticization Efficiencies of 15 Mol % 4th Generation PEO Internally Plasticized PVC Ranked By Descending $E\Delta T_g$ Values

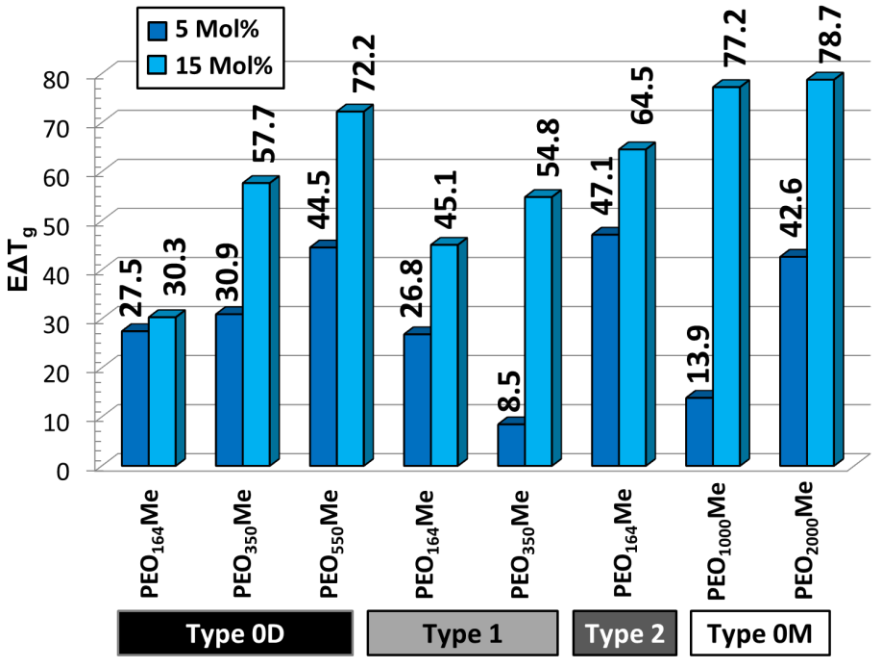

Figure 4.17 Efficiency Values ($E\Delta T_g$) of 4th Generation Internally Plasticized PVC

At 5 mole percent, Type 2 PVC-TRZ-DiHexyl-TRZ-DiPEO$_{164}$Me gives the highest $E\Delta T_g$ value ($E\Delta T_g$ = 47.1). Type 0D PVC-TRZ-DiPEO$_{550}$Me ($E\Delta T_g$ = 44.5) and Type 0M PVC-TRZ-PEO$_{2000}$Me ($E\Delta T_g$ = 42.6) furnished similar plasticization efficiency values to the Type 2 PEO sample. A notable efficiency decrease in Type 0D PVC-TRZ-DiPEO$_{350}$Me ($E\Delta T_g$ = 30.9) represents an 11.7% drop compared to Type 0M PVC-TRZ-PEO$_{2000}$Me. Type 0D PVC-TRZ-DiPEO$_{164}$Me ($E\Delta T_g$ = 27.5) has a similar $E\Delta T_g$ to its relative, PVC-TRZ-DiPEO$_{350}$Me. Type 1 PVC-TRZ-Hexyl-TRZ-DiPEO$_{164}$Me possessing three ethylene oxide repeat units, gives an efficiency value of 26.8. A significantly worse $E\Delta T_g$ was calculated for PVC-TRZ-PEO$_{1000}$Me ($E\Delta T_g$ = 13.9), representing a 13.0% decrease from PVC-TRZ-Hexyl-TRZ-DiPEO$_{164}$Me. The lowest efficiency value belongs to Type 1 PVC-TRZ-Hexyl-TRZ-DiPEO$_{350}$Me ($E\Delta T_g$ = 8.5) with approximately 7 to 8 ethylene oxide repeat units. Its analogue, Type 1 PVC-TRZ-Hexyl-TRZ-DiPEO$_{164}$Me, is 18.4% more efficient.

Miscibility of the internal plasticizer plays a key role in its ability to soften PVC. While Type 1 PVC-TRZ-Hexyl-TRZ-DiPEO$_{350}$Me contains a greater mass of plasticizer than PVC-

TRZ-Hexyl-TRZ-DiPEO$_{164}$Me, the longer PEO chain does not necessarily equate to better efficiencies and depressed glass transition temperatures, especially when functionalized at 5 mole percent. In externally plasticized polyether-based systems,[6] miscibility with PVC plays a major role in how efficiently an emollient engenders flexibility.[7] The increase in ethylene oxide repeat units in combination with the hexyl tether may decrease the compatibility of the Type 1 PEO plasticizers with PVC.[6] In addition, the diminished presence of chain ends with respect to the increasing size of the PEO chains in the polymer may contribute to elevated glass transition temperatures and significant decreases in $E\Delta T_g$: the scarcity of chain ends may impede the ability of these Type 1 PEO plasticizers to optimally generate space between PVC chains at 5 mole percent in PVC-TRZ-Hexyl-TRZ-DiPEO$_{164}$Me and PVC-TRZ-Hexyl-TRZ-DiPEO$_{350}$Me.

At 15 mole percent, Type 0M PVC-TRZ-PEO$_{2000}$Me ($E\Delta T_g$ = 78.7) and PVC-TRZ-PEO$_{1000}$Me ($E\Delta T_g$ = 77.2) exhibited the two highest $E\Delta T_g$ values of all 4th generation PEO triazole-plasticizers. Type 0D PVC-TRZ-DiPEO$_{550}$Me ($E\Delta T_g$ = 72.2) gave the next highest efficiency value, followed by Type 2 PVC-TRZ-DiHexyl-TRZ-DiPEO$_{164}$Me ($E\Delta T_g$ = 64.5) and Type 0D PVC-TRZ-DiPEO$_{350}$Me ($E\Delta T_g$ = 57.7). Type 1 PVC-TRZ-Hexyl-TRZ-DiPEO$_{350}$Me ($E\Delta T_g$ = 54.8) and PVC-TRZ-Hexyl-TRZ-DiPEO$_{164}$Me ($E\Delta T_g$ = 45.1) reveal inverted efficiency values compared to their 5 mole percent analogues. Finally, Type 0D PVC-TRZ-DiPEO$_{164}$Me ($E\Delta T_g$ = 30.3) displays the lowest plasticization efficiency value of the 4th generation plasticizers at 15 mole percent.

Branching at the PVC backbone appears to be imperative to enhanced plasticization efficiencies at 5 mole percent. Type 2 PVC-TRZ-DiHexyl-TRZ-DiPEO$_{164}$Me ($E\Delta T_g$ = 47.1), containing two hexyl tethers and PEO chains with three repeat units proved more efficient than Type 0D PVC-TRZ-DiPEO$_{550}$Me ($E\Delta T_g$ = 44.5) and Type 0M PVC-TRZ-PEO$_{2000}$Me ($E\Delta T_g$ = 42.6). Analyzing the structural Type of these PEO plasticizers, Type 0D TRZ-DiPEO$_{550}$Me is branched at the primary triazole with two PEO$_{550}$Me chains, while Type 0M

TRZ-PEO_{2000}Me is functionalized with a single PEO chain and is comparatively linear. The high weight percentage of internal plasticizer in PVC-TRZ-PEO_{2000}Me (61.0 Wt% Plasticizer) compared to PVC-TRZ-DiPEO_{550}Me (47.7 Wt% Plasticizer) compensates for the lack of branching at the primary triazole, yielding similar T_g values. The next two most efficient samples were also branched Type 0D PEO plasticizers. In contrast, the samples with the lowest efficiencies are Type 1 and Type 0M. Inversion of $E\Delta T_g$ values between Type 1 PEO samples at 5 and 15 mole percent plasticizer illustrates that at different levels of functionalization, branching and long PEO chains are required to impart enhanced plasticization efficiencies. At 5 mole percent, compatibility of TRZ-Hexyl-TRZ-DiPEO_{164}Me may be better than that of TRZ-Hexyl-TRZ-DiPEO_{350}Me, while at 15 mole percent, the plasticizer mass increase between TRZ-Hexyl-TRZ-DiPEO_{350}Me (72.3 Wt% Plasticizer) and TRZ-Hexyl-TRZ-DiPEO_{164}Me (62.3 Wt% Plasticizer) takes precedence. The hexyl-tether does not seem to be essential in enhancing plasticization efficiency in PEO-functionalized triazole-plasticizers at 5 mole percent. However, a synergism of primary triazole branching and the hexyl-tether in Type 2 PVC-TRZ-DiHexyl-TRZ-DiPEO_{164}Me gives the best $E\Delta T_g$ value, showing that the optimal internal plasticizer design contains a combination of these structural attributes.

In contrast, at 15 mole percent, high plasticizer molecular weight per anchoring unit takes precedence over structural branching. Long PEO chains are present in the top three samples. The highest $E\Delta T_g$ values belong to Type 0M PEO polymers. Compared to Type 0D TRZ-DiPEO_{550}Me ($E\Delta T_g$ = 72.2), a 7.7% $E\Delta T_g$ decrease in Type 2 PVC-TRZ-DiHexyl-TRZ-DiPEO_{164}Me ($E\Delta T_g$ = 64.5) shows that while branching at the primary triazole is key in enhancing plasticizing efficiency, the relative amount of PEO incorporated into the plasticizer is more important at high mole percentages.

4.8 Cumulative Thermal Analysis and Plasticizer Efficiencies: Triazole-Based Internally Plasticized PVC Versus DEHP-PVC

DSC results of all PVC samples containing triazole-plasticizers are illustrated in **Figure 4.18**. Glass transition temperatures versus weight percent plasticizer of the 4th generation analogues with DEHP-PVC standards are presented in **Figure 4.19**. Cumulative T_g values and weight percentages for all generations of plasticizer are listed in **Table 4.5**. $E\Delta T_g$ values for all samples are given in **Table 4.6** and **Table 4.7**. $E\Delta T_g$ values for PVC samples plasticized by all generations of triazole emollients are depicted in **Figure 4.20**.

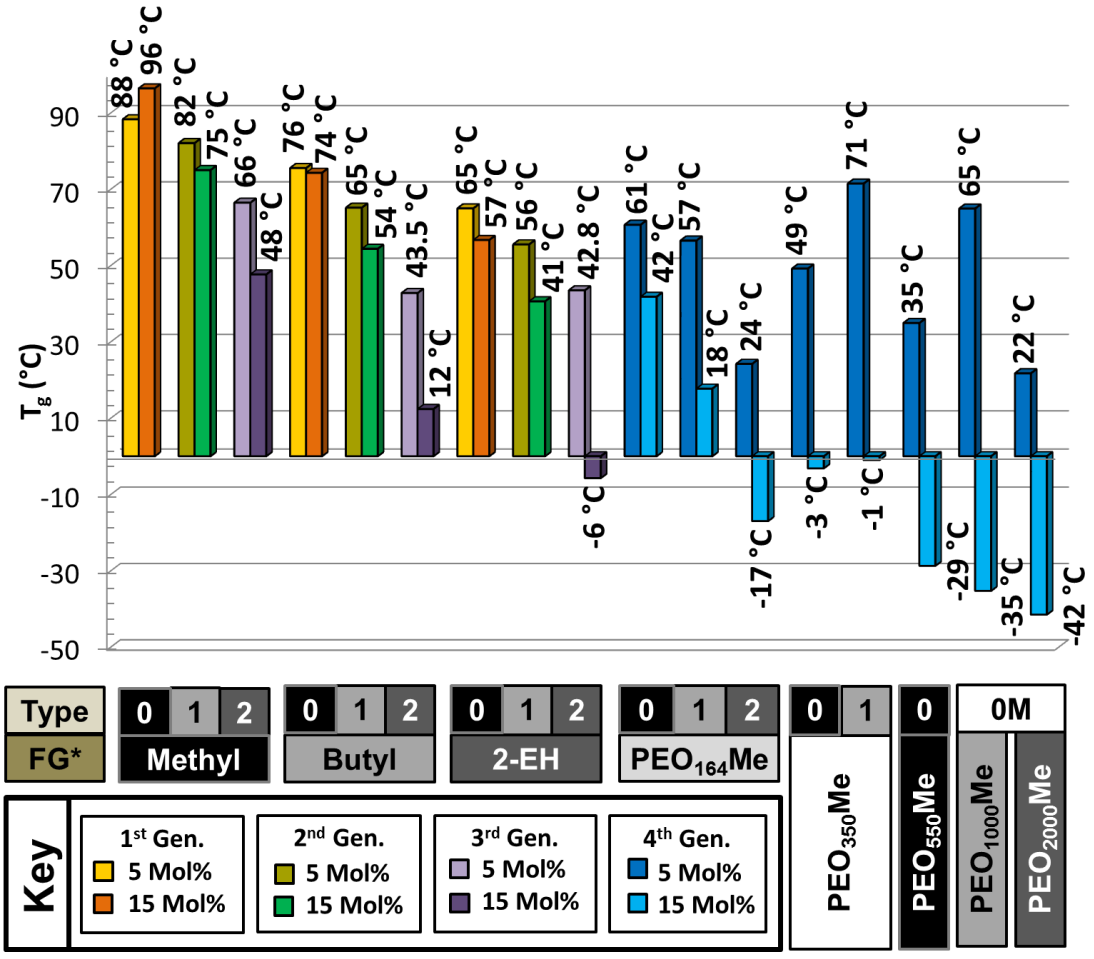

Figure 4.18 DSC Data for All Triazole Internally Plasticized PVC
(**FG = Functional Group*)

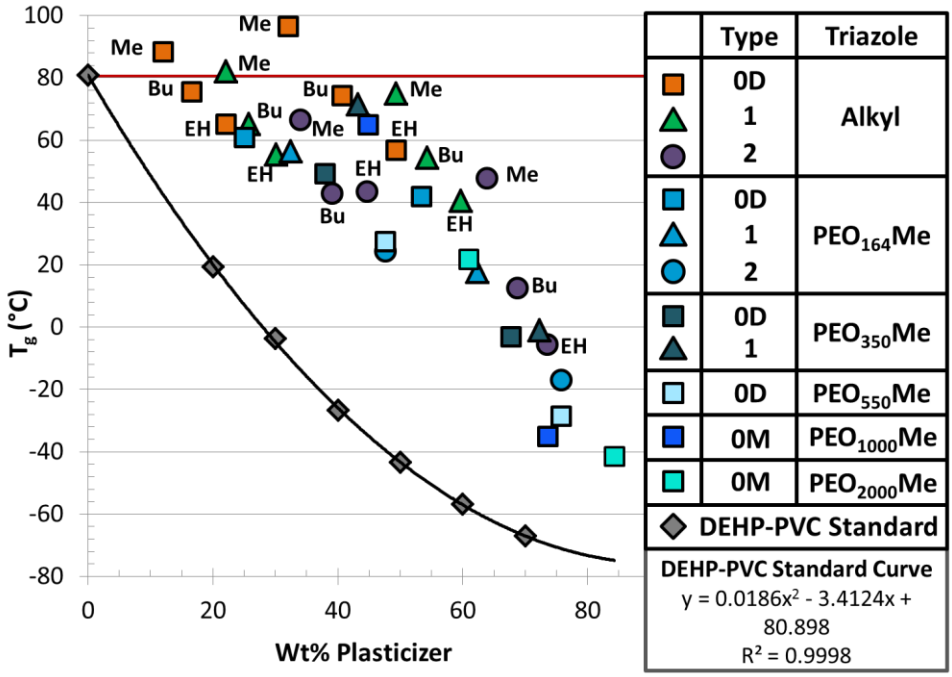

Figure 4.19 T_g Values Versus Weight Percent Plasticizer with DEHP-PVC Standard Mixtures and All Triazole Internally Plasticized PVC

As a whole, the triazole-plasticizer systems exhibiting higher efficiencies favor poly(ethylene oxide) moieties. For Type 0D PVC-TRZ-DiMe containing only methyl ester groups (at 5 and 15 mole percent triazole), significant *anti*-plasticization is observed (T_g = 88 °C and 96 °C). At 5 mole percent, PVC-TRZ-DiMe displays an $E\Delta T_g$ of -19.0, and -17.1 at 15 mole percent. This is due to the rigid aromatic nature of the primary triazole anchor: π-π stacking of these triazole rings in the three-dimensional matrix of PVC can impart crystallization and stiffness to the modified polymer. DSC data gathered from PVC samples containing Type 0D alkyl emollients implies that plasticization occurs, albeit less efficiently, due to the inability to move about the polymeric matrix, stemming from anchoring the short alkyl plasticizing motifs directly to PVC. When utilizing alkyl groups, long, bulky, sterically hindered chains are necessary to obtain lower glass transition temperatures. This is apparent with the 1st generation Type 0D PVC-TRZ-DiEH ($E\Delta T_g$ 5 Mol% = 24.1 and $E\Delta T_g$ 15 Mol% = 19.7) showing improved plasticizing efficacy over PVC-TRZ-DiBu ($E\Delta T_g$ 5 Mol% = 10.5 and $E\Delta T_g$ 15 Mol% = 6.2). The 4th generation Type 0D PEO system exhibits significant enhancements in plasticization efficiencies compared to the 1st generation Type 0D alkyl

Gen.	Polymer	Mol %	Wt %	T_g (°C)	Type	FG*
4	PVC-TRZ-PEO_{2000}Me	15	84.3	-42	0M	PEO
4	PVC-TRZ-PEO_{1000}Me	15	73.7	-35	0M	PEO
4	PVC-TRZ-DiPEO_{550}Me	15	75.8	-29	0D	PEO
4	PVC-DiHexyl-TRZ-DiPEO_{164}Me	15	75.8	-17	2	PEO
3	PVC-DiHexyl-TRZ-DiEH	15	73.5	-6	2	Alkyl
4	PVC-TRZ-DiPEO_{350}Me	15	67.8	-3	0D	PEO
4	PVC-TRZ-Hexyl-TRZ-DiPEO_{350}Me	15	72.3	-1	1	PEO
3	PVC-TRZ-DiHexyl-TRZ-DiBu	15	68.8	12	2	Alkyl
4	PVC-TRZ-Hexyl-TRZ-DiPEO_{164}Me	15	62.3	18	1	PEO
4	PVC-TRZ-PEO_{2000}Me	5	61.0	22	0M	PEO
4	PVC-TRZ-DiHexyl-TRZ-DiPEO_{164}Me	5	47.7	24	2	PEO
4	PVC-TRZ-DiPEO_{550}Me	5	47.7	27	0D	PEO
2	PVC-TRZ-Hexyl-TRZ-DiEH	15	59.6	41	1	Alkyl
4	PVC-TRZ-DiPEO_{164}Me	15	53.5	42	0D	PEO
3	PVC-TRZ-DiHexyl-TRZ-DiBu	5	39.1	42.8	2	Alkyl
3	PVC-TRZ-DiHexyl-TRZ-DiEH	5	44.7	43.5	2	Alkyl
3	PVC-TRZ-DiHexyl-TRZ-DiMe	15	63.9	48	2	Alkyl
4	PVC-TRZ-DiPEO_{350}Me	5	38.0	49	0D	PEO
2	PVC-TRZ-Hexyl-TRZ-DiBu	15	54.3	54	1	Alkyl
2	PVC-TRZ-Hexyl-TRZ-DiEH	5	30.1	56	1	Alkyl
4	PVC-TRZ-Hexyl-TRZ-DiPEO_{164}Me	5	32.5	57	1	PEO
1	PVC-TRZ-DiEH	15	49.4	57	0D	Alkyl
4	PVC-TRZ-DiPEO_{164}Me	5	25.1	61	0D	PEO
4	PVC-TRZ-PEO_{1000}Me	5	45.0	65	0M	PEO
1	PVC-TRZ-DiEH	5	22.1	65	0D	Alkyl
2	PVC-TRZ-Hexyl-TRZ-DiBu	5	25.7	65	1	Alkyl
3	PVC-TRZ-DiHexyl-TRZ-DiMe	5	34.0	66	2	Alkyl
4	PVC-TRZ-Hexyl-TRZ-DiPEO_{350}Me	5	43.1	71	1	PEO
1	PVC-TRZ-DiBu	15	40.8	74	0D	Alkyl
2	PVC-TRZ-Hexyl-TRZ-DiMe	15	49.3	75	1	Alkyl
1	PVC-TRZ-DiBu	5	16.7	76	0D	Alkyl
2	PVC-TRZ-Hexyl-TRZ-DiMe	5	22.1	82	1	Alkyl
1	PVC-TRZ-DiMe	5	12.1	88	0D	Alkyl
1	PVC-TRZ-DiMe	15	32.1	96	0D	Alkyl

Table 4.5 Glass Transition Temperatures of All Triazole Internally Plasticized PVC Ordered By Ascending T_g Values
(**FG = Functional Group*)

Gen.	Polymer	Wt %	T_g (°C)	EΔT_g	Type	FG*
4	PVC-TRZ-DiHexyl-TRZ-DiPEO$_{164}$Me	47.7	24	47.1	2	PEO
4	PVC-TRZ-DiPEO$_{550}$Me	47.7	27	44.5	0D	PEO
4	PVC-TRZ-PEO$_{2000}$Me	61.0	22	42.6	0M	PEO
3	PVC-TRZ-DiHexyl-TRZ-DiBu	39.1	42.8	36.4	2	Alkyl
3	PVC-TRZ-DiHexyl-TRZ-DiEH	44.7	43.5	32.5	2	Alkyl
4	PVC-TRZ-DiPEO$_{350}$Me	38.0	49	30.9	0D	PEO
2	PVC-TRZ-Hexyl-TRZ-DiEH	30.1	56	29.7	1	Alkyl
4	PVC-TRZ-DiPEO$_{164}$Me	25.1	61	27.5	0D	PEO
4	PVC-TRZ-Hexyl-TRZ-DiPEO$_{164}$Me	32.5	57	26.8	1	PEO
1	PVC-TRZ-DiEH	22.1	65	24.1	0D	Alkyl
2	PVC-TRZ-Hexyl-TRZ-DiBu	25.7	65	21.0	1	Alkyl
3	PVC-TRZ-DiHexyl-TRZ-DiMe	34.0	66	15.4	2	Alkyl
4	PVC-TRZ-PEO$_{1000}$Me	45.0	65	13.9	0M	PEO
1	PVC-TRZ-DiBu	16.7	76	10.5	0D	Alkyl
4	PVC-TRZ-Hexyl-TRZ-DiPEO$_{350}$Me	43.1	71	8.5	1	PEO
2	PVC-TRZ-Hexyl-TRZ-DiMe	22.1	82	-1.6	1	Alkyl
1	PVC-TRZ-DiMe	12.1	88	-19.0	0D	Alkyl

Table 4.6 Plasticization Efficiencies of All 5 Mol% Triazole Internally Plasticized PVC Ranked By Descending EΔT_g Values
(**FG = Functional Group*)

Gen.	Polymer	Wt %	T_g (°C)	EΔT_g	Type	FG*
4	PVC-TRZ-PEO$_{2000}$Me	84.3	-42	78.7	0M	PEO
4	PVC-TRZ-PEO$_{1000}$Me	73.7	-35	77.2	0M	PEO
4	PVC-TRZ-DiPEO$_{550}$Me	75.8	-29	72.2	0D	PEO
4	PVC-TRZ-DiHexyl-TRZ-DiPEO$_{164}$Me	75.8	-17	64.5	2	PEO
4	PVC-TRZ-DiPEO$_{350}$Me	67.8	-3	57.7	0D	PEO
3	PVC-TRZ-DiHexyl-TRZ-DiEH	73.5	-6	57.6	2	Alkyl
4	PVC-TRZ-Hexyl-TRZ-DiPEO$_{350}$Me	72.3	-1	54.8	1	PEO
3	PVC-TRZ-DiHexyl-TRZ-DiBu	68.8	12	46.7	2	Alkyl
4	PVC-TRZ-Hexyl-TRZ-DiPEO$_{164}$Me	62.3	18	45.1	1	PEO
4	PVC-TRZ-DiPEO$_{164}$Me	53.5	42	30.3	0D	PEO
2	PVC-TRZ-Hexyl-TRZ-DiEH	59.6	41	29.4	1	Alkyl
3	PVC-TRZ-DiHexyl-TRZ-DiMe	63.9	48	23.4	2	Alkyl
2	PVC-TRZ-Hexyl-TRZ-DiBu	54.3	54	20.4	1	Alkyl
1	PVC-TRZ-DiEH	49.4	57	19.7	0D	Alkyl
1	PVC-TRZ-DiBu	40.8	74	6.2	0D	Alkyl
2	PVC-TRZ-Hexyl-TRZ-DiMe	49.3	75	4.9	1	Alkyl
1	PVC-TRZ-DiMe	32.1	96	-17.1	0D	Alkyl

Table 4.7 Plasticization Efficiencies of All 15 Mol% Triazole Internally Plasticized PVC Ranked By Descending EΔT_g Values
(**FG = Functional Group*)

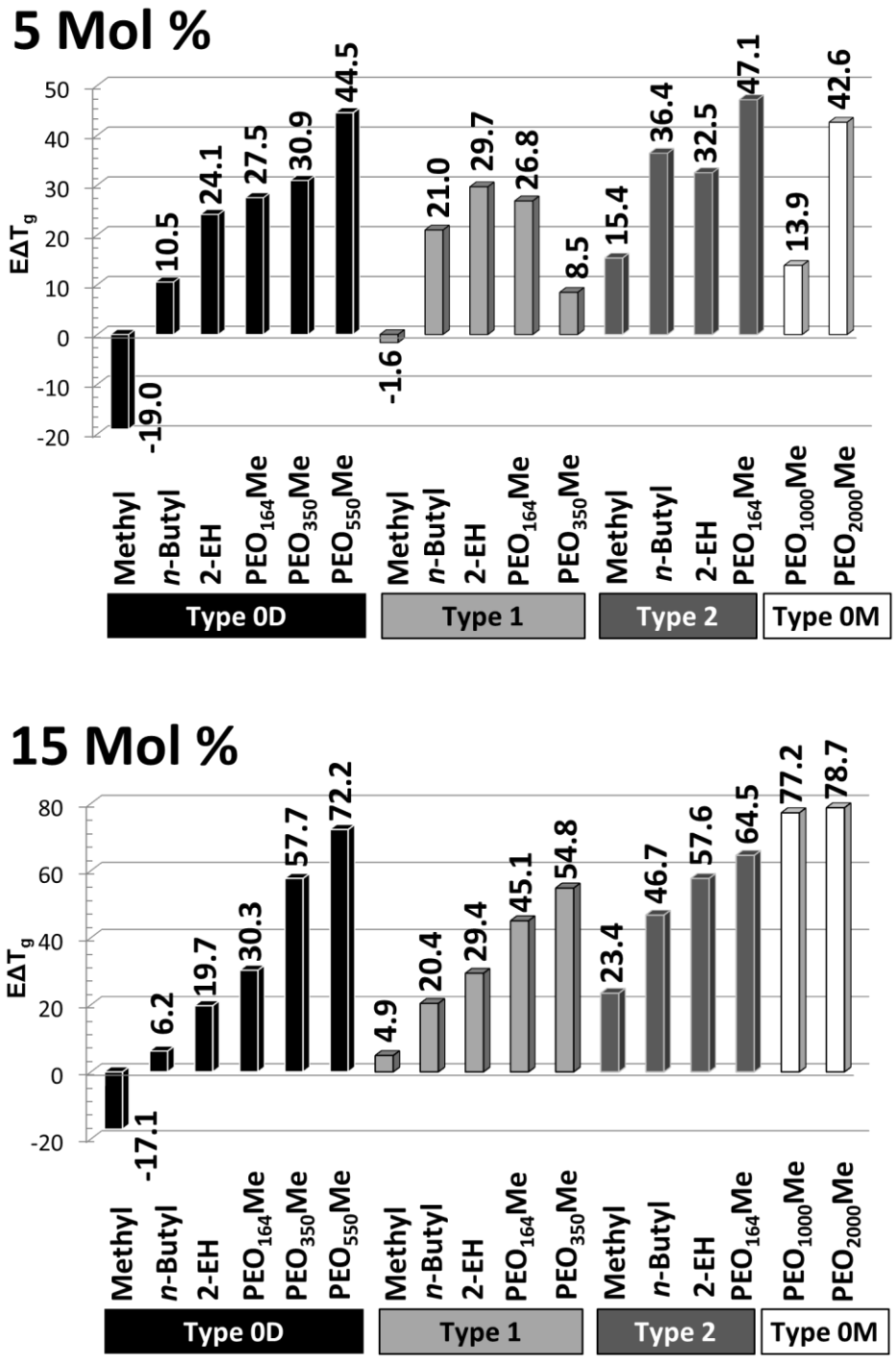

Figure 4.20 Efficiency Values of All Triazole Internally Plasticized PVC
Top: 5 Mol % $E\Delta T_g$ Values Grouped by Type
Bottom: 15 Mol % $E\Delta T_g$ Values Grouped by Type

analogues. PVC-TRZ-DiPEO$_{164}$Me, with three ethylene oxide repeat units, give EΔT_g values of 27.5 at 5 mole percent and 30.3 at 15 mole percent, while PVC-TRZ-DiPEO$_{350}$Me (EΔT_g 5 Mol% = 30.9 and EΔT_g 15 Mol% = 57.7) and PVC-TRZ-DiPEO$_{550}$Me (EΔT_g 5 Mol% = 44.5 and EΔT_g 15 Mol% = 72.2) displays EΔT_g values surpassing all Type 0D alkyl derivatives. Longer PEO chains improves plasticization efficacy, which is further amplified at higher mole percentages.

The Type 1 system containing a single hexyl tether enhanced the efficacy of the triazole-plasticizers over the Type 0D emollients. This is presumably due to the space created between PVC and the secondary triazole, which was designed to maximize the mobility of the plasticizer amongst the polymeric matrix. Out of the 2nd generation Type 1 alkyl derivatives, PVC-TRZ-Hexyl-TRZ-DiEH possesses the highest efficiency values (EΔT_g 5 Mol% = 29.7 and EΔT_g 15 Mol% = 29.4) over the *n*-butyl and methyl relatives. Type 1 PVC-TRZ-Hexyl-TRZ-DiEH shows improvement over the Type 0D predecessor, PVC-TRZ-DiEH, notably at 15 mole percent. The anti-plasticization effect of the rigid primary triazole directly on PVC is quelled with the addition of the hexyl tether. Comparatively, at 5 mole percent, Type 1 PEO samples PVC-TRZ-Hexyl-TRZ-DiPEO$_{164}$Me (EΔT_g 5 Mol% = 26.8) and PVC-TRZ-Hexyl-TRZ-DiPEO$_{350}$Me (EΔT_g 5 Mol% = 8.5) are less efficient than PVC-TRZ-Hexyl-TRZ-DiEH. Nonetheless, efficiencies are restored at 15 mole percent with both PVC-TRZ-Hexyl-TRZ-DiPEO$_{164}$Me (EΔT_g 15 Mol% = 45.1) and PVC-TRZ-Hexyl-TRZ-DiPEO$_{350}$Me (EΔT_g 15 Mol% = 54.8) displaying EΔT_g values greater than PVC-TRZ-Hexyl-TRZ-DiEH.

Type 2 triazole-plasticizers demonstrate superior EΔT_g values over the Type 1 system. These covalently-bound plasticizers contain a branch point at the primary triazole created by two hexyl tethers. Alkyl functionalized Type 2 PVC-TRZ-DiHexyl-TRZ-DiBu (EΔT_g 5 Mol% = 36.4 and EΔT_g 15 Mol% = 46.7) and PVC-TRZ-DiHexyl-TRZ-DiEH (EΔT_g 5 Mol% = 32.5 and EΔT_g 15 Mol% = 57.6) display greater efficiencies over Type 1 alkyl PVC-TRZ-Hexyl-TRZ-DiBu and PVC-TRZ-Hexyl-TRZ-DiEH, and Type 0D PVC-TRZ-DiBu and PVC-

TRZ-DiEH. Extended branching and lengthy alkyl chains present in both the primary and secondary triazoles are imperative in conveying the maximum plasticizing efficiency when utilizing alkyl moieties to internally plasticize PVC. Type 2 PVC-TRZ-DiHexyl-TRZ-DiPEO$_{164}$Me ($E\Delta T_g$ 5 Mol% = 47.1 and $E\Delta T_g$ 15 Mol% = 64.5), which has PEO-functionalized secondary triazole esters, have the highest $E\Delta T_g$ out of all 5 mole percent samples, and is the most efficient Type 2 analogue. At 15 mole percent, PVC-TRZ-DiHexyl-TRZ-DiPEO$_{164}$Me has nearly the same plasticizer weight percentage as Type 0D PVC-TRZ-DiPEO$_{550}$Me; despite this, the Type 2 sample, PVC-TRZ-DiHexyl-TRZ-DiPEO$_{164}$Me (T_g = -17 °C) exhibits a glass transition temperature approximately 12 °C higher than Type 0D PVC-TRZ-DiPEO$_{550}$Me (T_g = -29 °C), with a concomitant $E\Delta T_g$ decrease of 7.7%. Taken together, the higher abundance of PEO at elevated levels of substitution takes precedence over increasing the distance and mobility of the secondary triazole with PVC. Type 0M PEO triazole-plasticizers PVC-TRZ-PEO$_{2000}$Me and PVC-TRZ-PEO$_{1000}$Me were synthesized to test this observation.

Poly(ethylene oxide) mono methyl ethers, with an average molecular weight of 1000 and 2000 g/mol, were employed to create Type 0M triazole plasticizers which are predominantly comprised of PEO. These propiolates are readily synthesized and cyclized onto PVC-azide, furnishing PVC-TRZ-PEO$_{1000}$Me and PVC-TRZ-PEO$_{2000}$Me. At 15 mole percent, the Type 0M PEO system gives the two highest $E\Delta T_g$ values. At 5 mole percent, disparate $E\Delta T_g$ values between Type 0M PEO plasticizers highlights the prerequisite for covalently-bound plasticizers to possess large molecular weights per anchoring point (**Figure 4.16**)

Due to the reduced amount of anchoring points at 5 mole percent, an amplified effect on efficiency and glass transition temperatures takes place with structural branching, spacing, and compatibility with PVC. **Table 4.6** shows that at 5 mole percent, many other polymers ranging from Type 0D, 1, and 2 containing less plasticizer by weight, give lower glass

transition temperatures and better $E\Delta T_g$ values than Type 0M PVC-TRZ-PEO_{1000}Me ($E\Delta T_g$ 5 Mol% = 13.9, 45.0 Wt% Plasticizer), which has no hexyl tether or appreciable structural branching. The best $E\Delta T_g$ values observed at 5 mole percent are with Type 2 PVC-TRZ-DiHexyl-TRZ-DiPEO_{164}Me ($E\Delta T_g$ 5 Mol% = 47.7), which possesses two hexyl tethers with pendant PEO secondary triazoles, and Type 0D PVC-TRZ-DiPEO_{550}Me ($E\Delta T_g$ 5 Mol% = 44.5), incorporating two esters of PEO_{550}Me, branching off the primary triazole.

At 15 mole percent, structural aspects are less important to achieve enhanced plasticizer efficiency. The greater abundance of covalently-bound emollient partially compensates for the lack of branching and spacing that is imperative to plasticizing efficacy at low mole and weight percentages. The upper half of **Table 4.7** is dominated by PEO-functionalized plasticizers: the top five polymers exhibiting the highest $E\Delta T_g$ values contain PEO chains. Within this subcategory, the two samples displaying the best efficiencies are Type 0M PEO plasticizers, which have no branching at the primary triazole. The most efficient alkyl-based triazole-plasticizer is Type 2 PVC-TRZ-DiHexyl-TRZ-DiEH (T_g = -6 °C, $E\Delta T_g$ 15 Mol% = 57.6, 73.5 Wt% Plasticizer). At nearly the same weight percent plasticizer (73.72 Wt% Plasticizer), Type 0M PVC-TRZ-PEO_{1000}Me displays a superior plasticization efficiency value ($E\Delta T_g$ 15 Mol% = 77.2) and lower glass transition temperature (T_g = -35 °C) than PVC-TRZ-DiHexyl-TRZ-DiEH. At 15 mole percent, the only alkyl-based polymers that rank within the top ten $E\Delta T_g$ values belong to 3rd generation, Type 2 plasticizers: PVC-TRZ-DiHexyl-TRZ-DiEH and PVC-TRZ-DiHexyl-TRZ-DiBu (**Table 4.7**). When utilizing alkyl functionalized plasticizing groups, triazole branching points, spacing the secondary triazole away from the PVC backbone, and long branched alkyl chains are necessary to obtain optimized PVC internal plasticizers regardless of weight percentage of emollient. In contrast, for PEO-based plasticizers at high mole percentages, the length of the PEO chain influences the plasticizing efficiency and glass transition temperature more than branching and distancing of the emollient from PVC.

4.9 Thermogravimetric Analysis: PEO-Triazole Internal Plasticizers

The thermal stability of 4th generation PEO triazole internally plasticized PVC was measured by our collaborators at IBM Almaden Research Center through derivative thermogravimetry (DTG) and thermogravimetric analyses (TGA) with a TA Instruments TGA Q500. A scanning range between 30 °C to 500 °C with a heating rate of 10 °C per minute was implemented in both air and nitrogen atmospheres. Degradation temperatures of PVC internally plasticized by the 4th generation system are given in **Table 4.8**.

All 4th generation PEO triazole internal plasticizers exhibit decreased $T_{d,PVC1}$ temperatures compared to unmodified PVC. However, many of these samples containing high weight percentages of triazole-plasticizer produce a DTG peak adjacent to $T_{d,PVC1}$ at elevated temperatures ranging from 270 °C to 309 °C. One possibility for this second peak may stem from a secondary dehydrochlorination event, where the PEO-based emollient retards the elimination of HCl at a lower temperatures: this phenomenon is labeled as $T_{d,PVC1.5}$ in **Table 4.8**.

For many PEO 4th generation samples, two unique DTG peaks appear between 336 °C to 366 °C and 383 °C to 418 °C (**Table 4.8**). These degradation events relate to PEO. PEO peaks in the range of 336 °C to 366 °C occur exclusively in Type 0D, Type 1 and Type 2 samples. All but one of these polymers (5% PVC-TRZ-PEO_{550}Me) with this peak is functionalized with 15 mole percent triazole-plasticizer. In addition, this event was measured primarily in nitrogen, with the exception of two samples exhibiting peaks in this range when measured in air (15% PVC-TRZ-Hexyl-TRZ-DiPEO_{164}Me and 15% PVC-TRZ-DiHexyl-TRZ-DiPEO_{164}Me). These samples share identical secondary triazoles and contain hexyl tethers belonging to Type 1 and 2 PEO plasticizers. Slightly lower degradation temperatures(~340 °C) were observed in these samples compared to Type 0D PEO samples (~350 °C to 360 °C). At 15 mole percent, alkyl-based triazole-plasticized PVC from the 2nd

Polymer	Atm	T_d PVC1 (°C)	T_d PVC1.5 (°C)	T_d PVC2 (°C)	T_d Hexyl (°C)	T_d PEO (°C)	T_d PEO2 (°C)	T_d TRZ (°C)	T_d TRZ1 (°C)	T_d TRZ2 (°C)
5% PVC-TRZ-DiPEO$_{164}$Me	N_2	262	-	441	-	-	-	-	453	-
	Air	269	-	444	-	-		434	451	463
15% PVC-TRZ-DiPEO$_{164}$Me	N_2	269	-	-	-	-	-	438	-	-
	Air	273	-	446	-	-	-	431	456	-
5% PVC-TRZ-DiPEO$_{350}$Me	N_2	256	-	437	-	-	-	-	-	-
	Air	266	-	442	-	-	-	434	-	459
15% PVC-TRZ-DiPEO$_{350}$Me	N_2	265	300	442	-	361	-	429	-	-
	Air	271	302	447	-	-	409	436	-	-
5% PVC-TRZ-DiPEO$_{550}$Me	N_2	265	-	-	-	366	-	433	-	-
	Air	N/A	N/A	N/A	-	N/A	N/A	N/A	N/A	N/A
15% PVC-TRZ-DiPEO$_{550}$Me	N_2	253	291	-	-	350	418	432	-	-
	Air	262	299	442	-	-	413	-	-	463
5% PVC-TRZ-Hexyl-TRZ-DiPEO$_{164}$Me	N_2	263	-	443	-	-	-	432	-	-
	Air	268	-	445	-	-	-	435	-	468
15% PVC-TRZ-Hexyl-TRZ-DiPEO$_{164}$Me	N_2	267	-	439	-	-	-	-	-	-
	Air	271	-	445	343	-	415	-	-	-
5% PVC-TRZ-Hexyl-TRZ-DiPEO$_{350}$Me	N_2	253	-	442	-	-	-	-	-	-
	Air	N/A	N/A	N/A	-	N/A	N/A	N/A	N/A	N/A
15% PVC-TRZ-Hexyl-TRZ-DiPEO$_{350}$Me	N_2	245	270	-	345	-	-	432	-	-
	Air	253	278	444	-	-	410		457	-
5% PVC-TRZ-DiHexyl-TRZ-DiPEO$_{164}$Me	N_2	261	284	447	-	-	-	435	-	-
	Air	266	285	443	-	-	-	432	454	-
15% PVC-TRZ-iHexyl-TRZ-DiPEO$_{164}$Me	N_2	276	307	446	-	-	-	434	-	-
	Air	282	-	441	336	-	398	-	-	-
5% PVC-TRZ-PEO$_{1000}$Me	N_2	261	-	442	-	-	-	430	-	-
	Air	264	-	443	-	-	-	435	-	461
15% PVC-TRZ-PEO$_{1000}$Me	N_2	254	-	449	-	-	383	433	-	-
	Air	260	309	-	-	-	398	-	-	470
5% PVC-TRZ-PEO$_{2000}$Me	N_2	249	-	443	-	-	-	-	-	-
	Air	255	-	448	-	-	-	428	-	465
15% PVC-TRZ-PEO$_{2000}$Me	N_2	247	-	-	-	-	388	434	-	-
	Air	N/A	N/A	N/A	-	N/A	N/A	N/A	N/A	N/A

Table 4.8 TGA/DTG Degradation Temperatures of 4th Generation PEO-Functionalized Internally Plasticized PVC

and 3rd generation showed similar degradation events in samples containing n-butyl or 2-ethylhexyl groups as the Type 1 and 2 PEO samples. In *Chapter 2*, 15% PVC-TRZ-Hexyl-TRZ-DiBu gave a DTG peak at 325 °C, while 15% PVC-TRZ-Hexyl-TRZ-DiEH displayed a peak 340 °C when measured in air (**Table 2.16**). Likewise, 3rd generation polymers displayed comparable degradation temperatures in air: 15% PVC-TRZ-Hexyl-TRZ-DiBu produced a peak at 337 °C and 15% PVC-TRZ-Hexyl-TRZ-DiEH gave a peak at 351 °C (**Table 3.10**). All 4th generation Type 1 and 2 polymers at 15 mole percent exhibit DTG peaks in this range: 336 °C (15% PVC-TRZ-DiHexyl-TRZ-DiPEO$_{164}$Me), 343 °C (15% PVC-TRZ-Hexyl-TRZ-DiPEO$_{164}$Me) and 345 °C (15% PVC-TRZ-Hexyl-TRZ-DiPEO$_{350}$Me). Another degradation event stemming from PEO occurs at marginally higher temperatures in Type 0D PEO plasticizers: 15% PVC-TRZ-DiPEO$_{550}$Me (350 °C, N_2), 15% PVC-TRZ-DiPEO$_{350}$Me (361 °C, N_2), and 5% PVC-TRZ-DiPEO$_{550}$Me (366 °C, N_2). Although the DTG peaks of Type 0D, Type 1 and Type 2 4th generation analogues appear similar, it is evident that the degradation events of Type 1 and 2 PEO samples between 336 °C and 345 °C must originate from the hexyl-tether ($T_{d,Hexyl}$), while the events between 350 °C and 366 °C belonging to Type 0D PEO polymers are specific to poly(ethylene oxide) monomethyl ether chains ($T_{d,PEO}$).

A secondary degradation event unique to PEO occurs at elevated temperatures between 383 °C and 398 °C ($T_{d,PEO2}$). All emollients possessing a PEO peak ($T_{d,PEO}$) at approximately 360 °C contain relatively short PEO chains compared to Type 0M derivatives which possess long chains of 1000 g/mol or 2000 g/mol. This is particularly apparent in Type 0M plasticized PVC, which have DTG spectra dominated by peaks originating from PEO. Both 15% PVC-TRZ-PEO$_{1000}$Me (383 °C N_2, 398 °C air) and 15% PVC-TRZ-PEO$_{2000}$Me (388 °C, N_2) are principally comprised of PEO, exhibiting substantial degradation events in this range. Polymers with intermediate length PEO chains (PEO$_{350}$Me and PEO$_{550}$Me) containing 15 mole percent plasticizer produce DTG peaks similar to Type 0M derivatives, albeit weaker and at an elevated temperature range between 409 °C and 418 °C. $T_{d,PEO2}$ of

Type 0M plasticized PVC is quite large and broad, which appear to overshadow degradation events between approximately 410 °C and 420 °C, observed in samples containing intermediate length PEO chains.

Many 4th generation polymers did not have a distinctive $T_{d,PVC2}$ peak at 442 °C. Broad DTG peaks were measured between 428 °C to 438 °C. Numerous samples displayed extremely weak $T_{d,PVC2}$ peaks, which overlap with a triazole degradation event ($T_{d,TRZ}$ = ~430 °C) transpiring at temperatures near $T_{d,PVC2}$. TGA and DTG data from the first three generations of internally plasticized PVC implies that degradation in this temperature range arise from ester hydrolysis on the primary or secondary triazole. Hydrolysis at approximately 430 °C was not as prevalent in the alkyl-based emollients compared to the 4th generation PEO polymers. Another explanation for this broadened degradation event may originate from the increase in polarity of the polymeric matrix. In juxtaposition to the 3rd generation analogue containing two non-polar hexyl tethers with 2-ethylhexyl triazole esters (15% PVC-TRZ-DiHexyl-TRZ-DiEH), the 4th generation samples possess polar PEO chains. In the first degradation event stemming from PVC ($T_{d,PVC1}$), hydrochloric acid (HCl) is liberated through the dehydrochlorination of PVC. The reactivity of HCl would increase in this relatively polar environment. Therefore, ester hydrolysis mediated by catalytic HCl should ensue at lower temperatures. This reasoning also predicts the ubiquitous decrease in $T_{d,PVC1}$ of all polymers incorporating PEO chains.

4.10 Plasticizer Migration: *n*-Hexane Extraction of Triazole-Based Internally Plasticized PVC Versus DEHP-PVC

The degree of plasticizer migration was determined by a process derived from an ASTM International standard test method (ASTM-D5227). This method describes an extraction/gravimetric procedure for determination of the amount of hexane-soluble low molecular weight material in a polymer matrix. Samples were extracted as thin square films

(approximately 15 x 15 mm), dried by high vacuum overnight and weighed. A Berzelius beaker (150 mL) with a stir bar (25mm x 8mm diameter) was utilized as the extraction apparatus. The procedure involved pre-heating 50 mL of *n*-hexane (Alfa Aesar, 95% HPLC distilled in glass at 50 °C for 15 minutes, prior to placing the polymer in the beaker. A stir rate of 100 revolutions per minute was used for all extractions. Each sample was extracted for 2 hours at 50 °C. After the extraction, the solvent was decanted. The polymer was placed in a 20 mL scintillation vial and dried at room temperature under high vacuum overnight. The mass of each sample post-extraction was determined. The degree of plasticizer migration was calculated using **Equation 4.1**:

Equation 4.1

$$Degree\ of\ Plasticizer\ Migration\ (\%) = \frac{Initial\ Mass - Mass\ After\ Extraction}{Initial\ Mass \times Weight\ Fraction\ Plasticizer} \times 100$$

where the "weight fraction plasticizer" is the weight percentage of plasticizer, divided by 100. The top 3 polymers with the highest plasticizing efficiency values ($E\Delta T_g$) were chosen for this migration study. Traditional DEHP-PVC (containing 60 weight percent DEHP) was used as a standard. Each polymer sample was extracted in triplicate. Plasticizer migration data are shown in **Table 4.9**. A stacked bar graph comparing average plasticizer migration percentages between DEHP-PVC standard (60 Wt% DEHP), 15% PVC-TRZ-PEO_{2000}Me, 15% PVC-TRZ-PEO_{1000}Me and 15% PVC-TRZ-DiPEO_{550}Me is illustrated in **Figure 4.21**.

The traditional DEHP-PVC blend containing 60 percent DEHP by weight exhibits complete plasticizer migration (99.96 ± 0.07%). In contrast, PVC internally plasticized by triazole emollients display no appreciable plasticizer migration: 15% PVC-TRZ-PEO_{2000}Me (0.68 ± 0.15%), 15% PVC-TRZ-PEO_{1000}Me (1.00 ± 0.14%) and 15% PVC-TRZ-DiPEO_{550}Me (0.78 ± 0.11%). These samples are substantially more stable under these conditions than the DEHP-PVC standard.

DEHP-PVC (60 Wt% DEHP)		
Before (mg)	*After (mg)*	*% Migration*
39.02	15.59	100.08
42.18	16.91	99.85
40.27	16.12	99.95
Average (% Migration)		**99.96**
Standard Error		**0.07**

15% PVC-TRZ-PEO$_{2000}$Me		
Before (mg)	*After (mg)*	*% Migration*
54.31	54.13	0.39
55.83	55.46	0.79
54.69	54.29	0.87
Average (% Migration)		**0.68**
Standard Error		**0.15**

15% PVC-TRZ-PEO$_{1000}$Me		
Before (mg)	*After (mg)*	*% Migration*
61.38	60.83	1.22
60.52	60.05	1.05
61.86	61.52	0.75
Average (% Migration)		**1.00**
Standard Error		**0.14**

15% PVC-TRZ-DiPEO$_{550}$Me		
Before (mg)	*After (mg)*	*% Migration*
57.57	57.31	0.60
56.85	56.52	0.77
56.37	55.95	0.98
Average (% Migration)		**0.78**
Standard Error		**0.11**

Table 4.9 Plasticizer Migration Data (*n*-Hexane) of DEHP-PVC (60 Wt % DEHP) Versus 15% PVC-TRZ-PEO$_{2000}$Me, 15% PVC-TRZ-PEO$_{1000}$Me and 15% PVC-TRZ-DiPEO$_{550}$Me

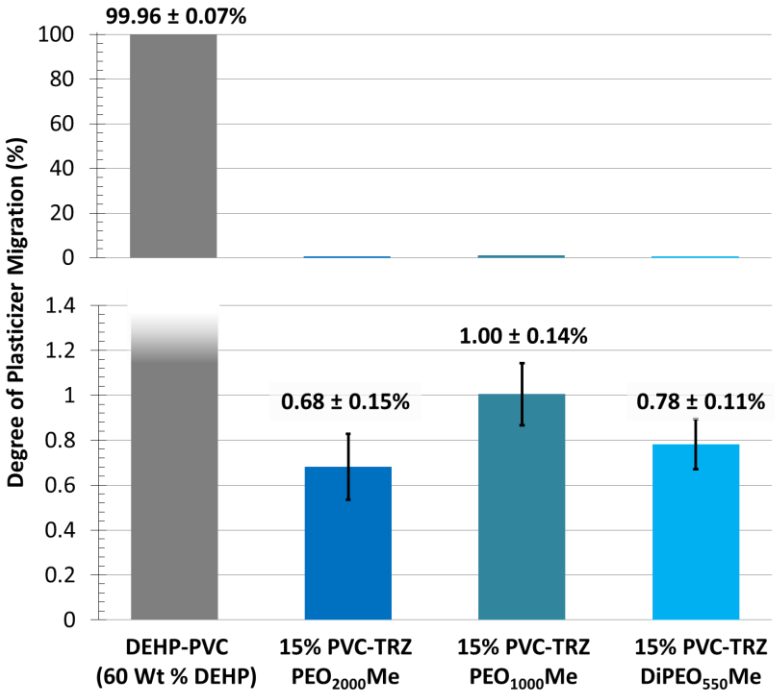

Figure 4.21 Degree of Plasticizer Migration (*n*-Hexane). Average Migration Percentages of DEHP-PVC (60 Wt % DEHP), 15% PVC-TRZ-PEO$_{2000}$Me, 15% PVC-TRZ-PEO$_{1000}$Me and 15% PVC-TRZ-DiPEO$_{550}$Me

4.11 Conclusion

Type 0D methyl esters directly appended to PVC displays the inherent anti-plasticization effect of the triazole ring, which diminishes with increasing molecular weight and branching of the alkyl ester chains. Introduction of a flexible hexyl tether to the secondary triazole group (Type 1) acts as additional molecular weight and branching, further lowering T_g values. Attachment of two hexyl tethered secondary triazoles (Type 2) follows this trend by enforcing another branch point and increasing molecular weight. Utilization of PEO esters in all architectural types significantly enhances T_g depressions, with longer PEO chains exhibiting remarkable results. Single PEO ester triazoles (Type 0M) readily prepared from propiolic esters using low-cost, commercially available materials combine excellent plasticization with straightforward synthesis, making these non-migratory internal plasticizers extremely attractive for industrial applications.

4.12 References

1. da Silva Neiro, S. M.; Dragunski, D. C.; Rubira, A. F.; Muniz, E. C. Miscibility of PVC/PEO Blends by Viscosimetric, Microscopic and Thermal Analyses. *European Polymer Journal* **2000,** *36* (3), 583-589.

2. Sun, Z.; Wang, W.; Feng, Z. Criterion of Polymer-Polymer Miscibility Determined By Viscometry. *European Polymer Journal* **1992,** *28* (10), 1259-1261.

3. Castro, R. E. N.; Toledo, E. A.; Rubira, A. F.; Muniz, E. C. Crystallisation and Miscibility of Poly(Ethylene Oxide)/Poly(Vinyl Chloride) Blends. *Journal of Materials Science* **2003,** *38* (4), 699-703.

4. Hoffmann, J. D. W., J. J. Melting Process and the Equilibrium Melting Temperature of Polychlorotrifluoroethylene. *Journal of Research of the National Bureau of Standards-A. Physics and Chemistry* **1962,** *66A* (1), 13-28.

5. Marco, C.; Gömez, M. A.; Fatou, J. G.; Etxeberria, A.; Elorza, M. M.; Iruin, J. J. Miscibility of Poly(Vinyl Chloride)/Poly(Ethylene Oxide) blends—I. Thermal Properties and Solid State ^{13}C-NMR Study. *European Polymer Journal* **1993,** *29* (11), 1477-1481.

6. Lee, K. W.; Chung, J. W.; Kwak, S.-Y. Synthesis and Characterization of Bio-Based Alkyl Terminal Hyperbranched Polyglycerols: A Detailed Study of Their Plasticization Effect and Migration resistance. *Green Chemistry* **2016,** *18* (4), 999-1009.

7. Jang, B. N.; Wang, D.; Wilkie, C. A. Relationship Between the Solubility Parameter of Polymers and the Clay Dispersion in Polymer/Clay Nanocomposites and the Role of the Surfactant. *Macromolecules* **2005,** *38* (15), 6533-6543.

8. Wooley, K. L.; Hawker, C. J.; Pochan, J. M.; Frechet, J. M. J. Physical Properties of Dendritic Macromolecules: A Glass Transition Temperature Study. *Macromolecules* **1993,** *26* (7), 1514-1519.

9. (a) Lee, K. W.; Chung, J. W.; Kwak, S. Y. Structurally Enhanced Self-Plasticization of Poly(vinyl chloride) via Click Grafting of Hyperbranched Polyglycerol. *Macromolecular Rapid Communications* **2016,** *37* (24), 2045-2051; (b) Navarro, R.; Gacal, T.; Ocakoglu, M.; Garcia, C.; Elvira, C.; Gallardo, A.; Reinecke, H. Nonmigrating Equivalent Substitutes for PVC/DOP Formulations as Shown by a TG Study of PVC with Covalently Bound PEO-PPO Oligomers. *Macromolecular Rapid Communications* **2017,** *38* (6).

10. Technical Bulletin: JEFFAMINE™ Polyetheramines. http://www.huntsman.com/performance_products/a/Products/Amines/Polyetheramines%20%20%20JEFFAMINE_R (accessed Sept 7, 2017).

11. (a) Navarro, R.; Perrino, M. P.; Garcia, C.; Elvira, C.; Gallardo, A.; Reinecke, H. Opening New Gates for the Modification of PVC or Other PVC Derivatives: Synthetic Strategies for the Covalent Binding of Molecules to PVC. *Polymers* **2016,** *8* (4), 152-165; (b) Navarro, R.; Perrino, M. P.; Garcia, C.; Elvira, C.; Gallardo, A.; Reinecke, H. Highly Flexible PVC Materials Without Plasticizer Migration as Obtained by Efficient One-Pot Procedure Using Trichlorotriazine Chemistry. *Macromolecules* **2016,** *49* (6), 2224-2227.

12. (a) Charlton, J. L.; Chee, G. Synthesis of Chiral Esters of Acetylenedicarboxylic Acid. *Tetrahedron Letters* **1994,** *35* (34), 6243-6246; (b) Charlson, J. L.; Chee, G.; McColeman, H. Synthesis of Acetylenedicarboxylic Acid Esters and Asymmetric Diels-Alder Reactions of the Bis(methyl (S)-lactyl) Ester. *Canadian Journal of Chemistry* **1995,** *73* (9), 1454-1462.

13. Ott, E. Über Symmetrische und Asymmetrische Dicarbonsäurechloride. *Justus Liebigs Annalen der Chemie* **1912,** *392* (3), 245-285.

5 Plasticizing Triazole Monomers For Copolymerization With Vinyl Chloride

5.1 Synthesis of Vinyl Acetate Triazole Phthalate Mimics

An alternative strategy to post-polymerization direct modification of poly(vinyl chloride) (PVC) to obtain internally plasticized materials involves the copolymerization of vinyl chloride monomer (VCM) with a monomer functionalized with a triazole-phthalate mimic. It was envisaged that an electron-rich monomer such as vinyl acetate (VAc) with an appended triazole-plasticizer could be synthesized for this purpose.

Azidation of vinyl chloroacetate *via* typical S_N2 conditions was not trivial. Relatively high temperatures required for this S_N2 reaction caused vinyl chloroacetate to autopolymerize. Inspired by chemistry applied to sensitive carbohydrates, use of phase transfer catalysis (PTC) was investigated.[1] Conceivably, a PTC would decrease the amount of thermal energy required to displace chloride by the azide nucleophile. Initially, tetrabutylammonium hydrogensulfate (TBAHS) was utilized in a two-phase benzene-water system, but did not adequately transfer sodium azide (NaN_3) into the benzene phase. Aliquat 336 was subsequently adapted and demonstrated successful azide displacement of chloride as monitored by ^{1}H-NMR. However, ^{1}H-NMR also revealed significant reductions in signal intensity of both vinyl chloroacetate and vinyl azidoacetate **5.1** as the reaction progressed. Realization that the aqueous phase caused hydrolysis of the vinyl acetates to acetaldehyde and acetic acid by-products[2] prompted a change in reaction conditions. Eventually, acetonitrile was found to be the optimal polar aprotic solvent for the azidation, due to its relatively low boiling point (82 °C) compared to other alternatives such as dimethylformamide (153 °C) or dimethyl sulfoxide (189 °C). High boiling solvents are challenging to remove during workup. The S_N2 reaction between vinyl chloroacetate and NaN_3 in acetonitrile requires TBAHS as a solubilization reagent for successful azide substitution. ^{1}H-NMR monitoring of vinyl chloroacetate, TBAHS, NaN_3, and $NaHCO_3$ in CD_3CN revealed complete displacement of the chloride after 1 hour at room temperature, furnishing vinyl azidoacetate

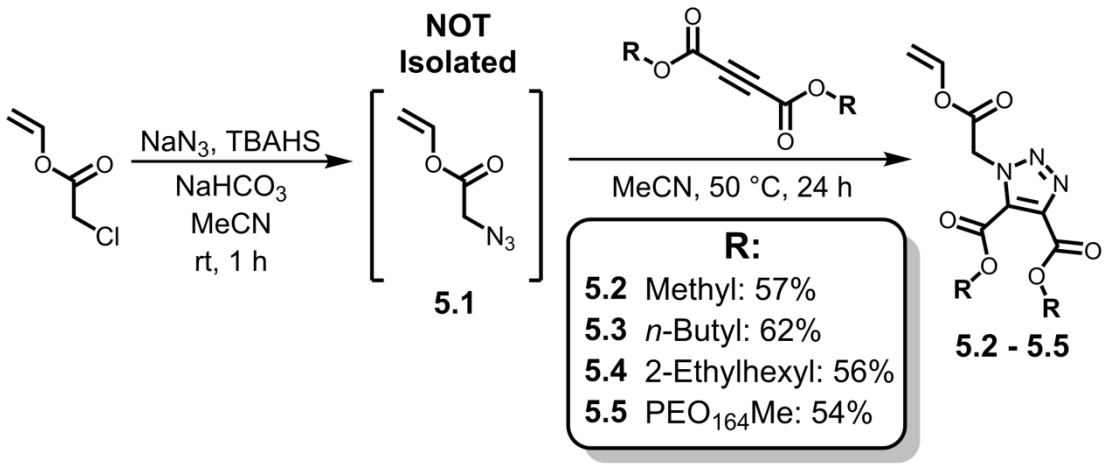

Scheme 5.1 Synthesis of Vinyl Acetate Containing Pendant Triazole-Phthalate Mimics

5.1 (**Scheme 5.1**). Subsequent azidations were scaled up and utilized non-deuterated acetonitrile. The azide **5.1** was not isolated due to its dangerous nature: low molecular weight organic azides have a propensity to decompose violently. A formula to indicate if an organic azide is likely safe to handle has been created:[3] $(N_{Carbon} + N_{Oxygen}) / N_{Azide\ Nitrogen} \geq 3$, where N = number of atoms. Using this formula, vinyl azidoacetate **5.1** gives a value of 1.6 and *should not be handled in its pure form*. After the azidation was complete, the reaction was filtered via glass sintered funnel into another round bottom flask and diluted with acetonitrile. Acetylenedicarboxylates containing alkyl and poly(ethylene oxide) diesters were combined with azide **5.1** and stirred for 24 hours at 50 °C (**Scheme 5.1**). After the azide-alkyne cycloaddition was complete, the volatiles were concentrated *in vacuo* and purified via column chromatography to furnish vinyl acetates **5.2 - 5.5** functionalized with pendant triazole-phthalate mimics in 54% to 62% yield. For extended storage of vinyl acetates **5.2 - 5.5**, 4-methoxyphenol (MEHQ) was used as a stabilizer.

^{1}H-NMR of the vinyl acetate monomers **5.2 - 5.5** bearing pendant triazole-phthalate mimics were acquired in $CDCl_3$ (**Figure 5.1**). All derivatives gave vinylic proton signals indicative of vinyl acetates. Vinylic proton **a** produces a signal at approximately δ 4.70 ppm,

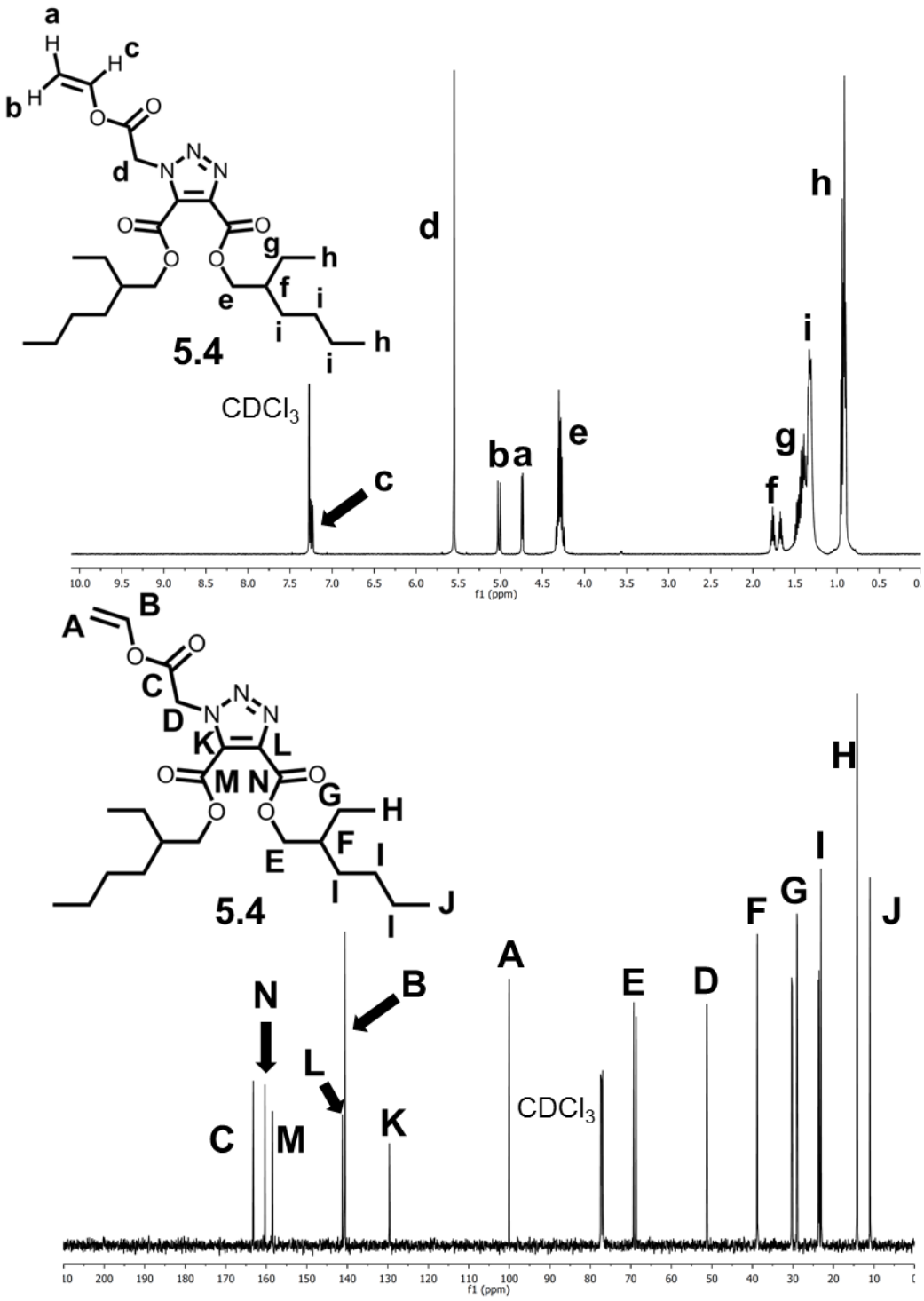

Figure 5.1 ^{1}H-NMR and ^{13}C-NMR Spectra of VAc-TRZ-DiEH **5.4**

while **b** appears at δ 5.0 ppm: both **a** and **b** are split as doublet of doublets. Vinylic proton **c** is noted at δ 7.25 ppm as a doublet of doublets, and shows the typical vinyl coupling constants. Methylene protons **d** between the acetate ester and triazole give a singlet at δ 5.55 ppm. Regioisomeric triazole esters functionalized with *n*-butyl **5.3** or 2-ethylhexyl groups **5.4** both display peaks **e** between δ 4.20 to δ 4.40 ppm, originating from the methylene protons adjacent to the triazole ester oxygen atoms. VAc-TRZ-DiMe **5.2** gives two singlets at δ 3.98 ppm and δ 4.00 ppm, representing the regioisomeric methyl esters. Unique peaks to VAc-TRZ-DiEH **5.4** belong to methine protons **f** on the 2-ethylhexyl chain, appearing as heptets at δ 1.67 ppm and δ 1.76 ppm. Signals between δ 1.27 ppm and δ 1.51 ppm are alkyl chain methylenes **i**, which overlap with methylene protons **g**. VAc-TRZ-DiBu **5.3** displays analogous methylene signals between δ 1.39 ppm to δ 1.51 ppm. Methyl protons **h** of the 2-ethylhexyl chain in **5.4** are present as multiplets between δ 0.79 ppm and δ 1.00 ppm.

^{13}C-NMR of all vinyl acetate derivatives exhibit signals originating from the alkene (**Figure 5.1**). Terminal vinyl carbon **A** appears at approximately δ 100 ppm, while carbon **B** gives a signal at δ 140 ppm. The acetate carbonyl **C** displays a signal at δ 163 ppm. Peaks at δ 158 ppm and δ 160 ppm belong to regioisomeric triazole carbonyls **M** and **N**. Methylene carbon **D** is observed around δ 51 ppm. Quaternary triazole carbons **K** and **L** appear at δ 130 ppm and δ 141 ppm. In VAc-TRZ-DiEH **5.4**, signals at δ 68.7 and δ 69.3 ppm represent the methylenes **E** adjacent to the triazole esters. VAc-TRZ-DiBu **5.3** shows comparable triazole ester methylene peaks to **5.4**, albeit shifted upfield to δ 65.9 ppm and δ 68.8 ppm, while VAc-TRZ-DiMe **5.2** produce methyl triazole signals at δ 52.9 ppm and δ 53.5 ppm. ^{13}C signals unique to VAc-TRZ-DiEH **5.4** appearing at δ 38.8 ppm and δ 38.9 ppm belong to methine **F** on the 2-ethylhexyl chain. Methylene carbons **G** in monomer **5.4** are observed between δ 28.9 and δ 30.3 ppm, while methylenes **I** are present in the range of δ 23.0 and δ 23.7 ppm. Monomer **5.3** containing *n*-butyl chains show similar methylene signals to **5.4** (δ 18.9 ppm to δ 19.1 ppm and δ 30.3 ppm to δ 30.6 ppm). Methyl carbons **H** and **J** in VAc-TRZ-DiEH **5.4**

are noted at δ 11.0 ppm and δ 14.2 ppm. Likewise, VAc-TRZ-DiBu **5.3** has methyl peaks at δ 13.6 ppm and δ 13.7 ppm.

5.2 Polymerization Experiments of Vinyl Acetate Triazole-Phthalate Mimics

Vinyl acetate monomers **5.2 - 5.5** were sent to our collaborators Dr. Jorge Coelho and Dr. Armenio Serra at the University of Coimbra, Portugal, for polymerization experiments. Vinyl chloride is a toxic gas (bp = -13.4 °C) and can only be handled safely with specialized equipment. Coelho and Serra at the Department of Chemical Engineering have the required equipment and years of experience working with vinyl chloride free radical polymerizations. Homopolymerizations of vinyl acetate (VAc) and vinyl chloride monomer (VCM) provided preliminary polymerization conditions. Copolymerizations of equal parts VAc and VCM (1 part monomer to 3 parts solvent) using Trigonox/AIBN as an initiator at 50 °C were conducted for 19 hours to establish optimized conditions in DMSO or DMF (**Scheme 5.2**). The highest level of VAc incorporation with VCM used 0.5% Trigonox/0.5% AIBN initiator in DMSO (**Table 5.1**: Exp 9). With these preliminary optimized reaction parameters, copolymerizations of vinyl acetates **5.3 - 5.4** and VCM were performed (**Scheme 5.3**).

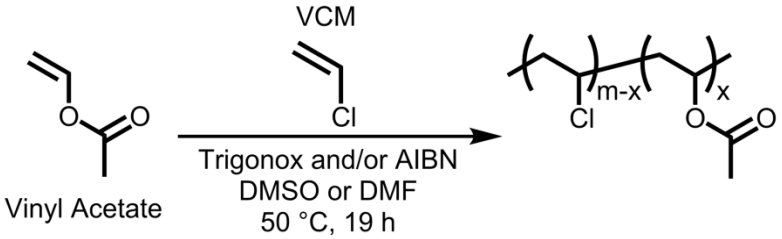

Scheme 5.2 Copolymerization of Vinyl Chloride Monomer (VCM) and Vinyl Acetate (VAc)

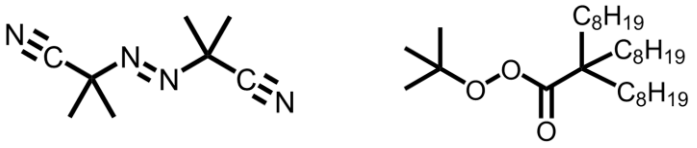

Figure 5.2 Structures of Azobisisobutyronitrile (AIBN, Left) and Trigonox 23 (Right)

Exp	Monomer*	Initiator (%)	Solvent	Conv. VC (%)	Conv. VAc (%)	$M_{n,SEC}$ x 10^{-3}	PDI	% (m/m) VC
1	VCM	0.1 Trigonox	DMSO	30		8.9	2.19	
2	VAc + VCM	0.1 Trigonox	DMSO	~0	~0			
3	VAc + VCM	0.05 Trigonox + 0.05 AIBN	DMSO	~0	~0			
4	Vac	0.1 Trigonox	DMSO		24	102.7	1.62	
5	VAc + VCM	0.1 Trigonox	DMSO	~0	~0			
6	VAc + VCM	0.1 Trigonox	DMF	~0	~0			
7	VAc + VCM	1 Trigonox	DMSO	53	28	12.3	1.78	82
8	VAc + VCM	1 Trigonox	DMF	54	6	7.4	2.16	86
9	VAc + VCM	0.5 Trigonox + 0.5 AIBN	DMSO	84	42	16.9	1.76	73
10	VAc + VCM	0.25 Trigonox + 0.75 AIBN	DMSO	82	42	20.7	1.67	79
11	VAc + VCM	1 AIBN	DMSO	82	37	8.9	1.79	74
12	VAc + VCM	0.5 Trigonox + 0.5 AIBN	DMF	81	22	8.8	1.74	79

Table 5.1 (Co)Polymerization Results of Vinyl Chloride and Vinyl Acetate at 50 °C
*Monomer Ratio= 1:1; Monomer to Solvent Ratio (v/v) = 1:3

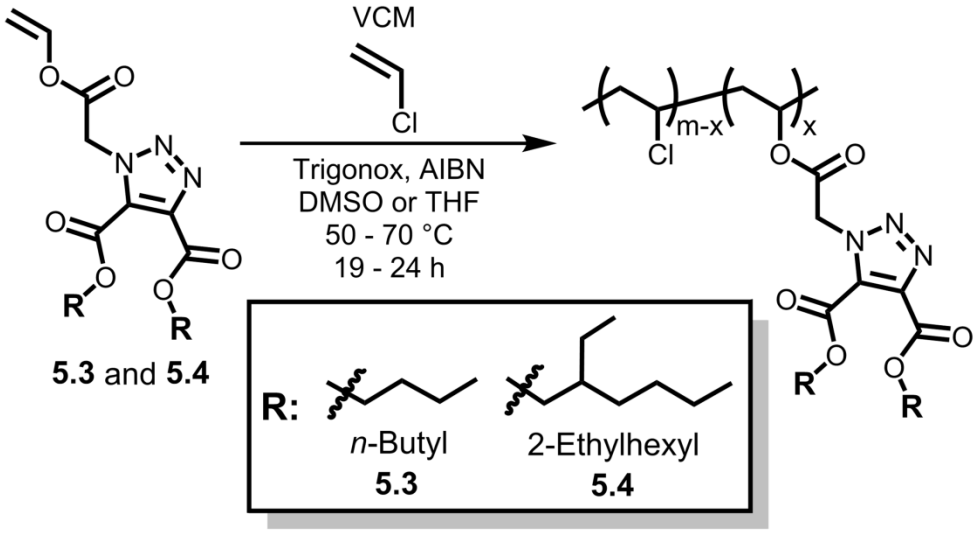

Scheme 5.3 Copolymerization of Vinyl Chloride and Vinyl Acetates Containing Pendant Triazole-Phthalate Mimics

Exp	Monomer*	Time (h)	Temp. (°C)	Solvent	Conv. VC (%)	Conv. VAc (%)	$M_{n,SEC}$ x 10^{-3}	PDI	% (m/m) VC
0	VAc + VCM	19	50	DMSO	87	91	19.6	2.04	80
1	**5.4** + VCM	19	50	DMSO	36	0	13.2	1.81	100
2	**5.4**	24	50	DMSO	-	0.88	-	-	-
		24	70	DMSO	-	61.4	12.6	1.72	-
		24	90	DMSO	-	**77.2**	9.9	1.98	**-**
3	**5.4** + VCM	19	70	DMSO	63	0	15.6	2.26	100
4	**5.4** + VCM	19	70	DMF	88	0	8.0	2.00	100
5	**5.4** + VCM	19	65	THF	87	0	6.3	1.87	100
6	**5.3** + VCM	22	70	DMSO	42	0	12.3	1.87	100
7	**5.3** + VCM (90/10)	19	70	DMSO	73	6.54	12.4	1.75	29

Table 5.2 (Co)Polymerization Results of Vinyl Chloride and Vinyl Acetates Containing Pendant Triazole-Phthalate Mimics
*Monomer Ratio= 1:1 Unless Otherwise Stated; Monomer to Solvent Ratio (v/v) = 1:1.5

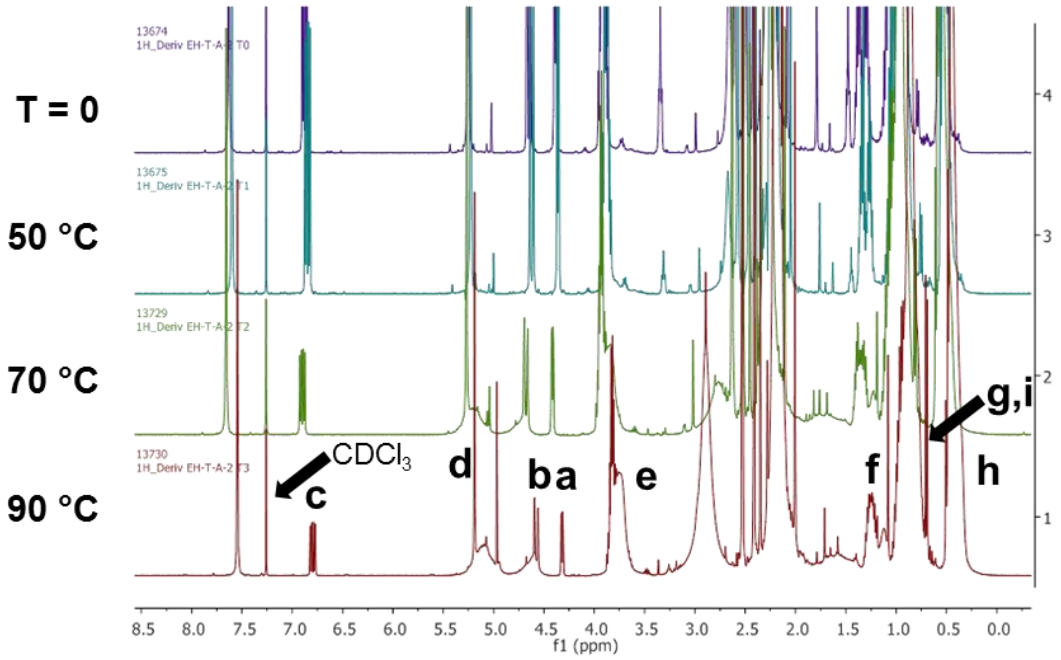

Figure 5.3 ^{1}H-NMR Spectra of Exp 2: VAc-TRZ-DiEH **5.4** Homopolymerizations as a Function of Temperature After 24 Hours

All polymerization experiments were carried out in a 15 mL reactor by graduate student Carlos Abren at the University of Coimbra. The results are displayed in **Table 5.2**. Exp 0 (**Table 5.2**) utilized the optimized conditions from the initial copolymerizations of vinyl chloride and vinyl acetate (**Table 5.1**: Exp 9). An analogous result to Exp 9 using a 50 mL reactor was observed with the 15 mL reactor (**Table 5.2**: Exp 0). Exp 1 (**Table 5.2**) showed no incorporation of VAc-TRZ-DiEH **5.4** with VCM (36% VCM conversion) during the attempted copolymerization. Because of this, homopolymerizations of VAc-TRZ-DiEH **5.4** were investigated at increasing temperatures for 24 hours (**Table 5.2**: Exp 2). ^{1}H-NMR spectra provided by our collaborators of VAc-TRZ-DiEH **5.4** indicates that homopolymerization does occur (**Figure 5.3**). Enhanced conversions were observed as the temperature increased. After 24 hours at 90 °C, monomer **5.4** exhibited 77.2% conversion (**Table 5.2**: Exp 2). Optimization of polymerization solvents utilizing DMSO, DMF and THF were investigated (**Table 5.2**: Exp 3, Exp 4, Exp 5).

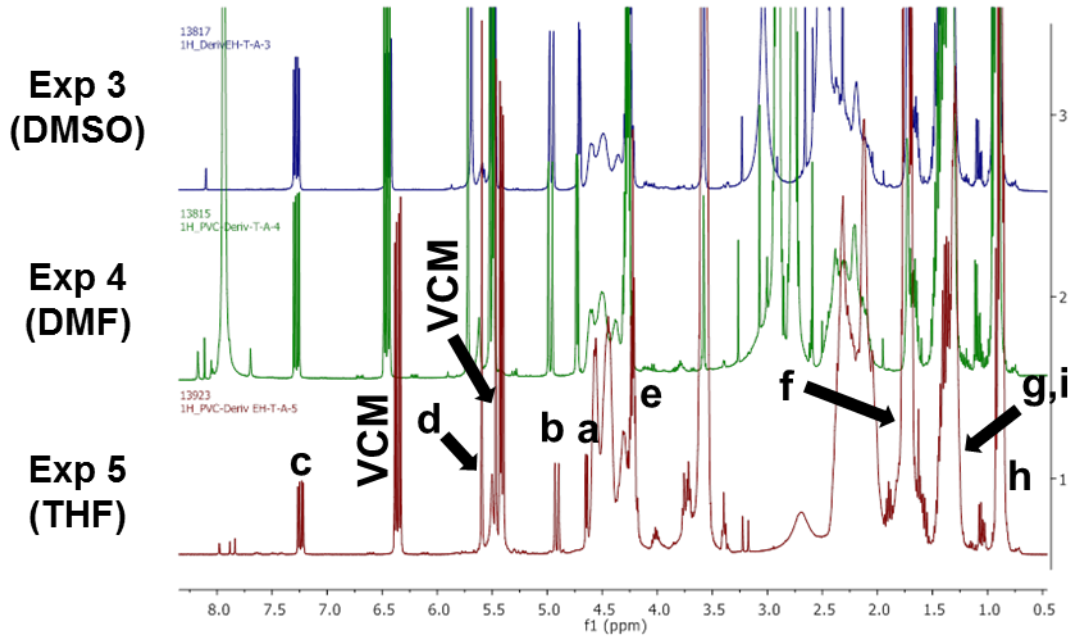

Figure 5.4 ^{1}H-NMR Spectra of VCM and VAc-TRZ-DiEH **5.4** Copolymerizations as a Function of Solvent (Top DMSO, Middle: DMF, Bottom: THF)

However, moving to copolymerization with VCM at 70 °C, no conversion of VAc-TRZ-DiEH **5.4** with VCM (63 to 88% VCM conversion) occurred after 19 hours. ^{1}H-NMR spectra of solvent optimization copolymerization experiments are presented in **Figure 5.4**. Regardless of solvent, no appreciable incorporation of VAc-TRZ-DiEH **5.4** into PVC was noted by ^{1}H-NMR. The presence of peaks at approximately δ 5.5 ppm and δ 6.5 ppm originate from VCM trapped in the polymeric matrix. While there appears to be signal broadening from the formation of poly(vinyl chloride) at δ 2.0 – 2.4 ppm and δ 4.2 – 4.6 ppm, the vinylic protons **a-c** of monomer **5.4** at δ 4.70 ppm (**a**), δ 5.0 ppm (**b**) and δ 7.25 ppm (**c**) (**Figure 5.1**) do not diminish nor form broadened peaks indicative of successful copolymerization (**Figure 5.4**).

Subsequently, copolymerization in DMSO (Exp 6, **Table 5.2**) was performed with VAc-TRZ-DiBu **5.3** and VCM. No incorporation of monomer **5.3** with VCM (42% VCM conversion) was observed during this attempted copolymerization. The ^{1}H-NMR spectrum of Exp 6 in THF-d_8 exhibits VCM peaks at δ 5.5 ppm and δ 6.5 ppm (**Figure 5.5**). Broad PVC signals between ~ δ 2.0 – 2.4 ppm and δ 4.4 – 4.6 ppm are also present. There appears to be a new broadened peak at approximately δ 5.6 ppm; this may stem from monomer methylene protons **d** (**Figure 5.1**) integrated into the copolymer, which inherently experiences anisotropic tumbling. However, vinylic proton signals **a** and **b** of monomer **5.3** remain in the ^{1}H-NMR spectrum, indicating incomplete incorporation of the vinyl acetate triazole with VCM. Methylene peaks belonging to the *n*-butyl triazole ester chains are present at δ 1.39 – 1.51 ppm and δ 1.68 – 1.81 ppm. Terminal methyl groups of the *n*-butyl chains are observed at δ 0.96 ppm.

In Exp 7, VAc-TRZ-DiBu **5.3** was copolymerized with VCM in a 9 to 1 ratio ([VAc-TRZ-DiBu]/[VCM]) at 70 °C in DMSO (**Table 5.2**). According to our collaborator, the ^{1}H-NMR spectrum indicates formation of copolymer, with approximately 6.5% conversion of VAc-TRZ-DiBu **5.3** and 73% conversion of VCM (**Figure 5.6**). The broadened signal appearing at δ 5.6 ppm in Exp 6 (**Figure 5.5**) is also present in Exp 7 (**Figure 5.6**). As with Exp 6, PVC signals

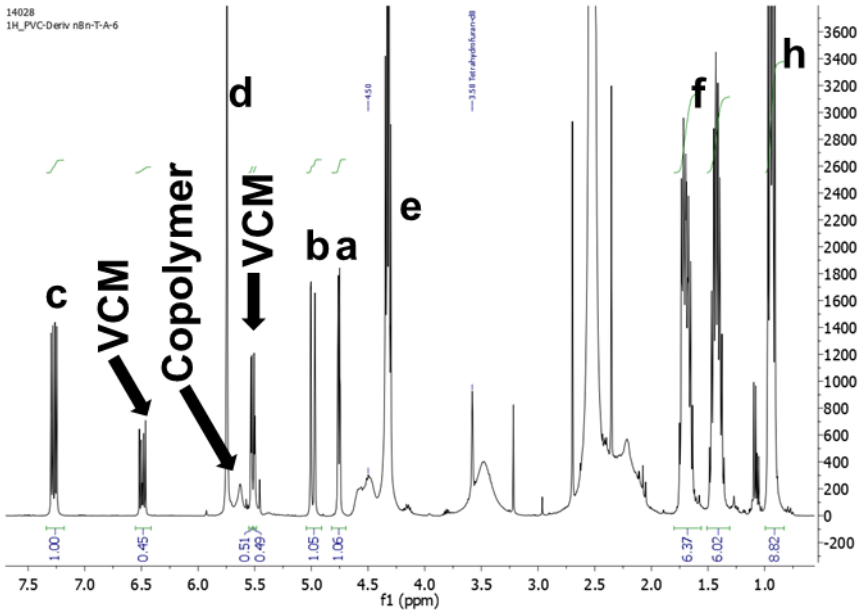

Figure 5.5 ^{1}H-NMR of Exp 6: VCM and VAc-TRZ-DiBu **5.3** Copolymerization (in THF-d_8)

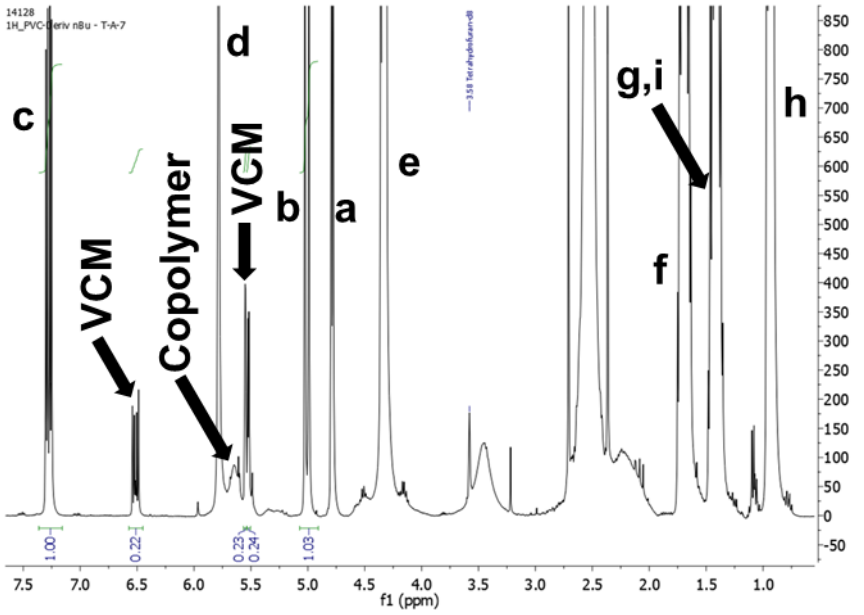

Figure 5.6 ^{1}H-NMR of Exp 7: VCM and VAc-TRZ-DiBu **5.3** Copolymerization at 70 °C Using DMSO ([VAc-TRZ-DiBu]/[VCM] = 90/10)

between ~ δ 2.0 – 2.4 ppm and δ 4.4 – 4.6 ppm are observed. The presence of methylene signals belonging to the triazole ester *n*-butyl chains between δ 1.39 – 1.51 ppm and δ 1.68 – 1.81 ppm are diminished, due to partial consumption of VAc-TRZ-DiBu **5.3** during polymerization. Consequently, signal broadening of copolymer regions incorporating the vinyl acetate derivative **5.3** occurs. Additionally, well-defined signals due to isotropic tumbling of monomer **5.3** decrease in intensity compared to Exp 6.

5.3 Synthesis of Acrylate Hexyl Tethered Triazole Phthalate Mimics

Our collaborators suggested that an acrylate derivative might remedy the low reactivity of vinyl acetate monomers **5.2 - 5.5** toward VCM copolymerization. Apparently, the appended triazole-phthalate mimic decreases the activity of the vinyl acetate. An acrylate incorporating a hexyl-tethered triazole-phthalate mimic was envisaged to serve two purposes: 1) generate space between the triazole and polymerizing vinyl group to prevent monomer deactivation and, 2) enhance the plasticization efficiency of the triazole, as demonstrated in *Chapter 2*. A synthesis derived from the double-arm hexyl-tethered acetylenedicarboxylates outlined in *Chapter 3* was implemented to obtain the desired acrylate. Under anhydrous conditions, the triazolo-alcohol containing 2-ethylhexyl triazole esters (TRZ-DiEH hexanol, **2.10**) was combined with Et_3N in anhydrous THF at 0 °C. Acryloyl chloride was slowly added

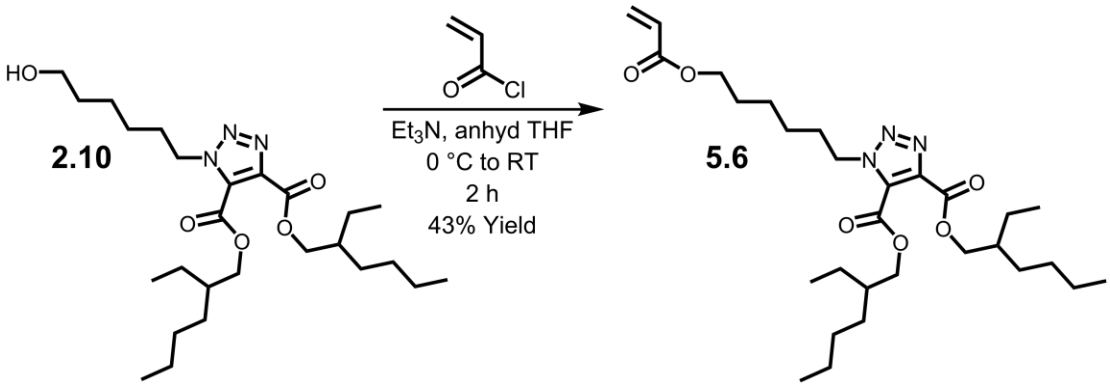

Scheme 5.5 Synthesis of Acrylate Containing Hexyl Tethered 2-Ethylhexyl Triazole Phthalate Mimic **5.6**

and stirred for 2 hours (**Scheme 5.5**). Acidic aqueous workup and subsequent purification via column chromatography furnished acrylate **5.6** as a clear oil in 43% yield.

^{1}H-NMR and ^{13}C-NMR of Acrylate-Hexyl-TRZ-DiEH **5.6** was acquired in $CDCl_3$ (**Figure 5.7**). ^{1}H-NMR of Acrylate-Hexyl-TRZ-DiEH **5.6** exhibits characteristic vinylic signals: **a** appears as a doublet at δ 6.41 ppm, while **b** is present as a doublet of doublets at δ 6.13 ppm. Vinylic proton **c** produces a doublet at δ 5.84 ppm and shows the typical vinyl coupling constants. Methylene protons **d** adjacent to the acrylate carbonyl gives a triplet at δ 4.16 ppm. Signal **h** at δ 4.60 ppm is indicative of methylene protons neighboring the triazole. The multiplet at δ 4.29 ppm represents methylene protons **i** bound to the oxygen in the 2-ethylhexyl ester. Hexyl tether methylene **e** overlaps with 2-ethylhexyl methines **j** between δ 1.64 – 1.79 ppm. A multiplet between δ 1.28 – 1.51 ppm belongs to the overlapping signals of the hexyl tether methylene **f** and 2-ethylhexyl methylenes **k** and **m**. Methyl groups **l** and **n** of the 2-ethylhexyl chains appear as a multiplet in the range of δ 0.87 – 0.98 ppm.

^{13}C-NMR of Acrylate-Hexyl-TRZ-DiEH **5.6** exhibits a signal indicative of the terminal vinylic acrylate carbon **A** at δ 130.6 ppm. Neighboring vinylic carbon **B** gives a peak at δ 128.5 ppm. The acrylate carbonyl **C** exhibits a signal at δ 166.2 ppm. Further upfield are carbonyl peaks of the triazole esters **L** (δ 158.9 ppm) and **M** (δ 160.6 ppm). Quaternary triazole carbons **J** and **K** are present at δ 129.6 ppm and δ 140.5 ppm. The 2-ethylhexyl groups display a myriad of carbon signals corresponding to each chain on the triazole. Methylene carbons **N** and **N'** give peaks at δ 68.4 ppm and δ 69.1 ppm. Methines **I** and **I'** appear at δ 38.70 ppm and δ 38.73 ppm, while **P** and **P'** are represented by signals at δ 23.5 ppm and δ 23.6 ppm. Methylene carbons **R** and **R'** are present at δ 30.17 and δ 30.21 ppm. Adjacent methylenes **S** and **S'** are observed at δ 28.86 ppm and δ 28.89 ppm. Peaks at δ 22.94 ppm and δ 22.96 ppm are indicative of methylenes **T** and **T'**. Signals **Q** and **U** appear at δ 10.9 ppm and δ 14.0 ppm, accounting for two methyl groups each.

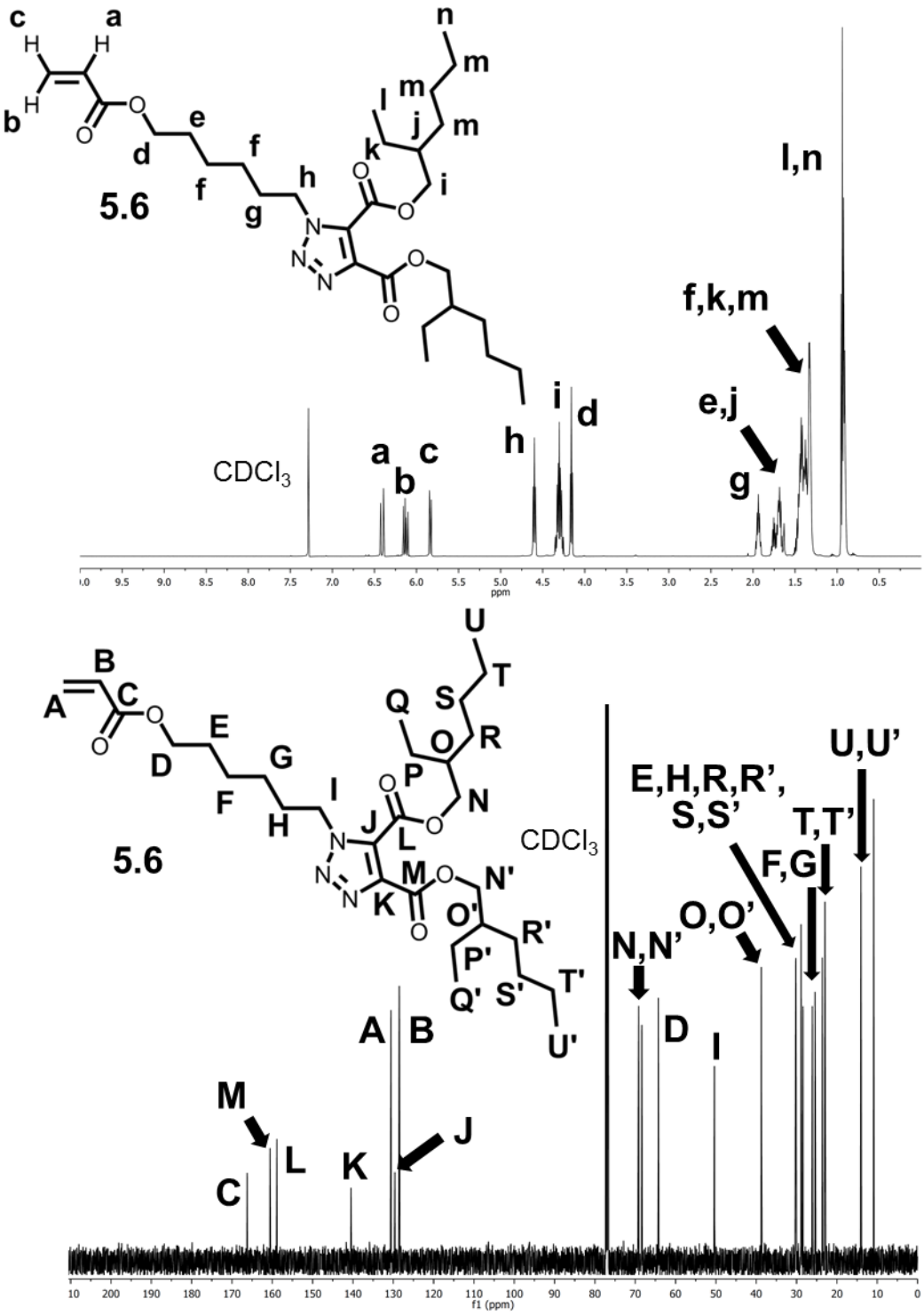

Figure 5.7 ^{1}H-NMR and ^{13}C-NMR Spectra of Acrylate-Hexyl-TRZ-DiEH **5.6**

Acrylate-Hexyl-TRZ-DiEH **5.6** and commercially available poly(ethylene oxide) monomethyl ether (PEO) acrylate and methacrylate will be sent to our collaborator copolymerizations with VCM, to act as internal PVC plasticizers (**Scheme 5.6** and **Scheme 5.7**). These polymerization experiments are currently ongoing.

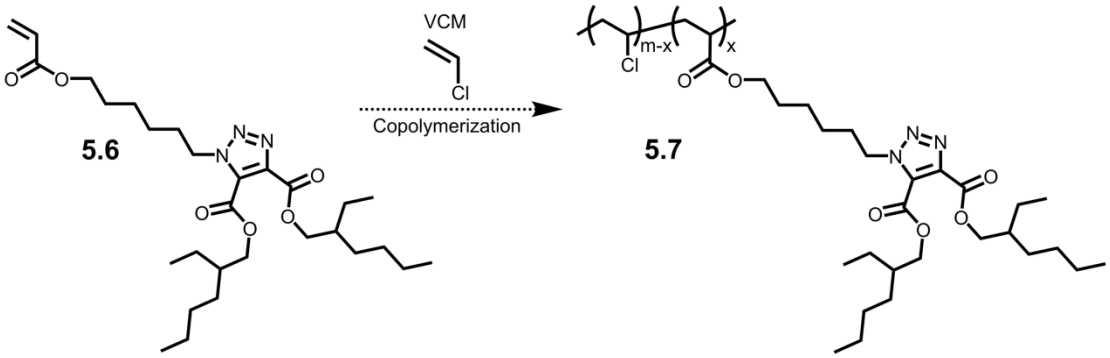

Scheme 5.6 Copolymerization of Vinyl Chloride and Acrylate **5.6** Containing Hexyl Tethered 2-Ethylhexyl Triazole Phthalate Mimic

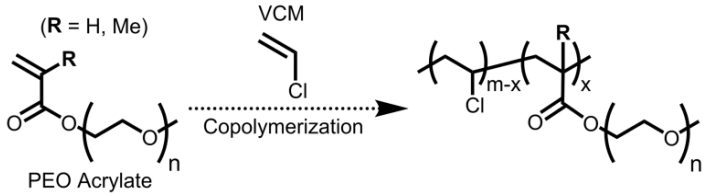

Scheme 5.7 Copolymerization of Vinyl Chloride and PEO Acrylate and PEO Methacrylate

5.4 Conclusion

Difficulties were encountered when attempting to copolymerize VCM and vinyl acetates containing triazole-phthalate mimics. To remedy the inactivity found with vinyl acetate triazoles, acrylate derivatives were sent, and are presently undergoing polymerization studies. While the copolymerization strategy is promising, it is currently easier to modify PVC with triazole-based phthalate mimics to obtain internally plasticized materials. VCM requires many safety protocols as it is a toxic gas under ambient conditions. Specialized equipment is required to copolymerize VCM with a monomer containing an appended plasticizing moiety. In comparison, post-polymerization direct modification of PVC using the triazole attachment

strategy outlined in *Chapters 2, 3* and *4* relies on minimal laboratory equipment. The copolymerization method may prove amiable to industry once reaction conditions involving VCM and a pre-plasticizing monomer are optimized. If the copolymers exhibit characteristics of internally plasticized PVC, this approach may be preferred in some applications to the post-polymerization functionalization strategy.

5.5 References

1. Kumar, R.; Tiwari, P.; Maulik, P. R.; Misra, A. K. A Generalized Procedure for the One-Pot Preparation of Glycosyl Azides and Thioglycosides Directly from Unprotected Reducing Sugars under Phase‐Transfer Reaction Conditions. *European Journal of Organic Chemistry* **2005,** (1), 74-79.

2. (a) Fujii, K.; Matsumoto, M.; Ukida, J. Hydrolysis of Poly(vinyl acetate)s of Various Tacticities. *Journal of Polymer Science Part B-Polymer Letters* **1963,** *1* (12), 687-691; (b) Noyce, D. S.; Pollack, R. M. Mechanisms for the Acid-Catalyzed Hydrolysis of Vinyl Acetate and Isopropenyl Acetate. *Journal of the American Chemical Society* **1969,** *91* (25), 7158-7163.

3. Brase, S.; Gil, C.; Knepper, K.; Zimmermann, V. Organic Azides: An Exploding Diversity of a Unique Class of Compounds. *Angewandte Chemie-International Edition* **2005,** *44* (33), 5188-5240.

6 Experimental Section

6.1 General Materials and Methods

PVC (M_w: 43000 g/mol, PDI: 1.95) was purchased from Sigma-Aldrich and purified by dissolution of 20.00 grams of PVC in 240 mL of THF at 50 °C. This solution was allowed to cool to room temperature and precipitated in 800 mL of methanol. The mother liquor was filtered and the dissolution-precipitation process was repeated two more times. Tetrahydrofuran (Fisher Scientific, HPLC grade, submicron filtered, uninhibited) was dried over sodium and benzophenone, under argon when anhydrous conditions were required. Silica gel (Sorbent Technologies, Fisher Scientific, or Sigma-Aldrich; grade 60, 230-400 mesh, 40-63 μm particle size) was utilized for column chromatography. All other chemicals were used as received.

The following chemicals were purchased from Fisher Scientific: hexanes (ACS certified, 4.2% methylpentanes), ethyl acetate (ACS certified), dichloromethane (stabilized HPLC grade, submicron filtered), methanol (ACS certified), ethanol (absolute, 200 proof, molecular biology grade), acetonitrile (Optima™, LC/MS grade), tetrahydrofuran (HPLC grade, submicron filtered, uninhibited), toluene (HPLC grade, ACS certified), acetone (HPLC grade), dimethylformamide (sequencing grade), pentanes (HPLC grade, submicron filtered), diethyl ether (BHT stabilized, ACS certified), sodium chloride (crystalline, ACS certified), sodium bromide (granular, ACS certified), sodium bicarbonate (granular powder, ACS certified), potassium hydroxide (pellets, ACS certified), magnesium sulfate (anhydrous, certified powder), sodium sulfate (anhydrous, granular ACS certified), concentrated hydrochloric acid (36.9%, ACS Certified), concentrated sulfuric acid (certified ACS Plus), bromine (ACS certified), zinc powder (99.2%), *n*-butanol (HPLC grade), Celite™ 545 filtering aid (non-acid washed). The following chemicals were purchased from Sigma-Aldrich: dimethylsulfoxide (≥99.9% ACS Reagent), carbon tetrachloride (anhydrous, ≥99.5%), 3-pentanone (≥99%), phosphorous pentachloride (≥98.0%, purum p.a.), pyridine (anhydrous,

99.8%), triethylamine (anhydrous, ≥99.5%), iodine (≥99.99% trace metals basis), tri(ethylene glycol) monomethyl ether (95%), poly(ethylene glycol) monomethyl ether 350, poly(ethylene glycol) monomethyl ether 550, acryloyl chloride (≥97%, 400 ppm phenothiazine stabilizer). The following chemicals were purchased from Tokyo Chemical Industries (TCI): 6-chlorohexanol (>96%), poly(ethylene glycol) monomethyl ether 1000, poly(ethylene glycol) monomethyl ether 2000, acetylenedicarboxylate monopotassium salt (>95%), tetrabutylammonium hydrogensulfate (>98%), vinyl chloroacetate (>99%, MEHQ stabilizer), 3-pentanone (>98.0%).The following chemicals were purchased from Acros Organics: sodium azide (99%, extra pure), acetylenedicarboxylic acid (98%), propiolic acid (98%), p-toluenesulfonic acid monohydrate (99%, extra pure), pyridine (99%), potassium bromide (ACS certified). The following chemicals were purchased from Alfa Aesar: dimethyl acetylenedicarboxylate (98%), 2-ethyl-1-hexanol (99%), propiolic acid (>98%). The following chemicals were purchased from Spectrum: dioctyl phthalate (CAS: 117-81-7), sodium bisulfite (granular, F.C.C.). The following chemicals were purchased from Cambridge Isotope Laboratories, Inc.: chloroform-D (D, 99.8%), benzene-d_6 (D, 99.5%).

6.2 Instrumentation

Nuclear Magnetic Resonance (NMR) spectra were recorded with a Bruker Avance III HD 4 channel 500 MHz Oxford Magnet NMR Spectrometer with Automation, Varian Unity Plus 500 MHz Oxford Magnet NMR Spectrometer, or Bruker Avance III HD 800 MHz NMR Spectrometer. ^{1}H-NMR spectra taken in deuterated chloroform ($CDCl_3$) used the $CHCl_3$ signal (δ 7.26 ppm) as an internal standard, and the $CDCl_3$ triplet (δ 77.27 ppm) for ^{13}C-NMR. ^{1}H-NMR spectra taken in benzene-d_6 utilized the C_6H_6 (δ 7.15 ppm) as an internal standard, and the C_6D_6 triplet (δ 127.68 ppm) for ^{13}C-NMR. Fourier Transform Infrared Spectroscopy (FTIR) was recorded with a Perkin-Elmer Spectrum One Spectrometer, with sodium chloride (NaCl) plates. Liquids were measured neat. Polymers were measured as dried thin films. Solid molecules were combined, ground and pressed into potassium bromide (KBr) plates using a

Carver press. High Resolution Mass Spectroscopy (HRMS) was recorded with a Thermo Scientific LTQ-Orbitrap Velos Pro MS. HRMS was taken with samples dissolved in acetonitrile (CH_3CN). Elemental analysis was performed by MHW Laboratories, P.O. Box 15149, Phoenix, AZ, 85060. Modulated Differential Scanning Calorimetry (MDSC) was performed on each polymer using a TA Instruments DSC Q2000 with a heat-cool-heat protocol. The general scanning ranges of MDSC analyses ranged from -90 °C to 200 °C, with a heating rate of 10 °C per minute. Derivative thermogravimetry (DTG) and thermal gravimetric analyses (TGA) were performed with a TA Instruments TGA Q500. TGA was performed within a scanning range of 30 °C to 500 °C, with a heating rate of 10 °C per minute in air or nitrogen.

6.3 Plasticizer Migration Studies

The degree of plasticizer migration was determined by a process derived from an ASTM International standard test method (ASTM-D5227). This method describes an extraction/gravimetric procedure for determination of the amount of hexane soluble low molecular weight material in a myriad of polymers. Samples were extracted as square films (~15 x 15 mm^2), dried by high vacuum overnight and weighed. A Berzelius beaker (150 mL) with a stir bar (25 mm x 8 mm diameter) was utilized as the extraction apparatus. 50 mL of *n*-hexane (Alfa Aesar, 95% HPLC distilled in glass) was pre-heated at 50 °C for 15 minutes prior to placing the polymer in the beaker. A stir rate of 100 revolutions per minute was used for all extractions. Each sample was extracted for 2 hours at 50 °C. After the extraction, the solvent was decanted. The polymer was placed in a 20 mL scintillation vial and dried under high vacuum at room temperature overnight. The mass of each sample post-extraction was determined. The degree of plasticizer migration was calculated using **Equation 4.1**. Traditional DEHP-PVC (containing 60 weight percent DEHP) was used as a standard. Each polymer sample was extracted in triplicate. Plasticizer migration data is shown in **Table 4.9**.

6.4 Warning on Organic Azides

Organic azides can be dangerous in nature: low molecular weight organic azides have a propensity to violently decompose. A formula to indicate if an organic azide is likely safe to handle has been created:[1] $(N_{Carbon} + N_{Oxygen}) / N_{Azide\ Nitrogen} \geq 3$, where N = number of atoms. Using this formula, vinyl azidoacetate **5.1** gives a value of 1.6 and *should not be handled in its pure form*. While 6-azidohexanol and PVC-azide did not show signs of violent decomposition, it should be noted that extreme caution should be taken at all times when synthesizing or handling organic azides.

6.5 Chapter 2 Experimental Section

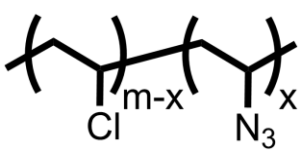

Preparation of 5% PVC-Azide.[2] Purified poly(vinyl chloride) (2.000 g, 21.68 mmol) was added to a 100 mL round bottom flask and dissolved in 20 mL of dimethylformamide at 62 °C. Sodium azide (2.000 g, 30.764 mmol) was subsequently added and stirred for 30 min. The reaction was immediately filtered through a large Buchner funnel with a WHATMAN™ grade 1 qualitative filter paper into a vacuum flask. The reaction solution was slowly precipitated into 200 mL of MeOH then filtered through a Buchner funnel and WHATMAN™ grade 1 qualitative filter paper into a vacuum flask. The polymer was dried for 15 min under house vacuum, then dissolved in 20 mL of THF. The dissolved polymer was slowly precipitated into 100 mL of MeOH then filtered through a Buchner funnel and WHATMAN™ grade 1 qualitative filter paper into a vacuum flask. This process was repeated once more with MeOH. The dissolved PVC was dissolved into 10 mL of THF and slowly precipitated in 100 mL of a 3:1 mixture of MeOH:H_2O, filtered and dried for 15 min under house vacuum then dissolved in 20 mL of THF. The final precipitation was performed in 100 mL of MeOH. The isolated polymer was dried under house vacuum for 5 days *via* Buchner funnel to give 1.4314 g of the title compound as a flocculent white solid.

^{1}H NMR (500 MHz, $CDCl_3$): δ 4.68 – 4.26 (br m, *Cl-C-H*), 4.21 (br s, *N-C-H*), 4.08 (br s, *N-C-H*), 2.45 – 2.02 (br m, *Cl-C-CH_2-C-Cl*), 1.94 – 1.77 (br m, *Cl-C-CH_2-C-N_3* and *N_3-C-CH_2-C-N_3*).

^{13}C NMR (125 MHz, $CDCl_3$, DEPT): δ 57.0 – 56.9 (CH syndio), 56.1 – 55.9 (CH hetero), 55.1 – 54.9 (CH iso), 47.3 – 44.8 (family of CH_2 peaks), 44.1 (N-C-CH_2).

IR (Neat): 2974 (m, alkane CH), 2911 (m, alkane CH), 2875 (m, alkane CH), 2114 (s, N_3), 1435 (m, methylene stretch CH_2), 615 (w, C-Cl) cm^{-1}.

DSC (T_g): 83 °C.

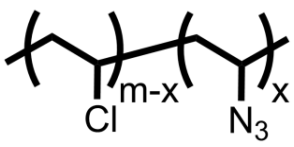

Preparation of 15% PVC-Azide.[2] Purified poly(vinyl chloride) (2.000 g, 21.68 mmol) was added to a 100 mL round bottom flask and dissolved in 20 mL of dimethylformamide at 62 °C. Sodium azide (2.000 g, 30.764 mmol) was subsequently added and stirred for 2 h. The reaction was immediately filtered through a large Buchner funnel with a WHATMAN™ grade 1 qualitative filter paper into a vacuum flask. The reaction solution was slowly precipitated into 200 mL of MeOH then filtered through a Buchner funnel and WHATMAN™ grade 1 qualitative filter paper into a vacuum flask. The polymer was dried for 15 min under house vacuum, then dissolved in 20 mL of THF. The dissolved polymer was slowly precipitated into 100 mL of MeOH then filtered through a Buchner funnel and WHATMAN™ grade 1 qualitative filter paper into a vacuum flask. This process was repeated once more with MeOH. The dissolved PVC was dissolved into 10 mL of THF and slowly precipitated in 100 mL of a 3:1 mixture of MeOH:H_2O, filtered and dried for 15 min under house vacuum then dissolved in 20 mL of THF. The final precipitation was performed in MeOH. The isolated polymer was dried under house vacuum for 5 days *via* Buchner funnel to give 1.2058 g of the title compound as a flocculent white solid.

^{1}H NMR (500 MHz, $CDCl_3$): δ 4.68 – 4.26 (br m, *Cl-C-H*), 4.20 (br s, *N-C-H*), 4.09 (br s, *N-C-H*), 2.51 – 2.02 (br m, *Cl-C-CH_2-C-Cl*), 1.98 – 1.77 (br m, *Cl-C-CH_2-C-N_3* and *N_3-C-CH_2-C-N_3*).

^{13}C NMR (125 MHz, $CDCl_3$, DEPT): δ 57.0 – 56.9 (CH syndio), 56.1 – 55.7 (CH hetero), 55.1 – 54.9 (CH iso), 47.3 – 44.8 (family of CH_2 peaks), 44.0 – 42.8 (N-C-CH_2).

IR (Neat): 2975 (m, alkane CH), 2911 (m, alkane CH), 2114 (s, N_3), 1435 (m, methylene stretch CH_2), 615 (w, C-Cl) cm^{-1}.

DSC (T_g): 78 °C.

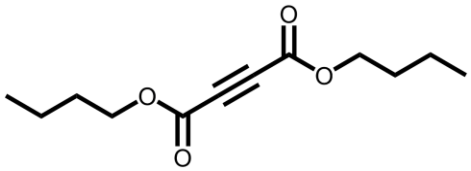

Preparation of 1,4-dibutyl but-2-ynedioate.[2] But-2-ynedioic acid (4.000 g, 35.07 mmol) was added to a 100 mL round bottom flask. *n*-Butanol (7.798 g, 105.21 mmol) was then added along with 4-methylbenzenesulfonic acid (0.400 g, 2.104 mmol) and 50 mL of dry toluene. Using a Dean-Stark apparatus, the reaction was heated and stirred at reflux for 1.5 h. The organic layer was concentrated *in vacuo* to give a crude brown oil. purified *via* flash chromatography using 95:5 hexanes:ethyl acetate affording 7.538 g (33.314 mmol, 94.99% yield) of the title compound as a colorless oil.

TLC: 95:5 hexanes:ethyl acetate, R_f=0.43, UV, $KMnO_4$ stain, *p*-anisealdehyde stain, blue spot.

^{1}H NMR (500 MHz, $CDCl_3$): δ 4.25 (t, *J* = 6.6 Hz, 4H), 1.68 (p, *J* = 6.6 Hz, 4H), 1.42 (h, *J* = 7.3 Hz, 4H), 0.96 (t, *J* = 7.3 Hz, 6H).

^{13}C NMR (125 MHz, $CDCl_3$, DEPT): δ 152.0 (C=O), 74.7 (4°), 66.8 (O-CH_2), 30.3 (CH_2), 18.9 (CH_2), 13.5 (CH_3).

IR: 2963 (s, alkane CH), 2938 (s, alkane CH), 2876 (s, alkane CH), 1728 (s, ester C=O), 1467 (s, methylene bending CH_2), 1252 (s, ester stretch C-O) cm^{-1}.

HRMS: Calcd. for $C_{12}H_{18}O_4$ $[M+H]^+$ 227.1278; Found 227.1283.

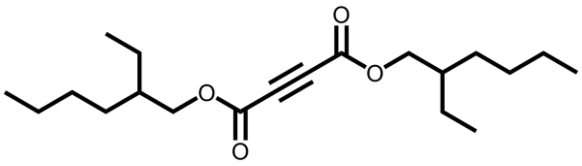

Preparation of 1,4-bis(2-ethylhexyl) but-2-ynedioate.[2] But-2-ynedioic acid (3.422 g, 30.00 mmol) was added to a 100 mL round bottom flask. 2-Ethylhexan-1-ol (8.595 g, 66.00 mmol) was then added along with 4-methylbenzenesulfonic acid (0.342 g, 1.800 mmol) and 42 mL of dry toluene. Using a Dean-Stark apparatus, the reaction was heated and stirred at reflux for 1 h. The organic layer was concentrated *in vacuo* to give a crude brown oil. Purification *via* flash chromatography using 95:5 hexanes:ethyl acetate afforded 9.211 g (27.213 mmol, 73.69% yield) of a colorless oil, as a mixture of diastereomers.

TLC: 95:5 hexanes:ethyl acetate, R_f=0.80, UV, $KMnO_4$ stain, *p*-anisealdehyde stain, blue spot.

^{1}H NMR (500 MHz, $CDCl_3$): δ 4.19 – 4.13 (m, 4H), 1.66 – 1.61 (m, 2H), 1.42 – 1.36 (m, 4H), 1.35 – 1.25 (m, 12H), 0.91 (t, 12H).

^{13}C NMR (125 MHz, $CDCl_3$, DEPT): δ 152.0 (C=O), 74.7 (4°), 69.2 (O-CH_2), 38.6 (CH), 30.1 (CH_2), 28.8 (CH_2), 23.5 (CH_2), 22.9 (CH_2), 14.0 (CH_3), 10.8 (CH_3).

IR: 2962 (s, alkane CH), 2932 (s, alkane CH), 2875 (s, alkane CH), 2862 (s, alkane CH), 1725 (s, ester C=O), 1464 (s, methylene bending CH_2), 1255 (s, ester stretch C-O) cm^{-1}.

HRMS: Calcd. for $C_{20}H_{35}O_4$ $[M+H]^+$ 339.2529; Found 339.2525.

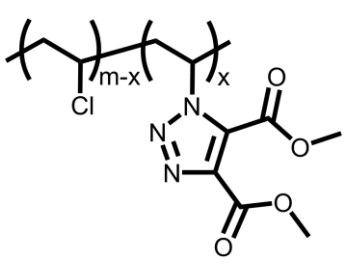

Preparation of 5% PVC-TRZ-DiMe. Poly(vinyl chloride) 5% azide (1.000 g, 16.00 mmol) was added to a 100 mL round bottom flask and dissolved in 20 mL of 3-pentanone at 90 °C. Dimethyl acetylenedicarboxylate (0.284g, 2.0 mmol) dissolved in 10 mL 3-pentanone was added to the PVC solution and

stirred for 24 h. The reaction was precipitated in 80 mL of MeOH, three times each. The isolated polymer was dried under house vacuum for 2 days to yield 0.850 g of a flocculent white solid.

^{1}H NMR (500 MHz, $CDCl_3$): δ 5.65 – 5.50 (br m, *C-C<u>H</u>-triazole*), 4.66 – 4.24 (br m, *Cl-C-<u>H</u>*), 4.08 – 4.02 (br m, *O-C<u>H₃</u>*), 4.00 (br s, *O-C<u>H₃</u>*), 2.93 – 2.55 (br m, *Cl-C-C<u>H₂</u>-C-triazole* and *triazole-C-C<u>H₂</u>-C-triazole*), 2.50 – 1.90 (br m, *Cl-C-C<u>H₂</u>-C-Cl*).

^{13}C NMR (125 MHz, $CDCl_3$): δ 139.0 (4°), 130.7 (4°), 57.0 – 56.9 (CH syndio), 56.1 – 55.9 (CH hetero), 55.1 – 54.9 (CH iso), 52.8 (O-CH_3), 47.3 – 44.8 (family of CH_2 peaks).

IR (Neat): 2976 (w, alkane CH), 2955 (w, alkane CH), 2912 (w, alkane CH), 1728 (s, ester C=O), 1556 (w, triazole C=C), 1436 (m, methylene stretch CH_2), 1268 (s, ester stretch C-O), 614 (w, C-Cl) cm^{-1}.

DSC (T_g): 88 °C.

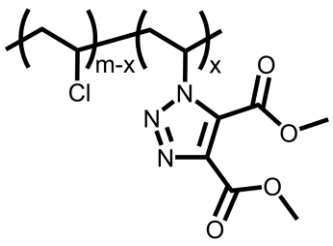

Preparation of 15% PVC-TRZ-DiMe. Poly(vinyl chloride) 15% azide (1.000 g, 16.00 mmol) was added to a 100 mL round bottom flask and dissolved in 20 mL of 3-pentanone at 90 °C. Dimethyl acetylenedicarboxylate (1.023 g, 7.2 mmol) was added to the PVC solution and stirred for 24 h. The reaction was precipitated in 80 mL of MeOH, three times each. The isolated polymer was dried under house vacuum for 2 days to yield 1.1 g of a flocculent white solid.

^{1}H NMR (500 MHz, $CDCl_3$): δ 5.65 – 5.35 (br m, *C-C<u>H</u>-triazole*), 4.65 – 4.15 (br m, *Cl-C-<u>H</u>*), 4.07 – 4.02 (br m, *O-C<u>H₃</u>*), 4.00 (br s, *O-C<u>H₃</u>*), 2.92 – 2.52 (br m, *Cl-C-C<u>H₂</u>-C-triazole* and *triazole-C-C<u>H₂</u>-C-triazole*), 2.50 – 1.85 (br m, *Cl-C-C<u>H₂</u>-C-Cl*).

^{13}C NMR (125 MHz, $CDCl_3$, DEPT): δ 160.1 (C=O), 158.7 (C=O), 139.0 (4°), 132.9 (4°), 57.0 – 56.9 (CH syndio), 56.4 (CH-triazole syndio), 56.1 – 55.9 (CH hetero), 55.1 – 54.9 (CH iso), 53.9 – 53.8 (CH-triazole iso), 52.8 (O-<u>C</u>H_3), 47.3 – 44.8 (family of CH_2 peaks).

IR (Neat): 2956 (w, alkane CH), 2912 (w, alkane CH), 2845 (w, alkane CH), 1729 (s, ester C=O), 1556 (w, triazole C=C), 1436 (m, methylene stretch CH_2), 1269 (s, ester stretch C-O), 615 (w, C-Cl) cm^{-1}.

DSC (T_g): 96 °C.

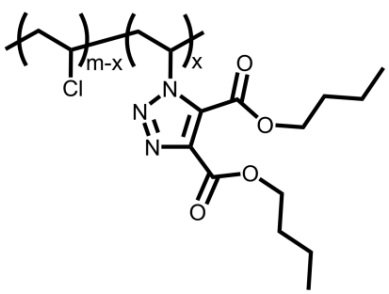

Preparation of 5% PVC-TRZ-DiBu. Poly(vinyl chloride) 5% azide (1.000 g, 16.00 mmol) was added to a 100 mL round bottom flask and dissolved in 30 mL of 3-pentanone at 90 °C. 1,4-Dibutyl but-2-ynedioate (0.452 g, 2.0 mmol) was added to the PVC solution and stirred for 24 h. The reaction was concentrated to approximately half its volume *in vacuo*, then precipitated in 80 mL of MeOH, three times each. The isolated polymer was dried under house vacuum for 2 days to yield 0.7 g of a flocculent white solid.

^{1}H NMR (500 MHz, $CDCl_3$): δ 5.64 – 5.40 (br m, *C-C<u>H</u>-triazole*), 4.65 – 4.42 (br m, *Cl-C-<u>H</u>*), 4.41 – 4.35 (br m, *O-C<u>H_2</u>-C*), 4.34 – 4.24 (br m, *Cl-C-<u>H</u>*), 2.92 – 2.81 (br t, *Cl-C-C<u>H_2</u>-C-triazole* and *triazole-C-C<u>H_2</u>-C-triazole*), 2.80 – 2.69 (br m, *Cl-C-C<u>H_2</u>-C-triazole* and *triazole-C-C<u>H_2</u>-C-triazole*), 2.50 – 1.85 (br m, *Cl-C-C<u>H_2</u>-C-Cl*), 1.82 – 1.72 (br m, *O-C-C<u>H_2</u>-C*), 1.52 – 1.40 (br m, *O-C-C-C<u>H_2</u>-C*), 0.98 (t, *J* = 7.2, *C<u>H_3</u>*).

^{13}C NMR (125 MHz, $CDCl_3$): δ 159.9 (C=O), 158.5 (C=O), 139.3 (4°), 132.8 (4°), 67.4 (O-CH_2), 65.8 (O-CH_2), 57.0 – 56.9 (CH syndio), 56.4 (CH-triazole syndio), 56.1 – 55.9 (CH hetero), 55.1 – 54.9 (CH iso), 53.9 – 53.8 (CH-triazole iso), 47.3 – 44.8 (family of CH_2 PVC peaks), 30.6 (CH_2), 30.3 (CH_2), 19.1 (CH_2), 13.74 (CH_2), 13.68 (CH_2).

IR (Neat): 2963 (w, alkane CH), 2936 (w, alkane CH), 2875 (w, alkane CH), 1723 (s, ester C=O), 1551 (w, triazole C=C), 1465 (m, methylene stretch CH_2), 1256 (s, ester C-O) cm^{-1}.

DSC (T_g): 76 °C.

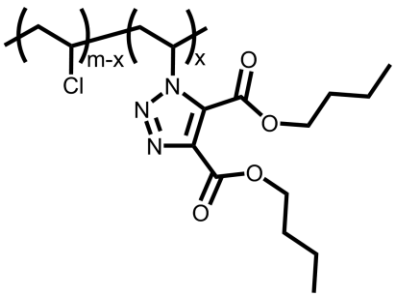

Preparation of 15% PVC-TRZ-DiBu. Poly(vinyl chloride) 15% azide (1.000 g, 16.00 mmol) was added to a 100 mL round bottom flask and dissolved in 20 mL of 3-pentanone at 90 °C. 1,4-Dibutyl but-2-ynedioate (1.6291 g, 7.2 mmol) was added to the PVC solution and stirred for 24 h. The reaction was precipitated in 80 mL of MeOH, three times each. The isolated polymer was dried under house vacuum for 2 days to yield 0.97 g of a flocculent white solid.

^{1}H NMR (500 MHz, $CDCl_3$): δ 5.65 – 5.45 (br m, *C-C<u>H</u>-triazole*), 4.67 – 4.41 (br m, *Cl-C-<u>H</u>*), 4.40 – 4.34 (br m, *O-C<u>H$_2$</u>-C*), 4.34 – 4.10 (br m, *Cl-C-<u>H</u>*), 2.92 – 2.81 (br t, *Cl-C-C<u>H$_2$</u>-C-triazole* and *triazole-C-C<u>H$_2$</u>-C-triazole*), 2.80 – 2.67 (br m, *Cl-C-C<u>H$_2$</u>-C-triazole* and *triazole-C-C<u>H$_2$</u>-C-triazole*), 2.50 – 1.85 (br m, *Cl-C-C<u>H$_2$</u>-C-Cl*), 1.82 – 1.65 (br m, *O-C-C<u>H$_2$</u>-C*), 1.52 – 1.35 (br m, *O-C-C-C<u>H$_2$</u>-C*), 0.98 (t, *J* = 7.3, *C<u>H$_3$</u>*).

^{13}C NMR (125 MHz, $CDCl_3$, DEPT): δ 159.9 (C=O), 158.5 (C=O), 139.3 (4°), 132.8 (4°), 67.4 (O-CH_2), 67.3 (O-CH_2), 65.8 (O-CH_2), 57.0 – 56.9 (CH syndio), 56.4 (CH-triazole syndio), 56.1 – 55.9 (CH hetero), 55.1 – 54.9 (CH iso), 53.9 – 53.8 (CH-triazole iso), 47.3 – 44.8 (family of CH_2 PVC peaks), 30.6 (CH_2), 30.3 (CH_2), 19.1 (CH_2), 19.0 (CH_2), 13.73 (CH_2), 13.67 (CH_2).

IR (Neat): 2963 (w, alkane CH), 2937 (w, alkane CH), 2876 (w, alkane CH), 1725 (s, ester C=O), 1552 (w, triazole C=C), 1466 (m, methylene stretch CH_2), 1255 (s, ester stretch C-O) cm^{-1}.

DSC (T_g): 74 °C.

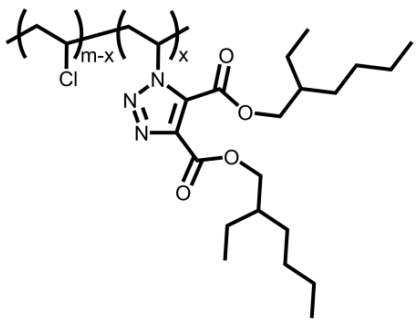

Preparation of 5% PVC-TRZ-DiEH. Poly(vinyl chloride) 5% azide (1.000 g, 16.00 mmol) was added to a 100 mL round bottom flask and dissolved in 30 mL of 3-pentanone at 90 °C. 1,4-Bis(2ethylhexyl) but-2-ynedioate (0.676 g, 2.0 mmol) was added to the PVC solution and stirred for 24 h. The reaction was precipitated in 80 mL of MeOH, three times each. The isolated polymer was dried under house vacuum for 2 days to yield 0.8216 g of a flocculent white solid.

^{1}H NMR (500 MHz, $CDCl_3$): δ 5.65 – 5.45 (br m, *C-C<u>H</u>-triazole*), 4.66 – 4.40 (br m, *Cl-C-<u>H</u>*), 4.39 – 4.20 (br m, *Cl-C-<u>H</u>* and *O-C<u>H$_2$</u>-C*), 2.92 – 2.81 (br t, *Cl-C-C<u>H$_2$</u>-C-triazole* and *triazole-C-C<u>H$_2$</u>-C-triazole*), 2.81 – 2.67 (br m, *Cl-C-C<u>H$_2$</u>-C-triazole* and *triazole-C-C<u>H$_2$</u>-C-triazole*), 2.50 – 1.85 (br m, *Cl-C-C<u>H$_2$</u>-C-Cl*), 1.80 – 1.69 (br m, *O-C-C<u>H</u>-C*), 1.52 – 1.36 (br m, *O-C-C-C<u>H$_2$</u>*), 1.35 – 1.26 (br s, *O-C-C-C-C<u>H$_2$</u>-C<u>H$_2$</u>*), 0.98 – 0.87 (m, *C<u>H$_3$</u>*).

^{13}C NMR (125 MHz, $CDCl_3$): δ 160.1 (C=O), 158.7 (C=O), 139.5 (4°), 132.5 (4°), 70.1 (O-CH_2), 69.9 (O-CH_2), 68.5 (O-CH_2), 57.0 – 56.9 (CH syndio), 56.5 – 56.4 (CH-triazole syndio), 56.1 – 55.9 (CH hetero), 55.2 – 54.9 (CH iso), 47.3 – 44.8 (family of CH_2 PVC peaks), 38.7 (CH), 38.6 (CH), 30.2 (CH_2), 30.1 (CH_2), 28.9 (CH_2), 23.6 (CH_2), 23.5 (CH_2), 23.0 (CH_2), 14.1 (CH_3), 10.9 (CH_3).

IR (Neat): 2961 (w, alkane CH), 2931 (w, alkane CH), 2873 (w, alkane CH), 2861 (w, alkane CH), 1725 (s, ester C=O), 1553 (w, triazole C=C), 1460 (m, methylene stretch CH_2), 1256 (s, ester stretch C-O), 613 (w, C-Cl) cm^{-1}.

DSC (T_g): 65 °C.

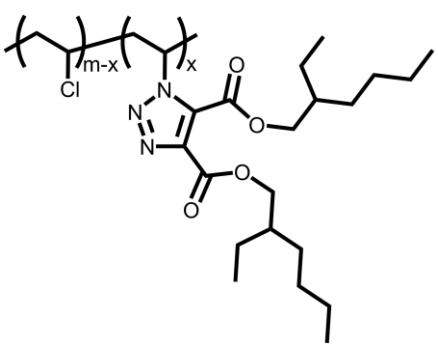

Preparation of 15% PVC-TRZ-DiEH. Poly(vinyl chloride) 15% azide (1.000 g, 16.00 mmol) was added to a 100 mL round bottom flask and dissolved in 20 mL of 3-pentanone at 90 °C. 1,4-Bis(2ethylhexyl) but-2-ynedioate (2.4369 g, 7.2 mmol) was added to the PVC solution and stirred for 24 h. The reaction was precipitated in 80 mL of MeOH, three times each. The isolated polymer was dried under house vacuum for 2 days to yield 0.93 g of a flocculent white solid.

^{1}H NMR (500 MHz, $CDCl_3$): δ 5.65 – 5.40 (br m, *C-C<u>H</u>-triazole*), 4.67 – 4.40 (br m, *Cl-C-<u>H</u>*), 4.39 – 4.10 (br m, *Cl-C-<u>H</u>* and *O-C<u>H$_2$</u>-C*), 2.92 – 2.81 (br t, *Cl-C-C<u>H$_2$</u>-C-triazole* and *triazole-C-C<u>H$_2$</u>-C-triazole*), 2.81 – 2.67 (br m, *Cl-C-C<u>H$_2$</u>-C-triazole* and *triazole-C-C<u>H$_2$</u>-C-triazole*), 2.50 – 1.85 (br m, *Cl-C-C<u>H$_2$</u>-C-Cl*), 1.80 – 1.60 (br m, *O-C-C<u>H</u>-C*), 1.52 – 1.36 (br m, *O-C-C-C<u>H$_2$</u>*), 1.35 – 1.26 (br s, *O-C-C-C-C<u>H$_2$</u>-C<u>H$_2$</u>*), 0.97 – 0.85 (m, *C<u>H$_3$</u>*).

^{13}C NMR (125 MHz, $CDCl_3$, DEPT): δ 160.1 (C=O), 158.7 (C=O), 139.5 (4°), 132.6 (4°), 70.0 (O-CH_2), 69.9 (O-CH_2), 68.5 (O-CH_2), 57.0 – 56.9 (CH syndio), 56.4 (CH-triazole syndio), 56.1 – 55.9 (CH hetero), 55.2 – 54.9 (CH iso), 47.3 – 44.8 (family of CH_2 PVC peaks), 38.7 (CH), 38.6 (CH), 30.2 (CH_2), 30.1 (CH_2), 28.9 (CH_2), 28.8 (CH2), 23.6 (CH_2), 23.5 (CH_2), 23.0 (CH_2), 14.1 (CH_3), 10.9 (CH_3).

IR (Neat): 2961 (s, alkane CH), 2932 (s, alkane CH), 2874 (s, alkane CH), 2862 (s, alkane CH), 1721 (s, ester C=O), 1555 (w, triazole C=C), 1463 (m, methylene stretch CH_2), 1255 (s, ester stretch C-O), 616 (w, C-Cl) cm^{-1}.

DSC (T_g): 57 °C.

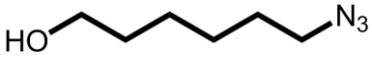

Preparation of 6-azidohexan-1-ol.[3] 6-chlorohexan-1-ol (1.500 g, 10.98 mmol) was added to a 100 mL round bottom flask with 20 mL of dimethyl sulfoxide. NaN_3 (1.071 g, 16.47 mmol) was carefully added to the reaction flask and stirred at 50 °C for 24 h. Water (40 mL) was added to the reaction to quench NaN_3. The reaction mixture was extracted five times using 30 mL each of ethyl acetate. The organic layers were washed with brine four times using 20 mL each, then dried with Na_2SO_4. The volatiles were evaporated *in vacuo* affording 1.572 g (10.98 mmol, quantitative yield) of the title compound as a colorless oil.

TLC: 3:2 hexanes:ethyl acetate, R_f=0.46, *p*-anisealdehyde stain, green-orange spot.

^{1}H NMR (500 MHz, $CDCl_3$): δ 3.60 (t, *J* = 6.6 Hz, 2H), 3.24 (t, *J* = 6.9 Hz, 2H), 1.61 – 1.52 (m, 4H), 1.41 – 1.31 (m, 4H).

^{13}C NMR (125 MHz, $CDCl_3$, DEPT): δ 62.7 (CH_2-OH), 51.4 (CH_2-N_3), 32.5 (CH_2), 28.8 (CH_2), 26.5 (CH_2), 25.3 (CH_2).

IR (Neat): 3351 (s, OH), 2937 (s, alkane CH), 2862 (s, alkane CH), 2097 (s, N_3), 1457 (m, methylene bending CH_2), 1056 (s, 1° alcohol stretch C-O) cm^{-1}.

HRMS: Calcd. for $C_6H_{13}N_3O$ $[M+H]^+$ 144.1131; Found 144.9812.

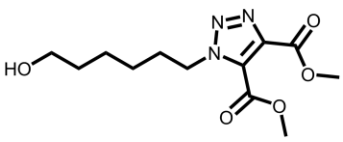

Preparation of 4,5-dimethyl 1-(6-hydroxyhexyl)-1H-1,2,3-triazole-4,5-dicarboxylate. 6-Azidohexan-1-ol (1.570 g, 10.98 mmol) was added to a 100 mL round bottom flask with 35 mL of $CHCl_3$. Dimethyl acetylenedicarboxylate (2.028 g, 14.27 mmol) was added to the reaction flask and stirred at 50 °C for 24 h. The volatiles were evaporated *in vacuo* affording a crude pale yellow oil. Purification *via* flash chromatography using 7:3 ethyl acetate:hexanes furnished 3.125 g (10.953 mmol, 99.76% yield) of the title compound as a pale yellow oil.

TLC: 7:3 ethyl acetate:hexanes, R_f=0.34, UV, *p*-anisealdehyde stain, purple spot.

^{1}H NMR (500 MHz, $CDCl_3$): δ 4.59 (t, *J* = 7.3 Hz, 2H), 3.99 (s, 3H), 3.96 (s, 3H), 3.63 (t, *J* = 6.4 Hz, 2H), 1.91 (p, *J* = 7.3 Hz, 2H), 1.55 (p, *J* = 6.4 Hz, 2H), 1.43 – 1.32 (m, 5H).

^{13}C NMR (125 MHz, $CDCl_3$, DEPT): δ 160.6 (C=O), 159.0 (C=O), 139.9 (4°), 129.8 (4°), 62.5 (CH_2), 53.5 (CH_3), 52.7 (CH_3), 50.5 (CH_2), 32.3 (CH_2), 30.1 (CH_2), 26.1 (CH_2), 25.1 (CH_2).

IR (Neat): 3429 (s, OH), 3006 (s, alkane CH), 2938 (s, alkane CH), 2862 (s, alkane CH), 1733 (s, ester C=O), 1555 (m, triazole C=C), 1469 (s, methylene bending CH_2), 1283 (s, ester stretch C-O), 1224 (s, ester stretch C-O), 1063 (s, 1°alcohol stretch C-O) cm^{-1}.

HRMS: Calcd. for $C_{12}H_{18}N_3O_5$ $[M+H]^+$ 286.1397; Found 286.1393.

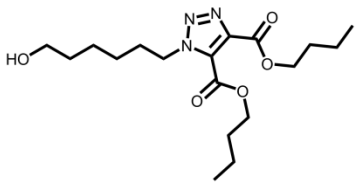

Preparation of 4,5-dibutyl 1-(6-hydroxyhexyl)-1H-1,2,3-triazole-4,5-dicarboxylate. 6-Azidohexan-1-ol (1.570 g, 10.98 mmol) was added to a 100 mL round bottom flask with 35 mL of $CHCl_3$. 1,4-Dibutyl but-2-ynedioate (3.229 g, 14.27 mmol) was added to the reaction flask and stirred at 50 °C for 24 h. The volatiles were evaporated *in vacuo* affording a colorless crude oil. Purification *via* flash chromatography using 3:2 hexanes:ethyl acetate furnished 4.013 g (10.862 mmol, 98.9% yield) of the title compound as a colorless oil.

TLC: 3:2 hexanes:ethyl acetate, R_f=0.25, UV, *p*-anisealdehyde stain, purple spot.

^{1}H NMR (500 MHz, $CDCl_3$): δ 4.57 (t, *J* = 7.2 Hz, 2H), 4.36 (overlapping t, *J* = 6.9 Hz, 4H), 3.62 (t, *J* = 6.4 Hz, 2H), 1.90 (p, *J* = 7.2 Hz, 2H), 1.74 (overlapping p, *J* = 6.9 Hz, 4H), 1.55 (p, *J* = 6.6 Hz, 2H), 1.49 – 1.30 (m, 9H), 1.02 – 0.85 (m, 6H).

^{13}C NMR (125 MHz, $CDCl_3$, DEPT): δ 160.5 (C=O), 158.8 (C=O), 140.3 (4°), 129.8 (4°), 66.7 (CH_2), 65.7 (CH_2), 62.6 (CH_2), 50.4 (CH_2), 32.4 (CH_2), 30.6 (CH_2), 30.3 (CH_2), 30.2 (CH_2), 26.1 (CH_2), 25.1 (CH_2), 19.1 (CH_3), 19.0 (CH_3), 13.7 (CH_3), 13.6 (CH_3).

IR (Neat): 3439 (s, OH), 2961 (s, alkane CH), 2936 (s, alkane CH), 2874 (s, alkane CH), 1732 (s, ester C=O), 1553 (m, triazole C=C), 1467 (s, methylene bending CH_2), 1280 (s, ester stretch C-O), 1065 (s, 1° alcohol stretch C-O) cm^{-1}.

HRMS: Calcd. for $C_{18}H_{31}N_3O_5$ $[M+H]^+$ 370.2336; Found 370.2330.

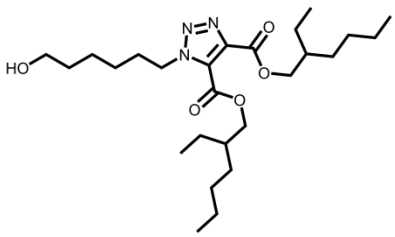

Preparation of 4,5-bis(2-ethylhexyl) 1-(6-hydroxyhexyl)-1H-1,2,3-triazole-4,5-dicarboxylate. 6-Azidohexan-1-ol (1.570 g, 10.98 mmol) was added to a 100 mL round bottom flask with 35 mL of $CHCl_3$. 1,4-Bis(2-ethylhexyl) but-2-ynedioate (4.830 g, 14.27 mmol) was added to the reaction flask and stirred at 50 °C for 24 h. The volatiles were evaporated *in vacuo* affording a colorless crude oil. Purification *via* flash chromatography using 7:3 hexanes:ethyl acetate furnished 5.2641 g (10.929 mmol, 99.5% yield) of a colorless oil, as a mixture of diastereomers.

TLC: 7:3 hexanes:ethyl acetate, R_f=0.29, UV, *p*-anisealdehyde stain, purple spot.

^{1}H NMR (500 MHz, $CDCl_3$): δ 4.58 (t, *J* = 7.3 Hz, 2H), 4.33 – 4.22 (m, 4H), 3.63 (t, *J* = 6.5 Hz, 2H), 1.91 (p, *J* = 7.5 Hz, 2H), 1.77 – 1.64 (m, 2H), 1.55 (p, *J* = 6.6 Hz, 2H), 1.44 – 1.26 (m, 21H), 0.97 – 0.80 (m, 12H).

^{13}C NMR (125 MHz, $CDCl_3$, DEPT): δ 160.5 (C=O), 158.8 (C=O), 140.4 (4°), 129.7 (4°), 69.1 (CH_2), 68.3 (CH_2), 62.5 (CH_2), 50.4 (CH_2), 38.7 (CH), 38.7 (CH), 32.4 (CH_2), 30.2 (CH_2), 28.9 (CH_2), 26.1 (CH_2), 25.1 (CH_2), 23.6 (CH_2), 23.5 (CH_2), 22.9 (CH_2), 14.0 (CH_3), 10.9 (CH_3).

IR (Neat): 3436 (s, OH), 2959 (s, alkane CH), 2932 (s, alkane CH), 2861 (s, alkane CH), 1733 (s, ester C=O), 1555 (m, triazole C=C), 1466 (s, methylene bending CH_2), 1279 (m, ester stretch C-O), 1060 (1° alcohol stretch C-O) cm^{-1}.

HRMS: Calcd. for $C_{26}H_{47}N_3O_5$ $[M+H]^+$ 482.3588; Found 482.3588.

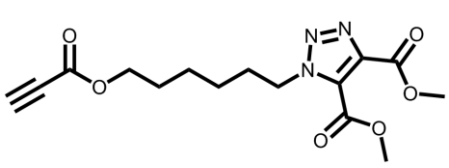

Preparation of 4,5-dimethyl-1-[6-(prop-2-ynoyloxy)hexyl]-1H-1,2,3-triazole-4,5-dicarboxylate. Propiolic acid (0.500 g, 7.138 mmol) was added to a 25 mL round bottom flask with 7 mL of toluene. 4,5-Dimethyl 1-(6-hydroxyhexyl)-1H-1,2,3-triazole-4,5-dicarboxylate (2.6472 g, 9.279 mmol) and 4-methylbenzenesulfonic acid (0.0815 g, 0.428 mmol) was added to the reaction flask and stirred at reflux for 2 h. The volatiles were evaporated *in vacuo*, affording a light brown crude oil. Purification *via* flash chromatography using 1:1 hexanes:ethyl acetate furnished 1.5981 g (4.738 mmol, 66.37% yield) of the title compound as a colorless oil.

TLC: 1:1 hexanes:ethyl acetate, R_f=0.61, UV, $KMnO_4$ stain, *p*-anisealdehyde stain, yellow spot.

^{1}H NMR (500 MHz, $CDCl_3$): δ 4.62 (t, *J* = 7.2 Hz, 2H), 4.20 (t, *J* = 6.5 Hz, 2H), 4.03 (s, 3H), 4.00 (s, 3H), 2.90 (s, 1H), 1.95 (p, *J* = 7.2 Hz, 2H), 1.70 (p, *J* = 6.7 Hz, 2H), 1.47 – 1.36 (m, 4H).

^{13}C NMR (125 MHz, $CDCl_3$, DEPT): δ 160.5 (C=O), 159.0 (C=O), 152.7 (C=O), 140.0 (4°), 129.7 (4°), 74.7 (alkyne 4°), 74.67 (alkyne CH), 66.0 (CH_2), 53.4 (CH_3), 52.7 (CH_3), 50.4 (CH_2), 30.0 (CH_2), 28.1 (CH_2), 25.9 (CH_2), 25.2 (CH_2).

IR (Neat): 3255 (s, alkyne CH) 2955 (s, alkane CH), 2864 (s, alkane CH), 2117 (s, alkyne CC), 1735 (s, ester C=O), 1716 (s, ester C=O), 1554 (m, triazole C=C), 1466 (s, methylene bending CH_2), 1267 (s, ester stretch C-O), 1235 (s, ester stretch C-O) cm^{-1}.

HRMS: Calcd. for $C_{15}H_{20}N_3O_6$ $[M+H]^+$ 338.1347; Found 338.1340.

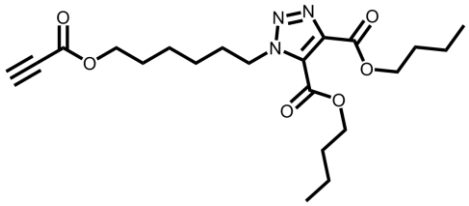

Preparation of 4,5-dibutyl-1-[6-(prop-2-ynoyloxy)hexyl]-1H-1,2,3-triazole-4,5-dicarboxylate. Propiolic acid (1.500 g, 21.413 mmol) was added to a 25 mL round bottom flask with 21 mL of toluene. 4,5-Dibutyl 1-(6-hydroxyhexyl)-1H-1,2,3-triazole-4,5-dicarboxylate (9.4935 g, 25.6956 mmol) and 4-methylbenzenesulfonic acid (0.2443 g, 1.2847 mmol) was added to the reaction flask and stirred at reflux for 2 h. The volatiles were evaporated *in vacuo*, affording a light brown crude oil. Purification *via* flash chromatography using 7:3 hexanes:ethyl acetate afforded 6.3370 g (15.0349 mmol, 70.21% yield) of the title compound as a colorless oil.

TLC: 7:3 hexanes:ethyl acetate, R_f=0.53, UV, $KMnO_4$ stain, *p*-anisealdehyde stain, yellow spot.

^{1}H NMR (500 MHz, $CDCl_3$): δ 4.60 (t, *J* = 7.2 Hz, 2H), 4.39 (overlapping t, *J* = 7.0 Hz, 4H), 4.20 (t, *J* = 6.5 Hz, 2H), 2.90 (s, 1H), 1.94 (p, *J* = 7.2 Hz, 2H), 1.77 (overlapping p, *J* = 7.0 Hz, 4H), 1.69 (p, *J* = 6.7 Hz, 2H), 1.51 – 1.35 (m, 8H), 1.00 – 0.96 (m, 6H).

^{13}C NMR (125 MHz, $CDCl_3$, DEPT): δ 160.4 (C=O), 158.7 (C=O), 152.7 (C=O), 140.4 (4°), 129.7 (4°), 74.7 (alkyne 4°), 74.6 (alkyne CH), 66.7 (CH_2), 66.0 (CH_2), 65.7 (CH_2), 50.3 (CH_2), 30.6 (CH_2), 30.0 (CH_2), 28.1 (CH_2), 25.9 (CH_2), 25.2 (CH_2), 19.1 (CH_2), 19.0 (CH_2), 13.6 (CH_3), 13.0 (CH_3).

IR (Neat): 3254 (s, alkyne CH), 2961 (s, alkane CH), 2937 (s, alkane CH), 2874 (s, alkane CH), 2117 (s, alkyne CC), 1718 (s, ester C=O), 1553 (m, triazole C=C), 1467 (s, methylene bending CH_2), 1267 (s, ester stretch C-O), 1235 (s, ester stretch C-O) cm^{-1}.

HRMS: Calcd. for $C_{21}H_{31}N_3O_6$ $[M+H]^+$ 422.2286; Found 422.2274.

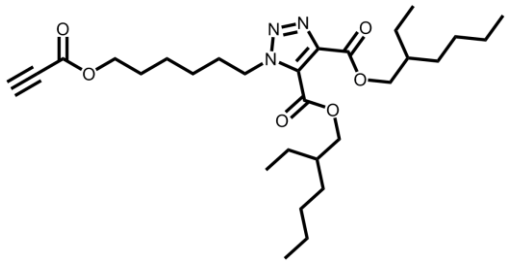

Preparation of 4,5-bis(2-ethylhexyl)-1-[6-(prop-2-ynoyloxy)hexyl]-1H-1,2,3-triazole-4,5-dicarboxylate. Propiolic acid (0.500 g, 7.138 mmol) was added to a 25 mL round bottom flask with 7 mL of toluene. 4,5-Bis(2-ethylhexyl) 1-(6-hydroxyhexyl)-1H-1,2,3-triazole-4,5-dicarboxylate (4.1256 g, 8.5652 mmol) and 4-methylbenzenesulfonic acid (0.0815 g, 0.428 mmol) was added to the reaction flask and stirred at reflux for 2 h. The volatiles were evaporated *in vacuo*, affording a light brown crude oil. Purification *via* flash chromatography using 4:1 hexanes:ethyl acetate afforded 2.7286 g (5.1126 mmol, 71.64% yield) of a colorless oil, as a mixture of diastereomers.

TLC: 4:1 hexanes:ethyl acetate, R_f=0.56, UV, $KMnO_4$ stain, *p*-anisealdehyde stain, blue-yellow spot.

^{1}H NMR (500 MHz, $CDCl_3$): δ 4.59 (t, *J* = 7.3 Hz, 2H), 4.35 – 4.23 (m, 4H), 4.19 (t, *J* = 6.6 Hz, 2H), 2.90 (s, 1H), 1.93 (p, *J* = 7.3 Hz, 2H), 1.71 (m, 4H), 1.50 – 1.27 (m, 20H), 0.96 – 0.87 (m, 12H).

^{13}C NMR (125 MHz, $CDCl_3$, DEPT): δ 160.5 (C=O), 158.8 (C=O), 152.7 (C=O), 140.5 (4°), 129.6 (4°), 74.7 (alkyne 4°), 74.6 (alkyne CH), 69.2 (CH_2), 68.4 (CH_2), 66.0 (CH_2), 50.3 (CH_2), 38.73 (CH), 38.70 (CH), 30.20 (CH_2), 30.15 (CH_2), 30.1 (CH_2), 28.9 (CH_2), 28.9 (CH_2), 28.1 (CH_2), 26.0 (CH_2), 25.3 (CH_2), 23.6 (CH_2), 23.5 (CH_2), 22.94 (CH_2), 22.93 (CH_2), 14.0 (CH_3), 10.88 (CH_3), 10.87 (CH_3).

IR (Neat): 3255 (s, alkyne CH), 2960 (s, alkane CH), 2931 (s, alkane CH), 2862 (s, alkane CH), 2117 (s, alkyne CC), 1717 (s, ester C=O), 1555 (m, triazole C=C), 1465 (s, methylene bending CH_2), 1268 (s, ester stretch C-O), 1220 (s, ester stretch C-O) cm^{-1}.

HRMS: Calcd. for $C_{29}H_{47}N_3O_6$ $[M+H]^+$ 534.3538; Found 534.3521.

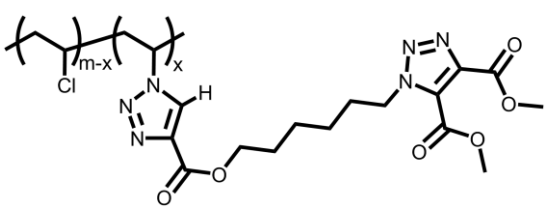

Preparation of 5% PVC-TRZ-Hexyl-TRZ-DiMe. Poly(vinyl chloride) 5% azide (1.000 g, 16.00 mmol) was added to a 100 mL round bottom flask and dissolved in 20 mL of 3-pentanone at 90 °C. 4,5-Dimethyl-1-[6-(prop-2-ynoyloxy)hexyl]-1H-1,2,3-triazole-4,5-dicarboxylate (0.674 g, 2.0 mmol) was added to the PVC solution and stirred for 36 h. The reaction was precipitated in 80 mL of MeOH, two times each. The isolated polymer was dried under house vacuum for 2 days to yield 0.880 g of a flocculent white solid.

^{1}H NMR (500 MHz, $CDCl_3$): δ 8.27 – 8.23 (br m, *PVC-triazole-H*), 8.19 – 8.16 (br m, *PVC-triazole-H*), 5.31 – 5.18 (br m, *C-CH-triazole*), 4.66 – 4.55 (br m, *Cl-C-H* and *PVC-linker-C-CH_2-triazole*), 4.46 (br s, *Cl-C-H*), 4.40 – 4.34 (br m, *PVC-triazole-O-CH_2-linker*), 4.34 – 4.25 (br m, *Cl-C-H*), 4.02 (br s, *O-CH_3*), 3.98 (br s, *O-CH_3*), 2.85 – 2.80 (br m, *Cl-C-CH_2-C-triazole* and *triazole-C-CH_2-C-triazole*), 2.76 – 2.71 (br t, *Cl-C-CH_2-C-triazole* and *triazole-C-CH_2-C-triazole*), 2.69 – 2.60 (br m, *Cl-C-CH_2-C-triazole* and *triazole-C-CH_2-C-triazole*), 2.50 – 1.99 (br m, *Cl-C-CH_2-C-Cl*), 1.99 – 1.90 (br m, *PVC-linker-CH_2-C-triazole*), 1.85 – 1.75 (br m, *PVC-triazole-O-C-CH_2-linker*), 1.55 – 1.36 (br m, *linker CH_2's*).

^{13}C NMR (125 MHz, $CDCl_3$): δ 160.6 (C=O), 159.0 (C=O), 140.0 (4°), 129.8 (4°), 65.2 (O-CH_2), 65.1 (O-CH_2), 57.0 – 56.9 (CH syndio), 56.1 – 55.9 (CH hetero), 55.2 – 54.9 (CH iso), 53.5 (CH_3), 52.7 (CH_3), 50.5 (CH_2) 47.3 – 44.8 (family of CH_2 PVC peaks), 30.0 (CH_2), 28.4 (CH_2), 26.0 (CH_2), 25.3 (CH_2).

IR (Neat): 3140 (w, triazole CH), 2975 (m, alkane CH), 2938 (m, alkane CH), 2912 (m, alkane CH), 1733 (s, ester C=O), 1714 (s, ester C=O), 1547 (w, triazole C=C), 1459 (m, methylene stretch CH_2), 1435 (m, methyl stretch CH), 1254 (s, ester stretch C-O), 1230 (s, ester stretch C-O), 611 (w, C-Cl) cm^{-1}.

DSC (T_g): 82 °C.

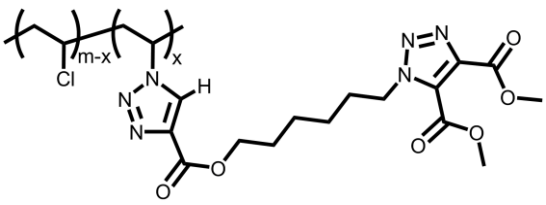

Preparation of 15% PVC-TRZ-Hexyl-TRZ-DiMe. Poly(vinyl chloride) 15% azide (1.000 g, 16.00 mmol) was added to a 100 mL round bottom flask and dissolved in 20 mL of 3-pentanone at 90 °C. 4,5-Dimethyl-1-[6-(prop-2-ynoyloxy)hexyl]-1H-1,2,3-triazole-4,5-dicarboxylate (2.4287 g, 7.2 mmol) was added to the PVC solution and stirred for 24 h. The reaction was precipitated in 80 mL of MeOH, three times each. The isolated polymer was dried under house vacuum for 2 days to yield 0.5 g of a flocculent white solid.

^{1}H NMR (500 MHz, $CDCl_3$): δ 8.27 – 8.23 (br m, *PVC-triazole-H*), 8.18 – 8.10 (br m, *PVC-triazole-H*), 5.31 – 5.10 (br m, *C-CH-triazole*), 4.66 – 4.55 (br m, *Cl-C-H* and *PVC-linker-C-CH_2-triazole*), 4.44 (br s, *Cl-C-H*), 4.40 – 4.25 (br m, *PVC-triazole-O-CH_2-linker* and *Cl-C-H*), 4.01 (br s, *O-CH_3*), 3.97 (br s, *O-CH_3*), 2.85 – 2.60 (br m, *Cl-C-CH_2-C-triazole* and *triazole-C-CH_2-C-triazole*), 2.50 – 1.99 (br m, *Cl-C-CH_2-C-Cl*), 1.94 (br s, *PVC-linker-CH_2-C-triazole*), 1.79 (br s, *PVC-triazole-O-C-CH_2-linker*), 1.49 – 1.41 (br m, *linker CH_2's*).

^{13}C NMR (125 MHz, $CDCl_3$, DEPT): δ 160.6 (C=O), 159.0 (C=O), 139.9 (4°), 129.8 (4°), 65.2 (O-CH_2), 65.1 (O-CH_2), 57.0 – 56.9 (CH syndio), 56.1 – 55.9 (CH hetero), 55.1 – 54.9 (CH iso), 53.5 (CH_3), 52.7 (CH_3), 50.5 (CH_2) 47.3 – 44.8 (family of CH_2 PVC peaks), 30.0 (CH_2), 28.4 (CH_2), 26.0 (CH_2), 25.3 (CH_2).

IR (Neat): 3138 (w, triazole CH), 2953 (m, alkane CH), 2863 (m, alkane CH), 1734 (s, ester C=O), 1546 (w, triazole C=C), 1464 (m, methylene stretch CH_2), 1435 (m, methyl stretch CH), 1225 (s, ester stretch C-O), 615 (w, C-Cl) cm^{-1}.

DSC (T_g): 75 °C.

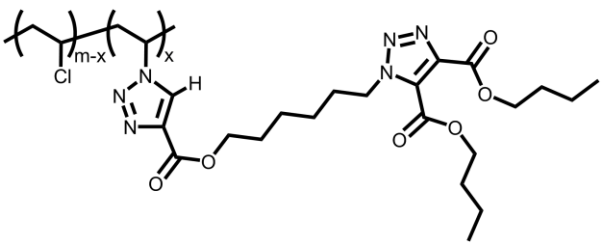

Preparation of 5% PVC-TRZ-Hexyl-TRZ-DiBu. Poly(vinyl chloride) 5% azide (1.000 g, 16.00 mmol) was added to a 100 mL round bottom flask and dissolved in 20 mL of 3-pentanone at 90 °C. 4,5-Dibutyl-1-[6-(prop-2-ynoyloxy)hexyl]-1H-1,2,3-triazole-4,5-dicarboxylate (0.8427 g, 2.0 mmol) was added to the PVC solution and stirred for 48 h. The reaction was precipitated in 80 mL of MeOH, three times each. The isolated polymer was dried under house vacuum for 2 days to yield 0.96 g of a flocculent white solid.

^{1}H NMR (500 MHz, $CDCl_3$): δ 8.29 – 8.23 (br m, *PVC-triazole-H*), 8.19 – 8.16 (br m, *PVC-triazole-H*), 5.30 – 5.20 (br m, *C-CH-triazole*), 4.66 – 4.55 (br s, *Cl-C-H* and *PVC-linker-C-CH_2-triazole*), 4.46 (br s, *Cl-C-H*), 4.42 – 4.35 (br m, *Cl-C-H* and *PVC-linker-triazole-O-CH_2*), 4.34 – 4.26 (br m, *PVC-triazole-O-CH_2-linker*), 2.85 – 2.80 (br m, *Cl-C-CH_2-C-triazole* and *triazole-C-CH_2-C-triazole*), 2.78 – 2.69 (br t, *Cl-C-CH_2-C-triazole* and *triazole-C-CH_2-C-triazole*), 2.68 – 2.60 (br m, *Cl-C-CH_2-C-triazole* and *triazole-C-CH_2-C-triazole*), 2.50 – 1.99 (br m, *Cl-C-CH_2-C-Cl*), 1.98 – 1.90 (br m, *PVC-linker-CH_2-C-triazole*), 1.80 – 1.72 (br m, *PVC-triazole-O-C-CH_2-linker* and *linker-triazole-O-C-CH_2*), 1.54 – 1.37 (br m, *linker CH_2's* and *linker-triazole-O-C-CH_2-CH_2-C*), 1.01 – 0.95 (br m, *CH_3*).

^{13}C NMR (125 MHz, $CDCl_3$): δ 160.4 (C=O), 158.7 (C=O), 140.3 (4°), 129.7 (4°), 66.7 (O-CH_2), 65.7 (O-CH_2), 57.0 – 56.9 (CH syndio), 56.1 – 55.9 (CH hetero), 55.2 – 54.9 (CH iso), 50.4 (CH_2), 47.3 – 44.8 (family of CH_2 PVC peaks), 30.6 (CH_2), 30.3 (CH_2), 30.0 (CH_2), 28.4 (CH_2), 28.3 (CH_2), 26.0 (CH_2), 25.4 (CH_2), 25.2 (CH_2), 19.1 (CH_2), 19.0 (CH_2), 13.74 (CH_3), 13.71 (CH_3), 13.7 (CH_3), 13.6 (CH_3).

IR (Neat): 3140 (w, triazole CH), 2962 (m, alkane CH), 2937 (m, alkane CH), 2873 (m, alkane CH), 1732 (s, ester C=O), 1552 (w, triazole C=C), 1464 (m, methylene stretch CH_2), 1435 (m, methyl stretch CH), 1255 (m, ester stretch C-O), 1202 (s, ester stretch C-O) cm^{-1}.

DSC (T_g): 65 °C.

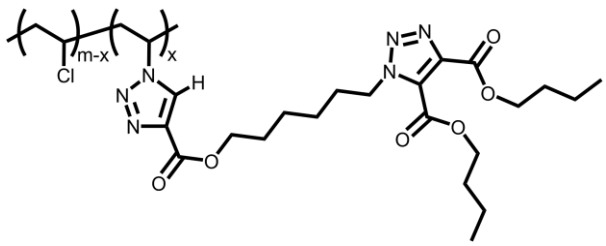

Preparation of 15% PVC-TRZ-Hexyl-TRZ-DiBu. Poly(vinyl chloride) 15% azide (1.000 g, 16.00 mmol) was added to a 100 mL round bottom flask and dissolved in 20 mL of 3-pentanone at 90 °C. 4,5-Dibutyl-1-[6-(prop-2-ynoyloxy)hexyl]-1H-1,2,3-triazole-4,5-dicarboxylate (3.0347 g, 7.2 mmol) was added to the PVC solution and stirred for 24 h. The reaction was precipitated in 80 mL of MeOH, three times each. The isolated polymer was dried under house vacuum for 1 day, then in a vacuum oven at 40 °C for 2 days to yield 0.80 g of an off-white solid.

^{1}H NMR (500 MHz, $CDCl_3$): δ 8.29 – 8.23 (br m, *PVC-triazole-H*), 8.17 – 8.10 (br m, *PVC-triazole-H*), 5.30 – 5.10 (br m, *C-CH-triazole*), 4.65 – 4.55 (br m, *Cl-C-H* and *PVC-linker-C-CH_2-triazole*), 4.45 (br s, *Cl-C-H*), 4.42 – 4.34 (br m, *Cl-C-H* and *PVC-triazole-O-CH_2-linker* and *PVC-linker-triazole-O-CH_2*), 2.85 – 2.80 (br m, *Cl-C-CH_2-C-triazole* and *triazole-C-CH_2-C-triazole*), 2.78 – 2.69 (br t, *Cl-C-CH_2-C-triazole* and *triazole-C-CH_2-C-triazole*), 2.68 – 2.51 (br m, *Cl-C-CH_2-C-triazole* and *triazole-C-CH_2-C-triazole*), 2.50 – 1.99 (br m, *Cl-C-CH_2-C-Cl*), 1.98 – 1.85 (br s, *PVC-linker-CH_2-C-triazole*), 1.85 – 1.71 (br m, *PVC-triazole-O-C-CH_2-linker* and *linker-triazole-O-C-CH_2*), 1.54 – 1.37 (br m, *linker CH_2's* and *linker-triazole-O-C-CH_2-CH_2-C*), 1.01 – 0.94 (br m, *CH_3*).

^{13}C NMR (125 MHz, $CDCl_3$, DEPT): δ 160.4 (C=O), 158.7 (C=O), 140.3 (4°), 129.7 (4°), 66.7 (O-CH_2), 65.7 (O-CH_2), 65.2 (O-CH_2), 57.1 – 56.9 (CH syndio), 56.1 – 55.9 (CH hetero), 55.1 – 54.9 (CH iso), 50.4 (CH_2), 47.3 – 44.8 (family of CH_2 PVC peaks), 30.6 (CH_2), 30.3 (CH_2),

30.0 (CH_2), 28.4 (CH_2), 28.3 (CH_2), 26.0 (CH_2), 25.4 (CH_2), 19.1 (CH_2), 19.0 (CH_2), 13.72 (CH_3), 13.65 (CH_3).

IR (Neat): 3138 (w, triazole CH), 2961 (m, alkane CH), 2937 (m, alkane CH), 2873 (m, alkane CH), 1732 (s, ester C=O), 1551 (m, triazole C=C), 1465 (m, methylene stretch CH2 stretch CH_2), 1435 (m, methyl stretch CH), 1203 (s, ester stretch C-O), 616 (w, C-Cl) cm^{-1}.

DSC (T_g): 54 °C.

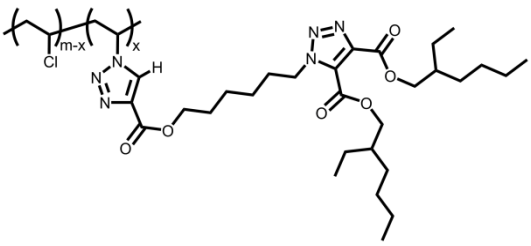

Preparation of 5% PVC-TRZ-Hexyl-TRZ-DiEH. Poly(vinyl chloride) 5% azide (1.000 g, 16.00 mmol) was added to a 100 mL round bottom flask and dissolved in 20 mL of 3-pentanone at 90 °C. 4,5-Bis(2-ethylhexyl)-1-[6-(prop-2-ynoyloxy)hexyl]-1H-1,2,3-triazole-4,5-dicarboxylate (1.0674 g, 2.0 mmol) was added to the PVC solution and stirred for 36 h. The reaction was precipitated in 80 mL of MeOH, three times each. The isolated polymer was dried under house vacuum for 2 days to yield 0.96 g of a flocculent white solid.

^{1}H NMR (500 MHz, $CDCl_3$): δ 8.28 – 8.23 (br m, *PVC-triazole-H*), 8.19 – 8.16 (br m, *PVC-triazole-H*), 5.25 (br s, *C-CH-triazole*), 4.65 – 4.55 (br m, *Cl-C-H* and *PVC-linker-C-CH_2-triazole*), 4.46 (br s, *Cl-C-H*), 4.40 – 4.24 (br m, *Cl-C-H* and *PVC-triazole-O-CH_2-linker* and *PVC-linker-triazole-O-CH_2*), 2.88 – 2.79 (br m, *Cl-C-CH_2-C-triazole* and *triazole-C-CH_2-C-triazole*), 2.78 – 2.69 (br t, *Cl-C-CH_2-C-triazole* and *triazole-C-CH_2-C-triazole*), 2.68 – 2.51 (br m, *Cl-C-CH_2-C-triazole* and *triazole-C-CH_2-C-triazole*), 2.50 – 1.98 (br m, *Cl-C-CH_2-C-Cl*), 1.98 – 1.86 (br m, *PVC-linker-CH_2-C-triazole*), 1.85 – 1.77 (br m, *PVC-triazole-O-C-CH_2-linker*), 1.76 – 1.68 (br m, *PVC-linker-triazole-O-C-CH-C*), 1.54 – 1.29 (br m, *linker CH_2's* and *linker-triazole-O-C-C-CH_2-CH_2-CH_2-C*), 0.96 – 0.89 (br m, *CH_3*).

^{13}C NMR (125 MHz, $CDCl_3$, DEPT): δ 160.6 (C=O), 158.8 (C=O), 140.4 (4°), 129.6 (4°), 69.2 (O-CH_2), 68.4 (O-CH_2), 65.2 (O-CH_2), 57.1 – 56.9 (CH syndio), 56.1 – 55.9 (CH hetero), 55.2 – 54.9 (CH iso), 50.4 (CH_2), 47.3 – 44.8 (family of CH_2 PVC peaks), 38.73 (CH), 38.69 (CH), 30.19 (CH_2), 30.16 (CH_2), 30.1 (CH_2), 28.88 (CH_2), 28.86 (CH_2), 28.4 (CH_2), 26.1 (CH_2), 25.4 (CH_2), 23.0 (CH_2), 22.96 (CH_2), 22.95 (CH_2), 14.1 (CH_3), 14.0 (CH_3), 10.9 (CH_3).

IR (Neat): 3144 (w, triazole CH), 2960 (s, alkane CH), 2931 (s, alkane CH), 2861 (s, alkane CH), 1732 (s, ester C=O), 1553 (m, triazole C=C), 1465 (m, methylene stretch CH_2), 1435 (m, methyl stretch CH), 1254 (m, ester stretch C-O), 1201 (s, ester stretch C-O), 615 (w, C-Cl) cm^{-1}.

DSC (T_g): 56 °C.

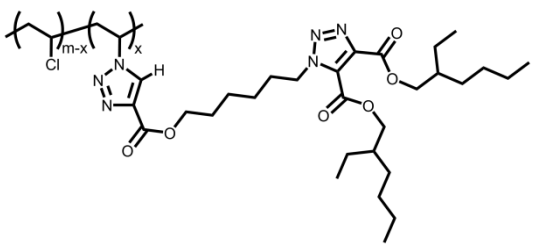

Preparation of 15% PVC-TRZ-Hexyl-TRZ-DiEH. Poly(vinyl chloride) 15% azide (1.000 g, 16.00 mmol) was added to a 100 mL round bottom flask and dissolved in 20 mL of 3-pentanone at 90 °C. 4,5-Bis(2-ethylhexyl)-1-[6-(prop-2-ynoyloxy)hexyl]-1H-1,2,3-triazole-4,5-dicarboxylate (3.8426 g, 7.2 mmol) was added to the PVC solution and stirred for 24 h. The reaction was precipitated in 80 mL of MeOH, three times each. The isolated polymer was dried under house vacuum for 1 day, then in a vacuum oven at 40 °C for 2 days to yield 1.11 g of an off-white solid.

^{1}H NMR (500 MHz, $CDCl_3$): δ 8.25 – 8.20 (br m, *PVC-triazole-H*), 8.19 – 8.07 (br m, *PVC-triazole-H*), 5.26 – 5.10 (br m, *C-CH-triazole*), 4.65 – 4.52 (br m, *Cl-C-H* and *PVC-linker-C-CH_2-triazole*), 4.45 (br s, *Cl-C-H*), 4.40 – 4.22 (br m, *Cl-C-H* and *PVC-triazole-O-CH_2-linker* and *PVC-linker-triazole-O-CH_2*), 2.87 – 2.79 (br m, *Cl-C-CH_2-C-triazole* and *triazole-C-CH_2-C-triazole*), 2.78 – 2.69 (br s, *Cl-C-CH_2-C-triazole* and *triazole-C-CH_2-C-triazole*), 2.68 – 2.51 (br m, *Cl-C-CH_2-C-triazole* and *triazole-C-CH_2-C-triazole*), 2.50 – 1.99 (br m, *Cl-C-CH_2-C-Cl*),

1.98 – 1.86 (br s, *PVC-linker-C<u>H₂</u>-C-triazole*), 1.85 – 1.77 (br s, *PVC-triazole-O-C-C<u>H₂</u>-linker*), 1.76 – 1.65 (br m, *PVC-linker-triazole-O-C-C<u>H</u>-C*), 1.55 – 1.25 (br m, *linker C<u>H₂</u>'s* and *linker-triazole-O-C-C-C<u>H₂</u>-C<u>H₂</u>-C<u>H₂</u>-C*), 0.97 – 0.86 (br m, *C<u>H₃</u>*).

^{13}C NMR (125 MHz, $CDCl_3$, DEPT) δ 160.6 (C=O), 158.8 (C=O), 140.4 (4°), 129.6 (4°), 69.2 (O-CH_2), 68.4 (O-CH_2), 65.2 (O-CH_2), 57.1 – 56.9 (CH syndio), 56.1 – 55.9 (CH hetero), 55.0 – 54.9 (CH iso), 50.4 (CH_2), 47.3 – 44.8 (family of CH_2 PVC peaks), 38.72 (CH), 38.69 (CH), 30.19 (CH_2), 30.16 (CH_2), 30.1 (CH_2), 28.88 (CH_2), 28.86 (CH_2), 28.4 (CH_2), 26.0 (CH_2), 25.4 (CH_2), 23.6 (CH_2), 23.5 (CH_2), 22.96 (CH_2), 22.94 (CH_2), 14.1 (CH_3), 10.9 (CH_3).

IR (Neat): 3139 (w, triazole CH), 2960 (s, alkane CH), 2932 (s, alkane CH), 2861 (s, alkane CH), 1733 (s, ester C=O), 1552 (m, triazole C=C), 1465 (m, methylene stretch CH_2), 1436 (m, methyl stretch CH), 1202 (s, ester stretch C-O), 616 (w, C-Cl) cm^{-1}.

DSC (T_g): 41 °C.

6.6 Chapter 3 Experimental Section

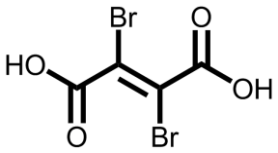

Preparation of Dibromofumaric Acid.[4] Acetylenedicarboxylic acid monopotassium salt (5.522 g, 36.30 mmol) was added to a 500 mL round bottom flask and dissolved into ~20 mL of 2M aqueous KOH solution while stirring. NaBr (102.89 g, 26.149 mmol) was dissolved in 80 mL of H_2O *via* sonication. Br_2 (6.381 g, 39.93 mmol) was quickly added to the NaBr aqueous solution. The resulting orange NaBr/Br_2 solution was subsequently added to the acetylenedicarboxylate solution. Stirring was ceased for the remainder of the reaction to prevent Br_2 degradation. The reaction flask was covered in aluminum foil, and an additional 50 mL of H_2O was added to bring the total volume to 150 mL, and was left for 24 h at room temperature. After 24 h, a transparent colorless solution was observed. To the reaction flask, 3 mL of saturated aqueous $Na_2S_2O_3$ solution was added to quench the excess Br_2 while stirring. The reaction was saturated with NaCl and acidified with 12 mL of concentrated HCl

and extracted with 50 mL of ethyl acetate each four times. The organic layers were dried with Na_2SO_4. The volatiles were evaporated *in vacuo* to afford a white solid. After recrystallization in chloroform, 8.000 g (29.21 mmol, 80.47% yield) of the title compound was recovered as colorless needles: mp 239 – 240 °C.

Alternative Purification Method: A faster method providing purer product involved dissolving the crude solid into a minimal amount of Et_2O, which was subsequently slowly rotavapped to deposit solid on the sides of a pear shaped flask. The solid was washed with $CHCl_3$, carefully avoiding pushing the deposited solid down the flask. The light brown to orange mother liquor was pipetted out and placed into a beaker. This washing process was repeated three times. The dissolution-washing process was repeated until the $CHCl_3$ mother liquor became colorless.

TLC: Not UV Active nor Stain Active.

^{1}H NMR (500 MHz, d_6-Acetone): No Detectable Protons.

^{13}C NMR (125 MHz, d_6-Acetone): δ 162.8 (C=O), 111.7 (C-Br).

IR (KBr Pellet): 3013 (s, OH stretch), 1699 (s, carboxylic acid C=O), 1405 (m, alcohol bending OH), 686 (m, C-Br) cm^{-1}.

HRMS: Not Detectable.

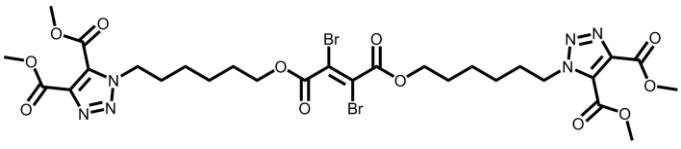

Preparation of 4,5-dimethyl 1-(6-{[(2E)-4-({6-[4,5-bis(methoxycarbonyl)-1H-1,2,3-triazol-1-yl]hexyl}oxy)-2,3-dibromo-4-oxobut-2-enoyl]oxy}hexyl)-1H-1,2,3-triazole-4,5-dicarboxylate.[4-5] Dibromofumaric acid (1.5000 g, 5.4765 mmol) and PCl_5 (2.3370 g, 11.226 mmol) was added to a 25 mL round bottom flask with 5 mL of pentane. The reaction was refluxed for 2 h while stirring. Reaction completeness was determined by observing the

dissolution of solids into a clear yellow solution. After the dissolution of solids was noted, the reaction was immediately diluted with 5 mL of pentane. The diluted reaction was added slowly to a 150 mL beaker of crescent-cube ice, and was allowed to stand for 10 min with occasional swirling. The quenched reaction solution was transferred to a 150 mL separatory funnel. The organic layer was collected and dried with Na_2SO_4. The volatiles were evaporated *in vacuo*, affording a clear yellow oil (1.6457g, 5.2959 mmol, 96.7% yield) of (2E)-dibromobut-2-enedioyl dichloride. The acid chloride was immediately diluted with 30 mL of CCl_4 under N_2 in a 250 mL pear flask. Next, 4,5-dimethyl 1-(6-hydroxyhexyl)-1H-1,2,3-triazole-4,5-dicarboxylate (3.1729 g, 11.121 mmol) and pyridine (0.8797 g, 11.121 mmol) were added to a 250 mL round bottom flask with 60 mL of CCl_4 and cooled to 0 °C under N_2 with stirring. The acid chloride solution was slowly added *via* syringe over 10 min, noting the formation of pyridine salts in solution. After the addition of the acid chloride, the reaction was allowed to stir at 0 °C for 30 min, then at room temperature for an additional 1 h. The reaction was poured into a 500 mL separatory funnel and washed with 20 mL of 5% aqueous HCl, two times each. The organic layer was collected, dried with $MgSO_4$ and filtered. The volatiles were then evaporated *in vacuo*, affording a clear yellow oil. Purification *via* flash chromatography using 7:3 ethyl acetate:hexanes furnishing 3.6947 g (4.5702 mmol, 86.29% yield) of the title compound as a clear pale yellow oil.

TLC: 7:3 ethyl acetate:hexanes, R_f=0.53, UV, *p*-anisealdehyde stain, purple spot.

^{1}H NMR (500 MHz, $CDCl_3$): δ 4.55 (t, *J* = 7.2 Hz, 4H), 4.23 (t, *J* = 6.5 Hz, 4H), 3.95 (s, 6H), 3.92 (s, 6H), 1.88 (p, *J* = 7.3 Hz, 4H), 1.68 (p, *J* = 6.5 Hz, 4H), 1.45 – 1.39 (m, 4H), 1.36 – 1.30 (m, 4H).

^{13}C NMR (125 MHz, $CDCl_3$, DEPT): δ 162.2 (C=O), 160.5 (C=O), 159.0 (C=O), 140.0 (4°), 129.7 (4°), 112.7 (C-Br), 66.9 (CH_2), 53.5 (CH_3), 52.7 (CH_3), 50.4 (CH_2), 30.0 (CH_2), 28.1 (CH_2), 25.8 (CH_2), 25.2 (CH_2).

IR (Neat): 3003 (s, alkane CH), 2954 (s, alkane CH), 2863 (s, alkane CH), 1733 (s, ester C=O), 1554 (m, triazole C=C), 1468 (s, methylene bending CH_2), 1272 (s, ester stretch C-O), 1231 (s, ester stretch C-O), 914 (s, alkene bending C=C), 733 (s, alkene bending C=C) cm^{-1}.

HRMS: Calcd. for $C_{28}H_{36}Br_2N_6O_{12}$ $[M+H]^+$ 807.0831; Found 807.0831. (Br isotopes): 809.0804, 811.0782, 812.0808.

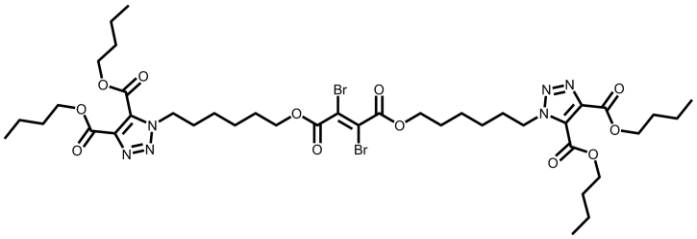

Preparation of 4,5-dibutyl 1-(6-{[(2E)-4-({6-[4,5-bis(butoxycarbonyl)-1H-1,2,3-triazol-1-yl]hexyl}oxy)-2,3-dibromo-4-oxobut-2-enoyl]oxy}hexyl)-1H-1,2,3-triazole-4,5-dicarboxylate.[4-5]

Dibromofumaric acid (1.5000 g, 5.4765 mmol) and PCl_5 (2.3940 g, 11.496 mmol) was added to a 25 mL round bottom flask with 5 mL of pentane. The reaction was refluxed for 2 h while stirring. Reaction completeness was determined by observing the dissolution of solids into a clear yellow solution. After the dissolution of solids was noted, the reaction was immediately diluted with 5 mL of pentane. The diluted reaction was added slowly to a 150 mL beaker of crescent-cube ice, and was allowed to stand for 10 min with occasional swirling. The quenched reaction solution was transferred to a 150 mL separatory funnel. The organic layer was collected and dried with Na_2SO_4. The volatiles were evaporated *in vacuo*, affording a clear yellow oil (1.6605 g, 5.3434 mmol, 97.5% yield) of (2E)-dibromobut-2-enedioyl dichloride. The acid chloride was immediately diluted with 30 mL of CCl_4 under N_2 in a 250 mL pear flask. Next, 4,5-dibutyl 1-(6-hydroxyhexyl)-1H-1,2,3-triazole-4,5-dicarboxylate (4.1457 g, 11.221 mmol) and pyridine (0.8870 g, 11.221 mmol) were added to a 250 mL round bottom flask with 60 mL of CCl_4 and cooled to 0 °C under N_2 with stirring. The acid chloride solution was slowly added *via* syringe over 10 min, noting an orange color and the formation of pyridine salts in solution. After the addition of the acid chloride, the reaction was allowed to stir at 0 °C for 30 min, then at room temperature for an additional 2 h. The reaction

was poured into a 500 mL separatory funnel and washed with 20 mL of 5% aqueous HCl, two times each. The organic layer was collected, dried with $MgSO_4$ and filtered. The volatiles were then evaporated *in vacuo*, affording a dark red oil. Purification *via* flash chromatography using 1:1 hexanes:ethyl acetate was performed, furnishing 4.4136 g (4.5186 mmol, 84.56% yield) of the title compound as a colorless oil.

TLC: 1:1 hexanes:ethyl acetate, R_f=0.78, UV, *p*-anisealdehyde stain, purple spot.

^{1}H NMR (500 MHz, $CDCl_3$): δ 4.56 (t, *J* = 7.2 Hz, 4H), 4.34 (overlapping t, *J* = 6.8 Hz, 8H), 4.25 (t, *J* = 6.4 Hz, 4H), 1.90 (p, *J* = 7.2 Hz, 4H), 1.77 – 1.63 (m, 12H), 1.48 – 1.30 (m, 16H), 0.99 – 0.75 (m, 12H).

^{13}C-NMR (125 MHz, $CDCl_3$, DEPT): δ 162.2 (C=O), 160.4 (C=O), 158.7 (C=O), 140.4 (4°), 129.6 (4°), 112.7 (C-Br), 66.9 (CH_2), 66.7 (CH_2), 65.7 (CH_2), 50.3 (CH_2), 30.6 (CH_2), 30.3 (CH_2), 30.0 (CH_2), 28.1 (CH_2), 25.9 (CH_2), 25.2 (CH_2), 19.1 (CH_2), 19.0 (CH_2), 13.7 (CH_3), 13.6 (CH_3).

IR (Neat): 2961 (s, alkane CH), 2937 (s, alkane CH), 2873 (s, alkane CH), 1733 (s, ester C=O), 1553 (m, triazole C=C), 1467 (s, methylene bending CH_2), 1267 (s, ester stretch C-O), 1214 (s, ester stretch C-O), 755 (m, alkene bending C=C) cm^{-1}.

HRMS: Calcd. for $C_{40}H_{60}Br_2N_6O_{12}$ $[M+H]^+$ 975.2708; Found 975.2708. (Br isotopes): 976.2737, 977.2684, 979.2668, 980.2695.

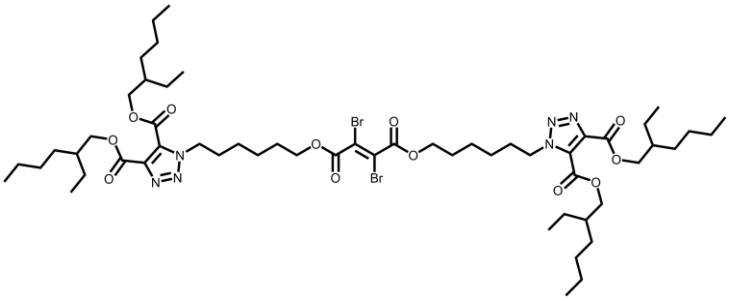

Preparation of 4,5-bis(2-ethylhexyl) 1-(6-{[(2E)-4-({6-[4,5-bis({[(2-ethylhexyl)oxy]carbonyl})-1H-1,2,3-triazol-1-yl]hexyl}oxy)-2,3-dibromo-4-oxobut-2-enoyl]oxy}hexyl)-1H-1,2,3-triazole-4,5-dicarboxylate.[4-5] Dibromofumaric acid (1.5200 g, 5.5502 mmol) and PCl_5 (2.4270 g, 11.655 mmol) was added to a 25 mL round bottom flask with 5 mL of pentane. The reaction was refluxed for 2 h while stirring. Reaction completeness was determined by observing the dissolution of solids into a clear yellow solution. After the dissolution of solids was noted, the reaction was immediately diluted with 5 mL of pentane. The diluted reaction was added slowly to a 150 mL beaker of crescent-cube ice, and was allowed to stand for 10 min with occasional swirling. The quenched reaction solution was transferred to a 150 mL separatory funnel. The organic layer was collected and dried with Na_2SO_4. The volatiles were evaporated *in vacuo*, affording a clear yellow oil (1.6563 g, 5.3299 mmol, 96.0% yield) of (2E)-dibromobut-2-enedioyl dichloride. The acid chloride was immediately diluted with 30 mL of CCl_4 under N_2 in a 250 mL pear flask. Next, 4,5-bis(2-ethylhexyl) 1-(6-hydroxyhexyl)-1H-1,2,3-triazole-4,5-dicarboxylate (5.3913 g, 11.193 mmol) and pyridine (0.8853 g, 11.193 mmol) were added to a 250 mL round bottom flask with 60 mL of CCl_4 and cooled to 0 °C under N_2 with stirring. The acid chloride solution was slowly added *via* syringe over 10 min, noting an orange-brown color and the formation of pyridine salts in solution. After the addition of the acid chloride, the reaction was allowed to stir at 0 °C for 30 min, then at room temperature for an additional 2 h. The reaction was poured into a 500 mL separatory funnel and washed with 20 mL of 5% aqueous HCl, two times each. The organic layer was collected, dried with $MgSO_4$ and filtered. The volatiles were then evaporated *in vacuo*, affording a dark red oil. Purification *via* flash chromatography using 7:3 hexanes:ethyl acetate was performed,

furnishing 5.1462 g (4.2842 mmol, 80.38% yield) of a colorless oil, as a mixture of diastereomers.

TLC: 7:3 hexanes:ethyl acetate, R_f=0.64, UV, *p*-anisealdehyde stain, blue spot.

^{1}H NMR (500 MHz, $CDCl_3$): δ 4.55 (t, *J* = 7.3 Hz, 4H), 4.30 – 4.19 (m, 12H), 1.89 (p, *J* = 7.4 Hz, 4H), 1.73 – 1.62 (m, 8H), 1.47 – 1.21 (m, 40H), 0.93 – 0.79 (m, 24H).

^{13}C-NMR (125 MHz, $CDCl_3$, DEPT): δ 162.2 (C=O), 160.6 (C=O), 158.8 (C=O), 140.5 (4°), 129.6 (4°), 112.7 (C-Br), 69.1 (CH_2), 68.4 (CH_2), 66.9 (CH_2), 50.3 (CH_2), 38.7 (CH), 30.2 (CH_2), 30.2 (CH_2), 30.1 (CH_2), 28.9 (CH_2), 28.1 (CH_2), 25.9 (CH_2), 25.2 (CH_2), 23.6 (CH_2), 23.5 (CH_2), 22.9 (CH_2), 14.0 (CH_3), 10.9 (CH_3).

IR (Neat): 2959 (s, alkane CH), 2932 (s, alkane CH), 2872 (s, alkane CH), 2861 (s, alkane CH), 1736 (s, ester C=O), 1554 (m, triazole C=C), 1466 (s, methylene bending CH_2), 1267 (s, ester stretch C-O), 1235 (s, ester stretch C-O), 758 (m, alkene bending C=C) cm^{-1}.

HRMS: Calcd. for $C_{56}H_{92}Br_2N_6O_{12}$ $[M+H]^+$ 1199.5213; Found 1199.5212. (Br isotopes): 1201.5193, 1203.5179, 1204.5198.

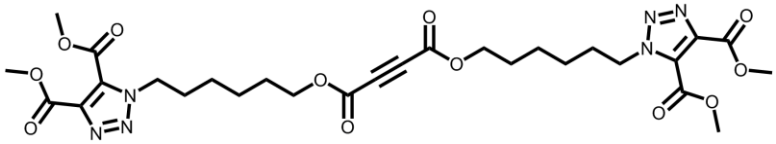

Preparation of 4,5-dimethyl 1-(6-{[4-({6-[4,5-bis(methoxycarbonyl)-1H-1,2,3-triazol-1-yl]hexyl}oxy)-4-oxobut-2-ynoyl]oxy}hexyl)-1H-1,2,3-triazole-4,5-dicarboxylate.[6] To a 250 mL round bottom flask, 4,5-dimethyl 1-(6-{[(2E)-4-({6-[4,5-bis(methoxycarbonyl)-1H-1,2,3-triazol-1-yl]hexyl}oxy)-2,3-dibromo-4-oxobut-2-enoyl]oxy}hexyl)-1H-1,2,3-triazole-4,5-dicarboxylate (1.000 g, 1.236 mmol) was added to 12 mL of anhydrous THF. Subsequently, Zn metal (0.4849 g, 7.416 mmol) and I_2 (0.020 g, 0.0787 mmol) were added and stirred at reflux for 5 h under N_2. The reaction was cooled and filtered through CELITE™ then concentrated *in vacuo* with 80 mL of ethyl acetate. The

solution was poured into a 500 mL separatory funnel and washed with 20 mL of 10% aqueous $Na_2S_2O_3$, two times each. The organic layer was collected and dried with $MgSO_4$. The volatiles were then evaporated *in vacuo*, and immediately purified *via* flash chromatography using 7:3 ethyl acetate:hexanes, affording 0.711 g (1.0928 mmol, 88.41% yield) of the title compound as a viscous clear yellow oil.

TLC: 7:3 ethyl acetate:hexanes, UV, R_f=0.54, $KMnO_4$ stain, *p*-anisealdehyde stain, blue spot.

^{1}H NMR (500 MHz, $CDCl_3$): δ 4.59 (t, *J* = 7.2 Hz, 4H), 4.21 (t, *J* = 6.5 Hz, 4H), 4.00 (s, 6H), 3.97 (s, 6H), 1.92 (p, *J* = 7.3 Hz, 4H), 1.67 (p, *J* = 6.6 Hz, 4H), 1.44 – 1.33 (m, 8H).

^{13}C-NMR (125 MHz, $CDCl_3$, DEPT): δ 160.5 (C=O), 159.0 (C=O), 151.8 (C=O), 139.9 (4°), 129.7 (4°), 74.7 (alkyne 4°), 66.6 (CH_2), 53.4 (CH_3), 52.7 (CH_3), 50.4 (CH_2), 29.9 (CH_2), 28.0 (CH_2), 25.8 (CH_2), 25.1 (CH_2).

IR (Neat): 3010 (s, alkane CH), 2954 (s, alkane CH), 2863 (s, alkane CH), 1729 (s, ester C=O), 1552 (m, triazole C=C), 1468 (methylene bending CH_2), 1259 (s, ester stretch C-O), 1227 (s, ester stretch C-O) cm^{-1}.

HRMS: Calcd. for $C_{28}H_{36}N_6O_{12}$ $[M+H]^+$ 649.2463; Found 649.2463.

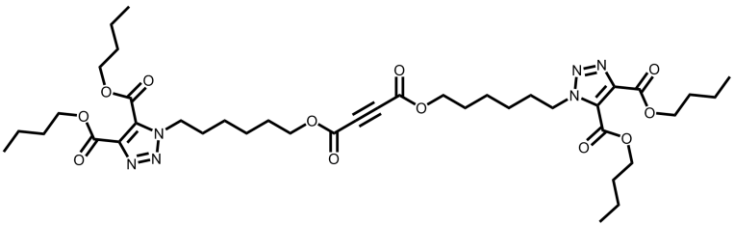

Preparation of 4,5-dibutyl 1-(6-{[4-({6-[4,5-bis(butoxycarbonyl)-1H-1,2,3-triazol-1-yl]hexyl}oxy)-4-oxobut-2-ynoyl]oxy}hexyl)-1H-1,2,3-triazole-4,5-dicarboxylate.[6] To a 250 mL round bottom flask, 4,5-dibutyl 1-(6-{[(2E)-4-({6-[4,5-bis(butoxycarbonyl)-1H-1,2,3-triazol-1-yl]hexyl}oxy)-2,3-dibromo-4-oxobut-2-enoyl]oxy}hexyl)-1H-1,2,3-triazole-4,5-dicarboxylate (7.780 g, 8.057 mmol) was added to 70 mL of anhydrous THF. Subsequently, Zn metal (3.1607 g, 48.343 mmol) and I_2 (0.1226 g, 0.48342 mmol) were added and stirred at reflux for

5 h under N_2. The reaction was cooled and filtered through CELITE^{TM} then concentrated *in vacuo* with 80 mL of ethyl acetate. The solution was poured into a 500 mL separatory funnel and washed with 20 mL of 10% aqueous $Na_2S_2O_3$, two times each. The organic layer was collected and dried with $MgSO_4$. The volatiles were then evaporated *in vacuo*, and immediately purified *via* flash chromatography using 7:3 hexanes:ethyl acetate, affording 5.2953 g (6.4817 mmol, 80.44% yield) of the title compound as a viscous colorless oil.

TLC: 7:3 hexanes:ethyl acetate, R_f=0.39, UV, $KMnO_4$ stain, *p*-anisealdehyde stain, blue spot.

^{1}H NMR (500 MHz, $CDCl_3$): δ 4.55 (t, *J* = 7.3 Hz, 4H), 4.34 (overlapping t, *J* = 6.7 Hz, 8H), 4.18 (t, *J* = 6.6 Hz, 4H), 1.89 (p, *J* = 7.3 Hz, 4H), 1.72 (overlapping p, *J* = 6.7, 8H), 1.65 (p, *J* = 6.6, 4H), 1.45 – 1.32 (m, 16H), 0.98 – 0.88 (m, 12H).

^{13}C-NMR (125 MHz, $CDCl_3$, DEPT): δ 160.2 (C=O), 158.7 (C=O), 151.8 (C=O), 140.4 (4°), 129.7 (4°), 74.7 (alkyne 4°), 66.7 (CH_2), 66.7 (CH_2), 65.7 (CH_2), 50.3 (CH_2), 30.6 (CH_2), 30.3 (CH_2), 30.0 (CH_2), 28.1 (CH_2), 25.9 (CH_2), 25.2 (CH_2), 19.1 (CH_2), 19.0 (CH_2), 13.7 (CH_3), 13.6 (CH_3).

IR (Neat): 2961 (s, alkane CH), 2937 (s, alkane CH), 2873 (s, alkane CH), 1725 (s, ester C=O), 1553 (triazole alkene, C=C), 1467 (methylene bending CH_2), 1259 (s, ester stretch C-O), 1207 (s, ester stretch, C-O) cm^{-1}.

HRMS: Calcd. for $C_{40}H_{60}N_6O_{12}$ $[M+H]^+$ 817.4342; Found 817.4326.

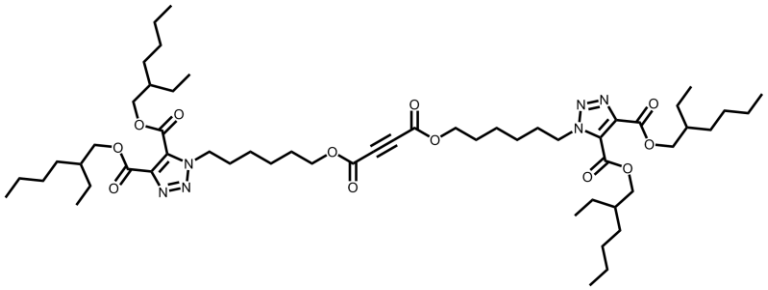

Preparation of 4,5-bis(2-ethylhexyl) 1-(6-{[4-({6-[4,5-bis({[(2-ethylhexyl)oxy]carbonyl})-1H-1,2,3-triazol-1-yl]hexyl}oxy)-4-oxobut-2-ynoyl]oxy}hexyl)-1H-1,2,3-triazole-4,5-dicarboxylate.[6] To a 250 mL round bottom flask, 4,5-bis(2-ethylhexyl) 1-(6-{[(2E)-4-({6-[4,5-bis({[(2-ethylhexyl)oxy]carbonyl})-1H-1,2,3-triazol-1-yl]hexyl}oxy)-2,3-dibromo-4-oxobut-2-enoyl]oxy}hexyl)-1H-1,2,3-triazole-4,5-dicarboxylate (7.207 g, 6.0 mmol) was added to 60 mL of anhydrous THF. Subsequently, Zn metal (2.353 g, 36.0 mmol) and I_2 (0.1827 g, 0.72 mmol) were added and stirred at reflux for 5 h under N_2. The reaction was cooled and filtered through CELITE™ then concentrated *in vacuo* with 80 mL of ethyl acetate. The solution was poured into a 500 mL separatory funnel and washed with 20 mL of 10% aqueous $Na_2S_2O_3$, two times each. The organic layer was collected and dried with $MgSO_4$. The volatiles were then evaporated *in vacuo*, and immediately purified *via* flash chromatography using 7:3 hexanes:ethyl acetate, affording 5.3218 g (5.1104 mmol, 85.17% yield) of a colorless oil, as a mixture of diastereomers.

TLC: 7:3 hexanes:ethyl acetate, R_f=0.63, UV, $KMnO_4$ stain, *p*-anisealdehyde stain, blue spot.

^{1}H NMR (500 MHz, $CDCl_3$): δ 4.56 (t, *J* = 7.2 Hz, 4H), 4.31 – 4.22 (m, 8H), 4.19 (t, *J* = 6.6 Hz, 4H), 1.90 (p, *J* = 7.2 Hz, 4H), 1.74 – 1.63 (m, 8H), 1.48 – 1.28 (m, 40H), 0.91 – 0.87 (m, 24H).

^{13}C-NMR (125 MHz, $CDCl_3$, DEPT): δ 160.6 (C=O), 158.8 (C=O), 151.8 (C=O), 140.5 (4°), 129.6 (4°), 74.7 (alkyne 4°), 69.2 (CH_2), 68.4 (CH_2), 66.7 (CH_2), 50.3 (CH_2), 38.7 (CH), 30.2 (CH_2), 30.2 (CH_2), 30.0 (CH_2), 28.9 (CH_2), 28.1 (CH_2), 25.9 (CH_2), 25.2 (CH_2), 23.6 (CH_2), 23.6 (CH_2), 23.0 (CH_2), 14.1 (CH_3), 10.9 (CH_3).

IR (Neat): 2959 (s, alkane CH), 2932 (s, alkane CH), 2872 (s, alkane CH), 2862 (s, alkane CH), 1727 (s, ester C=O), 1554 (m, triazole C=C), 1466 (s, methylene bending CH_2), 1256 (s, ester stretch C-O), 1215 (s, ester stretch C-O) cm^{-1}.

HRMS: Calcd. for $C_{56}H_{92}N_6O_{12}$ $[M+H]^+$ 1041.6846; Found 1041.6843.

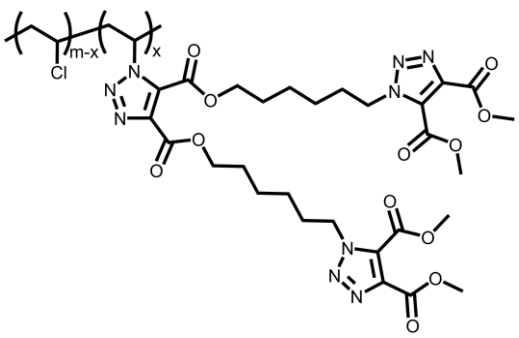

Preparation of 5% PVC-TRZ-DiHexyl-TRZ-DiMe. Poly(vinyl chloride) 5% azide (0.500 g, 8.00 mmol) was added to a 50 mL round bottom flask and dissolved in 20 mL of 3-pentanone at 90 °C. 4,5-Dimethyl 1-(6-{[4-({6-[4,5-bis(methoxycarbonyl)-1H-1,2,3-triazol-1-yl]hexyl}oxy)-4-oxobut-2-ynoyl]oxy}hexyl)-1H-1,2,3-triazole-4,5-dicarboxylate (0.520 g, 0.80 mmol) was added to the PVC solution and stirred for 24 h. The reaction was precipitated in 80 mL of MeOH, three times each. The isolated polymer was dried under house vacuum for 2 days to yield 0.413 g of a flocculent white solid.

^{1}H NMR (500 MHz, $CDCl_3$): δ 5.62 – 5.42 (br m, *C-C<u>H</u>-triazole*), 4.66 – 4.54 (br m, *Cl-C-<u>H</u>* and *PVC-linker-C-C<u>H$_2$</u>-triazole*), 4.45 (br s, *Cl-C-<u>H</u>*), 4.37 – 4.34 (br m, *PVC-triazole-O-C<u>H$_2$</u>-linker*), 4.33 – 4.25 (br m, *Cl-C-<u>H</u>*), 4.01 (br s, *O-CH$_3$*), 3.97 (br s, *O-CH$_3$*), 2.91 – 2.80 (br m, *Cl-C-C<u>H$_2$</u>-C-triazole* and *triazole-C-C<u>H$_2$</u>-C-triazole*), 2.74 (br s, *Cl-C-C<u>H$_2$</u>-C-triazole* and *triazole-C-C<u>H$_2$</u>-C-triazole*), 2.49 – 1.99 (br m, *Cl-C-C<u>H$_2$</u>-C-Cl*), 1.98 – 1.89 (br m, *PVC-linker-C<u>H$_2$</u>-C-triazole*), 1.83 – 1.73 (br m, *PVC-triazole-O-C-C<u>H$_2$</u>-linker*), 1.55 – 1.36 (br m, *linker C<u>H$_2$</u>'s*).

^{13}C NMR (125 MHz, $CDCl_3$): δ 160.6 (C=O), 159.0 (C=O), 139.9 (4°), 129.8 (4°), 67.3 (O-CH_2), 65.7 (O-CH_2), 57.1 – 56.9 (CH syndio), 56.1 – 55.9 (CH hetero), 55.2 – 54.9 (CH iso), 53.5 (CH_3), 52.7 (CH_3), 50.5 (CH_2), 47.3 – 44.8 (family of CH_2 PVC peaks), 30.0 (CH_2), 28.3 (CH_2), 28.1 (CH_2), 26.0 (CH_2), 25.9 (CH_2), 25.3 (CH_2), 25.2 (CH_2).

IR (Neat): 2942 (s, alkane CH), 2864 (s, alkane CH), 1733 (s, ester C=O), 1556 (m, triazole C=C), 1462 (m, methylene stretch CH_2), 1436 (m, methyl stretch CH), 1230 (s, ester stretch C-O) cm^{-1}.

DSC (T_g): 66 °C.

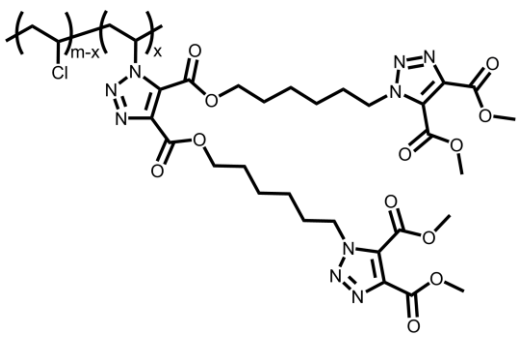

Preparation of 15% PVC-TRZ-DiHexyl-TRZ-DiMe. Poly(vinyl chloride) 15% azide (1.000 g, 16.00 mmol) was added to a 100 mL round bottom flask and dissolved in 20 mL of 3-pentanone at 90 °C. 4,5-Dimethyl 1-(6-{[4-({6-[4,5-bis(methoxycarbonyl)-1H-1,2,3-triazol-1-yl]hexyl}oxy)-4-oxobut-2-ynoyl]oxy}hexyl)-1H-1,2,3-triazole-4,5-dicarboxylate (3.6098 g, 7.2 mmol) was added to the PVC solution and stirred for 20 h. The reaction was concentrated to approximately half its volume *in vacuo*, then precipitated in 80 mL of MeOH, three times each. The isolated polymer was dried under house vacuum for 1 day, then in a vacuum oven at 40 °C for 2 days to yield 1.6847 g of an off-white solid.

^{1}H NMR (500 MHz, $CDCl_3$): δ 5.62 – 5.35 (br m, *C-C<u>H</u>-triazole*), 4.66 – 4.54 (br m, *Cl-C-<u>H</u>* and *PVC-linker-C-C<u>H$_2$</u>-triazole*), 4.45 (br s, *Cl-C-<u>H</u>*), 4.35 (br s, *PVC-triazole-O-C<u>H$_2$</u>-linker*), 4.33 – 4.25 (br m, *Cl-C-<u>H</u>*), 4.00 (br s, *O-C<u>H$_3$</u>*), 3.97 (br s, *O-C<u>H$_3$</u>*), 2.91 – 2.80 (br m, *Cl-C-C<u>H$_2$</u>-C-triazole* and *triazole-C-C<u>H$_2$</u>-C-triazole*), 2.73 (br s, *Cl-C-C<u>H$_2$</u>-C-triazole* and *triazole-C-C<u>H$_2$</u>-C-triazole*), 2.40 – 1.99 (br m, *Cl-C-C<u>H$_2$</u>-C-Cl*), 1.98 – 1.89 (br m, *PVC-linker-C<u>H$_2$</u>-C-triazole*), 1.78 (br s, *PVC-triazole-O-C-C<u>H$_2$</u>-linker*), 1.53 – 1.34 (br m, *linker C<u>H$_2$</u>'s*).

^{13}C NMR (125 MHz, $CDCl_3$, DEPT): δ 160.6 (C=O), 159.0 (C=O), 139.9 (4°), 129.8 (4°), 67.3 (O-CH_2), 67.1 (O-CH_2), 65.7 (O-CH_2), 57.1 – 56.9 (CH syndio), 56.1 – 55.9 (CH hetero), 55.2 – 54.9 (CH iso), 53.5 (CH_3), 52.7 (CH_3), 50.5 (CH_2), 47.3 – 44.8 (family of CH_2 PVC peaks), 30.0 (CH_2), 28.3 (CH_2), 28.1 (CH_2), 26.0 (CH_2), 25.9 (CH_2), 25.3 (CH_2), 25.2 (CH_2).

IR (Neat): 2953 (s, alkane CH), 2863 (s, alkane CH), 1733 (s, ester C=O), 1553 (m, triazole C=C), 1468 (m, methylene stretch CH_2), 1435 (m, methyl stretch CH), 1280 (m, ester stretch C-O), 1219 (s, ester stretch C-O), 615 (w, C-Cl) cm^{-1}.

DSC (T_g): 48 °C.

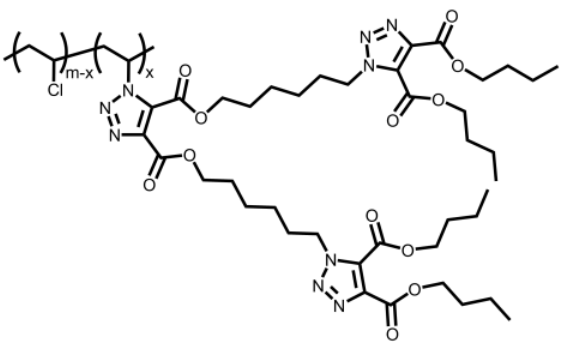

Preparation of 5% PVC-TRZ-DiHexyl-TRZ-DiBu. Poly(vinyl chloride) 5% azide (1.000 g, 16.00 mmol) was added to a 100 mL round bottom flask and dissolved in 30 mL of 3-pentanone at 90 °C. 4,5-Dibutyl 1-(6-{[4-({6-[4,5-bis(butoxycarbonyl)-1H-1,2,3-triazol-1-yl]hexyl}oxy)-4-oxobut-2-ynoyl]oxy}hexyl)-1H-1,2,3-triazole-4,5-dicarboxylate (1.307 g, 1.6 mmol) was added to the PVC solution and stirred for 24 h. The reaction was concentrated to approximately half its volume *in vacuo*, then precipitated in 80 mL of MeOH, three times each. The isolated polymer was dried under house vacuum for 1 day, then in a vacuum oven at 40 °C for 2 days to yield 1.2034 g of an off-white solid.

^{1}H NMR (500 MHz, $CDCl_3$): δ 5.62 – 5.40 (br m, *C-C<u>H</u>-triazole*), 4.65 – 4.55 (br m, *Cl-C-<u>H</u>* and *PVC-linker-C-C<u>H$_2$</u>-triazole*), 4.45 (br s, *Cl-C-<u>H</u>*), 4.40 – 4.24 (br m, *Cl-C-<u>H</u>* and *PVC-triazole-O-C<u>H$_2$</u>-linker* and *PVC-linker-triazole-O-C<u>H$_2$</u>*), 2.90 – 2.80 (br m, *Cl-C-C<u>H$_2$</u>-C-triazole* and *triazole-C-C<u>H$_2$</u>-C-triazole*), 2.74 (br s, *Cl-C-C<u>H$_2$</u>-C-triazole* and *triazole-C-C<u>H$_2$</u>-C-triazole*), 2.50 – 1.98 (br m, *Cl-C-C<u>H$_2$</u>-C-Cl*), 1.98 – 1.89 (br m, *PVC-linker-C<u>H$_2$</u>-C-triazole*), 1.85 – 1.71 (br m, *PVC-triazole-O-C-C<u>H$_2$</u>-linker* and *linker-triazole-O-C-C<u>H$_2$</u>*), 1.54 – 1.36 (br m, *linker C<u>H$_2$</u>'s* and *linker-triazole-O-C-C<u>H$_2$</u>-C<u>H$_2$</u>-C*), 1.01 – 0.94 (br t, *C<u>H$_3$</u>*).

^{13}C NMR (125 MHz, $CDCl_3$): δ 160.4 (C=O), 158.7 (C=O), 140.3 (4°), 129.7 (4°), 66.7 (O-CH_2), 65.7 (O-CH_2), 65.2 (O-CH_2), 57.0 – 56.9 (CH syndio), 56.1 – 55.9 (CH hetero), 55.1 – 54.9 (CH iso), 50.4 (CH_2), 47.3 – 44.8 (family of CH_2 PVC peaks), 30.6 (CH_2), 30.4 (CH_2), 30.1

(CH_2), 28.4 (CH_2), 28.1 (CH_2), 26.1 (CH_2), 26.0 (CH_2), 25.3 (CH_2), 25.2 (CH_2), 19.1 (CH_2), 19.0 (CH_2), 13.72 (CH_3), 13.65 (CH_3).

IR (Neat): 2961 (s, alkane CH), 2937 (s, alkane CH), 2873 (s, alkane CH), 1729 (s, ester C=O), 1552 (m, triazole C=C), 1466 (m, methylene stretch CH_2), 1435 (m, methyl stretch CH), 1264 (s, ester stretch C-O), 1203 (s, ester stretch C-O) cm^{-1}.

DSC (T_g): 43 °C.

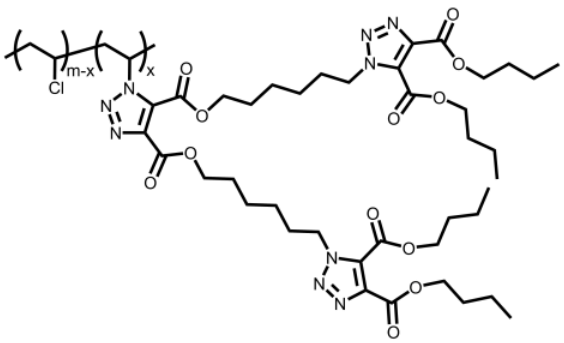

Preparation of 15% PVC-TRZ-DiHexyl-TRZ-DiBu. Poly(vinyl chloride) 15% azide (1.000 g, 16.00 mmol) was added to a 100 mL round bottom flask and dissolved in 20 mL of 3-pentanone at 90 °C. 4,5-Dibutyl 1-(6-{[4-({6-[4,5-bis(butoxycarbonyl)-1H-1,2,3-triazol-1-yl]hexyl}oxy)-4-oxobut-2-ynoyl]oxy}hexyl)-1H-1,2,3-triazole-4,5-dicarboxylate (5.50 g, 6.73 mmol) was added to the PVC solution and stirred for 27 h. The reaction was concentrated to approximately half its volume *in vacuo*, then precipitated in 80 mL of MeOH, three times each. The isolated polymer was dried under house vacuum for 1 day, then in a vacuum oven at 40 °C for 2 days to yield 2.0206 g of a flexible pale yellow solid.

^{1}H NMR (500 MHz, $CDCl_3$): δ 5.62 – 5.35 (br m, *C-C<u>H</u>-triazole*), 4.65 – 4.55 (br m, *Cl-C-<u>H</u>* and *PVC-linker-C-C<u>H$_2$</u>-triazole*), 4.45 – 4.20 (br m, *Cl-C-<u>H</u>* and *PVC-triazole-O-C<u>H$_2$</u>-linker* and *PVC-linker-triazole-O-C<u>H$_2$</u>*), 2.90 – 2.80 (br s, *Cl-C-C<u>H$_2$</u>-C-triazole* and *triazole-C-C<u>H$_2$</u>-C-triazole*), 2.79 – 2.64 (br s, *Cl-C-C<u>H$_2$</u>-C-triazole* and *triazole-C-C<u>H$_2$</u>-C-triazole*), 2.50 – 1.98 (br m, *Cl-C-C<u>H$_2$</u>-C-Cl*), 1.98 – 1.86 (br s, *PVC-linker-C<u>H$_2$</u>-C-triazole*), 1.83 – 1.68 (br s, *PVC-triazole-O-C-C<u>H$_2$</u>-linker* and *linker-triazole-O-C-C<u>H$_2$</u>*), 1.53 – 1.33 (br s, *linker C<u>H$_2$</u>'s* and *linker-triazole-O-C-C<u>H$_2$</u>-C<u>H$_2$</u>-C*), 1.02 – 0.91 (br s, *C<u>H$_3$</u>*).

^{13}C NMR (125 MHz, $CDCl_3$, DEPT): δ 160.4 (C=O), 159.8 (C=O), 158.7 (C=O), 140.3 (4°), 129.7 (4°), 66.7 (O-CH_2), 65.7 (O-CH_2), 57.0 – 56.9 (CH syndio), 56.1 – 55.9 (CH hetero), 55.1 – 54.9 (CH iso), 50.4 (CH_2), 47.3 – 45.3 (family of CH_2 PVC peaks), 30.6 (CH_2), 30.3 (CH_2), 30.1 (CH_2), 28.3 (CH_2), 28.1 (CH_2), 26.1 (CH_2), 26.0 (CH_2), 25.3 (CH_2), 25.2 (CH_2), 19.1 (CH_2), 19.0 (CH_2), 13.7 (CH_3), 13.6 (CH_3).

IR (Neat): 2961 (s, alkane CH), 2937 (s, alkane CH), 2873 (s, alkane CH), 1732 (s, ester C=O), 1552 (s, triazole C=C), 1467 (s, methylene stretch CH_2), 1436 (m, methyl stretch CH), 1267 (s, ester stretch C-O), 1203 (s, ester stretch C-O), 615 (w, C-Cl) cm^{-1}.

DSC (T_g): 12 °C.

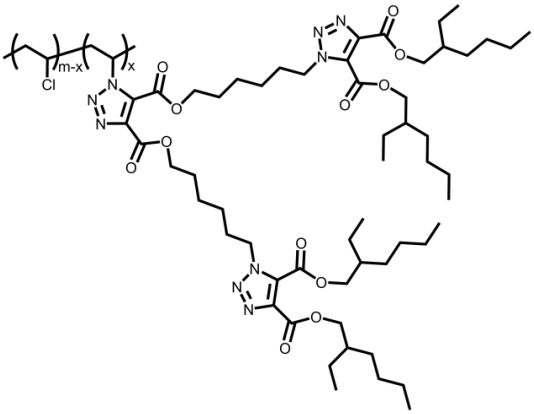

Preparation of 5% PVC-TRZ-DiHexyl-TRZ-DiEH. Poly(vinyl chloride) 5% azide (1.000 g, 16.00 mmol) was added to a 100 mL round bottom flask and dissolved in 20 mL of 3-pentanone at 90 °C. 4,5-Bis(2-ethylhexyl) 1-(6-{[4-({6-[4,5-bis({[(2-ethylhexyl)oxy]carbonyl})-1H-1,2,3-triazol-1-yl]hexyl}oxy)-4-oxobut-2-ynoyl]oxy}hexyl)-1H-1,2,3-triazole-4,5-dicarboxylate (2.0827 g, 2.0 mmol) was diluted with 10 mL of 3-pentanone and added to the PVC solution, then stirred for 36 h. The reaction was concentrated to approximately half its volume *in vacuo*, then precipitated in 80 mL of MeOH, two times each. The isolated polymer was dried under house vacuum for 1 day, then in a vacuum oven at 40 °C for 2 days to yield 1.02 g of an off-white solid.

^{1}H NMR (500 MHz, $CDCl_3$): δ 5.62 – 5.44 (br m, *C-C<u>H</u>-triazole*), 4.67 – 4.56 (br m, *Cl-C-<u>H</u>* and *PVC-linker-C-C<u>H$_2$</u>-triazole*), 4.54 – 4.39 (br m, *Cl-C-<u>H</u>* and *PVC-triazole-O-C<u>H$_2$</u>-linker* and *PVC-linker-triazole-O-C<u>H$_2$</u>-C*), 4.39 – 4.22 (br m, *Cl-C-<u>H</u>*), 2.92 – 2.81 (br m, *Cl-C-C<u>H$_2$</u>-C-*

triazole and *triazole-C-C<u>H₂</u>-C-triazole*), 2.81 – 2.66 (br s, *Cl-C-C<u>H₂</u>-C-triazole* and *triazole-C-C<u>H₂</u>-C-triazole*), 2.50 – 1.99 (br m, *Cl-C-C<u>H₂</u>-C-Cl*), 1.98 – 1.88 (br m, *PVC-linker-C<u>H₂</u>-C-triazole*), 1.85 – 1.77 (br m, *PVC-triazole-O-C-C<u>H₂</u>-linker*), 1.76 – 1.65 (br m, *PVC-linker-triazole-O-C-C<u>H</u>-C*), 1.54 – 1.26 (br m, *linker C<u>H₂</u>'s* and *linker-triazole-O-C-C-C<u>H₂</u>-C<u>H₂</u>-C<u>H₂</u>-C*), 0.97 – 0.88 (br m, *C<u>H₃</u>*).

^{13}C NMR (125 MHz, $CDCl_3$): δ 160.6 (C=O), 158.8 (C=O), 140.5 (4°), 129.6 (4°), 69.2 (O-CH_2), 68.4 (O-CH_2), 65.7 (O-CH_2), 57.0 – 56.9 (CH syndio), 56.1 – 55.9 (CH hetero), 55.2 – 54.9 (CH iso), 50.4 (CH_2), 47.3 – 44.8 (family of CH_2 PVC peaks), 38.72 (CH), 38.69 (CH), 30.19 (CH_2), 30.15 (CH_2), 30.1 (CH_2), 28.88 (CH_2), 28.86 (CH_2), 28.4 (CH_2), 28.1 (CH_2), 26.1 (CH_2), 26.0 (CH_2), 25.3 (CH_2), 25.23 (CH_2), 25.16 (CH_2), 23.6 (CH_2), 23.5 (CH_2), 22.96 (CH_2), 22.95 (CH_2), 14.1 (CH_3), 10.92 (CH_3), 10.90 (CH_3).

IR (Neat): 2960 (s, alkane CH), 2932 (s, alkane CH), 2872 (s, alkane CH), 2861 (s, alkane CH), 1729 (s, ester C=O), 1554 (s, triazole C=C), 1465 (s, methylene stretch CH_2), 1436 (m, methyl stretch CH), 1260 (s, ester stretch C-O), 1203 (s, ester stretch C-O) cm^{-1}.

DSC (T_g): 43 °C.

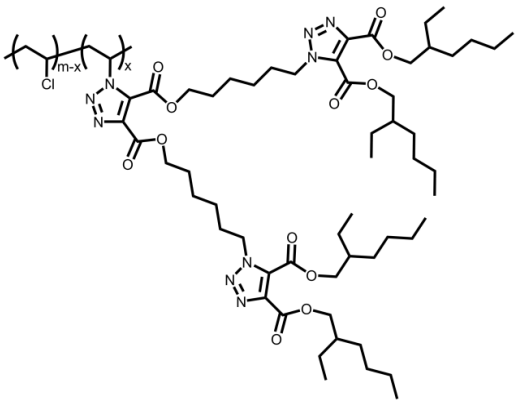

Preparation of 15% PVC-TRZ-DiHexyl-TRZ-DiEH. Poly(vinyl chloride) 15% azide (1.000 g, 16.00 mmol) was added to a 100 mL round bottom flask and dissolved in 20 mL of 3-pentanone at 90 °C. 4,5-Bis(2-ethylhexyl) 1-(6-{[4-({6-[4,5-bis({[(2-ethylhexyl)oxy]carbonyl})-1H-1,2,3-triazol-1-yl]hexyl}oxy)-4-oxobut-2-ynoyl]oxy}hexyl)-1H-1,2,3-triazole-4,5-dicarboxylate (7.4978 g, 7.2 mmol) was added to the PVC solution and stirred for 28 h. The reaction was concentrated to approximately half its volume *in vacuo*, then precipitated in 80 mL of MeOH, four times each. The isolated polymer

was dried under house vacuum for 1 day, then in a vacuum oven at 40 °C for 3 days to yield 2.3972 g of a flexible pale yellow solid.

^{1}H NMR (500 MHz, $CDCl_3$): δ 5.63 – 5.34 (br m, C-C*H*-triazole), 4.67 – 4.52 (br m, *Cl-C-H* and *PVC-linker-C-CH_2-triazole*), 4.51 – 4.38 (br m, *Cl-C-H* and *PVC-triazole-O-CH_2-linker* and *PVC-linker-triazole-O-CH_2-C*), 4.38 – 4.15 (br m, *Cl-C-H*), 2.92 – 2.80 (br s, *Cl-C-CH_2-C-triazole* and *triazole-C-CH_2-C-triazole*), 2.80 – 2.66 (br s, *Cl-C-CH_2-C-triazole* and *triazole-C-CH_2-C-triazole*), 2.50 – 1.98 (br m, *Cl-C-CH_2-C-Cl*), 1.98 – 1.87 (br s, *PVC-linker-CH_2-C-triazole*), 1.84 – 1.64 (br m, *PVC-triazole-O-C-CH_2-linker and PVC-linker-triazole-O-C-CH-C*), 1.54 – 1.24 (br m, *linker CH_2's* and *linker-triazole-O-C-C-CH_2-CH_2-CH_2-C*), 0.98 – 0.83 (br m, *CH_3*).

^{13}C NMR (125 MHz, $CDCl_3$, DEPT): δ 160.6 (C=O), 158.8 (C=O), 140.5 (4°), 129.6 (4°), 69.1 (O-CH_2), 68.3 (O-CH_2), 66.4 (O-CH_2), 65.7 (O-CH_2), 57.0 – 56.9 (CH syndio), 56.1 – 55.9 (CH hetero), 50.4 (CH_2), 47.3 – 45.2 (family of CH_2 PVC peaks), 38.72 (CH), 38.68 (CH), 30.2 (CH_2), 30.14 (CH_2), 30.1 (CH_2), 28.87 (CH_2), 28.85 (CH_2), 28.4 (CH_2), 28.1 (CH_2), 26.1 (CH_2), 26.0 (CH_2), 25.3 (CH_2), 25.2 (CH_2), 25.16 (CH_2), 23.6 (CH_2), 23.5 (CH_2), 22.95 (CH_2), 22.93 (CH_2), 14.0 (CH_3), 10.90 (CH_3), 10.88 (CH_3).

IR (Neat): 2960 (s, alkane CH), 2932 (s, alkane CH), 2861 (s, alkane CH), 1729 (s, ester C=O), 1553 (s, triazole C=C), 1465 (s, methylene stretch CH_2), 1437 (m, methyl stretch CH), 1260 (s, ester stretch C-O), 1204 (s, ester stretch C-O), 616 (w, C-Cl) cm^{-1}.

DSC (T_g): -6 °C.

6.7 Chapter 4 Experimental Section

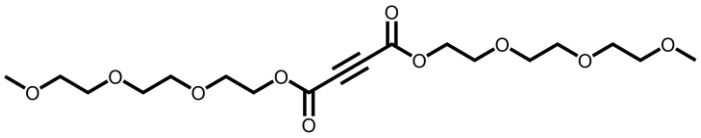

Preparation of 1,4-bis({2-[2-(2-methoxyethoxy)ethoxy]ethyl}) but-2-ynedioate. But-2-ynedioic acid (1.0000 g, 8.767 mmol) was added to a 50 mL round bottom flask. Triethylene glycol monomethyl ether (3.1670 g, 19.290 mmol) was then added along with 4-methylbenzenesulfonic acid (0.1667 g, 0.876 mmol) and 13 mL of dry toluene. Using a Dean-Stark apparatus, the reaction was heated and stirred at reflux for 5 h. The reaction was transferred to a 150 mL separatory funnel and diluted with 40 mL of toluene and washed with 20 mL of saturated $NaHCO_3$ three times each. The aqueous layer was extracted with 60 mL of ethyl acetate, three times each. The combined organic layers were dried with $MgSO_4$, filtered, and concentrated *in vacuo*. Purification *via* flash chromatography using 95:5 CH_2Cl_2:MeOH afforded 2.673 g (6.576 mmol, 75.02% yield) of the title compound as a colorless oil.

TLC: 95:5 CH_2Cl_2:MeOH, R_f=0.53, UV, $KMnO_4$ stain, *p*-anisealdehyde stain, blue spot. Blue fluorescence at 395 nm.

^{1}H NMR (500 MHz, $CDCl_3$): δ 4.39 – 4.31 (m, 4H), 3.74 – 3.70 (m, 4H), 3.65 – 3.60 (m, 12H), 3.56 – 3.49 (m, 4H), 3.37 – 3.33 (m, 6H).

^{13}C NMR (125 MHz, $CDCl_3$, DEPT): δ 151.6 (C=O), 74.7 (alkyne 4°), 71.9 (CH_2), 70.7 (CH_2), 70.6 (CH_2), 68.4 (CH_2), 65.8 (CH_2), 58.9 (CH_3).

IR (Neat): 2879 (s, alkane CH), 1725 (s, ester C=O), 1259 (s, ester stretch C-O), 1110 (s, ether stretch C-O) cm^{-1}.

HRMS: Calcd. for $C_{18}H_{30}O_{10}$ $[M+H]^+$ 407.1912; Found 407.1895. $[M+Na]^+$ 429.1731; Found 429.1708.

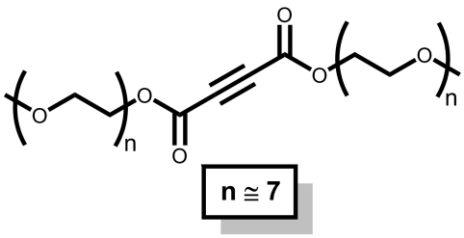

Preparation of 1,4-bis-[methoxy poly(ethylene glycol) 350]-but-2-ynedioate. But-2-ynedioic acid (4.000 g, 35.069 mmol) was added to a 250 mL round bottom flask. Poly(ethylene glycol) monomethyl ether 350 (28.231 g, 80.659 mmol) was added along with 0.2 mL H_2SO_4 and 40 mL of dry toluene. Using a Dean-Stark apparatus, the reaction was heated and stirred at reflux for 2 h. The reaction was concentrated *in vacuo*, and diluted with 100 mL ethyl acetate. The solution was transferred to a 500 mL separatory funnel and washed with 10 mL of saturated $NaHCO_3$ three times each. The aqueous layer was extracted with 60 mL of ethyl acetate, three times each. The combined organic layers were dried with $MgSO_4$, filtered, and concentrated *in vacuo*. Purification *via* flash chromatography using 93:7 CH_2Cl_2:MeOH afforded 16.750 g (21.502 mmol, 61.31% yield) of the title compound as a colorless oil.

TLC: 93:7 CH_2Cl_2:MeOH, R_f=0.71, UV, $KMnO_4$ stain, *p*-anisealdehyde stain, blue spot. Blue fluorescence at 395 nm.

^{1}H NMR (500 MHz, $CDCl_3$): δ 4.39 (t, 4H), 3.75 (t, 4H), 3.67 (br s, 36H), 3.59 – 3.53 (m, 4H), 3.41 – 3.37 (m, 6H).

^{13}C NMR (125 MHz, $CDCl_3$, DEPT): δ 151.6 (C=O), 74.9 (alkyne 4°), 71.9 (CH_2), 70.71 (CH_2), 70.66 (CH_2), 70.62 (CH_2), 70.59 (CH_2), 70.5 (CH_2), 68.4 (CH_2), 65.8 (CH_2), 59.0 (CH_3).

IR (Neat): 2874 (s, alkane CH), 1724 (s, ester C=O), 1257 (s, ester stretch C-O), 1107 (s, ether stretch C-O) cm^{-1}.

HRMS: Calcd. for (n=6,6) $C_{30}H_{54}O_{16}$ $[M+H]^+$ 671.3485; Found 671.3477.

Calcd. for (n=6,7) $C_{32}H_{58}O_{17}$ $[M+H]^+$ 715.3747; Found 715.3736.

Calcd. for (n=7,7) $C_{34}H_{62}O_{18}$ $[M+H]^+$ 759.4009; Found 759.3997.

Calcd. for (n=7,8) $C_{36}H_{66}O_{19}$ $[M+H]^+$ 803.4271; Found 803.4260.

Calcd. for (n=8,8) $C_{38}H_{70}O_{20}$ $[M+H]^+$ 847.4533; Found 847.4520.

Calcd. for (n=8,9) $C_{40}H_{74}O_{21}$ $[M+H]^+$ 891.4795; Found 891.4779.

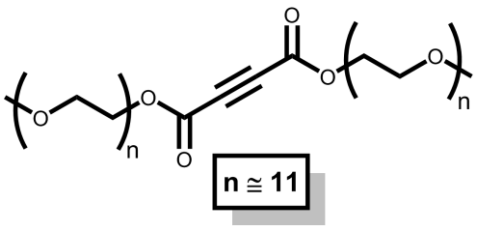

Preparation of 1,4-bis-[methoxy poly(ethylene glycol) 550]-but-2-ynedioate. But-2-ynedioic acid (2.000 g, 17.534 mmol) was added to a 250 mL round bottom flask. Poly(ethylene glycol) monomethyl ether 550 (20.252 g, 36.821 mmol) was then added along with 0.2 mL H_2SO_4 and 40 mL of dry toluene. Using a Dean-Stark apparatus, the reaction was heated and stirred at reflux for 2 h. The reaction was concentrated *in vacuo*, and diluted with 100 mL ethyl acetate. The solution was transferred to a 500 mL separatory funnel and washed with 10 mL of saturated $NaHCO_3$ three times each. The aqueous layer was extracted with 60 mL of ethyl acetate, three times each. The combined organic layers were dried with $MgSO_4$, filtered, and concentrated *in vacuo*. Purification *via* flash chromatography using 93:7 CH_2Cl_2:MeOH afforded 16.153 g (13.712 mmol, 78.20% gravimetric yield) of the title compound as a colorless oil.

TLC: 93:7 CH_2Cl_2:MeOH, R_f=0.65, UV, $KMnO_4$ stain, *p*-anisealdehyde stain, blue spot.

^{1}H NMR (500 MHz, $CDCl_3$): δ 4.39 (m, 2H), 4.35 (m, 1H), 3.75 (m, 4H), 3.66 (br s, 84H), 3.56 (m, 4H), 3.41 – 3.37 (m, 6H), 2.98 (br s, 0.36H).

^{13}C NMR (125 MHz, $CDCl_3$, DEPT): δ 152.6 (C=O, propiolic ester), 151.7 (C=O ADC ester), 75.3 (propiolic C-H), 74.9 (alkyne 4° ADC), 74.6 (alkyne 4° propiolic), 72.5 (CH_2), 71.9 (CH_2), 70.71 (CH_2), 70.66 (CH_2), 70.58 (CH_2), 70.52 (CH_2), 70.4 (CH_2), 68.6 (CH_2), 68.4 (CH_2), 65.8 (CH_2), 65.2 (CH_2), 61.8 (CH_2), 59.0 (CH_3).

IR (Neat): 2874 (s, alkane CH), 2111 (m, alkyne CH), 1720 (s, ester C=O), 1252 (s, ester stretch C-O), 1107 (s, ether stretch C-O) cm^{-1}.

HRMS: Calcd. for (n=10,11) $C_{48}H_{90}O_{25}$ $[M+H]^+$ 1067.5844; Found 1067.5823.

Calcd. for (n=11,11) $C_{50}H_{94}O_{26}$ $[M+H]^+$ 1111.6106; Found 1111.6086.

Calcd. for (n=11,12) $C_{52}H_{98}O_{27}$ $[M+H]^+$ 1155.6368; Found 1155.6348.

Calcd. for (n=12,12) $C_{54}H_{102}O_{28}$ $[M+H]^+$ 1199.6630; Found 1199.6608.

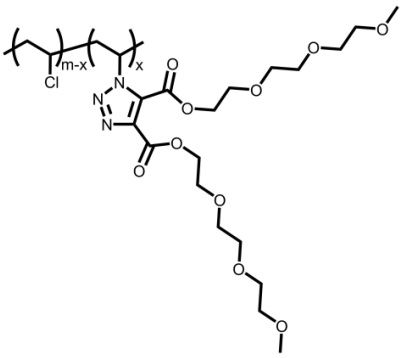

Preparation of 5% PVC-TRZ-DiPEO$_{164}$Me. Poly(vinyl chloride) 5% azide (1.000 g, 16.00 mmol) was added to a 100 mL round bottom flask and dissolved in 30 mL of 3-pentanone at 90 °C. 1,4-Bis({2-[2-(2-methoxyethoxy)ethoxy]ethyl})but-2-ynedioate (2.0827 g, 2.0 mmol) was added to the PVC solution and stirred for 24 h. The reaction was concentrated to approximately half its volume *in vacuo*, then precipitated in 80 mL of MeOH, three times each. The isolated polymer was dried under house vacuum for 1 day, then in a vacuum oven at 40 °C for 2 days to yield 0.970 g of a flocculent white solid.

^{1}H NMR (500 MHz, $CDCl_3$): δ 5.66 – 5.48 (br m, *C-C<u>H</u>-triazole*), 4.66 – 4.55 (br s, *Cl-C-<u>H</u>*), 4.55 – 4.39 (br s, *Cl-C-<u>H</u>* and *triazole-O-C<u>H$_2$</u>),* 4.38 – 4.24 (br m, *Cl-C-<u>H</u>*), 3.87 – 3.81 (br m, *triazole-O-C-C<u>H$_2$</u>-O*), 3.73 – 3.60 (br m, *triazole-O-C-C-O-C<u>H$_2$</u>-C<u>H$_2$</u>-O-C<u>H$_2$</u>-C*), 3.57 – 3.52 (br m, *C-C<u>H$_2$</u>-O-CH$_3$*), 3.40 – 3.34 (br s, *O-C<u>H$_3$</u>*), 2.90 – 2.80 (br s, *Cl-C-C<u>H$_2$</u>-C-triazole* and *triazole-C-C<u>H$_2$</u>-C-triazole*), 2.80 – 2.66 (br s, *Cl-C-C<u>H$_2$</u>-C-triazole* and *triazole-C-C<u>H$_2$</u>-C-triazole*), 2.50 – 1.85 (br m, *Cl-C-C<u>H$_2$</u>-C-Cl*).

^{13}C NMR (125 MHz, $CDCl_3$, DEPT): δ 159.7 (C=O), 158.3 (C=O), 139.4 (4°), 132.2 (4°), 71.9 (CH_2), 70.65 (CH_2), 70.6 (CH_2), 70.55 (CH_2), 68.7 (CH_2), 68.4 (CH_2), 66.2 (CH_2), 64.9 (CH_2),

59.0 (CH_3), 57.0 – 56.9 (CH syndio), 56.1 – 55.9 (CH hetero), 55.1 – 54.9 (CH iso), 47.3 – 44.8 (family of CH_2 peaks).

IR (Neat): 2910 (s, alkane CH), 1726 (s, ester C=O), 1551 (s, triazole C=C), 1451 (s, methylene stretch CH_2), 1437 (m, methyl stretch CH), 1256 (s, ester stretch C-O), 1200 (s, ester stretch C-O), 1107 (s, ether stretch C-O), 611 (w, C-Cl) cm^{-1}.

DSC (T_g): 61 °C.

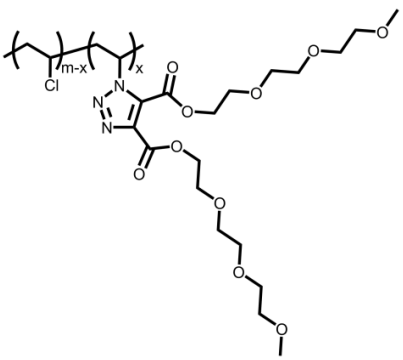

Preparation of 15% PVC-TRZ-DiPEO$_{164}$Me. Poly(vinyl chloride) 15% azide (1.000 g, 16.00 mmol) was added to a 100 mL round bottom flask and dissolved in 20 mL of 3-pentanone at 90 °C. 1,4-Bis({2-[2-(2-methoxyethoxy)ethoxy]ethyl})but-2-ynedioate (2.4238 g, 6.0 mmol) was added to the PVC solution and stirred for 72 h. The reaction was concentrated to approximately half its volume *in vacuo*, then precipitated in 80 mL of MeOH, three times each. The isolated polymer was dried under house vacuum for 1 day, then in a vacuum oven at 40 °C for 3 days to yield 1.33 g of a white solid.

^{1}H NMR (500 MHz, $CDCl_3$): δ 5.66 – 5.44 (br m, *C-C<u>H</u>-triazole*), 4.63 – 4.54 (br s, *Cl-C-<u>H</u>*), 4.54 – 4.39 (br s, *Cl-C-<u>H</u>* and *triazole-O-C<u>H$_2$</u>),* 4.36 – 4.24 (br m, *Cl-C-<u>H</u>*), 3.87 – 3.79 (br m, *triazole-O-C-C<u>H$_2$</u>-O*), 3.76 – 3.68 (br m, *triazole-O-C-C-O-C<u>H$_2$</u>-C<u>H$_2$</u>-O-C<u>H$_2$</u>-C*), 3.58 – 3.53 (br m, *C-C<u>H$_2$</u>-O-CH$_3$*), 3.40 – 3.36 (br s, *O-C<u>H$_3$</u>*), 2.92 – 2.81 (br m, *Cl-C-C<u>H$_2$</u>-C-triazole* and *triazole-C-C<u>H$_2$</u>-C-triazole*), 2.80 – 2.66 (br m, *Cl-C-C<u>H$_2$</u>-C-triazole* and *triazole-C-C<u>H$_2$</u>-C-triazole*), 2.50 – 1.95 (br m, *Cl-C-C<u>H$_2$</u>-C-Cl*).

^{13}C NMR (125 MHz, $CDCl_3$, DEPT): δ 159.7 (C=O), 158.3 (C=O), 138.6 (4°), 131.7 (4°), 71.9 (CH_2), 70.67 (CH_2), 70.62 (CH_2), 70.57 (CH_2), 68.7 (CH_2), 68.4 (CH_2), 66.2 (CH_2), 64.9 (CH_2),

59.0 (CH_3), 57.0 – 56.9 (CH syndio), 56.1 – 55.9 (CH hetero), 55.2 – 54.9 (CH iso), 47.3 – 44.8 (family of CH_2 peaks).

IR (Neat): 2879 (s, alkane CH), 1734 (s, ester C=O), 1549 (s, triazole C=C), 1452 (s, methylene stretch CH_2), 1259 (s, ester stretch C-O), 1200 (s, ester stretch C-O), 1107 (s, ether stretch C-O), 611 (w, C-Cl) cm^{-1}.

DSC (T_g): 42 °C.

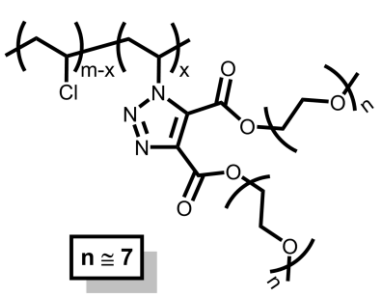

Preparation of 5% PVC-TRZ-DiPEO$_{350}$Me. Poly(vinyl chloride) 5% azide (1.000 g, 16.00 mmol) was added to a 100 mL round bottom flask and dissolved in 20 mL of 3-pentanone at 90 °C. 1,4-Bis-[methoxy poly(ethylene glycol) 350]-but-2-ynedioate (1.558 g, 2.0 mmol) was added to the PVC solution and stirred for 24 h. The reaction was concentrated to approximately half its volume *in vacuo*, then precipitated in 80 mL of MeOH, three times each. The isolated polymer was dried under house vacuum for 1 day, then in a vacuum oven at 40 °C for 2 days to yield 1.0872 g of a white solid.

^{1}H NMR (500 MHz, $CDCl_3$): δ 5.69 – 5.40 (br m, C-C*H*-*triazole*), 4.66 – 4.55 (br s, *Cl-C-H*), 4.55 – 4.39 (br s, *Cl-C-H* and *triazole-O-CH_2),* 4.38 – 4.12 (br s, *Cl-C-H*), 3.89 – 3.80 (br s, *triazole-O-C-CH_2-O*), 3.72 – 3.59 (br m, *triazole-O-C-C-O-CH_2-CH_2-O-*), 3.58 – 3.54 (br s, *C-CH_2-O-CH_3*), 3.41 – 3.37 (br s, *O-CH_3*), 2.92 – 2.81 (br m, *Cl-C-CH_2-C-triazole* and *triazole-C-CH_2-C-triazole*), 2.80 – 2.67 (br m, *Cl-C-CH_2-C-triazole* and *triazole-C-CH_2-C-triazole*), 2.50 – 1.90 (br m, *Cl-C-CH_2-C-Cl*).

^{13}C NMR (125 MHz, $CDCl_3$, DEPT): δ 71.9 (CH_2), 70.61 (CH_2), 70.58 (CH_2), 70.52 (CH_2), 68.9 (CH_2), 68.7 (CH_2), 68.4 (CH_2), 64.9 (CH_2), 59.0 (CH_3), 57.1 – 56.9 (CH syndio), 56.1 – 55.9 (CH hetero), 55.2 – 54.9 (CH iso), 47.3 – 44.9 (family of CH_2 peaks).

IR (Neat): 2910 (s, alkane CH), 1732 (s, ester C=O), 1551 (w, triazole C=C), 1435 (s, methylene stretch CH_2), 1254 (s, ester stretch C-O), 1202 (m, ester stretch C-O), 1105 (s, ether stretch C-O), 615 (w, C-Cl) cm^{-1}.

DSC (T_g): 49 °C.

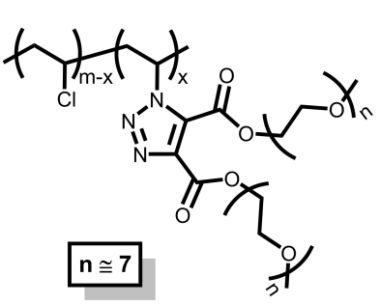

Preparation of 15% PVC-TRZ-DiPEO$_{350}$Me. Poly(vinyl chloride) 15% azide (1.000 g, 16.00 mmol) was added to a 100 mL round bottom flask and dissolved in 35 mL of 3-pentanone at 96 °C. 1,4-Bis-[methoxy poly(ethylene glycol) 350]-but-2-ynedioate (5.6088 g, 7.2 mmol) was added to the PVC solution and stirred for 48 h. The reaction was concentrated to approximately one-third its volume *in vacuo*. To a 250 mL beaker, 100 mL of MeOH was added, then placed in a dry ice-acetone bath for 2 min. The polymer was precipitated by dropwise addition of the reaction solution in 2 mL increments into the cooled MeOH. After the addition of reaction solution, the mother liquor was decanted and replaced with 100 mL of fresh MeOH. The beaker was cooled to -78 °C for 2 min, upon which another 2 mL of reaction solution was added dropwise. This process was repeated until the entire polymer was precipitated. When all of the reaction solution was precipitated, the last volume of mother liquor was decanted. Subsequently, the neat polymer was cooled to -78 °C and washed with 50 mL of MeOH four times each. The isolated polymer was dried under house vacuum for 1 day, then in a vacuum oven at 40 °C for 3 days to yield 2.0000 g of a flexible orange solid.

^{1}H NMR (500 MHz, $CDCl_3$): δ 5.67 – 5.40 (br m, C-C*H*-Triazole), 4.67 – 4.56 (br s, *Cl-C-H*), 4.56 – 4.50 (br s, *Cl-C-H* and *triazole-O-CH_2),* 4.50 – 4.40 (br s, *Cl-C-H* and *triazole-O-CH_2),* 4.38 – 4.15 (br m, *Cl-C-H*), 3.89 – 3.79 (br s, *triazole-O-C-CH_2-O*), 3.78 – 3.59 (br m, *triazole-O-C-C-O-CH_2-CH_2-O-*), 3.58 – 3.55 (br t, *C-CH_2-O-CH_3*), 3.41 – 3.38 (br s, *O-CH_3*), 2.92 –

2.81 (br m, *Cl-C-C<u>H</u>-C-triazole* and *triazole-C-C<u>H</u>-C-triazole*), 2.81– 2.65 (br m, *Cl-C-C<u>H</u>-C-triazole* and *triazole-C-C<u>H</u>-C-triazole*), 2.50 – 1.85 (br m, *Cl-C-C<u>H</u>-C-Cl*).

^{13}C NMR (200 MHz, $CDCl_3$): δ 161.0 (C=O), 159.8 (C=O), 158.3 (C=O), 139.3 (4°), 131.7 (4°), 72.5 (CH_2), 71.9 (CH_2), 70.6 (CH_2), 68.9 (CH_2), 68.7 (CH_2), 68.4 (CH_2), 66.2 (CH_2), 66.1 (CH_2), 64.9 (CH_2), 63.1 (CH_2), 61.7 (CH_2), 59.0 (CH_3), 56.9 – 56.5 (CH syndio), 56.0 – 55.6 (CH hetero), 55.0 – 54.5 (CH iso), 47.3 – 44.8 (family of CH_2 peaks).

IR (Neat): 2877 (s, alkane CH), 1729 (s, ester C=O), 1548 (w, triazole C=C), 1456 (s, methylene stretch CH_2), 1283 (s, ester stretch C-O), 1198 (s, ester stretch C-O), 1108 (s, ether stretch C-O), 615 (w, C-Cl) cm^{-1}.

DSC (T_g): -3 °C.

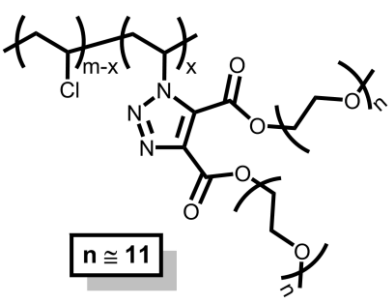

Preparation of 5% PVC-TRZ-DiPEO$_{550}$Me. Poly(vinyl chloride) 5% azide (1.000 g, 16.00 mmol) was added to a 100 mL round bottom flask and dissolved in 20 mL of 3-pentanone at 95 °C. 1,4-Bis-[methoxy poly(ethylene glycol) 550]-but-2-ynedioate (2.827 g, 2.4 mmol) was added to the PVC solution and stirred for 24 h. The reaction was concentrated to approximately half its volume *in vacuo*, then precipitated once in 80 mL of MeOH. The crude polymer was dissolved in 15 mL of 3-pentaone and 1,4-Bis-[methoxy poly(ethylene glycol) 550]-but-2-ynedioate (2.827 g, 2.4 mmol) was added to the PVC solution and stirred for 24 h. The reaction was concentrated to approximately half its volume *in vacuo*, then precipitated in 80 mL of MeOH, two times each. The isolated polymer was dried under house vacuum for 1 day, then in a vacuum oven at 40 °C for 2 days to yield 0.704 g of an off- white solid.

^{1}H NMR (500 MHz, $CDCl_3$): δ 8.30 – 8.20 (br m, *PVC-triazole-<u>H</u>*), 8.12 – 8.08 (br s, *PVC-triazole-<u>H</u>*), 5.66 – 5.50 (br m, *C-C<u>H</u>-triazole*), 5.30 – 5.15 (br m, *C-C<u>H</u>-triazole*), 4.67 – 4.56

(br s, *Cl-C-H*), 4.55 – 4.40 (br s, *Cl-C-H* and *triazole-O-CH$_2$-C-O*), 4.40 – 4.25 (br m, *Cl-C-H* and *triazole-O-CH$_2$-C-O*), 3.90 – 3.78 (br m, *triazole-O-C-CH$_2$-O*), 3.76 – 3.59 (br s, *triazole-O-C-C-O-CH$_2$-CH$_2$-O-*), 3.58 – 3.54 (br m, *C-CH$_2$-O-CH$_3$*), 3.41 – 3.37 (br s, *O-CH$_3$*), 2.92 – 2.81 (br m, *Cl-C-CH$_2$-C-triazole* and *triazole-C-CH$_2$-C-triazole*), 2.90 – 2.69 (br m, *Cl-C-CH$_2$-C-triazole* and *triazole-C-CH$_2$-C-triazole*), 2.50 – 1.80 (br m, *Cl-C-CH$_2$-C-Cl*).

^{13}C NMR (125 MHz, $CDCl_3$, DEPT): δ 71.9 (CH_2), 70.62 (CH_2), 70.59 (CH_2), 70.53 (CH_2), 68.9 (CH_2), 68.9 (CH_2), 68.4 (CH_2), 64.9 (CH_2), 63.1 (CH_2), 59.0 (CH_3), 57.1 – 56.9 (CH syndio), 56.1 – 55.9 (CH hetero), 55.2 – 54.9 (CH iso), 47.3 – 44.8 (family of CH_2 peaks).

IR (Neat): 2909 (s, alkane CH), 2877 (s, alkane CH), 1732 (s, ester C=O), 1551 (w, triazole C=C), 1435 (m, methylene stretch CH_2), 1254 (s, ester stretch C-O), 1200 (s, ester stretch C-O), 1106 (s, ether stretch C-O), 615 (w, C-Cl) cm^{-1}.

DSC (T_g): 27 °C.

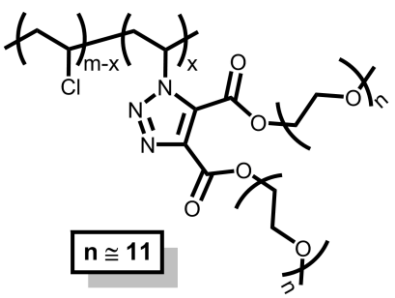

Preparation of 15% PVC-TRZ-DiPEO$_{550}$Me. Poly(vinyl chloride) 15% azide (1.000 g, 16.00 mmol) was added to a 100 mL round bottom flask and dissolved in 40 mL of 3-pentanone at 96 °C. 1,4-Bis-[methoxy poly(ethylene glycol) 550]-but-2-ynedioate (8.4816 g, 7.2 mmol) was added to the PVC solution and stirred for 48 h. The reaction was concentrated to approximately one-third its volume *in vacuo*. To a 250 mL beaker, 100 mL of MeOH was added, then placed in a dry ice-acetone bath for 2 min. The polymer was precipitated by dropwise addition of the reaction solution in 2 mL increments into the cooled MeOH. After the addition of reaction solution, the mother liquor was decanted and replaced with 100 mL of fresh MeOH. The beaker was cooled to -78 °C for 2 min, upon which another 2 mL of reaction solution was added dropwise. This process was repeated until the entire polymer was precipitated. When all of the reaction solution was precipitated, the last volume of mother

liquor was decanted. Subsequently, the neat polymer was cooled to -78 °C and washed with 50 mL of MeOH four times each. The isolated polymer was dried under house vacuum for 1 day, then in a vacuum oven at 40 °C for 3 days to yield 3.8272 g of a flexible orange solid.

^{1}H NMR (500 MHz, $CDCl_3$): δ 4.66 – 4.57 (br s, *Cl-C-H*), 4.56 – 4.50 (br s, *Cl-C-H* and *triazole-O-CH_2-C-O*), 4.49 – 4.43 (br m, *Cl-C-H* and *PVC-triazole-O-CH_2-C-O*), 4.37 – 4.28 (br m, *Cl-C-H* and *PVC-triazole-O-CH_2-C*), 3.91 – 3.78 (br m, *triazole-O-C-CH_2-O*), 3.77 – 3.60 (br m, *triazole-O-C-C-O-CH_2-CH_2-O-*), 3.59 – 3.55 (br m, *C-CH_2-O-CH_3*), 2.80 – 2.70 (br m, *Cl-C-CH_2-C-triazole* and *triazole-C-CH_2-C-triazole*), 2.50 – 1.85 (br m, *Cl-C-CH_2-C-Cl*).

^{13}C NMR (200 MHz, $CDCl_3$): δ 161.0 (C=O), 158.3 (C=O), 72.5 (CH_2), 71.9 (CH_2), 70.6 (CH_2), 68.9 (CH_2), 68.7 (CH_2), 68.4 (CH_2), 66.3 (CH_2), 66.1 (CH_2), 64.9 (CH_2), 63.1 (CH_2), 61.8 (CH_2), 59.0 (CH_3), 56.9 – 56.5 (CH syndio), 56.0 – 55.6 (CH hetero), 55.0 – 54.5 (CH iso), 47.3 – 44.7 (family of CH_2 peaks).

IR (Neat): 2873 (s, alkane CH), 1732 (s, ester C=O), 1540 (w, triazole C=C), 1452 (m, methylene stretch CH_2), 1253 (s, ester stretch C-O), 1201 (s, ester stretch C-O), 1105 (s, ether stretch C-O) cm^{-1}.

DSC (T_g): -29 °C.

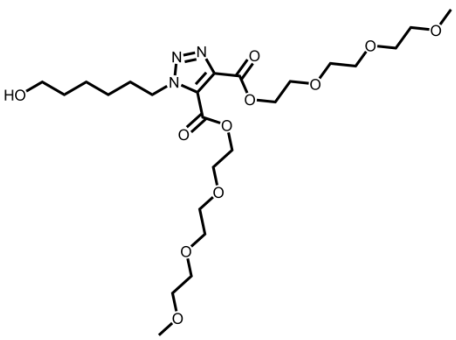

Preparation of 4,5-bis({2-[2-(2-methoxyethoxy)ethoxy]ethyl}) 1-(6-hydroxyhexyl)-1H-1,2,3-triazole-4,5-dicarboxylate. 6-Azidohexan-1-ol (1.0000 g, 6.983 mmol) was added to a 100 mL round bottom flask with 30 mL of $CHCl_3$. 1,4-Bis({2-[2-(2-methoxyethoxy)ethoxy]ethyl})but-2-ynedioate (3.4061 g, 8.381 mmol) was added to the reaction flask and stirred at 50 °C for 24 h. The volatiles were evaporated *in vacuo* affording a

colorless crude oil. Purification *via* flash chromatography using 95:5 CH_2Cl_2:MeOH afforded 2.8533 g (5.191 mmol, 74.34% yield) of the title compound as a colorless oil.

TLC: 95:5 CH_2Cl_2:MeOH, R_f=0.48, UV, $KMnO_4$ stain, *p*-anisealdehyde stain, dark blue spot.

^{1}H NMR (500 MHz, $CDCl_3$): δ 4.60 (t, *J* = 7.2 Hz, 2H), 4.55 (t, *J* = 4.5, 2H), 4.51 (t, *J* = 4.9 Hz, 2H), 3.82 (overlapping t, *J* = 4.8 Hz, 4H), 3.72 – 3.60 (m, 14H), 3.56 – 3.53 (m, 4H), 3.37 – 3.36 (m, 6H), 1.93 (p, *J* = 7.2 Hz, 2H), 1.69 (s, 1H), 1.56 (p, *J* = 6.7 Hz, 2H), 1.47 – 1.30 (m, 4H).

^{13}C NMR (125 MHz, $CDCl_3$, DEPT): δ 160.1 (C=O), 158.5 (C=O), 140.0 (4°), 130.1 (4°), 71.9 (CH_2), 70.7 (CH_2), 70.6 (CH_2), 70.6 (CH_2), 70.6 (CH_2), 70.5 (CH_2), 68.8 (CH_2), 68.5 (CH_2), 65.6 (CH_2), 64.8 (CH_2), 62.5 (CH_2), 59.0 (CH_3), 50.5 (CH_2), 32.4 (CH_2), 30.1 (CH_2), 26.0 (CH_2), 25.1 (CH_2).

IR (Neat): 3472 (s, OH), 2930 (s, alkane CH), 2874 (s, alkane CH), 1733 (s, ester C=O), 1552 (m, triazole C=C), 1468 (s, methylene bending CH_2), 1281 (s, ester stretch C-O), 1247 (s, ether stretch C-O), 1111 (s, ether stretch C-O), 1067 (s, 1° alcohol stretch C-O) cm^{-1}.

HRMS: Calcd. for $C_{24}H_{43}N_3O_{11}$ $[M+H]^+$ 550.2970; Found 550.2948.

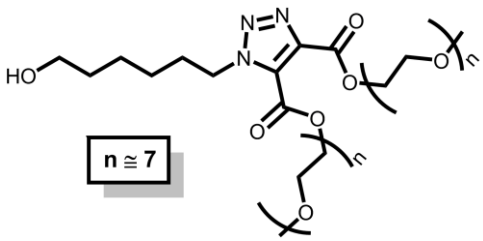

Preparation of 4,5-bis[methoxy poly(ethylene glycol) 350]-1-(6-hydroxyhexyl)-1H-1,2,3-triazole-4,5-dicarboxylate. 6-Azidohexan-1-ol (3.144 g, 21.958 mmol) was added to a 250 mL round bottom flask with 50 mL of $CHCl_3$. 1,4-Bis[methoxy poly(ethylene glycol) 350]-but-2-ynedioate (18.816 g, 24.154 mmol) was added to the reaction flask and stirred at 55 °C for 24 h. The volatiles were evaporated *in vacuo,* affording a pale yellow crude oil. Purification *via* flash chromatography using 93:7 CH_2Cl_2:MeOH afforded 17.473 g (18.947 mmol, 86.29% yield) of the title compound as a pale yellow oil.

TLC: 93:7 CH_2Cl_2:MeOH, R_f=0.48, UV, $KMnO_4$ stain, *p*-anisealdehyde stain, white spot.

^{1}H NMR (500 MHz, $CDCl_3$): δ 4.59 (t, *J* = 6.9 Hz, 2H), 4.54 (br s, 2H), 4.50 (br s, 2H), 3.81 (br s, 4H), 3.64 (br s, 50H), 3.55 (br s, 5H), 3.38 (br s, 6H), 1.98 – 1.87 (m, 2H), 1.55 (br s, 2H), 1.47 – 1.30 (m, 4H).

^{13}C NMR (125 MHz, $CDCl_3$, DEPT): δ 160.1 (C=O), 158.4 (C=O), 140.0 (4°), 130.1 (4°), 71.9 (CH_2), 70.7 (CH_2), 70.60 (CH_2), 70.56 (CH_2), 70.5 (CH_2), 68.7 (CH_2), 68.5 (CH_2), 65.6 (CH_2), 64.8 (CH_2), 62.4 (CH_2), 59.0 (CH_3), 50.5 (CH_2), 32.4 (CH_2), 30.1 (CH_2), 26.0 (CH_2), 25.1 (CH_2).

IR (Neat): 3501 (s, OH), 2873 (s, alkane CH), 1732 (s, ester C=O), 1552 (m, triazole C=C), 1470 (s, methylene bending CH_2), 1283 (s, ester stretch C-O), 1249 (s, ester stretch C-O), 1108 (s, ether stretch C-O) cm^{-1}.

HRMS: Calcd. for (n = 5,6) $C_{34}H_{63}N_3O_{16}$ $[M+H]^+$ 770.4281; Found 770.4272.

Calcd. for (n = 6,6) $C_{36}H_{67}N_3O_{17}$ $[M+H]^+$ 814.4543 Found 814.4531.

Calcd. for (n = 6,7) $C_{38}H_{72}N_3O_{18}$ $[M+H]^+$ 858.4805 Found 858.4791.

Calcd. for (n = 7,7) $C_{40}H_{75}N_3O_{19}$ $[M+H]^+$ 902.5068; Found 902.5054.

Calcd. for (n = 7,8) $C_{42}H_{79}N_3O_{20}$ $[M+H]^+$ 946.5330; Found 946.5315.

Calcd. for (n = 8,8) $C_{44}H_{83}N_3O_{21}$ $[M+H]^+$ 990.5592; Found 990.5573.

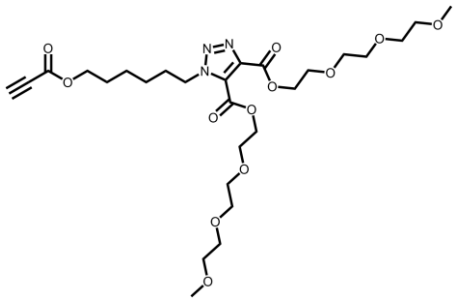

Preparation of 4,5-bis({2-[2-(2-methoxyethoxy)ethoxy]ethyl})-1-[6-(prop-2-ynoyloxy)hexyl]-1H-1,2,3-triazole-4,5-dicarboxylate. Propiolic acid (1.0000 g, 14.2755 mmol) was added to a 50 mL round bottom flask with 14 mL of toluene. 4,5-Bis({2-[2-(2-methoxyethoxy)ethoxy]ethyl})-1-(6-hydroxyhexyl)-1H-1,2,3-triazole-4,5-dicarboxylate (9.4152 g, 17.1306 mmol) and 4-methylbenzenesulfonic acid (0.2715 g, 1.4275 mmol) was added to the reaction flask and stirred at reflux for 3 h. The volatiles were evaporated *in vacuo*, affording a light brown crude oil. Purification *via* flash chromatography using 95:5 CH_2Cl_2:MeOH afforded 6.6122 g (10.9902 mmol, 76.99% yield) of the title compound as a colorless oil.

TLC: 95:5 CH_2Cl_2:MeOH, R_f=0.50, UV, $KMnO_4$ stain, *p*-anisealdehyde stain, blue-yellow spot.

^{1}H NMR (500 MHz, $CDCl_3$): δ 4.59 (t, *J* = 7.2 Hz, 2H), 4.54 (t, *J* = 4.8, 2H), 4.50 (t, *J* = 4.9 Hz, 2H), 4.18 (t, *J* = 6.5 Hz, 2H), 3.82 (overlapping t, *J* = 4.9 Hz, 4H), 3.72 – 3.60 (m, 12H), 3.57 – 3.49 (m, 4H), 3.37 (s, 3H), 3.36 (s, 3H), 2.93 (s, 1H), 1.93 (p, *J* = 7.2 Hz, 2H), 1.68 (p, *J* = 6.5 Hz, 2H), 1.45 – 1.34 (m, 4H).

^{13}C NMR (125 MHz, $CDCl_3$, DEPT): δ 160.1 (C=O), 158.4 (C=O), 152.7 (C=O), 140.0 (4°), 129.6 (4°), 74.7 (alkyne 4°), 74.6 (alkyne CH), 71.9 (CH_2), 70.7 (CH_2), 70.60 (CH_2), 70.56 (CH_2), 68.8 (CH_2), 68.5 (CH_2), 66.0 (CH_2), 65.6 (CH_2), 64.8 (CH_2), 59.0 (CH_3), 50.4 (CH_2), 30.0 (CH_2), 28.1 (CH_2), 25.9 (CH_2), 25.2 (CH_2).

IR (Neat): 3220 (m, alkyne CH), 2874 (s, alkane CH), 2114 (s, alkyne CC), 1732 (s, ester C=O), 1715 (s, ester C=O), 1552 (triazole C=C), 1469 (methylene bending CH_2), 1271 (m, ester stretch C-O), 1235 (s, ester stretch C-O), 1108 (s, ether stretch C-O) cm^{-1}.

HRMS: Calcd. for $C_{27}H_{43}N_3O_{12}$ $[M+H]^+$ 602.2920; Found 602.2917. $[M+Na]^+$ 624.2739; Found 624.2720.

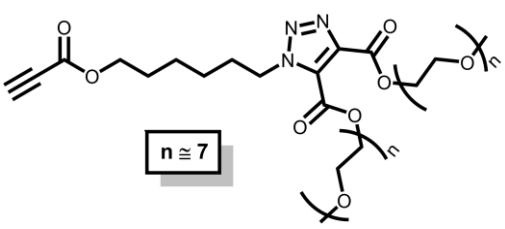

Preparation of 4,5-bis[methoxy poly(ethylene glycol) 350]-1-[6-(prop-2-ynoyloxy)hexyl]-1H-1,2,3-triazole-4,5-dicarboxylate. Propiolic acid (2.543 g, 36.3044 mmol) was added to a 100 mL round bottom flask with 30 mL of toluene. 4,5-Bis[methoxy poly(ethylene glycol) 350]-1-(6-hydroxyhexyl)-1H-1,2,3-triazole-4,5-dicarboxylate (11.160 g, 12.1015 mmol) and 0.15 mL H_2SO_4 was added to the reaction flask and stirred at reflux for 2 h. The volatiles were evaporated *in vacuo*, affording a light brown crude oil. Purification *via* flash chromatography using 95:5 CH_2Cl_2:MeOH afforded 7.073 g (7.2601 mmol, 59.97% yield) of the title compound as a pale yellow oil.

TLC: 95:5 CH_2Cl_2:MeOH, R_f=0.44, UV, $KMnO_4$ stain, *p*-anisealdehyde stain, blue-yellow spot.

^{1}H NMR (500 MHz, $CDCl_3$) δ 4.60 (t, *J* = 6.8 Hz, 2H), 4.55 (t, 2H), 4.51 (t, *J* = 4.2 Hz, 2H), 4.19 (t, *J* = 6.0 Hz, 2H), 3.85 – 3.81 (m, 4H), 3.68 – 3.63 (m, 50H), 3.57 – 3.54 (m, 4H), 3.39 (bs, 6H), 2.96 (s, 1H), 1.94 (p, *J* = 7.0 Hz, 2H), 1.69 (p, *J* = 6.7 Hz, 2H), 1.48 – 1.34 (m, 4H).

^{13}C NMR (125 MHz, $CDCl_3$, DEPT): δ 160.1 (C=O), 158.4 (C=O), 152.7 (C=O), 140.0 (4°), 130.0 (4°), 74.7 (alkyne 4°), 74.6 (alkyne CH), 71.9 (CH_2), 70.72 (CH_2), 70.67 (CH_2), 70.61 (CH_2), 70.58 (CH_2), 70.5 (CH_2), 68.8 (CH_2), 68.6 (CH_2), 68.5 (CH_2), 66.0 (CH_2), 65.6 (CH_2), 65.2 (CH_2), 64.8 (CH_2), 59.0 (CH_3), 50.4 (CH_2), 30.0 (CH_2), 28.1 (CH_2), 25.9 (CH_2), 25.2 (CH_2).

IR (Neat): 3214 (s, alkyne CH), 2873 (s, alkane CH), 2112 (s, alkyne CC), 1715 (s, ester C=O), 1551 (m, triazole C=C), 1467 (s, methylene bending CH_2), 1236 (s, ester stretch C-O), 1108 (s, ether stretch C-O) cm^{-1}.

HRMS: Calcd. for (n = 5,5) $C_{35}H_{59}N_3O_{16}$ $[M+H]^+$ 778.3968; Found 778.3958.

Calcd. for (n = 5,6) $C_{37}H_{63}N_3O_{17}$ $[M+H]^+$ 822.4230; Found 822.4221.

Calcd. for (n = 6,6) $C_{39}H_{67}N_3O_{18}$ $[M+H]^+$ 866.4492; Found 866.4481.

Calcd. for (n = 6,7) $C_{41}H_{71}N_3O_{19}$ $[M+H]^+$ 910.4755; Found 910.4741.

Calcd. for (n = 7,7) $C_{43}H_{75}N_3O_{20}$ $[M+H]^+$ 954.5017; Found 954.5000.

Calcd. for (n = 7,8) $C_{45}H_{79}N_3O_{21}$ $[M+H]^+$ 998.5279; Found 998.5264.

Calcd. for (n = 8,8) $C_{47}H_{83}N_3O_{22}$ $[M+H]^+$ 1042.5541; Found 1042.5521.

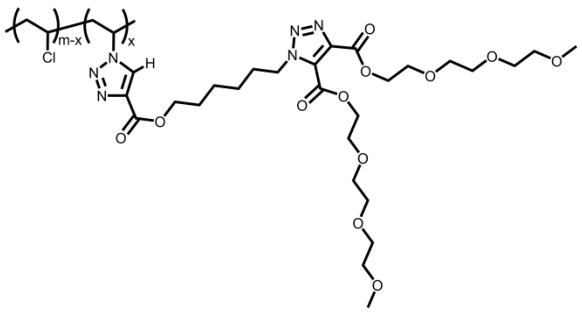

Preparation of 5% PVC-TRZ-Hexyl-TRZ-DiPEO$_{164}$Me. Poly(vinyl chloride) 5% azide (1.000 g, 16.00 mmol) was added to a 100 mL round bottom flask and dissolved in 30 mL of 3-pentanone at 90 °C. 4,5-Bis({2-[2-(2-methoxyethoxy)ethoxy]ethyl})-1-[6-(prop-2-ynoyloxy)hexyl]-1H-1,2,3-triazole-4,5-dicarboxylate (1.203 g, 2.0 mmol) was added to the PVC solution and stirred for 24 h. The reaction was concentrated to approximately half its volume *in vacuo*, then precipitated in 80 mL of MeOH, three times each. The isolated polymer was dried under house vacuum for 1 day, then in a vacuum oven at 40 °C for 2 days to yield 0.9573 g of a flocculent white solid.

^{1}H NMR (500 MHz, $CDCl_3$): δ 8.32 – 8.22 (br s, *PVC-triazole-H*), 8.18 – 8.14 (br m, *PVC-triazole-H*), 8.11 – 8.07 (br m, *PVC-triazole-H*), 5.32 – 5.17 (br m, *C-CH-triazole*), 4.67 – 4.57 (br m, *Cl-C-H* and *PVC-linker-C-CH$_2$-triazole*), 4.54 – 4.50 (br m, *Cl-C-H* and *PVC-triazole-O-CH$_2$-linker*), 4.50 – 4.41 (br m, *Cl-C-H*), 4.40 – 4.24 (br m, *Cl-C-H*), 3.87 – 3.80 (br m, *triazole-O-C-CH$_2$-O*), 3.73 – 3.61 (br m, *triazole-O-C-C-O-CH$_2$-CH$_2$-O-CH$_2$-C*), 3.58 – 3.52 (br m, *C-*

C<u>H₂</u>-O-CH₃), 3.384 (br s, *O-C<u>H₃</u>*), 3.377 (br s, *O-C<u>H₃</u>*), 2.87 – 2.78 (br m, *Cl-C-C<u>H₂</u>-C-triazole* and *triazole-C-C<u>H₂</u>-C-triazole*), 2.78 – 2.60 (br m, *Cl-C-C<u>H₂</u>-C-triazole* and *triazole-C-C<u>H₂</u>-C-triazole*), 2.50 – 1.99 (br m, *Cl-C-C<u>H₂</u>-C-Cl*), 1.86 – 1.75 (br m, *PVC-linker-C<u>H₂</u>-C-triazole*), 1.72 – 1.60 (br s, *PVC-triazole-O-C-C<u>H₂</u>-linker*), 1.56 – 1.34 (br m, *linker C<u>H₂</u>'s*).

^{13}C NMR (125 MHz, $CDCl_3$, DEPT): δ 160.1 (C=O), 158.4 (C=O), 140.0 (4°), 71.9 (CH_2), 70.67 (CH_2), 70.61 (CH_2), 70.57 (CH_2), 68.7 (CH_2), 68.5 (CH_2), 66.2 (CH_2), 65.6 (CH_2), 64.8 (CH_2), 59.0 (CH_3), 57.0 – 56.9 (CH syndio), 56.1 – 55.9 (CH hetero), 55.2 – 54.9 (CH iso), 50.5 (CH_2), 47.3 – 44.8 (family of CH_2 peaks), 30.0 (CH_2), 28.4 (CH_2), 26.0 (CH_2), 25.4 (CH_2).

IR (Neat): 3140 (w, triazole CH), 2973 (s, alkane CH), 2937 (s, alkane CH), 2911 (s, alkane CH), 1734 (s, ester C=O), 1551 (m, triazole C=C), 1459 (s, methylene stretch CH_2), 1435 (s, methyl stretch CH), 1254 (s, ester stretch C-O), 1201 (s, ester stretch C-O), 1121 (s, ether stretch C-O), 615 (w, C-Cl) cm^{-1}.

DSC (T_g): 57 °C.

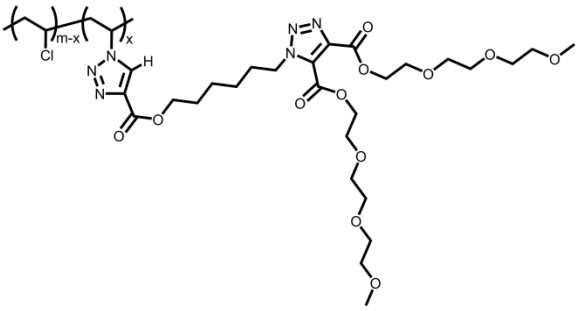

Preparation of 15% PVC-TRZ-Hexyl-TRZ-DiPEO$_{164}$Me. Poly(vinyl chloride) 15% azide (1.000 g, 16.00 mmol) was added to a 100 mL round bottom flask and dissolved in 30 mL of 3-pentanone at 90 °C. 4,5-Bis({2-[2-(2-methoxyethoxy)ethoxy]ethyl})-1-[6-(prop-2-ynoyloxy)hexyl]-1H-1,2,3-triazole-4,5-dicarboxylate (3.6098 g, 6.0 mmol) was added to the PVC solution and stirred for 24 h. The reaction was concentrated to approximately half its volume *in vacuo*, then precipitated in 80 mL of MeOH, three times each. The isolated polymer was dried under house vacuum for 1 day, then in a vacuum oven at 40 °C for 2 days to yield in a vacuum oven at 40 °C for 3 days to yield 1.9197 g of a white solid.

^{1}H NMR (500 MHz, $CDCl_3$): δ 8.35 – 8.05 (br m, *PVC-triazole-H*), 5.32 – 5.12 (br m, *C-CH-triazole*), 4.70 – 4.59 (br m, *Cl-C-H* and *PVC-linker-C-CH_2-triazole*), 4.58 – 4.54 (br s, *Cl-C-H* and *triazole-O-CH_2-C-O*), 4.54 – 4.50 (br m, *Cl-C-H* and *triazole-O-CH_2-C-O*), 4.49 – 4.42 (br s, *Cl-C-H*), 4.41 – 4.26 (br m, *Cl-C-H* and *PVC-triazole-O-CH_2-linker*), 3.90 – 3.81 (br m, *triazole-O-C-CH_2-O*), 3.73 – 3.62 (br m, *triazole-O-C-C-O-CH_2-CH_2-O-CH_2-C*), 3.58 – 3.53 (br m, *C-CH_2-O-CH_3*), 3.39 (br s, *O-CH_3*), 3.38 (br s, *O-CH_3*), 2.87 – 2.79 (br s, *Cl-C-CH_2-C-triazole* and *triazole-C-CH_2-C-triazole*), 2.78 – 2.61 (br m, *Cl-C-CH_2-C-triazole* and *triazole-C-CH_2-C-triazole*), 2.51 – 2.00 (br m, *Cl-C-CH_2-C-Cl*), 1.86 – 1.72 (br m, *PVC-linker-CH_2-C-triazole*), 1.72 – 1.62 (br s, *PVC-triazole-O-C-CH_2-linker*), 1.56 – 1.33 (br m, *linker CH_2's*).

^{13}C NMR (200 MHz, $CDCl_3$): δ 160.2 (C=O), 158.4 (C=O), 71.9 (CH_2), 70.67 (CH_2), 70.61 (CH_2), 70.57 (CH_2), 68.8 (CH_2), 68.5 (CH_2), 65.7 (CH_2), 64.8 (CH_2), 59.0 (CH_3), 57.0 – 56.9 (CH syndio), 50.5 (CH_2), 47.3 – 44.8 (family of CH_2 peaks), 30.0 (CH_2), 28.4 (CH_2), 26.0 (CH_2), 25.4 (CH_2).

IR (Neat): 3137 (w, triazole CH), 2936 (s, alkane CH), 2874 (s, alkane CH), 1733 (s, ester C=O), 1551 (m, triazole C=C), 1466 (s, methylene stretch CH_2), 1438 (s, methyl stretch CH), 1247 (s, ester stretch C-O), 1203 (s, ester stretch C-O), 1121 (s, ether stretch C-O), 615 (w, C-Cl) cm^{-1}.

DSC (T_g): 18 °C.

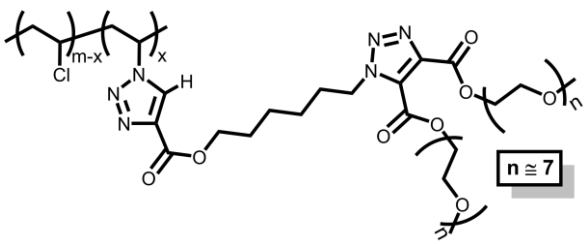

Preparation of 5% PVC-TRZ-Hexyl-TRZ-DiPEO$_{350}$Me. Poly(vinyl chloride) 5% azide (1.000 g, 16.00 mmol) was added to a 100 mL round bottom flask and dissolved in 15 mL of 3-pentanone at 90 °C. 4,5-Bis[methoxy poly(ethylene glycol) 350]-1-[6-(prop-2-ynoyloxy)hexyl]-1H-1,2,3-triazole-4,5-dicarboxylate (2.3381 g, 2.4 mmol) was added to the PVC solution and stirred for 24 h. The reaction was concentrated to

approximately one-third its volume *in vacuo* then precipitated once in 80 mL of MeOH. The crude polymer was dissolved in 15 mL of 3-pentaone and 4,5-Bis[methoxy poly(ethylene glycol) 350]-1-[6-(prop-2-ynoyloxy)hexyl]-1H-1,2,3-triazole-4,5-dicarboxylate (2.3381 g, 2.4 mmol) was added to the solution and stirred for 24 h. The reaction was once again concentrated to approximately one-third its volume *in vacuo* then precipitated once in 80 mL of MeOH, two times each. The isolated polymer was dried under house vacuum for 1 day, then in a vacuum oven at 40 °C for 2 days to yield 0.6447 of a white solid.

^{1}H NMR (500 MHz, $CDCl_3$): δ 8.37 – 8.21 (br m, *PVC-triazole-H*), 8.21 – 8.16 (br s, *PVC-triazole-H*), 8.16 – 8.08 (br s, *PVC-triazole-H*), 5.32 – 5.16 (br m, *C-CH-triazole*), 4.67 – 4.55 (br m, *Cl-C-H* and *PVC-linker-C-CH_2-triazole*), 4.55 – 4.40 (br m, *Cl-C-H* and *PVC-triazole-O-CH_2-linker*), 4.40 – 4.25 (br m, *Cl-C-H*), 3.92 – 3.80 (br m, *triazole-O-C-CH_2-O*), 3.73 – 3.60 (br s, *triazole-O-C-C-O-CH_2-CH_2-O-*), 3.58 – 3.55 (br m, *C-CH_2-O-CH_3*), 3.42 – 3.37 (br s, *O-CH_3*), 2.92 – 2.65 (br m, *Cl-C-CH_2-C-triazole* and *triazole-C-CH_2-C-triazole*), 2.50 – 1.90 (br m, *Cl-C-CH_2-C-Cl*), 1.86 – 1.74 (br s, *PVC-linker-CH_2-C-triazole*), 1.74 – 1.60 (br s, *PVC-triazole-O-C-CH_2-linker*), 1.56 – 1.34 (br m, *linker CH_2's*).

^{13}C NMR (125 MHz, $CDCl_3$, DEPT): δ 71.9 (CH_2), 70.6 (CH_2), 66.2 (CH_2), 66.0 (CH_2), 65.6 (CH_2), 64.3 (CH_2), 63.8 (CH_2), 59.0 (CH_3), 57.0 – 56.9 (CH syndio), 56.1 – 55.9 (CH hetero), 55.2 – 54.9 (CH iso), 50.5 (CH_2), 47.3 – 44.8 (family of CH_2 peaks).

IR (Neat): 3129 (w, triazole CH), 2975 (s, alkane CH), 2938 (s, alkane CH), 2911 (s, alkane CH), 1714 (s, ester C=O), 1548 (w, triazole C=C), 1459 (s, methylene stretch CH_2), 1435 (s, methyl stretch CH), 1283 (s, ester stretch C-O), 1198 (s, ester stretch C-O), 1108 (s, ether stretch C-O), 615 (w, C-Cl) cm^{-1}.

DSC (T_g): 71 °C.

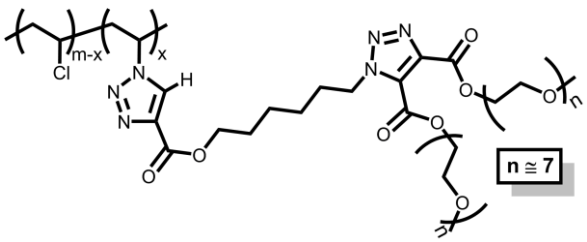

Preparation of 15% PVC-TRZ-Hexyl-TRZ-DiPEO$_{350}$Me. Poly(vinyl chloride) 15% azide (1.000 g, 16.00 mmol) was added to a 100 mL round bottom flask and dissolved in 35 mL of 3-pentanone at 96 °C. 4,5-Bis[methoxy poly(ethylene glycol) 350]-1-[6-(prop-2-ynoyloxy)hexyl]-1H-1,2,3-triazole-4,5-dicarboxylate (7.014 g, 7.2 mmol) was added to the PVC solution and stirred for 24 h. The reaction was concentrated to approximately one-third its volume *in vacuo*. To a 250 mL beaker, 100 mL of MeOH was added, then placed in a dry ice-acetone bath for 2 min. The polymer was precipitated by dropwise addition of the reaction solution in 2 mL increments into the cooled MeOH. After the addition of reaction solution, the mother liquor was decanted and replaced with 100 mL of fresh MeOH. The beaker was cooled to -78 °C for 2 min, upon which another 2 mL of reaction solution was added dropwise. This process was repeated until the entire polymer was precipitated. When all of the reaction solution was precipitated, the last volume of mother liquor was decanted. Subsequently, the neat polymer was cooled to -78 °C and washed with 50 mL of MeOH four times each. The isolated polymer was dried under house vacuum for 1 day, then in a vacuum oven at 40 °C for 3 days to yield 2.3169 g of a flexible orange solid.

^{1}H NMR (500 MHz, $CDCl_3$): δ 8.29 – 8.24 (br m, *PVC-triazole-H*), 8.20 – 8.15 (br s, *PVC-triazole-H*), 8.13 – 8.06 (br m, *PVC-triazole-H*), 5.40 – 5.10 (br m, *C-CH-triazole*), 4.70 – 4.57 (br m, *Cl-C-H* and *PVC-linker-C-CH$_2$-triazole*), 4.57 – 4.54 (br s, *Cl-C-H* and *PVC-triazole-O-CH$_2$-linker*), 4.54 – 4.41 (br m, *Cl-C-H*), 4.40 – 4.25 (br m, *PVC-triazole-O-CH$_2$-linker*), 4.25 – 4.10 (br m, *Cl-C-H*), 3.92 – 3.80 (br m, *triazole-O-C-CH$_2$-O*), 3.77 – 3.59 (br m, *triazole-O-C-C-O-CH$_2$-CH$_2$-O-CH$_2$-C*), 3.59 – 3.55 (br t, *C-CH$_2$-O-CH$_3$*), 3.41 – 3.38 (br s, *O-CH$_3$*), 2.87 – 2.60 (br m, *Cl-C-CH$_2$-C-triazole* and *triazole-C-CH$_2$-C-triazole*), 2.50 – 2.01 (br m, *Cl-C-CH$_2$-C-Cl*), 2.01– 1.85 (br s, *PVC-linker-CH$_2$-C-triazole*), 1.75 – 1.60 (br s, *PVC-triazole-O-C-CH$_2$-linker*), 1.56 – 1.34 (br m, *linker CH$_2$'s*).

^{13}C NMR (200 MHz, $CDCl_3$): δ 161.0 (C=O), 160.1 (C=O), 158.4 (C=O), 140.1 (4°), 129.9 (4°), 71.9 (CH_2), 70.6 (CH_2), 68.9 (CH_2), 68.8 (CH_2), 68.5 (CH_2), 65.6 (CH_2), 64.8 (CH_2), 59.0 (CH_3), 56.9 (CH syndio), 55.9 (CH hetero), 55.0 – 54.9 (CH iso), 50.5 (CH_2), 47.3 – 44.8 (family of CH_2 peaks), 30.0 (CH_2), 29.7 (CH_2), 28.3 (CH_2), 26.01 (CH_2), 25.92 (CH_2), 25.35 (CH_2), 25.28 (CH_2).

IR (Neat): 3133 (w, triazole CH), 2878 (s, alkane CH), 1732 (s, ester C=O), 1552 (w, triazole C=C), 1456 (m, methylene stretch CH_2), 1253 (s, ester stretch C-O), 1201 (s, ester stretch C-O), 1105 (s, ether stretch C-O) cm^{-1}.

DSC (T_g): -1 °C.

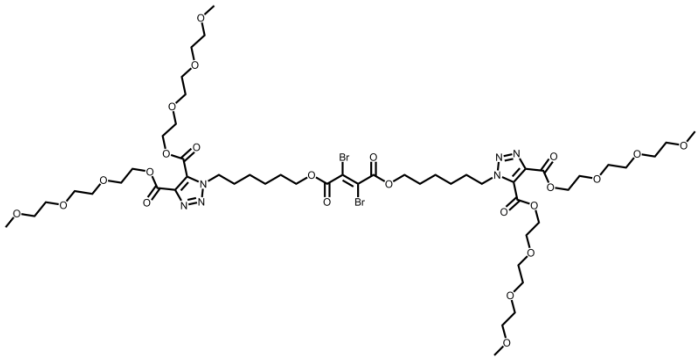

Preparation of 4,5-bis({2-[2-(2-methoxyethoxy)ethoxy]ethyl}) 1-(6-{[(2E)-4-({6-[bis(2,5,8,11-tetraoxadodecanoyl)-1H-1,2,3-triazol-1-yl]hexyl}oxy)-2,3-dibromo-4-oxobut-2-enoyl]oxy}hexyl)-1H-1,2,3-triazole-4,5-dicarboxylate.[4-5] Dibromofumaric acid (1.5000 g, 5.4765 mmol) and PCl_5 (2.394 g, 11.5007 mmol) was added to a 25 mL round bottom flask with 5 mL of pentane. The reaction was refluxed for 2 h while stirring. Reaction completeness was determined by observing the dissolution of solids into a clear yellow solution. After the dissolution of solids was noted, the reaction was immediately diluted with 5 mL of pentane. The diluted reaction was added slowly to a 150 mL beaker of crescent-cube ice, and was allowed to stand for 10 min with occasional swirling. The quenched reaction solution was transferred to a 150 mL separatory funnel. The organic layer was collected and dried with Na_2SO_4. The volatiles were evaporated *in vacuo* affording a clear yellow oil (1.701 g, 5.4765 mmol, quantitative yield) of (2E)-dibromobut-2-enedioyl dichloride. The acid chloride was

immediately diluted with 30 mL of CCl_4 under N_2 in a 250 mL pear flask. Next, 4,5-bis({2-[2-(2-methoxyethoxy)ethoxy]ethyl})-1-(6-hydroxyhexyl)-1H-1,2,3-triazole-4,5-dicarboxylate (6.3208 g, 11.5007 mmol) and pyridine (0.9097 g, 11.5007 mmol) were added to a 250 mL round bottom flask with 60 mL of CCl_4 and cooled to 0 °C under N_2 with stirring. The acid chloride solution was slowly added *via* syringe over 10 min, noting a light-yellow color and the formation of pyridine salts in solution. After the addition of the acid chloride, the reaction was allowed to stir at 0 °C for 2 hours, then at room temperature for an additional 22 hours. The reaction was poured into a 500 mL separatory funnel and washed with 20 mL 5% aqueous HCl two times each. The organic layer was collected, dried with $MgSO_4$ and filtered. The volatiles were then evaporated *in vacuo*. Purification *via* flash chromatography using 95:5 CH_2Cl_2:MeOH was performed, affording 5.2615 g (3.9350 mmol, 71.85% yield) of the title compound as a colorless oil.

TLC: 95:5 CH_2Cl_2:MeOH, R_f=0.47, UV, *p*-anisealdehyde stain, blue spot.

^{1}H NMR (500 MHz, Benzene-d_6): δ 4.36 (t, *J* = 4.9, 4H), 4.30 (t, 4H), 4.11 (t, *J* = 7.3 Hz, 4H), 3.91 (t, *J* = 6.5 Hz, 4H), 3.50 – 3.45 (m, 8H), 3.45 – 3.39 (m, 24H), 3.36 – 3.30 (m, 8H), 3.13 (s, 6H), 3.12 (s, 6H), 1.49 (p, *J* = 7.4 Hz, 4H), 1.22 (p, *J* = 6.6 Hz, 4H), 1.00 – 0.84 (m, 8H).

^{13}C NMR (125 MHz, Benzene-d_6, DEPT): δ 162.0 (C=O), 160.6 (C=O), 158.5 (C=O), 141.0 (4°), 129.5 (4°), 112.9 (C-Br), 72.0 (CH_2), 71.98 (CH_2), 70.63 (CH_2), 70.59 (CH_2), 70.51 (CH_2), 70.50 (CH_2), 70.47 (CH_2), 68.7 (CH_2), 68.3 (CH_2), 66.7 (CH_2), 65.3 (CH_2), 64.7 (CH_2), 58.3 (CH_3), 49.7 (CH_2), 29.6 (CH_2), 27.8 (CH_2), 25.5 (CH_2), 24.9 (CH_2).

IR (Neat): 2874 (s, alkane CH), 1733 (s, ester C=O), 1552 (m, triazole C=C), 1468 (methylene bending CH_2), 1270 (s, ester stretch C-O), 1242 (s, ester stretch C-O), 1111 (s, ether stretch C-O), 755 (m, alkene bending C=C) cm^{-1}.

HRMS: Calcd. for $C_{52}H_{84}Br_2N_6O_{24}$ $[M+H]^+$ 1335.3976; Found 1335.3981.

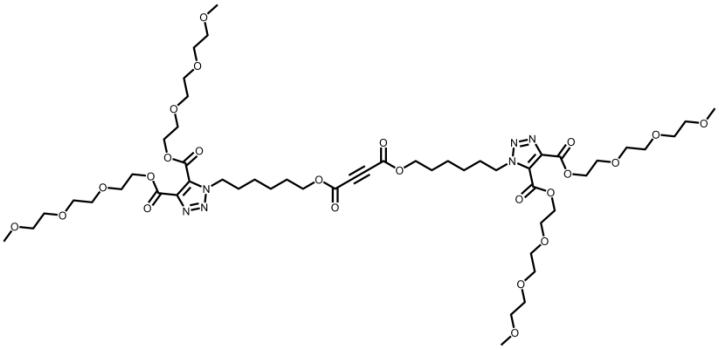

Preparation of 4,5-bis({2-[2-(2-methoxyethoxy)ethoxy]ethyl }) 1-(6-{[4-({6-[bis(2,5,8,11-tetraoxadodecanoyl)-1H-1,2,3-triazol-1-yl]hexyl}oxy)-4-oxobut-2-ynoyl]oxy}hexyl)-1H-1,2,3-triazole-4,5-dicarboxylate.[6] To a 250 mL round bottom flask, 4,5-bis({2-[2-(2-methoxyethoxy)ethoxy]ethyl}) 1-(6-{[(2E)-4-({6-[bis(2,5,8,11-tetraoxadodecanoyl)-1H-1,2,3-triazol-1-yl]hexyl}oxy)-2,3-dibromo-4-oxobut-2-enoyl]oxy}hexyl)-1H-1,2,3-triazole-4,5-dicarboxylate (5.2210 g, 3.9048 mmol) was added to 40 mL of anhydrous THF. Subsequently, Zn metal (1.5317 g, 23.4288 mmol) and I_2 (0.0471 g, 0.1857 mmol) were added and stirred at reflux for 5 h under N_2. The reaction was cooled and filtered through CELITE^{TM}. The reaction was concentrated *in vacuo* and diluted with 80 mL of ethyl acetate. The solution was poured into a 500 mL separatory funnel and washed with 10 mL of 10% aqueous $Na_2S_2O_3$, two times each. The organic layer was collected and dried with $MgSO_4$. The volatiles were then evaporated *in vacuo*, and immediately purified *via* flash chromatography using 95:5 CH_2Cl_2:MeOH, affording 3.8523 g (3.2723 mmol, 83.80% yield) of the title compound as a pale yellow oil.

TLC: 95:5 CH_2Cl_2:MeOH, R_f=0.47, UV, $KMnO_4$ stain, *p*-anisealdehyde stain, blue spot.

^{1}H NMR (500 MHz, Benzene-d_6) δ 4.36 (t, *J* = 4.9 Hz, 4H), 4.31 (t, *J* = 4.8 Hz, 4H), 4.09 (t, *J* = 7.3 Hz, 4H), 3.76 (t, *J* = 6.6 Hz, 4H), 3.47 (t, *J* = 4.9 Hz, 8H), 3.45 – 3.39 (m, 24H), 3.35 – 3.30 (m, 8H), 3.13 (s, 6H), 3.12 (s, 6H), 1.45 (p, *J* = 7.2 Hz, 4H), 1.10 (p, *J* = 6.7 Hz, 4H), 0.87 – 0.80 (m, 8H).

^{13}C-NMR (125 MHz, Benzene-d_6, DEPT): δ 160.6 (C=O), 158.5 (C=O), 151.6 (C=O), 140.9 (4°), 129.5 (4°), 74.9 (alkyne 4°), 72.0 (CH_2), 70.6 (CH_2), 70.6 (CH_2), 70.49 (CH_2), 70.48

(CH_2), 70.46 (CH_2), 68.7 (CH_2), 68.3 (CH_2), 66.3 (CH_2), 65.3 (CH_2), 64.7 (CH_2), 58.3 (CH_3), 49.7 (CH_2), 29.6 (CH_2), 27.7 (CH_2), 25.5 (CH_2), 24.7 (CH_2).

IR (Neat): 2874 (s, alkane CH), 1727 (s, ester C=O), 1552 (m, triazole C=C), 1469 (s, methylene bending CH_2), 1259 (s, ester stretch C-O), 1110 (s, ether stretch C-O) cm^{-1}.

HRMS: Calcd. for $C_{52}H_{84}N_6O_{24}$ $[M+H]^+$ 1177.5610; Found 1177.5616. $[M+Na]^+$ 1199.5429; Found 1199.5411.

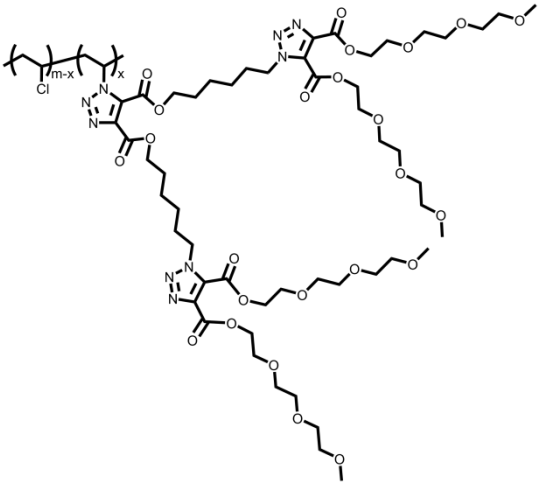

Preparation of 5% PVC-TRZ-DiHexyl-TRZ-DiPEO$_{164}$Me. Poly(vinyl chloride) 5% azide (1.000 g, 16.00 mmol) was added to a 100 mL round bottom flask and dissolved in 30 mL of 3-pentanone at 90 °C. 4,5-Bis({2-[2-(2-methoxyethoxy)ethoxy]ethyl}) 1-(6-{[4-({6-[bis(2,5,8,11-tetraoxadodecanoyl)-1H-1,2,3-triazol-1-yl]hexyl}oxy)-4-oxobut-2-ynoyl]oxy}hexyl)-1H-1,2,3-triazole-4,5-dicarboxylate (2.8253g, 2.4 mmol) was added to the PVC solution and stirred for 24 h. The reaction was concentrated to approximately half its volume *in vacuo*, then precipitated in 80 mL of MeOH, three times each. The isolated polymer was dried under house vacuum for 1 day, then in a vacuum oven at 40 °C for 2 days to yield 1.5201 g of a white solid.

^{1}H NMR (500 MHz, $CDCl_3$): δ 5.65 – 5.45 (br m, *C-C<u>H</u>-triazole*), 4.67 – 4.58 (br m, *Cl-C-<u>H</u>* and *PVC-linker-C-C<u>H$_2$</u>-triazole*), 4.57 – 4.54 (br s, *Cl-C-<u>H</u>* and *triazole-O-C<u>H$_2$</u>-C-O*), 4.54 – 4.50 (br m, *triazole-O-C<u>H$_2$</u>-C-O*), 4.50 – 4.41 (br s, *Cl-C-<u>H</u>*), 4.40 – 4.34 (br m, *PVC-triazole-O-C<u>H$_2$</u>-linker*), 4.34 – 4.25 (br m, *Cl-C-<u>H</u>*), 3.87 – 3.81 (br m, *triazole-O-C-C<u>H$_2$</u>-O*), 3.73 – 3.62 (br m, *triazole-O-C-C-O-C<u>H$_2$</u>-C<u>H$_2$</u>-O-C<u>H$_2$</u>-C*), 3.58 – 3.52 (br m, *C-C<u>H$_2$</u>-O-CH$_3$*), 3.39 (br s, *O-C<u>H$_3$</u>*), 3.38 (br s, *O-C<u>H$_3$</u>*), 2.92 – 2.82 (br m, *Cl-C-C<u>H$_2$</u>-C-triazole* and *triazole-C-C<u>H$_2$</u>-C-*

triazole), 2.82 – 2.68 (br s, *Cl-C-C<u>H₂</u>-C-triazole* and *triazole-C-C<u>H₂</u>-C-triazole*), 2.50 – 1.99 (br m, *Cl-C-C<u>H₂</u>-C-Cl*), 1.85 – 1.75 (br m, *PVC-linker-C<u>H₂</u>-C-triazole*), 1.72 – 1.60 (br s, *PVC-triazole-O-C-C<u>H₂</u>-linker*), 1.55 – 1.33 (br m, *linker C<u>H₂</u>'s*).

^{13}C NMR (125 MHz, $CDCl_3$, DEPT): δ 160.1 (C=O), 158.4 (C=O), 145.5 (4°), 71.9 (CH_2), 70.67 (CH_2), 70.61 (CH_2), 70.57 (CH_2), 68.7 (CH_2), 68.5 (CH_2), 65.6 (CH_2), 64.8 (CH_2), 59.0 (CH_3), 57.0 – 56.9 (CH syndio), 56.1 – 55.9 (CH hetero), 50.5 (CH_2), 47.3 – 44.9 (family of CH_2 peaks), 30.0 (CH_2), 28.4 (CH_2), 27.2 (CH_2), 27.0 (CH_2).

IR (Neat): 2934 (s, alkane CH), 2875 (s, alkane CH), 1733 (s, ester C=O), 1552 (m, triazole C=C), 1467 (s, methylene stretch CH_2), 1271 (s, ester stretch C-O), 1202 (s, ester stretch C-O), 1111 (s, ether stretch C-O), 615 (w, C-Cl) cm^{-1}.

DSC (T_g): 24 °C.

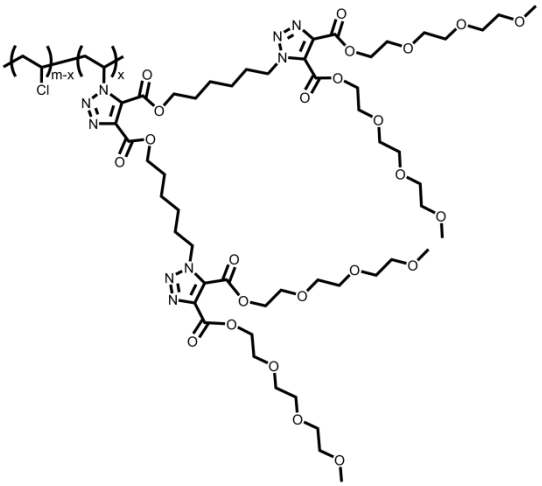

Preparation of 15% PVC-TRZ-DiHexyl-TRZ-DiPEO$_{164}$Me. Poly(vinyl chloride) 15% azide (1.000 g, 16.00 mmol) was added to a 100 mL round bottom flask and dissolved in 30 mL of 3-pentanone at 90 °C. 4,5-Bis({2-[2-(2-methoxyethoxy)ethoxy]ethyl}) 1-(6-{[4-({6-[bis(2,5,8,11-tetraoxadodecanoyl)-1H-1,2,3-triazol-1-yl]hexyl}oxy)-4-oxobut-2-ynoyl]oxy}hexyl)-1H-1,2,3-triazole-4,5-dicarboxylate (7.063 g, 6.0 mmol) was added to the PVC solution and stirred for 24 h. The reaction was concentrated to approximately one-third its volume *in vacuo*. To a 250 mL beaker, 100 mL of MeOH was added, then placed in a dry ice-acetone bath for 2 min. The polymer was precipitated by dropwise addition of the reaction solution in 2 mL increments into the cooled MeOH. After the addition of reaction solution, the mother liquor was decanted and replaced with 100 mL of fresh MeOH. The beaker was

cooled to -78 °C for 2 min, upon which another 2 mL of reaction solution was added dropwise. This process was repeated until the entire polymer was precipitated. When all of the reaction solution was precipitated, the last volume of mother liquor was decanted. Subsequently, the neat polymer was cooled to -78 °C and washed with 50 mL of MeOH four times each. The isolated polymer was dried under house vacuum for 1 day, then in a vacuum oven at 40 °C for 3 days to yield 3.3816 g of a flexible pale yellow solid.

^{1}H NMR (500 MHz, $CDCl_3$): δ 5.65 – 5.35 (br m, *C-C<u>H</u>-triazole*), 4.67 – 4.58 (br s, *Cl-C-<u>H</u>* and *PVC-linker-C-C<u>H$_2$</u>-triazole*), 4.58 – 4.54 (br s, *Cl-C-<u>H</u>* and *triazole-O-C<u>H$_2$</u>-C-O*), 4.54 – 4.48 (br m, *Cl-C-<u>H</u>* and *triazole-O-C<u>H$_2$</u>-C-O*), 4.39 – 4.24 (br m, *Cl-C-<u>H</u>* and *PVC-triazole-O-C<u>H$_2$</u>-linker*), 3.88 – 3.78 (br m, *triazole-O-C-C<u>H$_2$</u>-O*), 3.75 – 3.60 (br m, *triazole-O-C-C-O-C<u>H$_2$</u>-C<u>H$_2$</u>-O-C<u>H$_2$</u>-C*), 3.59 – 3.48 (br m, *C-C<u>H$_2$</u>-O-CH$_3$*), 3.43 – 3.31 (br s, *O-C<u>H$_3$</u>*), 2.90 – 2.80 (br s, *Cl-C-C<u>H$_2$</u>-C-triazole* and *triazole-C-C<u>H$_2$</u>-C-triazole*), 2.80 – 2.53 (br m, *Cl-C-C<u>H$_2$</u>-C-triazole* and *triazole-C-C<u>H$_2$</u>-C-triazole*), 2.50 – 1.90 (br m, *Cl-C-C<u>H$_2$</u>-C-Cl*), 1.89 – 1.60 (br m, *PVC-linker-C<u>H$_2$</u>-C-triazole* and *PVC-triazole-O-C-C<u>H$_2$</u>-linker*), 1.57 – 1.30 (br m, *linker C<u>H$_2$</u>'s*).

^{13}C NMR (200 MHz, $CDCl_3$): δ 160.1 (C=O), 158.4 (C=O), 140.0 (4°), 129.9 (4°), 129.5 (4°), 71.9 (CH_2), 70.67 (CH_2), 70.60 (CH_2), 70.56 (CH_2), 68.8 (CH_2), 68.5 (CH_2), 66.2 (CH_2), 65.6 (CH_2), 64.8 (CH_2), 59.0 (CH_3), 56.9 (CH syndio), 55.9 (CH hetero), 55.0 – 54.9 (CH iso), 50.5 (CH_2), 47.3 – 44.8 (family of CH_2 peaks), 30.0 (CH_2), 29.7 (CH_2), 28.4 (CH_2), 28.1 (CH_2), 26.04 (CH_2), 25.96 (CH_2), 25.3 (CH_2), 25.2 (CH_2).

IR (Neat): 2928 (s, alkane CH), 2874 (s, alkane CH), 1733 (s, ester C=O), 1552 (m, triazole C=C), 1464 (s, methylene stretch CH_2), 1279 (s, ester stretch C-O), 1202 (s, ester stretch C-O), 1111 (s, ether stretch C-O), 615 (w, C-Cl) cm^{-1}.

DSC (T_g): -17 °C.

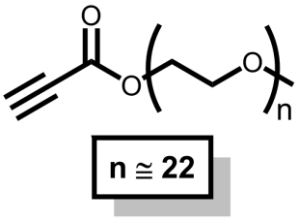

Preparation of methoxy poly(ethylene glycol) 1000 prop‐2‐ynoate. Propiolic acid (4.2000 g, 60.000 mmol) was added to a 250 mL round bottom flask with 40 mL of toluene. Methoxy poly(ethylene glycol) 1000 (20.0000 g, 20.000 mmol) and 0.2 mL H_2SO_4 was added to the reaction flask and stirred at reflux for 2 h. The reaction was concentrated *in vacuo*, and diluted with 100 mL ethyl acetate. The solution was transferred to a 500 mL separatory funnel and washed with 5 mL of saturated $NaHCO_3$ three times each. The aqueous layer was extracted with 60 mL of ethyl acetate, three times each. The combined organic layers were dried with $MgSO_4$, filtered, and concentrated *in vacuo*, affording 16.1738g (15.374 mmol, 76.87% gravimetric yield) of the title compound as a white waxy solid of varying chain lengths.

TLC: 93:7 CH_2Cl_2:MeOH, R_f=0.55, $KMnO_4$ stain, *p*-anisealdehyde stain, blue-yellow spot.

^{1}H NMR (500 MHz, $CDCl_3$): δ 4.37 – 4.32 (m, 2H), 3.76 – 3.72 (m, 2H), 3.72 – 3.58 (m, 82H), 3.58 – 3.53 (m, 2H), 3.42 – 3.35 (m, 3H), 2.99 (s, 1H).

^{13}C NMR (125 MHz, $CDCl_3$, DEPT): δ 152.6 (C=O), 75.3 (alkyne 4°), 74.5 (alkyne CH), 71.9 (CH_2), 70.7 (CH_2), 70.64 (CH_2), 70.55 (CH_2), 68.5 (CH_2), 65.2 (CH_2), 59.0 (CH_3).

IR (Neat): 3214 (m, alkyne CH), 2871 (s, alkane CH), 2112 (s, alkyne CC), 1716 (s, ester C=O), 1244 (s, ester stretch C-O), 1108 (s, ether stretch C-O) cm^{-1}.

HRMS: Calcd. for (n =19) $C_{42}H_{80}O_{21}$ $[M+H]^+$ 921.5265; Found 921.5288.

Calcd. for (n =20) $C_{44}H_{84}O_{22}$ $[M+H]^+$ 965.5527; Found 965.5550.

Calcd. for (n =21) $C_{46}H_{88}O_{23}$ $[M+H]^+$ 1009.5789; Found 1009.5815.

Calcd. for (n =22) $C_{48}H_{92}O_{24}$ $[M+H]^+$ 1053.6051; Found 1053.6075.

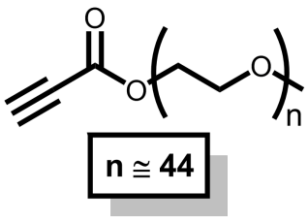

Preparation of methoxy poly(ethylene glycol) 2000 prop‐2‐ynoate. Propiolic acid (2.1000 g, 30.000 mmol) was added to a 250 mL round bottom flask with 40 mL of toluene. Methoxy poly(ethylene glycol) 2000 (20.0000 g, 10.000 mmol) and 0.2 mL H_2SO_4 was added to the reaction flask and stirred at reflux for 2 h. The reaction was concentrated *in vacuo*, and diluted with 100 mL ethyl acetate. The solution was transferred to a 500 mL separatory funnel and washed with 10 mL of saturated $NaHCO_3$ three times each. The aqueous layer was extracted with 100 mL ethyl acetate two times each. The organic layers were combined and dried with $MgSO_4$, filtered, and concentrated *in vacuo*, affording 11.5138g (5.611 mmol, 56.11% gravimetric yield) of the title compound as a white waxy solid of varying chain lengths.

TLC: 93:7 CH_2Cl_2:MeOH, R_f=0.45, $KMnO_4$ stain, *p*-anisealdehyde stain, blue-yellow spot.

^{1}H NMR (500 MHz, $CDCl_3$): δ 4.41 – 4.33 (m, 2H), 3.84 – 3.78 (m, 1H), 3.77 – 3.73 (m, 2H), 3.73 – 3.61 (m, 176H), 3.59 – 3.54 (m, 2H), 3.54 – 3.47 (m, 1H), 3.42 – 3.35 (m, 2H), 2.99 (s, 1H).

^{13}C NMR (125 MHz, $CDCl_3$, DEPT): δ 153.4 (C=O), 75.4 (alkyne 4°), 74.7 (alkyne CH), 71.8 (CH_2), 70.6 (CH_2), 70.5 (CH_2), 68.5 (CH_2), 65.1 (CH_2), 60.3 (CH_2), 58.9 (CH_3).

IR (Neat): 3216 (w, alkyne CH), 2876 (s, alkane CH), 2112 (m, alkyne CC), 1715 (m, ester C=O), 1244 (m, ester stretch C-O), 1111 (s, ether stretch C-O) cm^{-1}.

HRMS: Calcd. for (n=39) $C_{82}H_{160}O_{41}$ $[M+H]^+$ 1824.0327; Found 1824.0298.

Calcd. for (n=40) $C_{84}H_{164}O_{42}$ $[M+H]^+$ 1868.0589; Found 1868.0557.

Calcd. for (n=41) $C_{86}H_{168}O_{43}$ $[M+H]^+$ 1912.0852; Found 1912.0814.

Calcd. for (n=42) $C_{88}H_{172}O_{44}$ $[M+H]^+$ 1956.1114; Found 1956.1077.

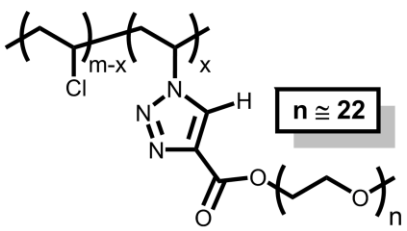

Preparation of 5% PVC-TRZ-PEO$_{1000}$Me. Poly(vinyl chloride) 5% azide (1.000 g, 16.00 mmol) was added to a 100 mL round bottom flask and dissolved in 15 mL of 3-pentanone at 96 °C. Methoxy poly(ethylene glycol) 1000-prop-2-ynoate (2.524 g, 2.4 mmol) was added to the PVC solution and stirred for 24 h. The reaction was precipitated once in 80 mL of MeOH. The crude polymer was dissolved in 15 mL of 3-pentaone and methoxy poly(ethylene glycol) 1000-prop-2-ynoate (2.524 g, 2.4 mmol) was added to the solution and stirred for 24 h. The reaction was concentrated to approximately half its volume *in vacuo*, then precipitated in 80 mL of MeOH, two times each. The isolated polymer was dried under house vacuum for 1 day, then in a vacuum oven at 40 °C for 2 days to yield 0.6690 g of a white solid.

^{1}H NMR (500 MHz, $CDCl_3$): δ 8.40 – 8.15 (br m, *PVC-triazole-H*), 5.32 – 5.10 (br m, *C-CH-triazole*), 4.70 – 4.56 (br m, *Cl-C-H*), 4.56 – 4.40 (br s, *Cl-C-H* and *triazole-O-CH$_2$),* 4.38 – 4.24 (br m, *Cl-C-H*), 3.92 – 3.83 (br m, *triazole-O-C-CH$_2$-O*), 3.83 – 3.59 (br m, *triazole-O-C-C-O-CH$_2$-CH$_2$-O-*), 3.58 – 3.55 (br m, *C-CH$_2$-O-CH$_3$*), 3.41 – 3.39 (br s, *O-CH$_3$*), 2.87 – 2.78 (br m, *Cl-C-CH$_2$-C-triazole* and *triazole-C-CH$_2$-C-triazole*), 2.78 – 2.69 (br m, *Cl-C-CH$_2$-C-triazole* and *triazole-C-CH$_2$-C-triazole*), 2.50 – 1.85 (br m, *Cl-C-CH$_2$-C-Cl*).

^{13}C NMR (125 MHz, $CDCl_3$, DEPT): δ 72.0 (CH_2), 70.6 (CH_2), 59.0 (CH_3), 57.0 – 56.9 (CH syndio), 56.1 – 55.9 (CH hetero), 55.0 – 54.9 (CH iso), 47.3 – 44.8 (family of CH_2 peaks).

IR (Neat): 2909 (s, alkane CH), 2874 (s, alkane CH), 1727 (s, ester C=O), 1541 (w, triazole C=C), 1435 (s, methylene stretch CH_2), 1253 (s, ester stretch C-O), 1199 (m, ester stretch C-O), 1106 (s, ether stretch C-O), 614 (w, C-Cl) cm^{-1}.

DSC (T_g): 65 °C.

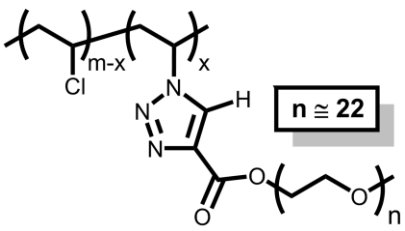

Preparation of 15% PVC-TRZ-PEO$_{1000}$Me. Poly(vinyl chloride) 15% azide (1.000 g, 16.00 mmol) was added to a 100 mL round bottom flask and dissolved in 30 mL of 3-pentanone at 96 °C. Methoxy poly(ethylene glycol) 1000-prop-2-ynoate (7.5746 g, 7.2 mmol) was added to the PVC solution and stirred for 24 h. The reaction was concentrated to approximately one-third its volume *in vacuo*. To a 250 mL beaker, 100 mL of MeOH was added, then placed in a dry ice-acetone bath for 2 min. The polymer was precipitated by dropwise addition of the reaction solution in 2 mL increments into the cooled MeOH. After the addition of reaction solution, the mother liquor was decanted and replaced with 100 mL of fresh MeOH. The beaker was cooled to -78 °C for 2 min, upon which another 2 mL of reaction solution was added dropwise. This process was repeated until the entire polymer was precipitated. When all of the reaction solution was precipitated, the last volume of mother liquor was decanted. Subsequently, the neat polymer was cooled to -78 °C and washed with 50 mL of MeOH four times each. The isolated polymer was dried under house vacuum for 1 day, then in a vacuum oven at 40 °C for 3 days to yield 2.2467 g of a flexible transparent yellow solid.

^{1}H NMR (500 MHz, $CDCl_3$): δ 8.29 – 8.07 (br m, *PVC-triazole-H*), 5.30 – 5.10 (br m, *C-CH-triazole*), 4.66 – 4.57 (br s, *Cl-C-H*), 4.56 – 4.50 (br s, *Cl-C-H* and *triazole-O-CH$_2$),* 4.49 – 4.40 (br s, *Cl-C-H*), 4.36 – 4.15 (br m, *Cl-C-H*), 3.95 – 3.82 (br s, *triazole-O-C-CH$_2$-O*), 3.82 – 3.59 (br m, *triazole-O-C-C-O-CH$_2$-CH$_2$-O-*), 3.58 – 3.54 (br m, *C-CH$_2$-O-CH$_3$*), 3.41 – 3.38 (br s, *O-CH$_3$*), 2.87 – 2.78 (br m, *Cl-C-CH$_2$-C-triazole* and *triazole-C-CH$_2$-C-triazole*), 2.78 – 2.68 (br m, *Cl-C-CH$_2$-C-triazole* and *triazole-C-CH$_2$-C-triazole*), 2.50 – 1.85 (br m, *Cl-C-CH$_2$-C-Cl*).

^{13}C NMR (200 MHz, $CDCl_3$): δ 161.0 (C=O), 160.4 (C=O), 138.1 (TRZ 4°), 129.7 (TRZ 4°) 72.5 (CH_2), 71.9 (CH_2), 70.6 (CH_2), 68.9 (CH_2), 64.3 (CH_2), 63.0 (CH_2), 61.8 (CH_2), 59.0 (CH_3), 56.9 (CH syndio), 56.1 – 55.9 (CH hetero), 55.0 – 54.9 (CH iso), 47.3 – 44.8 (family of CH_2 peaks).

IR (Neat): 2874 (s, alkane CH), 1725 (m, ester C=O), 1454 (m, methylene stretch CH_2), 1253 (m, ester stretch C-O), 1103 (s, ether stretch C-O) cm^{-1}.

DSC (T_g): -35 °C.

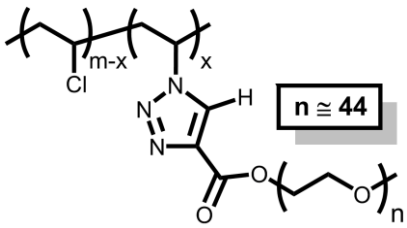

Preparation of 5% PVC-TRZ-PEO$_{2000}$Me. Poly(vinyl chloride) 5% azide (1.000 g, 16.00 mmol) was added to a 100 mL round bottom flask and dissolved in 15 mL of 3-pentanone at 96 °C. Methoxy poly(ethylene glycol) 2000-prop-2-ynoate (4.9248 g, 2.4 mmol) was added to the PVC solution and stirred for 24 h. The reaction was precipitated once in 80 mL of MeOH. The crude polymer was then dissolved in 15 mL of 3-pentaone and methoxy poly(ethylene glycol) 2000-prop-2-ynoate (4.9248g, 2.4 mmol) was added to the solution and stirred for 24 h. The reaction was concentrated to approximately half its volume *in vacuo*, then precipitated in 80 mL of MeOH, two times each. The isolated polymer was dried under house vacuum for 1 day, then in a vacuum oven at 40 °C for 2 days to yield 1.0484 g of a white solid.

^{1}H NMR (500 MHz, $CDCl_3$): δ 8.32 – 8.18 (br m, *PVC-triazole-H*), 5.30 – 5.15 (br m, *C-CH-triazole*), 4.66 – 4.57 (br m, *Cl-C-H*), 4.56 – 4.40 (br m, *Cl-C-H* and *triazole-O-CH_2),* 4.39 – 4.15 (br m, *Cl-C-H*), 3.82 – 3.58 (br m, *triazole-O-C-C-O-CH_2-CH_2-O-*), 3.58 – 3.54 (br t, *C-CH_2-O-CH_3*), 3.53 – 3.50 (br t, *C-CH_2-O-CH_3*), 3.40 – 3.39 (br s, *O-CH_3*), 2.87 – 2.77 (br m, *Cl-C-CH_2-C-triazole* and *triazole-C-CH_2-C-triazole*), 2.77 – 2.68 (br m, *Cl-C-CH_2-C-triazole* and *triazole-C-CH_2-C-triazole*), 2.50 – 1.85 (br m, *Cl-C-CH_2-C-Cl*).

^{13}C NMR (125 MHz, $CDCl_3$, DEPT): δ 161.0 (C=O), 72.0 (CH_2), 70.6 (CH_2), 68.9 (CH_2), 66.7 (CH_2), 63.0 (CH_2), 61.8 (CH_2), 59.0 (CH_3), 57.0 – 56.9 (CH syndio), 56.1 – 55.9 (CH hetero), 55.1 – 54.9 (CH iso), 47.3 – 44.8 (family of CH_2 peaks).

IR (Neat): 3120 (w, triazole CH), 2908 (s, alkane CH), 2873 (s, alkane CH), 1728 (m, ester C=O), 1528 (w, triazole C=C), 1435 (m, methylene stretch CH_2), 1253 (s, ester stretch C-O), 1199 (m, ester stretch C-O), 1106 (s, ether stretch C-O), 615 (w, C-Cl) cm^{-1}.

DSC (T_g): 22 °C.

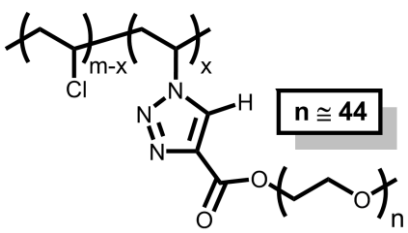

Preparation of 15% PVC-TRZ-PEO_{2000}Me. Poly(vinyl chloride) 15% azide (1.000 g, 16.00 mmol) was added to a 100 mL round bottom flask and dissolved in 25 mL of 3-pentanone at 90 °C. Methoxy poly(ethylene glycol) 2000-prop-2-ynoate (7.387 g, 3.600 mmol) was added to the PVC solution and stirred for 72 h. The reaction was concentrated to approximately half its volume *in vacuo*. To a 250 mL beaker, 100 mL of MeOH was added, then placed in a dry ice-acetone bath for 2 min. The polymer was precipitated by dropwise addition of the reaction solution in 2 mL increments into the cooled MeOH. After the addition of reaction solution, the mother liquor was decanted and replaced with 100 mL of fresh MeOH. The beaker was cooled to -78 °C for 2 min, upon which another 2 mL of reaction solution was added dropwise. This process was repeated until the entire polymer was precipitated. When all of the reaction solution was precipitated, the last volume of mother liquor was decanted. Subsequently, the neat polymer was cooled to -78 °C and washed with 50 mL of MeOH four times each. The isolated polymer was dried under house vacuum for 1 day, then in a vacuum oven at 40 °C for 3 days to yield 2.9260 g of a flexible transparent yellow solid.

^{1}H NMR (500 MHz, $CDCl_3$): δ 8.40 – 8.15 (br m, *PVC-triazole-H*), 5.35 – 5.05 (br m, *C-CH-triazole*), 4.65 – 4.55 (br s, *Cl-C-H*), 4.55 – 4.36 (br m, *Cl-C-H* and *triazole-O-CH_2),* 4.36 – 4.15 (br m, *Cl-C-H*), 3.95 – 3.40 (br s, *triazole-O-C-CH_2-O* and *triazole-O-C-C-O-CH_2-CH_2-O-* and *C-CH_2-O-CH_3*), 3.38 (br s, *O-CH_3*), 3.36 (br s, *O-CH_3*), 2.50 – 1.75 (br m, *Cl-C-CH_2-C-Cl*).

^{13}C NMR (125 MHz, $CDCl_3$, DEPT): δ 161.0 (C=O), 72.5 (CH_2), 71.9 (CH_2), 70.6 (CH_2), 68.9 (CH_2), 63.0 (CH_2), 61.7 (CH_2), 59.0 (CH_3), 57.0 (CH syndio), 55.9 (CH hetero), 54.9 (CH iso), 47.3 – 44.8 (family of CH_2 peaks).

IR (Neat): 3120 (w, triazole CH), 2871 (s, alkane CH), 1726 (m, ester C=O), 1544 (w, triazole C=C), 1455 (m, methylene stretch CH_2), 1251 (s, ester stretch C-O), 1111 (s, ether stretch C-O), 615 (w, C-Cl) cm^{-1}.

DSC (T_g): -42 °C.

6.8 Chapter 5 Experimental Section

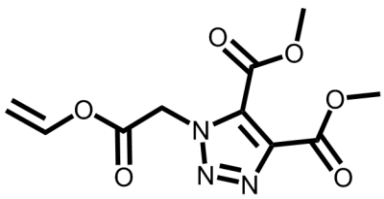

Preparation of 4,5-dimethyl 1-[2-(ethenyloxy)-2-oxoethyl]-1H-1,2,3-triazole-4,5-dicarboxylate. Vinyl chloroacetate (1.000 g, 8.296 mmol) was added to an aluminum foil covered 100 mL round bottom flask with 13 mL of CH_3CN. NaN_3 (1.618 g, 24.89 mmol) and $NaHCO_3$ (0.348 g, 4.15 mmol) were added to the flask with stirring. Next, tetrabutylammonium hydrogen sulfate (0.2816 g, 0.8296 mmol) was added to the reaction flask and stirred at room temperature for 1 h. The reaction mixture was filtered through a glass sintered funnel into another 100 mL round bottom flask. The residues were washed in an additional 13 mL of CH_3CN and filtered through the glass sintered funnel. Dimethyl acetylenedicarboxylate (1.886 g, 13.273 mmol) was added to the reaction flask and stirred at 50 °C for 24 h. The volatiles were evaporated *in vacuo*, affording a crude brown solid. The product was dry-loaded and purified via flash chromatography using 6:4 hexanes:ethyl acetate, furnishing 1.2617 g (4.6867 mmol, 56.5% yield) of the title compound as a colorless solid: mp 130-131 °C.

TLC: 6:4 hexanes:ethyl acetate, R_f=0.38, UV, $KMnO_4$ stain, *p*-anisealdehyde stain, light purple spot.

IR (KBr Pellet): 3028 (s, CH stretch alkene), 1768 (s, ester), 1749 (s, ester), 1725 (s, ester), 1651 (s, C=C alkene stretch) cm^{-1}.

^{1}H NMR (500 MHz, $CDCl_3$): δ 7.24 (dd, *J* = 13.8, 6.2 Hz, 1H), 5.55 (s, 2H), 5.01 (dd, *J* = 13.8, 2.2 Hz, 1H), 4.74 (dd, *J* = 6.2, 2.2 Hz, 1H), 4.00 (s, 3H), 3.98 (s, 3H).

^{13}C-NMR (125 MHz, $CDCl_3$, DEPT): δ 163.0 (C=O), 160.2 (C=O), 158.6 (C=O), 140.5 (CH), 140.4 (4^{o}), 129.8 (4^{o}), 100.1 (CH_2), 53.5 (CH_3), 52.9 (CH_3), 51.3 (CH_2).

HRMS: Calcd. for $C_{10}H_{11}N_3O_6$ $[M+H]^+$: 270.0721, found 270.0710.

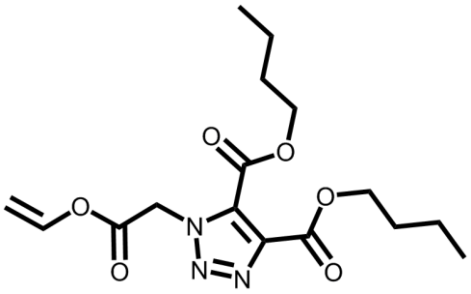

Preparation of 4,5-dibutyl 1-[2-(ethenyloxy)-2-oxoethyl]-1H-1,2,3-triazole-4,5-dicarboxylate. Vinyl chloroacetate (1.000 g, 8.296 mmol) was added to an aluminum foil covered 100 mL round bottom flask with 13 mL of CH_3CN. NaN_3 (1.618 g, 24.89 mmol) and $NaHCO_3$ (0.348 g, 4.15 mmol) were added to the flask with stirring. Next, tetrabutylammonium hydrogen sulfate (0.2816 g, 0.8296 mmol) was added to the reaction flask and stirred at room temperature for 1 h. The reaction mixture was filtered through a glass sintered funnel into another 100 mL round bottom flask. The residues were washed in an additional 13 mL of CH_3CN and filtered through the glass sintered funnel. 1,4-Dibutyl but-2-ynedioate (3.003 g, 13.273 mmol) was added to the reaction flask and stirred at 50 °C for 24 h. The volatiles were evaporated *in vacuo*, affording a crude brown liquid. Purification via flash chromatography using 8:2 hexanes:ethyl acetate, furnishing 1.8153 g (5.1371 mmol, 61.9% yield) of the title compound as an orange oil.

TLC: 8:2 hexanes:ethyl acetate, R_f=0.37, UV, $KMnO_4$ stain, *p*-anisealdehyde stain, light purple spot.

IR (Neat): 2962 (s, CH stretch alkane), 2936 (s, CH stretch alkane), 2875 (s, CH stretch alkane), 1773 (s, ester), 1730 (s, ester), 1648 (s, C=C alkene stretch) cm^{-1}.

^{1}H NMR (500 MHz, $CDCl_3$): δ 7.24 (dd, *J* = 13.8, 6.2 Hz, 1H), 5.54 (s, 2H), 5.01 (dd, *J* = 13.8, 2.2 Hz, 1H), 4.73 (dd, *J* = 6.2, 2.2 Hz, 1H), 4.39 (t, *J* = 6.7 Hz, 2H), 3.36 (t, *J* = 6.7, 2H), 1.81 – 1.68 (m, 4H), 1.51 – 1.39 (m, 4H), 0.96 (two overlapping t, 6H).

^{13}C-NMR (125 MHz, $CDCl_3$, DEPT): δ 163.1 (C=O), 160.1 (C=O), 158.1 (C=O), 141.0 (4^{o}), 140.5 (CH), 129.6 (4^{o}), 99.9 (CH_2), 66.8 (CH_2), 65.9 (CH_2), 51.2 (CH_2), 30.6 (CH_2), 30.3 (CH_2), 19.1 (CH_2), 18.9 (CH_2), 13.7 (CH_3), 13.6 (CH_3).

HRMS: Calcd for $C_{16}H_{23}N_3O_6$ $[M+H]^+$: 354.1659, found 354.1632.

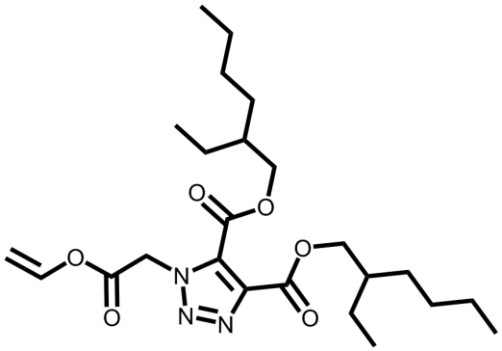

Preparation of 4,5-bis(2-ethylhexyl) 1-[2-(ethenyloxy)-2-oxoethyl]-1H-1,2,3-triazole-4,5-dicarboxylate. Vinyl chloroacetate (1.000 g, 8.296 mmol) was added to an aluminum foil covered 100 mL round bottom flask with 13 mL of CH_3CN. NaN_3 (1.618 g, 24.89 mmol) and $NaHCO_3$ (0.348 g, 4.15 mmol) were added to the flask with stirring. Next, tetrabutylammonium hydrogen sulfate (0.2816 g, 0.8296 mmol) was added to the reaction flask and stirred at room temperature for 1 h. The reaction mixture was filtered through a glass sintered funnel into another 100 mL round bottom flask. The residues were washed in an additional 13 mL of CH_3CN and filtered through the glass sintered funnel. 1,4-Dibutyl but-2-ynedioate (3.003 g, 13.273 mmol) was added to the reaction flask and stirred at 50 °C for 24 h. The volatiles were evaporated *in vacuo*, affording a crude brown liquid. Purification via flash chromatography using 8:2 hexanes:ethyl acetate, furnishing 1.8153 g (5.1371 mmol, 61.9% yield) of the title compound as an orange oil. 1,4-Bis(2-ethylhexyl) but-2-ynedioate (4.492 g, 13.273 mmol) was added to the reaction flask and stirred at 50 °C for 24 h. The

volatiles were evaporated *in vacuo* affording a crude brown liquid. Purification via flash chromatography using 9:1 hexanes:ethyl acetate, furnishing 2.171 g (4.6634 mmol, 56.2% yield) of the title compound as an orange oil.

TLC: 9:1 hexanes:ethyl acetate, R_f=0.30, UV, $KMnO_4$ stain, *p*-anisealdehyde stain, blue spot.

IR (Neat): 2961 (s, CH stretch alkane), 2931 (s, CH stretch alkane), 2873 (s, CH stretch alkane), 2861 (s, CH stretch alkane), 1774 (s, ester), 1734 (s, ester), 1648 (s, C=C alkene stretch) cm^{-1}.

^{1}H NMR (500 MHz, $CDCl_3$): δ 7.26 (dd, *J* = 13.8, 6.2 Hz, 1H), 5.55 (s, 2H), 5.01 (dd, *J* = 13.8, 2.1 Hz, 1H), 4.74 (dd, *J* = 6.2, 2.1 Hz, 1H), 4.36 – 4.22 (m, 4H), 1.76 (hept, *J* = 12.0, 5.8 Hz, 1H), 1.67 (hept, *J* = 12.1, 5.8 Hz, 1H), 1.51 – 1.27 (m, 16H), 1.00 – 0.79 (m, 12H).

^{13}C-NMR (125 MHz, $CDCl_3$, DEPT): δ 163.2 (C=O), 160.3 (C=O), 158.5 (C=O), 141.2 (4^o), 140.6 (CH), 129.6 (4^o), 100.0 (CH_2), 69.3 (CH_2), 68.7 (CH_2), 51.3 (CH_2), 38.9 (CH), 38.8 (CH), 30.3 (CH_2), 30.2 (CH_2), 29.0 (CH_2), 28.95 (CH_2), 23.7 (CH_2), 23.6 (CH_2), 23.08 (CH_2), 23.03 (CH_2), 14.2 (CH_3), 11.0 (CH_3).

HRMS: Calcd for $C_{24}H_{39}N_3O_6$ $[M+H]^+$: 466.2912, found 466.2884.

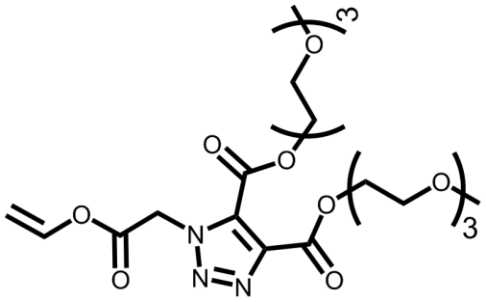

Preparation of 1-ethenyl 4,5-bis({2-[2-(2-methoxyethoxy)ethoxy]ethyl}) 1H-1,2,3-triazole-1,4,5-tricarboxylate. Vinyl chloroacetate (3.000 g, 24.89 mmol) was added to an aluminum foil covered 50 mL round bottom flask with 18 mL of CH_3CN. NaN_3 (4.854 g, 74.67 mmol) and $NaHCO_3$ (0.8360 g, 9.956 mmol) were added to the flask with stirring. Next, tetrabutylammonium hydrogen sulfate (0.8451 g, 2.489 mmol) was added to the reaction flask and stirred at room temperature for 1 h. The reaction mixture was filtered through a glass sintered funnel into another 100 mL round bottom flask. The

residues were washed in an additional 13 mL of CH_3CN and filtered through the glass sintered funnel. 1,4-bis({2-[2-(2-methoxyethoxy)ethoxy]ethyl})but-2-ynedioate (13.1506 g, 32.357 mmol) was added to the reaction flask and stirred at 50 °C for 24 h. The volatiles were evaporated *in vacuo*, affording a crude brown liquid. Purification via flash chromatography using 7:3 ethyl acetate:acetone furnished 7.1385 g (13.3798 mmol, 53.76% yield) of the title compound as a yellow oil.

TLC: 7:3 ethyl acetate:acetone, R_f=0.64, UV, $KMnO_4$ stain, *p*-anisealdehyde stain, blue-yellow spot.

IR (Neat): 2880 (s, CH stretch alkane), 1733 (s, ester), 1647 (s, C=C alkene stretch) cm^{-1}.

^1H NMR (500 MHz, $CDCl_3$): δ 7.26 (dd, *J* = 13.9, 6.2 Hz, 1H), 5.59 (s, 2H), 5.02 (dd, *J* = 13.8, 2.1 Hz, 1H), 4.75 (dd, *J* = 6.2, 2.1 Hz, 1H), 4.59 – 4.49 (m, 4H), 3.90 – 3.84 (m, 2H), 3.82 – 3.76 (m, 2H), 3.76 – 3.70 (m, 2H), 3.72 – 3.62 (m, 10H), 3.59 – 3.52 (m, 4H), 3.39 (s, 3H), 3.38 (s, 3H).

^{13}C-NMR (125 MHz, $CDCl_3$, DEPT): δ 163.1 (C=O), 159.7 (C=O), 157.5 (C=O), 140.7 (4^o), 140.6 (CH), 130.2 (4^o), 99.96 (CH_2), 71.9 (CH_2), 70.7 (CH_2), 70.6 (CH_2), 70.58 (CH_2), 70.55 (CH_2), 68.7 (CH_2), 68.2 (CH_2), 65.6 (CH_2), 65.0 (CH_2), 59.0 (CH_3), 51.3 (CH_2).

HRMS: Calcd. for $C_{22}H_{35}N_3O_{12}$ $[M+H]^+$: 534.2294, found 534.2277.

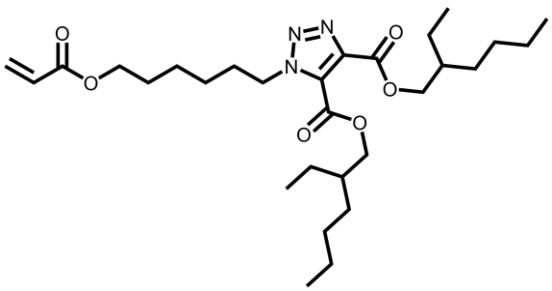

Preparation of 4,5-bis(2-ethylhexyl)-1-[6-(prop-2-enoyloxy)hexyl]-1H-1,2,3-triazole-4,5-dicarboxylate. Acryloyl chloride (5.4906 g, 60.6629 mmol) was diluted with 20 mL of anhydrous THF under N_2 in a 150 mL pear flask. Next, 4,5-bis(2-ethylhexyl) 1-(6-hydroxyhexyl)-1H-1,2,3-triazole-4,5-dicarboxylate (9.740 g, 20.2209 mmol) and triethylamine (3.0692 g, 30.3314 mmol) were combined in a

250 mL round bottom flask with 50 mL of anhydrous THF and stirred. This reaction was cooled to 0 °C under N_2 for 15 min. The acryloyl chloride solution was slowly added *via* syringe over 15 min. After the addition of acryloyl chloride, the reaction was allowed to stir at 0 °C for 1 hour, then at room temperature for an additional 1 hour. The reaction mixture was concentrated *in vacuo* and diluted with 80 mL of ethyl acetate, then washed twice with 10 mL of 10% aqueous HCl. The organic layer was dried with $MgSO_4$ and filtered, then evaporated *in vacuo*, affording a crude orange oil. Purification *via* flash chromatography using 7:3 hexanes:ethyl acetate furnished 4.680 g (8.735 mmol, 43.2% yield) of a clear oil, as a mixture of diastereomers.

TLC: 7:3 hexanes:ethyl acetate, R_f=0.71, UV, $KMnO_4$ and *p*-anisealdehyde stain, purple spot.

^{1}H NMR (500 MHz, $CDCl_3$): δ 6.41 (d, *J* = 17.2 Hz, 1H), 6.13 (dd, *J* = 17.2, 10.8 Hz, 1H), 5.84 (d, *J* = 10.8 Hz, 1H), 4.60 (t, *J* = 7.3 Hz, 2H), 4.29 (m, 4H), 4.16 (t, *J* = 6.5 Hz, 2H), 1.94 (m, *J* = 7.2 Hz, 2H), 1.79 – 1.64 (m, 4H), 1.51 – 1.28 (m, 20H), 0.98 – 0.87 (m, 12H).

^{13}C-NMR (125 MHz, $CDCl_3$, DEPT): δ 166.2 (Acrylate C=O), 160.6 (C=O), 158.9 (C=O), 140.5 (4°), 130.6 (CH_2 Alkene), 129.6 (4°), 128.5 (CH Alkene), 69.1 (CH_2), 68.4 (CH_2), 64.3 (O-CH_2 Acrylate), 50.4 (CH_2), 38.73 (CH), 38.70 (CH), 30.21 (CH_2), 30.17 (CH_2), 30.1 (CH_2), 28.89 (CH_2), 28.86 (CH_2), 28.4 (CH_2), 26.1 (CH_2), 25.4 (CH_2), 23.6 (CH_2), 23.5 (CH_2), 22.96 (CH_2), 22.94 (CH_2), 14.0 (CH_3), 10.9 (CH_3).

IR (Neat): 3439 (w, alkene CH), 2959 (s, alkane CH), 2932 (s, alkane CH), 2861 (s, alkane CH), 1738 (s, ester C=O), 1731 (s, ester C=O), 1636 (m, mono. sub. alkene C=C), 1620 (m, alkene C=C), 1557 (m, triazole C=C), 1463 (s, methylene bending CH_2), 1271 (s, ester stretch C-O), 1195 (s, ester stretch C-O), 985 (s, mono. sub. alkene bending C=C), 811 (s, mono. sub. alkene bending C=C) cm^{-1}.

HRMS: Calcd. for $C_{29}H_{49}N_3O_6$ $[M+H]^+$ 536.3694; Found 536.3686.

6.9 References

1. Brase, S.; Gil, C.; Knepper, K.; Zimmermann, V. Organic Azides: An Exploding Diversity of a Unique Class of Compounds. *Angewandte Chemie-International Edition* **2005,** *44* (33), 5188-5240.

2. Earla, A.; Braslau, R. Covalently Linked Plasticizers: Triazole Analogues of Phthalate Plasticizers Prepared by Mild Copper-Free "Click" Reactions with Azide-Functionalized PVC. *Macromolecular Rapid Communications* **2014,** *35* (6), 666-671.

3. Pak, H. K.; Han, J.; Jeon, M.; Kim, Y.; Kwon, Y.; Park, J. Y.; Rhee, Y. H.; Park, J. Synthesis of Enamides by Ruthenium-Catalyzed Reaction of Alkyl Azides with Acid Anhydrides in Ionic Liquid. *ChemCatChem* **2015,** *7* (24), 4030-4034.

4. Ott, E. Über Symmetrische und Asymmetrische Dicarbonsäurechloride. *Justus Liebigs Annalen der Chemie* **1912,** *392* (3), 245-285.

5. Charlton, J. L.; Chee, G. Synthesis of Chiral Esters of Acetylenedicarboxylic Acid. *Tetrahedron Letters* **1994,** *35* (34), 6243-6246.

6. Charlson, J. L.; Chee, G.; McColeman, H. Synthesis of Acetylenedicarboxylic Acid Esters and Asymmetric Diels-Alder Reactions of the Bis(methyl (S)-lactyl) Ester. *Canadian Journal of Chemistry* **1995,** *73* (9), 1454-1462.

Appendix

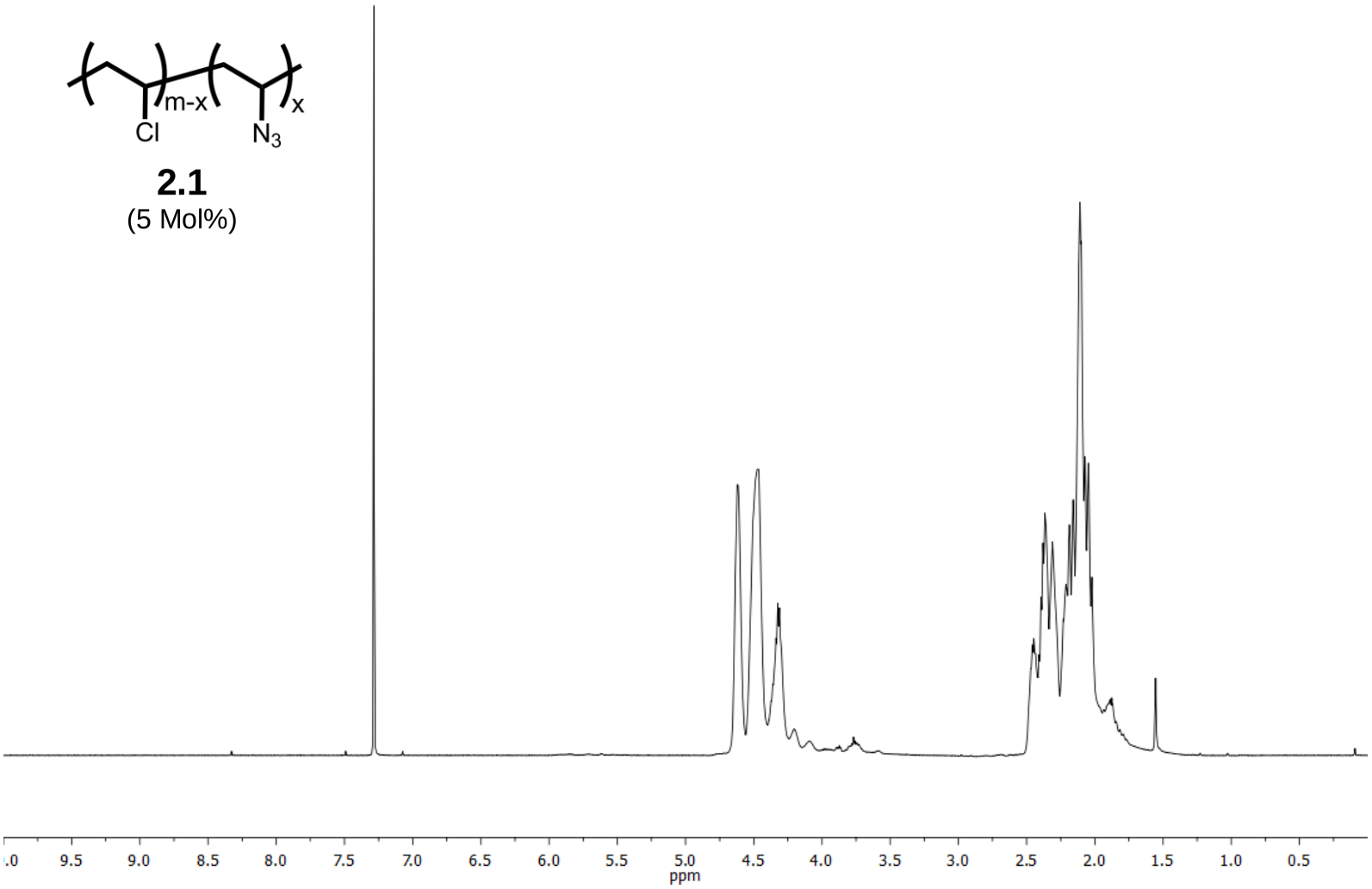
m-x
x
Cl
N3
2.1
(5 Mol%)
9.5
9.0
8.5
8.0
7.5
7.0
6.5
6.0
5.5
5.0
4.5
4.0
3.5
3.0
2.5
2.0
1.5
1.0
0.5
ppm

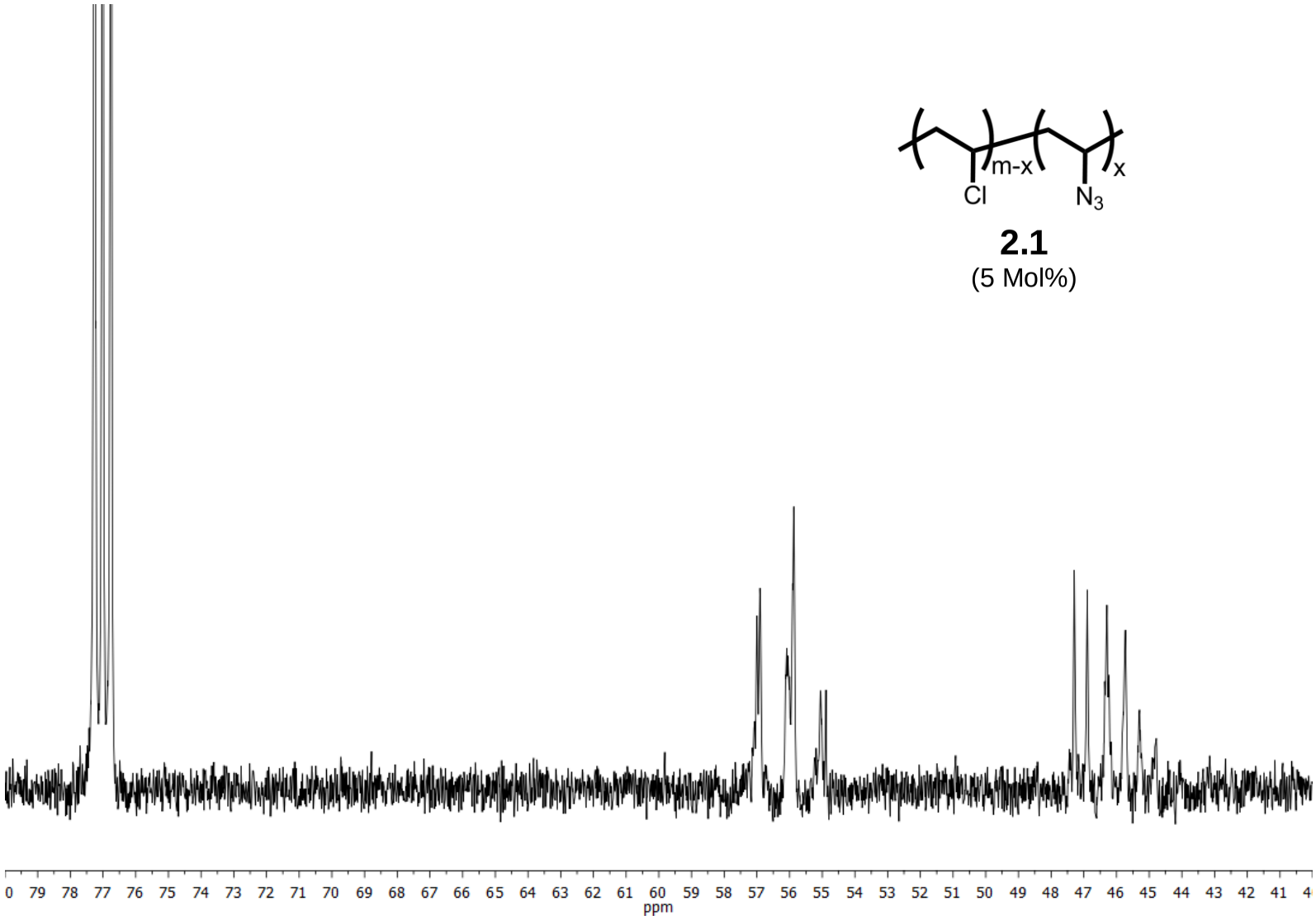
m-x
x
Cl
N3
2.1
(5 Mol%)
0 79 78 77 76 75 74 73 72 71 70 69 68 67 66 65 64 63 62 61 60 59 58 57 56 55 54 53 52 51 50 49 48 47 46 45 44 43 42 41 4
ppm

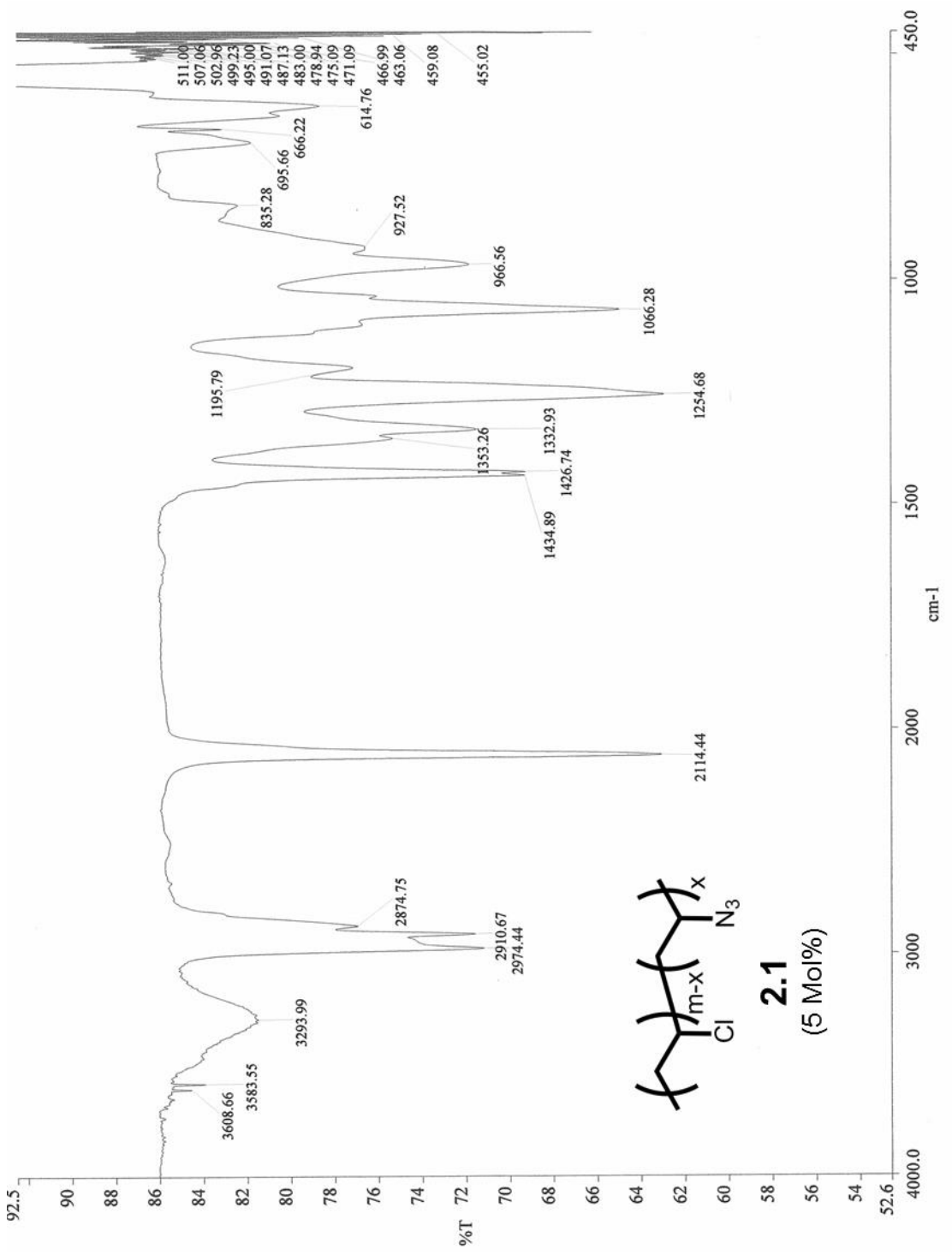
92.5
90
88
86
84
82
80
78
76
74
72
70
68
66
64
62
60
58
56
54
52.6
%T
4000.0
3000
2000
1500
1000
450.0
cm-1
3608.66
3583.55
3293.99
2874.75
2910.67
2974.44
2114.44
1434.89
1426.74
1353.26
1332.93
1254.68
1195.79
1066.28
966.56
927.52
835.28
695.66
666.22
614.76
511.00
507.06
502.96
499.23
495.00
491.07
487.13
483.00
478.94
475.09
471.09
466.99
463.06
459.08
455.02
m-x
Cl
N3
x
2.1
(5 Mol%)

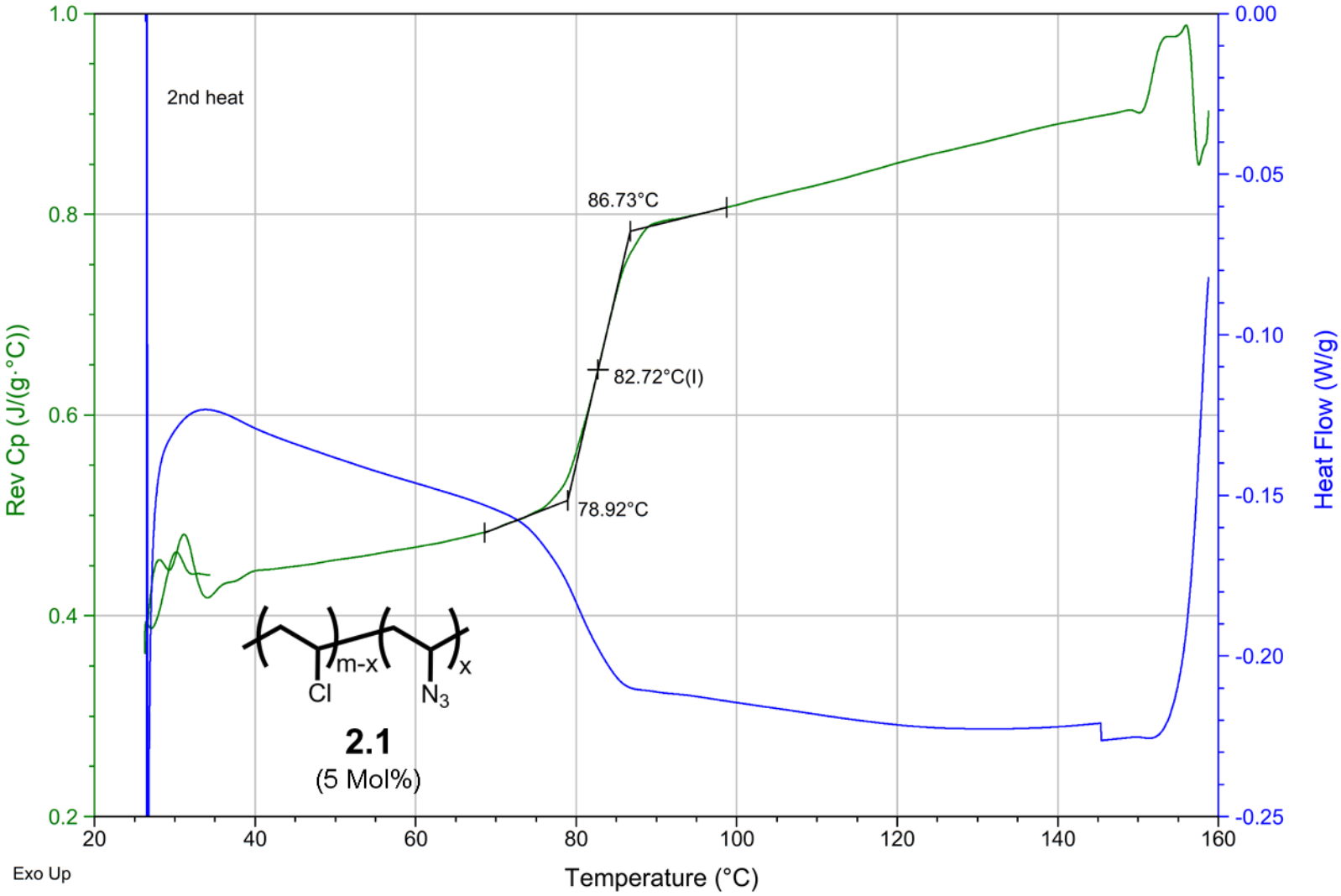
2nd heat
86.73°C
82.72°C(I)
78.92°C
m-x
x
Cl
N3
2.1
(5 Mol%)
Rev Cp (J/(g·°C))
Heat Flow (W/g)
Temperature (°C)
Exo Up
1.0
0.8
0.6
0.4
0.2
0.00
-0.05
-0.10
-0.15
-0.20
-0.25
20
40
60
80
100
120
140
160

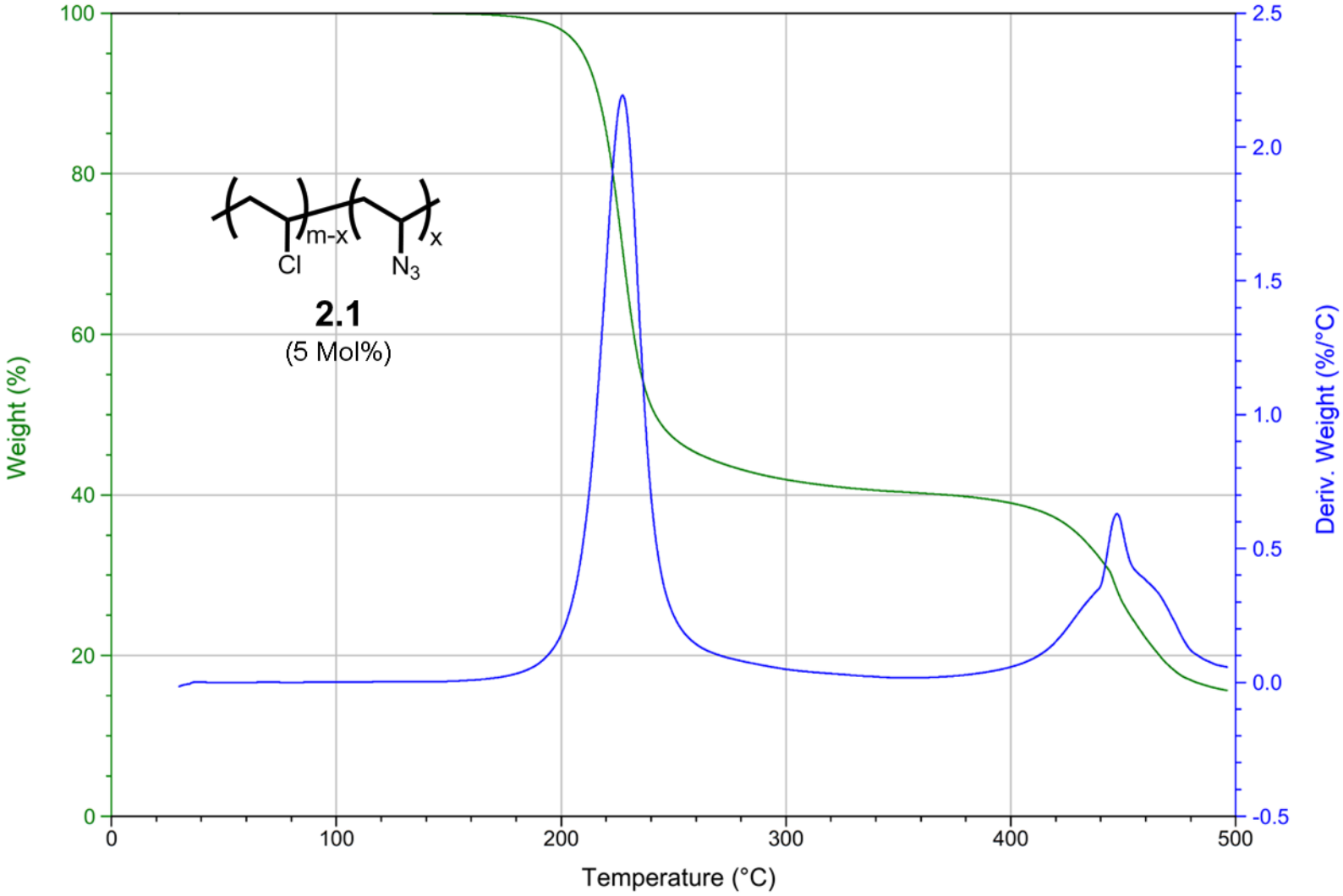
Weight (%)
Deriv. Weight (%/°C)
Temperature (°C)
100
80
60
40
20
0
2.5
2.0
1.5
1.0
0.5
0.0
-0.5
0
100
200
300
400
500
m-x
x
Cl
N3
2.1
(5 Mol%)

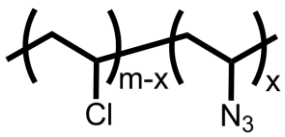

2.1
(15 Mol%)

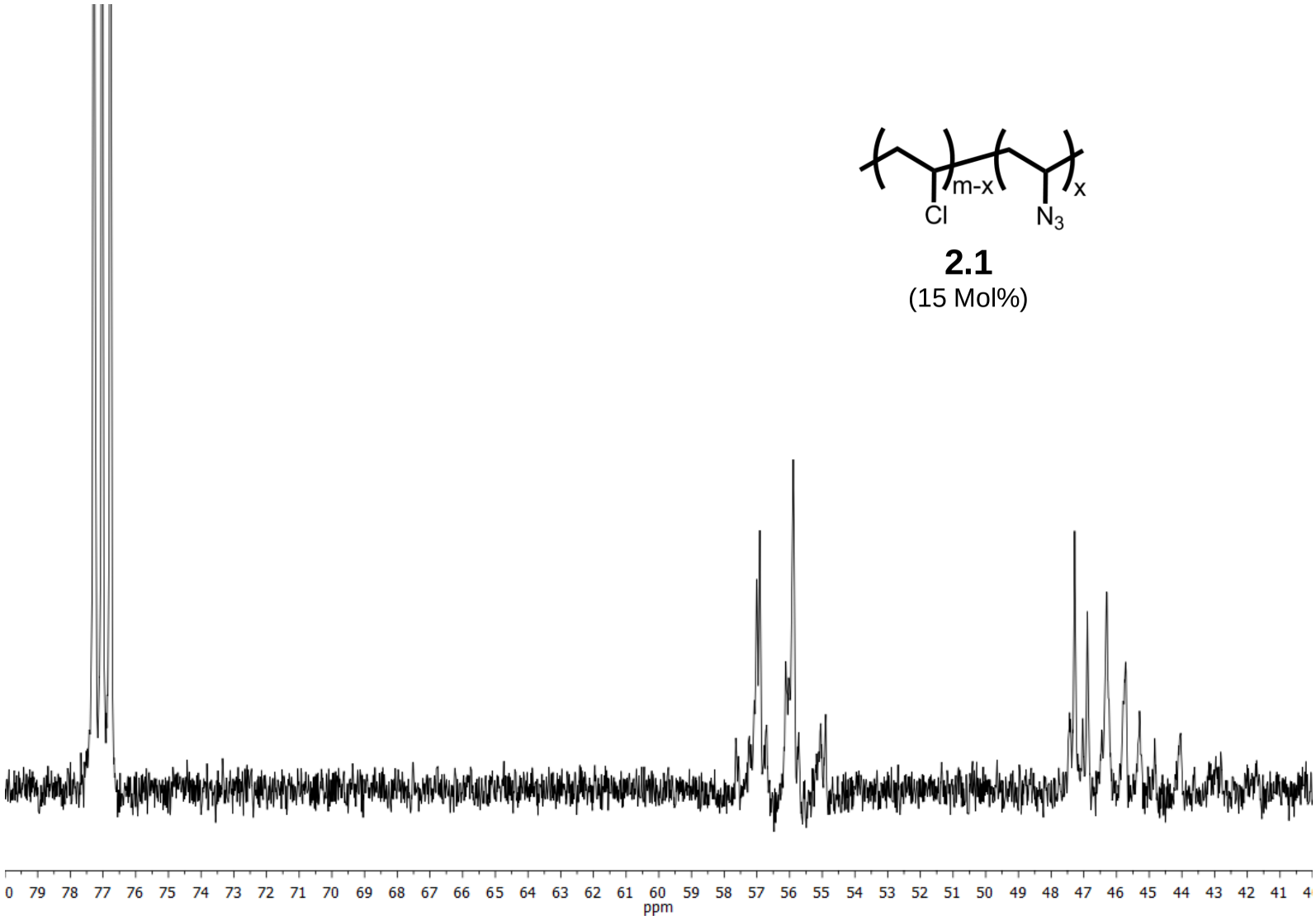
m-x
x
Cl
N3
2.1
(15 Mol%)
0 79 78 77 76 75 74 73 72 71 70 69 68 67 66 65 64 63 62 61 60 59 58 57 56 55 54 53 52 51 50 49 48 47 46 45 44 43 42 41 4
ppm

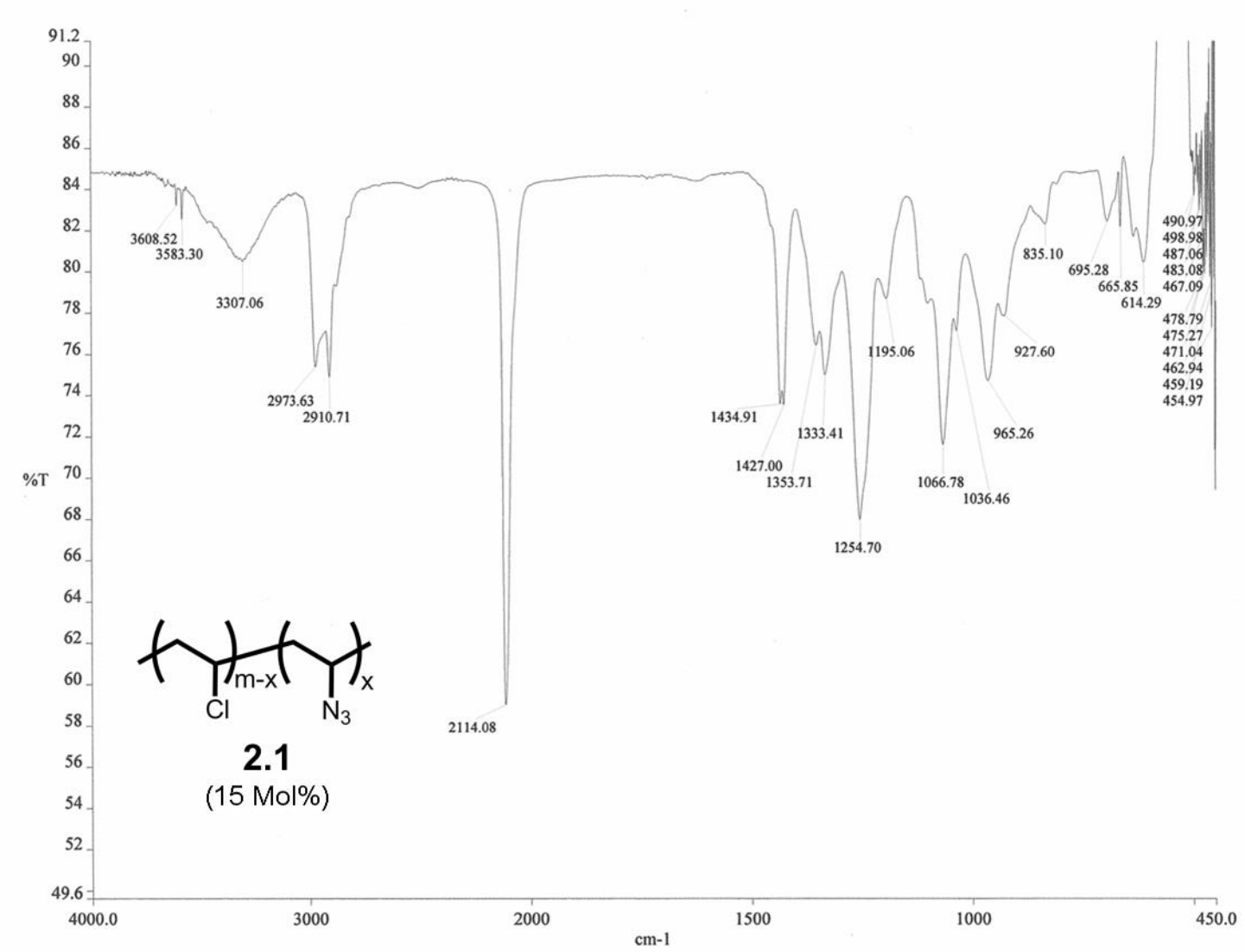
%T
cm-1
3608.52
3583.30
3307.06
2973.63
2910.71
2114.08
1434.91
1427.00
1353.71
1333.41
1254.70
1195.06
1066.78
1036.46
965.26
927.60
835.10
695.28
665.85
614.29
490.97
498.98
487.06
483.08
467.09
478.79
475.27
471.04
462.94
459.19
454.97
m-x
x
Cl
N3
2.1
(15 Mol%)

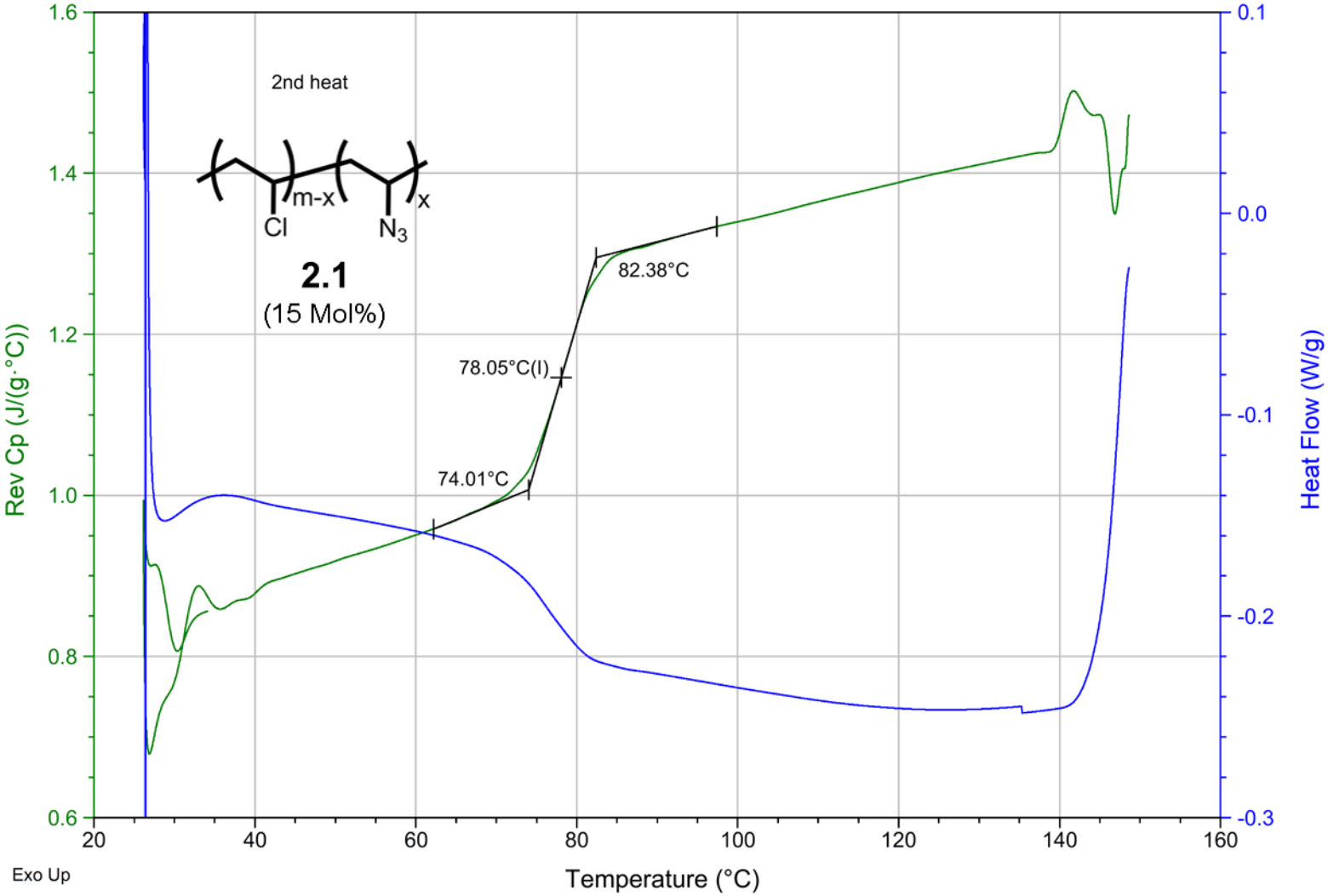
2nd heat
m-x
x
Cl
N3
2.1
(15 Mol%)
82.38°C
78.05°C(I)
74.01°C
Rev Cp (J/(g·°C))
Heat Flow (W/g)
Temperature (°C)
Exo Up
1.6
1.4
1.2
1.0
0.8
0.6
0.1
0.0
-0.1
-0.2
-0.3
20
40
60
80
100
120
140
160

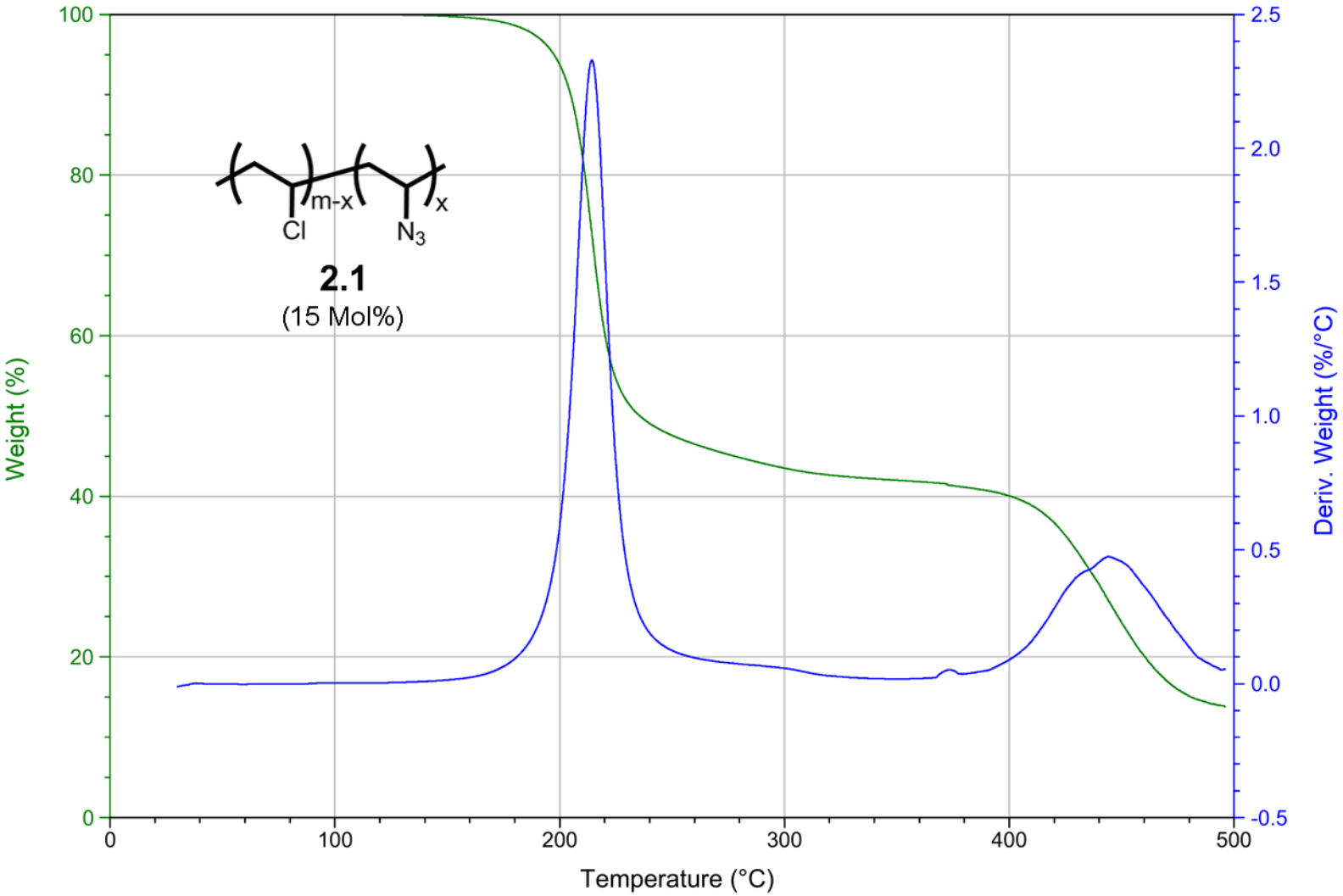
Weight (%)
Deriv. Weight (%/°C)
Temperature (°C)
100
80
60
40
20
0
2.5
2.0
1.5
1.0
0.5
0.0
-0.5
0
100
200
300
400
500
m-x
x
Cl
N3
2.1
(15 Mol%)

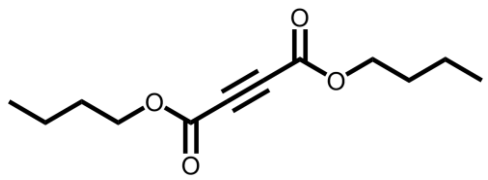

2.2

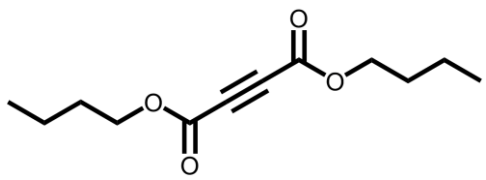
O
O
O
O

2.2

200
190
180
170
160
150
140
130
120
110
100
90
80
70
60
50
40
30
20
10
ppm

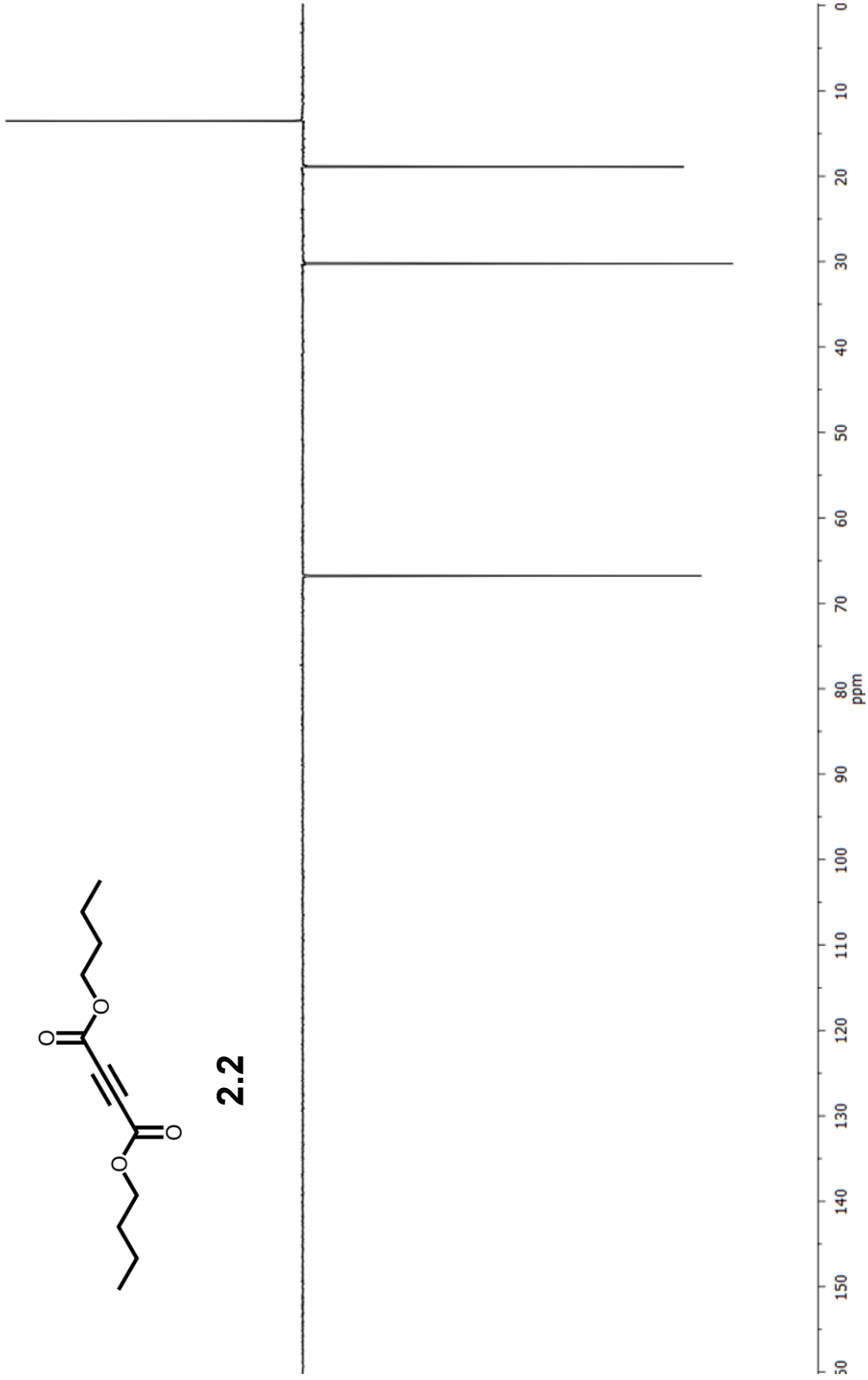
2.2
0
10
20
30
40
50
60
70
80
ppm
90
100
110
120
130
140
150

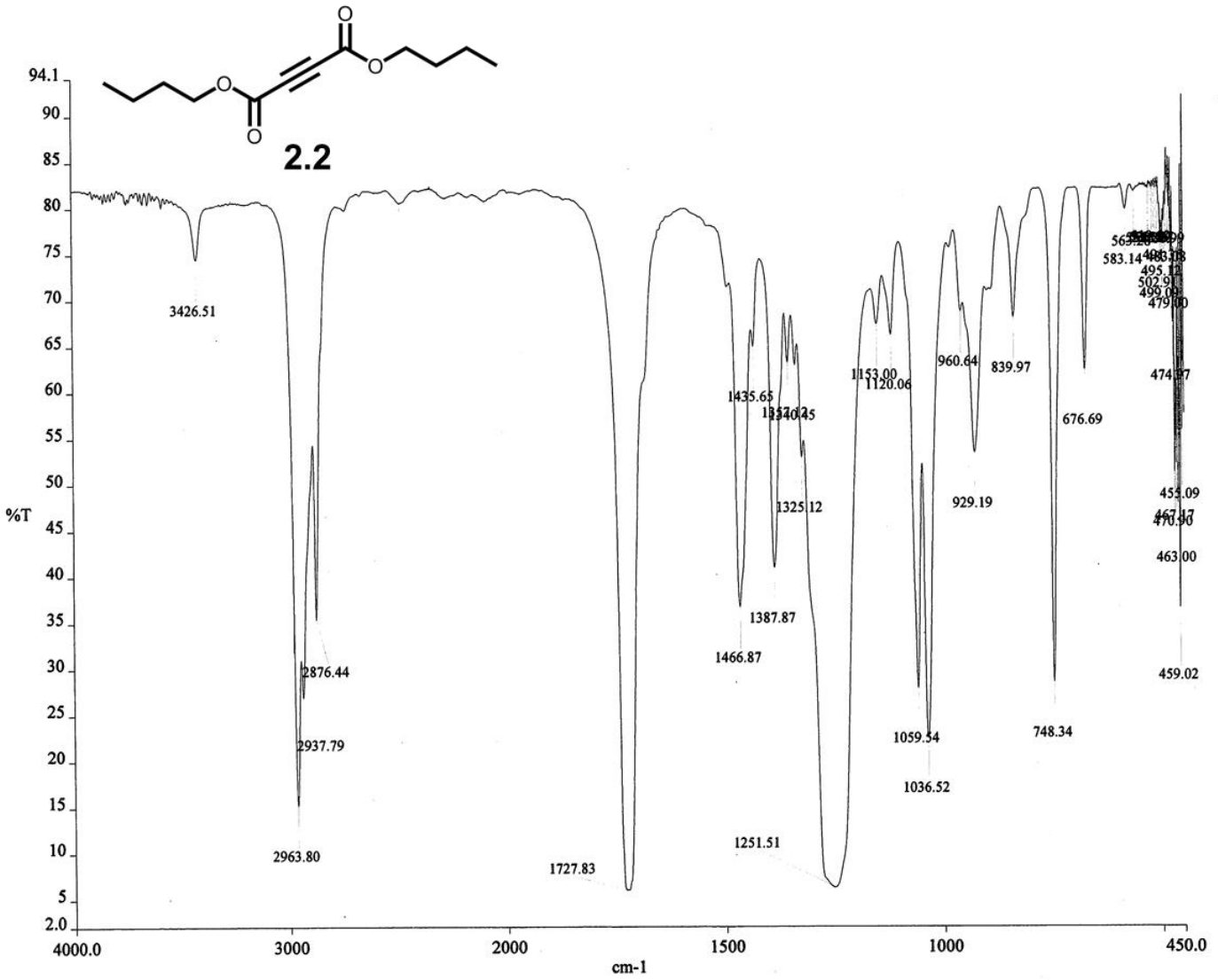
2.2
%T
cm-1
4000.0
3000
2000
1500
1000
450.0
94.1
90
85
80
75
70
65
60
55
50
45
40
35
30
25
20
15
10
5
2.0
3426.51
2963.80
2937.79
2876.44
1727.83
1466.87
1435.65
1387.87
1340.45
1325.12
1251.51
1153.00
1120.06
1059.54
1036.52
960.64
929.19
839.97
748.34
676.69
583.14
495.12
479.00
474.37
463.00
459.02
455.09

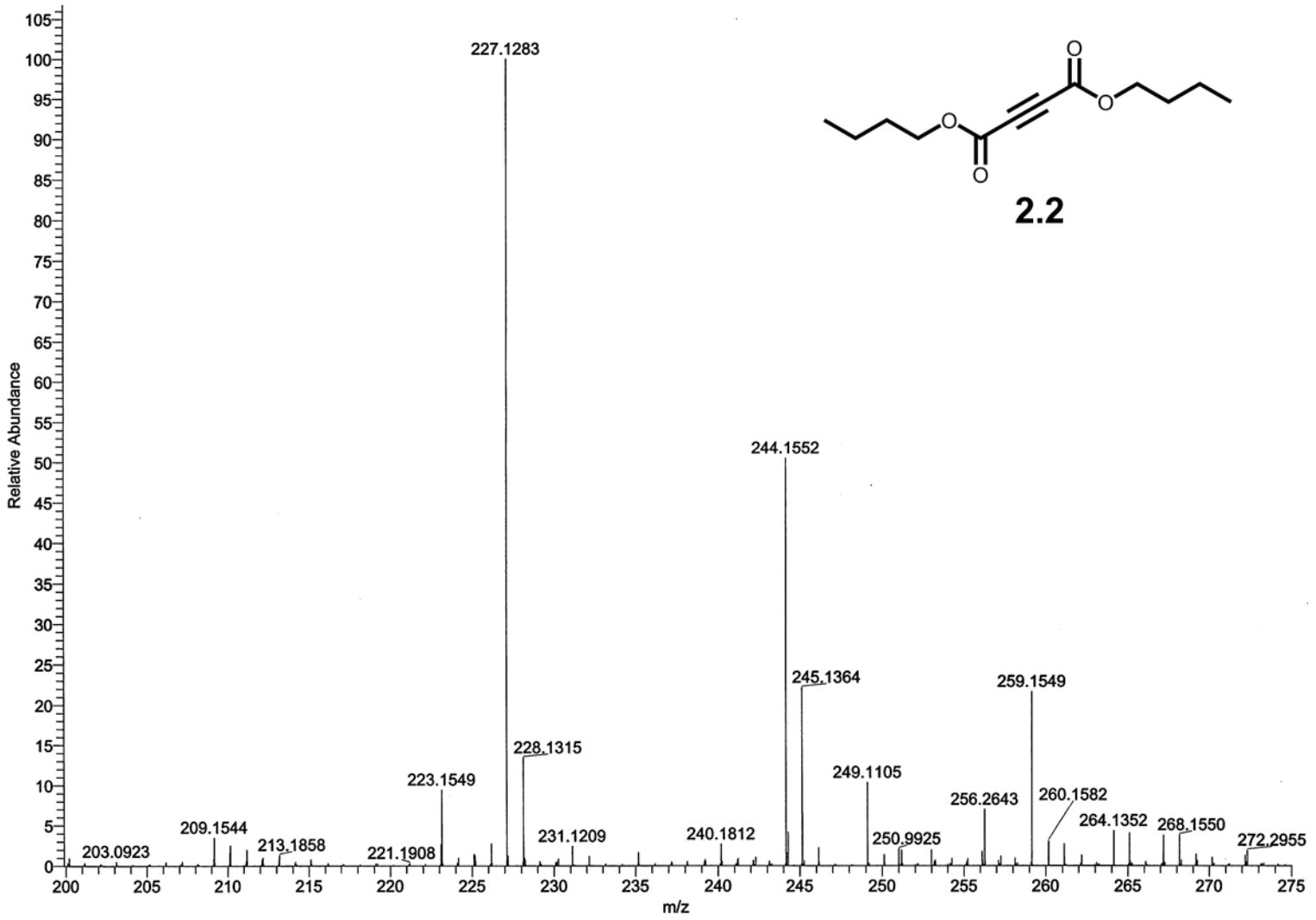
227.1283
244.1552
245.1364
259.1549
228.1315
249.1105
223.1549
256.2643
260.1582
264.1352
268.1550
209.1544
213.1858
231.1209
240.1812
250.9925
272.2955
203.0923
221.1908
Relative Abundance
m/z
2.2

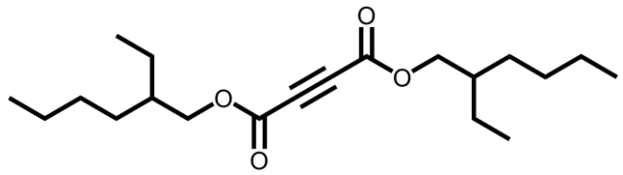

2.3

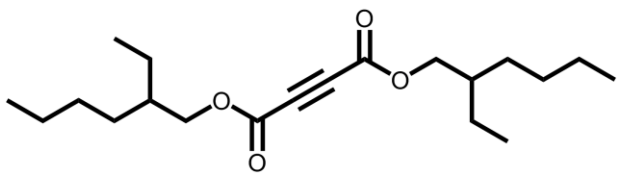

2.3

200
190
180
170
160
150
140
130
120
110
100
90
80
70
60
50
40
30
20
10
ppm

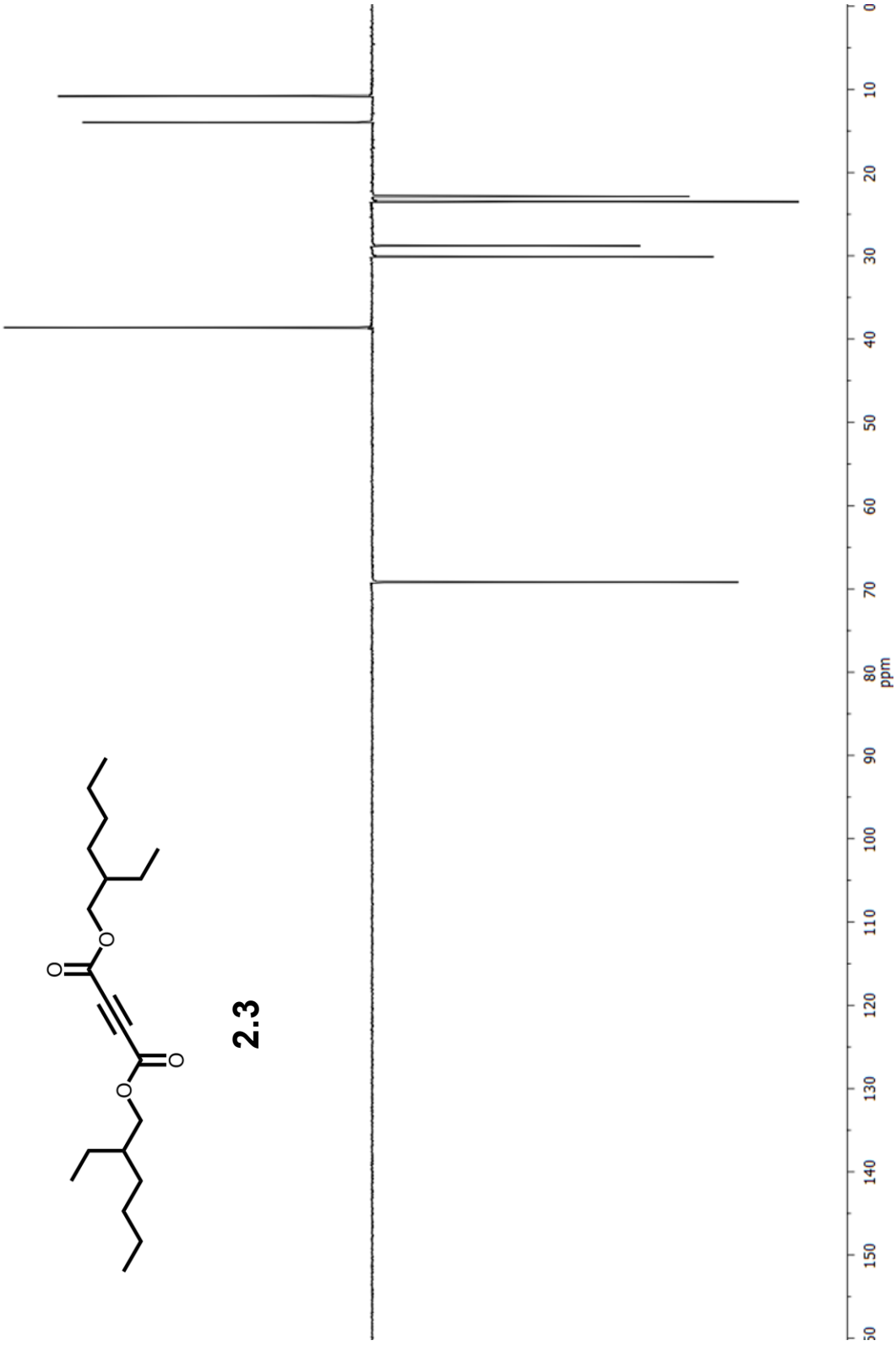
2.3
ppm
0
10
20
30
40
50
60
70
80
90
100
110
120
130
140
150

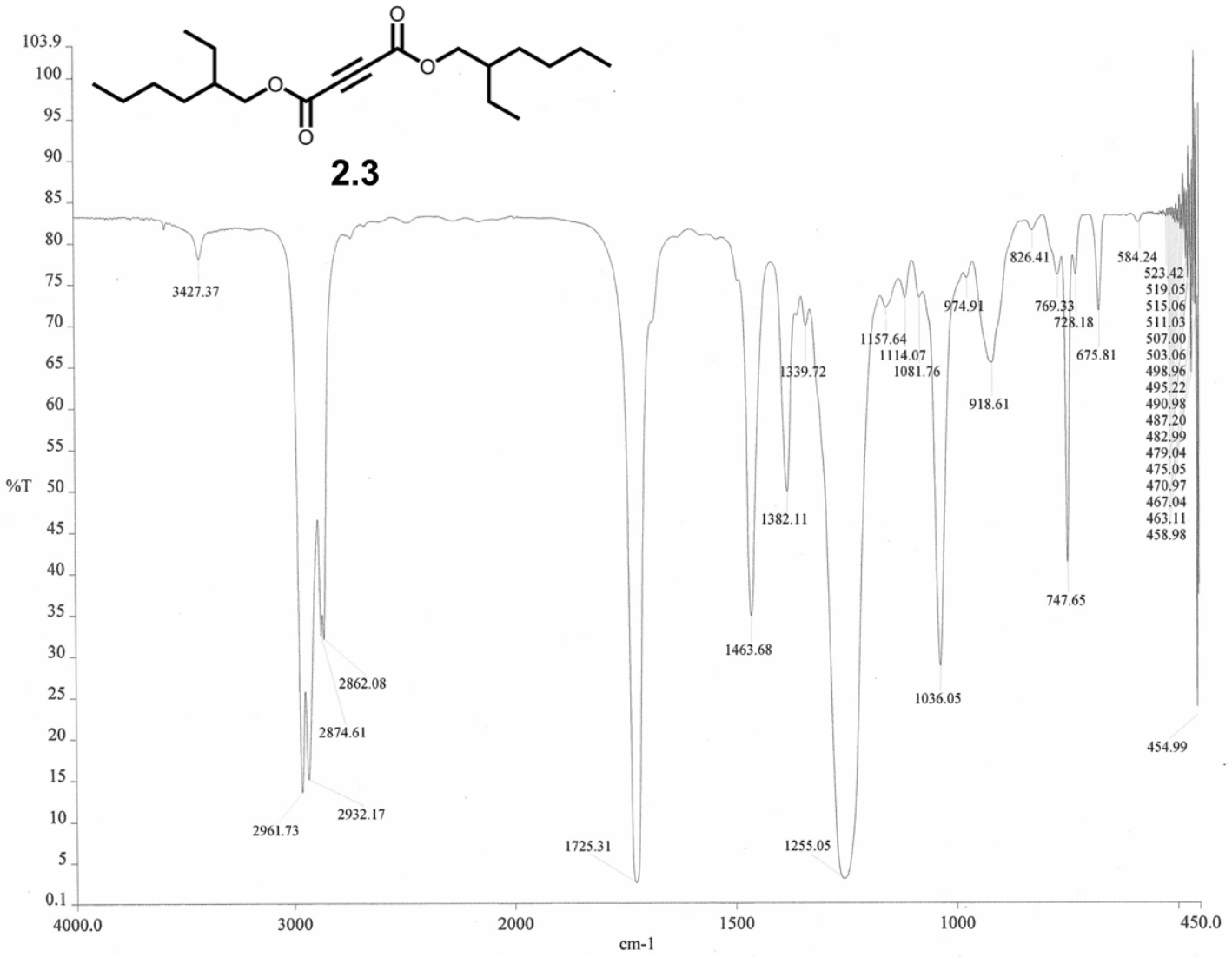
2.3
%T
cm-1
103.9
100
95
90
85
80
75
70
65
60
55
50
45
40
35
30
25
20
15
10
5
0.1
4000.0
3000
2000
1500
1000
450.0
3427.37
2961.73
2932.17
2874.61
2862.08
1725.31
1463.68
1382.11
1339.72
1255.05
1157.64
1114.07
1081.76
1036.05
974.91
918.61
826.41
769.33
747.65
728.18
675.81
584.24
523.42
519.05
515.06
511.03
507.00
503.06
498.96
495.22
490.98
487.20
482.99
479.04
475.05
470.97
467.04
463.11
458.98
454.99

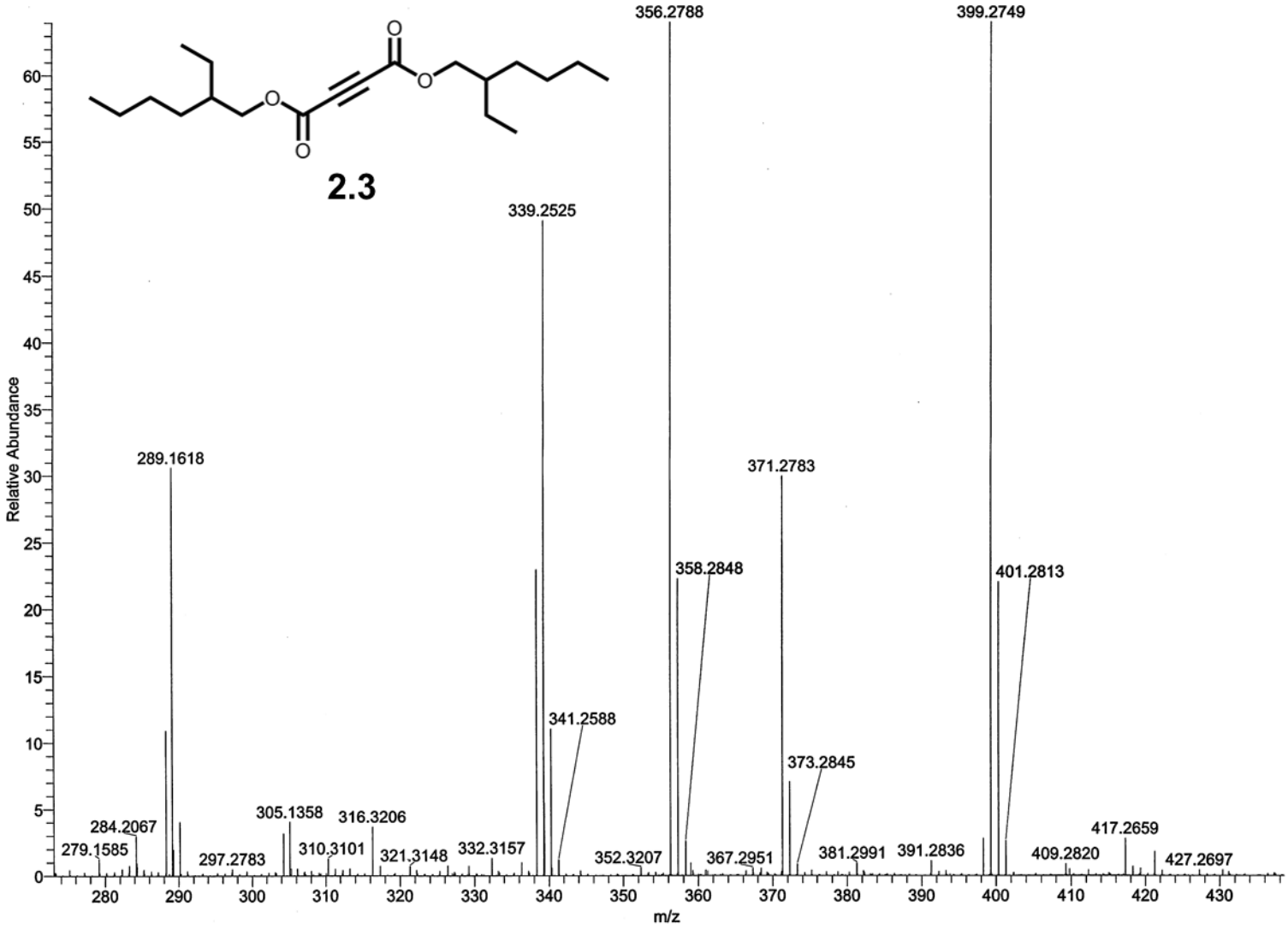
2.3
Relative Abundance
m/z
356.2788
399.2749
339.2525
289.1618
371.2783
358.2848
401.2813
341.2588
373.2845
284.2067
279.1585
305.1358
316.3206
297.2783
310.3101
321.3148
332.3157
352.3207
367.2951
381.2991
391.2836
409.2820
417.2659
427.2697

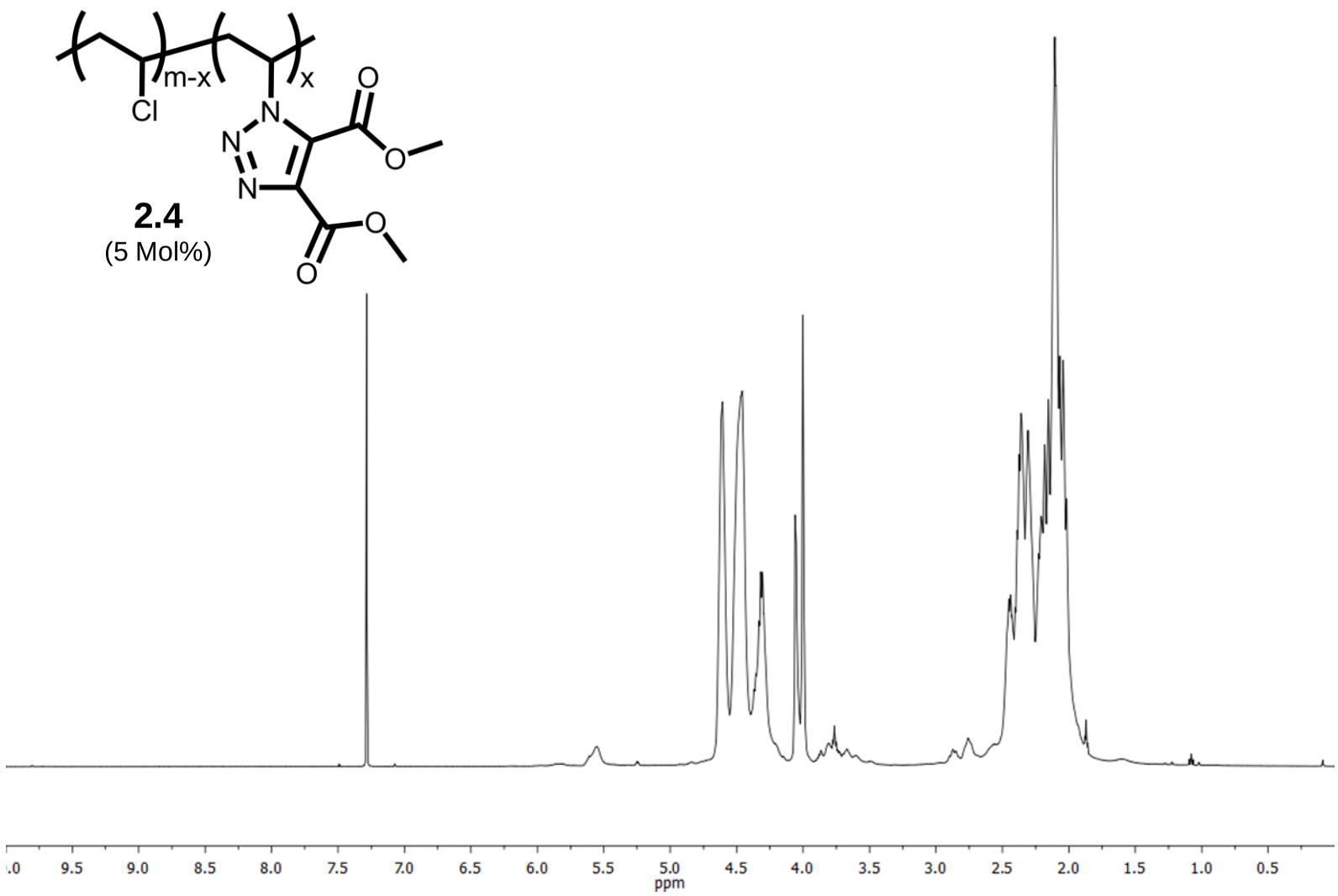
m-x
x
Cl
N
N
N
O
O
O
O
2.4
(5 Mol%)
9.5
9.0
8.5
8.0
7.5
7.0
6.5
6.0
5.5
5.0
4.5
4.0
3.5
3.0
2.5
2.0
1.5
1.0
0.5
ppm

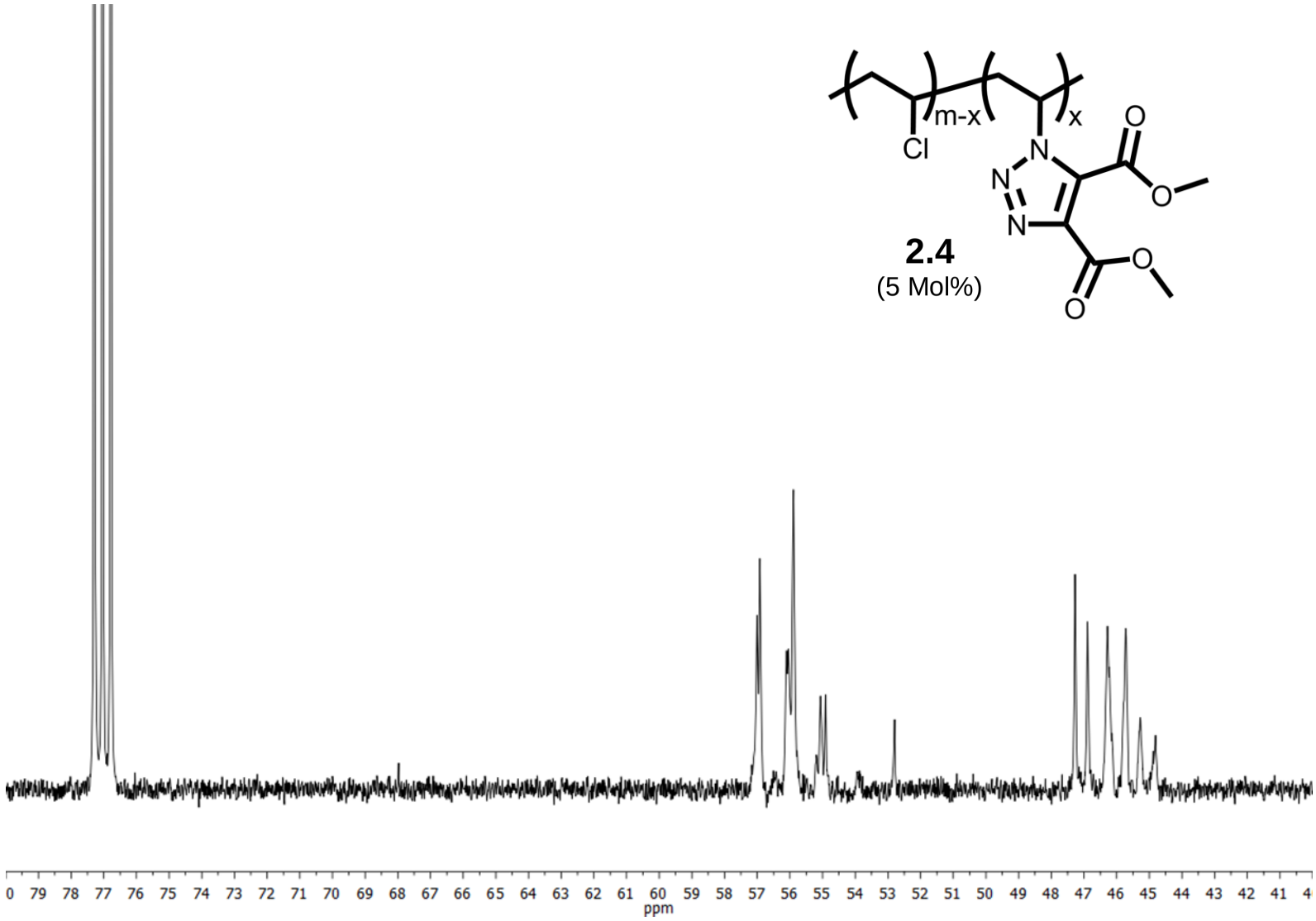
m-x
x
Cl
N
N
N
O
O
O
O
2.4
(5 Mol%)
0 79 78 77 76 75 74 73 72 71 70 69 68 67 66 65 64 63 62 61 60 59 58 57 56 55 54 53 52 51 50 49 48 47 46 45 44 43 42 41 4
ppm

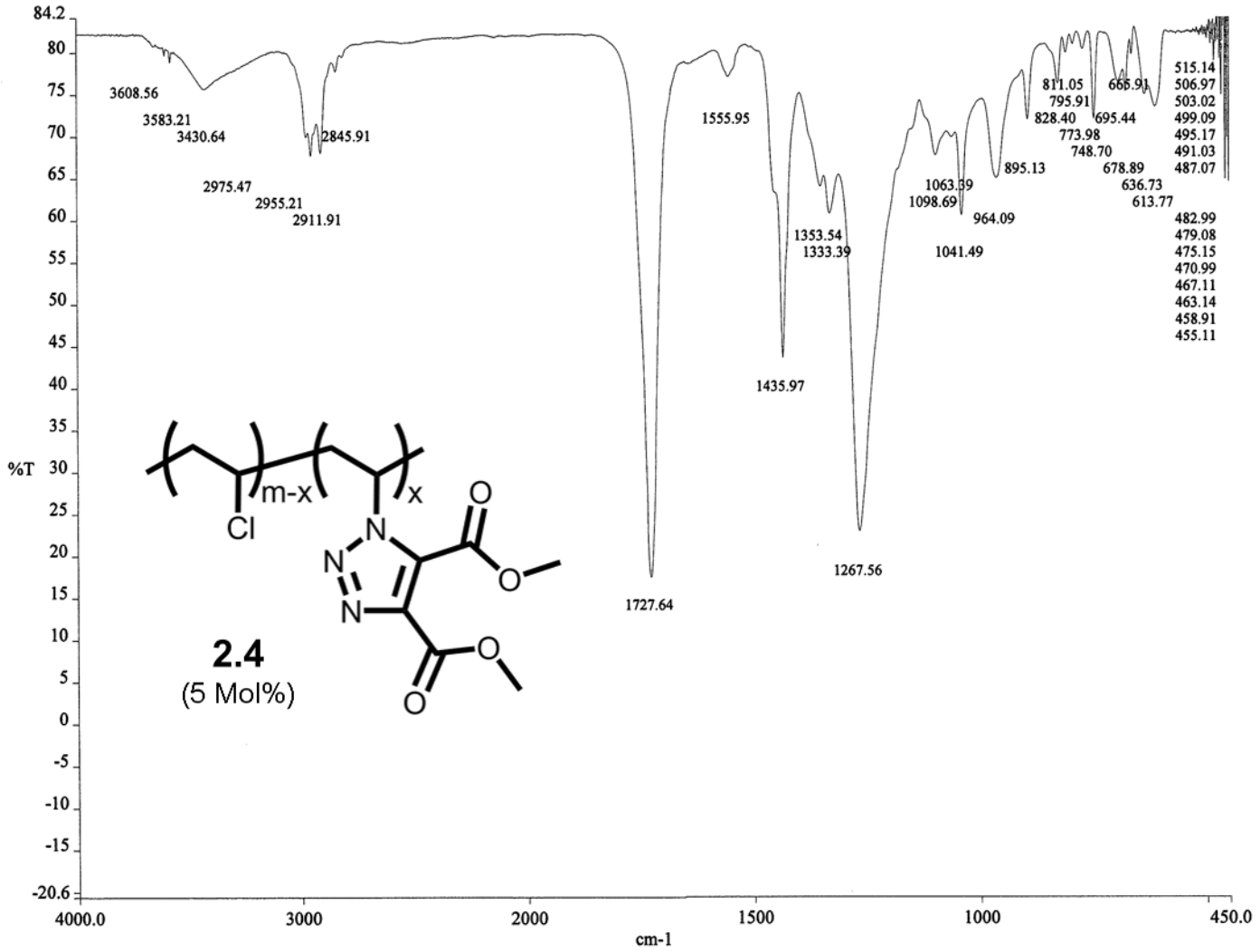
84.2
80
75
70
65
60
55
50
45
40
35
%T 30
25
20
15
10
5
0
-5
-10
-15
-20.6
4000.0
3000
2000
1500
1000
450.0
cm-1
3608.56
3583.21
3430.64
2975.47
2955.21
2911.91
2845.91
1727.64
1555.95
1435.97
1353.54
1333.39
1267.56
1098.69
1063.39
1041.49
964.09
895.13
828.40
811.05
795.91
773.98
748.70
695.44
678.89
665.91
636.73
613.77
515.14
506.97
503.02
499.09
495.17
491.03
487.07
482.99
479.08
475.15
470.99
467.11
463.14
458.91
455.11
m-x
x
Cl
N
N
N
O
O
O
O
2.4
(5 Mol%)

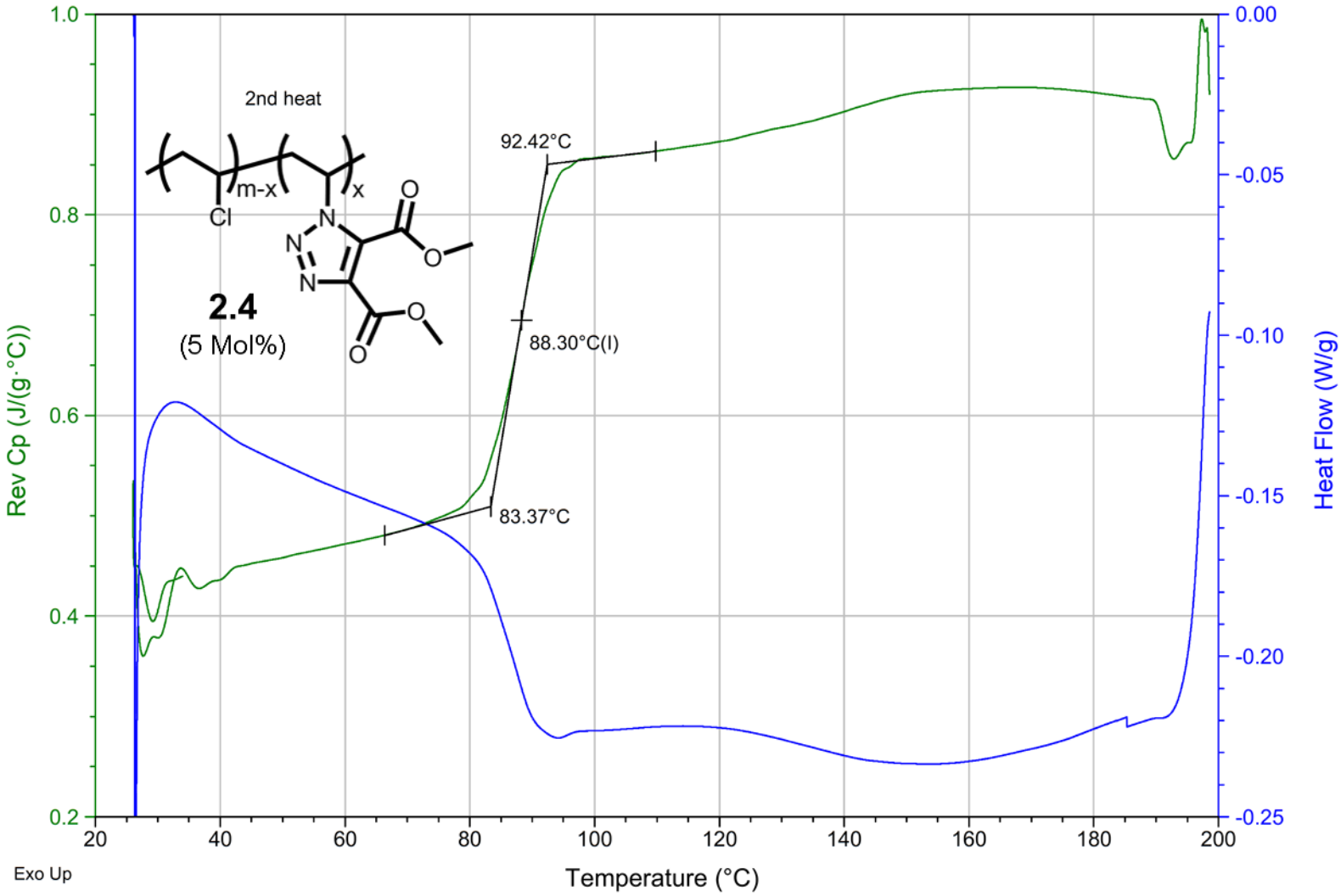
2nd heat
m-x
x
Cl
N
N
N
O
O
O
O
2.4
(5 Mol%)
92.42°C
88.30°C(I)
83.37°C
Rev Cp (J/(g·°C))
Heat Flow (W/g)
Temperature (°C)
Exo Up
1.0
0.8
0.6
0.4
0.2
0.00
-0.05
-0.10
-0.15
-0.20
-0.25
20
40
60
80
100
120
140
160
180
200

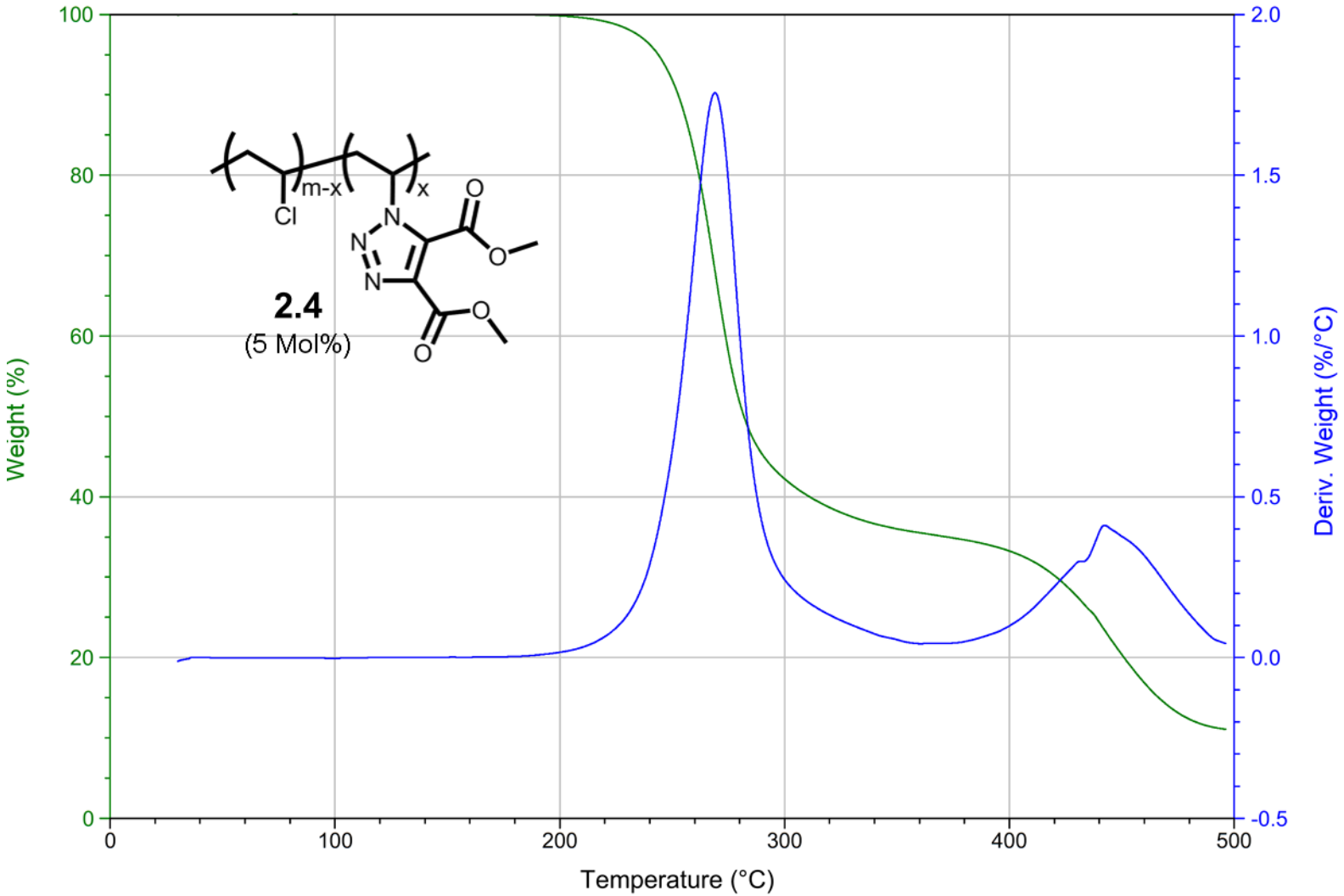
Weight (%)
Deriv. Weight (%/°C)
Temperature (°C)
100
80
60
40
20
0
2.0
1.5
1.0
0.5
0.0
-0.5
0
100
200
300
400
500
m-x
x
Cl
N
N
N
O
O
O
O
2.4
(5 Mol%)

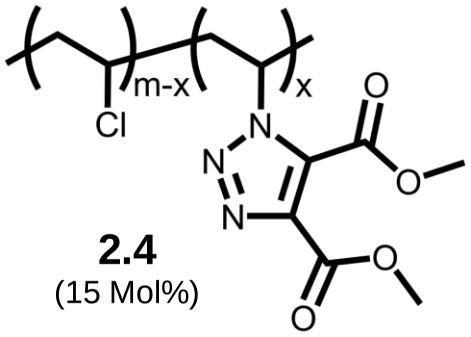
m-x
x
Cl
N
N
N
O
O
O
O

2.4
(15 Mol%)

9.5
9.0
8.5
8.0
7.5
7.0
6.5
6.0
5.5
5.0
4.5
4.0
3.5
3.0
2.5
2.0
1.5
1.0
0.5
ppm

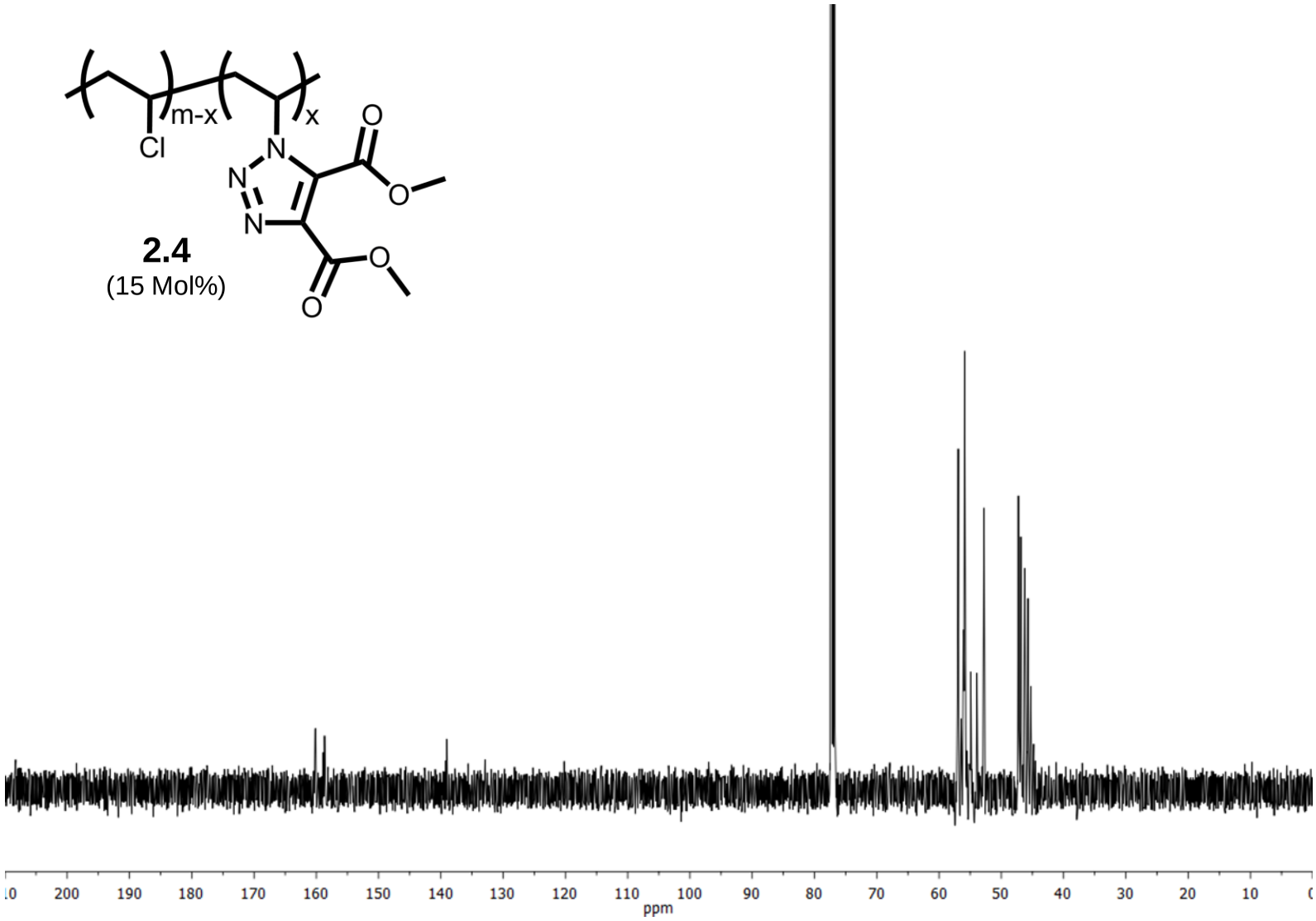
m-x
x
Cl
N
N
N
O
O
O
O
2.4
(15 Mol%)
ppm

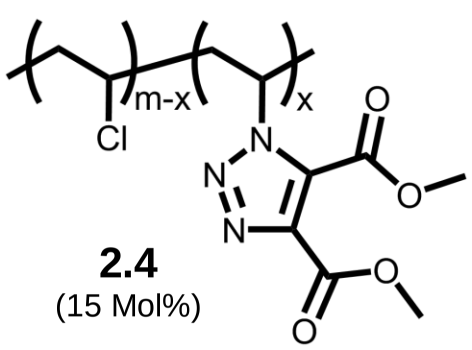
m-x
x
Cl
N
N
N
O
O
O
O

2.4
(15 Mol%)

150
140
130
120
110
100
90
80
70
60
50
40
30
20
10
0
ppm

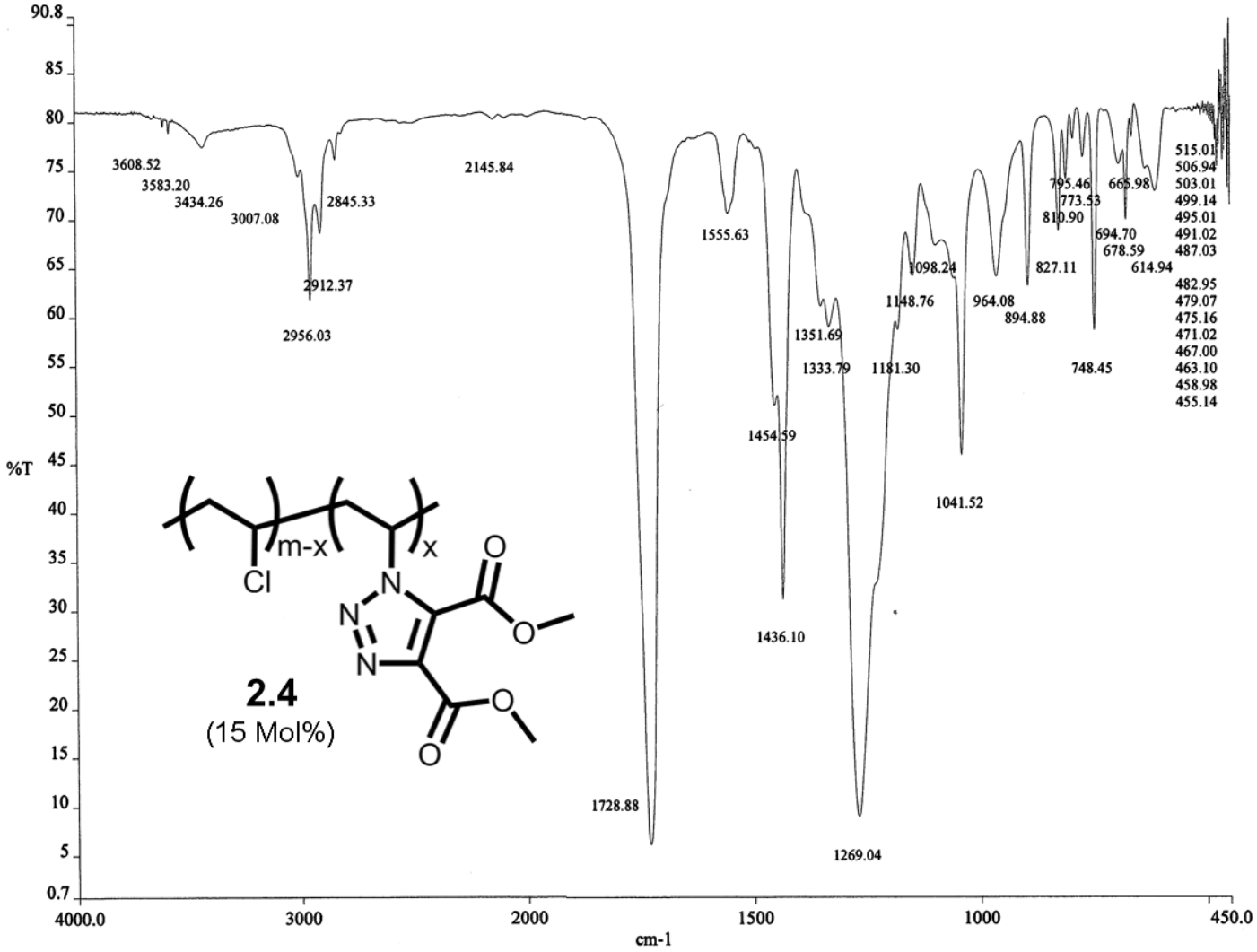
90.8
85
80
75
70
65
60
55
50
45
40
35
30
25
20
15
10
5
0.7
%T
4000.0
3000
2000
1500
1000
450.0
cm-1
3608.52
3583.20
3434.26
3007.08
2845.33
2912.37
2956.03
2145.84
1555.63
1454.59
1436.10
1351.69
1333.79
1728.88
1269.04
1181.30
1148.76
1098.24
1041.52
964.08
894.88
827.11
795.46
773.53
748.45
694.70
678.59
665.98
614.94
515.01
506.94
503.01
499.14
495.01
491.02
487.03
482.95
479.07
475.16
471.02
467.00
463.10
458.98
455.14
m-x
x
Cl
N
N
N
O
O
O
O
2.4
(15 Mol%)

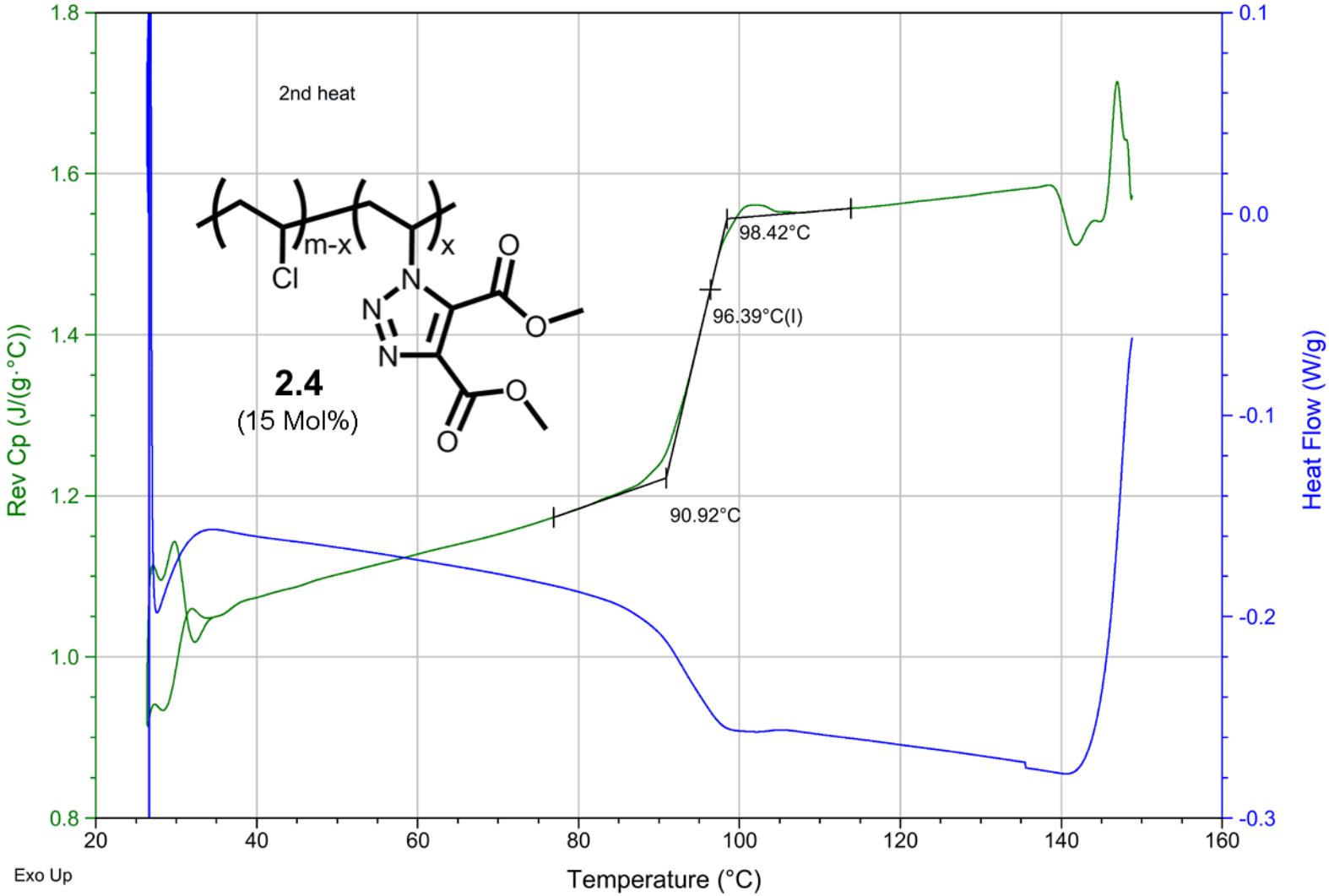
2nd heat
2.4
(15 Mol%)
m-x
x
Cl
98.42°C
96.39°C(I)
90.92°C
Rev Cp (J/(g·°C))
Heat Flow (W/g)
Temperature (°C)
Exo Up
1.8
1.6
1.4
1.2
1.0
0.8
0.1
0.0
-0.1
-0.2
-0.3
20
40
60
80
100
120
140
160

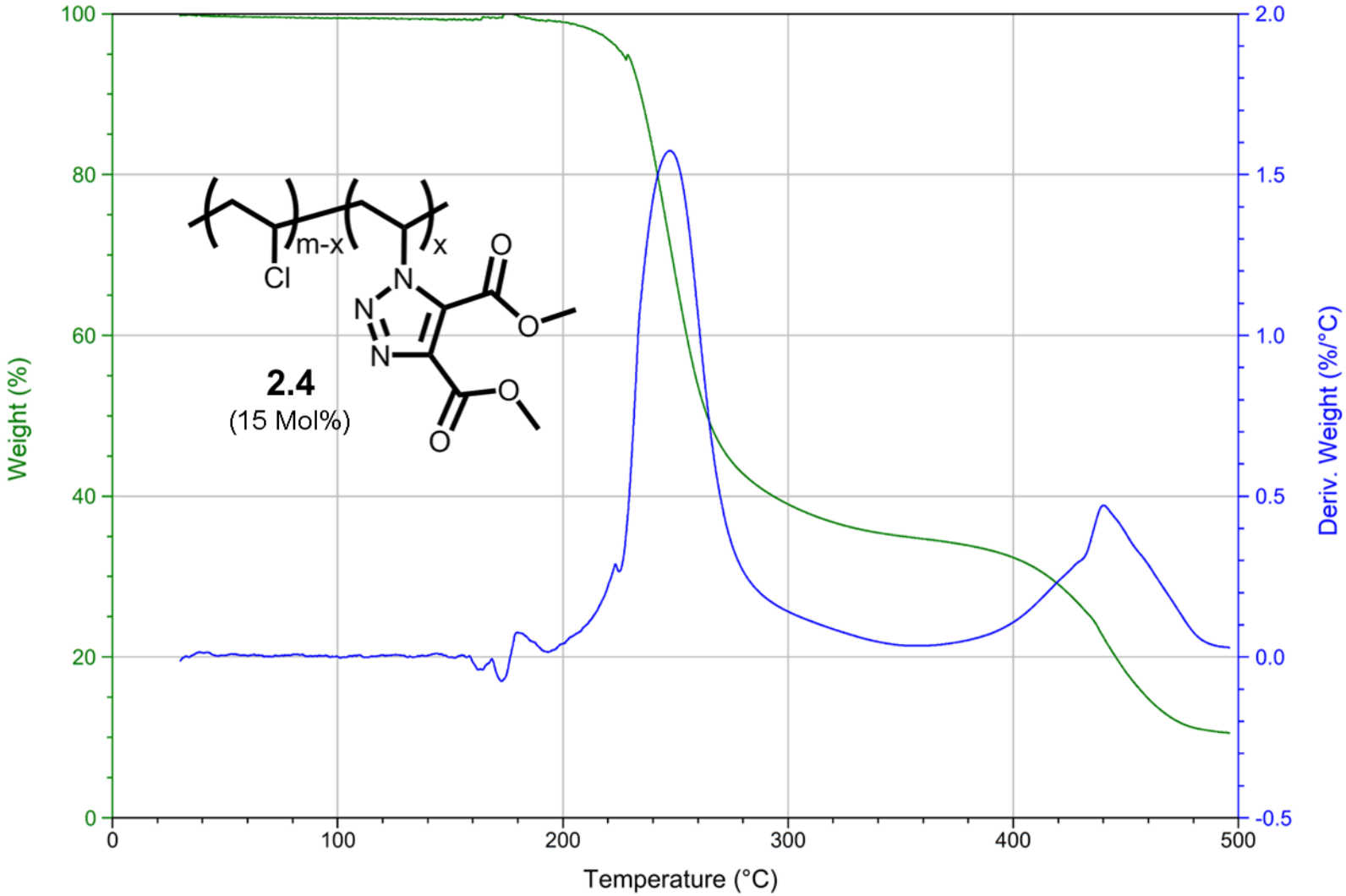
Weight (%)
Deriv. Weight (%/°C)
Temperature (°C)
0
20
40
60
80
100
-0.5
0.0
0.5
1.0
1.5
2.0
0
100
200
300
400
500
m-x
x
Cl
N
N
N
O
O
O
O
2.4
(15 Mol%)

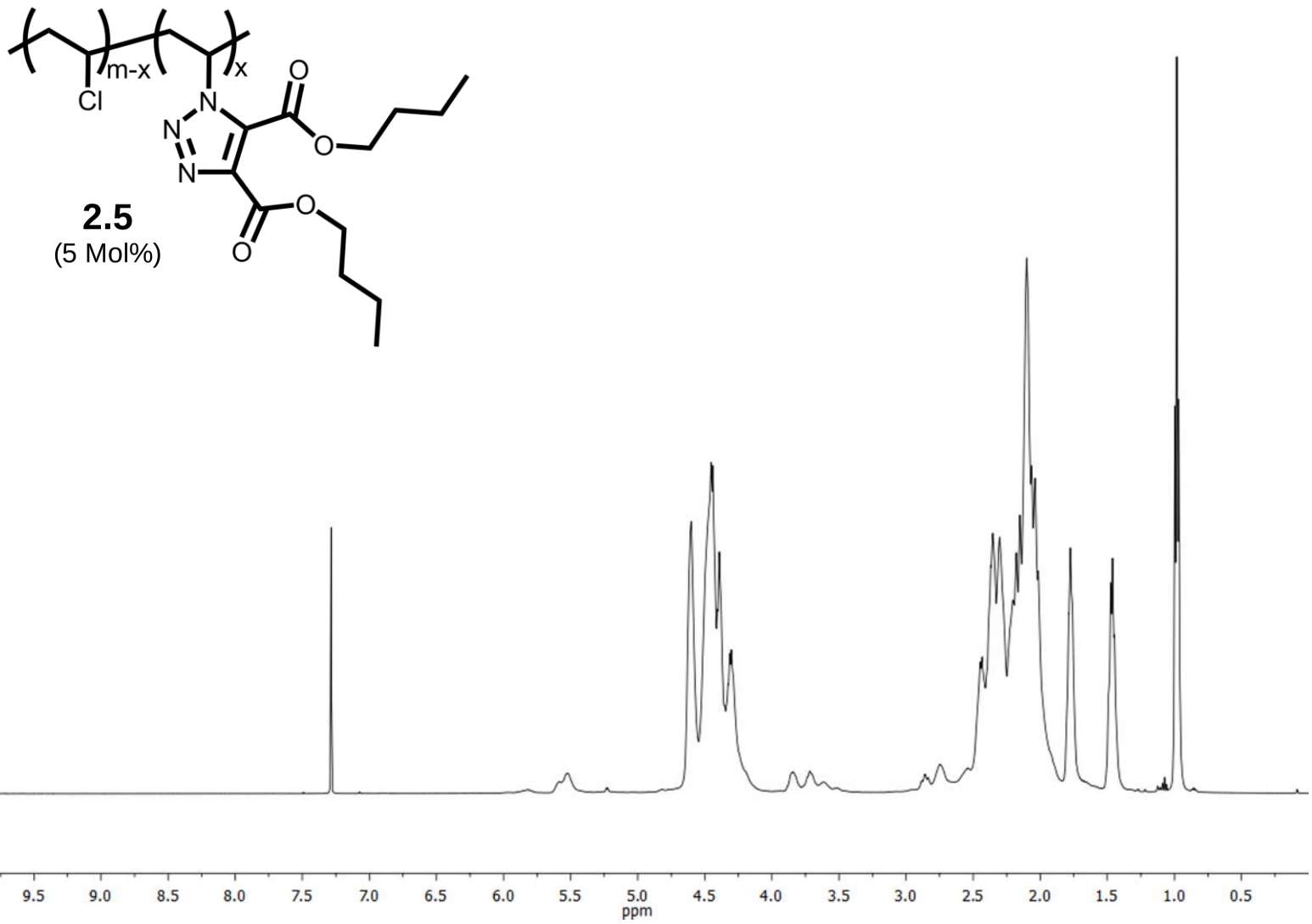
m-x
x
Cl
N
N
N
O
O
O
O
2.5
(5 Mol%)
9.5
9.0
8.5
8.0
7.5
7.0
6.5
6.0
5.5
5.0
4.5
4.0
3.5
3.0
2.5
2.0
1.5
1.0
0.5
ppm

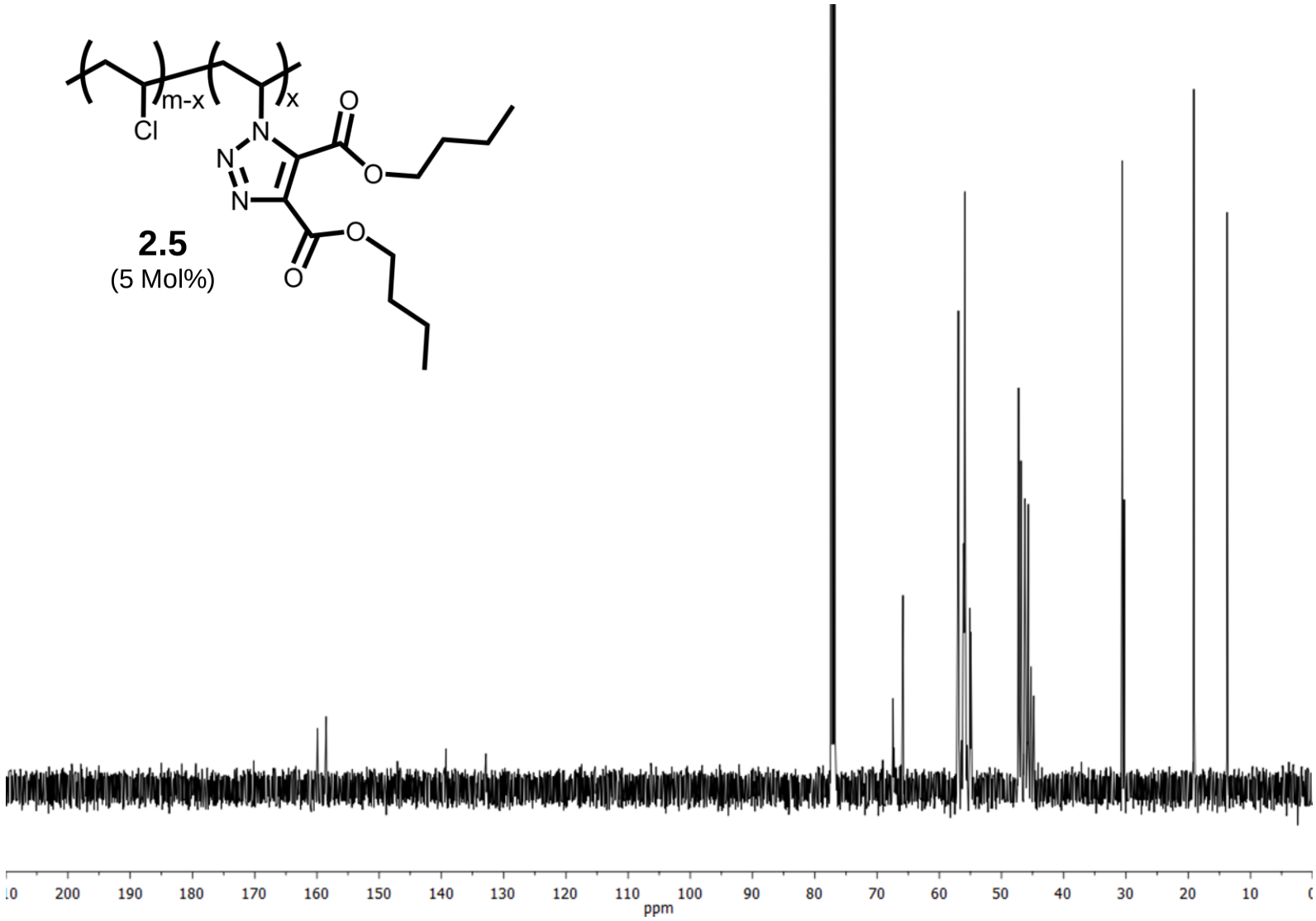
m-x
x
Cl
N
N
N
O
O
O
O
2.5
(5 Mol%)
200
190
180
170
160
150
140
130
120
110
100
90
80
70
60
50
40
30
20
10
ppm

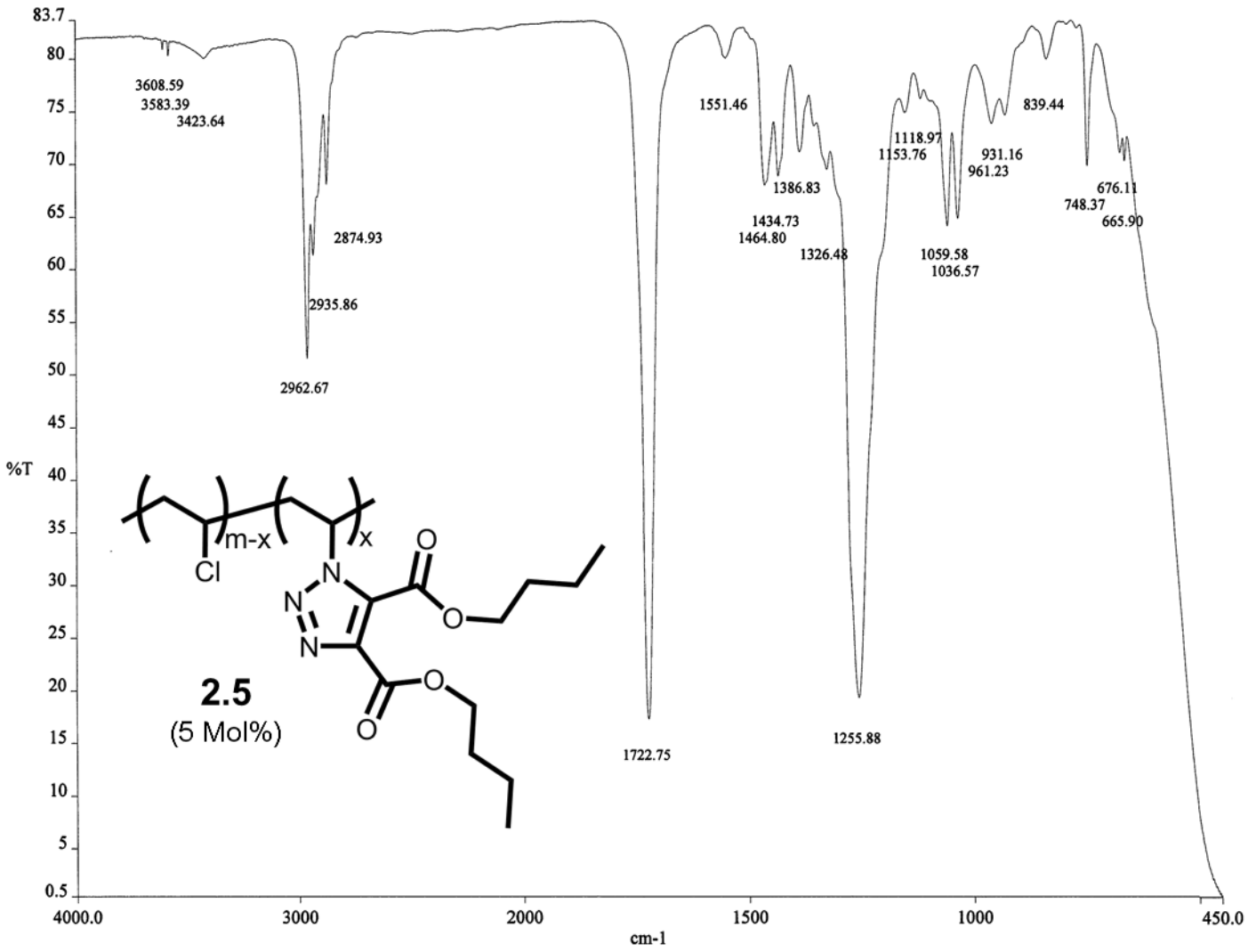
83.7
80
75
70
65
60
55
50
45
40
35
30
25
20
15
10
5
0.5
%T
4000.0
3000
2000
1500
1000
450.0
cm-1
3608.59
3583.39
3423.64
2874.93
2935.86
2962.67
1722.75
1551.46
1386.83
1434.73
1464.80
1326.48
1255.88
1118.97
1153.76
1059.58
1036.57
931.16
961.23
839.44
676.11
748.37
665.90
m-x
x
Cl
N
N
N
O
O
O
O
2.5
(5 Mol%)

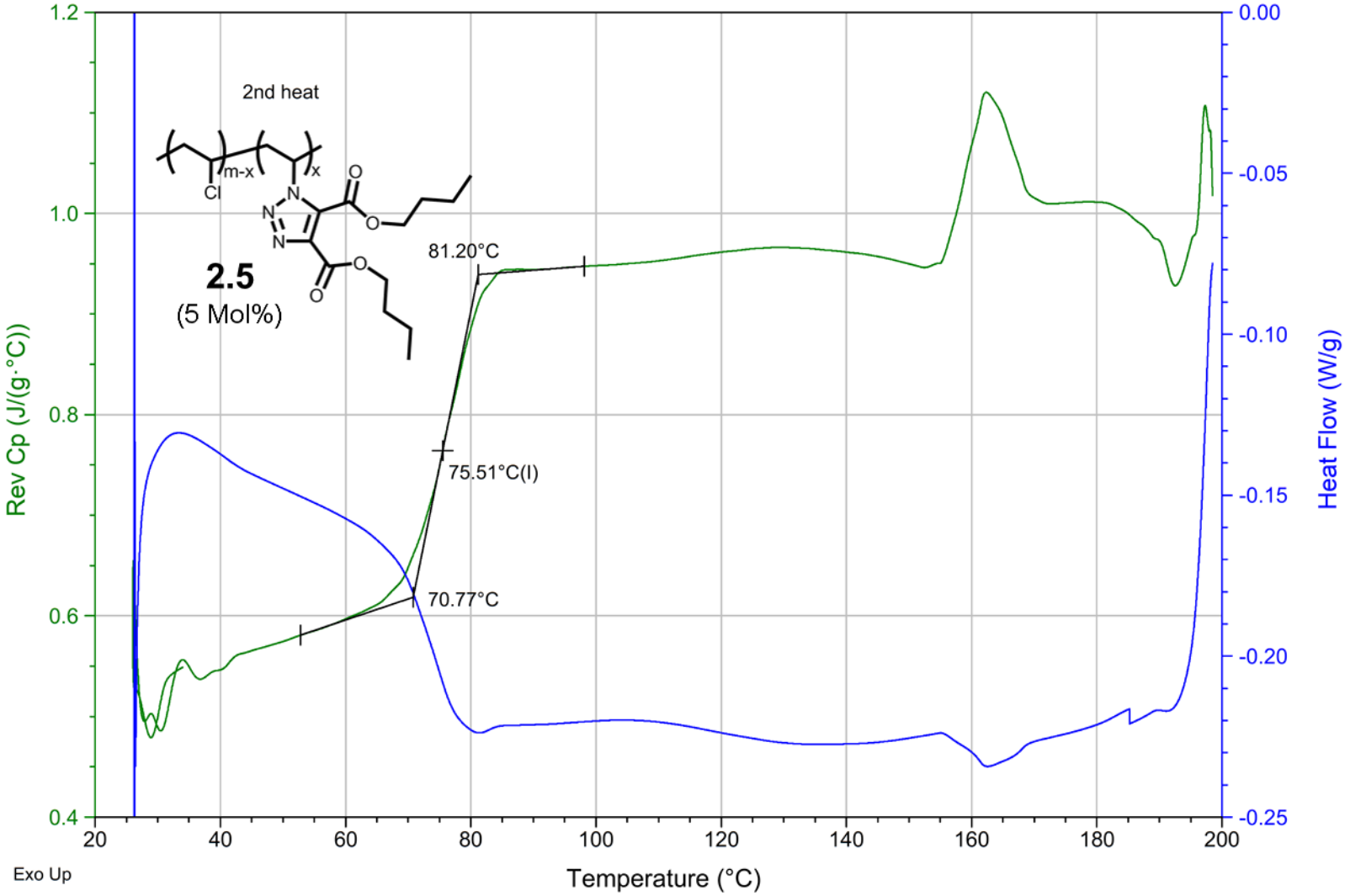
2nd heat
m-x
x
Cl
2.5
(5 Mol%)
81.20°C
75.51°C(I)
70.77°C
Rev Cp (J/(g·°C))
Heat Flow (W/g)
Temperature (°C)
Exo Up
1.2
1.0
0.8
0.6
0.4
0.00
-0.05
-0.10
-0.15
-0.20
-0.25
20
40
60
80
100
120
140
160
180
200

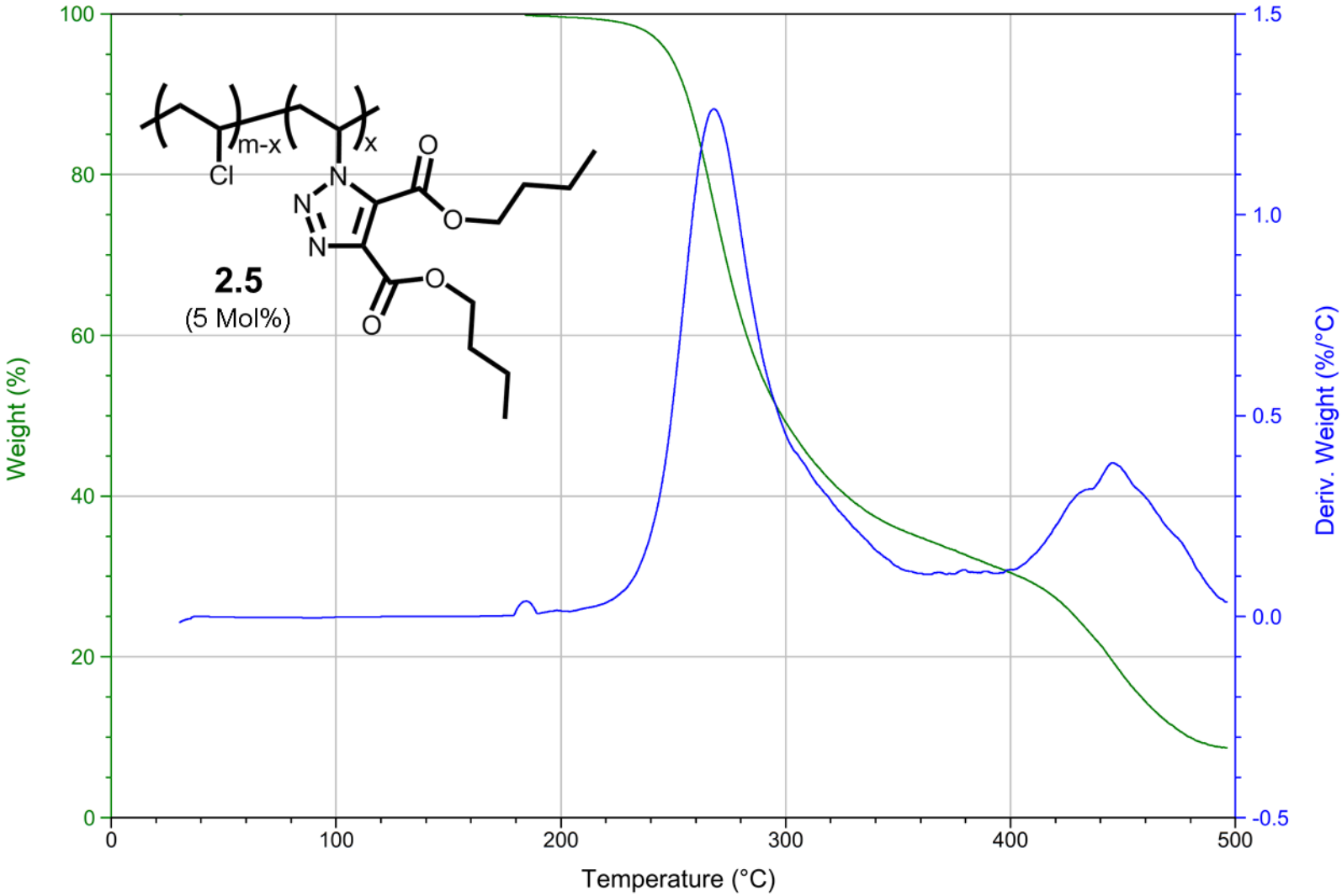
Weight (%)
Deriv. Weight (%/°C)
Temperature (°C)
100
80
60
40
20
0
1.5
1.0
0.5
0.0
-0.5
0
100
200
300
400
500
m-x
x
Cl
N
N
N
O
O
O
O
2.5
(5 Mol%)

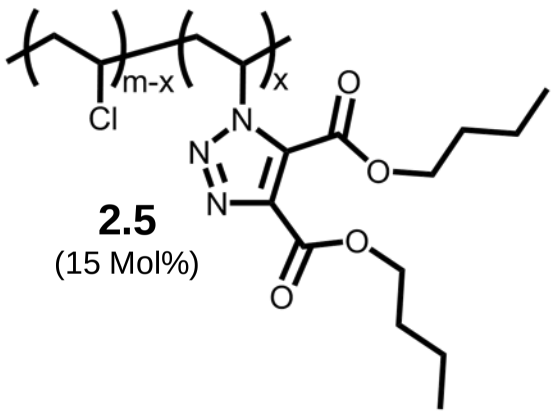
m-x
x
Cl
N
N
N
O
O
O
O

2.5
(15 Mol%)

9.5
9.0
8.5
8.0
7.5
7.0
6.5
6.0
5.5
5.0
4.5
4.0
3.5
3.0
2.5
2.0
1.5
1.0
0.5
ppm

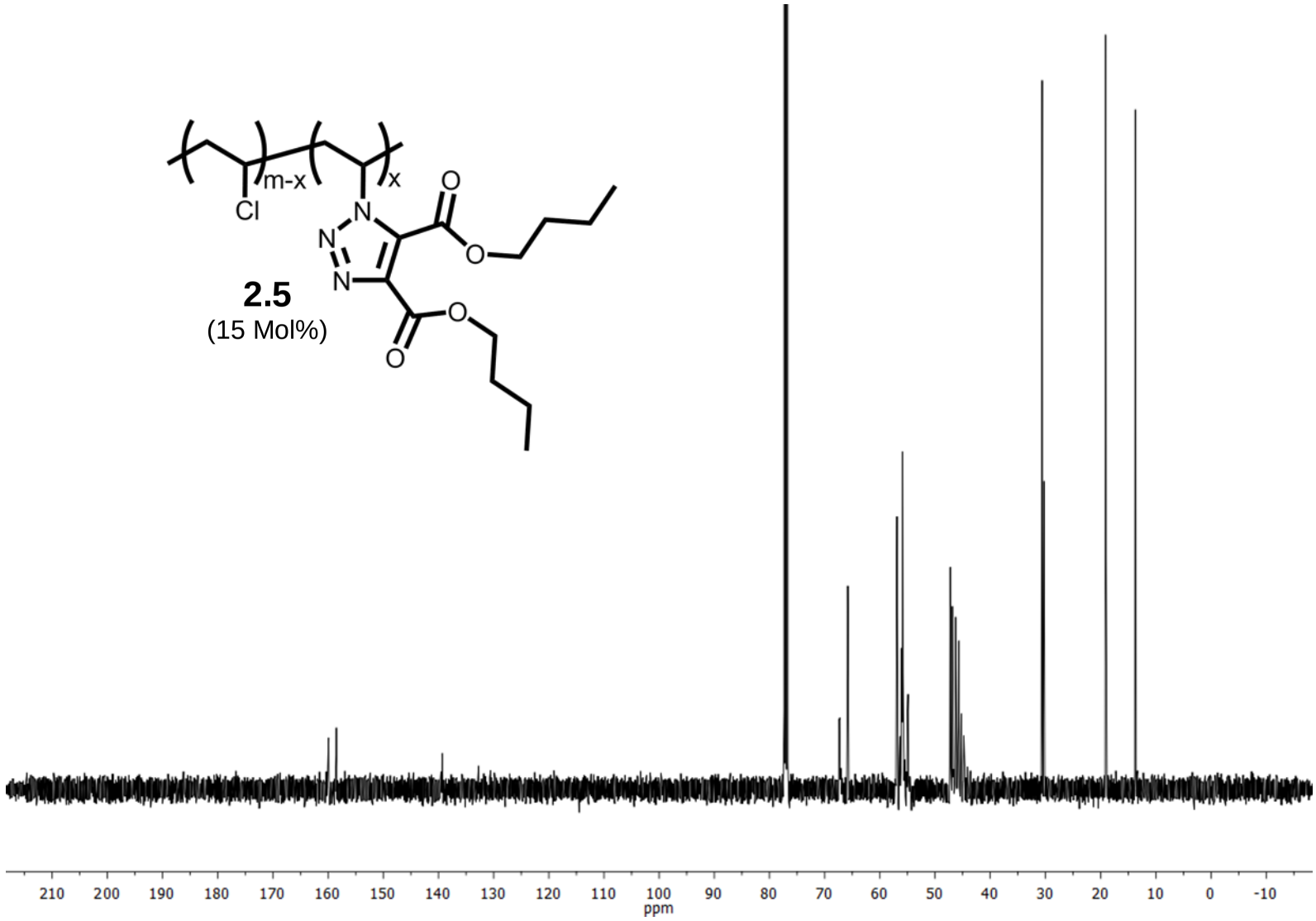
m-x
x
Cl
N
N
N
O
O
O
O
2.5
(15 Mol%)
210 200 190 180 170 160 150 140 130 120 110 100 90 80 70 60 50 40 30 20 10 0 -10
ppm

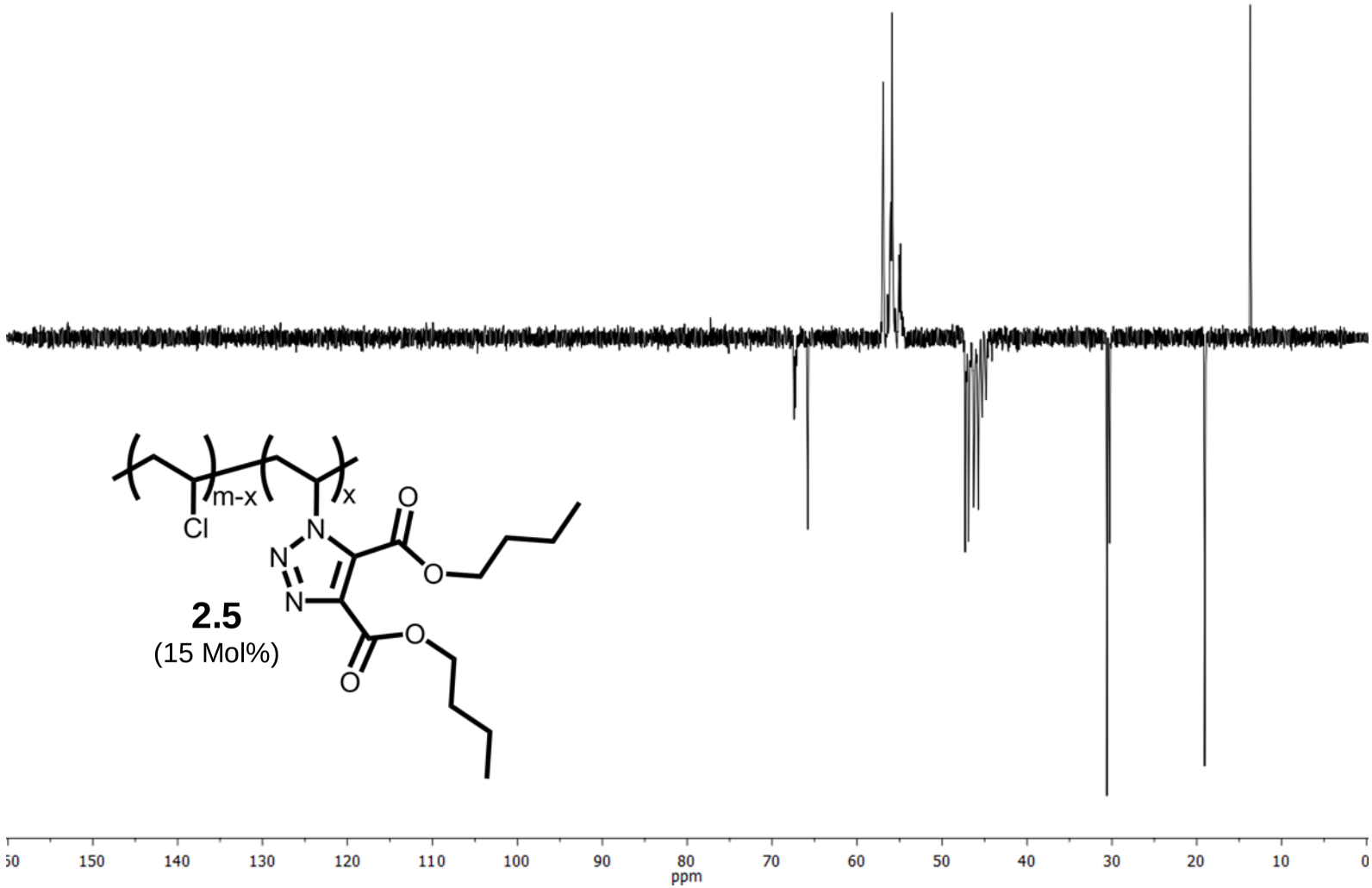
m-x
x
Cl
N
N
N
O
O
O
O
2.5
(15 Mol%)
150
140
130
120
110
100
90
80
70
60
50
40
30
20
10
ppm

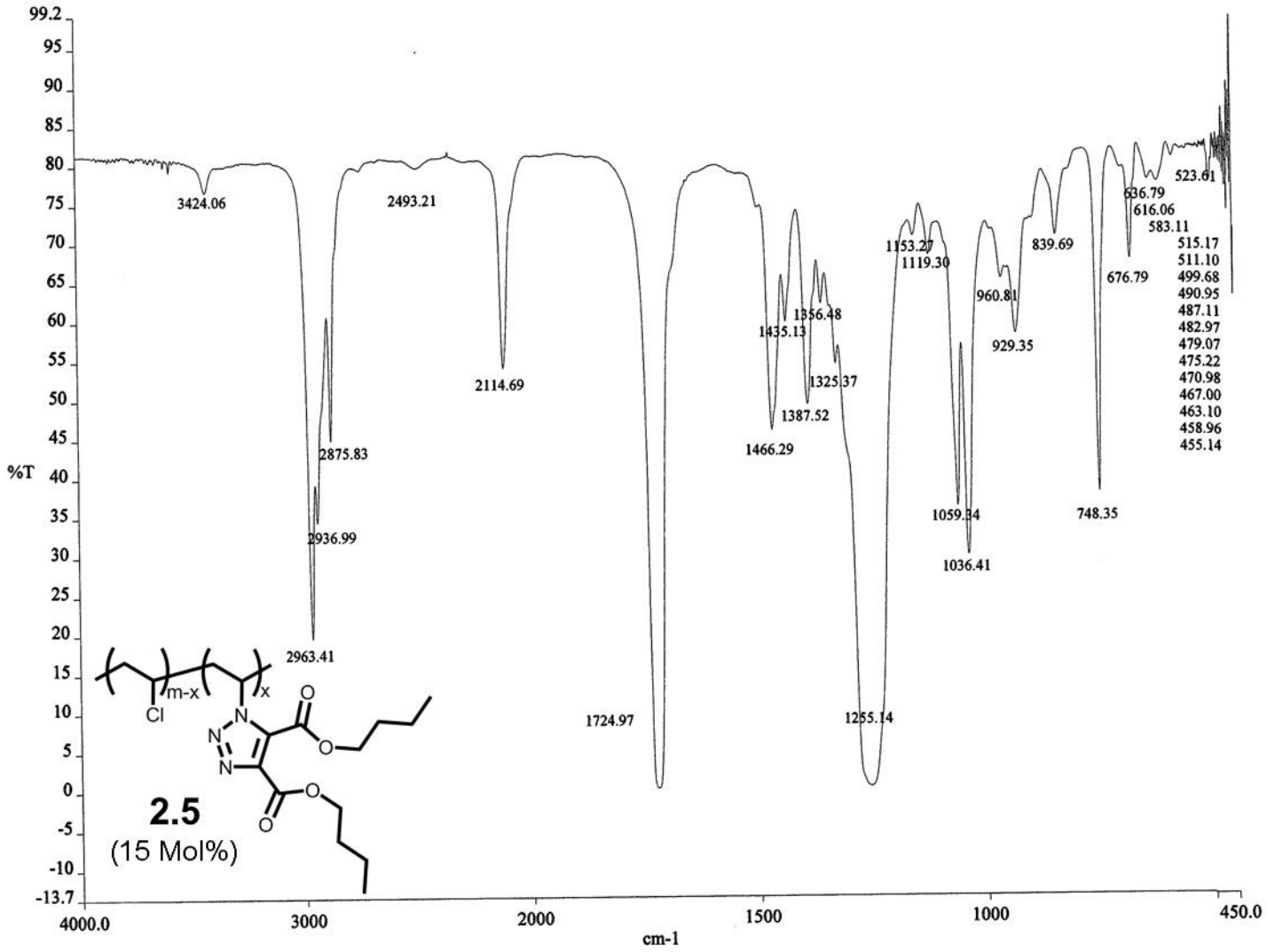
%T
cm-1
4000.0
3000
2000
1500
1000
450.0
99.2
95
90
85
80
75
70
65
60
55
50
45
40
35
30
25
20
15
10
5
0
-5
-10
-13.7
3424.06
2963.41
2936.99
2875.83
2493.21
2114.69
1724.97
1466.29
1435.13
1387.52
1356.48
1325.37
1255.14
1153.27
1119.30
1059.34
1036.41
960.81
929.35
839.69
748.35
676.79
636.79
616.06
583.11
523.61
515.17
511.10
499.68
490.95
487.11
482.97
479.07
475.22
470.98
467.00
463.10
458.96
455.14
m-x
x
Cl
N
N
N
O
O
O
O
2.5
(15 Mol%)

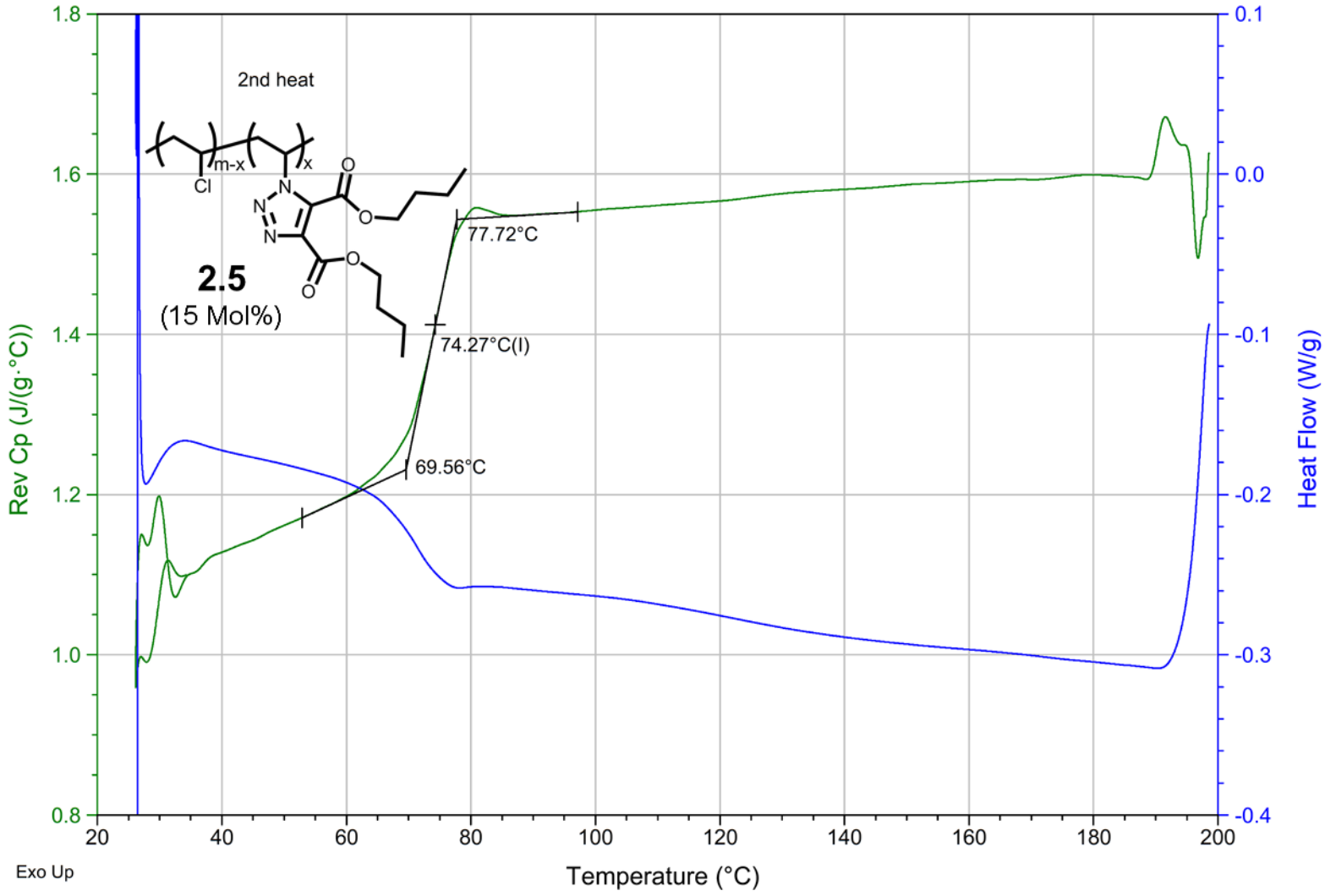
2nd heat
m-x
x
Cl
N
N
N
O
O
O
O
2.5
(15 Mol%)
77.72°C
74.27°C(I)
69.56°C
Rev Cp (J/(g·°C))
Heat Flow (W/g)
Temperature (°C)
Exo Up
1.8
1.6
1.4
1.2
1.0
0.8
0.1
0.0
-0.1
-0.2
-0.3
-0.4
20
40
60
80
100
120
140
160
180
200

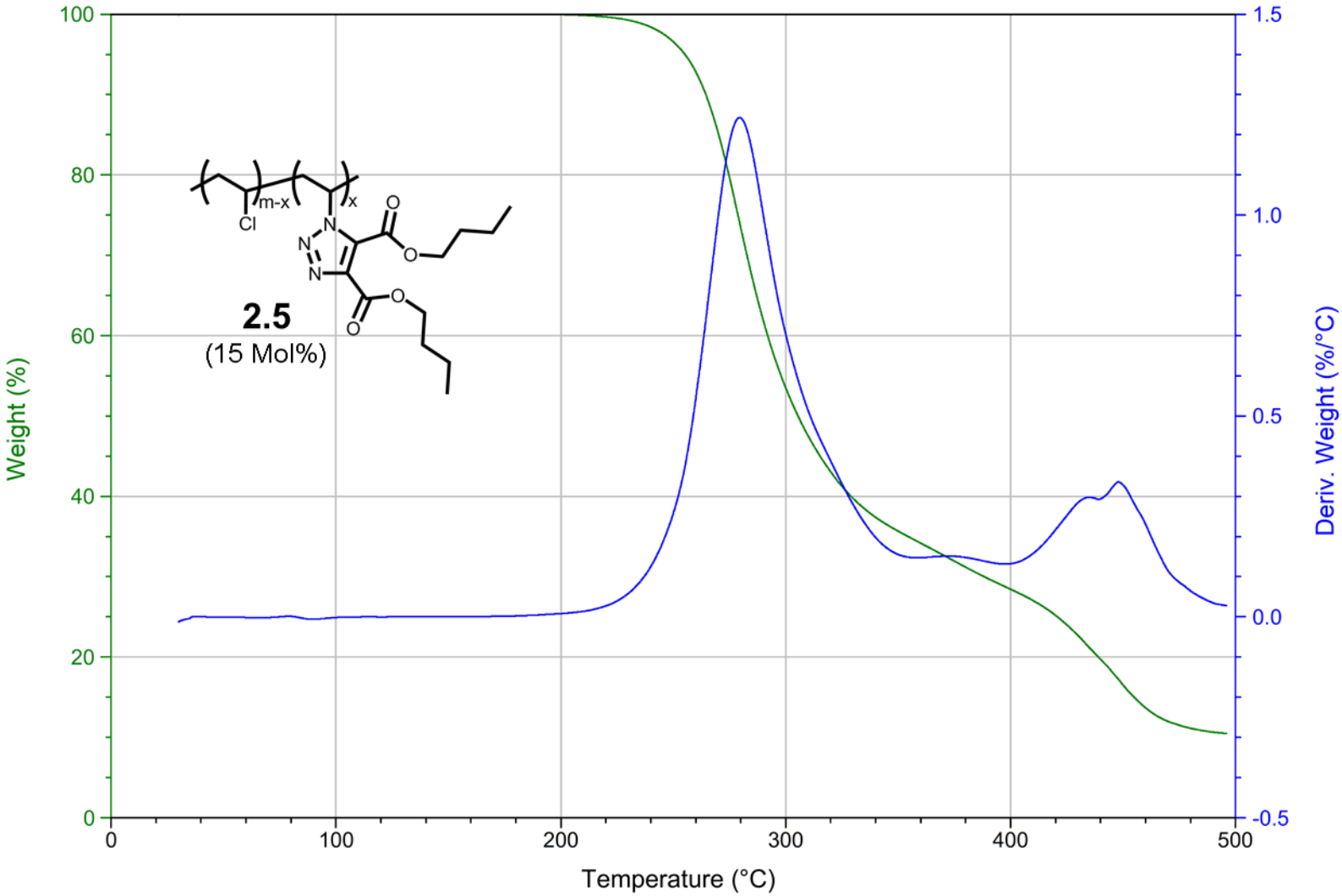
Weight (%)
Deriv. Weight (%/°C)
Temperature (°C)
100
80
60
40
20
0
1.5
1.0
0.5
0.0
-0.5
0
100
200
300
400
500
m-x
x
Cl
N
N
N
O
O
O
O
2.5
(15 Mol%)

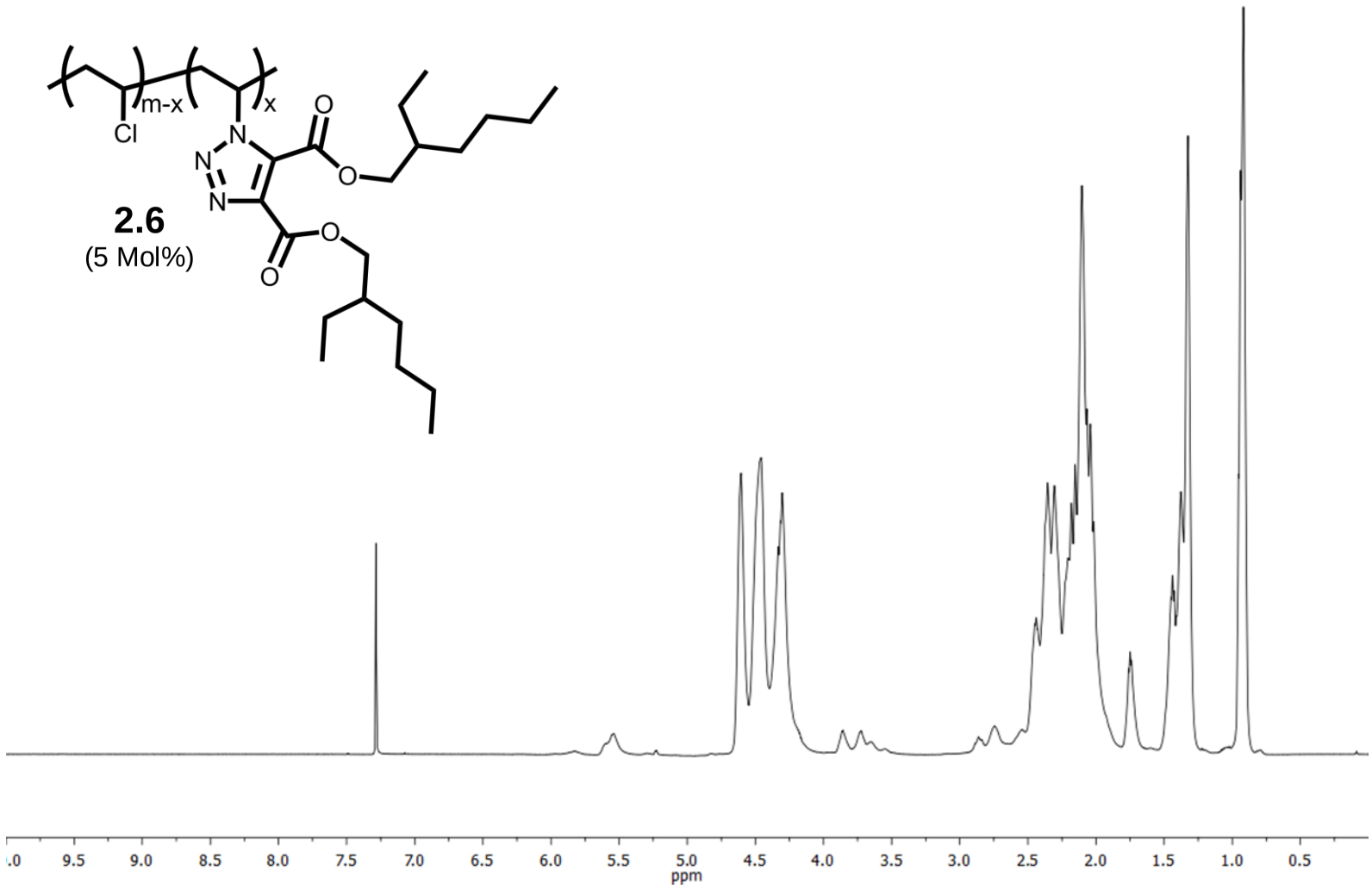
m-x
x
Cl
N
N
N
O
O
O
O
2.6
(5 Mol%)
9.5
9.0
8.5
8.0
7.5
7.0
6.5
6.0
5.5
5.0
4.5
4.0
3.5
3.0
2.5
2.0
1.5
1.0
0.5
ppm

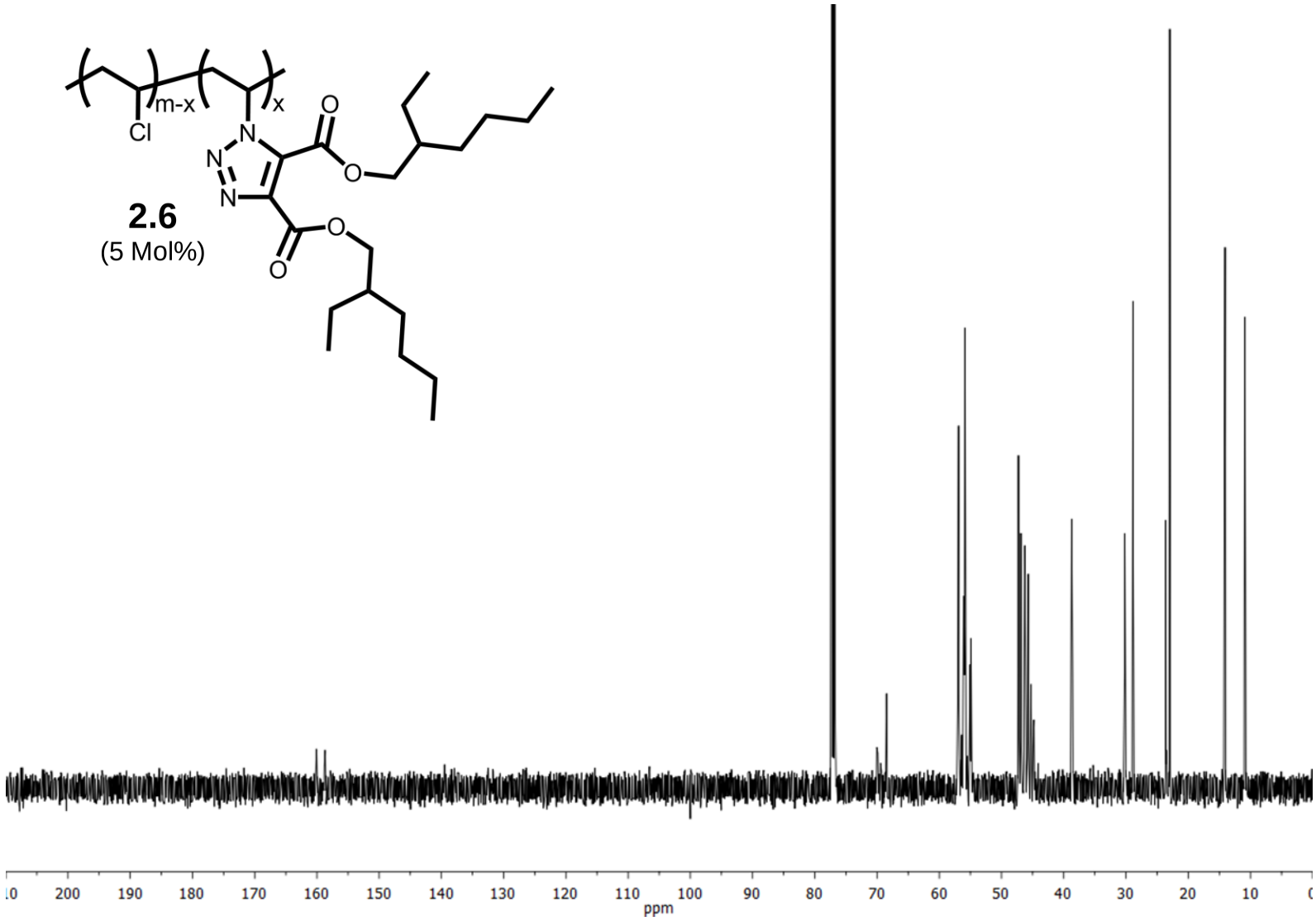
m-x
x
Cl
N
N
N
O
O
O
O
2.6
(5 Mol%)
200
190
180
170
160
150
140
130
120
110
100
90
80
70
60
50
40
30
20
10
ppm

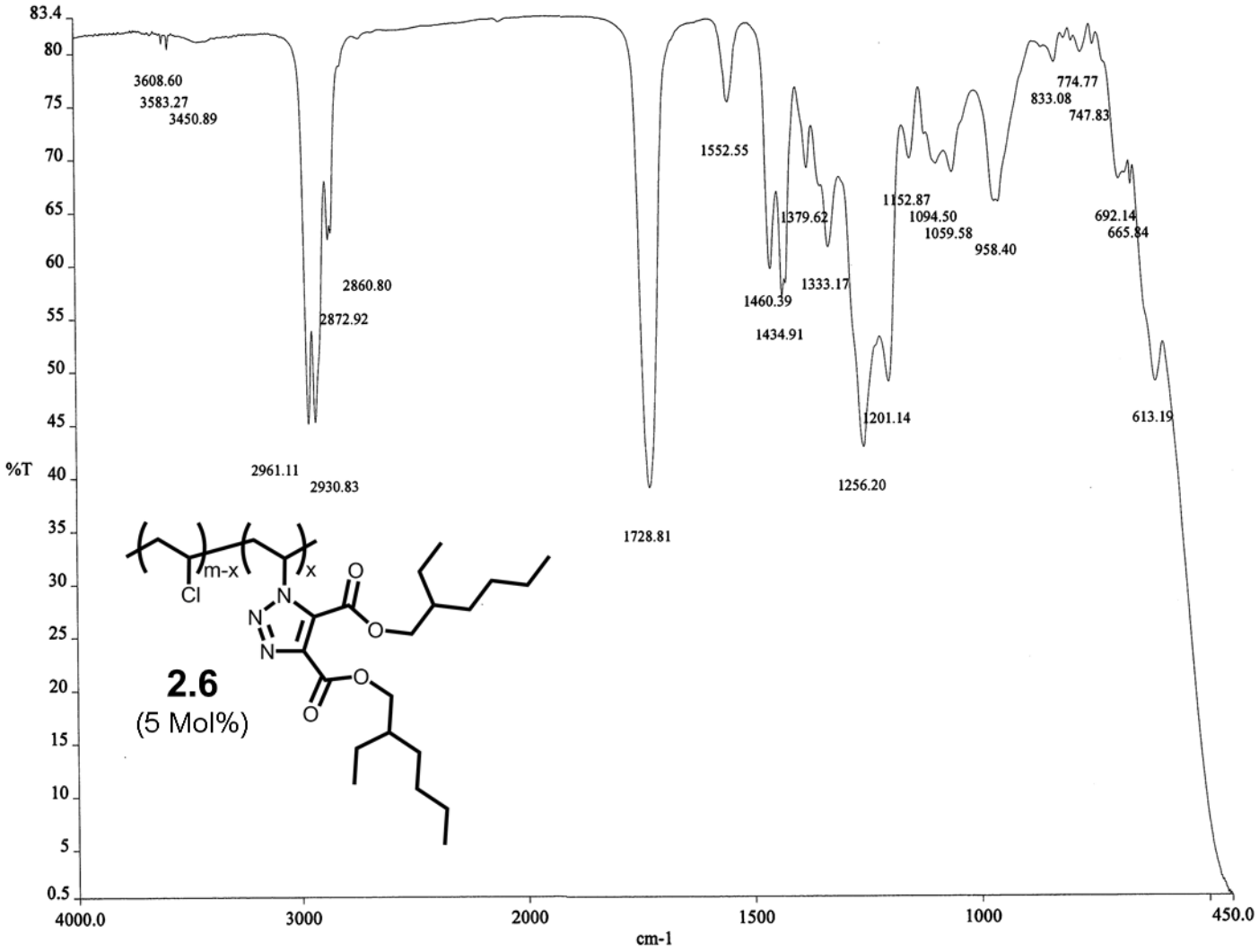
83.4
80
75
70
65
60
55
50
45
40
35
30
25
20
15
10
5
0.5
%T
3608.60
3583.27
3450.89
2961.11
2930.83
2872.92
2860.80
1728.81
1552.55
1460.39
1434.91
1379.62
1333.17
1256.20
1201.14
1152.87
1094.50
1059.58
958.40
774.77
833.08
747.83
692.14
665.84
613.19
4000.0
3000
2000
1500
1000
450.0
cm-1
m-x
x
Cl
N
N
N
O
O
O
O
2.6
(5 Mol%)

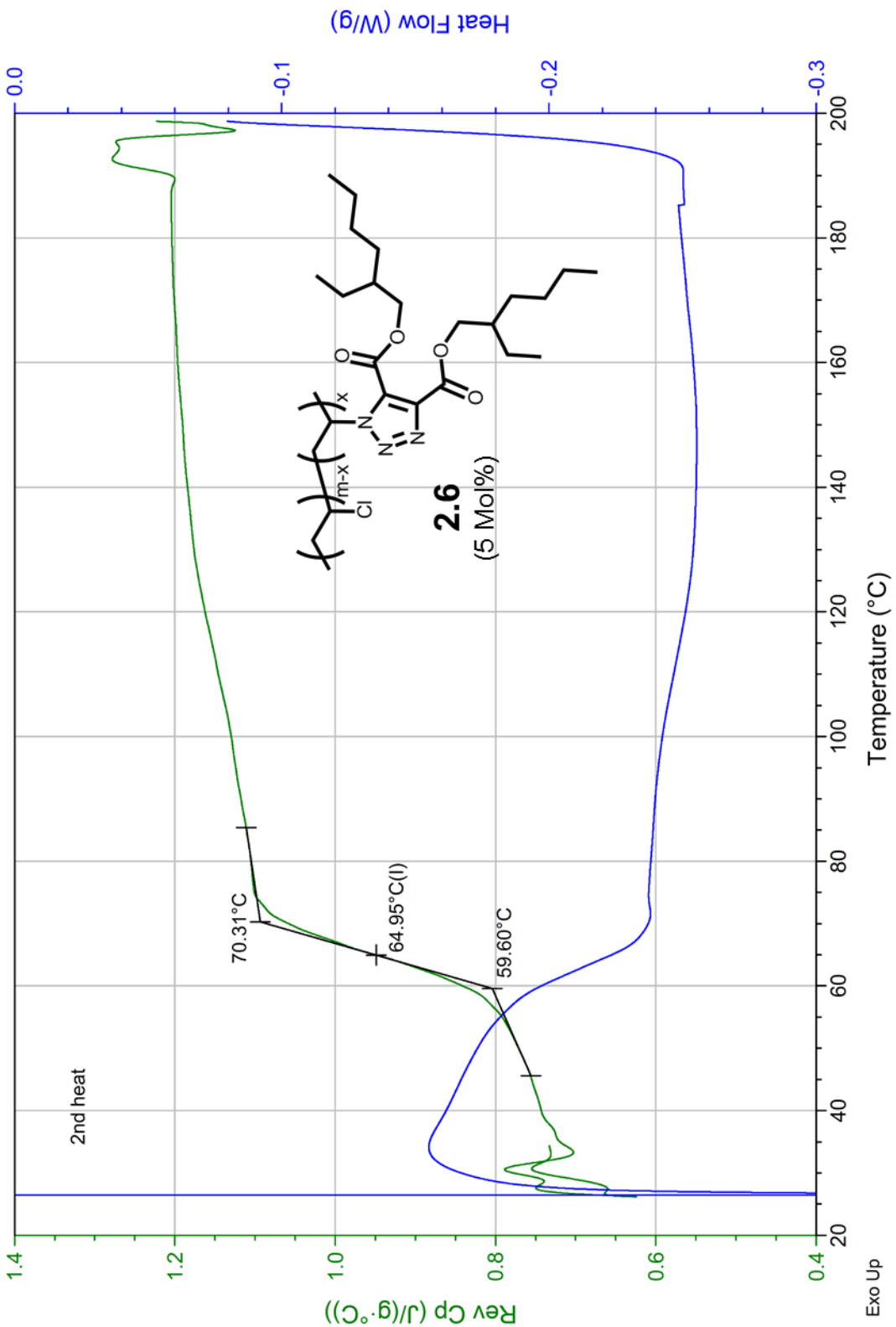
Heat Flow (W/g)
0.0
-0.1
-0.2
-0.3
Rev Cp (J/(g·°C))
1.4
1.2
1.0
0.8
0.6
0.4
Temperature (°C)
20
40
60
80
100
120
140
160
180
200
Exo Up
2nd heat
70.31°C
64.95°C(I)
59.60°C
2.6
(5 Mol%)
m-x
x
Cl
O
N
N
N

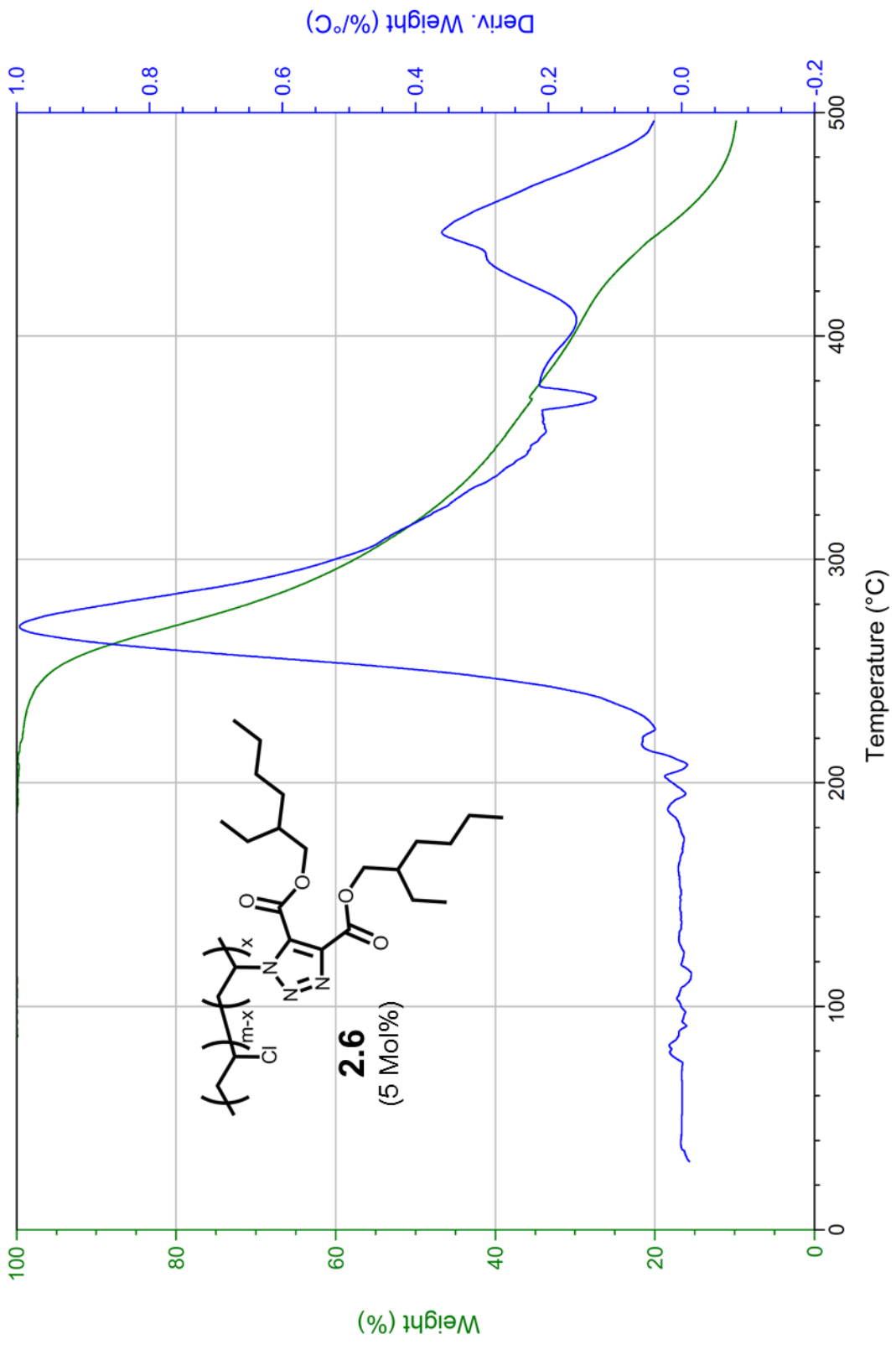
Weight (%)
Deriv. Weight (%/°C)
Temperature (°C)
2.6
(5 Mol%)

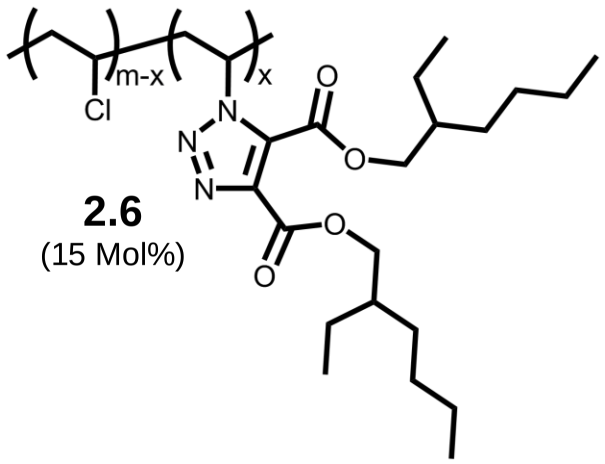
m-x
x
Cl
N
N
N
O
O
O
O

2.6
(15 Mol%)

9.5
9.0
8.5
8.0
7.5
7.0
6.5
6.0
5.5
5.0
4.5
4.0
3.5
3.0
2.5
2.0
1.5
1.0
0.5
ppm

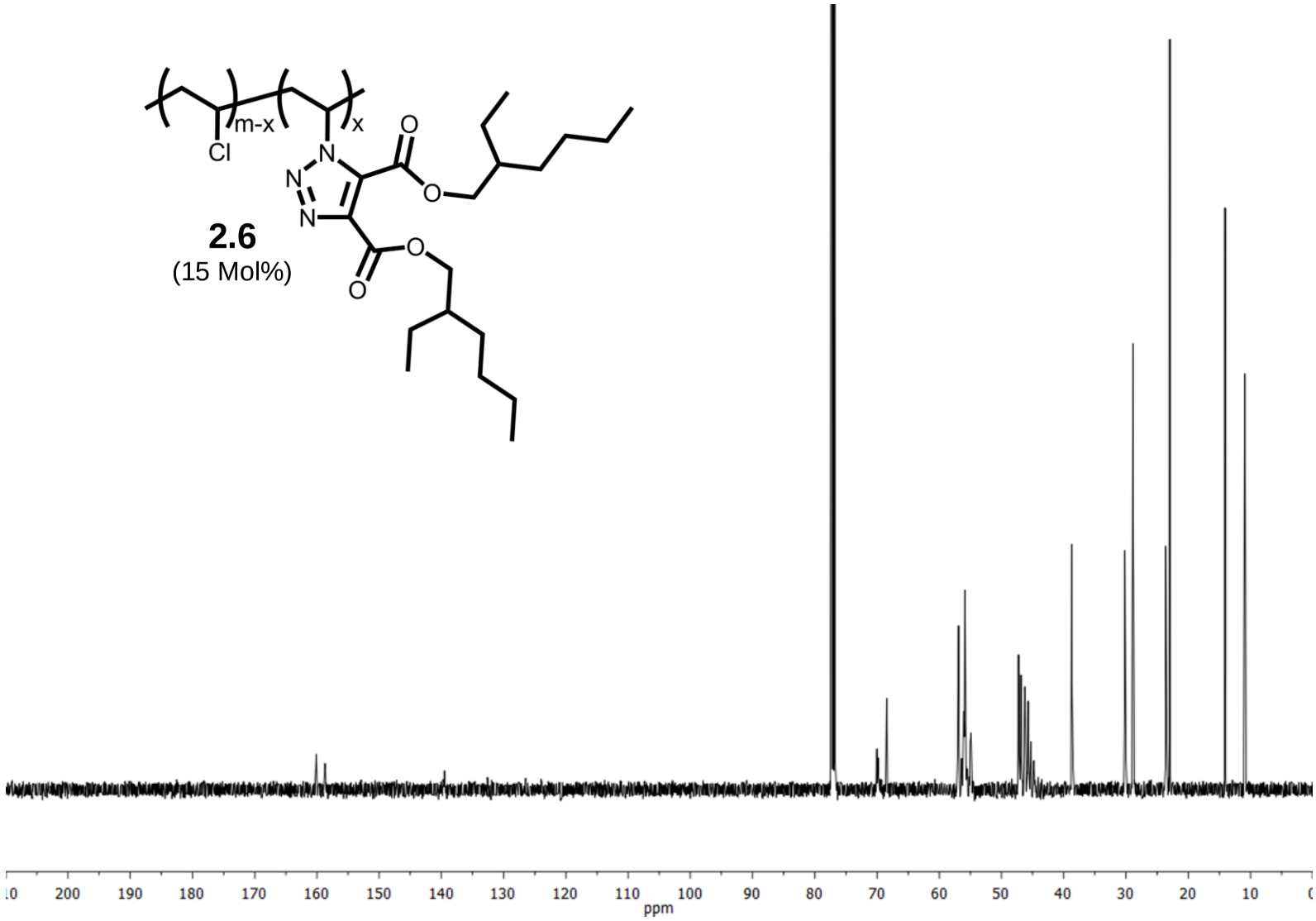
m-x
x
Cl
N
N
N
O
O
O
O
2.6
(15 Mol%)
200
190
180
170
160
150
140
130
120
110
100
90
80
70
60
50
40
30
20
10
ppm

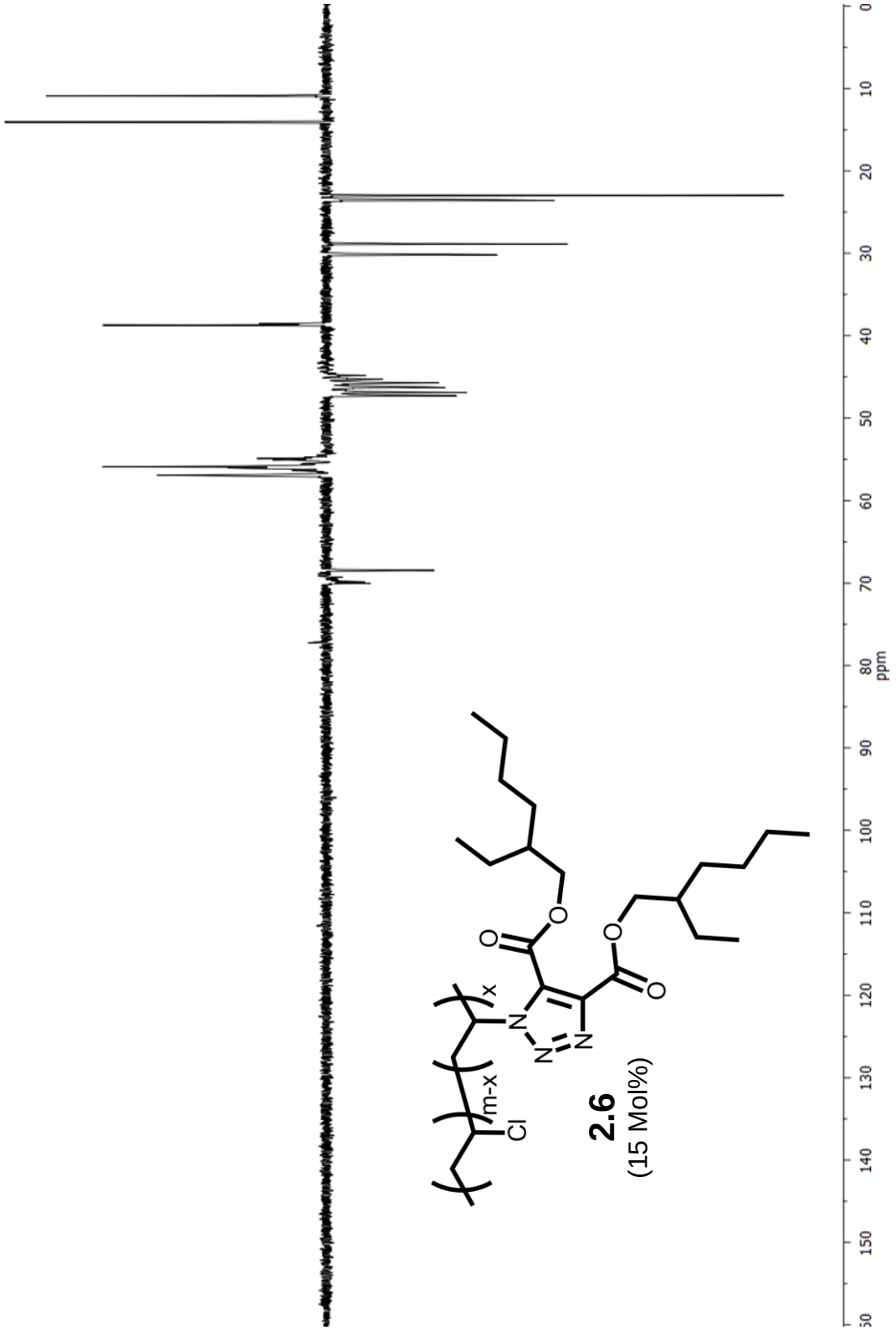
ppm
0
10
20
30
40
50
60
70
80
90
100
110
120
130
140
150
O
O
O
O
N
N
N
x
m-x
Cl

2.6
(15 Mol%)

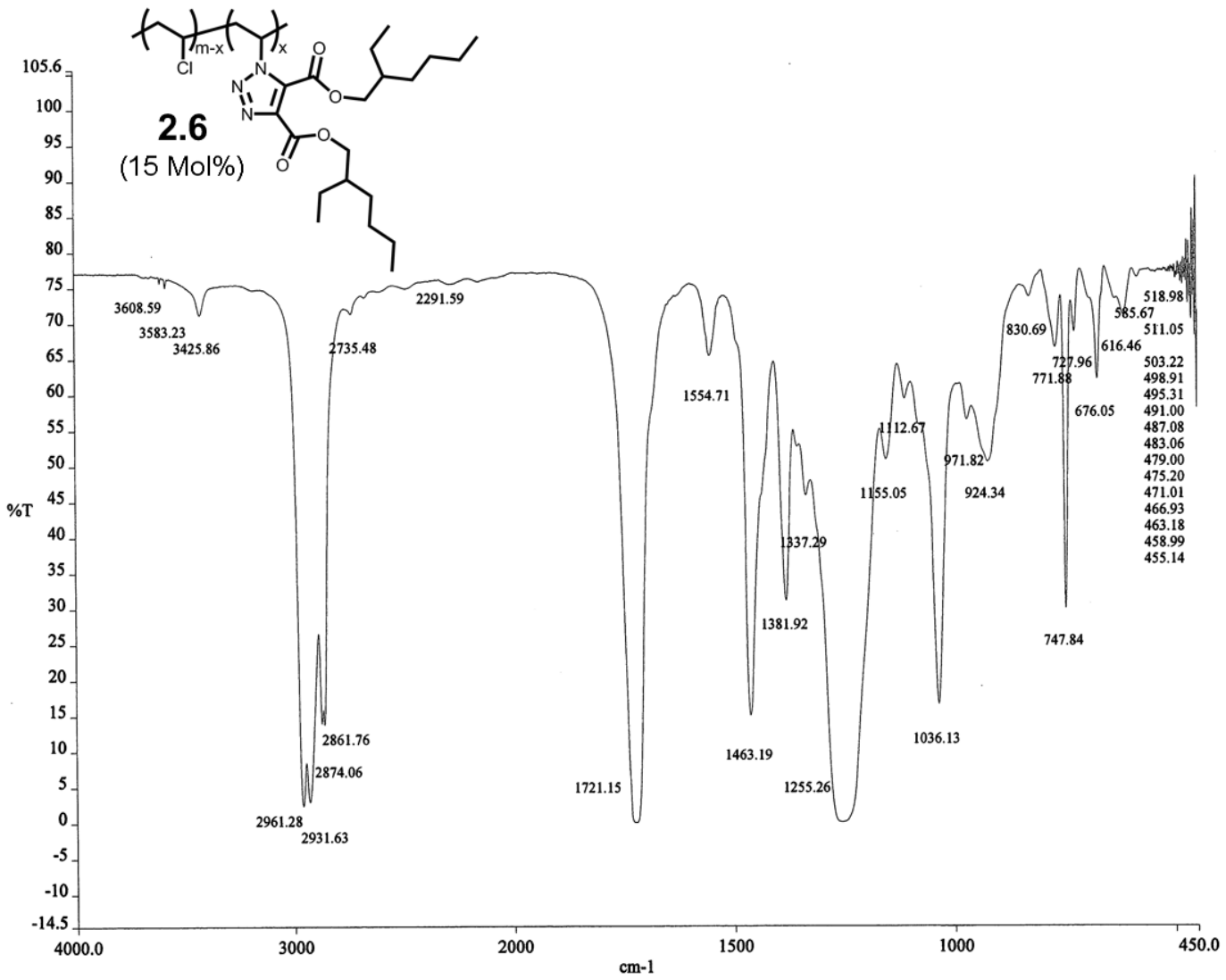
2.6
(15 Mol%)
%T
cm-1
3608.59
3583.23
3425.86
2735.48
2291.59
1554.71
1112.67
971.82
830.69
727.96
771.88
676.05
616.46
585.67
518.98
511.05
503.22
498.91
495.31
491.00
487.08
483.06
479.00
475.20
471.01
466.93
463.18
458.99
455.14
1155.05
924.34
1337.29
1381.92
747.84
2861.76
2874.06
2961.28
2931.63
1721.15
1463.19
1255.26
1036.13

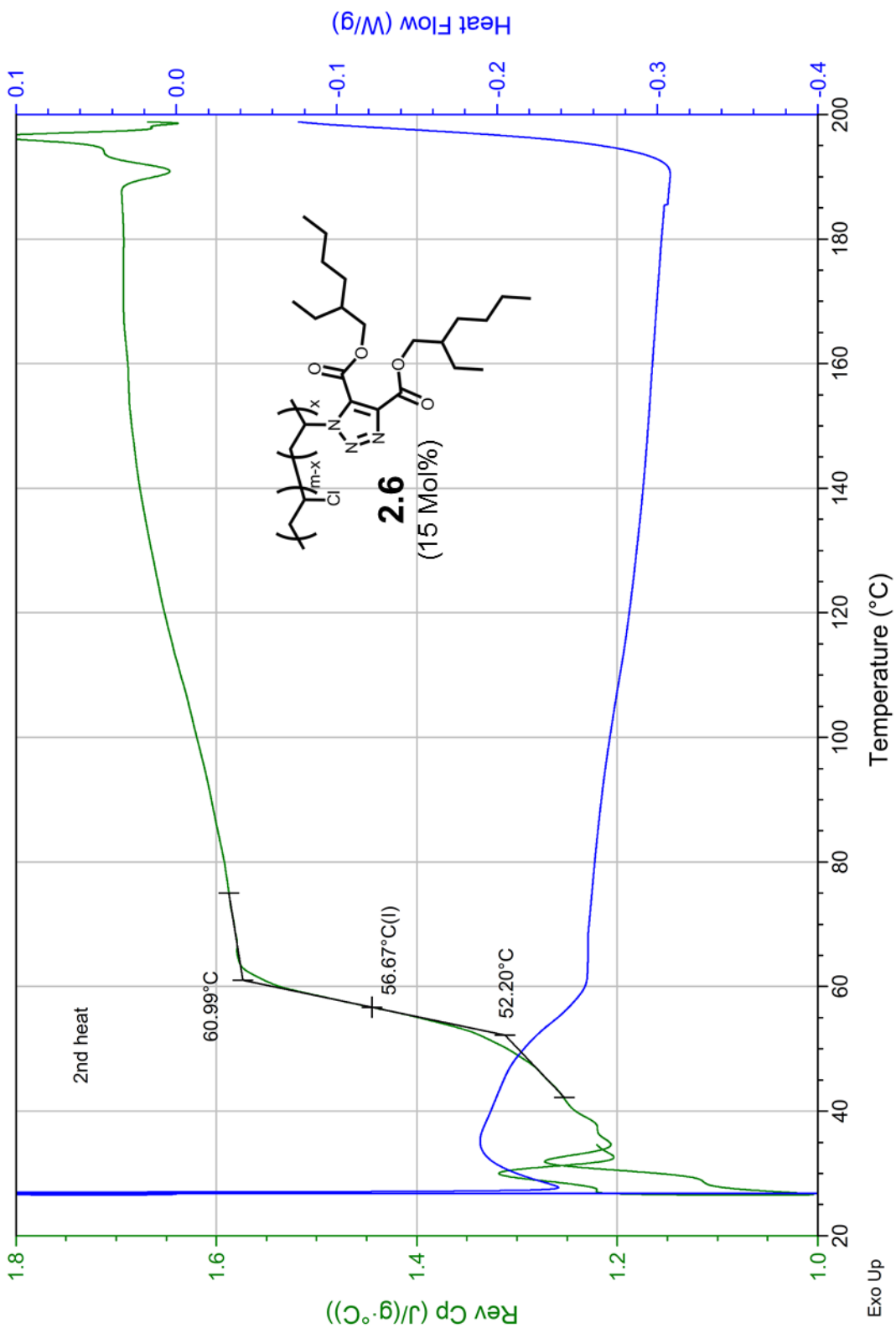
Heat Flow (W/g)
0.1
0.0
-0.1
-0.2
-0.3
-0.4
Rev Cp (J/(g·°C))
1.8
1.6
1.4
1.2
1.0
Temperature (°C)
20
40
60
80
100
120
140
160
180
200
Exo Up
2nd heat
60.99°C
56.67°C(I)
52.20°C
2.6
(15 Mol%)
m-x
x
Cl
O
N
N
N

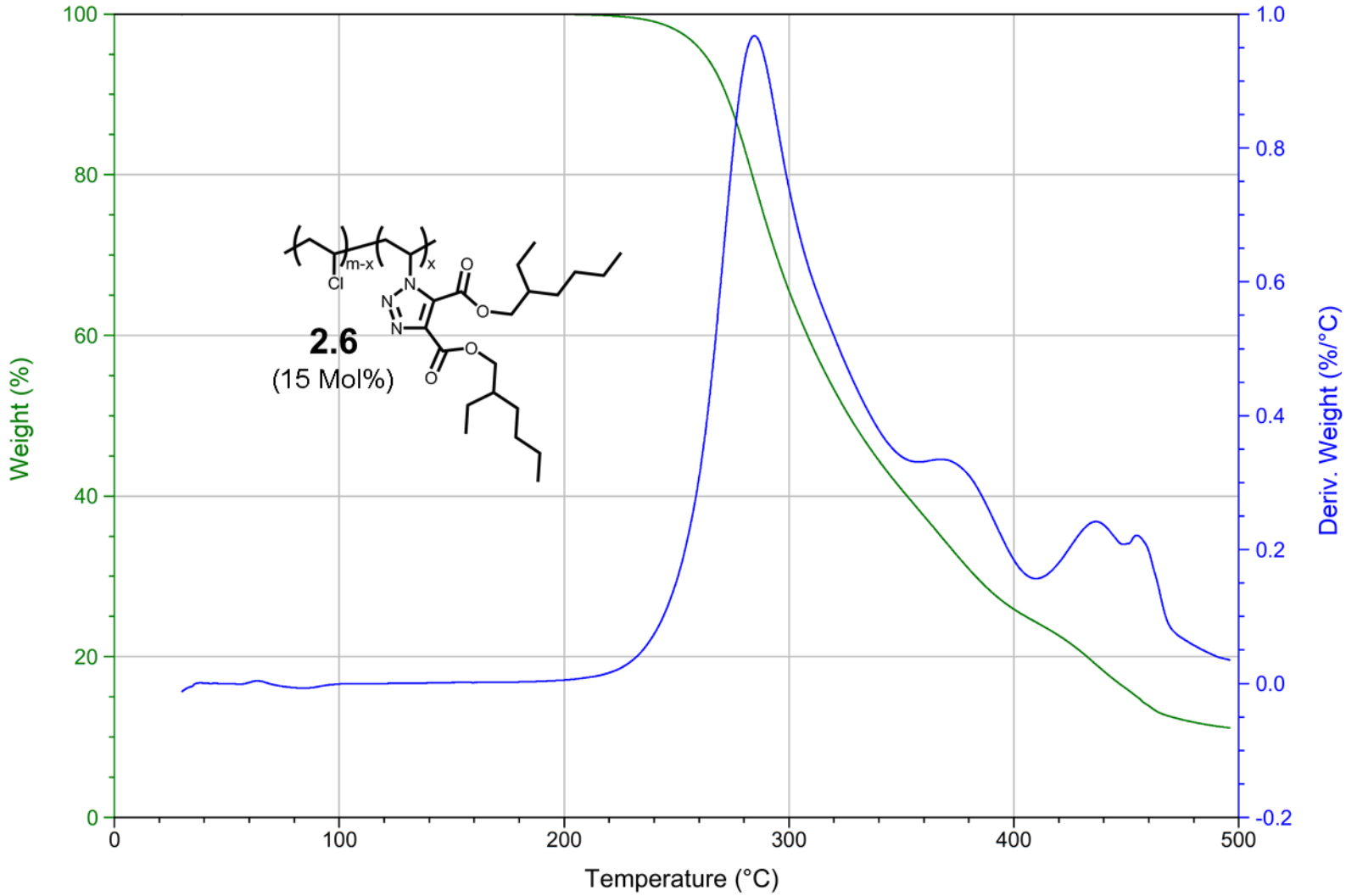
2.6
(15 Mol%)
Weight (%)
Deriv. Weight (%/°C)
Temperature (°C)
0
20
40
60
80
100
-0.2
0.0
0.2
0.4
0.6
0.8
1.0
0
100
200
300
400
500

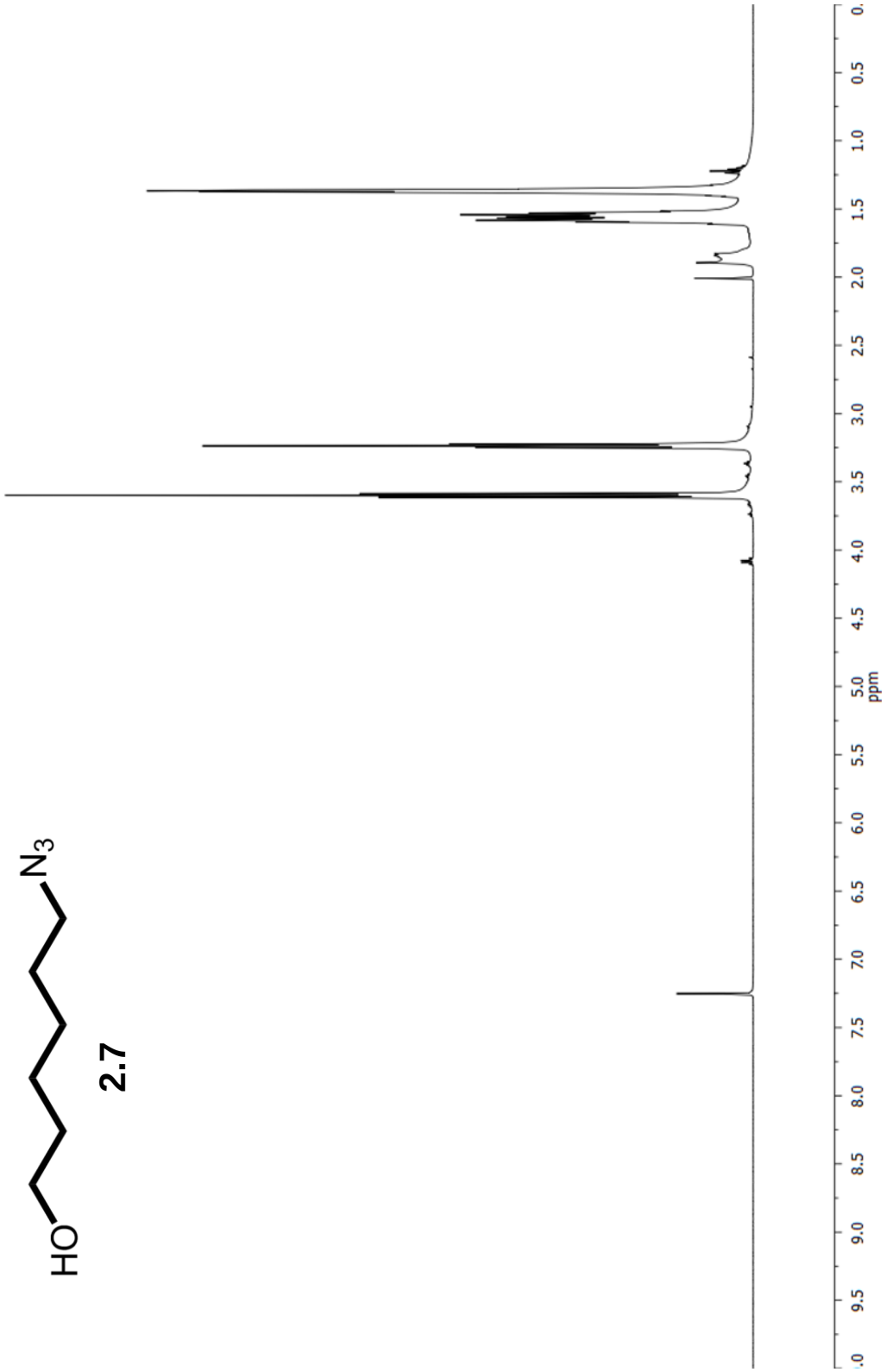
HO
N3
2.7
ppm

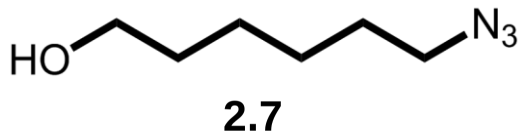
HO
N3

2.7

200
190
180
170
160
150
140
130
120
110
100
90
80
70
60
50
40
30
20
10
ppm

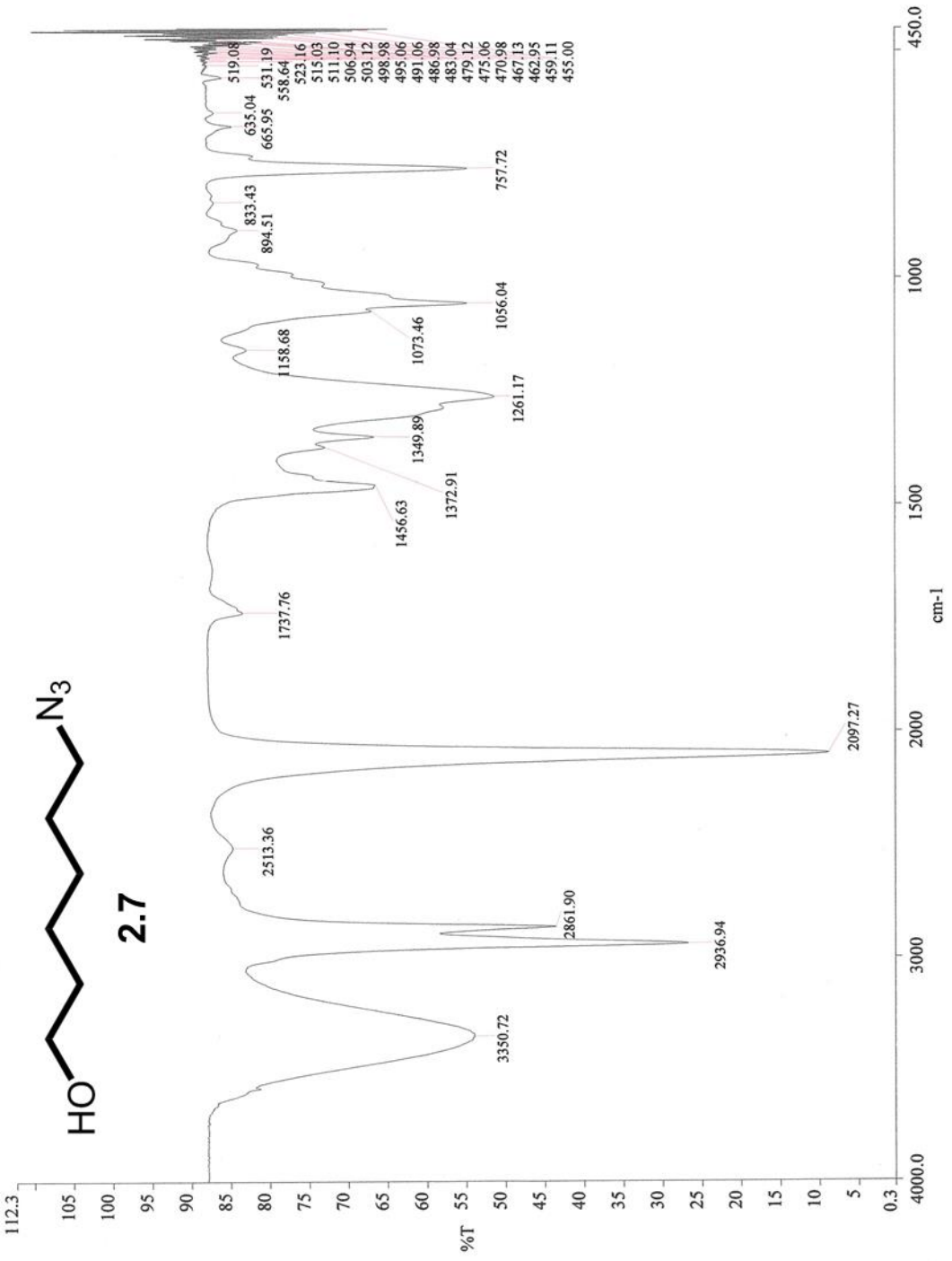
HO
N3
2.7
%T
cm-1
112.3
105
100
95
90
85
80
75
70
65
60
55
50
45
40
35
30
25
20
15
10
5
0.3
4000.0
3000
2000
1500
1000
450.0
3350.72
2936.94
2861.90
2513.36
2097.27
1737.76
1456.63
1372.91
1349.89
1261.17
1158.68
1073.46
1056.04
894.51
833.43
757.72
665.95
635.04
558.64
531.19
519.08
523.16
515.03
511.10
506.94
503.12
498.98
495.06
491.06
486.98
483.04
479.12
475.06
470.98
467.13
462.95
459.11
455.00

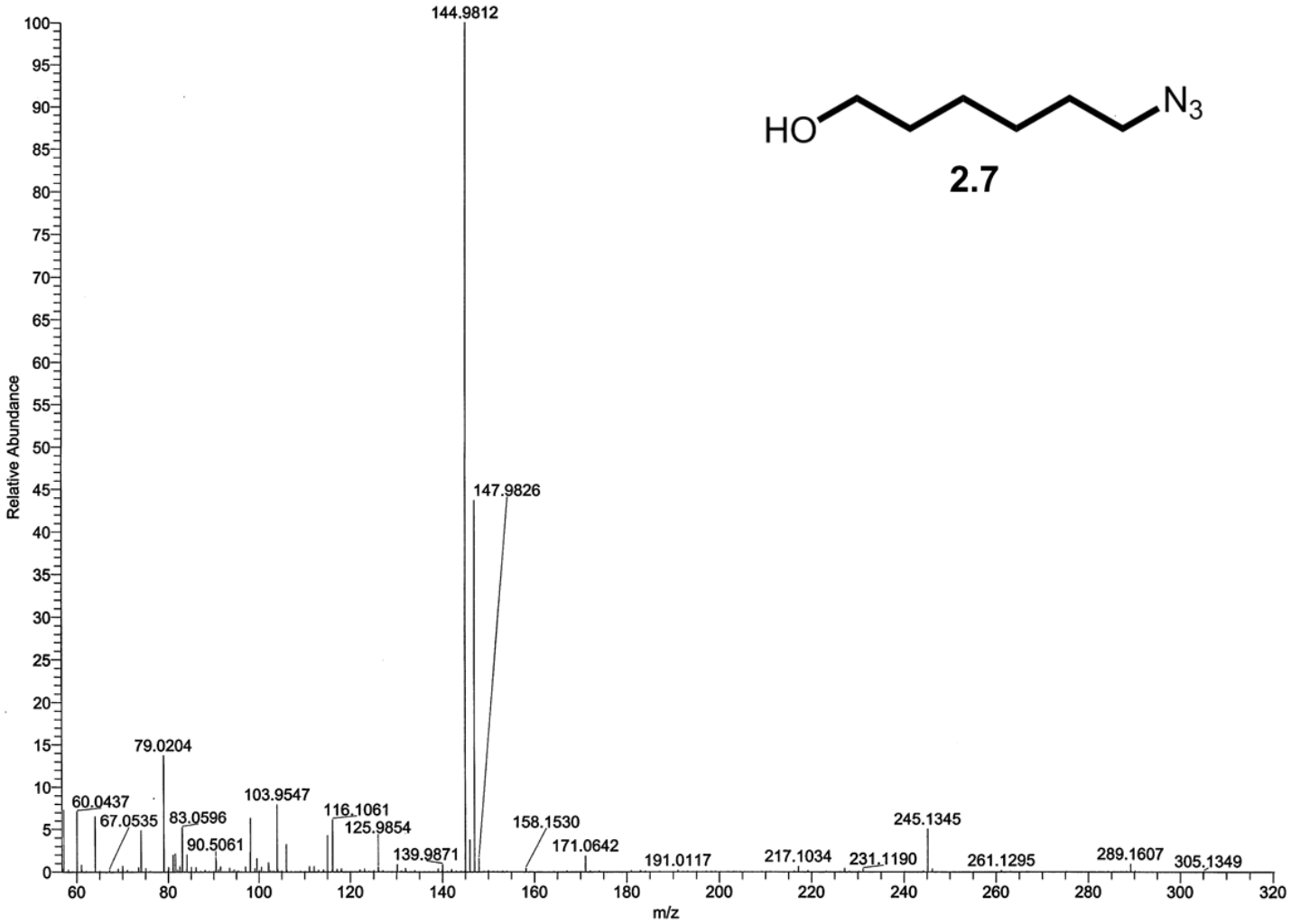
144.9812
147.9826
79.0204
60.0437
67.0535
83.0596
90.5061
103.9547
116.1061
125.9854
139.9871
158.1530
171.0642
191.0117
217.1034
231.1190
245.1345
261.1295
289.1607
305.1349
Relative Abundance
m/z
HO
N3

2.7

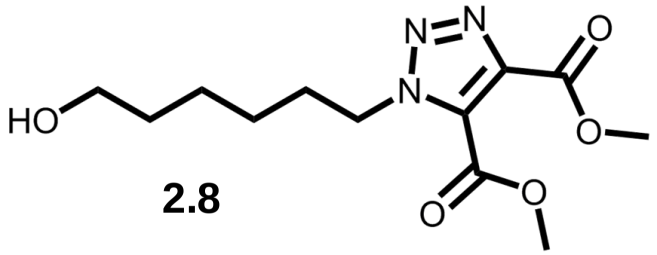
HO
N
N
N
O
O
O
O

2.8

9.5
9.0
8.5
8.0
7.5
7.0
6.5
6.0
5.5
5.0
4.5
4.0
3.5
3.0
2.5
2.0
1.5
1.0
0.5
ppm

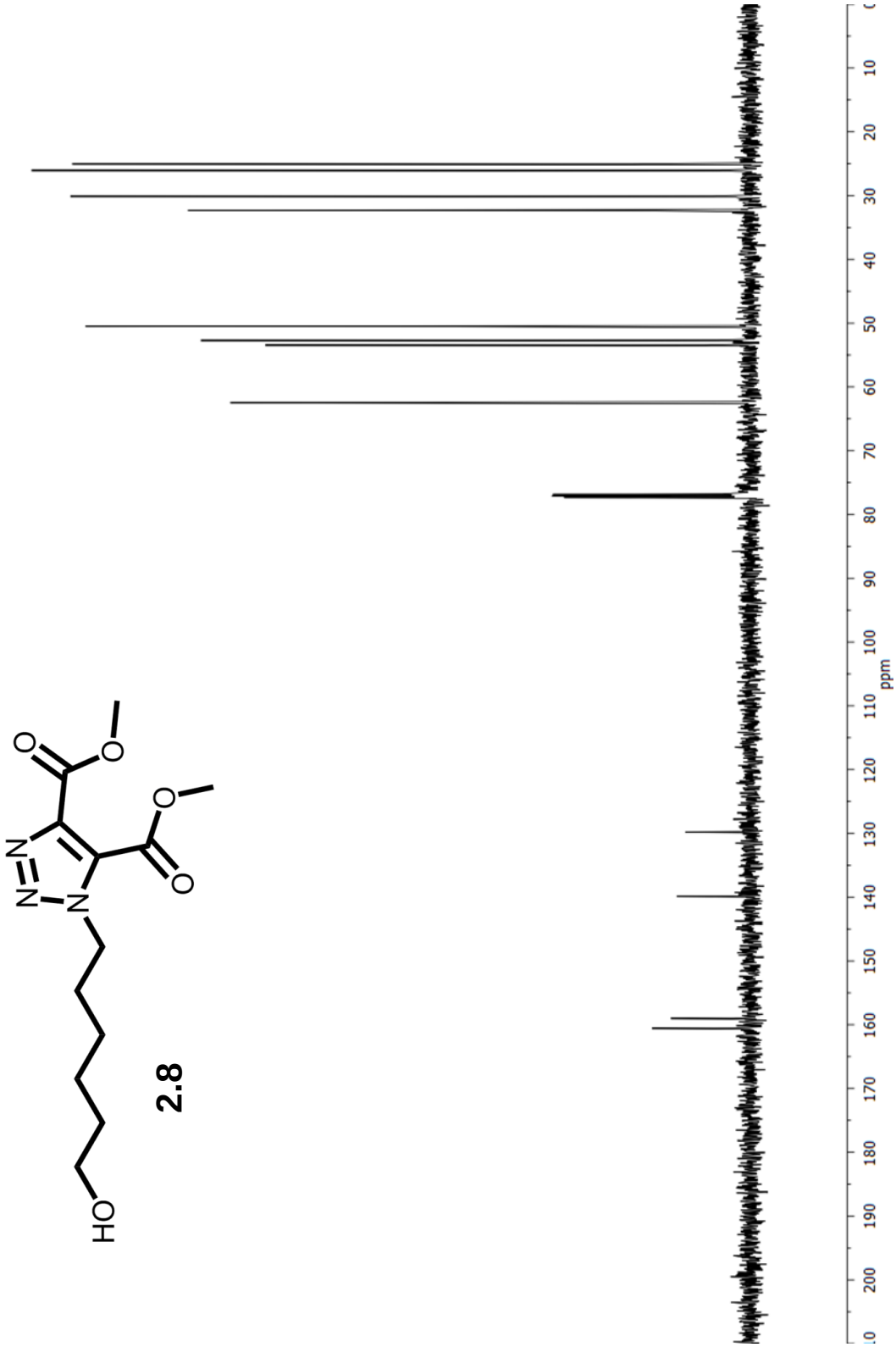
O
O
O
O
N
N
N
HO
2.8
ppm
10
20
30
40
50
60
70
80
90
100
110
120
130
140
150
160
170
180
190
200

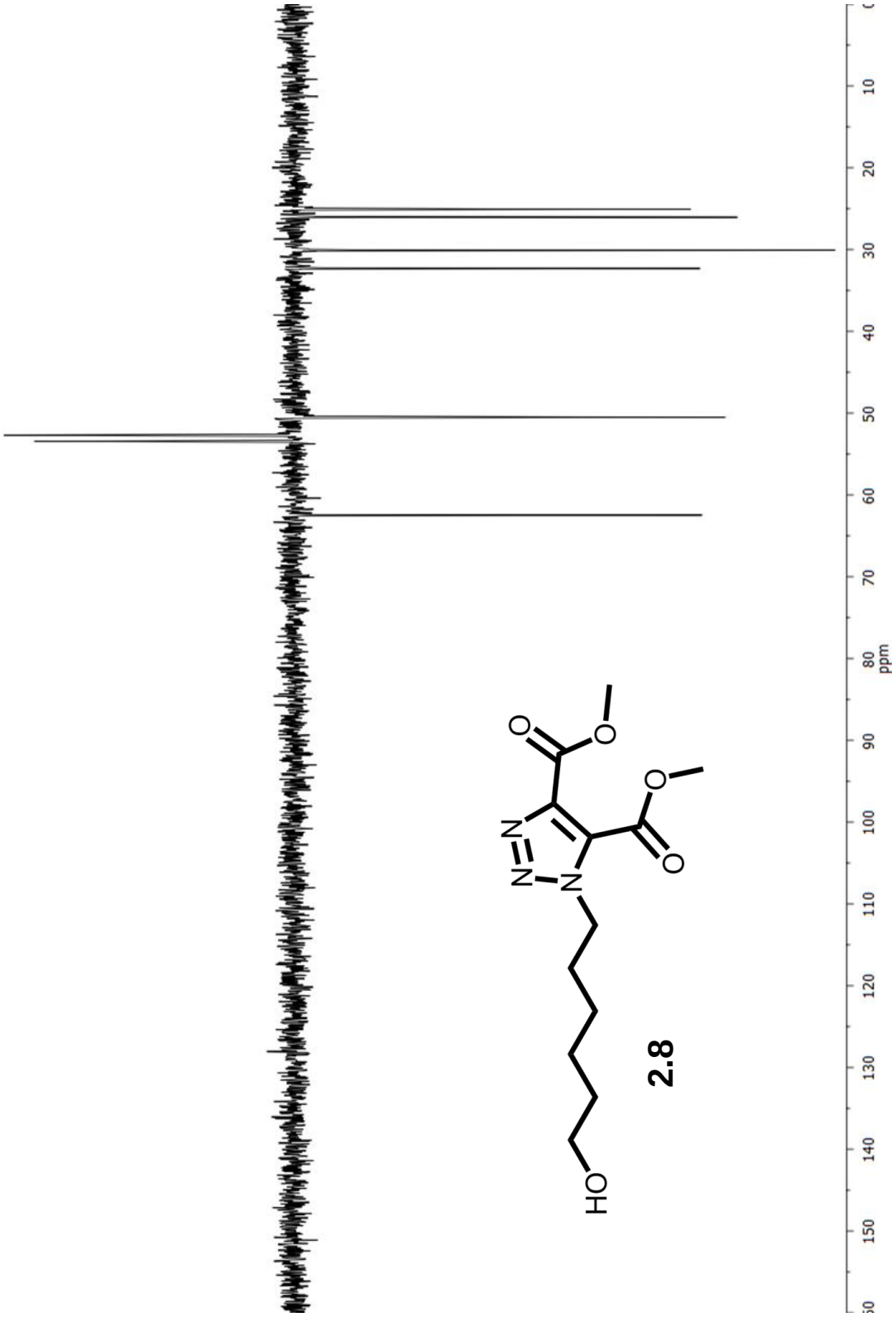

2.8

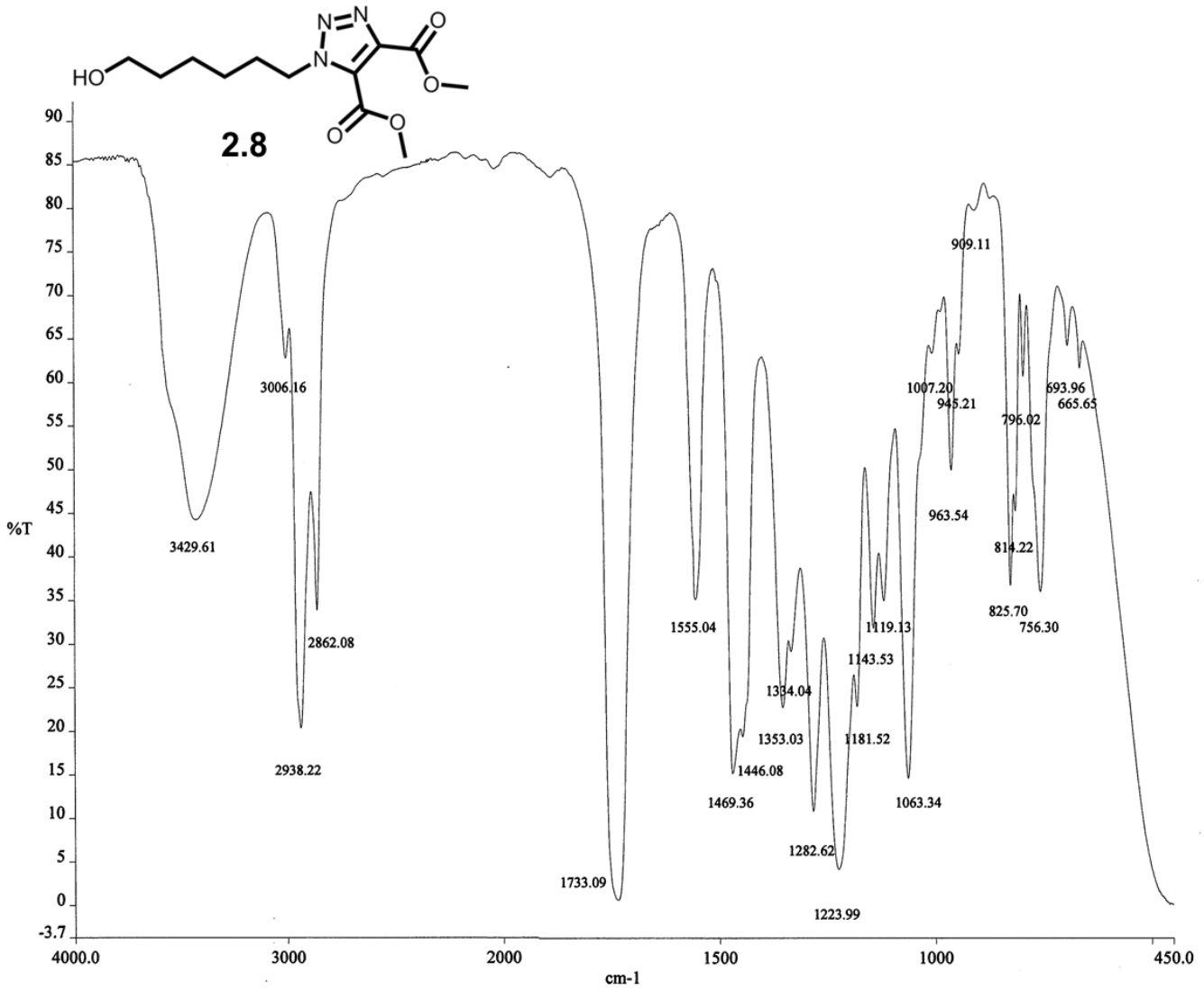
HO
N
N
N
O
O
O
O
2.8
%T
90
85
80
75
70
65
60
55
50
45
40
35
30
25
20
15
10
5
0
-3.7
4000.0
3000
2000
1500
1000
450.0
cm-1
3429.61
3006.16
2938.22
2862.08
1733.09
1555.04
1469.36
1446.08
1353.03
1334.04
1282.62
1223.99
1181.52
1143.53
1119.13
1063.34
1007.20
963.54
945.21
909.11
825.70
814.22
796.02
756.30
693.96
665.65

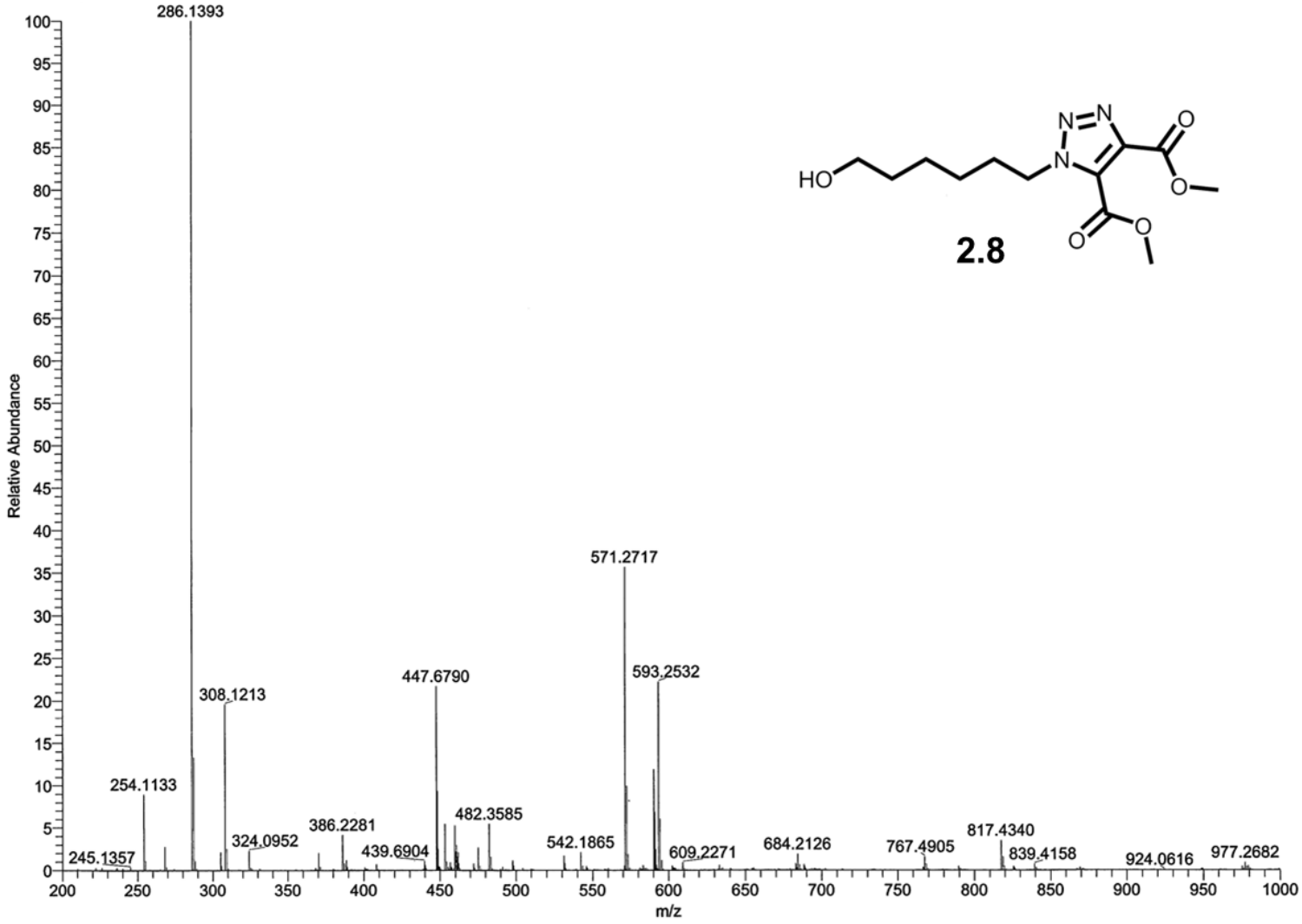
286.1393
571.2717
593.2532
447.6790
308.1213
254.1133
482.3585
386.2281
324.0952
439.6904
542.1865
609.2271
684.2126
767.4905
817.4340
839.4158
924.0616
977.2682
245.1357
Relative Abundance
m/z
HO
N
N
N
O
O
O
O

2.8

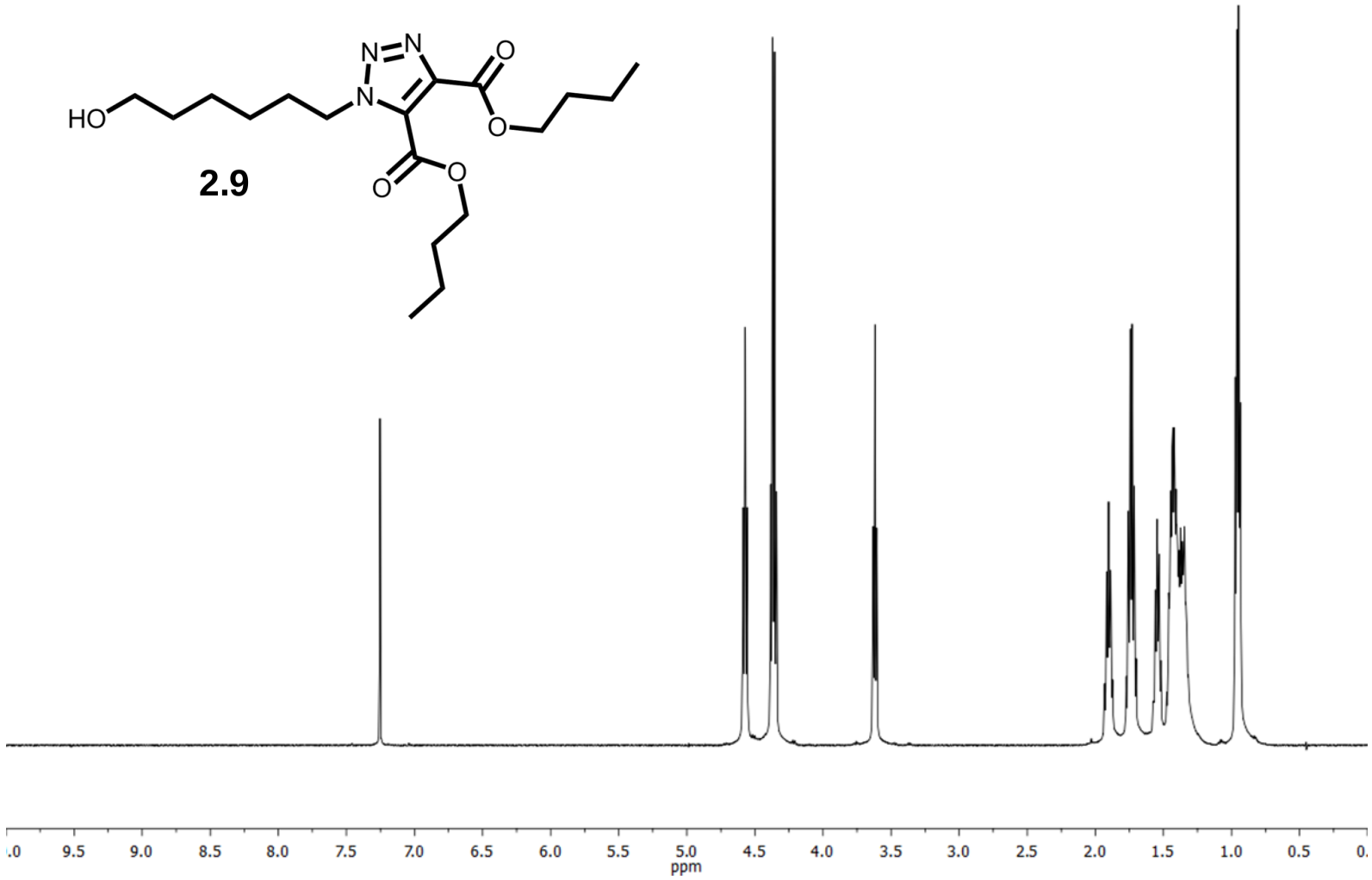
HO
N
N
N
O
O
O
O
2.9
9.5
9.0
8.5
8.0
7.5
7.0
6.5
6.0
5.5
5.0
4.5
4.0
3.5
3.0
2.5
2.0
1.5
1.0
0.5
ppm

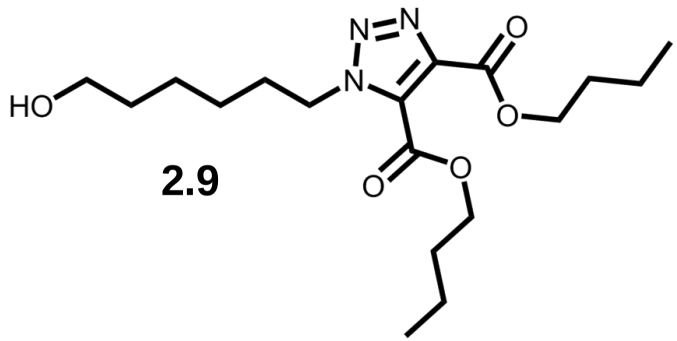
HO
N
N
N
O
O
O
O

2.9

200
190
180
170
160
150
140
130
120
110
100
90
80
70
60
50
40
30
20
10
ppm

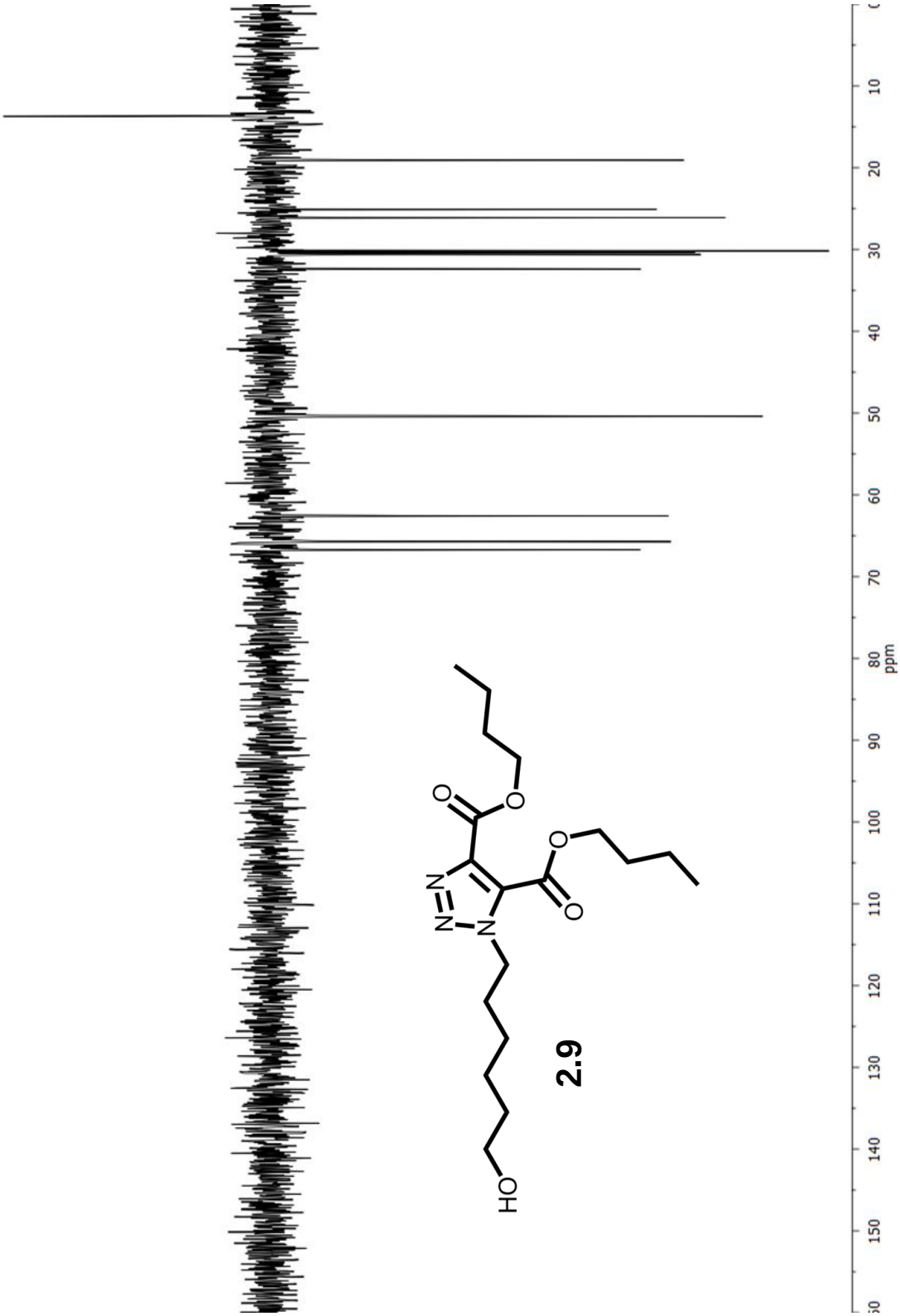
O
O
O
O
N
N
N
HO
2.9
ppm

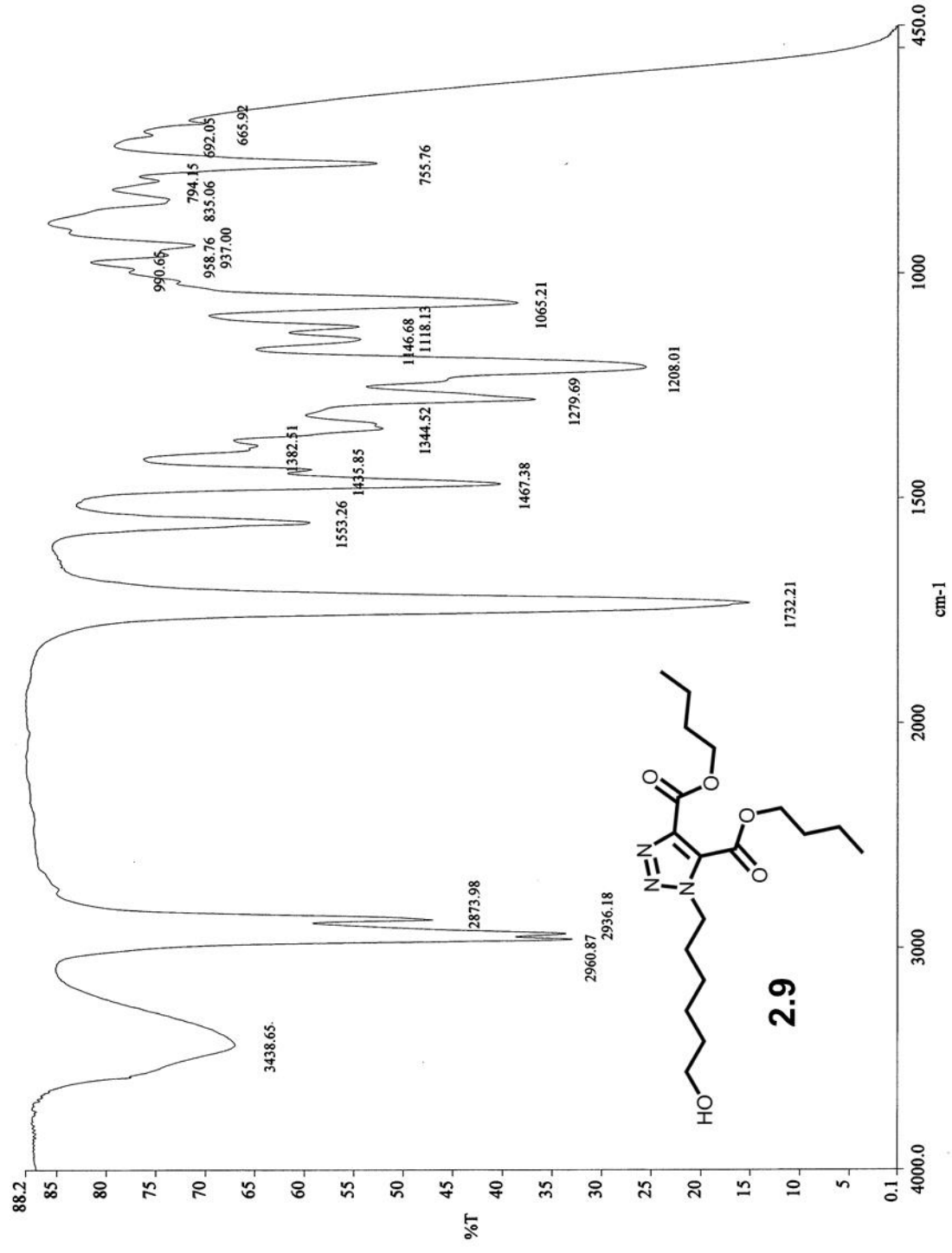
88.2
85
80
75
70
65
60
55
50
45
40
35
30
25
20
15
10
5
0.1
%T
4000.0
3000
2000
1500
1000
450.0
cm-1
3438.65
2960.87
2936.18
2873.98
1732.21
1553.26
1467.38
1435.85
1382.51
1344.52
1279.69
1208.01
1146.68
1118.13
1065.21
990.65
958.76
937.00
835.06
794.15
755.76
692.05
665.92
HO
2.9

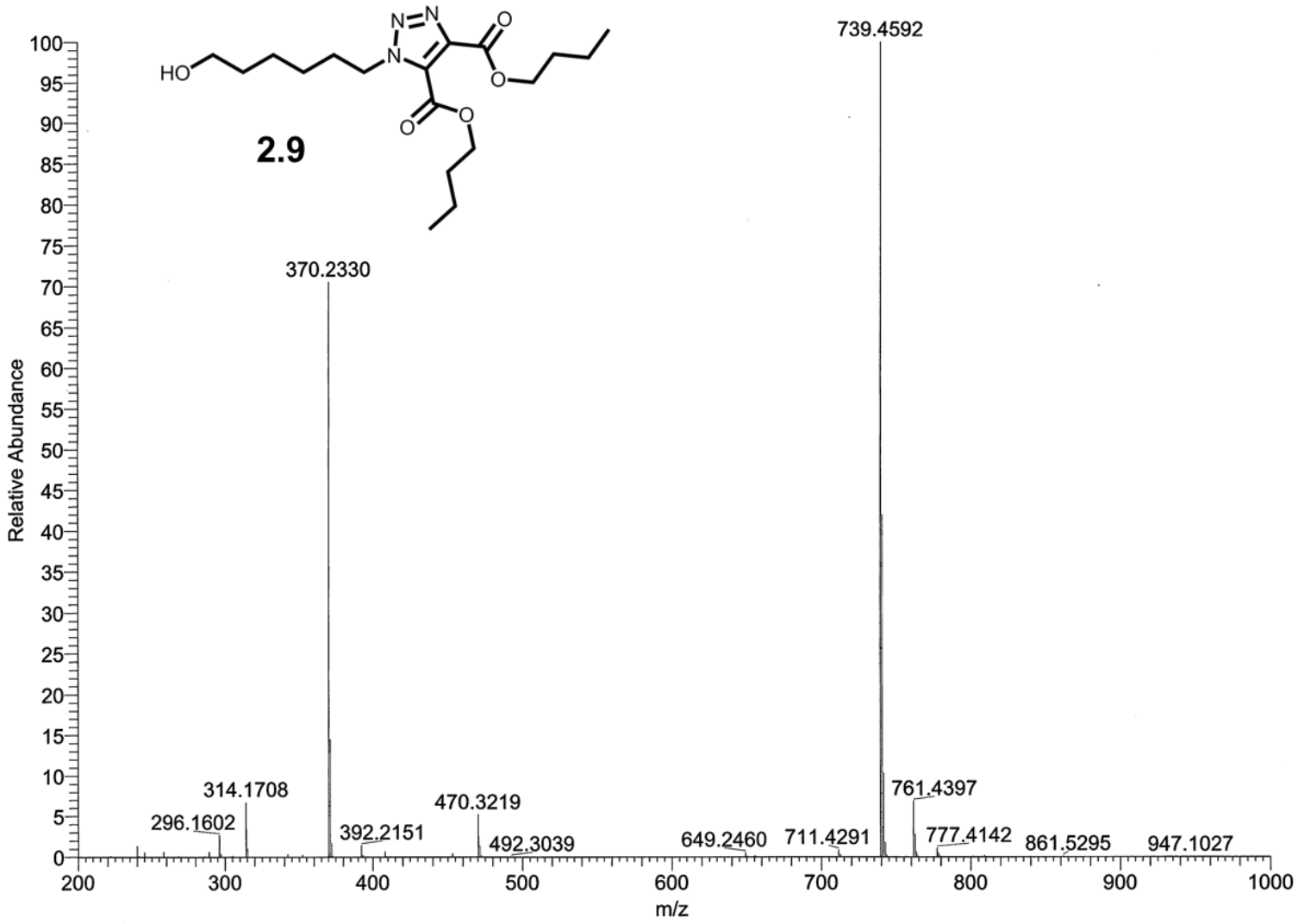
2.9
HO
N
N
N
O
O
O
O
739.4592
370.2330
314.1708
296.1602
392.2151
470.3219
492.3039
649.2460
711.4291
761.4397
777.4142
861.5295
947.1027
Relative Abundance
m/z
100
95
90
85
80
75
70
65
60
55
50
45
40
35
30
25
20
15
10
5
0
200
300
400
500
600
700
800
900
1000

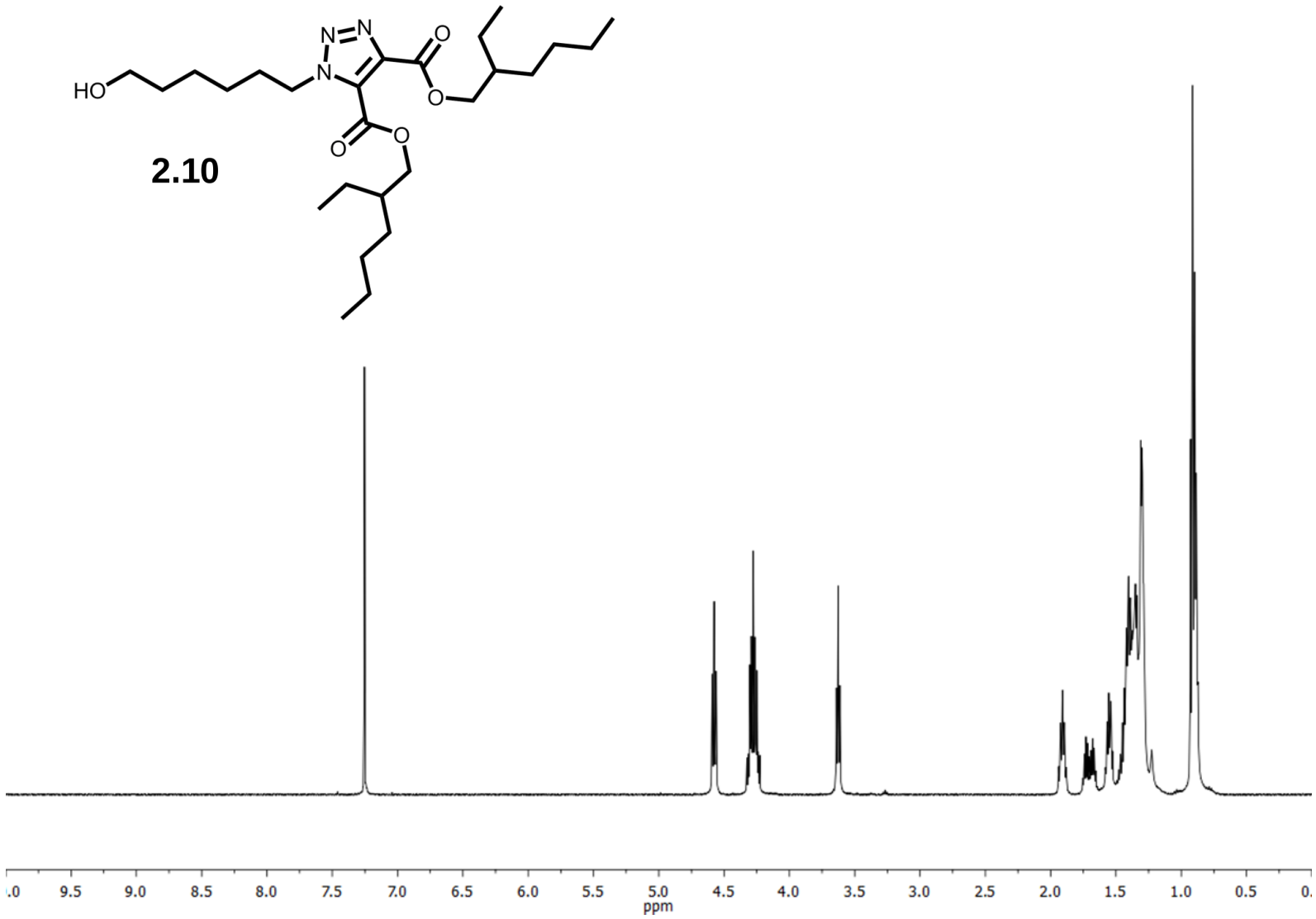
HO
N
N
N
O
O
O
O
2.10
9.5
9.0
8.5
8.0
7.5
7.0
6.5
6.0
5.5
5.0
4.5
4.0
3.5
3.0
2.5
2.0
1.5
1.0
0.5
ppm

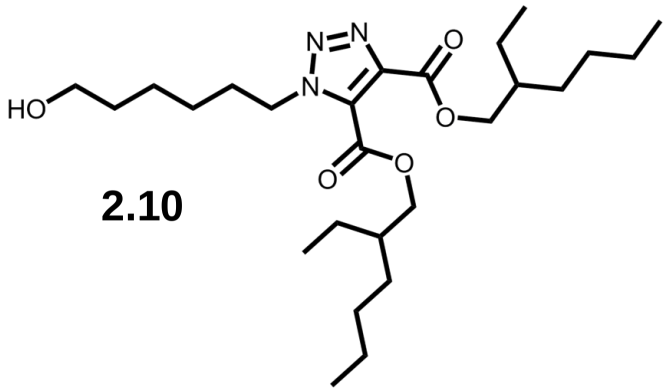
HO
N
N
N
O
O
O
O

2.10

200
190
180
170
160
150
140
130
120
110
100
90
80
70
60
50
40
30
20
10
ppm

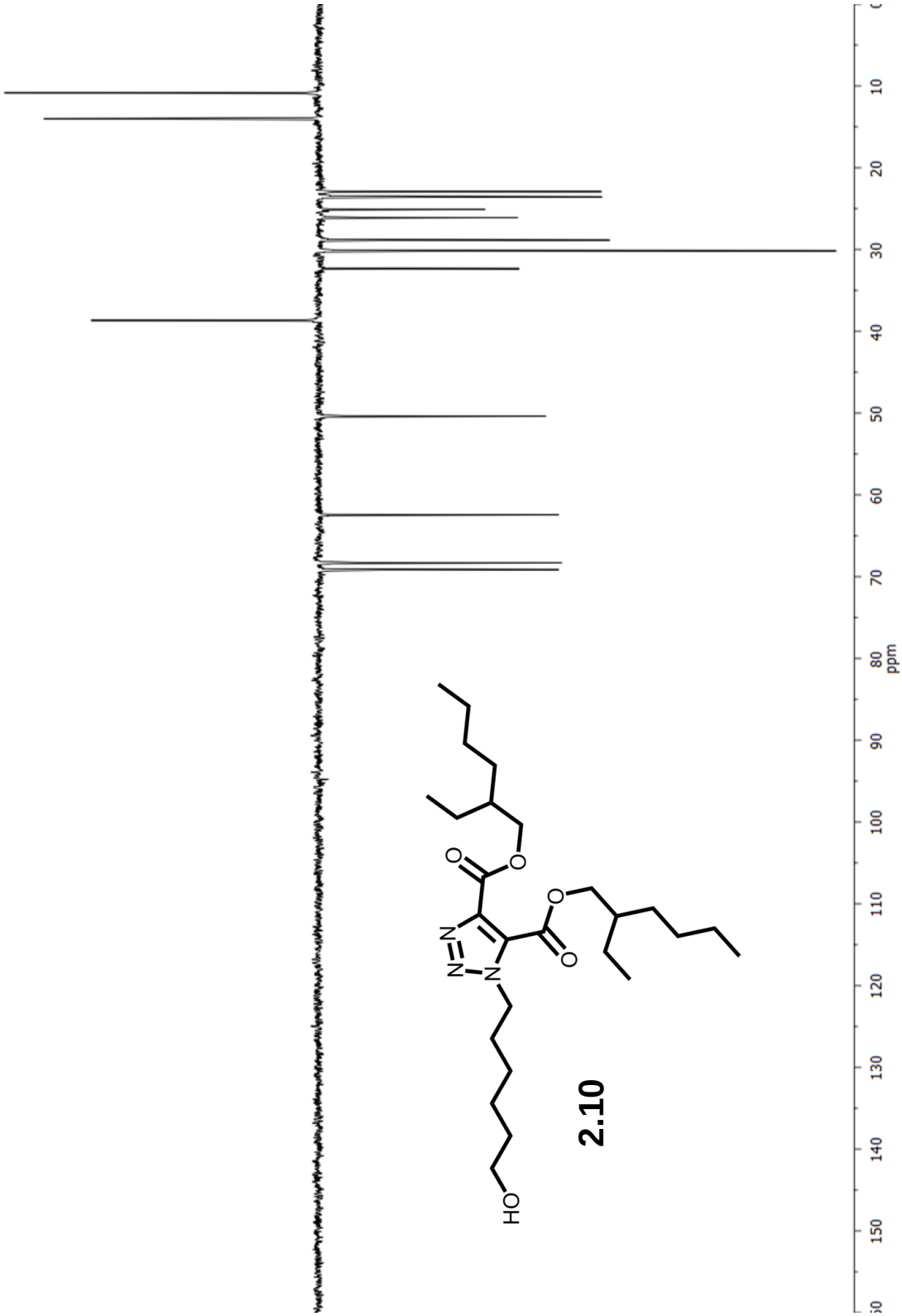
ppm
2.10

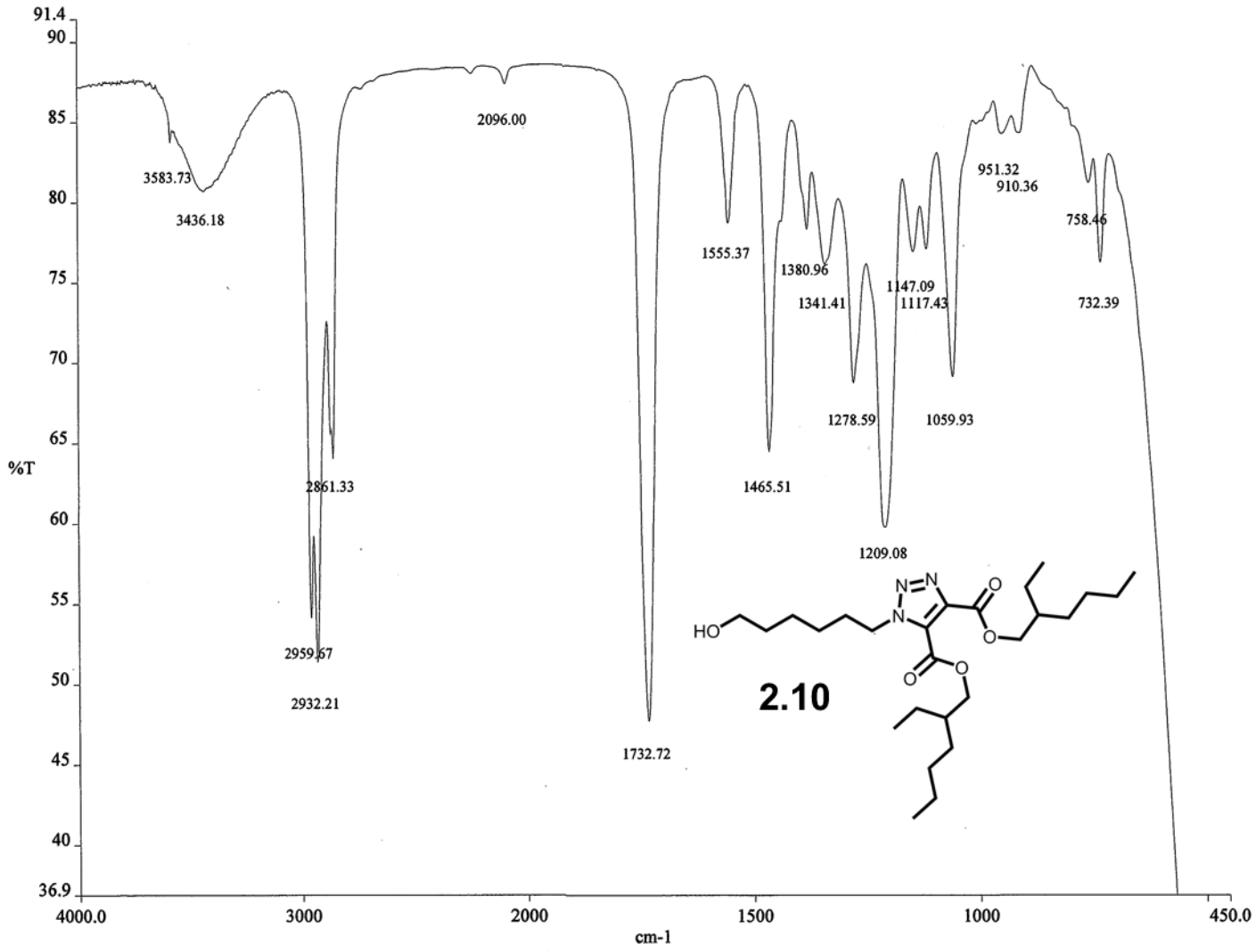
91.4
90
85
80
75
70
65
60
55
50
45
40
36.9
%T
4000.0
3000
2000
1500
1000
450.0
cm-1
3583.73
3436.18
2959.67
2932.21
2861.33
2096.00
1732.72
1555.37
1465.51
1380.96
1341.41
1278.59
1209.08
1147.09
1117.43
1059.93
951.32
910.36
758.46
732.39
HO
N
N
O
O
O
O
2.10

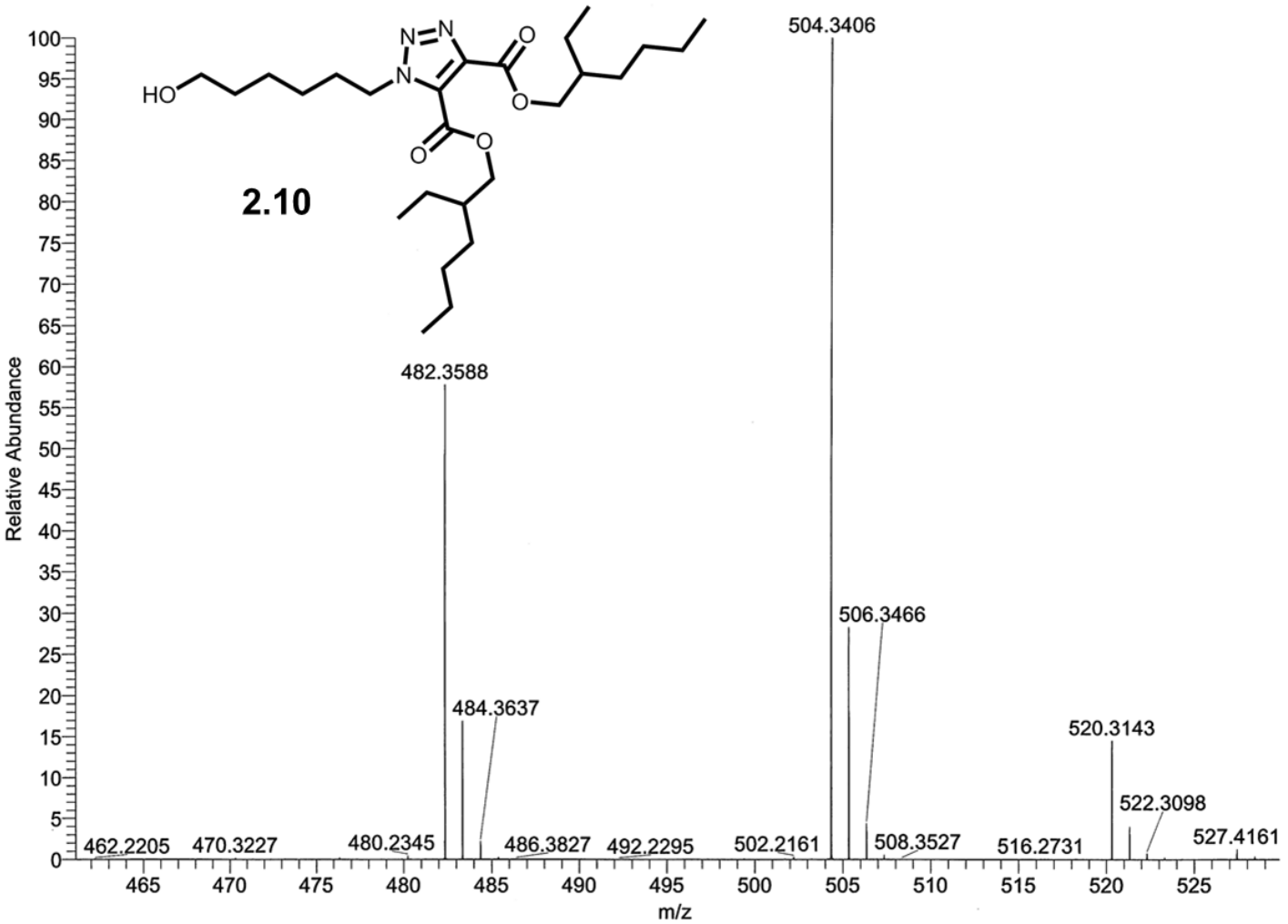
2.10
HO
N
N
N
O
O
O
O
Relative Abundance
m/z
504.3406
482.3588
506.3466
484.3637
520.3143
522.3098
527.4161
462.2205
470.3227
480.2345
486.3827
492.2295
502.2161
508.3527
516.2731

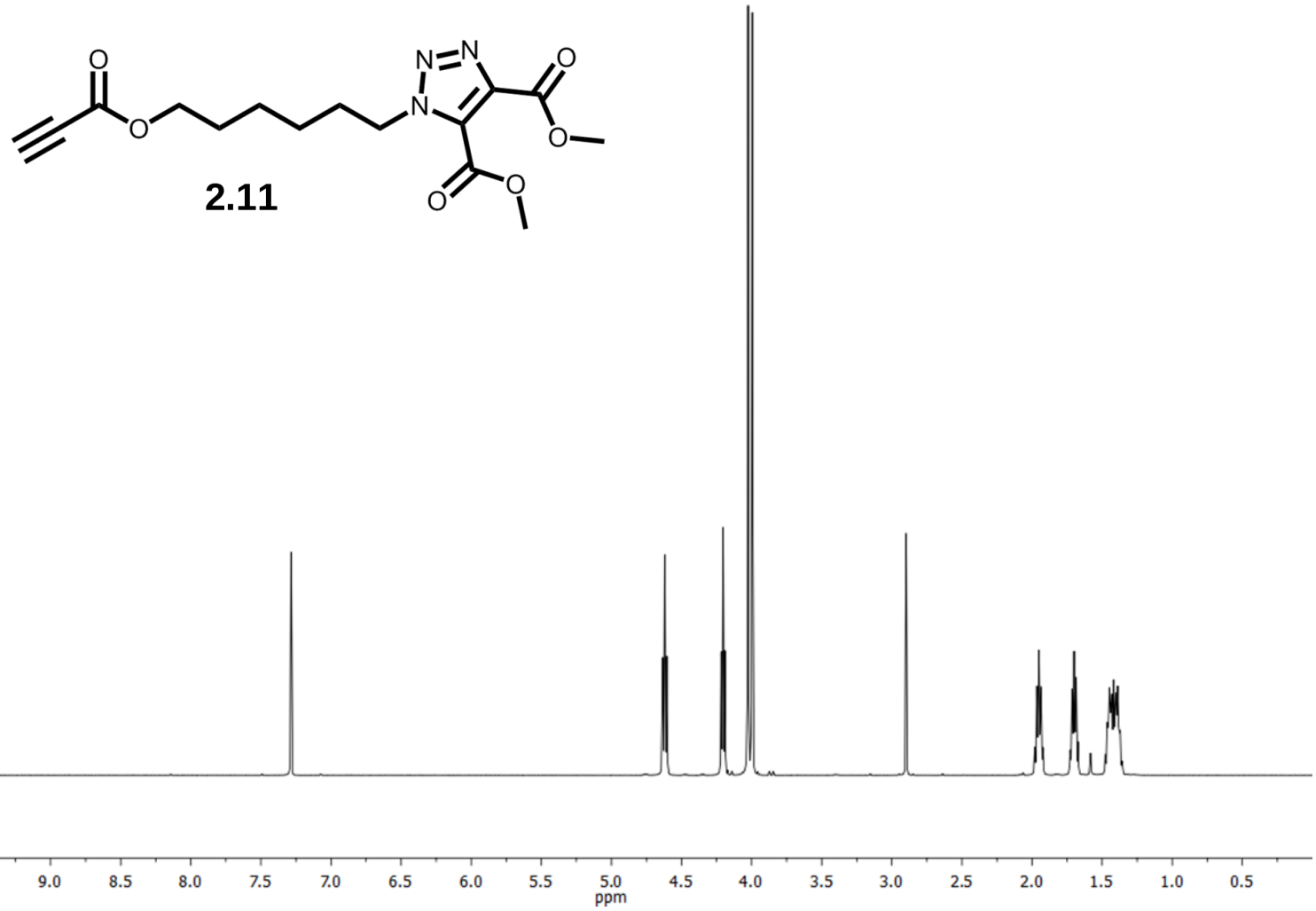
2.11
ppm

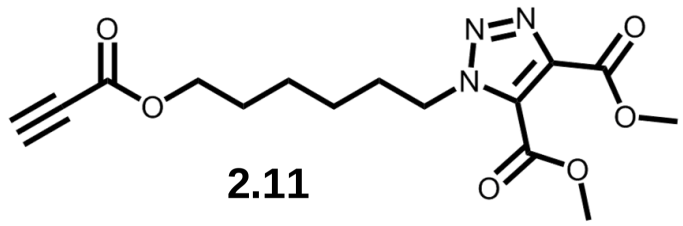
O
O
N
N
N
O
O
O
O

2.11

200
190
180
170
160
150
140
130
120
110
100
90
80
70
60
50
40
30
20
10
ppm

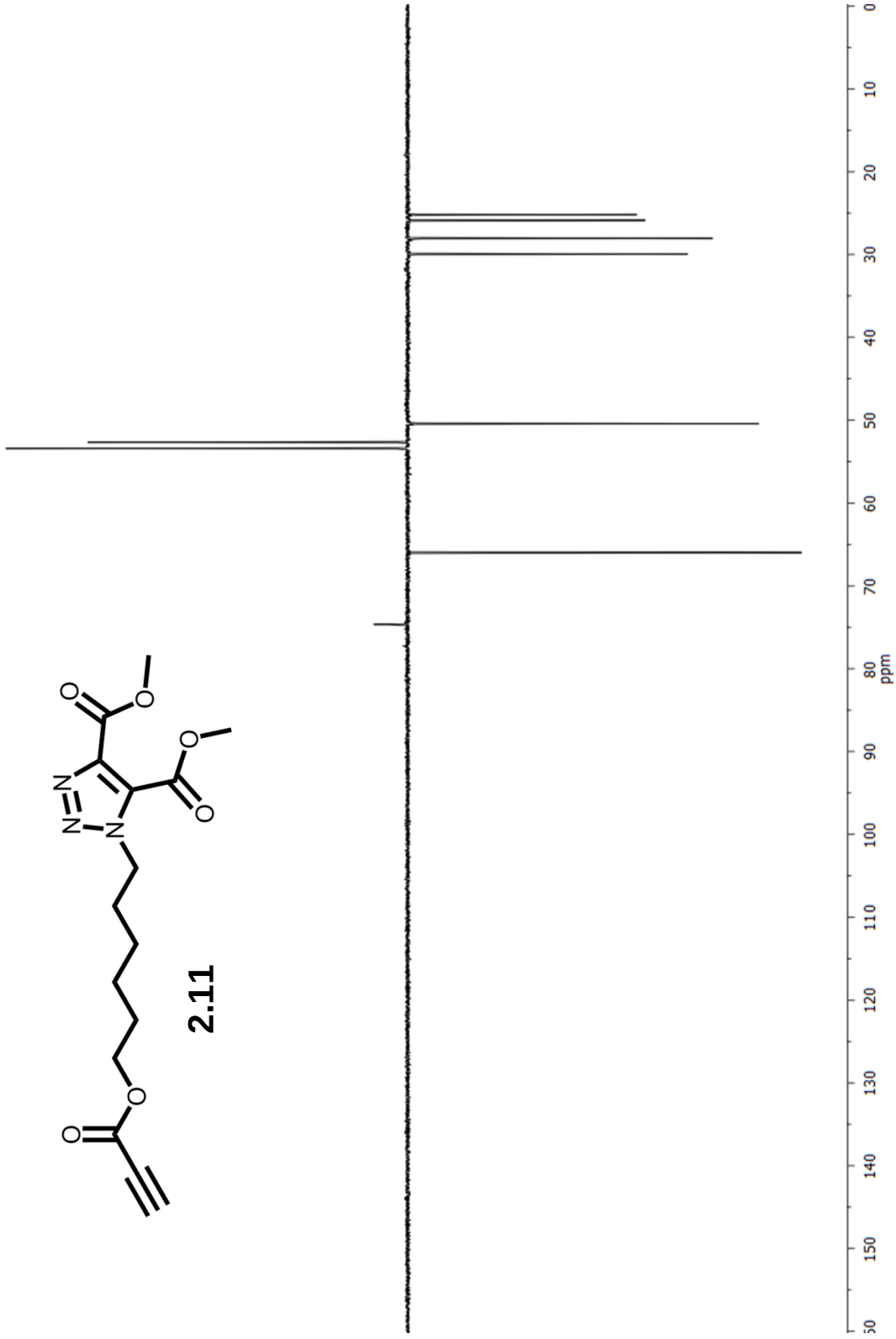
2.11
ppm

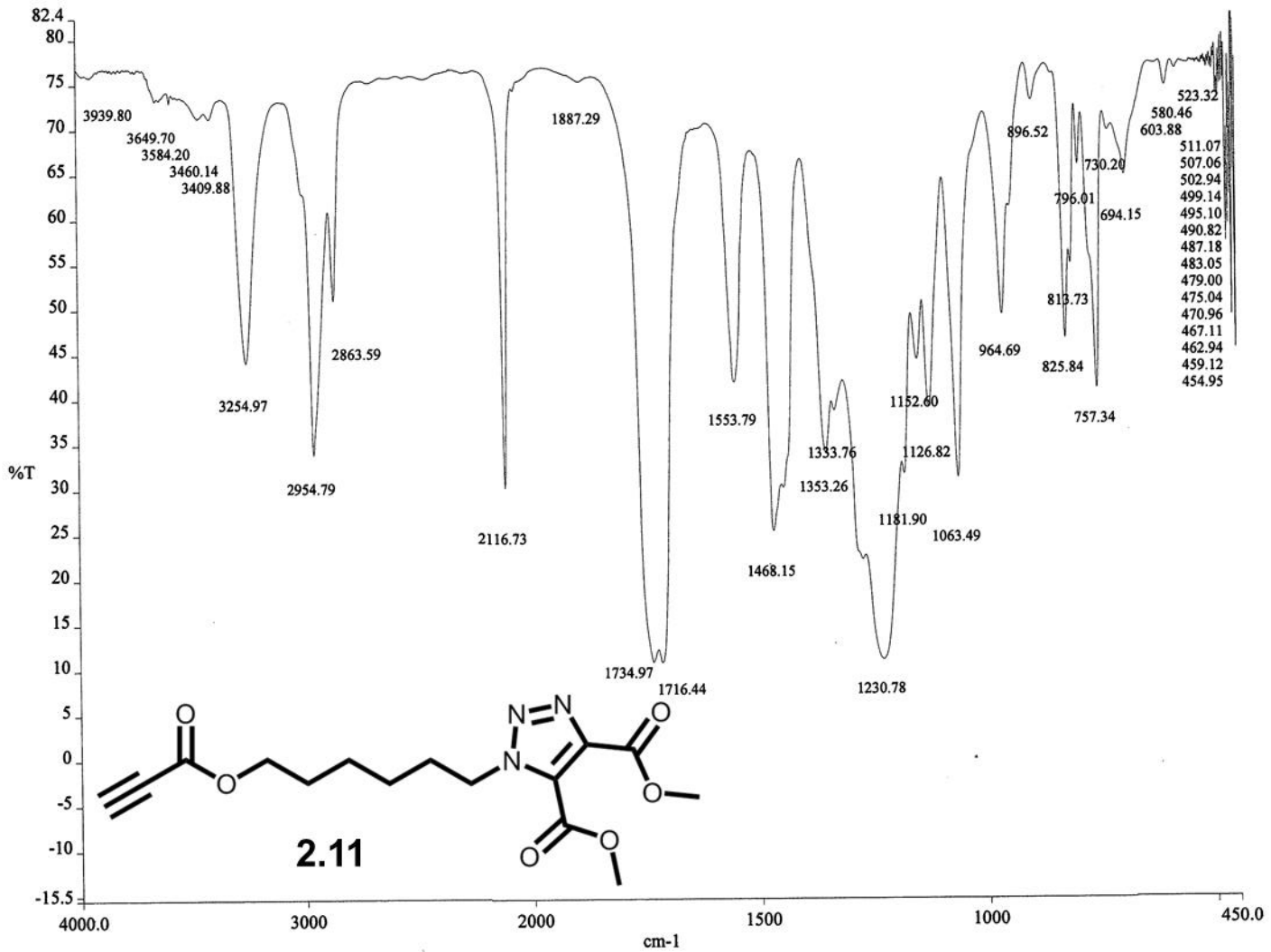
82.4
80
75
70
65
60
55
50
45
40
35
30
25
20
15
10
5
0
-5
-10
-15.5
%T
4000.0
3000
2000
1500
1000
450.0
cm-1
3939.80
3649.70
3584.20
3460.14
3409.88
3254.97
2954.79
2863.59
2116.73
1887.29
1734.97
1716.44
1553.79
1468.15
1353.26
1333.76
1230.78
1181.90
1152.60
1126.82
1063.49
964.69
896.52
825.84
813.73
796.01
757.34
730.20
694.15
603.88
580.46
523.32
511.07
507.06
502.94
499.14
495.10
490.82
487.18
483.05
479.00
475.04
470.96
467.11
462.94
459.12
454.95
O
O
O
N
N
N
O
O
O
2.11

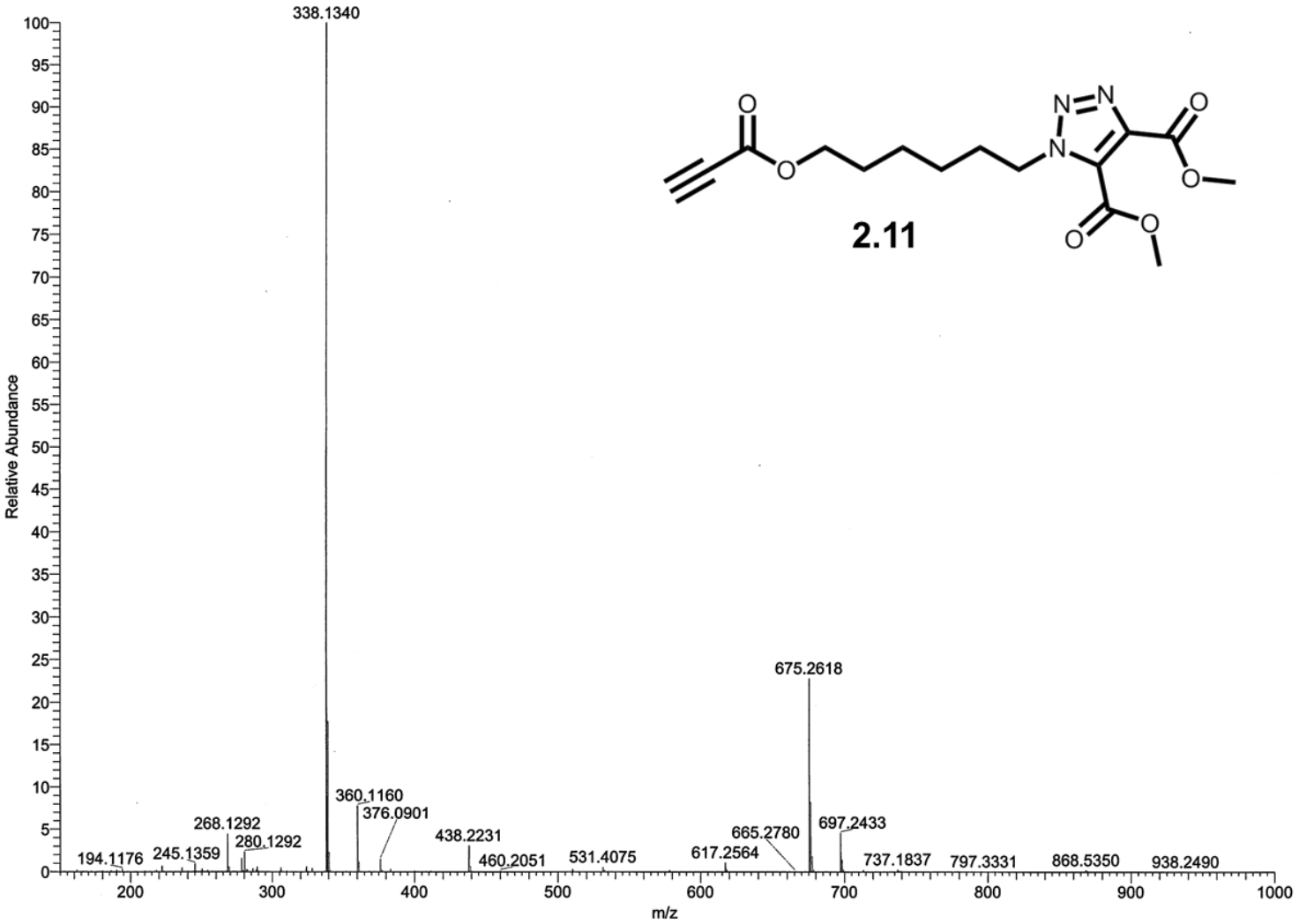
338.1340
675.2618
360.1160
376.0901
268.1292
280.1292
438.2231
194.1176
245.1359
460.2051
531.4075
617.2564
665.2780
697.2433
737.1837
797.3331
868.5350
938.2490
Relative Abundance
m/z
2.11

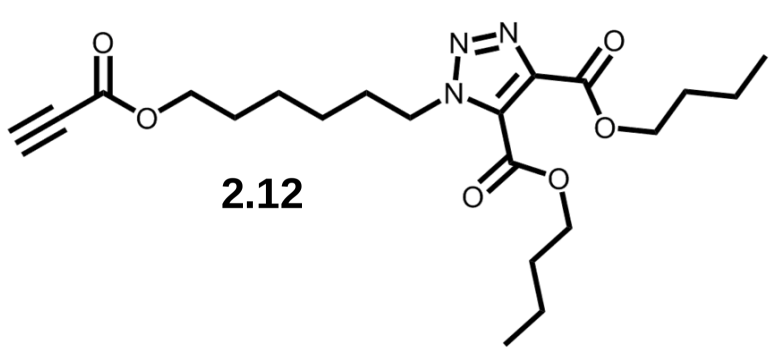
O
O
N=N
N
O
O
O
O

2.12

9.5
9.0
8.5
8.0
7.5
7.0
6.5
6.0
5.5
5.0
4.5
4.0
3.5
3.0
2.5
2.0
1.5
1.0
0.5
ppm

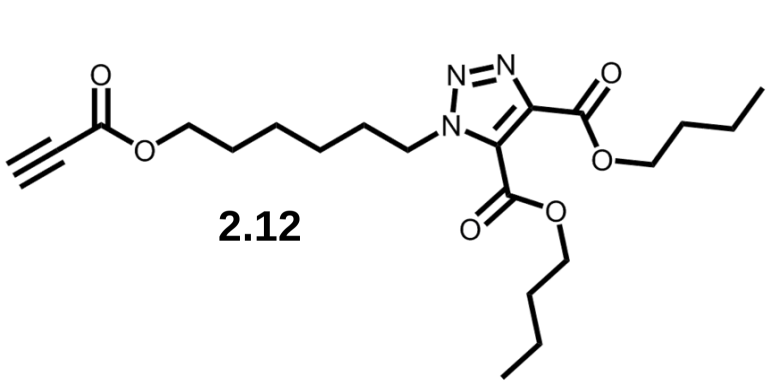
O
O
N
N
N
O
O
O
O

2.12

200
190
180
170
160
150
140
130
120
110
100
90
80
70
60
50
40
30
20
10
ppm

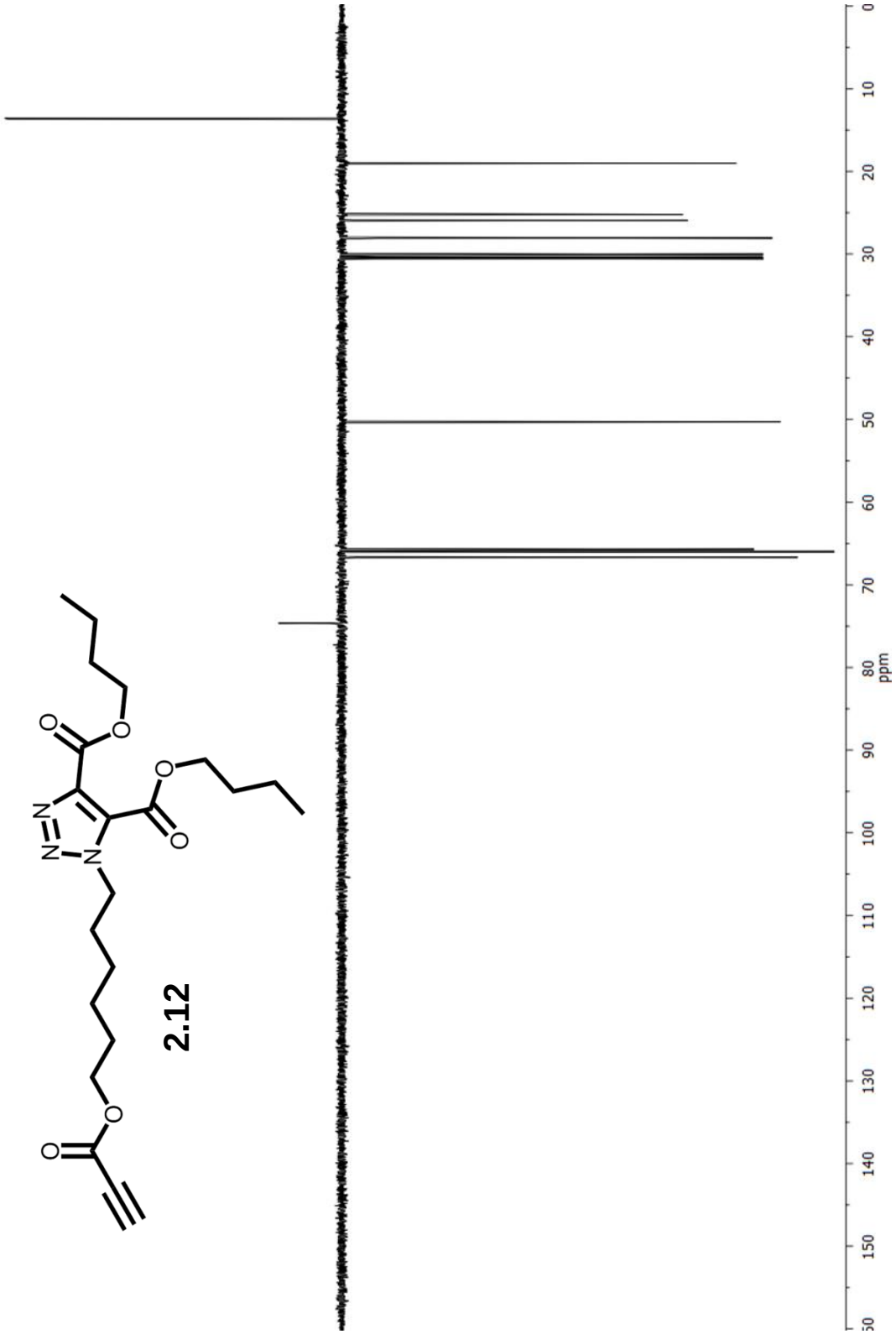
2.12
ppm

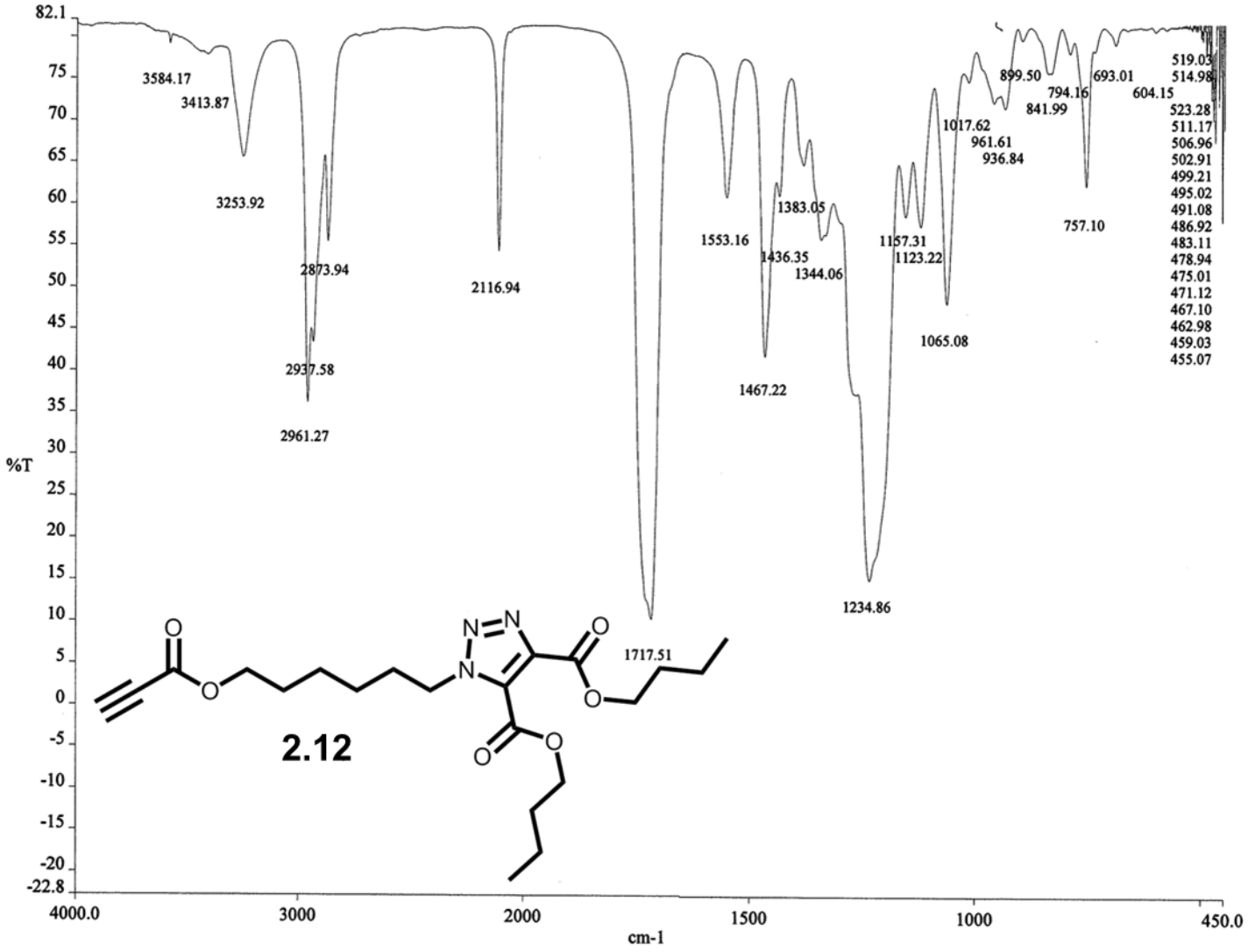
82.1
75
70
65
60
55
50
45
40
35
30
25
20
15
10
5
0
-5
-10
-15
-20
-22.8
%T
4000.0
3000
2000
1500
1000
450.0
cm-1
3584.17
3413.87
3253.92
2873.94
2937.58
2961.27
2116.94
1717.51
1553.16
1467.22
1436.35
1383.05
1344.06
1234.86
1157.31
1123.22
1065.08
1017.62
961.61
936.84
899.50
841.99
794.16
757.10
693.01
604.15
519.03
514.98
523.28
511.17
506.96
502.91
499.21
495.02
491.08
486.92
483.11
478.94
475.01
471.12
467.10
462.98
459.03
455.07
2.12

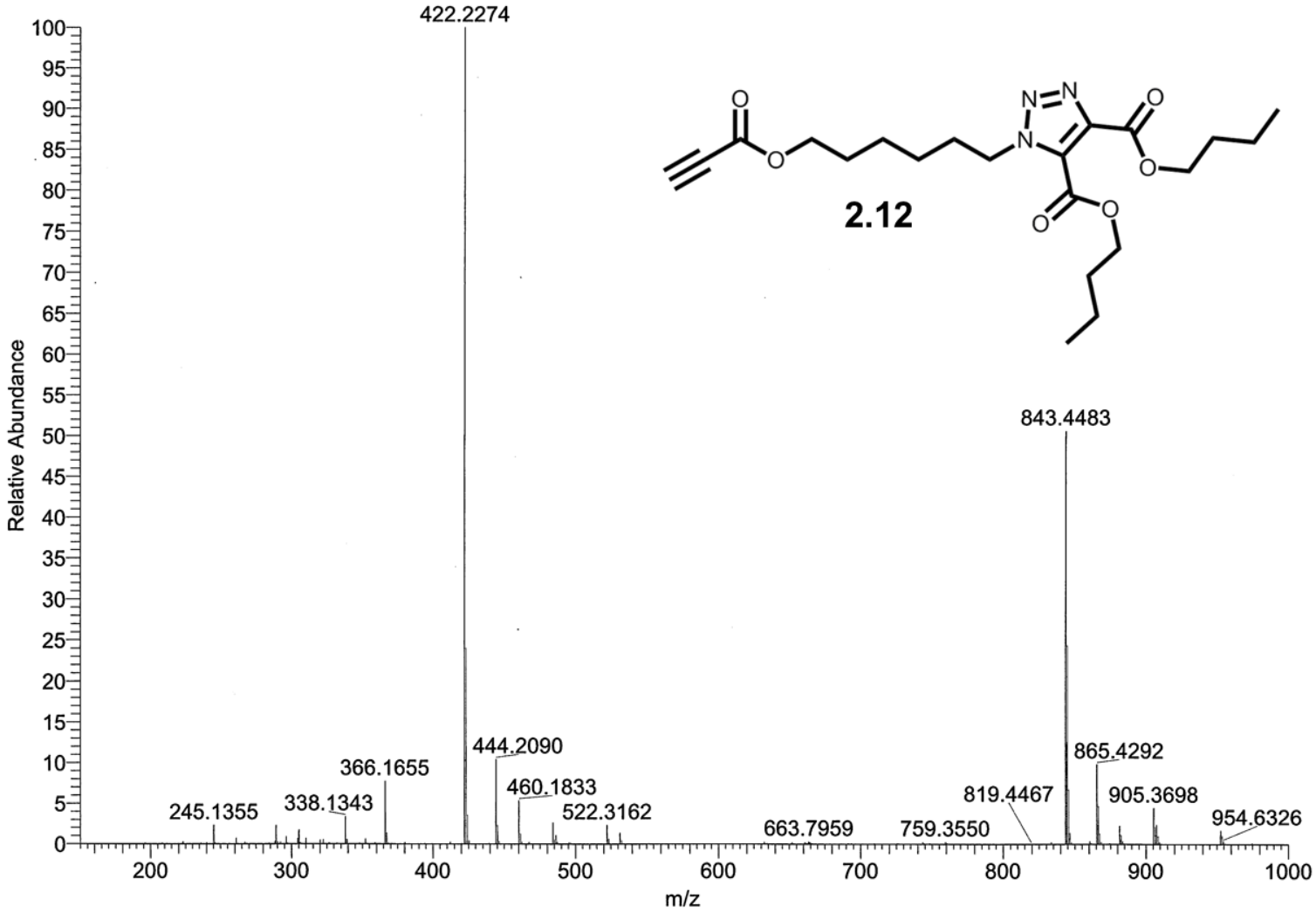
422.2274
843.4483
2.12
Relative Abundance
m/z
100
95
90
85
80
75
70
65
60
55
50
45
40
35
30
25
20
15
10
5
0
200
300
400
500
600
700
800
900
1000
245.1355
338.1343
366.1655
444.2090
460.1833
522.3162
663.7959
759.3550
819.4467
865.4292
905.3698
954.6326

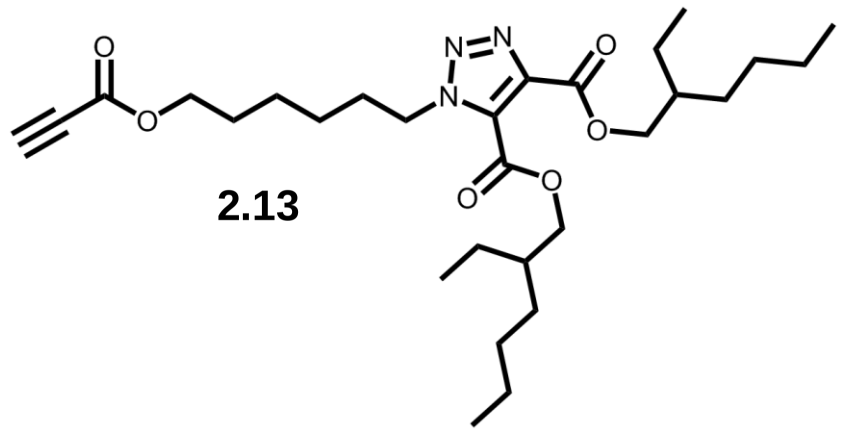
O
O
N
N
N
O
O
O
O
O

2.13

9.5
9.0
8.5
8.0
7.5
7.0
6.5
6.0
5.5
5.0
4.5
4.0
3.5
3.0
2.5
2.0
1.5
1.0
0.5
ppm

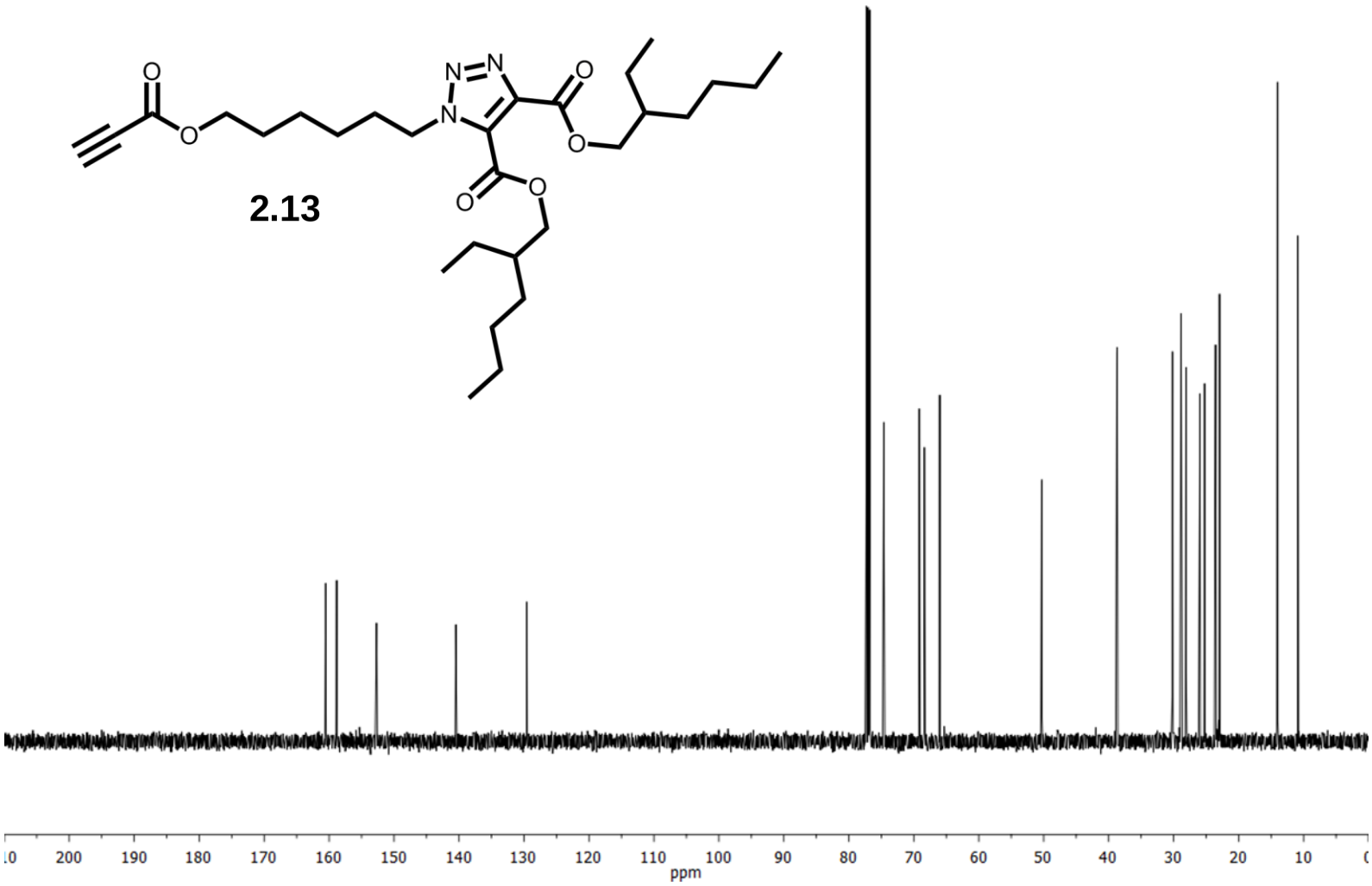
2.13
ppm

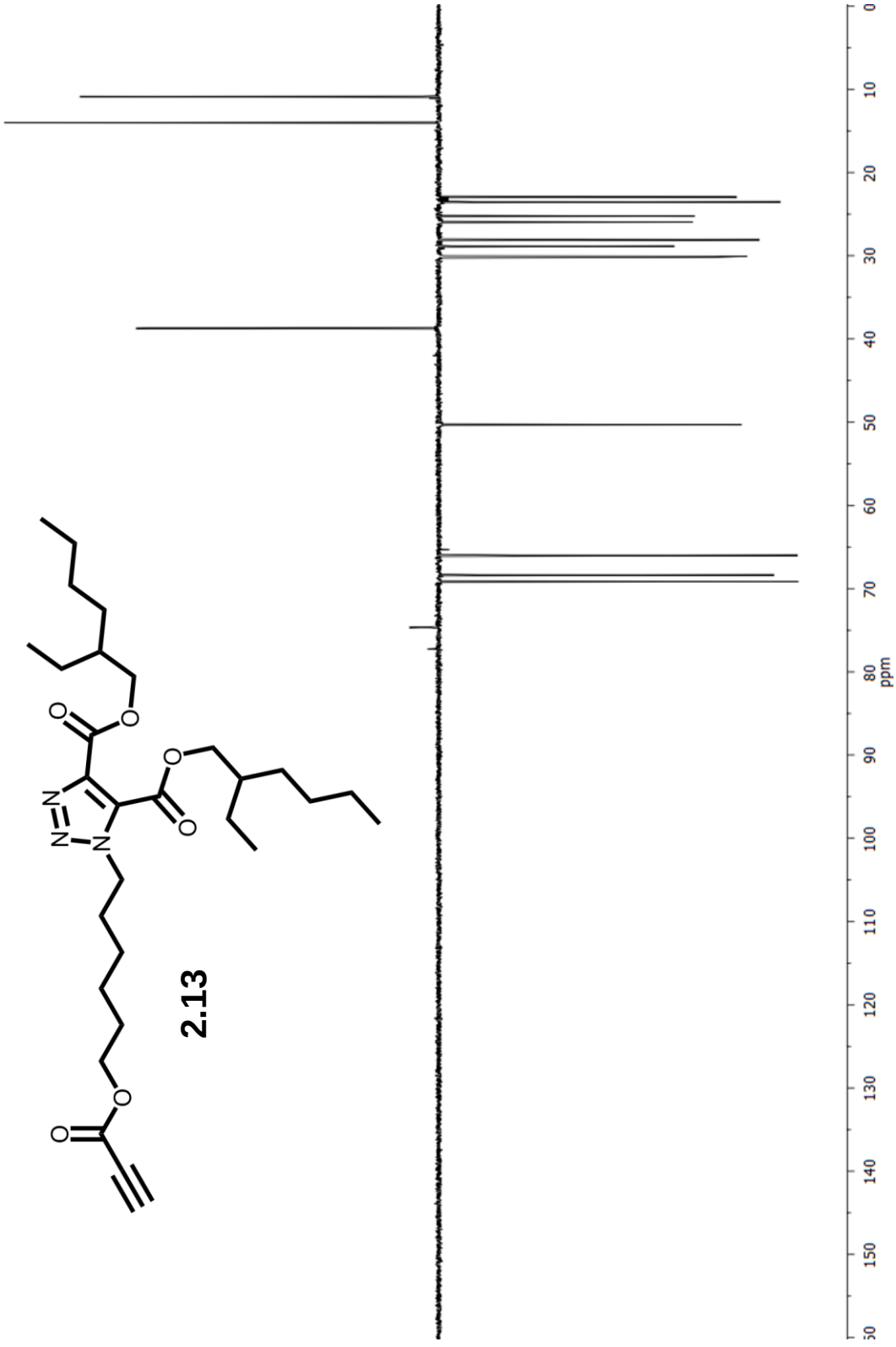
2.13
ppm

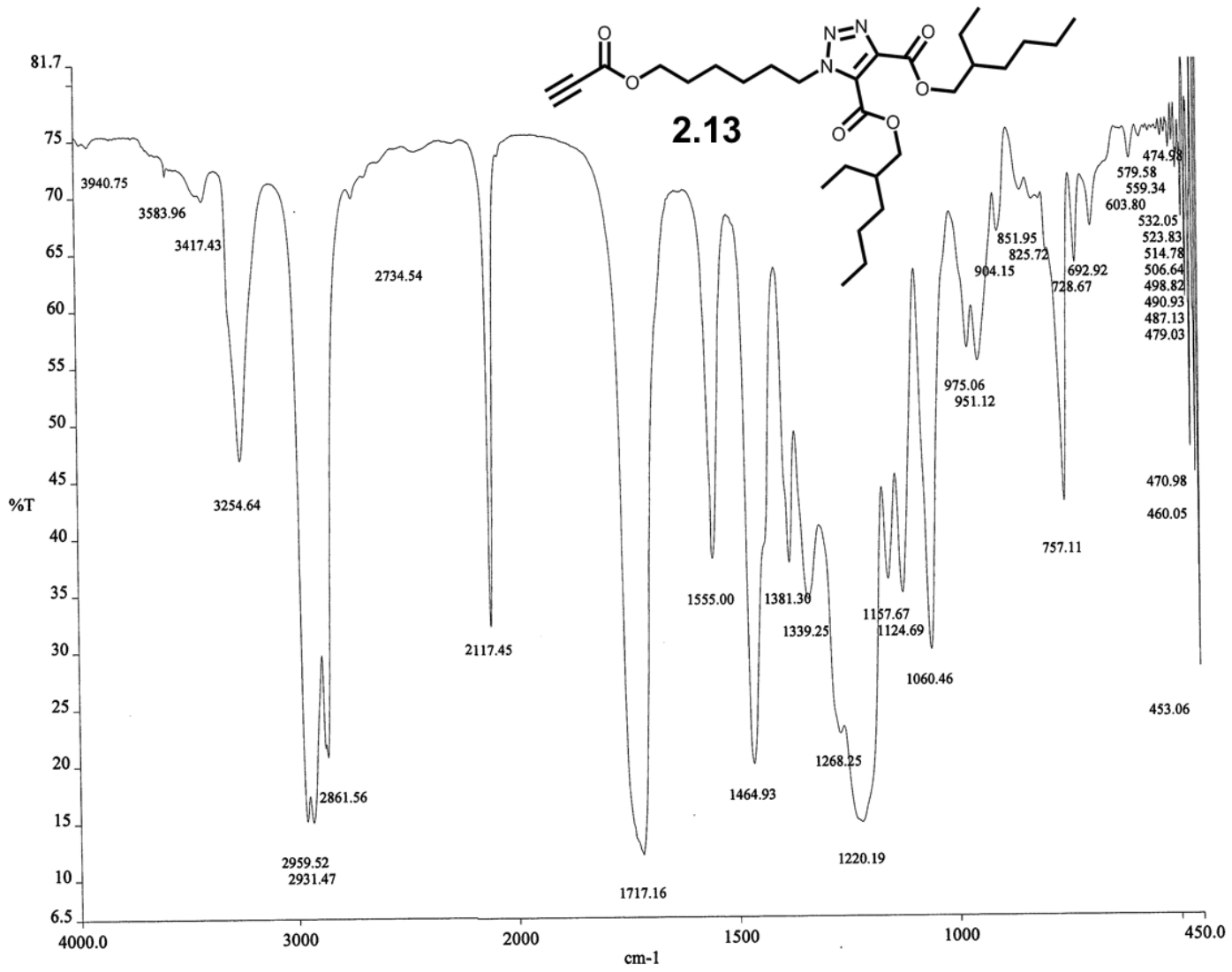
2.13
%T
cm-1
81.7
75
70
65
60
55
50
45
40
35
30
25
20
15
10
6.5
4000.0
3000
2000
1500
1000
450.0
3940.75
3583.96
3417.43
3254.64
2959.52
2931.47
2861.56
2734.54
2117.45
1717.16
1555.00
1464.93
1381.30
1339.25
1268.25
1220.19
1157.67
1124.69
1060.46
975.06
951.12
904.15
851.95
825.72
757.11
728.67
692.92
603.80
579.58
559.34
532.05
523.83
514.78
506.64
498.82
490.93
487.13
479.03
474.98
470.98
460.05
453.06

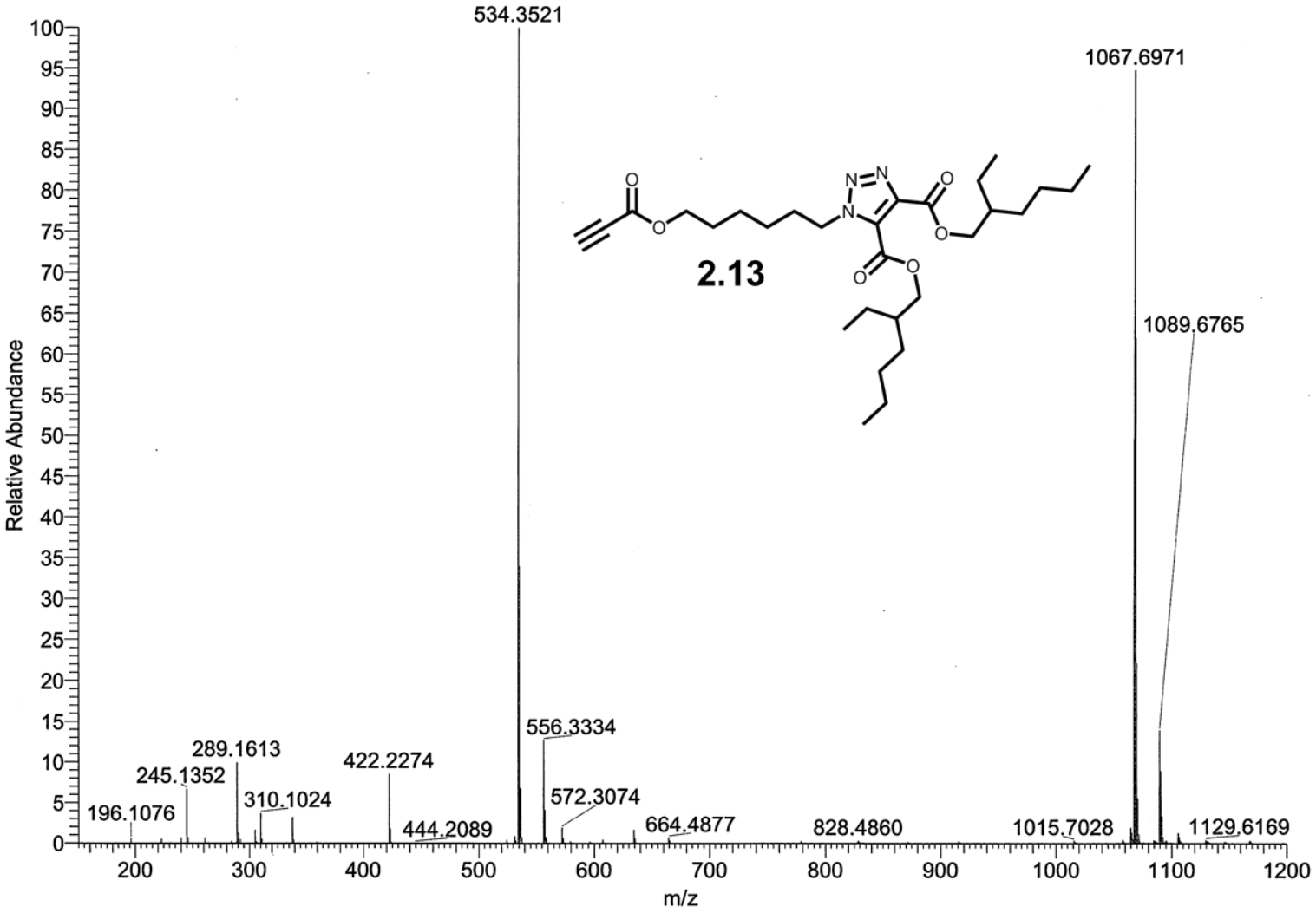
534.3521
1067.6971
1089.6765
2.13
556.3334
289.1613
422.2274
245.1352
572.3074
310.1024
196.1076
444.2089
664.4877
828.4860
1015.7028
1129.6169
Relative Abundance
m/z

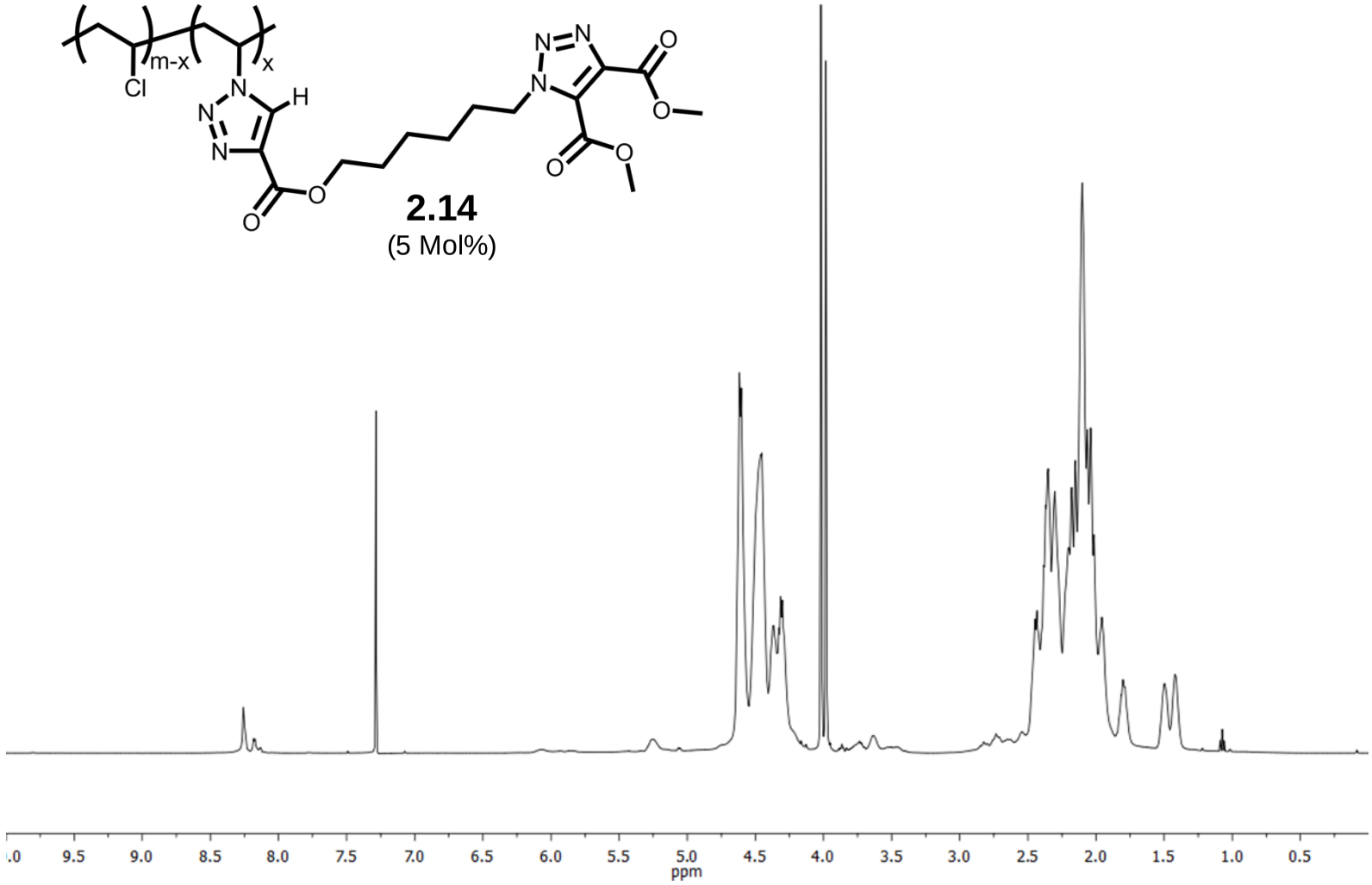
m-x
x
Cl
H
N
N
N
N
N
O
O
O
O
O
O
O
2.14
(5 Mol%)
9.5
9.0
8.5
8.0
7.5
7.0
6.5
6.0
5.5
5.0
4.5
4.0
3.5
3.0
2.5
2.0
1.5
1.0
0.5
ppm

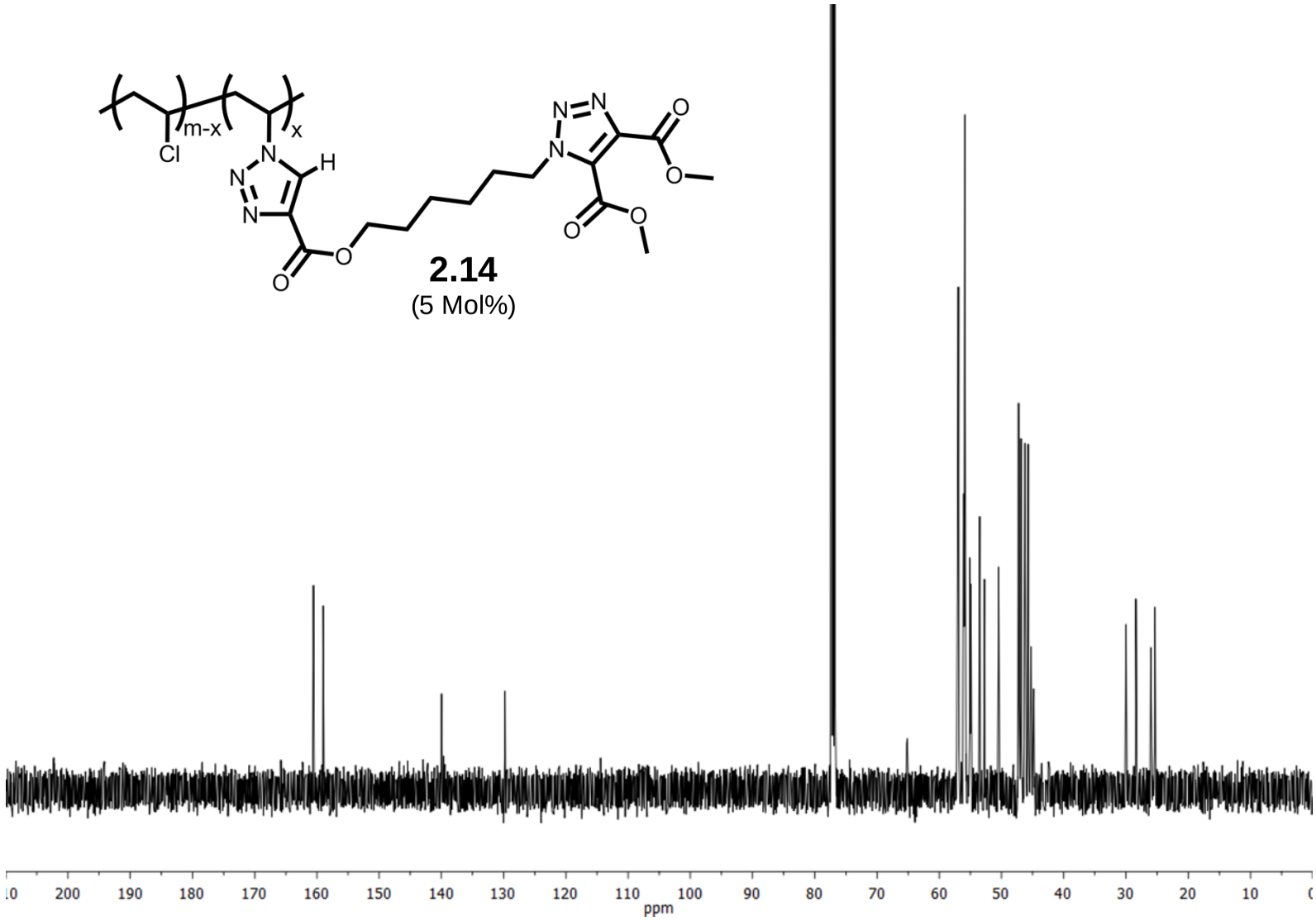
m-x
x
Cl
H
N
N
N
N
N
O
O
O
O
O
O
2.14
(5 Mol%)
200
190
180
170
160
150
140
130
120
110
100
90
80
70
60
50
40
30
20
10
ppm

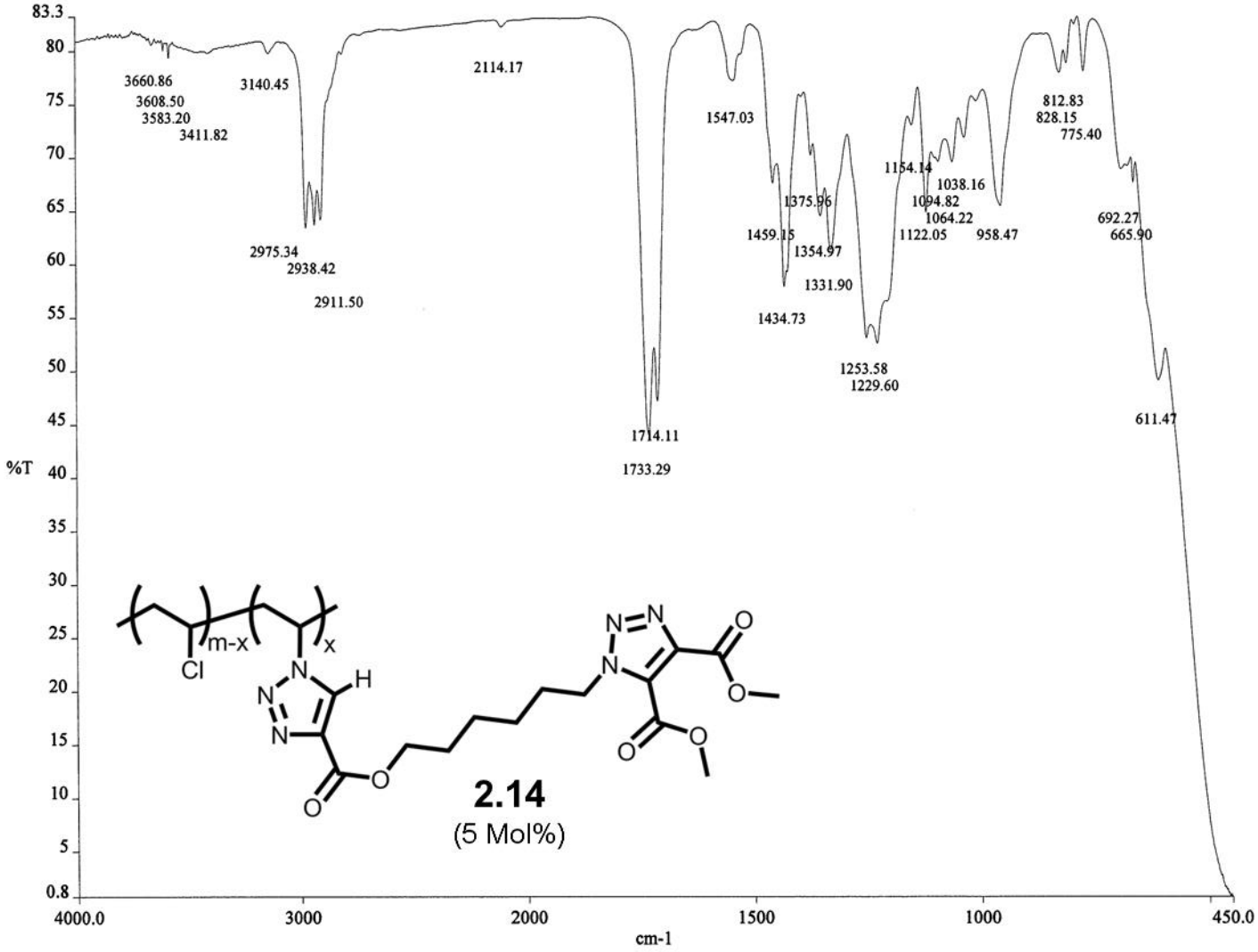
83.3
80
75
70
65
60
55
50
45
40
35
30
25
20
15
10
5
0.8
%T
4000.0
3000
2000
1500
1000
450.0
cm-1
3660.86
3608.50
3583.20
3411.82
3140.45
2975.34
2938.42
2911.50
2114.17
1733.29
1714.11
1547.03
1459.15
1434.73
1375.96
1354.97
1331.90
1253.58
1229.60
1154.14
1122.05
1094.82
1064.22
1038.16
958.47
812.83
828.15
775.40
692.27
665.90
611.47
m-x
x
Cl
H
N
O
2.14
(5 Mol%)

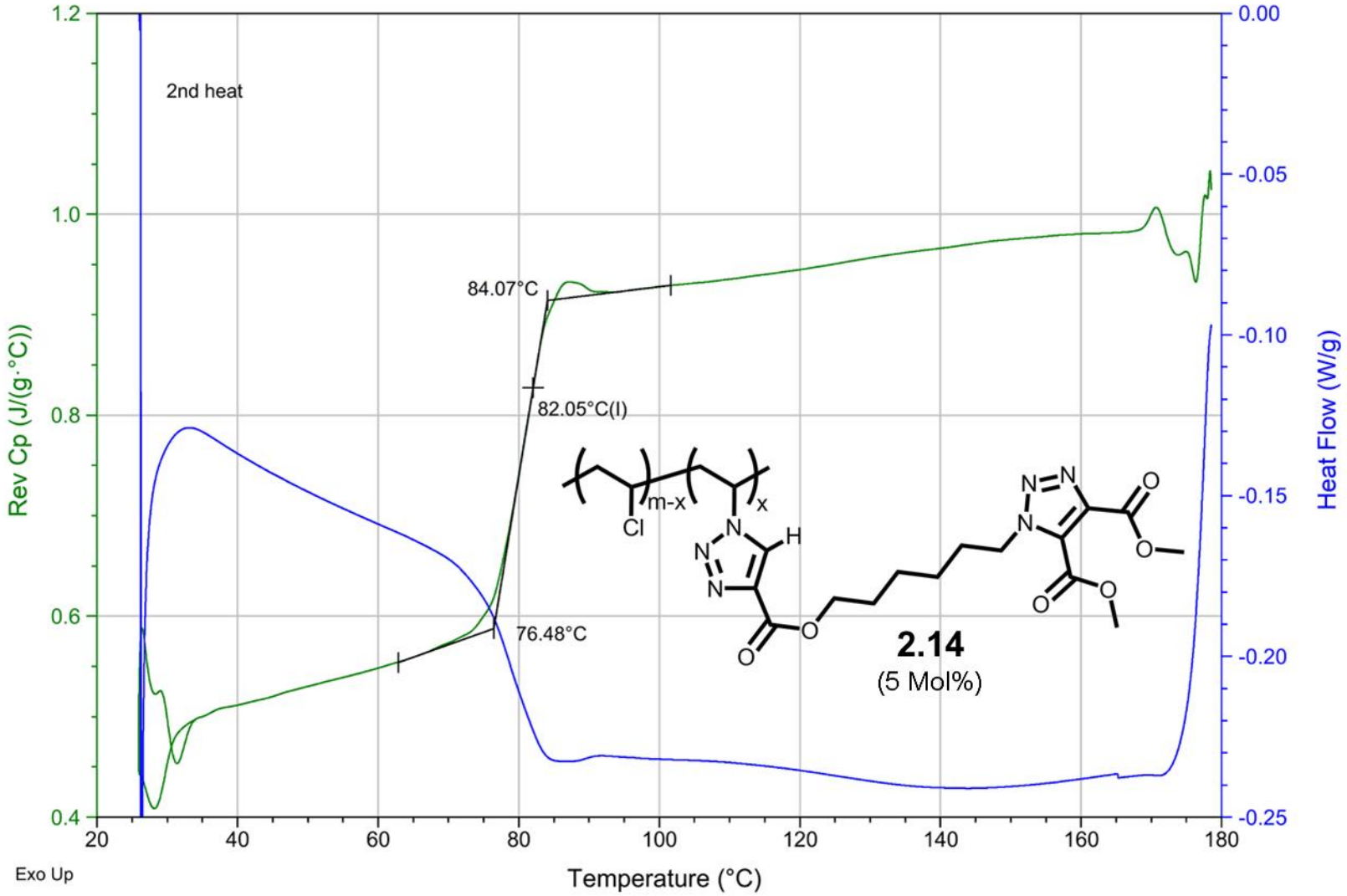
2nd heat
84.07°C
82.05°C(I)
76.48°C
Rev Cp (J/(g·°C))
Heat Flow (W/g)
Temperature (°C)
Exo Up
1.2
1.0
0.8
0.6
0.4
0.00
-0.05
-0.10
-0.15
-0.20
-0.25
20
40
60
80
100
120
140
160
180
m-x
x
Cl
H
N
O
2.14
(5 Mol%)

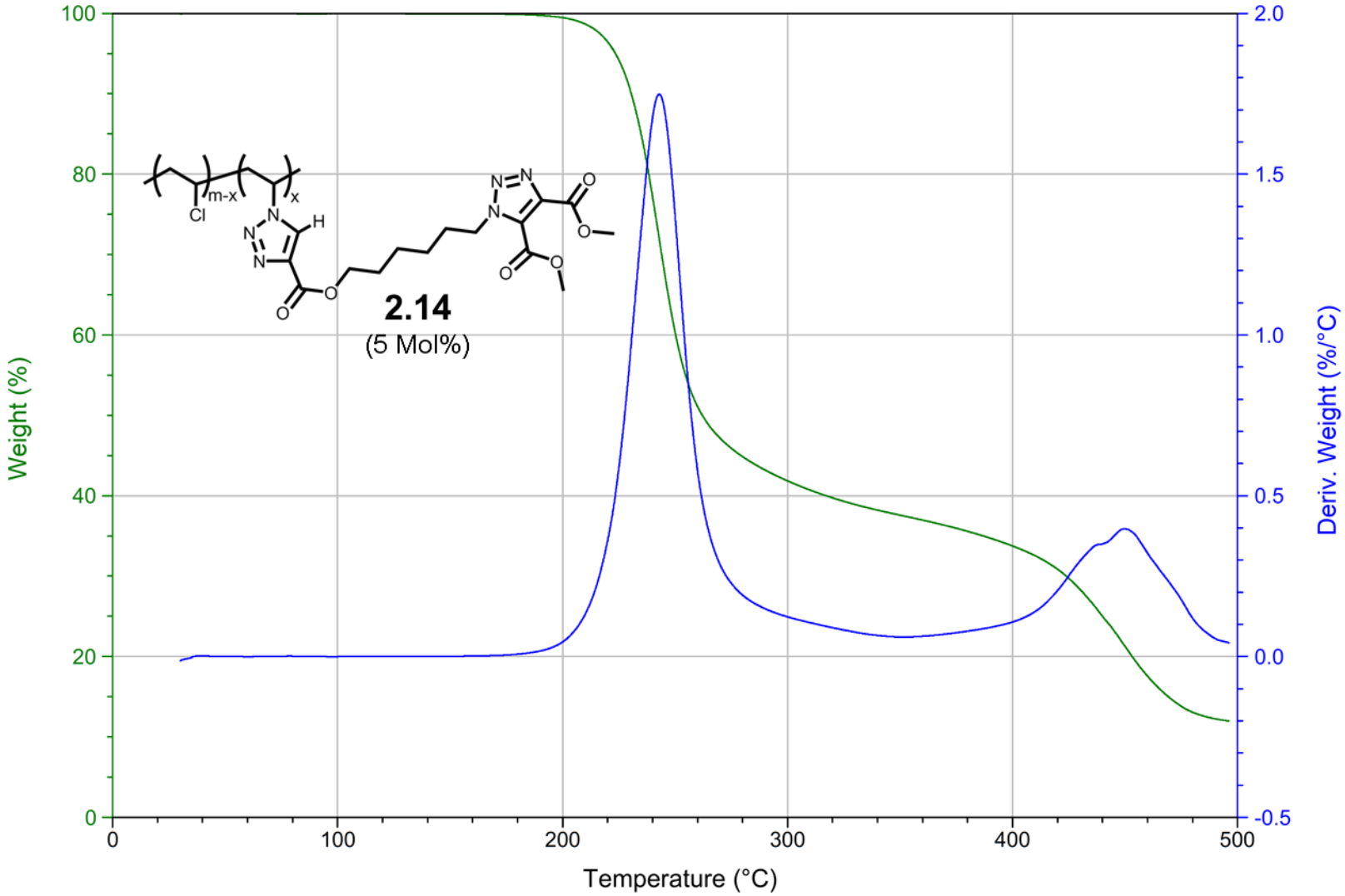
2.14
(5 Mol%)
Weight (%)
Deriv. Weight (%/°C)
Temperature (°C)
100
80
60
40
20
0
2.0
1.5
1.0
0.5
0.0
-0.5
0
100
200
300
400
500
Cl
m-x
x
H
N
O

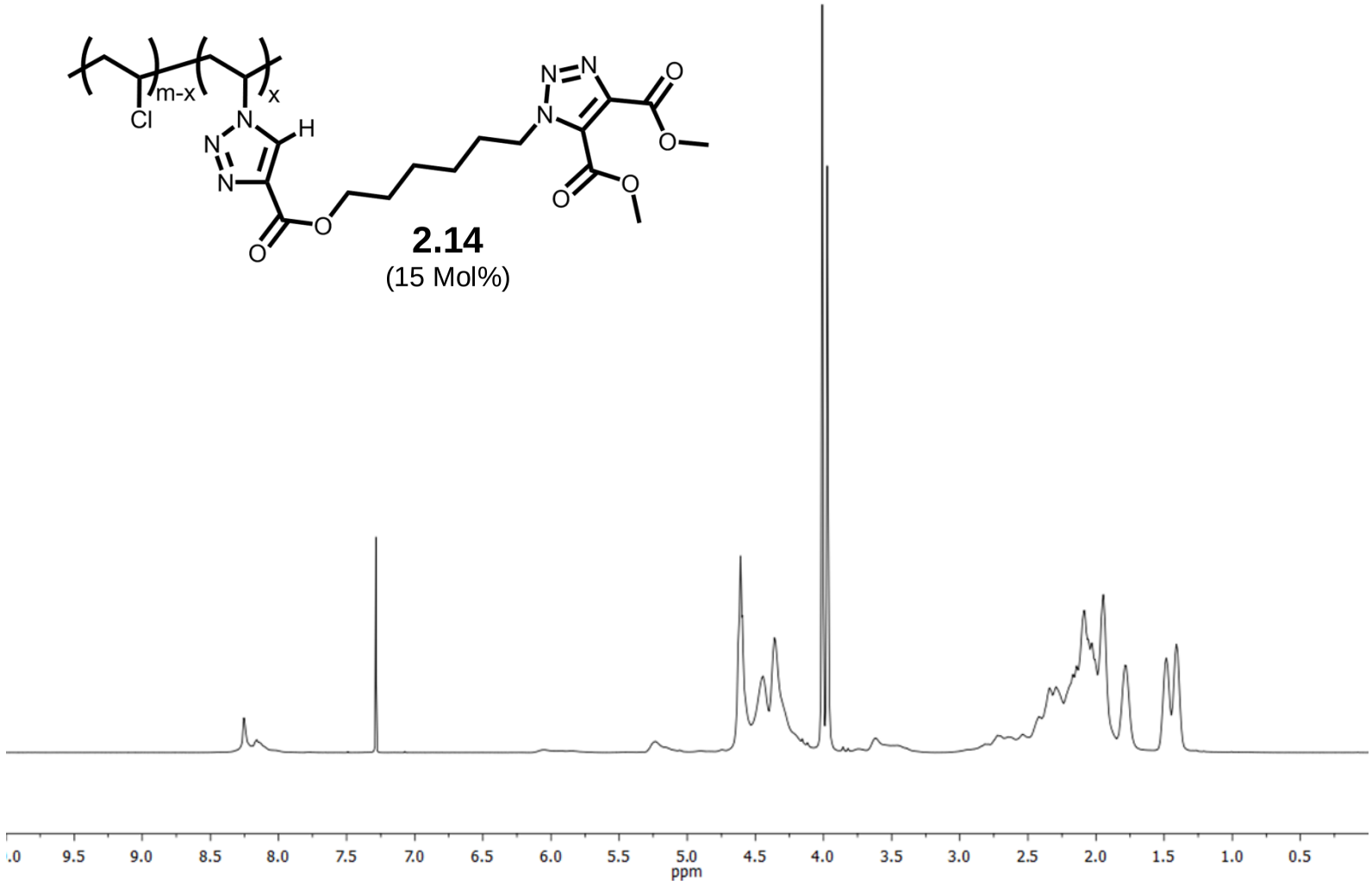
m-x
x
Cl
H
N
N
N
N
N
O
O
O
O
O
O
2.14
(15 Mol%)
9.5
9.0
8.5
8.0
7.5
7.0
6.5
6.0
5.5
5.0
4.5
4.0
3.5
3.0
2.5
2.0
1.5
1.0
0.5
ppm

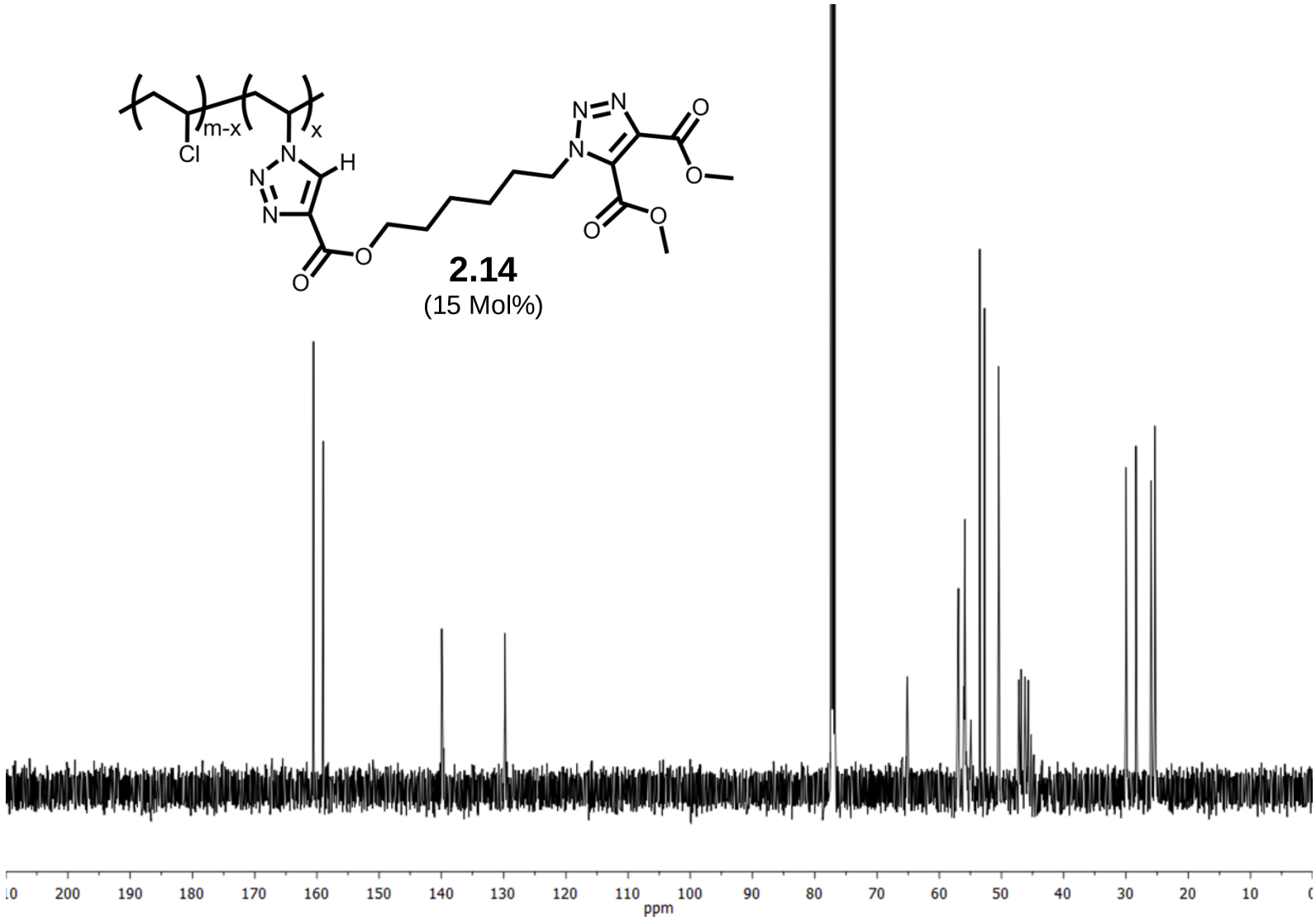
m-x
x
Cl
H
N
N
N
N
O
O
O
O
O
O
2.14
(15 Mol%)
200
190
180
170
160
150
140
130
120
110
100
90
80
70
60
50
40
30
20
10
ppm

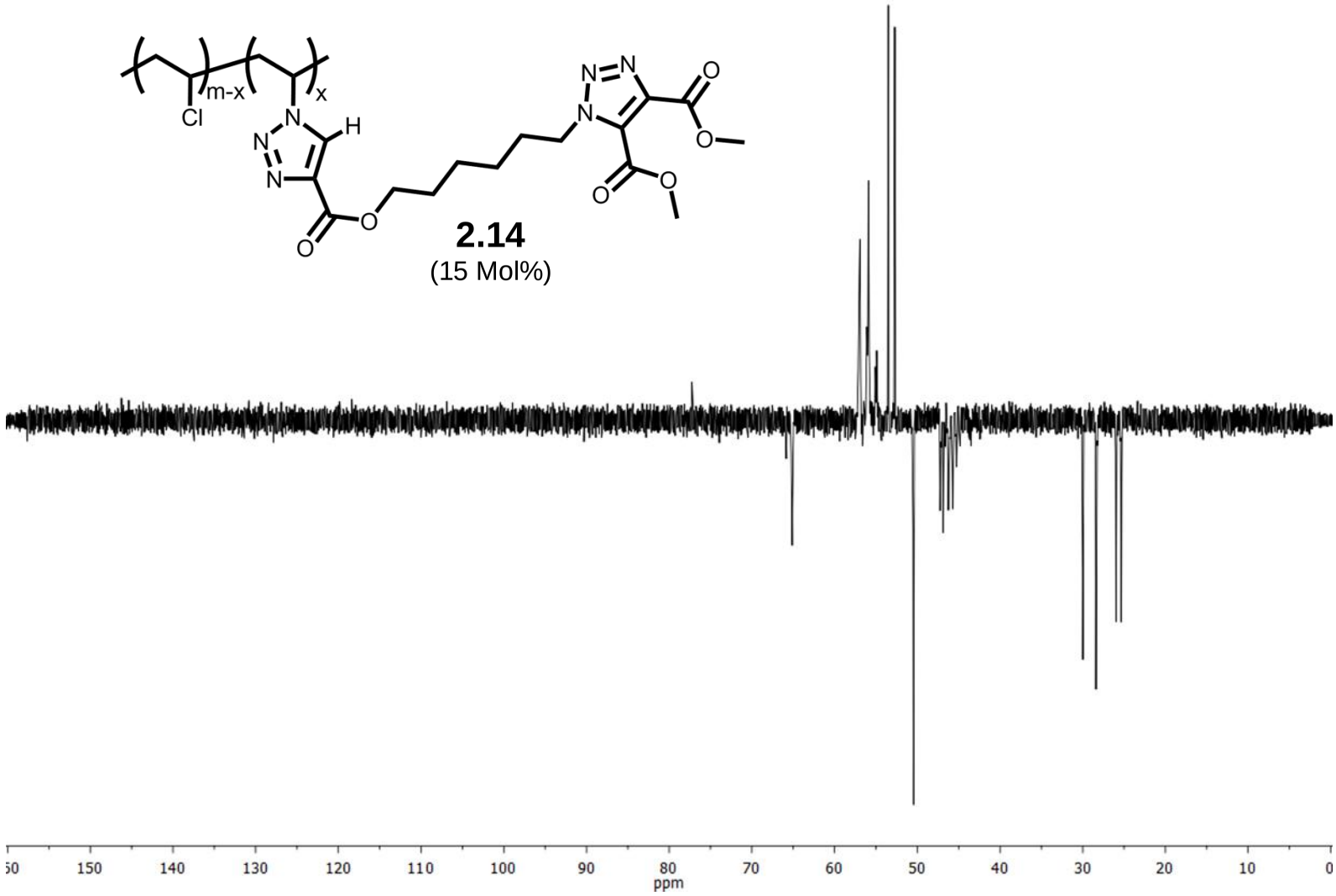
m-x
x
Cl
H
N
N
N
N
O
O
O
O
O
O
2.14
(15 Mol%)
150
140
130
120
110
100
90
80
70
60
50
40
30
20
10
0
ppm

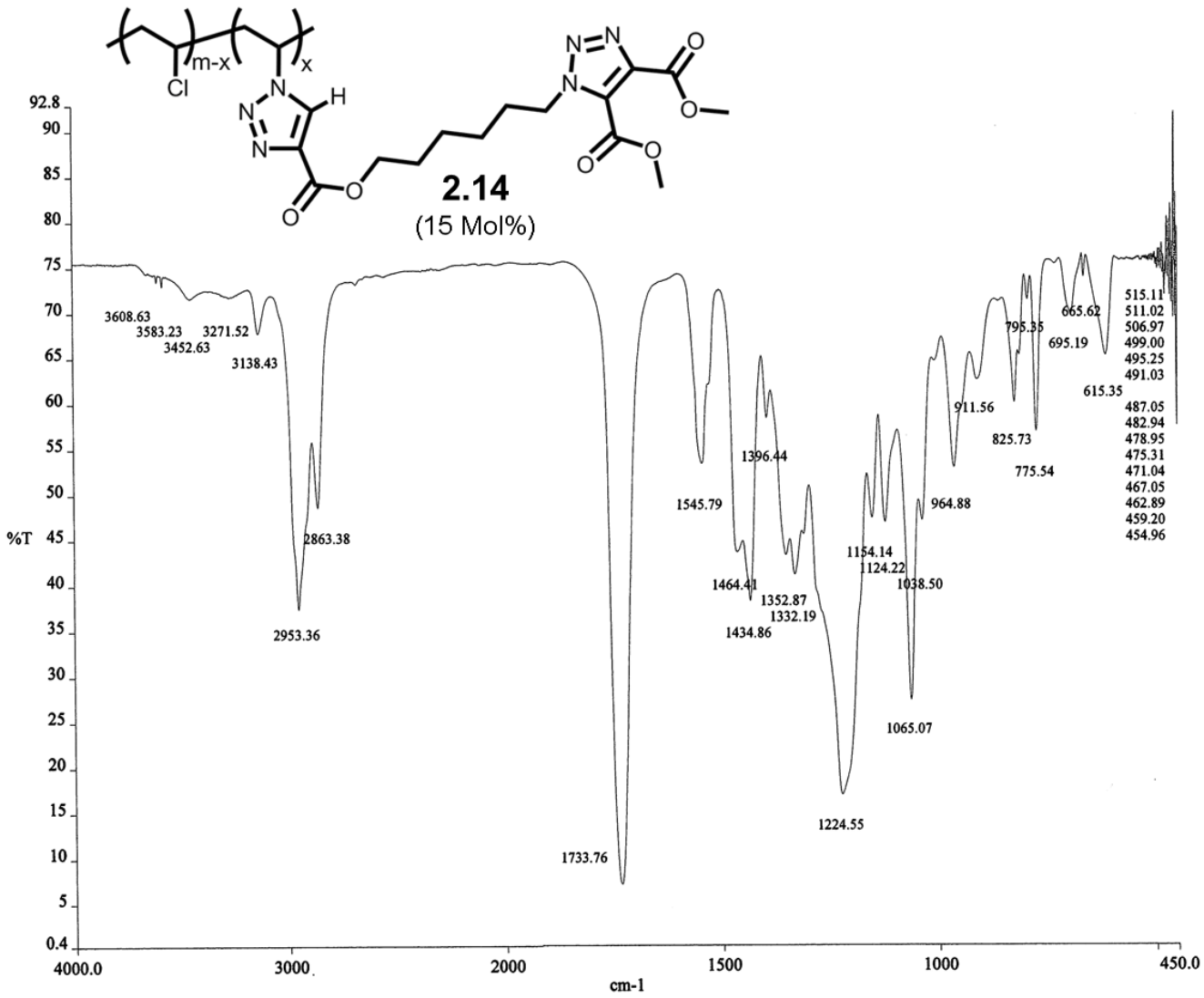
m-x
x
Cl
H
N
O
2.14
(15 Mol%)
92.8
90
85
80
75
70
65
60
55
50
45
40
35
30
25
20
15
10
5
0.4
%T
3608.63
3583.23
3452.63
3271.52
3138.43
2863.38
2953.36
1733.76
1545.79
1396.44
1464.41
1434.86
1352.87
1332.19
1224.55
1154.14
1124.22
1065.07
1038.50
964.88
911.56
825.73
795.35
775.54
695.19
665.62
615.35
515.11
511.02
506.97
499.00
495.25
491.03
487.05
482.94
478.95
475.31
471.04
467.05
462.89
459.20
454.96
4000.0
3000
2000
1500
1000
450.0
cm-1

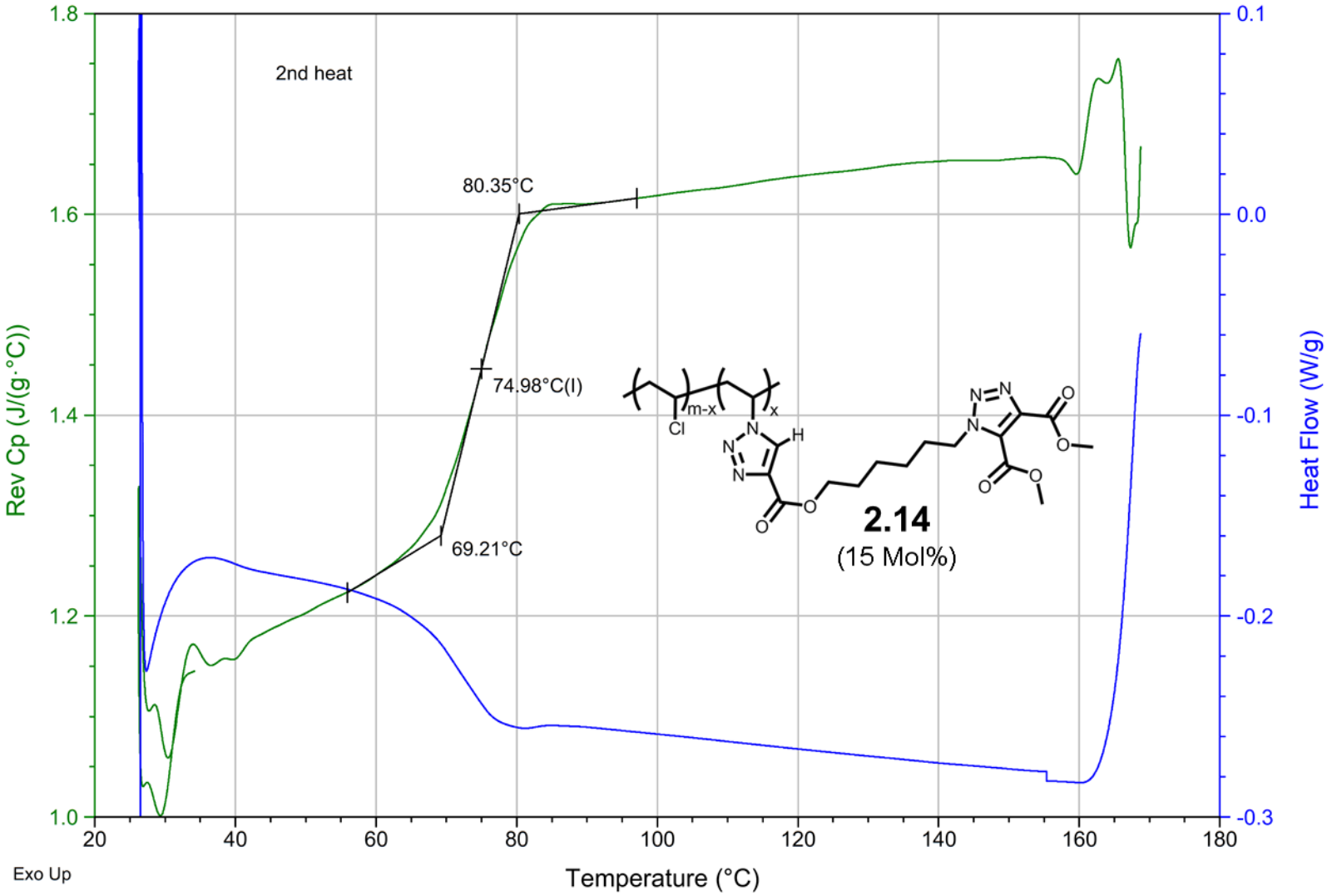
2nd heat
80.35°C
74.98°C(I)
69.21°C
2.14
(15 Mol%)
Rev Cp (J/(g·°C))
Heat Flow (W/g)
Temperature (°C)
Exo Up
1.8
1.6
1.4
1.2
1.0
0.1
0.0
-0.1
-0.2
-0.3
20
40
60
80
100
120
140
160
180

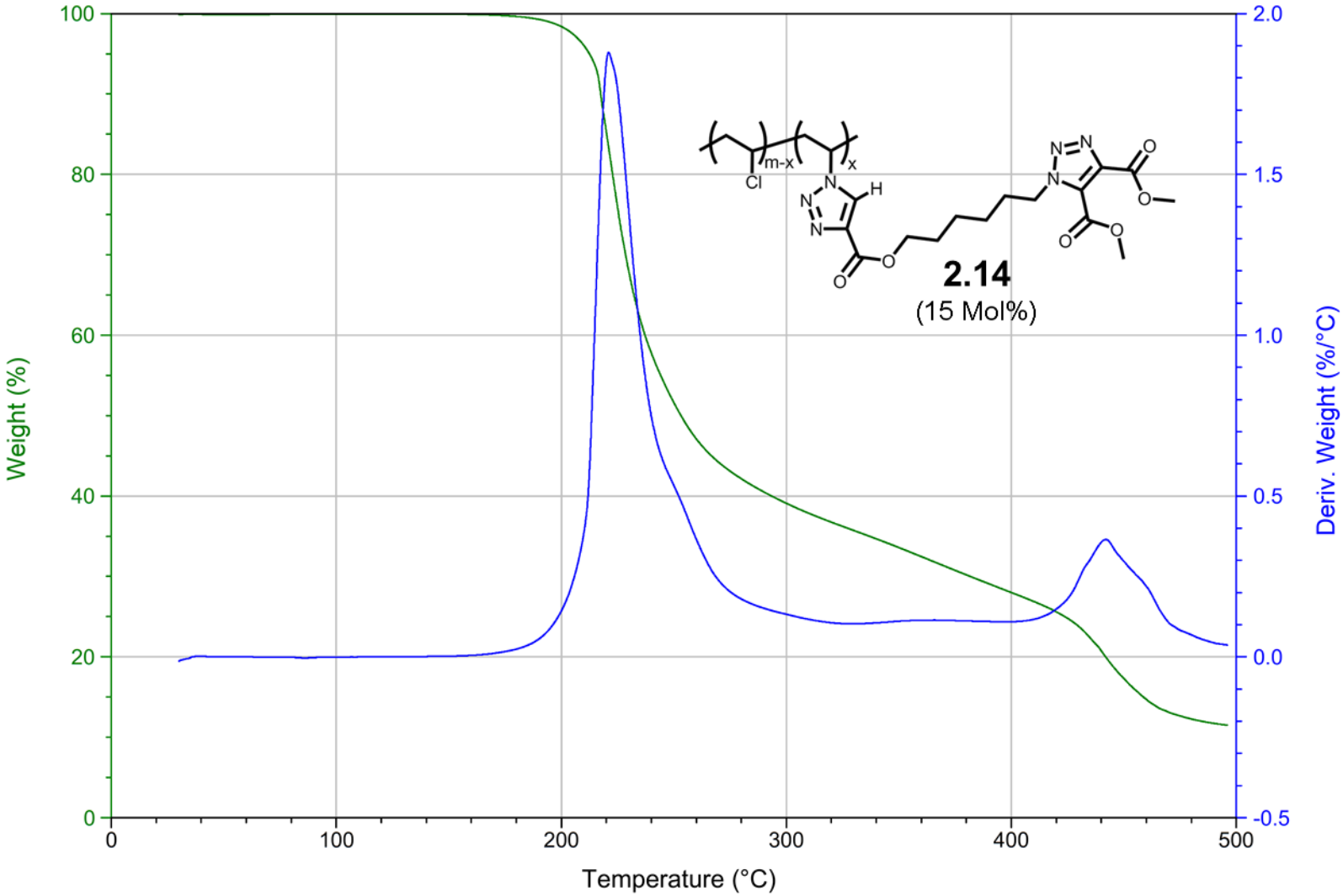
Weight (%)
Deriv. Weight (%/°C)
Temperature (°C)
0
20
40
60
80
100
-0.5
0.0
0.5
1.0
1.5
2.0
0
100
200
300
400
500
m-x
x
Cl
H
N
O
2.14
(15 Mol%)

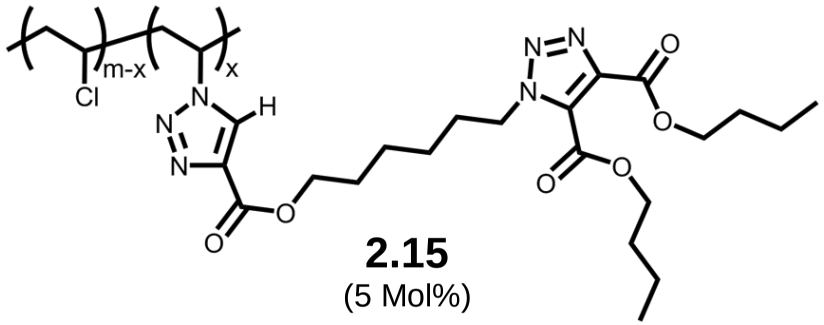
m-x
x
Cl
H
N
N
N
N
O
O
O
O
O
O

2.15
(5 Mol%)

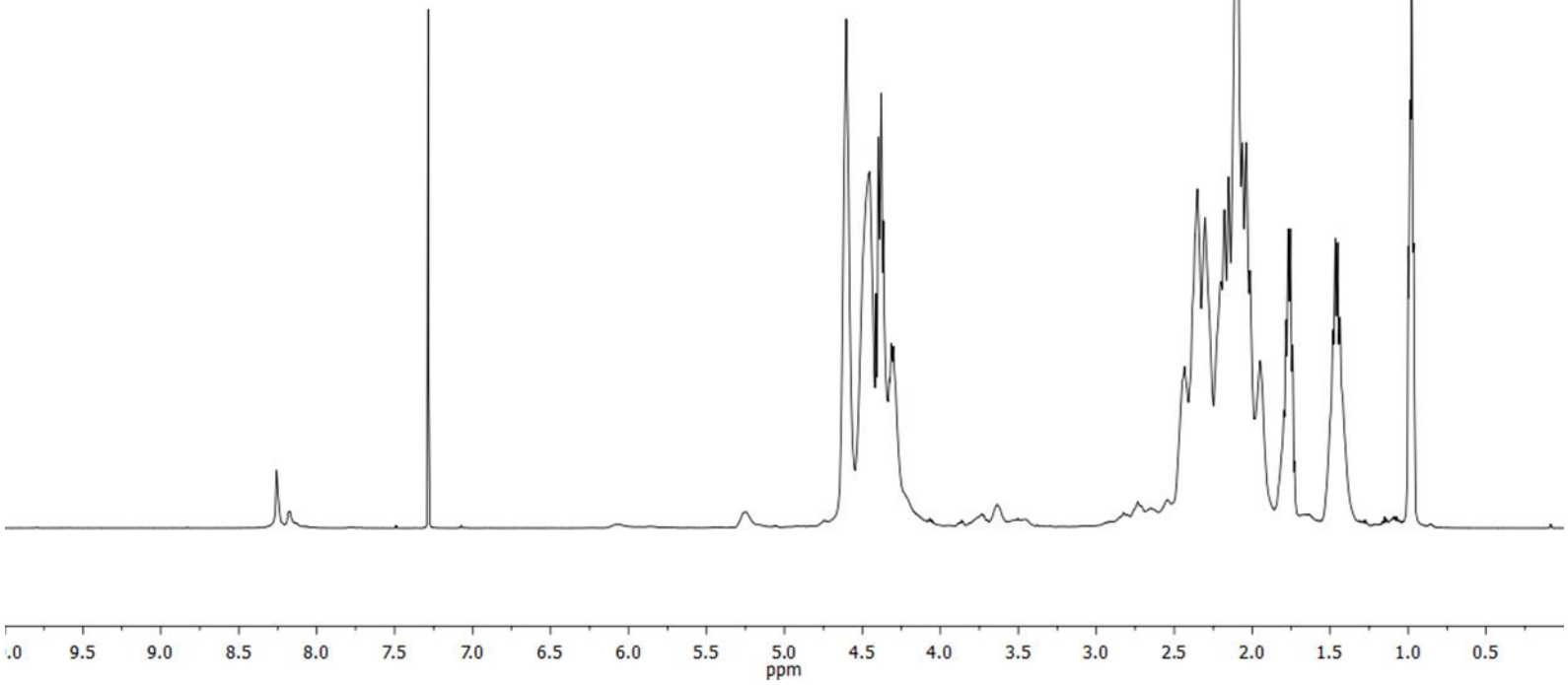
9.5
9.0
8.5
8.0
7.5
7.0
6.5
6.0
5.5
5.0
4.5
4.0
3.5
3.0
2.5
2.0
1.5
1.0
0.5
ppm

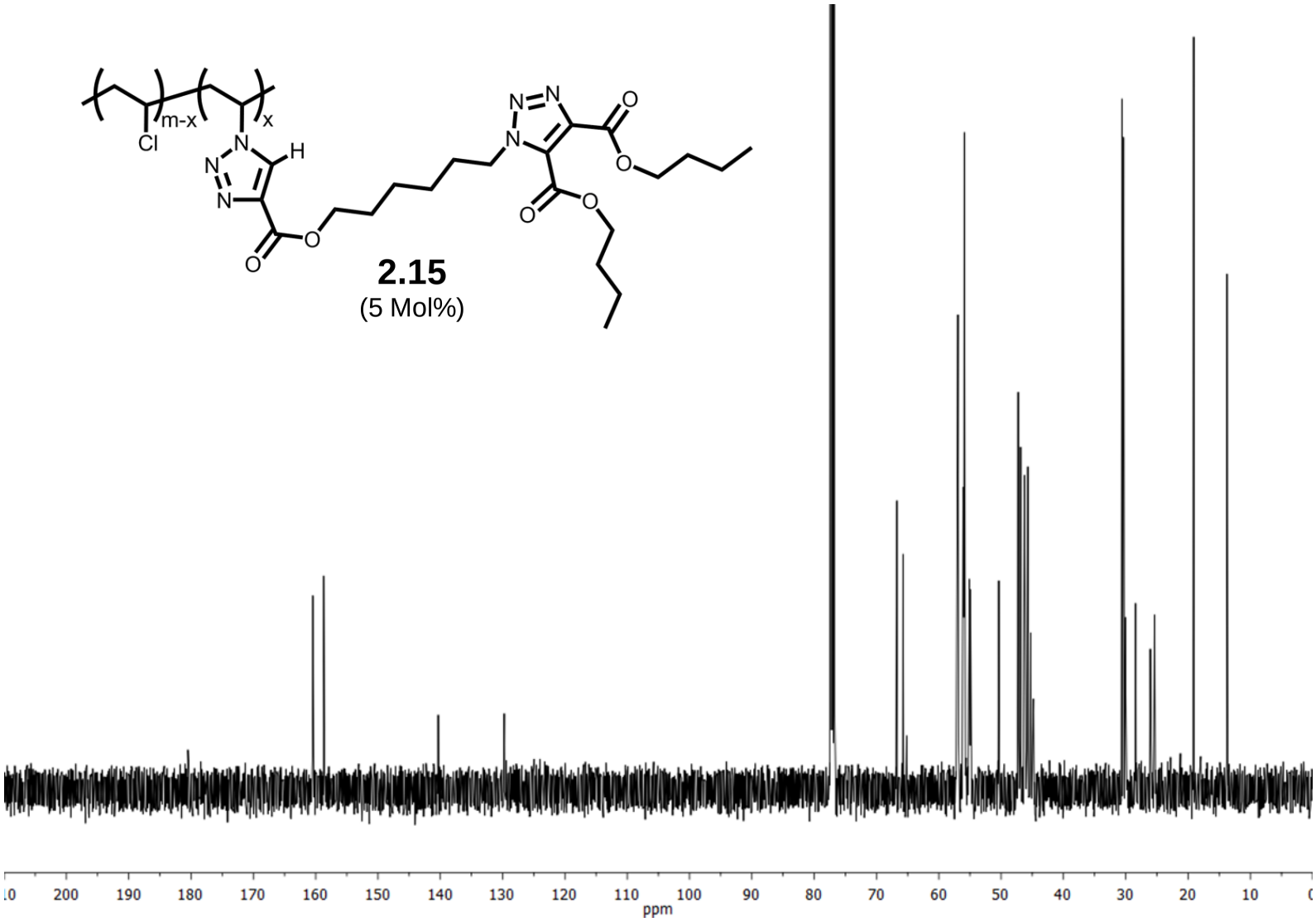
m-x
x
Cl
H
N
N
N
O
O
O
O
O
O
N
N
N
2.15
(5 Mol%)
200
190
180
170
160
150
140
130
120
110
100
90
80
70
60
50
40
30
20
10
ppm

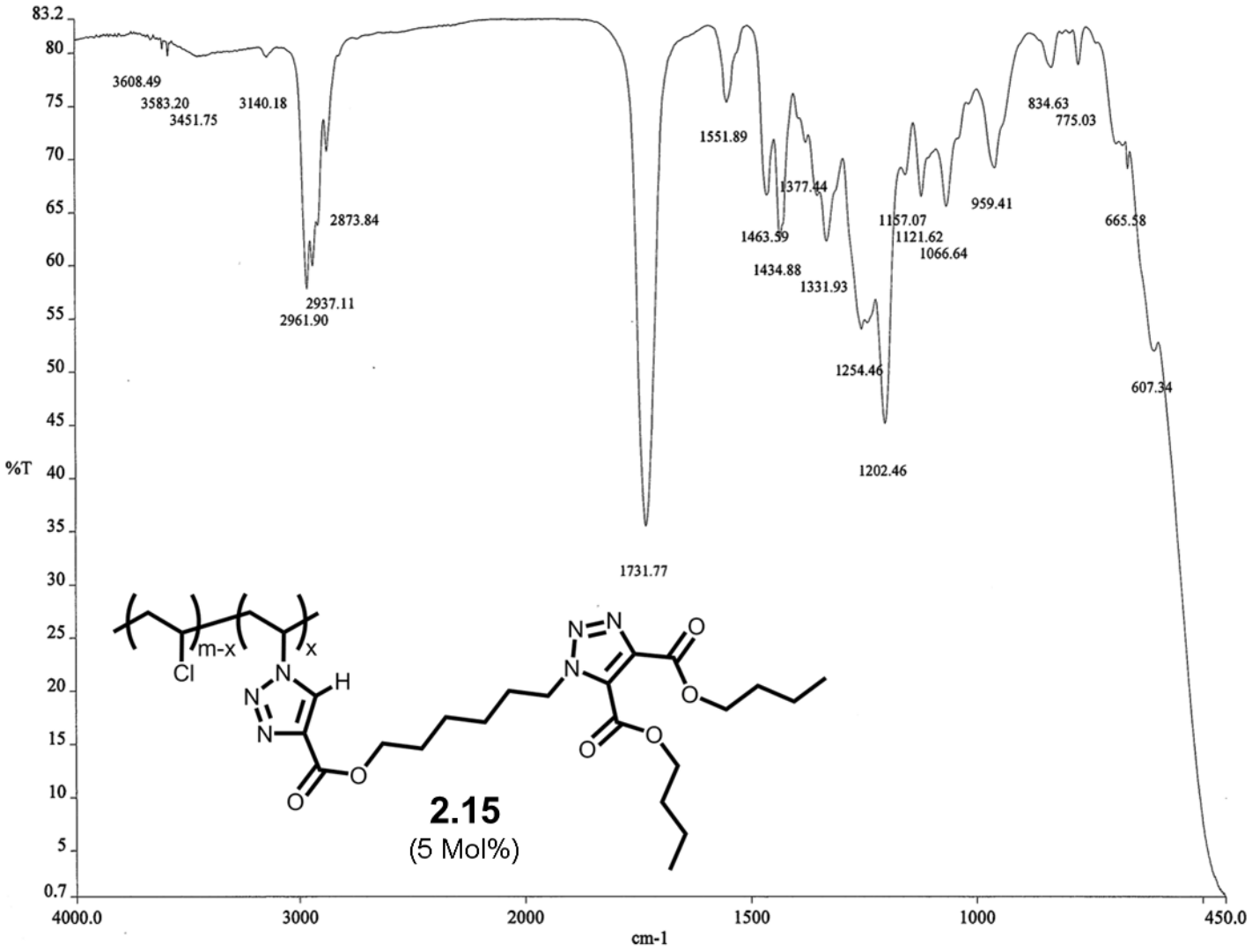
83.2
80
75
70
65
60
55
50
45
40
35
30
25
20
15
10
5
0.7
%T
4000.0
3000
2000
1500
1000
450.0
cm-1
3608.49
3583.20
3451.75
3140.18
2873.84
2937.11
2961.90
1731.77
1551.89
1463.59
1377.44
1434.88
1331.93
1254.46
1202.46
1157.07
1121.62
1066.64
959.41
834.63
775.03
665.58
607.34
m-x
x
Cl
H
N
O
2.15
(5 Mol%)

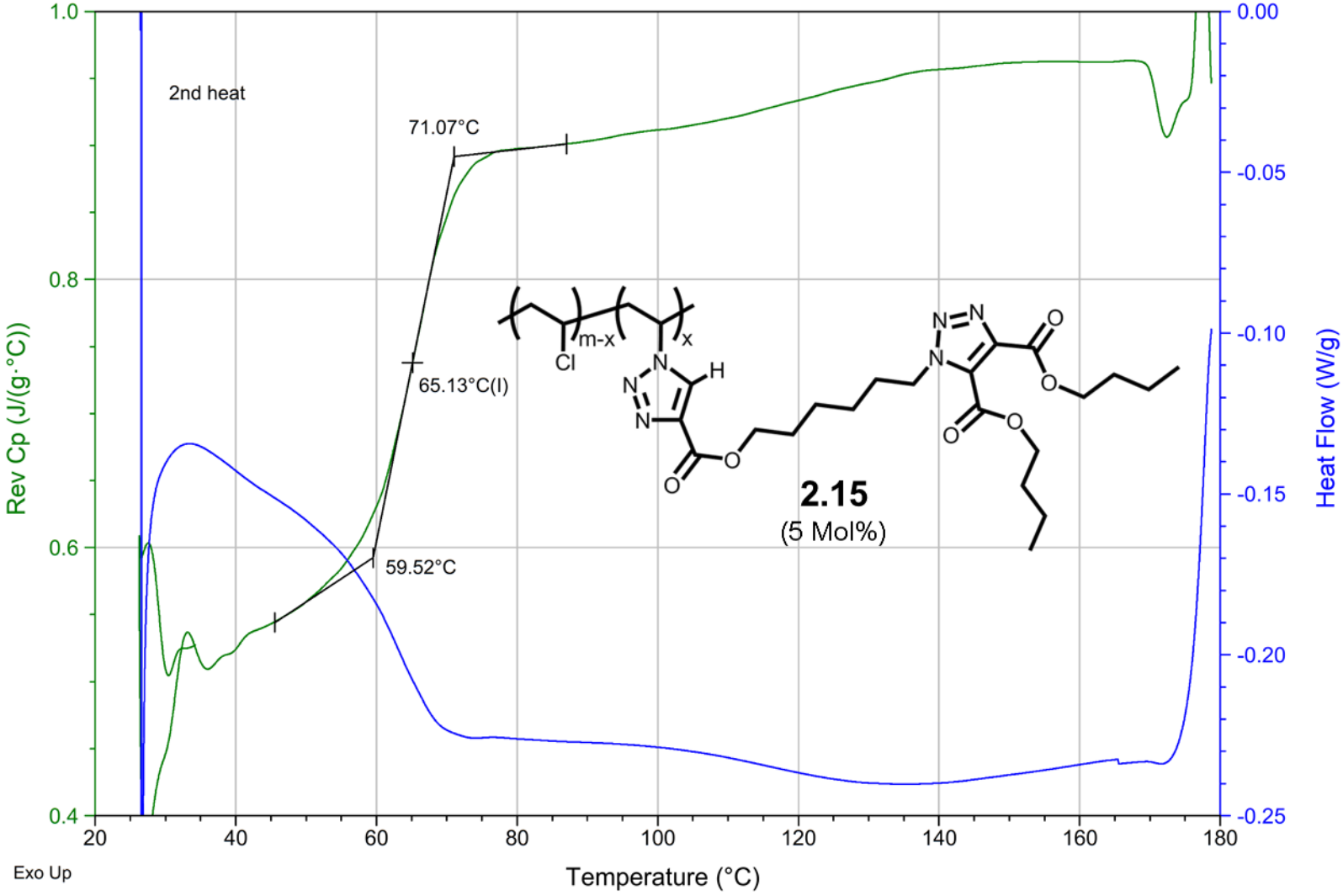
2nd heat
71.07°C
65.13°C(I)
59.52°C
m-x
x
Cl
H
N
O
2.15
(5 Mol%)
Rev Cp (J/(g·°C))
Heat Flow (W/g)
Temperature (°C)
Exo Up
1.0
0.8
0.6
0.4
0.00
-0.05
-0.10
-0.15
-0.20
-0.25
20
40
60
80
100
120
140
160
180

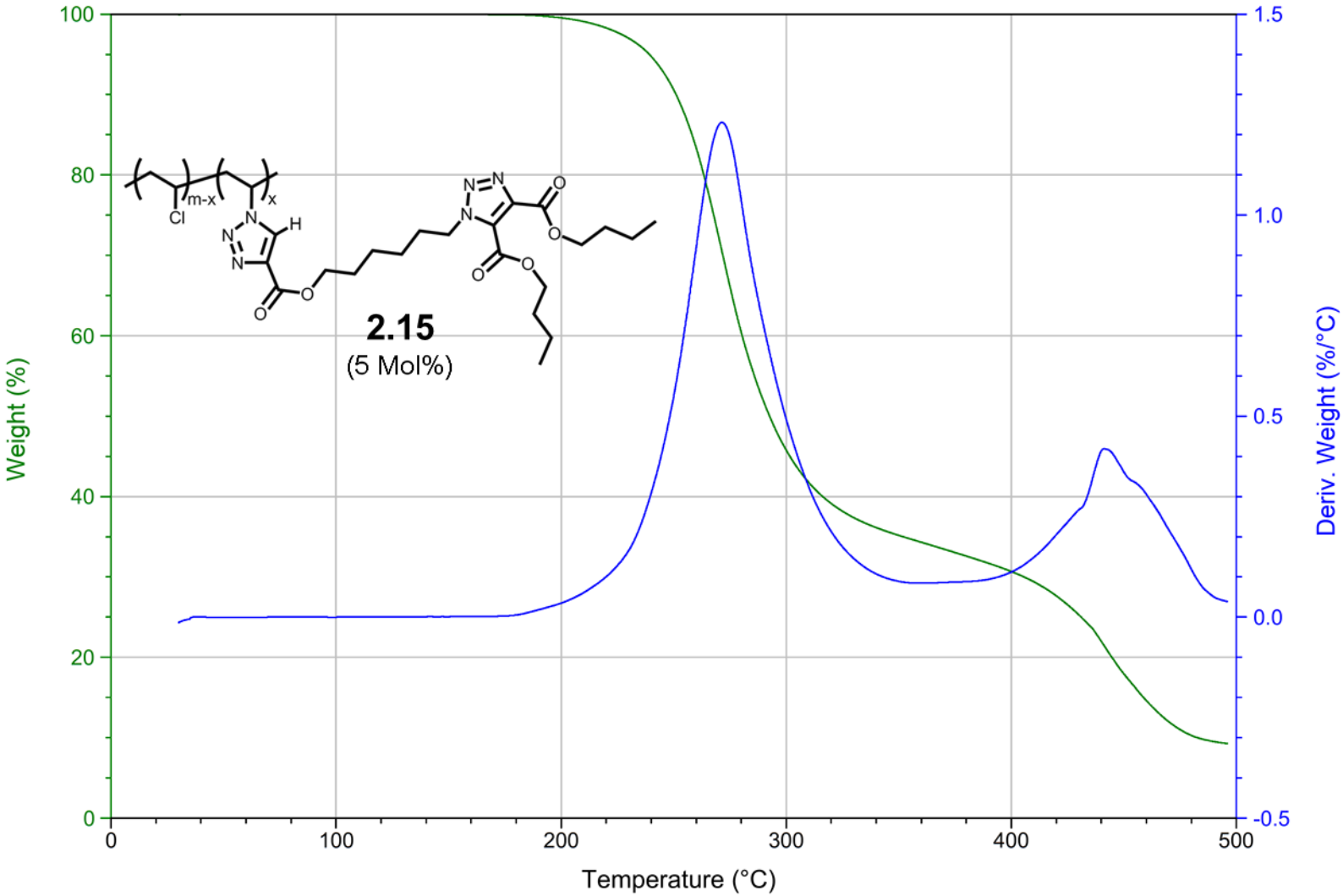
Weight (%)
Deriv. Weight (%/°C)
Temperature (°C)
100
80
60
40
20
0
1.5
1.0
0.5
0.0
-0.5
0
100
200
300
400
500
m-x
x
Cl
H
N
O
2.15
(5 Mol%)

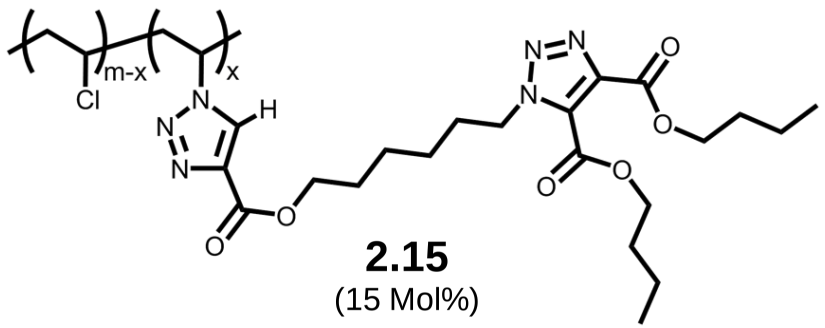
m-x
x
Cl
H
N
N
N
N
N
O
O
O
O
O
O

2.15
(15 Mol%)

9.5
9.0
8.5
8.0
7.5
7.0
6.5
6.0
5.5
5.0
4.5
4.0
3.5
3.0
2.5
2.0
1.5
1.0
0.5
ppm

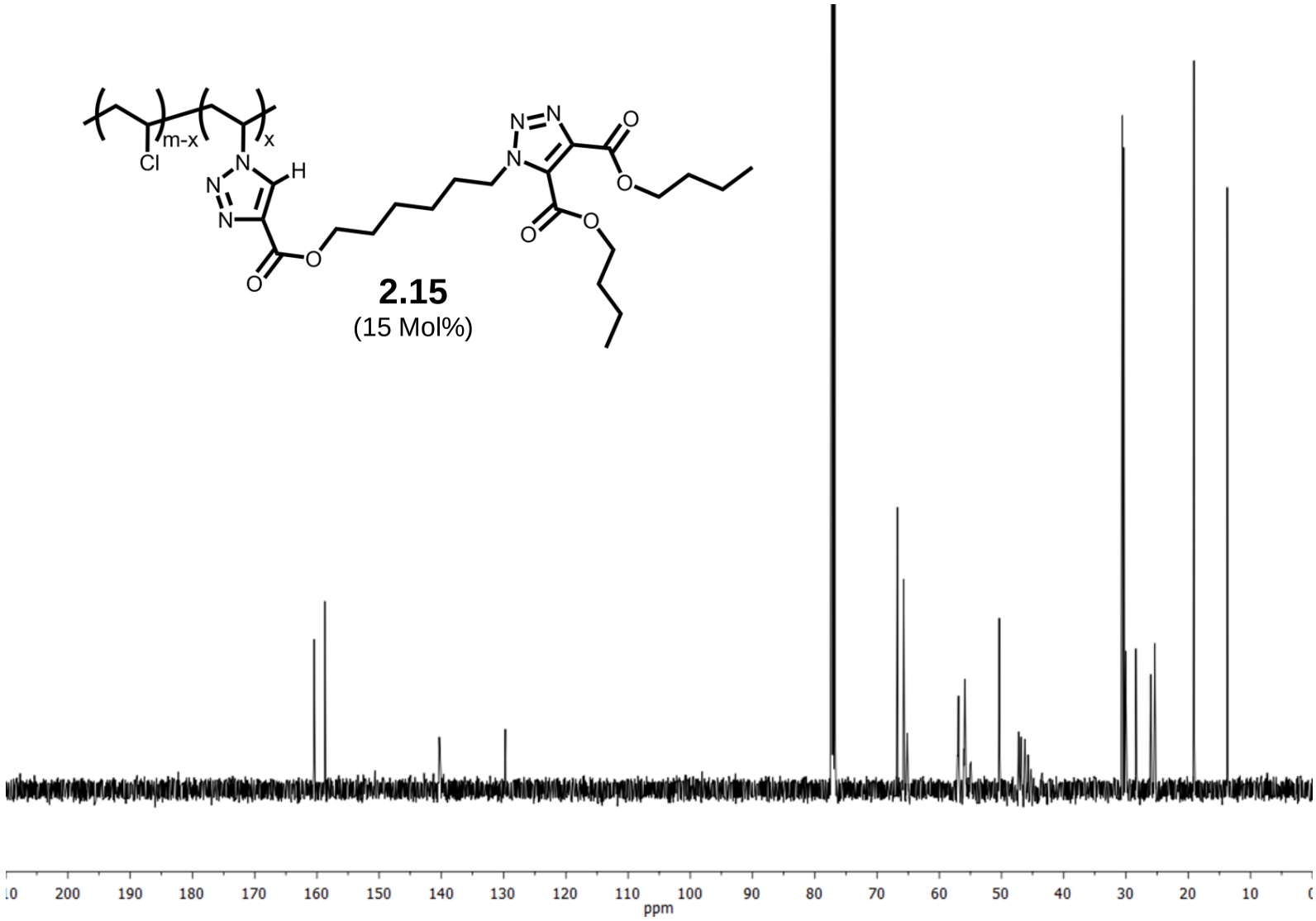
m-x
x
Cl
H
N
N
N
O
O
O
O
O
O
N
N
N
2.15
(15 Mol%)
ppm
200
190
180
170
160
150
140
130
120
110
100
90
80
70
60
50
40
30
20
10

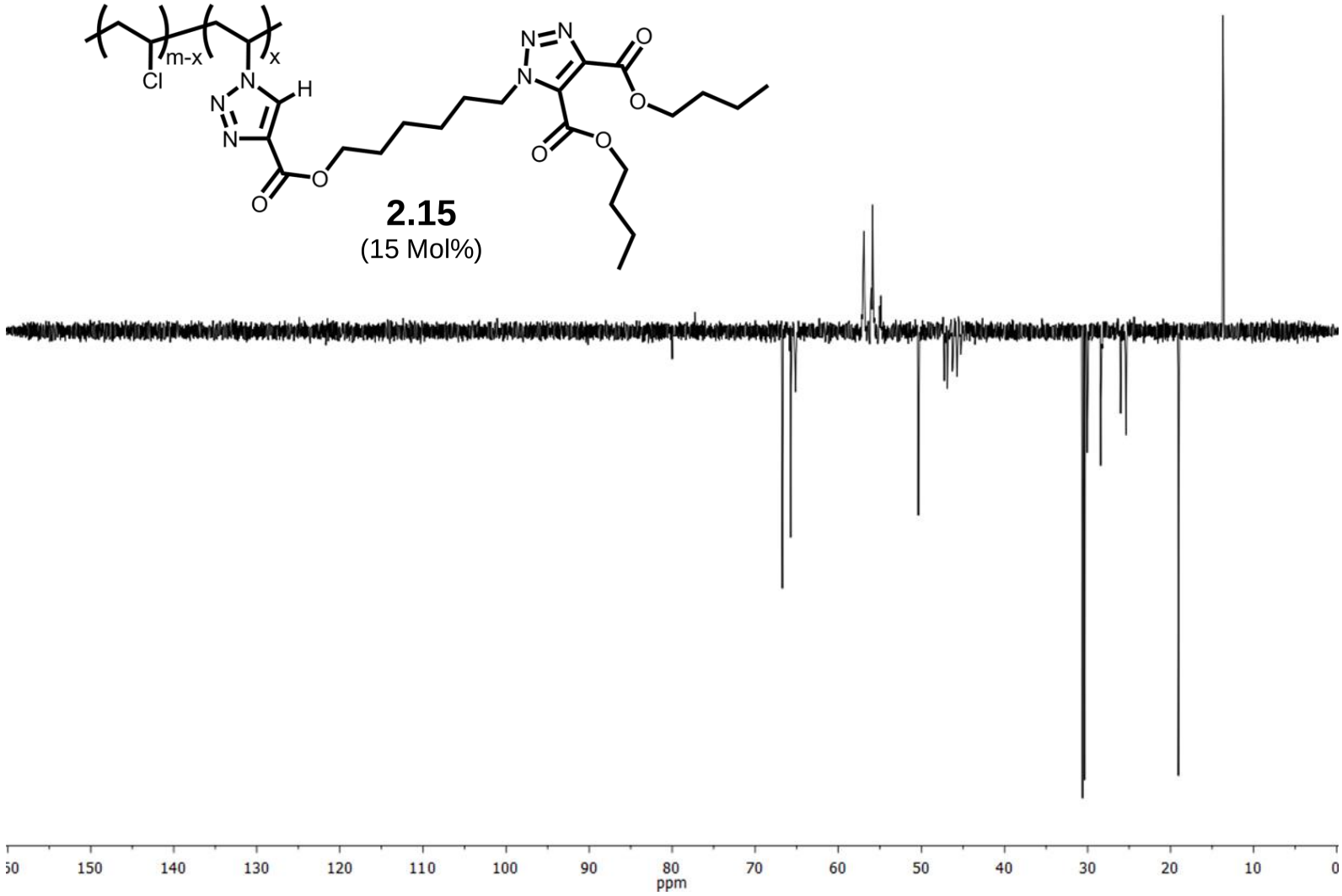
m-x
x
Cl
H
N
N
N
N
O
O
O
O
O
O
2.15
(15 Mol%)
150
140
130
120
110
100
90
80
70
60
50
40
30
20
10
ppm

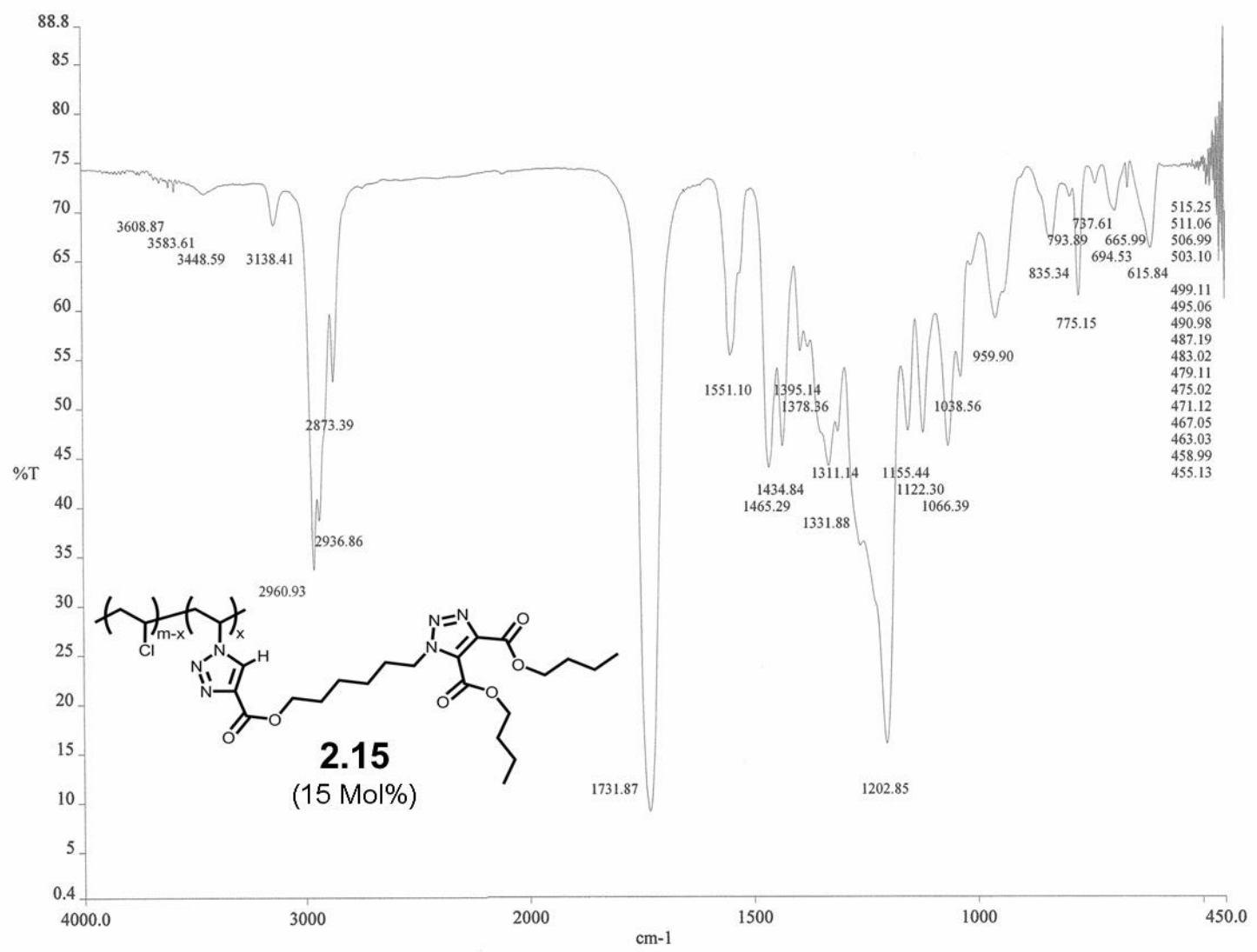
88.8
85
80
75
70
65
60
55
50
45
40
35
30
25
20
15
10
5
0.4
%T
4000.0
3000
2000
1500
1000
450.0
cm-1
3608.87
3583.61
3448.59
3138.41
2873.39
2936.86
2960.93
1731.87
1551.10
1395.14
1378.36
1434.84
1465.29
1311.14
1331.88
1202.85
1155.44
1122.30
1066.39
1038.56
959.90
835.34
793.89
775.15
737.61
694.53
665.99
615.84
515.25
511.06
506.99
503.10
499.11
495.06
490.98
487.19
483.02
479.11
475.02
471.12
467.05
463.03
458.99
455.13
m-x
x
Cl
H
2.15
(15 Mol%)

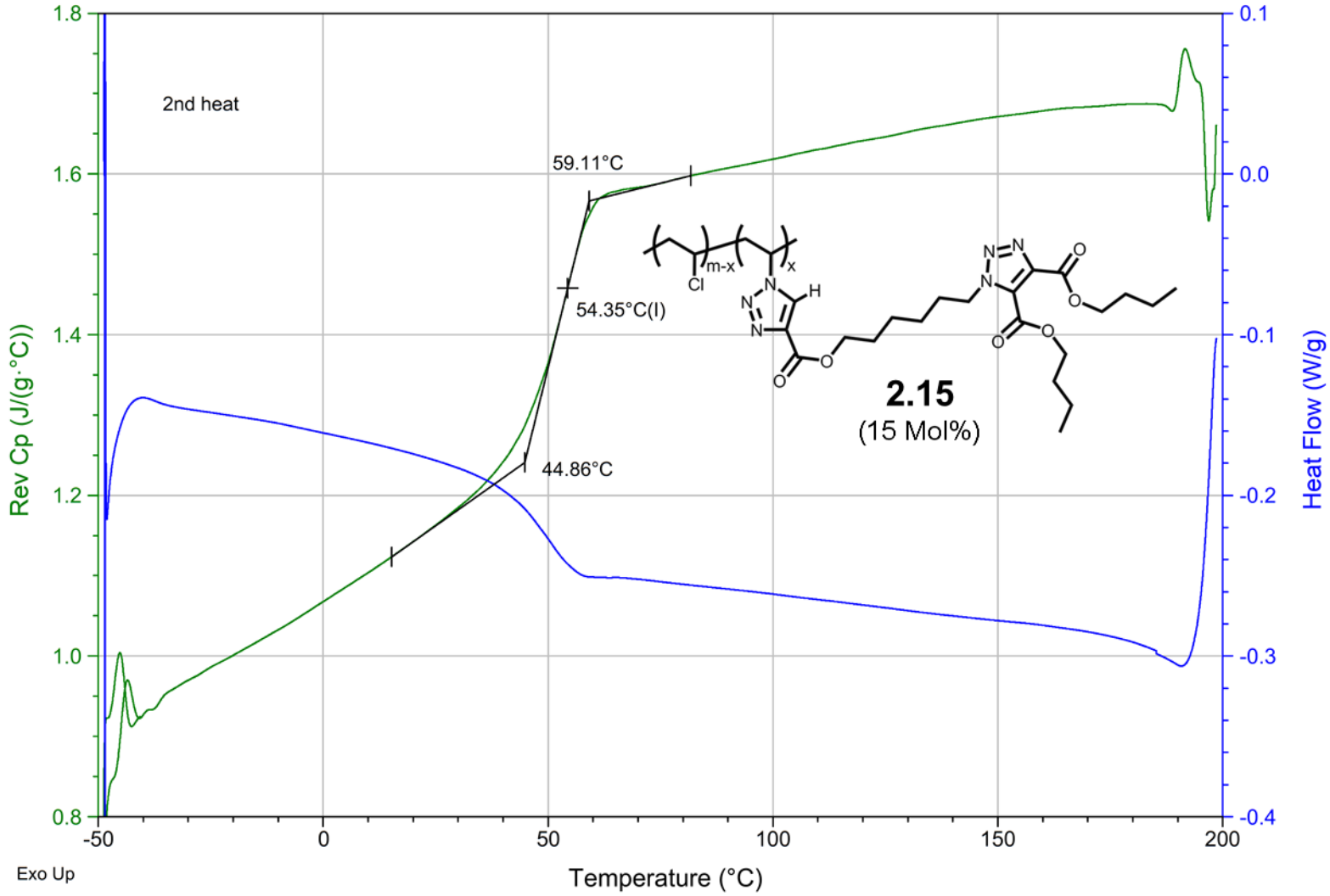
2nd heat
59.11°C
54.35°C(I)
44.86°C
2.15
(15 Mol%)
Rev Cp (J/(g·°C))
Heat Flow (W/g)
Temperature (°C)
Exo Up
1.8
1.6
1.4
1.2
1.0
0.8
0.1
0.0
-0.1
-0.2
-0.3
-0.4
-50
0
50
100
150
200

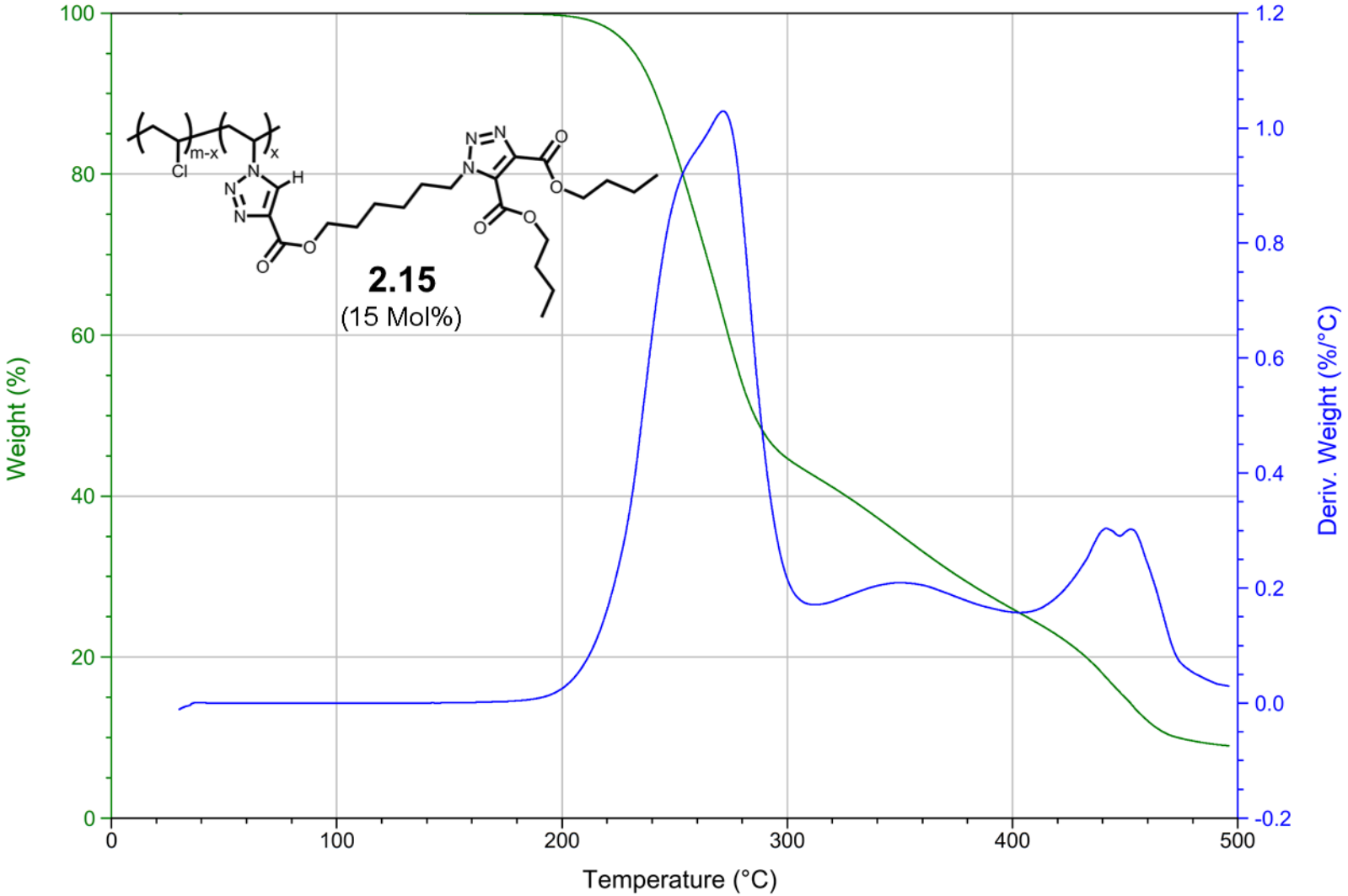
2.15
(15 Mol%)
Weight (%)
Deriv. Weight (%/°C)
Temperature (°C)
100
80
60
40
20
0
1.2
1.0
0.8
0.6
0.4
0.2
0.0
-0.2
0
100
200
300
400
500

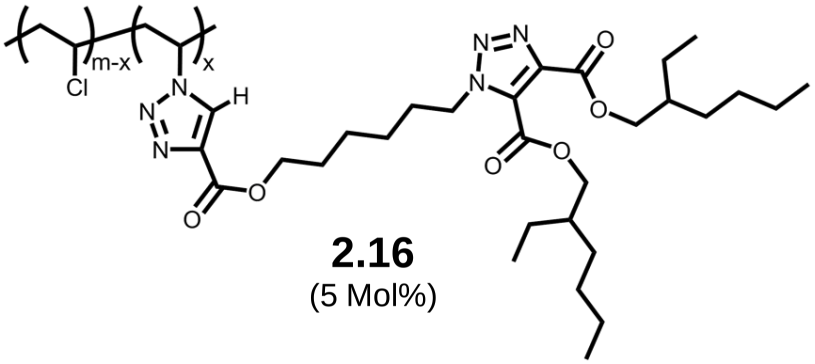

2.16
(5 Mol%)

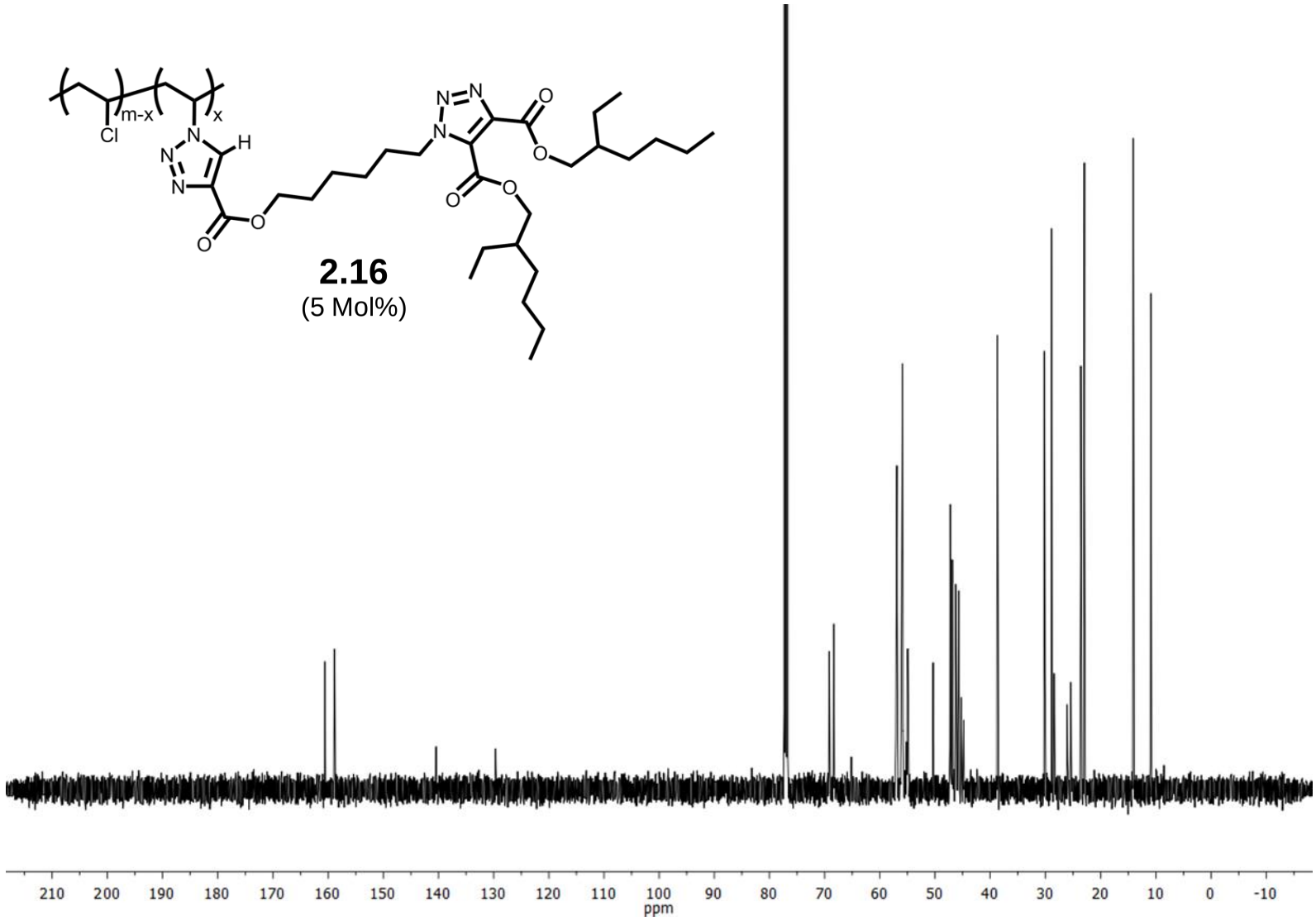
m-x
x
Cl
H
N
O
2.16
(5 Mol%)
210 200 190 180 170 160 150 140 130 120 110 100 90 80 70 60 50 40 30 20 10 0 -10
ppm

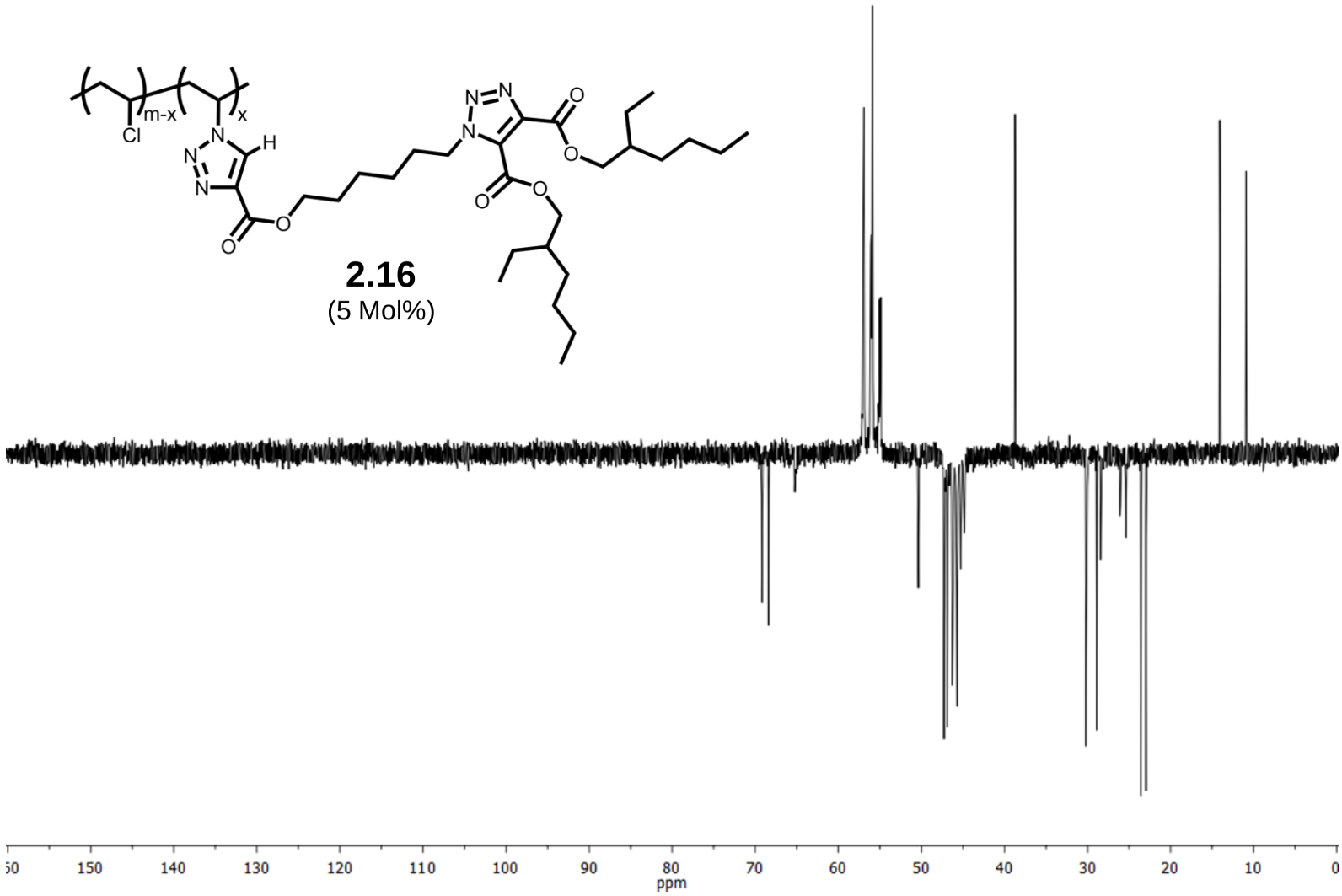
m-x
x
Cl
H
N
O
2.16
(5 Mol%)
150
140
130
120
110
100
90
80
70
60
50
40
30
20
10
0
ppm

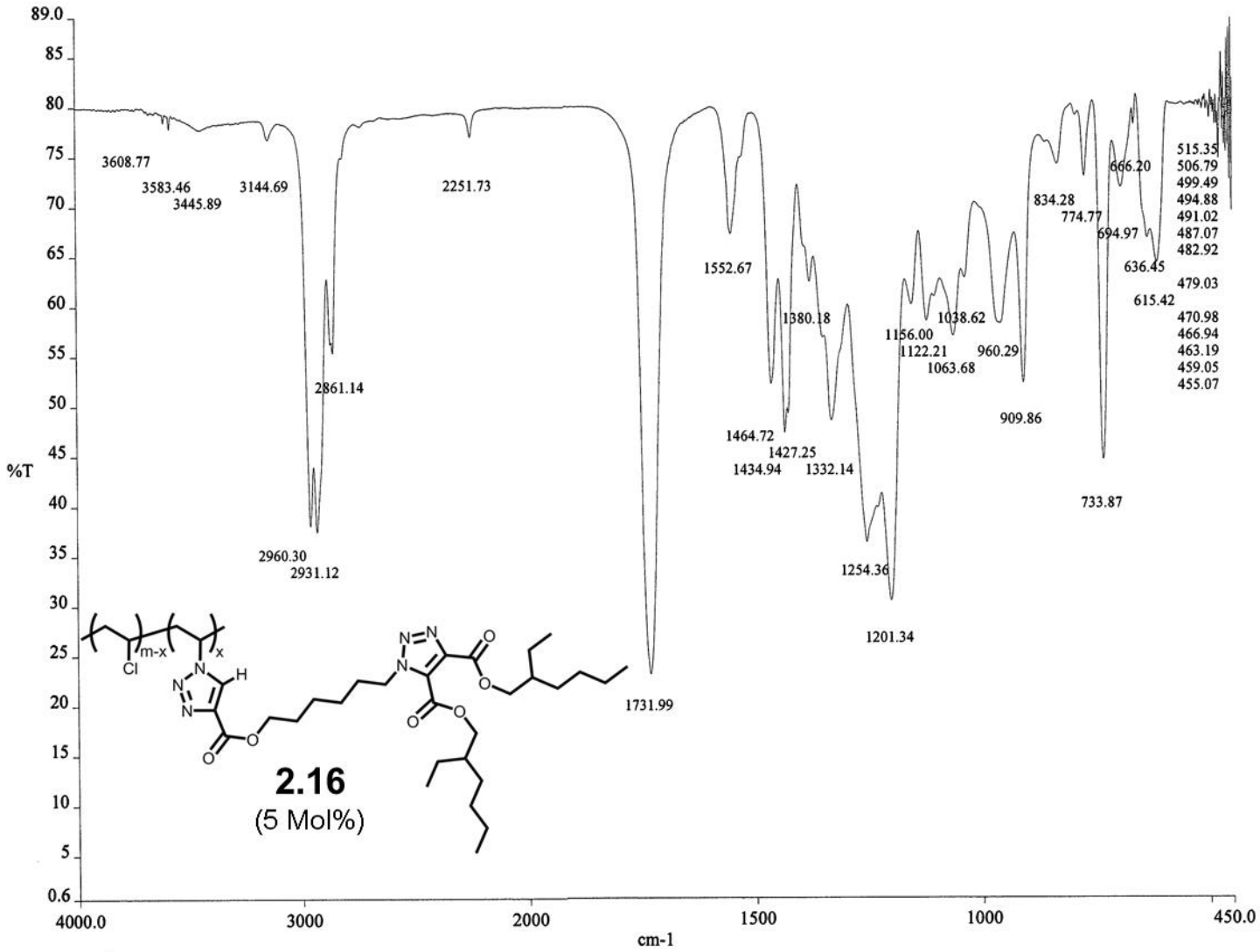
89.0
85
80
75
70
65
60
55
50
45
40
35
30
25
20
15
10
5
0.6
%T
4000.0
3000
2000
1500
1000
450.0
cm-1
3608.77
3583.46
3445.89
3144.69
2251.73
2861.14
2960.30
2931.12
1731.99
1552.67
1464.72
1427.25
1434.94
1380.18
1332.14
1254.36
1201.34
1156.00
1122.21
1063.68
1038.62
960.29
909.86
834.28
774.77
733.87
694.97
666.20
636.45
615.42
515.35
506.79
499.49
494.88
491.02
487.07
482.92
479.03
470.98
466.94
463.19
459.05
455.07
Cl
m-x
x
H
2.16
(5 Mol%)

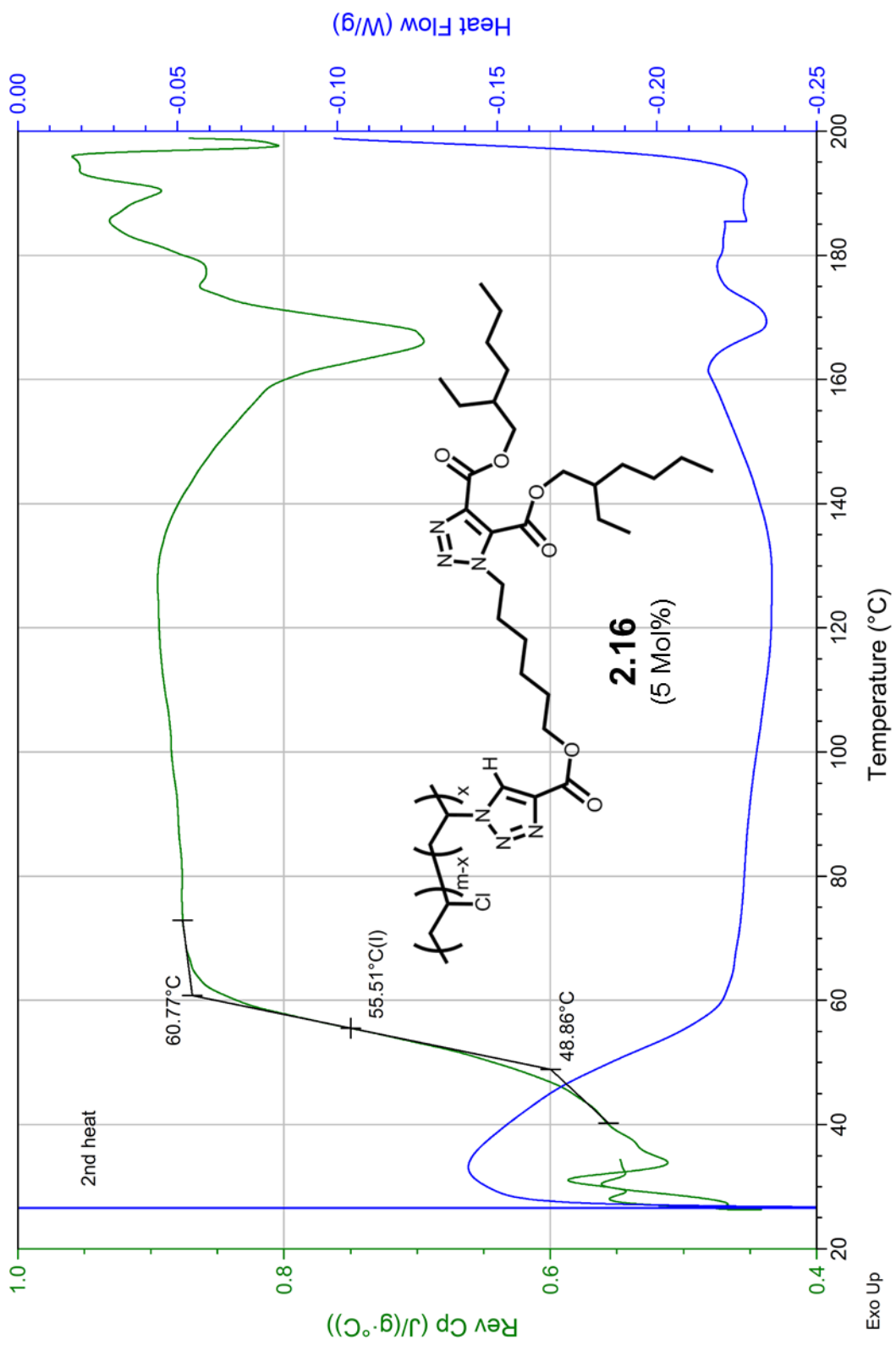
Heat Flow (W/g)
0.00
-0.05
-0.10
-0.15
-0.20
-0.25
Rev Cp (J/(g·°C))
1.0
0.8
0.6
0.4
Exo Up
20
40
60
80
100
120
140
160
180
200
Temperature (°C)
2nd heat
60.77°C
55.51°C(l)
48.86°C
2.16
(5 Mol%)
m-x
x
Cl

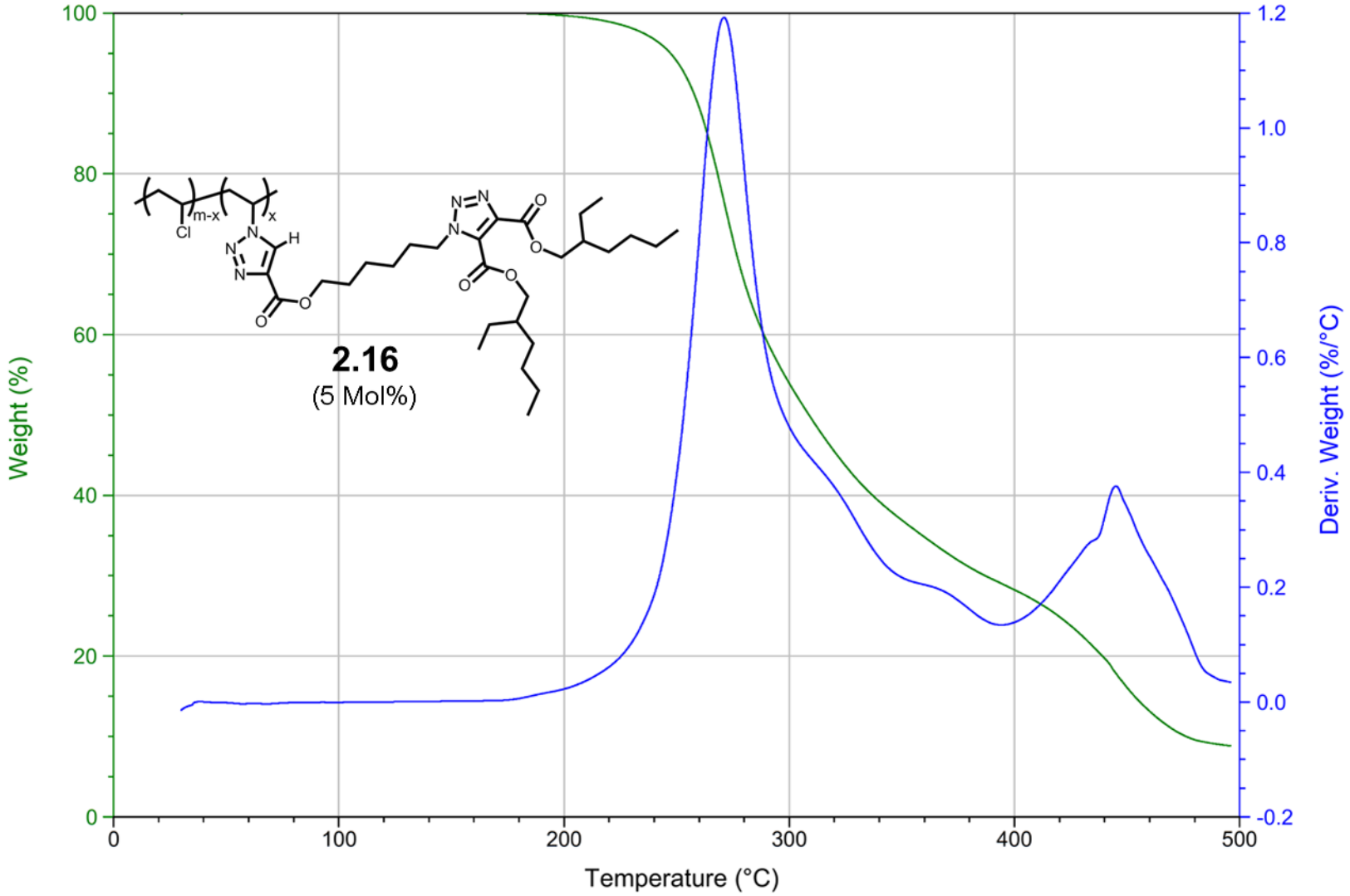
2.16
(5 Mol%)
Weight (%)
Deriv. Weight (%/°C)
Temperature (°C)
100
80
60
40
20
0
1.2
1.0
0.8
0.6
0.4
0.2
0.0
-0.2
0
100
200
300
400
500

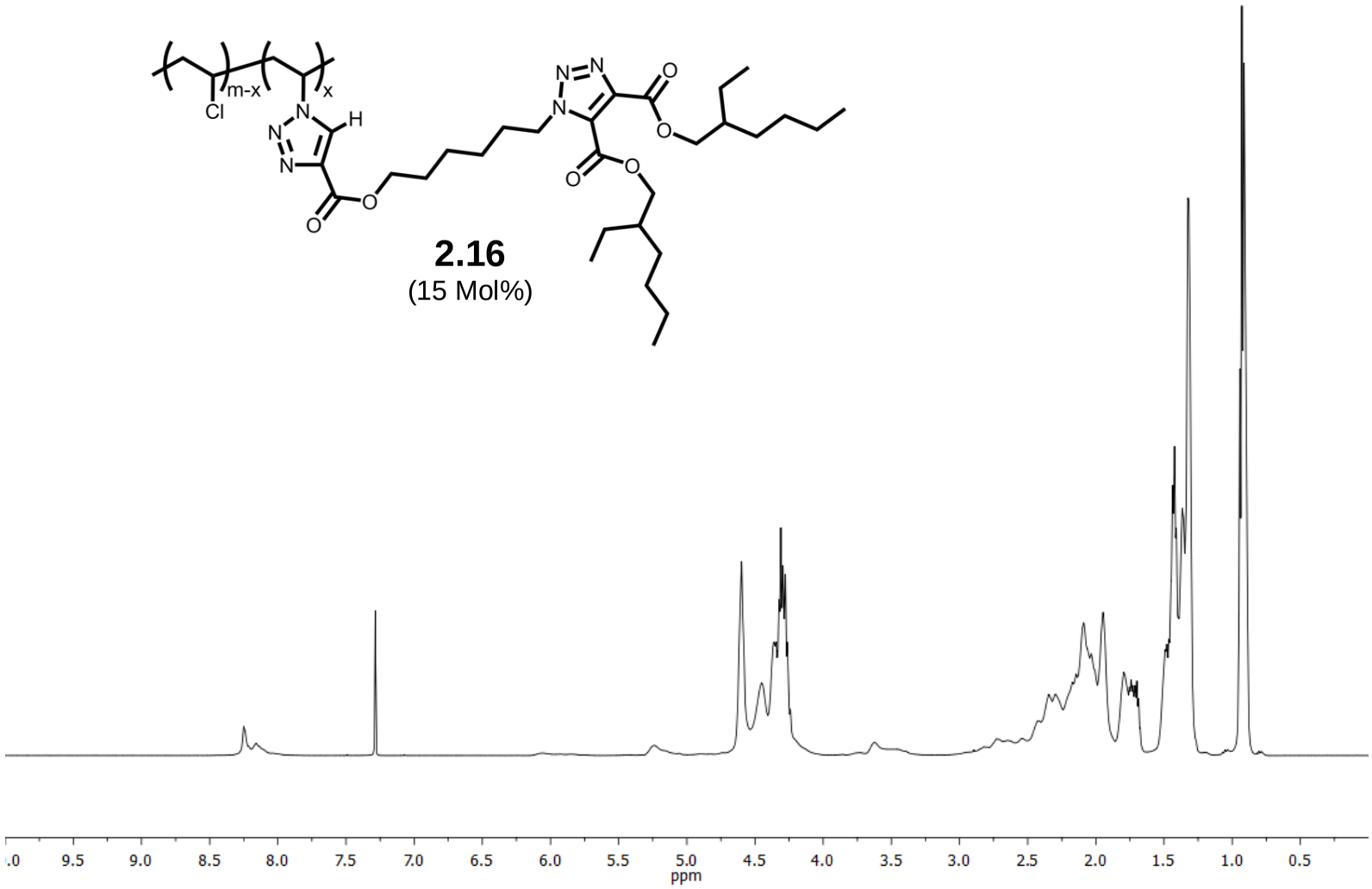
m-x
x
Cl
H
N
O
2.16
(15 Mol%)
9.5
9.0
8.5
8.0
7.5
7.0
6.5
6.0
5.5
5.0
4.5
4.0
3.5
3.0
2.5
2.0
1.5
1.0
0.5
ppm

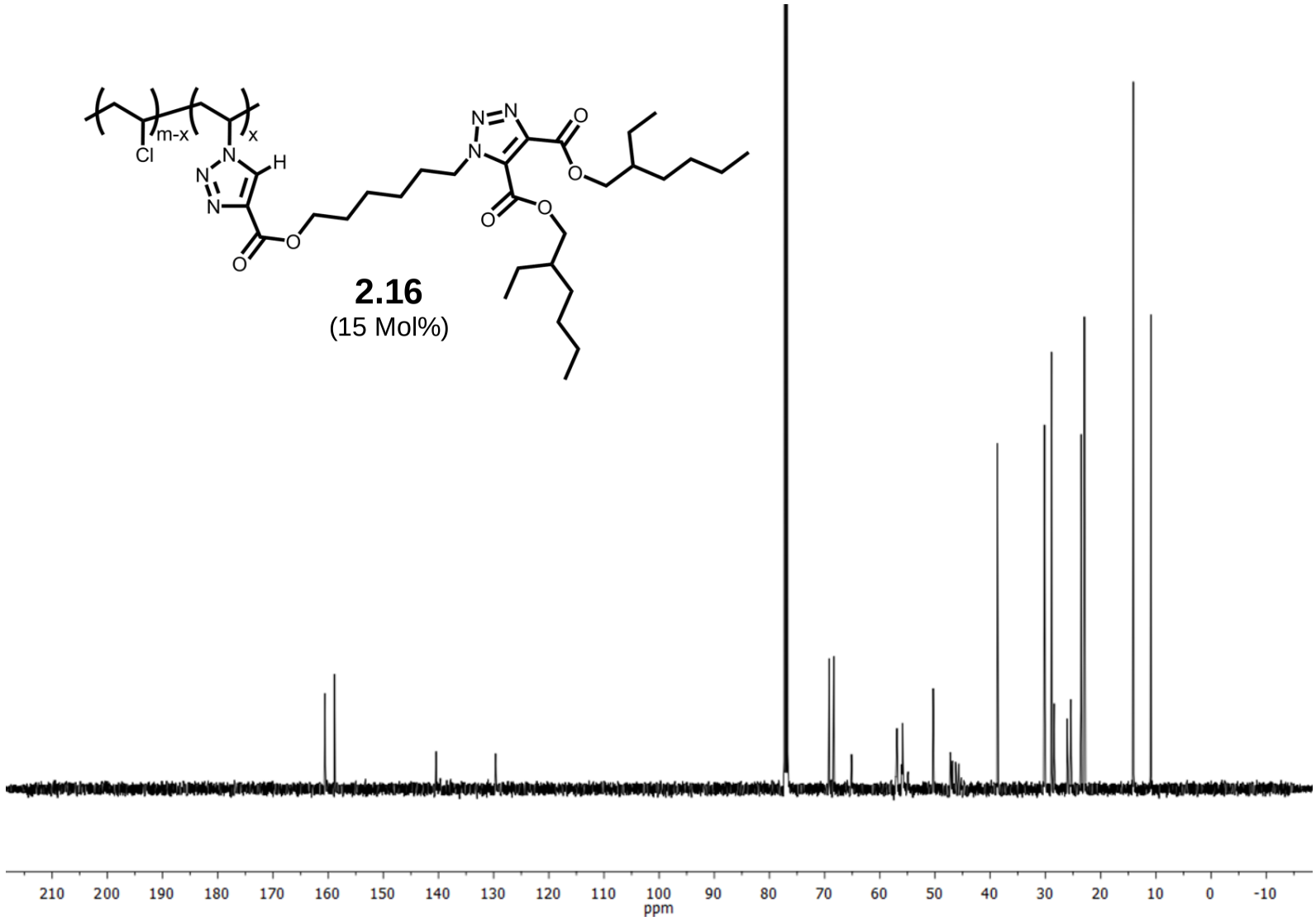
m-x
x
Cl
H
N
N
N
N
O
O
O
O
O
O
2.16
(15 Mol%)
210
200
190
180
170
160
150
140
130
120
110
100
90
80
70
60
50
40
30
20
10
0
-10
ppm

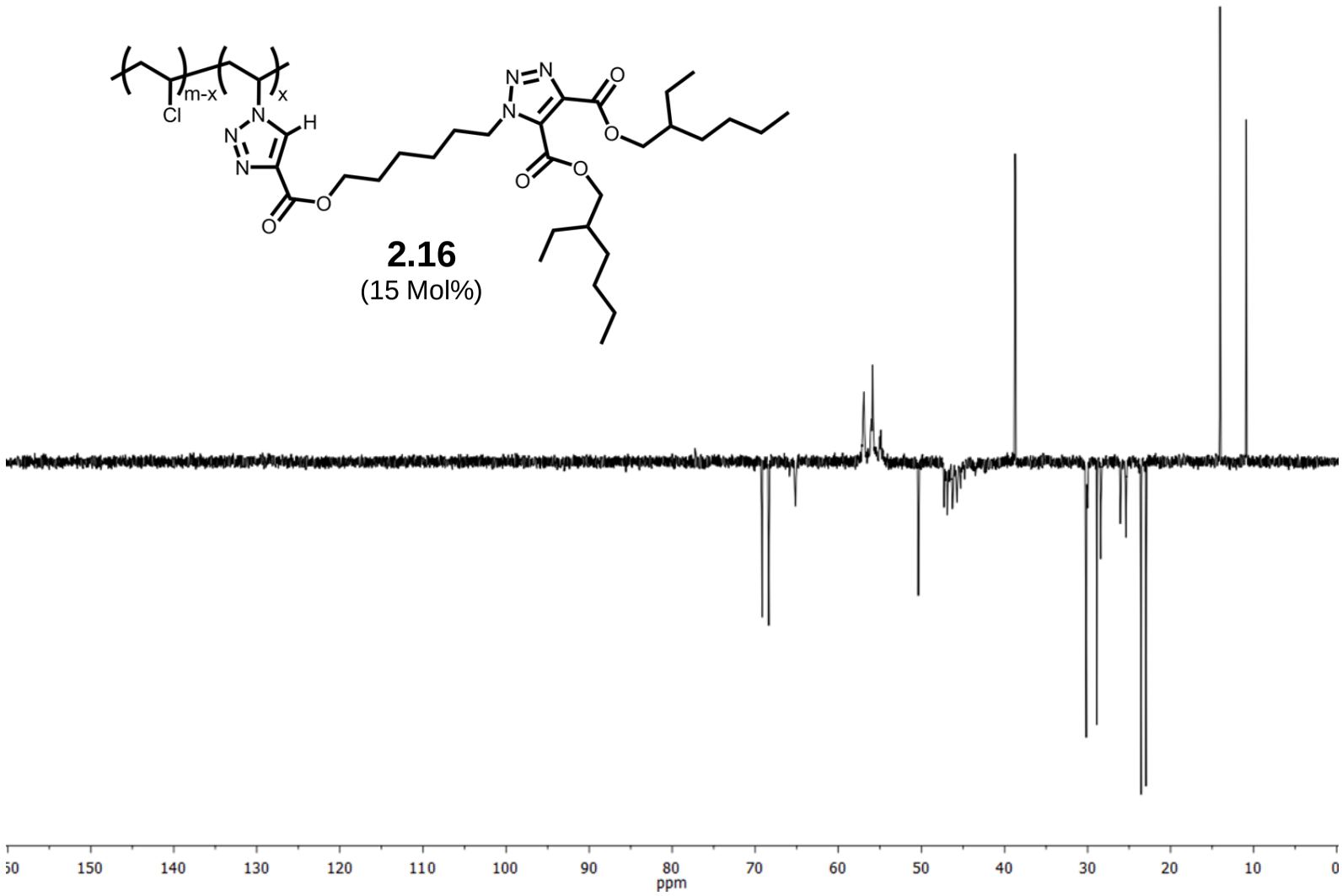
m-x
x
Cl
H
N
N
N
N
O
O
O
O
O
O
2.16
(15 Mol%)
150
140
130
120
110
100
90
80
70
60
50
40
30
20
10
0
ppm

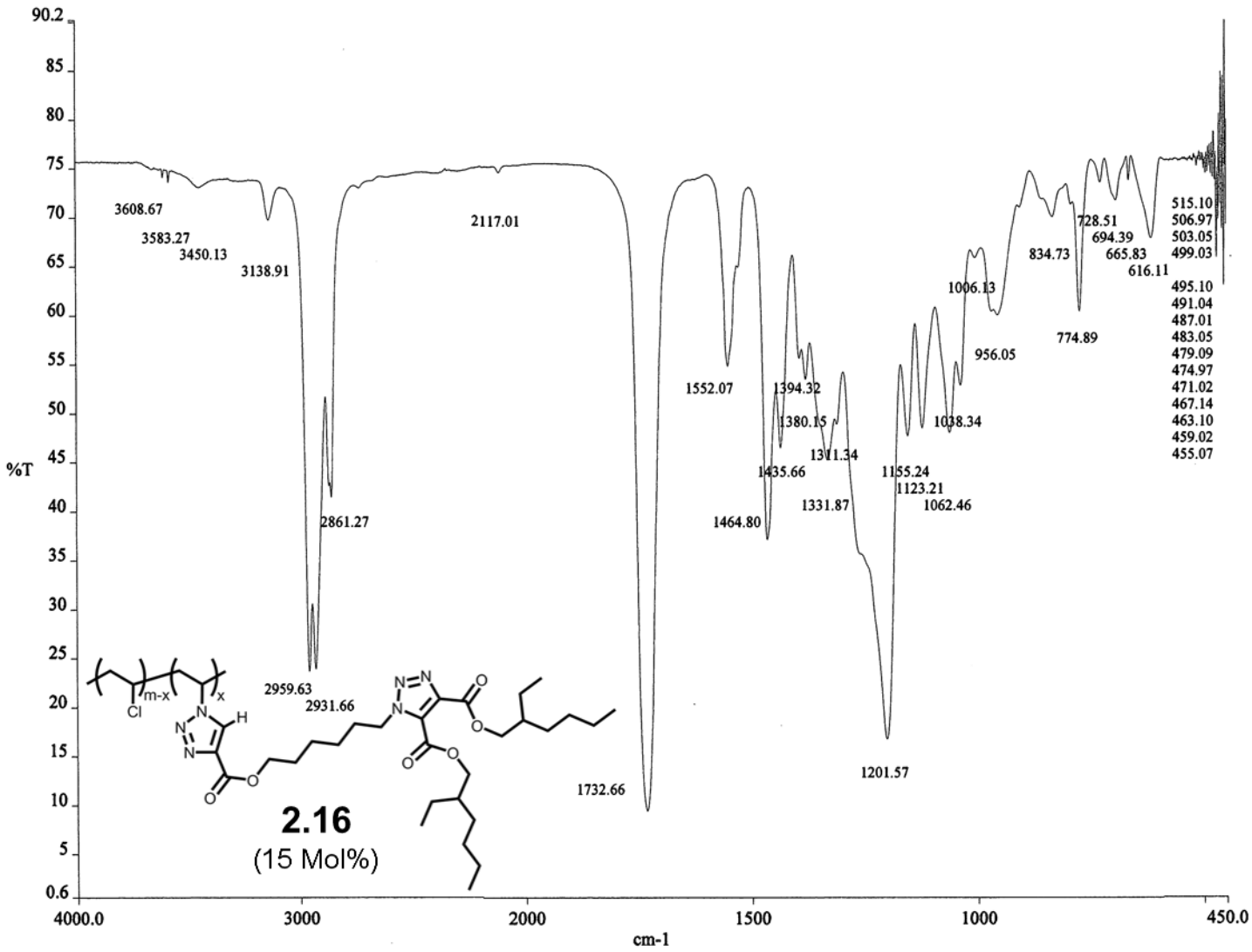
%T
cm-1
4000.0
3000
2000
1500
1000
450.0
90.2
85
80
75
70
65
60
55
50
45
40
35
30
25
20
15
10
5
0.6
3608.67
3583.27
3450.13
3138.91
2959.63
2931.66
2861.27
2117.01
1732.66
1552.07
1464.80
1435.66
1394.32
1380.15
1331.87
1311.34
1201.57
1155.24
1123.21
1062.46
1038.34
1006.13
956.05
834.73
774.89
728.51
694.39
665.83
616.11
515.10
506.97
503.05
499.03
495.10
491.04
487.01
483.05
479.09
474.97
471.02
467.14
463.10
459.02
455.07
Cl
m-x
x
H
O
N
2.16
(15 Mol%)

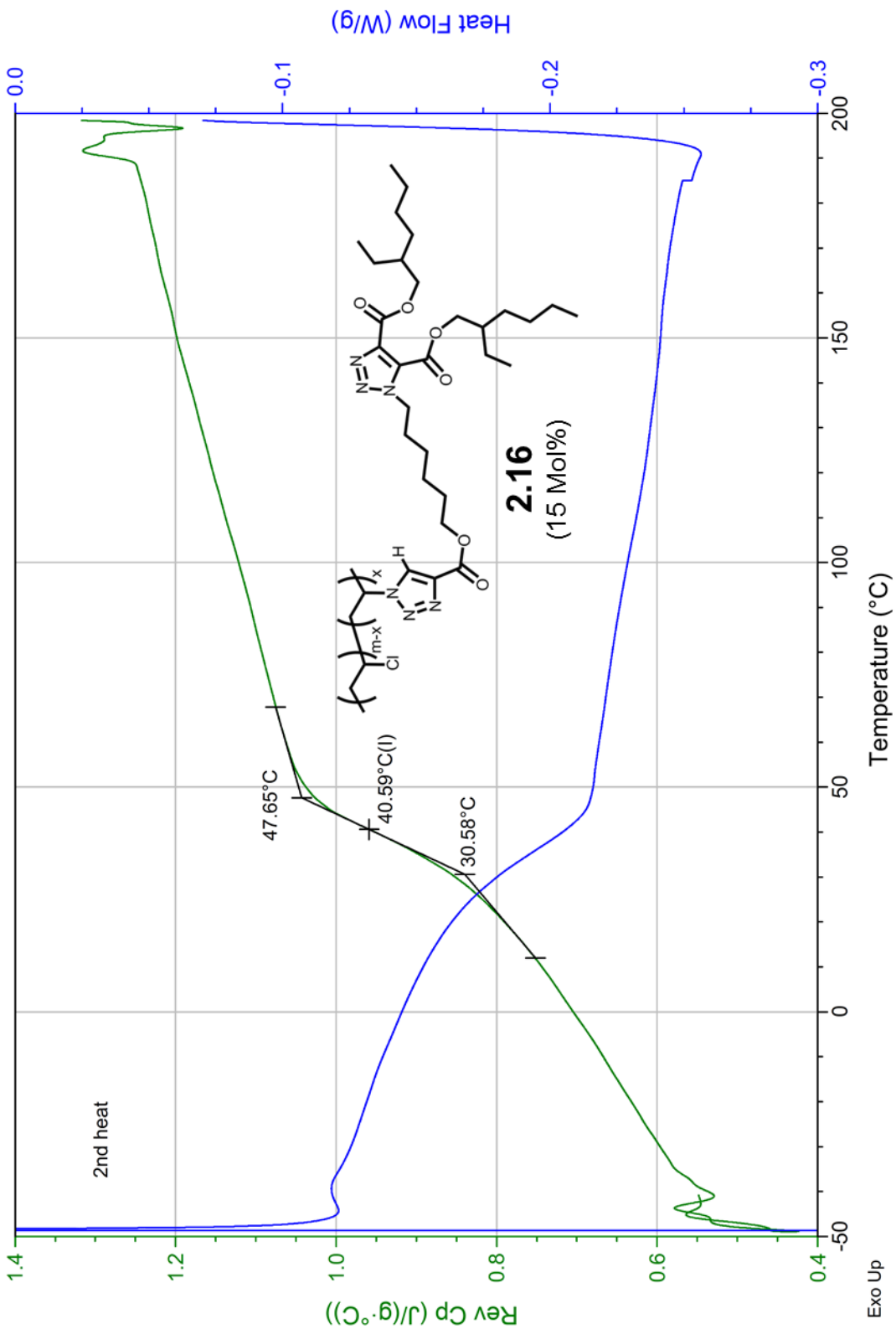
Heat Flow (W/g)
0.0
-0.1
-0.2
-0.3
Rev Cp (J/(g·°C))
1.4
1.2
1.0
0.8
0.6
0.4
Exo Up
-50
0
50
100
150
200
Temperature (°C)
2nd heat
47.65°C
40.59°C(I)
30.58°C
2.16
(15 Mol%)

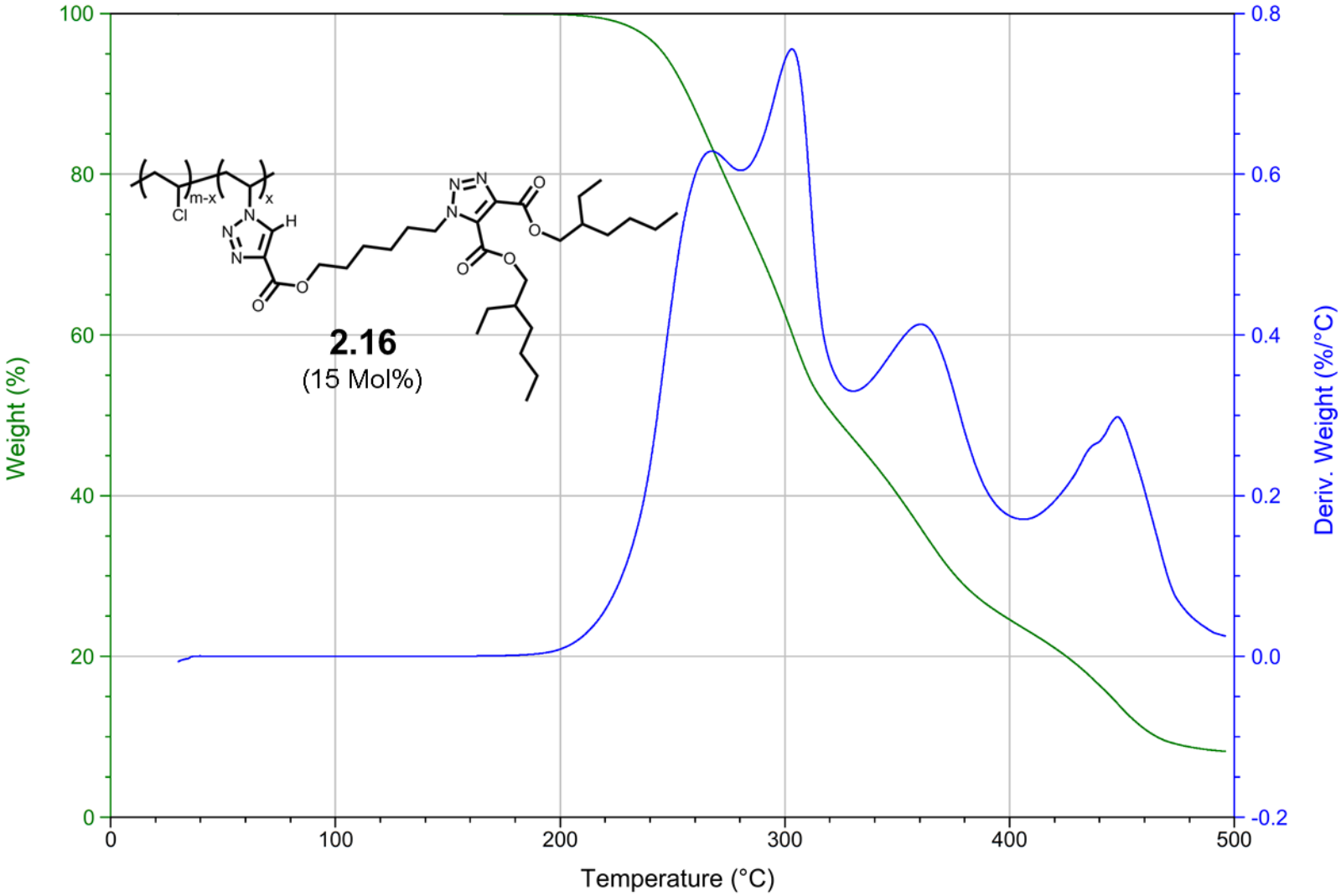
2.16
(15 Mol%)
Weight (%)
Deriv. Weight (%/°C)
Temperature (°C)
100
80
60
40
20
0
0.8
0.6
0.4
0.2
0.0
-0.2
0
100
200
300
400
500

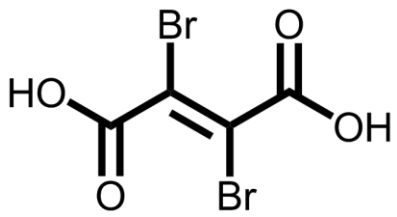
Br
O
HO
OH
O
Br

3.1

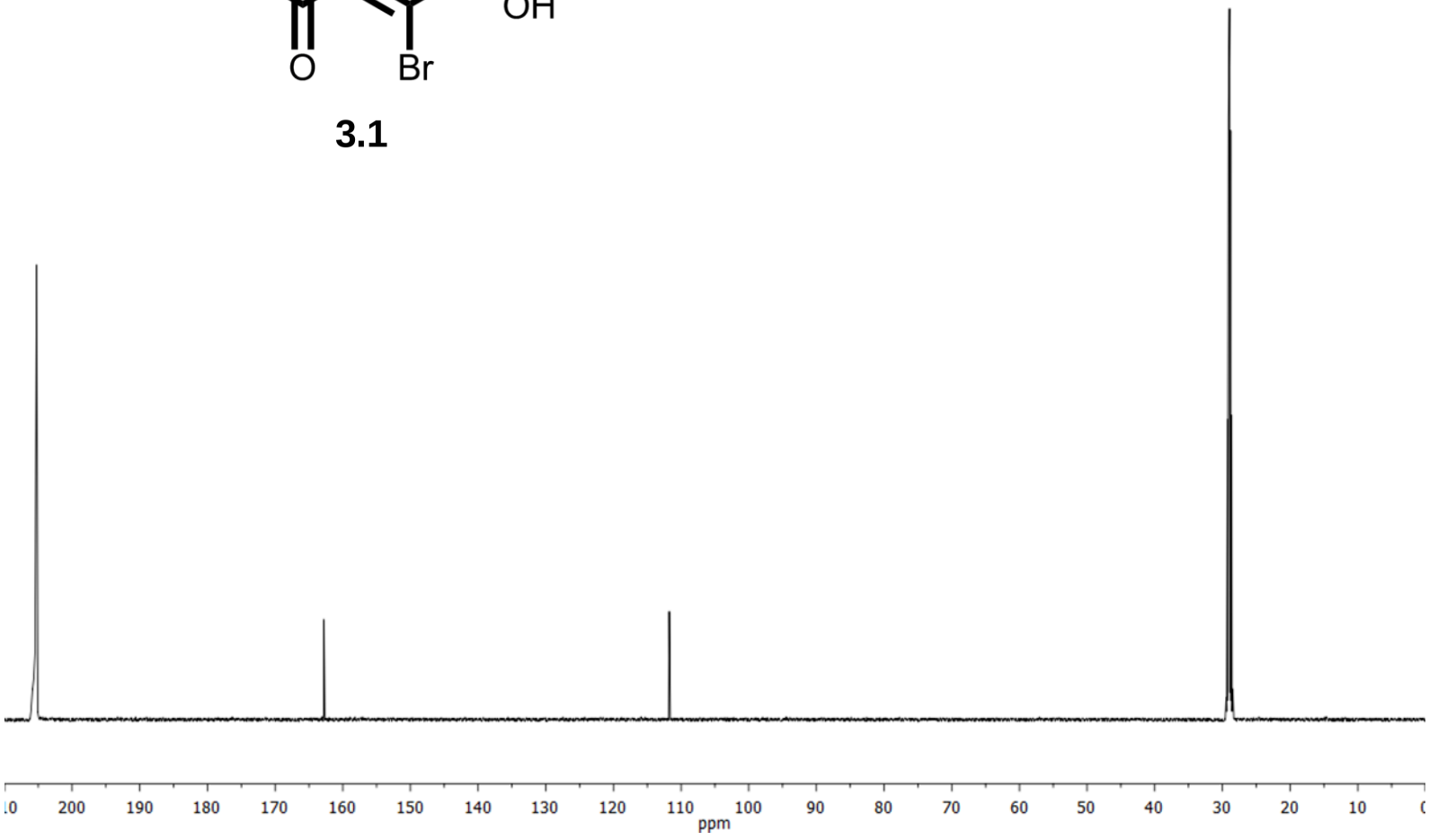
200
190
180
170
160
150
140
130
120
110
100
90
80
70
60
50
40
30
20
10
ppm

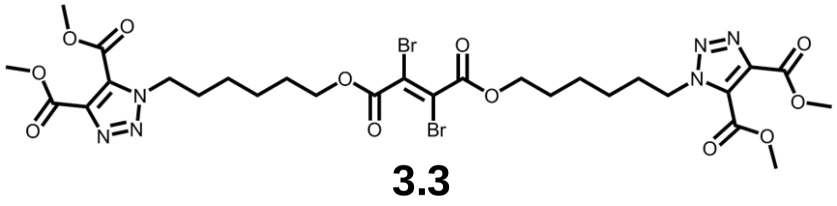

3.3

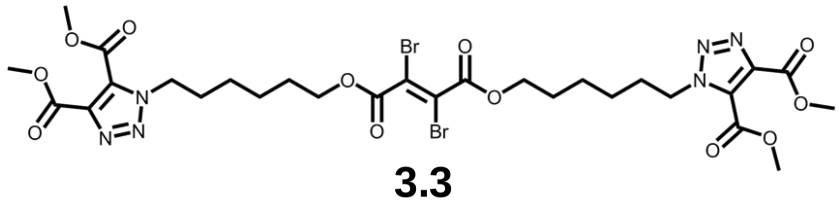
Br
Br

3.3

200
190
180
170
160
150
140
130
120
110
100
90
80
70
60
50
40
30
20
10
ppm

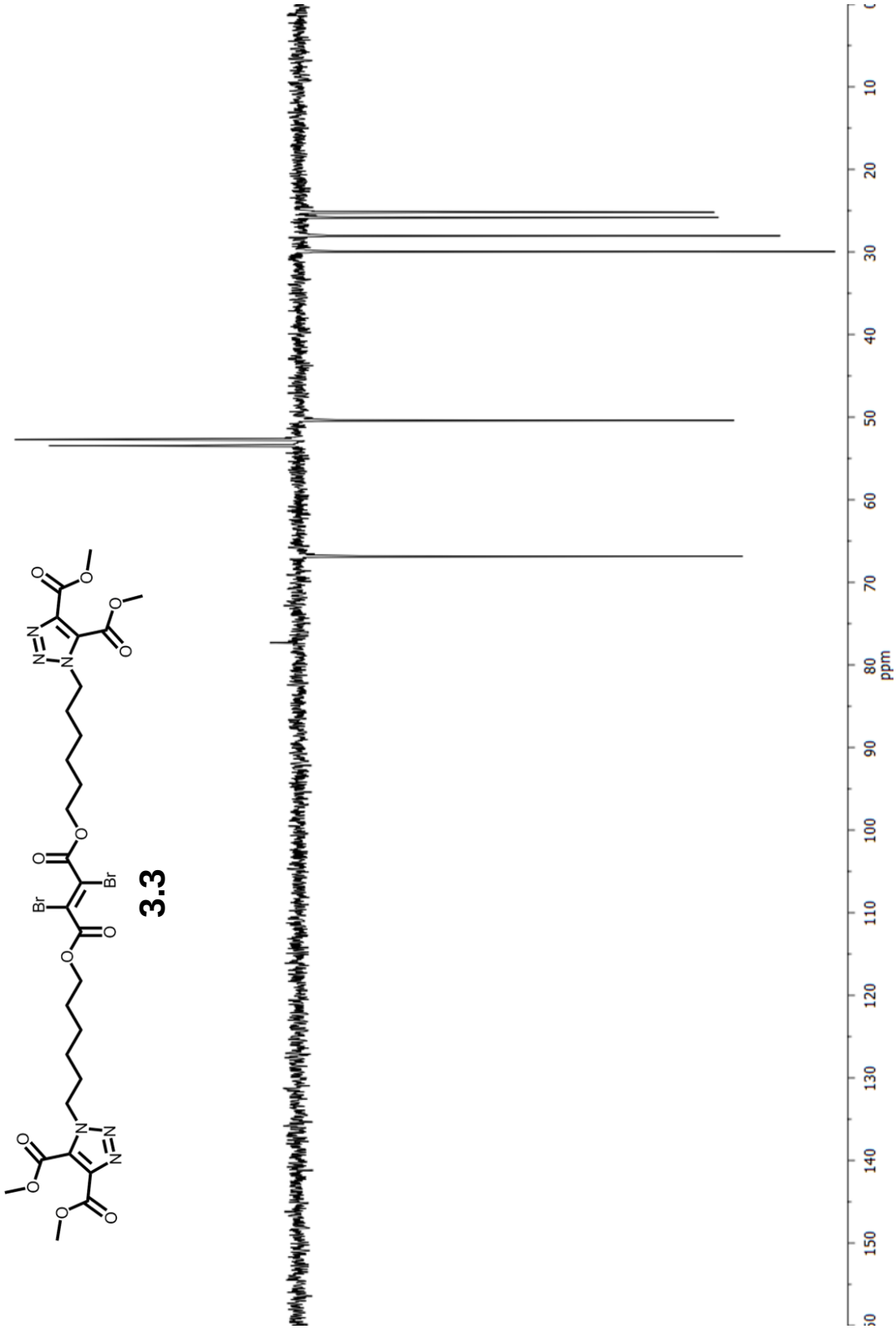
3.3
ppm

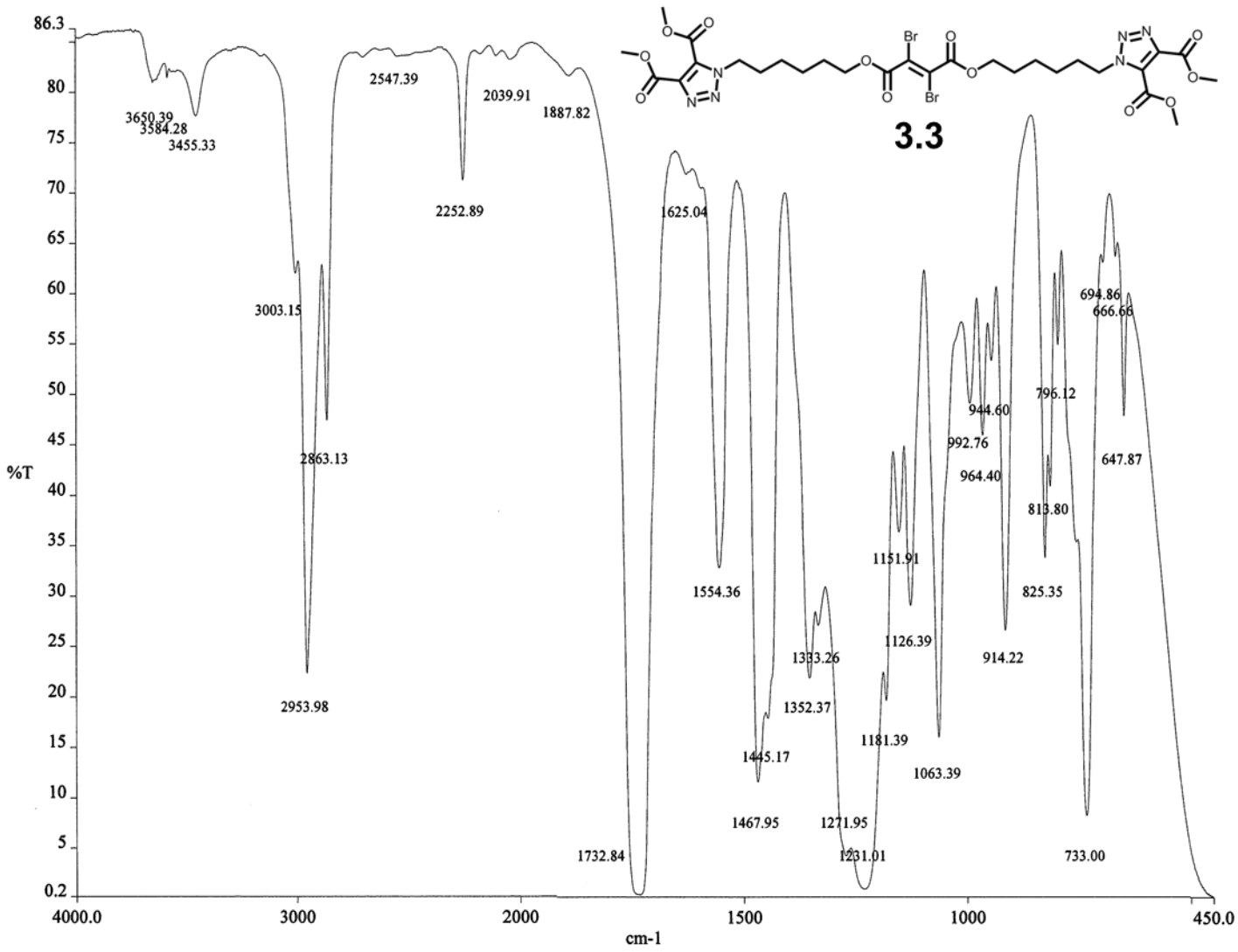
3.3
86.3
80
75
70
65
60
55
50
45
40
35
30
25
20
15
10
5
0.2
%T
4000.0
3000
2000
1500
1000
450.0
cm-1
3650.39
3584.28
3455.33
2547.39
2039.91
1887.82
2252.89
1625.04
3003.15
2863.13
2953.98
1554.36
1445.17
1467.95
1732.84
1333.26
1352.37
1271.95
1231.01
1151.91
1126.39
1181.39
1063.39
992.76
964.40
944.60
914.22
796.12
825.35
813.80
694.86
666.66
647.87
733.00

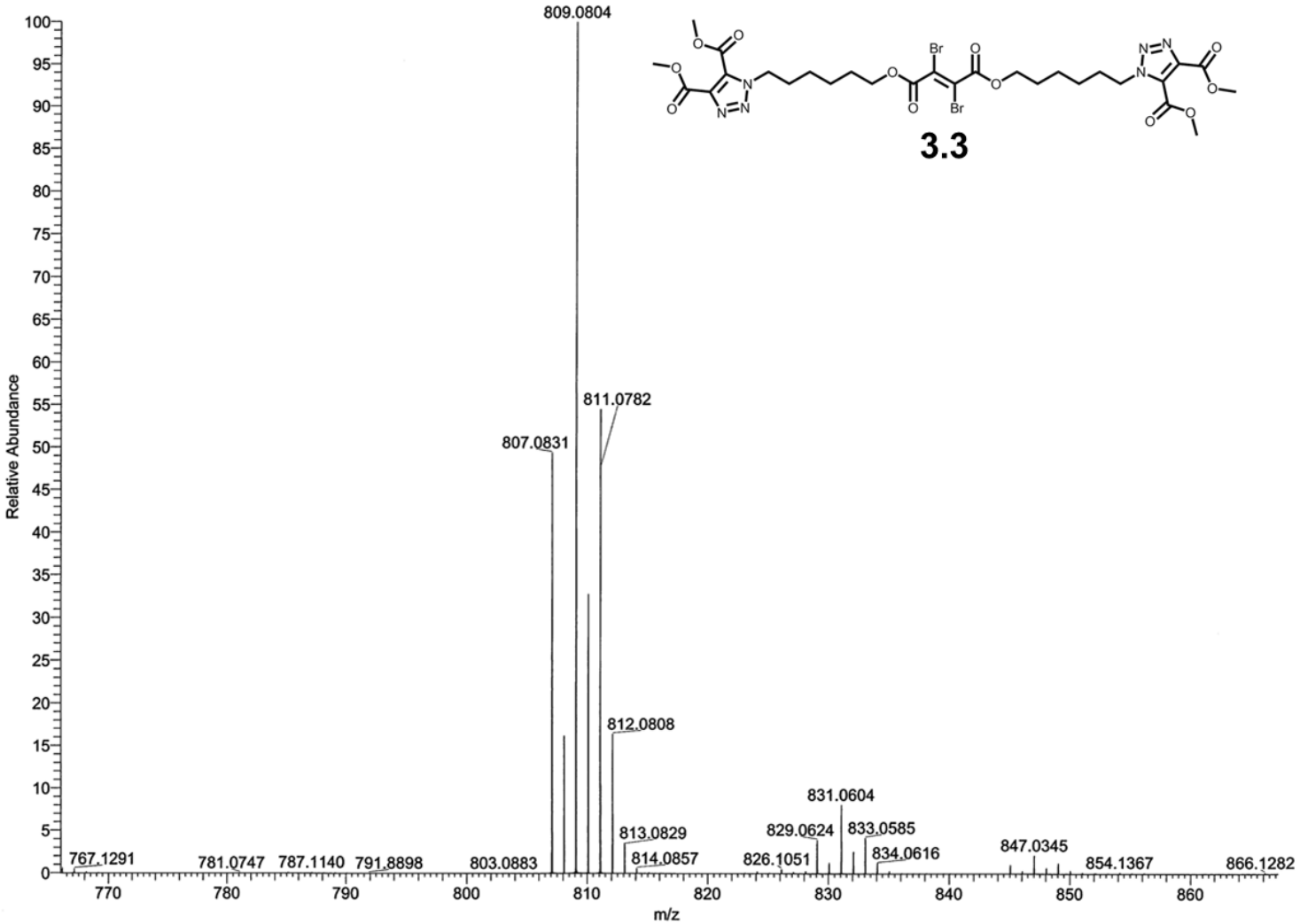
809.0804
811.0782
807.0831
812.0808
831.0604
813.0829
829.0624
833.0585
814.0857
826.1051
834.0616
847.0345
767.1291
781.0747
787.1140
791.8898
803.0883
854.1367
866.1282
Relative Abundance
m/z
3.3

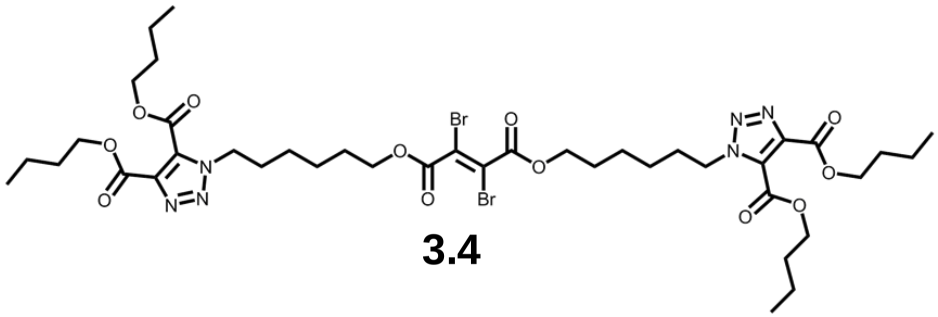

3.4

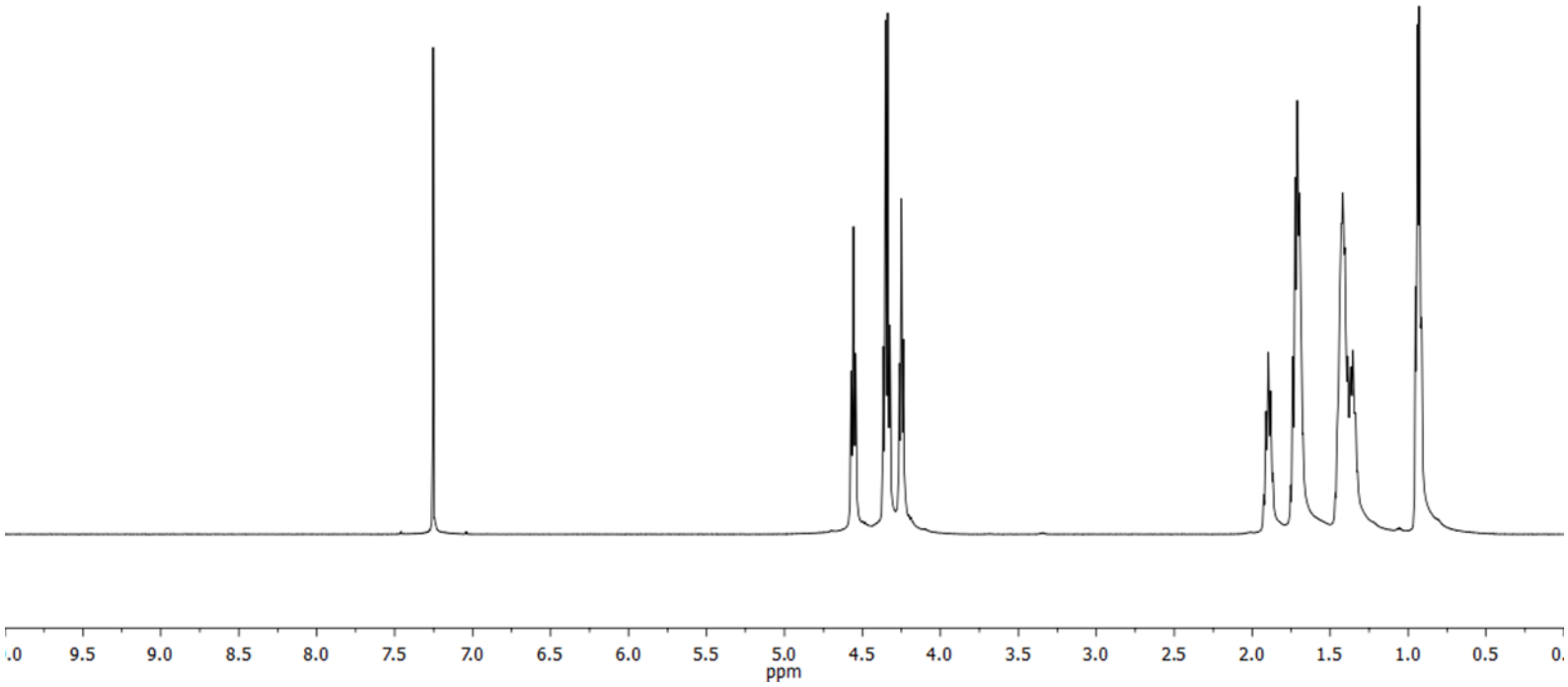

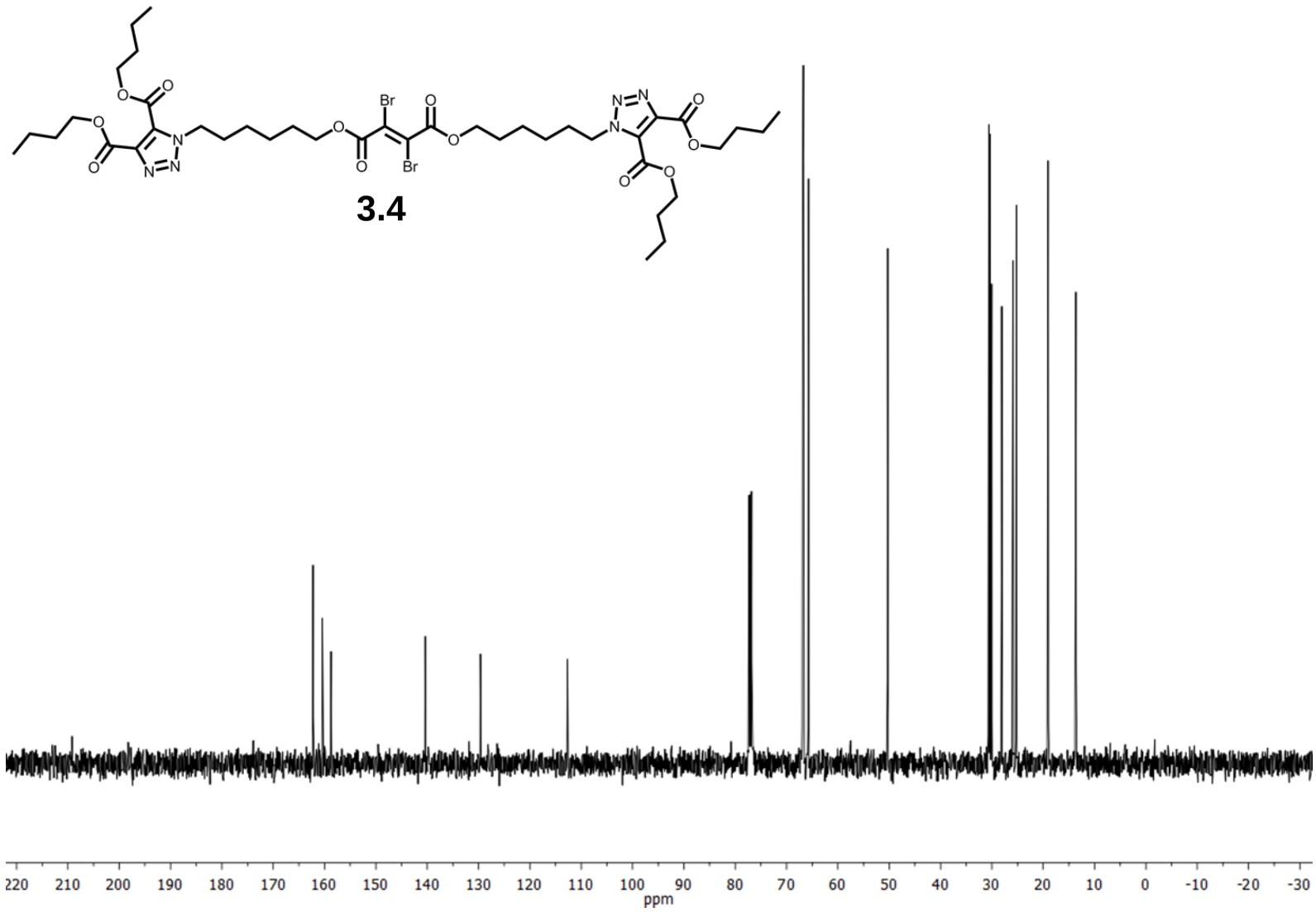
Br
Br
3.4
220
210
200
190
180
170
160
150
140
130
120
110
100
90
80
70
60
50
40
30
20
10
0
-10
-20
-30
ppm

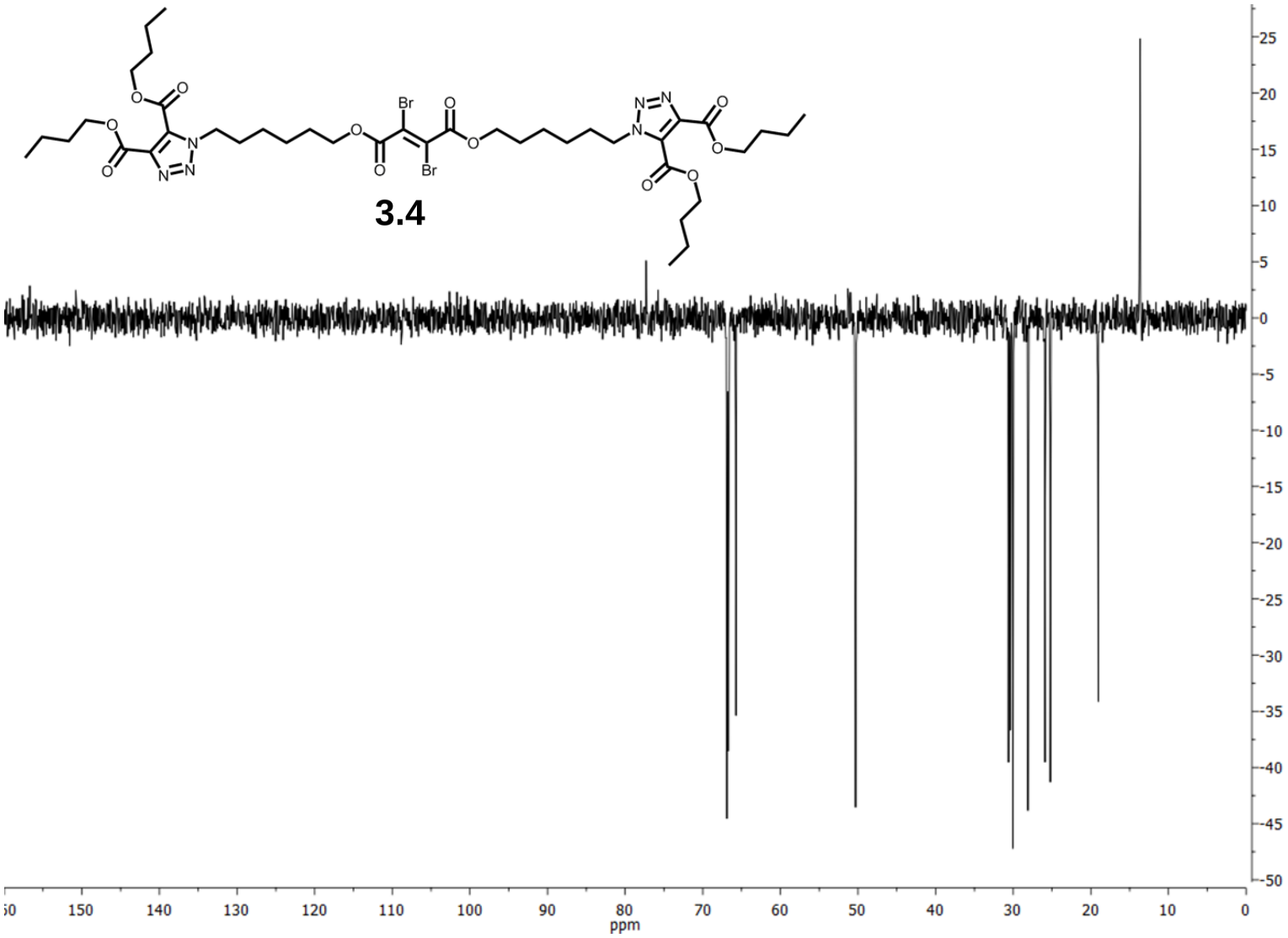
3.4
ppm

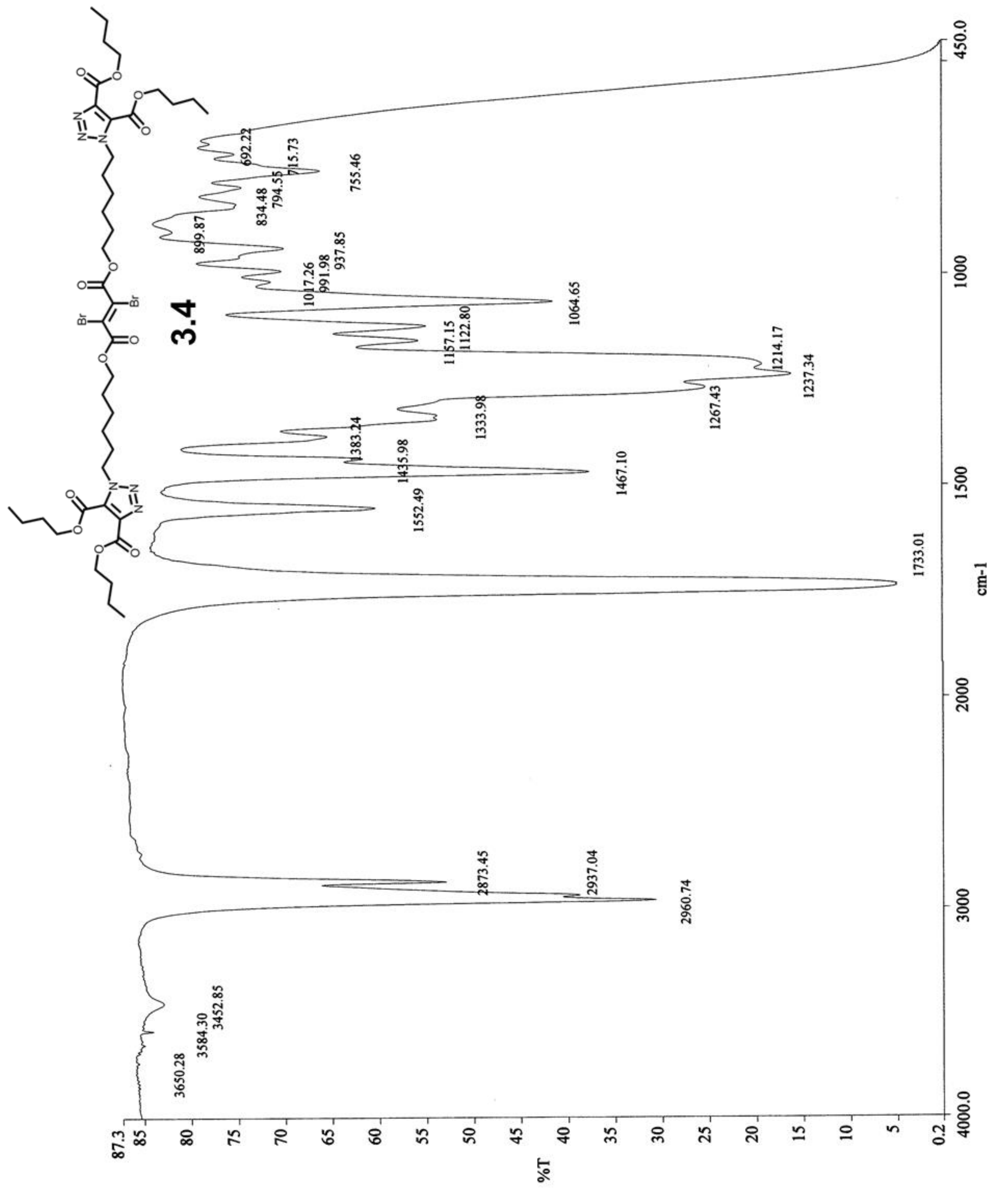
3.4
Br
Br
%T
cm-1
87.3
0.2
4000.0
3000
2000
1500
1000
450.0
3650.28
3584.30
3452.85
2960.74
2937.04
2873.45
1733.01
1552.49
1467.10
1435.98
1383.24
1333.98
1267.43
1237.34
1214.17
1157.15
1122.80
1064.65
1017.26
991.98
937.85
899.87
834.48
794.55
755.46
715.73
692.22

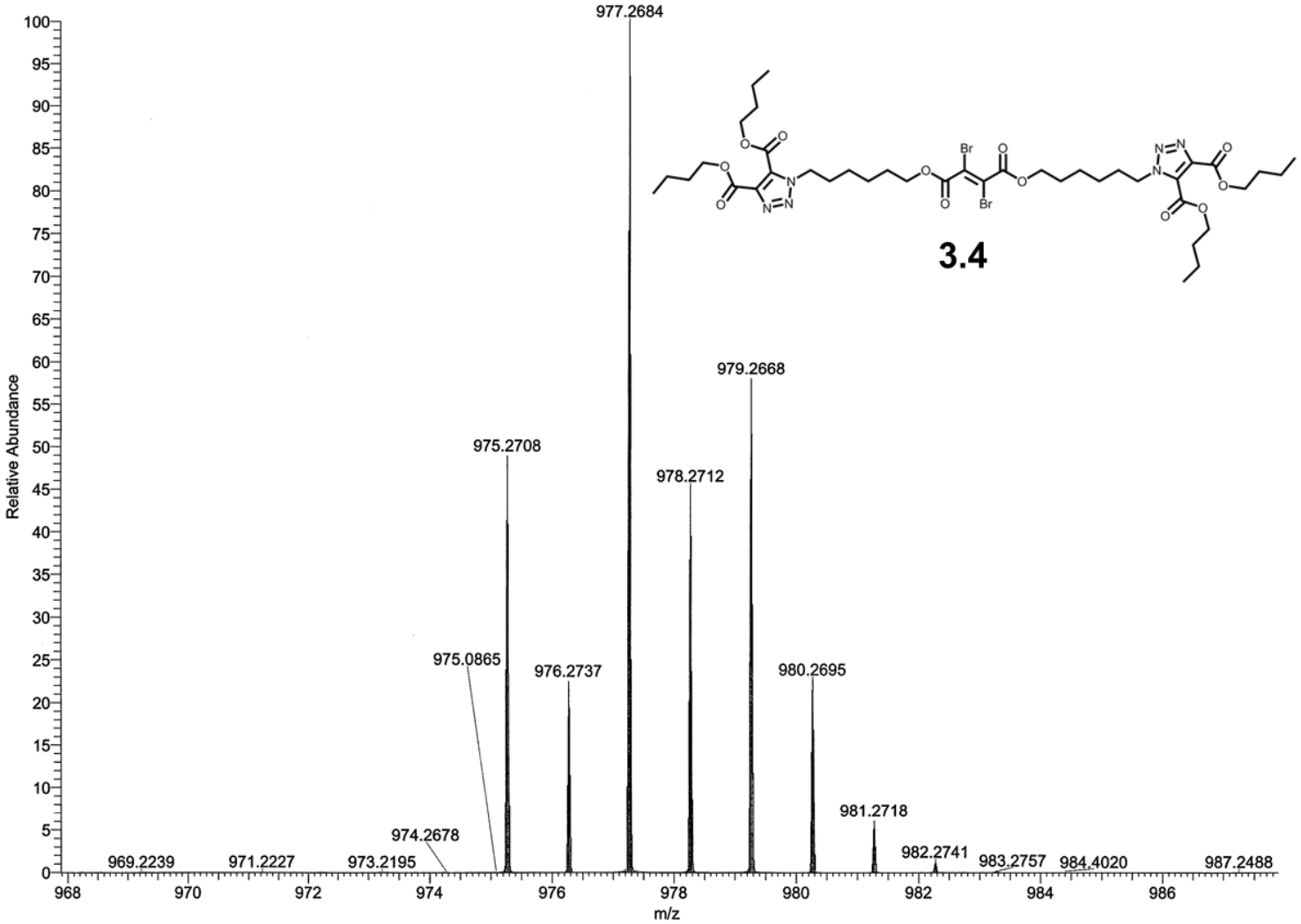
977.2684
979.2668
975.2708
978.2712
975.0865
976.2737
980.2695
981.2718
974.2678
982.2741
969.2239
971.2227
973.2195
983.2757
984.4020
987.2488
Relative Abundance
m/z
3.4

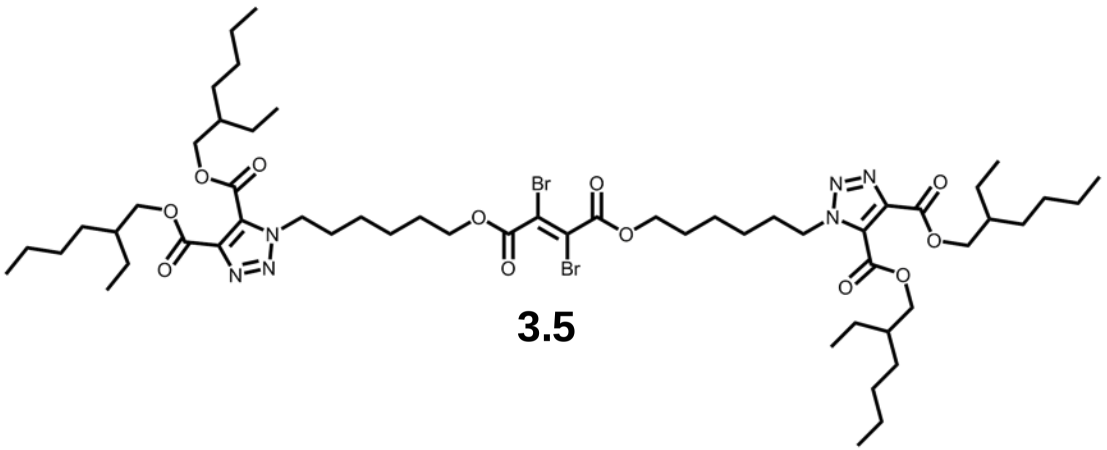

3.5

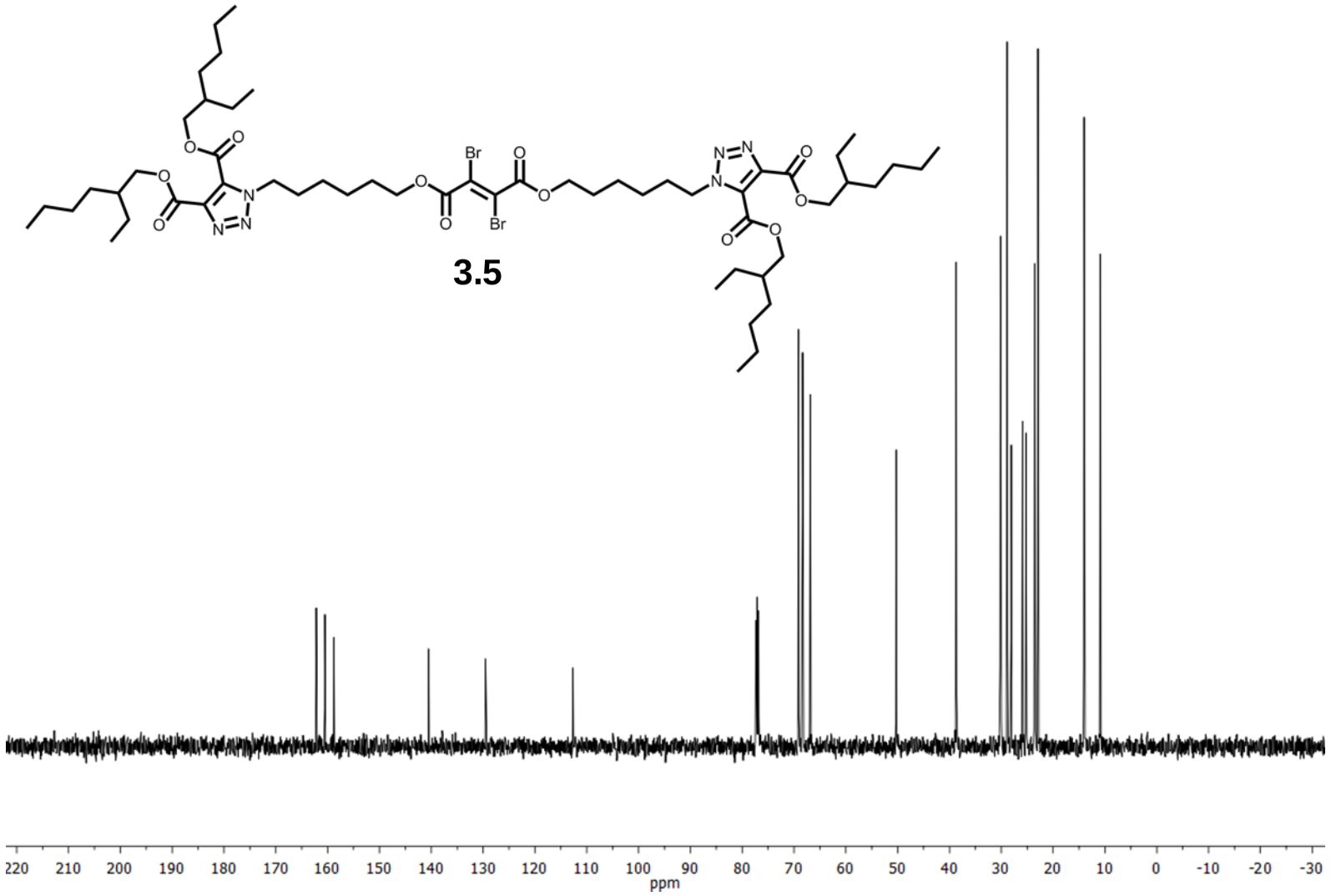
Br
Br
3.5
220
210
200
190
180
170
160
150
140
130
120
110
100
90
80
70
60
50
40
30
20
10
0
-10
-20
-30
ppm

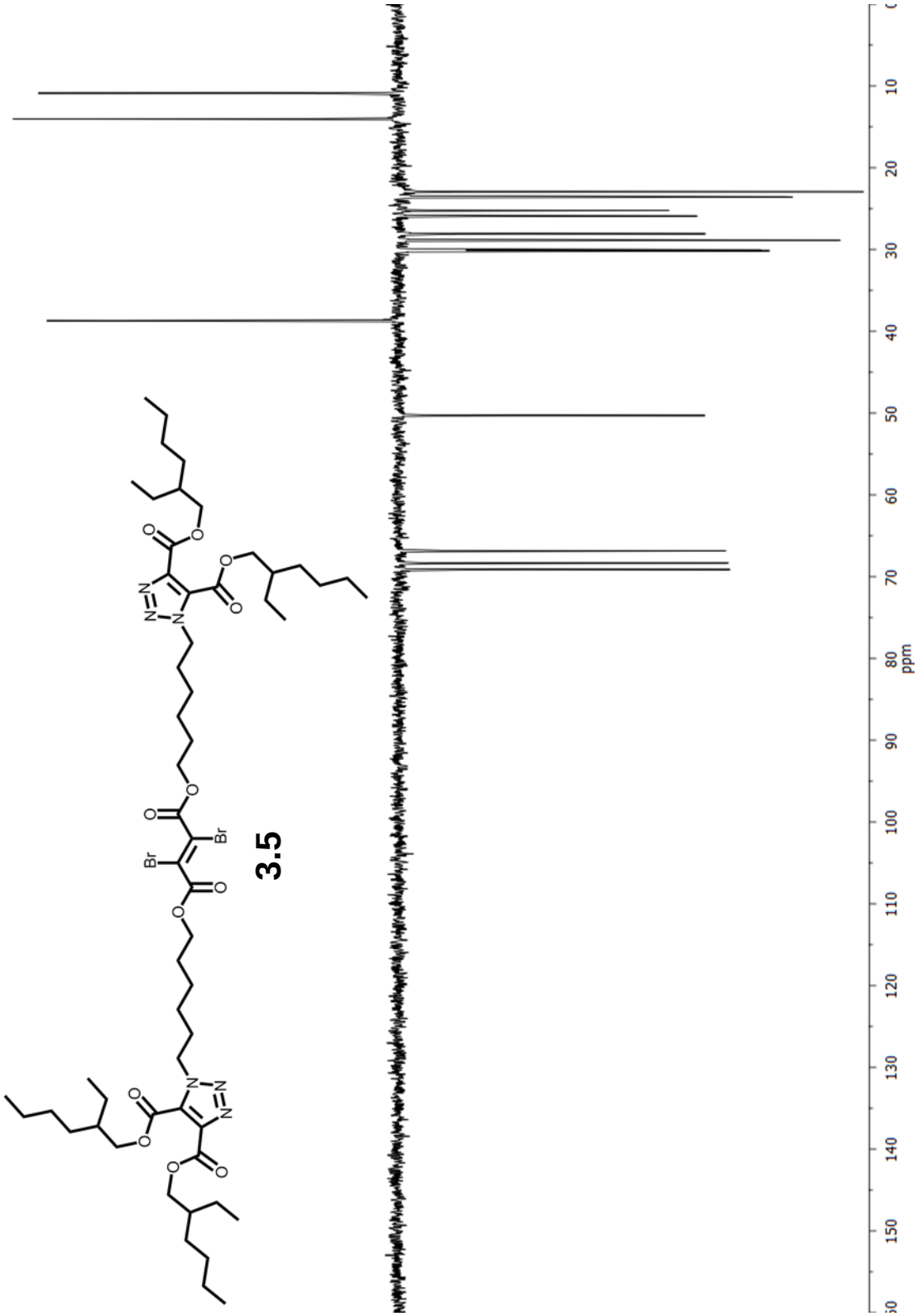
3.5
ppm

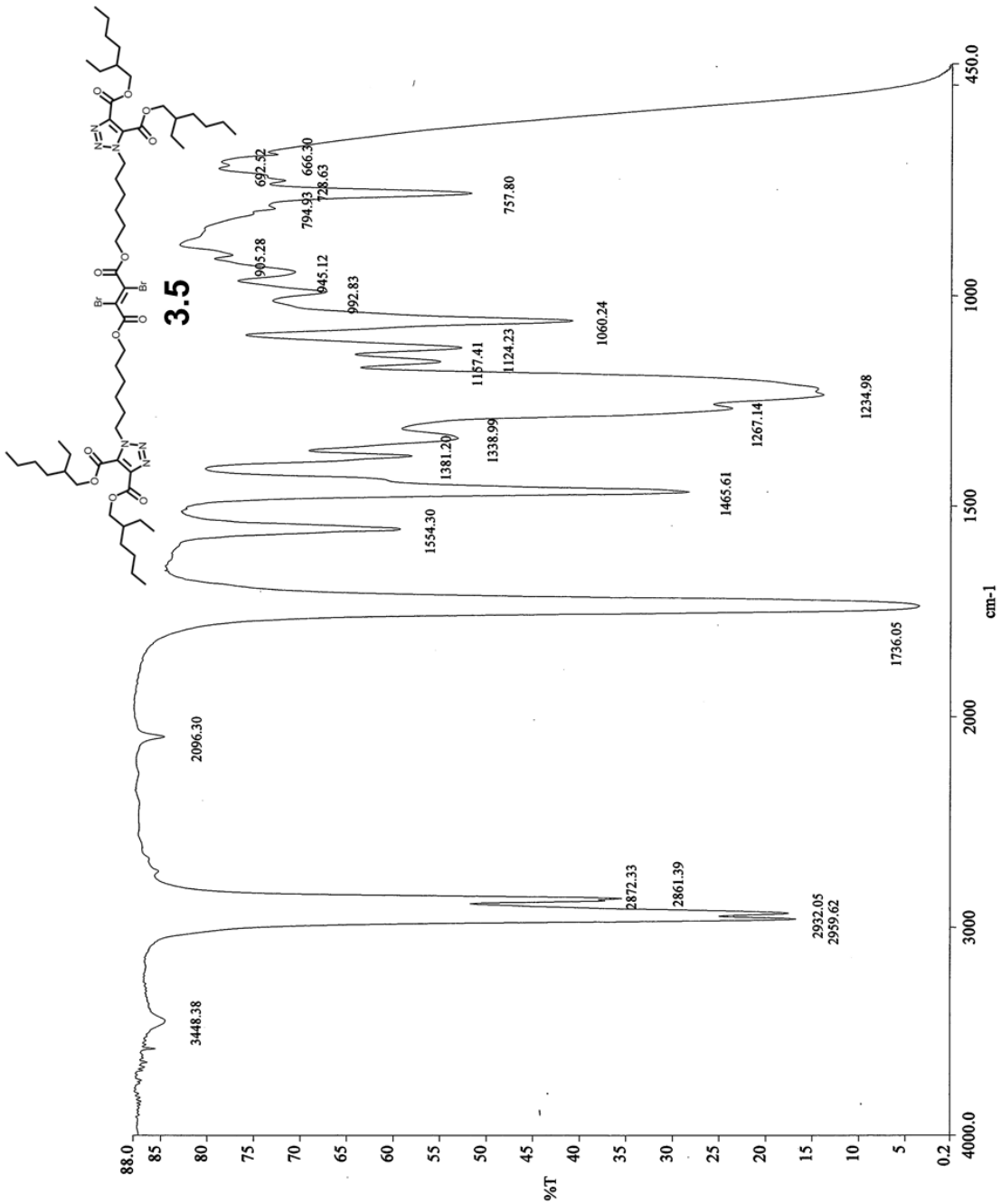
3.5
3448.38
2096.30
2872.33
2861.39
2932.05
2959.62
1736.05
1554.30
1465.61
1381.20
1338.99
1267.14
1234.98
1157.41
1124.23
1060.24
992.83
945.12
905.28
794.93
757.80
728.63
666.30
692.52
%T
cm-1
4000.0
3000
2000
1500
1000
450.0
88.0
85
80
75
70
65
60
55
50
45
40
35
30
25
20
15
10
5
0.2

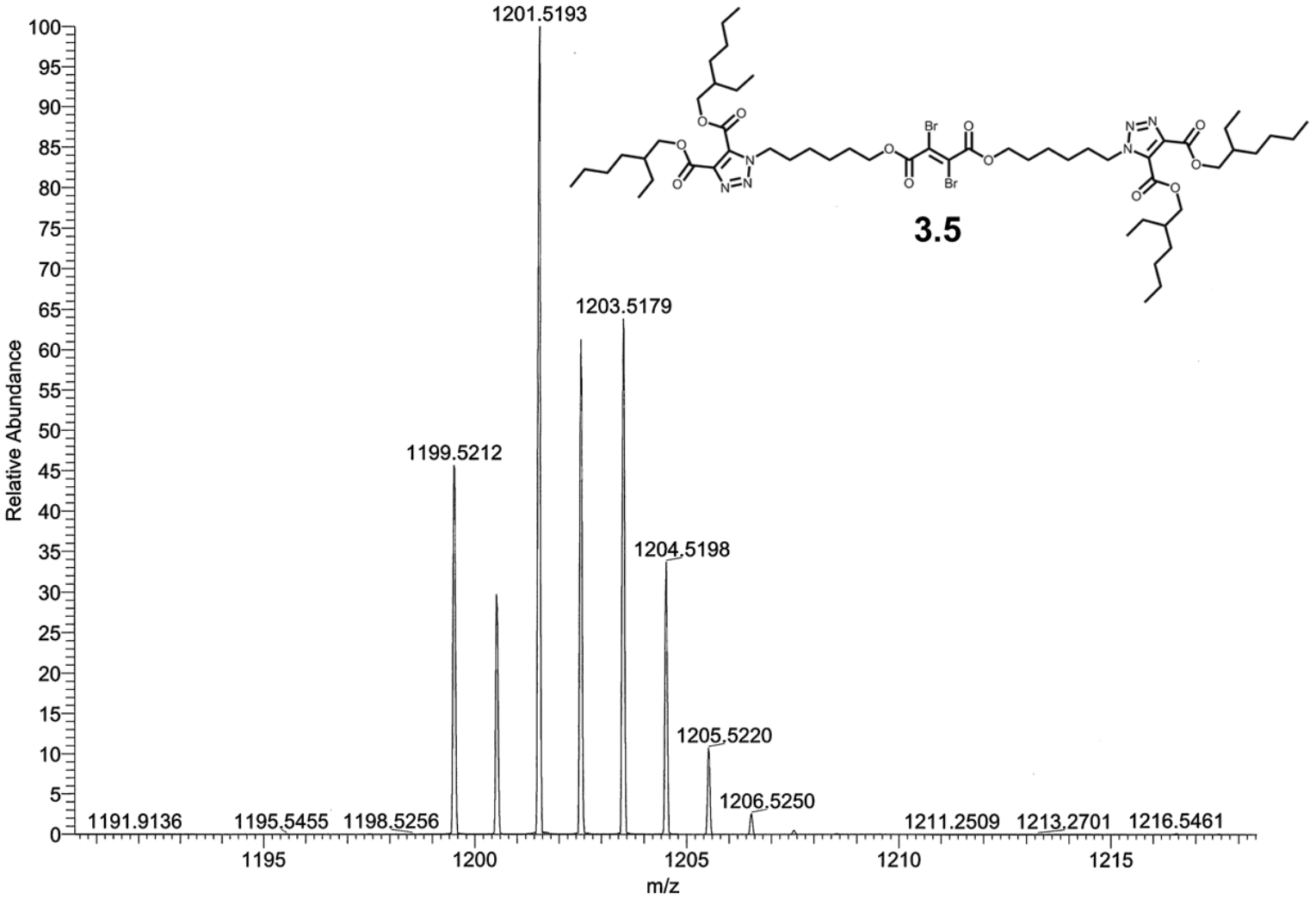
1201.5193
1203.5179
1199.5212
1204.5198
1205.5220
1206.5250
1191.9136
1195.5455
1198.5256
1211.2509
1213.2701
1216.5461
Relative Abundance
m/z
3.5

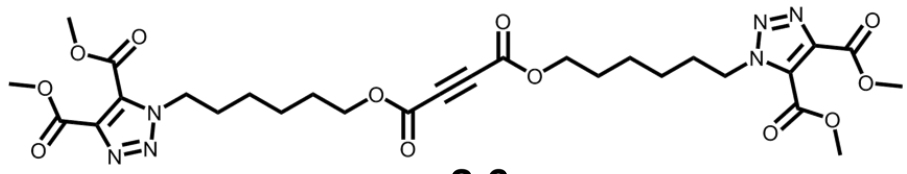

3.6

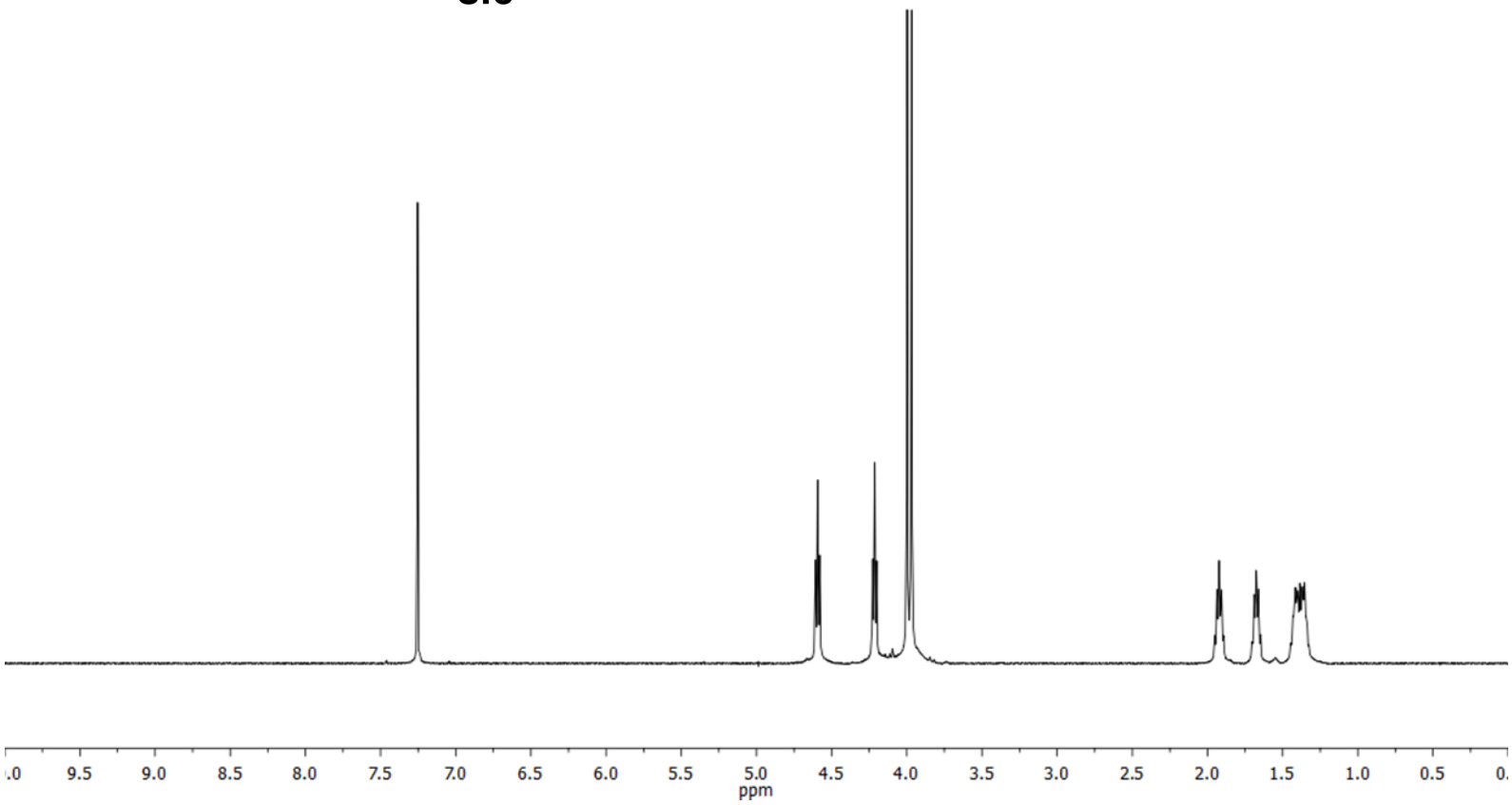

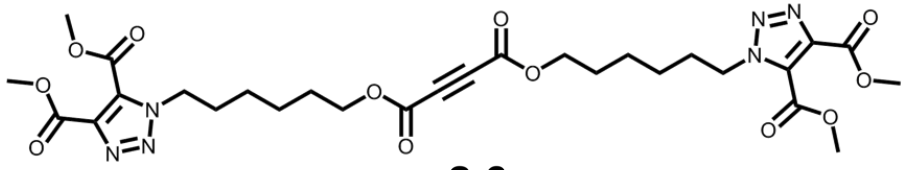

3.6

200
190
180
170
160
150
140
130
120
110
100
90
80
70
60
50
40
30
20
10
ppm

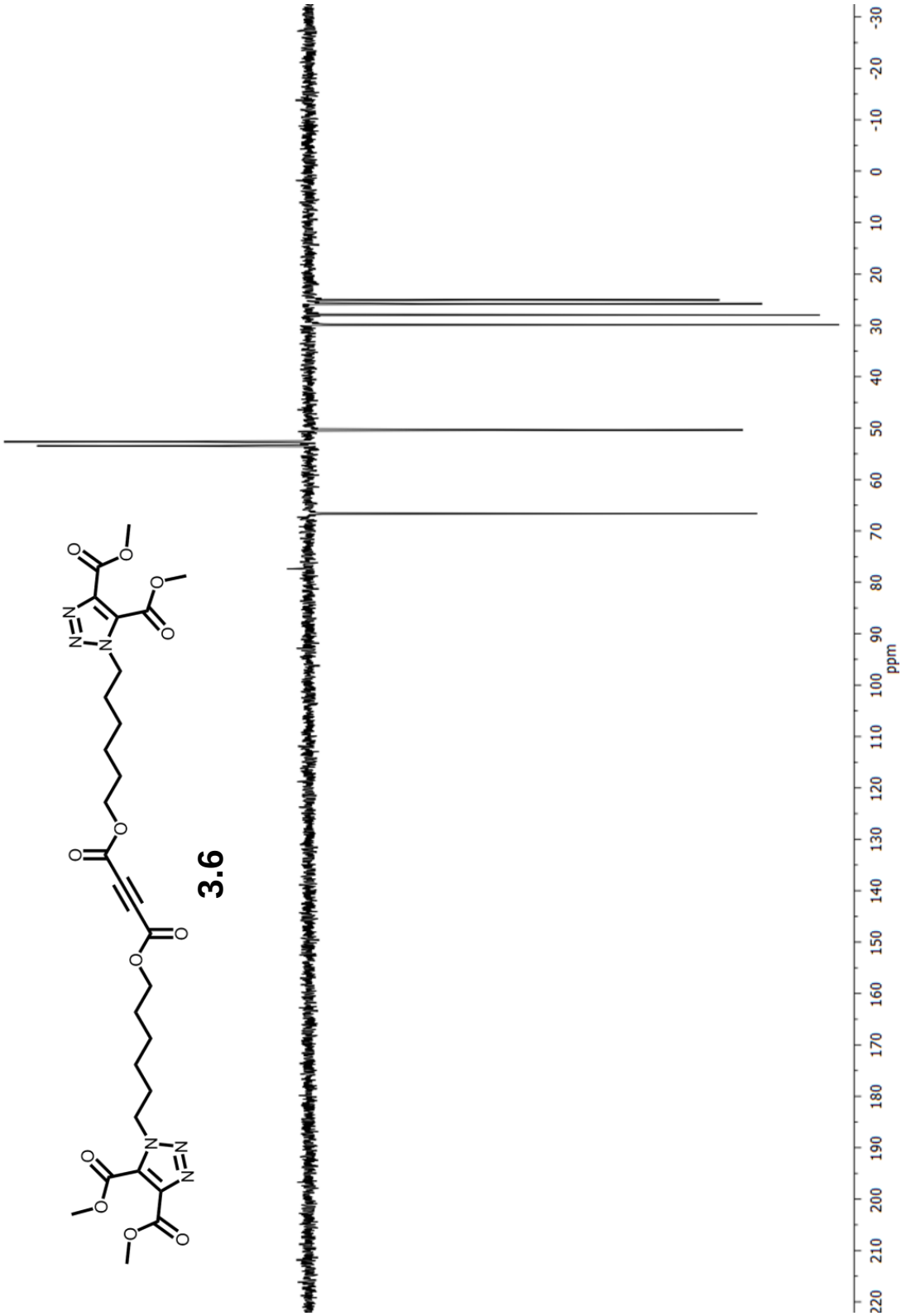
3.6
ppm

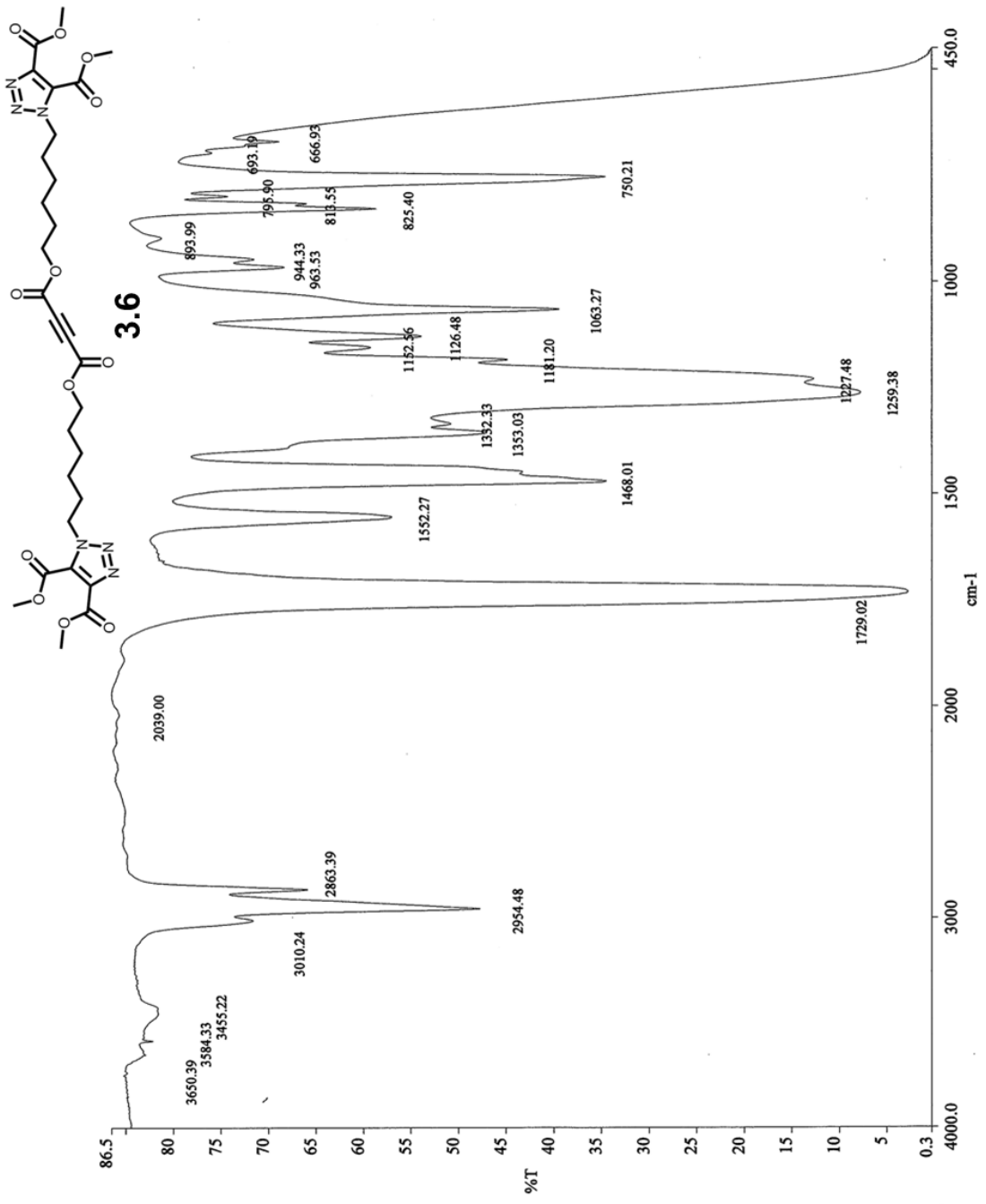
3.6
%T
cm-1
86.5
80
75
70
65
60
55
50
45
40
35
30
25
20
15
10
5
0.3
4000.0
3000
2000
1500
1000
450.0
3650.39
3584.33
3455.22
3010.24
2954.48
2863.39
2039.00
1729.02
1552.27
1468.01
1353.03
1352.33
1259.38
1227.48
1181.20
1152.56
1126.48
1063.27
963.53
944.33
893.99
825.40
813.55
795.90
750.21
693.19
666.93

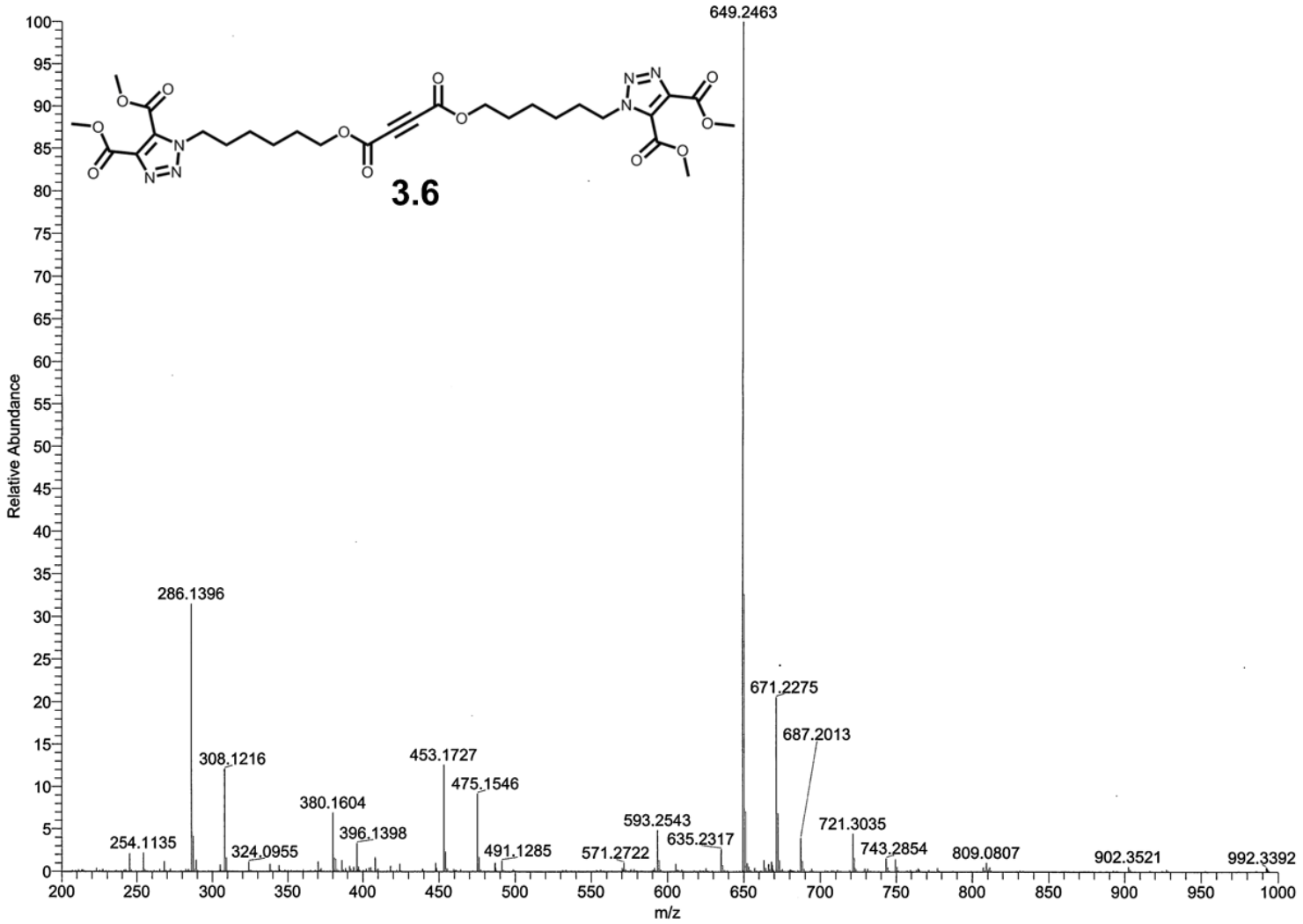
3.6
649.2463
286.1396
671.2275
687.2013
308.1216
453.1727
475.1546
380.1604
396.1398
593.2543
635.2317
721.3035
254.1135
324.0955
491.1285
571.2722
743.2854
809.0807
902.3521
992.3392
Relative Abundance
m/z

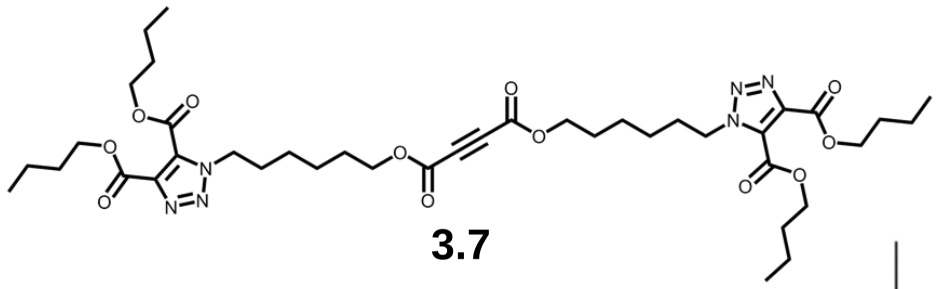

3.7

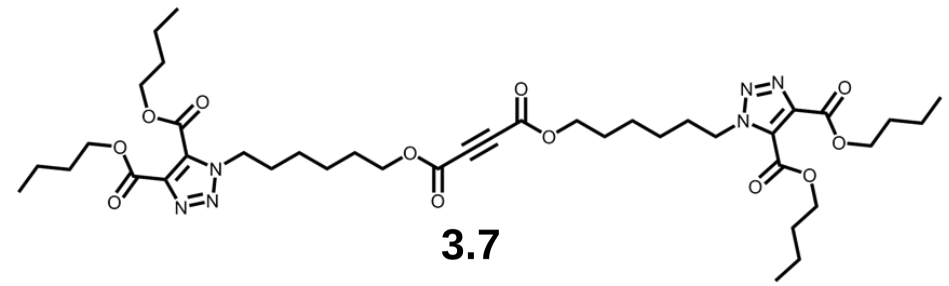

3.7

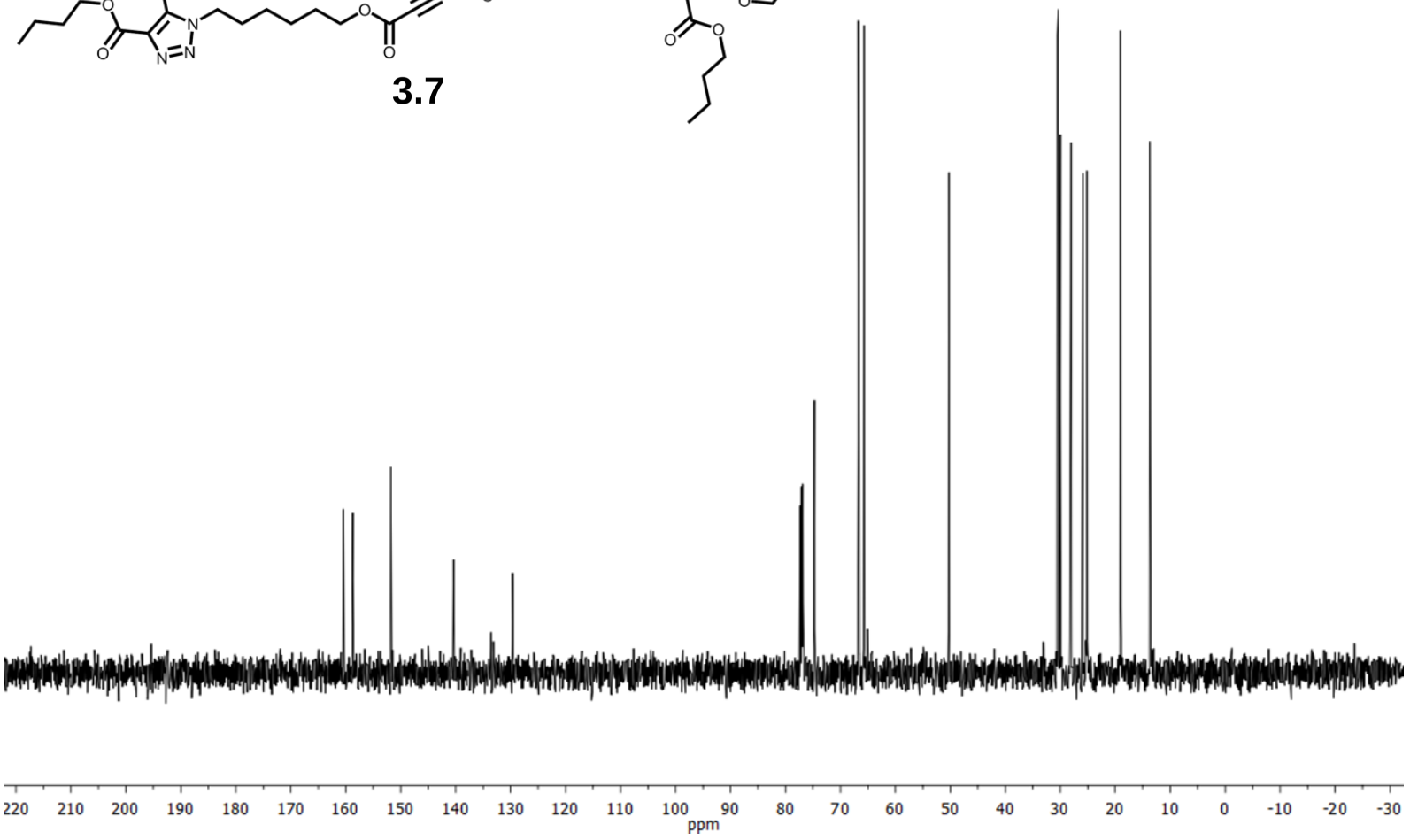
220
210
200
190
180
170
160
150
140
130
120
110
100
90
80
70
60
50
40
30
20
10
0
-10
-20
-30
ppm

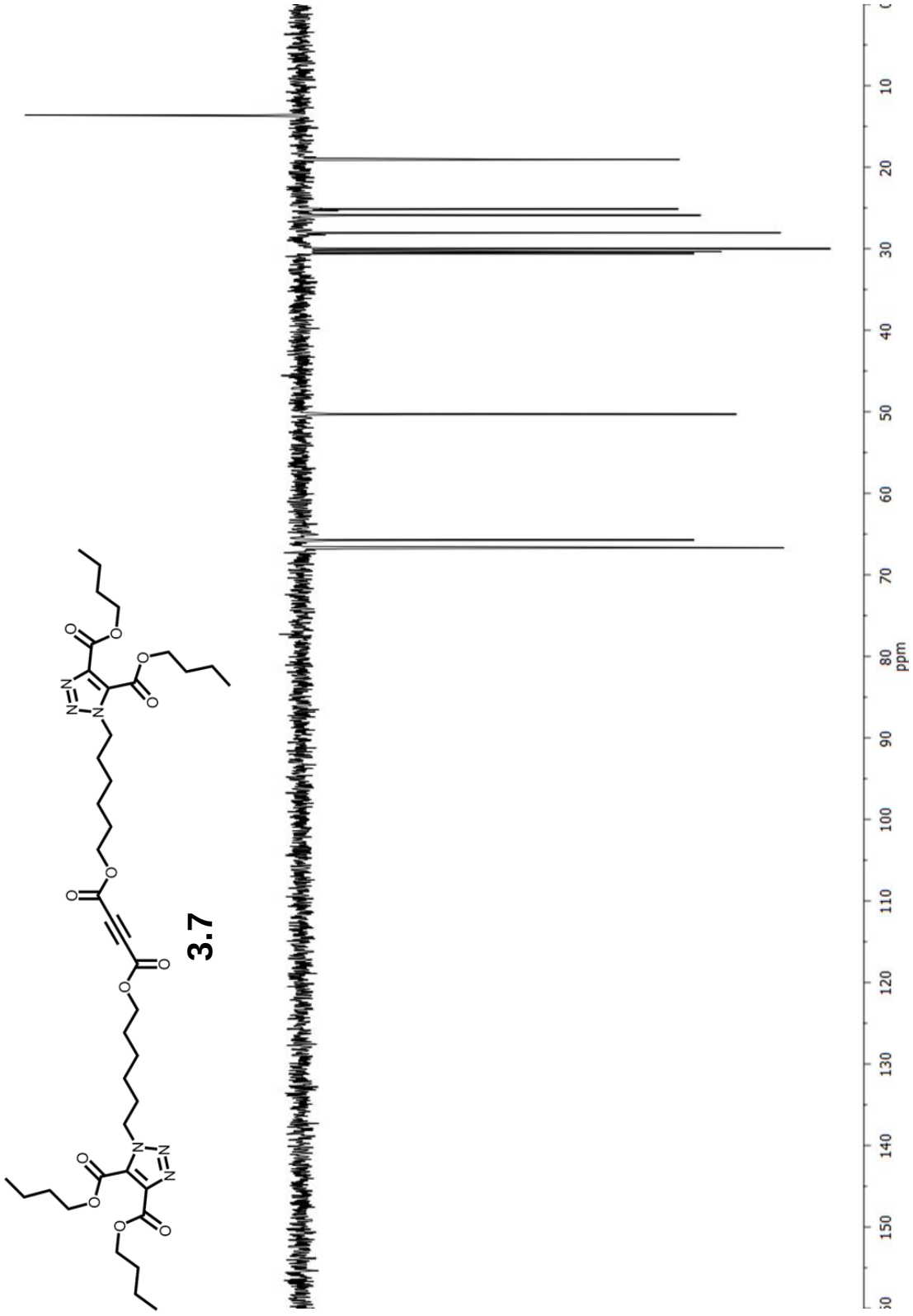
3.7
ppm

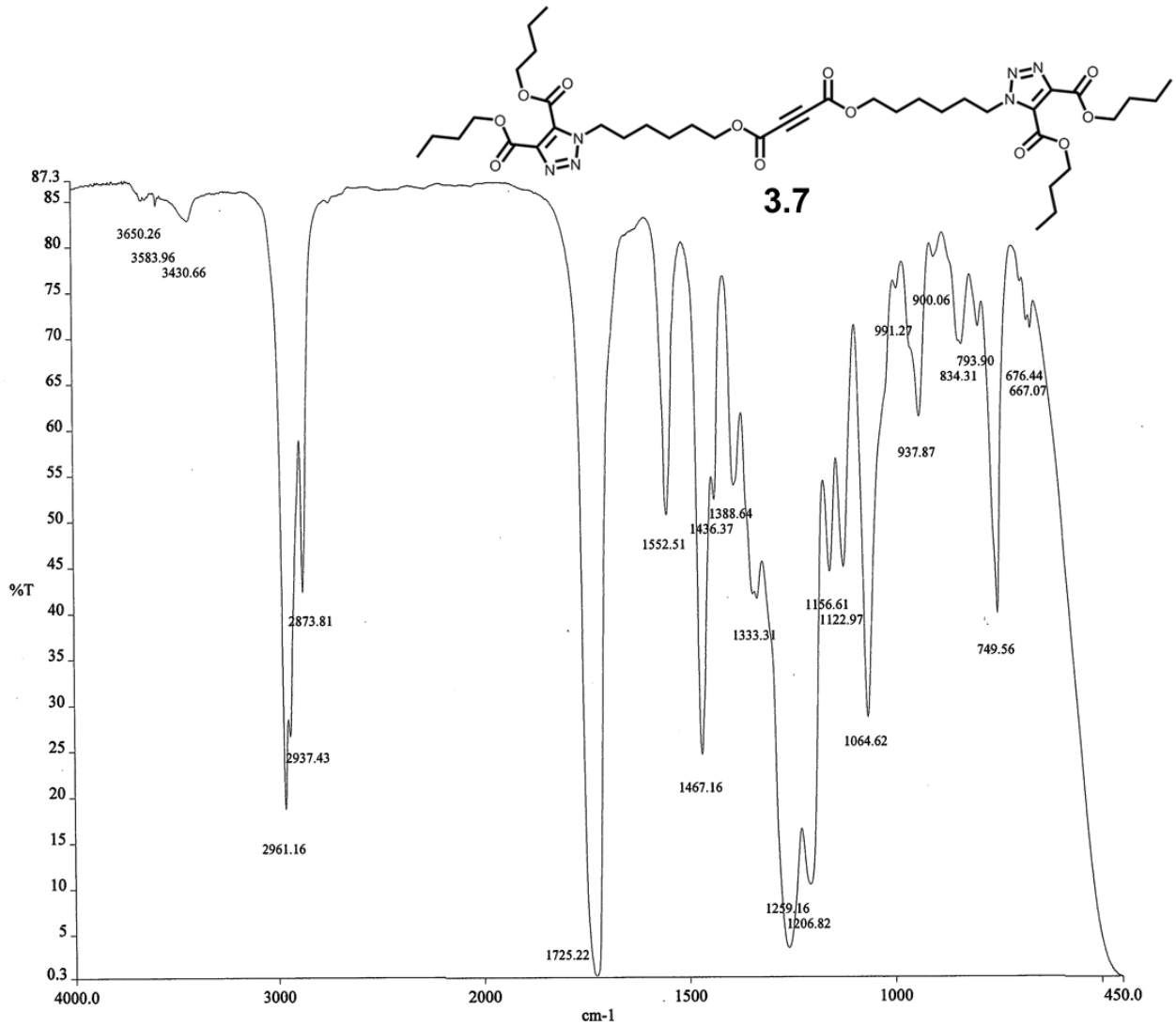
3.7
%T
cm-1
87.3
85
80
75
70
65
60
55
50
45
40
35
30
25
20
15
10
5
0.3
4000.0
3000
2000
1500
1000
450.0
3650.26
3583.96
3430.66
2873.81
2937.43
2961.16
1725.22
1552.51
1388.64
1436.37
1467.16
1333.31
1259.16
1206.82
1156.61
1122.97
1064.62
991.27
900.06
937.87
793.90
834.31
749.56
676.44
667.07

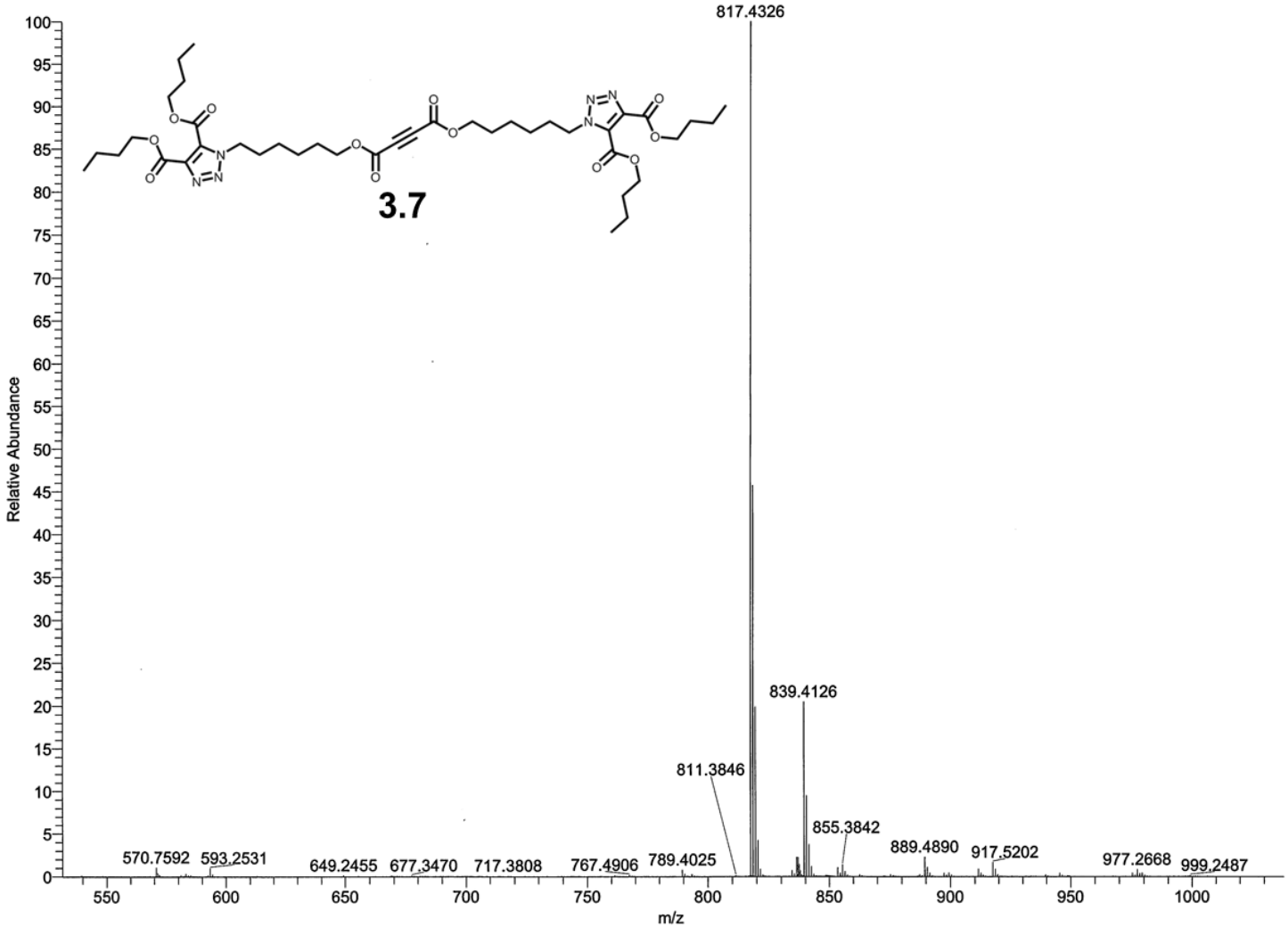
3.7
817.4326
839.4126
811.3846
855.3842
889.4890
917.5202
977.2668
999.2487
570.7592
593.2531
649.2455
677.3470
717.3808
767.4906
789.4025
Relative Abundance
m/z

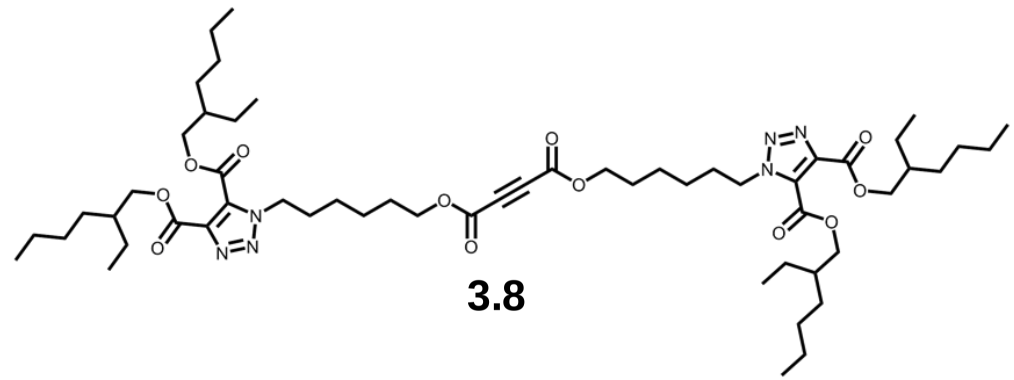

3.8

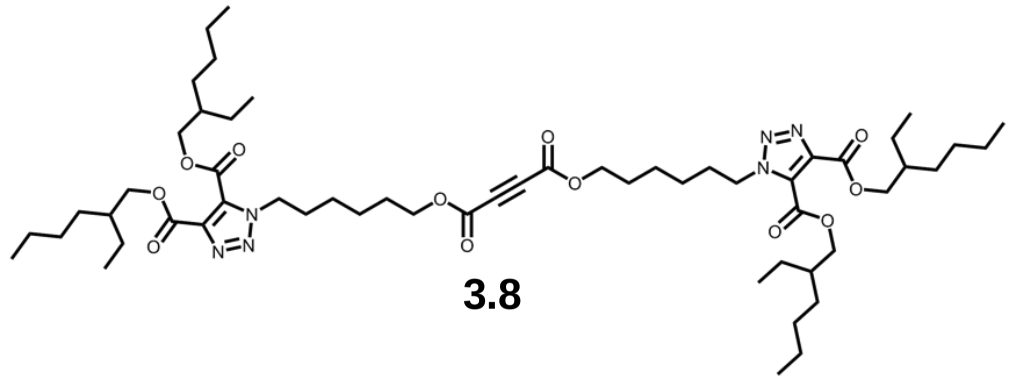

3.8

200
190
180
170
160
150
140
130
120
110
100
90
80
70
60
50
40
30
20
10
ppm

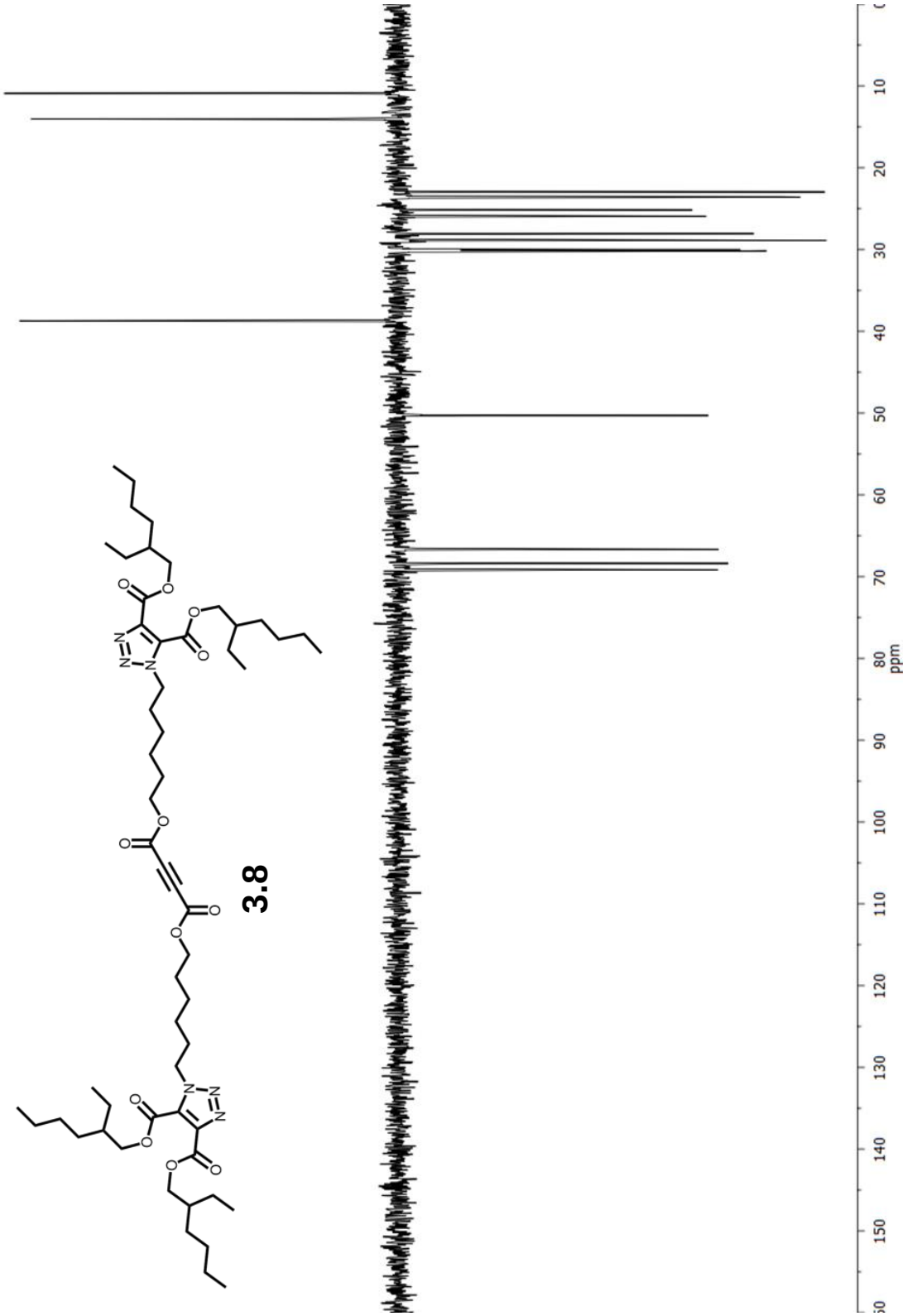
3.8
10
20
30
40
50
60
70
80
ppm
90
100
110
120
130
140
150

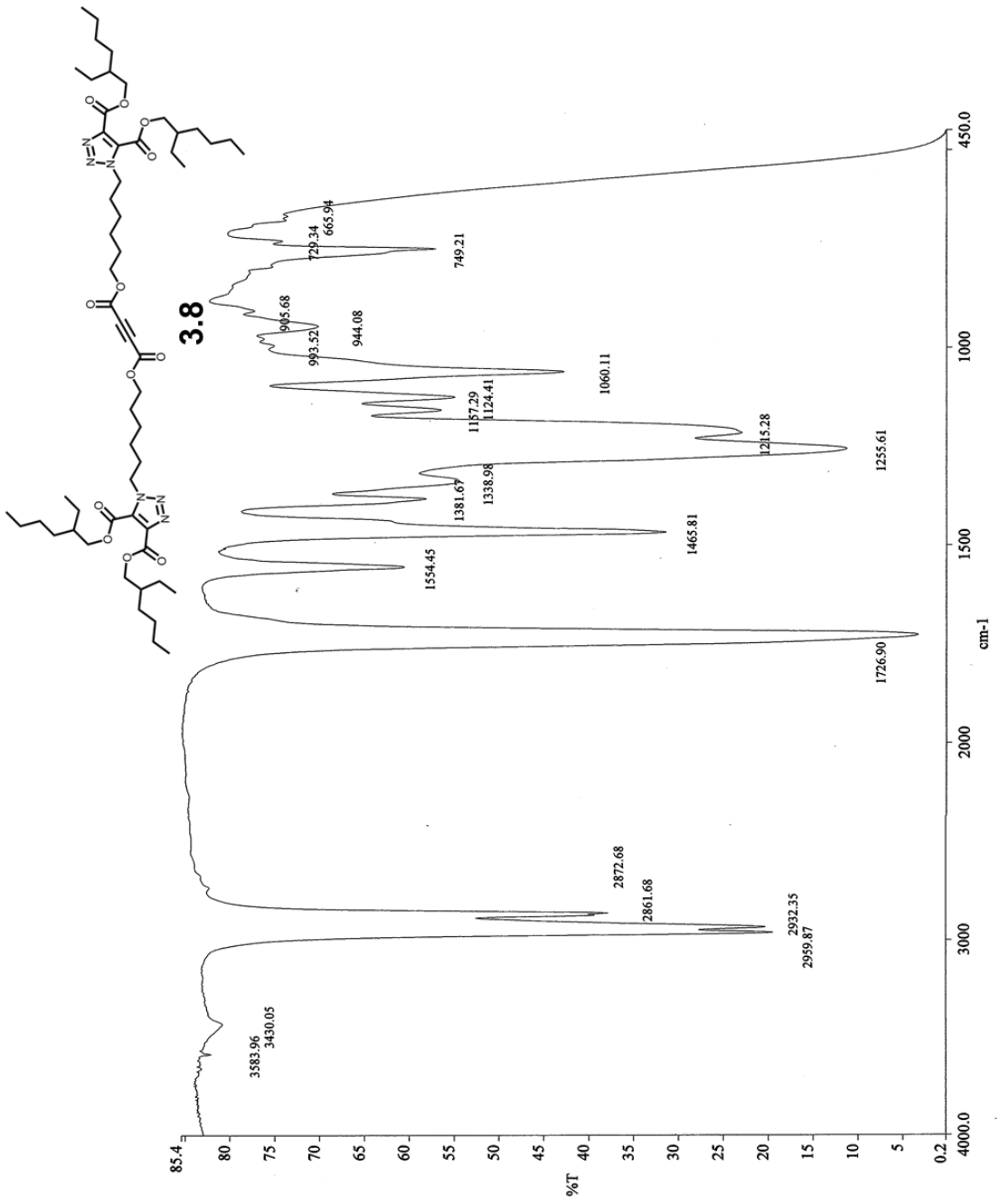
3.8
85.4
80
75
70
65
60
55
50
45
40
35
30
25
20
15
10
5
0.2
%T
4000.0
3000
2000
1500
1000
450.0
cm-1
3583.96
3430.05
2872.68
2861.68
2932.35
2959.87
1726.90
1554.45
1465.81
1381.67
1338.98
1255.61
1215.28
1157.29
1124.41
1060.11
993.52
965.68
944.08
749.21
729.34
665.94

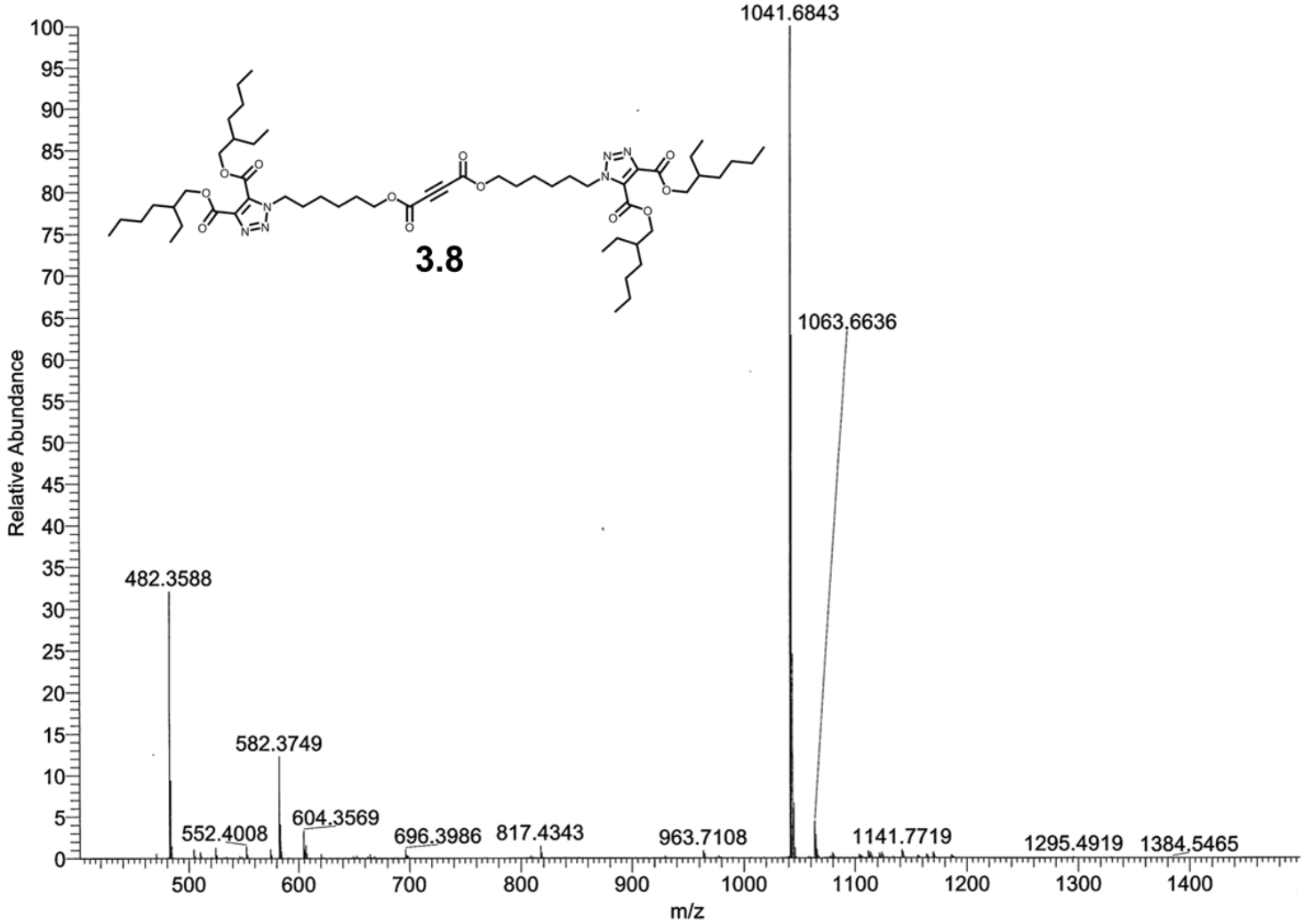
3.8
Relative Abundance
m/z
1041.6843
1063.6636
482.3588
582.3749
604.3569
552.4008
696.3986
817.4343
963.7108
1141.7719
1295.4919
1384.5465

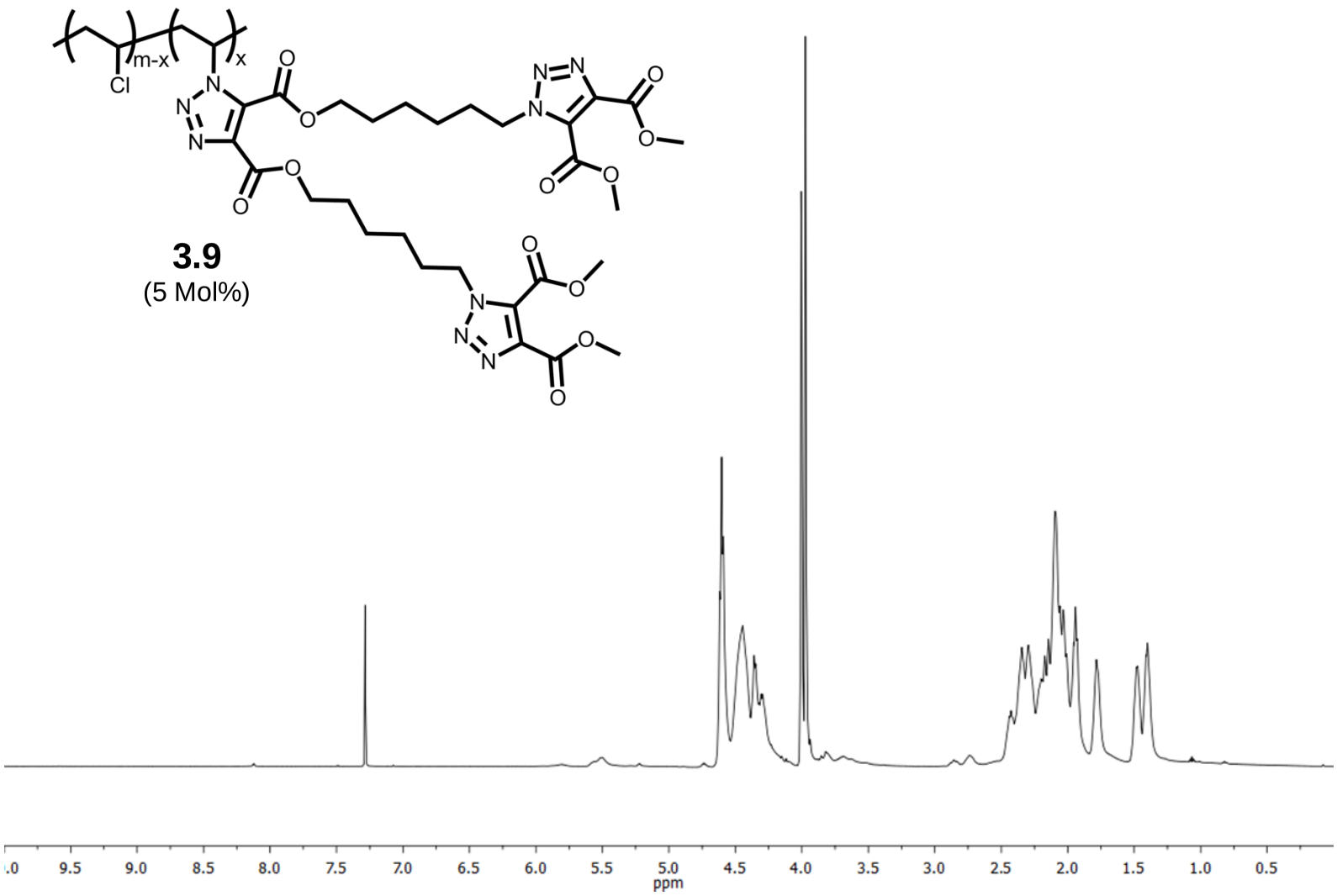
m-x
x
Cl
3.9
(5 Mol%)
9.5
9.0
8.5
8.0
7.5
7.0
6.5
6.0
5.5
5.0
4.5
4.0
3.5
3.0
2.5
2.0
1.5
1.0
0.5
ppm

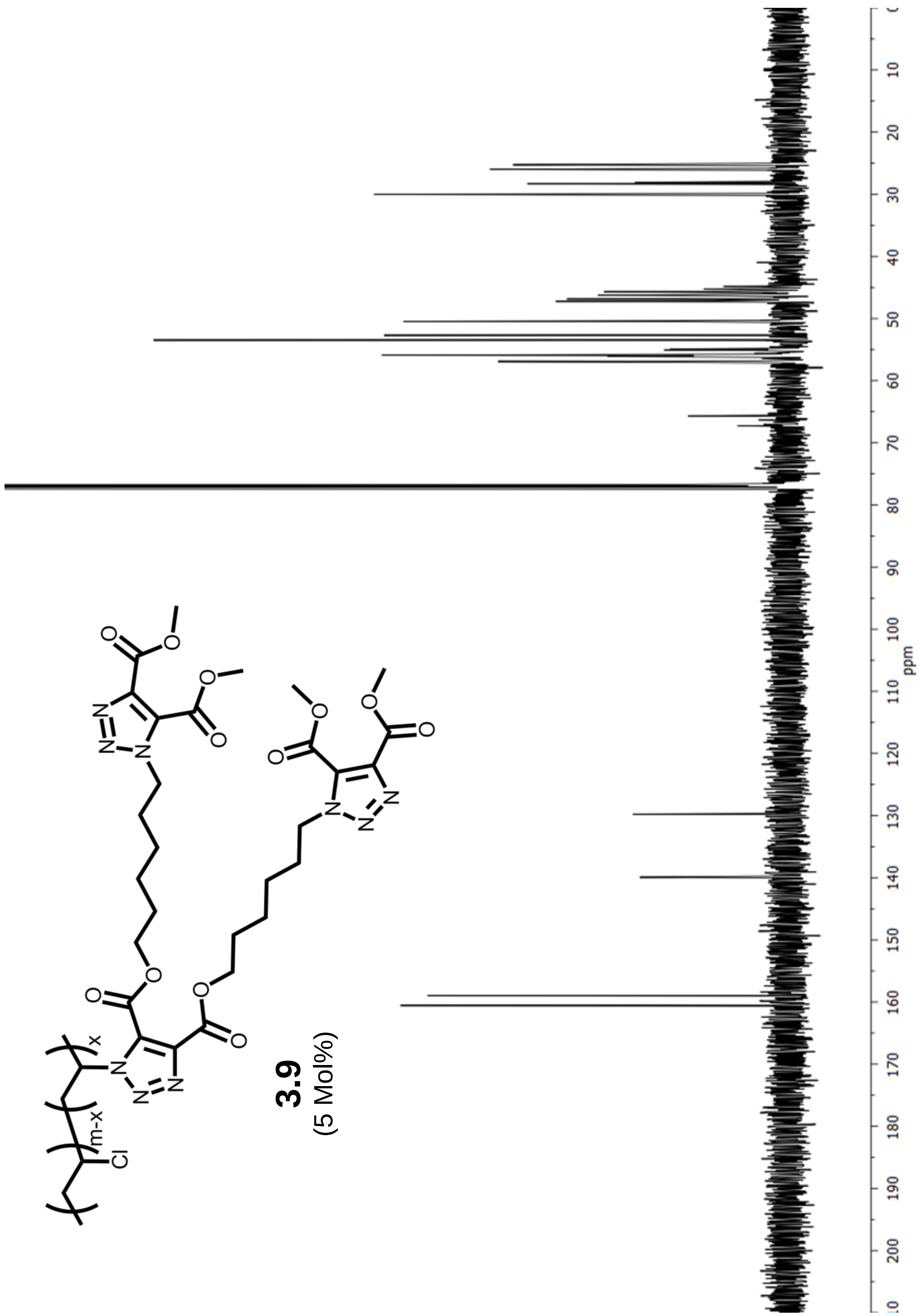
3.9
(5 Mol%)
Cl
m-x
x
ppm
0
10
20
30
40
50
60
70
80
90
100
110
120
130
140
150
160
170
180
190
200
210

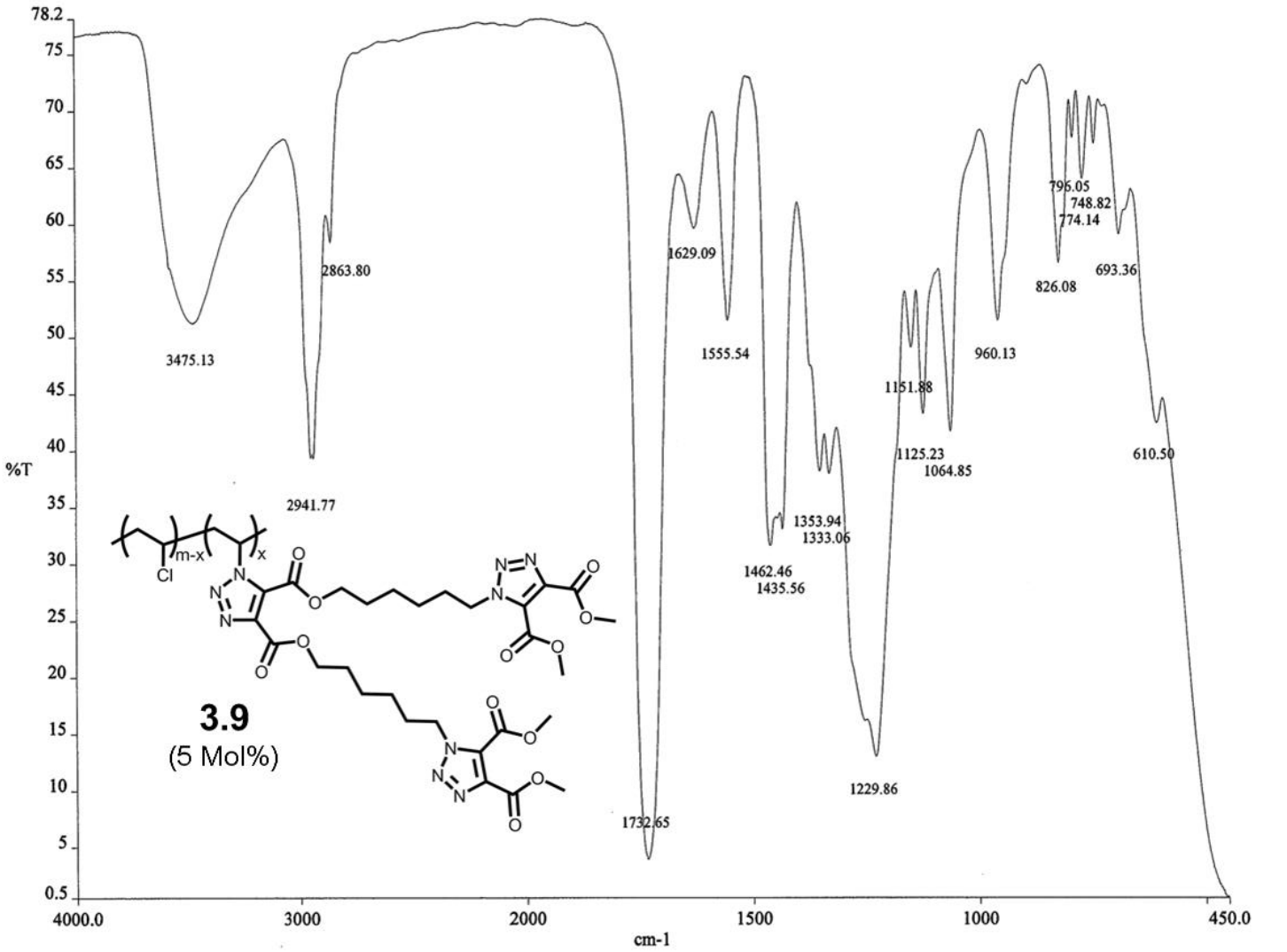
78.2
75
70
65
60
55
50
45
40
35
30
25
20
15
10
5
0.5
%T
4000.0
3000
2000
1500
1000
450.0
cm-1
3475.13
2863.80
2941.77
1629.09
1555.54
1462.46
1435.56
1353.94
1333.06
1732.65
1229.86
1151.88
1125.23
1064.85
960.13
826.08
796.05
774.14
748.82
693.36
610.50
m-x
x
Cl
3.9
(5 Mol%)

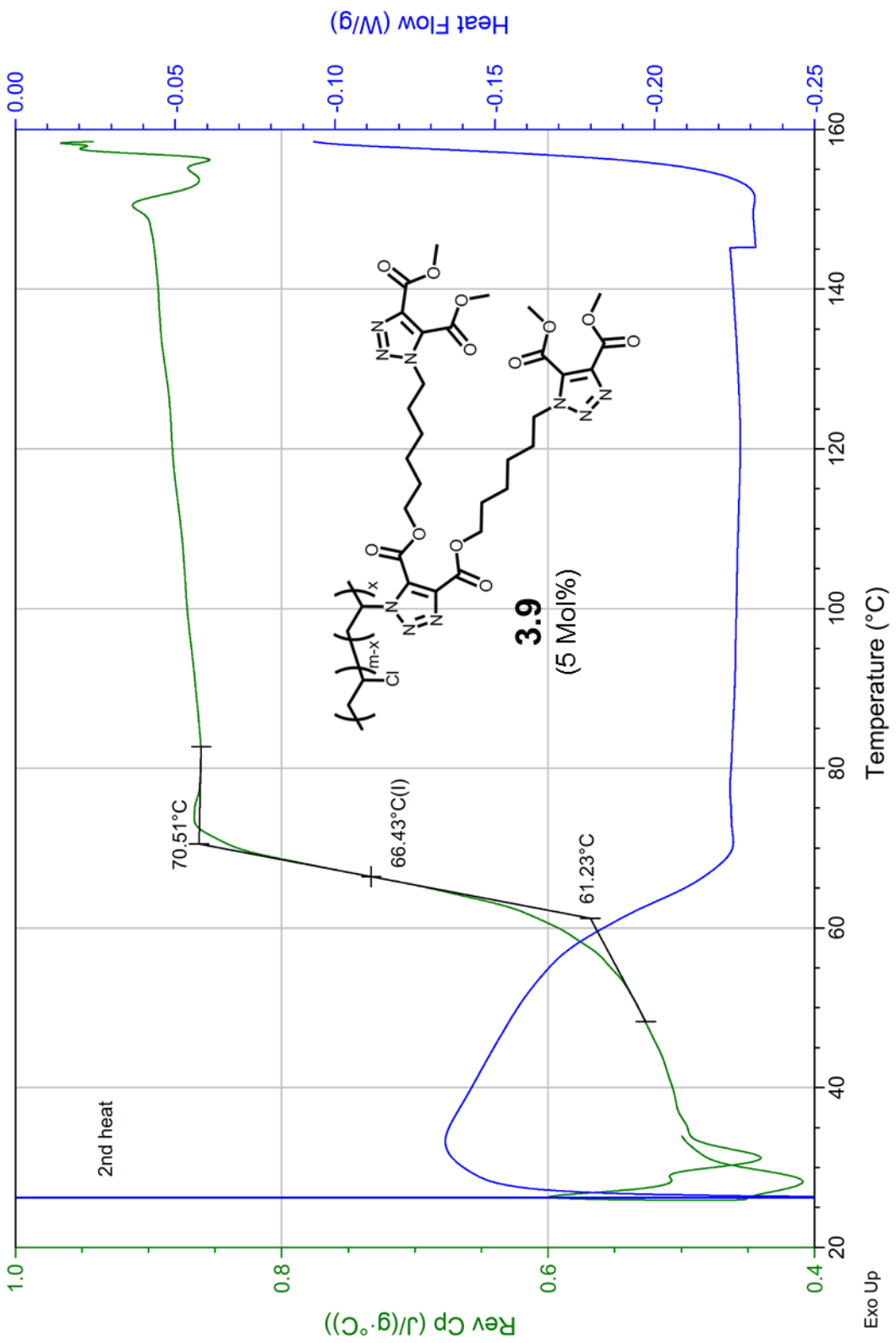
Heat Flow (W/g)
0.00
-0.05
-0.10
-0.15
-0.20
-0.25
Rev Cp (J/(g·°C))
1.0
0.8
0.6
0.4
Exo Up
Temperature (°C)
20
40
60
80
100
120
140
160
2nd heat
70.51°C
66.43°C(I)
61.23°C
3.9
(5 Mol%)

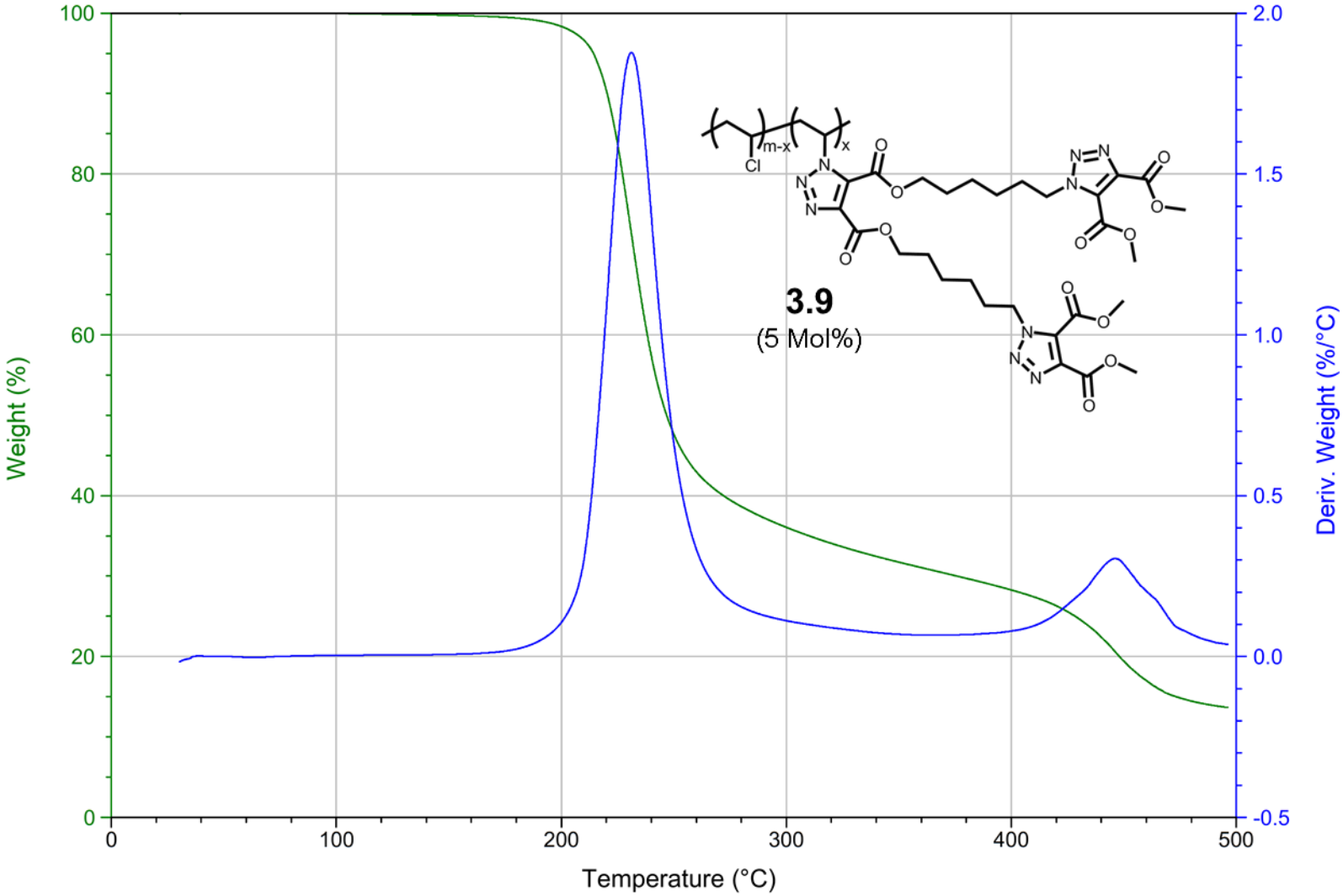
Weight (%)
Deriv. Weight (%/°C)
Temperature (°C)
0
20
40
60
80
100
-0.5
0.0
0.5
1.0
1.5
2.0
0
100
200
300
400
500
m-x
x
Cl
3.9
(5 Mol%)

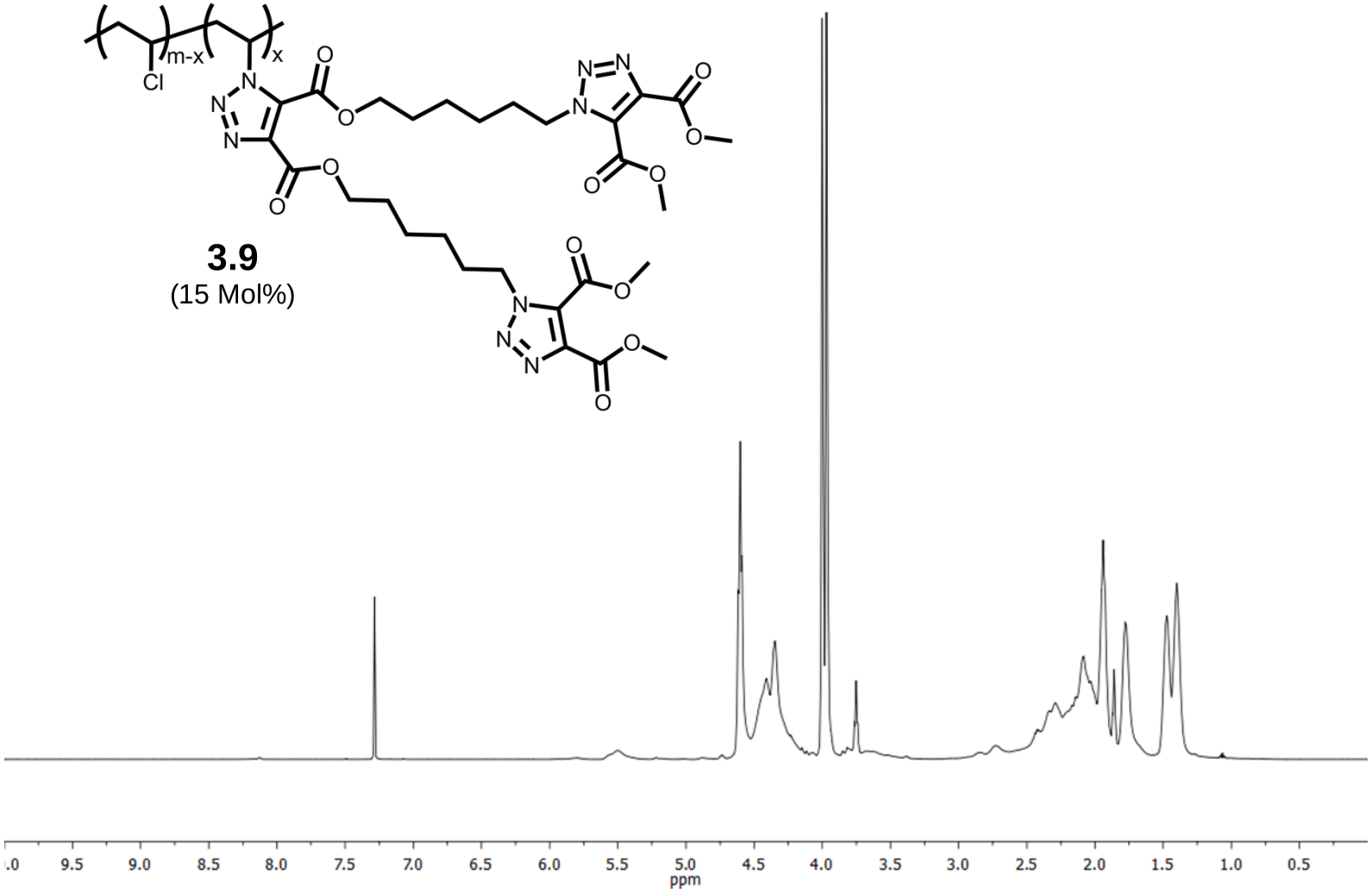
m-x
x
Cl
3.9
(15 Mol%)
9.5
9.0
8.5
8.0
7.5
7.0
6.5
6.0
5.5
5.0
4.5
4.0
3.5
3.0
2.5
2.0
1.5
1.0
0.5
ppm

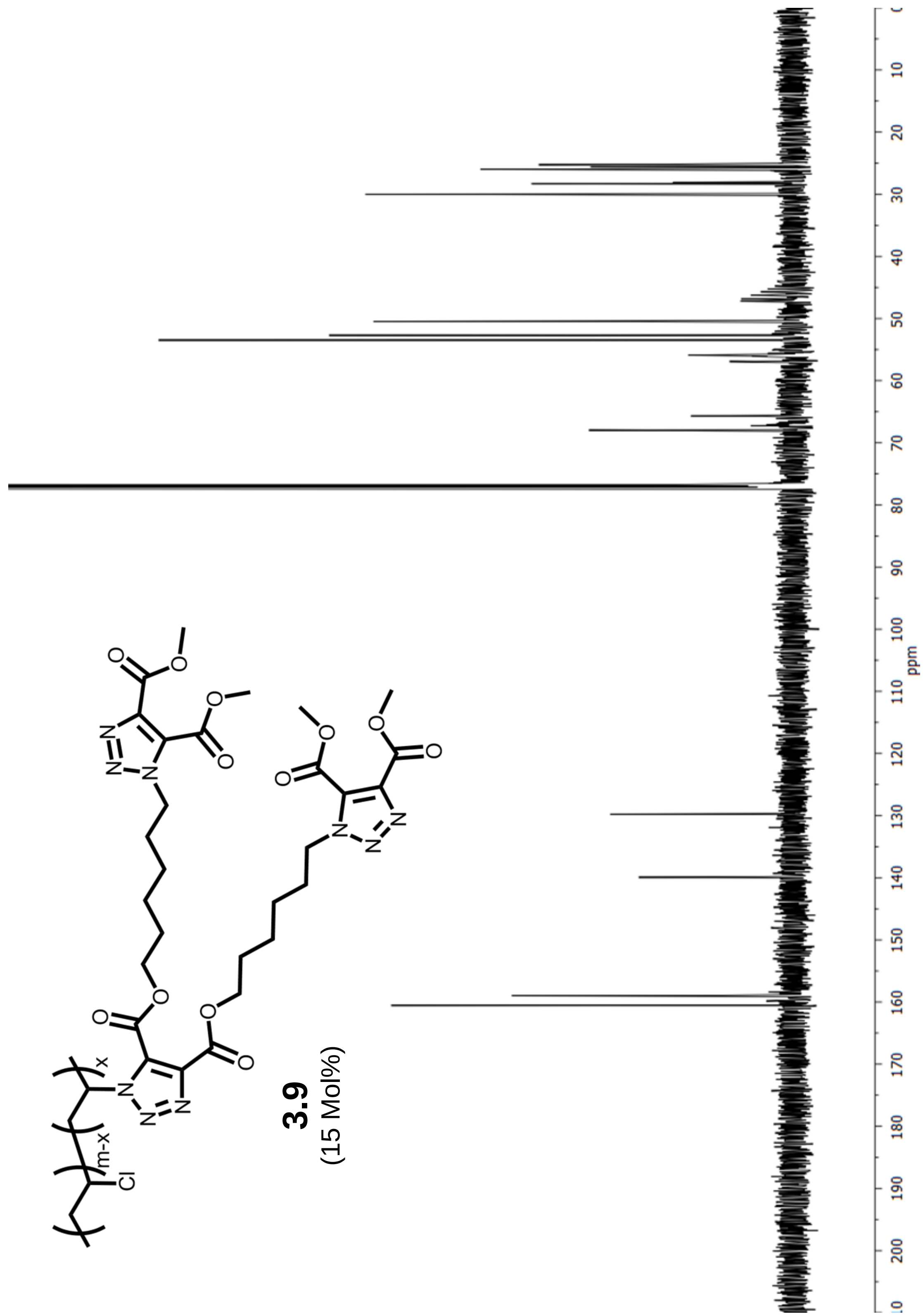
3.9
(15 Mol%)
ppm

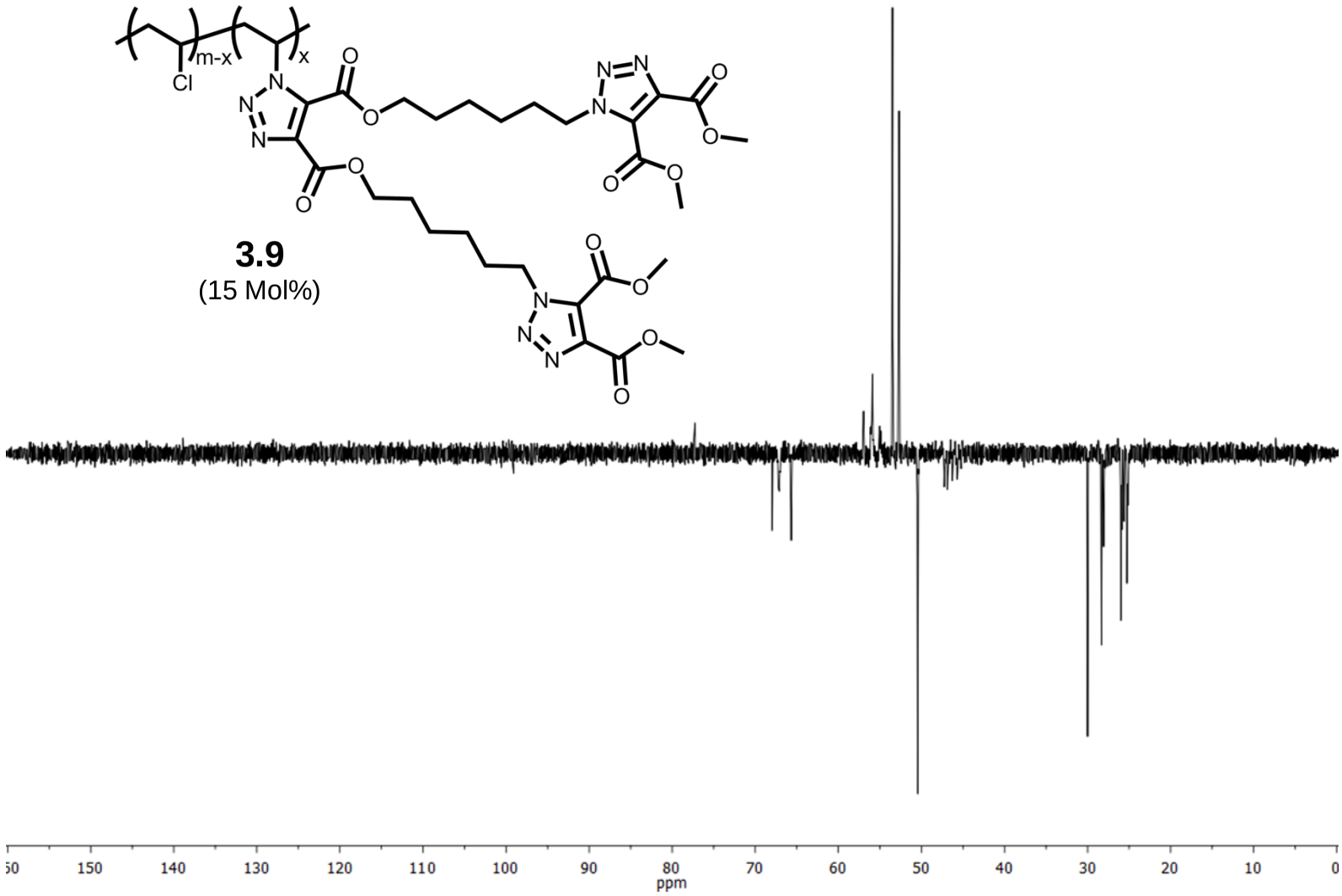
m-x
x
Cl
N
N
N
O
O
O
O
N
N
N
O
O
O
O
N
N
N
O
O
O
O
3.9
(15 Mol%)
150
140
130
120
110
100
90
80
70
60
50
40
30
20
10
0
ppm

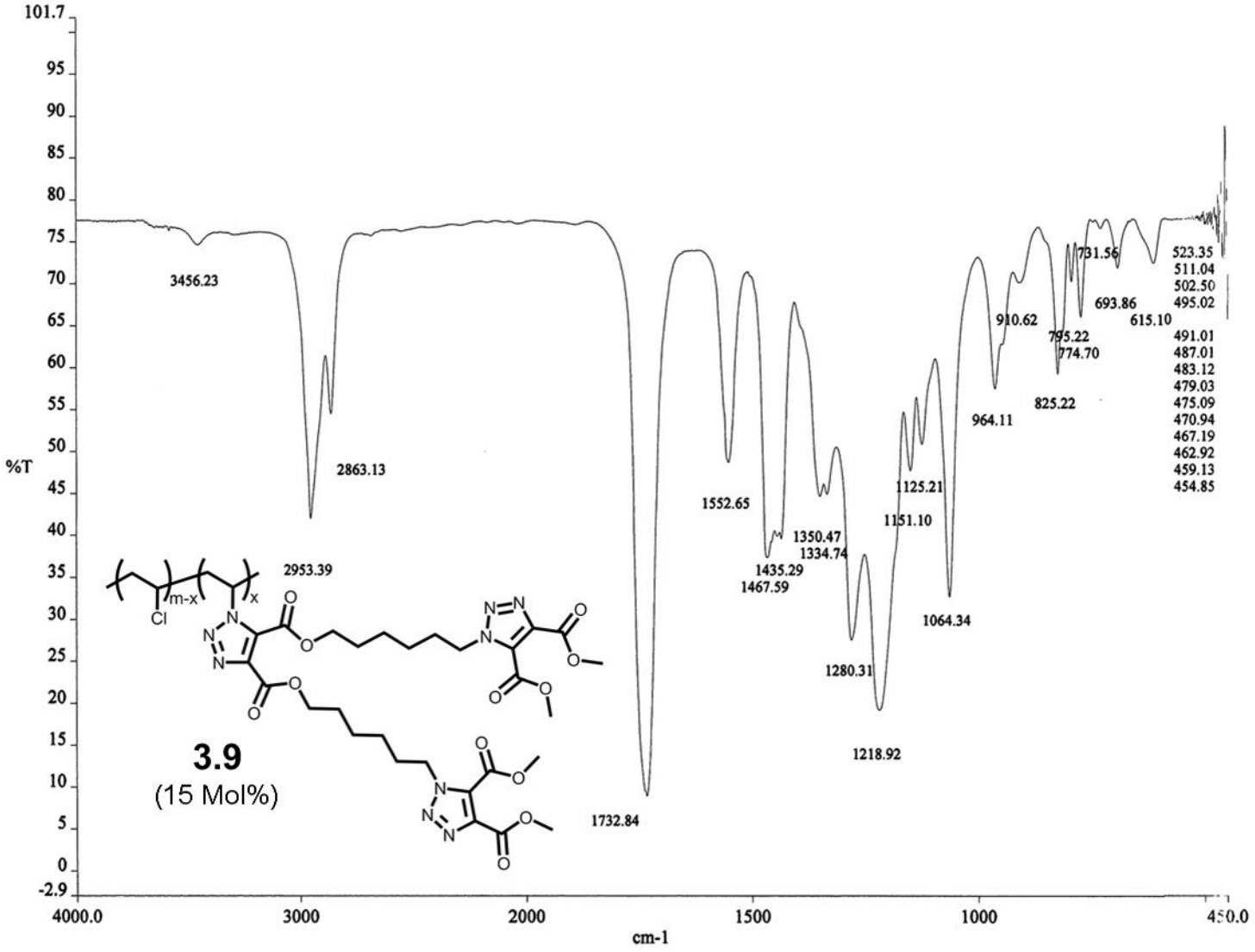
101.7
95
90
85
80
75
70
65
60
55
50
45
40
35
30
25
20
15
10
5
0
-2.9
%T
4000.0
3000
2000
1500
1000
450.0
cm-1
3456.23
2863.13
2953.39
1732.84
1552.65
1467.59
1435.29
1350.47
1334.74
1280.31
1218.92
1151.10
1125.21
1064.34
964.11
910.62
825.22
795.22
774.70
731.56
693.86
615.10
523.35
511.04
502.50
495.02
491.01
487.01
483.12
479.03
475.09
470.94
467.19
462.92
459.13
454.85
m-x
x
Cl
3.9
(15 Mol%)

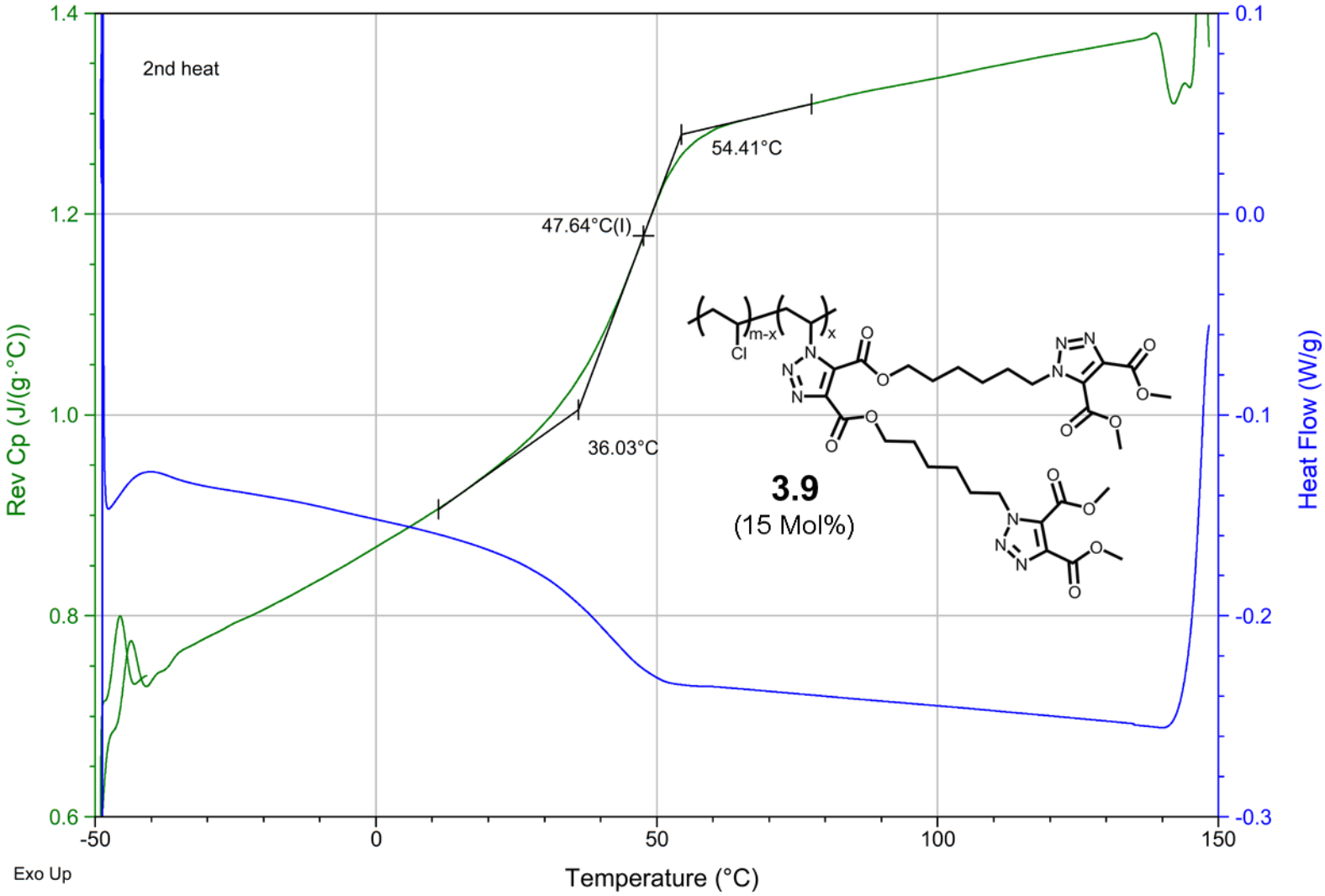
2nd heat
54.41°C
47.64°C(I)
36.03°C
3.9
(15 Mol%)
Rev Cp (J/(g·°C))
Heat Flow (W/g)
Temperature (°C)
Exo Up
1.4
1.2
1.0
0.8
0.6
0.1
0.0
-0.1
-0.2
-0.3
-50
0
50
100
150

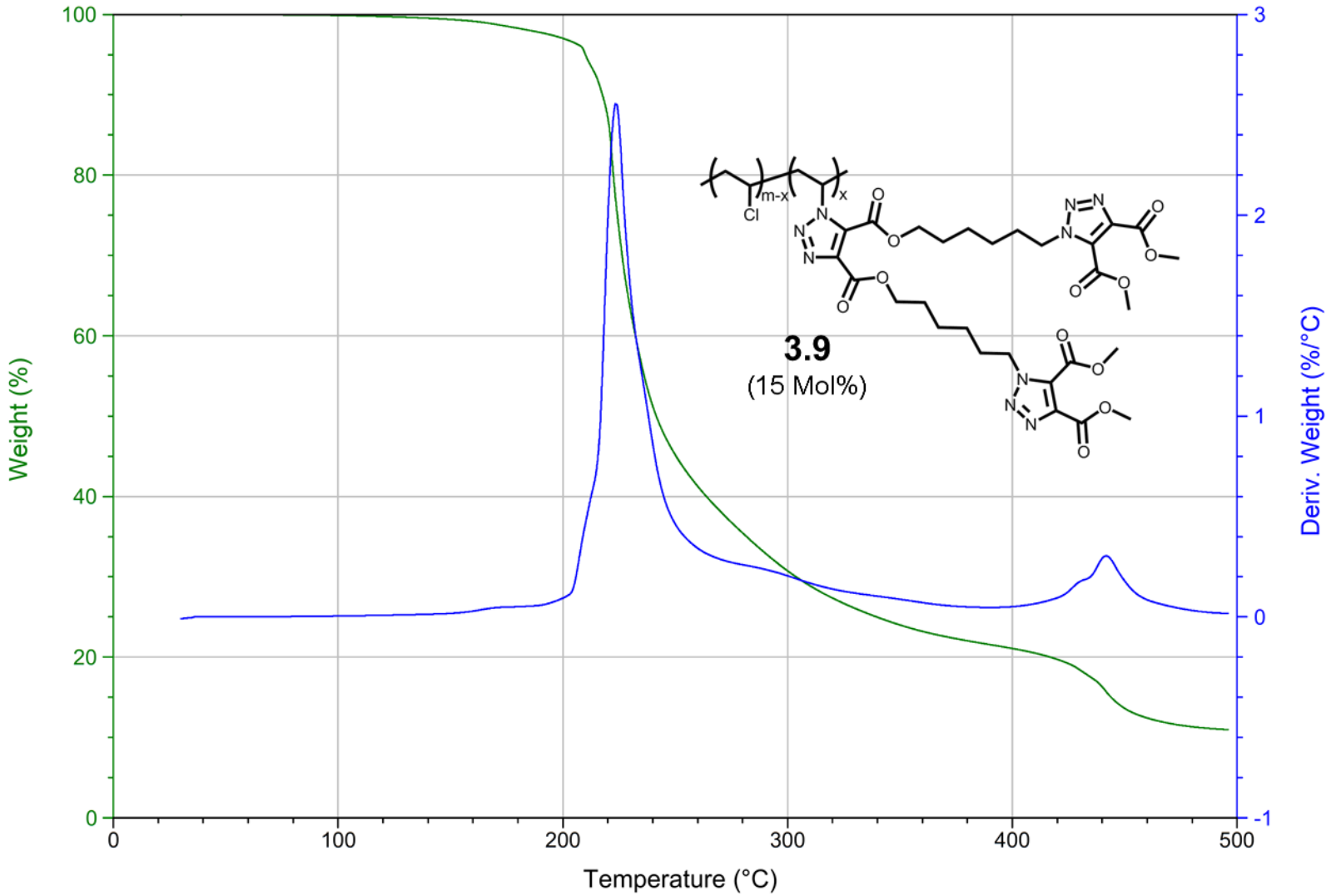
Weight (%)
Deriv. Weight (%/°C)
Temperature (°C)
0
20
40
60
80
100
-1
0
1
2
3
0
100
200
300
400
500
m-x
x
Cl
3.9
(15 Mol%)

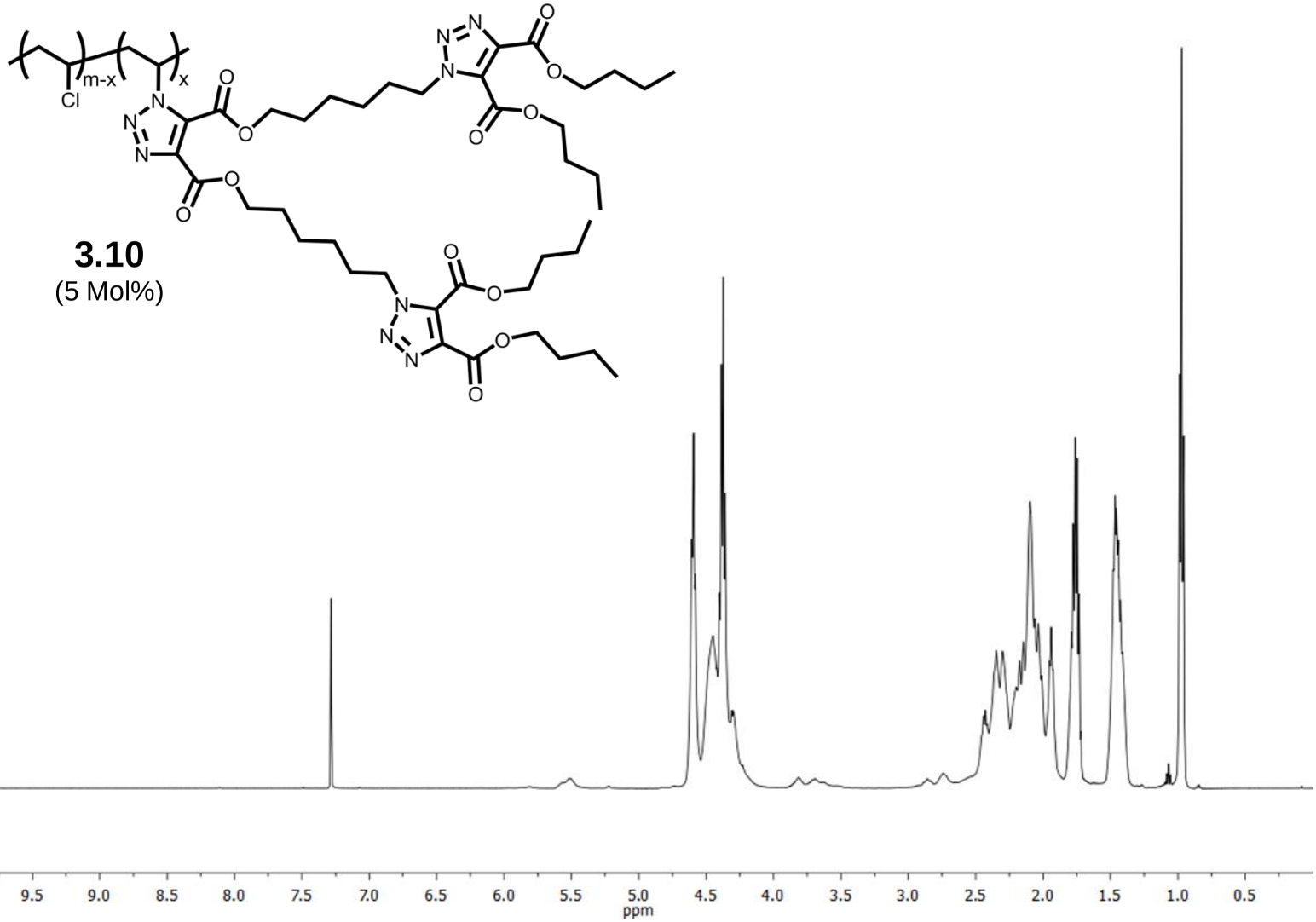
m-x
x
Cl
3.10
(5 Mol%)
9.5
9.0
8.5
8.0
7.5
7.0
6.5
6.0
5.5
5.0
4.5
4.0
3.5
3.0
2.5
2.0
1.5
1.0
0.5
ppm

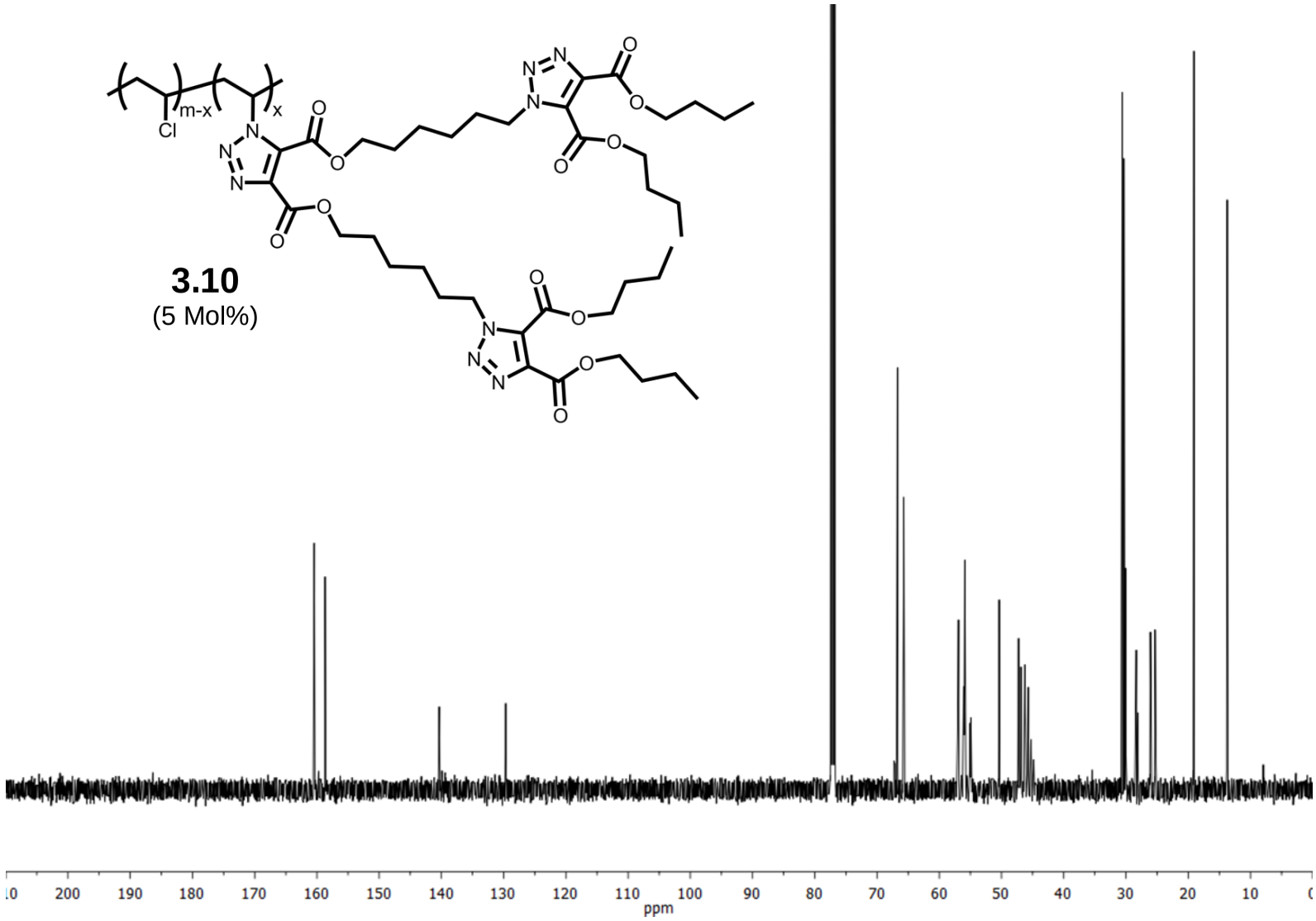
m-x
x
Cl
3.10
(5 Mol%)
ppm

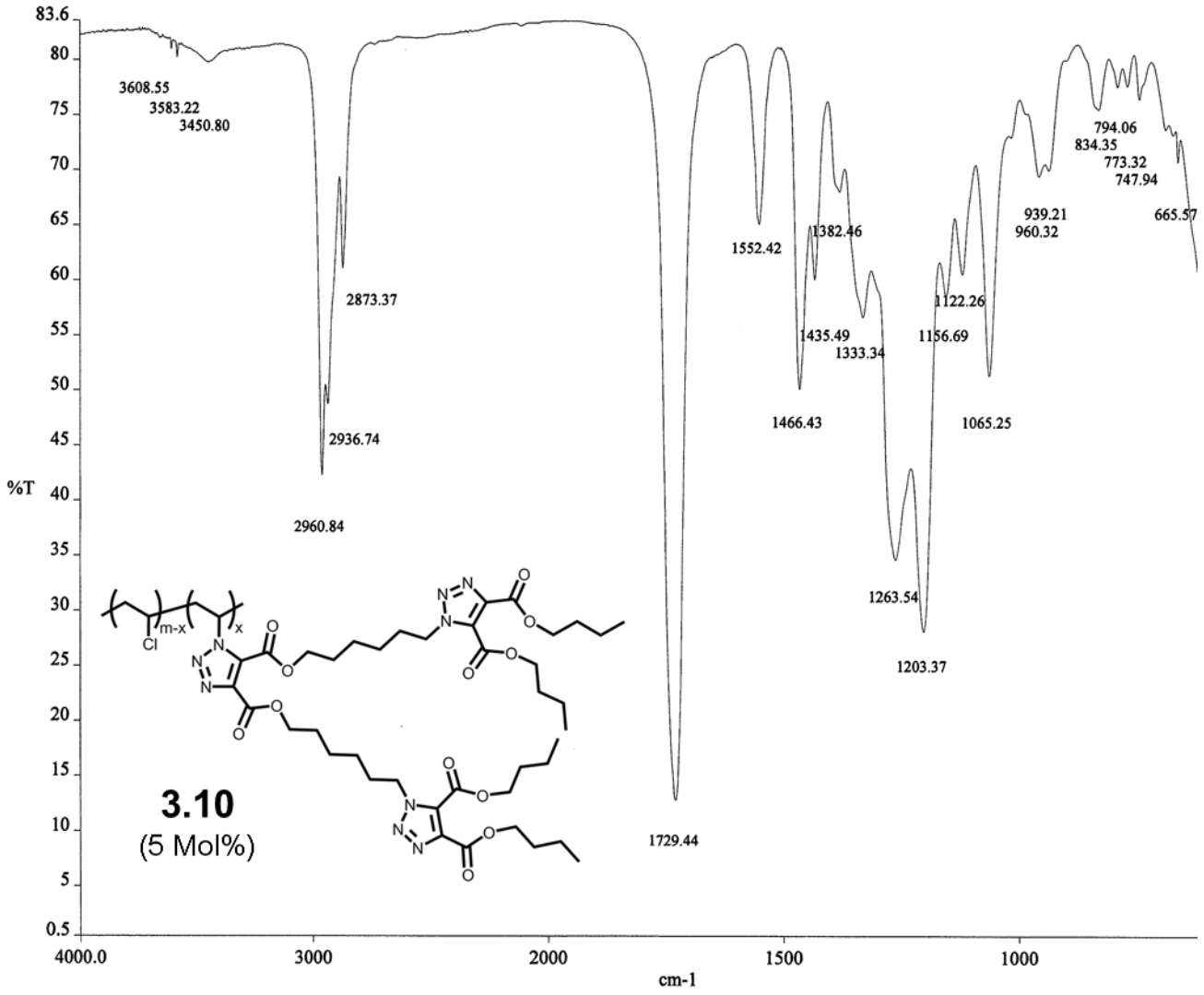
83.6
80
75
70
65
60
55
50
45
40
35
30
25
20
15
10
5
0.5
%T
4000.0
3000
2000
1500
1000
cm-1
3608.55
3583.22
3450.80
2873.37
2936.74
2960.84
1729.44
1552.42
1382.46
1435.49
1333.34
1466.43
1263.54
1203.37
1122.26
1156.69
1065.25
939.21
960.32
794.06
834.35
773.32
747.94
665.57
m-x
x
Cl
3.10
(5 Mol%)

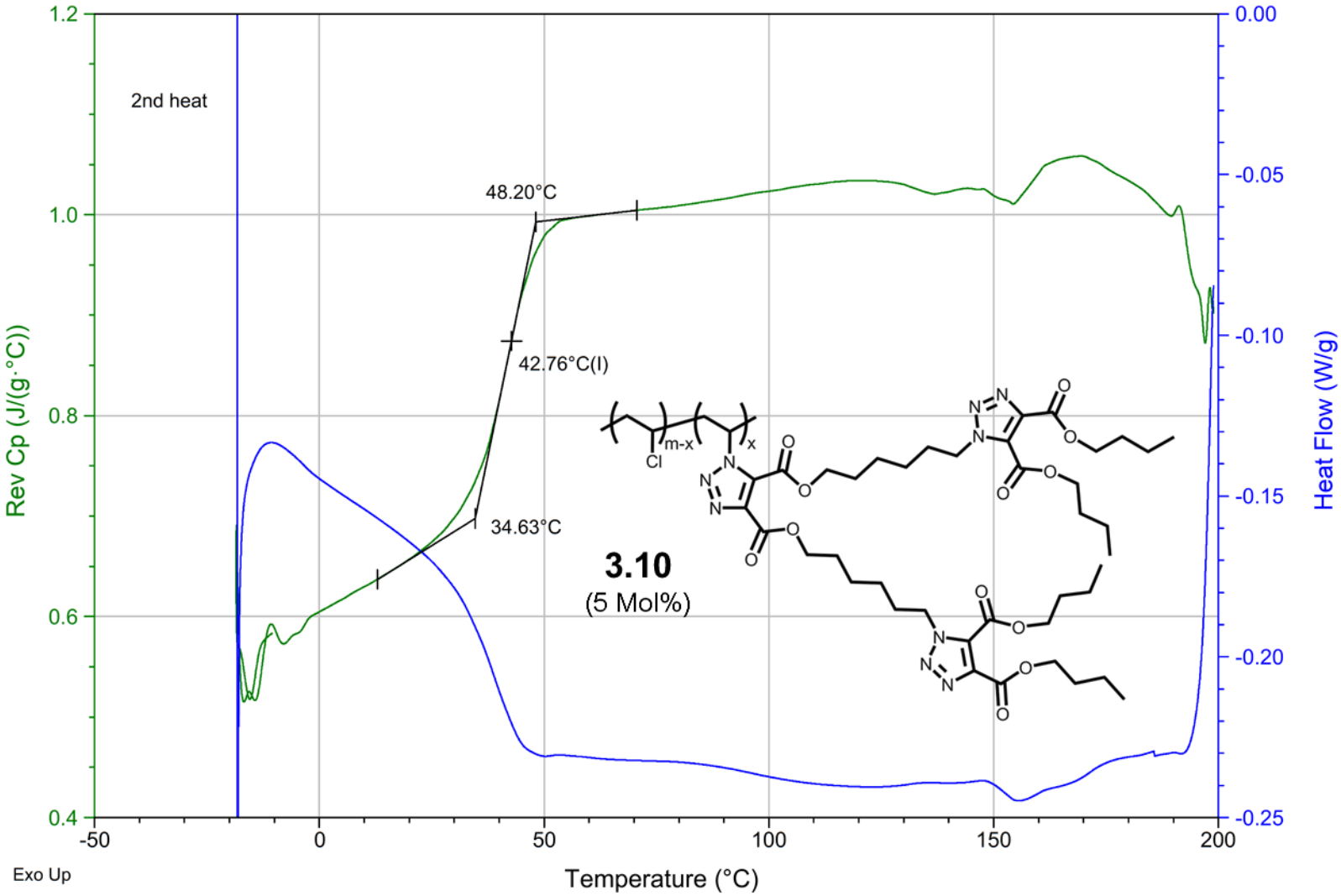
2nd heat
48.20°C
42.76°C(I)
34.63°C
3.10
(5 Mol%)
Rev Cp (J/(g·°C))
Heat Flow (W/g)
Temperature (°C)
Exo Up
1.2
1.0
0.8
0.6
0.4
0.00
-0.05
-0.10
-0.15
-0.20
-0.25
-50
0
50
100
150
200

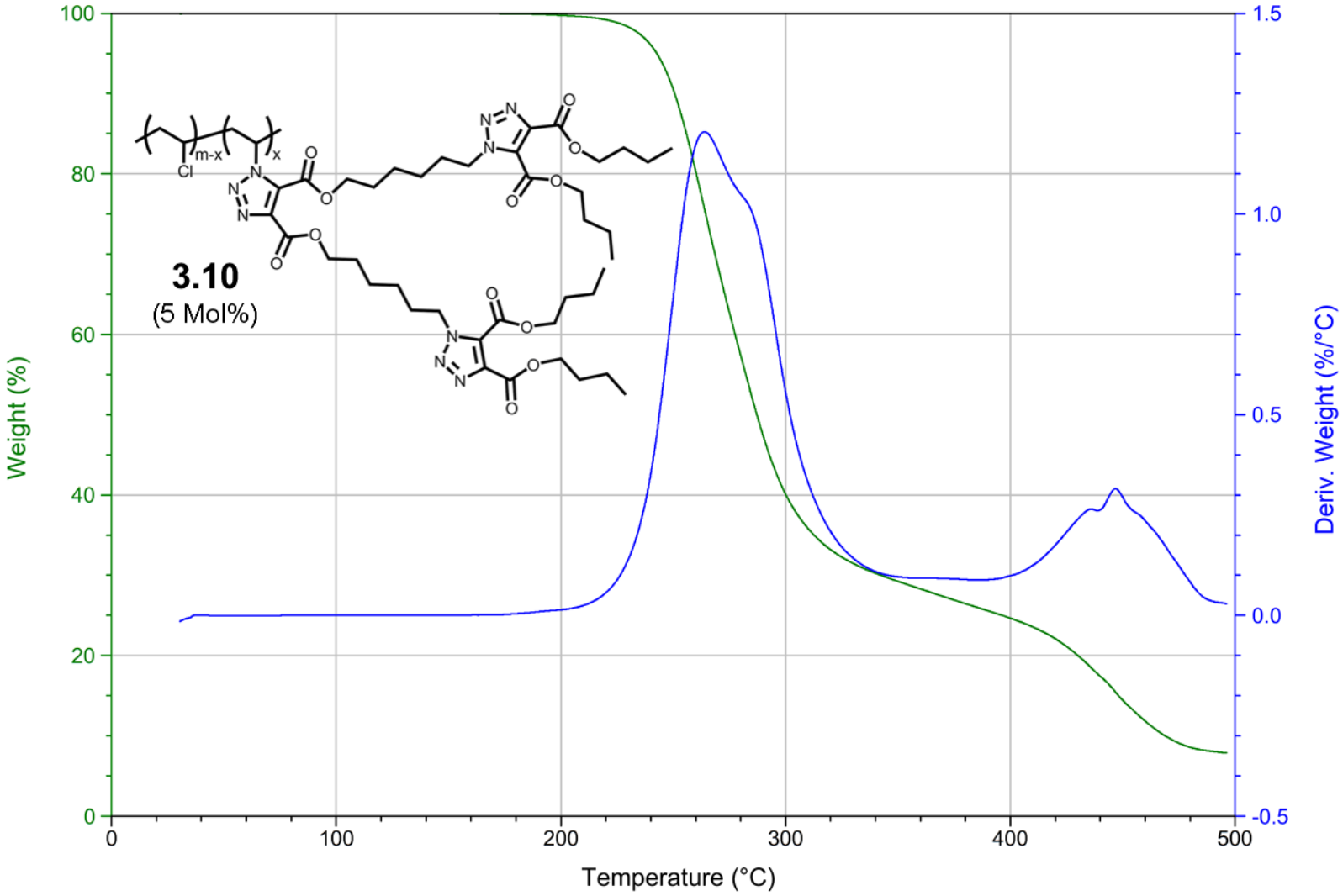
3.10
(5 Mol%)
Weight (%)
Deriv. Weight (%/°C)
Temperature (°C)
100
80
60
40
20
0
1.5
1.0
0.5
0.0
-0.5
0
100
200
300
400
500

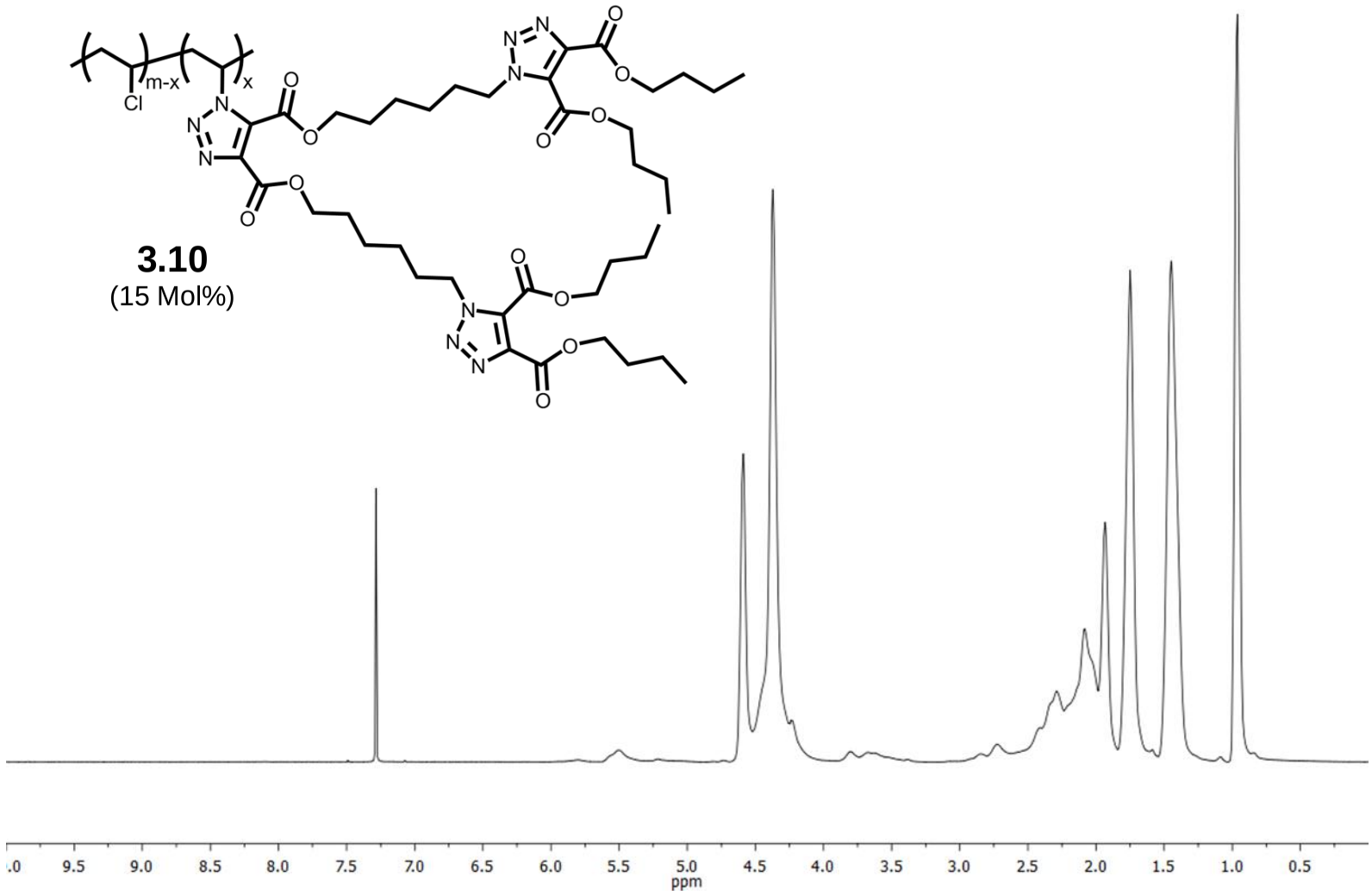
Cl
m-x
x
3.10
(15 Mol%)
9.5
9.0
8.5
8.0
7.5
7.0
6.5
6.0
5.5
5.0
4.5
4.0
3.5
3.0
2.5
2.0
1.5
1.0
0.5
ppm

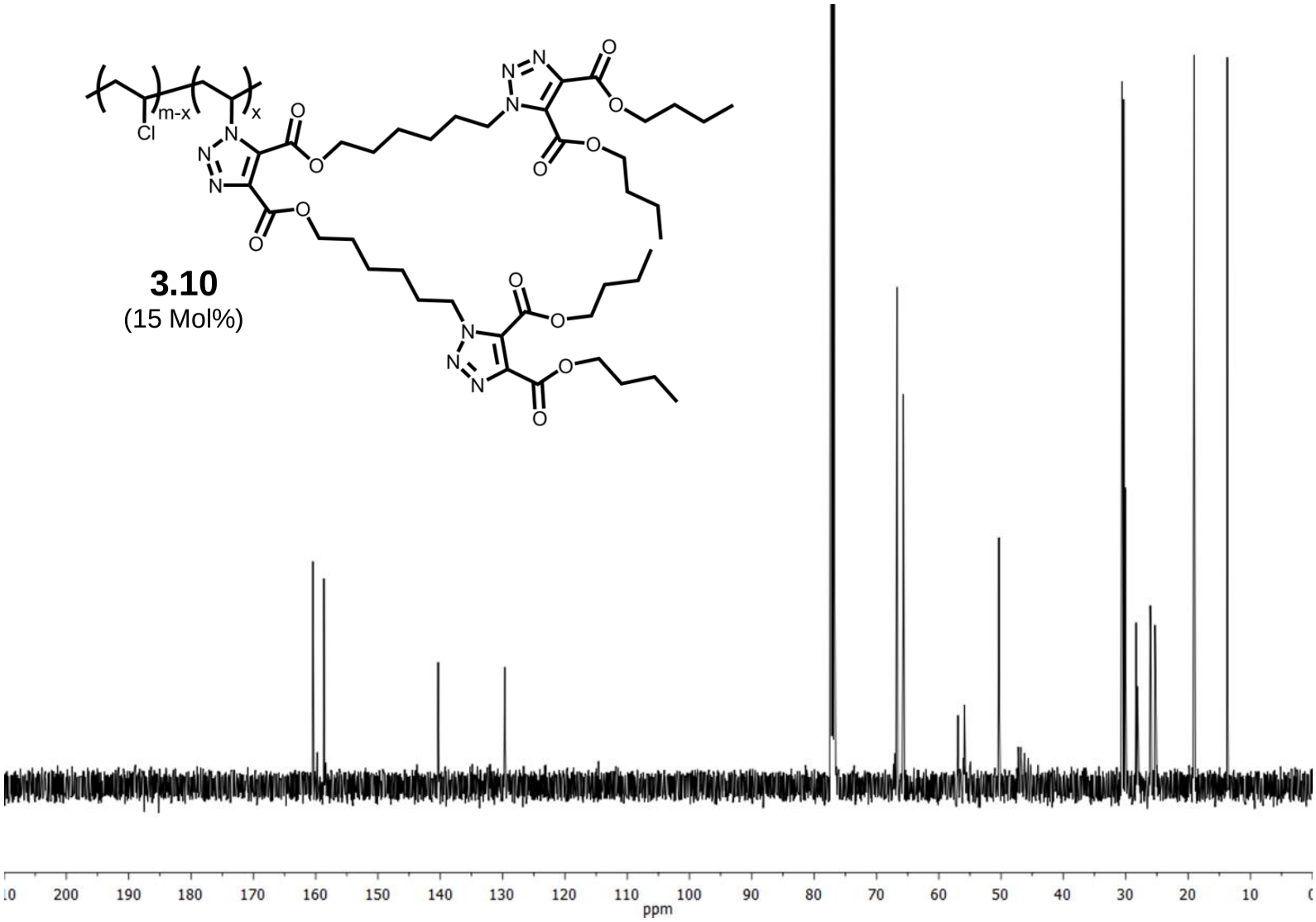
3.10
(15 Mol%)
Cl
m-x
x
ppm

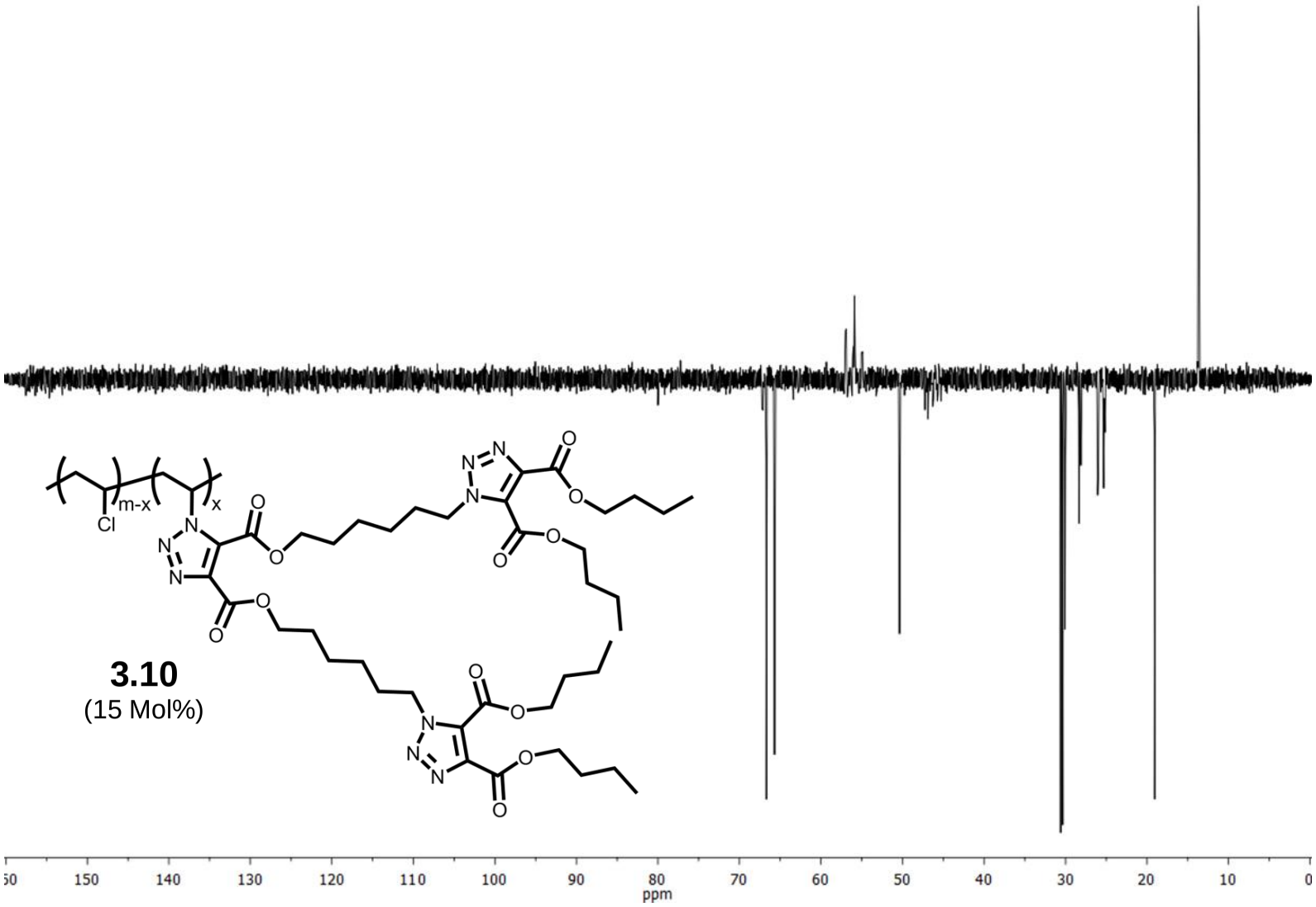
m-x
x
Cl
3.10
(15 Mol%)
150
140
130
120
110
100
90
80
70
60
50
40
30
20
10
ppm

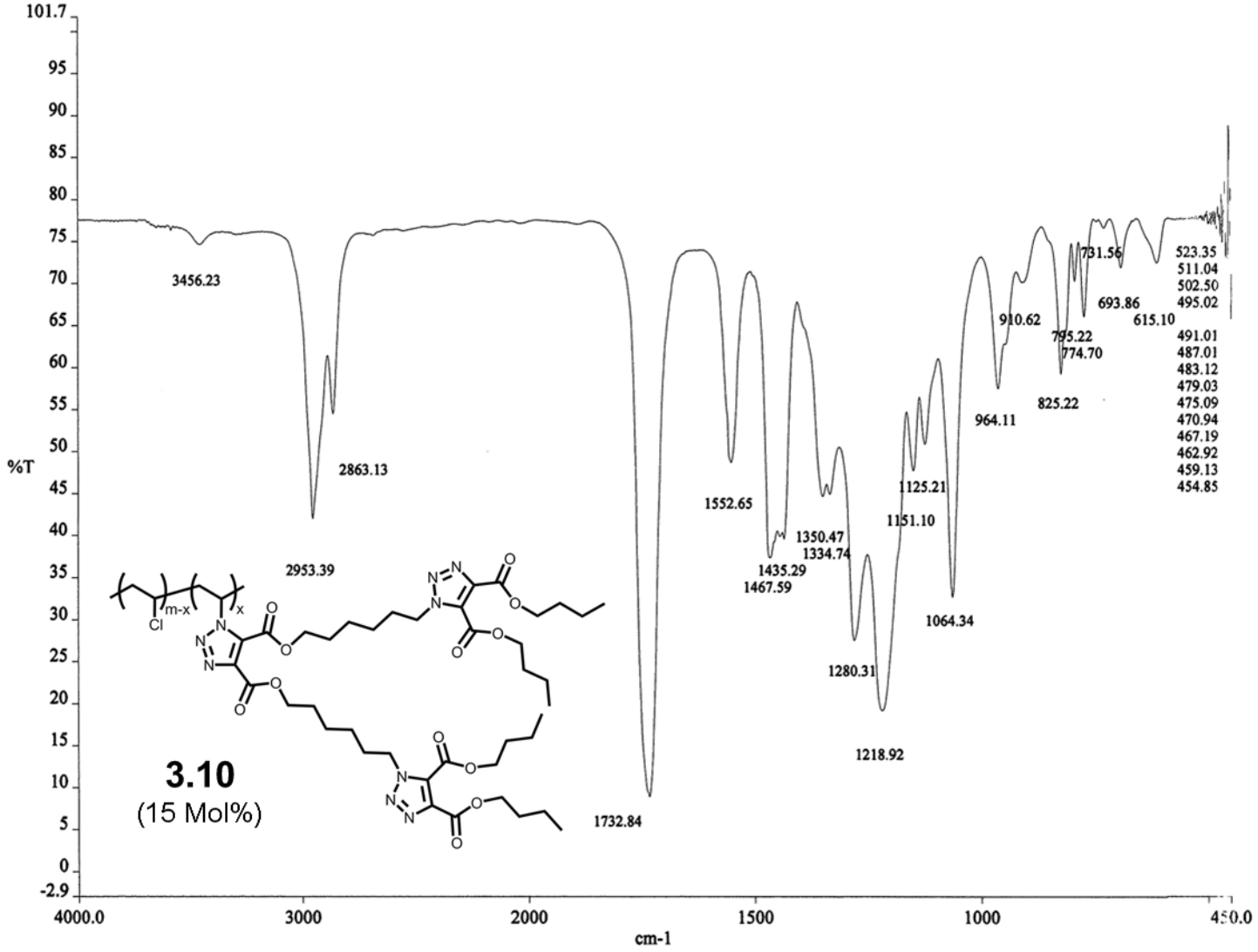
101.7
95
90
85
80
75
70
65
60
55
50
45
40
35
30
25
20
15
10
5
0
-2.9
%T
4000.0
3000
2000
1500
1000
450.0
cm-1
3456.23
2863.13
2953.39
1552.65
1435.29
1467.59
1350.47
1334.74
1280.31
1218.92
1732.84
1125.21
1151.10
1064.34
964.11
910.62
825.22
795.22
774.70
731.56
693.86
615.10
523.35
511.04
502.50
495.02
491.01
487.01
483.12
479.03
475.09
470.94
467.19
462.92
459.13
454.85
m-x
x
Cl
3.10
(15 Mol%)

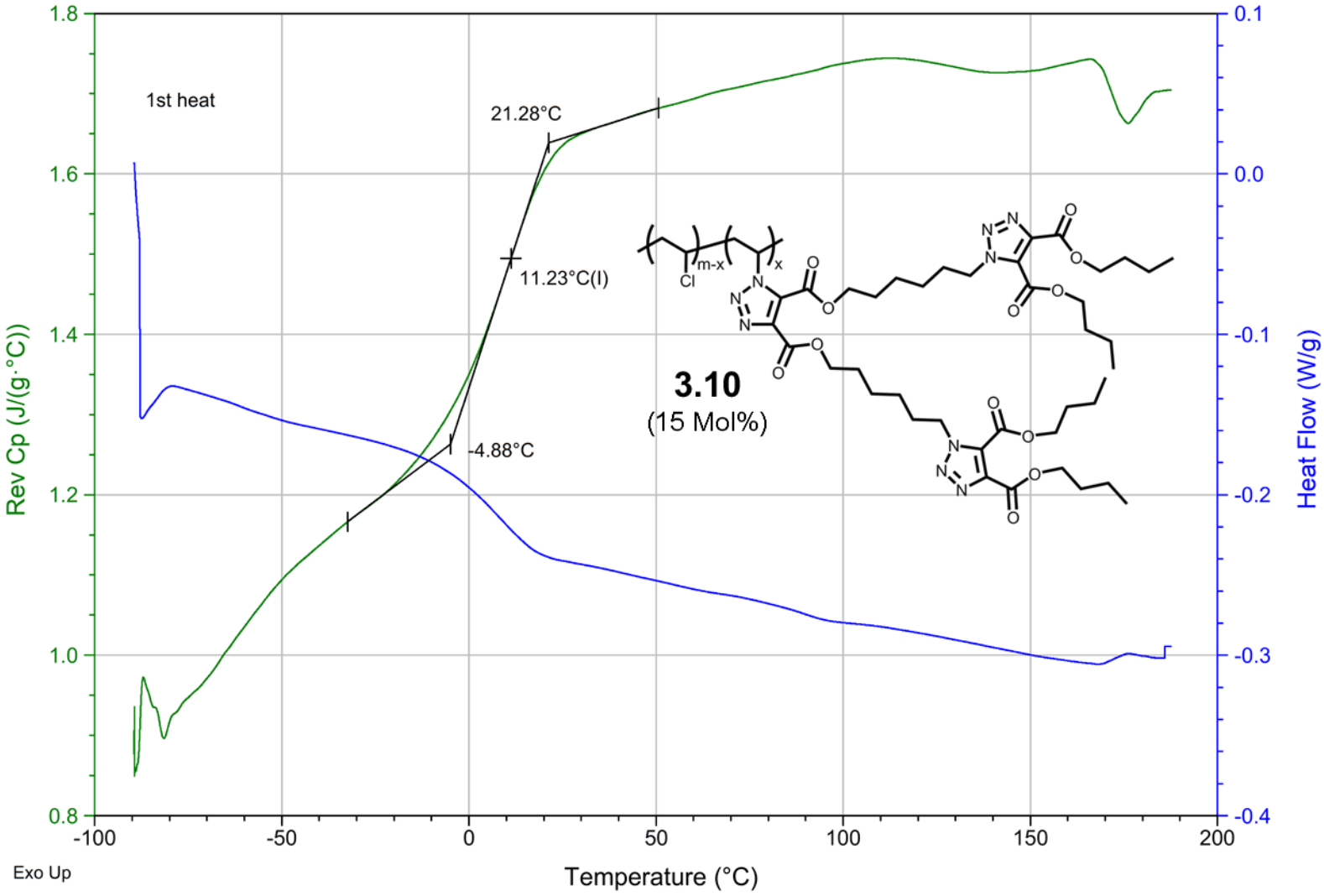
1st heat
21.28°C
11.23°C(I)
-4.88°C
3.10
(15 Mol%)
Rev Cp (J/(g·°C))
Heat Flow (W/g)
Temperature (°C)
Exo Up
1.8
1.6
1.4
1.2
1.0
0.8
0.1
0.0
-0.1
-0.2
-0.3
-0.4
-100
-50
0
50
100
150
200

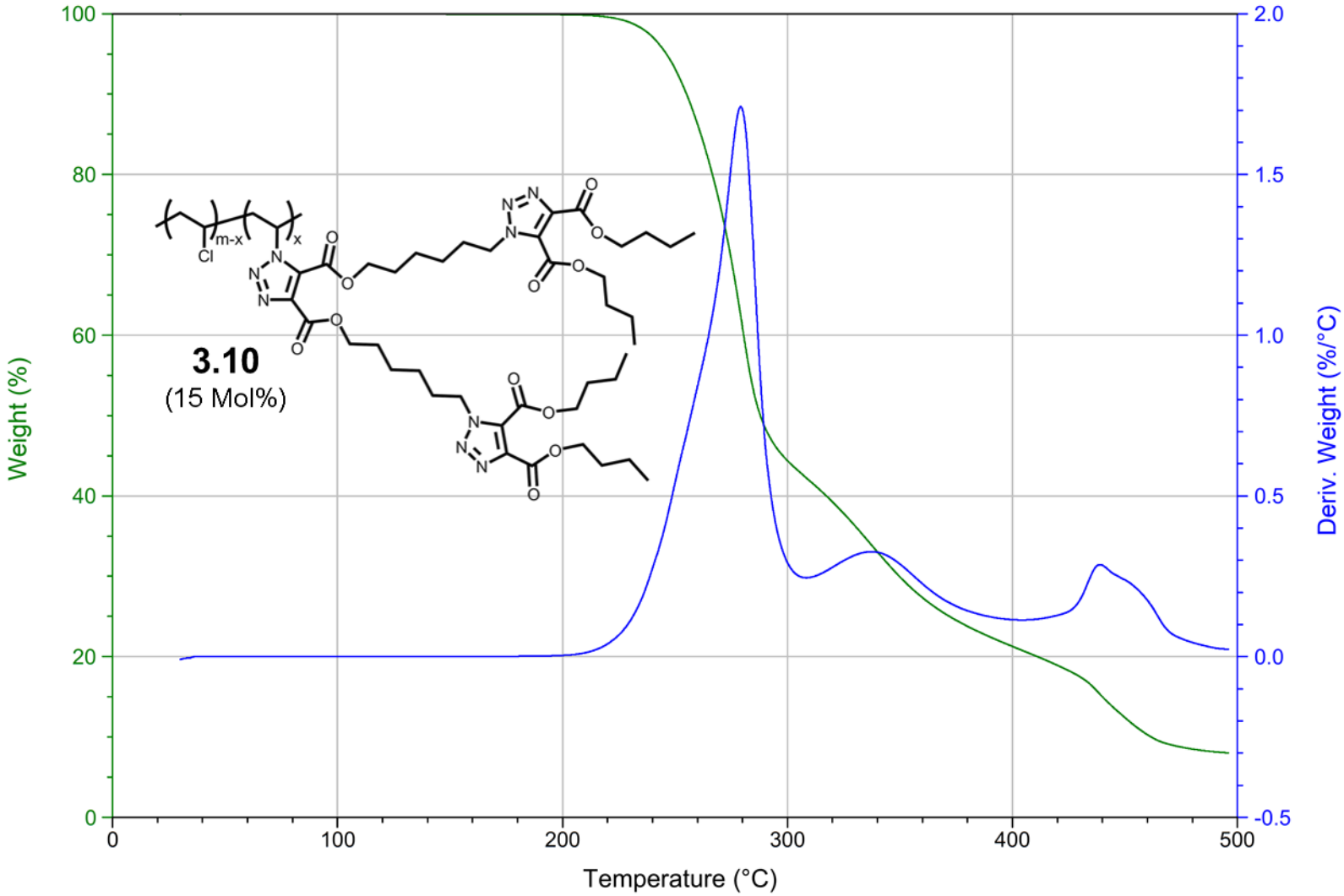
3.10
(15 Mol%)
Weight (%)
Deriv. Weight (%/°C)
Temperature (°C)
100
80
60
40
20
0
2.0
1.5
1.0
0.5
0.0
-0.5
0
100
200
300
400
500

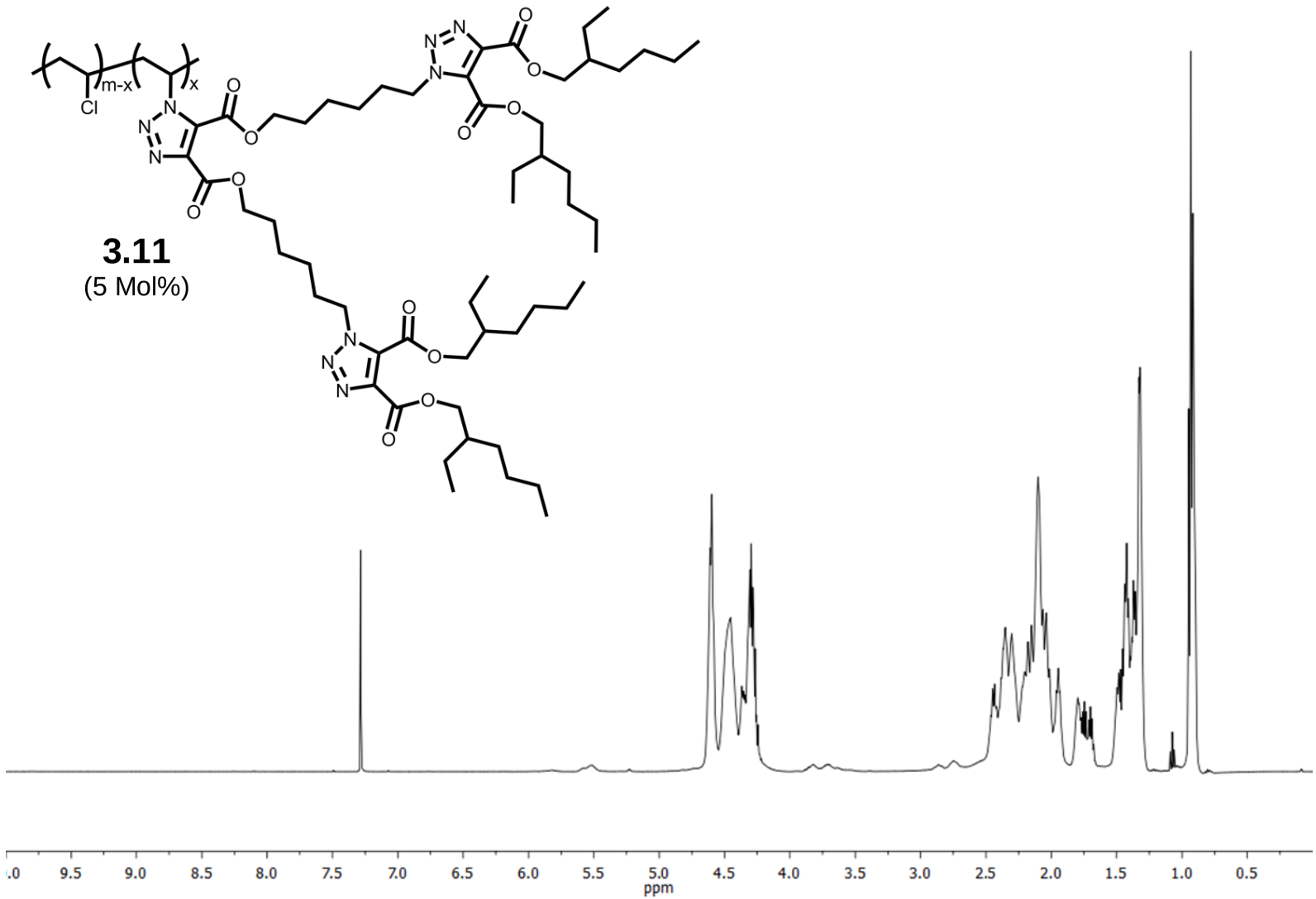
m-x
x
Cl
3.11
(5 Mol%)
9.5
9.0
8.5
8.0
7.5
7.0
6.5
6.0
5.5
5.0
4.5
4.0
3.5
3.0
2.5
2.0
1.5
1.0
0.5
ppm

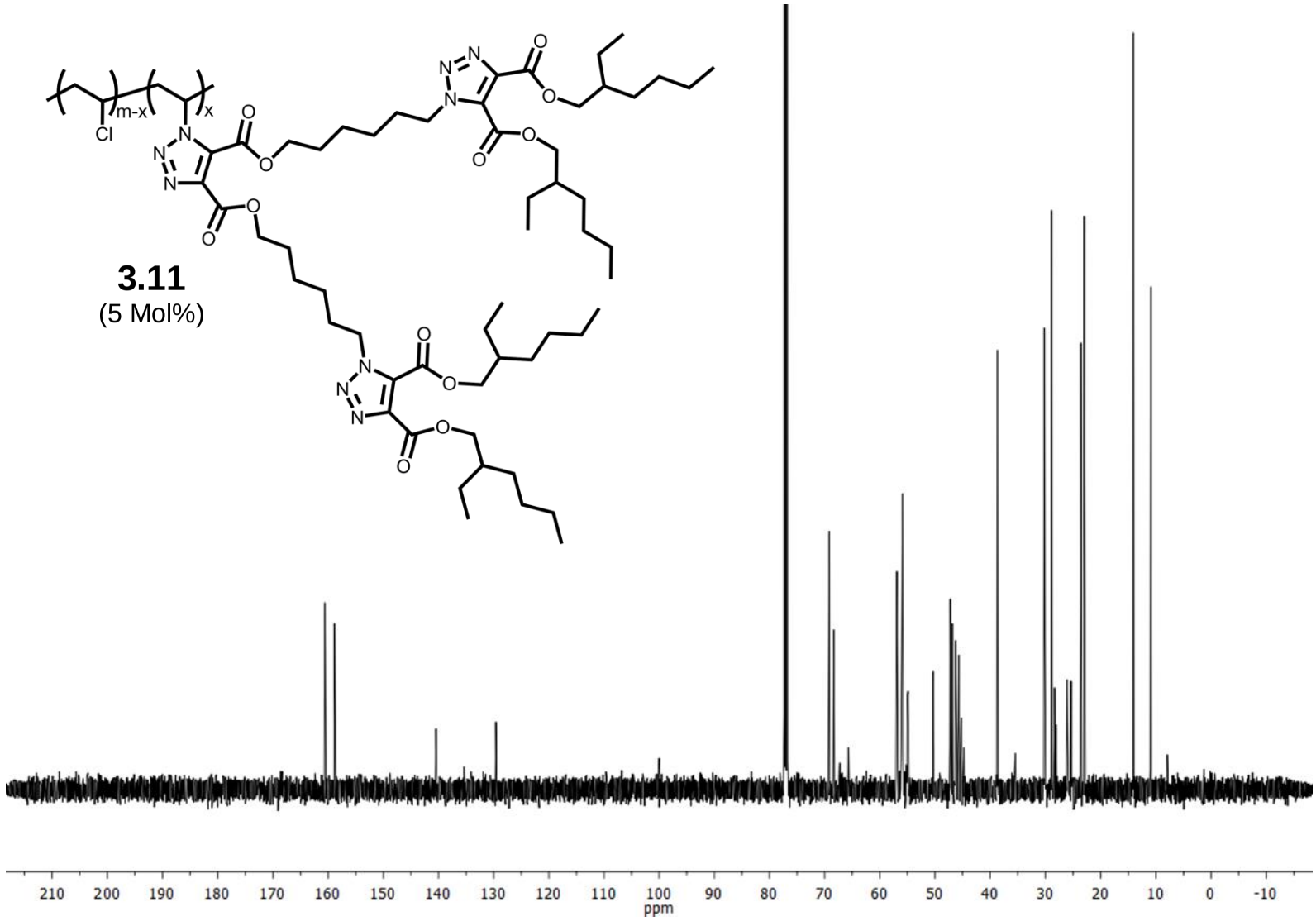
m-x
x
Cl
3.11
(5 Mol%)
210 200 190 180 170 160 150 140 130 120 110 100 90 80 70 60 50 40 30 20 10 0 -10
ppm

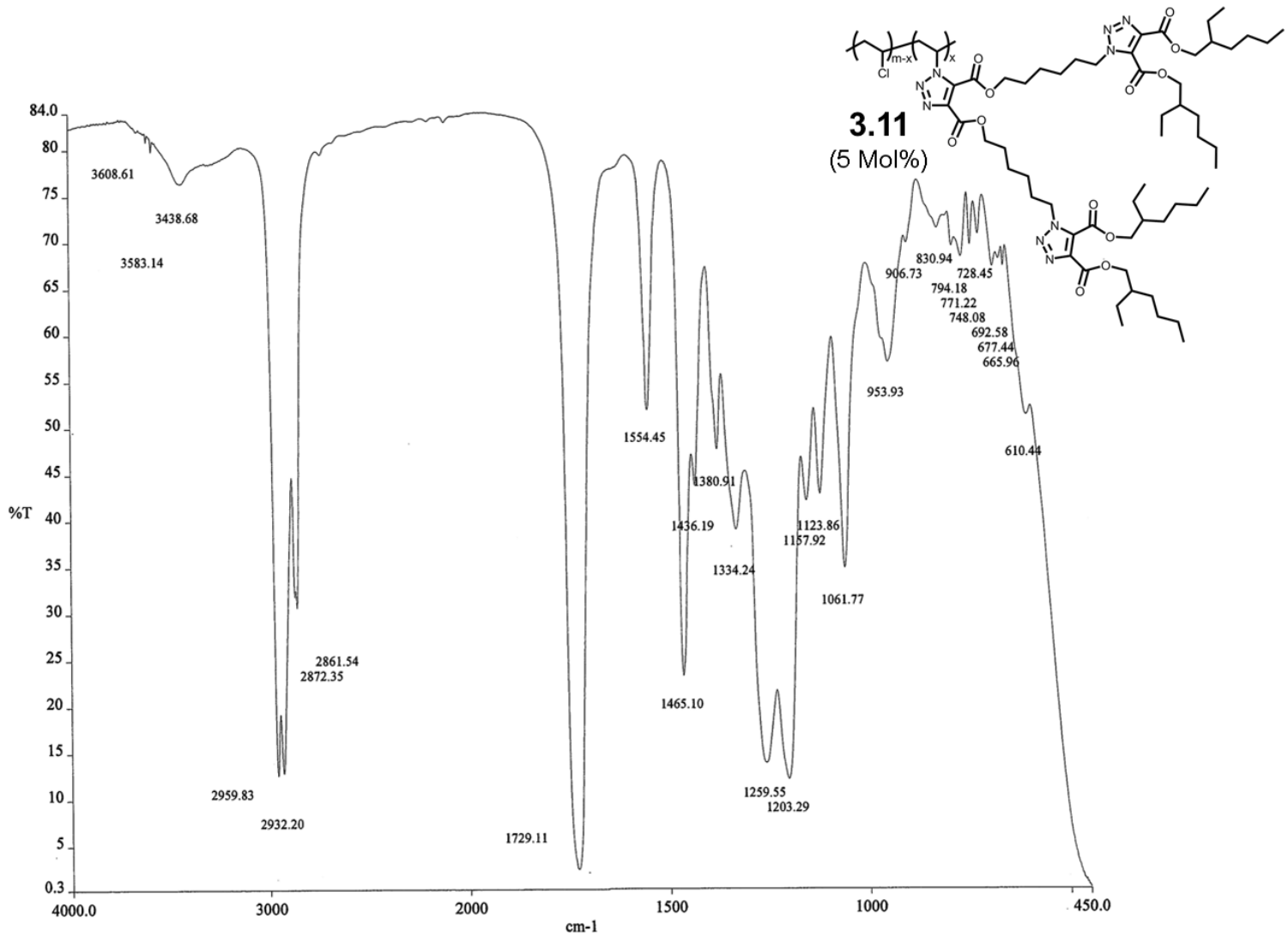
3.11
(5 Mol%)
%T
cm-1
84.0
80
75
70
65
60
55
50
45
40
35
30
25
20
15
10
5
0.3
4000.0
3000
2000
1500
1000
450.0
3608.61
3438.68
3583.14
2959.83
2932.20
2861.54
2872.35
1729.11
1554.45
1465.10
1436.19
1380.91
1334.24
1259.55
1203.29
1157.92
1123.86
1061.77
953.93
906.73
830.94
794.18
771.22
748.08
728.45
692.58
677.44
665.96
610.44

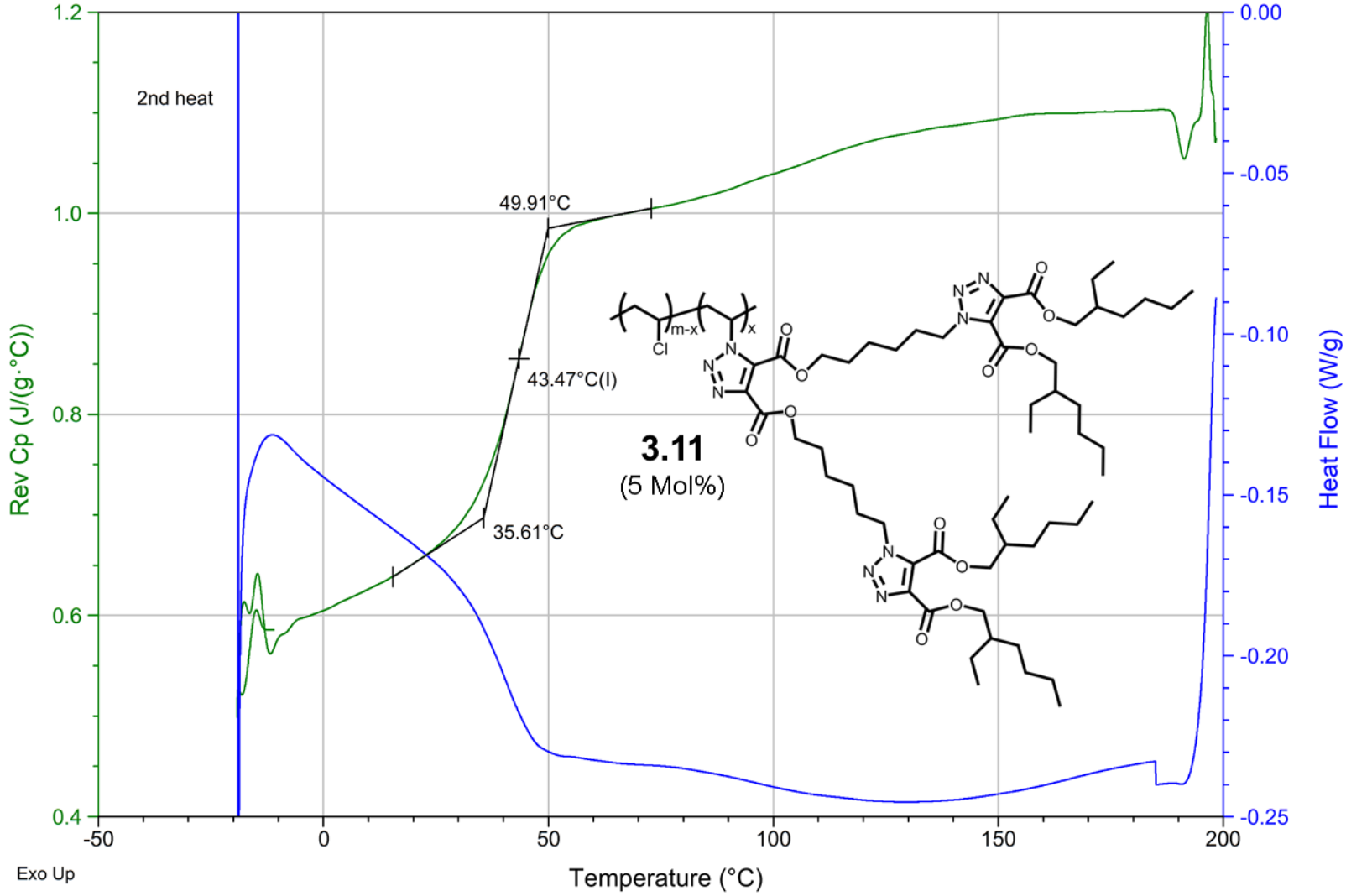
2nd heat
49.91°C
43.47°C(I)
35.61°C
3.11
(5 Mol%)
Rev Cp (J/(g·°C))
Heat Flow (W/g)
Temperature (°C)
Exo Up
1.2
1.0
0.8
0.6
0.4
0.00
-0.05
-0.10
-0.15
-0.20
-0.25
-50
0
50
100
150
200

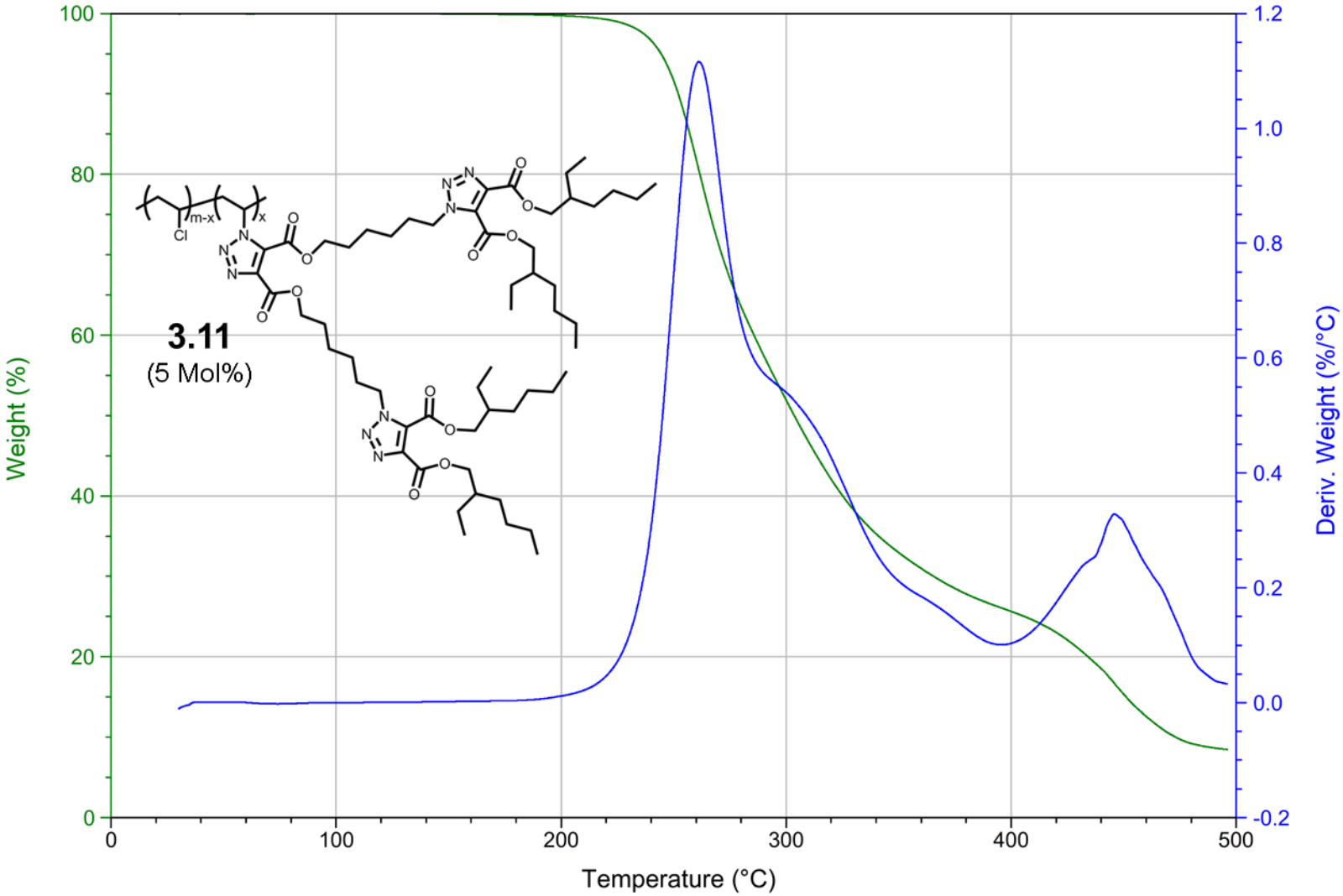
3.11
(5 Mol%)
Weight (%)
Deriv. Weight (%/°C)
Temperature (°C)
100
80
60
40
20
0
1.2
1.0
0.8
0.6
0.4
0.2
0.0
-0.2
0
100
200
300
400
500

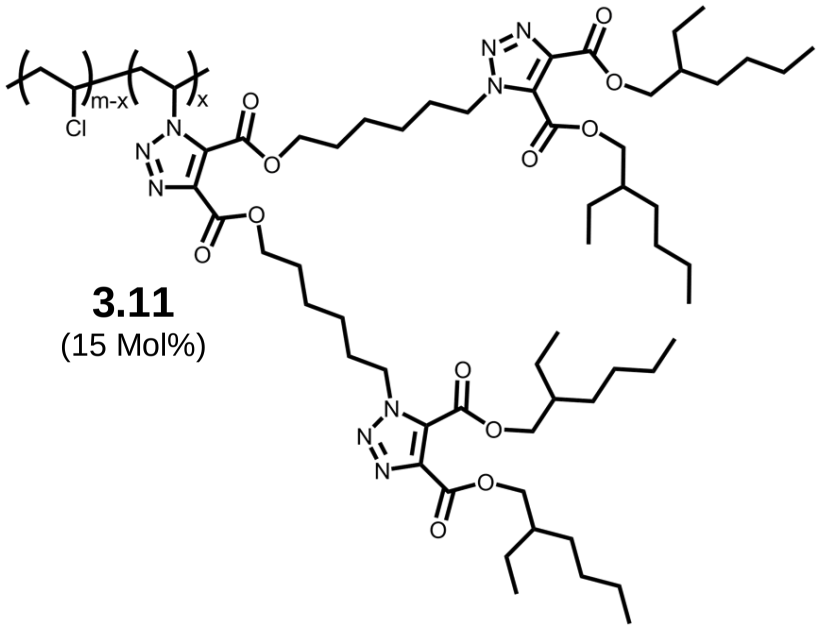

3.11
(15 Mol%)

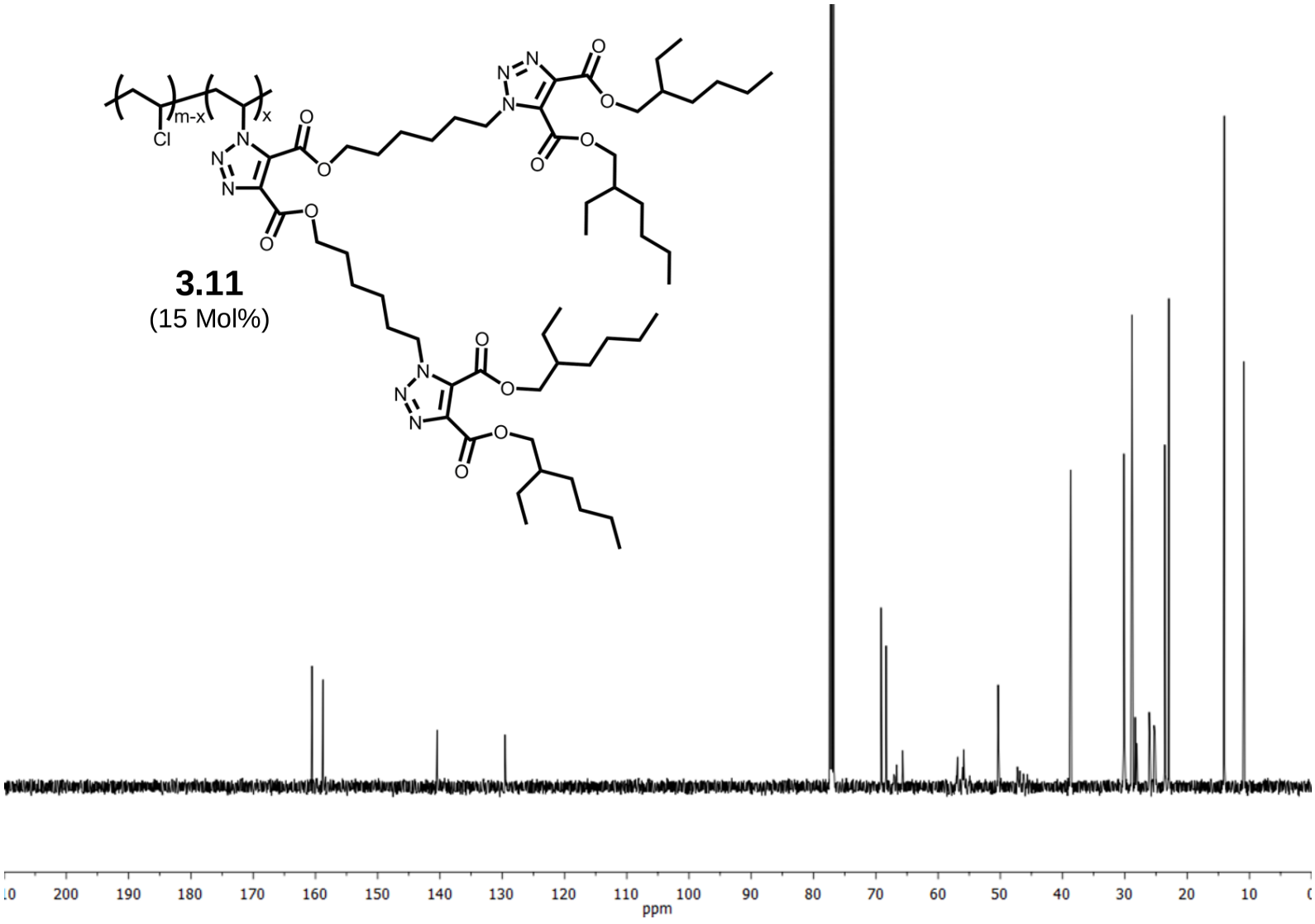
3.11
(15 Mol%)
m-x
x
Cl
ppm

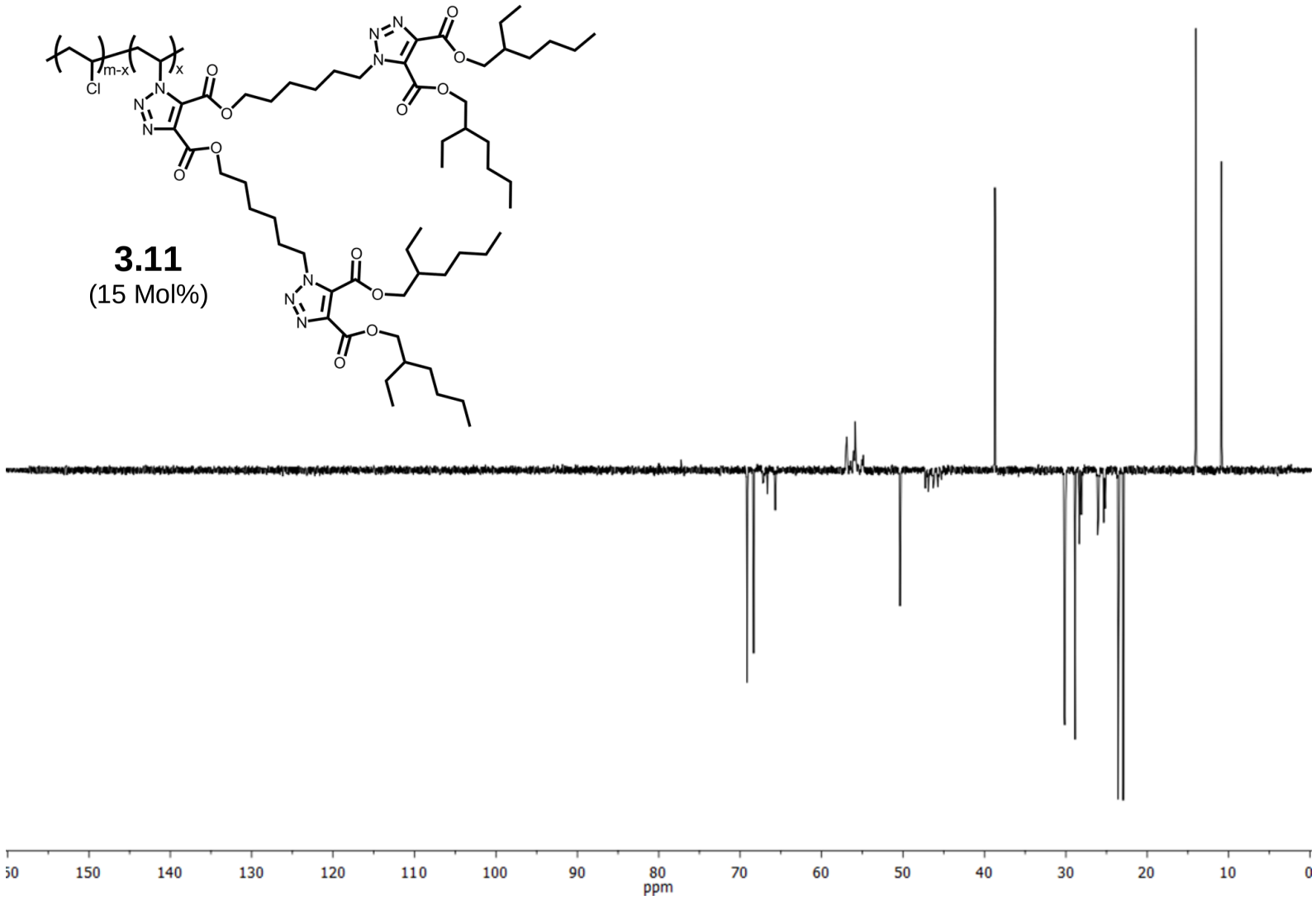
3.11
(15 Mol%)
m-x
x
Cl
ppm

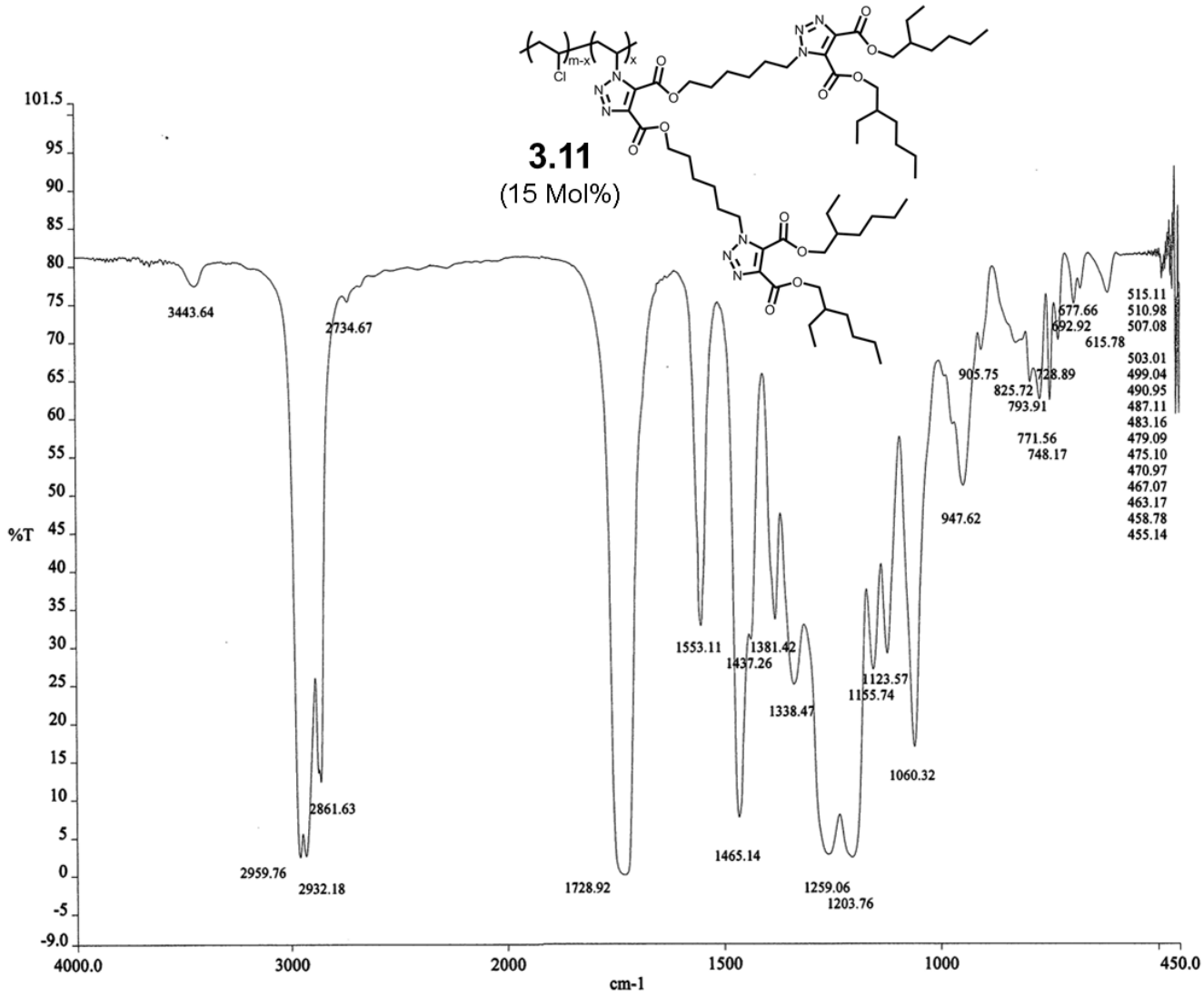
3.11
(15 Mol%)
%T
cm-1
4000.0
3000
2000
1500
1000
450.0
3443.64
2959.76
2932.18
2861.63
2734.67
1728.92
1553.11
1465.14
1437.26
1381.42
1338.47
1259.06
1203.76
1155.74
1123.57
1060.32
947.62
905.75
825.72
793.91
771.56
748.17
728.89
692.92
677.66
615.78
515.11
510.98
507.08
503.01
499.04
490.95
487.11
483.16
479.09
475.10
470.97
467.07
463.17
458.78
455.14

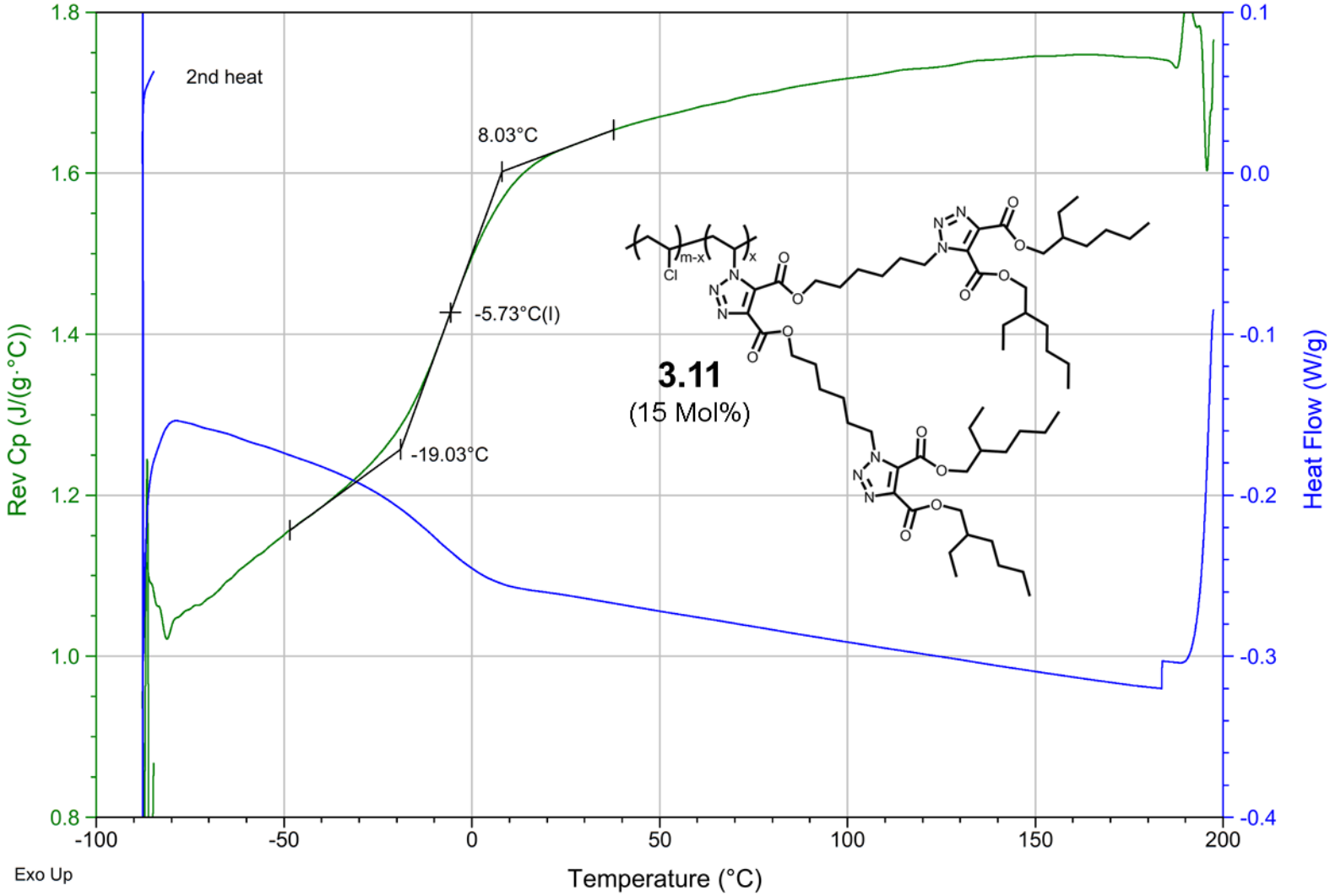
2nd heat
8.03°C
-5.73°C(I)
-19.03°C
3.11
(15 Mol%)
Rev Cp (J/(g·°C))
Heat Flow (W/g)
Temperature (°C)
Exo Up
1.8
1.6
1.4
1.2
1.0
0.8
0.1
0.0
-0.1
-0.2
-0.3
-0.4
-100
-50
0
50
100
150
200

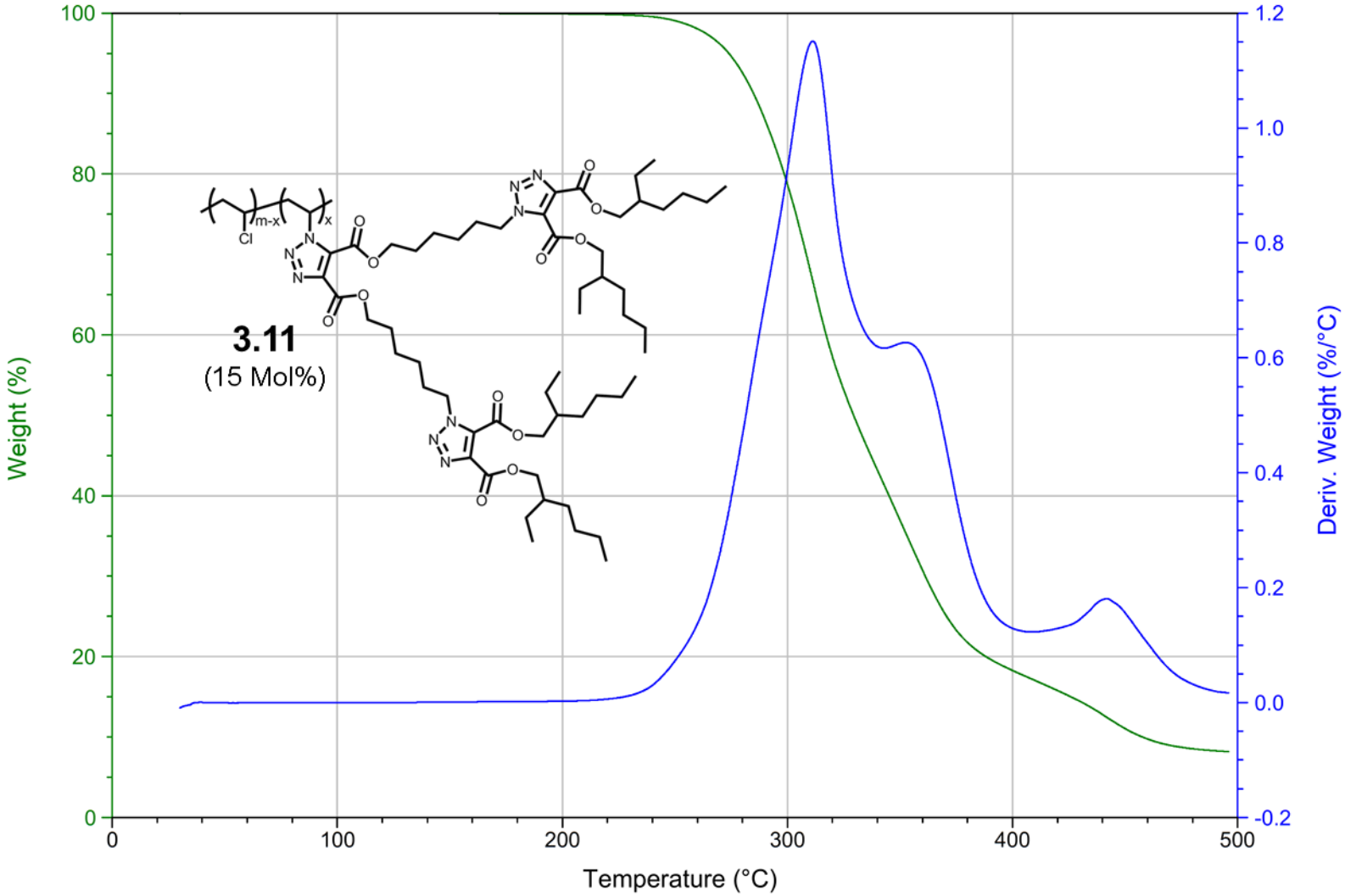
3.11
(15 Mol%)
Weight (%)
Deriv. Weight (%/°C)
Temperature (°C)
100
80
60
40
20
0
1.2
1.0
0.8
0.6
0.4
0.2
0.0
-0.2
0
100
200
300
400
500

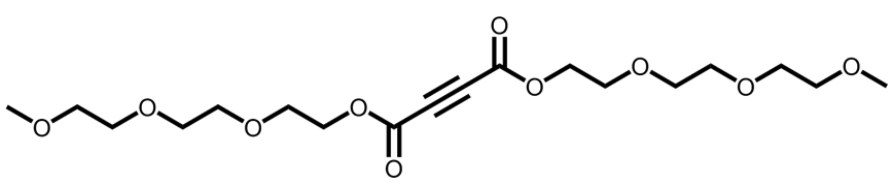

4.1

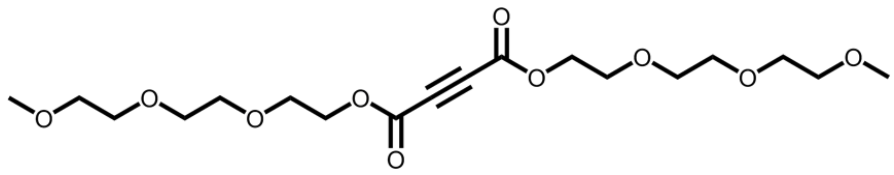

4.1

200
190
180
170
160
150
140
130
120
110
100
90
80
70
60
50
40
30
20
10
ppm

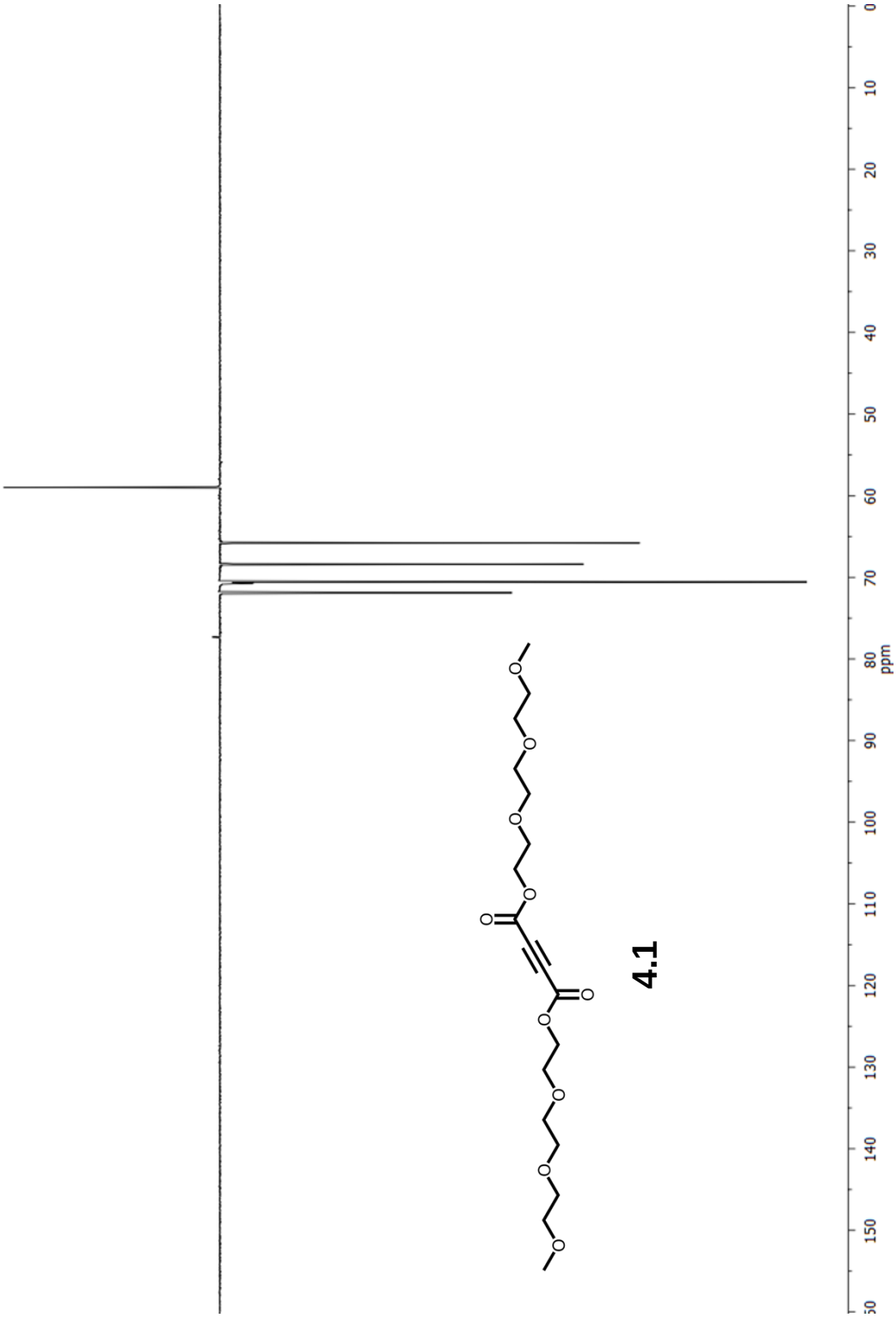

4.1

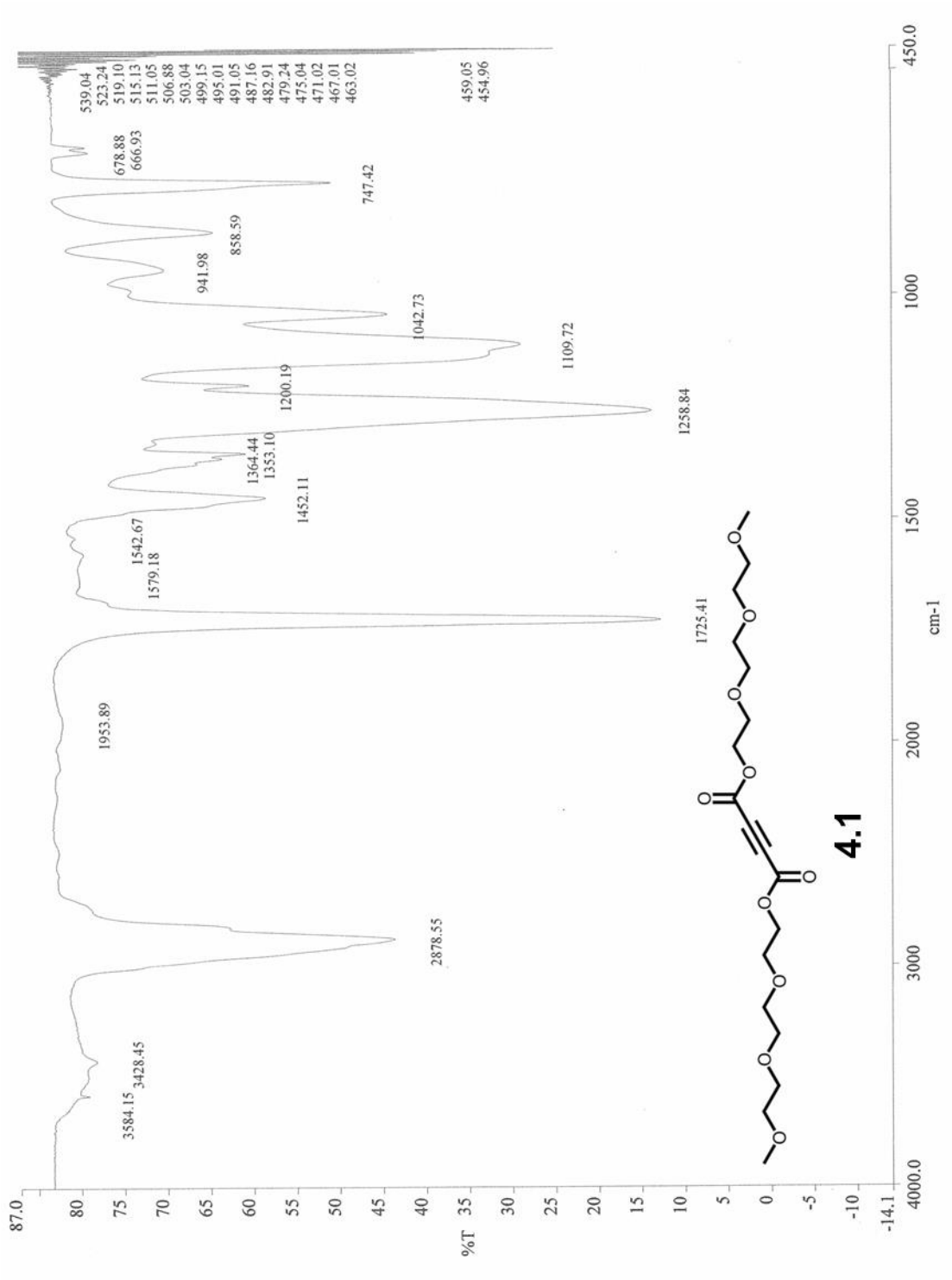
4.1
%T
cm-1
4000.0
3000
2000
1500
1000
450.0
87.0
80
75
70
65
60
55
50
45
40
35
30
25
20
15
10
5
0
-5
-10
-14.1
3584.15
3428.45
2878.55
1953.89
1725.41
1579.18
1542.67
1452.11
1364.44
1353.10
1258.84
1200.19
1109.72
1042.73
941.98
858.59
747.42
678.88
666.93
539.04
523.24
519.10
515.13
511.05
506.88
503.04
499.15
495.01
491.05
487.16
482.91
479.24
475.04
471.02
467.01
463.02
459.05
454.96

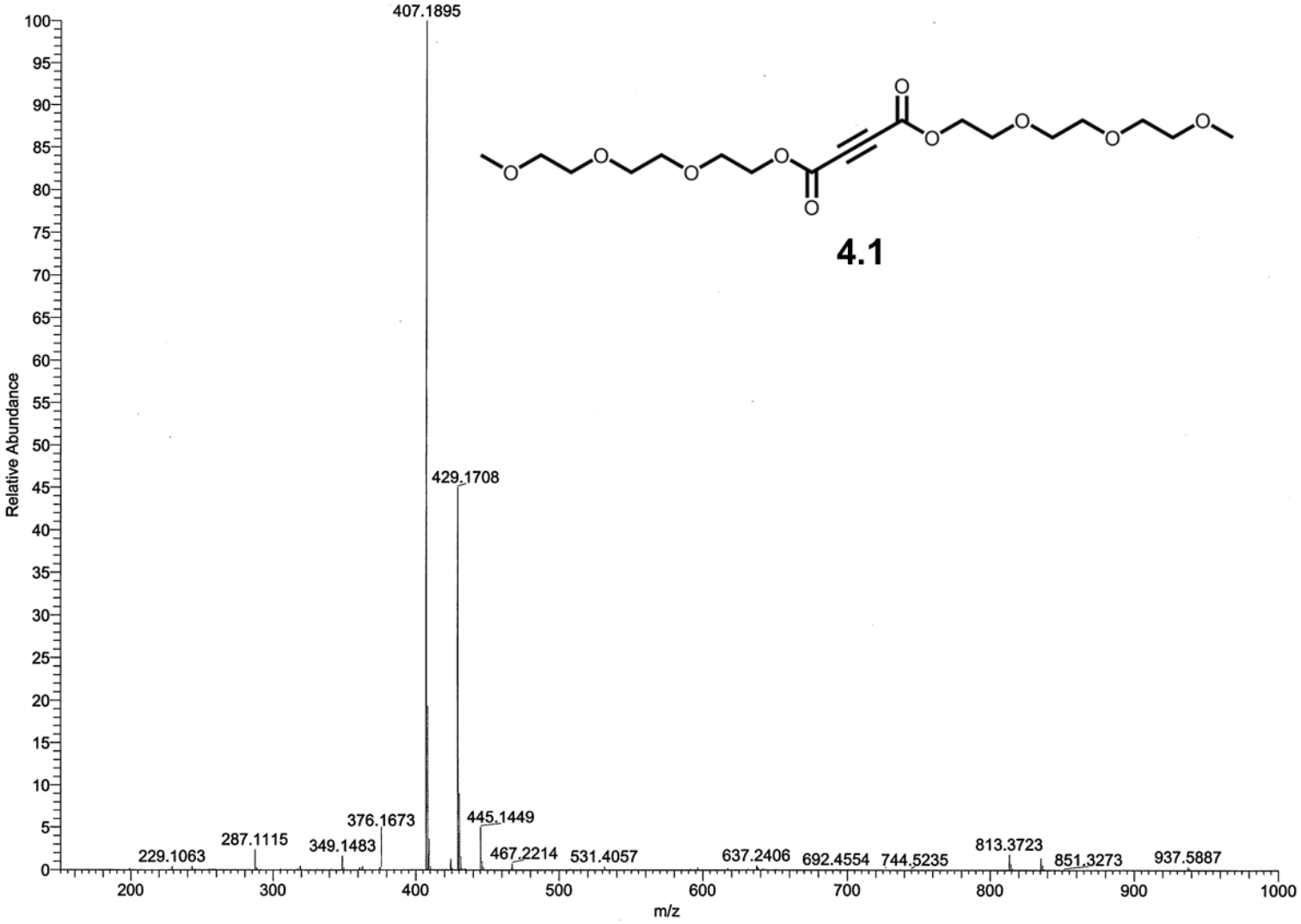
407.1895
429.1708
376.1673
445.1449
287.1115
349.1483
229.1063
467.2214
531.4057
637.2406
692.4554
744.5235
813.3723
851.3273
937.5887
Relative Abundance
m/z
100
95
90
85
80
75
70
65
60
55
50
45
40
35
30
25
20
15
10
5
0
200
300
400
500
600
700
800
900
1000

4.1

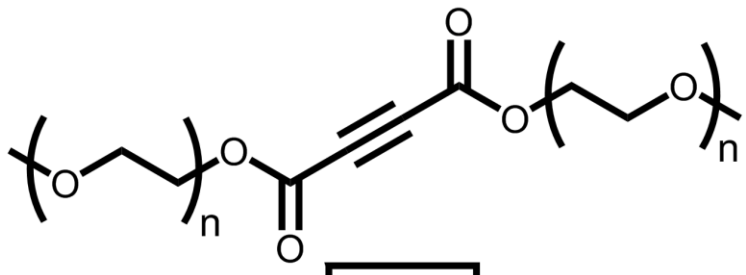

n ≅ 7

4.2

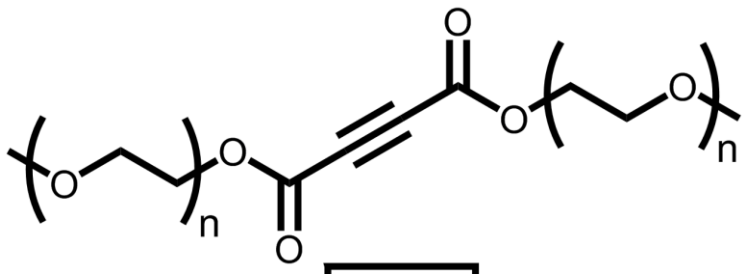
O
O
n
O
O
O
n

n ≅ 7

4.2

200
190
180
170
160
150
140
130
120
110
100
90
80
70
60
50
40
30
20
10
ppm

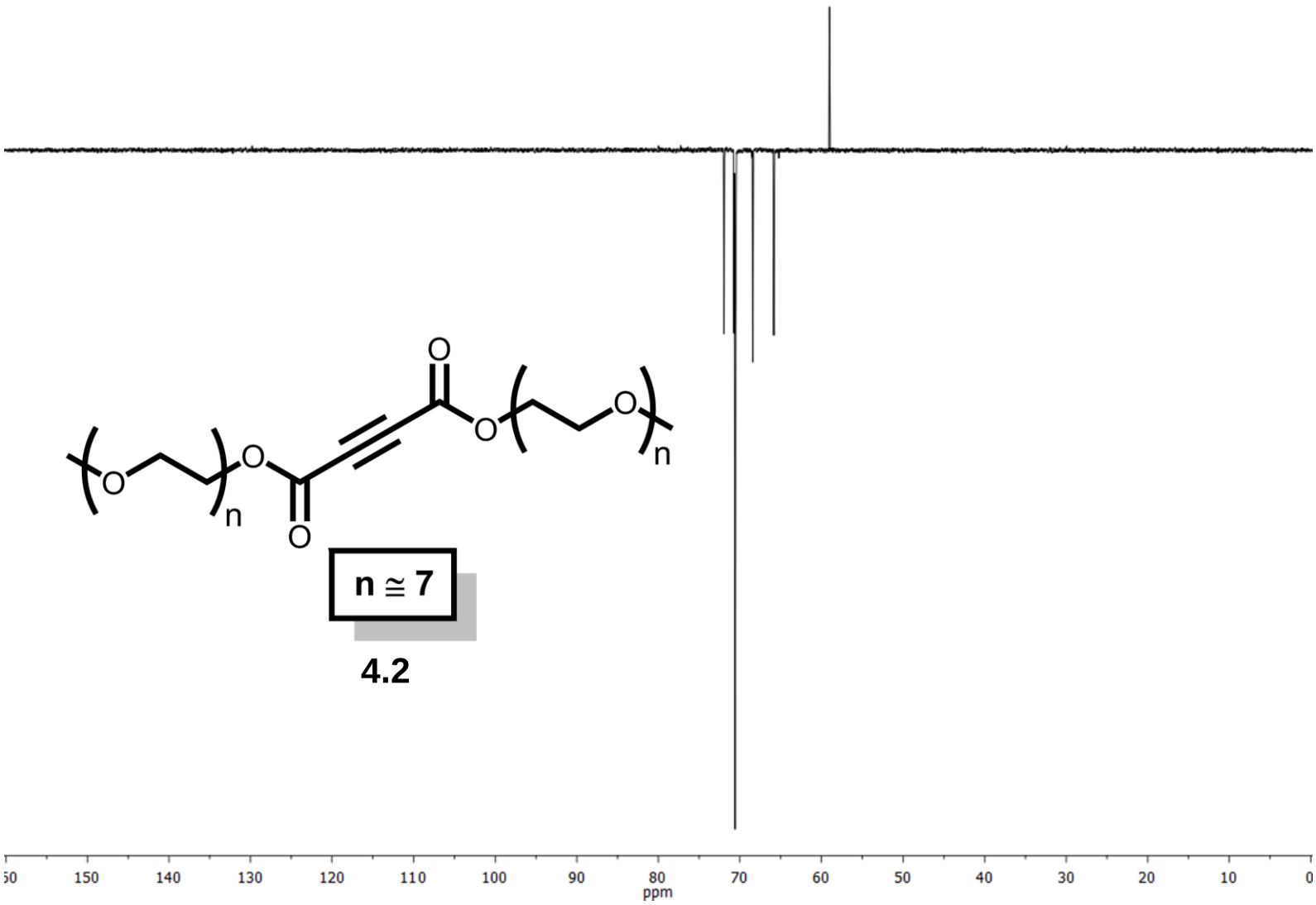
O
O
O
O
n
O
O
n
n ≅ 7
150
140
130
120
110
100
90
80
70
60
50
40
30
20
10
0
ppm

4.2

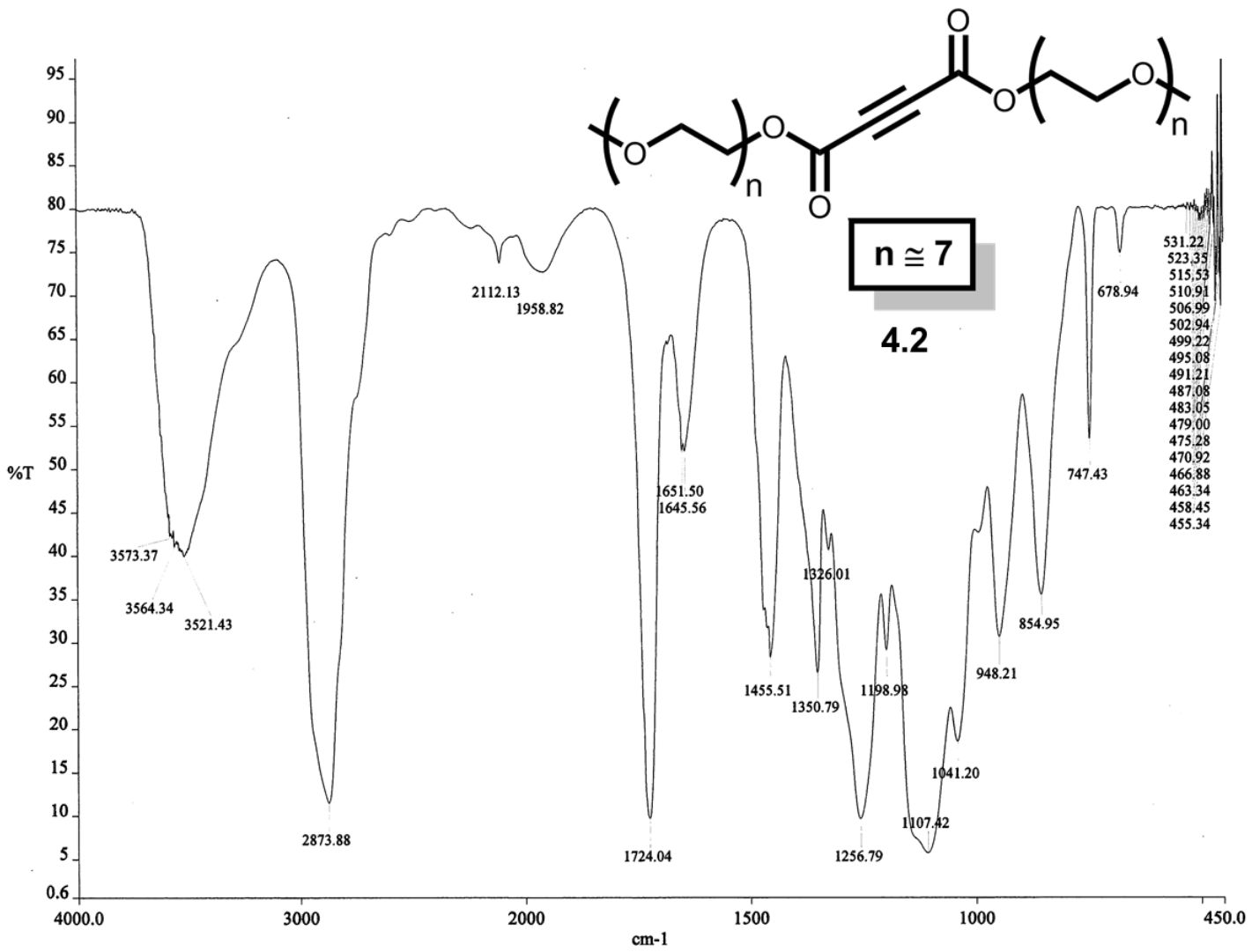
n ≅ 7
4.2
%T
cm-1
4000.0
3000
2000
1500
1000
450.0
3573.37
3564.34
3521.43
2873.88
2112.13
1958.82
1724.04
1651.50
1645.56
1455.51
1350.79
1326.01
1256.79
1198.98
1107.42
1041.20
948.21
854.95
747.43
678.94
531.22
523.35
515.53
510.91
506.99
502.94
499.22
495.08
491.21
487.08
483.05
479.00
475.28
470.92
466.88
463.34
458.45
455.34

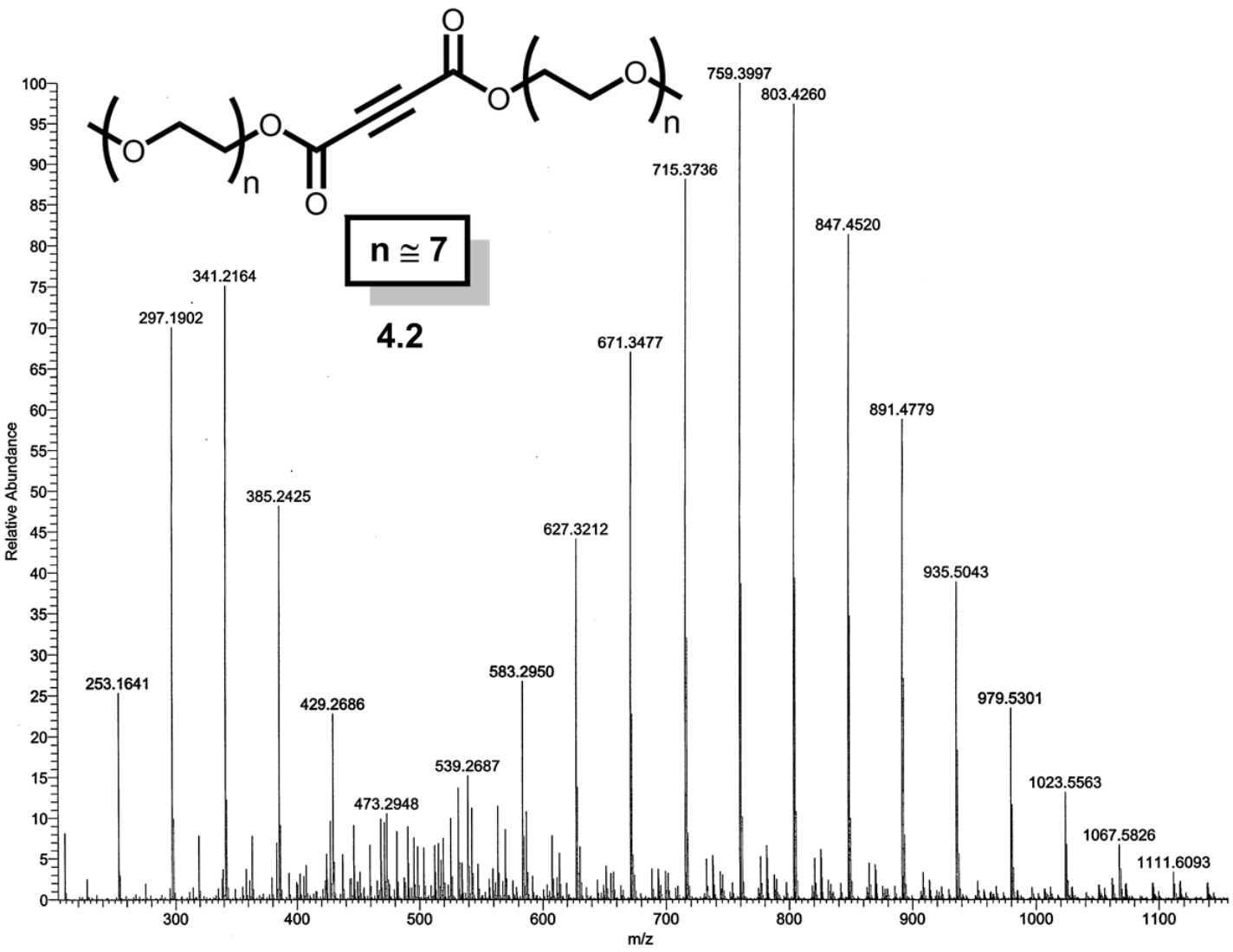
n ≅ 7
4.2
Relative Abundance
m/z
759.3997
803.4260
715.3736
847.4520
341.2164
297.1902
671.3477
891.4779
385.2425
627.3212
935.5043
253.1641
583.2950
429.2686
979.5301
539.2687
1023.5563
473.2948
1067.5826
1111.6093

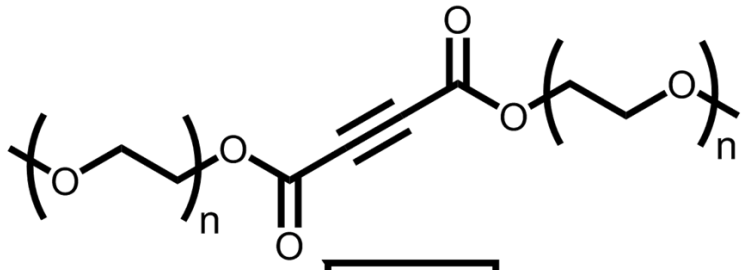

n ≅ 11

4.3

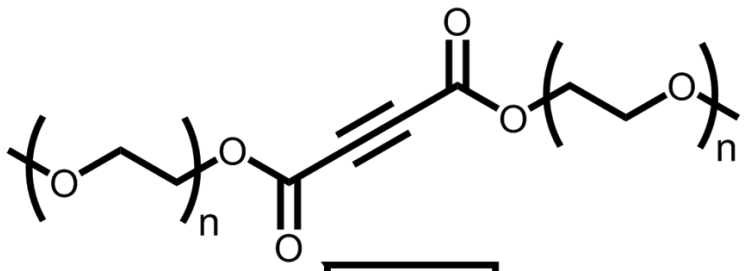
O
O
O
n
O
O
O
n

n ≅ 11

4.3

200
190
180
170
160
150
140
130
120
110
100
90
80
70
60
50
40
30
20
10
ppm

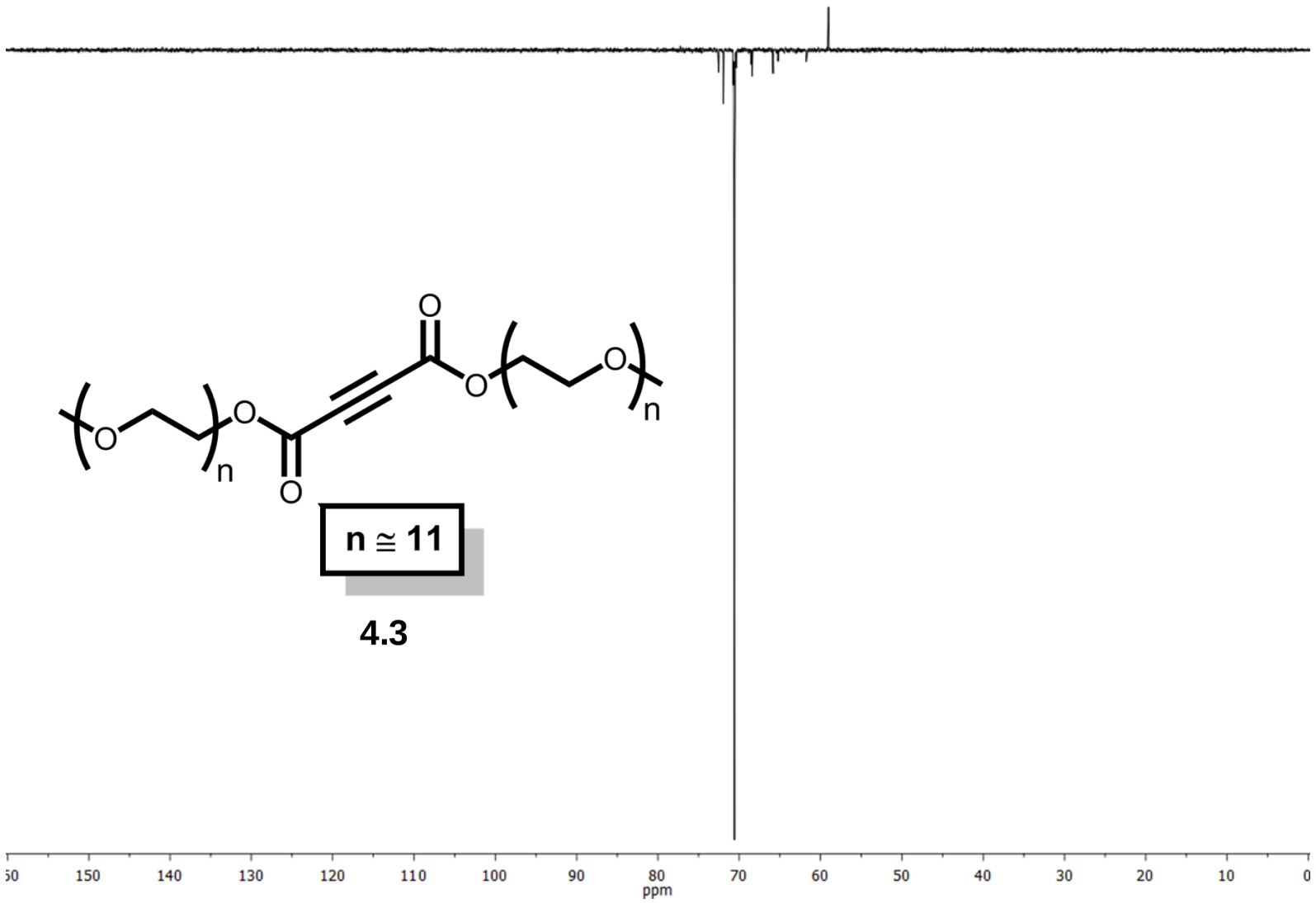
O
O
O
n
O
O
O
n
n ≅ 11
150
140
130
120
110
100
90
80
70
60
50
40
30
20
10
ppm

4.3

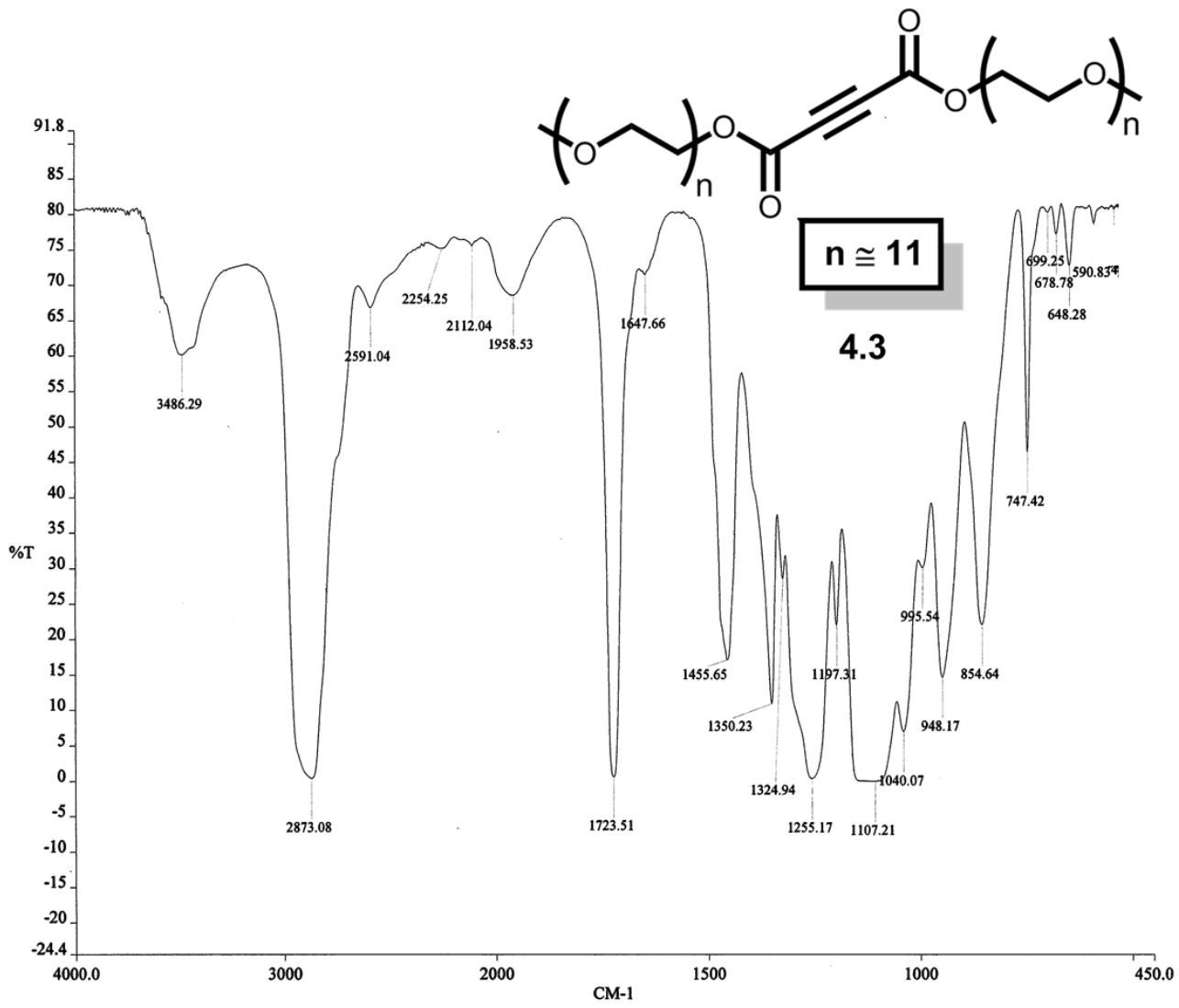
n ≅ 11
4.3
%T
CM-1
91.8
85
80
75
70
65
60
55
50
45
40
35
30
25
20
15
10
5
0
-5
-10
-15
-20
-24.4
4000.0
3000
2000
1500
1000
450.0
3486.29
2873.08
2591.04
2254.25
2112.04
1958.53
1723.51
1647.66
1455.65
1350.23
1324.94
1255.17
1197.31
1107.21
1040.07
995.54
948.17
854.64
747.42
699.25
678.78
648.28
590.83

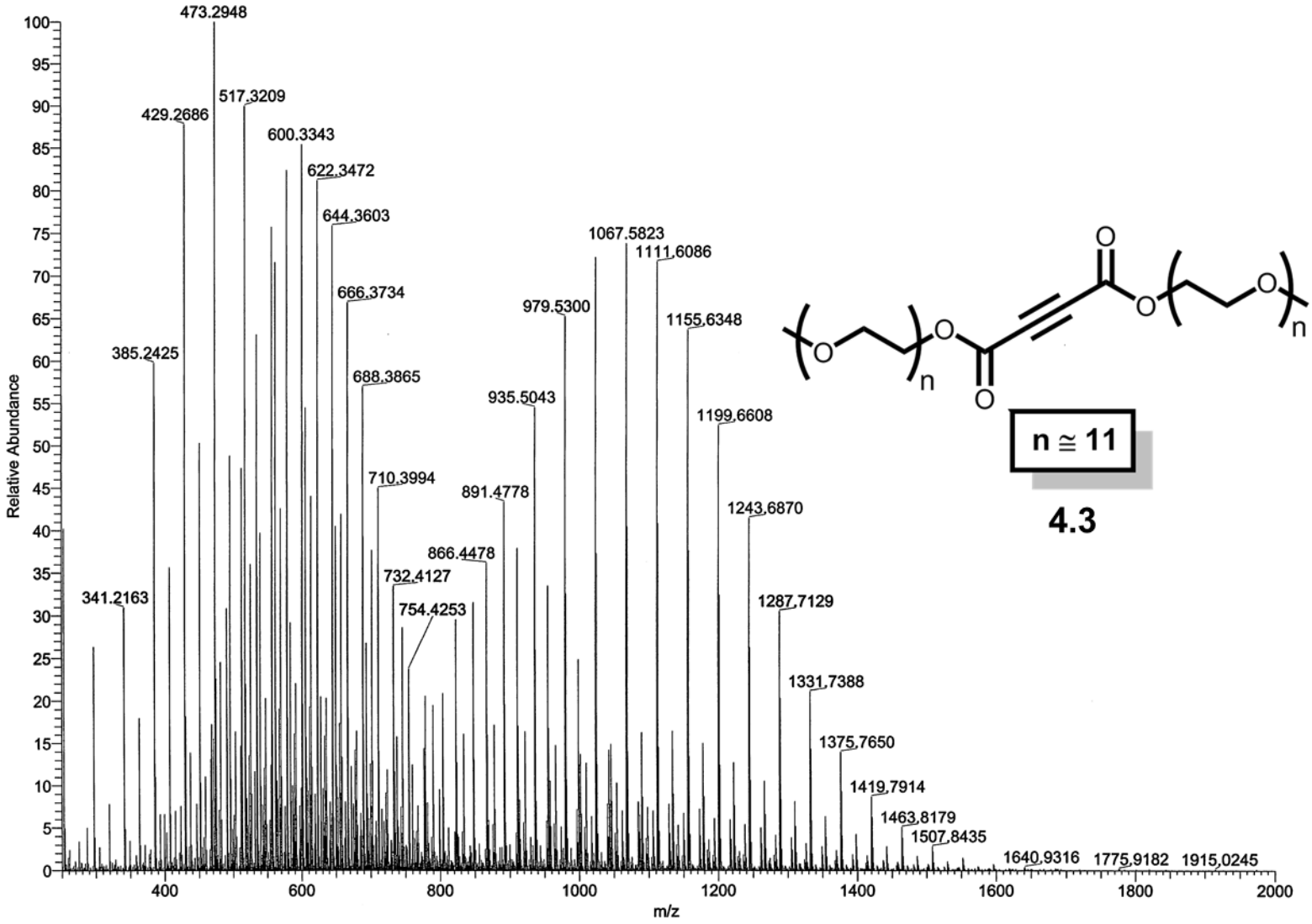
473.2948
517.3209
429.2686
600.3343
622.3472
644.3603
666.3734
385.2425
688.3865
710.3994
341.2163
754.4253
732.4127
866.4478
891.4778
935.5043
979.5300
1067.5823
1111.6086
1155.6348
1199.6608
1243.6870
1287.7129
1331.7388
1375.7650
1419.7914
1463.8179
1507.8435
1640.9316
1775.9182
1915.0245
Relative Abundance
m/z
n ≅ 11
4.3

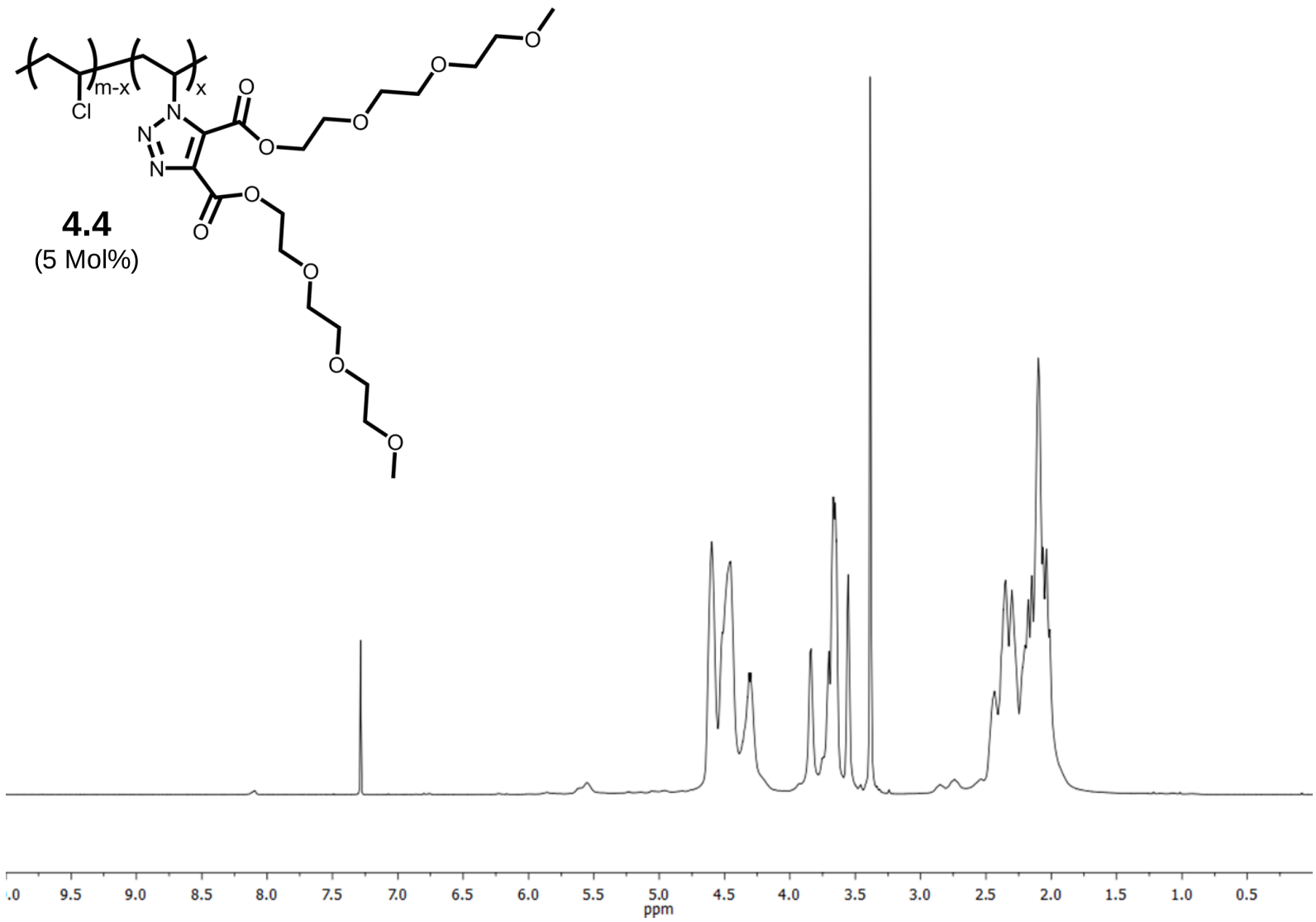
m-x
x
Cl
N
N
N
O
O
O
O
O
O
O
O
O
O
O
O
O
4.4
(5 Mol%)
9.5
9.0
8.5
8.0
7.5
7.0
6.5
6.0
5.5
5.0
4.5
4.0
3.5
3.0
2.5
2.0
1.5
1.0
0.5
ppm

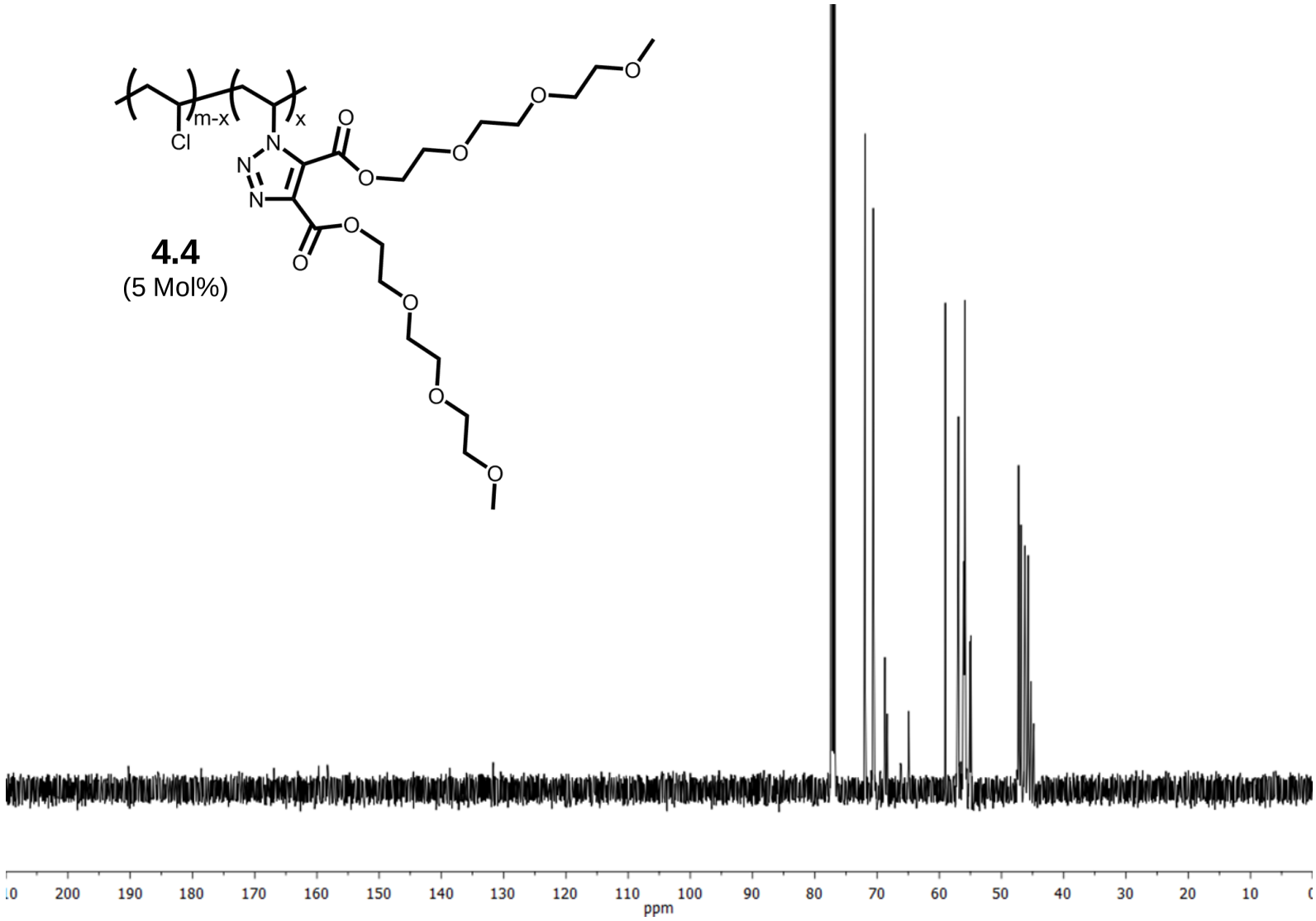
m-x
x
Cl
N
N
N
O
O
O
O
O
O
O
O
O
O
O
4.4
(5 Mol%)
200
190
180
170
160
150
140
130
120
110
100
90
80
70
60
50
40
30
20
10
ppm

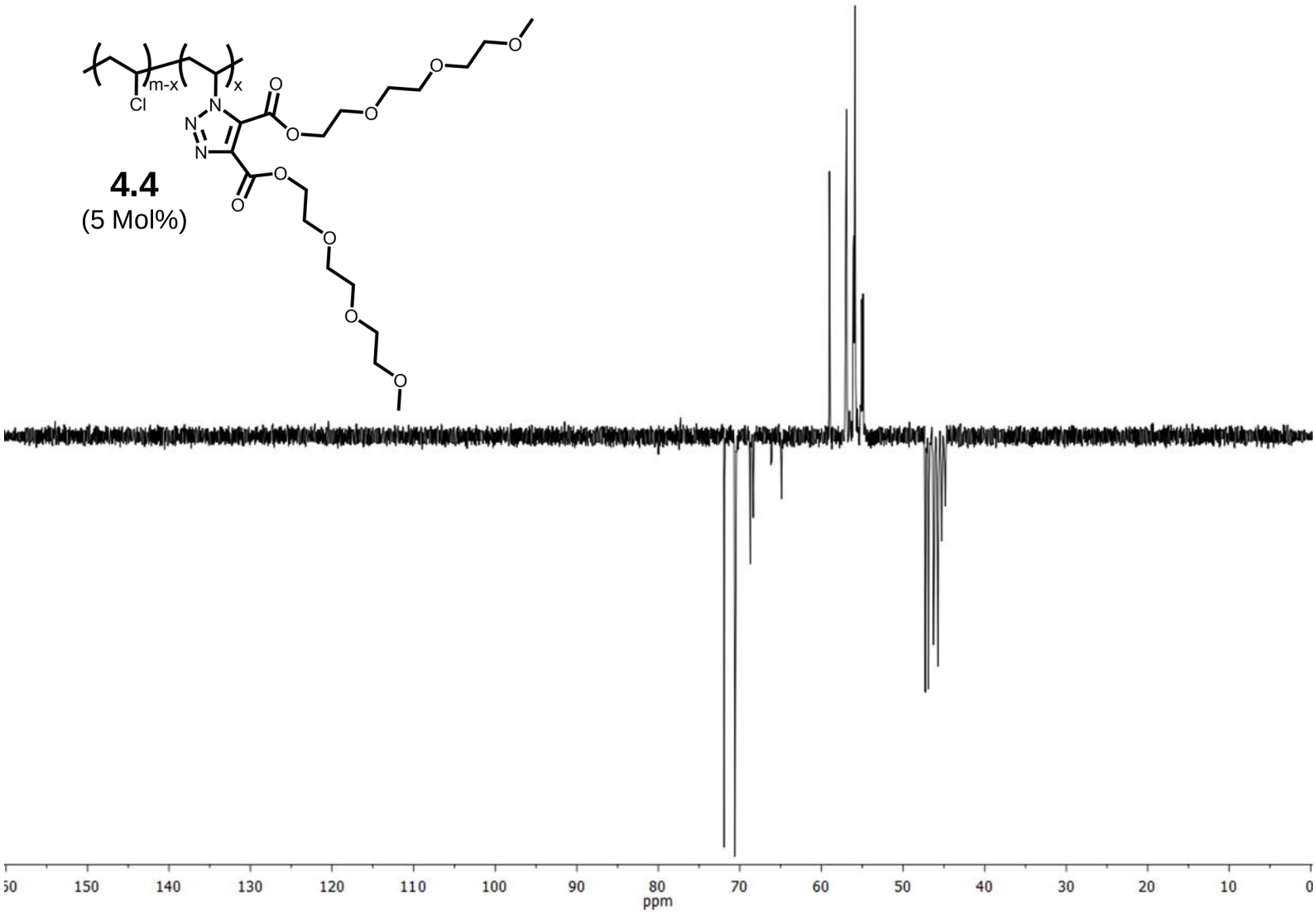
m-x
x
Cl
N
N
N
O
O
O
O
O
O
O
O
O
O
O
O
4.4
(5 Mol%)
150
140
130
120
110
100
90
80
70
60
50
40
30
20
10
0
ppm

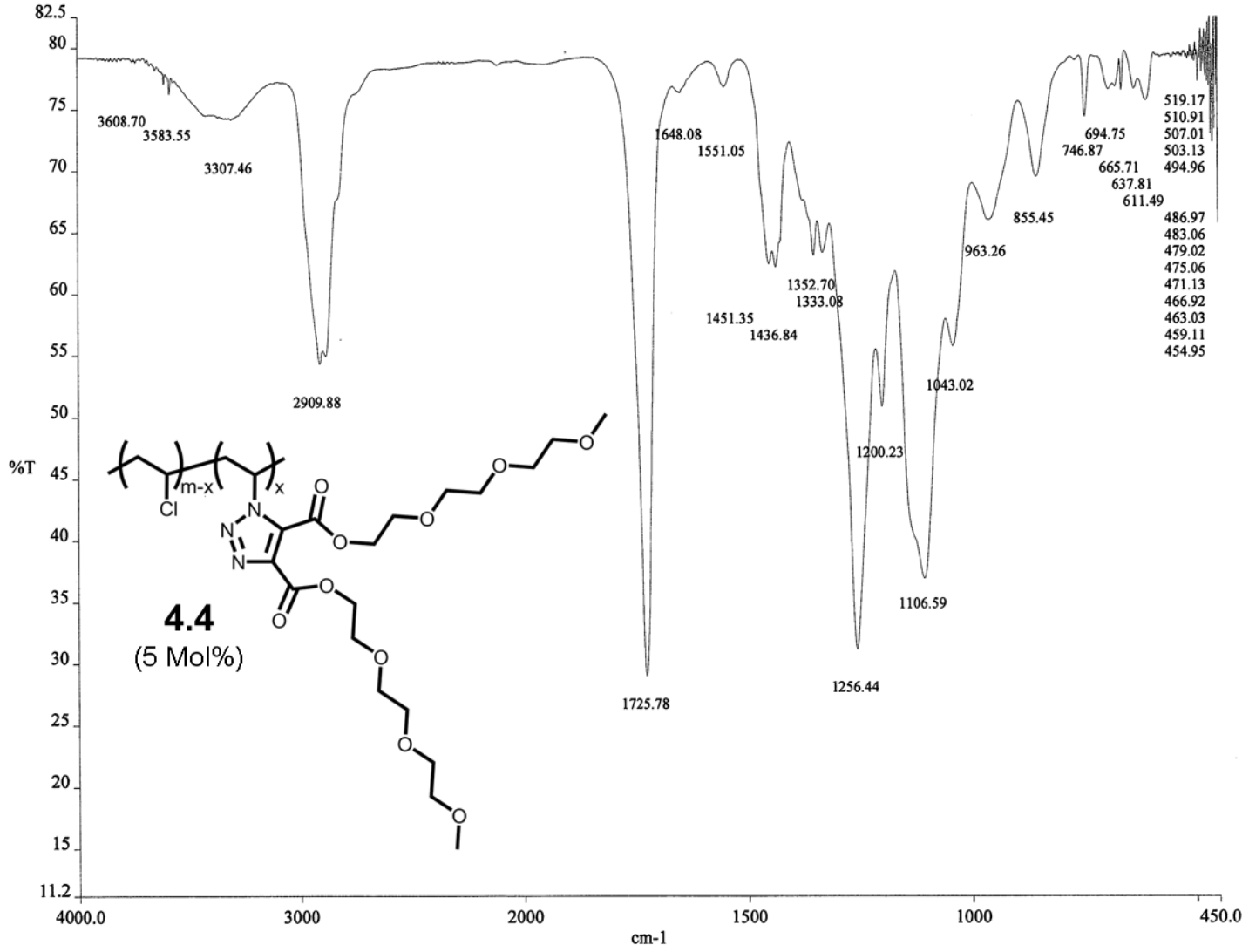
82.5
80
75
70
65
60
55
50
45
40
35
30
25
20
15
11.2
%T
4000.0
3000
2000
1500
1000
450.0
cm-1
3608.70
3583.55
3307.46
2909.88
1648.08
1551.05
1451.35
1436.84
1352.70
1333.08
1200.23
1256.44
1725.78
1106.59
1043.02
963.26
855.45
746.87
694.75
665.71
637.81
611.49
519.17
510.91
507.01
503.13
494.96
486.97
483.06
479.02
475.06
471.13
466.92
463.03
459.11
454.95
m-x
x
Cl
4.4
(5 Mol%)

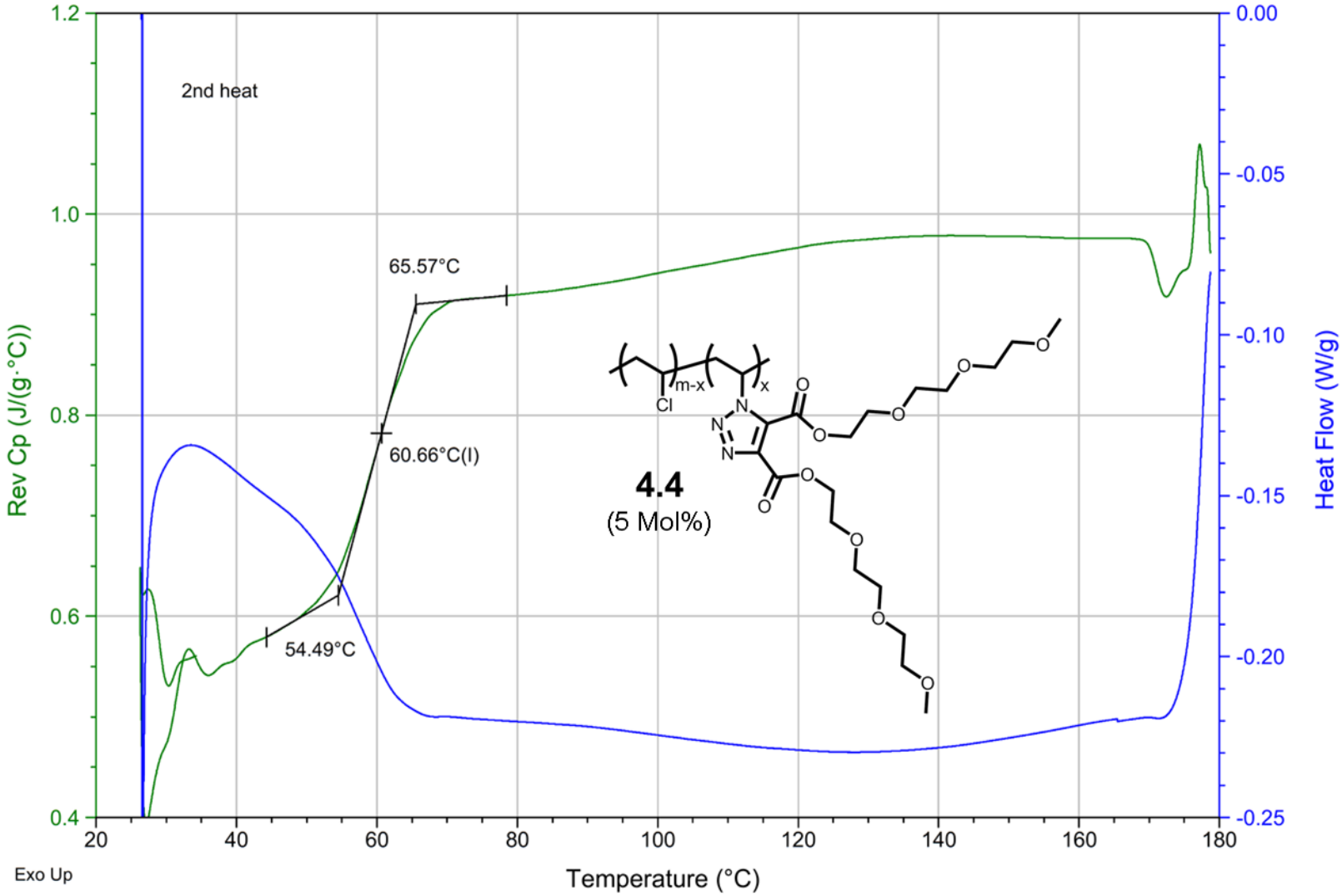
2nd heat
65.57°C
60.66°C(I)
54.49°C
4.4
(5 Mol%)
Rev Cp (J/(g·°C))
Heat Flow (W/g)
Temperature (°C)
Exo Up
1.2
1.0
0.8
0.6
0.4
0.00
-0.05
-0.10
-0.15
-0.20
-0.25
20
40
60
80
100
120
140
160
180

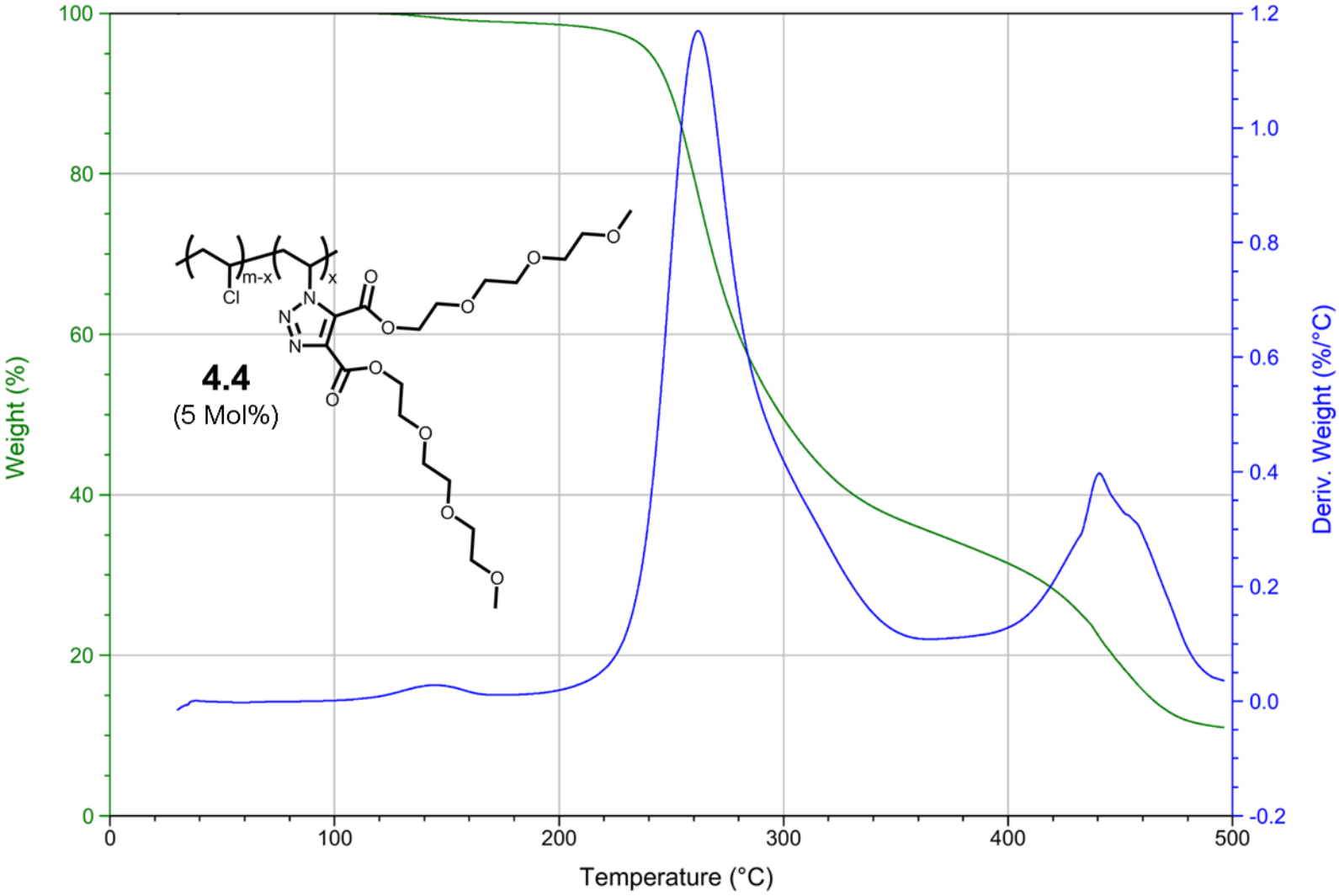
4.4
(5 Mol%)
Cl
m-x
x
N
N
O
O
O
O
O
O
O
O
O
Weight (%)
Deriv. Weight (%/°C)
Temperature (°C)
100
80
60
40
20
0
1.2
1.0
0.8
0.6
0.4
0.2
0.0
-0.2
0
100
200
300
400
500

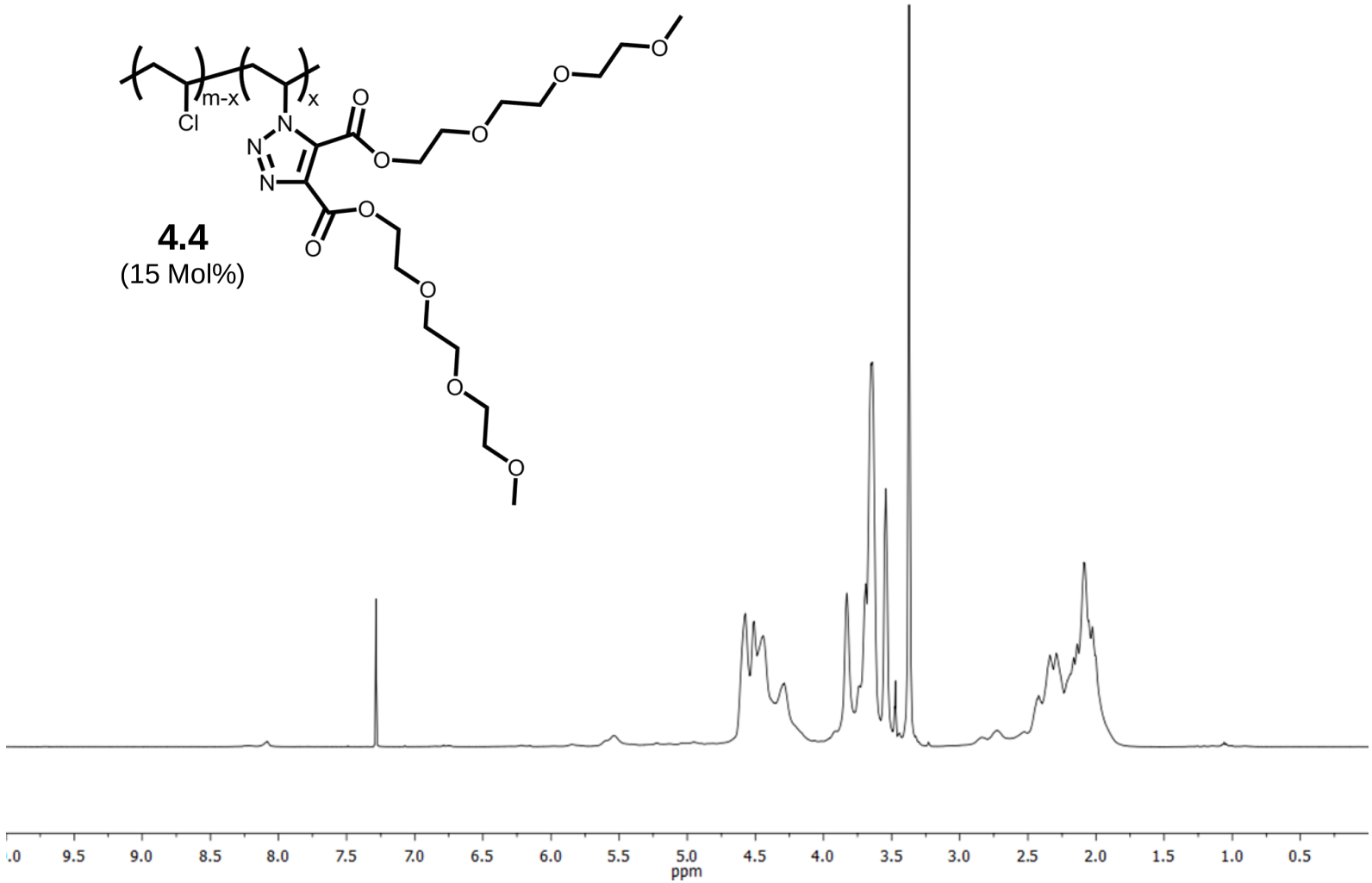
m-x
x
Cl
N
N
N
O
O
O
O
O
O
O
O
O
O
O
O
4.4
(15 Mol%)
9.5
9.0
8.5
8.0
7.5
7.0
6.5
6.0
5.5
5.0
4.5
4.0
3.5
3.0
2.5
2.0
1.5
1.0
0.5
ppm

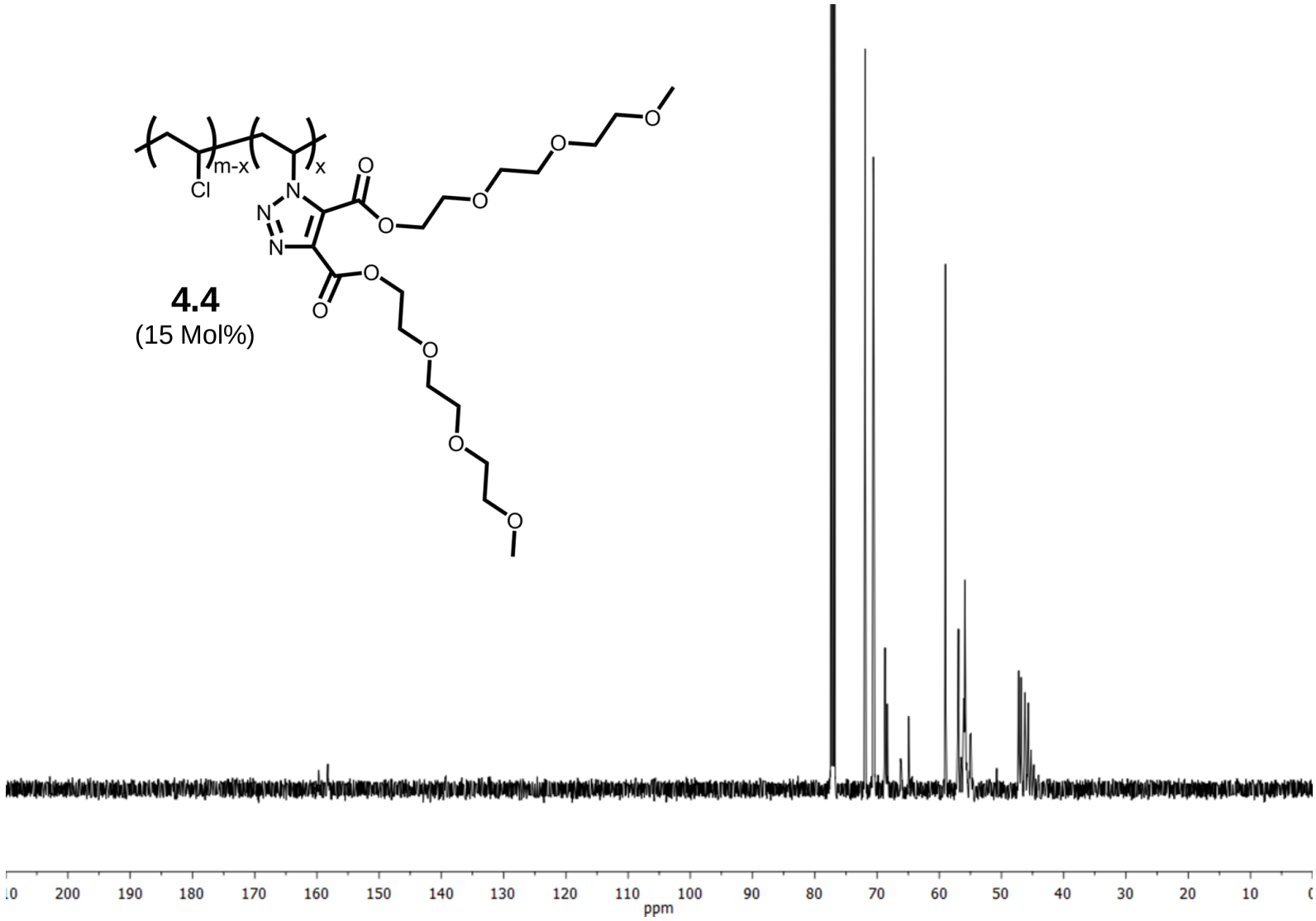
m-x
x
Cl
N
N
N
O
O
O
O
O
O
O
O
O
O
O
4.4
(15 Mol%)
200
190
180
170
160
150
140
130
120
110
100
90
80
70
60
50
40
30
20
10
ppm

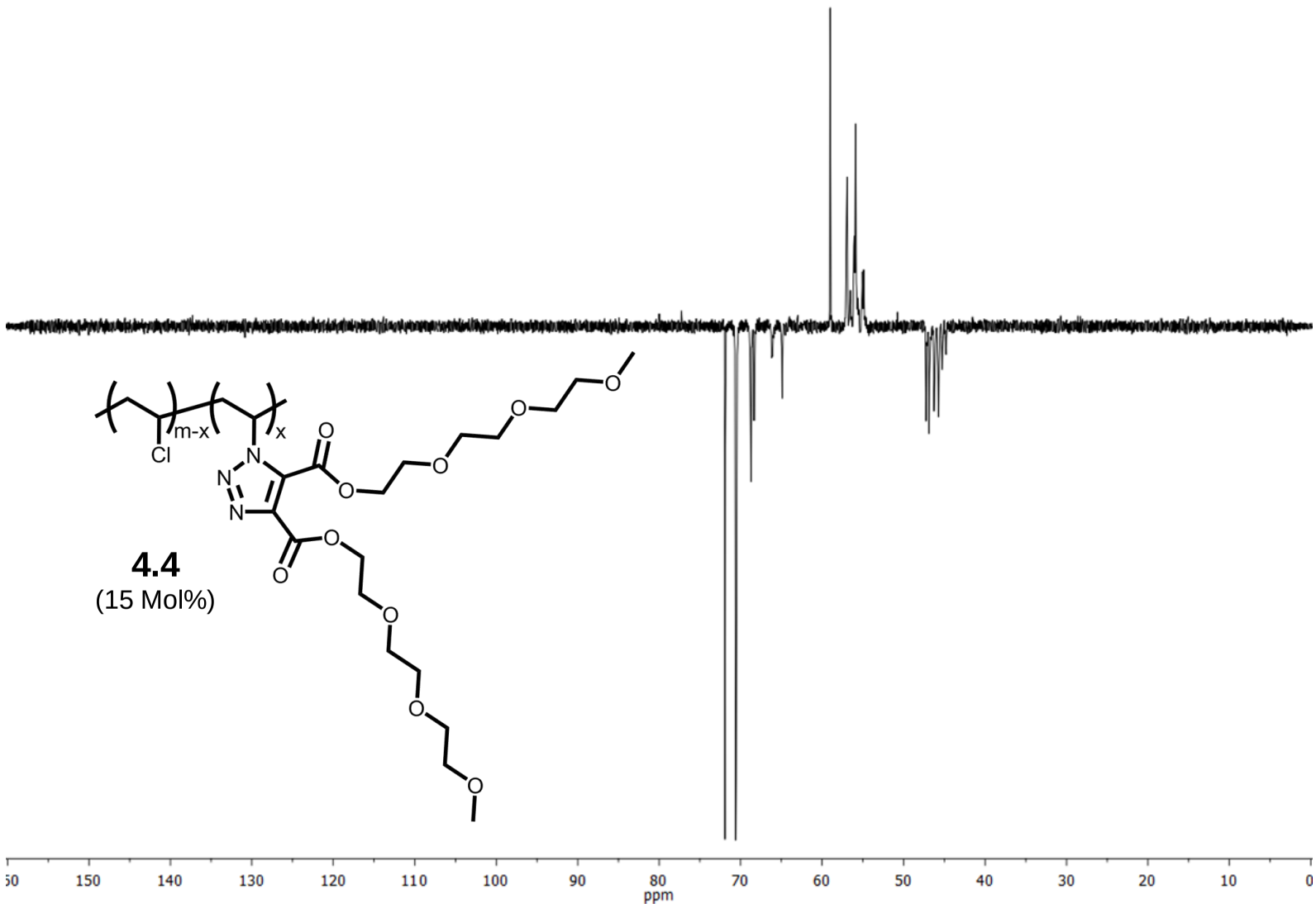
m-x
x
Cl
N
N
N
O
O
O
O
O
O
O
O
O
O
O
O
4.4
(15 Mol%)
150
140
130
120
110
100
90
80
70
60
50
40
30
20
10
ppm

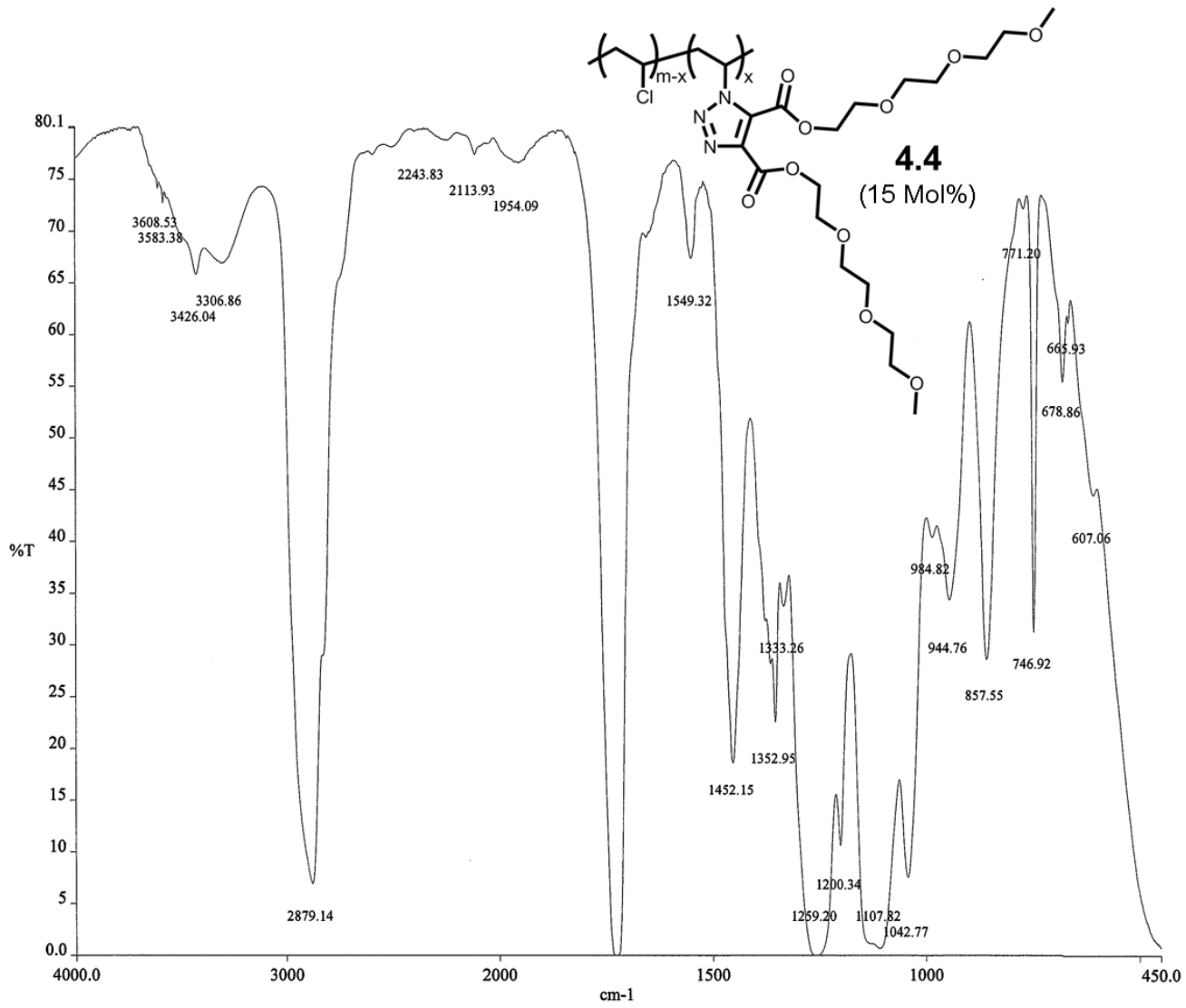
4.4
(15 Mol%)
%T
cm-1
3608.53
3583.38
3306.86
3426.04
2879.14
2243.83
2113.93
1954.09
1549.32
1452.15
1352.95
1333.26
1200.34
1259.20
1107.82
1042.77
984.82
944.76
857.55
771.20
746.92
665.93
678.86
607.06

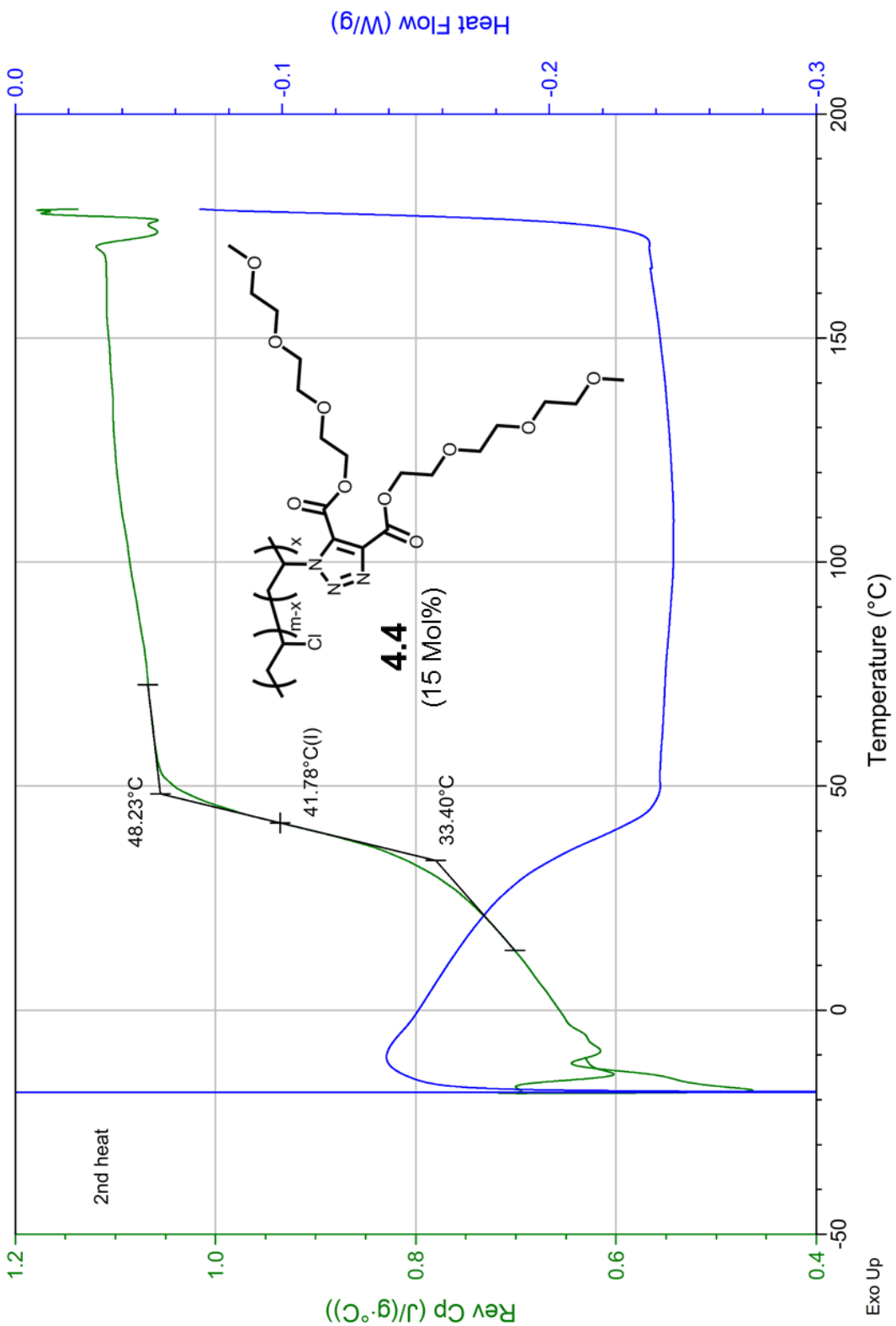
Heat Flow (W/g)
0.0
-0.1
-0.2
-0.3
Rev Cp (J/(g·°C))
1.2
1.0
0.8
0.6
0.4
Exo Up
-50
0
50
100
150
200
Temperature (°C)
2nd heat
48.23°C
41.78°C(I)
33.40°C
4.4
(15 Mol%)
m-x
x
Cl

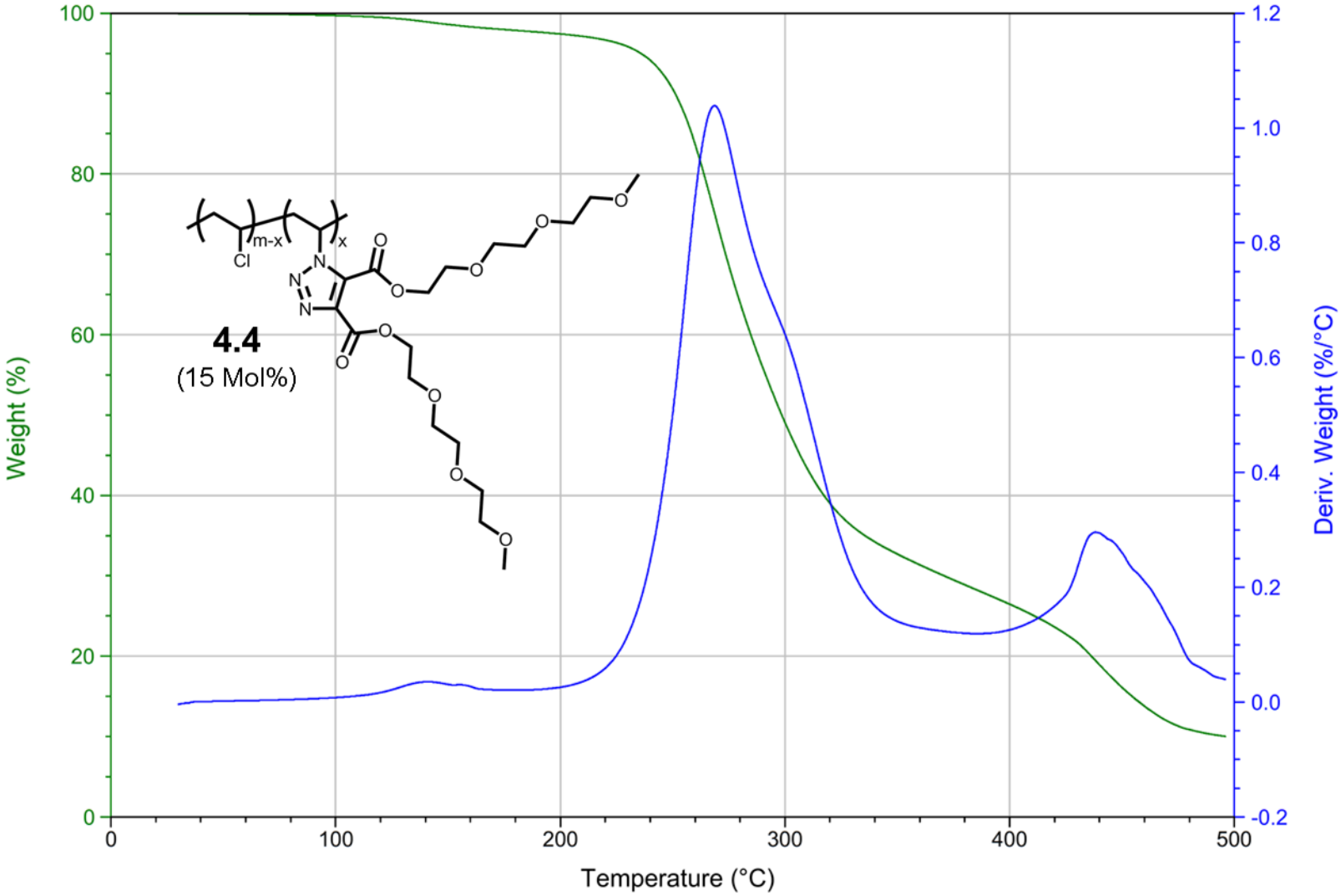
4.4
(15 Mol%)
Weight (%)
Deriv. Weight (%/°C)
Temperature (°C)
100
80
60
40
20
0
1.2
1.0
0.8
0.6
0.4
0.2
0.0
-0.2
0
100
200
300
400
500

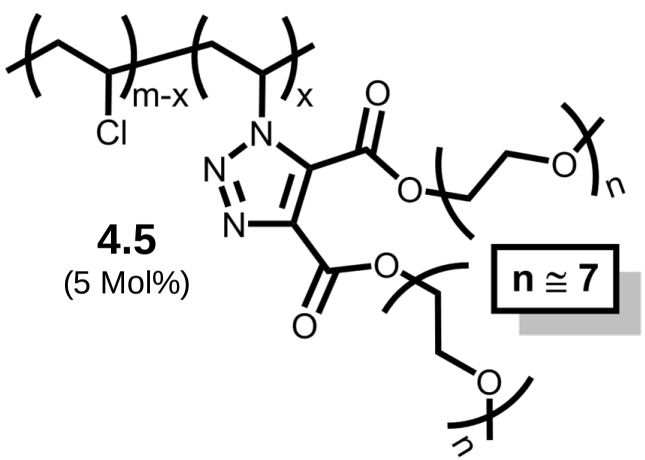
m-x
x
Cl
N
N
N
O
O
O
O
O
n
O
O
n
4.5
(5 Mol%)
n ≅ 7

9.5
9.0
8.5
8.0
7.5
7.0
6.5
6.0
5.5
5.0
4.5
4.0
3.5
3.0
2.5
2.0
1.5
1.0
0.5
ppm

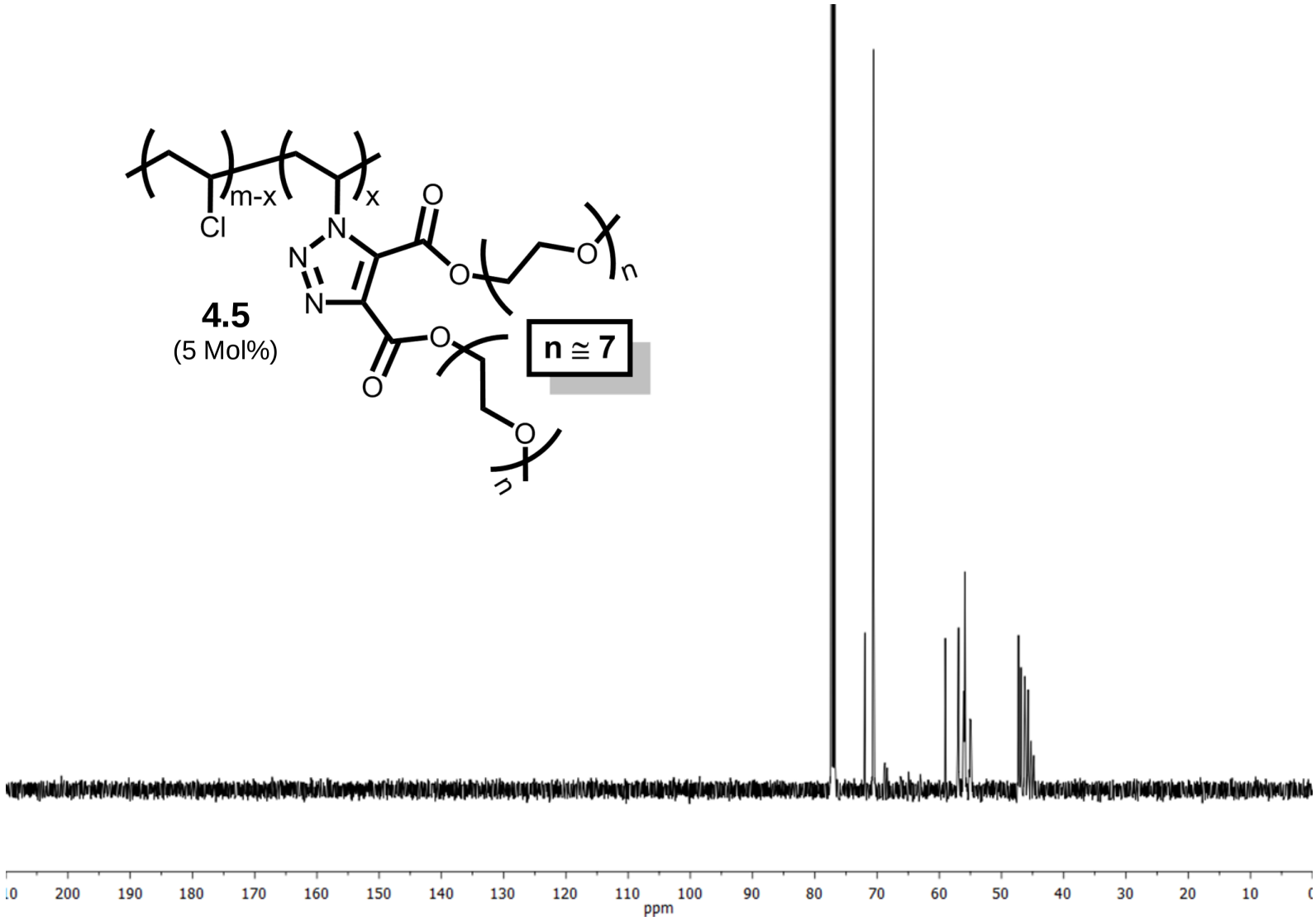
m-x
x
Cl
N
N
N
O
O
O
O
O
O
n
n
4.5
(5 Mol%)
n ≅ 7
ppm
200
190
180
170
160
150
140
130
120
110
100
90
80
70
60
50
40
30
20
10

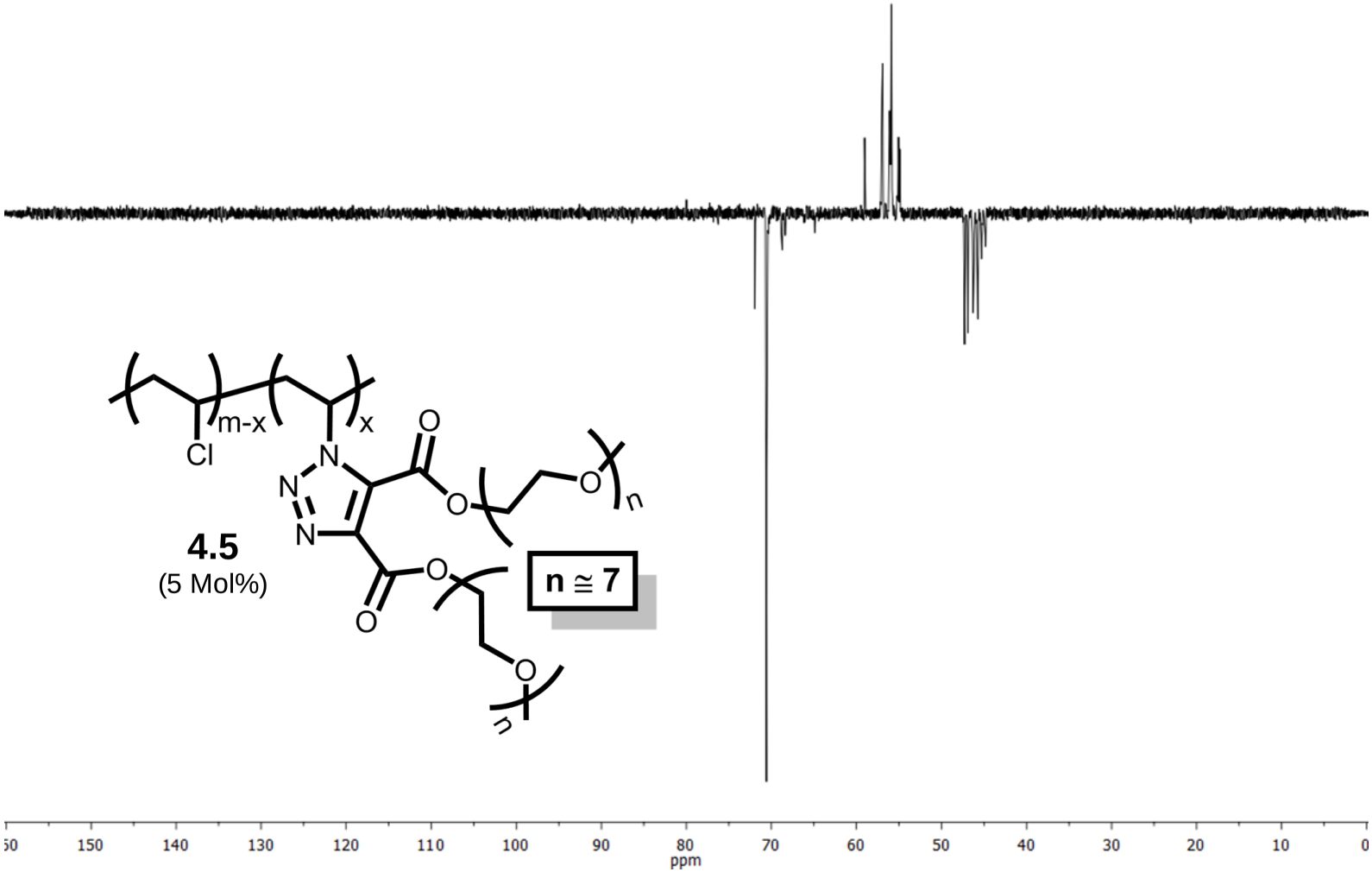
m-x
x
Cl
N
N
N
O
O
O
n
O
O
O
n
4.5
(5 Mol%)
n ≅ 7
150
140
130
120
110
100
90
80
70
60
50
40
30
20
10
0
ppm

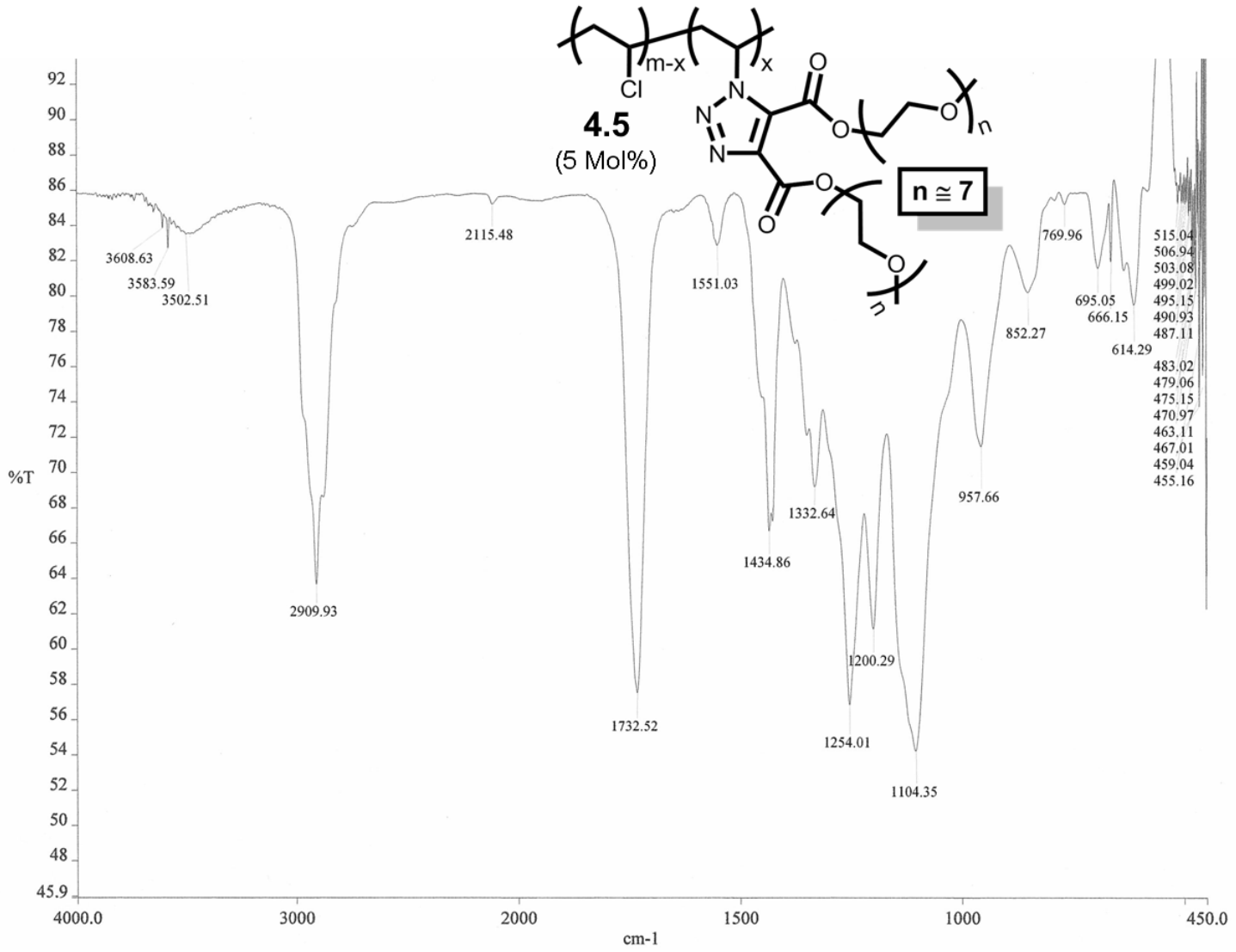
4.5
(5 Mol%)
n ≅ 7
%T
cm-1
4000.0
3000
2000
1500
1000
450.0
3608.63
3583.59
3502.51
2909.93
2115.48
1732.52
1551.03
1434.86
1332.64
1254.01
1200.29
1104.35
957.66
852.27
769.96
695.05
666.15
614.29
515.04
506.94
503.08
499.02
495.15
490.93
487.11
483.02
479.06
475.15
470.97
463.11
467.01
459.04
455.16

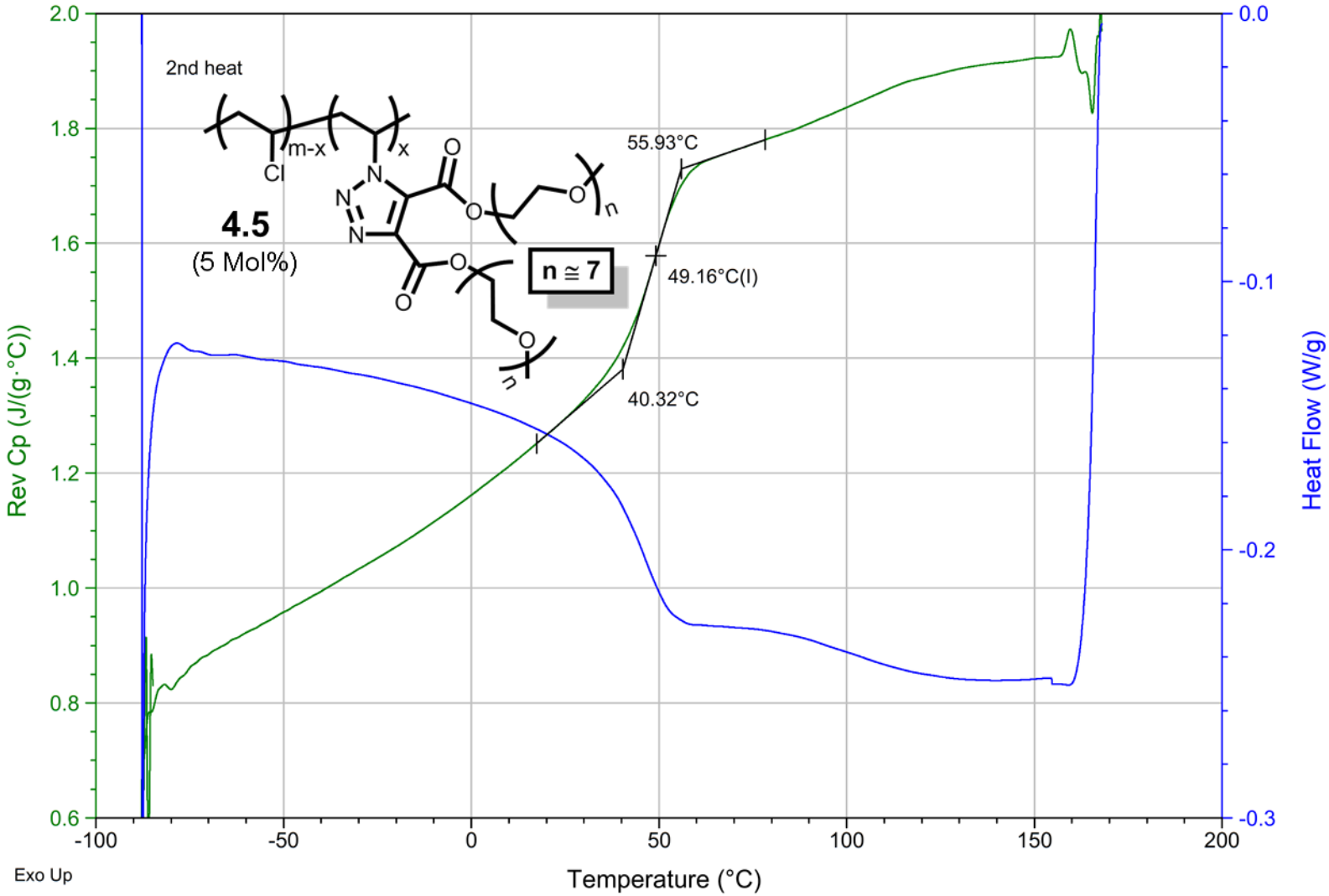
2nd heat
4.5
(5 Mol%)
n ≅ 7
55.93°C
49.16°C(I)
40.32°C
Rev Cp (J/(g·°C))
Heat Flow (W/g)
Temperature (°C)
Exo Up
2.0
1.8
1.6
1.4
1.2
1.0
0.8
0.6
0.0
-0.1
-0.2
-0.3
-100
-50
0
50
100
150
200

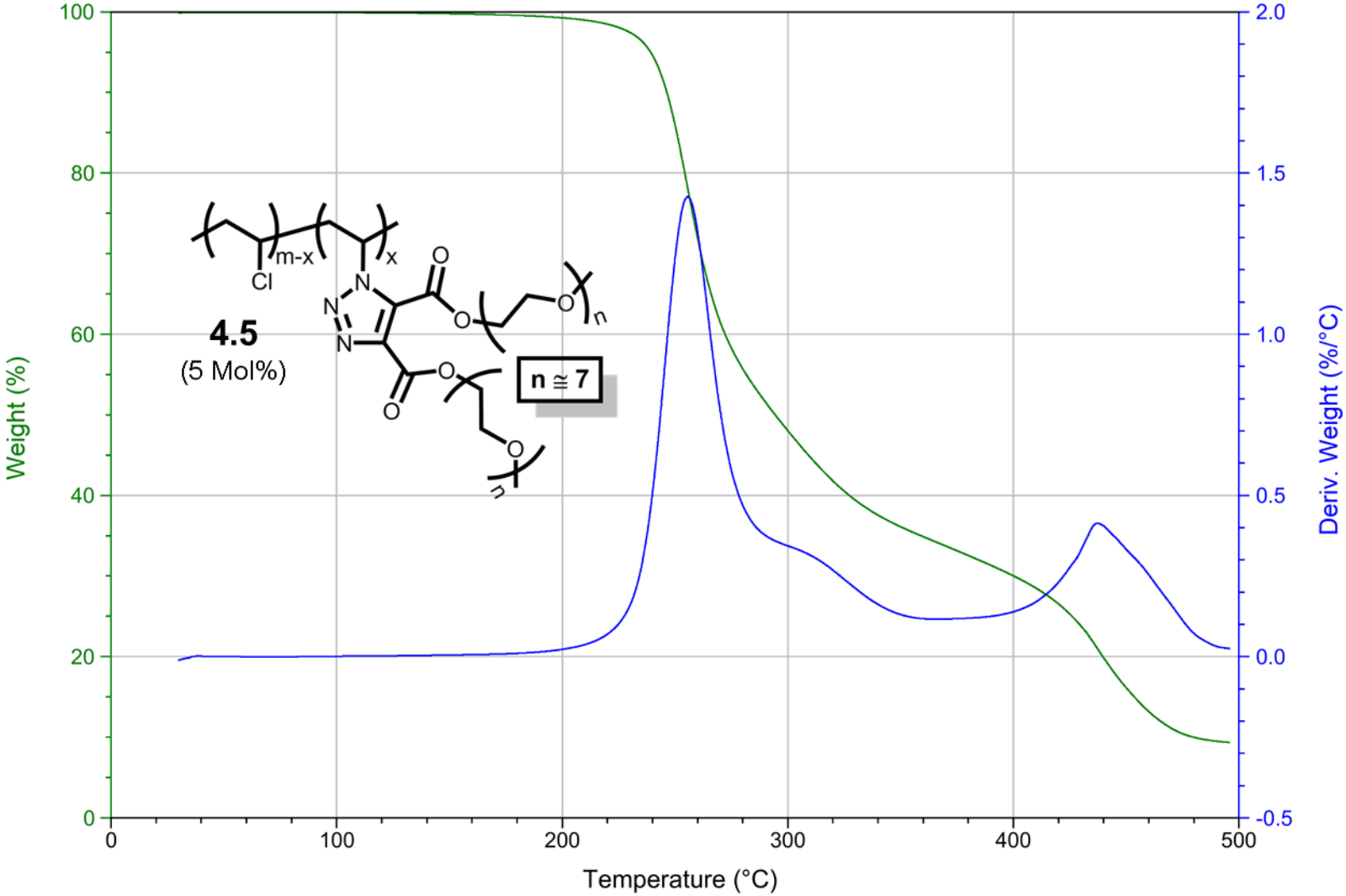
Weight (%)
Deriv. Weight (%/°C)
Temperature (°C)
100
80
60
40
20
0
2.0
1.5
1.0
0.5
0.0
-0.5
0
100
200
300
400
500
m-x
x
Cl
4.5
(5 Mol%)
n ≅ 7

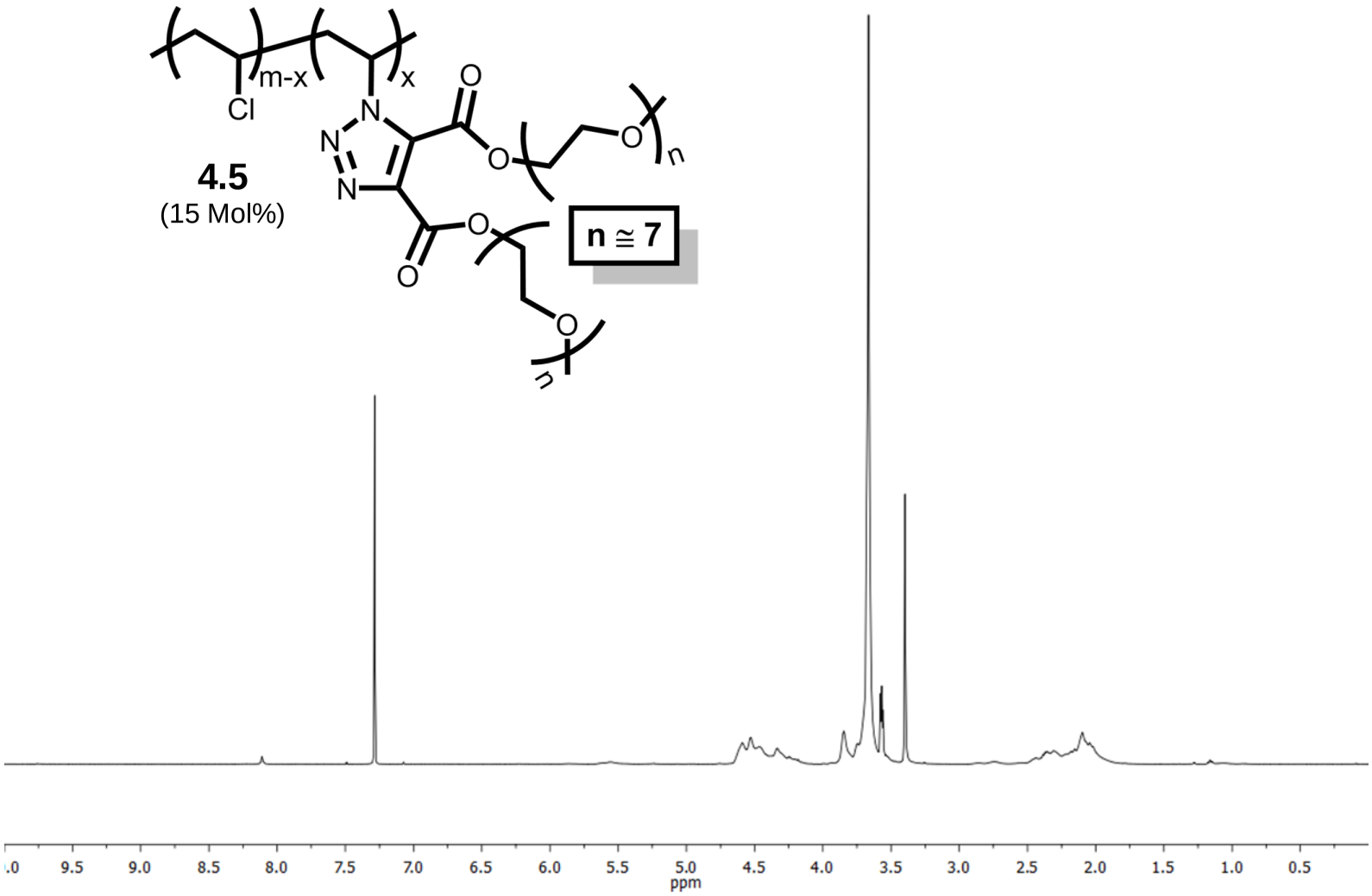
m-x
x
Cl
N
N
N
O
O
O
O
O
O
n
n
4.5
(15 Mol%)
n ≅ 7
9.5
9.0
8.5
8.0
7.5
7.0
6.5
6.0
5.5
5.0
4.5
4.0
3.5
3.0
2.5
2.0
1.5
1.0
0.5
ppm

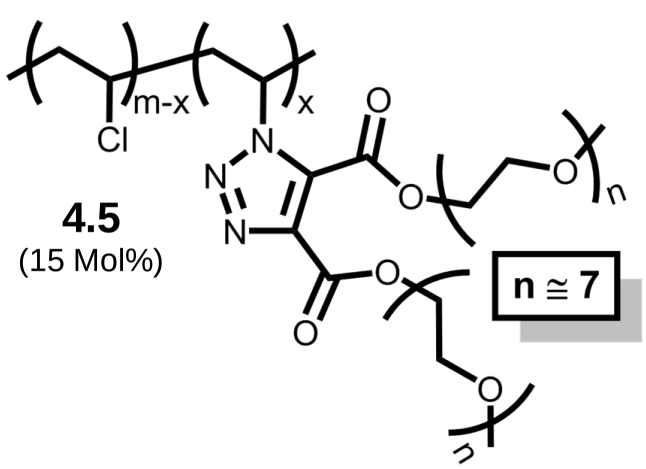
m-x
x
Cl
N
N
N
O
O
O
O
O
O
n
n
4.5
(15 Mol%)
n ≅ 7

200
190
180
170
160
150
140
130
120
110
100
90
80
70
60
50
40
30
20
10
ppm

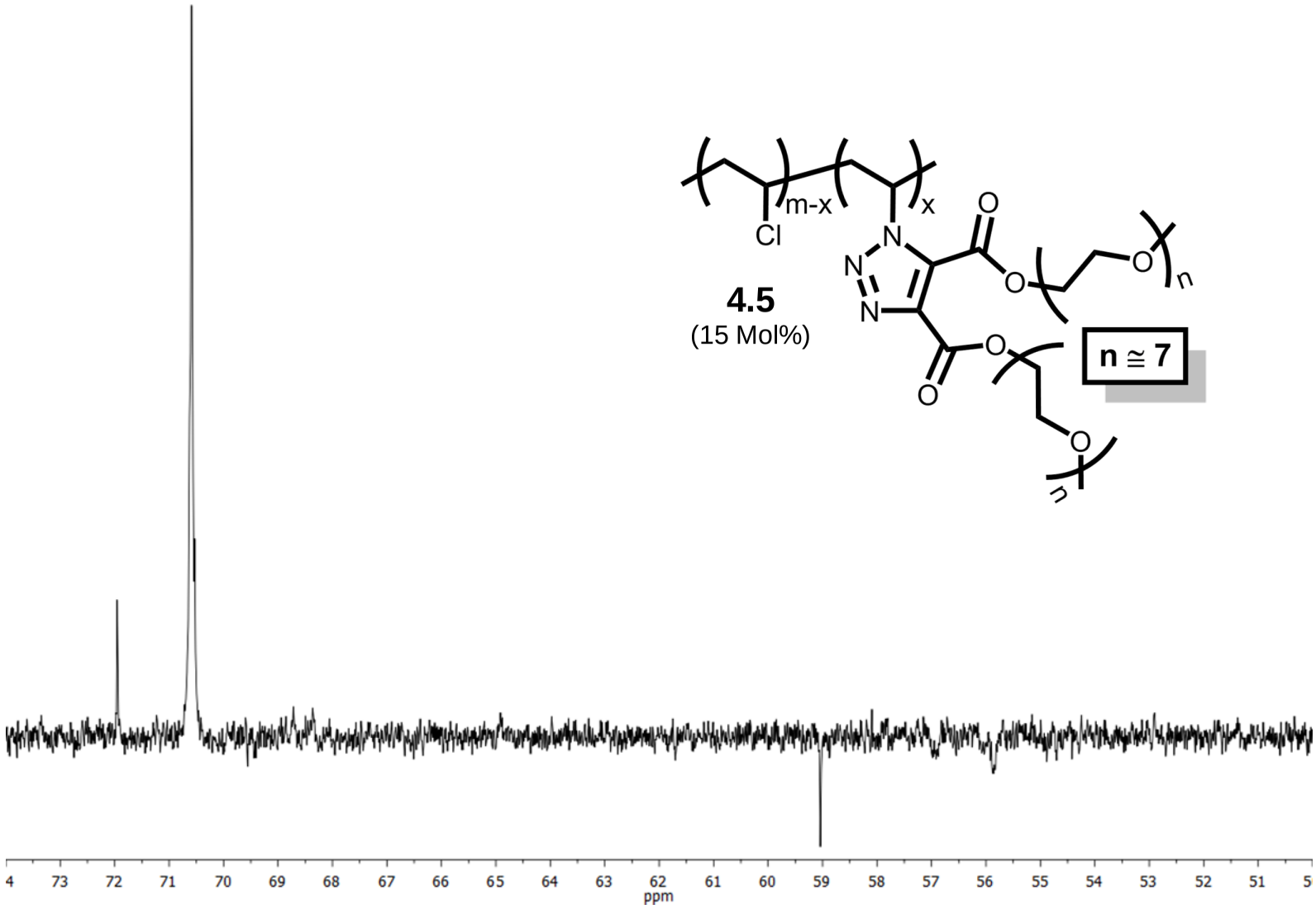
m-x
x
Cl
N
N
N
O
O
O
O
O
O
n
n
4.5
(15 Mol%)
n ≅ 7
4
73
72
71
70
69
68
67
66
65
64
63
62
61
60
59
58
57
56
55
54
53
52
51
5
ppm

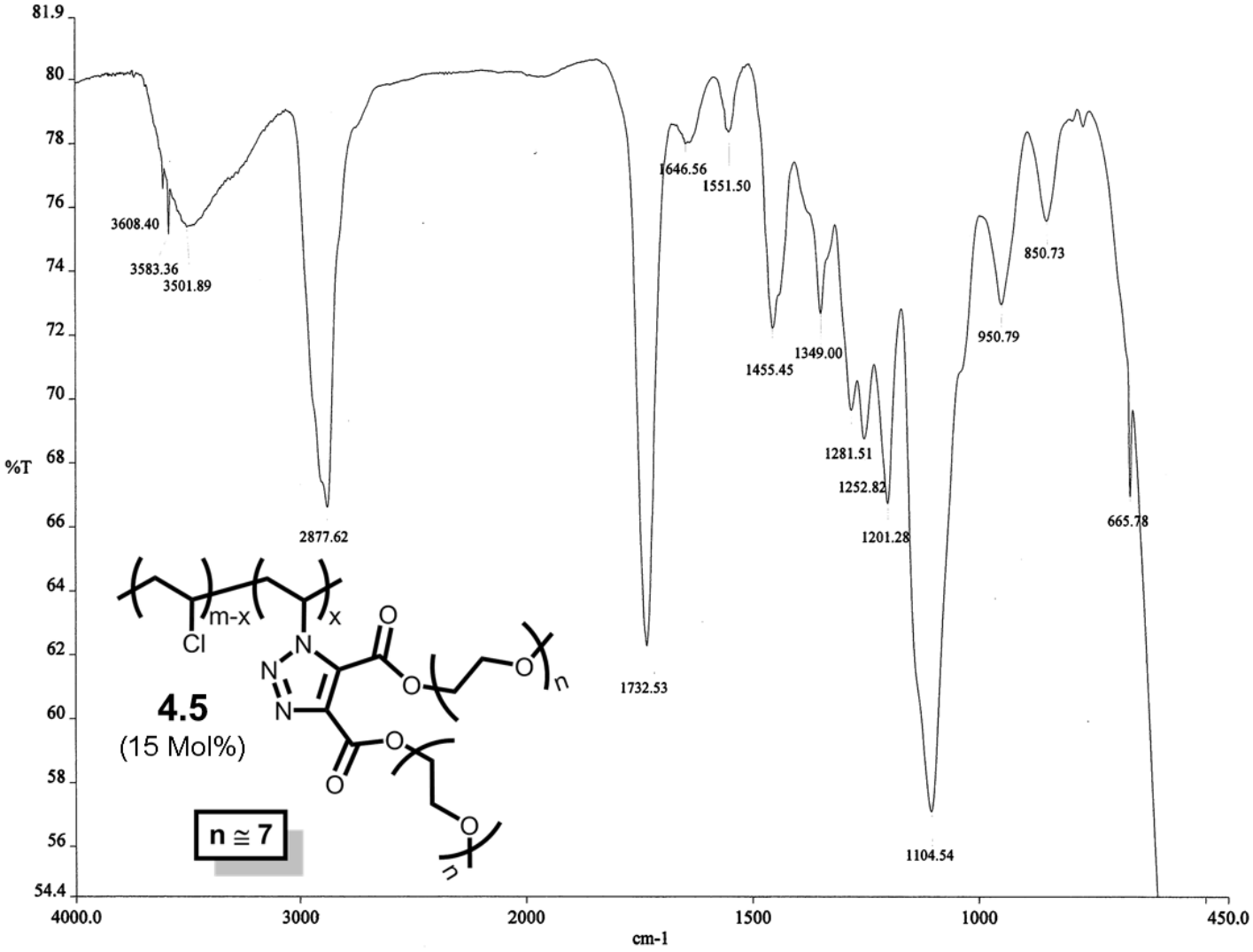
81.9
80
78
76
74
72
70
68
66
64
62
60
58
56
54.4
%T
4000.0
3000
2000
1500
1000
450.0
cm-1
3608.40
3583.36
3501.89
2877.62
1646.56
1551.50
1455.45
1349.00
1281.51
1252.82
1201.28
1732.53
1104.54
950.79
850.73
665.78
m-x
x
Cl
N
N
N
O
O
O
O
O
O
n
n
4.5
(15 Mol%)
n ≅ 7

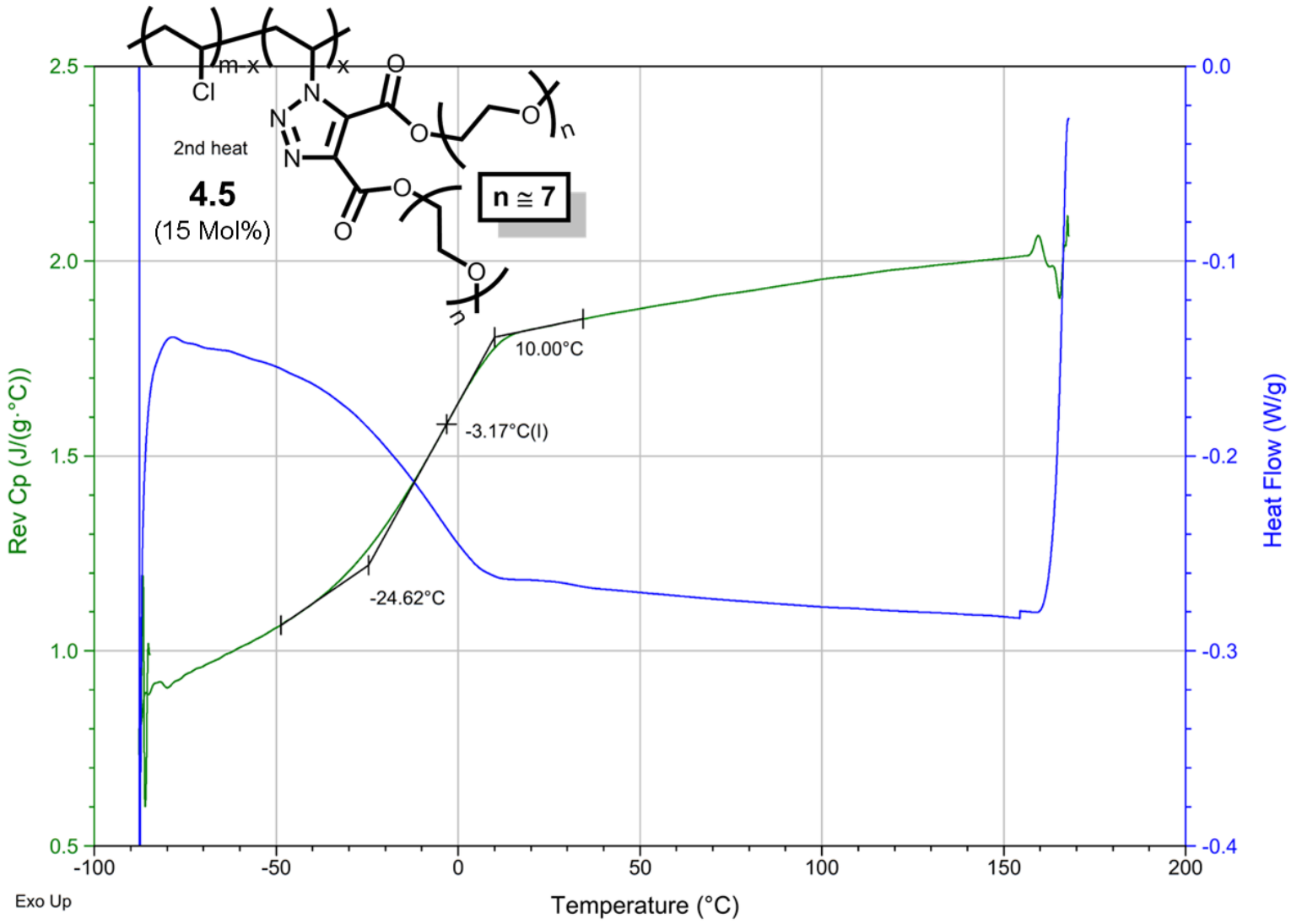
2nd heat
4.5
(15 Mol%)
n ≅ 7
10.00°C
-3.17°C(I)
-24.62°C
Rev Cp (J/(g·°C))
Heat Flow (W/g)
Temperature (°C)
Exo Up
2.5
2.0
1.5
1.0
0.5
0.0
-0.1
-0.2
-0.3
-0.4
-100
-50
0
50
100
150
200

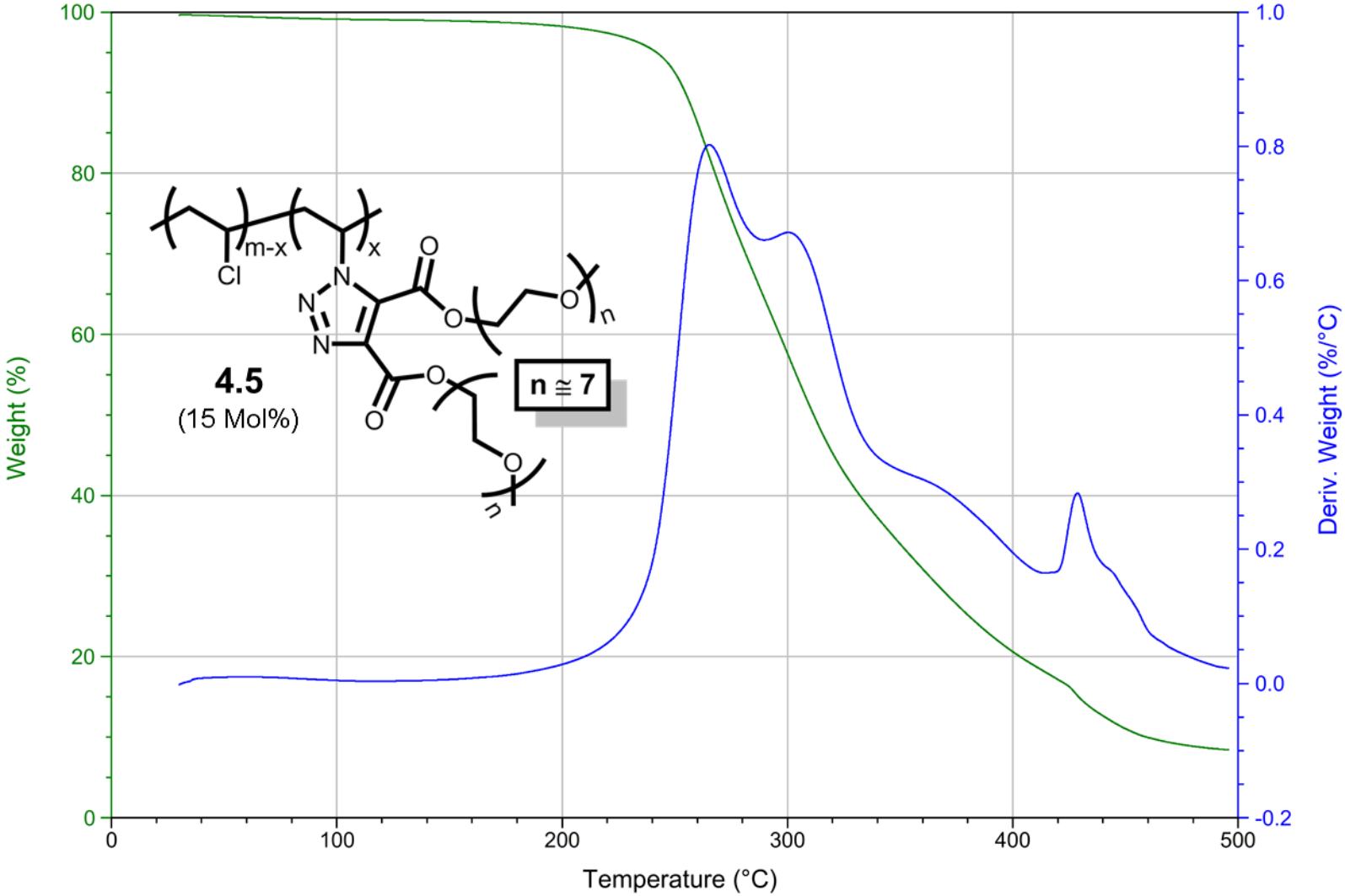
Weight (%)
Deriv. Weight (%/°C)
Temperature (°C)
0
20
40
60
80
100
-0.2
0.0
0.2
0.4
0.6
0.8
1.0
0
100
200
300
400
500
m-x
x
Cl
N
N
N
O
O
O
O
O
n
4.5
(15 Mol%)
n ≅ 7

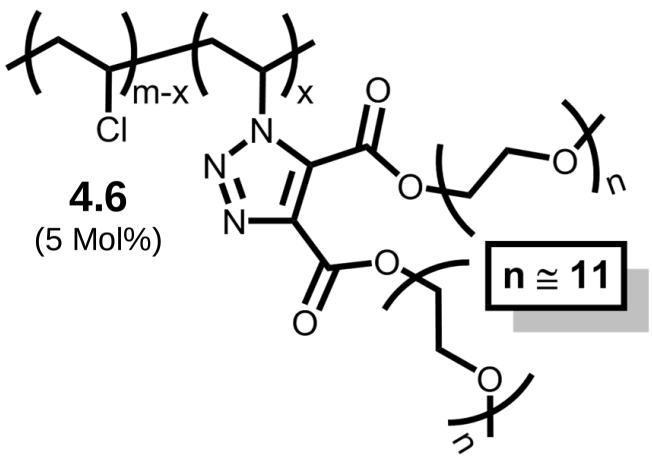
m-x
x
Cl
N
N
N
O
O
O
O
O
n
n
O
n ≅ 11

4.6
(5 Mol%)

9.5
9.0
8.5
8.0
7.5
7.0
6.5
6.0
5.5
5.0
4.5
4.0
3.5
3.0
2.5
2.0
1.5
1.0
0.5
ppm

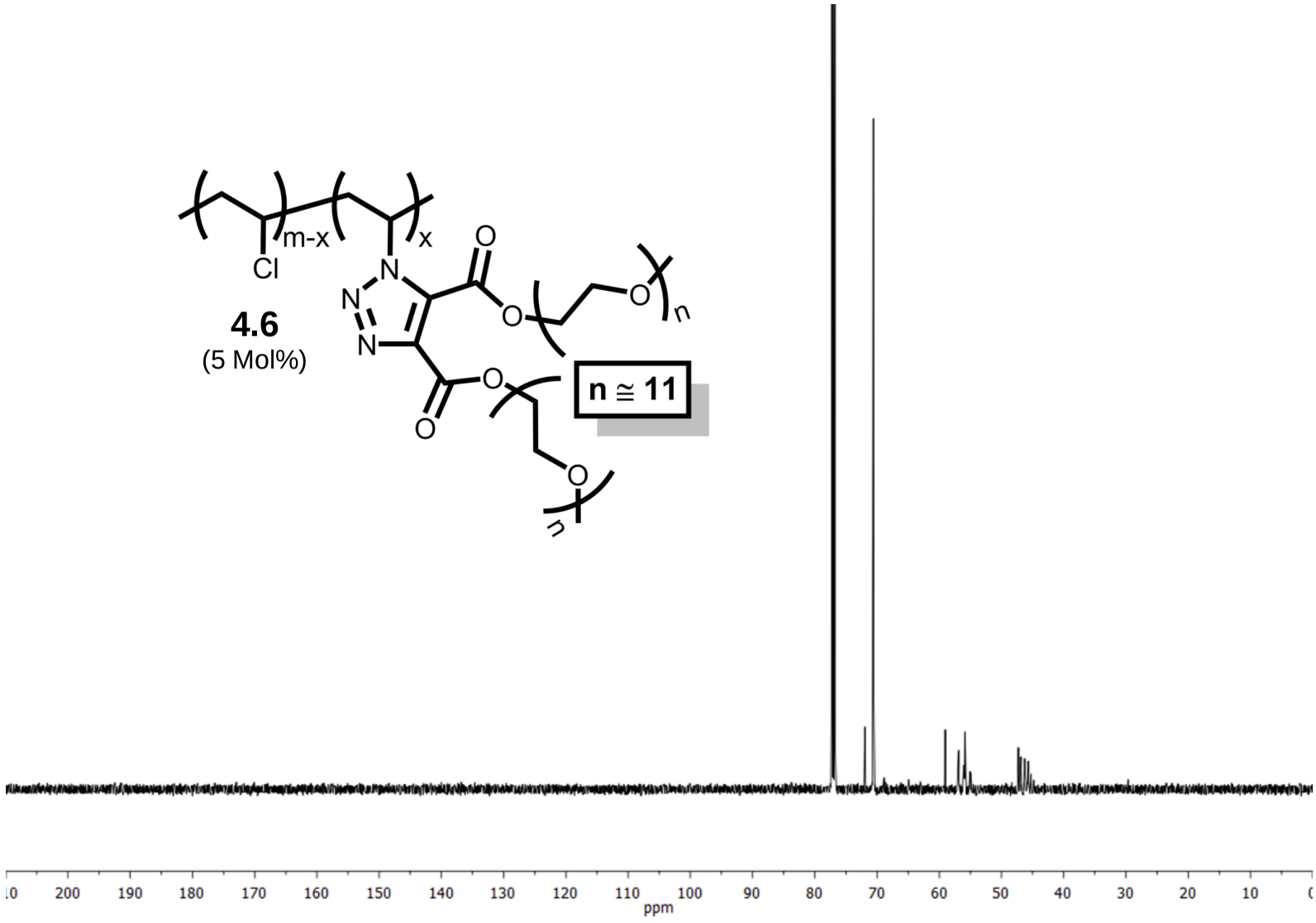
m-x
x
Cl
N
N
N
O
O
O
O
O
n
n
4.6
(5 Mol%)
n ≅ 11
ppm

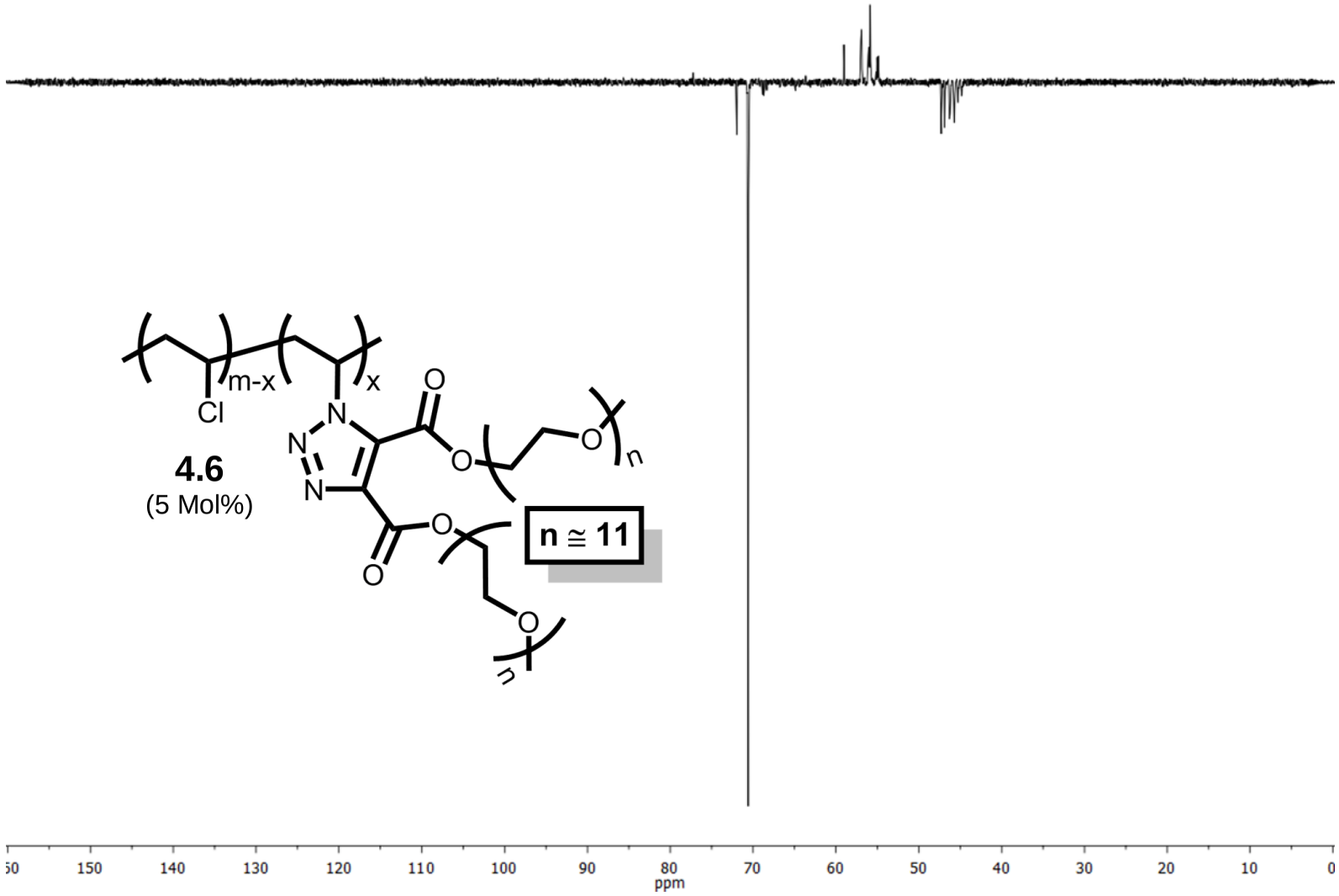
m-x
x
Cl
N
N
N
O
O
O
O
O
O
n
n
4.6
(5 Mol%)
n ≅ 11
150
140
130
120
110
100
90
80
70
60
50
40
30
20
10
0
ppm

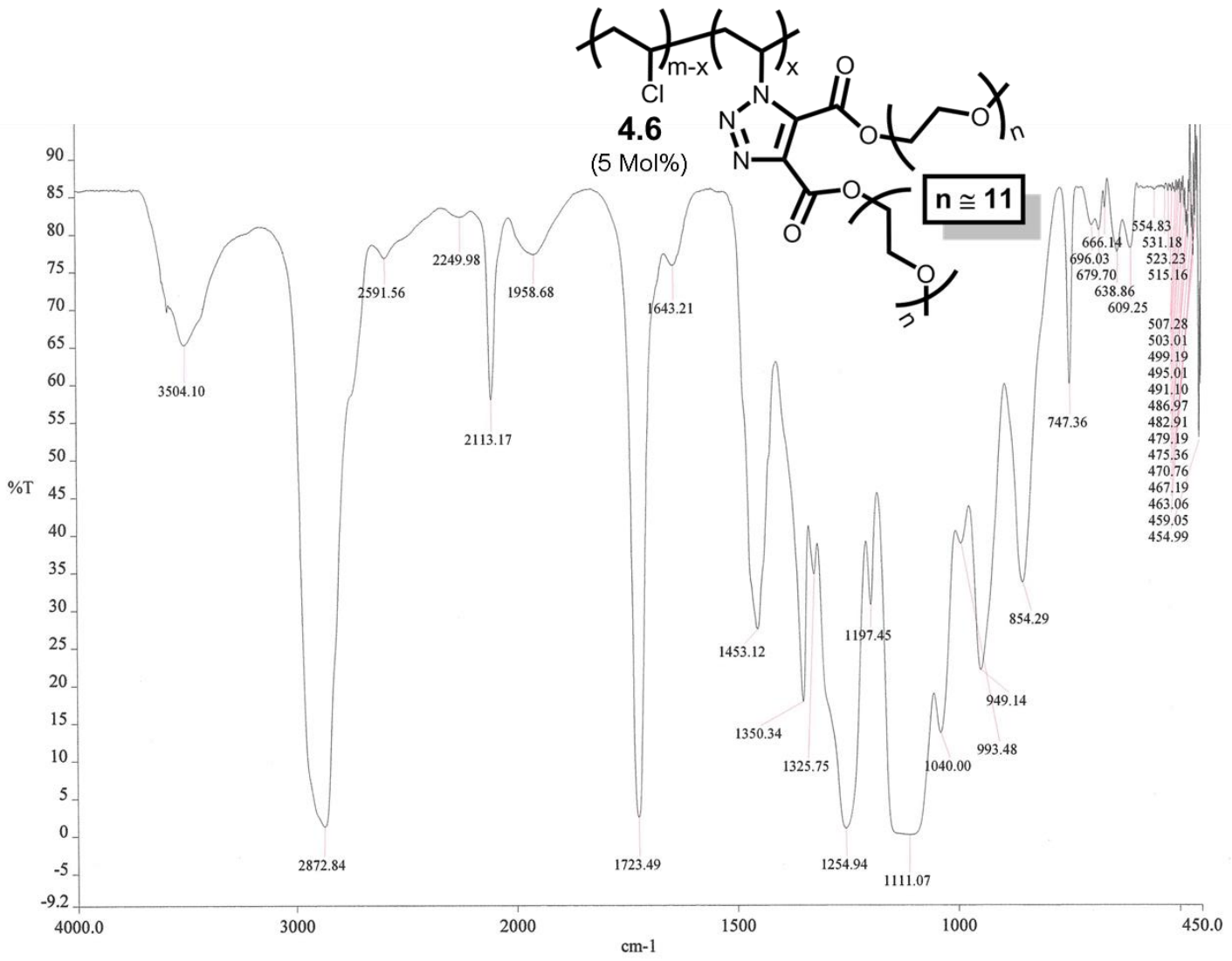
4.6
(5 Mol%)
n ≅ 11
%T
cm-1
3504.10
2872.84
2591.56
2249.98
2113.17
1958.68
1723.49
1643.21
1453.12
1350.34
1325.75
1254.94
1197.45
1111.07
1040.00
993.48
949.14
854.29
747.36
666.14
696.03
679.70
638.86
609.25
554.83
531.18
523.23
515.16
507.28
503.01
499.19
495.01
491.10
486.97
482.91
479.19
475.36
470.76
467.19
463.06
459.05
454.99

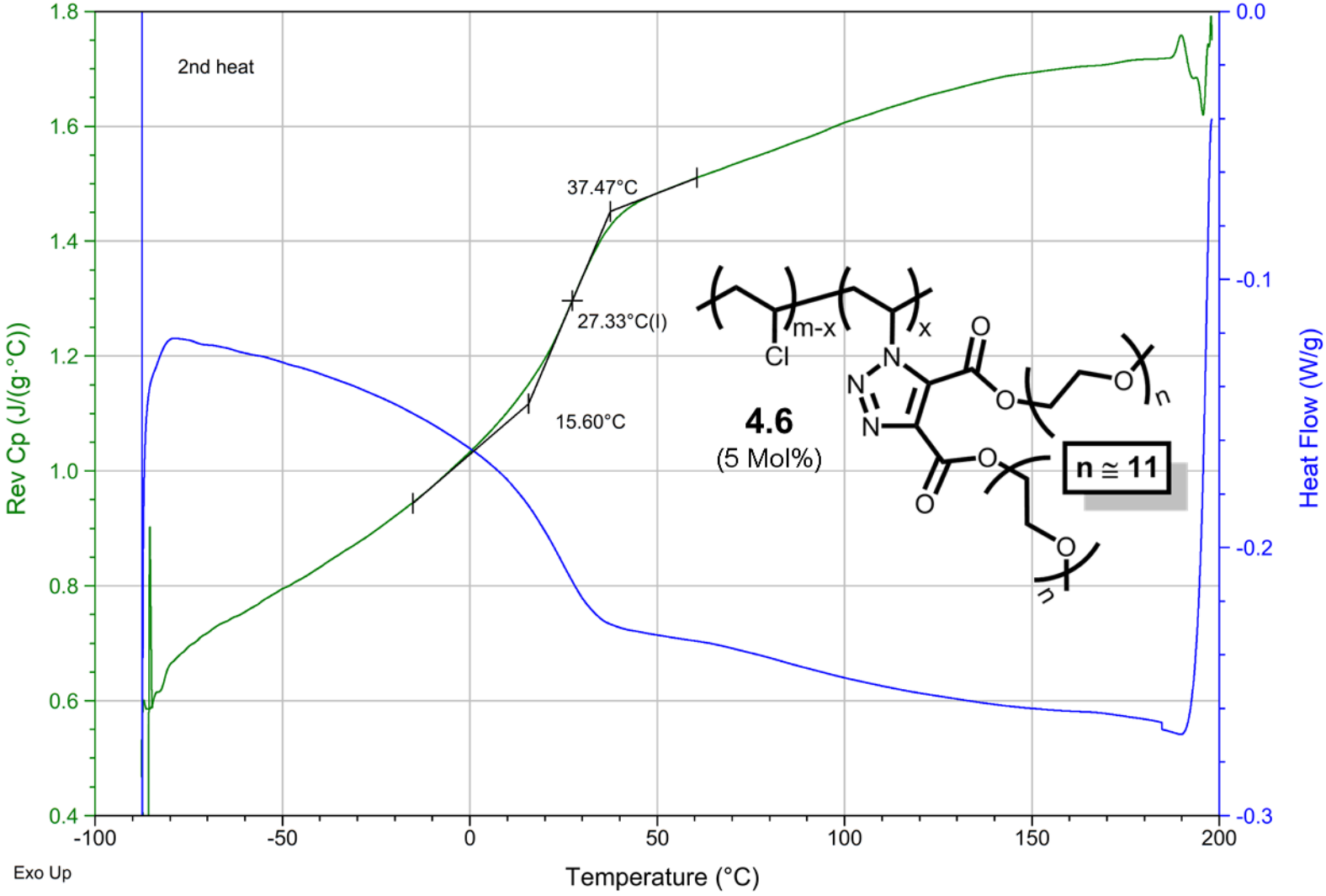
2nd heat
37.47°C
27.33°C(I)
15.60°C
4.6
(5 Mol%)
m-x
x
Cl
n ≅ 11
Rev Cp (J/(g·°C))
Heat Flow (W/g)
Temperature (°C)
Exo Up
1.8
1.6
1.4
1.2
1.0
0.8
0.6
0.4
0.0
-0.1
-0.2
-0.3
-100
-50
0
50
100
150
200

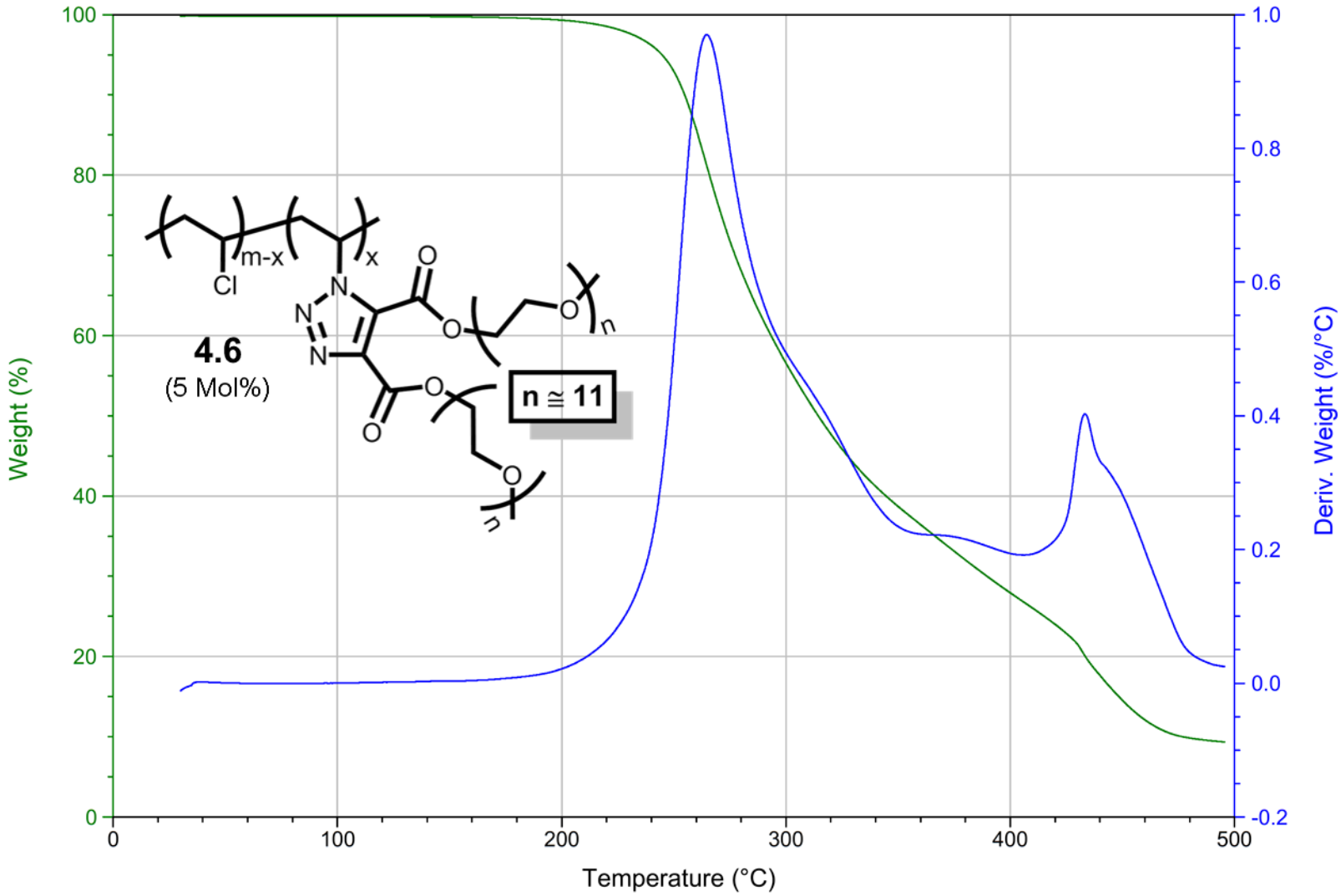
Weight (%)
Deriv. Weight (%/°C)
Temperature (°C)
0
20
40
60
80
100
-0.2
0.0
0.2
0.4
0.6
0.8
1.0
0
100
200
300
400
500
m-x
x
Cl
N
N
N
O
O
O
O
O
n
n ≅ 11
4.6
(5 Mol%)

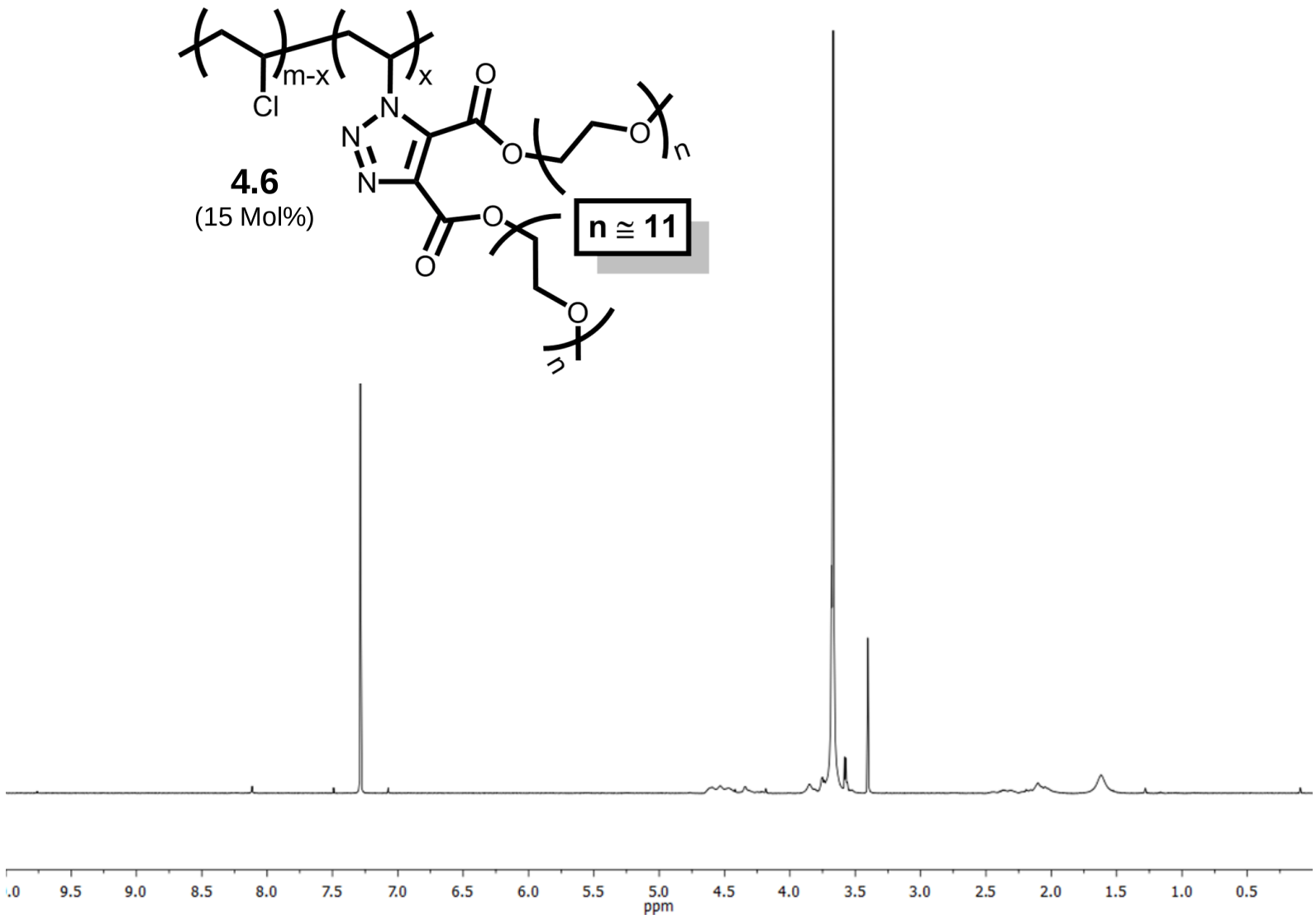
m-x
x
Cl
N
N
N
O
O
O
O
O
n
n
4.6
(15 Mol%)
n ≅ 11
9.5
9.0
8.5
8.0
7.5
7.0
6.5
6.0
5.5
5.0
4.5
4.0
3.5
3.0
2.5
2.0
1.5
1.0
0.5
ppm

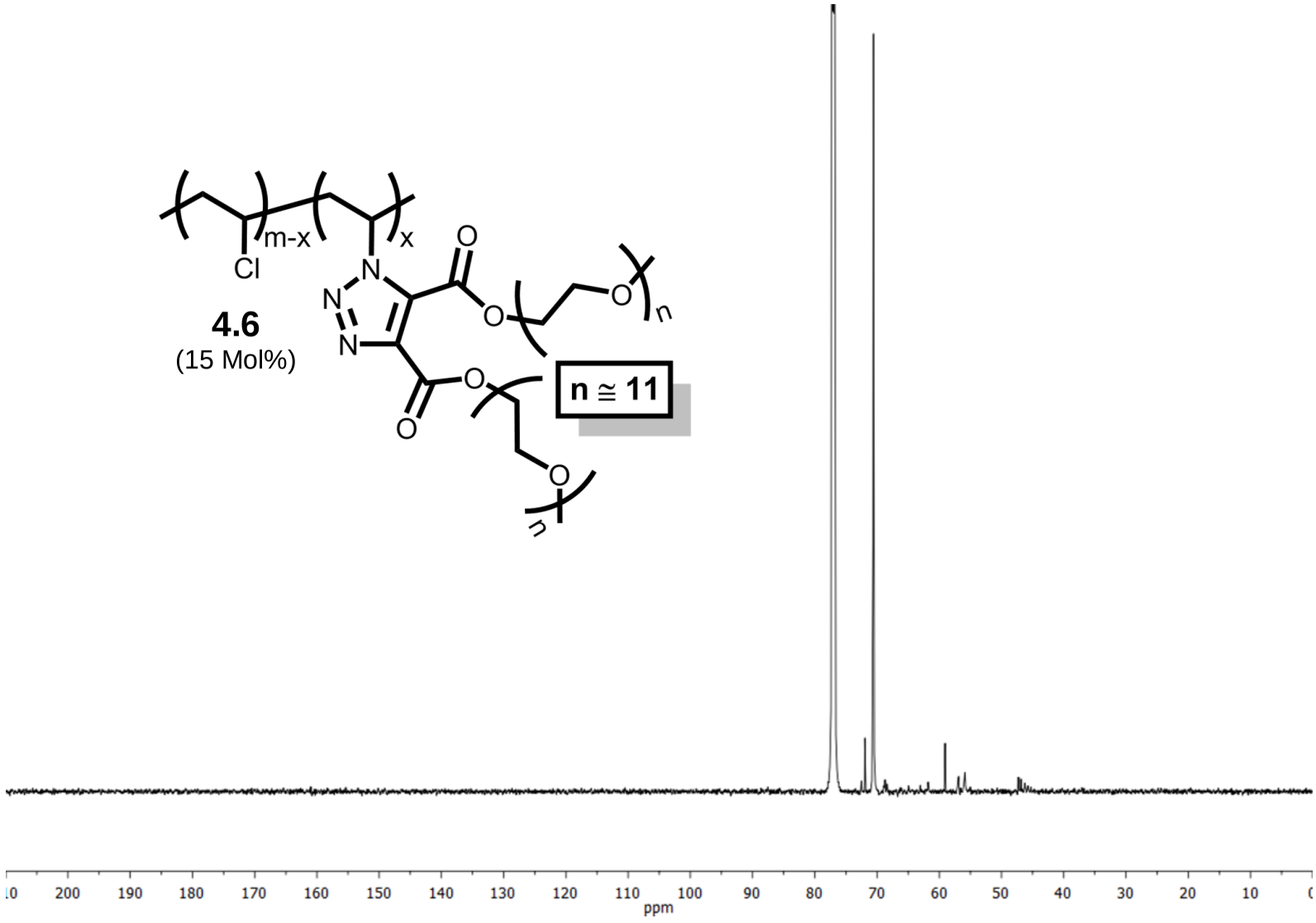
m-x
x
Cl
N
N
N
O
O
O
O
O
n
O
O
n
4.6
(15 Mol%)
n ≅ 11
ppm

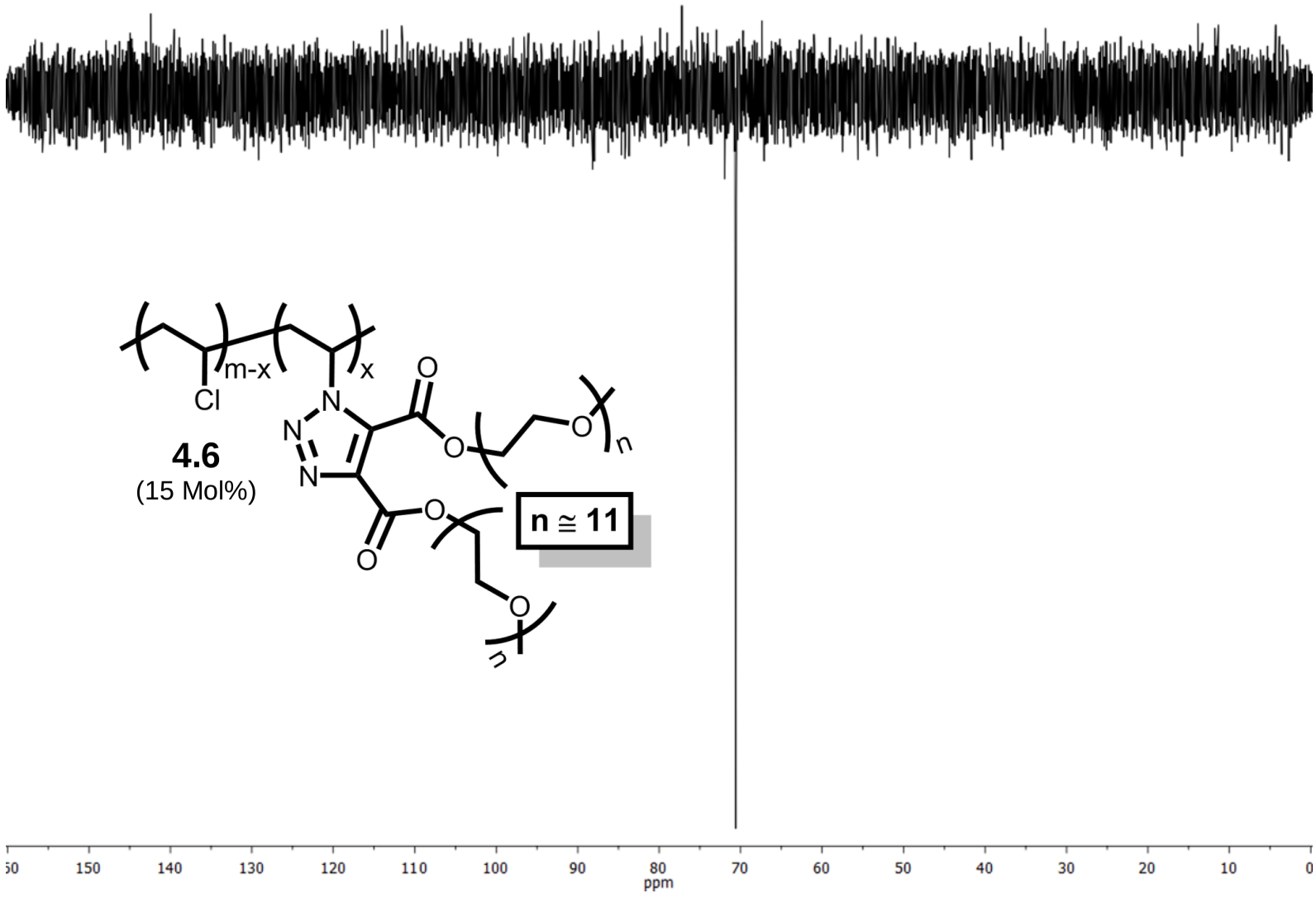
m-x
x
Cl
4.6
(15 Mol%)
N
N
N
O
O
O
O
O
O
n
n ≅ 11
n
150
140
130
120
110
100
90
80
70
60
50
40
30
20
10
0
ppm

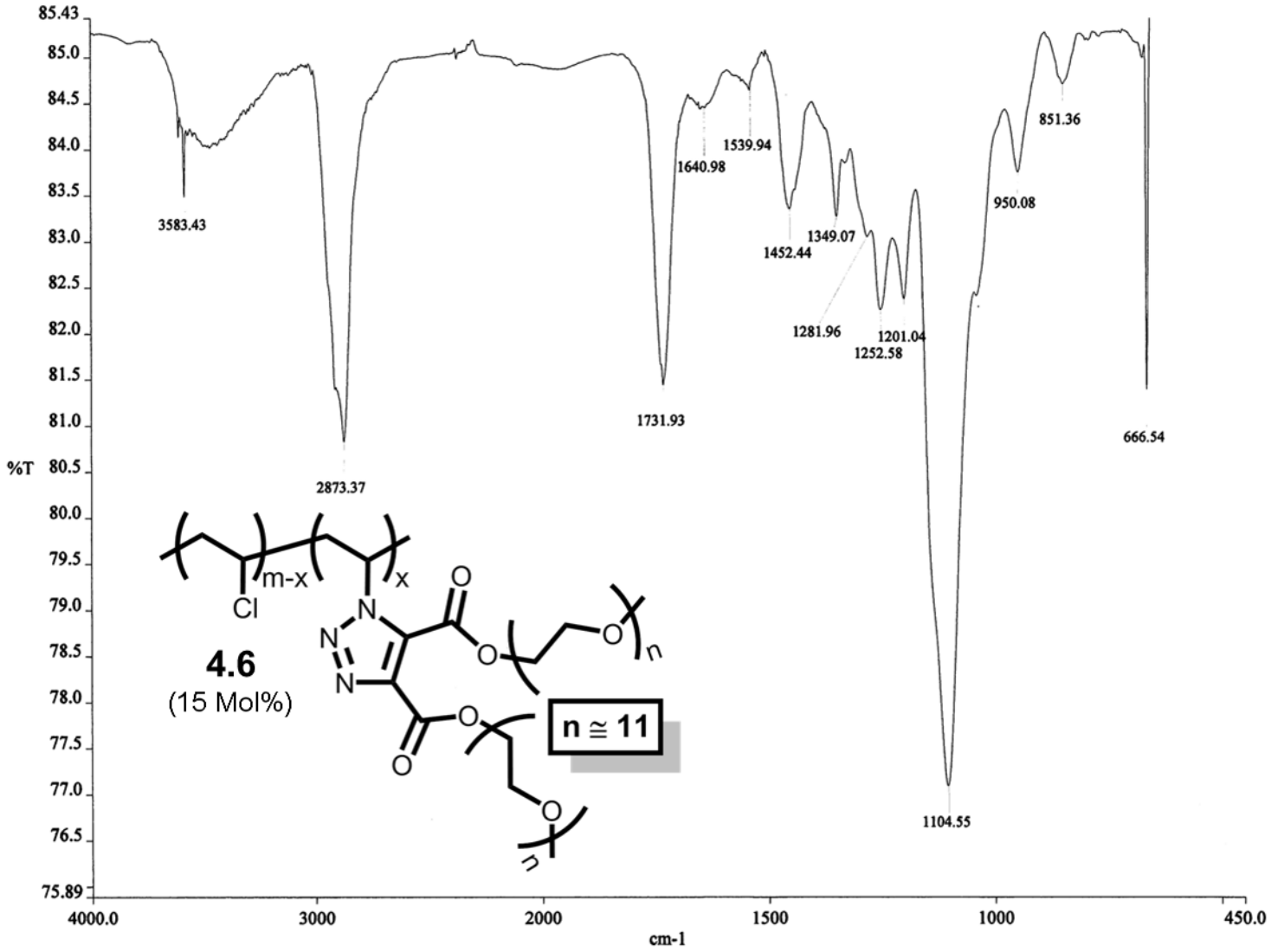
85.43
85.0
84.5
84.0
83.5
83.0
82.5
82.0
81.5
81.0
80.5
80.0
79.5
79.0
78.5
78.0
77.5
77.0
76.5
75.89
%T
4000.0
3000
2000
1500
1000
450.0
cm-1
3583.43
2873.37
1731.93
1640.98
1539.94
1452.44
1349.07
1281.96
1252.58
1201.04
1104.55
950.08
851.36
666.54
m-x
x
Cl
4.6
(15 Mol%)
n ≅ 11

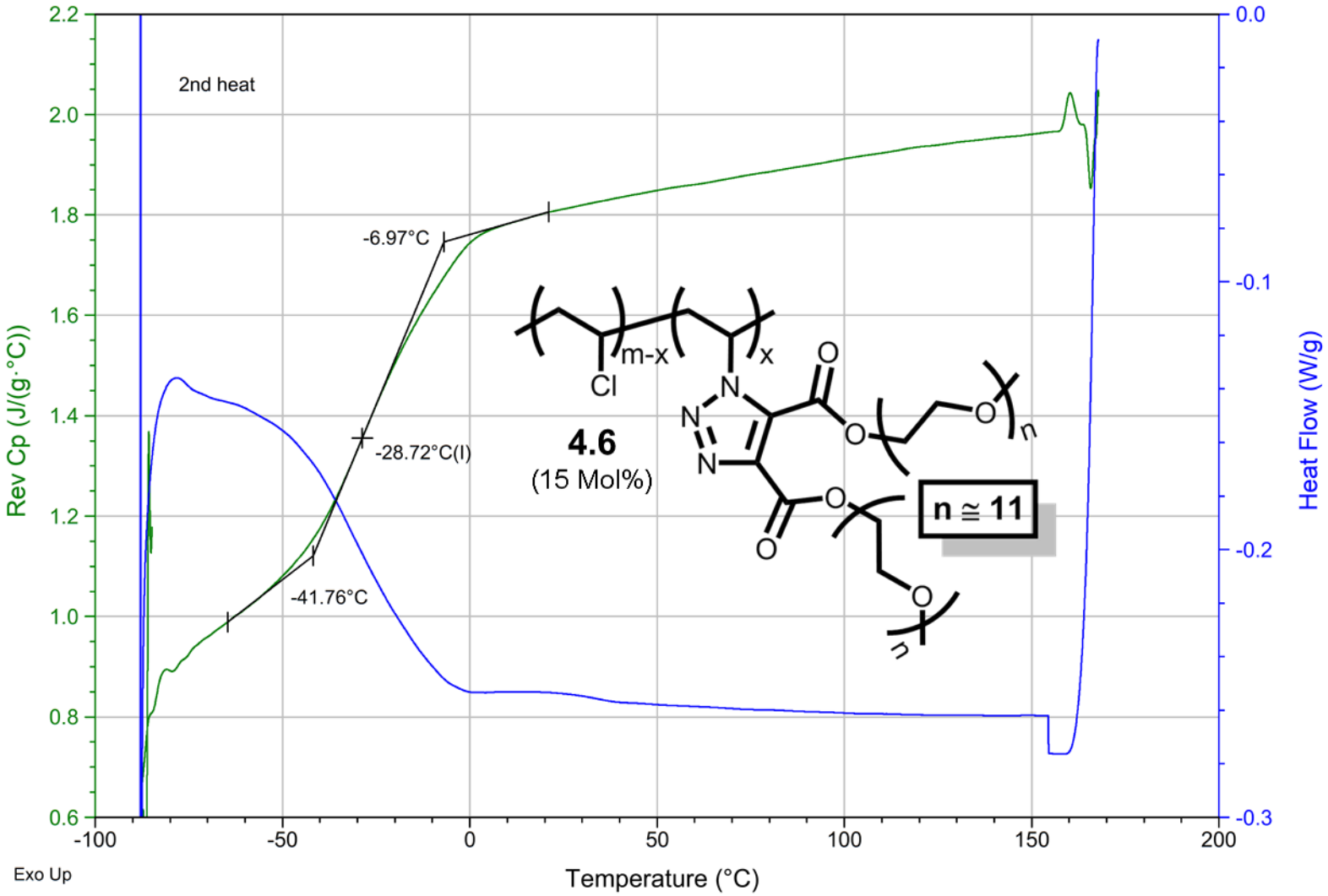
2nd heat
-6.97°C
-28.72°C(I)
-41.76°C
4.6
(15 Mol%)
m-x
x
Cl
n ≅ 11
Rev Cp (J/(g·°C))
Heat Flow (W/g)
Temperature (°C)
Exo Up
2.2
2.0
1.8
1.6
1.4
1.2
1.0
0.8
0.6
0.0
-0.1
-0.2
-0.3
-100
-50
0
50
100
150
200

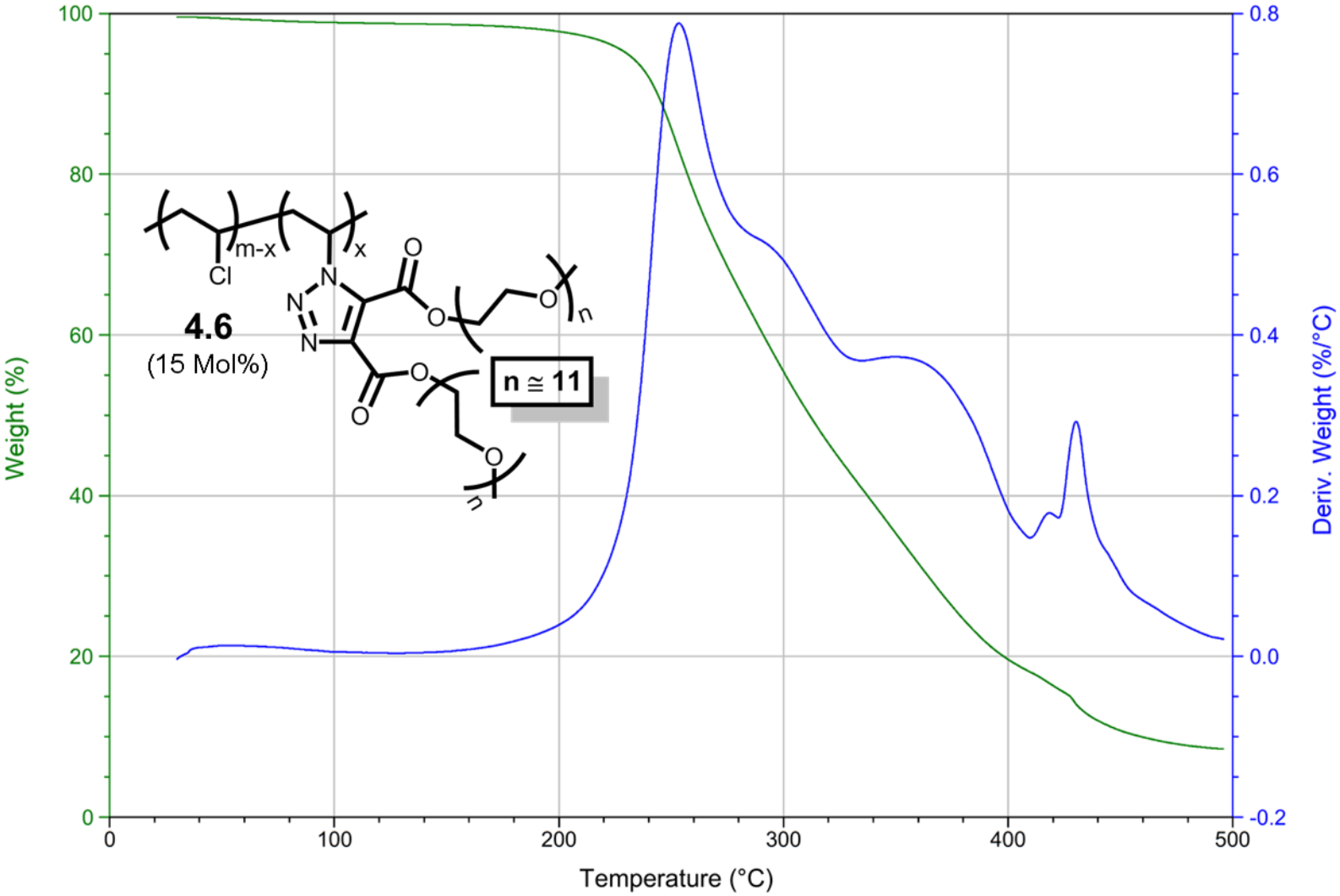
Weight (%)
Deriv. Weight (%/°C)
Temperature (°C)
0
20
40
60
80
100
-0.2
0.0
0.2
0.4
0.6
0.8
0
100
200
300
400
500
m-x
x
Cl
4.6
(15 Mol%)
n ≅ 11

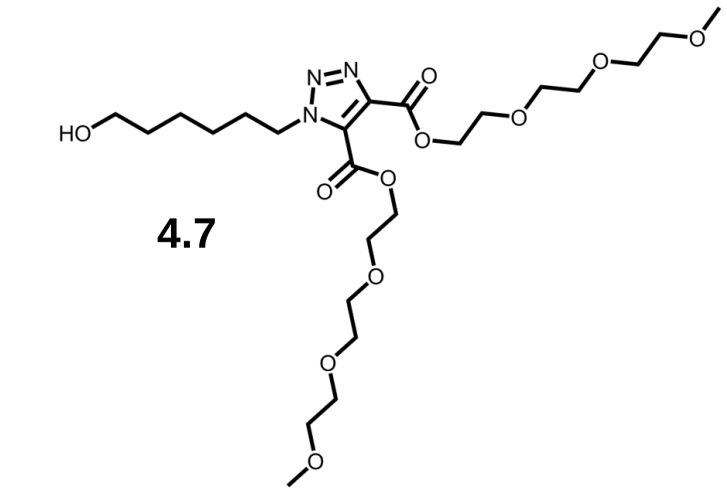
HO
N
N
N
O
O
O
O
O
O
O
O
O
O
O
O
O

4.7

9.5
9.0
8.5
8.0
7.5
7.0
6.5
6.0
5.5
5.0
4.5
4.0
3.5
3.0
2.5
2.0
1.5
1.0
0.5
ppm

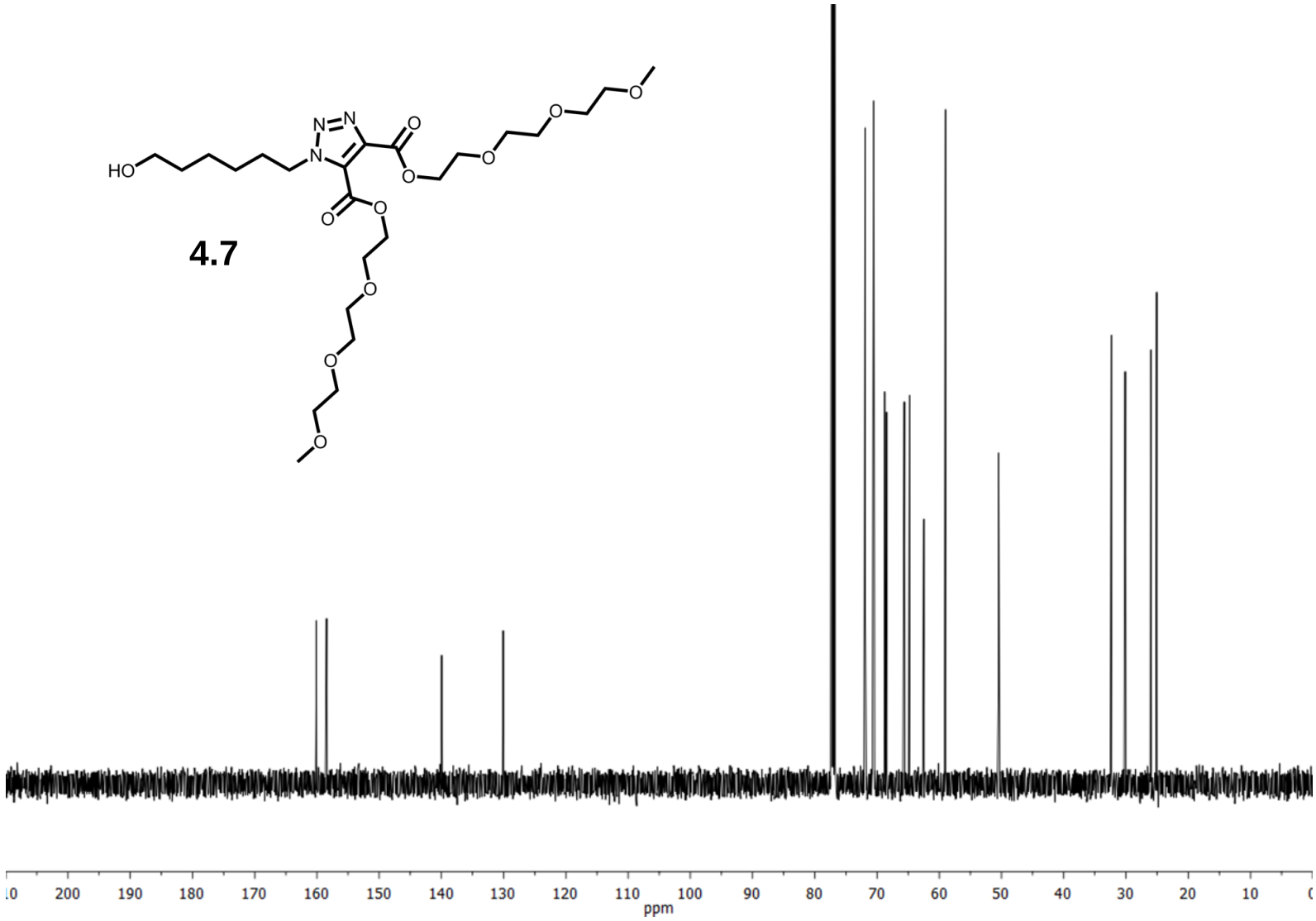
HO
N
N
N
O
O
O
O
O
O
O
O
O
O
O
O
4.7
ppm

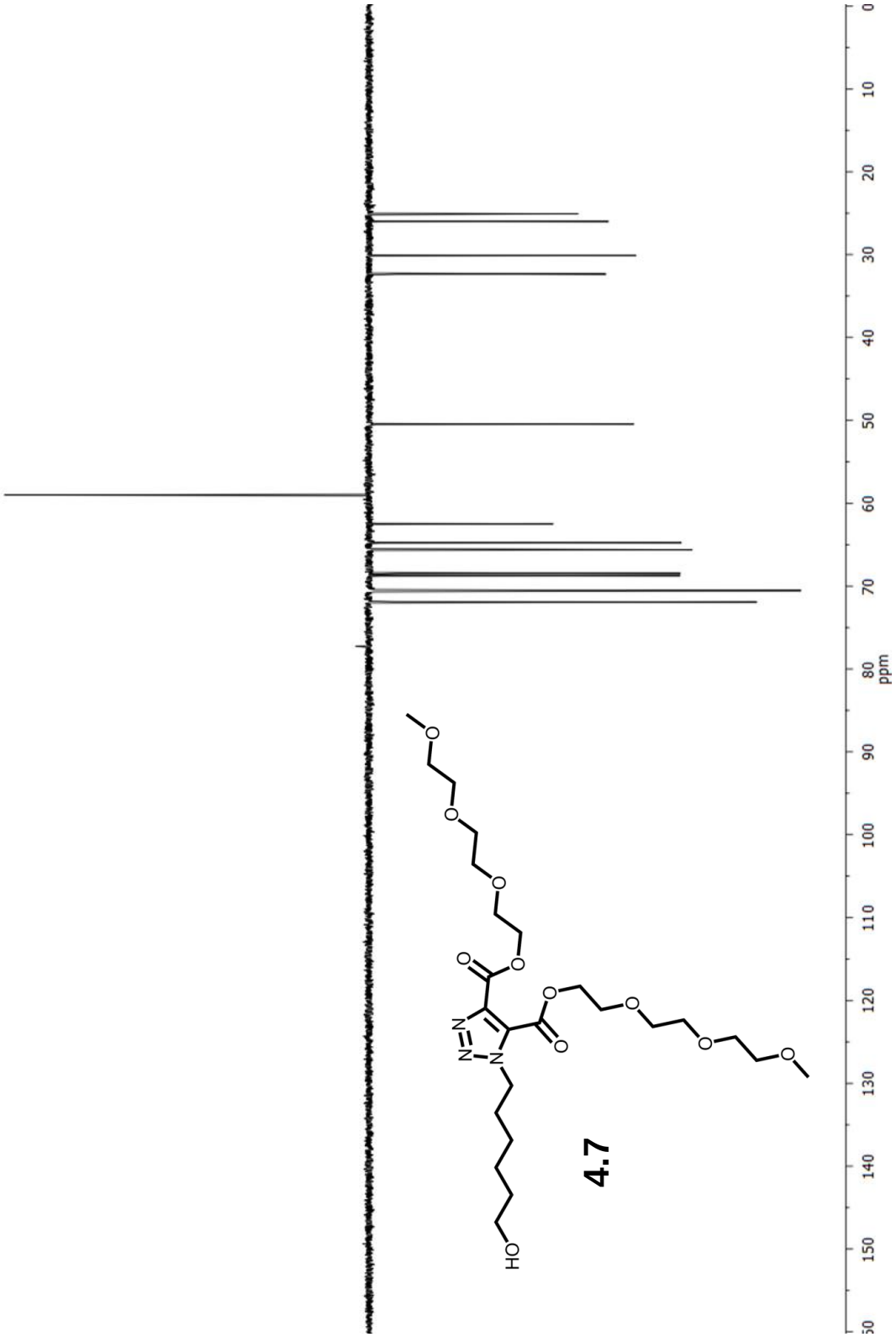
4.7
HO
ppm

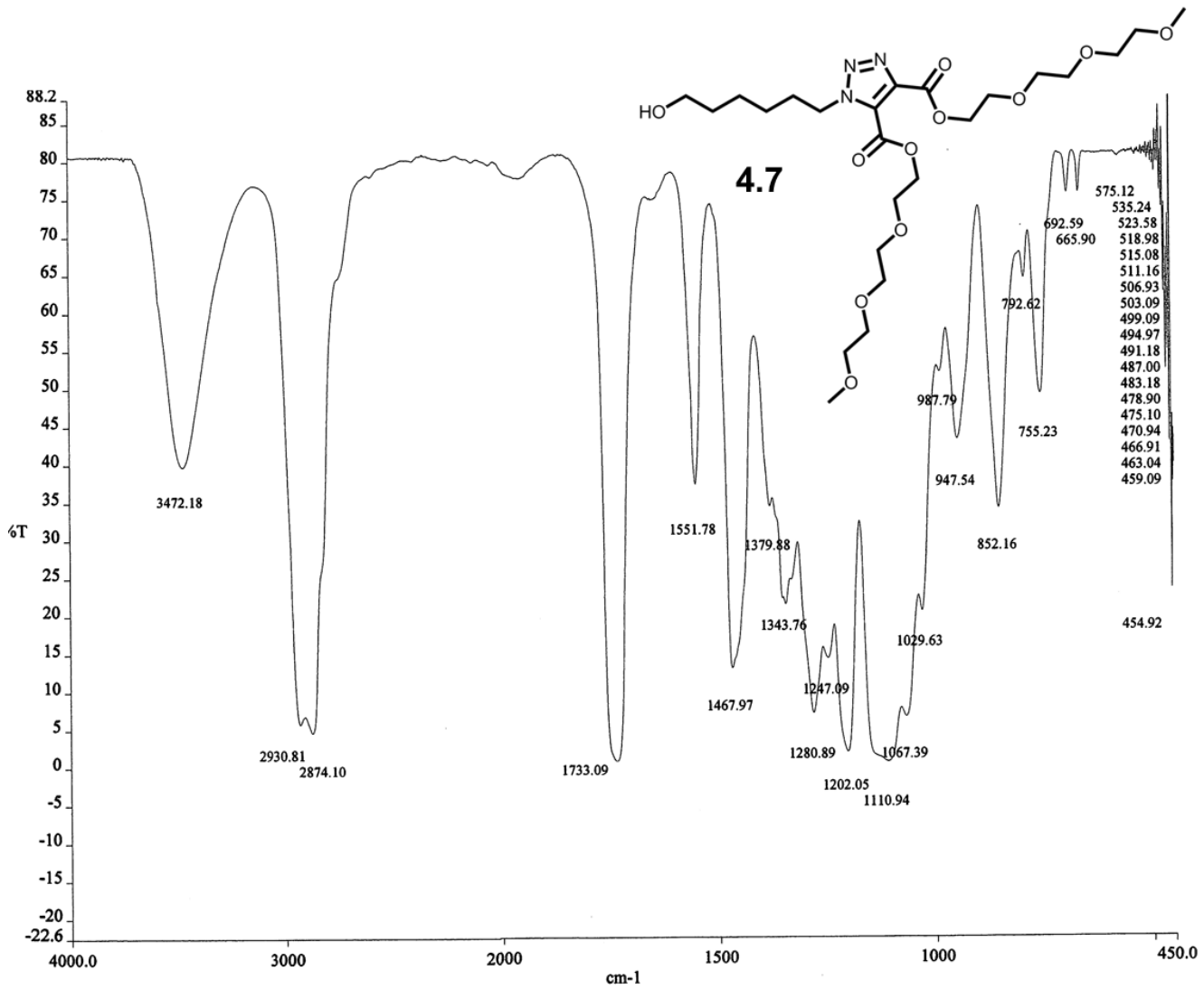
4.7
%T
cm-1
3472.18
2930.81
2874.10
1733.09
1551.78
1467.97
1379.88
1343.76
1280.89
1247.09
1202.05
1110.94
1067.39
1029.63
987.79
947.54
852.16
792.62
755.23
692.59
665.90
575.12
535.24
523.58
518.98
515.08
511.16
506.93
503.09
499.09
494.97
491.18
487.00
483.18
478.90
475.10
470.94
466.91
463.04
459.09
454.92

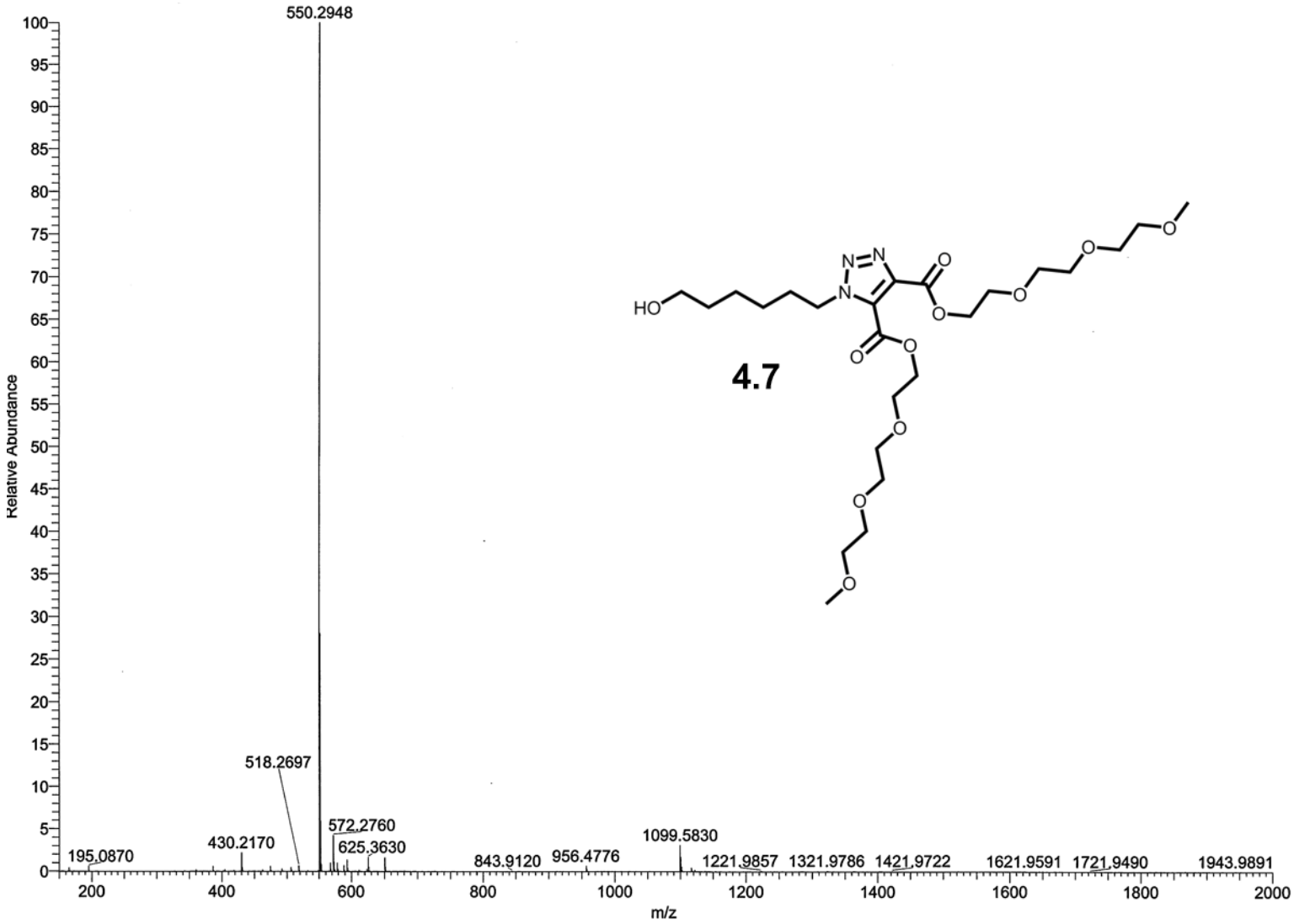
550.2948
518.2697
572.2760
625.3630
430.2170
195.0870
843.9120
956.4776
1099.5830
1221.9857
1321.9786
1421.9722
1621.9591
1721.9490
1943.9891
Relative Abundance
m/z
HO
4.7

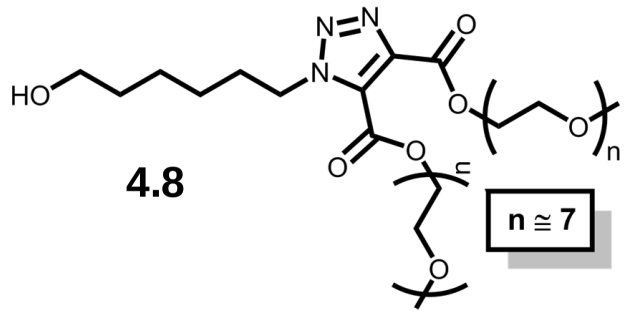
HO
N
N
N
O
O
O
O
O
n
O
n ≅ 7

4.8

10.0
9.5
9.0
8.5
8.0
7.5
7.0
6.5
6.0
5.5
5.0
4.5
4.0
3.5
3.0
2.5
2.0
1.5
1.0
0.5
ppm

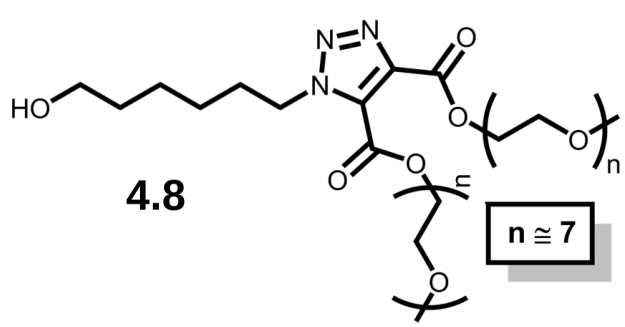
HO
N
N
N
O
O
O
O
n
O
O
n
O
n ≅ 7

4.8

200
190
180
170
160
150
140
130
120
110
100
90
80
70
60
50
40
30
20
10
ppm

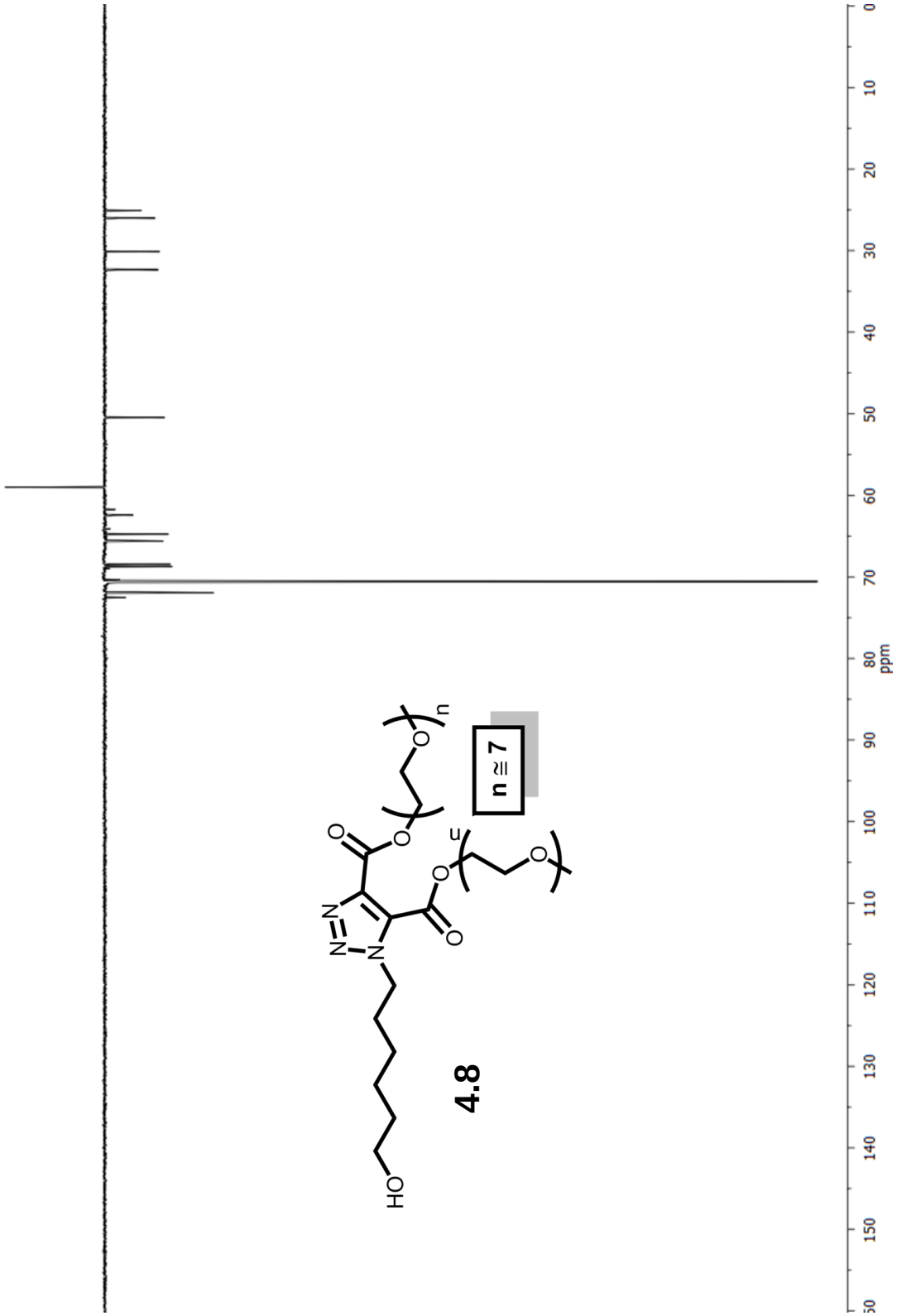
n ≅ 7
HO
4.8
ppm

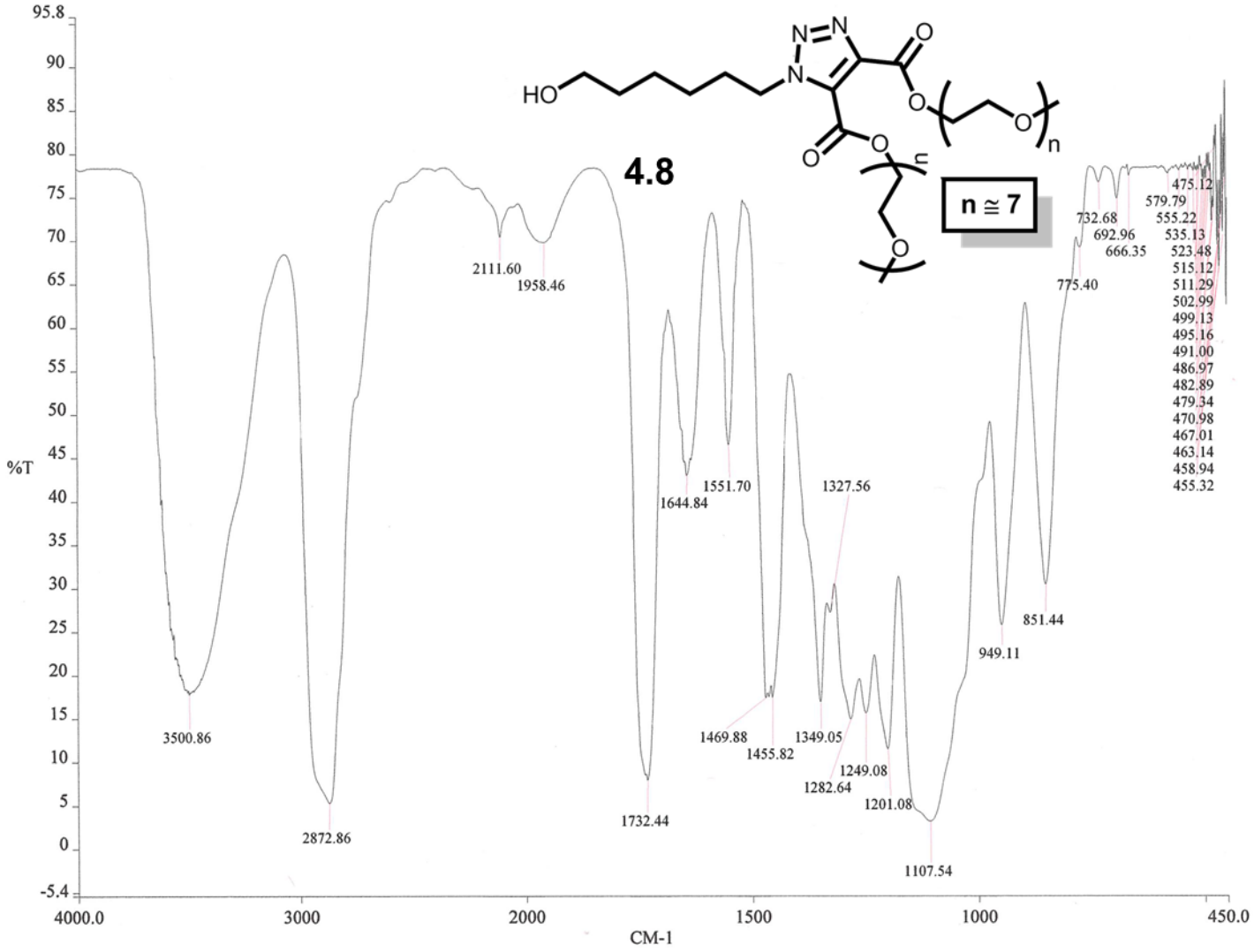
4.8
n ≅ 7
%T
CM-1
95.8
90
85
80
75
70
65
60
55
50
45
40
35
30
25
20
15
10
5
0
-5.4
4000.0
3000
2000
1500
1000
450.0
3500.86
2872.86
2111.60
1958.46
1732.44
1644.84
1551.70
1469.88
1455.82
1349.05
1327.56
1282.64
1249.08
1201.08
1107.54
949.11
851.44
775.40
732.68
692.96
666.35
579.79
555.22
535.13
523.48
515.12
511.29
502.99
499.13
495.16
491.00
486.97
482.89
479.34
475.12
470.98
467.01
463.14
458.94
455.32

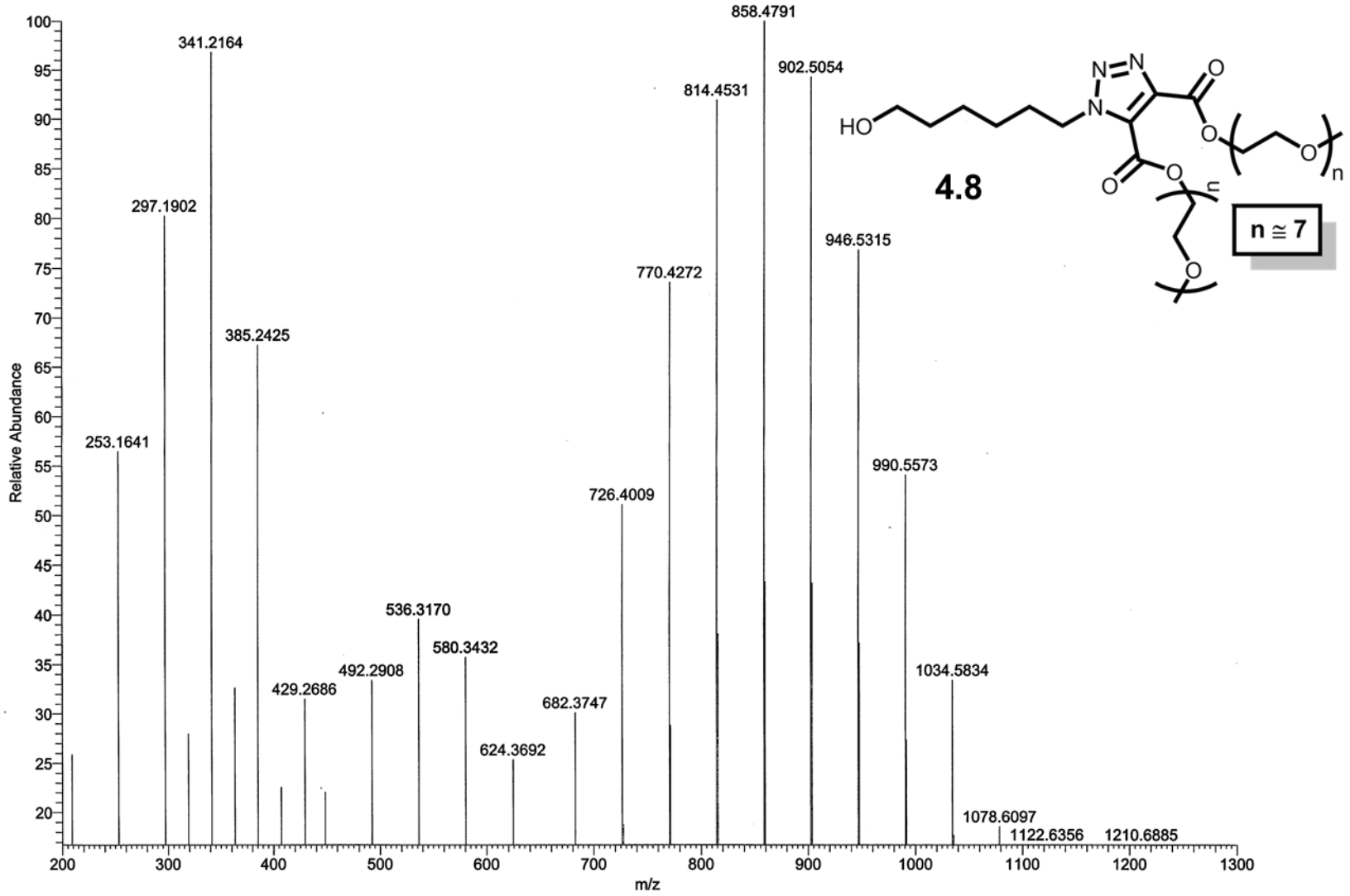
858.4791
341.2164
902.5054
814.4531
297.1902
946.5315
770.4272
385.2425
253.1641
990.5573
726.4009
536.3170
580.3432
492.2908
1034.5834
429.2686
682.3747
624.3692
1078.6097
1122.6356
1210.6885
Relative Abundance
m/z
HO
4.8
n ≅ 7

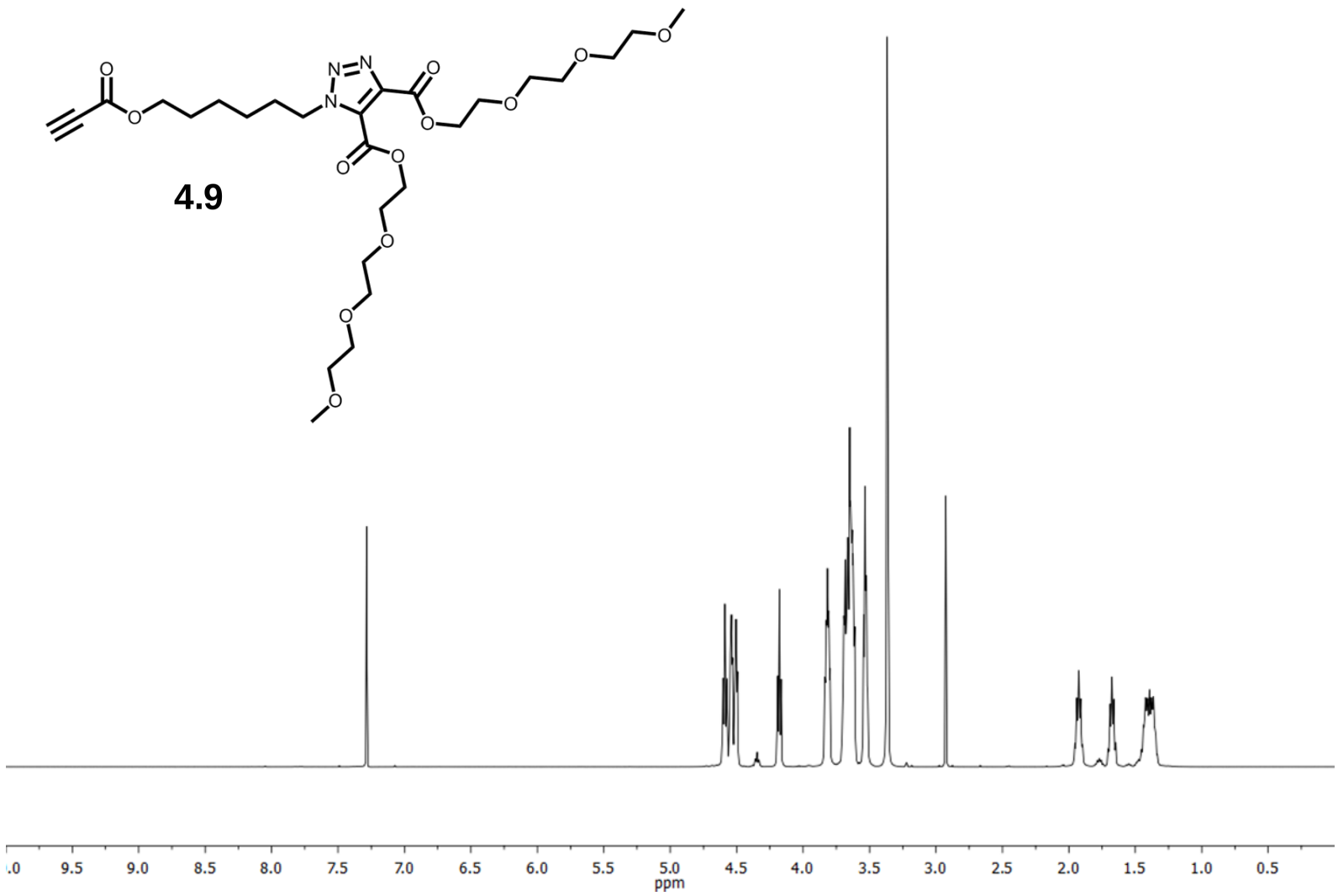
4.9
ppm

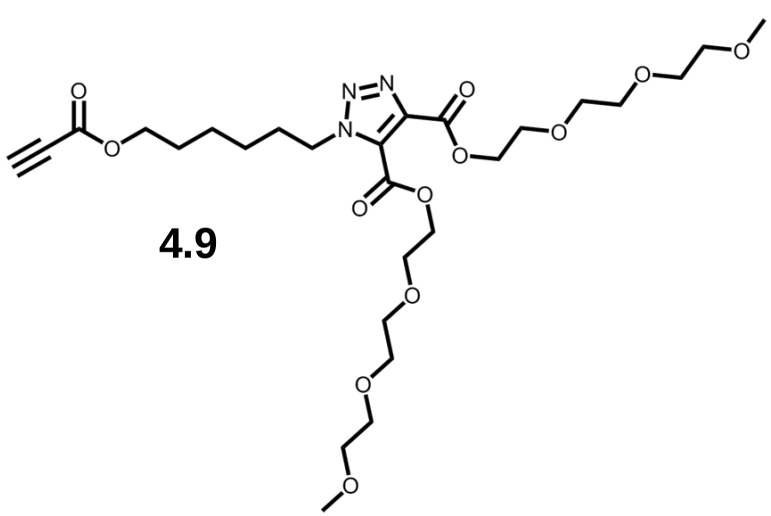
4.9

200
190
180
170
160
150
140
130
120
110
100
90
80
70
60
50
40
30
20
10
ppm

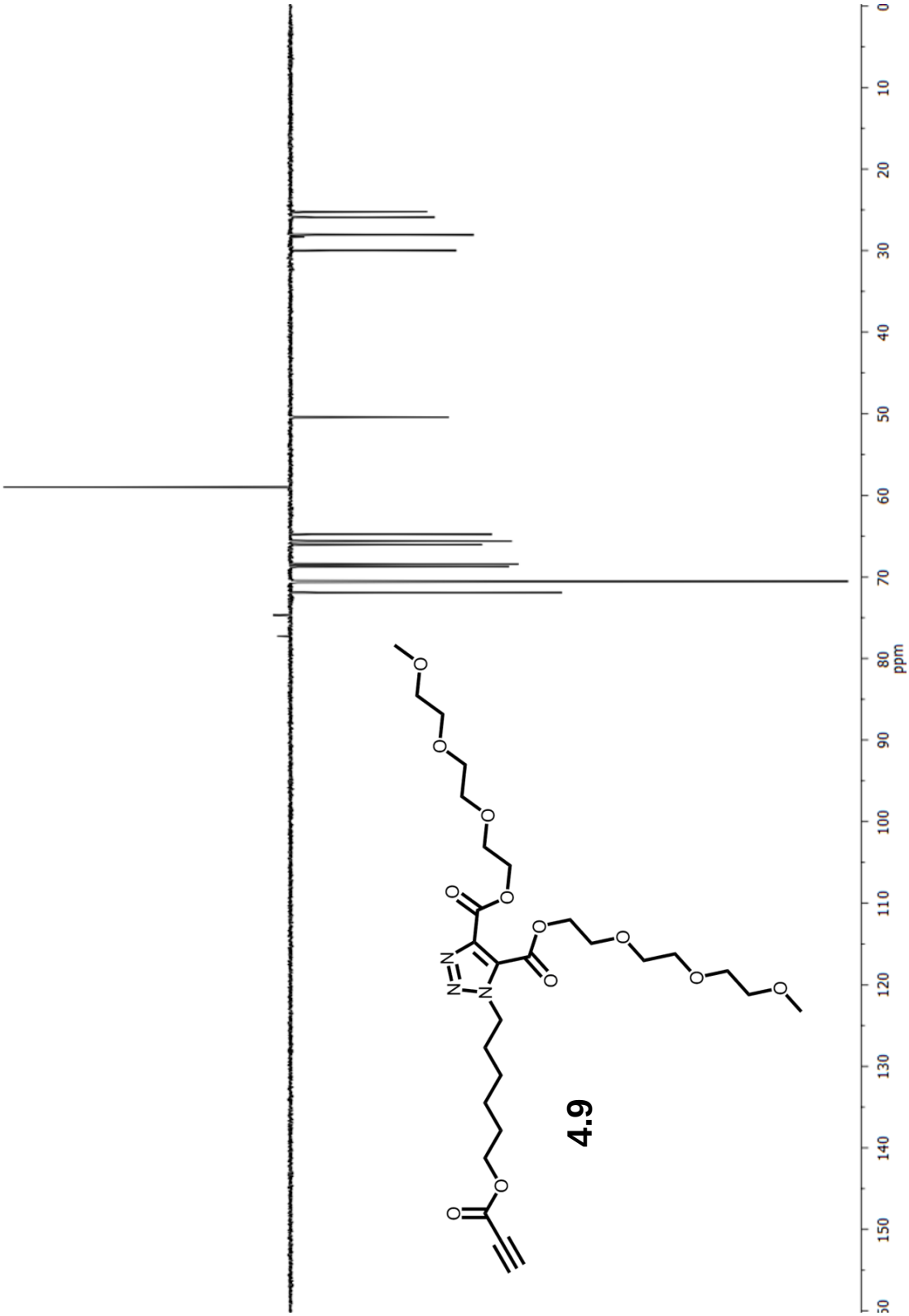
4.9
ppm

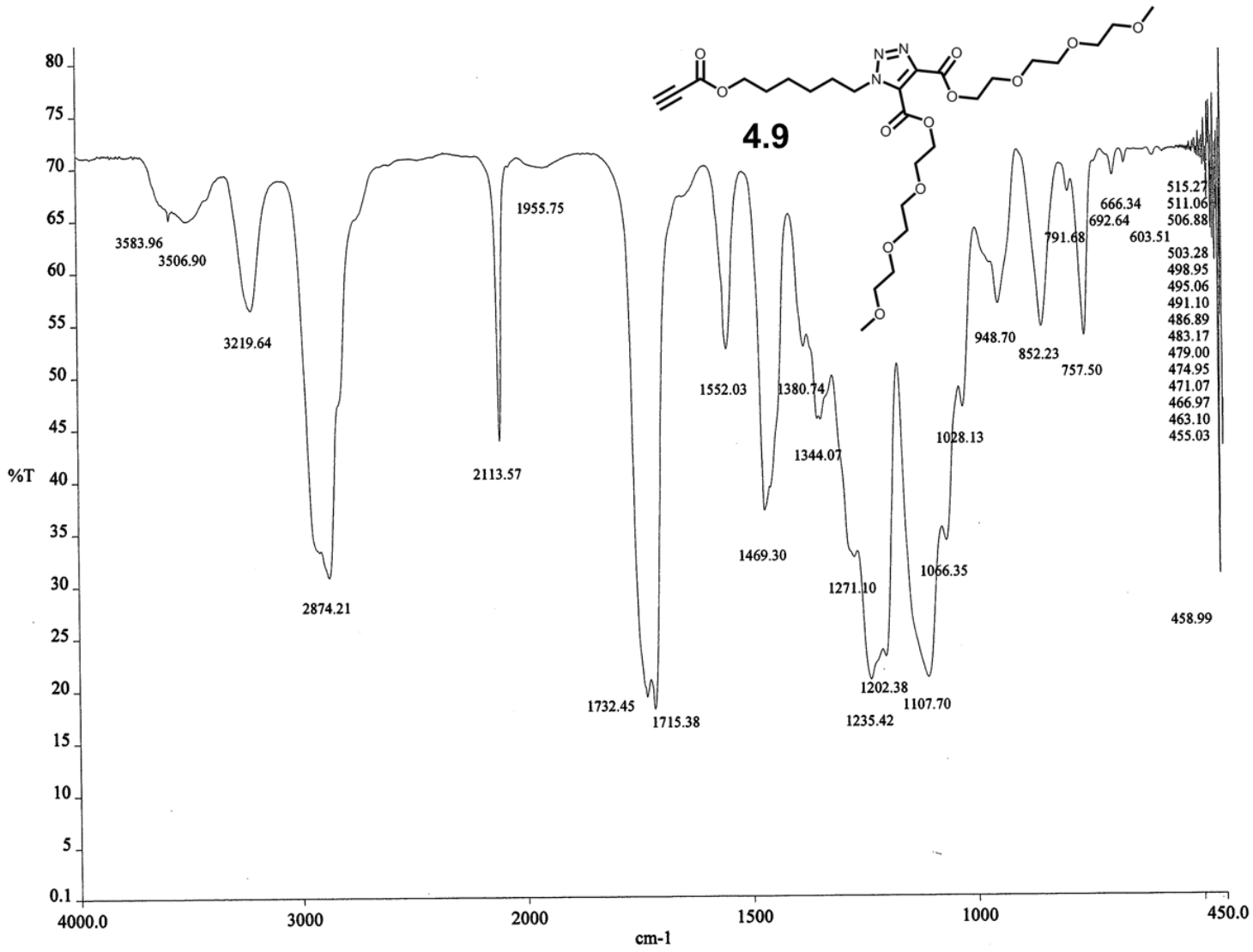
4.9
%T
cm-1
4000.0
3000
2000
1500
1000
450.0
3583.96
3506.90
3219.64
2874.21
2113.57
1955.75
1732.45
1715.38
1552.03
1469.30
1380.74
1344.07
1271.10
1235.42
1202.38
1107.70
1066.35
1028.13
948.70
852.23
791.68
757.50
692.64
666.34
603.51
515.27
511.06
506.88
503.28
498.95
495.06
491.10
486.89
483.17
479.00
474.95
471.07
466.97
463.10
458.99
455.03

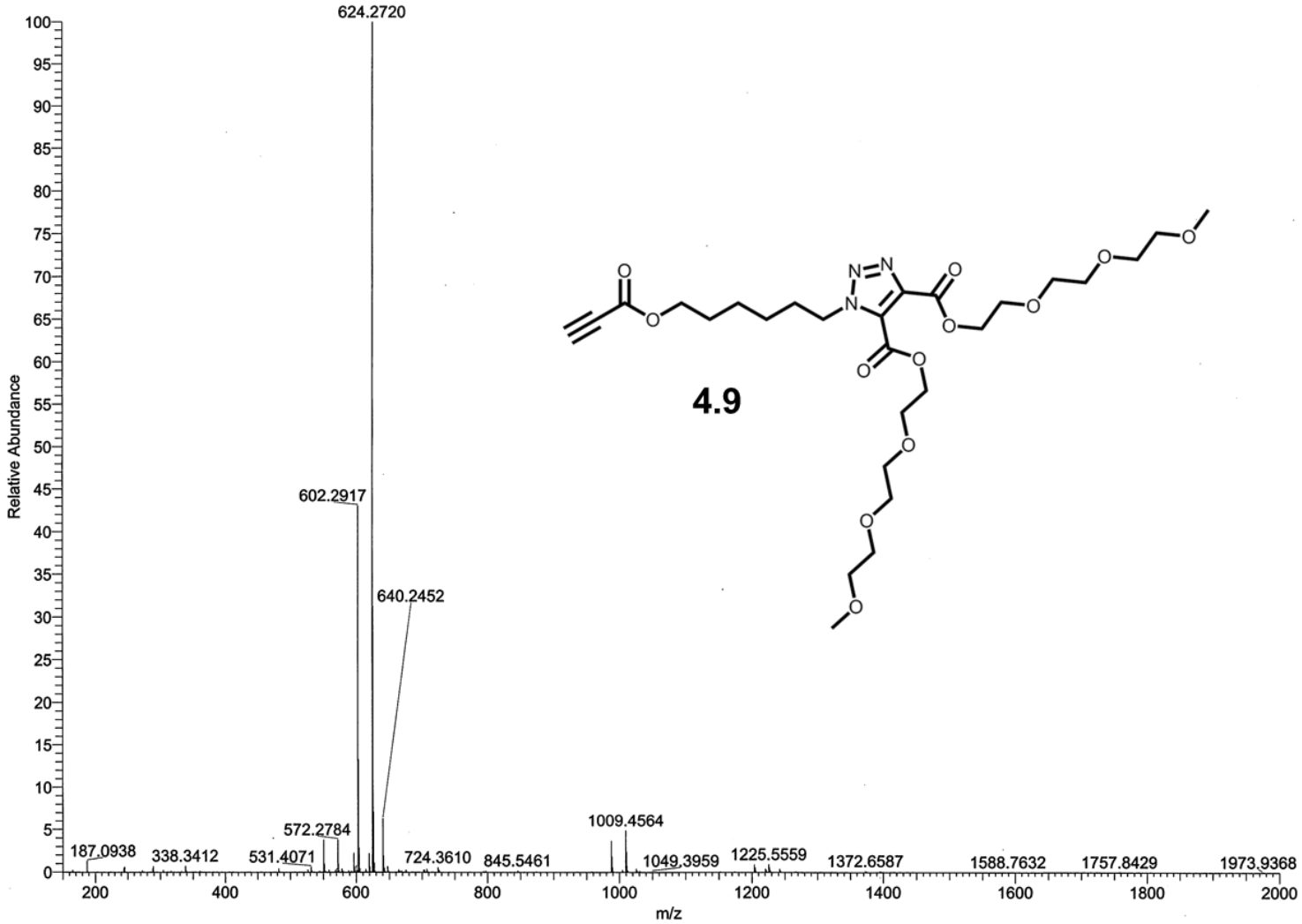
624.2720
602.2917
640.2452
572.2784
1009.4564
187.0938
338.3412
531.4071
724.3610
845.5461
1049.3959
1225.5559
1372.6587
1588.7632
1757.8429
1973.9368
Relative Abundance
m/z
4.9

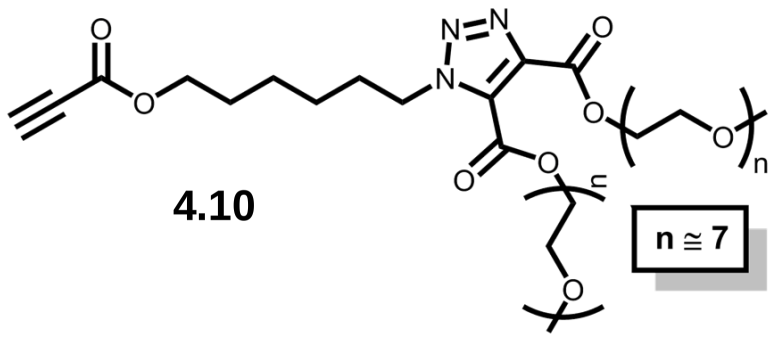
4.10
n ≅ 7

9.5
9.0
8.5
8.0
7.5
7.0
6.5
6.0
5.5
5.0
ppm
4.5
4.0
3.5
3.0
2.5
2.0
1.5
1.0
0.5

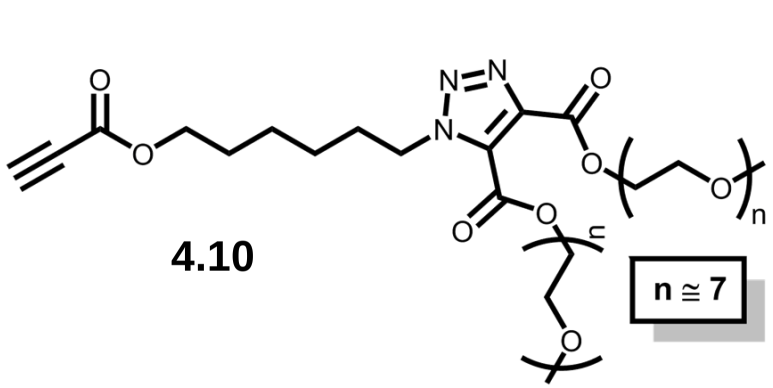
4.10
n ≅ 7

200
190
180
170
160
150
140
130
120
110
100
90
80
70
60
50
40
30
20
10
ppm

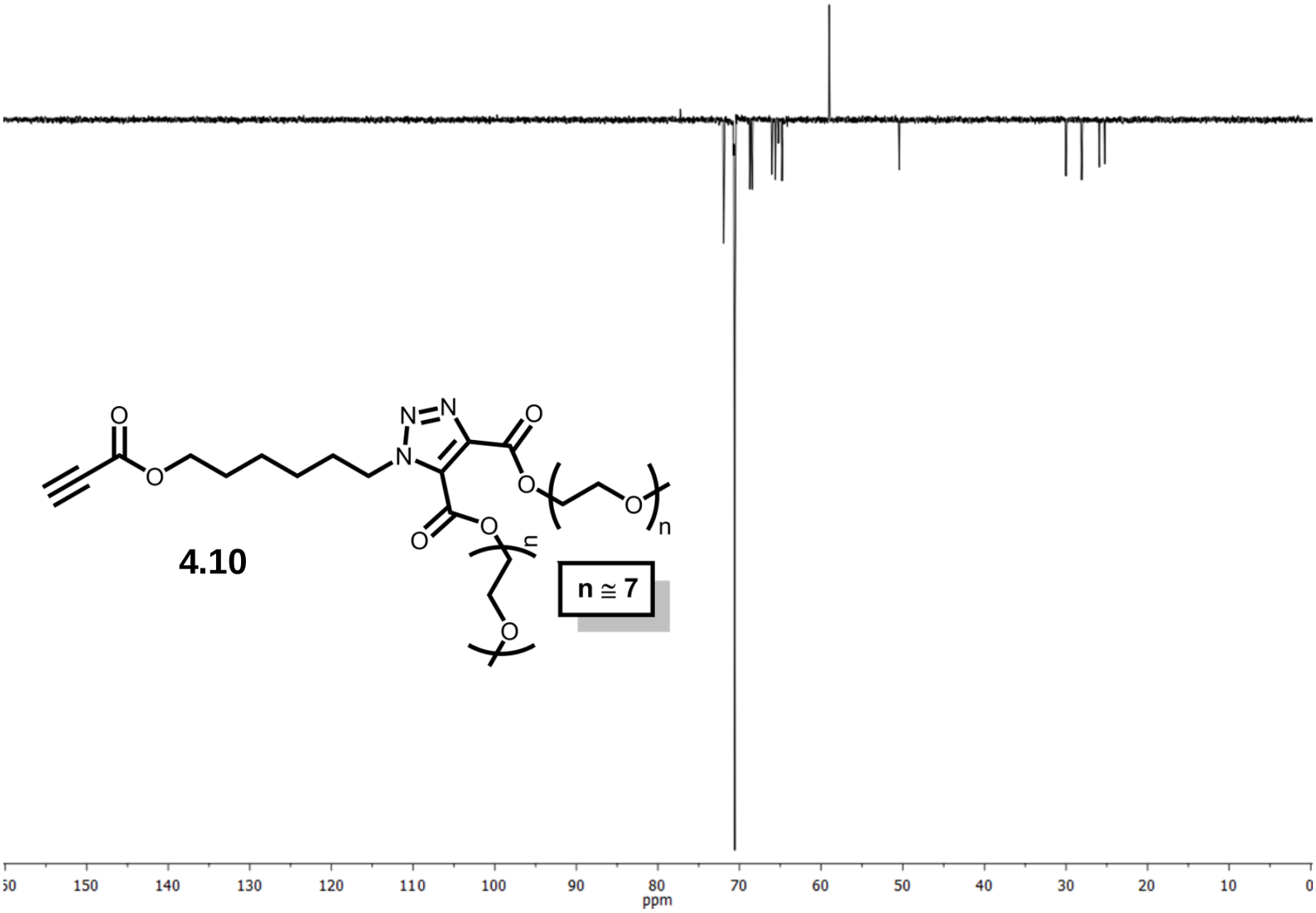
4.10
n ≅ 7
150
140
130
120
110
100
90
80
70
60
50
40
30
20
10
ppm

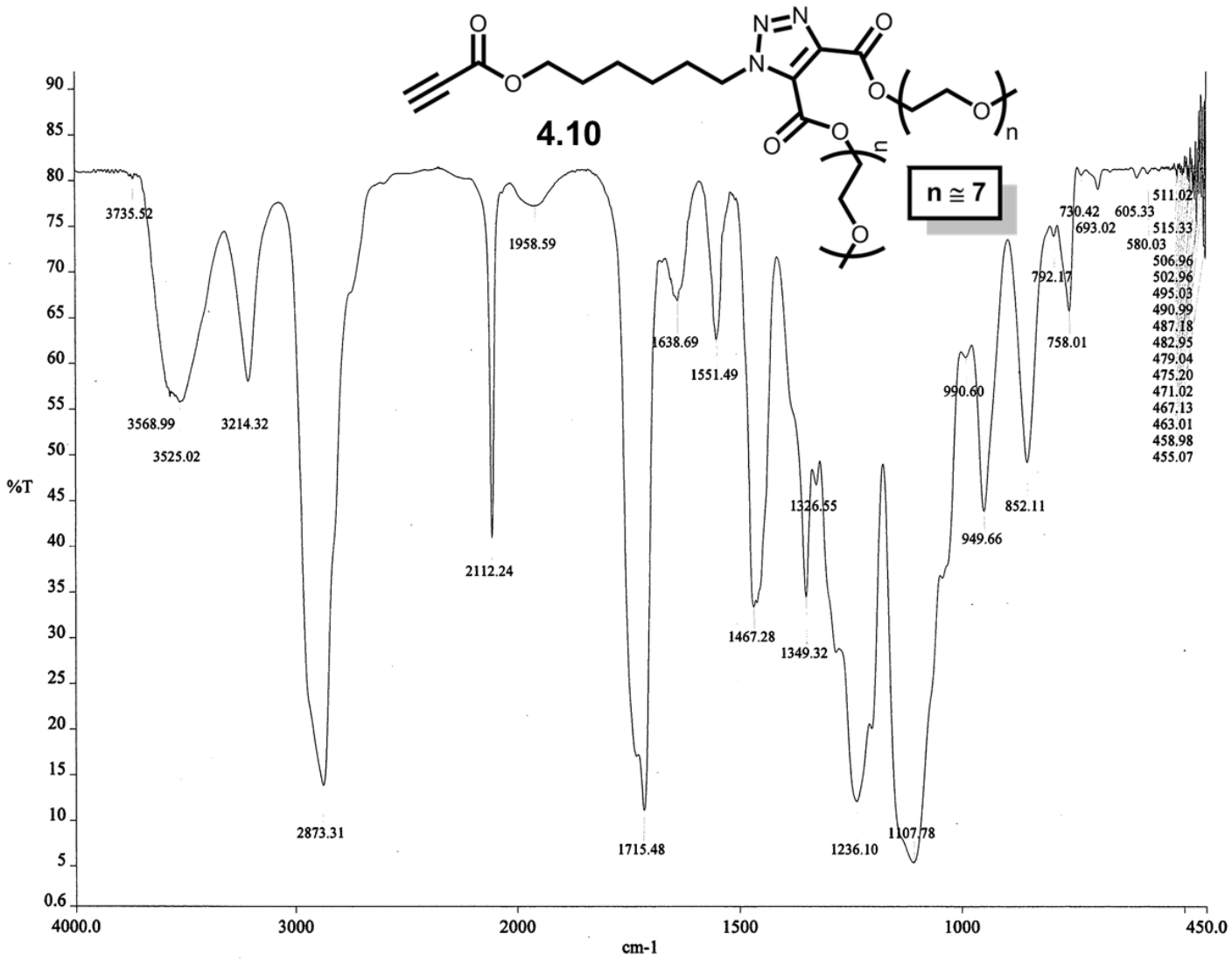
4.10
n ≅ 7
%T
cm-1
4000.0
3000
2000
1500
1000
450.0
3735.52
3568.99
3525.02
3214.32
2873.31
2112.24
1958.59
1715.48
1638.69
1551.49
1467.28
1349.32
1326.55
1236.10
1107.78
990.60
949.66
852.11
792.17
758.01
730.42
693.02
605.33
580.03
511.02
515.33
506.96
502.96
495.03
490.99
487.18
482.95
479.04
475.20
471.02
467.13
463.01
458.98
455.07

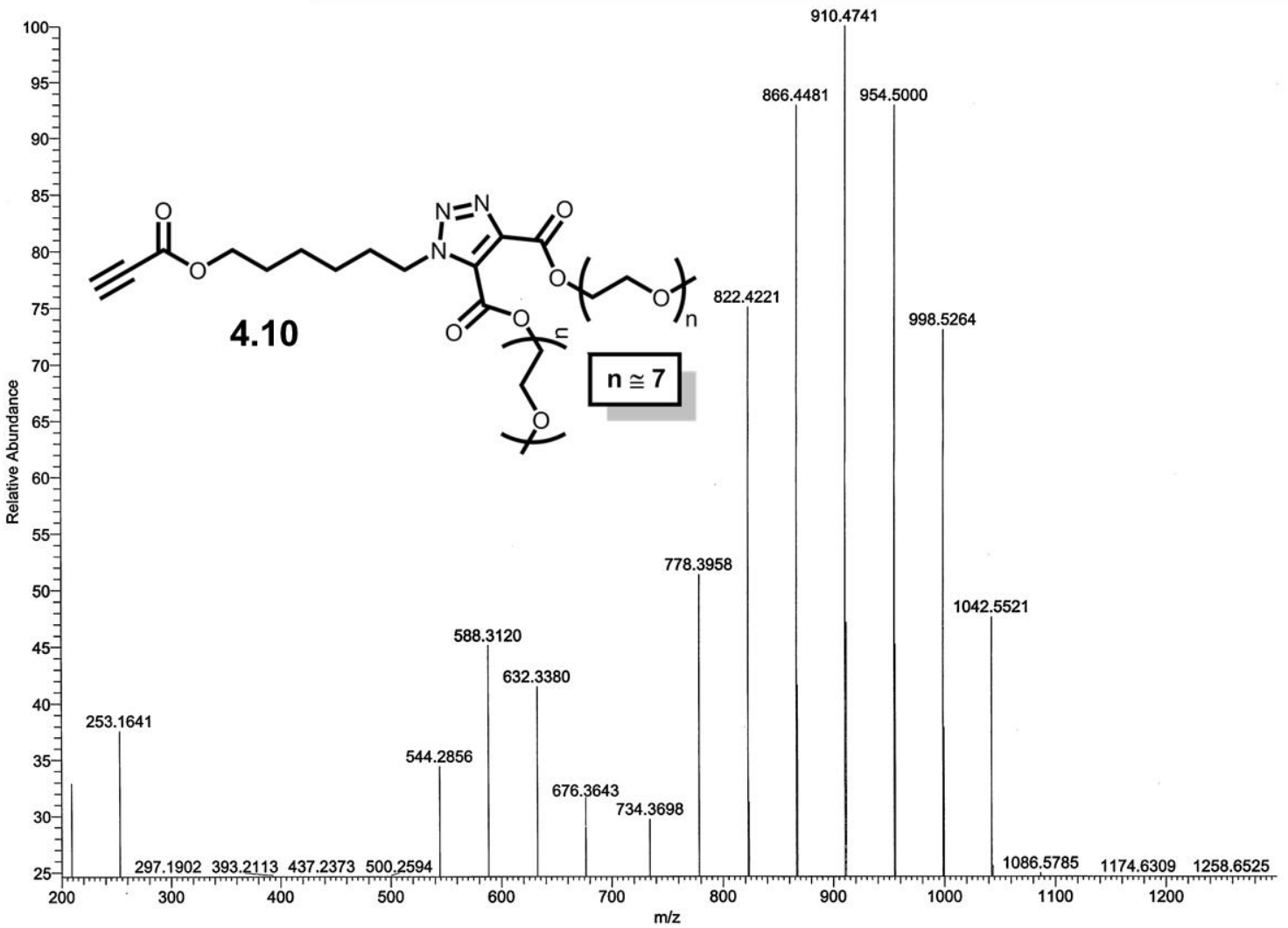
4.10
n ≅ 7
Relative Abundance
m/z
910.4741
866.4481
954.5000
822.4221
998.5264
778.3958
1042.5521
588.3120
632.3380
253.1641
544.2856
676.3643
734.3698
297.1902
393.2113
437.2373
500.2594
1086.5785
1174.6309
1258.6525

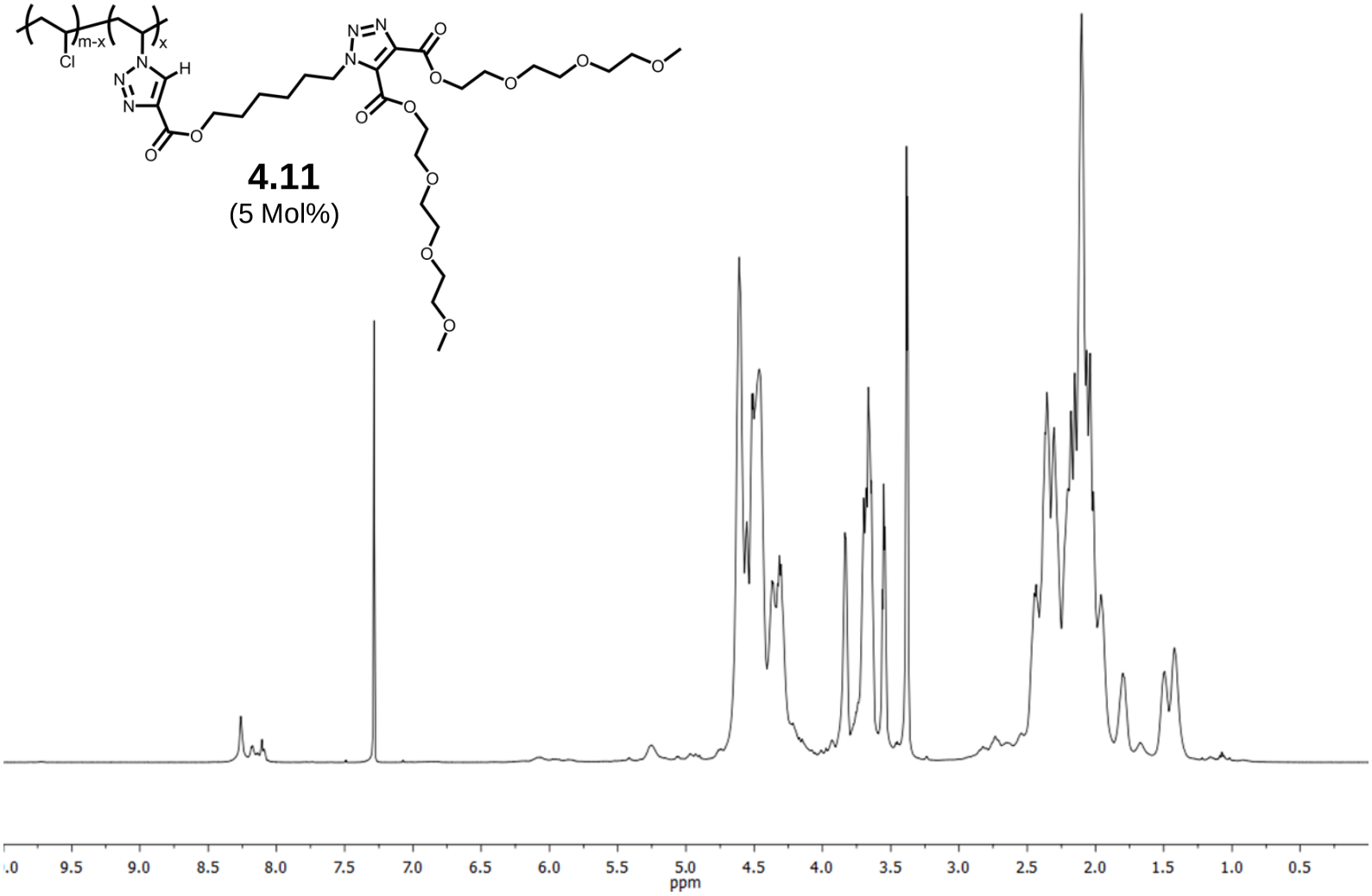
m-x
x
Cl
H
N
O
4.11
(5 Mol%)
9.5
9.0
8.5
8.0
7.5
7.0
6.5
6.0
5.5
5.0
4.5
4.0
3.5
3.0
2.5
2.0
1.5
1.0
0.5
ppm

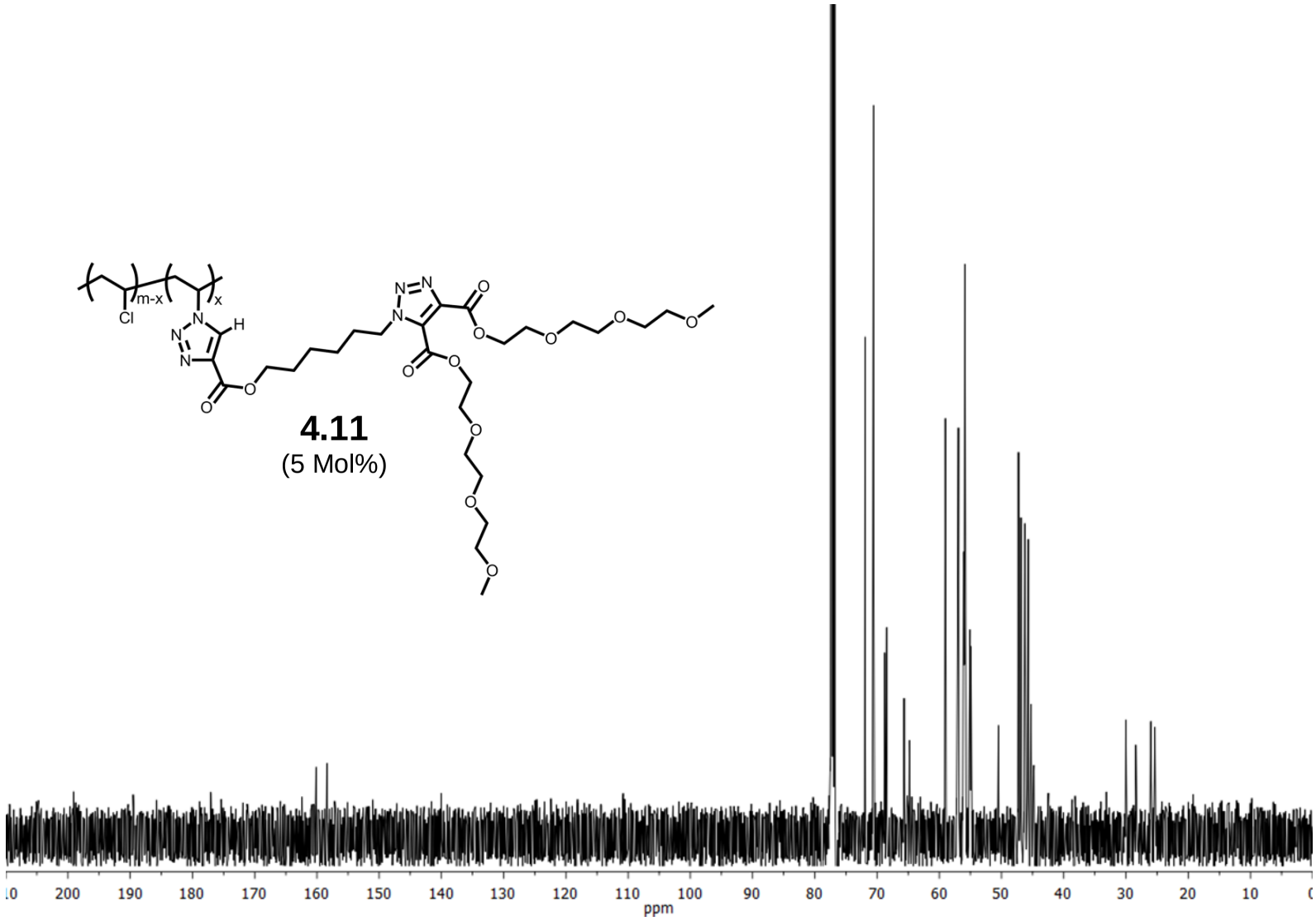
m-x
x
Cl
H
N
O
4.11
(5 Mol%)
ppm
200
190
180
170
160
150
140
130
120
110
100
90
80
70
60
50
40
30
20
10

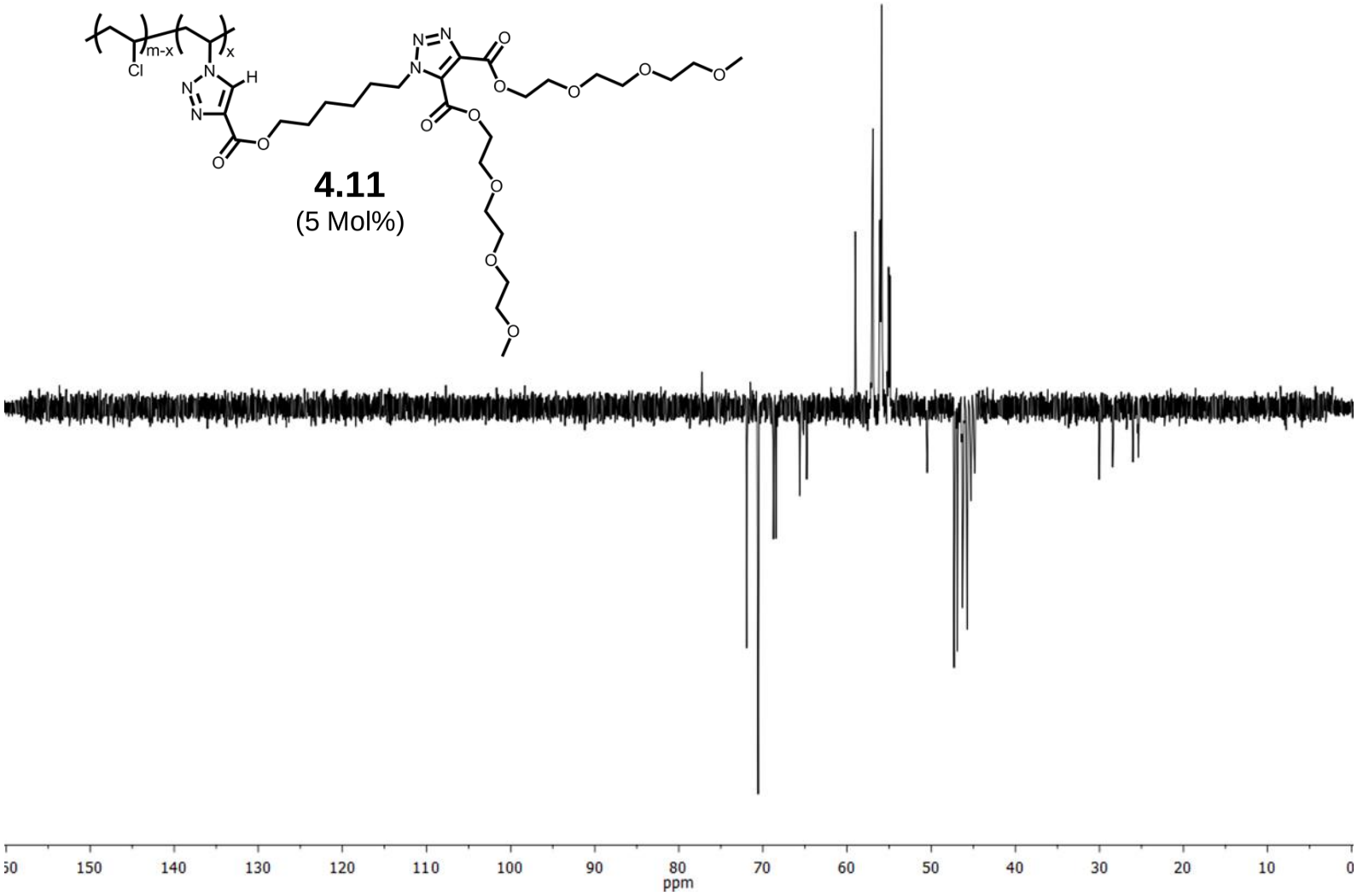
4.11
(5 Mol%)
ppm

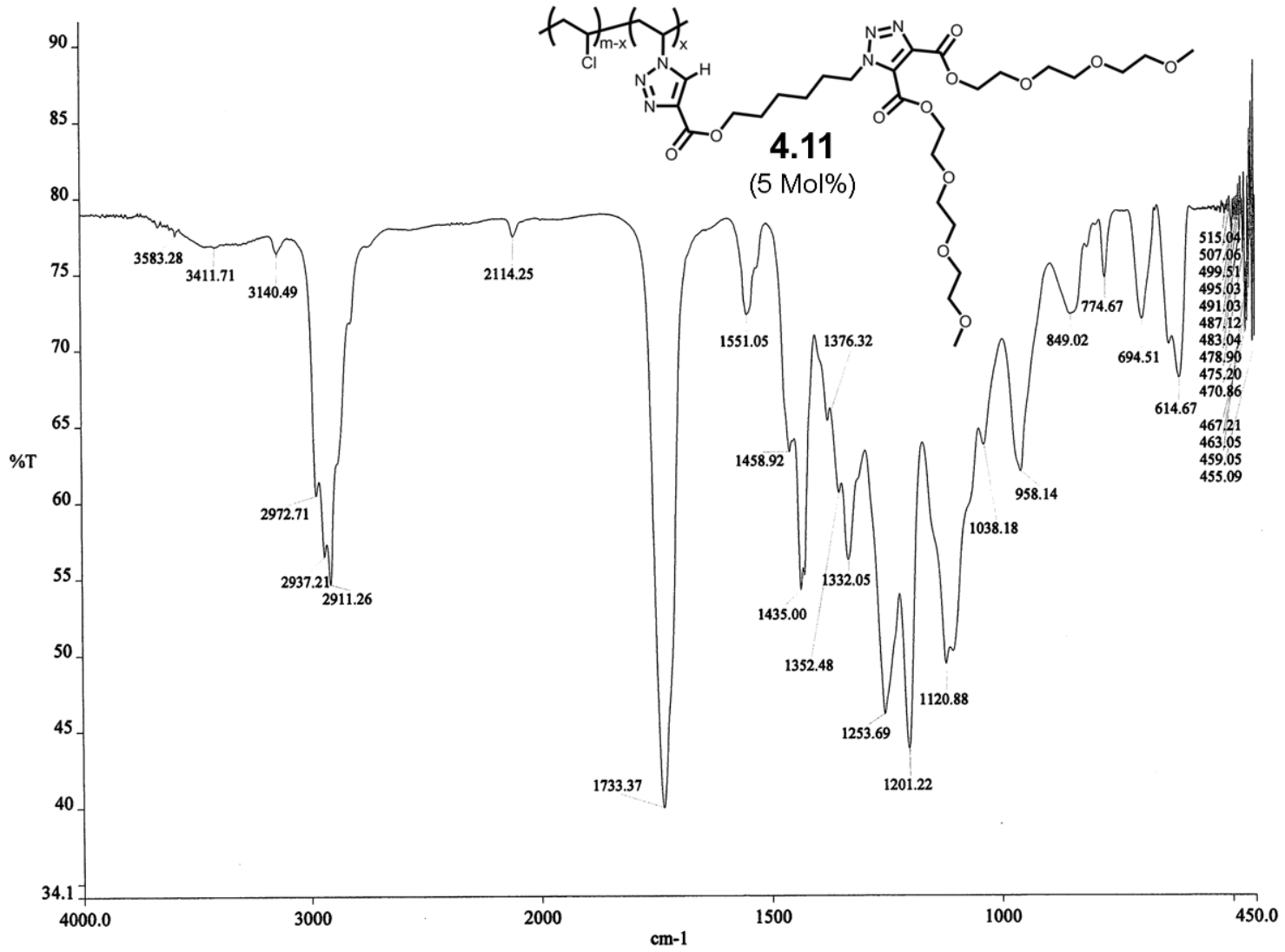
4.11
(5 Mol%)
%T
cm-1
3583.28
3411.71
3140.49
2972.71
2937.21
2911.26
2114.25
1733.37
1551.05
1458.92
1435.00
1376.32
1352.48
1332.05
1253.69
1201.22
1120.88
1038.18
958.14
849.02
774.67
694.51
614.67
515.04
507.06
499.51
495.03
491.03
487.12
483.04
478.90
475.20
470.86
467.21
463.05
459.05
455.09

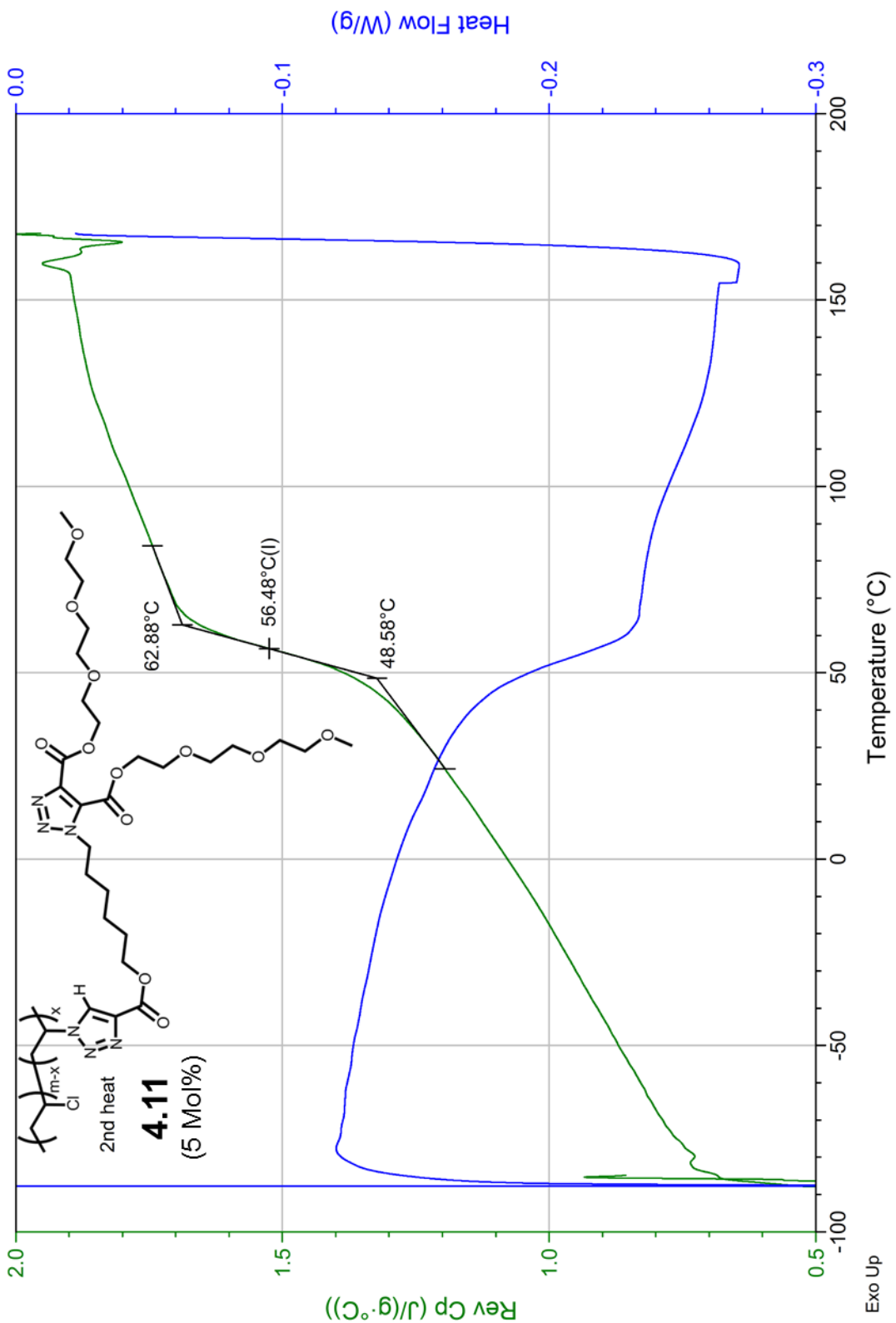
Heat Flow (W/g)
0.0
-0.1
-0.2
-0.3
Rev Cp (J/(g·°C))
2.0
1.5
1.0
0.5
Temperature (°C)
200
150
100
50
0
-50
-100
Exo Up
62.88°C
56.48°C(I)
48.58°C
2nd heat
4.11
(5 Mol%)

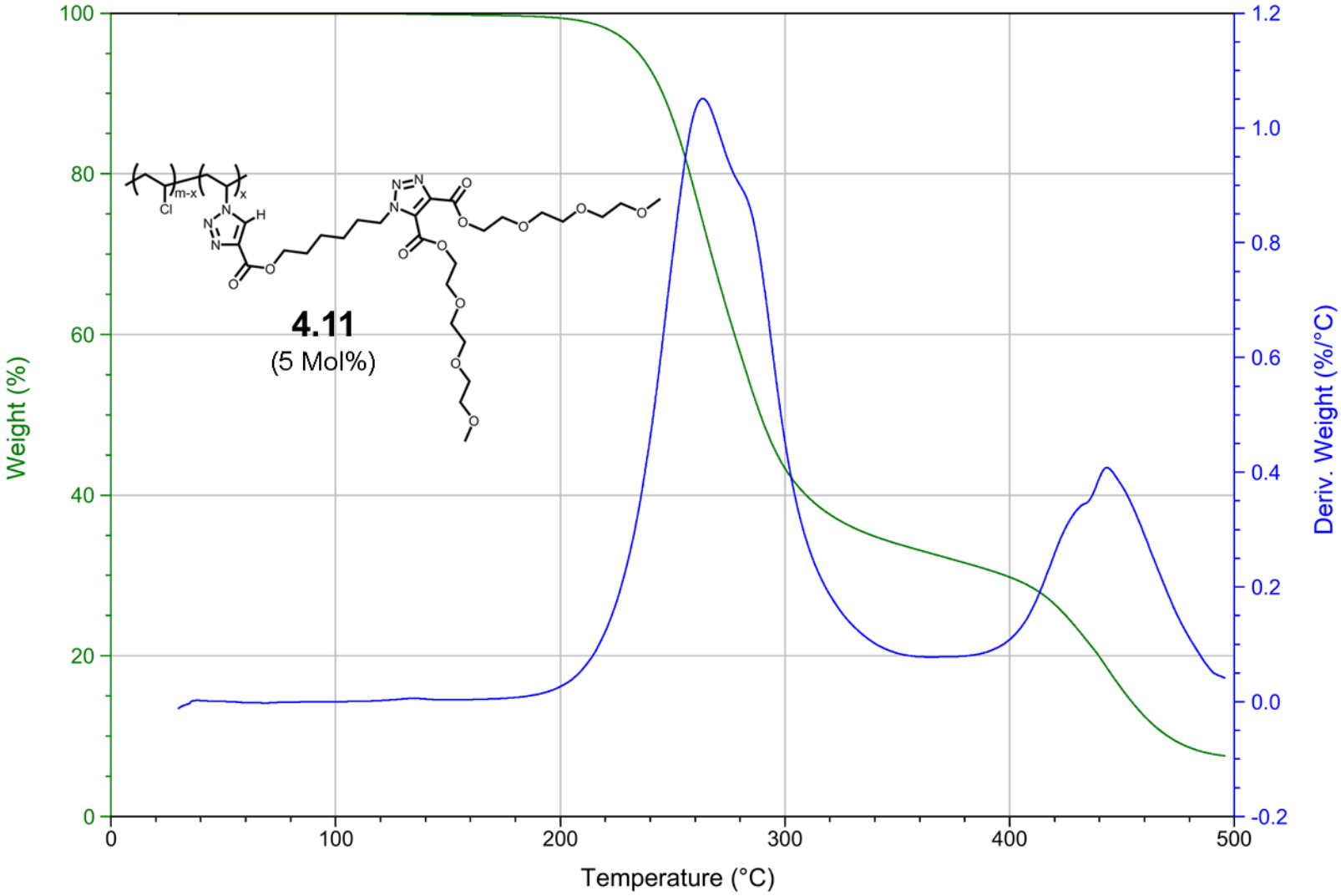
4.11
(5 Mol%)
Weight (%)
Deriv. Weight (%/°C)
Temperature (°C)
100
80
60
40
20
0
1.2
1.0
0.8
0.6
0.4
0.2
0.0
-0.2
0
100
200
300
400
500

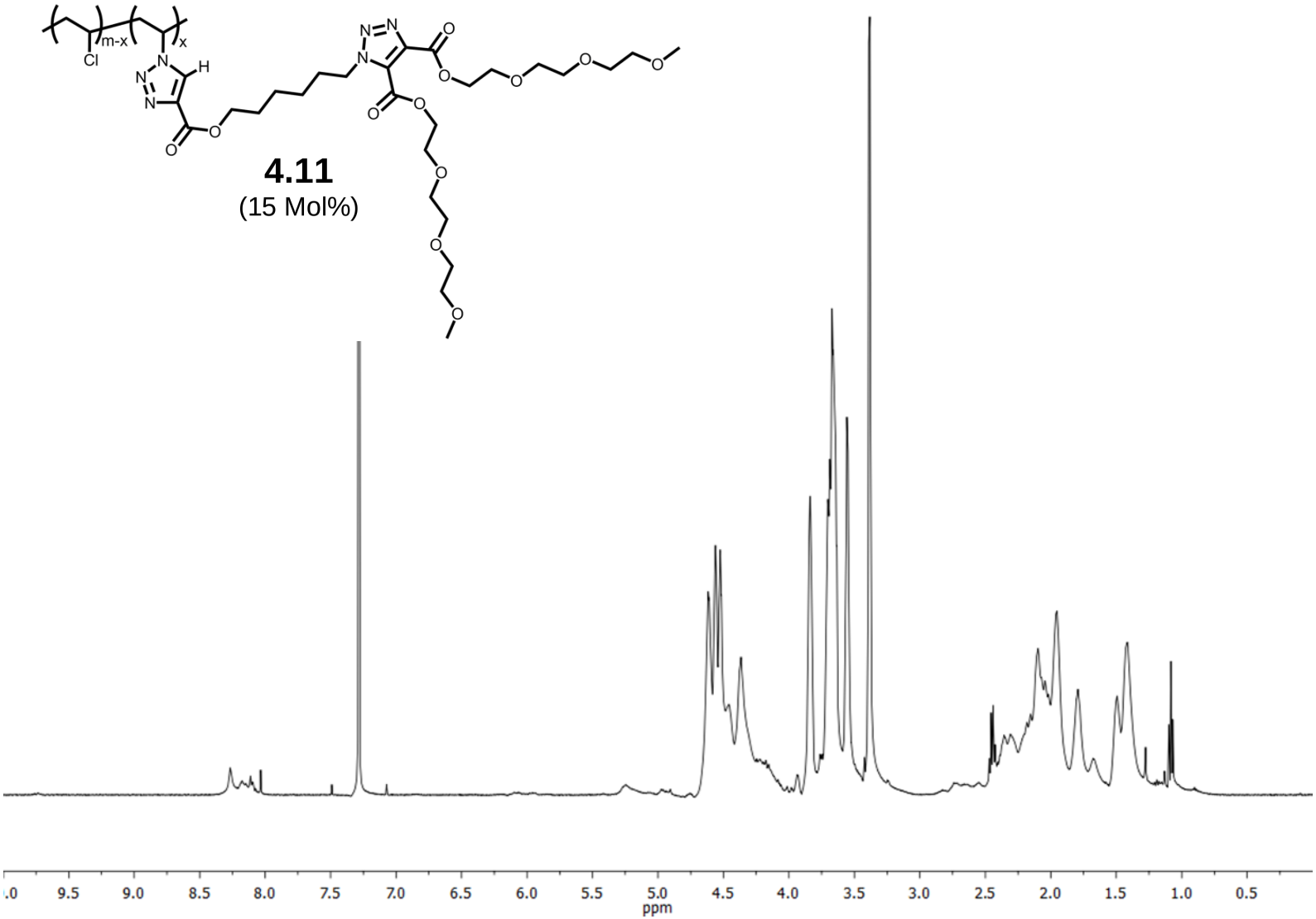
4.11
(15 Mol%)
ppm

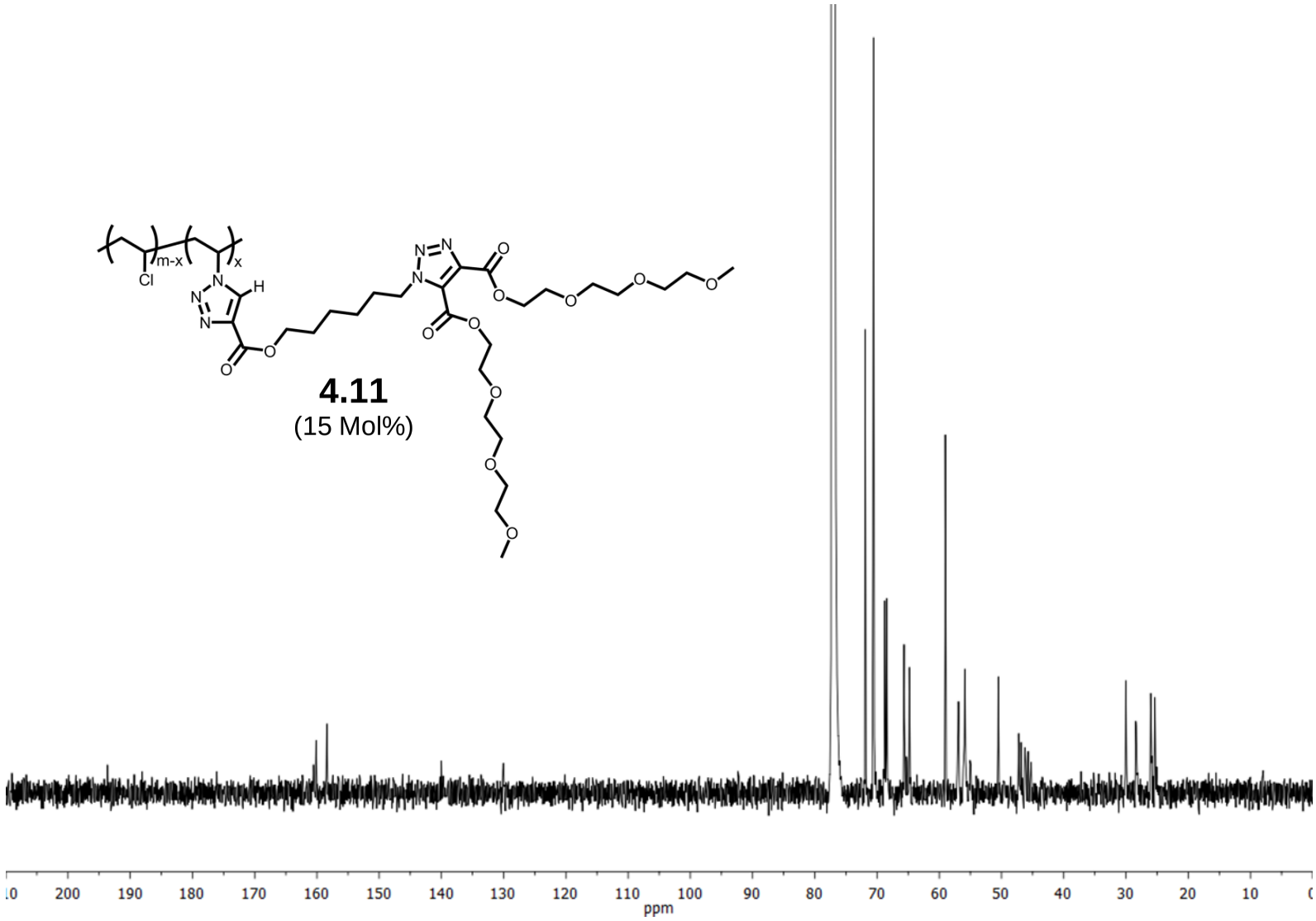
m-x
x
Cl
H
4.11
(15 Mol%)
ppm

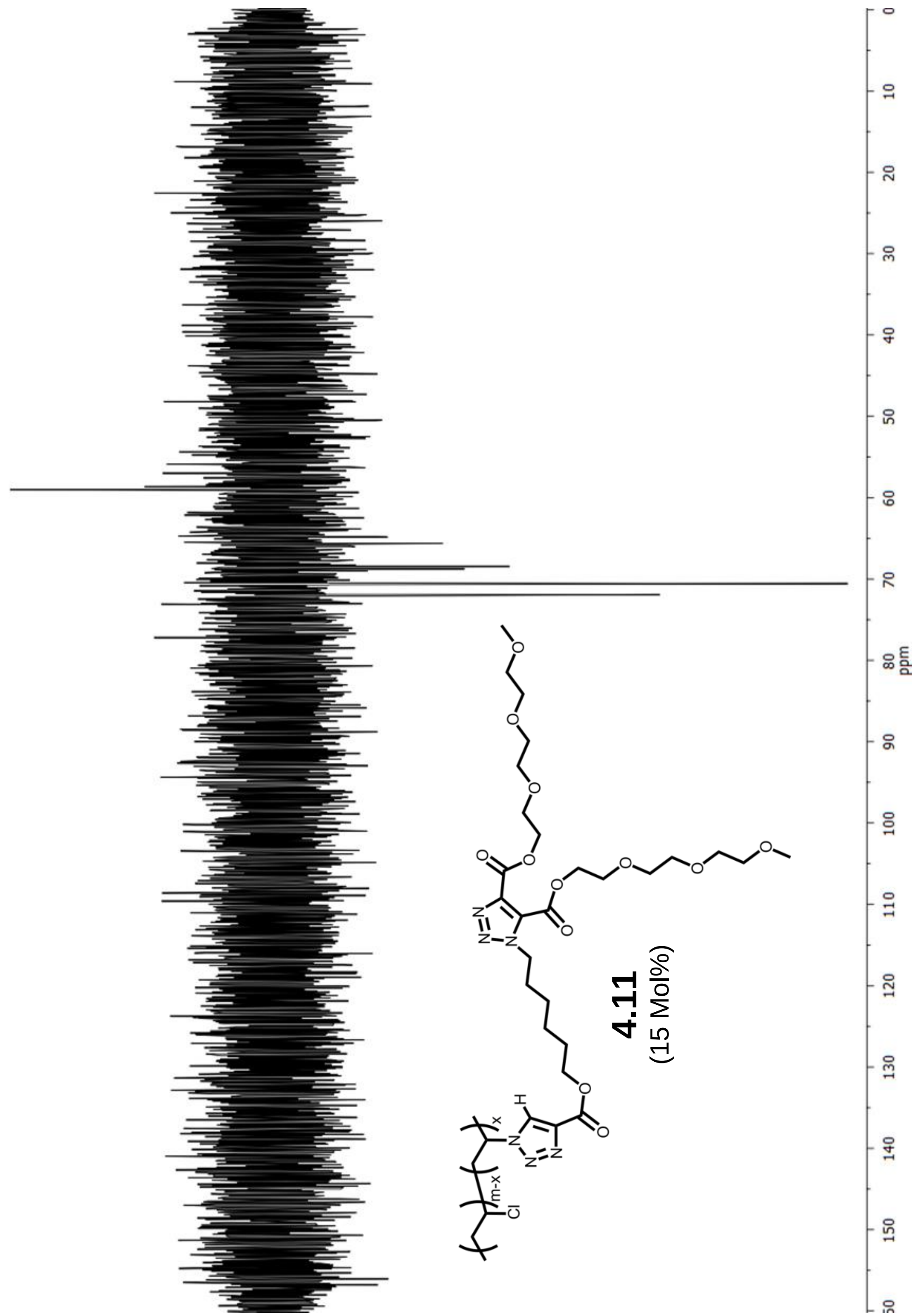
4.11
(15 Mol%)
ppm
0
10
20
30
40
50
60
70
80
90
100
110
120
130
140
150

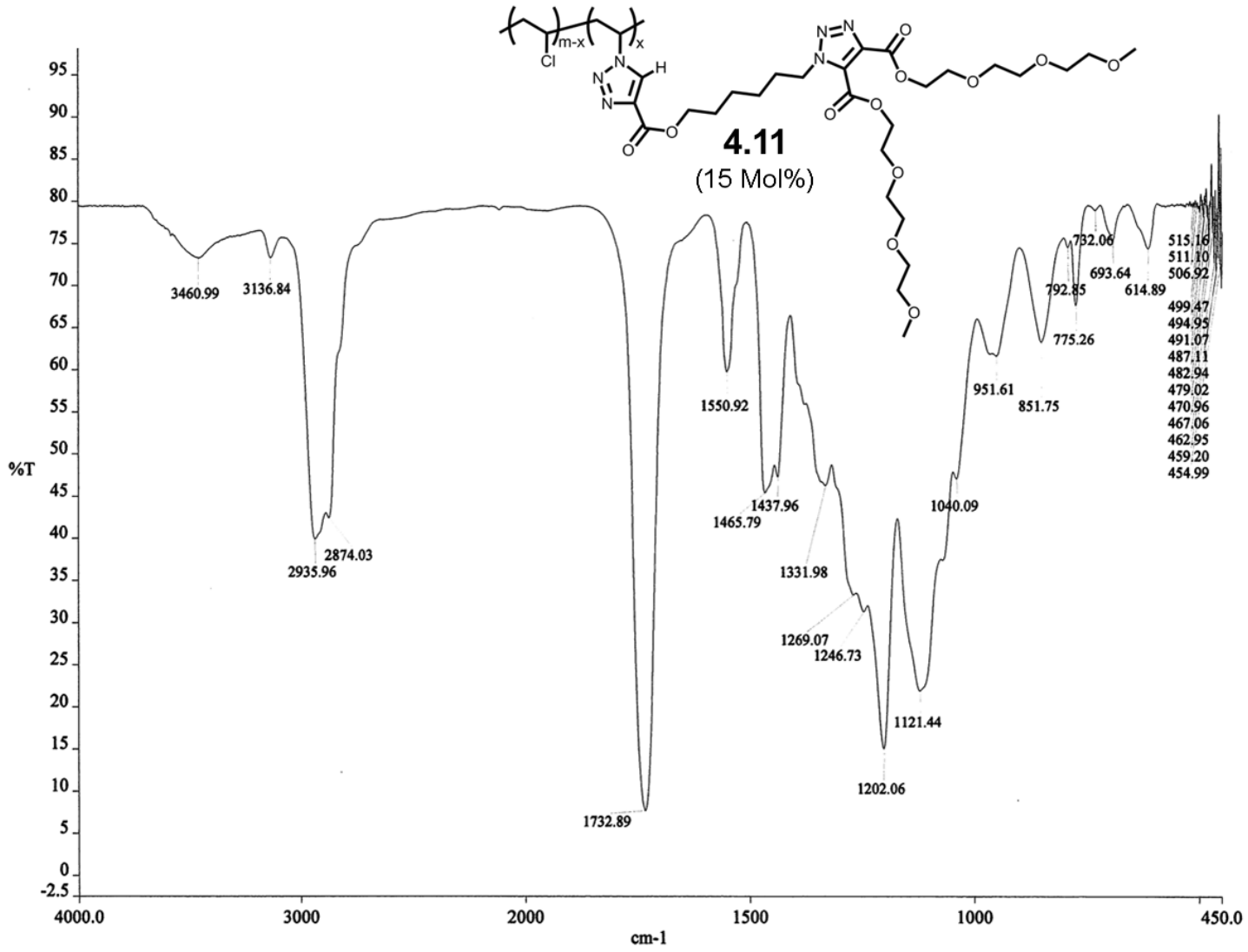
4.11
(15 Mol%)
%T
cm-1
4000.0
3000
2000
1500
1000
450.0
3460.99
3136.84
2935.96
2874.03
1732.89
1550.92
1465.79
1437.96
1331.98
1269.07
1246.73
1202.06
1121.44
1040.09
951.61
851.75
792.85
775.26
732.06
693.64
614.89
515.16
511.10
506.92
499.47
494.95
491.07
487.11
482.94
479.02
470.96
467.06
462.95
459.20
454.99

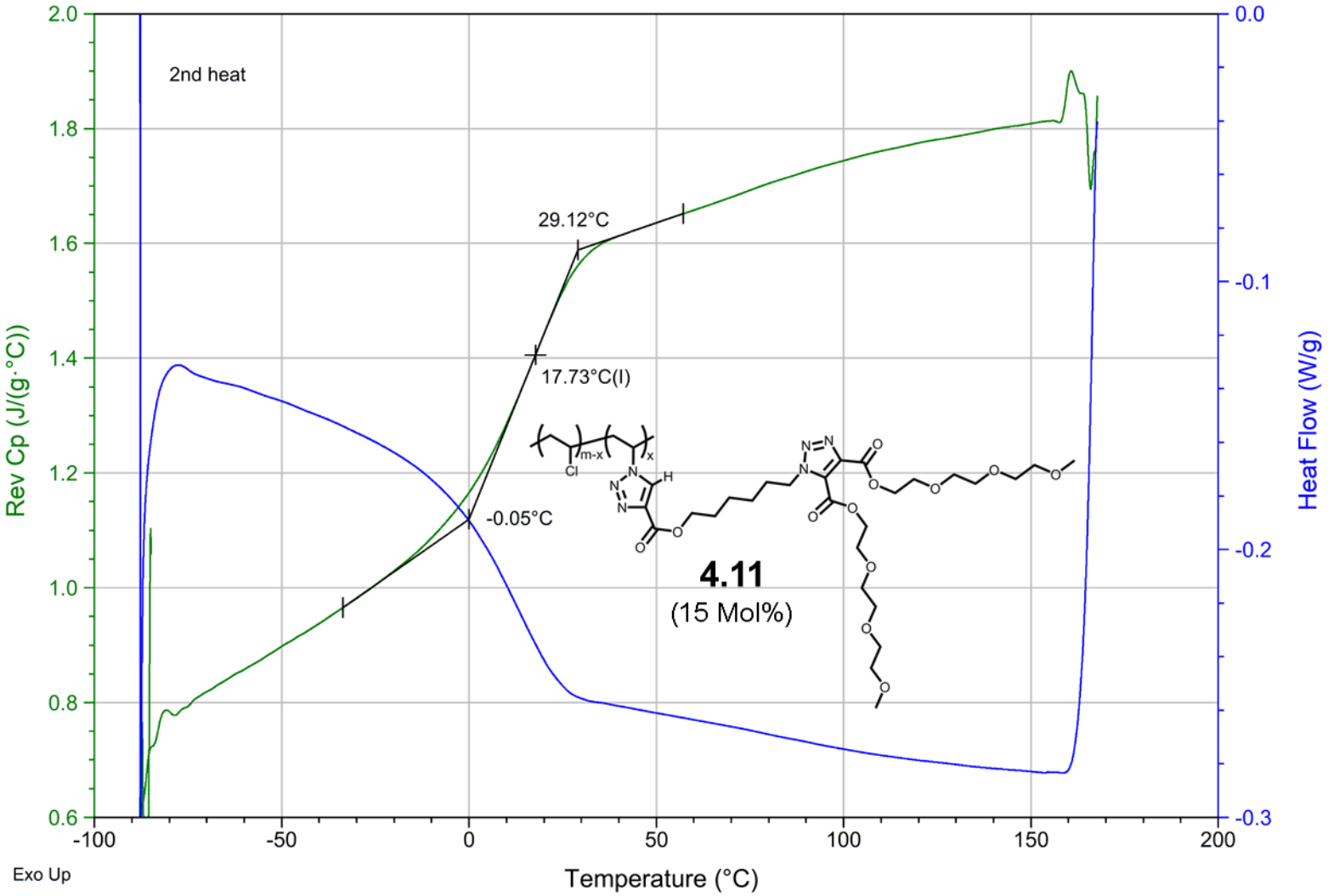
2nd heat
29.12°C
17.73°C(I)
-0.05°C
4.11
(15 Mol%)
Rev Cp (J/(g·°C))
Heat Flow (W/g)
Temperature (°C)
Exo Up
2.0
1.8
1.6
1.4
1.2
1.0
0.8
0.6
0.0
-0.1
-0.2
-0.3
-100
-50
0
50
100
150
200

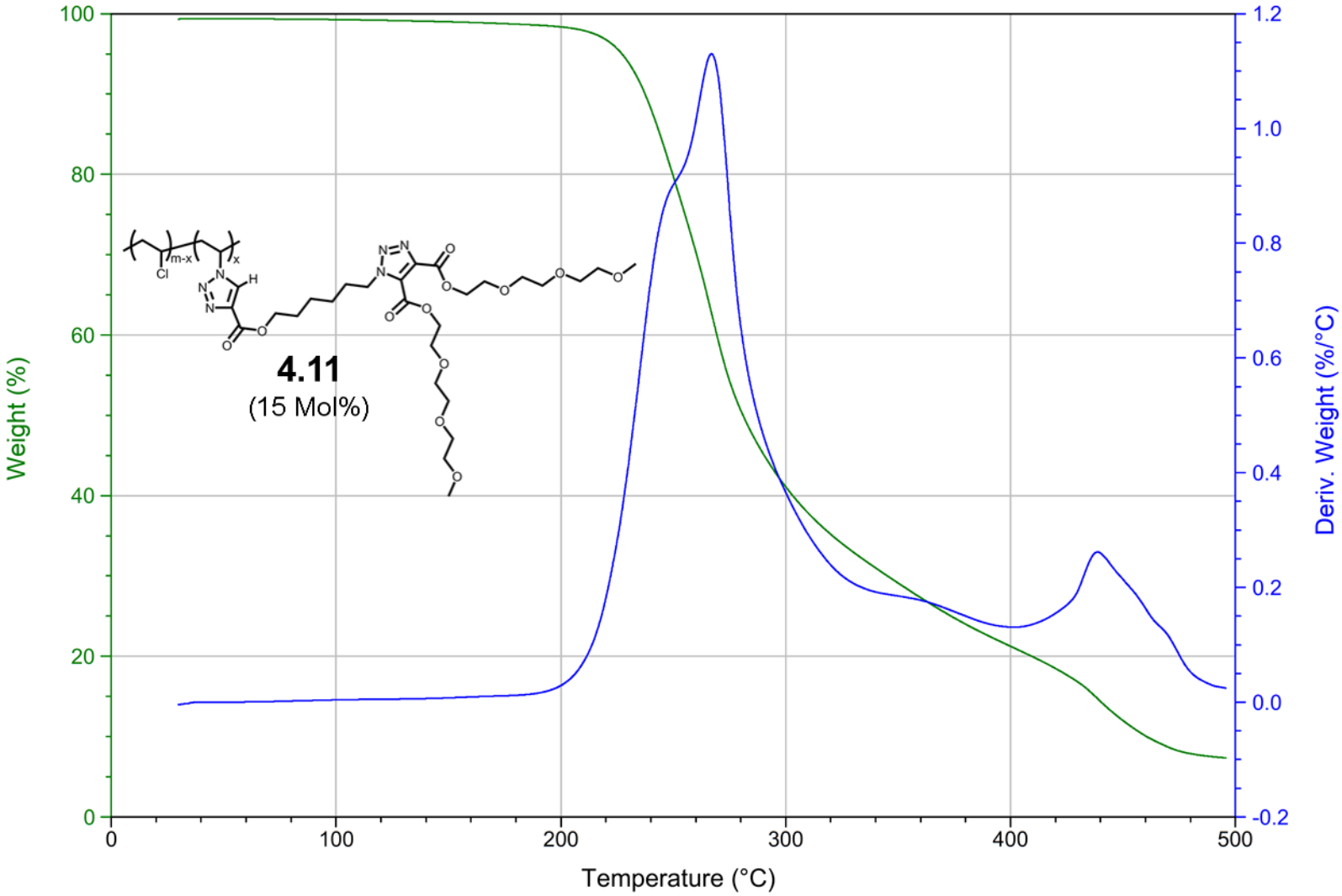
4.11
(15 Mol%)
Weight (%)
Deriv. Weight (%/°C)
Temperature (°C)
100
80
60
40
20
0
1.2
1.0
0.8
0.6
0.4
0.2
0.0
-0.2
0
100
200
300
400
500

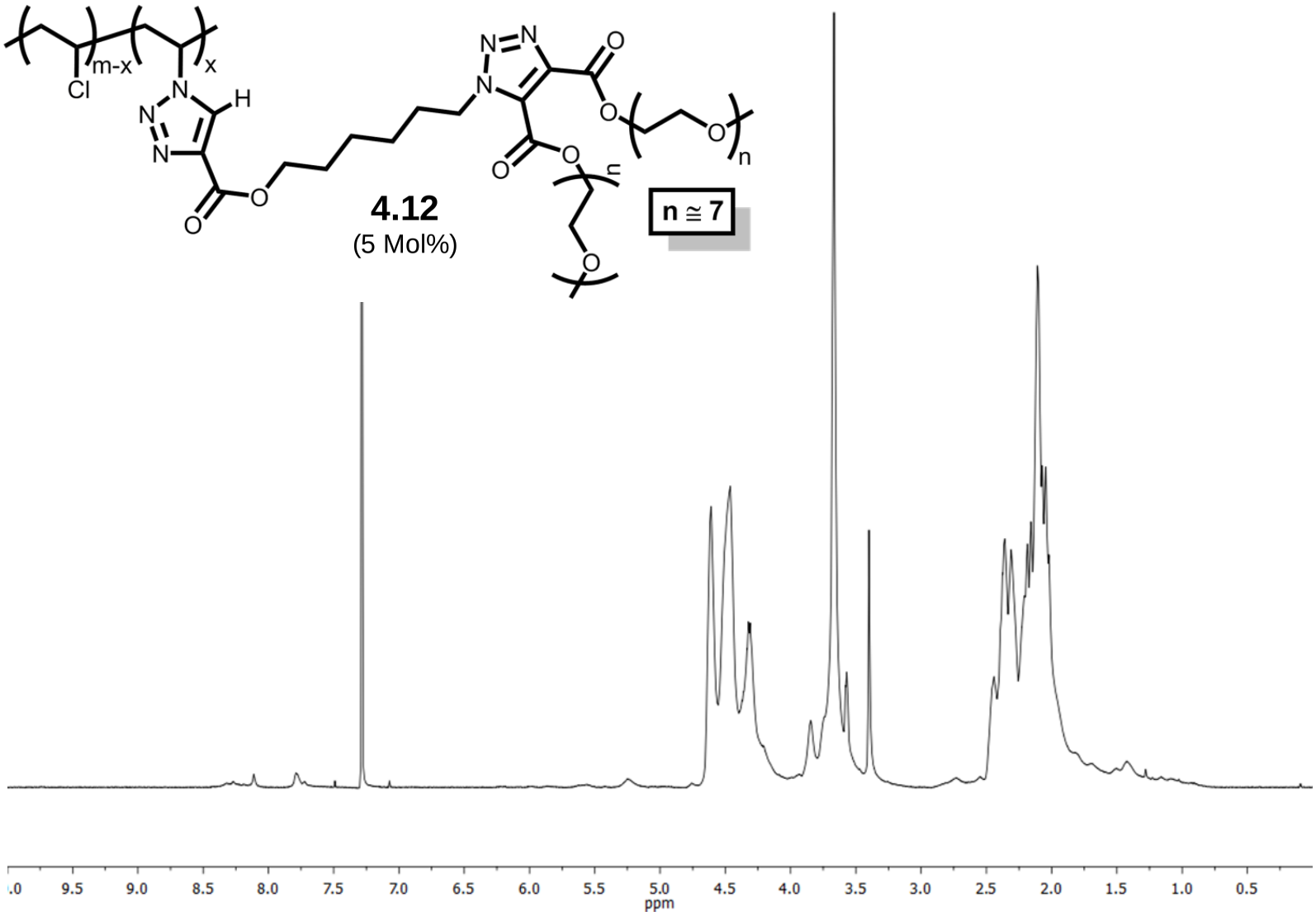
m-x
x
Cl
H
N
N
N
N
O
O
O
O
O
O
O
n
4.12
(5 Mol%)
n ≅ 7
9.5
9.0
8.5
8.0
7.5
7.0
6.5
6.0
5.5
5.0
4.5
4.0
3.5
3.0
2.5
2.0
1.5
1.0
0.5
ppm

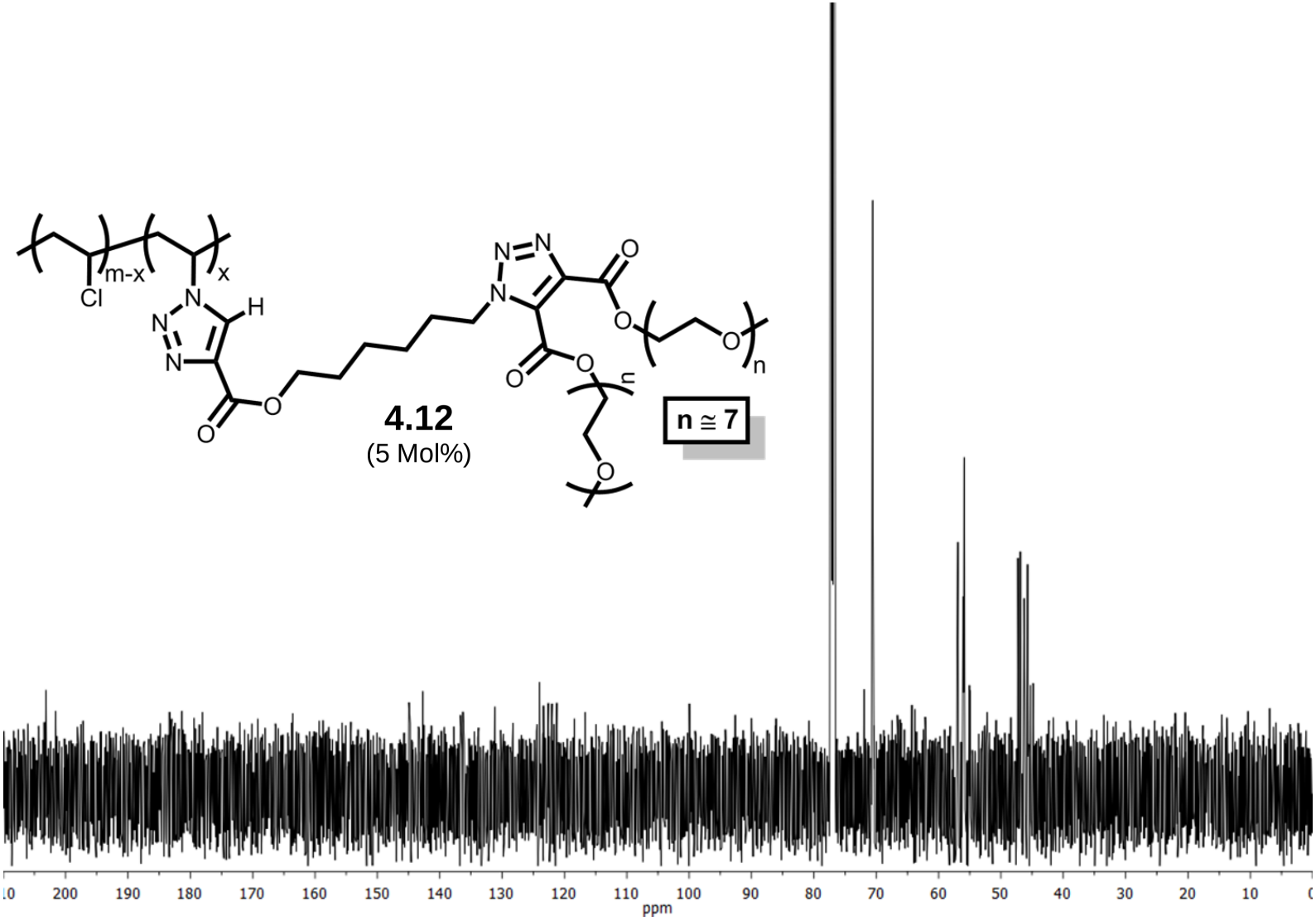
m-x
x
Cl
H
N
O
n
4.12
(5 Mol%)
n ≅ 7
ppm

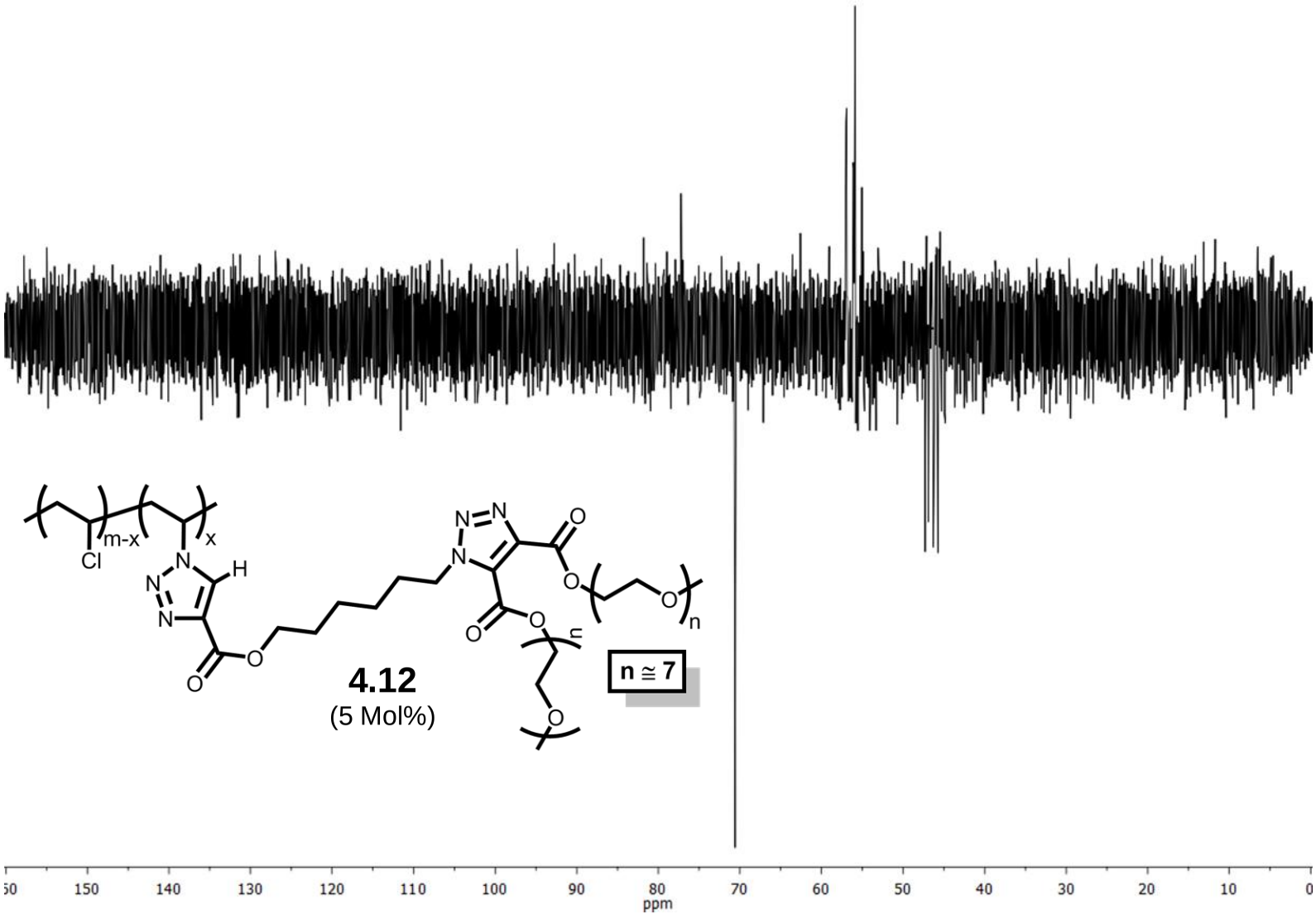
m-x
x
Cl
H
N
O
n
4.12
(5 Mol%)
n ≅ 7
150
140
130
120
110
100
90
80
70
60
50
40
30
20
10
0
ppm

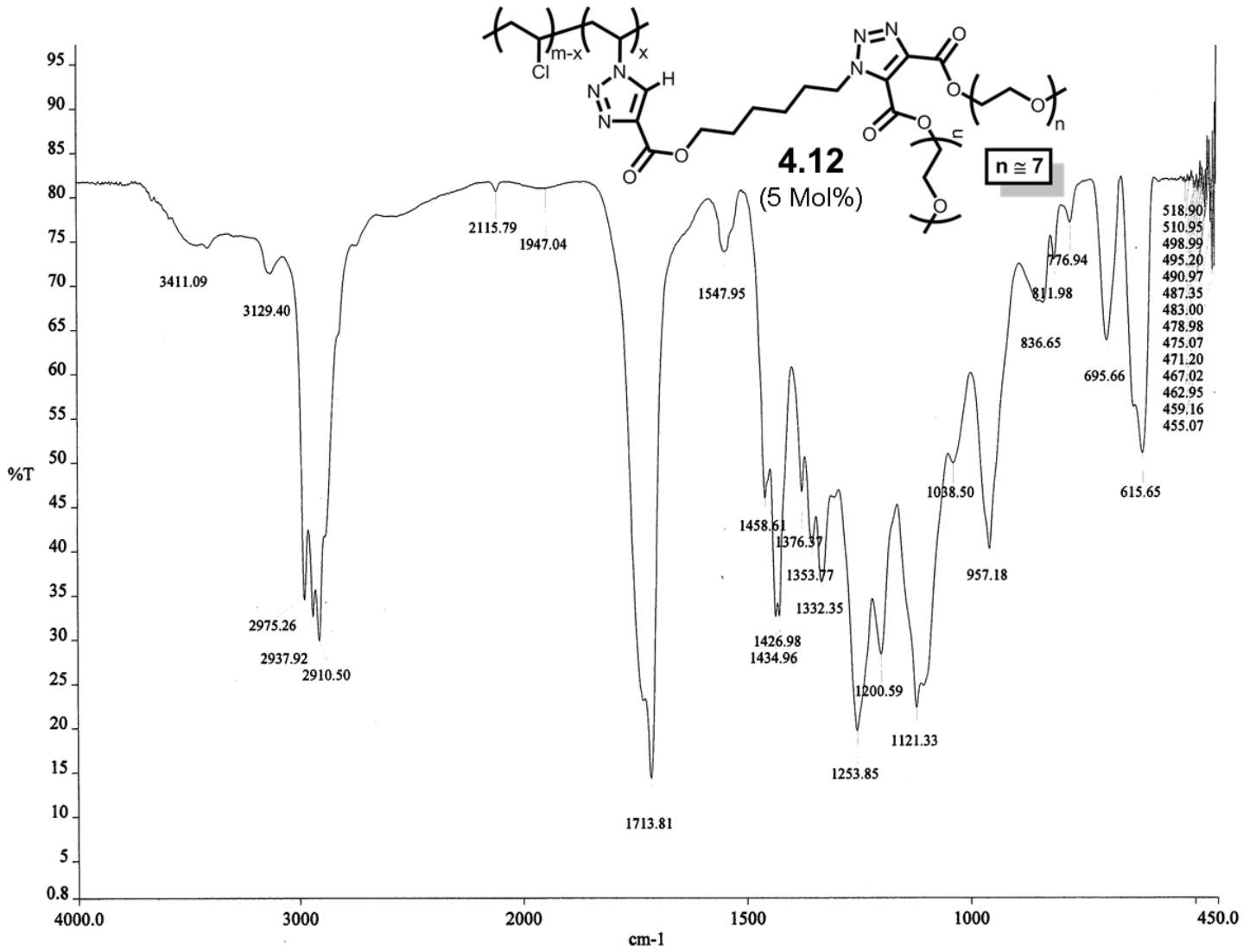
4.12
(5 Mol%)
n ≅ 7
%T
cm-1
4000.0
3000
2000
1500
1000
450.0
3411.09
3129.40
2975.26
2937.92
2910.50
2115.79
1947.04
1713.81
1547.95
1458.61
1376.37
1353.77
1332.35
1426.98
1434.96
1253.85
1200.59
1121.33
1038.50
957.18
836.65
811.98
776.94
695.66
615.65
518.90
510.95
498.99
495.20
490.97
487.35
483.00
478.98
475.07
471.20
467.02
462.95
459.16
455.07

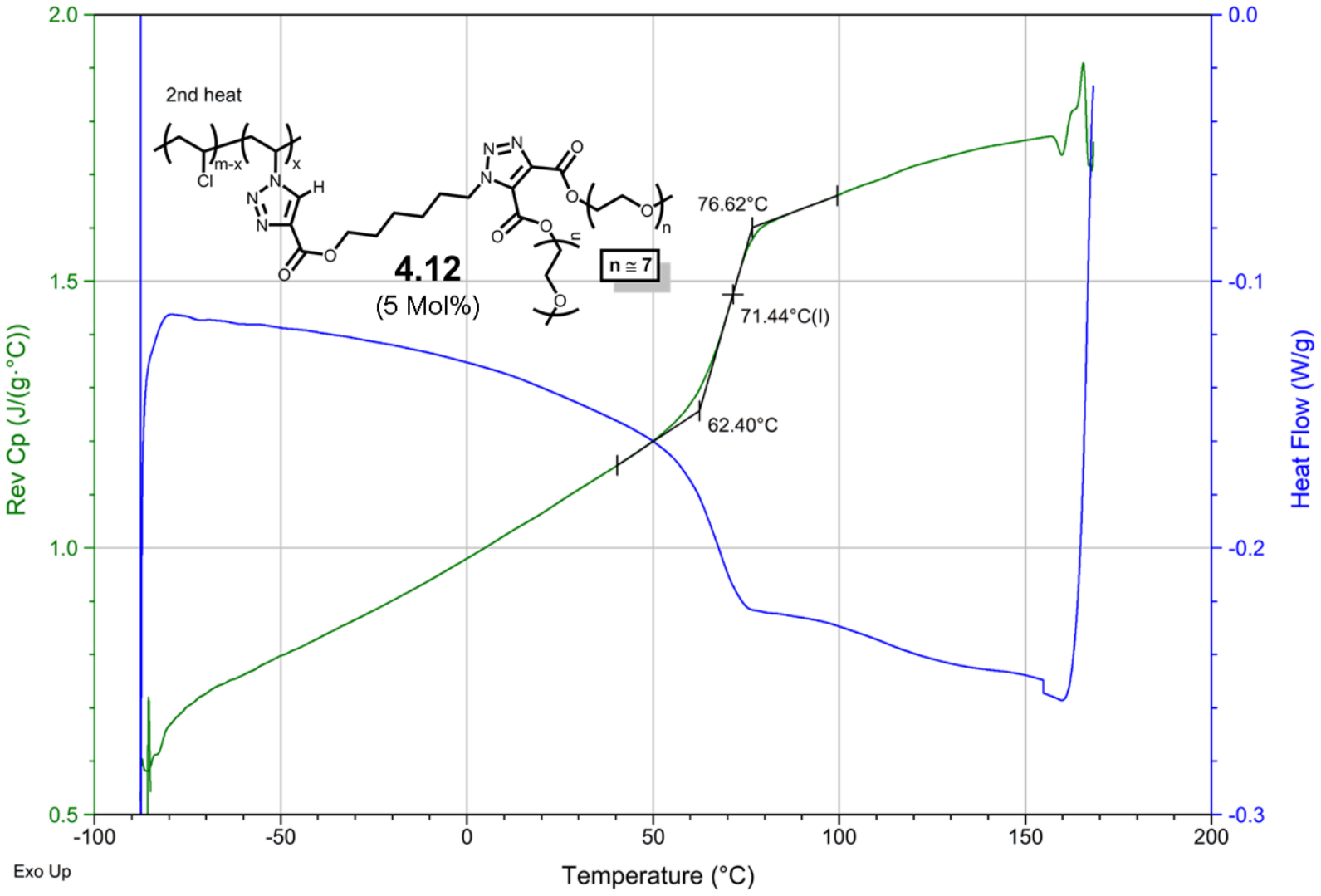
2nd heat
4.12
(5 Mol%)
n ≅ 7
76.62°C
71.44°C(I)
62.40°C
Rev Cp (J/(g·°C))
Heat Flow (W/g)
Temperature (°C)
Exo Up
2.0
1.5
1.0
0.5
0.0
-0.1
-0.2
-0.3
-100
-50
0
50
100
150
200

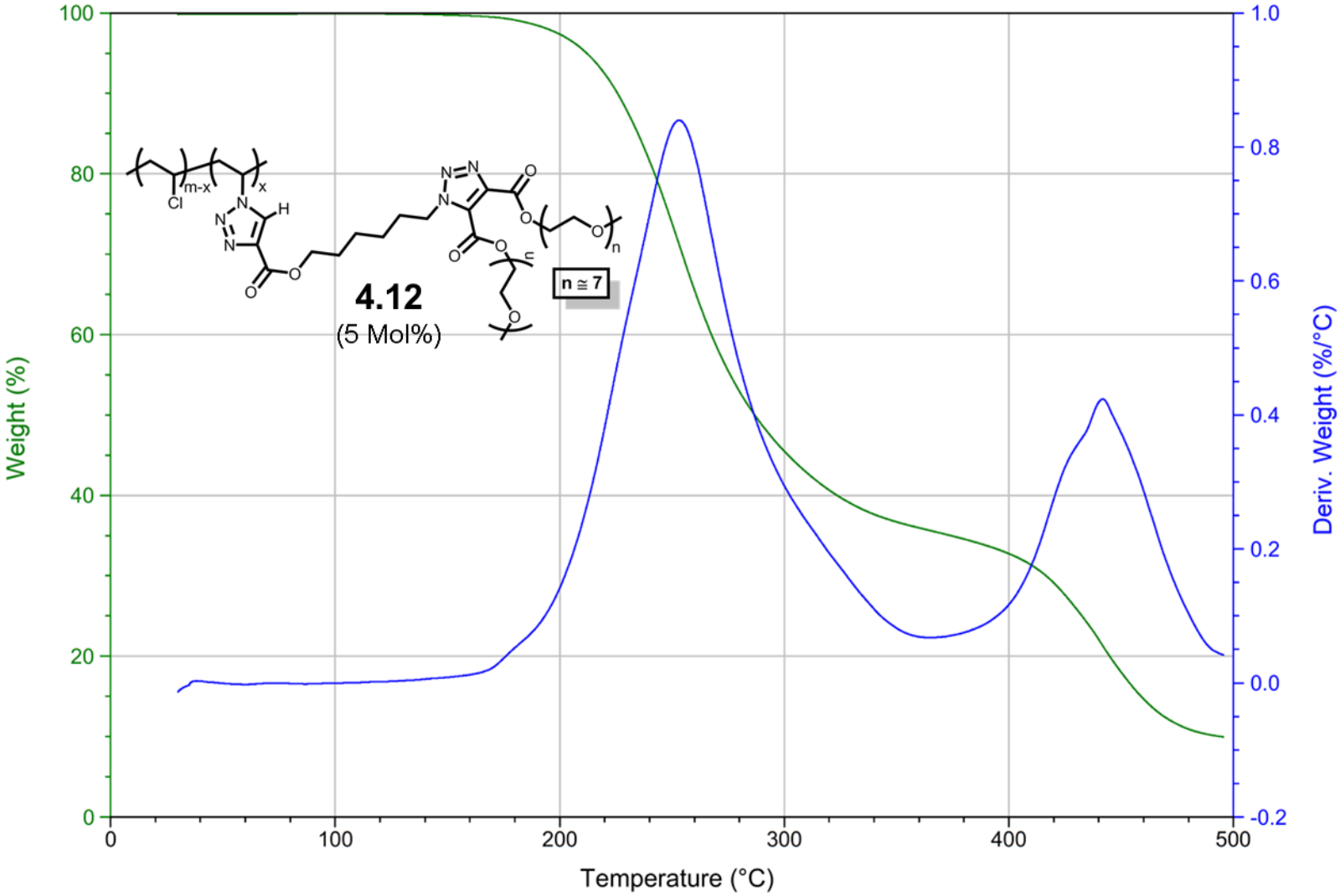
4.12
(5 Mol%)
n ≅ 7
Weight (%)
Deriv. Weight (%/°C)
Temperature (°C)
0
20
40
60
80
100
-0.2
0.0
0.2
0.4
0.6
0.8
1.0
0
100
200
300
400
500

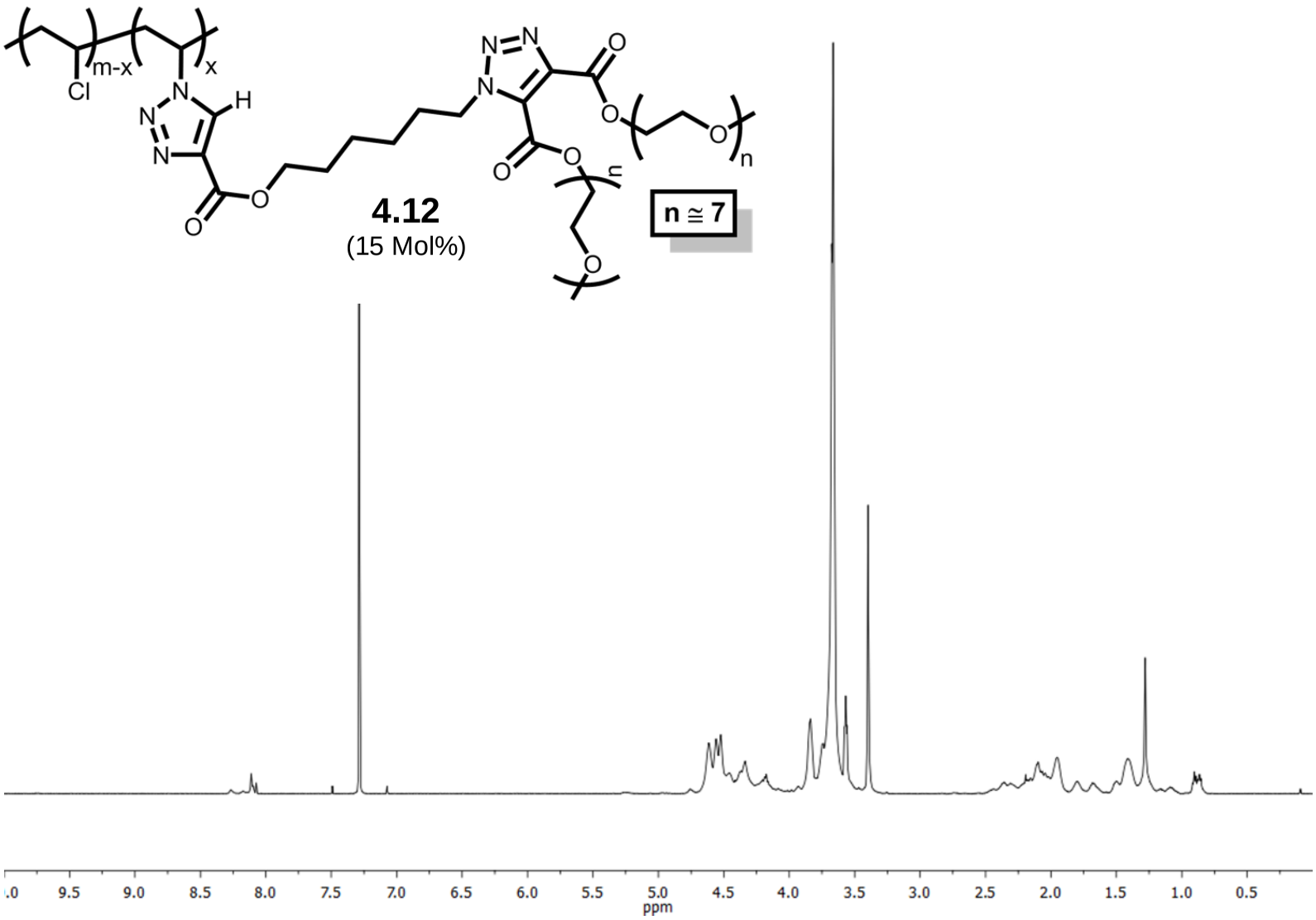
m-x
x
Cl
H
N
N
N
N
O
O
O
O
O
O
n
n
O
4.12
(15 Mol%)
n ≅ 7
9.5
9.0
8.5
8.0
7.5
7.0
6.5
6.0
5.5
5.0
4.5
4.0
3.5
3.0
2.5
2.0
1.5
1.0
0.5
ppm

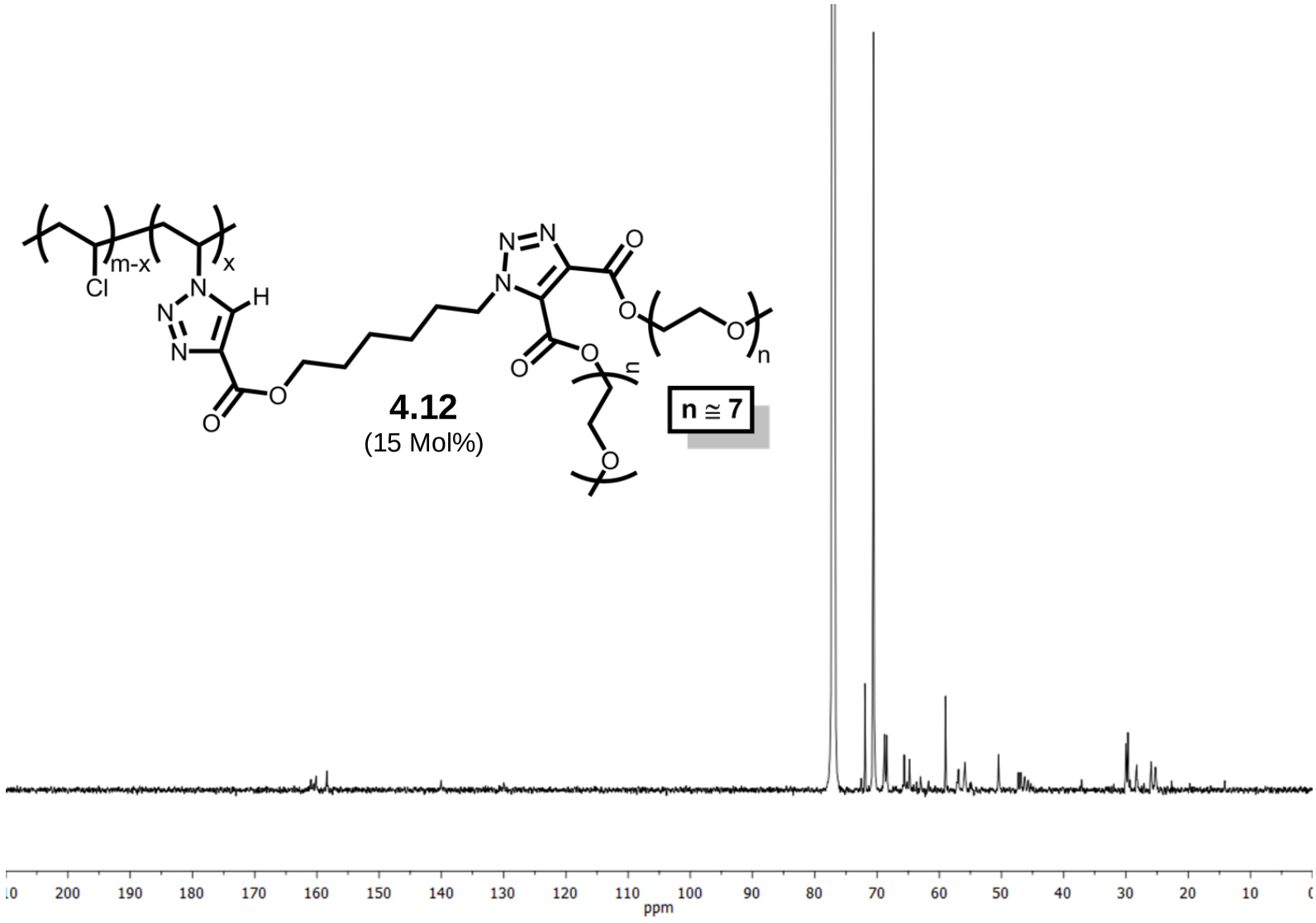
m-x
x
Cl
H
N
O
O
n
4.12
(15 Mol%)
n ≅ 7
ppm
200
190
180
170
160
150
140
130
120
110
100
90
80
70
60
50
40
30
20
10

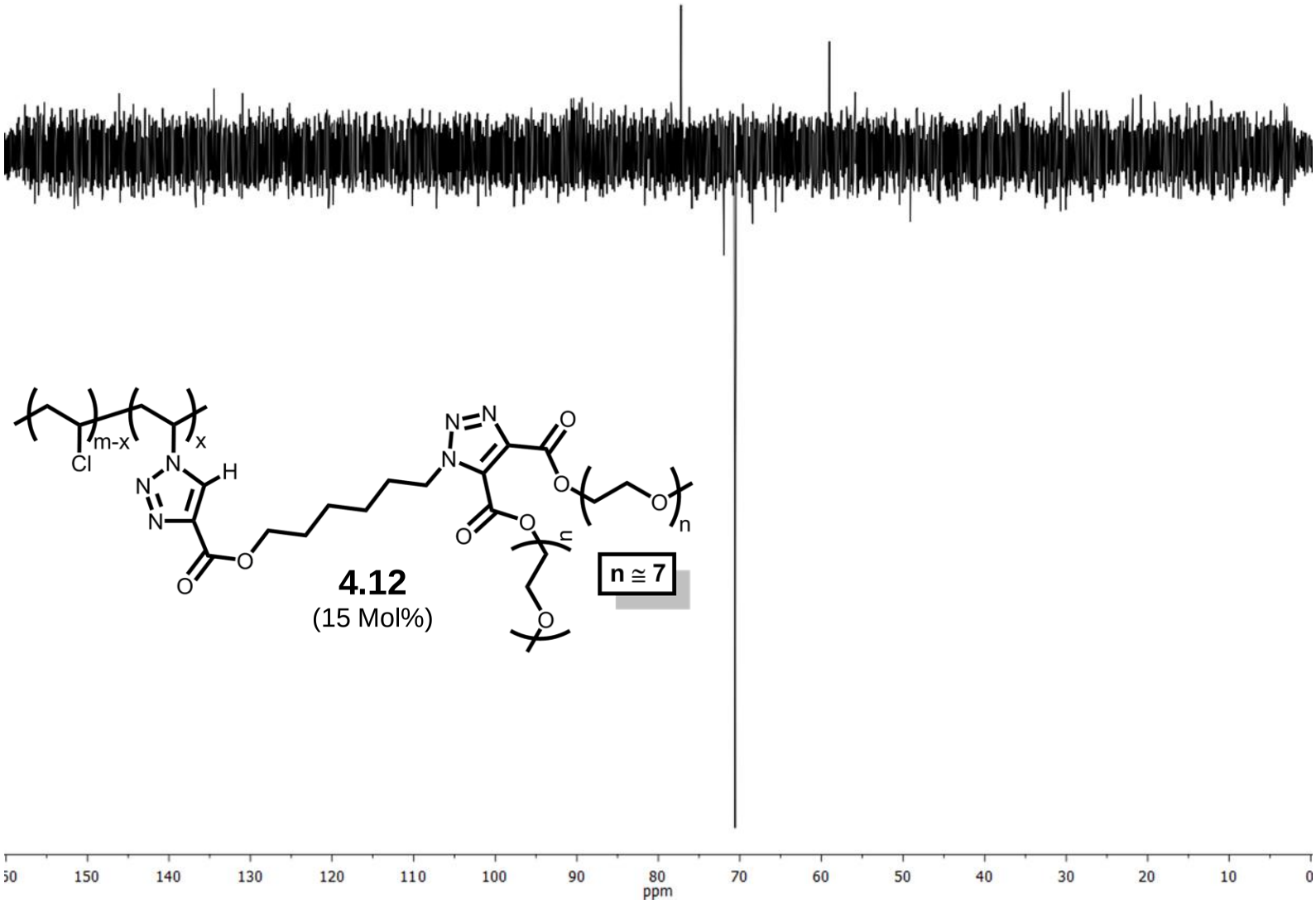
Cl
m-x
x
N
N
N
H
O
O
N
N
O
O
O
O
n
O
O
n
O
n ≅ 7
150
140
130
120
110
100
90
80
70
60
50
40
30
20
10
ppm

4.12
(15 Mol%)

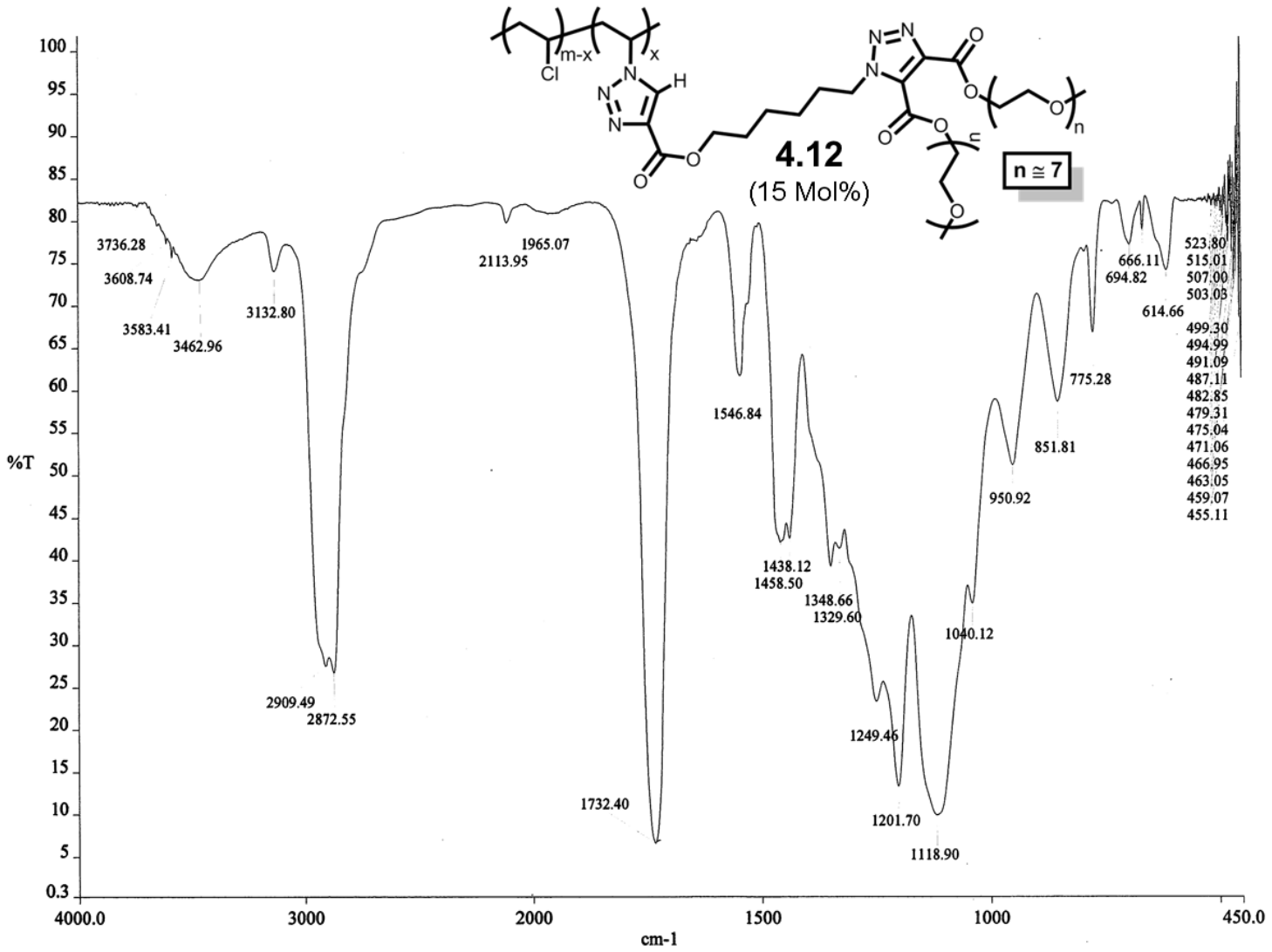
4.12
(15 Mol%)
n ≅ 7
%T
cm-1
4000.0
3000
2000
1500
1000
450.0
3736.28
3608.74
3583.41
3462.96
3132.80
2909.49
2872.55
2113.95
1965.07
1732.40
1546.84
1438.12
1458.50
1348.66
1329.60
1249.46
1201.70
1118.90
1040.12
950.92
851.81
775.28
694.82
666.11
614.66
523.80
515.01
507.00
503.03
499.30
494.99
491.09
487.11
482.85
479.31
475.04
471.06
466.95
463.05
459.07
455.11

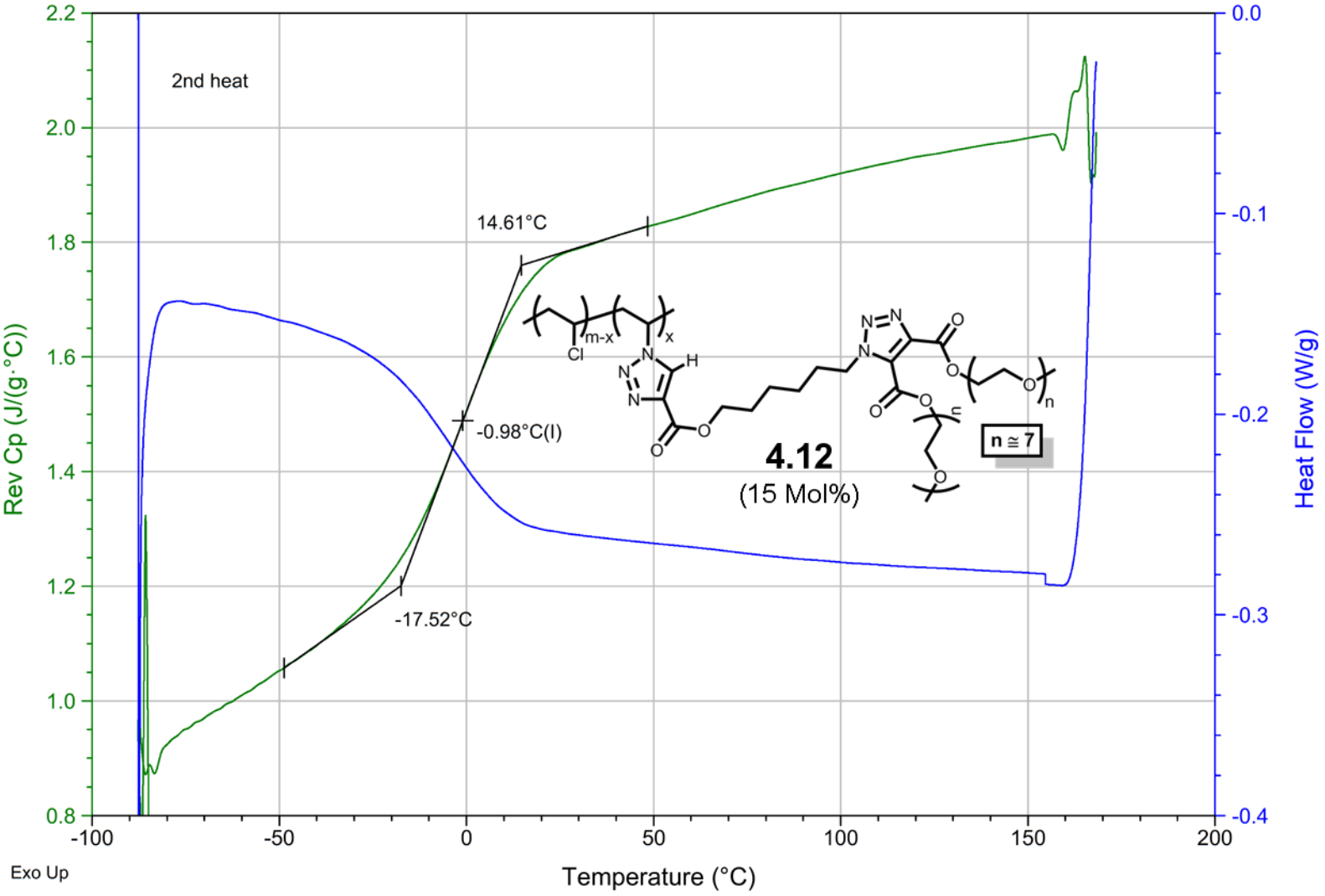
2nd heat
14.61°C
-0.98°C(I)
-17.52°C
4.12
(15 Mol%)
n ≅ 7
Rev Cp (J/(g·°C))
Heat Flow (W/g)
Temperature (°C)
Exo Up
2.2
2.0
1.8
1.6
1.4
1.2
1.0
0.8
0.0
-0.1
-0.2
-0.3
-0.4
-100
-50
0
50
100
150
200

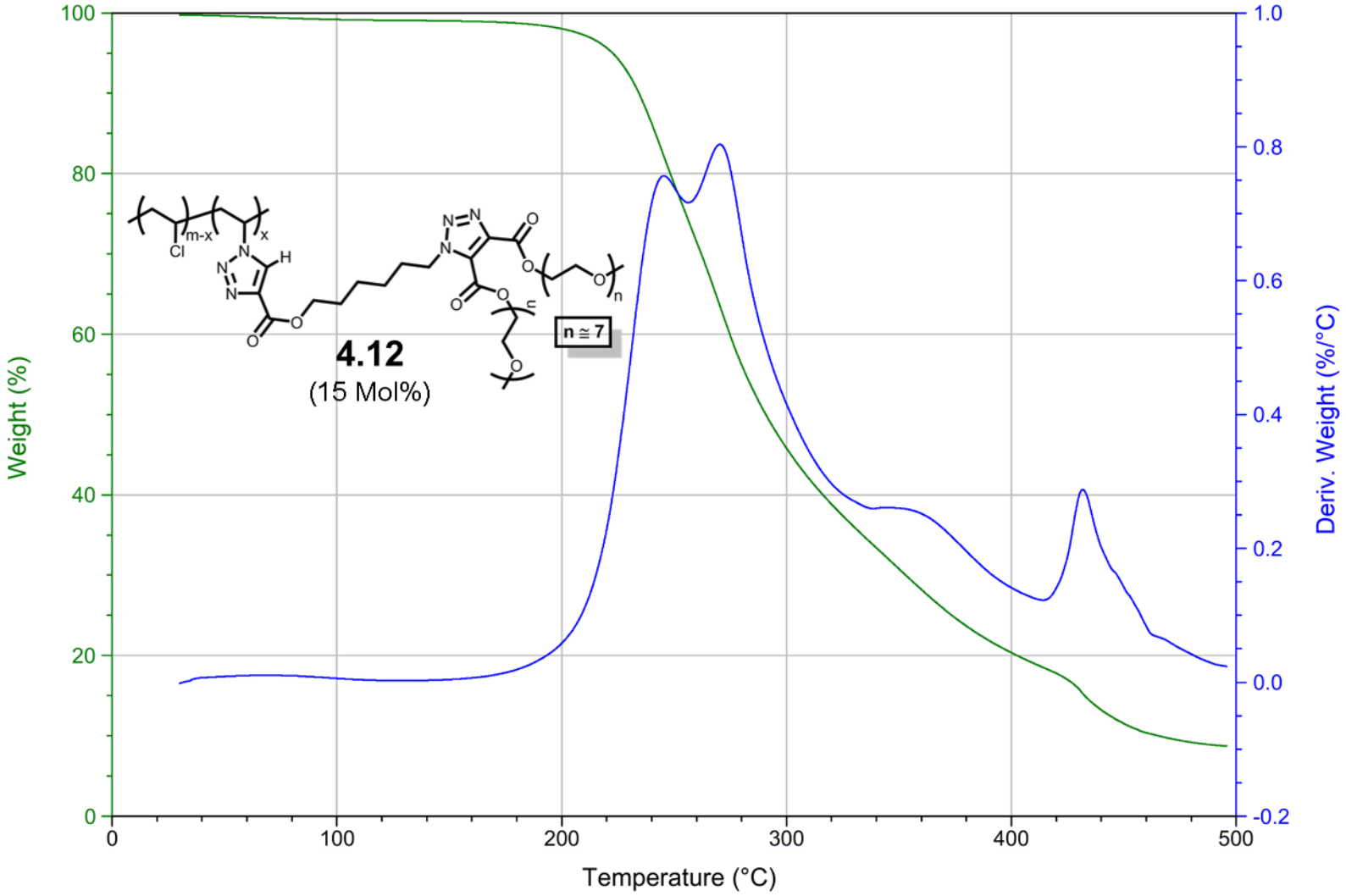
Weight (%)
Deriv. Weight (%/°C)
Temperature (°C)
100
80
60
40
20
0
1.0
0.8
0.6
0.4
0.2
0.0
-0.2
0
100
200
300
400
500
m-x
x
Cl
H
n ≅ 7
4.12
(15 Mol%)

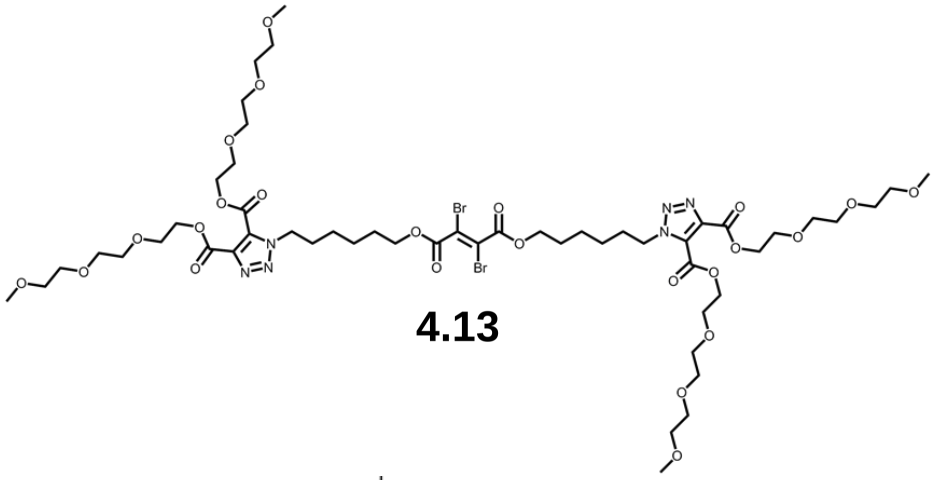

4.13

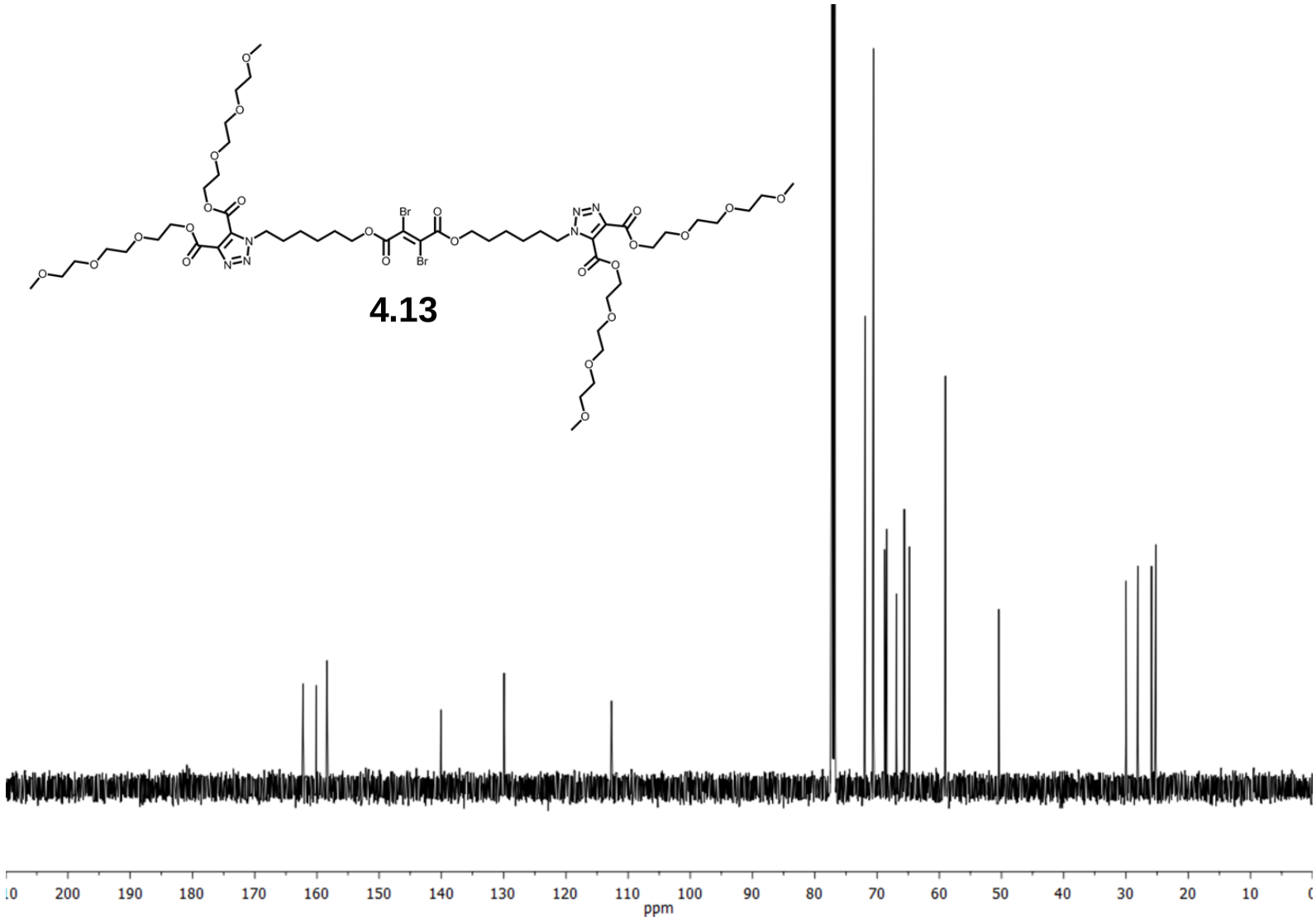
4.13
ppm

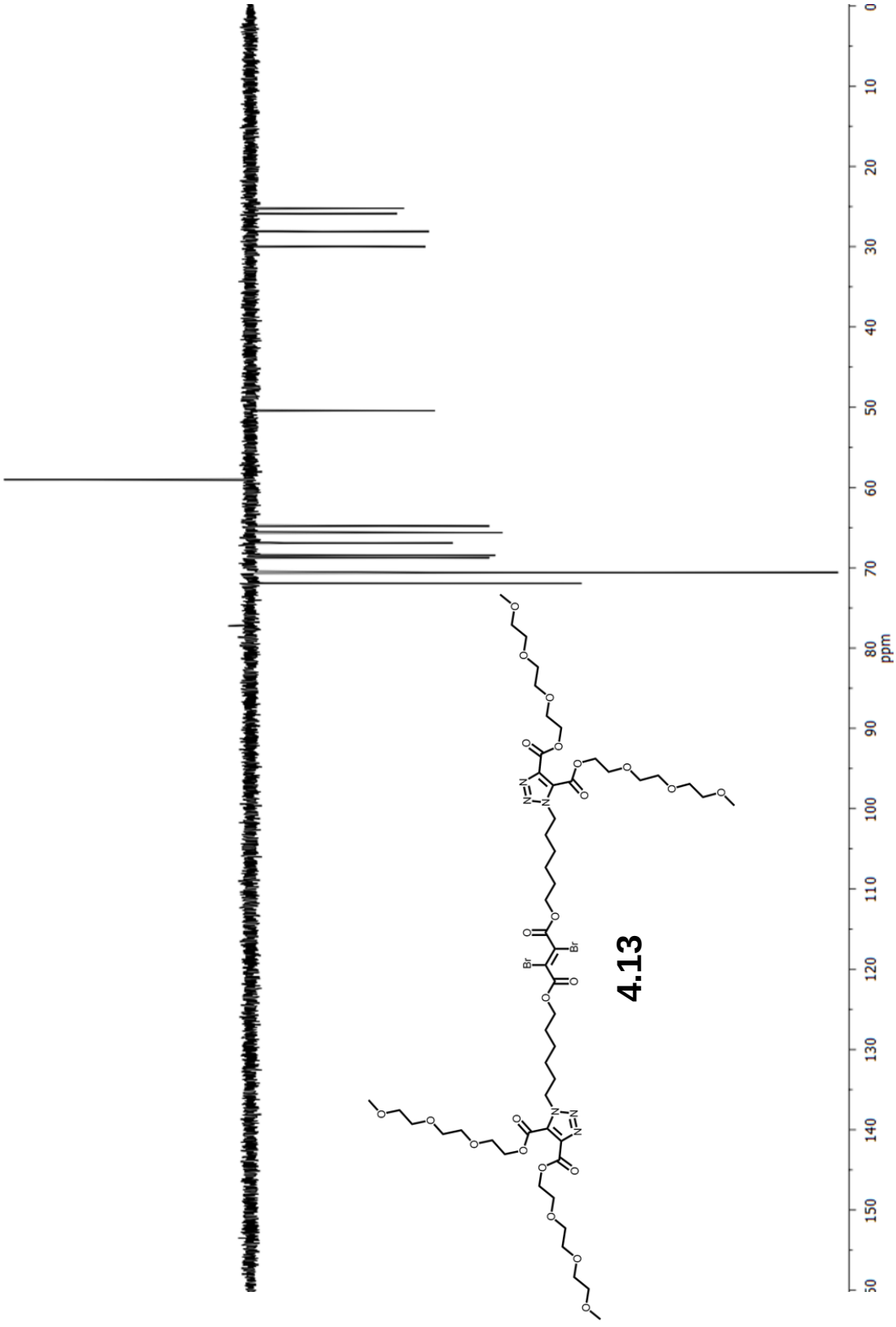
4.13
ppm
0
10
20
30
40
50
60
70
80
90
100
110
120
130
140
150
50

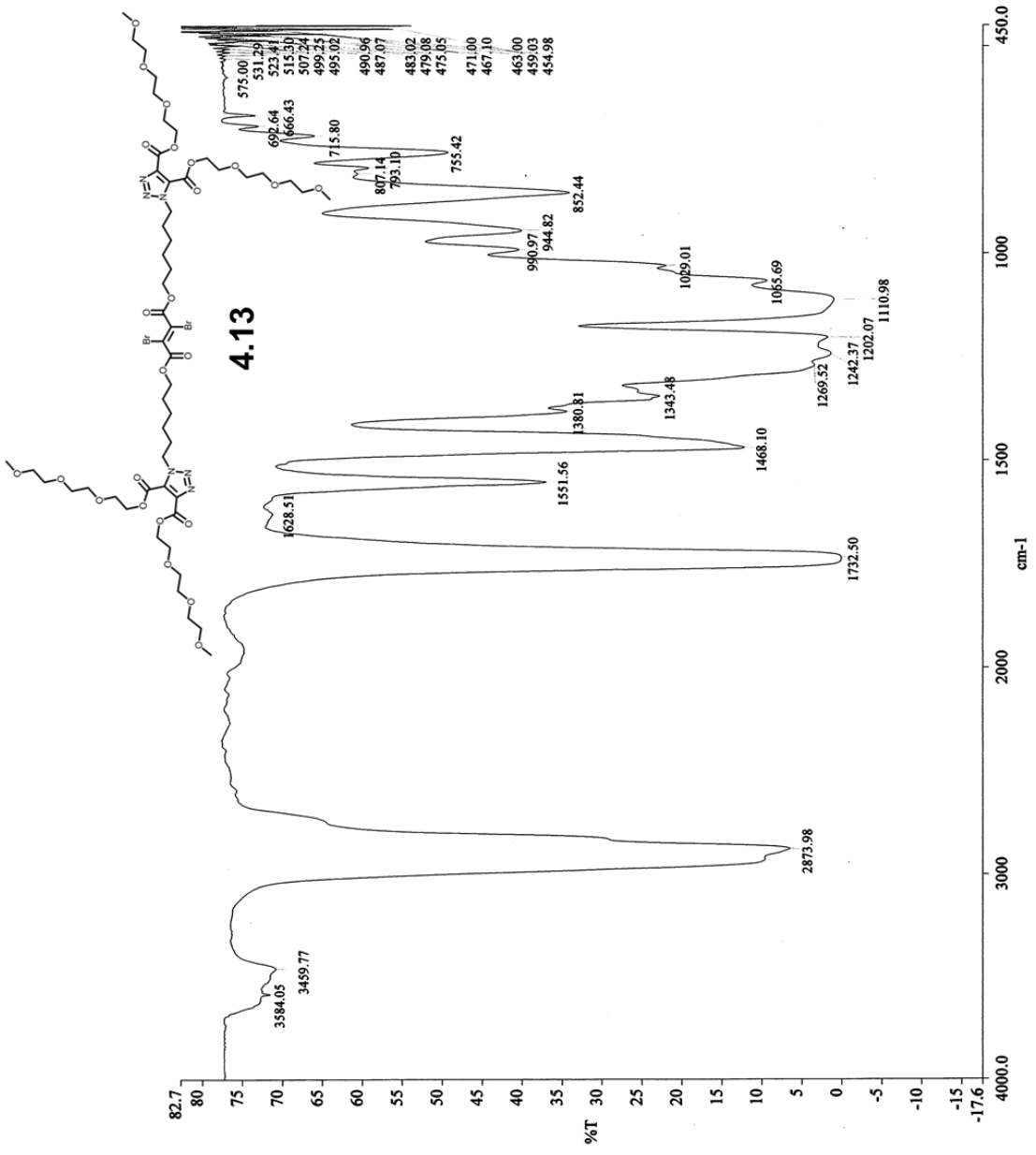
4.13
3584.05
3459.77
2873.98
1732.50
1628.51
1551.56
1468.10
1380.81
1343.48
1269.52
1242.37
1202.07
1110.98
1063.69
1029.01
990.97
944.82
852.44
807.14
793.10
755.42
715.80
692.64
666.43
575.00
531.29
523.41
515.30
507.24
499.25
495.02
490.96
487.07
483.02
479.08
475.05
471.00
467.10
463.00
459.03
454.98
%T
cm-1
82.7
-17.6
4000.0
450.0

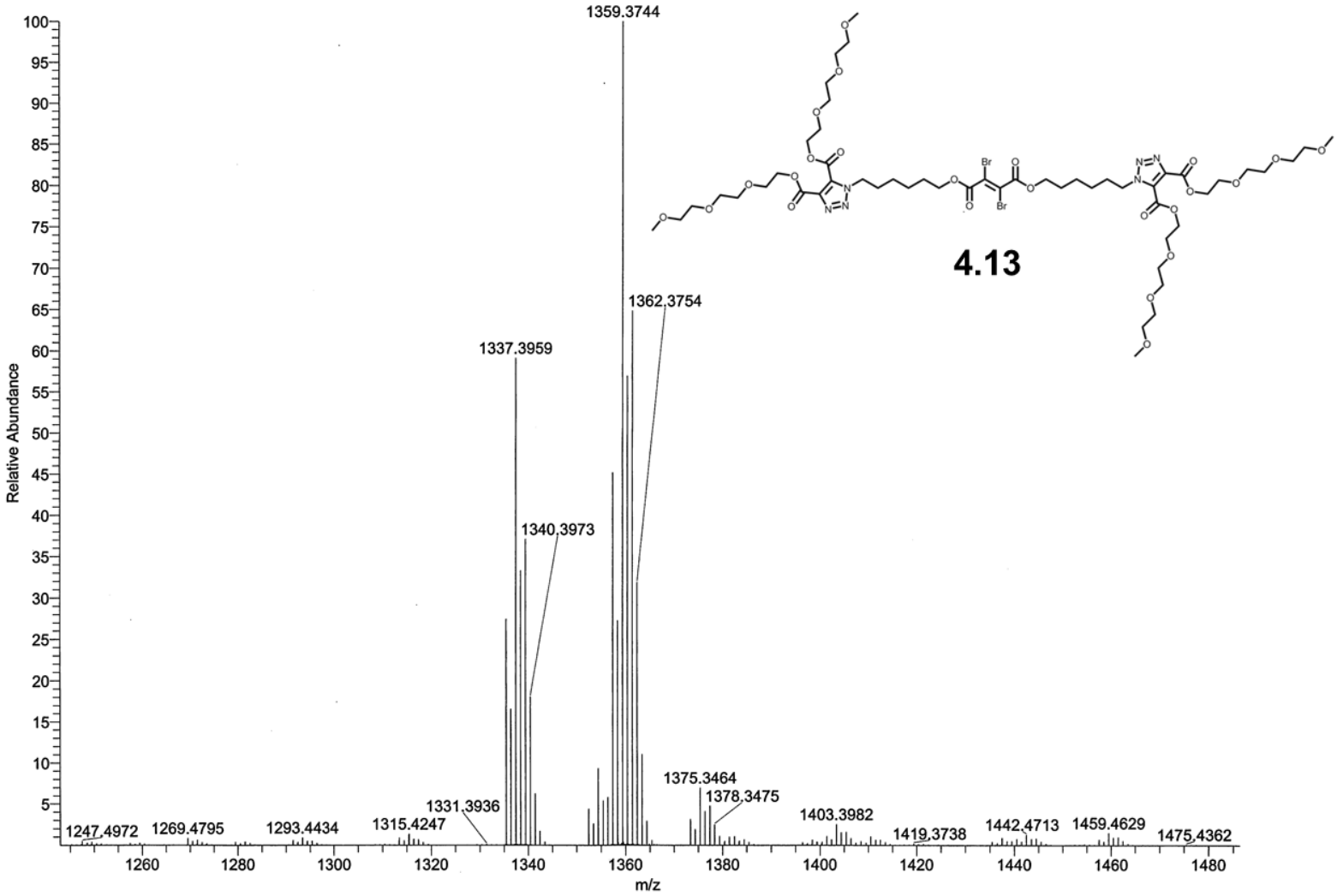
1359.3744
1362.3754
1337.3959
1340.3973
1375.3464
1378.3475
1331.3936
1315.4247
1247.4972
1269.4795
1293.4434
1403.3982
1419.3738
1442.4713
1459.4629
1475.4362
Relative Abundance
m/z
4.13

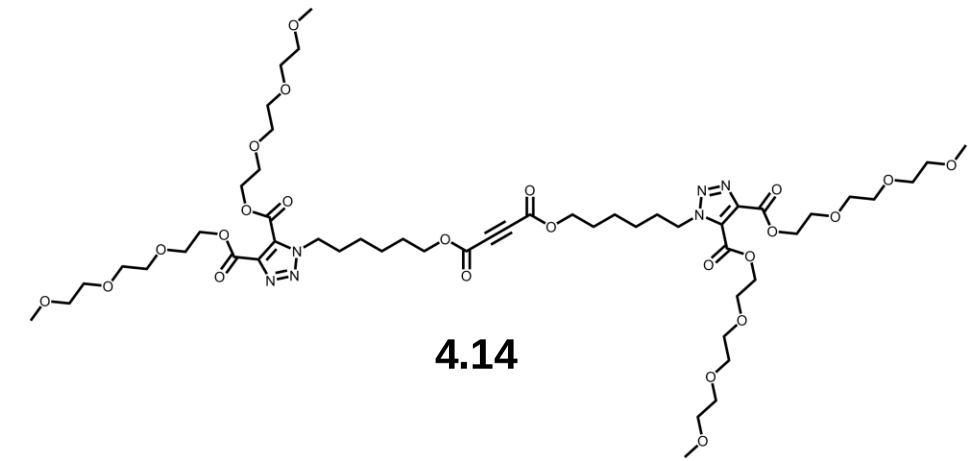

4.14

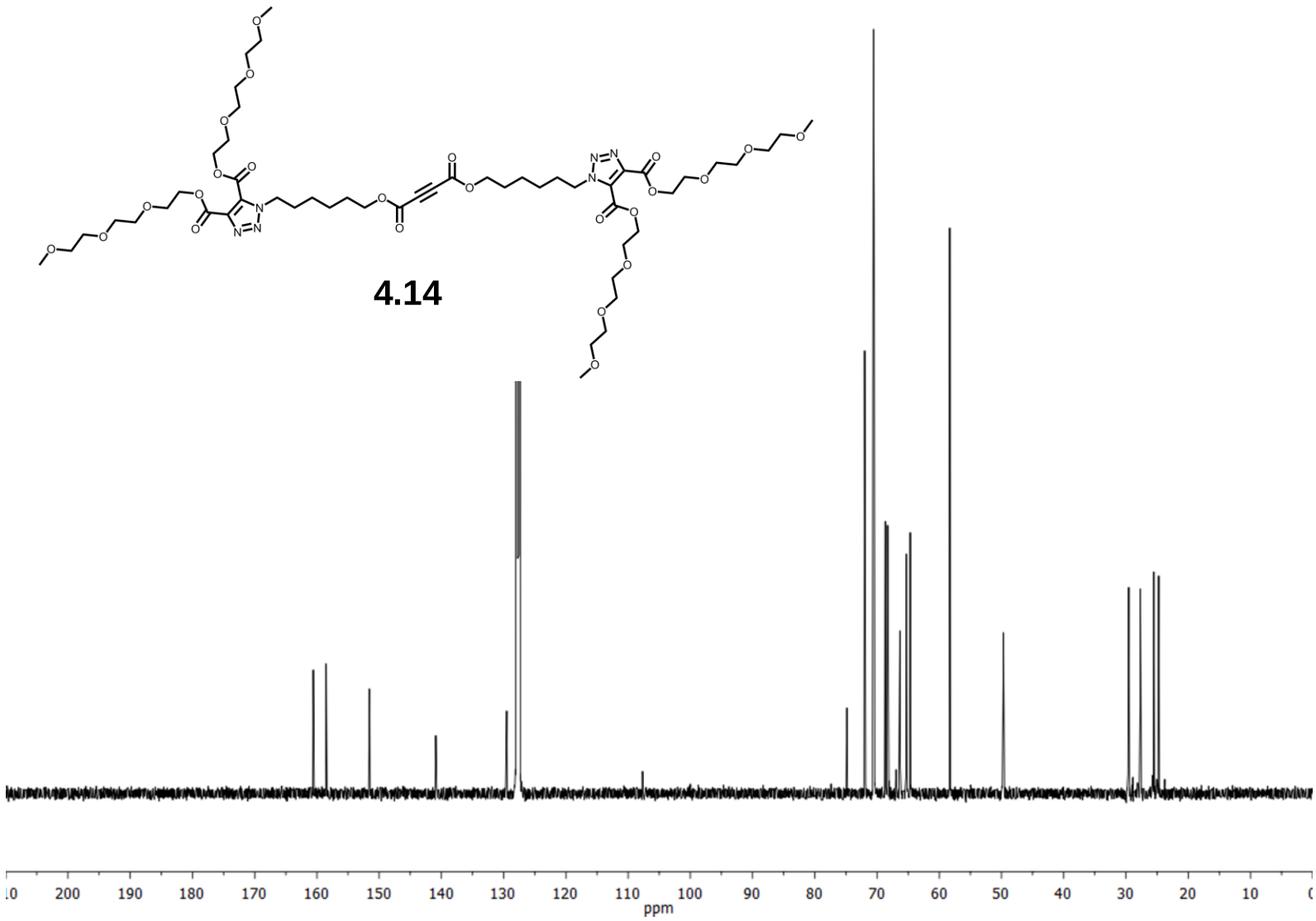
4.14
ppm

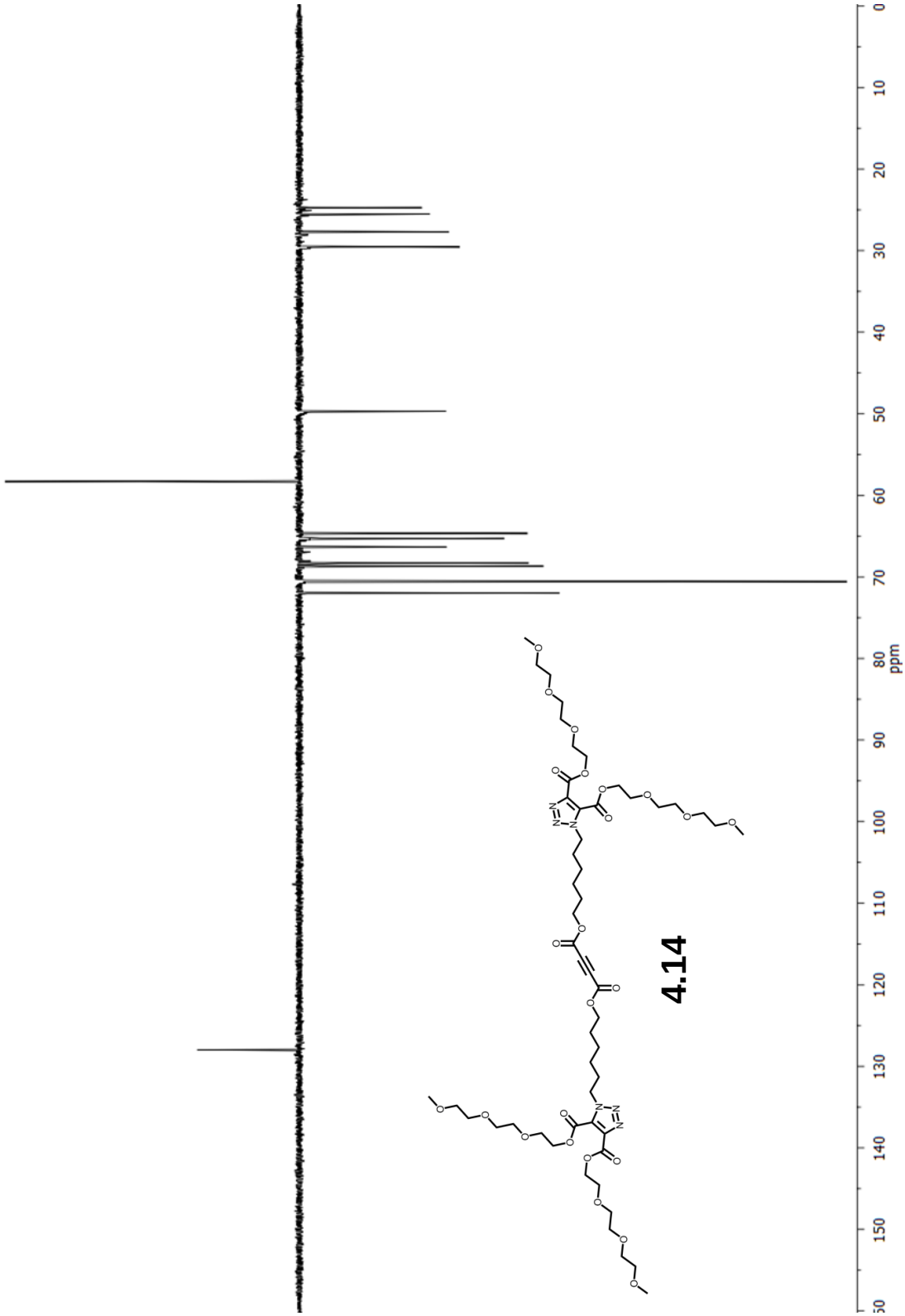
4.14
ppm

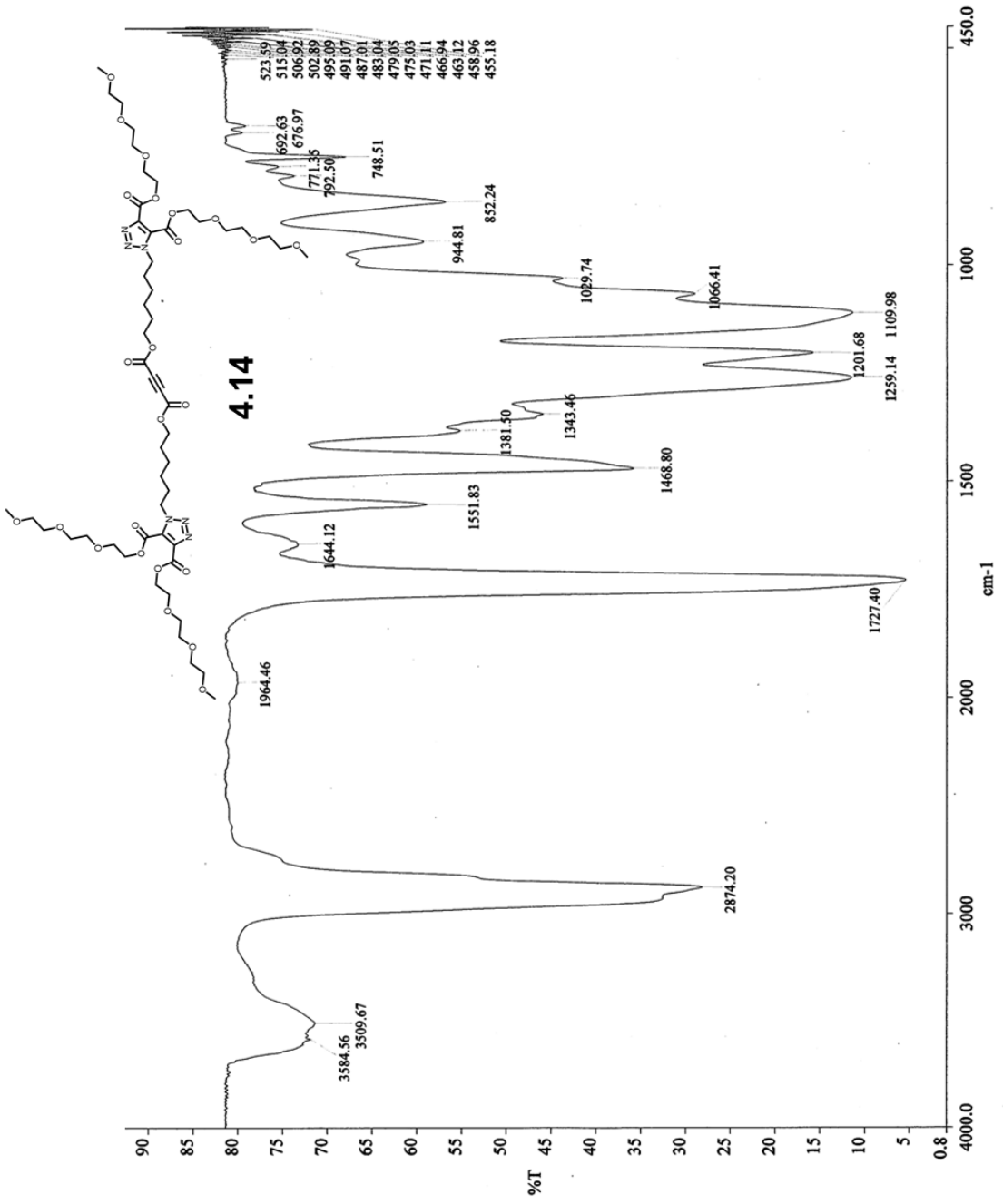
4.14
%T
cm-1
4000.0
3000
2000
1500
1000
450.0
0.8
5
10
15
20
25
30
35
40
45
50
55
60
65
70
75
80
85
90
3584.56
3509.67
2874.20
1964.46
1727.40
1644.12
1551.83
1468.80
1381.50
1343.46
1259.14
1201.68
1109.98
1066.41
1029.74
944.81
852.24
792.50
771.35
748.51
692.63
676.97
523.59
515.04
506.92
502.89
495.09
491.07
487.01
483.04
479.05
475.03
471.11
466.94
463.12
458.96
455.18

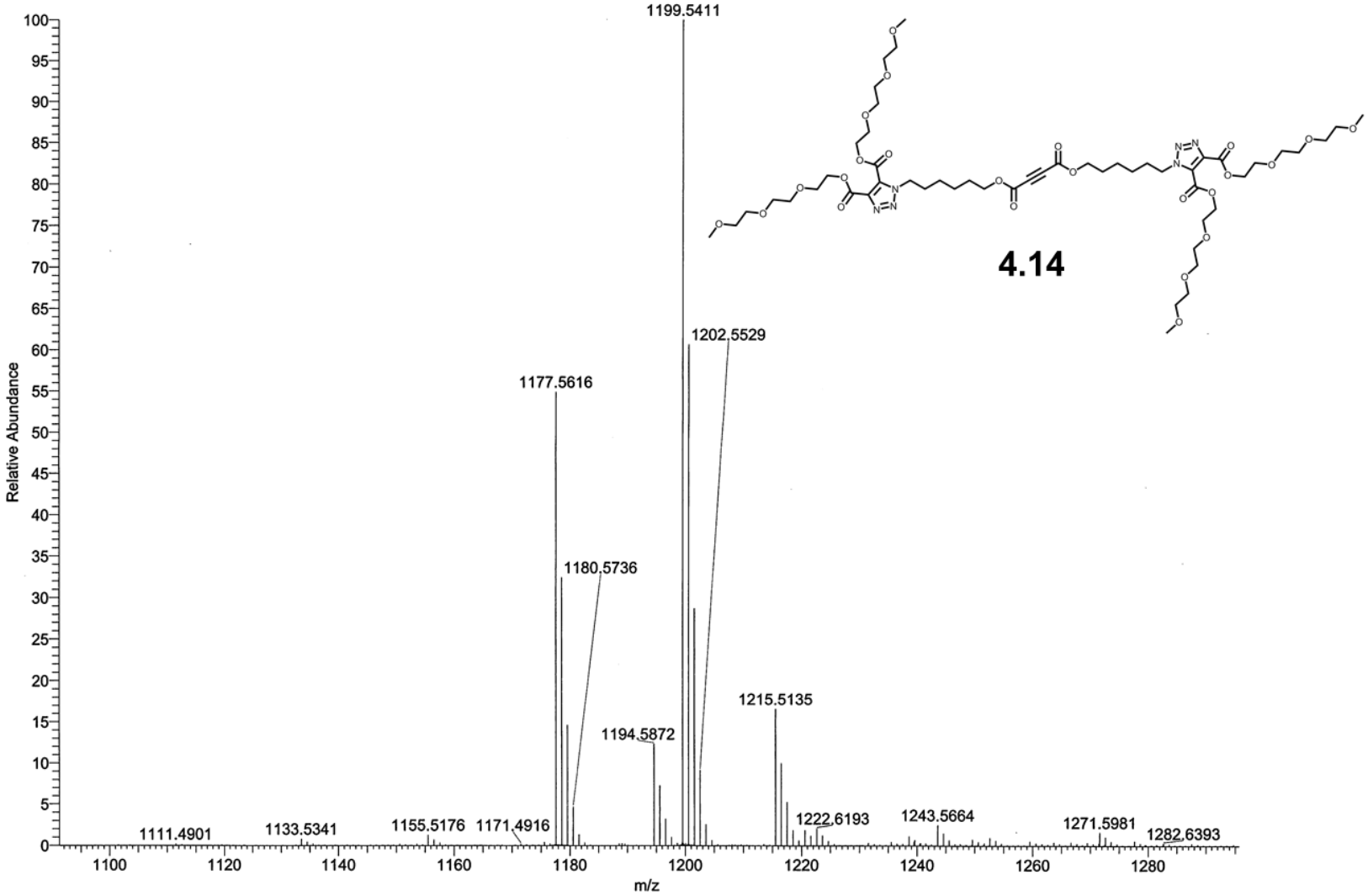
1199.5411
1202.5529
1177.5616
1180.5736
1215.5135
1194.5872
1111.4901
1133.5341
1155.5176
1171.4916
1222.6193
1243.5664
1271.5981
1282.6393
Relative Abundance
m/z
4.14

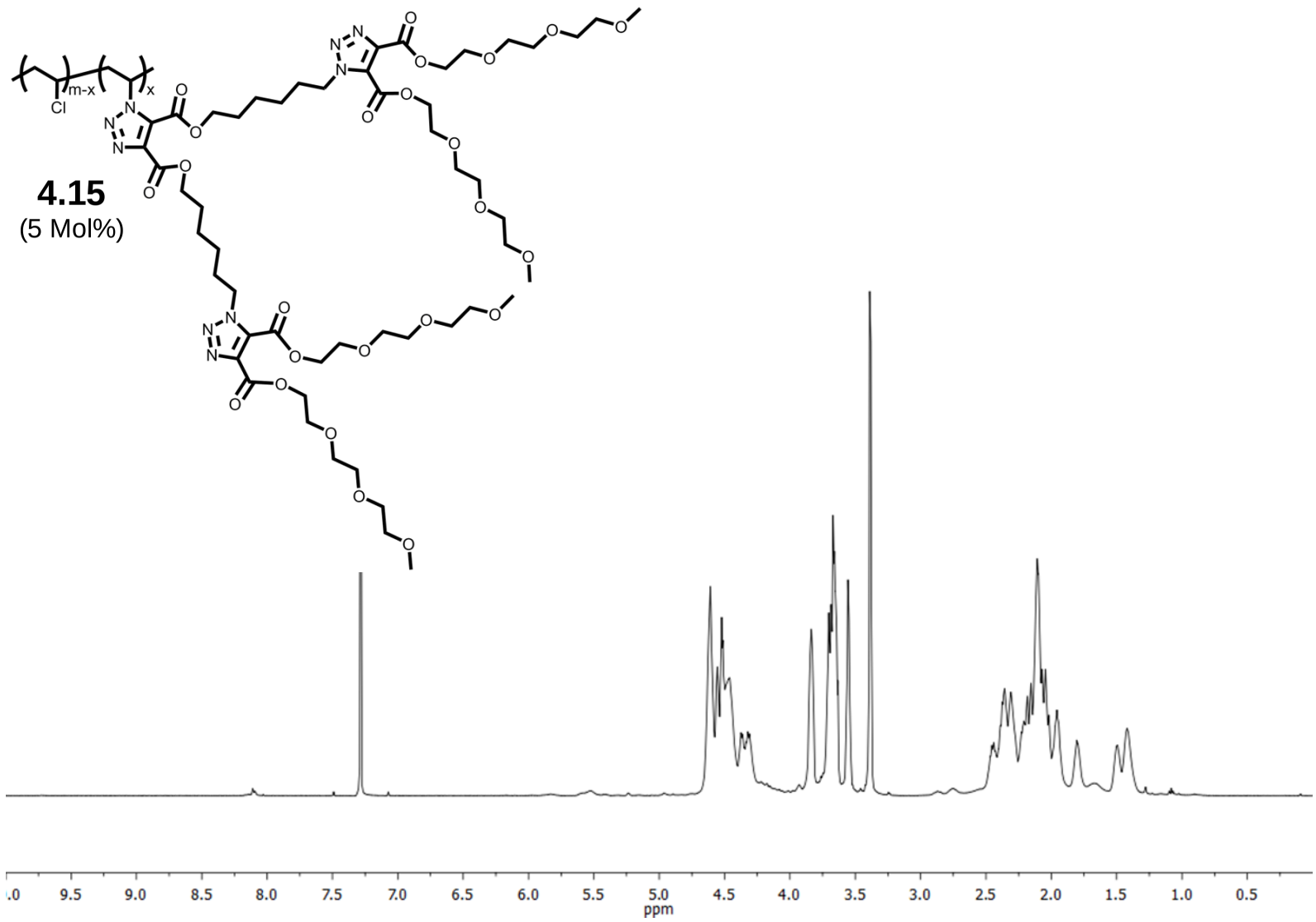
4.15
(5 Mol%)
m-x
x
Cl
ppm

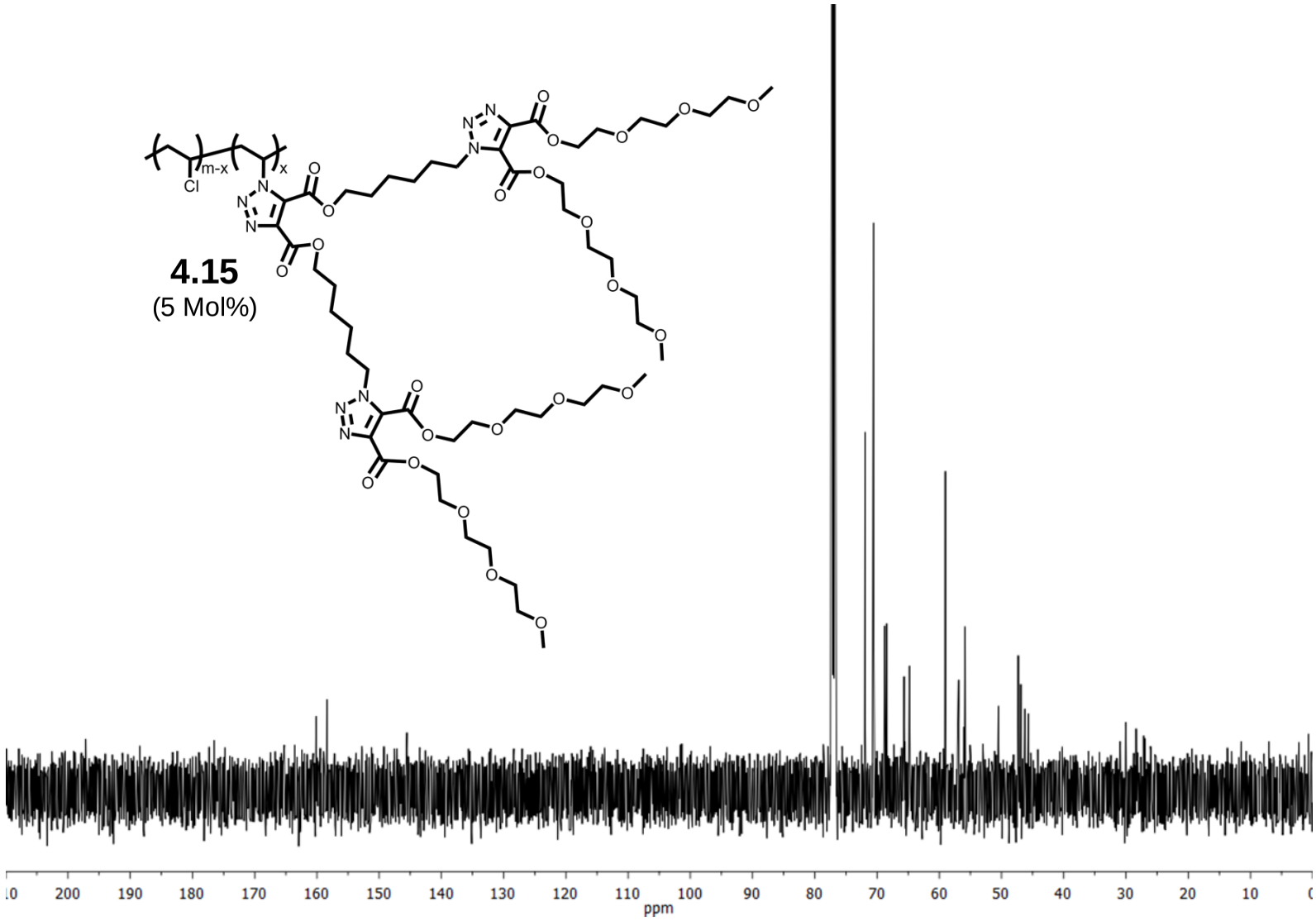
4.15
(5 Mol%)
m-x
x
Cl
ppm

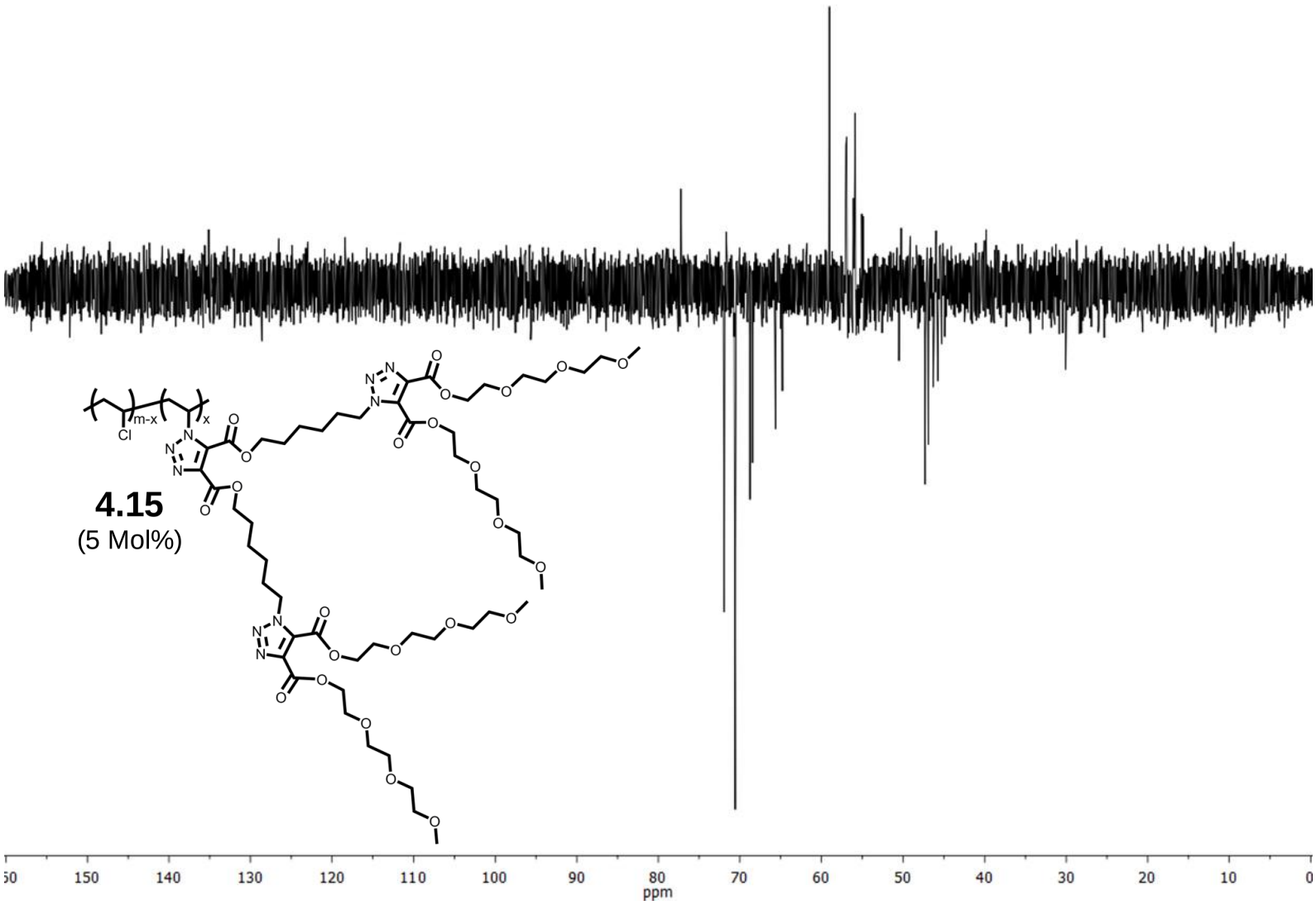
4.15
(5 Mol%)
m-x
x
Cl
150
140
130
120
110
100
90
80
70
60
50
40
30
20
10
ppm

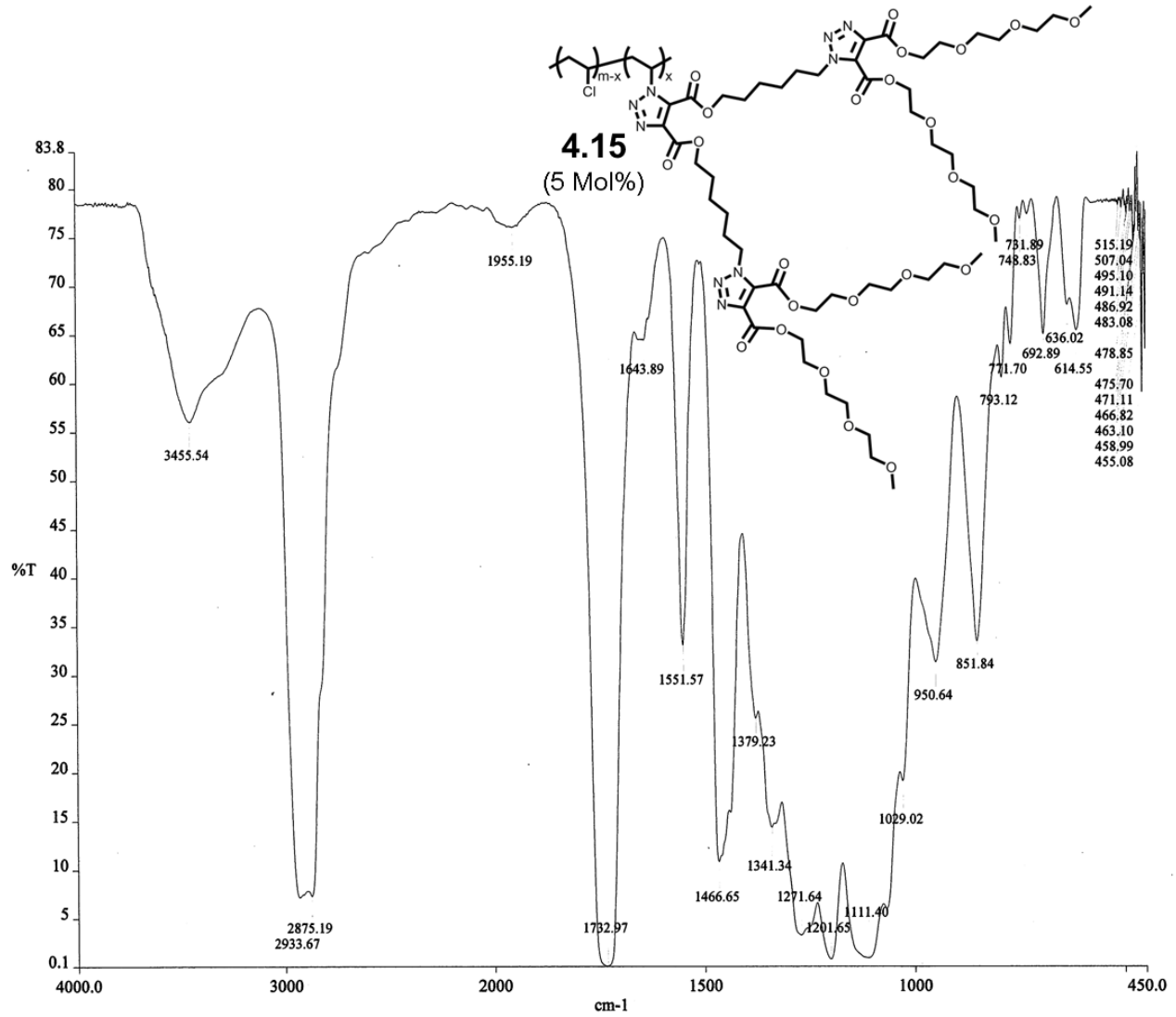
4.15
(5 Mol%)
%T
cm-1
3455.54
2933.67
2875.19
1955.19
1732.97
1643.89
1551.57
1466.65
1379.23
1341.34
1271.64
1201.65
1111.40
1029.02
950.64
851.84
793.12
771.70
748.83
731.89
692.89
636.02
614.55
515.19
507.04
495.10
491.14
486.92
483.08
478.85
475.70
471.11
466.82
463.10
458.99
455.08

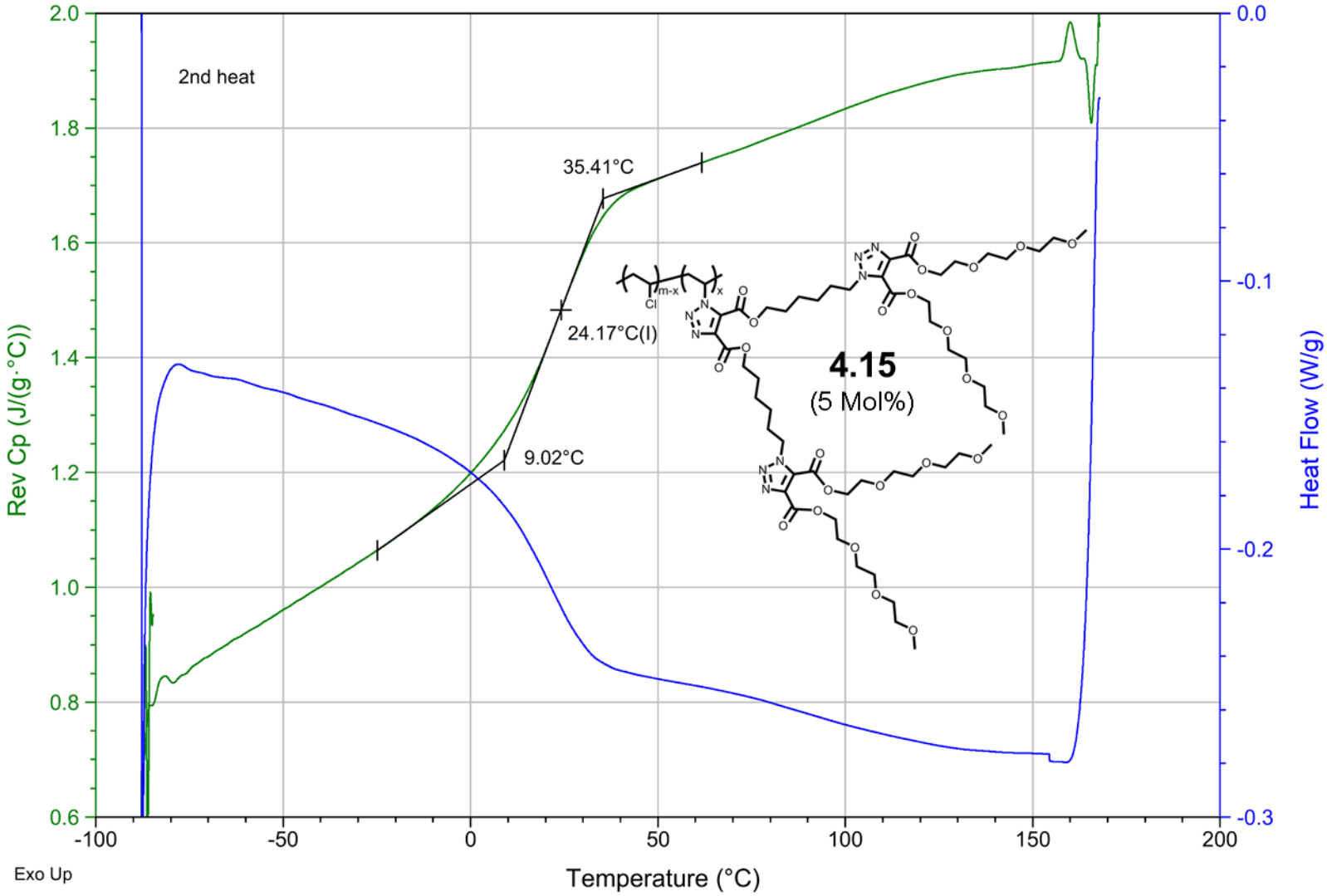
2nd heat
35.41°C
24.17°C(I)
9.02°C
4.15
(5 Mol%)
Rev Cp (J/(g·°C))
Heat Flow (W/g)
Temperature (°C)
Exo Up
2.0
1.8
1.6
1.4
1.2
1.0
0.8
0.6
0.0
-0.1
-0.2
-0.3
-100
-50
0
50
100
150
200

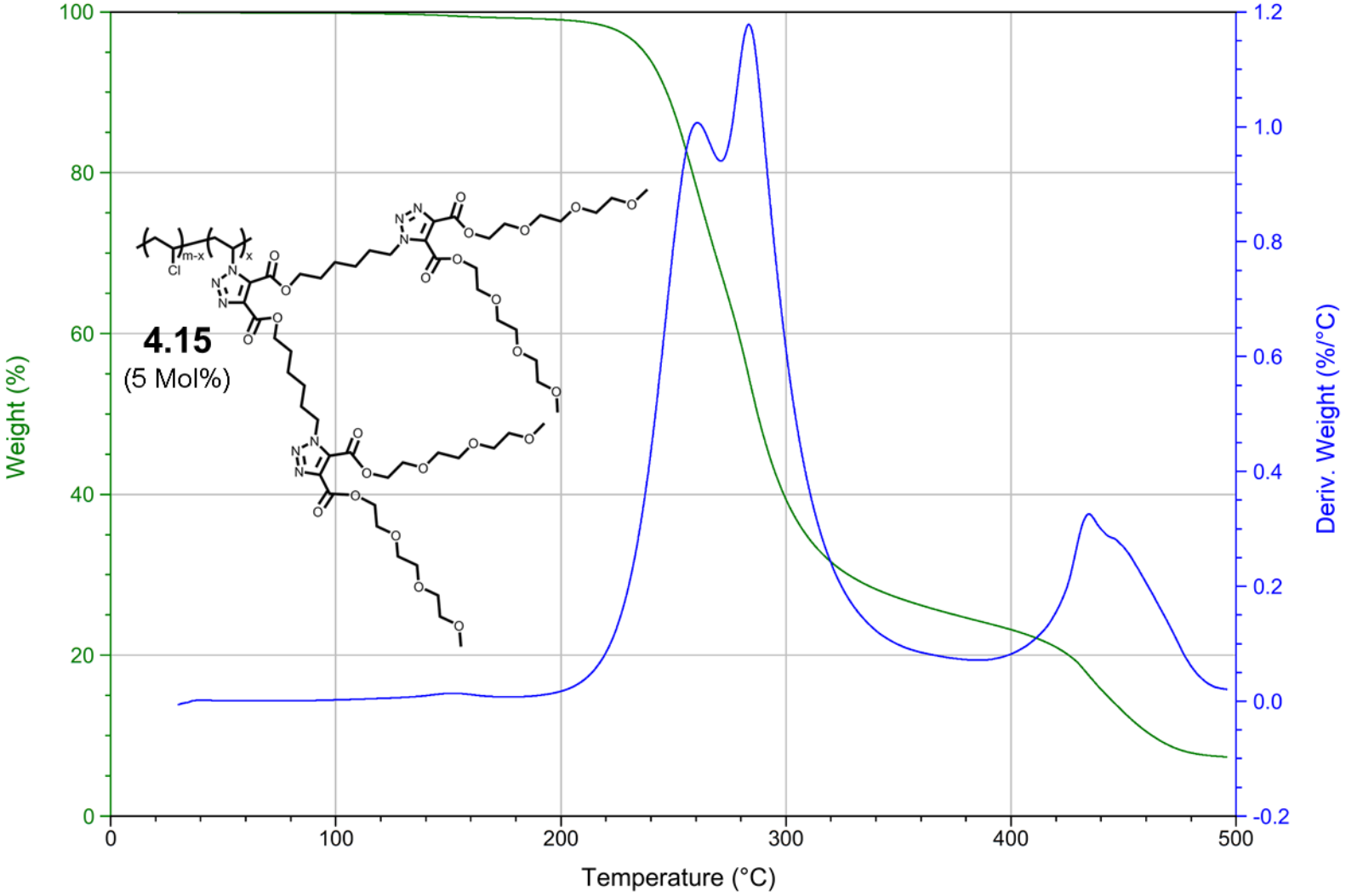
4.15
(5 Mol%)
Weight (%)
Deriv. Weight (%/°C)
Temperature (°C)
100
80
60
40
20
0
1.2
1.0
0.8
0.6
0.4
0.2
0.0
-0.2
0
100
200
300
400
500

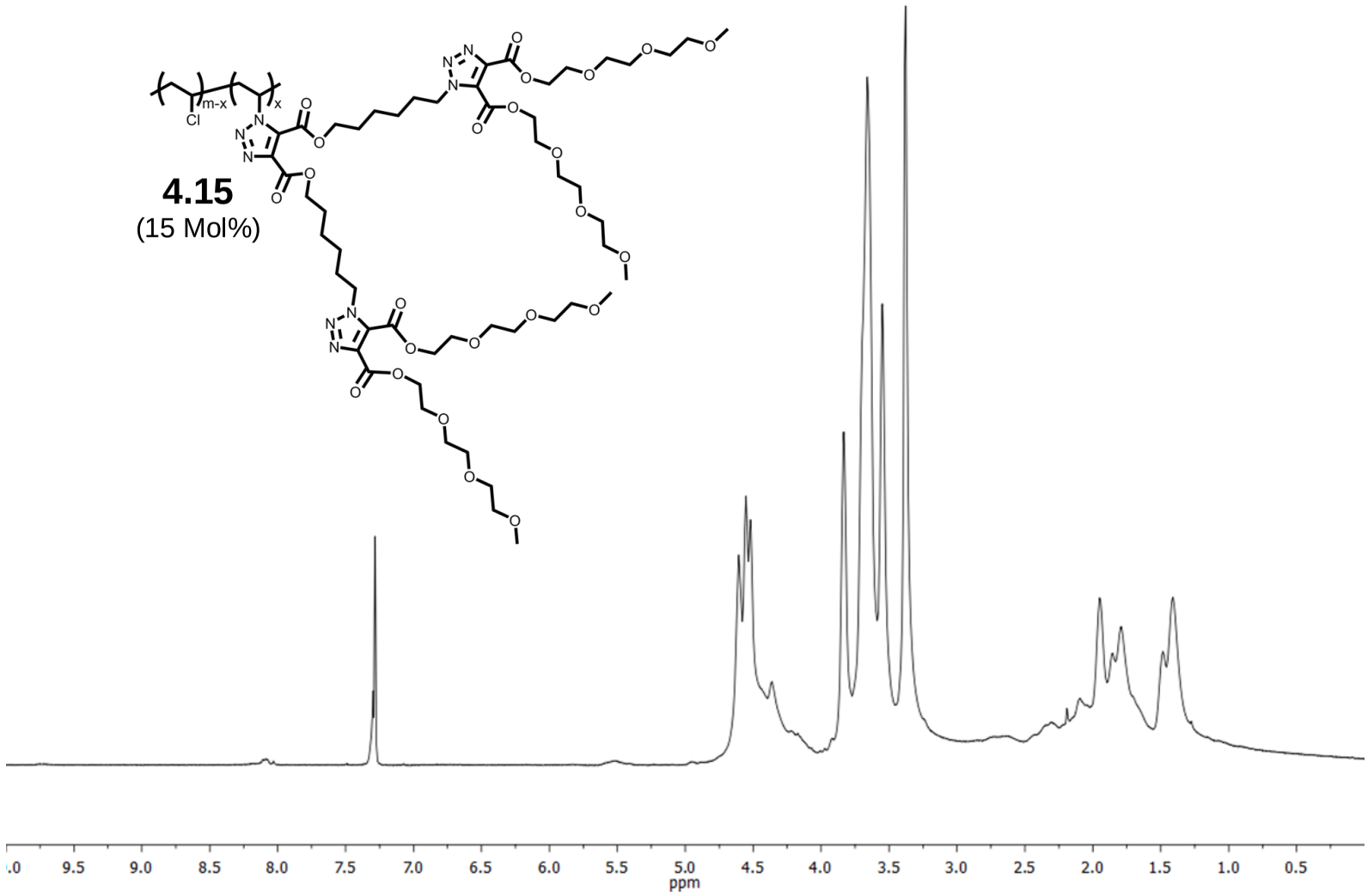
4.15
(15 Mol%)
Cl
m-x
x
ppm

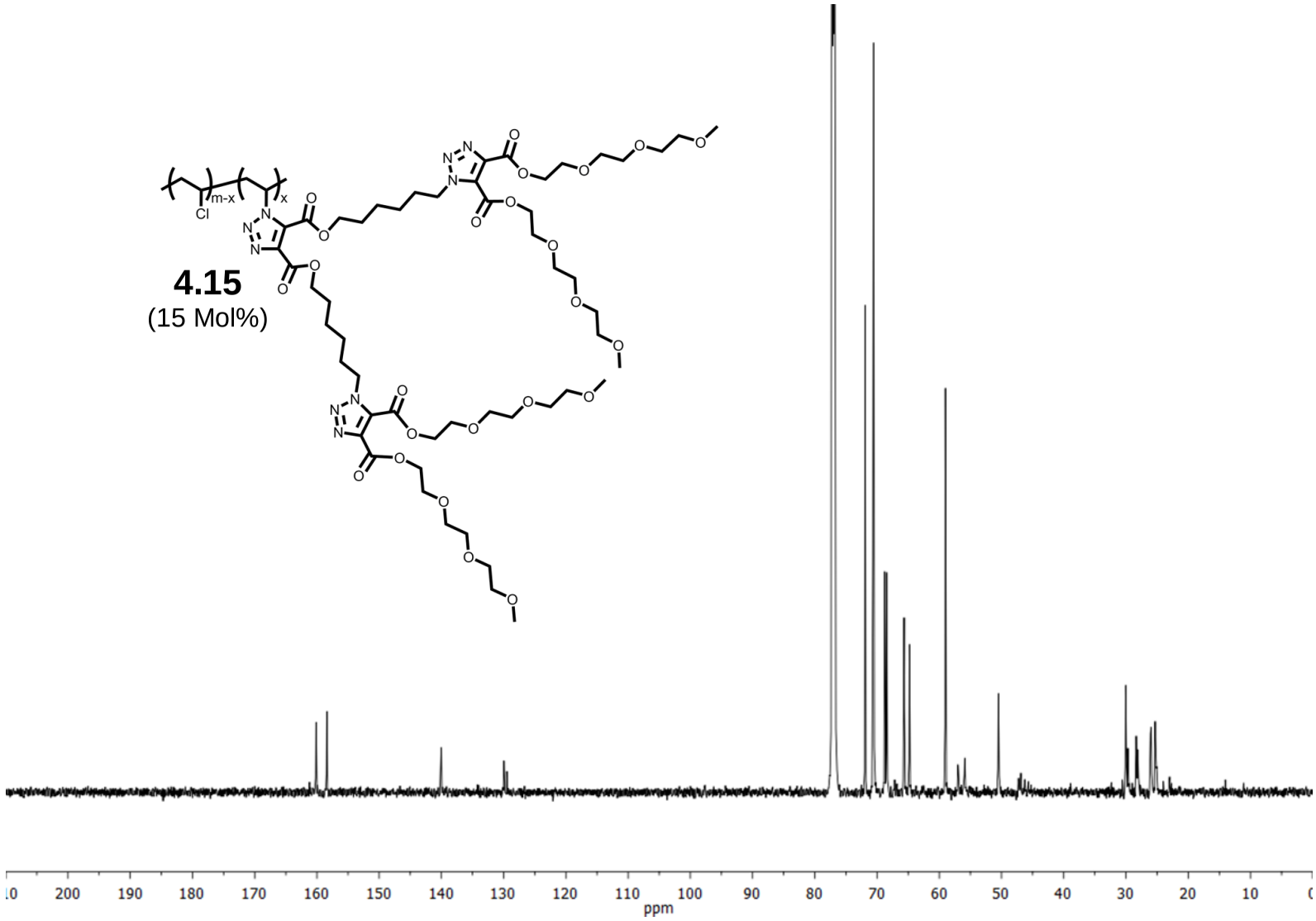
4.15
(15 Mol%)
Cl
m-x
x
ppm

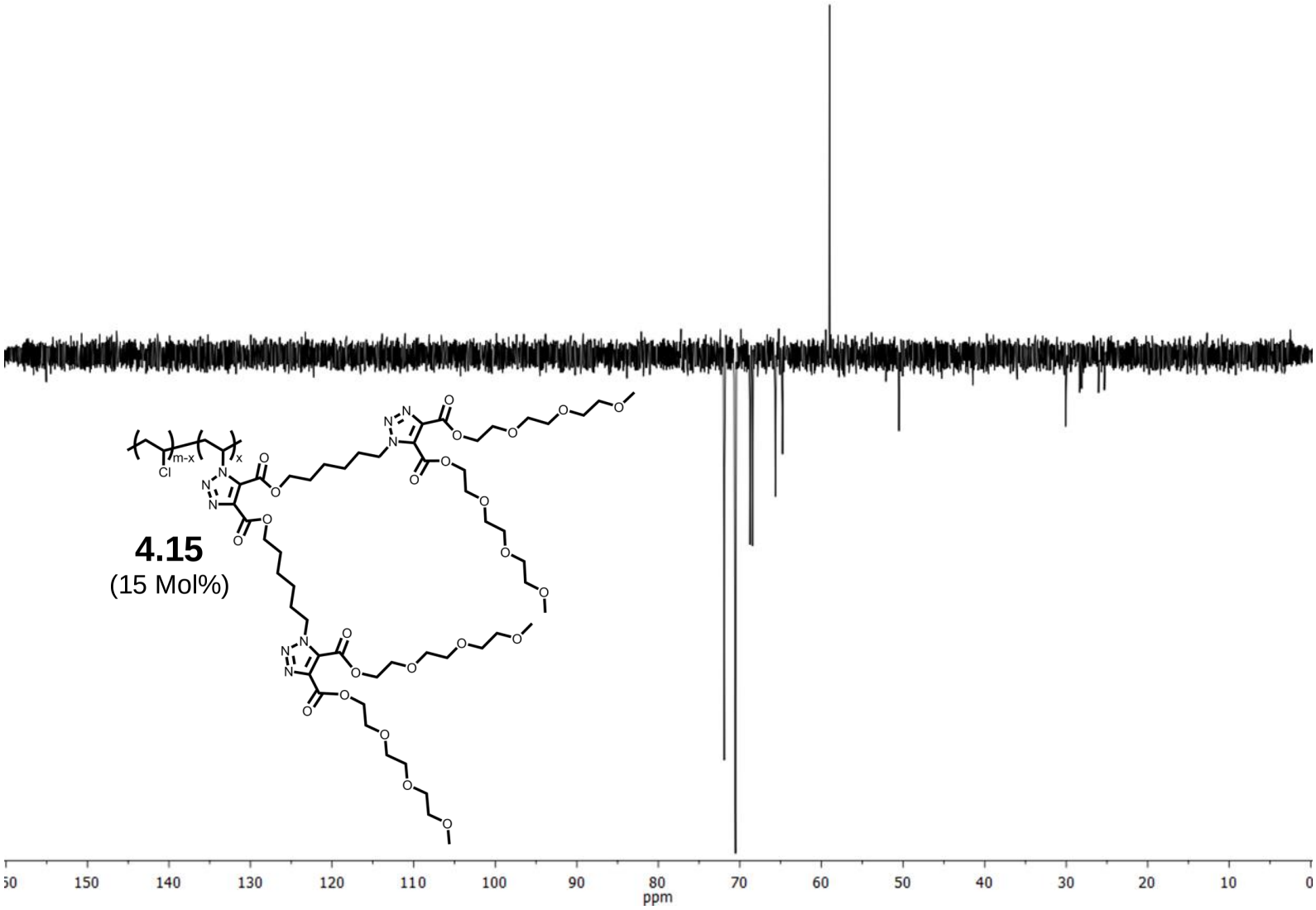
4.15
(15 Mol%)
m-x
x
Cl
150
140
130
120
110
100
90
80
70
60
50
40
30
20
10
0
ppm

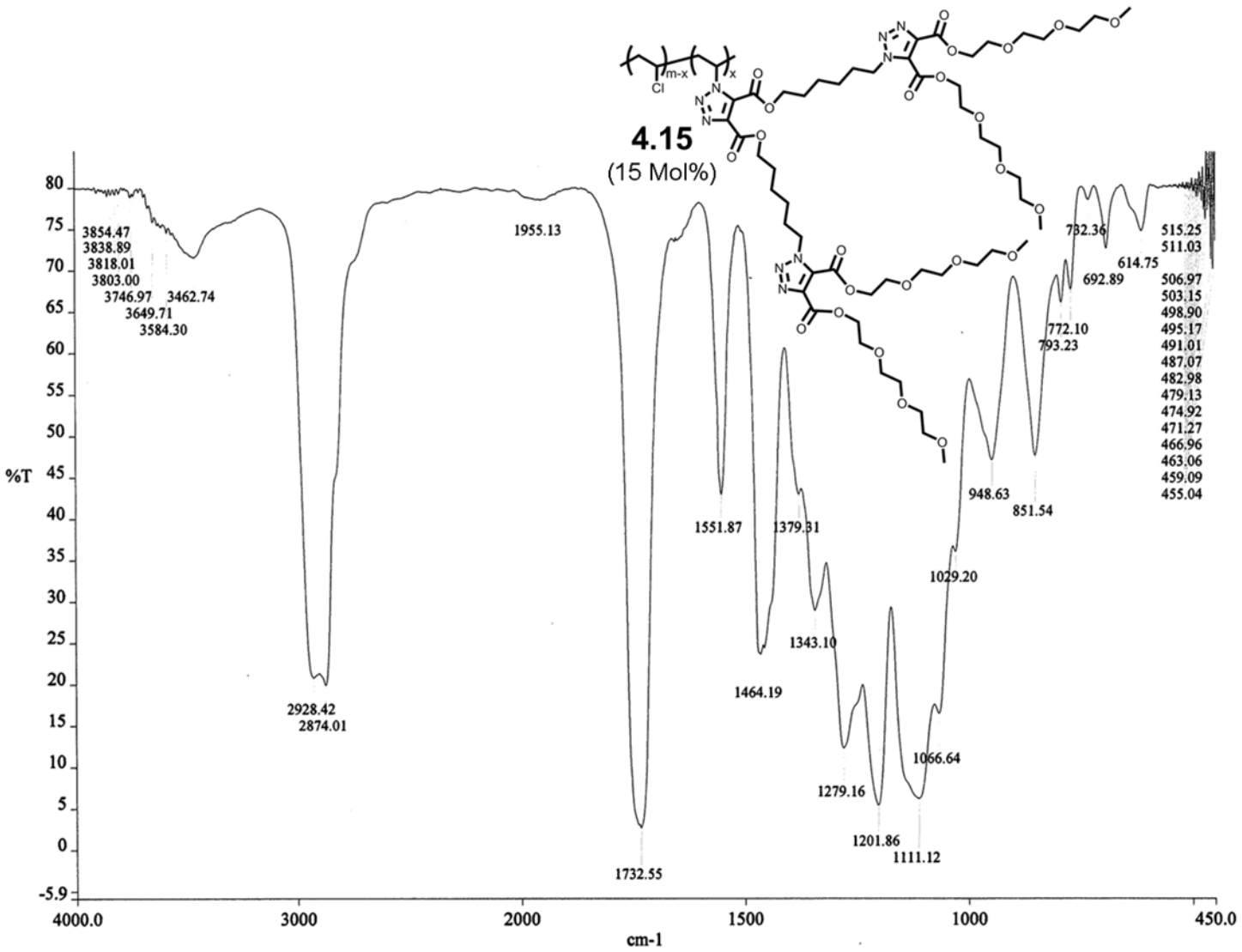
4.15
(15 Mol%)
%T
cm-1
3854.47
3838.89
3818.01
3803.00
3746.97
3462.74
3649.71
3584.30
2928.42
2874.01
1955.13
1732.55
1551.87
1464.19
1379.31
1343.10
1279.16
1201.86
1111.12
1066.64
1029.20
948.63
851.54
793.23
772.10
732.36
692.89
614.75
515.25
511.03
506.97
503.15
498.90
495.17
491.01
487.07
482.98
479.13
474.92
471.27
466.96
463.06
459.09
455.04

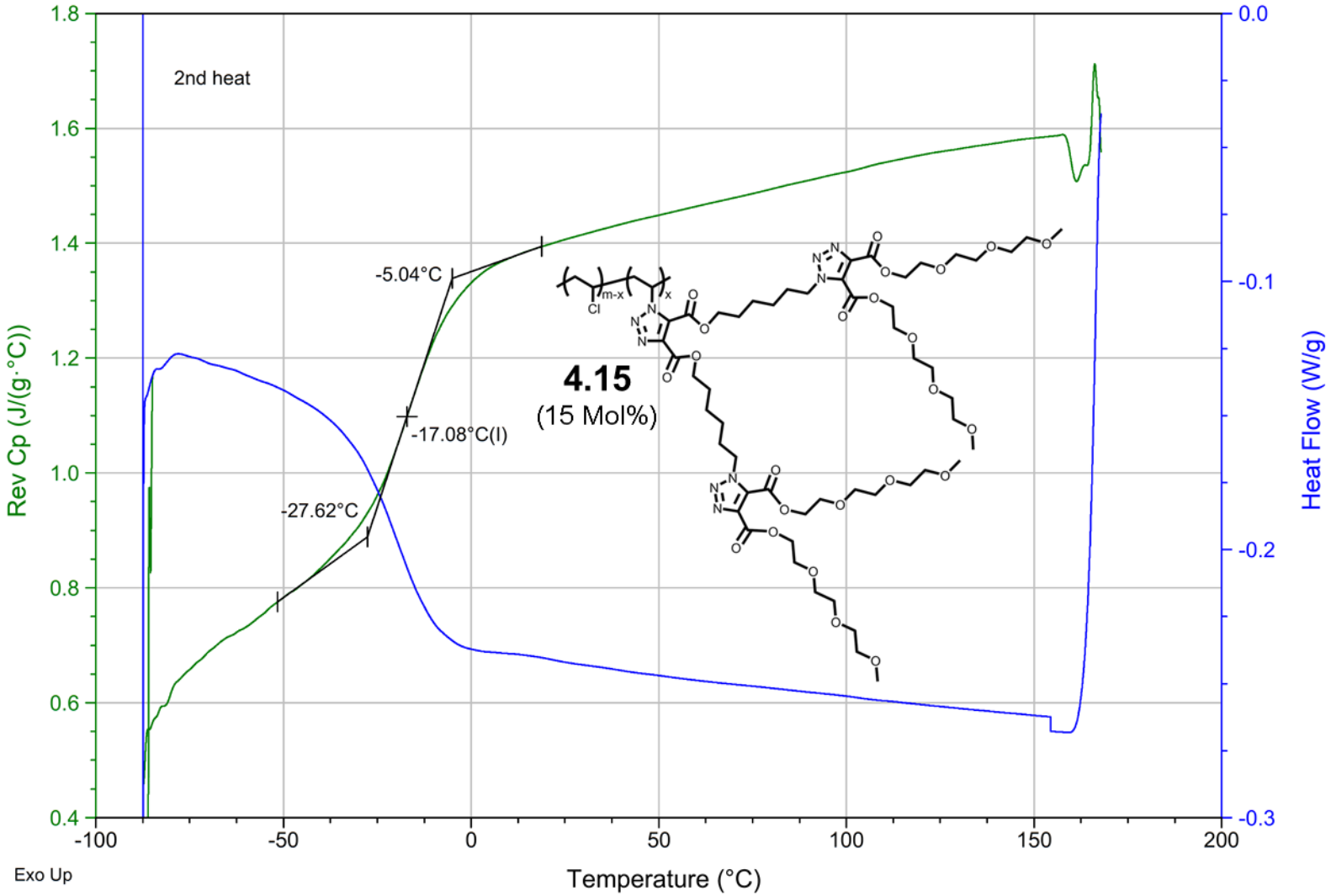
2nd heat
-5.04°C
-17.08°C(I)
-27.62°C
4.15
(15 Mol%)
Rev Cp (J/(g·°C))
Heat Flow (W/g)
Temperature (°C)
Exo Up
1.8
1.6
1.4
1.2
1.0
0.8
0.6
0.4
0.0
-0.1
-0.2
-0.3
-100
-50
0
50
100
150
200

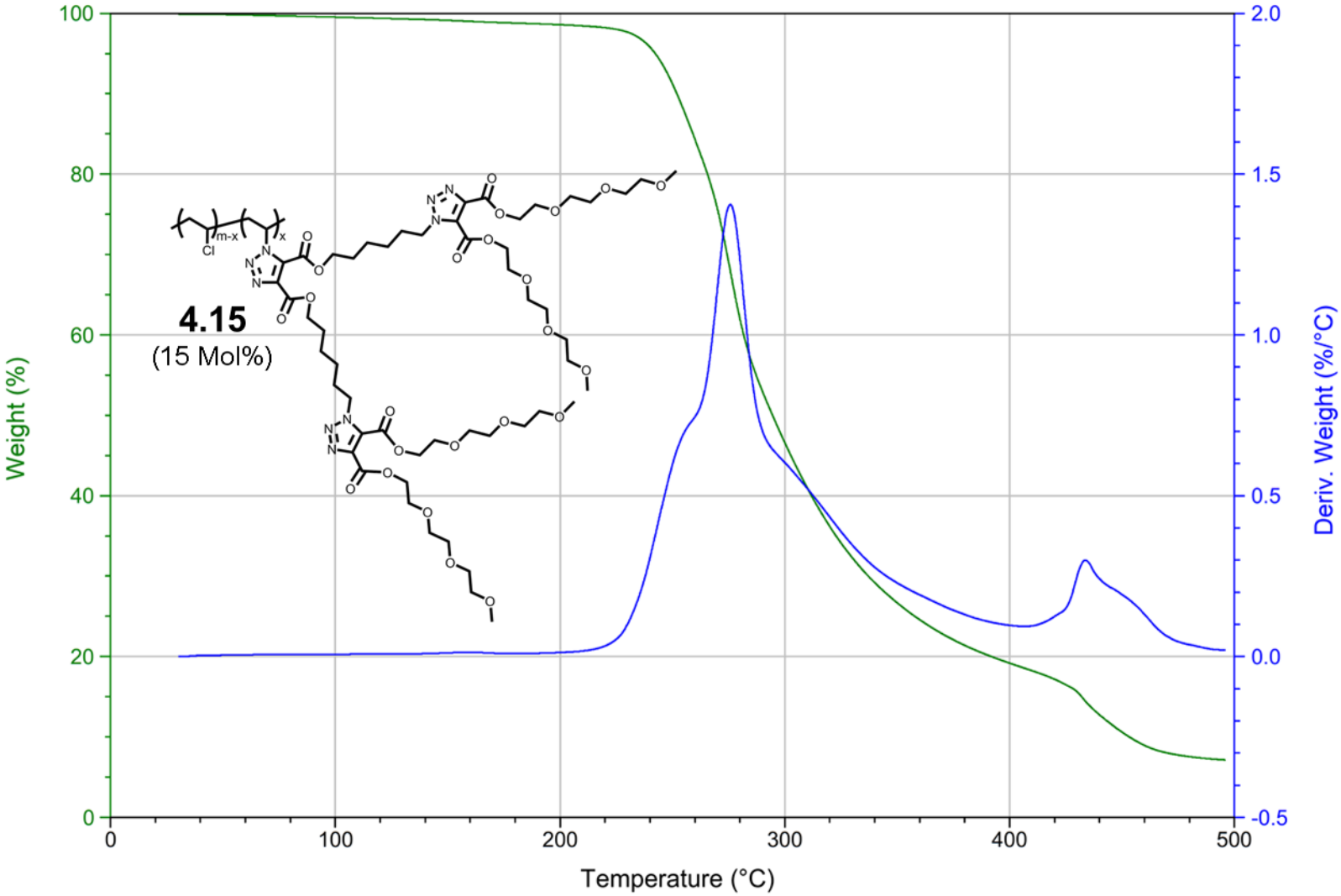
4.15
(15 Mol%)
Weight (%)
Deriv. Weight (%/°C)
Temperature (°C)
100
80
60
40
20
0
2.0
1.5
1.0
0.5
0.0
-0.5
0
100
200
300
400
500

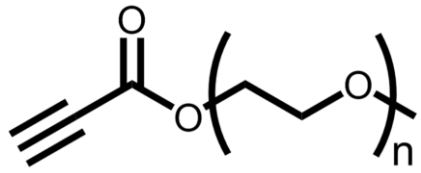

n ≅ 22

4.16

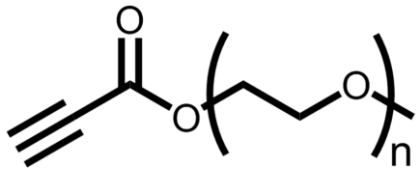
O
O
O
n

n ≅ 22

4.16

200
190
180
170
160
150
140
130
120
110
100
90
80
70
60
50
40
30
20
10
ppm

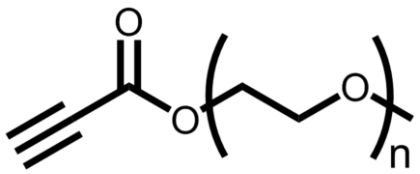

n ≅ 22

4.16

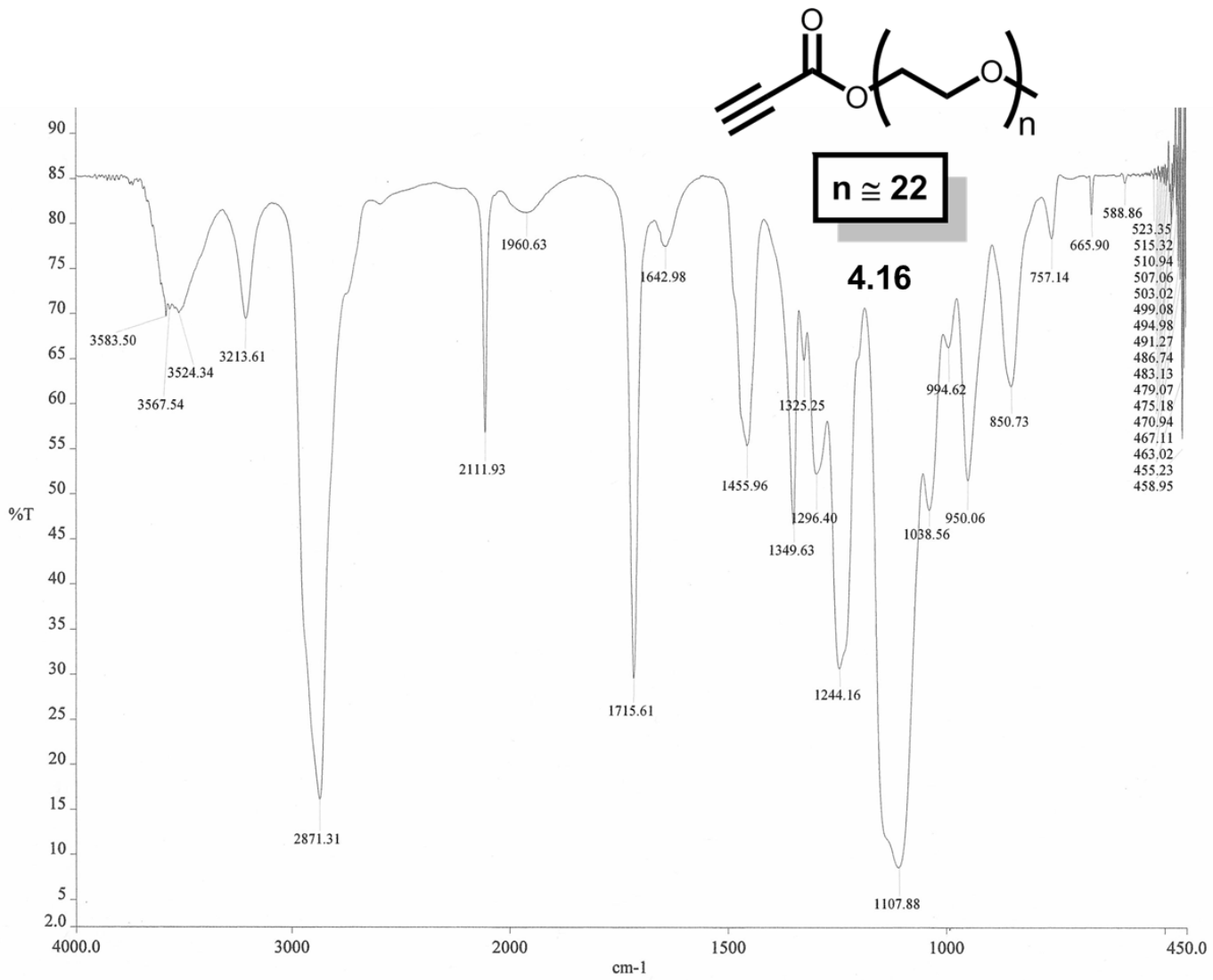
n ≅ 22
4.16
%T
cm-1
4000.0
3000
2000
1500
1000
450.0
3583.50
3567.54
3524.34
3213.61
2871.31
1960.63
2111.93
1642.98
1715.61
1455.96
1325.25
1349.63
1296.40
1244.16
1107.88
1038.56
994.62
950.06
850.73
757.14
665.90
588.86
523.35
515.32
510.94
507.06
503.02
499.08
494.98
491.27
486.74
483.13
479.07
475.18
470.94
467.11
463.02
455.23
458.95

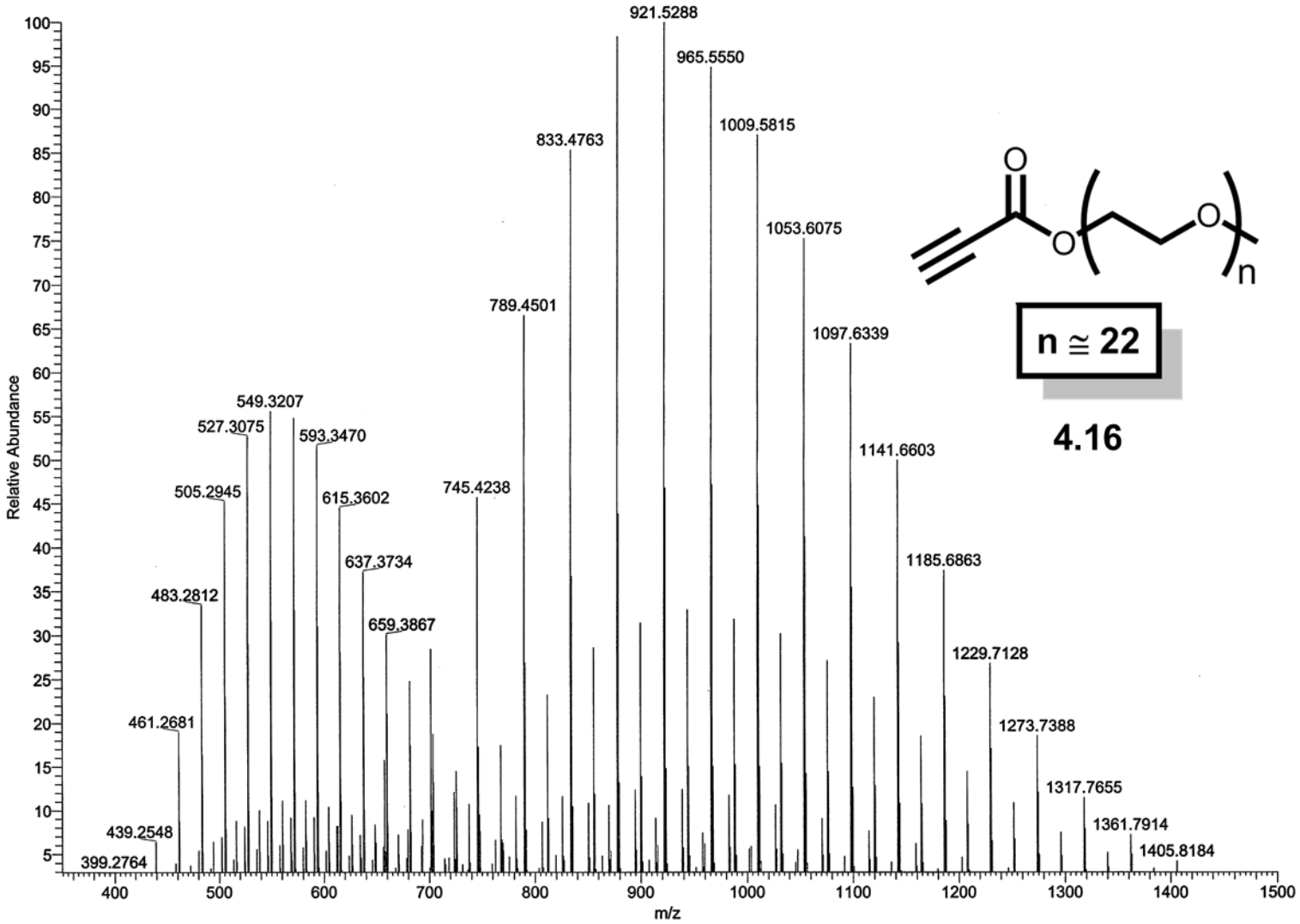
921.5288
965.5550
1009.5815
833.4763
1053.6075
789.4501
1097.6339
549.3207
527.3075
593.3470
1141.6603
505.2945
615.3602
745.4238
637.3734
1185.6863
483.2812
659.3867
1229.7128
461.2681
1273.7388
1317.7655
439.2548
1361.7914
399.2764
1405.8184
Relative Abundance
m/z
n ≅ 22
4.16

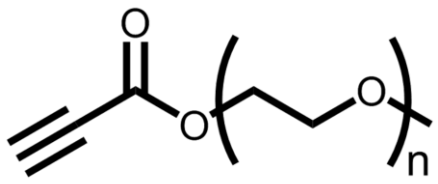

4.17

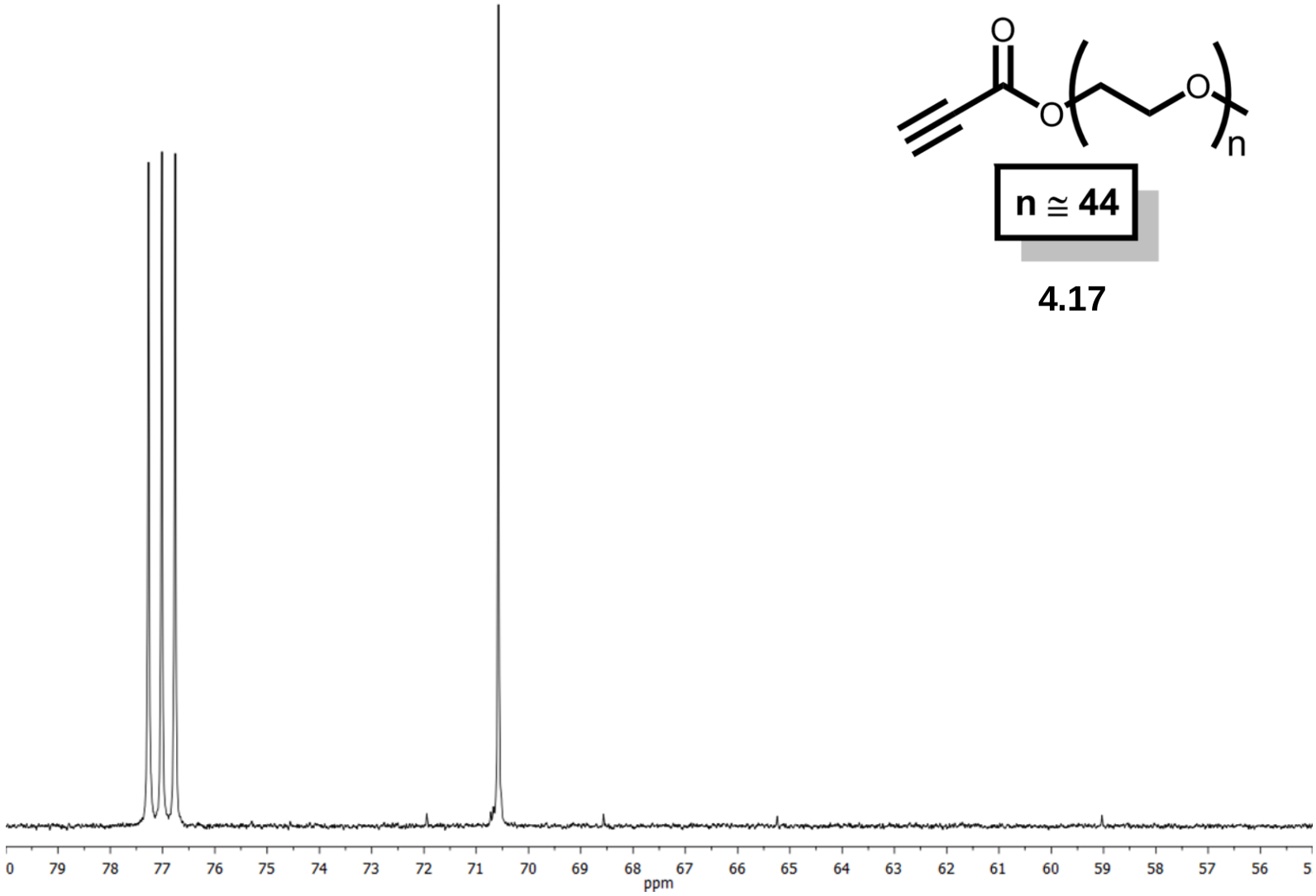
O
O
O
n
n ≅ 44
0
79
78
77
76
75
74
73
72
71
70
69
68
67
66
65
64
63
62
61
60
59
58
57
56
5
ppm

4.17

n ≅ 44
4.17
ppm

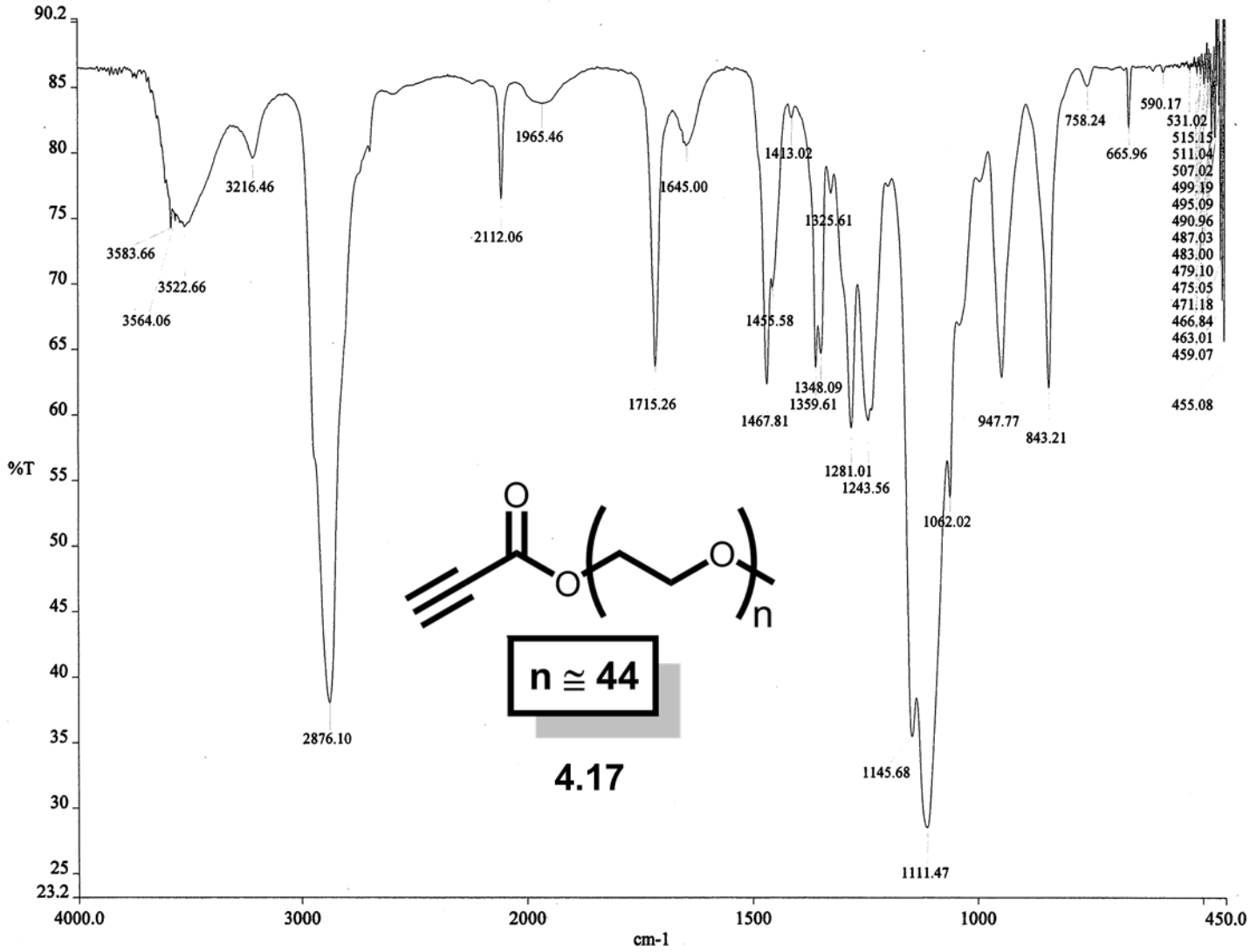
90.2
85
80
75
70
65
60
55
50
45
40
35
30
25
23.2
%T
4000.0
3000
2000
1500
1000
450.0
cm-1
3583.66
3564.06
3522.66
3216.46
2876.10
1965.46
2112.06
1715.26
1645.00
1467.81
1455.58
1413.02
1359.61
1348.09
1325.61
1281.01
1243.56
1145.68
1111.47
1062.02
947.77
843.21
758.24
665.96
590.17
531.02
515.15
511.04
507.02
499.19
495.09
490.96
487.03
483.00
479.10
475.05
471.18
466.84
463.01
459.07
455.08
O
O
O
n
n ≅ 44
4.17

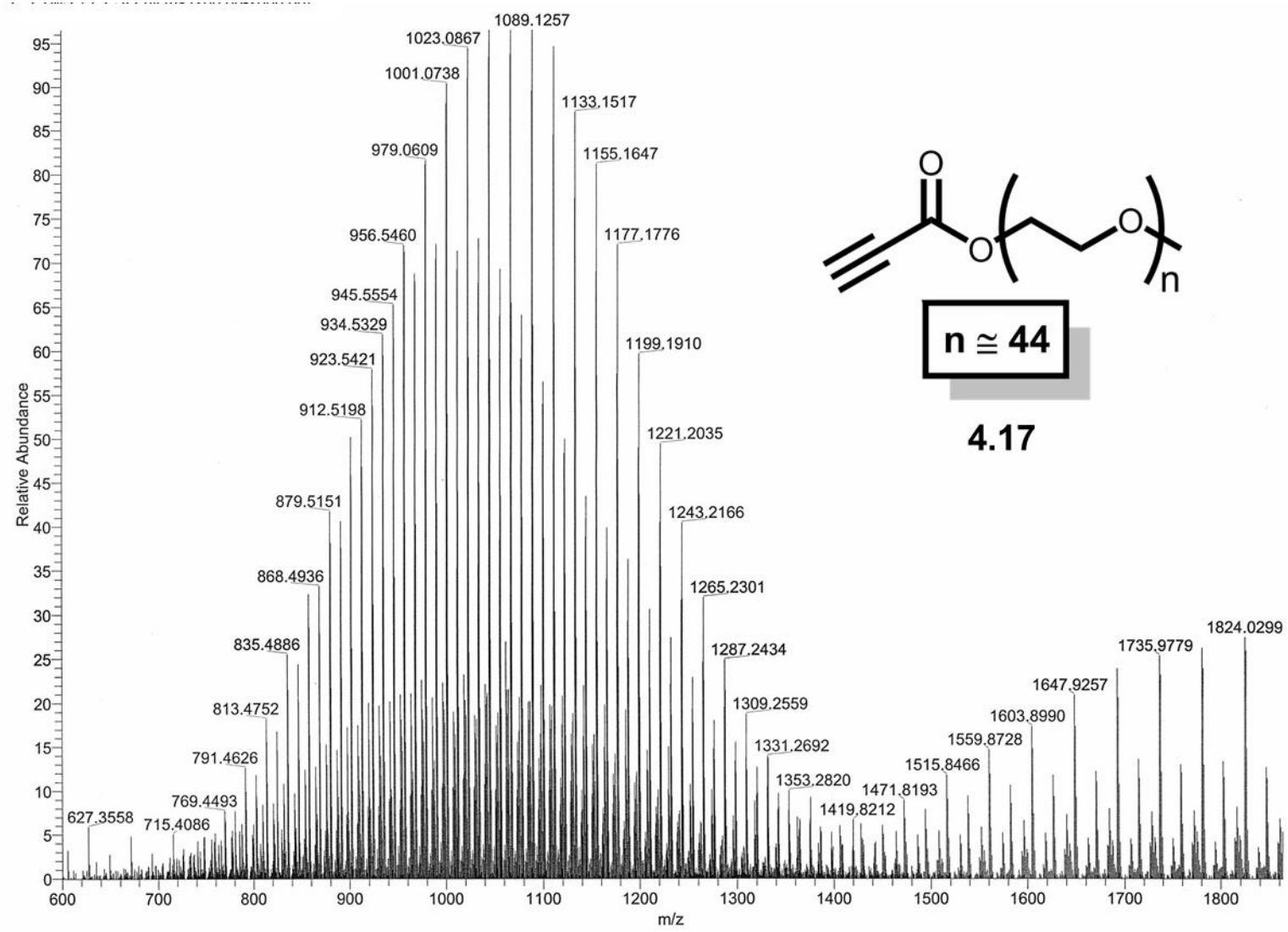
1089.1257
1023.0867
1001.0738
1133.1517
979.0609
1155.1647
956.5460
1177.1776
945.5554
934.5329
1199.1910
923.5421
912.5198
1221.2035
879.5151
1243.2166
868.4936
1265.2301
835.4886
1287.2434
813.4752
1309.2559
791.4626
1331.2692
769.4493
1353.2820
627.3558
715.4086
1419.8212
1471.8193
1515.8466
1559.8728
1603.8990
1647.9257
1735.9779
1824.0299
Relative Abundance
m/z
n ≅ 44
4.17

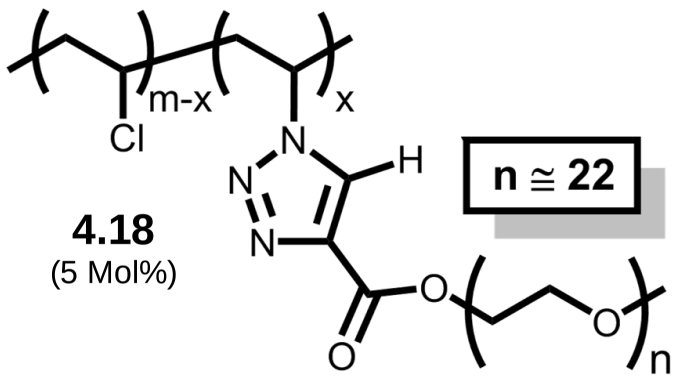
m-x
x
Cl
N
N
N
H
O
O
O
n
n ≅ 22

4.18
(5 Mol%)

9.5
9.0
8.5
8.0
7.5
7.0
6.5
6.0
5.5
5.0
4.5
4.0
3.5
3.0
2.5
2.0
1.5
1.0
0.5
ppm

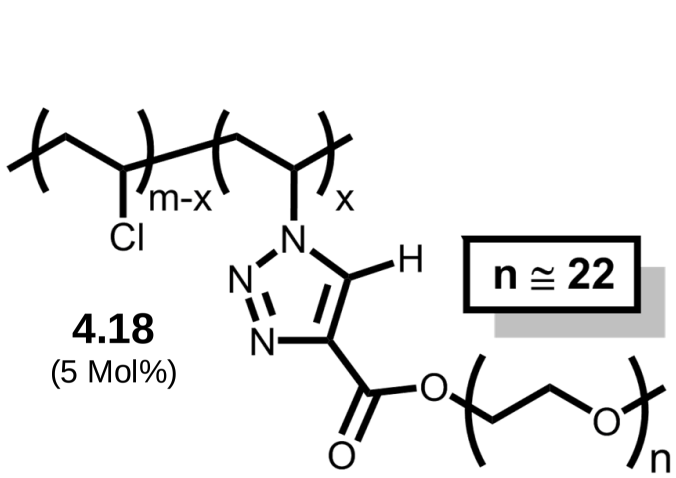
m-x
x
Cl
N
N
N
H
O
O
O
n
n ≅ 22

4.18
(5 Mol%)

200
190
180
170
160
150
140
130
120
110
100
90
80
70
60
50
40
30
20
10
ppm

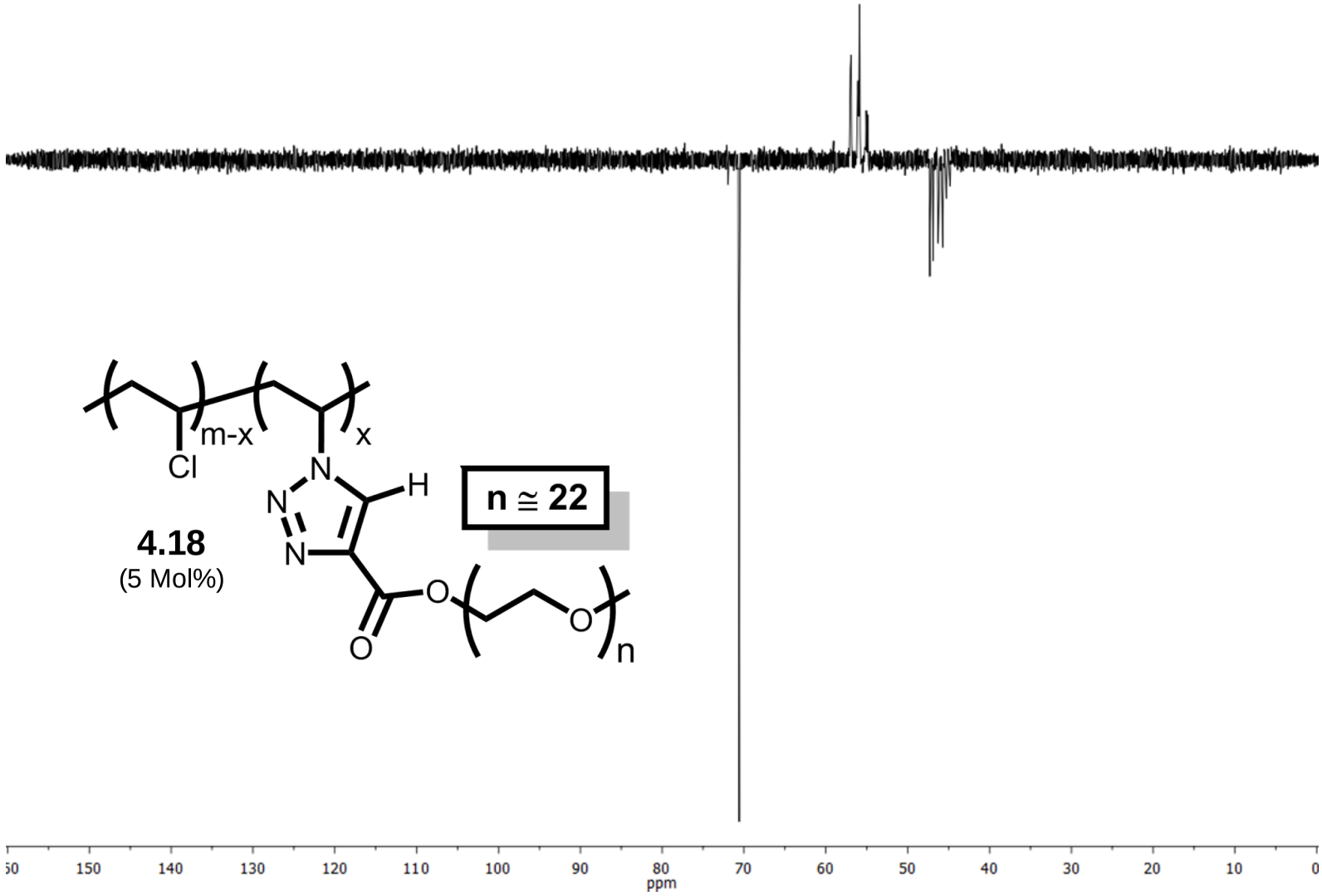
m-x
x
Cl
N
N
N
H
O
O
O
n
n ≅ 22
4.18
(5 Mol%)
150
140
130
120
110
100
90
80
70
60
50
40
30
20
10
0
ppm

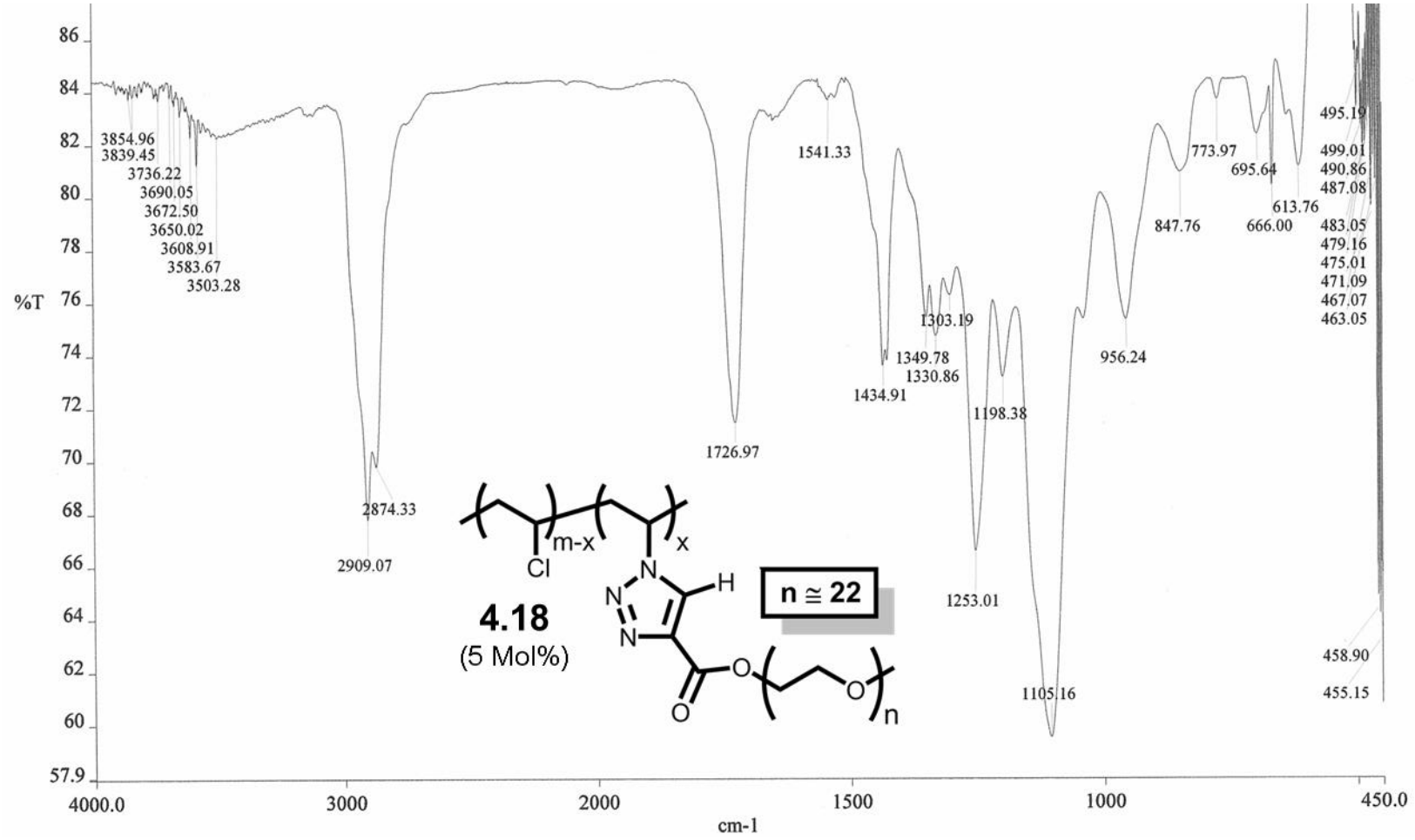
%T
cm-1
4000.0
3000
2000
1500
1000
450.0
86
84
82
80
78
76
74
72
70
68
66
64
62
60
57.9
3854.96
3839.45
3736.22
3690.05
3672.50
3650.02
3608.91
3583.67
3503.28
2909.07
2874.33
1726.97
1541.33
1434.91
1349.78
1330.86
1303.19
1198.38
1253.01
1105.16
956.24
847.76
773.97
695.64
666.00
613.76
495.19
499.01
490.86
487.08
483.05
479.16
475.01
471.09
467.07
463.05
458.90
455.15
m-x
x
Cl
H
N
N
N
O
O
O
n
4.18
(5 Mol%)
n ≅ 22

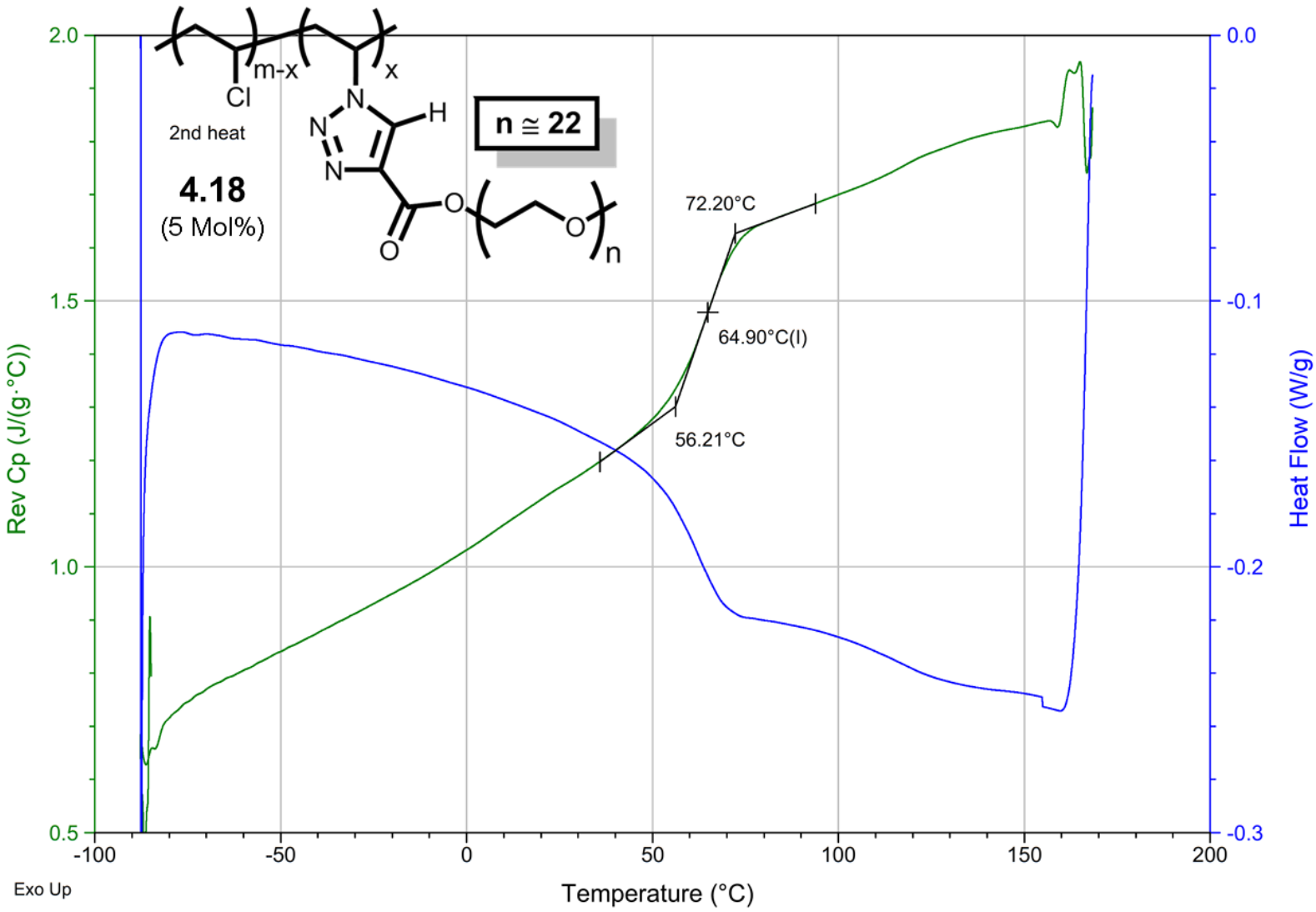
2nd heat
4.18
(5 Mol%)
n ≅ 22
72.20°C
64.90°C(I)
56.21°C
Rev Cp (J/(g·°C))
Heat Flow (W/g)
Temperature (°C)
Exo Up
2.0
1.5
1.0
0.5
0.0
-0.1
-0.2
-0.3
-100
-50
0
50
100
150
200

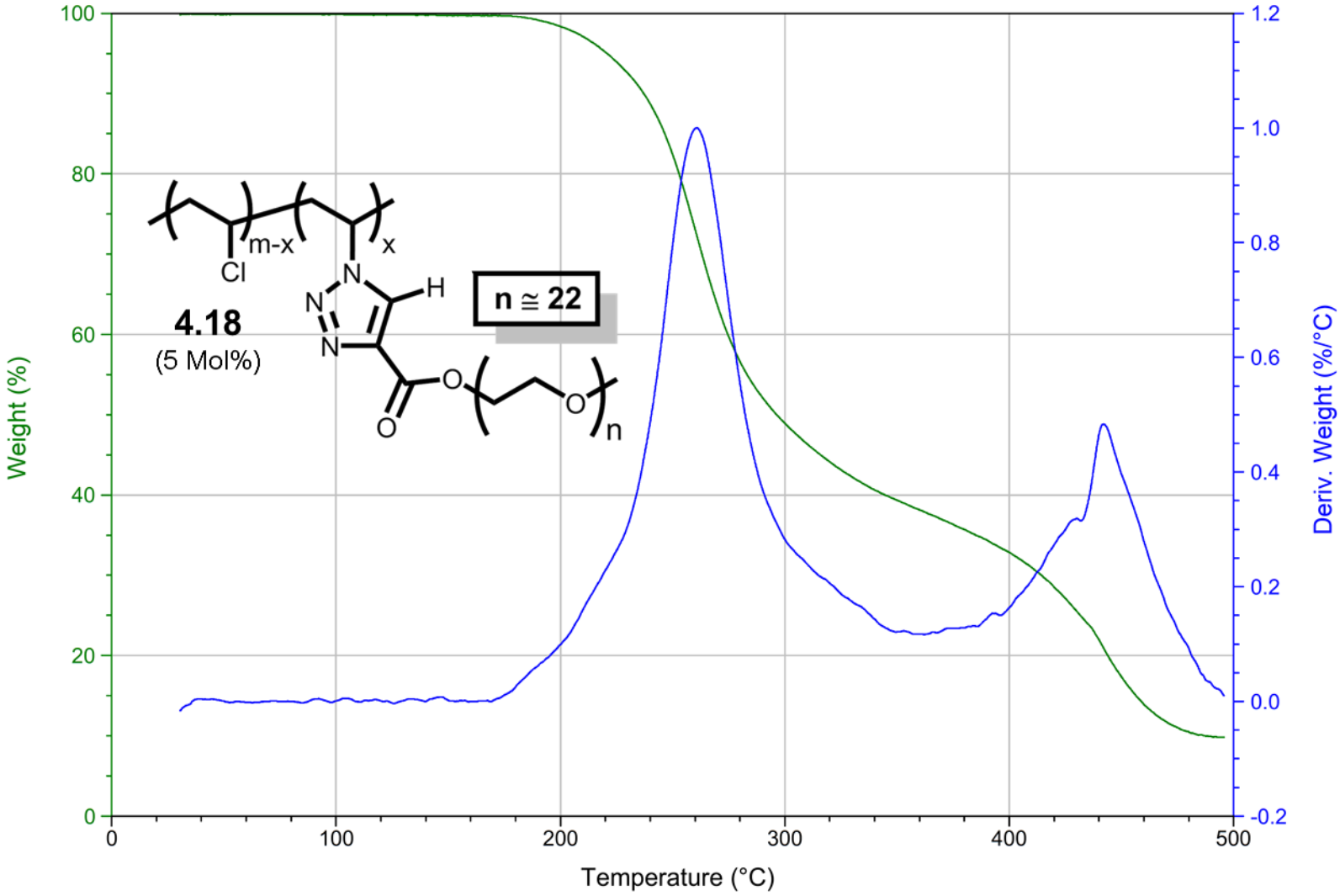
Weight (%)
Deriv. Weight (%/°C)
Temperature (°C)
0
20
40
60
80
100
-0.2
0.0
0.2
0.4
0.6
0.8
1.0
1.2
0
100
200
300
400
500
m-x
x
Cl
N
N
H
O
O
O
n
4.18
(5 Mol%)
n ≅ 22

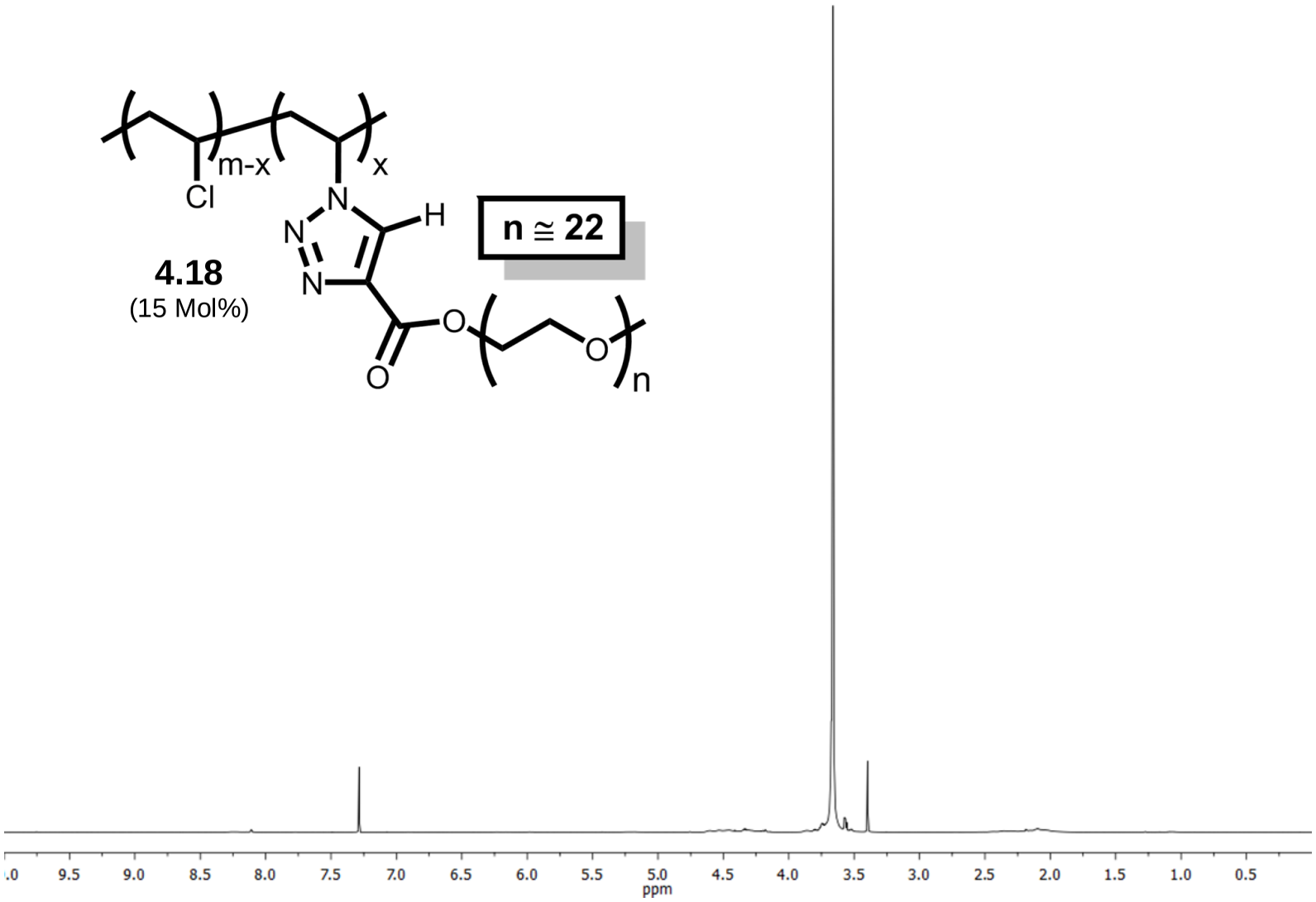
m-x
x
Cl
N
N
N
H
O
O
O
n
n ≅ 22
4.18
(15 Mol%)
9.5
9.0
8.5
8.0
7.5
7.0
6.5
6.0
5.5
5.0
4.5
4.0
3.5
3.0
2.5
2.0
1.5
1.0
0.5
ppm

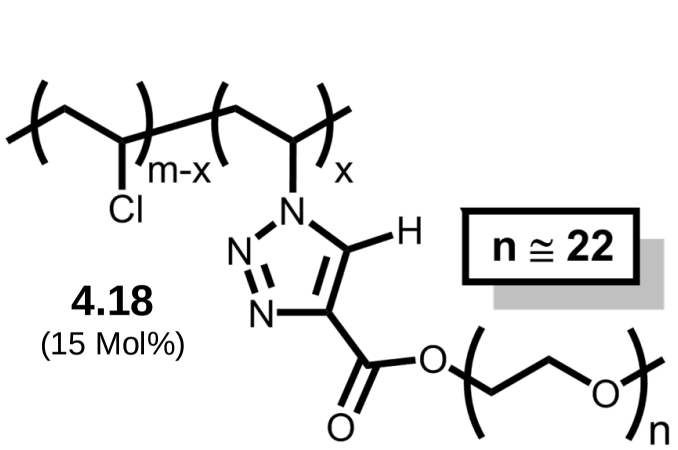

4.18
(15 Mol%)

n ≅ 22

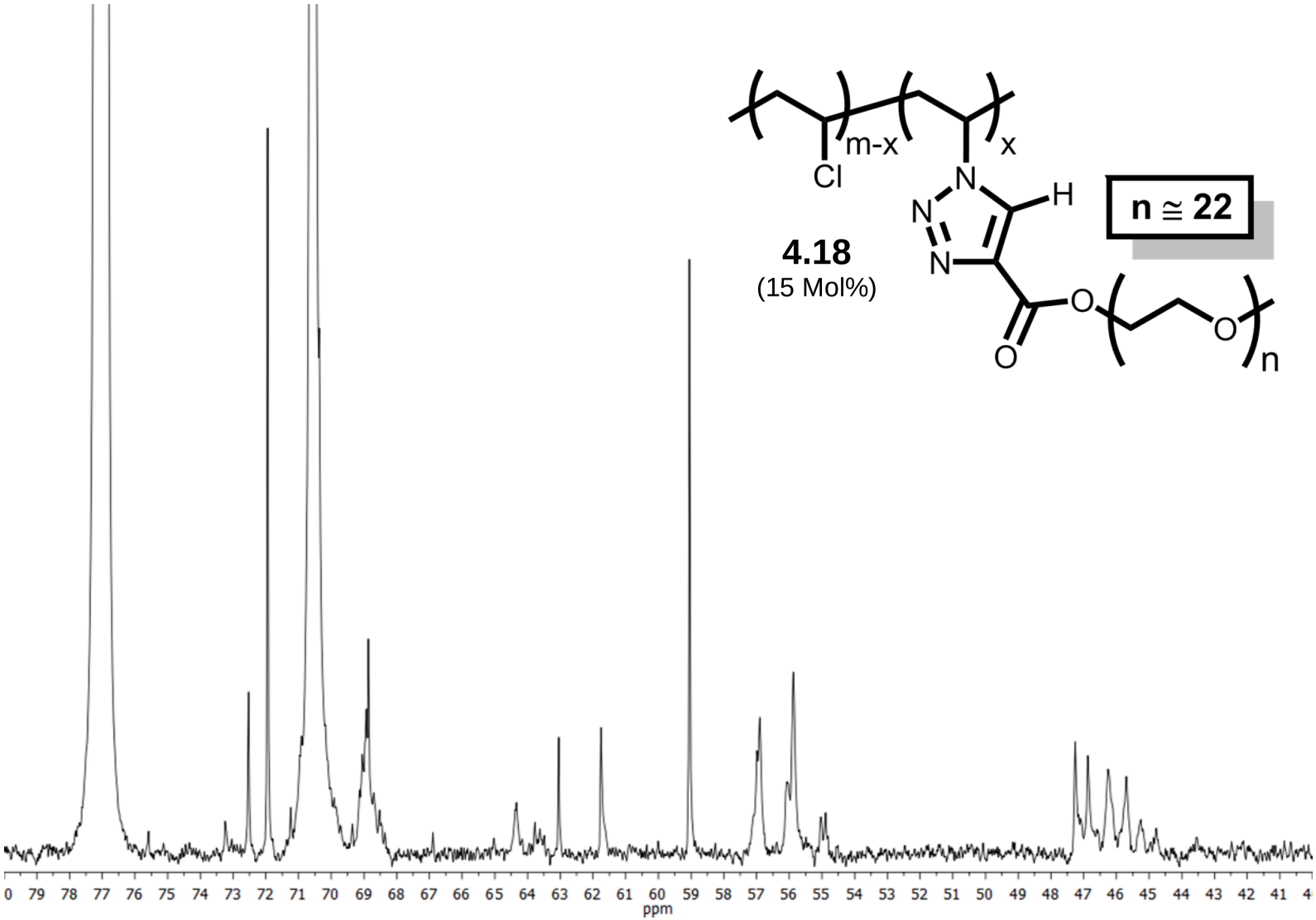
m-x
x
Cl
N
N
N
H
O
O
O
n
n ≅ 22
4.18
(15 Mol%)
0 79 78 77 76 75 74 73 72 71 70 69 68 67 66 65 64 63 62 61 60 59 58 57 56 55 54 53 52 51 50 49 48 47 46 45 44 43 42 41 4
ppm

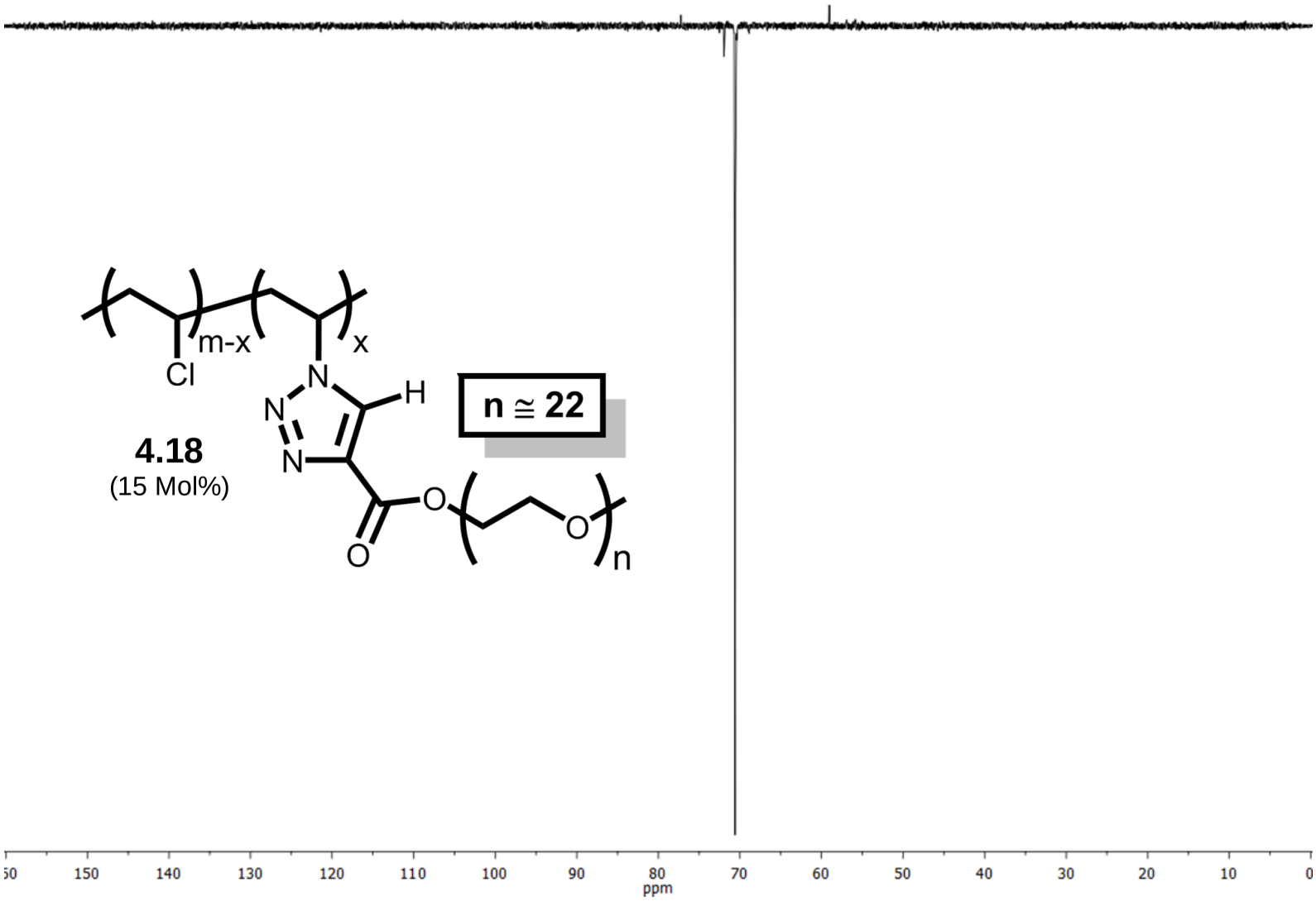
m-x
x
Cl
N
N
N
H
O
O
O
n
n ≅ 22
4.18
(15 Mol%)
150
140
130
120
110
100
90
80
70
60
50
40
30
20
10
0
ppm

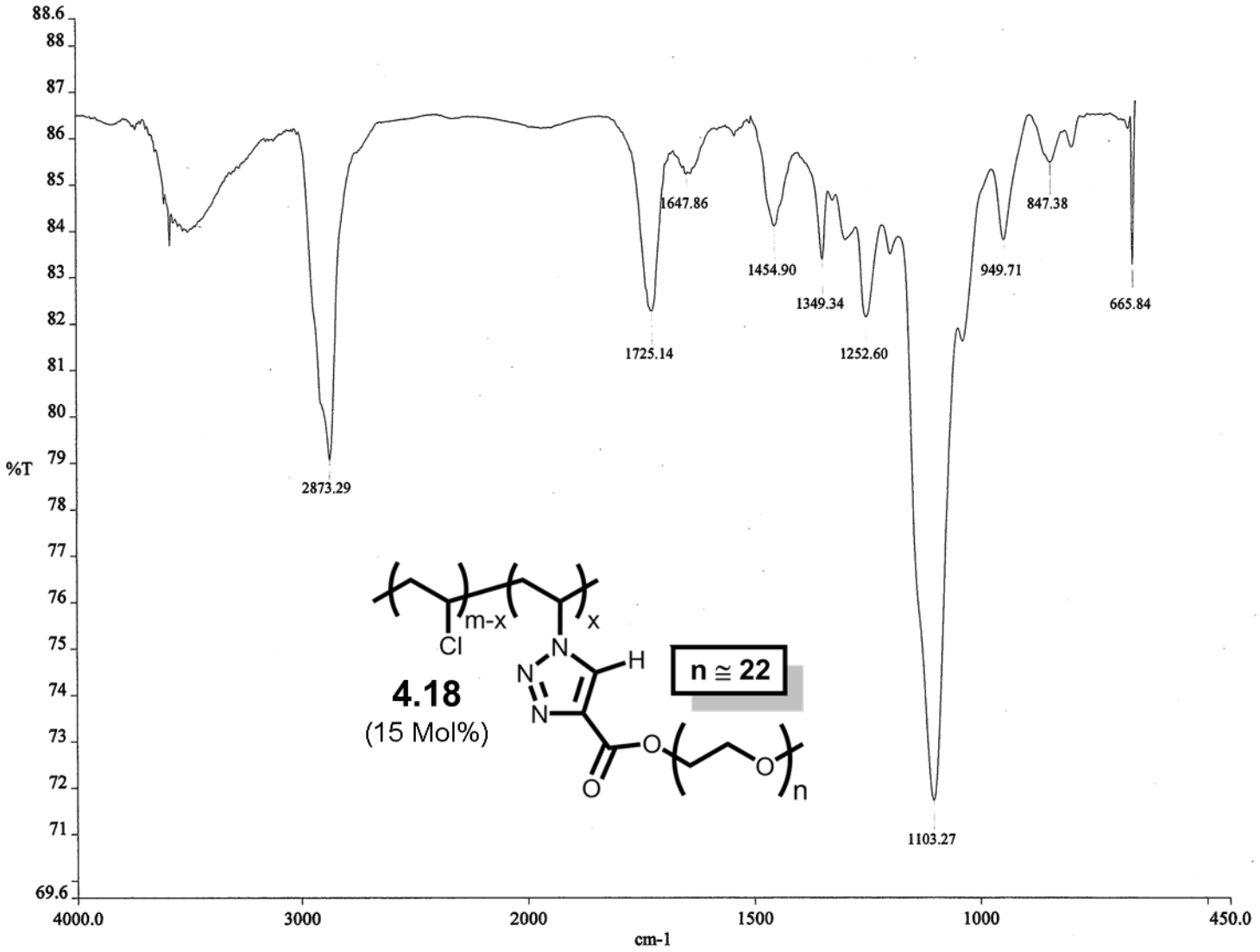
88.6
88
87
86
85
84
83
82
81
80
79
78
77
76
75
74
73
72
71
69.6
%T
4000.0
3000
2000
1500
1000
450.0
cm-1
2873.29
1725.14
1647.86
1454.90
1349.34
1252.60
1103.27
949.71
847.38
665.84
m-x
x
Cl
N
N
N
H
O
O
O
n
4.18
(15 Mol%)
n ≅ 22

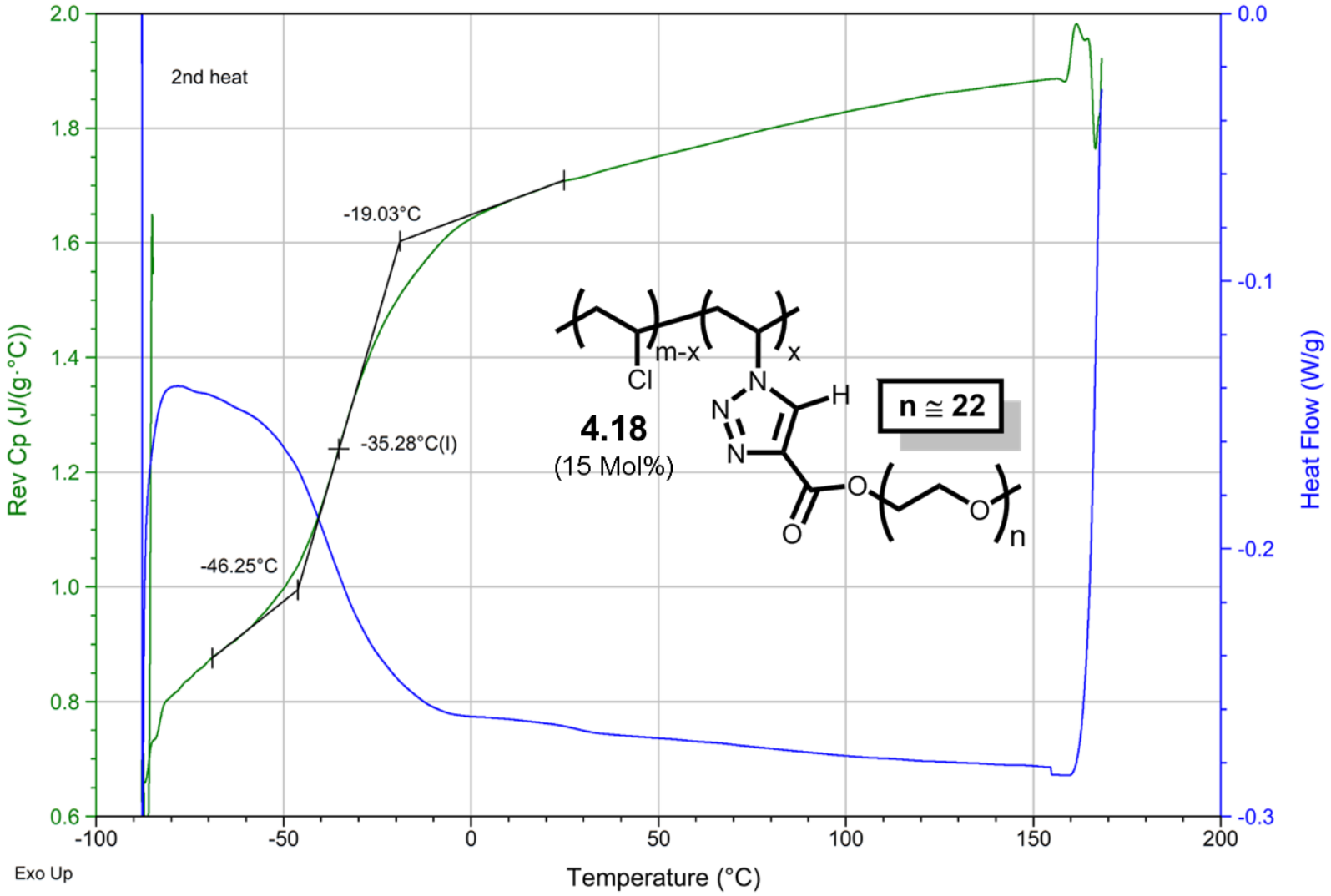
2nd heat
-19.03°C
-35.28°C(I)
-46.25°C
4.18
(15 Mol%)
m-x
x
Cl
H
n ≅ 22
n
Rev Cp (J/(g·°C))
Heat Flow (W/g)
Temperature (°C)
Exo Up
2.0
1.8
1.6
1.4
1.2
1.0
0.8
0.6
0.0
-0.1
-0.2
-0.3
-100
-50
0
50
100
150
200

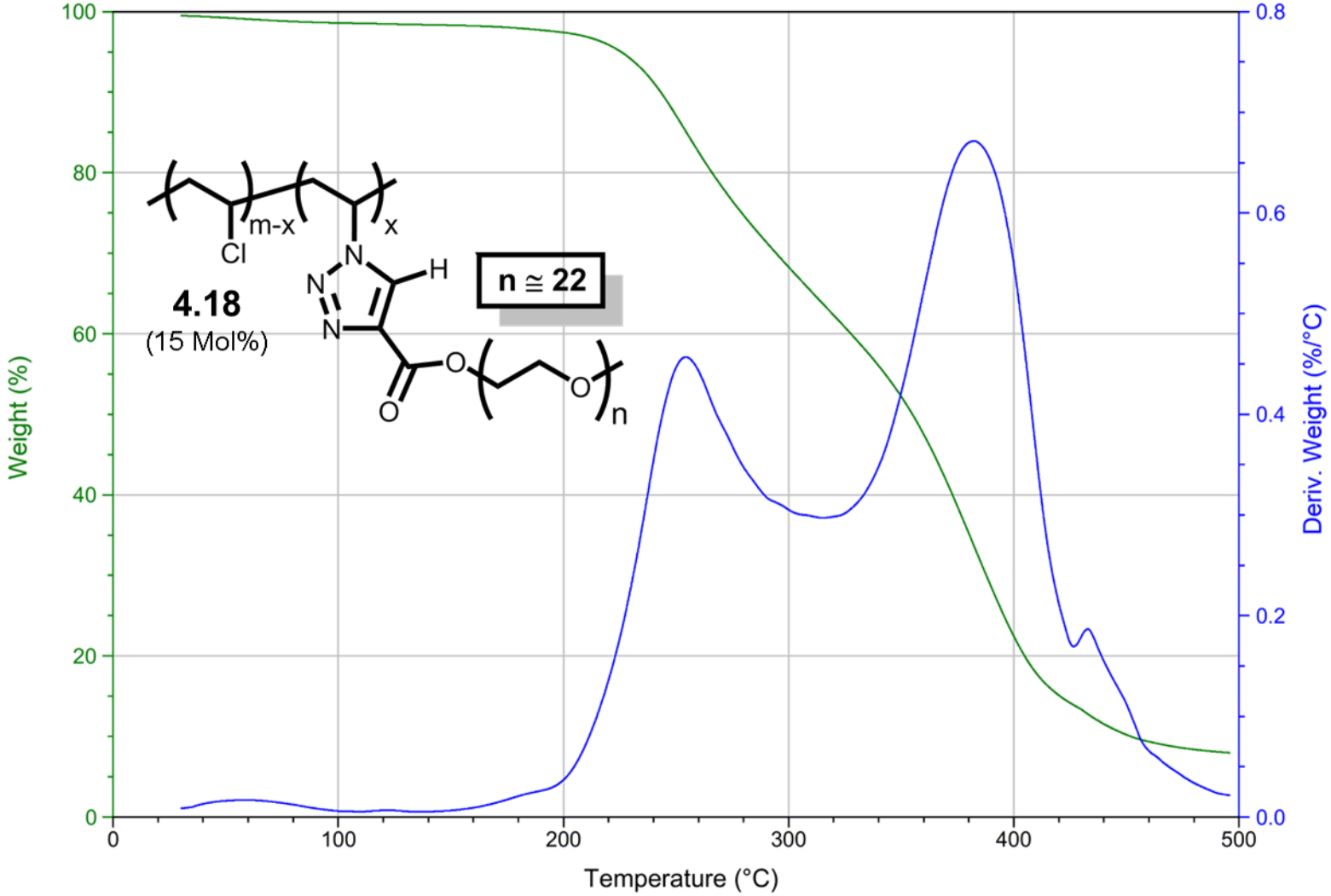
Weight (%)
Deriv. Weight (%/°C)
Temperature (°C)
0
20
40
60
80
100
0.0
0.2
0.4
0.6
0.8
0
100
200
300
400
500
m-x
x
Cl
N
N
H
O
O
O
n
4.18
(15 Mol%)
n ≅ 22

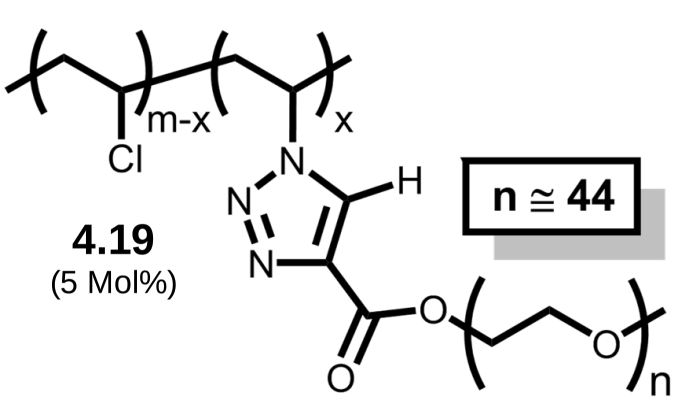
m-x
x
Cl
N
N
N
H
O
O
O
n
n ≅ 44

4.19
(5 Mol%)

9.5
9.0
8.5
8.0
7.5
7.0
6.5
6.0
5.5
5.0
4.5
4.0
3.5
3.0
2.5
2.0
1.5
1.0
0.5
ppm

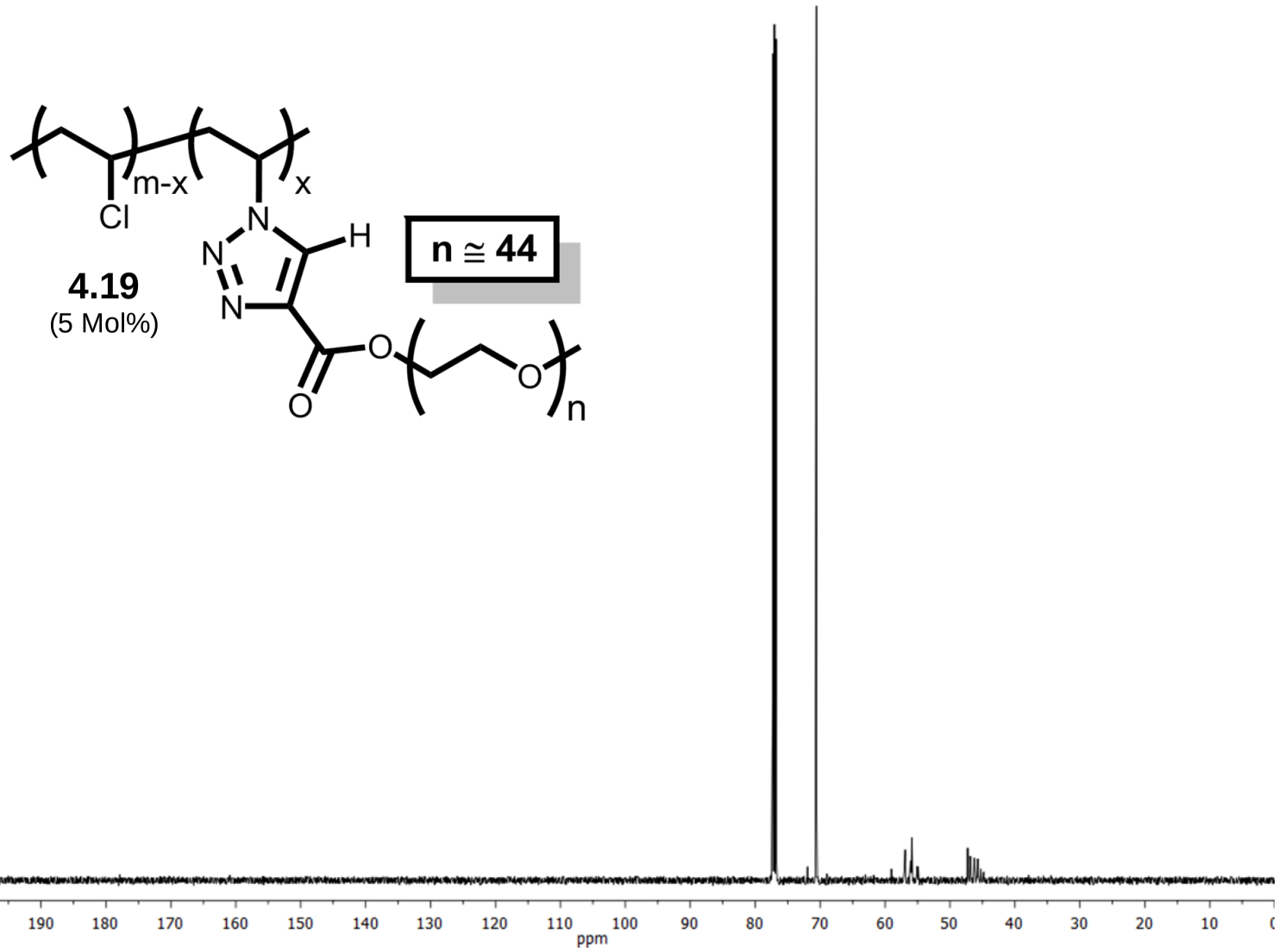
m-x
x
Cl
N
N
N
H
O
O
O
n
n ≅ 44
4.19
(5 Mol%)
200
190
180
170
160
150
140
130
120
110
100
90
80
70
60
50
40
30
20
10
ppm

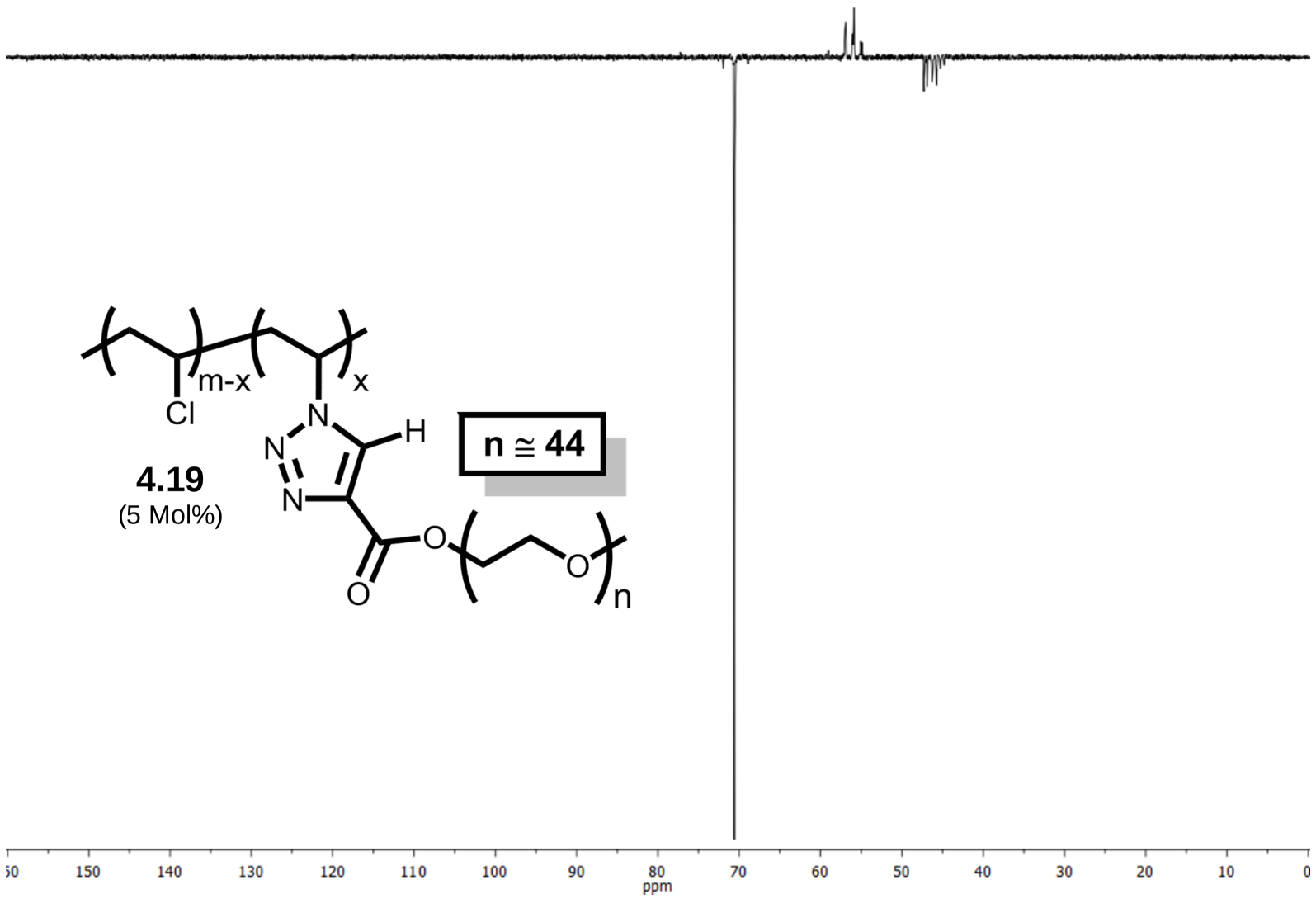
m-x
x
Cl
N
N
N
H
O
O
O
n
4.19
(5 Mol%)
n ≅ 44
150
140
130
120
110
100
90
80
70
60
50
40
30
20
10
0
ppm

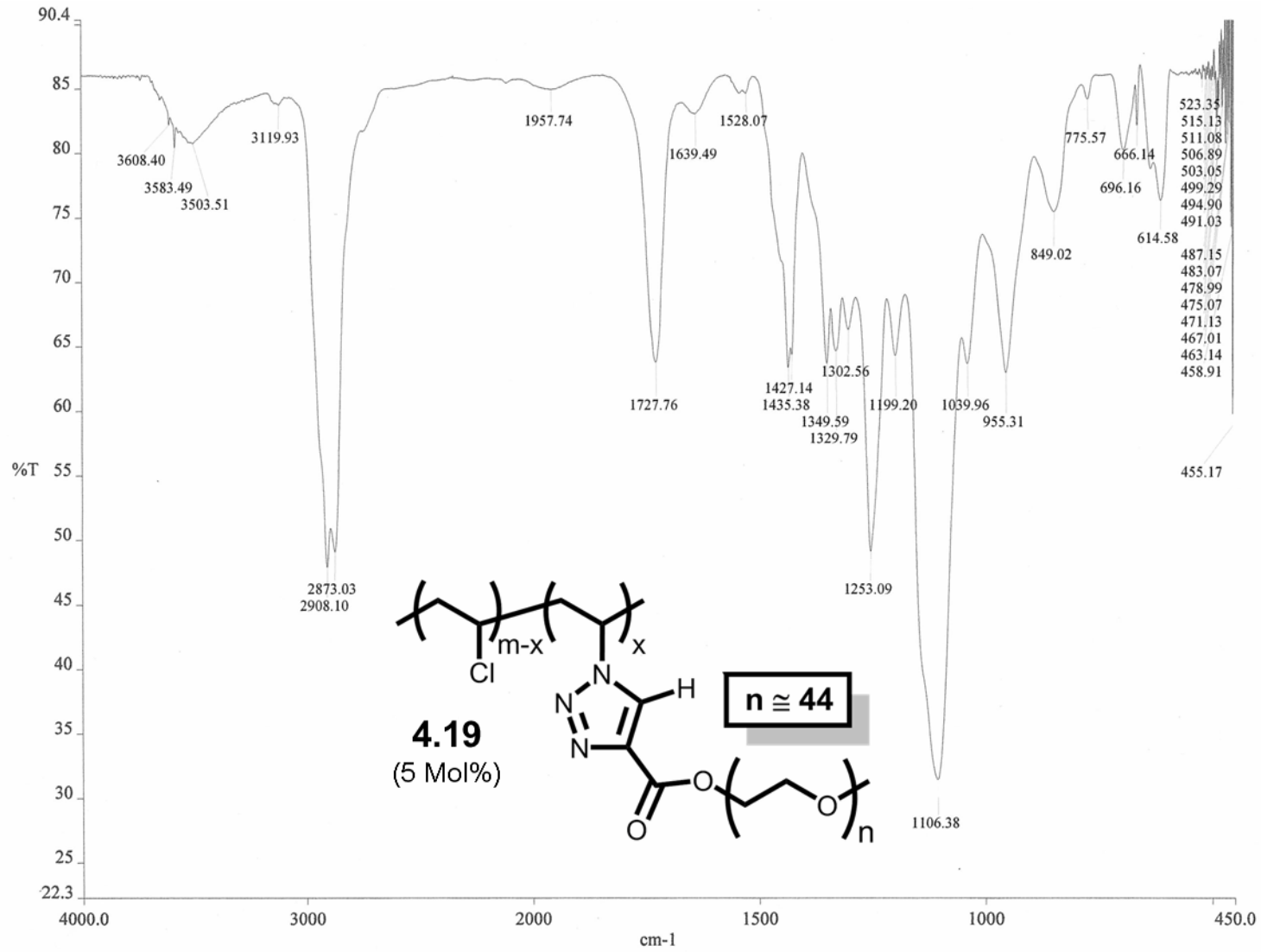
90.4
85
80
75
70
65
60
55
50
45
40
35
30
25
22.3
%T
4000.0
3000
2000
1500
1000
450.0
cm-1
3608.40
3583.49
3503.51
3119.93
2873.03
2908.10
1957.74
1727.76
1639.49
1528.07
1427.14
1435.38
1349.59
1329.79
1302.56
1253.09
1199.20
1106.38
1039.96
955.31
849.02
775.57
696.16
666.14
614.58
523.35
515.13
511.08
506.89
503.05
499.29
494.90
491.03
487.15
483.07
478.99
475.07
471.13
467.01
463.14
458.91
455.17
m-x
x
Cl
N
N
N
H
O
O
O
n
n ≅ 44
4.19
(5 Mol%)

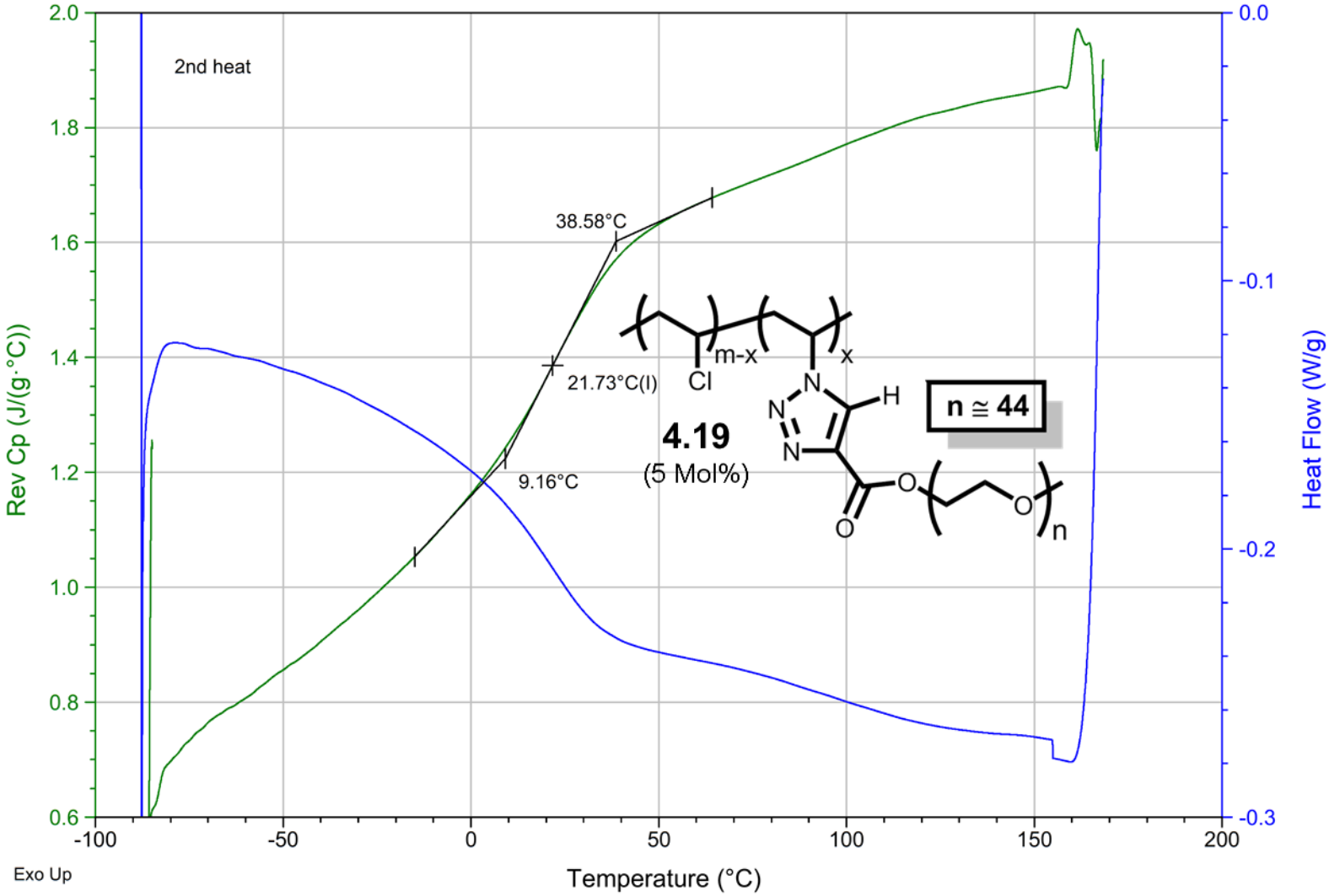
2nd heat
38.58°C
21.73°C(I)
9.16°C
4.19
(5 Mol%)
m-x
x
Cl
H
n ≅ 44
n
Rev Cp (J/(g·°C))
Heat Flow (W/g)
Temperature (°C)
Exo Up
2.0
1.8
1.6
1.4
1.2
1.0
0.8
0.6
0.0
-0.1
-0.2
-0.3
-100
-50
0
50
100
150
200

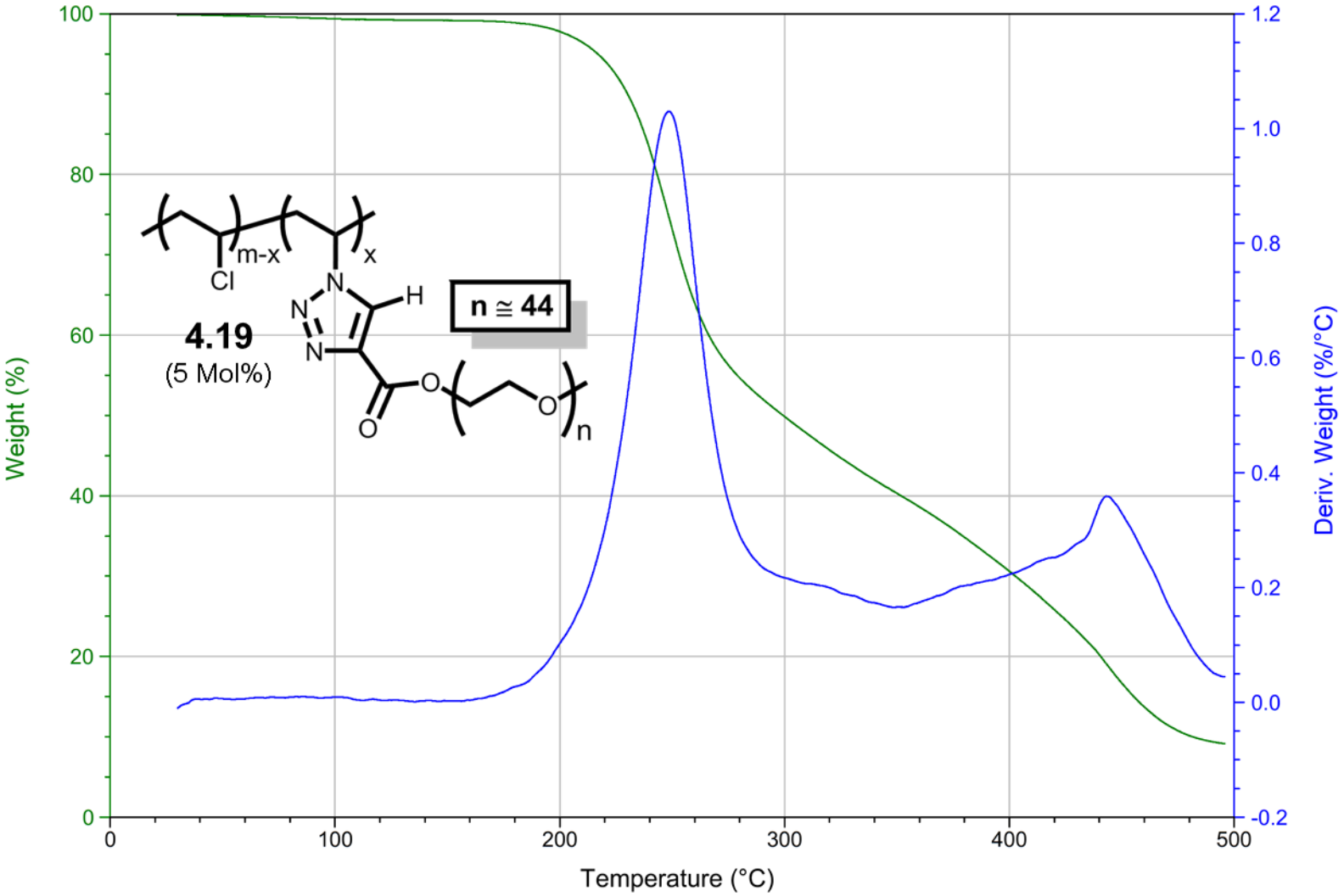
Weight (%)
Deriv. Weight (%/°C)
Temperature (°C)
0
20
40
60
80
100
-0.2
0.0
0.2
0.4
0.6
0.8
1.0
1.2
0
100
200
300
400
500
m-x
x
Cl
N
N
N
H
O
O
O
n
4.19
(5 Mol%)
n ≅ 44

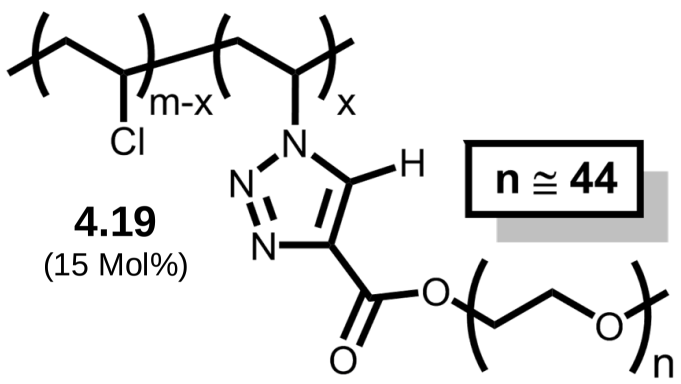

4.19
(15 Mol%)

n ≅ 44

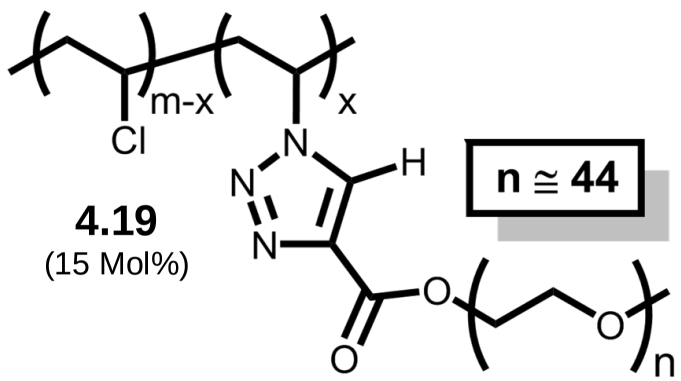
m-x
x
Cl
N
N
N
H
O
O
O
n
n ≅ 44

4.19
(15 Mol%)

200
190
180
170
160
150
140
130
120
110
100
90
80
70
60
50
40
30
20
10
ppm

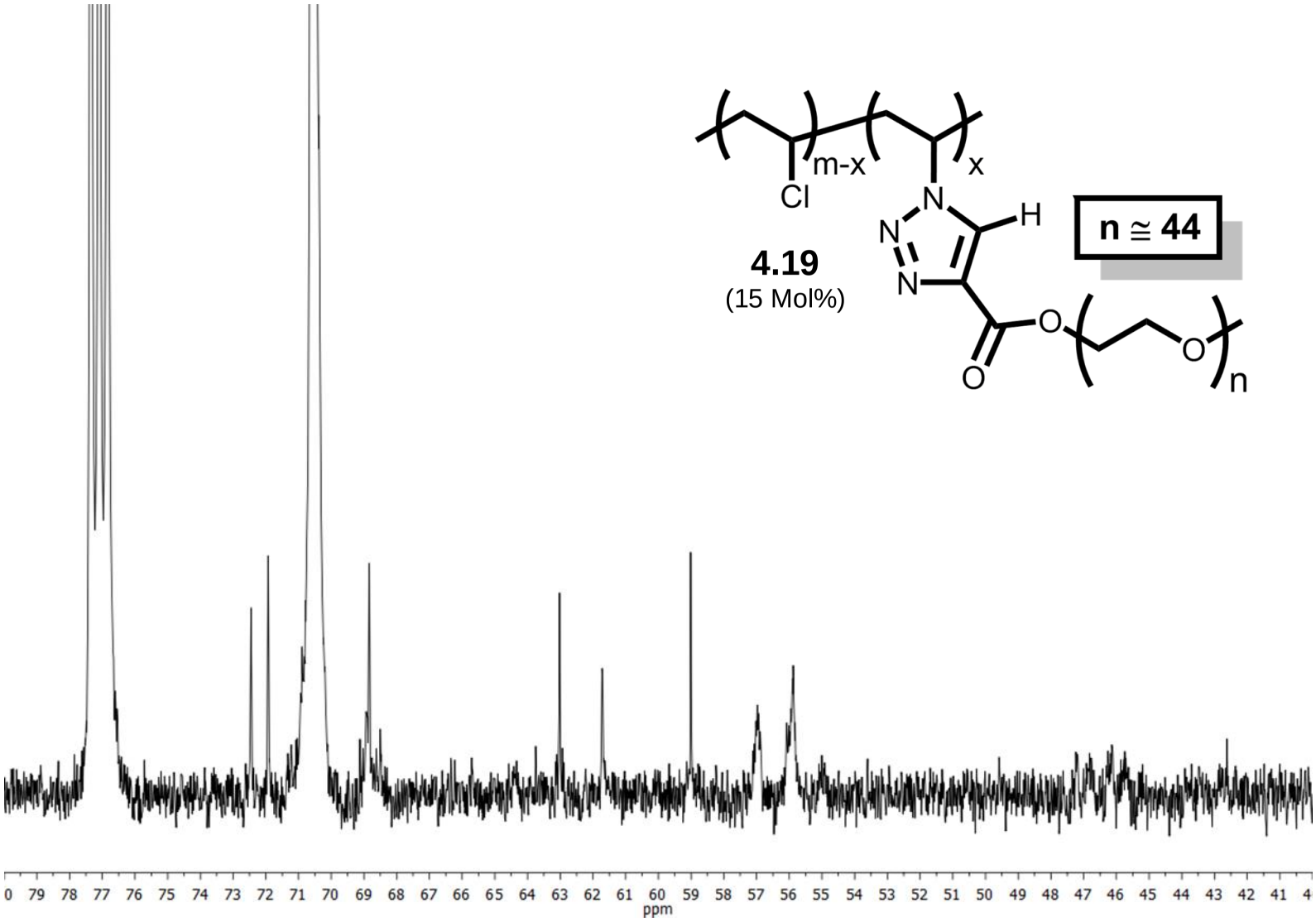
m-x
x
Cl
N
N
N
H
n ≅ 44
O
O
O
n
4.19
(15 Mol%)
0 79 78 77 76 75 74 73 72 71 70 69 68 67 66 65 64 63 62 61 60 59 58 57 56 55 54 53 52 51 50 49 48 47 46 45 44 43 42 41 4
ppm

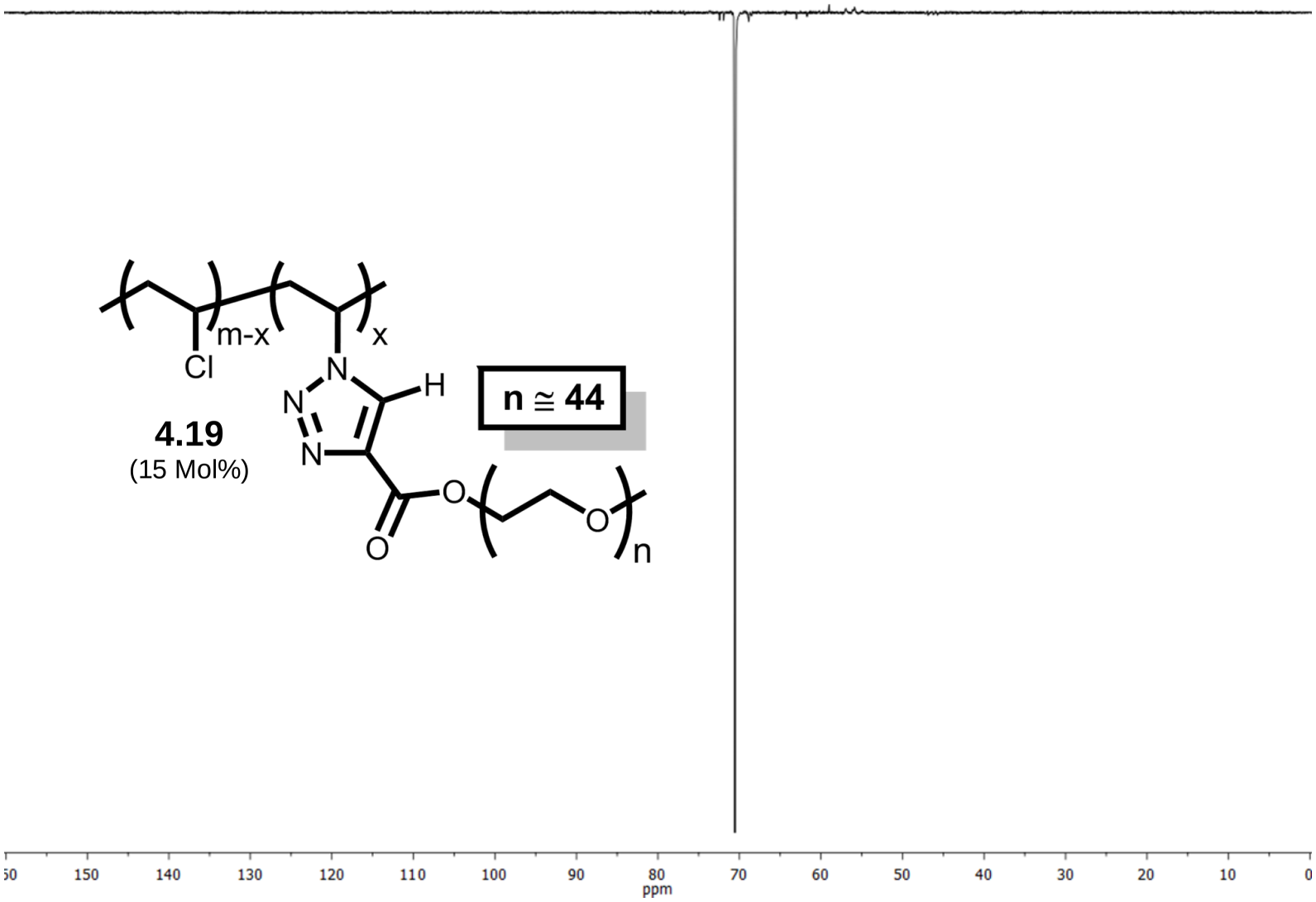
m-x
x
Cl
N
N
N
H
O
O
O
n
4.19
(15 Mol%)
n ≅ 44
150
140
130
120
110
100
90
80
70
60
50
40
30
20
10
0
ppm

969

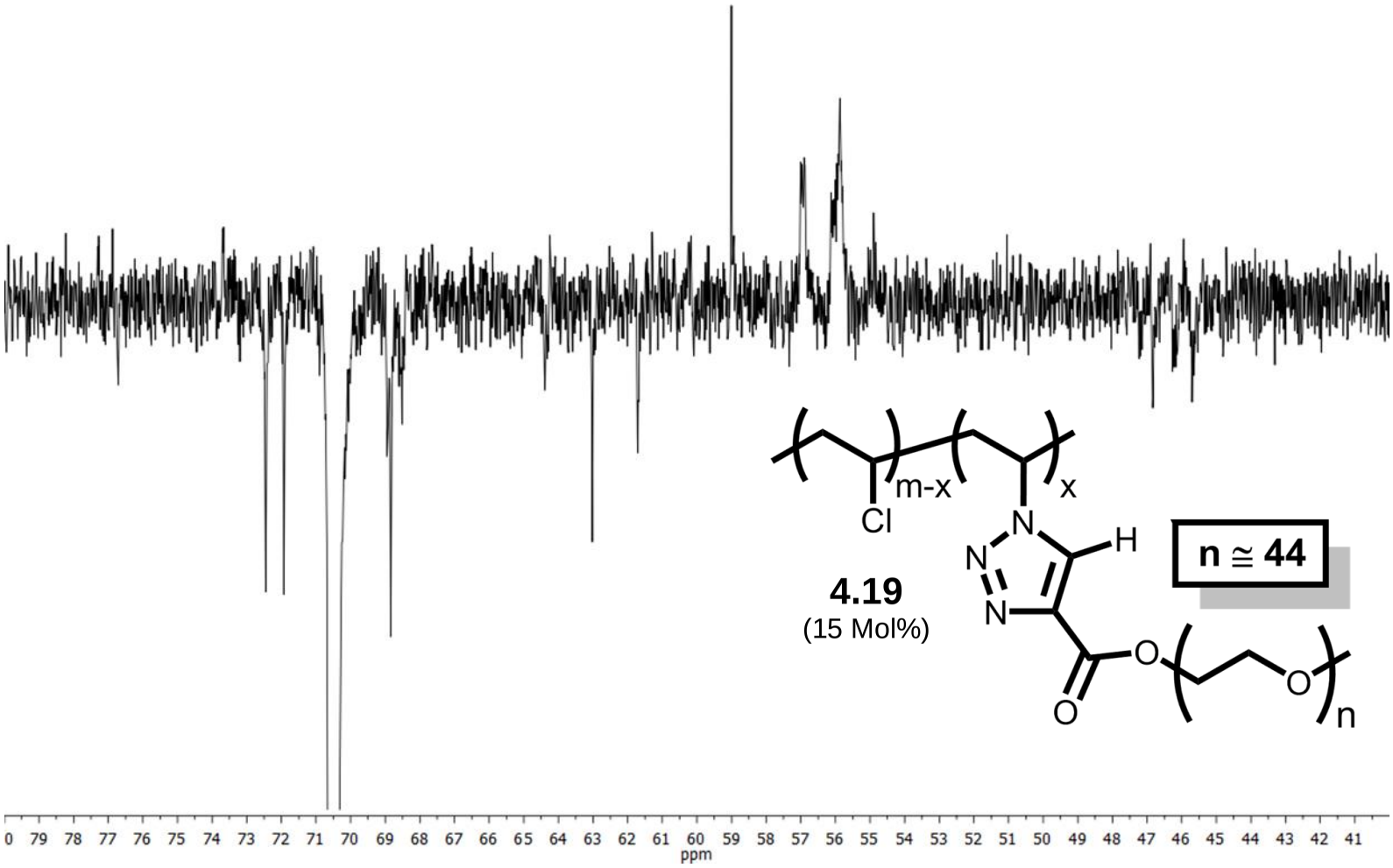
0 79 78 77 76 75 74 73 72 71 70 69 68 67 66 65 64 63 62 61 60 59 58 57 56 55 54 53 52 51 50 49 48 47 46 45 44 43 42 41
ppm
m-x
x
Cl
N
N
N
H
O
O
O
n
n ≅ 44
4.19
(15 Mol%)

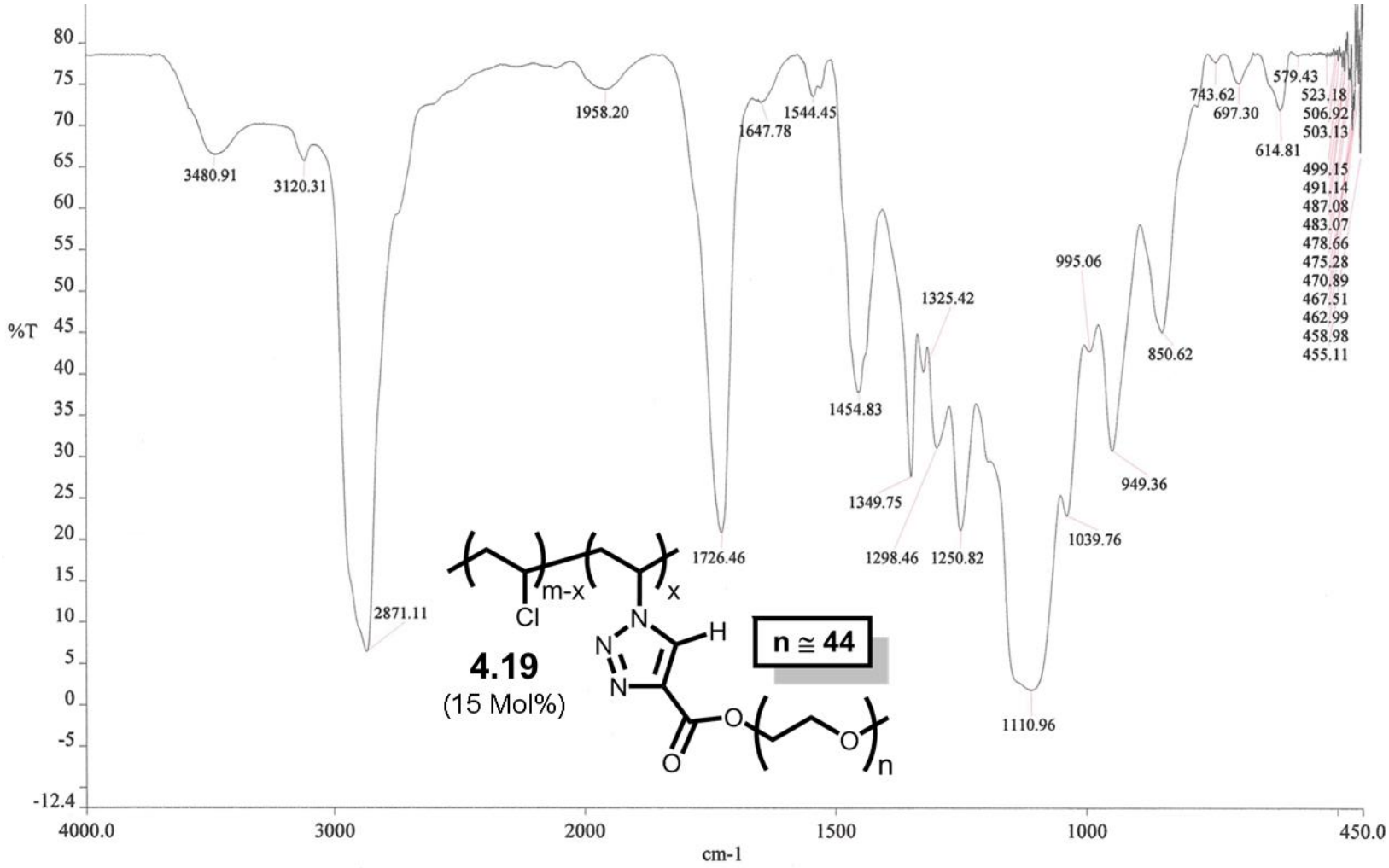
%T
cm-1
4000.0
3000
2000
1500
1000
450.0
80
75
70
65
60
55
50
45
40
35
30
25
20
15
10
5
0
-5
-12.4
3480.91
3120.31
2871.11
1958.20
1726.46
1647.78
1544.45
1454.83
1349.75
1325.42
1298.46
1250.82
1110.96
1039.76
995.06
949.36
850.62
743.62
697.30
614.81
579.43
523.18
506.92
503.13
499.15
491.14
487.08
483.07
478.66
475.28
470.89
467.51
462.99
458.98
455.11
m-x
x
Cl
N
N
N
H
O
O
O
n
4.19
(15 Mol%)
n ≅ 44

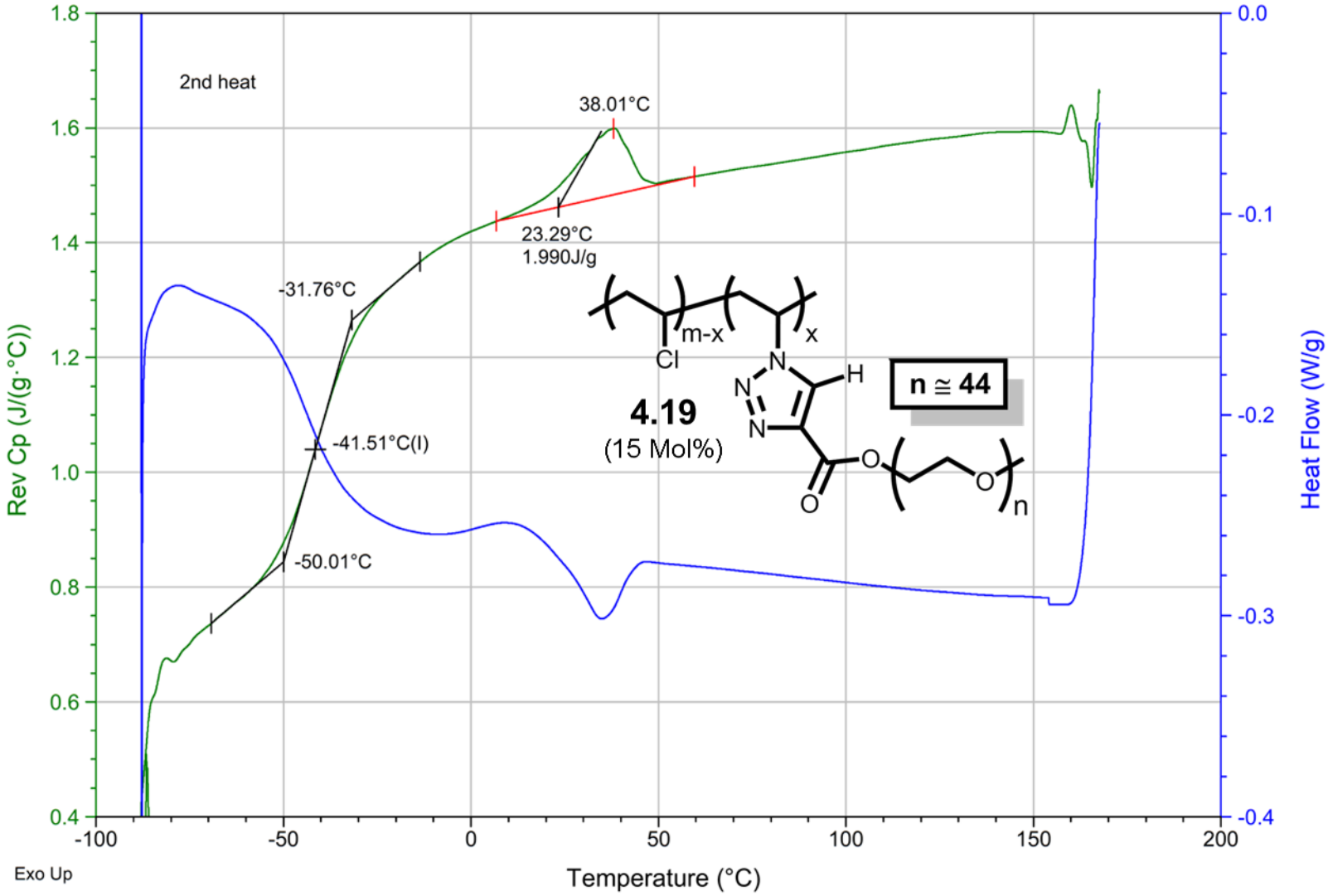
2nd heat
38.01°C
23.29°C
1.990J/g
-31.76°C
-41.51°C(I)
-50.01°C
4.19
(15 Mol%)
n ≅ 44
Rev Cp (J/(g·°C))
Heat Flow (W/g)
Temperature (°C)
Exo Up
1.8
1.6
1.4
1.2
1.0
0.8
0.6
0.4
0.0
-0.1
-0.2
-0.3
-0.4
-100
-50
0
50
100
150
200

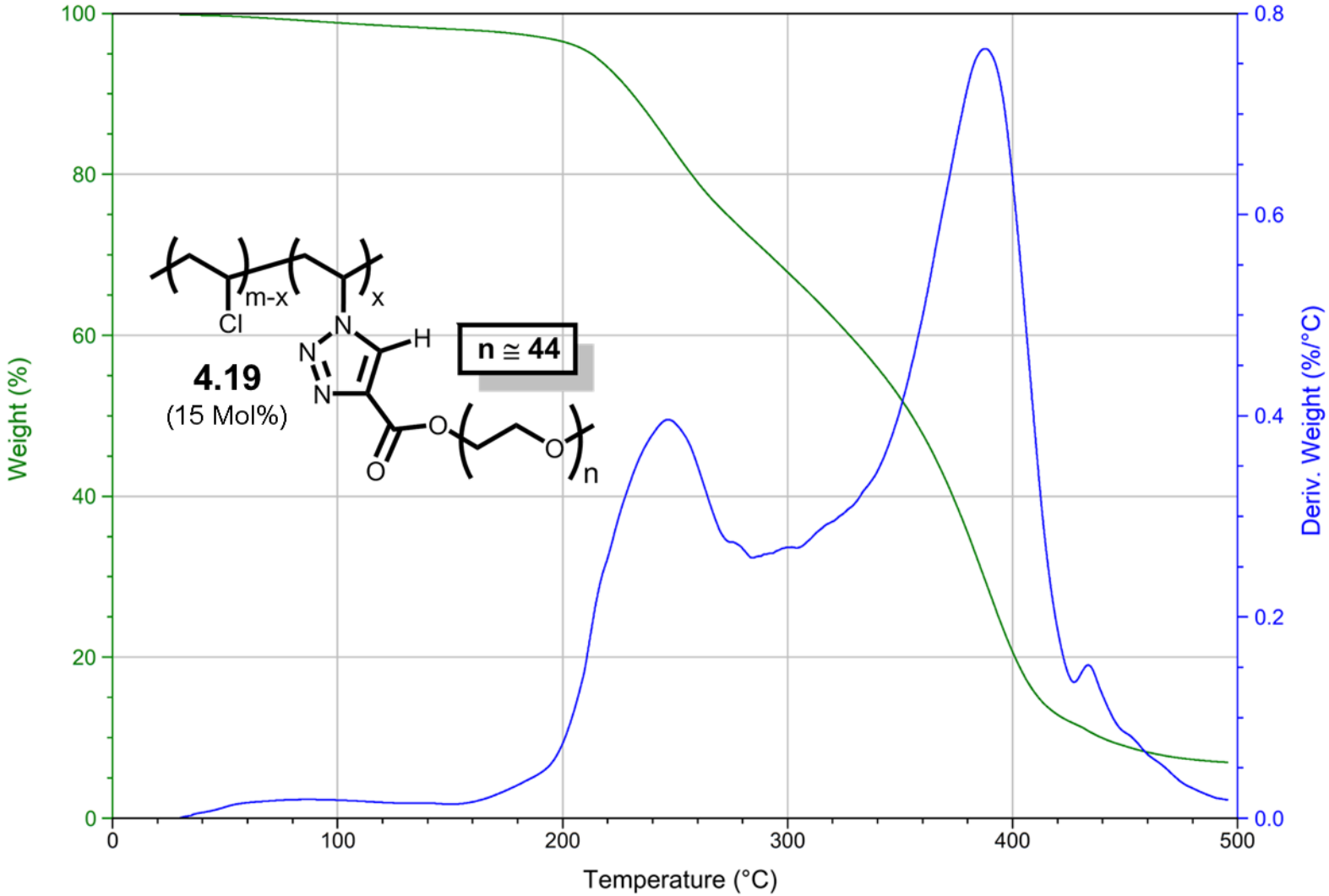
Weight (%)
Deriv. Weight (%/°C)
Temperature (°C)
0
20
40
60
80
100
0.0
0.2
0.4
0.6
0.8
0
100
200
300
400
500
m-x
x
Cl
N
N
H
O
O
O
n
4.19
(15 Mol%)
n ≅ 44

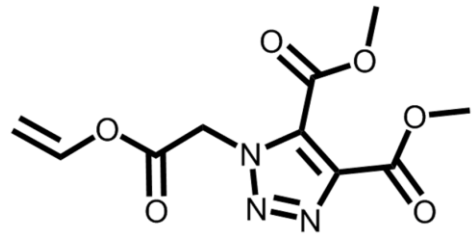

5.2

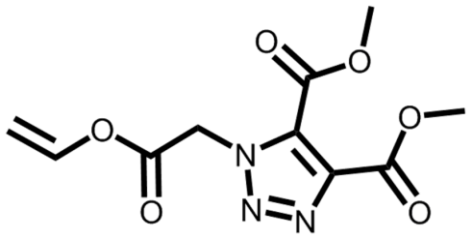

5.2

ppm
200
190
180
170
160
150
140
130
120
110
100
90
80
70
60
50
40
30
20
10

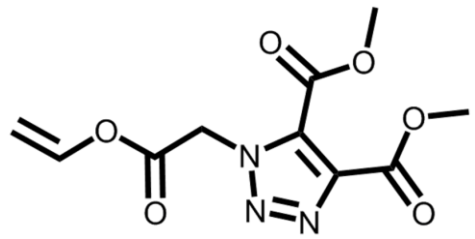

5.2

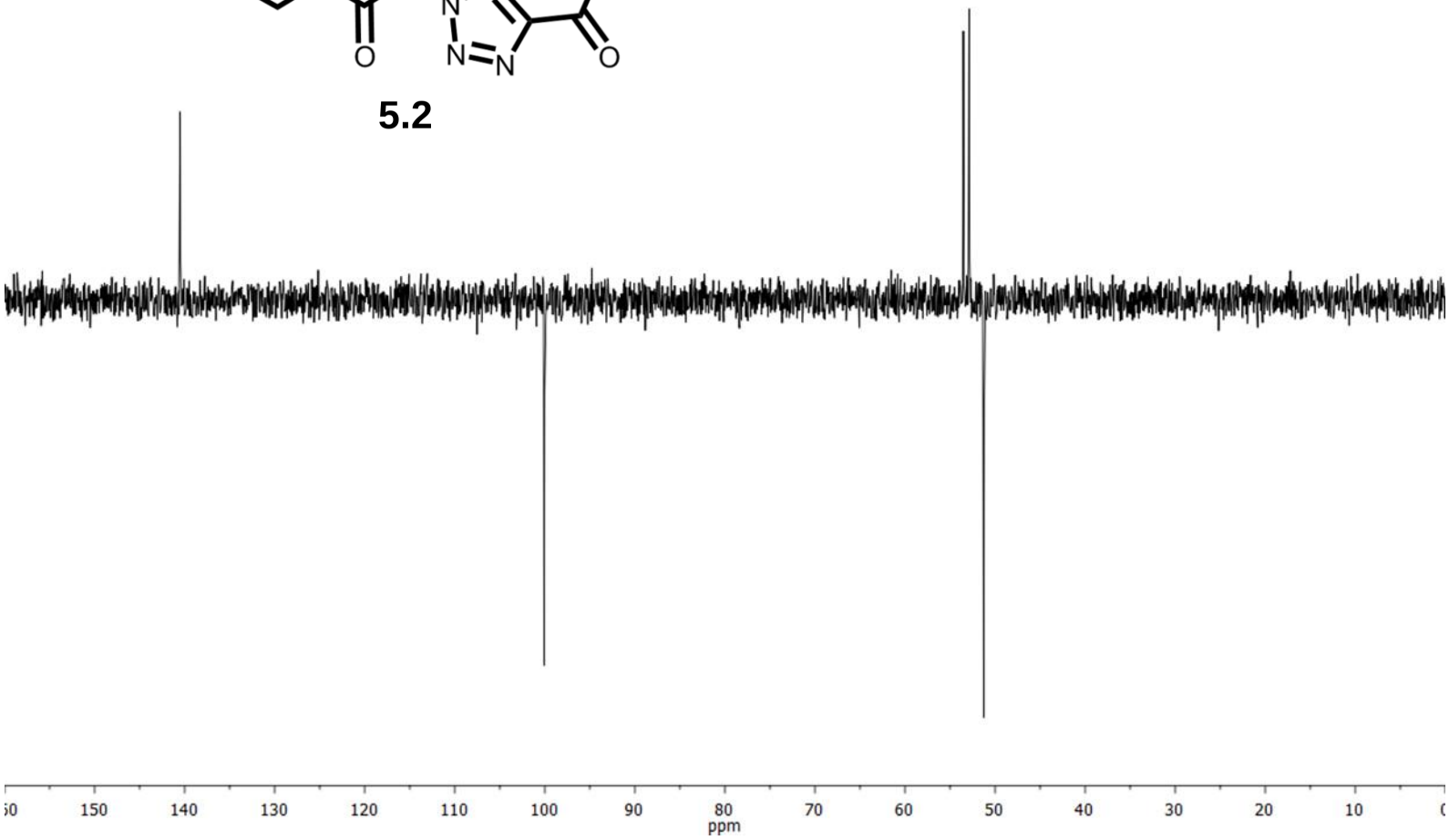

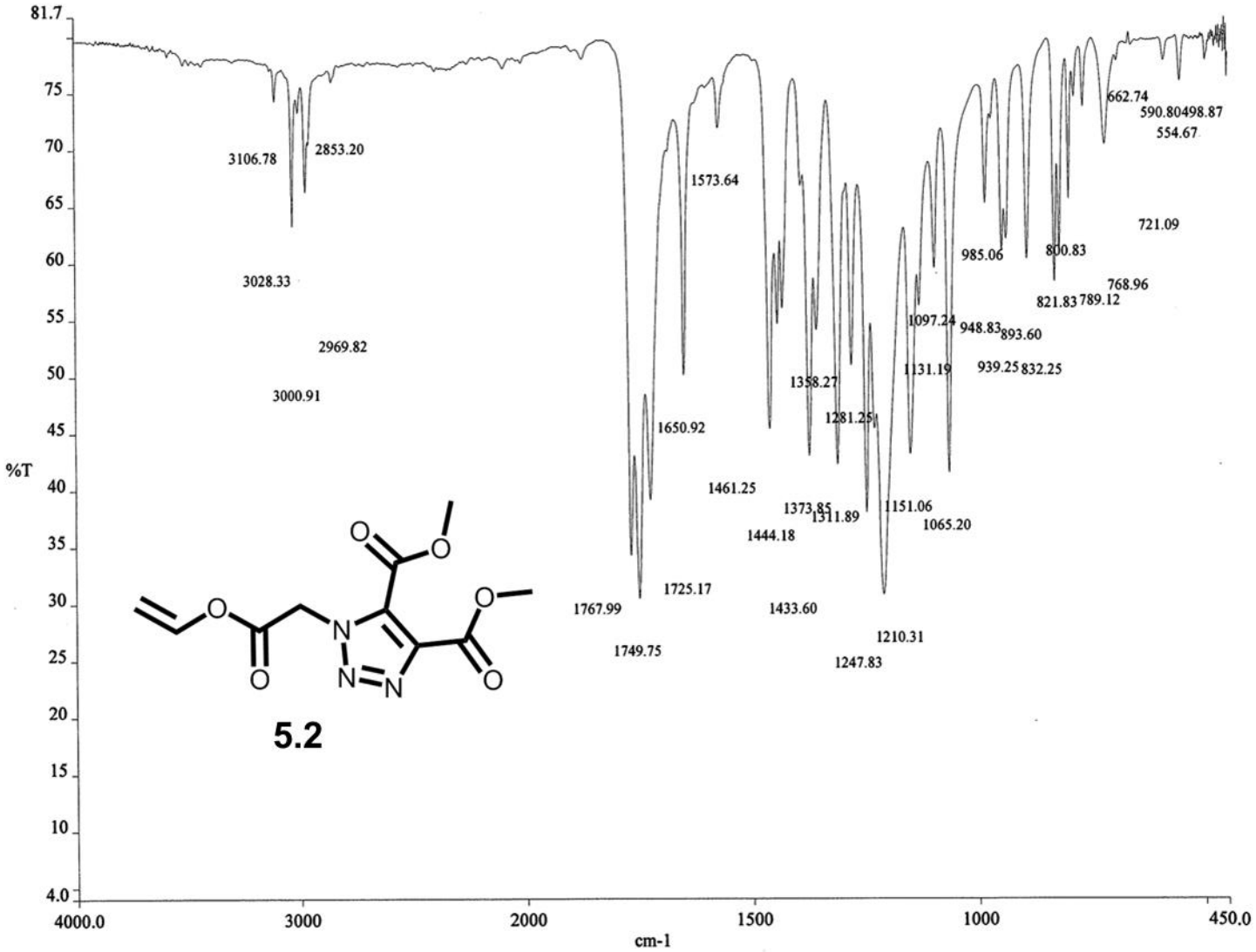
81.7
75
70
65
60
55
50
45
40
35
30
25
20
15
10
4.0
%T
4000.0
3000
2000
1500
1000
450.0
cm-1
3106.78
2853.20
3028.33
2969.82
3000.91
1573.64
1650.92
1725.17
1767.99
1749.75
1461.25
1444.18
1433.60
1358.27
1373.85
1311.89
1281.25
1247.83
1210.31
1151.06
1131.19
1097.24
1065.20
985.06
948.83
939.25
893.60
832.25
821.83
800.83
789.12
768.96
721.09
662.74
590.80
498.87
554.67
O
O
O
O
O
N
N
N

5.2

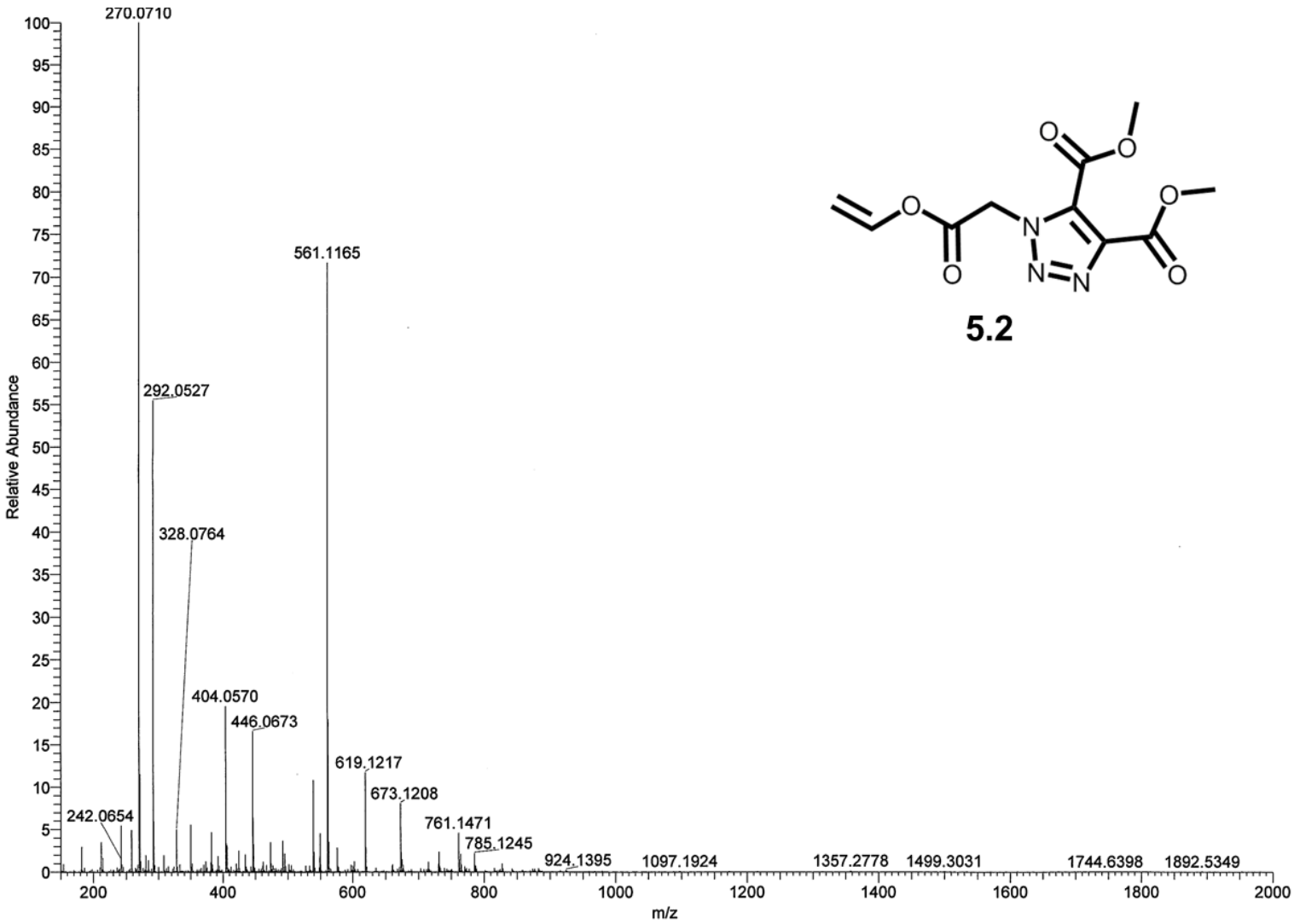
270.0710
561.1165
292.0527
328.0764
404.0570
446.0673
619.1217
673.1208
761.1471
785.1245
242.0654
924.1395
1097.1924
1357.2778
1499.3031
1744.6398
1892.5349
Relative Abundance
m/z
100
95
90
85
80
75
70
65
60
55
50
45
40
35
30
25
20
15
10
5
0
200
400
600
800
1000
1200
1400
1600
1800
2000

5.2

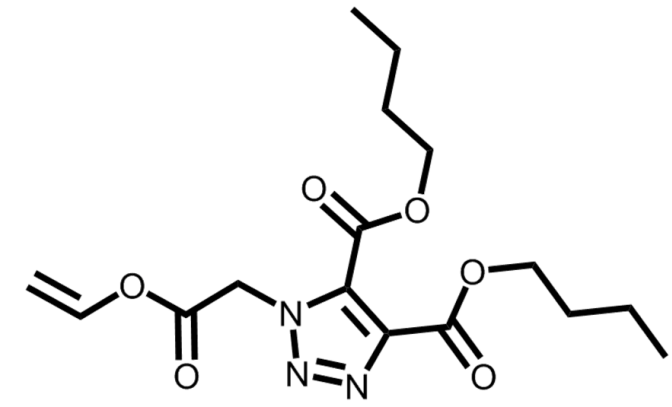
O
O
O
N
N
N
O
O
O

5.3

9.5
9.0
8.5
8.0
7.5
7.0
6.5
6.0
5.5
5.0
4.5
4.0
3.5
3.0
2.5
2.0
1.5
1.0
0.5
ppm

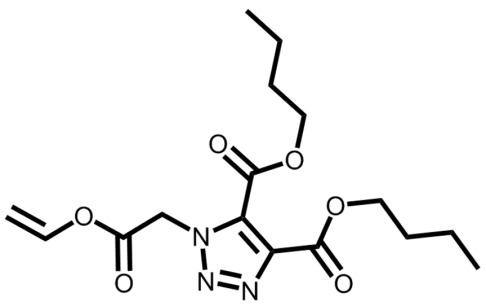

5.3

200
190
180
170
160
150
140
130
120
110
100
90
80
70
60
50
40
30
20
10
ppm

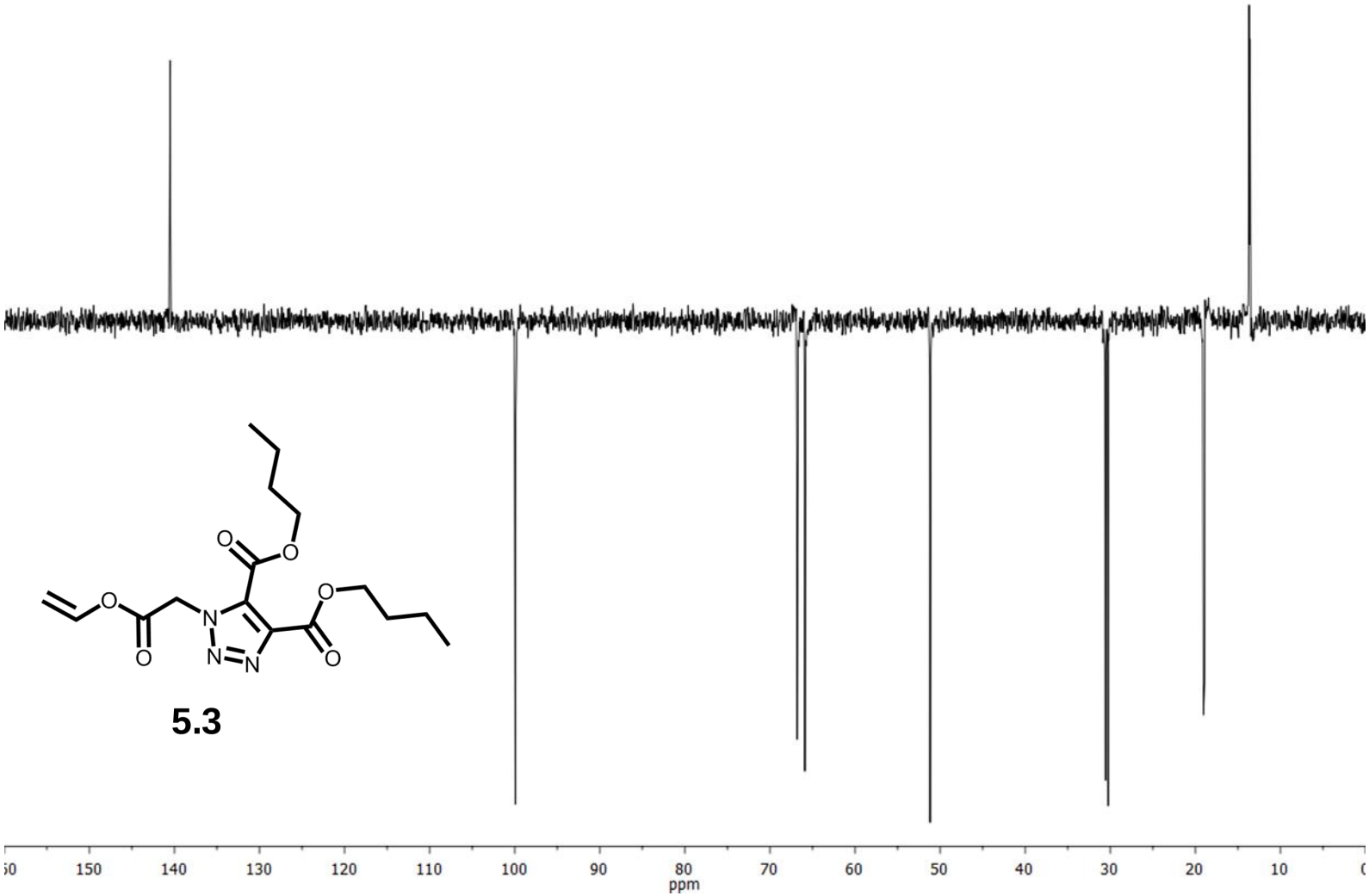

5.3

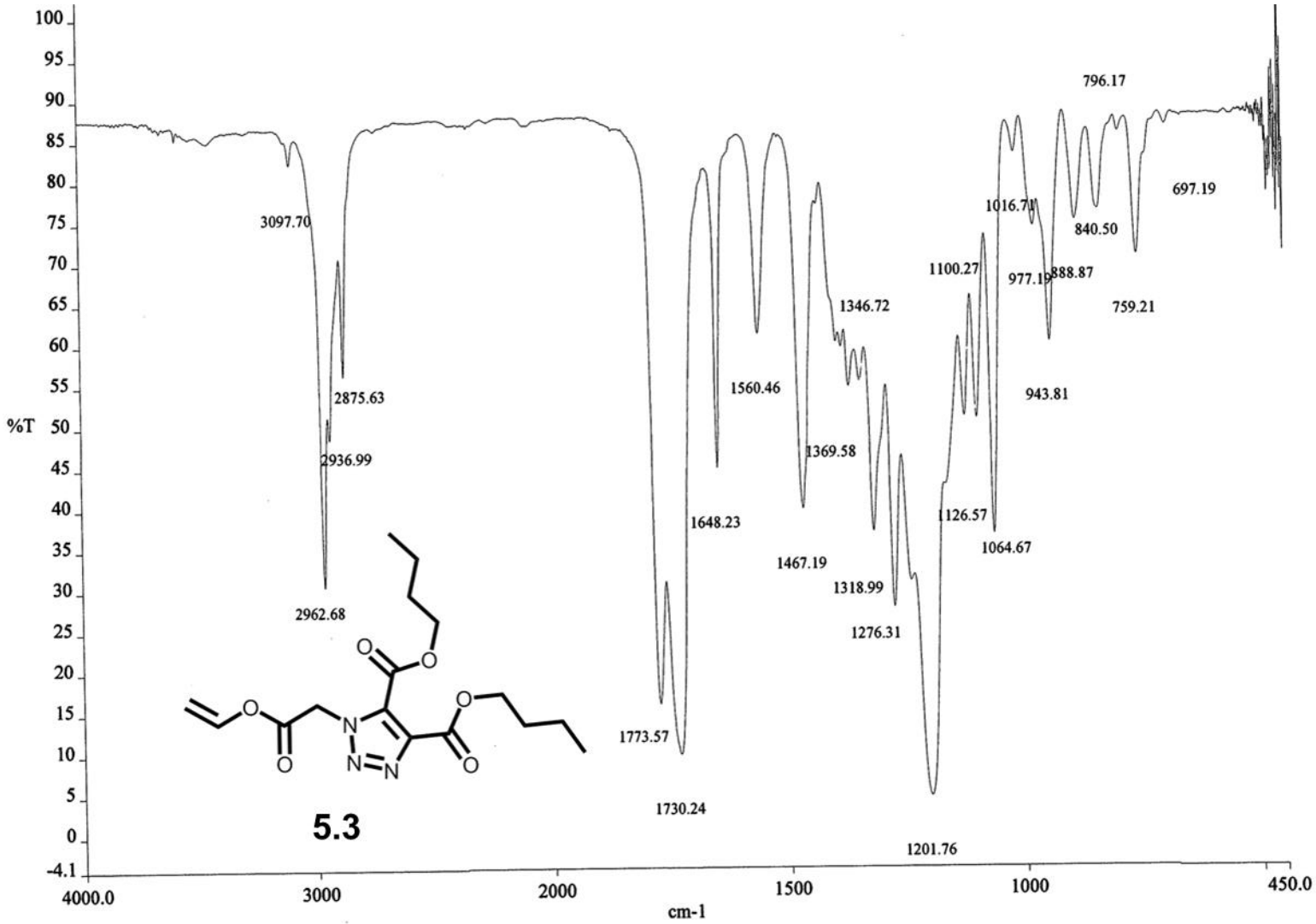
%T
cm-1
4000.0
3000
2000
1500
1000
450.0
3097.70
2962.68
2936.99
2875.63
1773.57
1730.24
1648.23
1560.46
1467.19
1369.58
1346.72
1318.99
1276.31
1201.76
1126.57
1100.27
1064.67
1016.71
977.19
943.81
888.87
840.50
796.17
759.21
697.19
5.3

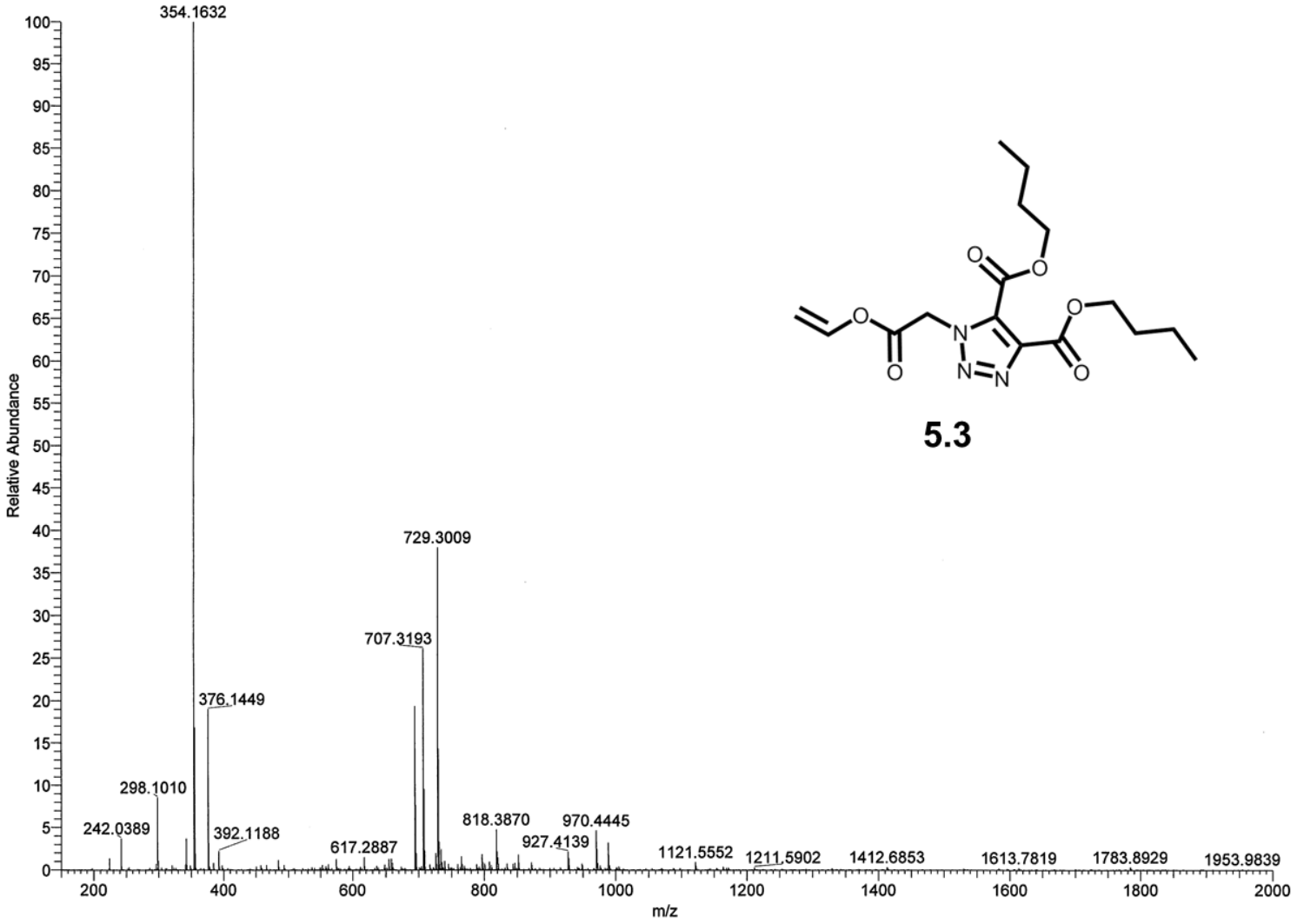
354.1632
729.3009
707.3193
376.1449
298.1010
242.0389
392.1188
617.2887
818.3870
970.4445
927.4139
1121.5552
1211.5902
1412.6853
1613.7819
1783.8929
1953.9839
Relative Abundance
m/z

5.3

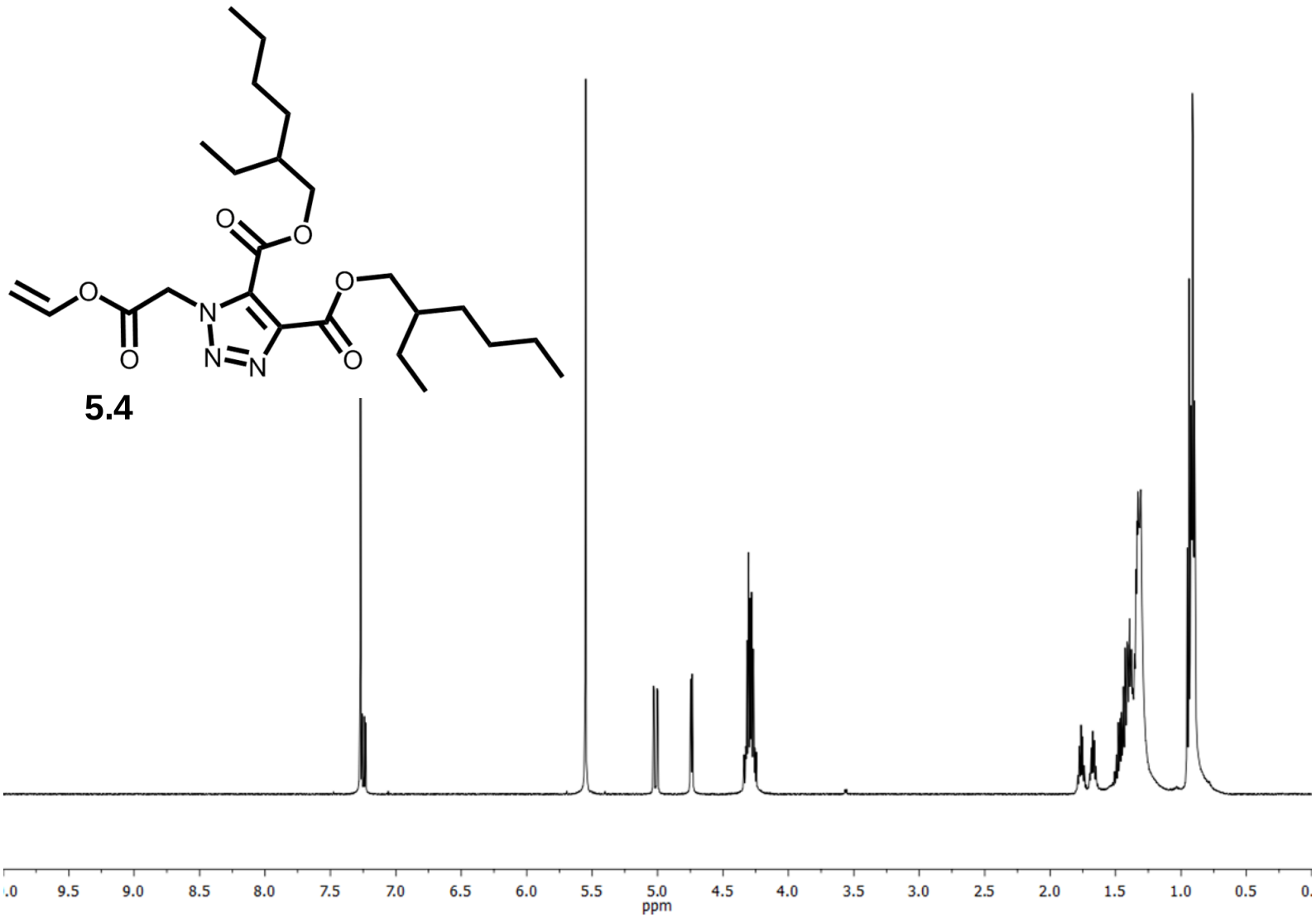
O
O
O
O
N
N
N
O
O
O
5.4
10.0
9.5
9.0
8.5
8.0
7.5
7.0
6.5
6.0
5.5
5.0
4.5
4.0
3.5
3.0
2.5
2.0
1.5
1.0
0.5
ppm

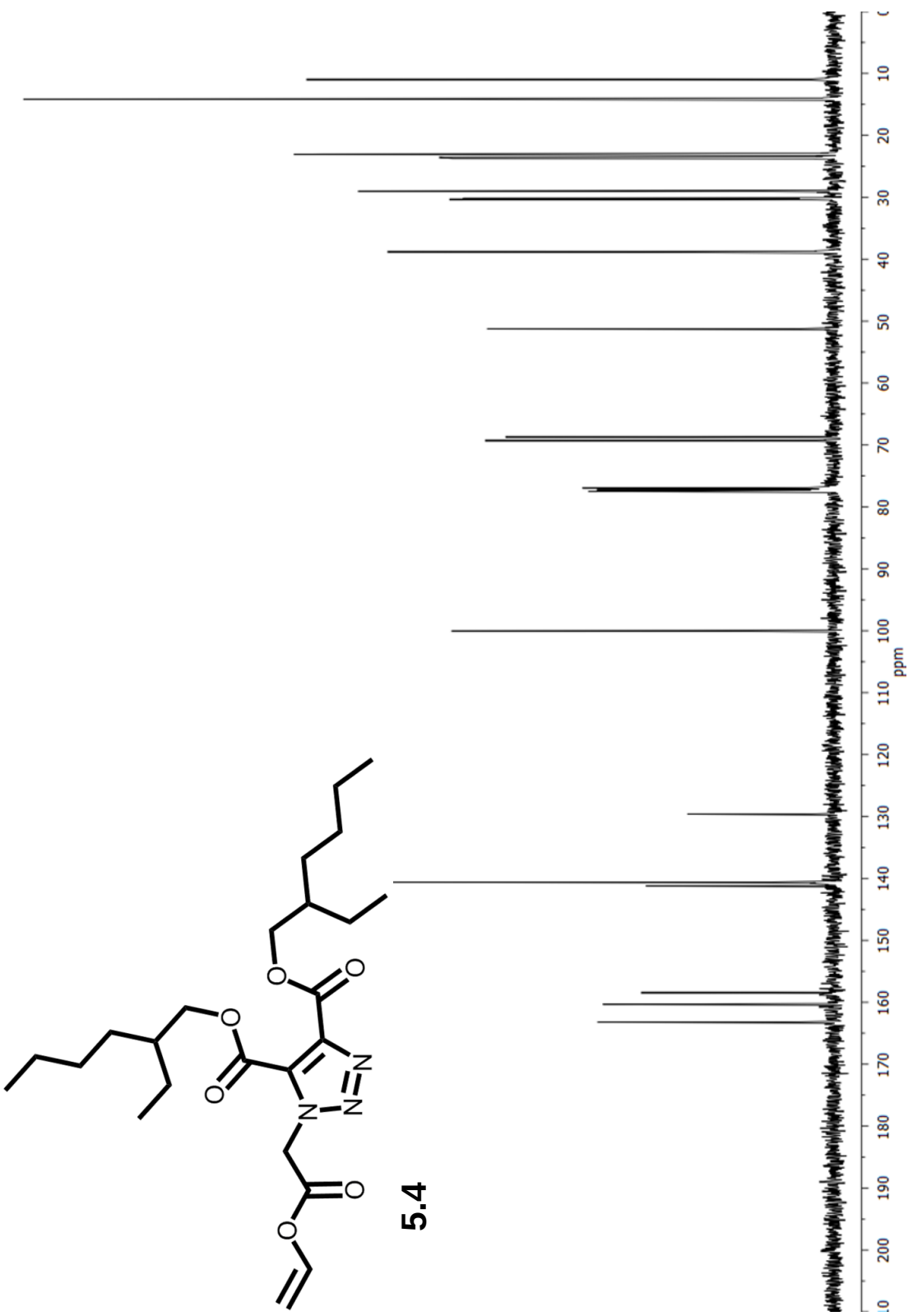
O
O
O
O
N
N
N
O
O
O
ppm
10
20
30
40
50
60
70
80
90
100
110
120
130
140
150
160
170
180
190
200

5.4

ppm
5.4

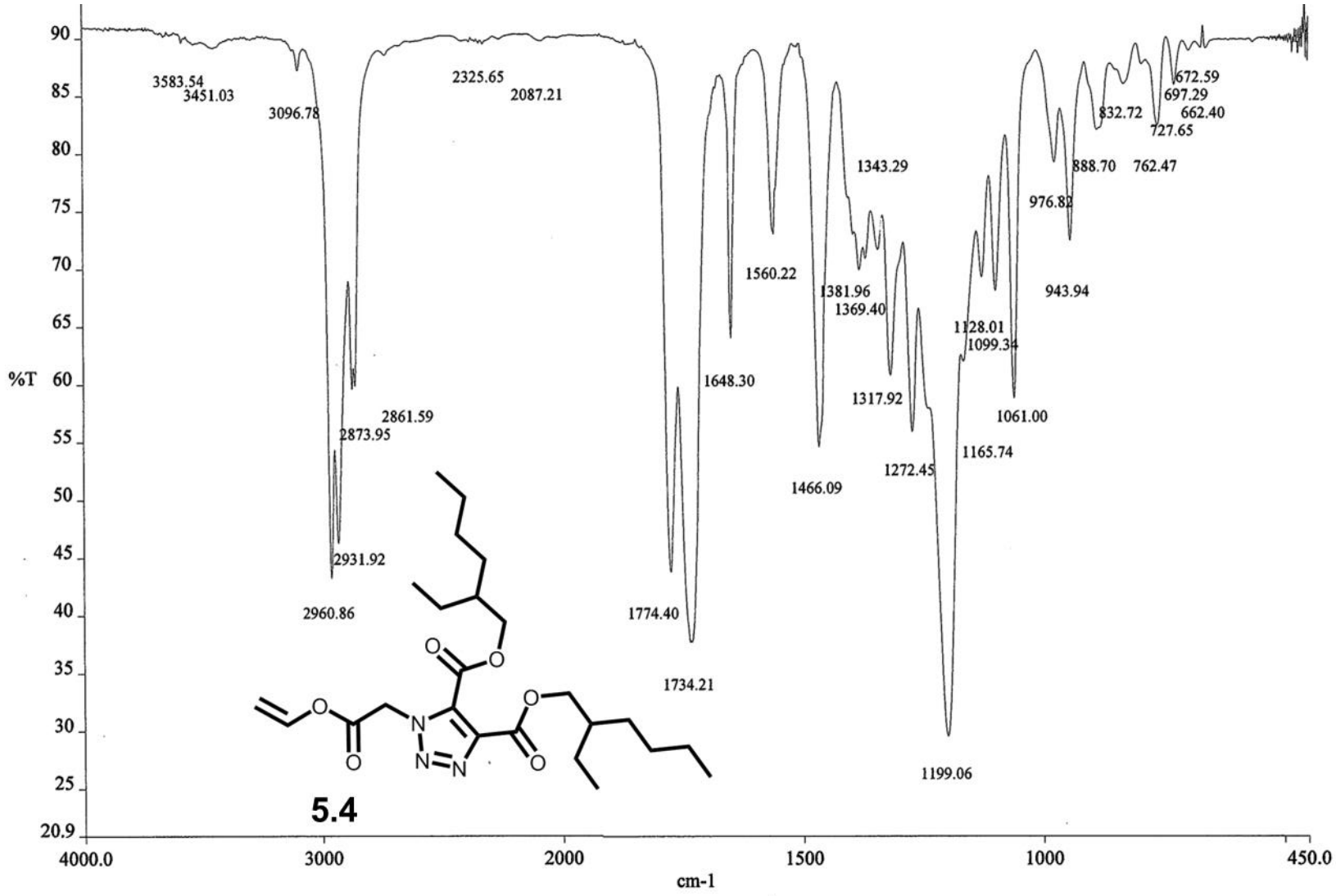
%T
cm-1
4000.0
3000
2000
1500
1000
450.0
90
85
80
75
70
65
60
55
50
45
40
35
30
25
20.9
3583.54
3451.03
3096.78
2325.65
2087.21
1343.29
976.82
888.70
762.47
832.72
727.65
672.59
697.29
662.40
1560.22
1381.96
1369.40
943.94
1128.01
1099.34
1648.30
1317.92
1061.00
2861.59
2873.95
1165.74
1466.09
1272.45
2931.92
2960.86
1774.40
1734.21
1199.06
5.4

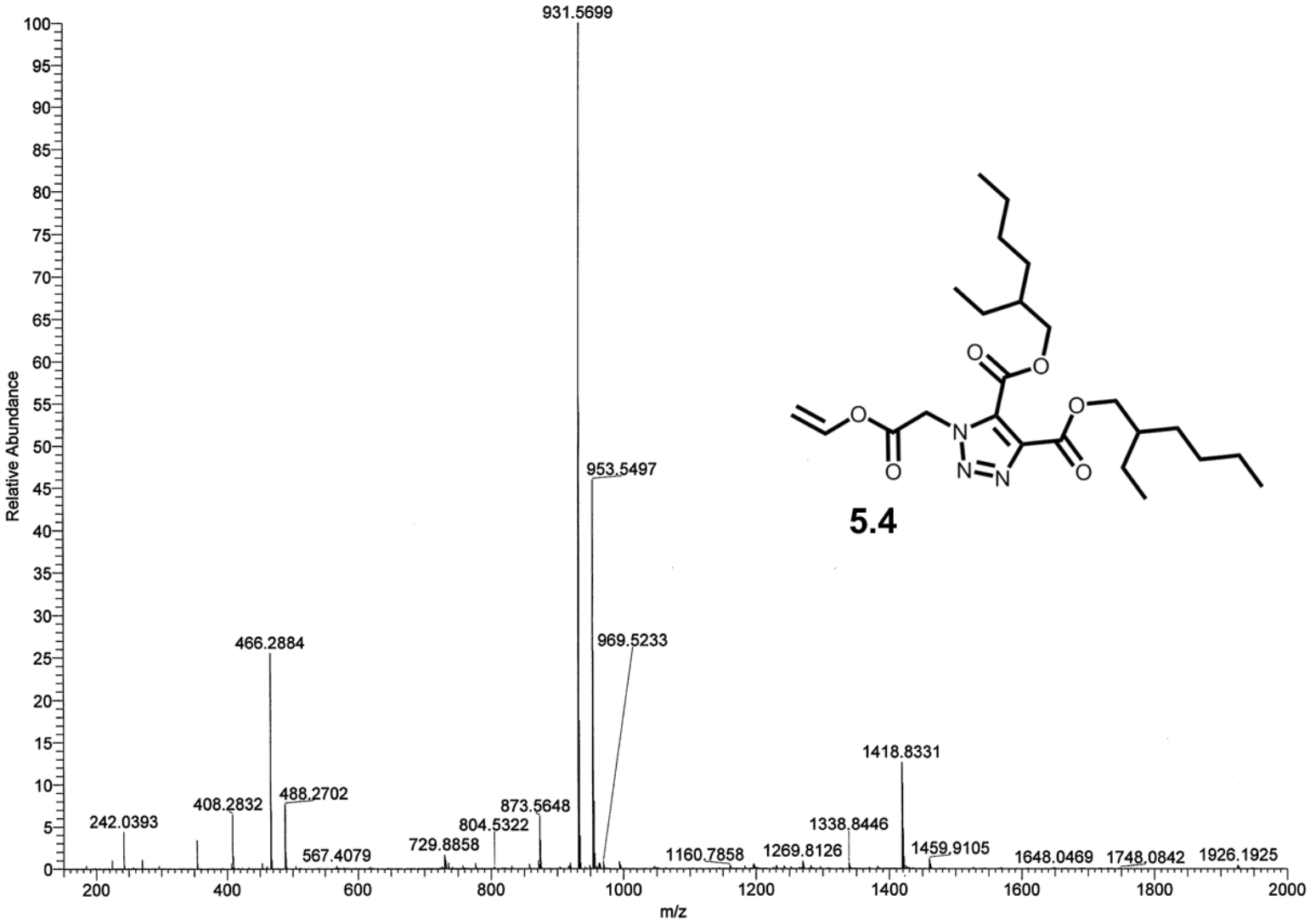
931.5699
953.5497
969.5233
466.2884
488.2702
408.2832
242.0393
567.4079
873.5648
804.5322
729.8858
1418.8331
1338.8446
1459.9105
1160.7858
1269.8126
1648.0469
1748.0842
1926.1925
Relative Abundance
m/z
5.4

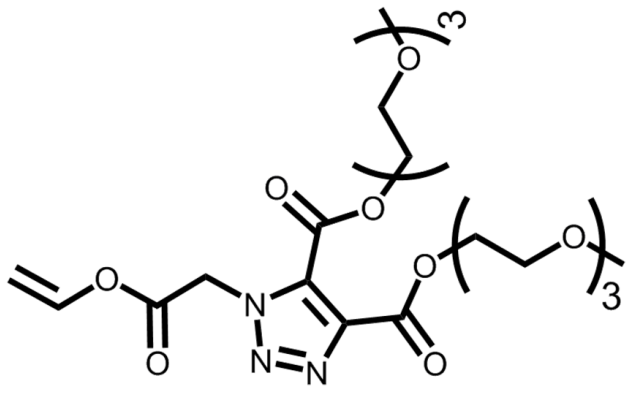
O
3
O
O
O
O
N
N
N
O
O
O
3

5.5

9.5
9.0
8.5
8.0
7.5
7.0
6.5
6.0
5.5
5.0
4.5
4.0
3.5
3.0
2.5
2.0
1.5
1.0
0.5
ppm

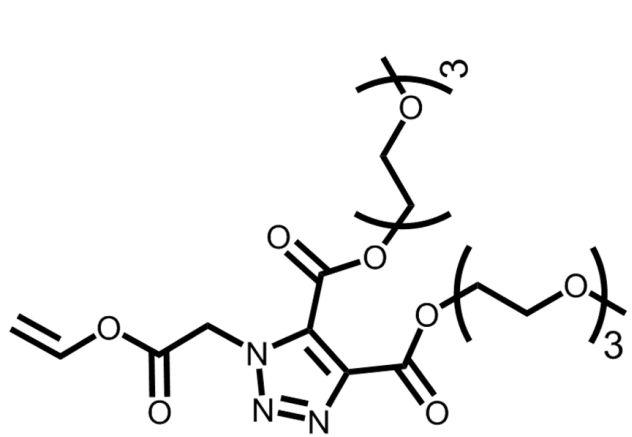

5.5

200
190
180
170
160
150
140
130
120
110
100
90
80
70
60
50
40
30
20
10
ppm

ppm
5.5

5.5
%T
cm-1
81.0
75
70
65
60
55
50
45
40
35
30
25
20
15
10
5
0
-5
-11.5
4000.0
3000
2000
1500
1000
450.0
3583.92
3510.42
3096.20
2879.62
2343.99
2259.53
2111.93
1953.24
1763.52
1732.85
1678.89
1647.17
1556.94
1464.16
1411.11
1366.84
1351.49
1316.81
1276.97
1244.26
1202.82
1103.37
1064.38
1027.89
983.20
946.60
851.44
795.34
757.56
704.50
665.93
559.59
531.20
515.24
511.15
506.91
503.11
499.08
494.99
491.14
486.84
483.29
479.06
474.95
471.02
466.89
462.93
458.79
455.02

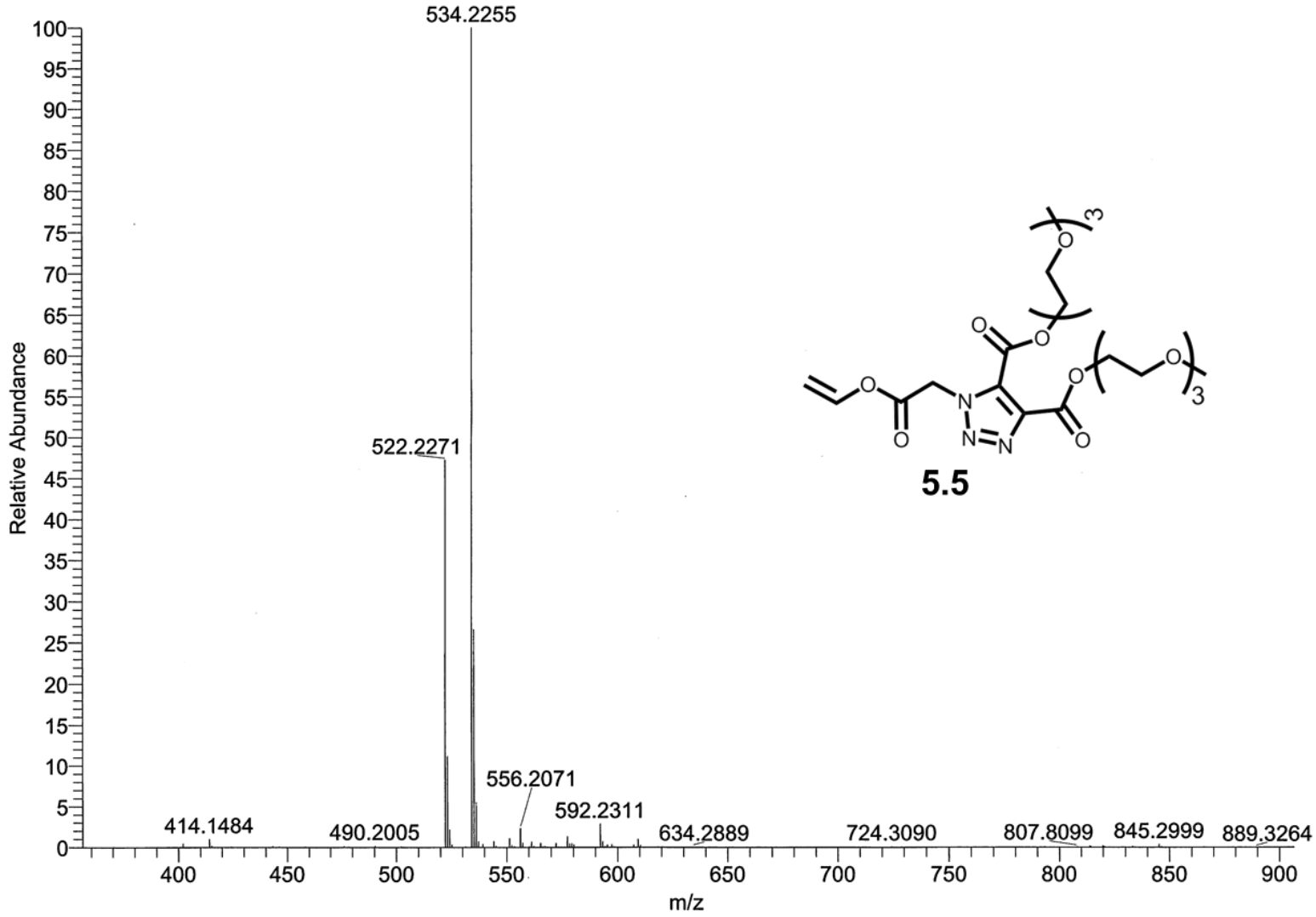
534.2255
522.2271
556.2071
592.2311
414.1484
490.2005
634.2889
724.3090
807.8099
845.2999
889.3264
Relative Abundance
m/z
100
95
90
85
80
75
70
65
60
55
50
45
40
35
30
25
20
15
10
5
0
400
450
500
550
600
650
700
750
800
850
900

5.5

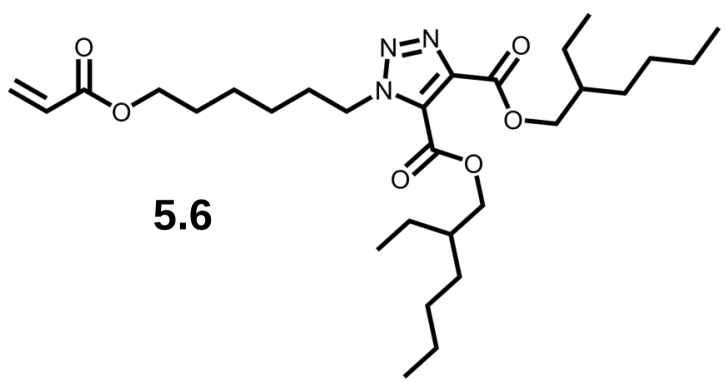
O
O
N
N
N
O
O
O
O
O

5.6

9.5
9.0
8.5
8.0
7.5
7.0
6.5
6.0
5.5
5.0
4.5
4.0
3.5
3.0
2.5
2.0
1.5
1.0
0.5
ppm

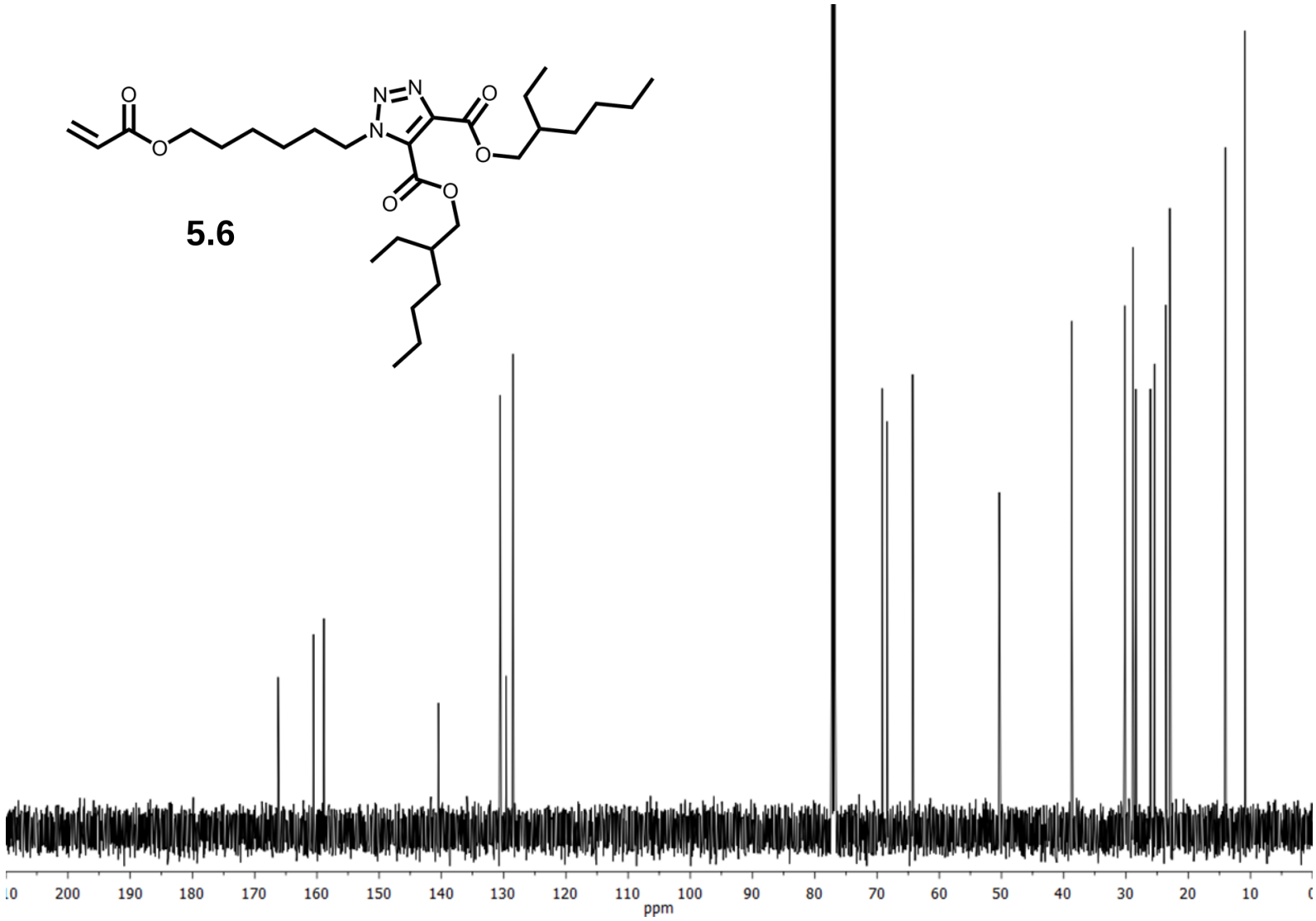
5.6
ppm

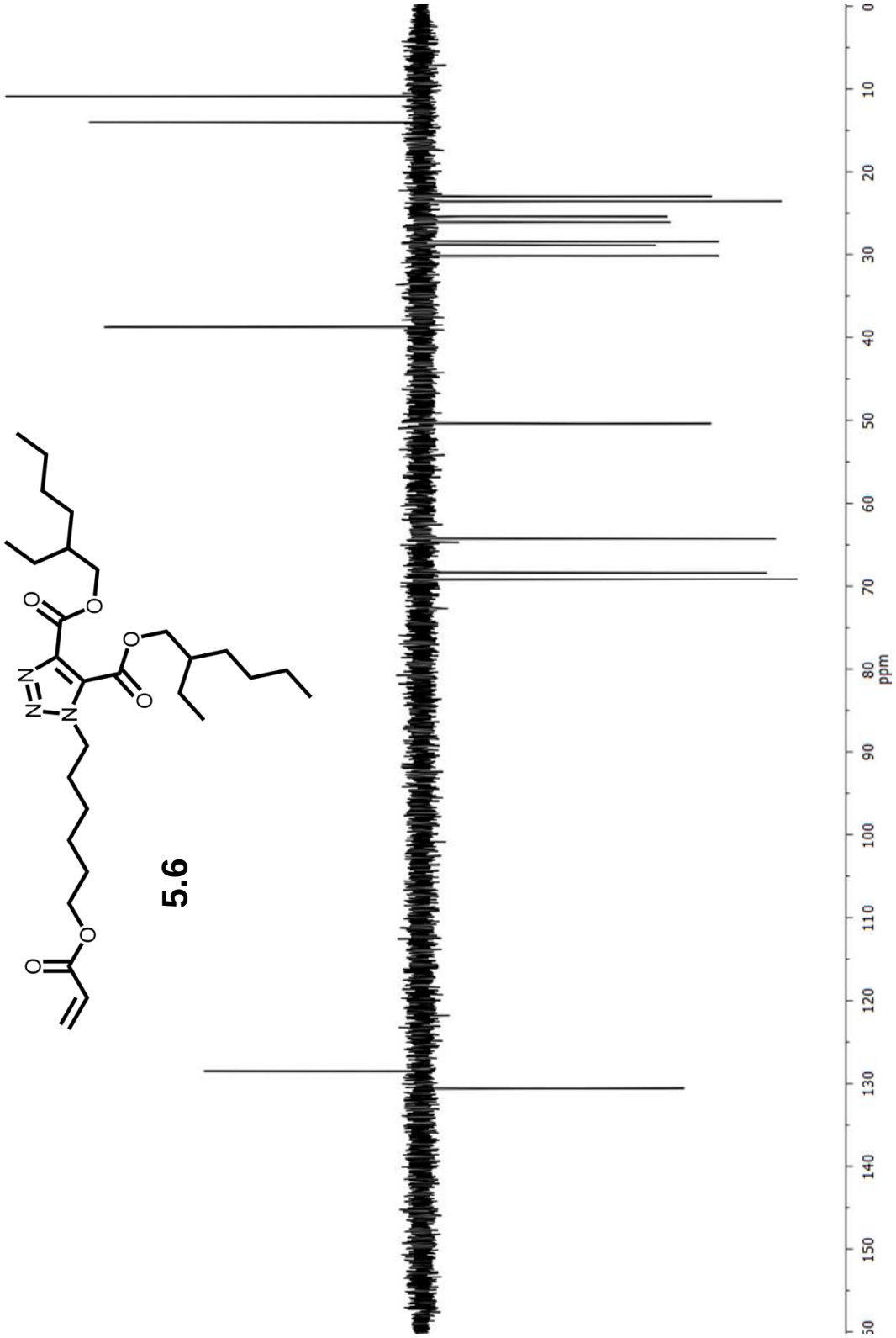
5.6
ppm

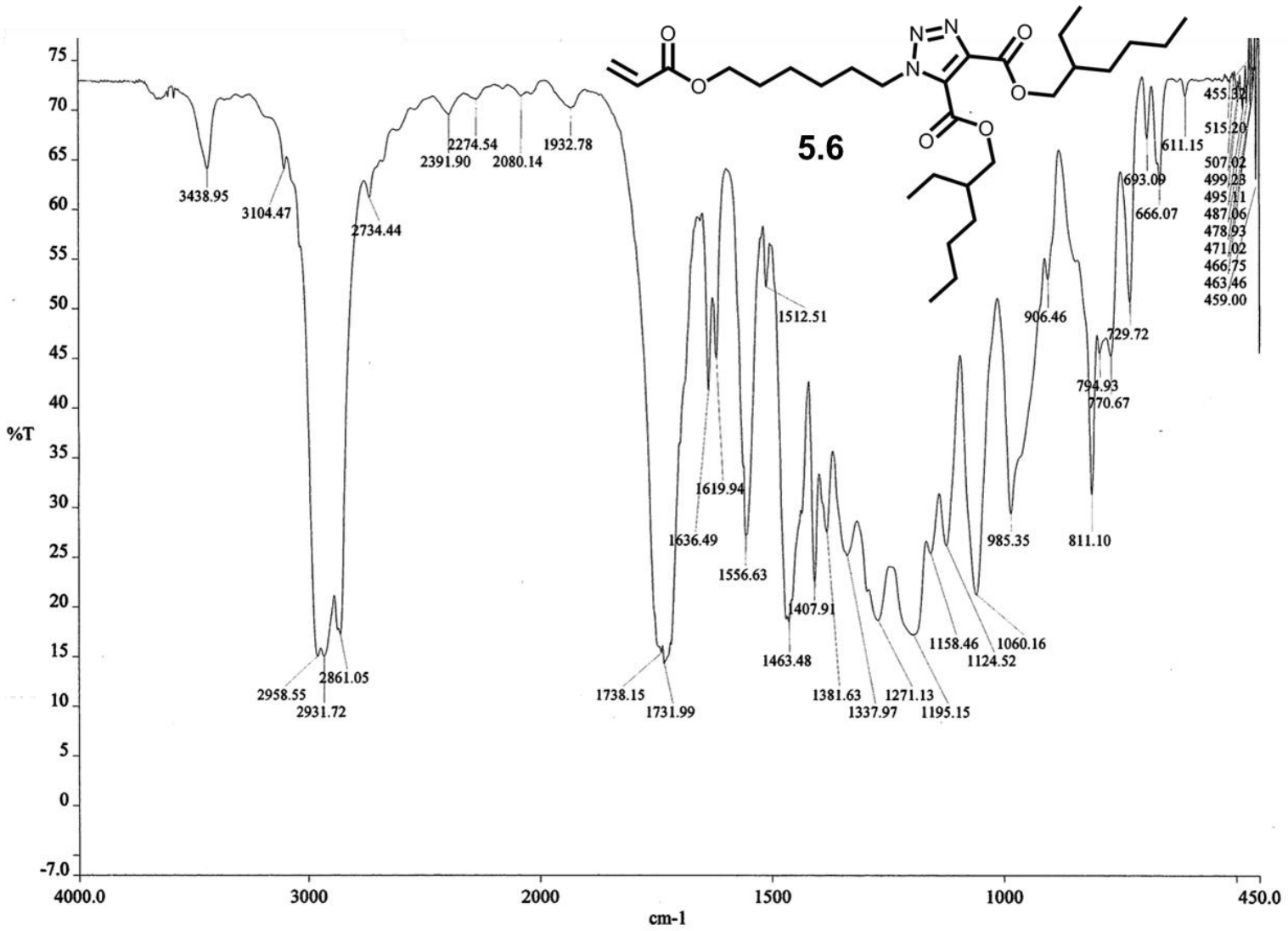
5.6
%T
cm-1
4000.0
3000
2000
1500
1000
450.0
75
70
65
60
55
50
45
40
35
30
25
20
15
10
5
0
-7.0
3438.95
3104.47
2734.44
2391.90
2274.54
2080.14
1932.78
2958.55
2931.72
2861.05
1738.15
1731.99
1636.49
1619.94
1556.63
1512.51
1463.48
1407.91
1381.63
1337.97
1271.13
1195.15
1158.46
1124.52
1060.16
985.35
906.46
811.10
794.93
770.67
729.72
693.09
666.07
611.15
515.20
507.02
499.23
495.11
487.06
478.93
471.02
466.75
463.46
459.00

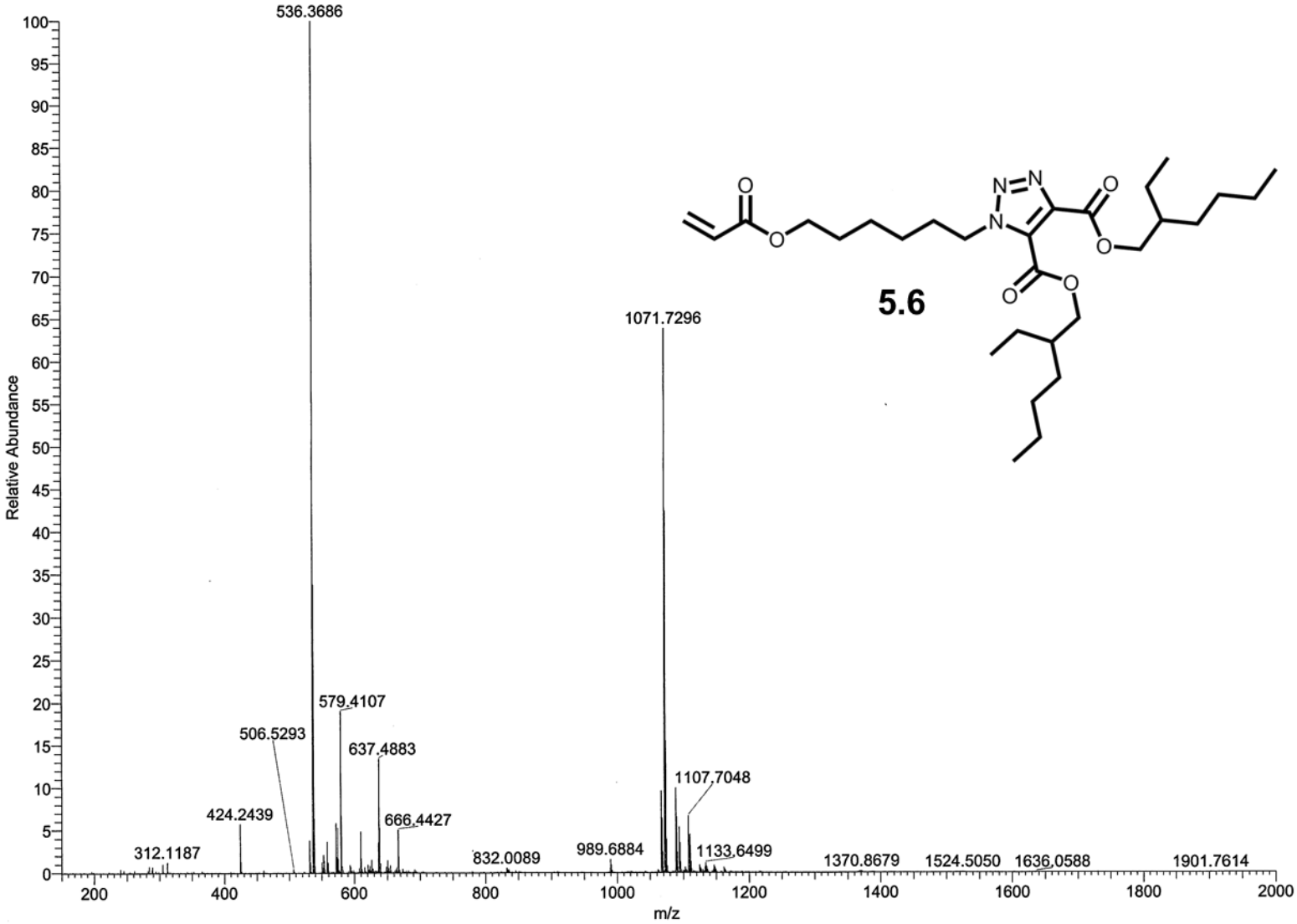
536.3686
1071.7296
579.4107
506.5293
637.4883
1107.7048
424.2439
666.4427
312.1187
832.0089
989.6884
1133.6499
1370.8679
1524.5050
1636.0588
1901.7614
Relative Abundance
m/z
5.6

Bibliography

1. 1999/815/EC: Commission Decision of 7 December 1999 Adopting Measures Prohibiting the Placing on the Market of Toys and Childcare Articles Intended to be Placed in the Mouth by Children Under Three Years of Age Made of Soft PVC Containing One or More of the Substances Di-iso-nonyl Phthalate (DINP), Di(2-ethylhexyl) Phthalate (DEHP), Dibutyl Phthalate (DBP), Di-iso-decyl Phthalate (DIDP), Di-n-octyl Phthalate (DNOP), and Butylbenzyl Phthalate (BBP). In *European Union*, 1999; Vol. L 315, pp 46-49.

2. Commission Directive 2004/93/EC of 21 September 2004 Amending Council Directive 76/768/EEC for the Purpose of Adapting Its Annexes II and III to Technical Progress. In *European Union*, 2004; Vol. L 300, pp 13-41.

3. Commission Directive 2007/19/EC of 30 March 2007 Amending Directive 2002/72/EC Relating to Plastic Materials and Articles Intended to Come into Contact with Food and Council Directive 85/572/EEC Laying Down the List of Simulants to Be Used for Testing Migration of Constituents of Plastic Materials and Articles Intended to Come into Contact with Foodstuffs. In *European Union*, 2007; Vol. L 91, pp 17-36.

4. Directive 2005/84/EC of the European Parliament and of the Council 14 December 2005 Amending for the 22nd time Council Directive 76/769/EEC on the Approximation of the Laws, Regulations and Administrative Provisions of the Member States Relating to Restrictions on the Marketing and Use of Certain Dangerous Substances and Preparations (Phthalates in Toys and Childcare Articles). In *European Union*, 2005; Vol. L 344, pp 40-43.

5. IHS Chemical. Chemical Economics Handbook: Plasticizers. https://www.ihs.com/products/plasticizers-chemical-economics-handbook.html (accessed September 25, 2017).

6. Safety Assessment of Di(2-Ethylhexyl) Phthalate (DEHP) Released From Medical Devices. United States Food and Drug Administration, United States of America, 2001.

7. Steady Growth Predicted in Global Markets for DINP and DOP Phthalate Plasticizers. *Additives for Polymers* **2015,** *2015* (9), 11.

8. Technical Bulletin: JEFFAMINE™ Polyetheramines. http://www.huntsman.com/performance_products/a/Products/Amines/Polyetheramines%20%20%20JEFFAMINE_R (accessed Sept 7, 2017).

9. The European Council of Vinyl Manufacturers, How is PVC Used? http://www.pvc.org/en/p/how-is-pvc-used (accessed Sept 13, 2017).

10. *U.S. Environmental Protection Agency: Child-Specific Exposure Factors Handbook (Final Report)*; United States of America, 2008.

11. *U.S. Resin Production & Sales 2016 vs. 2015.* https://plastics.americanchemistry.com/Sales-Data-by-Resin.pdf (accessed Sept 8, 2017).

12. Whitfield & Associates. The Economic Benefits of Polyvinyl Chloride in the United States and Canada. http://www.pvc.org/upload/documents/The_Economics_of_PVC.pdf. (accessed Sept 13, 2017).

13. *World Plastics Statistics 2015*. https://committee.iso.org/files/live/sites/tc61/files/The%20Plastic%20Industry%20Berlin%20Aug%202016%20-%20Copy.pdf. (accessed Sept 13, 2017).

14. Abraham, R. J.; Canton, M.; Griffiths, L. Proton Chemical Shifts In NMR: Part 17. Chemical Shifts In Alkenes And Anisotropic And Steric Effects Of The Double Bond. *Magnetic Resonance in Chemistry* **2001,** *39* (8), 421-431.

15. Abraham, R. J.; Reid, M. Proton Chemical Shifts In NMR. Part 16. Proton Chemical Shifts In Acetylenes And The Anisotropic And Steric Effects Of The Acetylene Group. *Journal of the Chemical Society-Perkin Transactions 2* **2001,** (7), 1195-1204.

16. Abreu, C. M. R.; Mendonça, P. V.; Serra, A. C.; Noble, B. B.; Guliashvili, T.; Nicolas, J.; Coote, M. L.; Coelho, J. F. J. Nitroxide-Mediated Polymerization of Vinyl Chloride at Low Temperature: Kinetic and Computational Studies. *Macromolecules* **2016,** *49* (2), 490-498.

17. Ahmed, S. A.; Moren, T.; Sehlstedt-Persson, M.; Blom, A. Effect of Oil Impregnation On Water Repellency, Dimensional Stability and Mold Susceptibility of Thermally Modified European Aspen and Downy Birch Wood. *Journal of Wood Science* **2017,** *63* (1), 74-82.

18. Aiken, W.; Alfrey, T., Jr.; Janssen, A.; Mark, H. Creep Behavior of Plasticized Vinylite VYNW. *Journal of Polymer Science* **1947,** *2*, 178-198.

19. Albro, P. W. Absorption, Metabolism, and Excretion of Di(2-ethylhexyl) Phthalate by Rats and Mice. *Environmental Health Perspectives* **1986,** *65*, 293-298.

20. Albro, P. W. The Metabolism of 2-Ethylhexanol in Rats. *Xenobiotica* **1975,** *5* (10), 625-636.

21. Albro, P. W.; Moore, B. Identification of the Metabolites of Simple Phthalate Diesters in Rat Urine. *Journal of Chromatography A* **1974,** *94* (1), 209-218.

22. Alfrey, T.; Price, C. C. Relative Reactivities in Vinyl Copolymerization *Journal of Polymer Science* **1947,** *2* (1), 101-106.

23. Alvaro, M.; García, H.; Miranda, M. A.; Primo, J. Preparation and Photolysis of Diaryl Esters of Acetylenedicarboxylic Acid. *Tetrahedron* **1992,** *48* (16), 3437-3444.

24. Anagnostopoulos, C. E.; Coran, A. Y.; Gamrath, H. R. Polymer–Diluent Interactions. I. A New Micromethod for Determining Polyvinyl Chloride-Diluent Interactions. *Journal of Applied Polymer Science* **1960,** *4* (11), 181-192.

25. Apelblat, A.; Korin, E.; Manzurola, E. Thermodynamic Properties of Aqueous Solutions with Citrate Ions. Compressibility Studies in Aqueous Solutions of Citric Acid. *Journal of Chemical Thermodynamics* **2013,** *64*, 14-21.

26. Arcadi, F. A.; Costa, C.; Imperatore, C.; Marchese, A.; Rapisarda, A.; Salemi, M.; Trimarchi, G. R.; Costa, G. Oral Toxicity of Bis(2-ethylhexyl) Phthalate During Pregnancy and Suckling in the Long-Evans Rat. *Food and Chemical Toxicology* **1998,** *36* (11), 963-970.

27. AuBuchon, J.; Estep, T.; Davey, R. The Effect of the Plasticizer Di-2-ethylhexyl Phthalate on the Survival of Stored RBCs. *Blood* **1988,** *71* (2), 448-452.

28. Barr, D. B.; Silva, M. J.; Kato, K.; Reidy, J. A.; Malek, N. A.; Hurtz, D.; Sadowski, M.; Needham, L. L.; Calafat, A. M. Assessing Human Exposure to Phthalates Using Monoesters and Their Oxidized Metabolites as Biomarkers. *Environmental Health Perspectives* **2003,** *111* (9), 1148-1151.

29. Becker, K.; Seiwert, M.; Angerer, J.; Heger, W.; Koch, H. M.; Nagorka, R.; Roßkamp, E.; Schlüter, C.; Seifert, B.; Ullrich, D. DEHP Metabolites in Urine of Children and DEHP in House Dust. *International Journal of Hygiene and Environmental Health* **2004,** *207* (5), 409-417.

30. Bellucci, M. C.; Marcelli, T.; Scaglioni, L.; Volonterio, A. Synthesis Of Diverse Spiroisoxazolidinohydantoins By Totally Regio- and Diasteroselective 1,3-Dipolar Cycloadditions. *RSC Advances* **2011,** *1* (7), 1250-1264.

31. Bentley, P.; Calder, I.; Elcombe, C.; Grasso, P.; Stringer, D.; Wiegand, H. J. Hepatic Peroxisome Proliferation in Rodents and its Significance for Humans. *Food and Chemical Toxicology* **1993,** *31* (11), 857-907.

32. Bigg, D. C. H. Comparison of Methods for Assessing the Degree of Interaction Between Plasticizers and Poly(vinyl chloride). *Journal of Applied Polymer Science* **1975,** *19* (11), 3119-3127.

33. Blotny, G. Recent Applications of 2,4,6-Trichloro-1,3,5-Triazine and its Derivatives in Organic Synthesis. *Tetrahedron* **2006,** *62* (41), 9507-9522.

34. Bonora, S.; Ercoli, L.; Torreggiani, A.; Fini, G. Influence of Sebacate Plasticizers on the Thermal Behaviour of Dipalmitoylphosphatidylcholine Liposomes. *Thermochimica Acta* **2002,** *385* (1-2), 51-61.

35. Borch, J.; Metzdorff, S. B.; Vinggaard, A. M.; Brokken, L.; Dalgaard, M. Mechanisms Underlying the Anti-Androgenic Effects of Diethylhexyl Phthalate in Fetal Rat Testis. *Toxicology* **2006,** *223* (1), 144-155.

36. Brase, S.; Gil, C.; Knepper, K.; Zimmermann, V. Organic Azides: An Exploding Diversity of a Unique Class of Compounds. *Angewandte Chemie-International Edition* **2005,** *44* (33), 5188-5240.

37. Braun, D. PVC - Origin, Growth, and Future. *Journal of Vinyl and Additive Technology* **2001,** *7* (4), 168-176.

38. Braun, D.; Böhringer, B.; Iván, B.; Kelen, T.; Tüdös, F. Structural Defects in Poly(vinyl chloride)—IV. Thermal Degradation of Vinyl Chloride/Acetylene Copolymers. *European Polymer Journal* **1986,** *22* (1), 1-4.

39. Brown, H. C.; McDaniel, D. H.; Hafliger, O. Chapter 14 - Dissociation Constants - Braude, E.A. In *Determination of Organic Structures by Physical Methods*, Nachod, F. C., Ed. Academic Press: 1955; pp 567-662.

40. Buchner, E.; Witter, H. III. Synthese der Pyrazolin-3,4,5-tricarbonsäure. *Justus Liebigs Annalen der Chemie* **1893,** *273* (2-3), 239-245.

41. Busse, W. F. The Physical Structure of Elastic Colloids. *The Journal of Physical Chemistry* **1932,** *36*, 2862-2879.

42. Cadet, J.; Davies, K. J. A.; Medeiros, M. H. G.; Di Mascio, P.; Wagner, J. R. Formation and Repair of Oxidatively Generated Damage in Cellular DNA. *Free Radical Biology and Medicine* **2017,** *107*, 13-34.

43. Caldas, V.; Radiotis, T.; Brown, G. R. Automated Microscopic Technique for Evaluating Poly(vinyl chloride)-Plasticizer Compatibility. *Journal of Applied Polymer Science* **1994,** *52* (13), 1939-1947.

44. Castro, R. E. N.; Toledo, E. A.; Rubira, A. F.; Muniz, E. C. Crystallisation and Miscibility of Poly(Ethylene Oxide)/Poly(Vinyl Chloride) Blends. *Journal of Materials Science* **2003,** *38* (4), 699-703.

45. Chan, L. C.; Cox, B. G. Kinetics of Amide Formation through Carbodiimide/N-Hydroxybenzotriazole (HOBt) Couplings. *The Journal of Organic Chemistry* **2007,** *72* (23), 8863-8869.

46. Charlson, J. L.; Chee, G.; McColeman, H. Synthesis of Acetylenedicarboxylic Acid Esters and Asymmetric Diels-Alder Reactions of the Bis(methyl (S)-lactyl) Ester. *Canadian Journal of Chemistry* **1995,** *73* (9), 1454-1462.

47. Charlton, J. L.; Chee, G. Synthesis of Chiral Esters of Acetylenedicarboxylic Acid. *Tetrahedron Letters* **1994,** *35* (34), 6243-6246.

48. Chiellini, F.; Ferri, M.; Morelli, A.; Dipaola, L.; Latini, G. Perspectives on Alternatives to Phthalate Plasticized Poly(vinyl chloride) in Medical Devices Applications. *Progress in Polymer Science* **2013,** *38* (7), 1067-1088.

49. Chubb, F. L.; Edward, J. T.; Wong, S. C. Simplex Optimization of Yields in the Bucherer-Bergs reaction. *Journal of Organic Chemistry* **1980,** *45* (12), 2315-2320.

50. Clark, F. W. Plasticizers. *Chemistry & Industry (London, U. K.)* **1941**, 228-230.

51. Crocker, J. F. S.; Safe, S. H.; Acott, P. Effects of Chronic Phthalate Exposure on the Kidney. *Journal of Toxicology and Environmental Health* **1988,** *23* (4), 433-444.

52. Crowther, M. W.; Szeverenyi, N. M.; Levy, G. C. Absolute Tacticity Assignments of Poly(vinyl chloride) via the Two-Dimensional NMR Spin-Lock RELAY Experiment. *Macromolecules* **1986,** *19* (5), 1333-1336.

53. da Silva Neiro, S. M.; Dragunski, D. C.; Rubira, A. F.; Muniz, E. C. Miscibility of PVC/PEO Blends by Viscosimetric, Microscopic and Thermal Analyses. *European Polymer Journal* **2000,** *36* (3), 583-589.

54. Daniels, P. H. A Brief Overview of Theories of PVC Plasticization and Methods Used to Evaluate PVC-Plasticizer Interaction. *Journal of Vinyl & Additive Technology* **2009,** *15* (4), 219-223.

55. Davis, B. J.; Maronpot, R. R.; Heindel, J. J. Di-(2-Ethylhexyl) Phthalate Suppresses Estradiol and Ovulation in Cycling Rats. *Toxicology and Applied Pharmacology* **1994,** *128* (2), 216-223.

56. Demirci, G.; Tasdelen, M. A. Synthesis and Characterization of Graft Copolymers by Photoinduced CuAAC Click Chemistry. *European Polymer Journal* **2015,** *66*, 282-289.

57. Desdoits-Lethimonier, C.; Albert, O.; Le Bizec, B.; Perdu, E.; Zalko, D.; Courant, F.; Lesne, L.; Guille, F.; Dejucq-Rainsford, N.; Jegou, B. Human Testis Steroidogenesis Is Inhibited by Phthalates. *Human Reproduction* **2012,** *27* (5), 1451-1459.

58. Deyo, J. A. Carcinogenicity and Chronic Toxicity of Di-2-Ethylhexyl Terephthalate (DEHT) Following a 2-Year Dietary Exposure in Fischer 344 Rats. *Food and Chemical Toxicology* **2008,** *46* (3), 990-1005.

59. Diels, O.; Alder, K. Synthesen in der Hydroaromatischen Reihe. *Justus Liebigs Annalen der Chemie* **1928,** *460* (1), 98-122.

60. Diels, O.; Thiele, W. E. Zur Kenntnis der Dien-Synthesen, XXX. Mitteil.: Über das Chlorid der Acetylendicarbonsäure. *Berichte der Deutschen Chemischen Gesellschaft (A and B Series)* **1938,** *71* (6), 1173-1178.

61. Doolittle, A. K. Application of a Mechanistic Theory of Solvent Action to Plasticizers and Plasticization. *Journal of Polymer Science* **1947,** *2*, 121-141.

62. Doolittle, A. K. Mechanism of Solvent Action. *Industrial & Engineering Chemistry* **1944,** *36*, 239-244.

63. Doolittle, A. K. Mechanism of Solvent Action. Influence of Molecular Size and Shape on Temperature Dependence of Solvent Ability. *Industrial & Engineering Chemistry* **1946,** *38*, 535-540.

64. Doty, P.; Zable, H. S. Determination of Polymer–Liquid Interaction by Swelling Measurements. *Journal of Polymer Science* **1946,** *1* (2), 90-101.

65. Earla, Aruna. Plasticization of PVC: Covalently Linked Plasticizers Using Thermal or Copper-Catalyzed Azide-Alkyne Cycloadditions. Ph.D. Dissertation. University of California Santa Cruz, United States of America, California, Santa Cruz, 2016.

66. Earla, A.; Braslau, R. Covalently Linked Plasticizers: Triazole Analogues of Phthalate Plasticizers Prepared by Mild Copper-Free "Click" Reactions with Azide-Functionalized PVC. *Macromolecular Rapid Communications* **2014,** *35* (6), 666-671.

67. Earla, A.; Li, L. B.; Costanzo, P.; Braslau, R. Phthalate Plasticizers Covalently Linked to PVC via Copper-Free or Copper Catalyzed Azide-Alkyne Cycloadditions. *Polymer* **2017,** *109*, 1-12.

68. Eckert, E.; Munch, F.; Goen, T.; Purbojo, A.; Muller, J.; Cesnjevar, R. Comparative Study On the Migration of Di-2-Ethylhexyl Phthalate (DEHP) and Tri-2-Ethylhexyl Trimellitate (TOTM) Into Blood From PVC Tubing Material of a Heart-Lung Machine. *Chemosphere* **2016,** *145*, 10-16.

69. Eichelberger, L. Iodination of Acetylene Derivatives. I. The Preparation of Diiodofumaric Acid. *Journal of the American Chemical Society* **1926,** *48*, 1320-1322.

70. Elakesh, E. O.; Richard Hull, T.; Price, D.; Carty, P. Thermal Decomposition of Chlorinated Poly(vinyl chloride) (CPVC). *Journal of Vinyl and Additive Technology* **2003,** *9* (3), 116-126.

71. Elsisi, A. E.; Carter, D. E.; Sipes, I. G. Dermal Absorbtion of Phthalate Diesters in Rats. *Fundamental and Applied Toxicology* **1989,** *12* (1), 70-77.

72. Endo, K. Synthesis and Structure of Poly(vinyl chloride). *Progress in Polymer Science* **2002,** *27* (10), 2021-2054.

73. Enomoto, S. Polymerization of Vinyl Chloride. *Journal of Polymer Science Part A: Polymer Chemistry* **1969,** *7*, 1255-1267.

74. Erythropel, H. C.; Maric, M.; Nicell, J. A.; Leask, R. L.; Yargeau, V. Leaching of the Plasticizer Di(2-ethylhexyl)phthalate (DEHP) From Plastic Containers and the Question of Human Exposure. *Applied Microbiology and Biotechnology* **2014,** *98* (24), 9967-9981.

75. Fankhauser-Noti, A.; Grob, K. Blank Problems In Trace Analysis of Diethylhexyl and Dibutyl Phthalate: Investigation of the Sources, Tips and Tricks. *Analytica Chimica Acta* **2007,** *582* (2), 353-360.

76. Fischer, I.; Schmitt, W. F.; Porth, H.-C.; Allsopp, M. W.; Vianello, G. Poly(Vinyl Chloride). In *Ullmann's Encyclopedia of Industrial Chemistry*, Wiley-VCH Verlag GmbH & Co. KGaA: 2000; pp 1-29.

77. Fischer, N. Morphology of Mass PVC. *Journal of Vinyl Technology* **1984,** *6* (1), 35-49.

78. Fisher, J. S. Environmental Anti-Androgens and Male Reproductive Health: Focus on Phthalates and Testicular Dysgenesis Syndrome. *Reproduction* **2004,** *127* (3), 305-315.

79. Fisher, J. S.; Macpherson, S.; Marchetti, N.; Sharpe, R. M. Human 'Testicular Dysgenesis Syndrome': A Possible Model Using In-Utero Exposure of the Rat to Dibutyl Phthalate. *Human Reproduction* **2003,** *18* (7), 1383-1394.

80. Fleming, I. Ionic Reactions—Reactivity. In *Molecular Orbitals and Organic Chemical Reactions*, John Wiley & Sons, Ltd: 2010; pp 145-203.

81. Flory, P. J. Kinetics of the Degradation of Polyesters by alcohols. *Journal of the American Chemical Society* **1940,** *62*, 2255-2261.

82. Flory, P. J. Thermodynamics of High Polymer Solutions. *The Journal of Chemical Physics* **1942,** *10* (1), 51-61.

83. Flory, P. J. Thermodynamics of High Polymer Solutions. *The Journal of Chemical Physics* **1941,** *9* (8), 660-661.

84. Flory, P. J. Viscosities of Linear Polyesters. An Exact Relationship between Viscosity and Chain Length. *Journal of the American Chemical Society* **1940,** *62* (5), 1057-1070.

85. Fordham, J. W. L. Stereoregulated Polymerization in the Free Propagating Species. I. Theory. *Journal of Polymer Science* **1959,** *39* (135), 321-334.

86. Foster, P. M. D. Disruption of Reproductive Development in Male Rat Offspring Following In Utero Exposure to Phthalate Esters. *International Journal of Andrology* **2006,** *29* (1), 140-147.

87. Foster, P. M. D.; Mylchreest, E.; Gaido, K. W.; Sar, M. Effects of Phthalate Esters on the Developing Reproductive Tract of Male Rats. *Human Reproduction Update* **2001,** *7* (3), 231-235.

88. Fox, T. G. Influence of Diluent and of Copolymer Composition on the Glass Temperature of a Polymer System. *Bull. Am. Phys. Soc. [2]* **1956,** *1*, 123.

89. Fox, T. G.; Flory, P. J. Viscosity-Molecular Weight and Viscosity-Temperature Relationships for Polystyrene and Polyisobutylene. *Journal of the American Chemical Society* **1948,** *70* (7), 2384-2395.

90. Fox, T. G., Jr.; Flory, P. J. Second-Order Transition Temperatures and Related Properties of Polystyrene. I. Influence of Molecular Weight. *Journal of Applied Physics* **1950,** *21*, 581-591.

91. Franz, R. G. Comparisons of pK_a and log P Values of Some Carboxylic and Phosphonic Acids: Synthesis and Measurement. *AAPS PharmSci* **2001,** *3* (2), 1-13.

92. Fujii, K.; Matsumoto, M.; Ukida, J. Hydrolysis of Poly(vinyl acetate)s of Various Tacticities. *Journal of Polymer Science Part B-Polymer Letters* **1963,** *1* (12), 687-691.

93. Gordon, M.; Taylor, J. S. Ideal Copolymers and the Second-Order Transitions of Synthetic Rubbers. i. Non-Crystalline Copolymers. *Journal of Applied Chemistry* **1952,** *2* (9), 493-500.

94. Gouinlock, E. V. The Fusion of Highly Crystalline Poly(vinyl chloride). *Journal of Polymer Science: Polymer Physics Edition* **1975,** *13* (8), 1533-1542.

95. Graham, P. R. Phthalate Ester Plasticizers--Why and How They Are Used. *Environmental Health Perspectives* **1973,** *3*, 3-12.

96. Griswold, M. D. The Central Role of Sertoli Cells in Spermatogenesis. *Seminars in Cell & Developmental Biology* **1998,** *9* (4), 411-416.

97. Hakkarainen, M. New PVC Materials for Medical Applications - The Release Profile of PVC/Polycaprolactone-Polycarbonate Aged in Aqueous Environments. *Polymer Degradation and Stability* **2003,** *80* (3), 451-458.

98. Hankett, J. M.; Collin, W. R.; Chen, Z. Molecular Structural Changes of Plasticized PVC After UV Light Exposure. *Journal of Physical Chemistry B* **2013,** *117* (50), 16336-16344.

99. Hannas, B. R.; Lambright, C. S.; Furr, J.; Howdeshell, K. L.; Wilson, V. S.; Gray, L. E. Dose-Response Assessment of Fetal Testosterone Production and Gene Expression Levels in Rat Testes Following In Utero Exposure to Diethylhexyl Phthalate, Diisobutyl Phthalate, Diisoheptyl Phthalate, and Diisononyl Phthalate. *Toxicological Sciences* **2011,** *123* (1), 206-216.

100. Hansen, C. M. The Three Dimensional Solubility Parameter and Solvent Diffusion Coefficient : Their Importance in Surface Coating Formulation. Copenhagen Danish Technical Press, Denmark, 1967.

101. Heger, N. E.; Hall, S. J.; Sandrof, M. A.; McDonnell, E. V.; Hensley, J. B.; McDowel, E. N.; Martin, K. A.; Gaido, K. W.; Johnson, K. J.; Boekelheide, K. Human Fetal Testis Xenografts Are Resistant to Phthalate-Induced Endocrine Disruption. *Environmental Health Perspectives* **2012,** *120* (8), 1137-1143.

102. Heudorf, U.; Mersch-Sundermann, V.; Angerer, J. Phthalates: Toxicology and Exposure. *International Journal of Hygiene and Environmental Health* **2007,** *210* (5), 623-634.

103. Heyl, D.; Fessner, W. D. Facile Direct Synthesis of Acetylenedicarboxamides. *Synthesis-Stuttgart* **2014,** *46* (11), 1463-1468.

104. Hildebrand, J. H. A Critique of the Theory of Solubility of Non-Electrolytes. *Chemical Reviews* **1949,** *44* (1), 37-45.

105. Hildebrand, J. H.; Scott, R. L. *The Solubility of Nonelectrolytes*. Dover Publications: New York, 1964.

106. Hill, S. S.; Shaw, B. R.; Wu, A. H. B. The Clinical Effects of Plasticizers, Antioxidants, and Other Contaminants in Medical Polyvinylchloride Tubing During Respiratory and Non-Respiratory Exposure. *Clinica Chimica Acta* **2001,** *304* (1-2), 1-8.

107. Himo, F.; Lovell, T.; Hilgraf, R.; Rostovtsev, V. V.; Noodleman, L.; Sharpless, K. B.; Fokin, V. V. Copper(I)-Catalyzed Synthesis of Azoles. DFT Study Predicts Unprecedented Reactivity and Intermediates. *Journal of the American Chemical Society* **2005,** *127* (1), 210-216.

108. Hjertberg, T.; Sörvik, E. M. Formation of Anomalous Structures in PVC and Their Influence on the Thermal Stability: 2. Branch Structures and Tertiary Chlorine. *Polymer* **1983,** *24* (6), 673-684.

109. Hjertberg, T.; Sörvik, E. M. Formation of Anomalous Structures in PVC and Their Influence on the Thermal Stability: 3. Internal Chloroallylic Groups. *Polymer* **1983,** *24* (6), 685-692.

110. Hjertberg, T.; Sörvik, E. M. Formation of Anomalous Structures in PVC and Their Influence on Thermal Stability. I. Endgroup Structures and Labile Chlorine Substituted by Phenol. *Journal of Macromolecular Science: Part A - Chemistry* **1982,** *17* (6), 983-1004.

111. Hoffmann, J. D. W., J. J. Melting Process and the Equilibrium Melting Temperature of Polychlorotrifluoroethylene. *Journal of Research of the National Bureau of Standards-A. Physics and Chemistry* **1962,** *66A* (1), 13-28.

112. Hofreiter, M.; Serre, D.; Poinar, H. N.; Kuch, M.; Paabo, S. Ancient DNA. *Nature Reviews Genetics* **2001,** *2* (5), 353-359.

113. Horowitz, B.; Stryker, M. H.; Waldman, A. A.; Woods, K. R.; Gass, J. D.; Drago, J. Stablization of Red Blood-Cells By the Plasticizer, Diethylhexylphthalate. *Vox Sanguinis* **1985,** *48* (3), 150-155.

114. Hoss, M.; Jaruga, P.; Zastawny, T. H.; Dizdaroglu, M.; Paabo, S. DNA Damage and DNA Sequence Retrieval From Ancient Tissues. *Nucleic Acids Research* **1996,** *24* (7), 1304-1307.

115. Houwink, R. *Proceedings of the XIth International Congress of Pure and Applied Chemistry: London, 17th-24th July, 1947*. Hepworth: London, 1947.

116. Howdeshell, K. L.; Furr, J.; Lambright, C. R.; Rider, C. V.; Wilson, V. S.; Gray, L. E. Cumulative Effects of Dibutyl Phthalate and Diethylhexyl Phthalate on Male Rat Reproductive Tract Development: Altered Fetal Steroid Hormones and Genes. *Toxicological Sciences* **2007,** *99* (1), 190-202.

117. Huggins, M. L. Solutions of Long Chain Compounds. *The Journal of Chemical Physics* **1941,** *9* (5), 440.

118. Huisgen, R. 1,3-Dipolar Cycloadditions. Past and Future. *Angewandte Chemie International Edition in English* **1963,** *2* (10), 565-598.

119. Huisgen, R. Kinetics and Mechanism of 1,3-Dipolar Cycloadditions. *Angewandte Chemie International Edition in English* **1963,** *2* (11), 633-645.

120. Huisgen, R.; Stangl, H.; Sturm, H. J.; Wagenhofer, H. Kinetik und Mechanismus der 1.3-dipolaren Additionen der Diazoalkane. *Angewandte Chemie* **1961,** *73* (5), 170.

121. Ito, M.; Nagai, K. Analysis of Degradation Mechanism of Plasticized PVC Under Artificial Aging Conditions. *Polymer Degradation and Stability* **2007,** *92* (2), 260-270.

122. Ivell, R.; Anand-Ivell, R. Biology of Insulin-Like Factor 3 in Human Reproduction. *Human Reproduction Update* **2009,** *15* (4), 463-476.

123. Jaeger , R. J.; Rubin , R. J. Migration of a Phthalate Ester Plasticizer from Polyvinyl Chloride Blood Bags into Stored Human Blood and Its Localization in Human Tissues. *New England Journal of Medicine* **1972,** *287* (22), 1114-1118.

124. Jaeger, R. J.; Rubin, R. J. Plasticizers From Plastic Devices: Extraction, Metabolism, and Accumulation By Biological Systems. *Science* **1970,** *170* (3956), 460-462.

125. Jang, B. N.; Wang, D.; Wilkie, C. A. Relationship Between the Solubility Parameter of Polymers and the Clay Dispersion in Polymer/Clay Nanocomposites and the Role of the Surfactant. *Macromolecules* **2005,** *38* (15), 6533-6543.

126. Jewett, J. C.; Bertozzi, C. R. Cu-free click cycloaddition reactions in chemical biology. *Chemical Society Reviews* **2010,** *39* (4), 1272-1279.

127. Jewett, J. C.; Sletten, E. M.; Bertozzi, C. R. Rapid Cu-Free Click Chemistry with Readily Synthesized Biarylazacyclooctynones. *Journal of the American Chemical Society* **2010,** *132* (11), 3688-3690.

128. Jia, P.; Hu, L.; Shang, Q.; Wang, R.; Zhang, M.; Zhou, Y. Self-Plasticization of PVC Materials via Chemical Modification of Mannich Base of Cardanol Butyl Ether. *ACS Sustainable Chemistry & Engineering* **2017,** *5* (8), 6665-6673.

129. Jia, P. Y.; Hu, L. H.; Feng, G. D.; Bo, C. Y.; Zhang, M.; Zhou, Y. H. PVC Materials Without Migration Obtained by Chemical Modification of Azide-Functionalized PVC and Triethyl Citrate Plasticizer. *Materials Chemistry and Physics* **2017,** *190*, 25-30.

130. Jia, P. Y.; Hu, L. H.; Yang, X. H.; Zhang, M.; Shang, Q. Q.; Zhou, Y. H. Internally Plasticized PVC Materials via Covalent Attachment of Aminated Tung Oil Methyl Ester. *RSC Advances* **2017,** *7* (48), 30101-30108.

131. Johnson, W. Final Report on the Safety Assessment of Acetyl Triethyl Citrate, Acetyl Tributyl Citrate, Acetyl Trihexyl Citrate, and Acetyl Trioctyl Citrate. *International Journal of Toxicology* **2002,** *21* (5), 1-17.

132. Kavlock, R.; Boekelheide, K.; Chapin, R.; Cunningham, M.; Faustman, E.; Foster, P.; Golub, M.; Henderson, R.; Hinberg, I.; Little, R.; Seed, J.; Shea, K.; Tabacova, S.; Tyl, R.; Williams, P.; Zacharewski, T. NTP Center for the Evaluation of Risks to Human Reproduction: Phthalates Expert Panel Report on the Reproductive and Developmental Toxicity of Di(2-ethylhexyl) Phthalate. *Reproductive Toxicology* **2002,** *16* (5), 529-653.

133. Kevy, S. V.; Jacobson, M. S. Hepatic Effects of a Phthalate Ester Plasticizer Leached from Poly(vinyl chloride) Blood Bags Following Transfusion. *Environmental Health Perspectives* **1982,** *45*, 57-64.

134. Kirkpatrick, A. Some Relations Between Molecular Structure and Plasticizing Effect. *Journal of Applied Physics* **1940,** *11* (4), 255-261.

135. Kobrosly, R. W.; Parlett, L. E.; Stahlhut, R. W.; Barrett, E. S.; Swan, S. H. Socioeconomic Factors and Phthalate Metabolite Concentrations Among United States Women of Reproductive Age. *Environmental Research* **2012,** *115*, 11-17.

136. Koch, H. M.; Bolt, H. M.; Preuss, R.; Angerer, J. New Metabolites of Di(2-ethylhexyl)phthalate (DEHP) in Human Urine and Serum After Single Oral Doses of Deuterium-Labelled DEHP. *Archives of Toxicology* **2005,** *79* (7), 367-376.

137. Koch, H. M.; Preuss, R.; Angerer, J. Di(2-ethylhexyl)phthalate (DEHP): Human Metabolism and Internal Exposure – An Update and Latest Results. *International Journal of Andrology* **2006,** *29* (1), 155-165.

138. Kolb, H. C.; Finn, M. G.; Sharpless, K. B. Click Chemistry: Diverse Chemical Function From A Few Good Reactions. *Angewandte Chemie-International Edition* **2001,** *40* (11), 2004-2021.

139. Kumar, R.; Tiwari, P.; Maulik, P. R.; Misra, A. K. A Generalized Procedure for the One-Pot Preparation of Glycosyl Azides and Thioglycosides Directly from Unprotected Reducing Sugars under Phase‐Transfer Reaction Conditions. *European Journal of Organic Chemistry* **2005,** (1), 74-79.

140. Kunishima, M.; Kawachi, C.; Hioki, K.; Terao, R.; Tani, S. Formation of Carboxamides by Direct Condensation of Carboxylic Acids and Amines in Alcohols Using a New Alcohol- and Water-Soluble Condensing Agent: DMT-MM. *Tetrahedron* **2001,** *57* (8), 1551-1558.

141. Kunishima, M.; Kawachi, C.; Morita, J.; Terao, K.; Iwasaki, F.; Tani, S. 4-(4,6-Dimethoxy-1,3,5-triazin-2-yl)-4-methyl-morpholinium Chloride: An Efficient Condensing Agent Leading to the Formation of Amides and Esters. *Tetrahedron* **1999,** *55* (46), 13159-13170.

142. Latini, G. Potential Hazards of Exposure to Di-(2-ethylhexyl)-Phthalate in Babies. *Biology of the Neonate* **2000,** *78* (4), 269-276.

143. Laurier, G. C.; Odriscoll, K. F.; Reilly, P. M. Estimating Reactivity in Free-Radical Copolymerizations. *Journal of Polymer Science-Polymer Symposia* **1985,** (72), 17-26.

144. Lee, K. W.; Chung, J. W.; Kwak, S.-Y. Synthesis and Characterization of Bio-Based Alkyl Terminal Hyperbranched Polyglycerols: A Detailed Study of Their Plasticization Effect and Migration resistance. *Green Chemistry* **2016,** *18* (4), 999-1009.

145. Lee, K. W.; Chung, J. W.; Kwak, S. Y. Structurally Enhanced Self-Plasticization of Poly(vinyl chloride) via Click Grafting of Hyperbranched Polyglycerol. *Macromolecular Rapid Communications* **2016,** *37* (24), 2045-2051.

146. Lhuguenot, J.-C.; Mitchell, A. M.; Milner, G.; Lock, E. A.; Elcombe, C. R. The Metabolism of Di(2-ethylhexyl) Phthalate (DEHP) and Mono-(2-ethylhexyl) Phthalate (MEHP) in Rats: In Vivo and In Vitro Dose and Time Dependency of Metabolism. *Toxicology and Applied Pharmacology* **1985,** *80* (1), 11-22.

147. Lhuguenot, J. C.; Mitchell, A. M.; Elcombe, C. R. The Metabolism of Mono-(2-Ethylhexyl) Phthalate (Mehp) and Liver Peroxisome Proliferation in the Hamster. *Toxicology and Industrial Health* **1988,** *4* (4), 431-441.

148. Lyche, J. L.; Gutleb, A. C.; Bergman, A.; Eriksen, G. S.; Murk, A. J.; Ropstad, E.; Saunders, M.; Skaare, J. U. Reproductive and Developmental Toxicity of Phthalates. *Journal of Toxicology and Environmental Health-Part B-Critical Reviews* **2009,** *12* (4), 225-249.

149. Maas, R. P.; Patch, S. C.; Pandolfo, T. J. Inhalation and Ingestion of Phthalate Compounds from Use of Synthetic Modeling Clays. *Bulletin of Environmental Contamination and Toxicology* **2004,** *73* (2), 227-234.

150. MacLeod, D. J.; Sharpe, R. M.; Welsh, M.; Fisken, M.; Scott, H. M.; Hutchison, G. R.; Drake, A. J.; van den Driesche, S. Androgen Action in the Masculinization Programming Window and Development of Male Reproductive Organs. *International Journal of Andrology* **2010,** *33* (2), 279-286.

151. Maier, G.; Jung, W. A. Acetylenedicarbonyl Dichloride. *Chemische Berichte-Recueil* **1982,** *115* (2), 804-807.

152. Marcelli, T.; Olimpieri, F.; Volonterio, A. Domino Synthesis of 1,3,5-Trisubstituted Hydantoins: A DFT Study. *Organic & Biomolecular Chemistry* **2011,** *9* (14), 5156-5161.

153. Marcilla, A.; Beltran, M. Wypych, G. Chapter 5 - Mechanisms of Plasticization. In *Handbook of Plasticizers (Third Edition)*, ChemTec Publishing: 2017; pp 119-134.

154. Marco, C.; Gömez, M. A.; Fatou, J. G.; Etxeberria, A.; Elorza, M. M.; Iruin, J. J. Miscibility of Poly(Vinyl Chloride)/Poly(Ethylene Oxide) blends—I. Thermal Properties and Solid State ^{13}C-NMR Study. *European Polymer Journal* **1993,** *29* (11), 1477-1481.

155. Marega, M.; Grob, K.; Moret, S.; Conte, L. Phthalate Analysis By Gas Chromatography-Mass Spectrometry: Blank Problems Related to the Syringe Needle. *Journal of Chromatography A* **2013,** *1273*, 105-110.

156. Martinez, G.; Mijangos, C.; Millan, J. Selective Substitution Reactions on PVC. Lability of Some Normal Structures. *Journal of Macromolecular Science Chemistry* **1982,** *A17* (7), 1129-1148.

157. McDonald, R. N.; Krueger, R. A. The Catalyzed Reaction of Acetylenedicarboxylic Acid and Thionyl Chloride. *The Journal of Organic Chemistry* **1963,** *28* (10), 2542-2544.

158. Meachem, S. J.; Nieschlag, E.; Simoni, M. Inhibin B in Male Reproduction: Pathophysiology and Clinical Relevance. *European Journal of Endocrinology* **2001,** *145* (5), 561-571.

159. Meek, M. E.; Chan, P. K. L. Bis(2-ethylhexyl)phthalate: Evaluation of Risks to Health From Environmental Exposure in Canada. *Journal of Environmental Science and Health, Part C* **1994,** *12* (2), 179-194.

160. Michael, A. Ueber die Einwirkung von Diazobenzolimid auf Acetylendicarbonsauremethylester. *Journal für praktische Chemie* **1893,** *48*, 94-95.

161. Mijangos, C.; Martinez, A.; Michel, A. Fonctionnalisation du Polychlorure de Vinyle: Greffage de Fonctions Plastifiantes (Type Ester d'Ethyle-Hexyle). *European Polymer Journal* **1986,** *22* (5), 417-421.

162. Minsker, K. S.; Lisitsky, V. V.; Kolesov, S. V.; Zaikov, G. E. New Developments in Degradation and Stabilization of Polymers Based on Vinyl Chloride. *Journal of Macromolecular Science, Part C* **1981,** *20* (2), 243-308.

163. Mitchell, R. T.; Childs, A. J.; Anderson, R. A.; van den Driesche, S.; Saunders, P. T. K.; McKinnell, C.; Wallace, W. H. B.; Kelnar, C. J. H.; Sharpe, R. M. Do Phthalates Affect Steroidogenesis by the Human Fetal Testis? Exposure of Human Fetal Testis Xenografts to Di-*n*-Butyl Phthalate. *The Journal of Clinical Endocrinology and Metabolism* **2012,** *97* (3), E341-E348.

164. Mylchreest, E.; Sar, M.; Cattley, R. C.; Foster, P. M. D. Disruption of Androgen-Regulated Male Reproductive Development by Di(*n*-Butyl) Phthalate During Late Gestation in Rats is Different from Flutamide. *Toxicology and Applied Pharmacology* **1999,** *156* (2), 81-95.

165. Natta, G. Une Nouvelle Classe de Polymeres d'α-Olefines Ayant une Régularité de Structure Exceptionnelle. *Journal of Polymer Science* **1955,** *16* (82), 143-154.

166. Natta, G.; Corradini, P. The Structure of Crystalline 1,2-Polybutadiene and of Other "Syndyotactic Polymers". *Journal of Polymer Science* **1956,** *20* (95), 251-266.

167. Navarro, R.; Bierbrauer, K.; Mijangos, C.; Goiti, E.; Reinecke, H. Modification of Poly(Vinyl Chloride) with New Aromatic Thiol Compounds. Synthesis and Characterization. *Polymer Degradation and Stability* **2008,** *93* (3), 585-591.

168. Navarro, R.; Gacal, T.; Ocakoglu, M.; Garcia, C.; Elvira, C.; Gallardo, A.; Reinecke, H. Nonmigrating Equivalent Substitutes for PVC/DOP Formulations as Shown by a TG Study of

PVC with Covalently Bound PEO-PPO Oligomers. *Macromolecular Rapid Communications* **2017,** *38* (6).

169. Navarro, R.; Perrino, M. P.; Garcia, C.; Elvira, C.; Gallardo, A.; Reinecke, H. Highly Flexible PVC Materials Without Plasticizer Migration as Obtained by Efficient One-Pot Procedure Using Trichlorotriazine Chemistry. *Macromolecules* **2016,** *49* (6), 2224-2227.

170. Navarro, R.; Perrino, M. P.; Garcia, C.; Elvira, C.; Gallardo, A.; Reinecke, H. Opening New Gates for the Modification of PVC or Other PVC Derivatives: Synthetic Strategies for the Covalent Binding of Molecules to PVC. *Polymers* **2016,** *8* (4), 152-165.

171. Navarro, R.; Perrino, M. P.; Tardajos, M. G.; Reinecke, H. Phthalate Plasticizers Covalently Bound to PVC: Plasticization with Suppressed Migration. *Macromolecules* **2010,** *43* (5), 2377-2381.

172. Noyce, D. S.; Pollack, R. M. Mechanisms for the Acid-Catalyzed Hydrolysis of Vinyl Acetate and Isopropenyl Acetate. *Journal of the American Chemical Society* **1969,** *91* (25), 7158-7163.

173. Oca, M. L.; Rubio, L.; Sarabia, L. A.; Ortiz, M. C. Dealing With the Ubiquity of Phthalates In the Laboratory When Determining Plasticizers By Gas Chromatography/Mass Spectrometry and PARAFAC. *Journal of Chromatography A* **2016,** *1464*, 124-140.

174. Ott, E. Über Symmetrische und Asymmetrische Dicarbonsäurechloride. *Justus Liebigs Annalen der Chemie* **1912,** *392* (3), 245-285.

175. Pak, H. K.; Han, J.; Jeon, M.; Kim, Y.; Kwon, Y.; Park, J. Y.; Rhee, Y. H.; Park, J. Synthesis of Enamides by Ruthenium-Catalyzed Reaction of Alkyl Azides with Acid Anhydrides in Ionic Liquid. *ChemCatChem* **2015,** *7* (24), 4030-4034.

176. Parks, L. G.; Ostby, J. S.; Lambright, C. R.; Abbott, B. D.; Klinefelter, G. R.; Barlow, N. J.; Gray, L. E. The Plasticizer Diethylhexyl Phthalate Induces Malformations by Decreasing Fetal Testosterone Synthesis During Sexual Differentiation in the Male Rat. *Toxicological Sciences* **2000,** *58* (2), 339-349.

177. Pascoal, M.; Brook, M. A.; Gonzaga, F.; Zepeda-Velazquez, L. Thermally controlled Silicone Functionalization Using Selective Huisgen Reactions. *European Polymer Journal* **2015,** *69* (Supplement C), 429-437.

178. Pawlak, M.; Mistlberger, G.; Bakker, E. In Situ Surface Functionalization of Plasticized Poly(Vinyl Chloride) Membranes by Click Chemistry. *Journal of Materials Chemistry* **2012,** *22* (25), 12796-12801.

179. Pham, Q.-T.; Millan, J.-L.; Madruga, E. L. Thermodynamics of the Stereosequence Propagations in the Radical Polymerization of Vinyl Chloride Studied by ^{13}C-NMR and IR. *Die Makromolekulare Chemie* **1974,** *175* (3), 945-952.

180. Pinal, R. Entropy of Mixing and the Glass Transition of Amorphous Mixtures. *Entropy* **2008,** *10* (3), 207-223.

181. Preuss, R.; Koch, H. M.; Angerer, J. Biological Monitoring of the Five Major Metabolites of Di-(2-ethylhexyl)phthalate (DEHP) in Human Urine Using Column-Switching

Liquid Chromatography–Tandem Mass Spectrometry. *Journal of Chromatography B* **2005,** *816* (1), 269-280.

182. Qi, D. H.; Yang, K.; Zhang, D.; Chen, B.; Wei, Q.; Zhang, C. H. Experimental Investigation of a Turbocharged CRDI Diesel Engine Fueled with Tung Oil-Diesel-Ethanol Microemulsion Fuel. *Renewable Energy* **2017,** *113*, 1201-1207.

183. Rathwell, K.; Sperry, J.; Brimble, M. A. Synthesis of Triazole Analogues of the Nanaomycin Antibiotics Using 'Click Chemistry'. *Tetrahedron* **2010,** *66* (23), 4002-4009.

184. Riemenschneider, W. Carboxylic Acids, Aliphatic. In *Ullmann's Encyclopedia of Industrial Chemistry*, Wiley-VCH Verlag GmbH & Co. KGaA: 2000; p 108.

185. Rock, G.; Labow, R. S.; Franklin, C.; Burnett, R.; Tocchi, M. Hypotension and Cardiac-Arrest in Rats After Infusion of Mono(2-Ethylhexyl)phthalate (MEHP), a Contaminant of Stored-Blood. *New England Journal of Medicine* **1987,** *316* (19), 1218-1219.

186. Rostovtsev, V. V.; Green, L. G.; Fokin, V. V.; Sharpless, K. B. A Stepwise Huisgen Cycloaddition Process: Copper(I)-Catalyzed Regioselective "Ligation" of Azides and Terminal Alkynes. *Angewandte Chemie International Edition* **2002,** *41* (14), 2596-2599.

187. Roth, B.; Herkenrath, P.; Lehmann, H. J.; Ohles, H. D.; Homig, H. J.; Benzbohm, G.; Kreuder, J.; Younossihartenstein, A. Di-(2-Ethylhexyl)-Phthalate as Plasticizer in PVC Respiratory Tubing Systems-Indications of Hazardous Effects on Pulmonary-Function in Mechanically Ventilated, Preterm Infants. *European Journal of Pediatrics* **1988,** *147* (1), 41-46.

188. Rubin, R. J.; Jaeger, R. J. Some Pharmacologic and Toxicologic Effects of Di-2-ethylhexyl Phthalate (DEHP) and Other Plasticizers. *Environmental Health Perspectives* **1973,** *3*, 53-59.

189. Rudel, R. A.; Brody, J. G.; Spengler, J. C.; Vallarino, J.; Geno, P. W.; Sun, G.; Yau, A. Identification of Selected Hormonally Active Agents and Animal Mammary Carcinogens in Commercial and Residential Air and Dust Samples. *Journal of the Air & Waste Management Association* **2001,** *51* (4), 499-513.

190. Ruggli, P. Uber Versuche zur Darstellung von Derivaten des Diamido-acetylens. 4. Mitteilung über Acetylenderivate. *Helvetica Chimica Acta* **1920,** *3*, 559-572.

191. Rusen, E.; Marculescu, B.; Butac, L.; Preda, N.; Mihut, L. The Synthesis and Characterization of Poly Vinyl Chloride Chemically Modified with C60. *Fullerenes, Nanotubes and Carbon Nanostructures* **2008,** *16* (3), 178-185.

192. Salazar-Martinez, E.; Romano-Riquer, P.; Yanez-Marquez, E.; Longnecker, M. P.; Hernandez-Avila, M. Anogenital Distance in Human Male and Female Newborns: A Descriptive, Cross-Sectional Study. *Environmental Health* **2004,** *3* (1), 8.

193. Sampson, J.; de Korte, D. DEHP-Plasticised PVC: Relevance to Blood Services*. *Transfusion Medicine* **2011,** *21* (2), 73-83.

194. Schettler, T. Human Exposure to Phthalates via Consumer Products. *International Journal of Andrology* **2006,** *29* (1), 134-139.

195. Scott, H. M.; Mason, J. I.; Sharpe, R. M. Steroidogenesis in the Fetal Testis and Its Susceptibility to Disruption by Exogenous Compounds. *Endocrine Reviews* **2009,** *30* (7), 883-925.

196. Scott, R. C.; Dugard, P. H.; Ramsey, J. D.; Rhodes, C. In Vitro Absorption of Some o-Phthalate Diesters Through Human and Rat Skin. *Environmental Health Perspectives* **1987,** *74*, 223-227.

197. Semon, W. L.; Stahl, G. A. History of Vinyl-Chloride Polymers. *Journal of Macromolecular Science-Chemistry* **1981,** *A 15* (6), 1263-1278.

198. Senichev, V. Y.; Tereshatov, V. V.; Wypych, G. Chapter 6 - Theories of Compatibility. In *Handbook of Plasticizers (Third Edition)*, ChemTec Publishing: 2017; pp 135-164.

199. Shamir, E. R.; Ewald, A. J. Three-Dimensional Organotypic Culture: Experimental Models of Mammalian Biology and Disease. *Nature Reviews Molecular Cell Biology* **2014,** *15* (10), 647-664.

200. Sharpe, R. M.; Franks, S. Environment, Lifestyle and Infertility - an Inter-Generational Issue. *Nature Medicine* **2002,** *8*, 33-40.

201. Shubhra, Q. T. H.; Alam, A. K. M. M.; Quaiyyum, M. A. Mechanical Properties of Polypropylene Composites: A Review. *Journal of Thermoplastic Composite Materials* **2013,** *26* (3), 362-391.

202. Silva, M. J.; Barr, D. B.; Reidy, J. A.; Malek, N. A.; Hodge, C. C.; Caudill, S. P.; Brock, J. W.; Needham, L. L.; Calafat, A. M. Urinary levels of Seven Phthalate Metabolites in the U.S. Population from the National Health and Nutrition Examination Survey (NHANES) 1999-2000. *Environ. Health Perspect.* **2004,** *112* (3), 331-338.

203. Simha, R. On A General Relation Involving Glass Temperature and Coefficients of Expansion of Polymers. *Journal of Chemical Physics* **1962,** *37* (5), 1003-1007.

204. Sinirlioglu, D.; Muftuoglu, A. E. Synthesis of an Inorganic-Organic Hybrid Material Based on Polyhedral Oligomeric Silsesquioxane and Polystyrene via Nitroxide-Mediated Polymerization and Click Reactions. *Designed Monomers and Polymers* **2011,** *14* (3), 273-286.

205. Skakkebaek, N. E.; Rajpert-De Meyts, E.; Main, K. M. Testicular Dysgenesis Syndrome: An Increasingly Common Developmental Disorder with Environmental Aspects. *Human Reproduction* **2001,** *16* (5), 972-978.

206. Sletten, E. M.; Bertozzi, C. R. From Mechanism to Mouse: A Tale of Two Bioorthogonal Reactions. *Accounts of Chemical Research* **2011,** *44* (9), 666-676.

207. Spade, D. J.; McDonnell, E. V.; Heger, N. E.; Sanders, J. A.; Saffarini, C. M.; Gruppuso, P. A.; De Paepe, M. E.; Boekelheide, K. Xenotransplantation Models to Study the Effects of Toxicants on Human Fetal Tissues. *Birth Defects Research Part B-Developmental and Reproductive Toxicology* **2014,** *101* (6), 410-422.

208. Starnes, W. H. Structural and Mechanistic Aspects of the Thermal Degradation of Poly(vinyl chloride). *Progress in Polymer Science* **2002,** *27* (10), 2133-2170.

209. Stroheker, T.; Cabaton, N.; Nourdin, G.; Regnier, J.-F.; Lhuguenot, J.-C.; Chagnon, M.-C. Evaluation of Anti-Androgenic Activity of Di-(2-ethylhexyl) Phthalate. *Toxicology* **2005,** *208* (1), 115-121.

210. Stuart, A.; McCallum, M. M.; Fan, D. M.; LeCaptain, D. J.; Lee, C. Y.; Mohanty, D. K. Poly(vinyl chloride) Plasticized With Succinate Esters: Synthesis and Characterization. *Polymer Bulletin* **2010,** *65* (6), 589-598.

211. Su, Y. C.; Lo, Y. L.; Hwang, C. C.; Wang, L. F.; Wu, M. H.; Wang, E. C.; Wang, Y. M.; Wang, T. P. Azide-Alkyne Cycloaddition For Universal Post-Synthetic Modifications of Nucleic Acids and Effective Synthesis of Bioactive Nucleic Acid Conjugates. *Organic & Biomolecular Chemistry* **2014,** *12* (34), 6624-6633.

212. Sun, Z.; Wang, W.; Feng, Z. Criterion of Polymer-Polymer Miscibility Determined By Viscometry. *European Polymer Journal* **1992,** *28* (10), 1259-1261.

213. Swan, S. H. Environmental Phthalate Exposure in Relation to Reproductive Outcomes and Other Health Endpoints in Humans. *Environmental Research* **2008,** *108* (2), 177-184.

214. Swan, S. H.; Main, K. M.; Liu, F.; Stewart, S. L.; Kruse, R. L.; Calafat, A. M.; Mao, C. S.; Redmon, J. B.; Ternand, C. L.; Sullivan, S.; Teague, J. L.; Study Future Families Res, T. Decrease in Anogenital Distance Among Male Infants with Prenatal Phthalate Exposure. *Environmental Health Perspectives* **2005,** *113* (8), 1056-1061.

215. ter Veld, M. G. R.; Schouten, B.; Louisse, J.; Es, D. S. van; Saag, P. T. van der; Rietjens, I. M. C. M.; Murk, A. J. Estrogenic Potency of Food-Packaging-Associated Plasticizers and Antioxidants As Detected in ERα and ERβ Reporter Gene Cell Lines. *Journal of Agricultural and Food Chemistry* **2006**, *54* (12), 4407-4416.

216. Tickner, J. A.; Schettler, T.; Guidotti, T.; McCally, M.; Rossi, M. Health Risks Posed by Use of Di-2-Ethylhexyl Phthalate (DEHP) in PVC Medical Devices: A Critical Review. *American Journal of Industrial Medicine* **2001,** *39* (1), 100-111.

217. Tiemblo, P.; Martinez, G.; Millan, J. L. A Verification by FTIR Spectroscopy of the Effect of Some Local Chain Conformations on the Specific Molecular Interactions of Solvents, Esters, and Polyesters with PVC. *Journal of Polymer Science Part A: Polymer Chemistry* **1995,** *33* (8), 1243-1255.

218. Tomaselli, F.; Gupta, V. P.; Calderon, H. S.; Brown, G. R. Poly(vinyl chloride)/Plasticizer-Mixture Interactions. Mixtures of Various Plasticizers of Industrial Importance. *Journal of Vinyl and Additive Technology* **1989,** *11* (1), 9-14.

219. Trasande, L.; Attina, T. M.; Sathyanarayana, S.; Spanier, A. J.; Blustein, J. Race/Ethnicity-Specific Associations of Urinary Phthalates with Childhood Body Mass in a Nationally Representative Sample. *Environmental Health Perspectives* **2013,** *121* (4), 501-506.

220. Tyman, J. H. P.; Wilczynski, D.; Kashani, M. A. Phenolic Lipids. Part XI. Compositional Studies on Technical Cashew Nutshell Liquid (CNSL) by Chromatography and Mass Spectroscopy. *Journal of the American Oil Chemists' Society* **1978,** *55* (9), 663-668.

221. Ugelstad, J.; Mork, P. C.; Dahl, P.; Rangnes, P. A Kinetic Investigation of the Emulsion Polymerization of Vinyl Chloride. *Journal of Polymer Science Part C: Polymer Symposia* **1969,** *27* (1), 49-68.

222. Volonterio, A.; Ramirez de Arellano, C.; Zanda, M. Synthesis of 1,3,5-Trisubstituted Hydantoins by Regiospecific Domino Condensation/Aza-Michael/O→N Acyl Migration of Carbodiimides with Activated α,β-Unsaturated Carboxylic Acids. *The Journal of Organic Chemistry* **2005,** *70* (6), 2161-2170.

223. Volonterio, A.; Zanda, M. Domino Condensation/Aza-Michael/O→N Acyl Migration of Carbodiimides with Activated α,β-Unsaturated Carboxylic Acids to Form Hydantoins. *Tetrahedron Letters* **2003,** *44* (47), 8549-8551.

224. Walter, C. W. Invention and Development of the Blood Bag. *Vox Sanguinis* **1984,** *47* (4), 318-324.

225. Winterfeldt, E. Additions to the Activated CC Triple Bond. *Angewandte Chemie-International Edition* **1967,** *6* (5), 423-434.

226. Wittassek, M.; Koch, H. M.; Angerer, J.; Bruening, T. Assessing Exposure to Phthalates - The Human Biomonitoring Approach. *Molecular Nutrition and Food Research* **2011,** *55* (1), 7-31.

227. Wittig, G.; Krebs, A. Zur Existenz Niedergliedriger Cycloalkine, I. *Chemische Berichte* **1961,** *94* (12), 3260-3275.

228. Wolf, C.; Lambright, C.; Mann, P.; Price, M.; Cooper, R. L.; Ostby, J.; L. Earl Gray, J. Administration of Potentially Antiandrogenic Pesticides (Procymidone, Linuron, Iprodione, Chlozolinate, p,p'-DDE, and Ketoconazole) and Toxic Substances (Dibutyl- and Diethylhexyl Phthalate, PCB 169, and Ethane Dimethane Sulphonate) During Sexual Differentiation Produces Diverse Profiles of Reproductive Malformations in the Male Rat. *Toxicology and Industrial Health* **1999,** *15* (1-2), 94-118.

229. Woodward, R. B.; Hoffmann, R. Stereochemistry of Electrocyclic Reactions. *Journal of the American Chemical Society* **1965,** *87* (2), 395-397.

230. Wooley, K. L.; Hawker, C. J.; Pochan, J. M.; Frechet, J. M. J. Physical Properties of Dendritic Macromolecules: A Glass Transition Temperature Study. *Macromolecules* **1993,** *26* (7), 1514-1519.

231. Wormuth, M.; Scheringer, M.; Vollenweider, M.; Hungerbühler, K. What Are the Sources of Exposure to Eight Frequently Used Phthalic Acid Esters in Europeans? *Risk Analysis* **2006,** *26* (3), 803-824.

232. Yang, J. B.; Feng, Y. Y.; Zeng, T.; Guo, X. T.; Li, L.; Hong, R. Y.; Qiu, T. Synthesis of Biodiesel via Transesterification of Tung Oil Catalyzed By New Bronsted Acidic Ionic Liquid. *Chemical Engineering Research & Design* **2017,** *117*, 584-592.

233. Yang, P.; Yan, J.; Sun, H. Z.; Fan, H. J.; Chen, Y.; Wang, F.; Shi, B. Novel Environmentally Sustainable Cardanol-Based Plasticizer Covalently Bound to PVC via Click Chemistry: Synthesis and Properties. *RSC Advances* **2015,** *5* (22), 16980-16985.

234. Yin, B.; Hakkarainen, M. Oligomeric Isosorbide Esters as Alternative Renewable Resource Plasticizers for PVC. *Journal of Applied Polymer Science* **2011,** *119* (4), 2400-2407.

235. Yoo, Y.; Youngblood, J. P. Tung Oil Wood Finishes with Improved Weathering, Durability, and Scratch Performance by Addition of Cellulose Nanocrystals. *ACS Applied Materials & Interfaces* **2017,** *9* (29), 24936-24946.

236. Zimmerman, H. E. On Molecular Orbital Correlation Diagrams, the Occurrence of Möbius Systems in Cyclization Reactions, and Factors Controlling Ground- and Excited-State Reactions. I. *Journal of the American Chemical Society* **1966,** *88* (7), 1564-1565.

237. Žlahtič, M.; Mikac, U.; Serša, I.; Merela, M.; Humar, M. Distribution and Penetration of Tung Oil in Wood Studied by Magnetic Resonance Microscopy. *Industrial Crops and Products* **2017,** *96*, 149-157.

238. Zota, A. R.; Calafat, A. M.; Woodruff, T. J. Temporal Trends in Phthalate Exposures: Findings from the National Health and Nutrition Examination Survey, 2001-2010. *Environmental Health Perspectives* **2014,** *122* (3), 235-241.